noble gases

noble gases

Edited by

RICHARD E. STANLEY, D.V.M.
U.S. Environmental Protection Agency

A. ALAN MOGHISSI, Ph.D.
U.S. Environmental Protection Agency

Technical Editor

JERRY J. LORENZ, B.A.
U.S. Environmental Protection Agency

NOBLE GASES

Edited by
RICHARD E. STANLEY
and
A. ALAN MOGHISSI

EDITORIAL NOTE

NOBLE GASES is based on a symposium which was held in Las Vegas, Nevada, from September 24 through 28, 1973, and was cosponsored by the U.S. Environmental Protection Agency's National Environmental Research Center at Las Vegas and the University of Nevada, Las Vegas.

The Symposium was attended by approximately 250 scientists, representing 11 countries. The intent of the Program Committee was to provide comprehensive coverage of the noble gases, including but not limited to, the properties, biokinetics, bioeffects, production and release to the environment, detection techniques, standards, and applications. The reader will note that this goal was adequately met, with all the intended areas of consideration being comprehensively addressed in this publication.

Although all the papers have been reviewed by the Editors, the views expressed are entirely the responsibility of the individual authors.

ORGANIZING COMMITTEES

Symposium Chairmen

D. S. Barth
Director
National Environmental Research Center - Las Vegas
U. S. Environmental Protection Agency
Las Vegas, NV 89114

R. B. Smith
Dean, College of Science and Mathematics
University of Nevada, Las Vegas
Las Vegas, NV 89109

Program Committee

A. Alan Moghissi, Chairman
Visiting Professor
Office of Interdisciplinary Programs
Georgia Institute of Technology
Atlanta, GA 30332

Richard E. Stanley, Deputy Chairman
Technical Advisor
Monitoring Systems Research & Development Laboratory
National Environmental Research Center - Las Vegas
U. S. Environmental Protection Agency
Las Vegas, NV 89114

Victor P. Bond
Associate Director
Life Sciences and Chemistry
Brookhaven National Laboratory
Upton, Long Island, NY 11973

Peter A. Morris
U. S. Atomic Energy Commission
Washington, DC 20545

Hans E. Suess
University of California
San Diego, CA 92412

Duncan A. Holaday
Mt. Sinai School of Medicine, New York
7 Carlton Road
Wellesley, MA 02181

Neil Bartlett
University of California
Lawrence Berkeley Laboratory
Department of Chemistry
Berkeley, CA 94720

Jack Russell
U. S. Environmental Protection Agency
Waterside Mall Bldg, Rm. 603
4th and M Streets, S. W.
Washington, DC 20460

Local Arrangements Committee: Richard E. Jaquish (EPA), Chairman

Publicity and Printing: Geneva S. Douglas (EPA), Co-chairman
R. Dennis Tate (EPA), Co-chairman

Protocol & International Relations Committee: Marianne Carpenter (EPA), Chairman

Finance Committee: Keith McNeil (UNLV), Chairman

Exhibits Committee: John S. Coogan (EPA), Chairman

TABLE OF CONTENTS

OPENING ADDRESS

Stanley M. Greenfield
Assistant Administrator for Research and Development
U. S. Environmental Protection Agency
Washington, DC 20460

For several reasons, I consider it a personal pleasure to welcome you here, and to present these introductory remarks to open this symposium on the Noble Gases.

Significantly, this symposium and the Tritium Symposium held here two years ago are two major events in a long list of cooperative ventures between the University of Nevada at Las Vegas and the Environmental Protection Agency. In fact, I am told that several research projects involving the joint efforts of the University are currently underway at the EPA's National Environmental Research Center here in Las Vegas.

At its inception, the EPA had acknowledged that, to attain its objectives, it must draw heavily on every source of relevant information. In its less than three years of existence, the EPA has acquired extensive operating capabilities in environmental monitoring and surveillance, in field and laboratory research, in standards development and implementation, and in design and engineering of control technologies and strategies. But these programs, effectual as they are, are not sufficient. In the urgency of the problems at hand, the EPA must turn for assistance to universities everywhere, to industrial and other business organizations, and to public and private research institutions — as well as to agencies within the various echelons of our own governmental structure. The willingness of these entities to make available the fruits of their research and to otherwise offer their resources to sustain the mission of the EPA is to me — speaking for the EPA — very much appreciated.

Now more often than not, the EPA is the prime mover in these joint ventures and mutual interest programs. And while it deposits a fair share into the world bank of knowledge, the EPA, in turn, recognizes certain reciprocal obligations to the many who serve in these various branches of inquiry.

Whatever the EPA does, however, has to be part and parcel of its prime commission to provide strong national leadership in identifying and controlling the hazards to health and welfare existent in man's physical and biological environment. Mahatma Ghandi once remarked on seeing a crowd of his people moving off in the distance,

"I must hurry and catch up with them for I am their leader...."

So, in its campaign against the environmental hazards to human health and welfare, the EPA must keep sharply alert to all developments conducive to that pursuit, especially to the explorations and findings of the total scientific community. It is the mounting accumulation of research achievements over the past decade, in fact, that has prompted the EPA to intensify its close scrutiny of Noble Gases. And now we are anxious to hear your views expressed in these eighty reports to be presented in this Symposium.

The adverse environmental effects of the Noble Gases are predominantly radiation effects. Hence, pollution from the Noble Gases, as from other nuclear materials, does not manifest itself so dramatically as a dead fish floating down a dark stream or as a pale yellow cloud hovering over the city park. Nonetheless, concern about radiation pollution is well justified on the basis of its potential lasting effects. Radiation pollution is brought to the attention of world citizenry by every means from science fiction drama to news articles and stories in popular magazines.

If I appear to be understating public concern about radioactivity, it is only in the context of comparison with that of the other forms of pollution. Nor do I mean to infer that environmental protection should be geared to popular demand. On the contrary, one cannot wait for the chickens to start squawking before setting out to track down the weasel suspected in the neighborhood. We have waited too long as it is. We waited until our waters became so befouled that whatever engineering genius we apply, whatever elaborate devices we employ, and whatever uncountable monies we expend, we have yet a long wait to reverse the processes of water degradation. We waited so long after the skyline of our most beautiful cities disappeared in the gray gloom of smog that whatever crash programs we implement and whatever sacrifices we make, we have yet to wait a longer time to get one deep lungful of wholesome refreshing air.

We are confronted with ample reasons to suspect that radiation may very well constitute a growing hazard to this and to unborn generations.

Thus a comprehensive evaluation of the contributions to our total radiation exposure from Noble Gases, now and in the future, is clearly indicated.

On reviewing my notes and other material on what I might include in these opening remarks, I thought about the document that will result from this Symposium. I foresee it as a valuable book very much in demand. The papers to be presented here provide a comprehensive report on what is known of the Noble Gases to date, and will undoubtedly raise a number of intriguing unknowns. The question-and-answer sessions may well provide some new challenges for further research and invention. Working scientists will most certainly find such a book of great interest, but — even more so — to the legion of aspiring scientists, the students, it will be a veritable textbook.

With your indulgence I would now like, for a moment, to address a few historical remarks to re-orient those who — like myself — a short while ago considered the Noble Gases little more than a brief and uninspiring lesson in elementary chemistry.

Although it was in 1785 that Henry Cavendish discovered the first mysterious footprint that evidenced the presence of a strange element, it was not until 1894 — a century later — that the first member of this new family was identified by Lord Rayleigh, He named it argon. By 1900, the other presently known five were isolated and characterized — helium, neon, krypton, xenon, and radon. By this time, radioactivity had been discovered by Becquerel, and radon, which had not really been identified as a Noble Gas until 1910, was shown to be a short-lived radioactive isotope that emanates from radium. Most of the productive experiments and studies of the Noble Gases during the following half century resulted from conjunctive developments in nuclear research. The findings of Rutherford, Soddy, Moseley, Thomson, and other investigators led to the identification of radioactive isotopes of all the other Noble Gases.

Almost simultaneously, the Noble Gases were being put to use. Argon went into light bulbs to retard filament disintegration and was used to create a neutral field to enhance shielded arc welding, the preparation of metallic titanium and the growing of pure crystals for transistors. Neon, xenon and krypton went into vapor lamps. Neon and helium mixtures went into gas lasers developed in 1960. Helium went into balloons, and all the Noble Gases were put into limited medical usages — radon, especially, until recently, was used in cancer therapy. Krypton-85 was used as a remarkably sensitive leak detector and in a number of medical applications in differential diagnosis. All usages, however, largely depended on the inertness of these elements. And, since the early days after the discovery of the Noble Gases, chemists tried to bring about compound formation to extend their possible uses.

Numberless experiments had reinforced the growing conviction that the Noble Gases were unquestionably inert. Experiments led only to clathrates — the "false" compounds formed by the entrapment of a Noble Gas atom within a structure of molecules of other elements. The matter was all but forgotten as chemists everywhere argued that the Noble Gases formed no compounds at all. Experiments became less and less often attempted. Possibly their colleagues were even embarrassed for the few philosopher-chemists who held doggedly to the tenet that nature would not tolerate a do-nothing element.

Then, in 1962, "The world of chemistry," in the words of one writer, "was thunderstruck!" It was then that Neil Bartlett, then at the University of British Columbia, furnished evidence for the existence of an ionic compound of a Noble Gas and consequently formed a solid product with xenon. I am pleased that this distinguished scientist is one of the participants of this symposium. His discovery "astounded the chemical world. The announcement," wrote another reporter, "was greeted with surprise and in some cases disbelief!"

Apparently, Howard Claassen, John Malm, and Henry Selig were quick to shake off the shock. At the Argonne National Laboratory, in the next few weeks, these three formed a confirming stable compound — **xenon tetrafluoride**. *Numerous other working scientists were lured back into theoretical and experimental researches of these gases which, yesterday, had no chemistry — and in which, at the beginning of the decade, few chemists were even interested. In a short while other ionic or covalent bonds with noble gases were formed with highly reactive elements, most often with xenon in combination with fluorine. And the investigations pursued over the next ten years culminated in this meeting of the minds.*

Lest I usurp material to be presented before this symposium and infringe on your right to discuss your own researches and findings and inventions, I shall try to confine my closing remarks to EPA's own interest in these Noble Gases and Noble Gas compounds.

Now, with all that will have been said of the Noble Gases by the end of this week and with all that is yet to be learned about them, it can be believed that the Noble Gases — like nuclear energy — are exceedingly more beneficial than harmful. Philosophically...

"... it adds a charm to mix the good a trifle with a little dust of harm."

But those romantic words of James Whitcomb Riley are not quite acceptable in terms of environmental protection. And therein lies the crux of EPA appreciation for the tedious and introspective efforts of all scientists, including EPA's own, who labor in the various fields of environmental concern. Though unheralded, rarely making the news headlines, our studies not only bring much to the bank of scientific knowledge, they put a few new wrinkles in the environmental impact of these Noble Gases. Our findings make it more plainly evident that the "little dust of harm" inherent in the Noble Gases can — if uncontrolled — encroach most seriously on public health. A case in point is the evidence that a high concentration of radon in inhaled air may be regarded as an etiologic agent in the cause of lung cancer.

EPA interest in radon stems from the production of this radioactive gas in uranium mining operations and from tailings. One area is already contaminated with this Noble Gas to such a level that corrective actions are being taken to protect the people involved. We shall be hearing reports of these activities in the course of this symposium.

EPA interest in krypton-85 results from its high fission yield and ten-year half-life. The large quantities of this radionuclide resulting from nuclear detonations and reactor operation have reached a present level of about 17 pCi/m^3 of air. The latest atmospheric inventory of approximately 60 megacuries is double that of ten years ago. Although the present concentration represents only a small radiation dose to the individual, at the present rate of production, the concentration of krypton-85 in the global atmosphere in the coming decades could be hazardous. Hence, there is a need for adequate methods for collecting and storing krypton-85 while

investigations into its biological kinetics and effects are pursued, particularly in the area of internal and external dose calculation and assessment. There is also an urgent need for methods of predicting the quantitative release of krypton-85 to the environment in conjunction with advances in nuclear technology.

The unfortunate occurrence of radiation damage to uranium miners, before sufficient knowledge was available to develop and implement preventive or corrective actions, produced human data in size comparable to that of the well-publicized radium-dial painters. It is of fundamental importance to develop accurate retroactive dose estimates to relate the occurring effects to the dose.

In summary, I should like to reiterate the importance of the interchange of information as demonstrated in this symposium and the crucial importance of mutual assistance, not only in pursuit of pollution-control technology, but also in the general advancement of science. Science in sometimes likened to a great labyrinth of mystery with occasional blind alleys. But too many philosopher-scientists disprove that notion. And as the story of the discovery of Noble Gas compounds so well illustrates, we must not allow complacency. One alley, long considered blind and barricaded, was opened finally by the astounding discovery of Noble Gas compounds. And I am confident that the EPA, with the cooperative assistance of all scientists, will one day light the way through all those seemingly blind alleys of environmental pollution and its control.

I. Atmospheric Levels of Noble Gases

ATMOSPHERIC CONCENTRATIONS OF FISSION PRODUCT NOBLE GASES

D. E. Bernhardt, A. A. Moghissi*, and J. A. Cochran
National Environmental Research Center
U. S. Environmental Protection Agency
Las Vegas, Nevada

Abstract

Electrical power production by nuclear reactors, in addition to other nuclear activities, results in the production of radioactive noble gases. The release of these radioactive gases, at their source of production or through reprocessing of the fissile materials, results in radiation exposure to the world population.

This paper considers past, present, and future fission-related radioactive noble gas production and releases. These releases of noble gases are then related to atmospheric concentrations, population exposures, and appropriate feasible control technologies.

Krypton-85, because of its long half-life and fission yield, presents the greatest potential radiation exposure to the world population. The primary sources of production are nuclear power generation and plutonium production reactors. Naval propulsion reactors, nuclear weapons testing, and the postulated peaceful uses of nuclear explosives are secondary sources of production. The other releases associated with reactors primarily take place during fuel reprocessing.

INTRODUCTION

The predominant quantities of radioactive noble gases found in the atmosphere, other than the radioisotopes of radon, result from mans' nuclear activities. The intent of this paper is to review the predominant sources of these radionuclides, their atmospheric concentrations, and the health implications of the most significant ones.

Table 1 is a list of the predominant noble gas radionuclides produced by the fission process prepared from the data of Lederer, *et al.*, (1968) and Weaver, *et al.*, (1963) with supplementary information on branching ratios from Katcoff (1960). The list of nuclides is not exhaustive, but does include those with the largest fission yields and radioactive half-lives.

The column on the right in Table 1 indicates the product of the integral from time zero to infinity ($\int_0^\infty e^{-\lambda t}\, dt$) and the decay energy. Since the human exposure pathway for all noble gases is essentially the same; i. e., predominantly external exposure to a gaseous cloud; this value is a general indication of the relative significance of the various radioactive noble gases.

Consideration of the data in Table 1 indicates that krypton-85 is the only fission product radioactive noble gas nuclide with long-term health implications. Due to its relatively long half-life, it accumulates in the environment for many years. Although krypton-85 has a lower fission yield than many of the other radionuclides, its half-life more than compensates for this. Furthermore, the fission product noble gas release pathways of the predominant fission product producing mechanisms today are such that most of the short half-life radionuclides undergo significant radioactive decay prior to release.

Krypton-85 is produced through the natural fission of uranium and the neutron activation of stable krypton (Diethron and Stockho, 1972). But, there is general agreement that because most of the krypton-85 from natural fission decays prior to being evolved to the earth's surface, the quantities of natural krypton-85 in the atmosphere are negligible and essentially zero in comparison to the quantities produced through man's activities(Diethorn and Stockho, 1972; Pannetier, 1968; and UN, 1971). Although a significant fraction of the past and present day atmospheric inventory of krypton-85 resulted from plutonium production reactors and nuclear weapons tests, the primary source of production and release today, and projected for the future, is the nuclear reactor fuel cycle (Coleman and Liberace, 1966; Pannetier, 1968; Unruh, 1970; UN, 1971; and Diethorn and Stockho, 1972). Griesser and Sittkus (1961) and Ehhalt, *et al.*, (1963) provided strong indications that reactor operations contributed a large fraction of the krypton-85 atmospheric inventory.

Table 2 contains the fission yields of krypton-85 (Lederer, *et al.*, 1968; Weaver, *et al.*, 1963; and Katcoff, 1960).

Many authors have estimated the krypton-85 production from power reactors and nuclear testing, but only a limited number of authors have attempted to estimate the production from all sources (Diethorn and Stockho, 1972 and Pannetier, 1968). Thus, although the krypton-85 projections for the future may have been fairly valid and only limited to the accuracy of energy projections, there has been poor agreement between the present atmospheric inventory estimated from samples and the production accounted for in source term estimates. Diethorn and Stockho (1972) and the UN (1971) accounted for less than 50% of the inventory estimate based on atmospheric samples.

*A. A. Moghissi is currently a visiting professor at the Georgia Institute of Technology on assignment from the U. S. Environmental Protection Agency.

PRODUCTION AND ATMOSPHERIC INVENTORY OF KRYPTON-85

The following items describe the sources of krypton-85 production. Several of the items; e. g., plutonium production reactors and propulsion reactors, are based on limited and incomplete information. The production from Plowshare projects (nuclear stimulation of natural gas) is particularly speculative in that their technical, economic, and political feasibilities have not been fully demonstrated. In order to give the best possible estimate for krypton-85 production and release to the atmosphere, all potential sources have been considered in this paper.

1. Commercial Power Reactors.

The contribution of krypton-85 from nuclear power reactors to the atmospheric inventory became significant in the late 1960's. Nucleonics Week's (1966-71) reports of power integrals (MW-h) indicate power reactor operations accounted for the production of about 15 MCi by 1970. Correcting for radioactive decay and delays in release, we estimate that this produced an atmospheric inventory of 7 MCi in 1970.

The computation of the future worldwide krypton-85 content of the earth's atmosphere is largely a projection based upon the energy needs of the world from 1970 to the year 2000. The best estimate of AEC (1972b) of the nuclear power capacity for the world is shown in Table 3. The estimate for east block countries excludes the People's Republic of China (PRC) because of the scarcity of data. The data for 1970 are based on the Nucleonics Week's (1966 and 1971) reports of actual power generated.

The krypton-85 inventory that is available for contribution to the atmospheric inventory is a function of the fission process, thermal power, and holdup time prior to fuel reprocessing and ultimate discharge to the atmosphere. Once discharged to the atmosphere, the krypton-85 inventory is a function of radioactive half-life.

Only about 0.02% of the krypton-85 is released in conjunction with the reactor operations, prior to fuel reprocessing (Logston and Chissler, 1970; UN, 1971; and Fowler and Voit, 1969). Fowler and Voit (1969) present an extensive review of releases associated with reactor operations and fuel reprocessing cycles.

The light water reactor (LWR), gas cooled reactor (GCR), and the advance gas reactor (AGR) are assumed to use uranium-235 (thermal neutron spectrum) as the primary fission process. The high-temperature gas cooled reactor (HTGR) will use an initial core with uranium-235 as the fissile material. Subsequent cores could be fueled with uranium-233 fuel. For purposes of krypton-85 projections, it has been assumed that the first five years of operation will use uranium-235 thermal fission, and that uranium-233 will be utilized for the remainder of plant life. The fast breeder reactor (FBR) will use plutonium-239 as the fissile material and the major fission process will be from plutonium-239 fission spectrum neutrons.

In order to convert the thermal power to curie quantities of krypton-85, the following factors were used in Table 2.

Fission yield expressed as MCi/GW-h:
- Uranium-235, thermal = 1.82×10^{-5}
- Uranium-233, thermal = 3.46×10^{-5}
- Plutonium-239, fission = 9.71×10^{-6}

The power capacities have been broken into reactor types, and the breakdown in electrical units is shown in the first five columns of Table 4 (AEC, 1972b). The last four columns of the table show the power projections in terms of thermal energy. The thermal listing assumes an 80% load factor for all reactor types. The electrical to thermal efficiencies used for the thermal conversion expressed as efficiency of electrical/thermal are as follows:

LWR, GCR	0.345
AGR, FBR	0.42
HTGR	0.39

Table 5 shows the result of the calculations for each reactor type for five year increments from 1970 to 2000. The total amount of krypton-85 produced in that thirty-year period is projected to be 13,000 megacuries.

Not all of the krypton-85 produced reaches the atmosphere. The fuel containing the krypton-85 is assumed to remain in the reactor core for approximately 12 to 18 months. After removal from the core, the fuel is cooled for one year prior to reprocessing. By the time the fuel is processed and the krypton released, some radioactive decay has taken place. The overall effect of holdup due to core life and cooling, as well as radioactive decay, is a three-year shift between the production and release of krypton. For example, in 1970, the total krypton-85 discharge to the atmosphere is essentially the same as the amount produced in the five-year period ending in 1967. The projected production is given in Table 5.

The atmospheric accumulation of krypton-85 for each five-year period from 1970 to 2000 is shown in Table 6. The values were based upon Table 5, corrected for holdup time and decay, and then accumulated. Based on this data, the atmospheric inventory of krypton-85 from nuclear power is estimated to be 7,500 MCi by 2000.

The nuclear power generation trend and the projected atmospheric accumulation of krypton-85 for the 30-year span from 1970 to 2000 are summarized in Figure 1. The contributions from the various reactor types are also shown. The U.S. contribution is about one-half of the total (AEC, 1972b).

2. Plutonium Production Reactors.

There is only limited unclassified information available that can be used to calculate krypton-85 inventory from production reactors. Diethorn and Stockho (1972) indicate estimated production reactor power levels for the United States, based on Hewlett and Anderson (1962) and Hewlett and Duncan (1969), for 1954 to 1972. From their information it can be estimated that the krypton-85 inventory was 6 MCi in 1965.

Testimony before the Joint Committee on Atomic Energy (JCAE)(1959) indicated that in 1959 there was roughly 25×10^7 l(65 million gallons) of high-level waste in the U.S. Upson (1966) indicated a value of over 28×10^7 l(75 million gallons) for 1966. Testimony before the JCAE (1959) indicated that the high-level wastes stored at Hanford contained 1.3 to 2.6 Ci/l (5-10 Ci/gal) of strontium-90. Using the value of 75 million gallons and an assumed average strontium-90 concentration of 5 Ci/gal, a quantity of 46 MCi of krypton-85 is indicated without correcting for differences in decay between strontium-90 and krypton-85.

$$75 \times 10^6 \text{ gal} \times \frac{5 \text{ Ci Sr}}{\text{gal}} \times 3.7 \times \frac{10^{10} \text{ dps}}{\text{Ci Sr}} \times \frac{\text{fis}}{0.0577 \text{ atom Sr}} \times$$

$$\frac{1}{7.85 \times 10^{-10} \text{ s}^{-1} \text{ Sr}} \times \frac{0.00274 \text{ atom Kr}}{\text{fis}} \times 2.043 \times 10^{-9} \text{ s}^{-1} \text{ (Kr)} \times$$

$$\frac{\text{Ci Kr}}{3.7 \times 10^{10} \text{ ds}} = 46 \times 10^6 \text{ Ci of krypton-85.}$$

Using the power profile indicated by Diethorn and Stockho (1972), this is indicative of an inventory of about 25 MCi in 1966.

Data from Diethorn and Stockho (1972) indicates a total production reactor power integral of 100,000 MWt-year. Correcting for the decay of krypton-85, this is equivalent to a power integral of about 50,000 MWt-year as of 1965 or 1966 (weighted decay factor of 2). Using their data on estimated atmospheric concentrations, and their postulated mixing model ($1.7 \text{ pCi/m}^3 \times 3.54 \times 10^{18} \text{ m}^3 = 6 \times 10^{18}$ pCi), an inventory of 6 MCi was indicated as of 1965.

Pannetier (1970) refers to a plutonium production number of some 60 tons as of 1966. He did not identify the country of origin, but for purposes of the calculation it is assumed to be the U.S. From this an estimate of krypton-85 production can be made as follows:

$$60 \text{ tons Pu} \times \frac{\text{Uranium Fission}}{\text{0.8 Pu Production}} \times \frac{9.09 \times 10^5 \text{ g}}{\text{Ton}} \times \frac{\text{Mole}}{239 \text{ g}} \times$$

(Glasstone, 1955)

$$\frac{6.023 \times 10^{23} \text{ atoms}}{\text{mole}} \times \frac{\text{MW-h}}{1.12 \times 10^{20} \text{ fis}} \times \frac{0.018 \text{ Ci } ^{85}\text{Kr}}{\text{MW-h}} =$$

28×10^6 Ci of ^{85}Kr.

Reducing this value by the power profile weighted decay factor of two (estimated from Diethorn and Stockho, 1972), gives an estimate for 1966 of 14 MCi.

The average of the above estimates is about 15 MCi of krypton-85 as of 1966 for the U.S.

There is even less data on worldwide production reactor operations than on the U.S. operations. Thus, it is assumed the Union of Soviet Socialist Republic (USSR) production was similar to that for the U.S., and that production for other countries; Great Britain, France, and the People's Republic of China was equivalent to an inventory of 15 MCi as of 1970 (roughly 100,000 MWt-h corrected for decay). The value of 15 MCi for other countries can also be considered to include some continued production for the U.S. and USSR. This indicates a worldwide inventory from plutonium production reactors of about 38 MCi for 1970.

It is assumed that plutonium production for weapons and nuclear explosives purposes (plutonium production other than from power reactors) for all countries in the world will continue at a rate of about two tons per year (AEC, 1972d). This will result in production of 4.7 MCi per five-year period. However, future production of plutonium for weapons use may be curtailed in the event of testing or disarmament agreements.

3. Plowshare — Peaceful Uses of Nuclear Explosives.

Nuclear explosives have been considered for use in civil engineering projects, recovery of natural resources, and waste disposal. To date, most of the U.S. efforts have been related to nuclear stimulation of natural gas wells. The technique is applicable to low permability gas bearing formations where the gas cannot be economically recovered by conventional well completion techniques.

The experiments named Gasbuggy, Rulison, and Rio Blanco have indicated the general technical feasibility of nuclear stimulation, but there are still uncertainties concerning the environmental consequences, competition from other technologies, and general economic feasibility.

Although nuclear stimulation of natural gas wells is still in the technical and financial feasibility evaluation phase, there have been several concepts for subsequent phases of implementing the program. Rubin, *et al.*, (1972) present one of the most current concepts.

Table 7 indicates a postulated U.S. development schedule and the resulting krypton-85 production. Tritium appears to be the limiting radionuclide for nuclear stimulation of natural gas, thus the emphasis is on fission versus thermonuclear devices (Rubin, *et al.*, 1972 and AEC, 1972a). The Diamond device, using uranium-235 as the fissile material, has been developed to limit tritium production and meet size limitations. Rubin, *et al.*, (1972) postulate that most of the stimulation projects will use several 100 kt devices with a yield of about 22 Ci of ^{85}Kr/kt. If plutonium is used, this value would be reduced to 13 Ci of ^{85}Kr/kt.

Although Table 7 only includes a program until 1983, it is postulated the program would continue until 2000. Continuing the program until 2000 assumes the development of other fields (Rubin, *et al.*, 1972) or could be considered to include other types of Plowshare technology. This schedule is probably optimistic.

4. Naval Propulsion Reactors.

The first U.S. Navy nuclear submarine was started up in 1954 (AEC, 1972c). As of June 1972, there were over 110 propulsion reactors aboard U.S. Navy ships (several ships, such as the Enterprise, have more than one reactor). Twenty-six ships, seven with two reactors each, were being built (AEC, 1972c and d) as of 1972.

The Nuclear Ship Savannah (operated 1961-1971) had an operating power of 80 MW. Assuming the same design technology was used for all of the propulsion units, and that a basic standard design was used for all of the reactors to simplify maintenance and stock piling of parts, it is assumed that all the propulsion reactors have a nominal power of 80 MW. Pannetier (1968) estimates a power of 50-60 MW.

Information from AEC (1972c) indicates about 500 reactor-years of operation by 1970 (corrected for decay of the krypton-85 inventory). Assuming 50 percent operating time, this is indicative of a krypton-85 inventory of about 3 MCi in 1970. It is then assumed that there will be about ten additional propulsion reactors beginning operation during each five-year period. The total for the world, after 1970, is assumed to be twice the U.S. total.

AEC (1972d) indicates increased power levels and core operating times for future ships. The aircraft carrier Nimitz will be powered by two reactors (versus eight for the Enterprise) with a 13-year core life. Long core-lives will result in decreased releases, due to decay, and additional delays in the release. The krypton-85 releases, based on these assumptions, are shown in Table 8.

5. Nuclear Testing.

Initial increases in worldwide atmospheric concentrations of krypton-85 were due to nuclear testing. But, with the general decrease in nuclear testing and the advent of underground testing, as well as the advent of nuclear power generation, nuclear testing now contributes a relatively small (compared to reactors) amount of krypton-85 to the atmospheric inventory.

Diethorn and Stockho (1972) present information indicating the ^{85}Kr atmospheric inventoy from nuclear testing just prior to 1965 was about (0.8 pCi/m^3 x 3.54 x 10^{18} m^3) 2.8 MCi. The UN (1971) estimated the ^{85}Kr production from nuclear testing from ^{90}Sr data. They estimated the production as 2.1-3.5 MCi, with the amount remaining in 1970 being 1.1-1.7 MCi. Unruh (1970) reports a value of only 0.05 MCi of ^{85}Kr for testing through the mid-sixties.

Unruh's (1970) value appears to be rather low, it accounts for roughly less than 10 Mt of fission products. Diethorn and Stockho's (1972) estimate is overlapped by the range of the UN (1970) estimate. Thus, a production of 3 MCi as of 1965 is used herein.

Since Limited Test Ban Treaty of 1963, there has been continued underground testing by the U.S., USSR, and France; cratering tests by several nations; and above ground tests by France and the People's Republic of China.

The decrease of the 1965 inventory of 3 MCi from radioactive decay is about 0.2 MCi per year. This is equivalent to the ^{85}Kr produced by 10-15 Mt of fission per year.

There is only limited information available on the fission yields for current nuclear testing. Although some U.S. and non-U.S. nuclear tests are publically announced, and the U.S. announces the detection of tests in other countries, there is usually only a general indication of the nuclear yield, and no indication of the fission yield. Furthermore, there are unannounced nuclear tests in the U.S. and USSR, and possibly other countries. Underground nuclear weapons tests carried out by the U.S. and USSR, and certain tests by other countries, are associated with limited releases of any fission products.

The following assumptions were used to estimate ^{85}Kr production from nuclear testing from 1965 to date:

(1). Nuclear tests announced by the U.S. (Vermillion, 1973) were assumed to be equal to the maximum yield of the announced range (i.e., if 20-200 kt, the yield was assumed to be 200 kt) and the yield was assumed to be all fission. The same assumptions were applied to USSR tests announced as detected by the U.S. The conservatism of these assumptions is intended to compensate for unannounced tests.

(2). Tests by the PRC or France were assumed to be equal to the maximum yield in the range of the announced (by the U.S. and/or respective country) yield, and yield was assumed to be all fission — except for several megaton range events which were indicated to be thermonuclear. For a thermonuclear event, the fission yield was assumed to be 100 kt, which is probably an overestimate.

(3). No attempt was made to distinguish between underground, cratering, and surface tests. Cowser, *et al.*, (1967) indicates that ^{85}Kr releases are reduced through radioactive decay by a factor of about 10^7 in passing through several hundred meters of impermeable formation.

Using the above assumptions, the total fission yield per year was roughly one-half of the yield necessary to compensate for the radioactive decay of the ^{85}Kr inventory from nuclear testing indicated for 1965.

Furthermore, the predominant portion of the yearly yield has been due to underground tests. Although the ^{85}Kr produced in underground tests may not be reduced by a factor of 10^7 before reaching the atmosphere, it will be reduced by several orders of magnitude.

Given the above discussion, it is assumed that the inventory as of 1965 (3 MCi) decreases due to radioactive decay, and is supplemented by the ^{85}Kr produced by 1 Mt of fission yield per year (0.02 MCi/year assumes most of the fissile material is ^{235}U, rather than 0.012 MCi/year for ^{239}Pu).

6. Miscellaneous Reactors.

There are numerous additional research, testing, and development reactors. But, the combination of their power levels, operating times, core-lives, and delays in fuel reprocessing are such that their contribution to the atmospheric krypton-85 inventory is insignificant.

7. Production and Atmospheric Release of Krypton-85 up to the Year 2000.

Table 8 summarizes production and release of krypton-85 from all sources. The total projected atmospheric inventory and the contributions from power reactors and other sources are plotted in Figure 2. As a matter of convenience, major assumptions relating to these values are also summarized as follows:

. . . . The "production" column indicates the actual production during the five-year period. The inventory numbers are carried forward to the next five-year period after correcting for decay. Apparent discrepancies between totals and the sum of items are due to rounding off the numbers.

The 1970 inventory for power reactors includes the effective release through 1970, thus, the total effective release through 1970 is also 7 MCi. The production estimates are based on the actual production during the five-year periods. The atmospheric values account for radioactive decay, holdup in the core, and the delay in reprocessing the fuel. The indicated values are for the total world. The U.S. accounts for a little less than 50% of the indicated values.

The atmospheric estimates for Pu production reactors are equal to the amount produced in the five-year increment, corrected for three years of decay. The three years of decay account for decay while the fuel is in the reactor, the delay in processing, and the decay of the krypton-85 produced in the early years of the five-year period.

The decay in the core of ship propulsion reactors, and from the early years of the five-year period, are included in the "production" value. The corrected figure accounts for only a year's delay for fuel reprocessing. The world value is assumed to be twice the U.S. value after 1970.

The atmospheric values for krypton-85 derived from gas stimulation are based on a year's lag between production and release.

No delay corrections are made for krypton-85 originating from nuclear weapons testing.

PROJECTED ATMOSPHERIC CONCENTRATIONS AND DOSES

Coleman and Liberace (1966), Diethorn and Stockho (1972), Whipple (1969), Cowser, *et al.*, (1966), and Dunster and Wagner (1970) have assumed that krypton-85 becomes essentially uniformly dispersed in the troposphere within a short period of time. Pannetier (1968) postulated a zonal mixing model, dividing the atmosphere into northern, southern, and intertropical regions. The northern region, which generally reflected the highest concentrations, also contained the major sources of krypton-85 releases. The latitudinal zonal distribution results from limited mixing along longitudes. The predominate wind patterns, and thus atmospheric transport, are along the latitudes. Global transit is measured in terms of several weeks; whereas interzonal transfer (direction of the poles) is measured in terms of months. Mixing between the troposphere and stratosphere approaches a year to years (Pannetier, 1968 and 1970).

Pannetier (1968) noted that stratospheric concentrations of krypton-85 were greater than those for the troposphere in the late 1960's. Since the stratosphere only accounts for about 25% of the atmospheric mass, versus about 75% for the troposphere, any uncertainties of the krypton-85 distribution or delays in mixing between these two segments of the atmosphere have a limited affect on long-term concentrations of krypton-85 in the troposphere. Only about 0.1% of the atmospheric mass is above 50 km (Verniani, 1966).

Pannetier (1968) relates the high concentrations of krypton-85 in the stratosphere to direct injection of krypton-85 from above ground nuclear weapons tests (due to thermal energy) into the stratosphere. He further notes that atmospheric thermal currents created by the continents might carry some of the krypton-85 releases (in addition to nuclear testing) directly to the stratosphere.

Given the uncertainties in estimates of krypton-85 production and release, and the long duration of releases, the uniform atmospheric mixing model is used herein.

Figure 3 indicates the estimated atmospheric concentrations based on the projected releases from Table 8. It has been assumed that krypton-85 becomes uniformly dispersed in the total atmospheric mass of 5.136×10^{21} g (Verniani, 1966) or 3.97×10^{18} m^3 (standard temperature and pressure).

Figure 3 includes data points from atmospheric measurements of krypton-85. A number of the data points, subsequent to 1960, are based on roughly six-month averages of results (range of results indicated by bar). It is evident that the concentrations estimated from the calculated inventories correspond very closely to the measured data points.

The envelope on the curve in Figure 3 indicates the postulated uncertainty of the "best estimate" reflected by the line. After about 1980, power reactor operations account for essentially all (over 90%) of the krypton-85 production, release, and atmospheric inventory. Thus, in general, the uncertainty in the atmospheric concentration of krypton-85 relates to uncertainties in the projections of nuclear power generation, and the radioactive decay of krypton-85 prior to its release. There are also the additional uncertainties of delay before release and the possibility of removal of krypton-85 from effluent streams. The uncertainties due to dilution and dispersion in the atmosphere are not included.

The indicated uncertainty in the early years, prior to 1970 to 1980, includes uncertainty in the power reactor production and release of krypton-85, but is primarily influenced by the unknowns related to plutonium production reactors and the nuclear propulsion of military ships. Although the sum of the estimated values correlate with the estimated inventory based on atmospheric samples, the general assumptions used in calculating the various releases easily have an uncertainty of 50% — especially when U.S. values are projected to worldwide values.

Thus, the correlation of the concentrations estimated from the production values with the measured values does not completely verify the production estimates. Rather, the correlation of the estimates may, in part, relate to compensating errors in the various calculations and projections.

Uncertainties in the projections for Plowshare applications and future nuclear testing have little impact on the future projections of atmospheric concentrations and dose due to the relatively small krypton-85 production from these sources.

Dose estimates for the whole body, basal layer of the skin, and the surface of the skin are indicated in Table 9. The dose calculations are based on the methods of Dunster and Wagner (1970) and Hendrickson (1970), modified for the effective energies recommended by Dillman (1970), and supplemented for the internal dose due to krypton-85 dissolved in body tissues after Lassen (1964).

As a matter of convenience, the factors are based on a dose received as a result of exposure to 1 pCi $^{85}Kr/m^3$ of air on an annual basis. The conversion factors are as follows:

Whole-body dose: 1.42×10^{-8} rad/year: This includes dose from krypton-85 in the body (Lassen, 1964) and external, bremsstrahlung and gamma dose (Dunster and Wagner, 1970).

Basal layer of skin: 1.04×10^{-6} rad/year: this includes beta dose (Hendrickson, 1970) and gamma and bremsstrahlung (Dunster and Wagner, 1970).

Skin surface: 2.08×10^{-6} rad/year (Dunster and Wagner, 1970. This is similar to the International Commission on Radiological Protection, ICRP, (1959) dose model.

Due to the present controversy concerning the appropriate dose model, the range of dose models (surface of the skin to whole body) is presented without concluding which is the appropriate model.

DISCUSSION

The data in Table 8 and Figure 2 indicates that the primary source of krypton-85 production has been, and will be, nuclear reactors (power generation and plutonium production). However, the actual release of krypton-85 from the reactor fuel cycle occurs during fuel reprocessing. Longston and Chissler (1970), UN (1971), and Fowler and Voit (1969) note that only about 0.02 percent is released during normal reactor operations.

The atmospheric concentration projections of this paper (Figure 3) show excellent agreement with the measured atmospheric concentrations for 1970 to 1973. Further, the measured concentrations (Figure 3) from 1954 to 1973 show a general trend of increase similar to that for the projections. The projections, which were only carried out to 2000, projected an average atmospheric concentration of 1,900 pCi/m^3 for 2000. This is related to yearly doses of 27 microrad for the whole body, and 2 mrad for the skin basal layer cells, and 4 mrad for the surface of the skin in accordance with ICRP (1959) model.

Table 10 presents a comparison of the year 2000 projections from this paper with those of others. The various values for the energy production, as well as krypton-85 production and the resulting dose are within a factor of two, with the values of this paper, based on recent power projections (AEC, 1972b) generally being slightly higher than previous year 2000 estimates; i. e., Coleman and Liberace (1966), 1,000 pCi/m^3; Cowser, *et al.*, (1966), 1,000 pCi/m^3; Pannetier (1968), 1,400 pCi/m^3; and Klement, *et al.*, (1972), 1,400 pCi/m^3.

The notable difference between this and previous papers is the accounting for the 1970 atmospheric inventory of krypton-85 based on analytical results. It is recognized, given the need for many assumptions, that the agreement might be due in part to happenstance; i. e., compensating errors in the assumptions.

The estimated atmospheric concentrations based on inventories from this paper are 13 pCi/m^3 for 1970 and 18 pCi/m^3 for 1973 versus averages from analytical results of about 15 pCi/m^3. Diethorn and Stockho (1972) only accounted for about 2 pCi/m^3 in 1971. Pannetier (1968) postulated that the difference between measured krypton-85 values and his estimates based on nuclear power and weapons tests was due to plutonium production reactors. Our estimates generally concur with this and indicate a small contribution (less than 10 percent for 1970) from nuclear ship propulsion.

The UN (1971), with reference to Pannetier (1968), indicates 28.7 MCi fo krypton-85 was produced in power reactors by 1970 (27 MCi if corrected for decay). Our estimate, based on actual reactor operating histories reported by Nucleonics Week (1966 and 1971), indicated production of 15 MCi by 1970, correcting for radioactive decay and delay for fuel reprocessing, results in an estimate of 7 MCi. It is assumed the differences in these estimates are due to the use of projected plant design capacities versus actual operating histories. An error of this nature may also be inherently included in our estimates, but, it is assumed that the delay between projected and on-line operating times and reduced load factors will be decreased for future plants. The UN

(1971) further notes a difference of 7-26 MCi in 1970 between the atmospheric inventory and sources. It assumes the difference is due to plutonium production reactors.

Plutonium production reactors, nuclear testing, and nuclear ship propulsion reactors have contributed significantly to the atmospheric inventory of ^{85}Kr. Our projections indicate that these sources will be important until about 1980, by which time atmospheric releases and inventory will be largely due to nuclear power. Fowler and Voit (1969), Mountain, *et al.*, (1968), Cowser, *et al.*, (1966), Coleman and Liberace (1966), Dunster and Wagner (1970), and Klement, *et al.*, (1972) have limited their evaluations primarily to power reactors, and, in most cases, the energy projections for one country or just the "free world." Coleman and Liberace (1966), Klement, *et al.*, (1972), and Dunster and Wagner (1970) included the whole world. Diethorn and Stockho (1972) include projections of essentially all of the source terms (only "free world"), but account for only about 20 percent of the inventory in 1970. Their projections are only carried to 1985. They project a krypton-85 atmospheric concentration for the "free world" of 350 pCi/m^3 for 1985. Since they assumed the instantaneous release of the produced ^{85}Kr, this may be compared to our 1988 estimate of 350 pCi/m^3 (built in three-year lag) versus our corrected value of 250 pCi/m^3 for 1985 (Figure 3). The projections used in this paper, as given in Table 3 (taken from AEC, 1972b), indicate that the "non-free world" contribution in only about 10 percent for 1985.

The uniform atmospheric mixing model has been used for the projections in this paper. This model is based on 3.97 x 10^{18} m^3 of air (5.136 x 10^{21}/1293 g/m^3, STP) according to Verniani (1966). Due to the long periods of release, the multiple point source type of release, and the 10.76 year half-life of krypton-85, it is felt that this model is adequate. The most limited atmospheric mixing takes place between the troposphere and the stratosphere, but the stratosphere accounts for only about 25 percent of the atmosphere. Further, it has been postulated (Pannetier, 1968) that the continents provide thermal currents which may result in higher than expected transport of releases from the continents to the stratosphere. Cowser, *et al.*, (1966) proposed uniform mixing up to about 13 km (8 miles), or essentially the top of the troposhere and Pannetier (1968) developed a zonal mixing model which indicates an effective dilution of about 15 percent less than the uniform mixing model. Given this information, the uniform model appears to be adequate for long-term releases.

REDUCTION OF KRYPTON-85 RELEASES

Projections of atmospheric concentrations of krypton-85 indicate that the dose to the surface of the skin will be several millirad and the whole body dose less than 0.1 millirad by 2000. Additional projections (from this paper and Coleman and Liberace, 1966) indicate these doses will increase by more than an order of magnitude by the middle of the 21st Century if the use of nuclear power continues, and efforts are not made to reduce krypton-85 releases to the atmosphere. The point at which the need for control of releases occurs will depend in part on social/political decisions, the economics of removal and retention of krypton-85, decisions as to the pertinent dose calculation procedures for krypton-85, and the degree of dependence on nuclear power. Furthermore, the local doses around a fuel reprocessing plant, about one mrad for the whole body and 50 mrad to the skin, may require some type of action before action is indicated for worldwide levels (Klement, *et al.*, 1972 and Shleien, 1970).

The krypton-85 doses today are at the microrad level, but krypton-85 releases to the atmosphere are a long-term dose commitment for the future, and fuel reprocessing plants (the actual source of release) being built today and tomorrow will be operating decades in the future. Thus, the time is approaching when decisions must be made on the need for krypton-85 isolation, and the basic technical information and technology should be available.

Dunster and Wagner (1970) note that removal and storage are basically a process of retention of the effluent stream, and removal of the krypton-85 with subsequent storage of a small volume of effluent. The volume of krypton-85 projected for production in the decade, 1990-2000, is several thousand cubic meters at one atmosphere or tens of cubic meters at 100 atmospheres.

Tadmor and Cowser (1967), Reist (1965), Pannetier (1968), and Cowser, *et al.*, (1967) investigated storing krypton-85 in underground formations. Cowser, *et al.*, (1967) indicates reduction factors of up to 10^7 for storage in impermeable geological formations. Mecca and Ludwick (1970) investigated entrapping noble gases in long-life foam. Keilholtz (1971) and Merriman, *et al.*, (1972) reported on systems for removing krypton from effluents.

Russell (1972) reviewed the status of various technologies and indicated the general feasibility of condensing krypton in liquid nitrogen with subsequent fractional distillation, adsorption of krypton on activated charcoal at cryogenic temperatures, and solvent extraction of krypton from effluent streams. He noted that disposal of the krypton was primarily a management versus a technical problem. Capital costs were estimated to be a small fraction of total plant costs, and operating costs a small fraction (less than 0.1 percent of power production costs.

CONCLUSIONS

The projected krypton-85 inventory for the year 2000 is 7,500 megacuries. Using the uniform distribution model for the atmosphere, the projected concentration is 1,900 pCi/m^3. The associated whole-body dose is less than one-tenth millirad, and the skin dose is about four mrad. These values are projected to increase by more than an order of magnitude by the middle of the 21st Century unless control techniques are used to isolate krypton-85 from the atmosphere. These conclusions are in general agreement with other reviewers; e. g., UN (1971), Diethorn and Stockho (1972), Klement, *et al.*, (1972), and Coleman and Liberace (1966).

The estimates of krypton-85 production and release up through 1973 account for the estimated atmospheric inventory based on sampling data. Our estimates indicate that the reprocessing of fuel from plutonium production reactors has been the primary source of atmospheric krypton-85. The projections indicate that reprocessing of fuel from power production reactors will be the primary source of krypton-85 after about 1975, and will account for more than 90 percent of the inventory and production after 1980.

Although there appears to be minimal justification for isolation of krypton-85 from the atmosphere today, projections indicate appropriate technology should be developed for the future. A precise estimate cannot be given as to when removal practices should be initiated because questions must be answered concerning the appropriate dose calculation procedures and the risk-cost-benefit analysis of applying removal techniques.

REFERENCES

Atomic Energy Commission (1972a), *Environmental Statement, Rio Blanco Gas Stimulation Project*, WASH-1519.

Atomic Energy Commission (1972b), *Nuclear Power 1973-2000*, Forecasting Branch, Office of Planning and Analysis, USAEC, WASH-1139(72).

Atomic Energy Commission (1972c), *Nuclear Reactors, Built, Being Built, or Planned*, TID-8200 (26th Rev).

Atomic Energy Commission (1972d), *Operating and Development Functions.*

Bruce, F. R. (1959, *Hearings Before the Special Subcommittee on Radiation, on Industrial Radioactive Waste Disposal*, Joint Committee Atomic Energy, U.S. Congress, Jan-Feb., 1959.

Coleman, J. R. and R. Liberace (1966), *Nuclear Power Production and Estimated Krypton-85 Levels*, Radiological Health Data Reports, 7:615-621, Nov. 66.

Cowser, K. E., W. J. Boegly, Jr., and D. G. Jacobs (1966), *^{85}Kr and Tritium in an Expanding World Nuclear Power Industry*, ORNL-4007.

Cowser, K. E., *et al.*, (1967), *Krypton-85 and Tritium in an Expanding World Nuclear Power Economy*, ORNL-4168.

Diethorn, W. S. and W. L. Stockho (1972), *The Dose to Man From Atmospheric ^{85}Kr*, Health Physics, 23:653-662.

Dillman, L. T. (1970), *Radionuclide Decay Schemes and Nuclear Parameters for Use in Radiation-Dose Estimates*, Part 2, Medical Internal Radiation Dose Committee, J. of Nuclear Medicine, Supp. 4, Pamph. 6.

Dunster, H. J. and B. F. Wagner (1970), *The Disposal of Noble Gas Fission Products From the Reprocessing of Nuclear Fuel*, AHSB (RP) R101, CONF 691039-1.

Ehhalt, D., K. L. Munnich, W. Roether, J. Schrolch, and W. Stich (1963), *Artificially Produced Radioactive Noble Gases in the Atmosphere*, J. Geophysics Res. 68 (13), 3817-3821. Includes data from deVries (1954); Suess (1958); Delibrias, *et al.*, (1959); Griesser and Sittkus (1961); and a private communication from C. Muhlemann (1962).

Fowler, T. W. and D. E. Voit (1969), *A Review of the Radiological and Environmental Aspects of Krypton-85*, Public Health Service, NF-69-16.

Glasstone, S. (1955), *Principles of Nuclear Engineering*, D. Van Nastrand Company, Inc.

Glueckauf, E. and G. P. Kitt (1956), *The Krypton and Xenon Contents of Atmospheric Air*, Proceedings of the Royal Society of London, Series A., Mathematical and Physical Sciences, Vol. 234, Royal Society Burlington House, March 6, 1956.

Griesser, O. and A. Sittkus (1961), *Bestimmung des ^{85}Kr Gehaltes der Luft*, Z. Naturforsch, 16a, 620.

Hendrickson, M. M. (1970), *The Dose From ^{85}Kr Released to the Earth's Atmosphere*, BNWL-SA-3233A, IAEA-SM-146/12, Battele Memorial Institute.

Hewlett, R. G. and O. E. Anderson (1962), *A History of the United States Atomic Energy Commission, Vol. I, The New World*, Pennsylvania State University Press, University Park, PA.

Hewlett, R. G. and F. Duncan (1969), *A History of the United States Atomic Energy Commission, Vol. II, Atomic Shield*, Pennsylvania State University Press, University Park, PA.

International Commission on Radiological Protection (1959), *Permissible Dose for International Radiation*, Report of Committee II, ICRP 2, Pergamon Press.

Jaquish, R. E. and F. B. Johns (1972), *Concentrations of Krypton-85 in Air*, Natural Radiation Environment-II, in Publication.

Joint Committee on Atomic Energy (1959), *Industrial Radioactive Waste Disposal*, 86th Congress, Jan-Feb. 1959, pp.21, 1832.

Katcoff, S. (1960), *Fission-Product Yields From Neutron-Induced Fission*, Nucleonics, 18:201-208, November 1960.

Keilholtz, G. W. (1971), *Krypton-Xenon Removal Systems, Nuclear Safety 12/6: 591-599.*

Kirk, W. P. (1972), *Krypton-85, A Review of the Literature and an Analysis of Radiation Hazard*, Environmental Protection Agency, Eastern Environmental Radiation Laboratory.

Klement, A. W., C. R. Miller, R. P. Minx, and B. Shleien (1972), *Estimates of Ionizing Radiation Doses in the United States, 1960-2000*, Environmental Protection Agency, ORP/CSD72)1.

Knox, J. B. and K. R. Peterson (1972), *Estimates of Doses to Northern Hemisphere Population Groups From ^{85}Kr Emitted by a Single Fuel-Reprocessing Plant*, Nuclear Safety, 13:130-135.

Lassen, N. A. (1964), *Assessment of Tissue Radiation Dose in Clinical Use of Radioactive Inert Gases, With Examples of Absorbed Doses From $^{3}H^{2}$, ^{85}Kr, and ^{133}Xe,* Minerva Nucleare, 8:211-217.

Lederer, C. M., J. M. Hollander, and I. Perlman (1968), *Table of Isotopes,* 6th ed., John Wiley and Sons, New York, N.Y.

Logston, J. E. and R. I. R. I. Chissler (1970), *Radioactive Waste Discharges to the Environment From Nuclear Power Facilities,* Public Health Service, Division of Environmental Health, BRH/DER 70)2.

Mecca, J. E. and J. D. Ludwick (1970), *The Development of a Long-Lived High Expansion Foam for Entrapping Air-Bearing Noble Gas,* DUN-SA-141, Douglas United Nuclear, Inc.

Merriman, J. R., M. J. Stephenson, J. R. Pashlsp, and D. I. Dunthorn (1972), *Removal of Radioactive Krypton and Xenon from Contaminated Off-Gas Systems,* Union Carbide Corp., Oakridge, Tennessee, K-L-6257.

Mountain, J. E., L. E. Eckart., and J. H. Leonard (1968), *Survey of Individual Radionuclides Production in Water-Cooled Reactors,* University of Cincinnati Summary Report, Phases I and II of Contract Ph 86-67-218, May 30, 1968.

National Environmental Research Center-Las Vegas (NERC-LV) (1973), Unpublished Environmental Surveillance Data, Environmental Protection Agency.

Nucleonics Week (1966 and 1971), Vol. 7, January to December 1966 and 12:4 January 28, 1971.

Pannetier, R. (1968), *Distribution, Atmospheric Transfer and Balance of Krypton-85,* (thesis) (CEN-Fontenay-aux-Roses, France), CEA-R-3591, translated by E. R. Appleby, BNWL-TR-34, July 1, 1969.

Pannetier, R. (1970), *Original Use of the Radioactive Tracer Gas Krypton-85 to Study Meridian Atmospheric Flow,* J. Geophys. Res., 75 (15), 2985-2989.

Poldervaart, A. (1955), Ed., *Crust of the Earth,* Geological Society of America, New York, N.Y.

Public Health Service (1970), *Radiological Health Handbook,* Dept. of Health, Education, and Welfare, Revised.

Reist, P. C. (1965), *The Disposal of Radioactive Krypton-85 in Porous Media,* NYO-841-7.

Rubin, B., L. Schwartz, and D. Montan (1972), *An Analysis of Gas Stimulation Using Nuclear Explosives,* UCRL-51226.

Russell, J. L. (1972), *A Review of the Actual and the Projected Offsite Doses at Fuel Reprocessing Plants,* Health Physics Society Annual Meeting, June 1972, Environmental Protection Agency.

Shleien, B. (1970), *An Estimate of Radiation Doses Received by Individuals Living in the Vicinity of a Nuclear Fuel Reprocessing Plant in 1968,* BRH/NERHL 70-1.

Shuping, R. E., C. R. Phillips, and A. A. Moghissi (1970), *^{85}Kr Levels in the Environment Determined From Dated Krypton Gas Samples,* Radiological Health Data and Reports, Vol II, Number 12, December 1970.

Silverman, L. (1959), *Hearings Before the Special Subcommittee on Radiation, on Industrial Radioactive Waste Disposal,* Joint Committee Atomic Energy, U. S. Congress.

Tadmor, J. and K. E. Cowser (1967), *Undergrounnd Disposal of Krypton-85 From Nuclear Fuel Reprocessing Plants,* Nuclear Engineering and Design, 6:243-250, North-Holland Publishing Comp.

United Nations (1971), *Scientific Committee on the Effects of Atomic Radiation, Environmental Radio-Activity,* A/AC, 82/R. 265, April 20, 1971.

Unruh, C. M. (1970), *Present and Projected Sources of Environmental Radiation (the Givens),* BNWL-SA-3354.

Upson, U. L. (1966), *Fixation of High-Level Radioactive Wastes in Phosphate Glass — Hot Cell Glass Experiment,* Battelle-Northwest, BNWL-200.

Vermillion, H. G. (1973), *Revised Nuclear Test Statistics,* Atomic Energy Commission, Nevada Operations Office, January 15, 1973.

Verniani, F. (1966), *The Total Mass of the Earth's Atmosphere,* J. Geophys. Res., 71 (2), 385-391.

Weaver, L. E., P. O. Strom, and P. A. Killeen (1963), *Estimated Total Chain and Independent Fission Yields for Several Neutron-Induced Fission Processes,* USNRDL-TR-633, March 5, 1963.

Whipple, G. H. (1969), *Approaches to the Calculation of Limitations on Nuclear Detonations for Peaceful Purposes,* Proceedings, Symposium Public Health Aspects of Peaceful Uses of Nuclear Explosives, Southwestern Radiological Health Laboratory, Las Vegas, Nevada, April 1969.

TABLE 1. Predominant Noble Gas Radionuclides Produced by the Fission Process.

Radionuclide	Half-Life (Years	Fission Yield ^{235}U Thermal Neutrons Atoms per 10^4 Fissions	Decay Energy (MeV)	Infinite Time Integral Times MeV (h-MeV)
Krypton				
85m	5.10×10^{-4}	130	1	7×10^{-4}
85	10.76	29.5	0.67	10
87	1.4×10^{-4}	250	4	8×10^{-4}
88	3.2×10^{-4}	350	3	1×10^{-3}
89	$3. \times 10^{-4}$	400	4	4×10^{-5}
90	1.0×10^{-6}	470	3	4×10^{-6}
Xenon				
131m	$3. \times 10^{-2}$	2	0.2	9×10^{-3}
132m	6.2×10^{-3}	16	0.2	2×10^{-3}
133	1.4×10^{-2}	660	0.4	8×10^{-3}
137	7.4×10^{-6}	530	4	4×10^{-5}
138	3.3×10^{-5}	420	4	2×10^{-4}

TABLE 2. Krypton-85 Production as a Result of Fission.

Fissile Material Neutron Energy	Atoms ^{85}Kr per 10^4 Fissions	Ci per 10^{22} Fissions	Ci/GWt-h	Ci Kiloton Fission
^{235}U thermal	29.5	1.63	18.2	23.6
^{235}U fission	27.4	1.51	16.9	22.0
^{238}U fission	22.6	1.25	13.9	18.1
^{239}Pu fission	15.8	0.87	9.71	12.6
^{239}Pu thermal	12.2	0.67	7.49	9.73
^{233}U thermal	56.2	3.10	34.6	45.0

TABLE 3. Forecast of Most Likely Power Capacity in Giga Watts-Electric (AEC, 1972b and 1972c).

Year	USA	Foreign	East Block	Total
1970	2	5.5	0.5	8
1975	54	39	8	101
1980	132	140	20	292
1985	280	303	56	639
1990	508	580	146	1,234
1995	811	968	318	2,097
2000	1,200	1,460	600	3,260

TABLE 4. Electric and Thermal Capacities by Reactor Types (AEC, 1972b) (Giga Watts-Electric Giga Watts-Thermal @ 80% Load Factor).

	GW-Electrical				GW-Thermal			
Year	LWR GCR	AGR	HTGR	FBR	LWR GCR	AGR	HTGR	FBR
1970	8	--	--	--	8	--	--	--
1975	92	9	--	--	213	17	--	--
1980	263	30	--	--	608	57	--	--
1985	543	60	36	--	1,259	114	74	--
1990	988	100	110	36	2,291	190	226	69
1995	1,454	150	225	268	3,372	286	462	510
2000	1,855	200	330	875	4,301	381	677	1,667

TABLE 5. Production of Krypton-85 in Various Reactor Types in Each Five-Year Period in MCi.

Year	LWR	AGR	HTGR	FBR	Total
1970	15	--	--	--	15
1975	170	14	--	--	184
1980	484	46	--	--	530
1985	1,002	91	59	--	1,152
1990	1,823	151	233	29	2,236
1995	2,683	226	531	216	3,656
2000	3,422	302	873	708	5,305

TABLE 6. Contribution of Various Reactors to the Atmospheric Inventory of Krypton-85.

	Megacuries				
Year	LWR	AGR	HTGR	FBR	Total
1970	7	--	--	--	7
1975	55	--	--	--	55
1980	322	29	--	--	356
1985	910	79	--	--	989
1990	1,960	168	130	--	2,258
1995	3,560	305	410	70	4,345
2000	5,580	495	965	435	7,475

TABLE 7. Nuclear Stimulation of Natural Gas.
(Rubin, *et al.*, 1972)

	Fiscal Year							
	1974-1977	1977	1978	1979	1980	1981	1982	1983
Number of Wells Stimulated								
Green River Basin Wyoming	--	--	10	30	50	70	70	70
Piceance Basin Colorado	--	20	20	30	30	30	30	30
Total Wells	3	20	30	60	80	100	100	100
Number of Explosives	10	60	100	210	290	370	370	370
Megacuries ^{85}Kr +	0.02	0.13	0.22	0.46	0.64	0.81	0.81	0.81

TABLE 8. Production and Atmospheric Release of Krypton-85 up to the Year 2000 in MCi.

Year	-70	71-75	76-80	81-85	86-90	91-95	96-00
Power Reactor							
Carry Over Inventory		5	40	258	717	1,636	3,148
Production	15	184	530	1,152	2,236	3,656	5,305
Release	7	50	316	731	1,541	2,709	4,327
Total Inventory	7	55	356	989	2,258	4,345	7,475
Pu Production Reactors							
Carry Over Inventory	38	27.5	22.9	19.5	17.0	15.2	13.9
Production		4.7	4.7	4.7	4.7	4.7	4.7
Release		4.0	4.0	4.0	4.0	4.0	4.0
Total Inventory	38	31.5	26.9	23.5	21.0	19.2	17.9
Ship Propulsion Reactors							
U.S. Navy, Carry Over Inv.	3	2.2	3.8	5.1	6.2	7.2	8.1
Production		3.2	3.4	3.7	4.0	3.2	4.5
Release		3.0	3.2	3.5	3.7	4.0	4.2
Total Inventory		5.2	7.0	8.6	9.9	11.2	12.3
World Inventory	3	10	14	17	20	22	25
Natural Gas Stimulation							
Carry Over Stimulation				0.6	2.8	4.5	5.7
Production			1.5	4.0	4.0	4.0	4.0
Release			0.8	3.2	3.4	3.4	3.4
Total			0.8	3.8	6.2	7.9	9.1
Nuclear Testing (World)							
Carry Over Inventory	2.2	1.63	1.24	0.97	0.76	0.61	0.5
Production		0.1	0.1	0.1	0.1	0.1	0.1
Release	0.09	0.09	0.09	0.09	0.09	0.09	0.09
Total	2.3	1.7	1.3	1.1	0.8	0.7	0.6
TOTAL IN ATMOSPHERE	50	98	395	1,034	2,306	4,395	7,528

TABLE 9. Projected Atmospheric Concentrations of Krypton-85 and Resulting Radiation Doses.

Year	Atmospheric Inventory (Megacuries)	Atmospheric Concentration pCi/m³ (s.t.p.)	Dose — microrad/year		
			Whole Body	Surface of Skin	Basal Layer of Skin
1970	50	13	0.18	26	13
1975	98	25	0.35	51	26
1980	395	99	1.41	207	103
1985	1,034	260	3.69	541	271
1990	2,306	581	8.23	1,207	604
1995	4,395	1,110	15.7	2,300	1,150
2000	7,528	1,900	26.9	3,940	1,970

TABLE 10. Comparison of Krypton-85 Projections for Year 2000.

Reference	Nuclear Power GWt	Atmospheric Inventory GCi	Average Atmospheric Concentration (pCi/m³)	Projected Doses (Millirad)		
				Whole Body	Skin Basal Layer	Skin Surface
This Paper	7,000	7.5	1,900	0.027	2	4
This Paper	3,000 USA	---	---	---	---	---
Klement, *et al.*, (1972)	5,000 Total	---	1,400	0.04	---	2
Coleman and Liberace (1966)	4,000 Total	4.0	1,000	---	---	2
Pannetier (1968)	5,000 Total	3.6	1,400	---	---	2
Unruh (1970)	3,000 USA	3.2	---	0.025	---	2
Cowser, *et al.*, (1966)	3,300 Free World	3.2	1,000	---	---	2
Dunster and Wagner (1970)	6,000 Total	---	---	0.04	---	4
United Nations (1971)	4,260 Total	9.4	2,300-3,000	0.03	---	4

Figure 1. PROJECTIONS FOR WORLD WIDE NUCLEAR POWER (0.8 Load Factor)

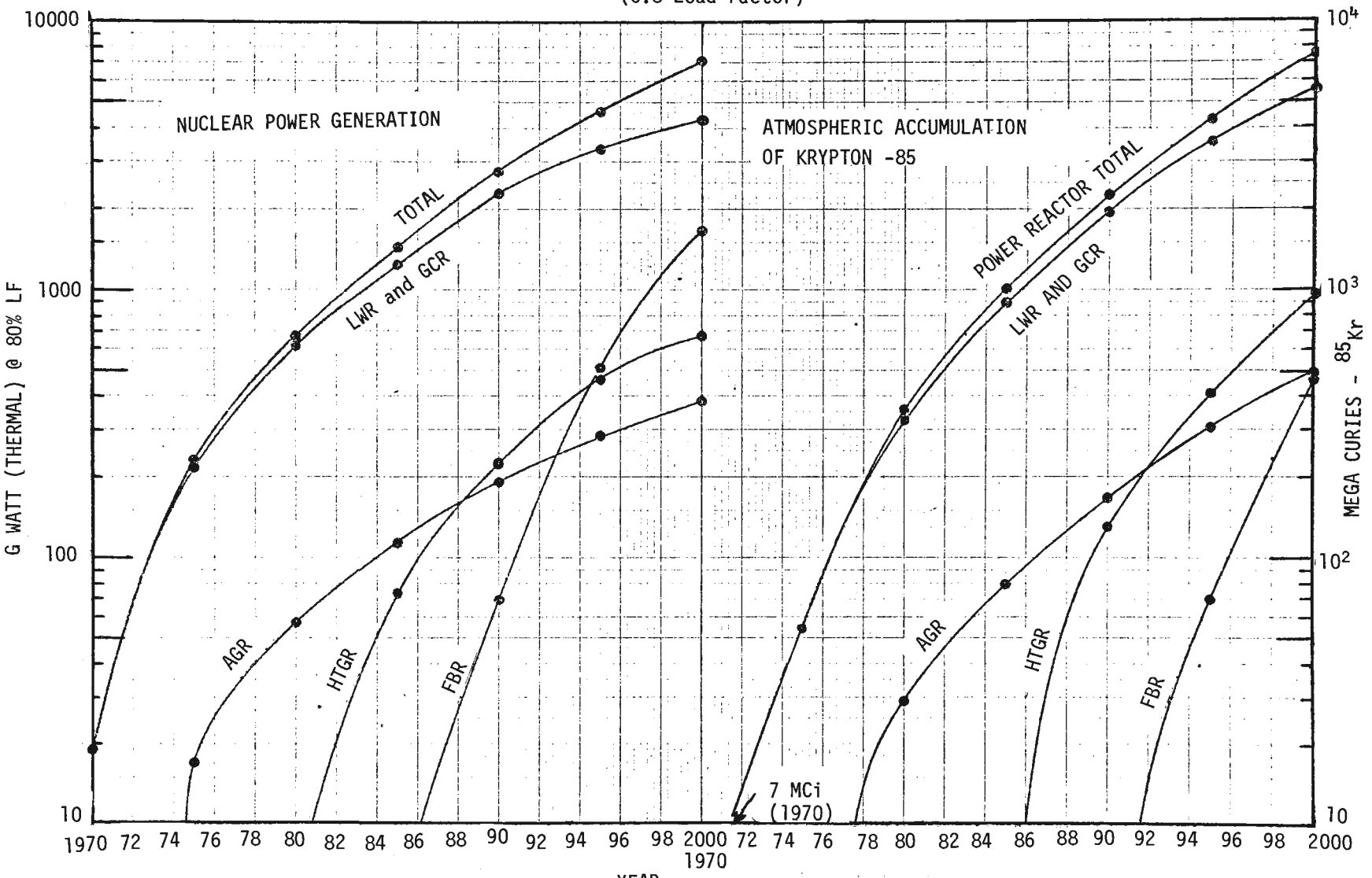

Figure 2.

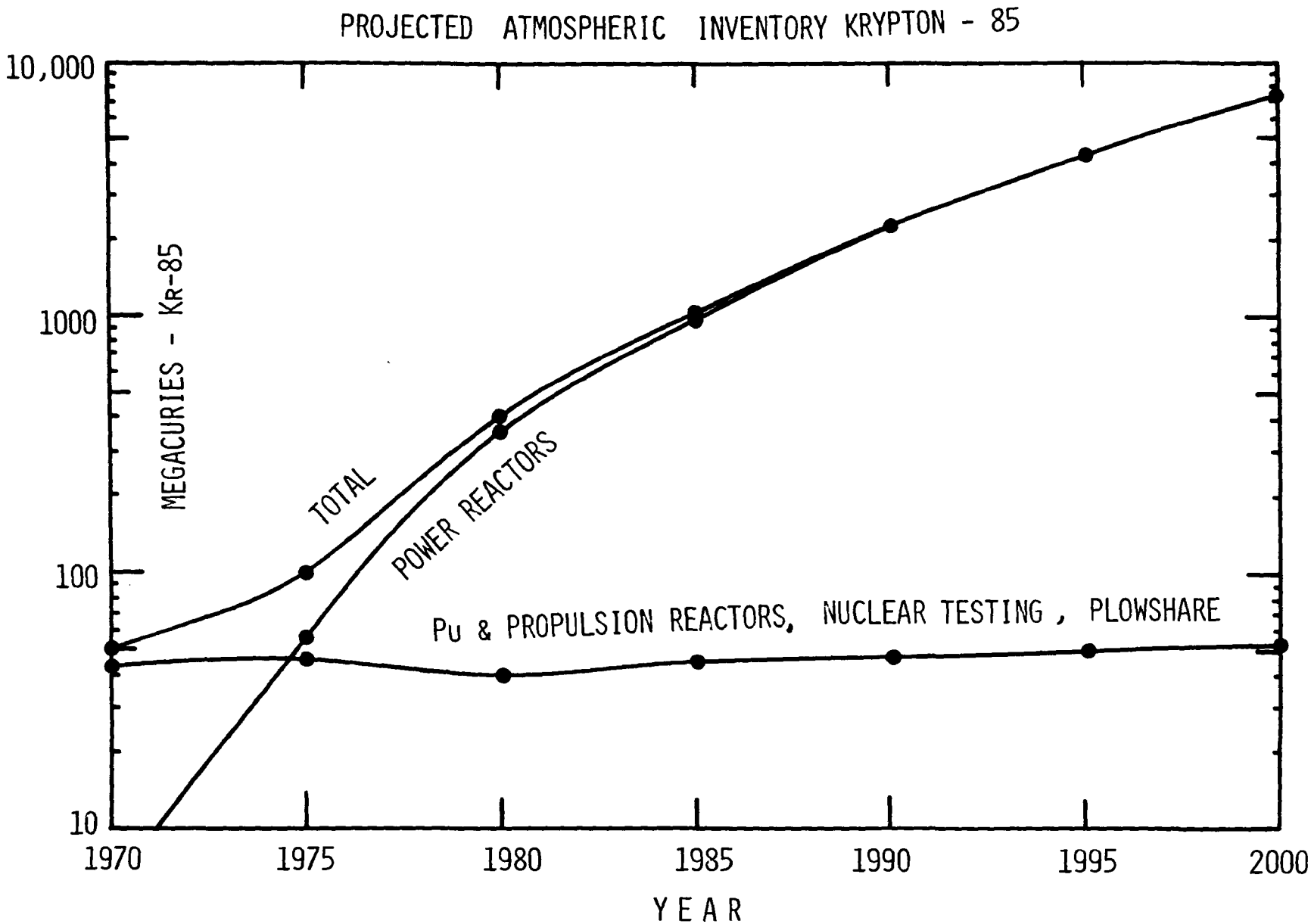
PROJECTED ATMOSPHERIC INVENTORY KRYPTON - 85
10,000
1000
100
10
MEGACURIES - KR-85
TOTAL
POWER REACTORS
Pu & PROPULSION REACTORS, NUCLEAR TESTING , PLOWSHARE
1970
1975
1980
1985
1990
1995
2000
YEAR

Figure 3.

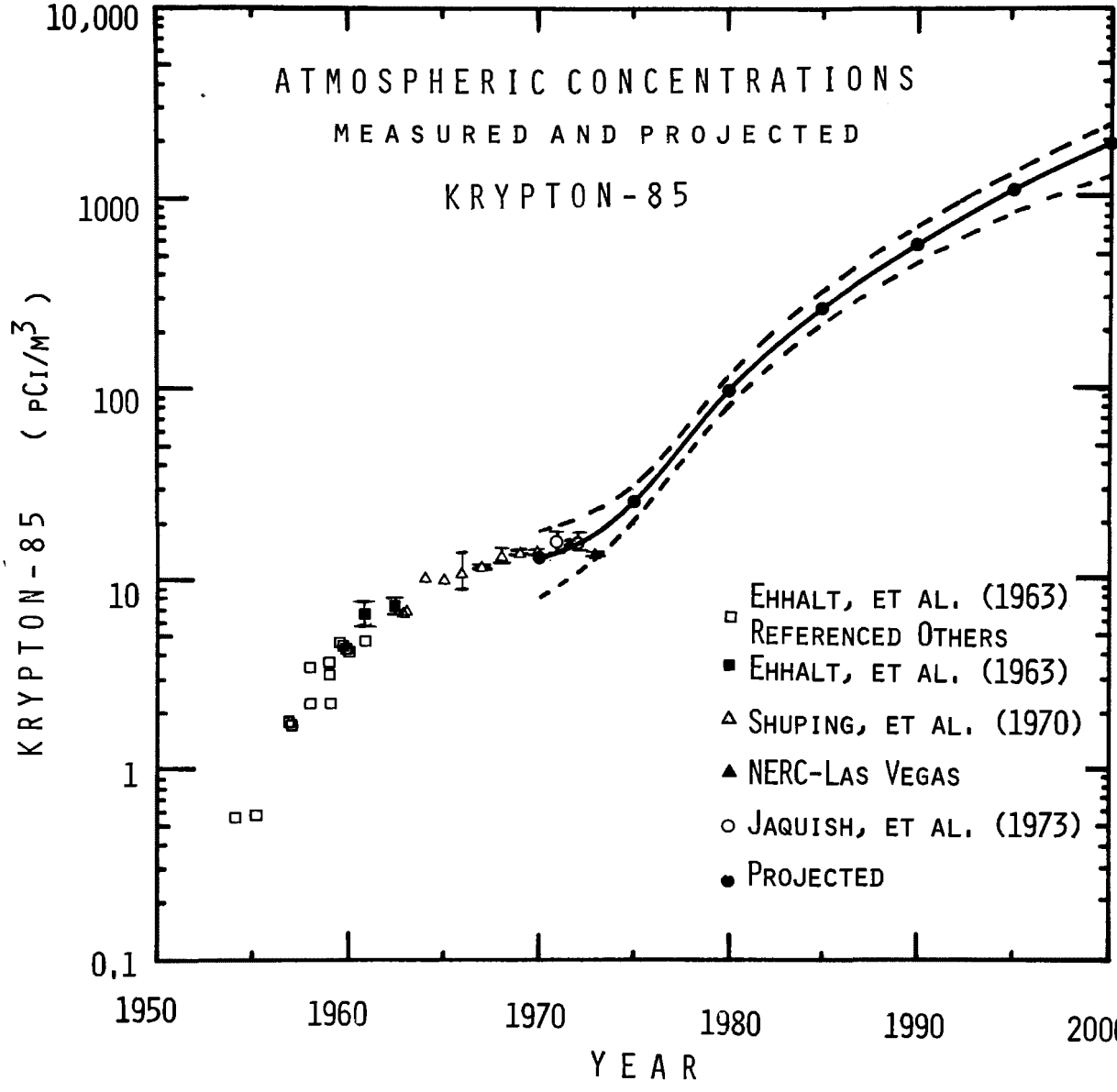
ATMOSPHERIC CONCENTRATIONS
MEASURED AND PROJECTED
KRYPTON-85
KRYPTON-85 (pCi/M3)
10,000
1000
100
10
1
0.1
1950
1960
1970
1980
1990
2000
YEAR
EHHALT, ET AL. (1963) REFERENCED OTHERS
EHHALT, ET AL. (1963)
SHUPING, ET AL. (1970)
NERC-LAS VEGAS
JAQUISH, ET AL. (1973)
PROJECTED

CONTAMINATION OF THE ATMOSPHERE WITH KRYPTON-85 IN POLAND

T. Wardaszko
Central Radiological Protection Laboratory
Warsaw, Poland

ACKNOWLEDGEMENTS

The keen interest and help of Dr. Jaworowski is gratefully acknowledged.

Abstract

The measurements of radioactive ^{85}Kr in atmospheric air have been conducted in Poland during the last three years using two different methods, one consisted of the application of large scintillation chambers, and the other consisted of gas chromatographic separation with purification of the krypton fraction.

The results obtained are similar to those so far reported for other European countries. They indicate that ^{85}Kr does not constitute a significant radiation hazard at the present time, but the tendency towards the increase of its atmospheric concentrations makes it one of the radionuclides of concern.

INTRODUCTION

The rapidly expanding nuclear power industry has released considerable quantities of fission-produced krypton-85 to the atmosphere. This relatively long-lived radioisotope readily diffuses by horizontal and vertical mixing of air masses and has an extremely low rate of depletion (Tadmor, 1973) due to its low-solubility in water and chemical inertness. This has led to the worldwide pollution of the atmosphere by this radionuclide. The relative uniformness of its distribution on a global scale is a fact known since the studies by Pannetier (1971).

Another important aspect of atmospheric contamination with ^{85}Kr is its increasing concentrations (Pannetier, 1971; Shuping, *et al.*, and Schroder, *et al.*, 1971) due to the growing nuclear power industry which includes nuclear fuel reprocessing, in a number of countries in the Northern Hemisphere. The predictions for the future decades indicate that, assuming the present gaseous waste disposal technology is not changed, and 75 per cent of the produced ^{85}Kr remains in this hemisphere, the average concentration of 100 pCi/m^3 will be reached as early as 1979 (Klement, *et al.*, 1972).

For these reasons, we are concerned with this type of radioactive pollution, although Poland is at an early stage in the development of nuclear power generation. The radiation doses to the population from this source are at present insignificant; however, attention must be paid to this radionuclide in order to get sufficient information on existing levels and trends for the future.

METHODS OF MEASUREMENT

At first the determinations of ^{85}Kr concentrations in air were carried out using the beta scintillation chambers described by Wardaszko, 1969 and Ilari, *et al.*, 1970, with later modifications. This consisted of cylindrical chambers with volumes of approximately one liter, fitted with thin plastic scintillators. These chambers were filled with enriched samples of atmospheric air and counted in a probe with 2 photomultiplier tubes (see Figure 1) connected to two scalers or a multichannel analyzer. Enrichment is made by two-stage adsorption on activated carbon at liquid nitrogen temperature with subsequent desorption allowing the unnecessary fractions to be vented.

As this method requires a rather large air sample, on the order of 5-6 m^3, another method was applied which is similar to that described by Stevenson and Johns (1971). This consisted of the application of gas chromatography for the separation of the krypton fraction of an enriched air sample, and its subsequent purification and radioactivity measurement in a liquid scintillation counter. The first stage of this process is in passing an air sample through a charcoal trap at liquid nitrogen temperature; then, a part of the adsorbed gases is passed through chromatographic columns for separation from other components, and subsequent purification accomplished with a platinum filament controlled by a thermal conductivity detector. A Polish-made gas chromatograph (type ICSO-571) was used for this purpose. The final fraction was introduced into the scintillation vial, and counted in a Packard Tri-Carb liquid scintillation counter with a technique elaborated by Shuping, *et al.*, (1969). This technique allows the use of a smaller air sample, about 1 m^3, without affecting the overall accuracy of the measurement.

The application of gas chromatography to the separation of radioactive noble gases was first introduced by Amadesi and Cervellati (1963), but this method was not used at first by other researchers. Artemenkowa, *et al.*, (1971) applied frontal chromatography for separating groups of radioactive noble gases in composite samples, although not at the trace level.

RESULTS

The results of measurements of ^{85}Kr concentrations in the atmospheric air in Warsaw for 1971 and 1972 presented in Table 1. At first these samples were measured using the scintillation technique just mentioned, whereas in the later samples the gas chromatographic technique was used. The overall error refers to each measurement; and is comprised of a 2 sigma counting error, as well as other errors due to manipulations with the gas sample.

As can be seen from this table, the ^{85}Kr concentrations do not vary greatly, but a tendency toward increases in concentrations is seen. The mean increase rate is 1.0 pCi/m^3 year, which is somewhat lower than that reported by Schroder, *et al.*, (1971) which was 1.3 pCi/m^3. year.

The results obtained are compared in temporal sequence to other data available from the literature mainly for European countries (see Table 2 and Figure 2). The first measurements of ^{85}Kr in Poland (Ostrowski and Jelen, 1965) made were at Cracow in Southern Poland in 1965. These measurements were not included because it was difficult to derive comparable values from the published data.

An apparently low scatter of concentration values is caused rather by incompletness of data than by the character of the phenomenon. In fact, a considerable dispersion of single values occurs due to temporal variations in ^{85}Kr emissions (Schroder, *et al.*, 1971) and their geographical distribution.

The data for Eastern Europe are scarce, but they indicate that the observed ^{85}Kr concentrations are similar to those encountered elsewhere. This confirms the above mentioned uniformity of radioactive krypton concentrations on a global scale.

At present, the radiation doses to the population from ^{85}Kr at existing concentrations are rather low, the order of 20 microrem/a skin dose, calculated as in Klement, *et al.*, (1971). This is only a small fraction of the total dose from the naturally occurring background radiation.

REFERENCES

Amadesi, P. and A. Cervellati, (1963), *Separation and Measurement of Rare Fission Gases by Gas Chromatography.* In: Proc. of the Colloquium on Radioactive Pollution of Gaseous Media, Saclay.

Artemenkova, L. V., *et al.*, (1971), *Ekspresnyje metody izotopnogo analiza radioaktivnykh gazov i aerozolej.* In: Rapid Methods for Measuring Radioactivity in the Environment; Proc. of a Symp. 1AEA, Vienna.

Bock, H. and C. M. Fleck, (1968), *Identification of Gaseous Beta Emitters in Low-Level Equipment.* In: Assessment of Airborne Radioactivity, Proc. of a Symp., IAEA, Vienna.

Csongor, E. (1972), *Issledovanie zagraznenija atmosfery izotopom ^{85}Kr.* In: Proc. of the 1st Radioecological Conf., St. Smokovec, Czechoslovakia.

Ilari, O., G. Sciocchietti and T. Wardaszko, (1970), *A High Sensitivity Method for the Beta-Active Gases Measurement in the Presence of Natural Radioactivity of the Air.* Giornale di Fisica Sanit. e Prot. c. le Rad. 14, 1, 38.

Jaquish, R. E. and F. B. Johns (1972), *Concentrations of Krypton-85 in Air.* Paper delivered at the Symp. on Natural Radioactivity of the Environment, Houston, Texas.

Klement, A. W., Jr., *et al.*, **(1972),** *Estimates of Ionizing Radiation Doses in the United States 1960-2000.* Rep. of the U.S., EPA, Office of Radiation Programs.

Ostrowski, K.W. and K. Jelen (1965), *On the Contamination of the Atmospheric Krypton by ^{85}Kr from Fission Products.* Nukleonika 10, 67 Warsaw.

Pannetier, R. (1971), *Distribution, transfert atmospherique et bilan du Krypton-85.* Rapport CEA-R-3591.

Schroder, J., K. O. Munnich and D. H. Ehhalt, (1971), *Krypton-85 in the Troposphere.* Nature 233, 5322, 614.

Shuping, R., C. R. Phillips and A. A. Moghissi, (1969), *Low-Level Counting of Environmental Krypton-85 by Liquid Scintillation.* Analyt. Chem. 41, 2082.

Shuping, R. E., C. R. Phillips and A. A. Moghissi, (1970), *Krypton-85 Levels in the Environment Determined from Dated Krypton Gas Samples.* Radiological Health Data and Reports 11, 671.

Stevenson, D. L. and F. B. Johns, (1971), *Separation Technique for the Determination of ^{85}Kr in the Environment.* In: Rapid Methods for Measuring Radioactivity in the Environment, Proc. of a Symp. IAEA, Vienna.

Tadmor, J. (1973), *Deposition of ^{85}Kr and Tritium Released from a Nuclear Fuel Reprocessing Plant.* Health Phys. 24, 1, 37.

Wardaszko, T. (1969), *A Principle of Low Concentrations Measurement of Beta and Gamma Active Gases in the Air.* In: Skazenia promieniotworcze otoczenia-Radioactive Contamination of the Environment, COPSP, Warszawa.

TABLE 1. Concentrations of ^{85}Kr in Warsaw, Poland.

Year	Number of Determinations	Mean Sample Volume, m^3	Mean concentration, pCi/m^3	Overall Error of Single Determination, %
1971	3	5	16.0	12
1972	8	5	17.4	12
1973	5	1.1	18.0	9

TABLE 2. Concentrations of ^{85}Kr in Atmospheric Air in the Period 1966-73 in Some Countries of the Northern Hemisphere.

Year	Country	Concentration pCi/m^3	References
1966	Hungary	11	Csongor (1972)
1966	Austria	10	Bock and Fleck (1968)
1967	France	12	Pannetier (1971)
1969	W. Germany	14.9	Schroder, *et al.*, (1971)
1971	Hungary	15	Csongor (1972)
1971*	U.S.A.	16.3	Jaquish and Johns (1972)
1971	Poland	16.0	This Paper
1972	Poland	17.4	This Paper
1973	Poland	18.0	This Paper

*Partly also 1972.

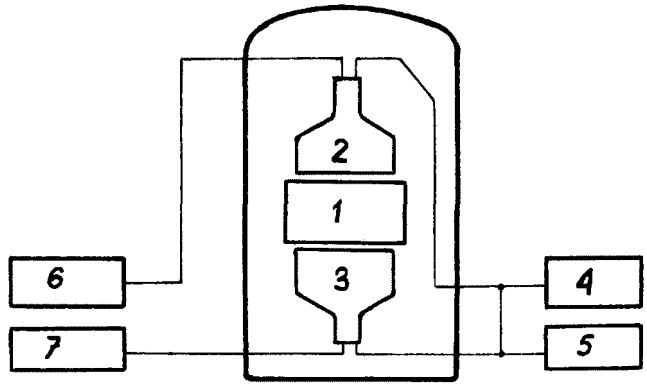

Figure 1. Block diagram of counting device with cylindrical scintillation chambers. (1 — Scintillation chamber; 2, 3 — PM tubes; 4, 5 — scalers or multichannel analyzer; and 6, 7 — HV supplies.)

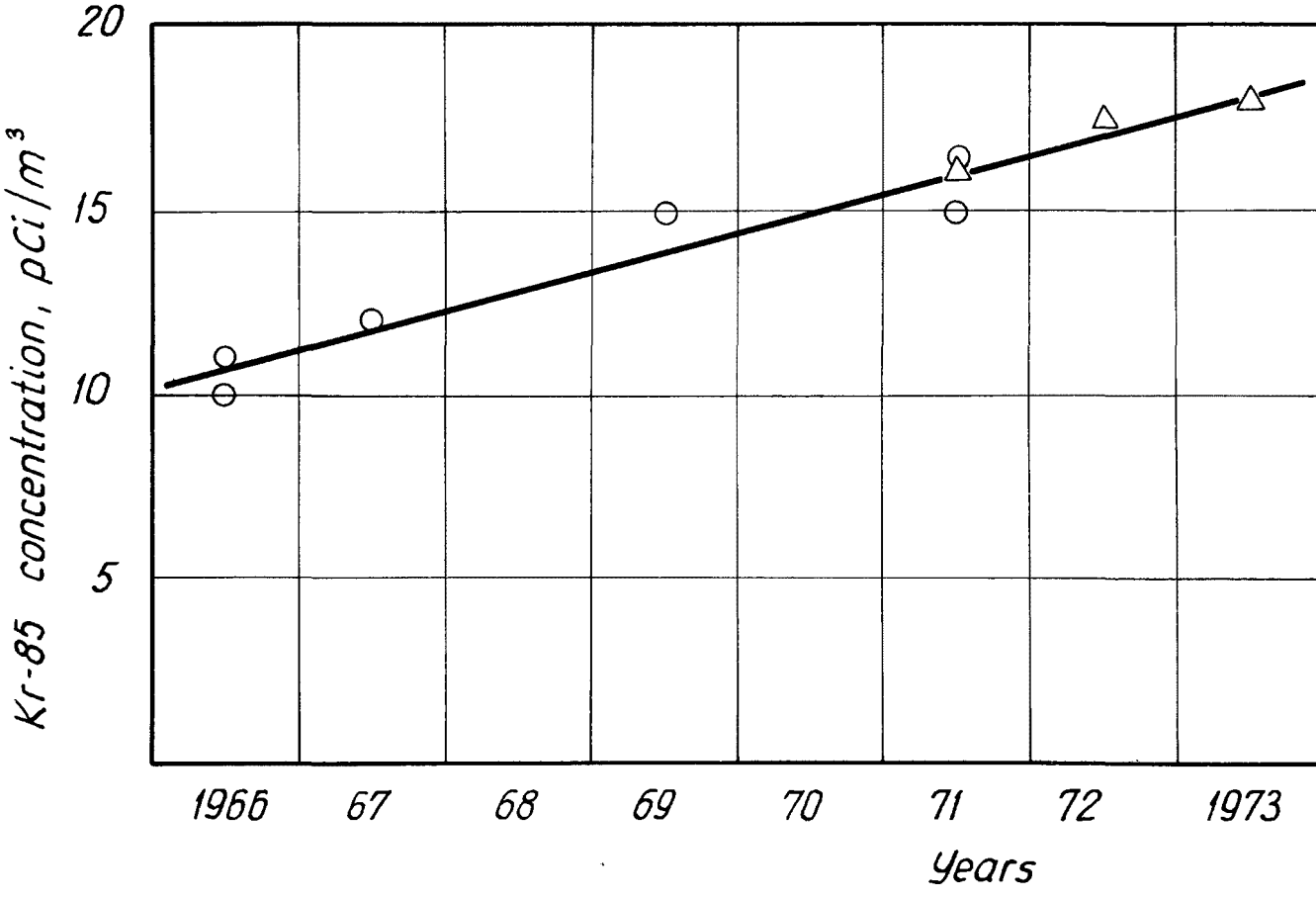

Figure 2. Temporal variations of the ^{85}Kr concentrations:
△ — Data for Warsaw, Poland.
O — Other data.

ATMOSPHERIC CONCENTRATIONS AND MIXING OF ARGON-37*

H. Loosli, H. Oeschger, R. Studer, M. Wahlen, and W. Wiest
Physikalisches Institute
Bern, Switzerland

ACKNOWLEDGEMENTS

The authors thank the CARBA Inc., Bern, Switzerland, and many other gas factories, and their coworkers, for supplying the dated argon samples. We are thankful to Dir. F. Wild, Drs. L. A. Currie, W. Shell, D. Lal, A. Nir, and Mr. N. Fong for their help to obtain argon samples from various locations.

Abstract

The ^{37}Ar activity in ground-level air samples from various countries (Switzerland, Denmark, USA, Canada, India, Australia, and Argentina) was monitored since 1969. Low-activity values of about 0.0025 dpm/l of argon were in agreement with the expected production rate by cosmic rays after mixing in altitude and latitude. However, high-activity values up to 1.8 dpm/l of Ar were observed several times. These were attributed to artificial sources, most probably to underground nuclear explosions. Estimates indicate that 0.7 to 2 MCi of ^{37}Ar must have been released into the atmosphere. Wind transportation and a two-dimensional multi-box eddy diffusion model were used to interpret the data in terms of atmospheric mixing. The best fit to the data was obtained with values between 1 and 3 x 10^{10} cm^2s^{-1} for an average latitudinal eddy diffusion coefficient between 20° and 70°N. Minor variations in the ^{37}Ar activity may be due to ^{37}Ar released from reactors or fuel reprocessing plants.

INTRODUCTION

Since 1969, we have continuously monitored the activity of ^{37}Ar (half-life = 35.1 d) in argon samples collected from ground-level air in Bern, Switzerland. In addition, a number of samples from various localities in the northern (Europe, USA, Canada, India) and southern (Sidney, Buenos Aires) hemispheres have been measured during this period. In the course of this investigation, we observed enormous fluctuations in the ^{37}Ar activity. Intermittently, the activity rose by up to 3 orders of magnitude above the values which are believed to be due to cosmic ray production; i.e., mainly from spallation reactions on ^{40}Ar and to neutron capture by ^{36}Ar (Lal and Peters, 1967 and Oeschger, *et al.*, 1970). These excess activities have been attributed to underground nuclear blasts (Loosli, *et al.*, 1969 and 1970), where massive amounts of ^{37}Ar, produced by the reaction $^{40}Ca(n,\alpha)^{37}Ar$, were thought to be vented into the atmosphere. These findings evidently make ^{37}Ar a very useful tracer for studies of atmospheric mixing processes.

In addition to meteorological methods, global atmospheric mixing can be studied by measurements of the atmospheric distributions of ozone, volcanic ash, cosmic ray produced nuclides, radioactive debris from nuclear explosions, and other tracers. For most of the conventional tracer isotopes, the geochemical and geophysical behavior (attachment to aerosols, scavenging, settling), and the exchange with other reservoirs besides the atmosphere, have to be known (e. g., Machta, *et al.*, 1970). Therefore, ^{37}Ar, a noble gas largely confined to the atmosphere, is useful in studying atmospheric mixing; also, its half-life corresponds to the mixing times involved. When cosmic ray produced ^{37}Ar activities are investigated, the mixing of a global stationary input can be unveiled, whereas bomb-produced ^{37}Ar activities yield information on mixing of a local changing-input. Repetitive inputs by nuclear blasts can be studied because, within about 6 months, the activity has decayed to the level of cosmic ray produced amounts; thus estimates can be made about the time required for reaching equilibrium in a given hemisphere. Because Ar is chemically inert, the monitoring of the ^{37}Ar activity, in combination with other nuclides, in turn allows the determination of wash-out parameters and exchange parameters (Machta, *et al.*, 1970).

EXPERIMENTAL PROCEDURE AND RESULTS

A detailed description of the experimental procedure of our ^{37}Ar measurements on tropospheric air samples is given by Oeschger (1963) and (1970); Loosli, *et al.*, (1969), (1969), and (1970); and Studer, (1973).

Most of the samples were measured in a proportional counter made of plexiglass with a volume of 1 l. A stainless steel counter with a total volume of 2.8 l was in use since the spring of 1972. Some characteristics of these counters are summarized in Table 1.

The overall counting efficiencies of our counters were determined using new ^{37}Ar standards provided by Drs. R. W. Stoenner and R. Davis, Jr. of Brookhaven National Laboratory. The results obtained with these standards were lower by 10% than the yields determined previously. Therefore, the ^{37}Ar results given by Loosli, *et al.*, (1969) and (1970); Oeschger, *et al.*, (1970); and Machta, *et al.*, (1970) need to be scaled up by a factor of 1.12.

**This work has been supported by the "Schweizerischer Nationalfonds zur Forderung der wissenschaftlichen Forschung".*

The results of the ^{37}Ar measurements on argon samples collected from near ground-level air for the period 1969-1973 are presented in Figures 1 to 4. Most of the samples were separated by A. G. Carba of Bern, Switzerland; and, for all of them, the actual dates of separation are known. The errors given are within one standard deviation. The arrows indicate the dates of nuclear explosions, both underground and in the atmosphere, which were obtained from press notices. We believe, that the low values in ^{37}Ar activity (around 0.0025 dpm/l Ar) as measured, e. g., in the summer of 1970, are representative for the cosmic ray produced activity found near ground-level after atmospheric mixing. This is discussed further in a subsequent section of this paper.

The pronounced peaks with high activities found in the autumns of 1969 through 1972 are attributed to artificial sources. Most plausibly, the massive ^{37}Ar excess is due to underground nuclear explosions, because each rise in activity was preceeded by an event amounting to about 1 megaton TNT. Figures 5 through 8 present the activity data from Figures 1 through 4, after corrections for a cosmic ray production contribution of 0.0025 dpm/l of Ar and for radioactive decay to the most probable date of the nuclear explosion. The reduced data were then used for the discussion of atmospheric mixing presented in a subsequent section of this paper.

COSMIC RAY PRODUCED ^{37}Ar ACTIVITY

The lowest ^{37}Ar activities (around 2.5×10^{-3} dpm/l Ar) were measured on a series of samples collected from air in the summers of 1970 and 1971 (Figures 1 to 4). These data suggest that no pronounced stratospheric or man-made input into the troposphere occurred during these periods. Therefore, they may represent the cosmic ray produced activity found at ground-level in a mixed atmosphere, after the activities remaining from the previous bomb explosions have decayed. Calculations of the weighted average value for the cosmic ray produced activity found at ground-level from data collected during the summers of 1970 and 1971 indicated $(2.3 \pm 0.3) \times 10^{-3}$ dpm/l of Ar and $(2.8 \pm 0.6) \times 10^{-3}$ dpm/l of Ar, respectively, with a weighted mean of $(2.4 \pm 0.3) \times 10^{-3}$ dpm/l of Ar. Four single measurements (out of 30) being up to a factor of 2 higher, were rejected in the evaluation of the above mean value. Their higher activities may be due to small stratospheric inputs by local leaks in the tropopause. The stated errors are within one standard deviation, and do not include the uncertainty introduced by neglecting possible man-made and stratospheric inputs.

The experimental results obtained may be compared to the values predicted by various models, combining estimated production rates and atmospheric mixing processes.

Within a mean life of ^{37}Ar ($\cong$ 50 d), the troposphere is rather well mixed. Therefore, assuming a completely mixed troposphere and no stratospheric input, we compared the observed ground-level activity with estimated average tropospheric production rates. Lal and Peters (1967) calculated an average tropospheric production rate of about 3×10^{-3} dpm/l of Ar with an estimated uncertainty of a factor of 3. Oeschger, *et al.,* (1970) give an average production rate between 200 and 1,000 g/cm^2 amounting to 7×10^{-3} dpm/l of Ar. This value is obtained for periods of sunspot maximum, and is uncertain up to a factor of 2. It is derived from the spallation reaction on ^{40}Ar, and includes a 10% contribution from the reaction $^{36}Ar(n,\gamma)^{37}Ar$. Within the uncertainties, the observed and estimated values agree.

Machta (1973) presents a two-dimensional model for atmospheric mixing, based on the production rates given by Lal and Peters (1967), and on average vertical tropospheric eddy diffusion coefficients of 6 to 8×10^4 cm^{2}s^{-1}. He predicts ^{37}Ar activity values between 0.0020 and 0.0025 dpm/l of Ar which are compatible with the observed data.

In order to improve the basic knowledge for these calculations, we plan to measure the absolute production rate of ^{37}Ar at mountain altitude by exposure experiments, and to determine the vertical activity distribution by collecting samples throughout the troposphere and stratosphere.

HIGH ^{37}Ar ACTIVITY VALUES

The high ^{37}Ar activities, exceeding the cosmic ray produced levels, are not only observed in samples from Europe. Correspondingly high activities were measured in samples from North America on December 18, 1970, in November and December 1971, and on March 23, 1972; and in samples from Bombay, India on February 12, 1972 and November 8, 1972, (cf. Figures 1 through 4). A few samples collected and analysed by Martin, (1973), seem to confirm the trend in activity variations as observed by us in samples from Bern in the period of September to November 1972. It is interesting to note that the high tritium activities observed by Oestlund, *et al.,* (1972) in air samples from Fairbanks, Alaska (November 1970 and October 1971) coincide with our results in high ^{37}Ar activities. These facts show that the enhanced ^{37}Ar activities could not have been caused by minor local releases, but that very large quantities of ^{37}Ar must have been released into the northern troposphere. Possible sources for massive ^{37}Ar inputs are (1) underground or atmospheric nuclear explosions; (2) nuclear reactors; and/or (3) plants for reprocessing nuclear fuel.

Sudden influxes of stratospheric air into the troposphere could cause only minor variations ranging to about 0.05 dpm/l of Ar (Lal and Peters, 1967), and thus cannot account for the top values measured in the autumns of 1969 through 1972. In periods with no indication of strong artificial ^{37}Ar inputs, sometimes ^{37}Ar activities are observed which are significantly higher than the level attributed to cosmic ray production; this was the case in the summer of 1970 (July 28), and in the summer of 1972 (July and August). These higher values may be caused by the release of ^{37}Ar during the reprocessing of nuclear fuel, by stratospheric inputs, or by low to intermediate yield underground nuclear explosions. In the following, we first estimate the yield of ^{37}Ar by the possible sources, and then we discuss atmospheric mixing.

POSSIBLE SOURCES FOR MAN-MADE ^{37}Ar

1. Reactors.

Matuszek (1973) reported measurements of ^{37}Ar activities released from different types of reactors. He found the ratio $^{37}Ar/^{85}Kr$ to be as high as 50 in gaseous effluents from a high-temperature gas-cooled reactor (116 MWt) in the US, and he concluded that the ^{37}Ar is mainly produced from Ca impurities. From this observation, he estimated that this particular reactor released about 6 x 10^3Ci of ^{37}Ar in 1971. Releases from gas-cooled reactors in France (total of 2,700 MWt), in the United Kingdom (total of 8,000 MWt) and in Russia are unknown. Since we observed high ^{37}Ar activities only once a year, and afterwards the activities decreased mostly to cosmic ray produced levels, we believe that the release of reactor produced ^{37}Ar is the reason for the minor fluctuations in activity, but does not account for the immense activities detected; e. g., in November 1970, in October 1971, and in September 1972. From our excess values measured in the summers of 1972 and 1973, we can estimate an upper limit of 300 kCi/a for a continuous release of ^{37}Ar from reactors.

2. Nuclear Explosions in the Atmosphere.

A rough estimate shows that the amount of ^{37}Ar produced by atmospheric nuclear tests by the reaction $^{36}Ar(n,\gamma)^{37}Ar$ is too small to account for the experimental data. Using an upper limit of 10% for the neutrons to escape from an event corresponding to 1 megaton of TNT or to 1.4 x 10^{27} neutrons (Teller, *et al.,* 1968), and assuming that 10% of the produced ^{37}Ar activity is found in the troposphere, we calculate an enhancement of the ^{37}Ar activity by 1 x 10^{-3} dpm/l of Ar in tropospheric air within 20°N and 70°N. This estimate is in agreement with our data from the period following the Chinese test of 1 to 3 megatons of TNT in June 27, 1973, when the ^{37}Ar activity remained below 0.01 dpm/l of Ar throughout July 1973.

3. Underground Nuclear Explosions.

Smith (1971) reported measurements of ^{37}Ar activities in the gases released from the cavity created by a fission explosion of 26 kt TNT (Gasbuggy project). These measurements imply a ^{37}Ar yield of 0.57 kCi/kt TNT for the particular limestone of the test site. This result, together with the facts that the neutron yield is 4 to 5 times higher in a fusion event than in a fission event of the same power (Teller, *et al.,* 1968); and that, in addition, the spectrum of fusion neutrons is harder, supports the conclusion that underground nuclear explosions can easily produce the large amounts of ^{37}Ar necessary to explain our measurements. In a different approach, Studer (1973) tried to estimate the ^{37}Ar production by underground fusion explosions. In this calculation, neutrons with an original energy distribution, as typically obtained in fusion, are followed in scattering and reaction processes in a medium with the average chemical composition of the earth's crust in order to obtain the production by the reaction $^{40}Ca(n,\alpha)^{37}Ar$. The cross-section measured by Barnes, *et al.,* (1973), and a Ca-content in the soil of 1.9 atom-%, were used. About 2% of the 14.1 MeV fusion produced neutrons were found to react with ^{40}Ca, thus leading to 1.8 x 10^8 Ci of ^{37}Ar produced by a fusion event equivalent to 1 Mt TNT. Several uncertainties and approximations involved in this investigation (e. g., escape probability of neutrons from the bomb device; mean energy of the spectra of escaped neutrons; and escape probability of ^{37}Ar from the well) all tend to lower the production of ^{37}Ar; and; therefore, the above result is not in disagreement with our values of up to 1.6 x 10^6 Ci of Ar derived from the measurements. These values were obtained from the activity data, measured after atmospheric mixing into a large part of the northern troposphere is completed (north of 20°N and below 200 g/cm^2); i. e., about 2 to 3 months after an input from an underground explosion. In Figures 5 through 8, average values for this excess equilibrium activity, as established 3 months after the explosions, are shown. In Table 2 the total amounts of ^{37}Ar activities, released from the 1969 through 1972 explosions, are listed as calculated from our data under the above assumptions.

GLOBAL MIXING OF BOMB-PRODUCED ^{37}Ar INPUT

The data given in Figures 1 through 8 shows that large variations occur within the first 1.5 to 2.5 months after the assumed dates of the ^{37}Ar releases. Later on, after 2 to 3 months, the ^{37}Ar activity generally decreases with a time constant comparable to its half-life; i. e., an "equilibrium" activity seems to be reached in most parts of the northern troposphere (see Table 2). Also, the relative concentrations are higher during the first period than later. These observations indicate, that during the first period of mixing, the distribution of ^{37}Ar is governed mainly by wind stream transport according to the actual meteorological situation, which is discussed below. In the second period of a large-scale mixing process throughout the northern troposphere has been achieved; this is discussed in terms of eddy diffusion in the next section of this paper.

Using meteorological data from weather maps of the nothern hemisphere, an attempt was made to predict the dates for the first or even the second passage of active air through Europe. The dates of the corresponding nuclear blasts, which are thought responsible for the input, are obtained from press information. An input duration Δt of one day was assumed. For the first 4 to 8 days surface winds were considered for the calculation of the transport, whereas afterwards the data on winds at a height of 500 mb were used. The area of the "activity cloud" was assumed to enlarge by 10% during transport, and different trajectories were considered if necessary. The dates of arrival as estimated under the above assumptions are given in Table 3, together with

the dates of the actually observed rise in ^{37}Ar activity. The agreement between the estimated and the observed arrival dates is fair, adding support to the assumption that the large ^{37}Ar inputs are due to underground nuclear explosions.

A moderate activity value obtained in a sample from Ohio on September 9, 1972 (Figure 4) is in agreement with the 500 mb wind calculations, namely Novaja Semlia-Canada-Greenland-Europe, for the first passage of the "activity cloud".

The estimated arrival date for a possible ^{37}Ar contribution from the USA explosion in Amchitka (November 6, 1971) coincides with an observed activity increase in samples from Bern after November 16, 1971 (see Figure 7). But, an argon sample collected in Vancouver, B.C., Canada, on November 9, 1971, did not show such an increase, although surface winds should have reached British Columbia by this day, according to the meteorological situation. We, therefore, conclude that by the Amchitka explosion, if any, less than 0.5 MCi of ^{37}Ar was released.

The fluctuations measured in the autumns of 1970 to 1972 indicate a time-span of about 2 weeks for air masses to circulate around the world. This is in agreement with generally adopted circulation times and with our estimates based on weather maps. An attempt to assay arrival dates for the second passage was not successful, because of the enlarged area of the "activity cloud", thus making many trajectories possible.

DISPERSION OF ^{37}Ar RELEASED FROM UNDERGROUND NUCLEAR EXPLOSIONS BY AN EDDY DIFFUSION MODEL

Atmospheric mixing processes in latitudes between 20° and 70° North and South are successfully explained by eddy diffusion models, whereas between 20°N and 20°S convective processes predominate. We, therefore, attempted to explain the dispersion of ^{37}Ar released from underground nuclear tests by an eddy diffusion model, and to derive values for the coefficients of latitudinal eddy diffusion. The diffusion equation is approximated by 213 stimultaneous first-order linear differential equations for 213 atmospheric boxes. The differential equations were solved numerically by an IBM-370 computer. The following assumptions were made:

(1) Zonal mixing is assumed to be fast. Therefore, the atmosphere is divided into well-mixed torus-shaped boxes around the globe, and only mixing in meridional and vertical directions are considered. This assumption is supported by the observation, that after the first passage of high-activity air masses, the activity does not, in general, decrease by more than a factor of two in the next few weeks.

(2) Only eddy diffusion is considered; transport along mean wind trajectories is neglected.

Torus-shaped boxes fill the space from the north pole to 20° South latitude, and from ground-level to an altitude of 13 km. Over each 10 degrees of latitude, 10 boxes with a height of 1.3 km each are piled up. Additional buffer boxes are used to simulate the exchange with the stratosphere and with the equatorial regions.

Parameters are the coefficients for meridional and vertical diffusion. The coefficients for vertical diffusion are adopted from the literature (Bolin, *et al.*, 1963 and 1970; Gudkson, *et al.*, 1968; Machta, *et al.*, 1970; and Hartwig, 1971). They vary between 10^4 and 5×10^5 cm^2/s as a function of the altitude. The main computer runs are made with vertical diffusion coefficients derived from Newell's (1963) time standard deviations of the vertical wind velocities, and the normalization factor given by Newell, *et al.*, (1969). The planned measurements of ^{37}Ar activities in samples from vertical profiles should allow determination of the vertical diffusion coefficients. The comparison of the measured and model calculated ^{37}Ar activities allow conclusions for the meridional diffusion coefficients. In the model, the coefficients are kept constant between 20°N and 70°N. Towards the equator, smaller values for the meridional diffusion coefficient are used in order to reduce the flux across the equator.

In Figure 9 the calculated activities for two latitudes and for two sets of diffusion coefficients are given, together with all measured values from Figures 6 to 8. Since all three artificial inputs lead to similar equilibrium activities, no adjustment of the measured values seems necessary. Good agreement between the measured and the calculated activities cannot be expected during the first 2 months. In the first weeks after an input the spreading of the ^{37}Ar activity is essentially determined by actual wind patterns, giving rise to fluctuations. Also, by then, the assumed zonal mixing has not been totally completed. Only thereafter is the random character of the mixing process reached which justifies the application of a diffusion model. Most of the samples were measured from air collected between 35° and 50°N. For these latitudes, the equilibrium activity, as obtained after about 2 months, does not show pronounced changes when calculated with diffusion coefficients between 1 and 3×10^{10} cm^2/s. This was expected because the inflow into these boxes nearly cancels the outflow; this is in agreement with the measurements. The increased scattering of the data, as observed about 120 to 200 days after an input, is mainly due to growing statistical uncertainties. More pronounced variations in activity are expected in samples from around 70°N (decrease) and from 25°N (increase).

The data from Bombay (20°N), therefore, give the best information about meridional diffusion coefficients. As shown in Figure 9, these data range between the activities calculated from the model with a meridional diffusion coefficient of 1 and 3×10^{10} cm^2/s. These two limits are in agreement with values given by Bolin, *et* al., (1963), Reed, *et al.*, (1965), and Hartwig (1971), and values calculated from the standard deviations of the meridional wind velocities in autumn (Newell, *et al.*, 1972).

CONCENTRATIONS OF ^{37}Ar IN THE SOUTHERN HEMISPHERE

If excess ^{37}Ar activities are monitored in both northern and southern hemispheres, conclusions can be drawn about tropospheric mixing across the equator. We could obtain only a few samples collected from the southern atmosphere (Sidney, Australia and Buenos Aires, Argentina — both 35°S; see Figures 3 and 4). An upper limit (95% confidence limit) obtained from a sample collected on November 22, 1972 agrees with expected cosmic ray produced activity levels. The two samples available from Australia and Argentina from January 1972 yielded values, which are definitely above these levels, but these data are still much lower than those obtained from samples collected in the northern hemisphere on comparable dates. These two samples were also measured after enrichment in ^{37}Ar by the thermal-diffusion technique of Currie (1973). His results, with lower errors, confirm that some excess activity had been introduced. The sparcity of data from the southern hemisphere, and possible disturbances caused by other contributors to the ^{37}Ar inventory (i. e., the French surface explosion input from the stratosphere into the southern troposphere on August 14, 1971), make the derivation of a trans-equatorial mixing rate uncertain. From December until February a large Hadley cell dominates the tropical region between 30°N and 10°S (Newell, *et al.*, 1972), displacing tropospheric air masses in the lower-level troposphere from north to south. Air masses, once released from this cell of circulation into the southern troposphere, are mixed zonally, and are continuously transported southwards. Provided that no other inputs of artificially produced ^{37}Ar into the southern troposphere occurred, an observed excess activity of 0.006 dpm/l of Ar has to be explained. Assuming that the exchange across the equator essentially took place between December and the end of January, and that, by then, the mixing was completed into half of the southern troposphere, a mean trans-equatorial flux of about 9×10^{13}/g of air/s would be required. This value in comparable to the generally adopted trans-equatorial fluxes at that time of the year — namely 1.15×10^{14}g/s (Newell, *et al.*, 1969) or 2.1×10^{14}g/s (Rao, 1964).

The excess activity might also be due to the French test of August 14, 1971, on Mururoa Island (21°S), where a fusion device of 1 Mt TNT was detonated at 500 to 600 m above ground-level (press information). If half of the fusion produced neutrons escaped from the bomb device into the air, and assuming 40% of the ^{37}Ar was consequently produced by the reaction $^{36}Ar(n,\gamma)^{37}Ar$, this ^{37}Ar activity would have mixed into 75% of the southern troposphere after re-entering the troposphere in summer; therefore, an upper limit in excess ^{37}Ar of 0.0011 dpm/l of Ar may be calculated for January 1972. This is well below the measured value of 0.006 dpm/l of Ar; consequently additional contributions are required. For example, 20 g of Ca, which might be present in the mantle of the device, would necessarily have been converted by the exothermal reaction $^{40}Ca(n,\alpha)^{37}Ar$. Also, if the height of the explosion is correct, it seems possible that enough neutrons could interact with Ca in the ground soil of the test site releasing about 0.7 MCi of ^{37}Ar (corresponding to the observed excess of 0.006 dpm/l of Ar from the heated soil into the atmosphere.

Besides there still remains the possibility of explaining the two high values found in the southern hemisphere by the input of stratospheric air into the troposphere, which usually takes place during summer time. A stratospheric ^{37}Ar activity of up to 0.05 dpm/l of Ar is expected according to Lal and Peters (1967). As the two samples collected within 14 days show high values, mixing or dilution must be considered. Estimates of the ^{37}Ar activity, orginating from the stratosphere, in a well-mixed troposphere range from 0.003 to 0.006 dpm/l of Ar, depending upon various assumptions. Partially completed mixing would raise these values. Therefore, considering the activity values of (0.0078 ± 0.0006 and 0.0084 ± 0.0005 dpm/l of Ar measured by Currie, 1973), the possibility of stratospheric input cannot be ruled out.

REFERENCES

Barnes, J. W., B. P. Bayhurst, J. S. Gilmore, R. J. Prestwood, and J. P. Balagna (1973), *Measurement of the $^{40}Ca(n,\alpha)^{37}Ar$ Excitation Function*; personal communication.

Bolin, B. and C. D. Keeling (1963), *Large-Scale Atmospheric Mixing Deduced from the Seasonal and Meridional Variations of Carbon Dioxide*, J. Geophys. Res. 68, 3899 - 3920.

Bolin, B. and W. Bischof (1970), *Variations of the Carbon Dioxide Content of the Atmosphere in the Northern Hemisphere*, Tellus 22, 431 - 442.

Currie, L. A. (1973), personal communication.

Gudikson, P. H., A. W. Fairhall,, and R. J. Reed (1968), *Roles of Mean Meridional Circulation and Eddy Diffusion in the Transport of Trace Substances in the Lower Stratosphere*, J. Geophys. Res. 73, 4461 - 4473.

Hartwig, S. (1971), *Bestimmung Atmospharischer Austauschgrossen aus Konzentrationsmessungen von Spallationsprodukten*, Dissertation Universitat Freiburg, Switzerland.

Lal, D. and B. Peters (1967), *Cosmic Ray Produced Radioactivity on the Earth*, Handbuch der Physik, Vol 46/2 Springer-Verlag, 551-612.

Loosli, H. H. and H. Oeschger (1968), *Detection of ^{39}Ar in Atmospheric Argon*, Earth Plan. Sci. Letters 5, 191 - 198.

Loosli, H. H. and H. Oeschger (1969), *^{37}Ar and ^{81}Kr in the Atmosphere*, Earth Plan. Sci. Letters 7, 67 - 71.

Loosli, H. H., H. Oeschger, and W. Wiest (1970), *Argon-37, Argon-39, and Krypton-81 in the Atmosphere and Tracer Studies Based on These Isotopes*, J. Geophys. Res. 75, 2895 - 2900.

Machta, L., R. J. List, M. E. Smith, Jr., and H. Oeschger (1970), *Use of Natural Radioactivities to Estimate Large-Scale Precipitation Scavenging*, Percipitation Scavenging, U. S. Atomic Energy Commission CONF-700601, pp 465 - 474.

Machta, L. (1973), *Argon-37 as a Measure of Atmospheric Vertical Mixing*. This Proceedings.

Matuszek, J. M., C. J. Paperiello, and Ch. O. Kunz (1973), *Reactor Contributions to Atmospheric Noble Gas Radioactivity Levels*. This Proceedings.

Martin, D. (1973), personal communication.

Newell, R. E. (1963), *The General Circulation of the Atmosphere and its Effects on the Movement of Trace Substances*, J. Geophys. Res. 68, 3949 - 3962.

Newell, R. E., D. G. Vincent, and J. W. Kidson (1969), *Interhemispheric Mass Exchange from Meteorological and Trace Substance Observations*, Tellus 21, 641 - 647.

Newell, R. E., J. W. Kidson, D. G. Vincent, and G. J. Boer (1972), *The General Circulation of the Tropical Atmosphere, Vol I, MIT-Press.*

Oeschger, H. (1963), *Low-Level Counting Methods: Radioactive Dating*, International Atomic Energy Agency, Vienna, pp 13 - 34.

Oeschger, H., J. Houtermans, H. Loosli, and M. Wahlen (1970), *The Constancy of Cosmic Radiation from Isotope Studies in Meteorites and on the Earth*, in Nobel Symposium 12, Radiocarbon Variations and Absolute Chronology by I. Olsson, Ed. Almqvist and Wiksell, pp 471 - 496.

Oestlund, H. G., A. S. Mason, and A. Ydfalk (1972), *Atmospheric HT and HTO 1968-71*, in Tritium Laboratory Data Report 2, December 1972 of the University of Miami, Rosenstiel School of Marine and Atmospheric Science.

Rao, Y. P. (1964), *Interhemispheric Circulation*, Quart. J. Roy. Met. Soc. 90, 190 - 194.

Reed, R. J. and K. E. German (1965), *A Contribution to the Problem of Stratospheric Diffusion by Large-Scale Mixing*, Month Weather Rev. 93, 313 - 321.

Smith, C. F., Jr. (1971), *Project Gasbuggy: Gas Quality Analysis and Evaluation Program, Tabulation of Radiochemical and Chemical Analytical Results*, UCRL 50635 (Rev. 2) 27.

Studer, R. (1973), *Produktion von ^{37}Ar durch unterirdisch gezundete Atombomben*, Lizentiatsarbeit, Universitat Bern, Switzerland.

Teller, E., W. K. Talley, G. H. Higgins, and G. W. Johnson (1968), *The Constructive Uses of Nuclear Explosives*, McGraw-Hill. Inc., New York, N.Y.

Wiest, W. (1973), *Messung von Argon-Isotopen in Luftproben und Vergleich mit Modellrechnungen*, Dissertation, Universitat Bern, Switzerland.

TABLE 1. Characteristics of ^{37}Ar Counters.

	1-liter Plexiglas Counter with External Anticoincidence	2.8-liter Stainless Steel Counter with Internal Anticoincidence
Gas mixture	98% Ar, 2% CH_4	90% Ar, 10% CH_4
Gas pressure	up to 5.2 atm	up to 8 atm
Gas in active volume	5.3-l Ar STP	10.1-l Ar STP (9-l in anticoincidence volume)
Shielding	15 m rock, 10 cm Pb	25 cm Pb
Background (full ^{37}Ar peak region)	0.07 cpm	0.25 cpm
Efficiency of ^{37}Ar source in total volume	65.6%	34.6%

TABLE 2. Total Released ^{37}Ar Activities from Underground Explosions in Novaja Semlia.

Date of Explosion	TNT Equivalent of Explosion (from Press Information) (MT)	Released ^{37}Ar Activity (MCi)
October 14, 1969	0.2 — 1	0.7
October 14, 1970	3 — 6	1.6
September 27, 1971	2 — 4	1.6
August 28, 1972	1	1.8

TABLE 3. Measured and Estimated First Arrival Dates of Air Masses with ^{37}Ar Activity.

Place and Date of Underground Explosions	^{37}Ar Activities Measured in Samples from Bern		Estimations Based on Weather Maps		
	Reduced activity (Figures 6-8) (dpm/l Ar)	Date of separation of first sample showing increased activity.	Arrival Date	Trajectory Used	Assumptions
Novaja Semlia Oct. 14, 1970	0.26	Oct. 27, 1970	Oct. 24	North Pole-Greenland	(a)
	0.46	Nov. 2, 1970	Oct. 29 - Nov. 1	Japan - USA	(a)
Novaja Semlia Sept. 27, 1971	0.032	Oct. 12, 1971	Oct. 13 - Oct. 15	Japan USA/ North Pole	(a)
	0.67	Oct. 19, 1971	Oct. 13 Oct. 19	Sibirie-Greenland Japan USA	(b)
Amchitka Nov. 6, 1971	0.81	Nov. 16, 1971	Nov. 13 - Nov. 15	USA	(a)
Novaja Semlia Aug. 28, 1972	2.40	Sept. 12, 1971	Sept. 11 - Sept. 13	Sibirie-Greenland (USA only in second passage)	(a)
			Sept. 13	Sibirie - Canada	(a)

Assumptions on transporting winds:
(a) First 4 days by surface winds; afterwards by winds in a height of 500 mb.
(b) First 8 days by surface winds; afterwards by winds in a height of 500 mb.

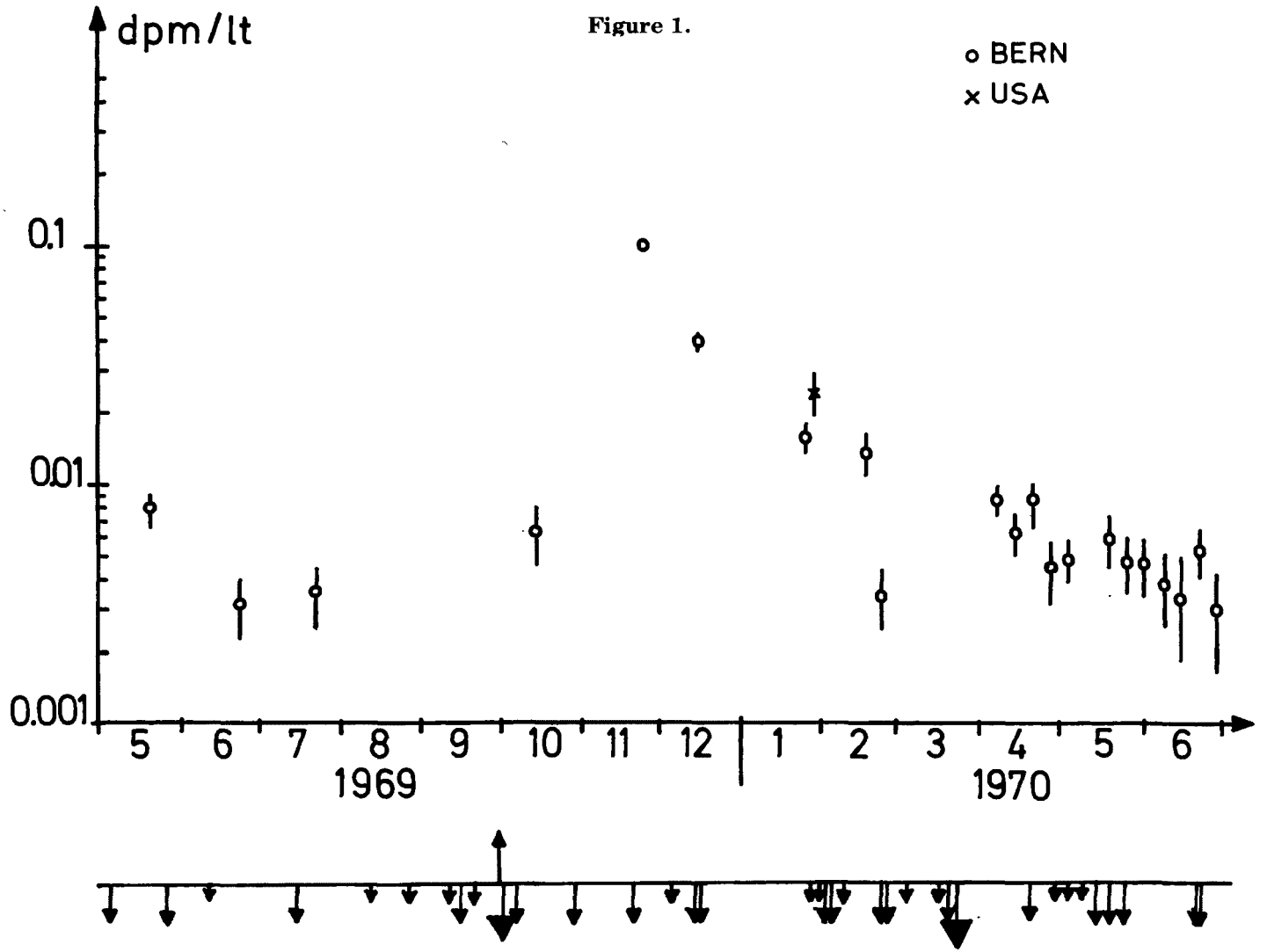

Figures 1 through 4. ^{37}Ar activities measured on argon samples collected at different locations from ground-level air for the period 1969 to 1973 are given as a function of collection dates. Large fluctuations are observed with peak values in autumns. Low-values around 2.5 x 10^{-3} dpm $^{37}Ar/l$ of Ar are representative for cosmic ray produced activity found near ground-level after atmospheric mixing. High-activities of up to 1.8 dpm/l of Ar are due to underground nuclear explosions. The arrows (length of arrows indicating the power of the bombs in a logarithmic scale) show the dates of nuclear explosions in the atmosphere (above the line) and underground (below the line).

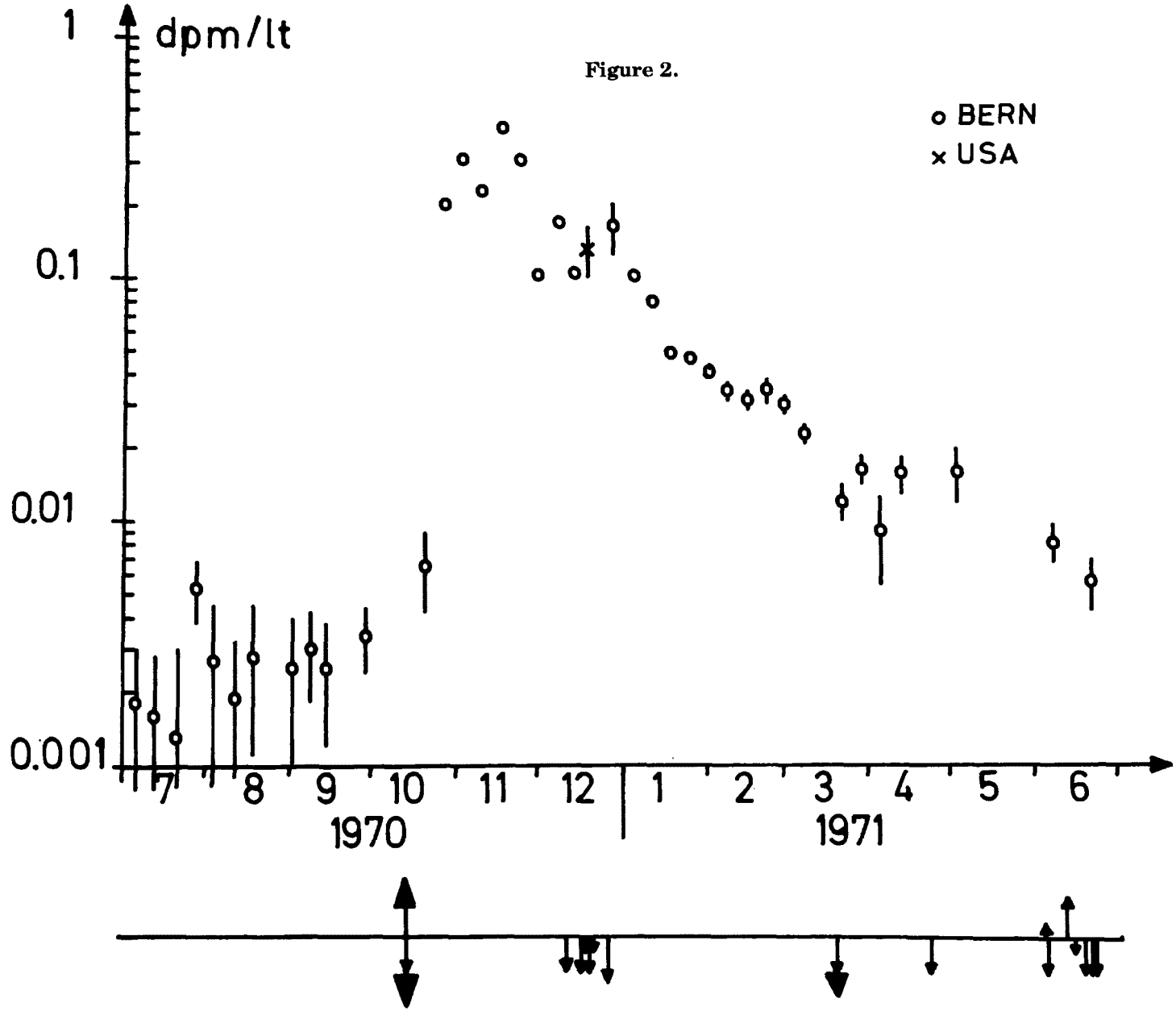

Figure 2.

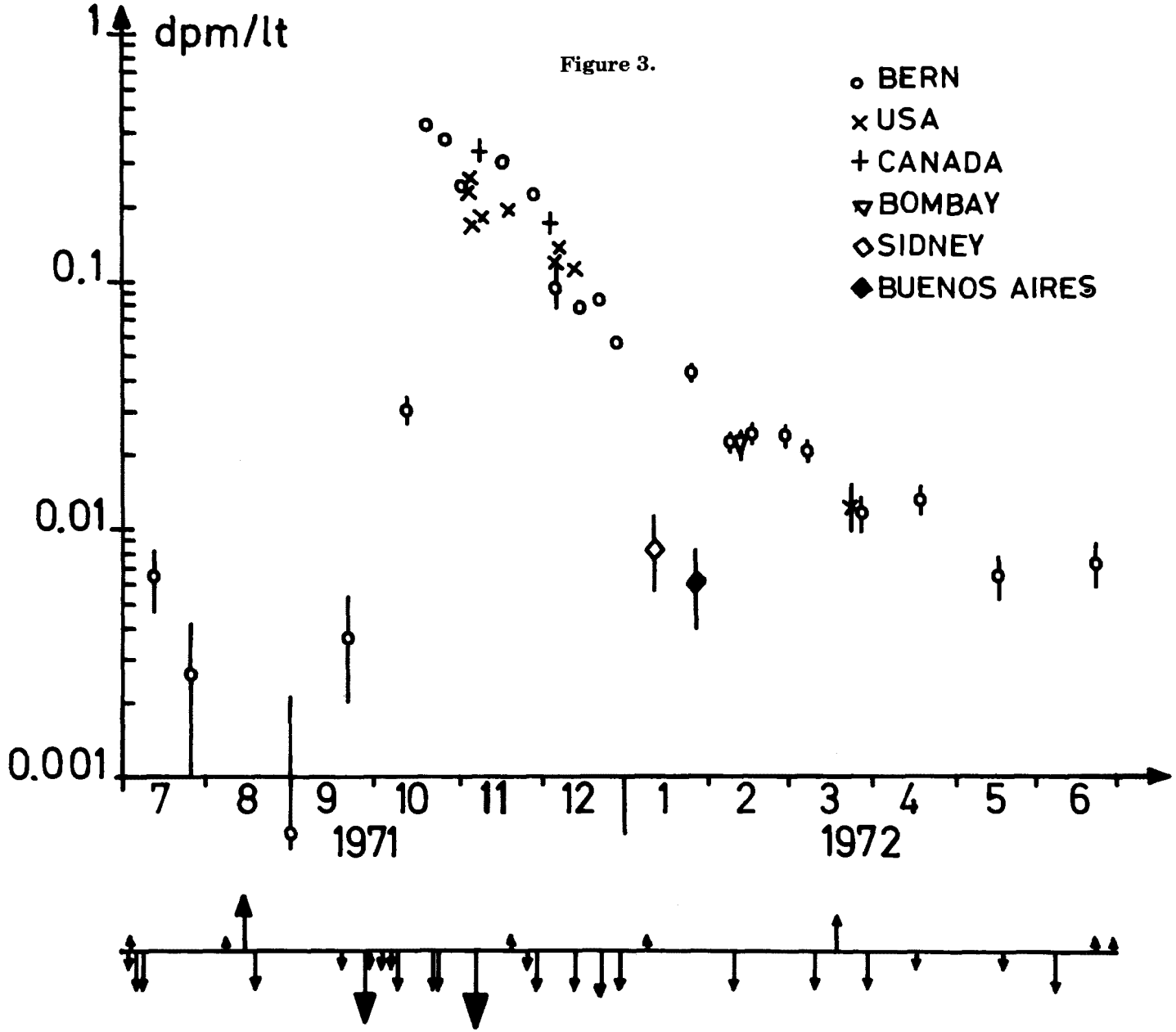
dpm/lt
1
0.1
0.01
0.001
BERN
USA
CANADA
BOMBAY
SIDNEY
BUENOS AIRES
7
8
9
10
11
12
1
2
3
4
5
6
1971
1972

Figure 3.

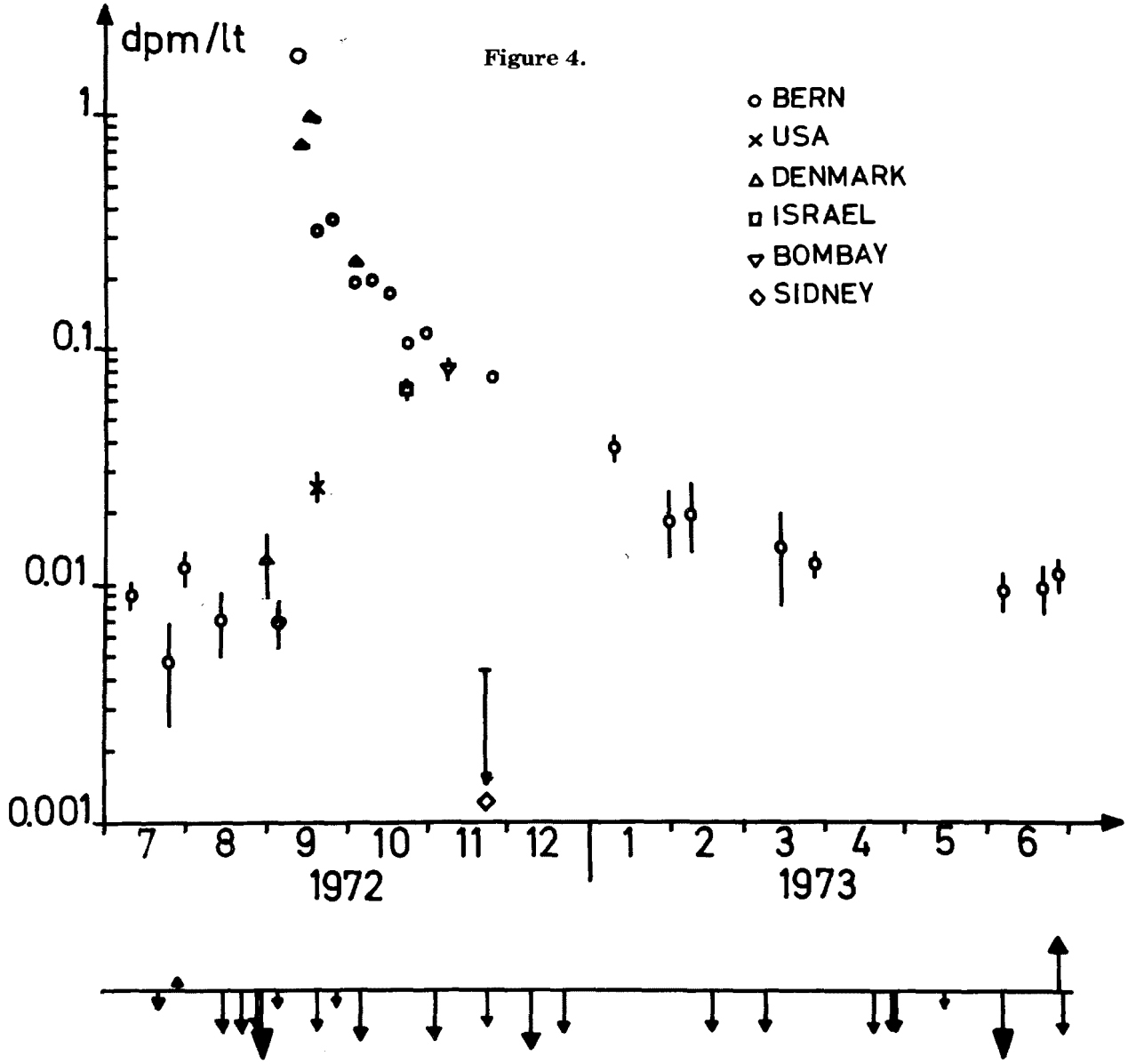
dpm/lt
1
0.1
0.01
0.001
7
8
9
10
11
12
1
2
3
4
5
6
1972
1973
BERN
USA
DENMARK
ISRAEL
BOMBAY
SIDNEY

Figure 4.

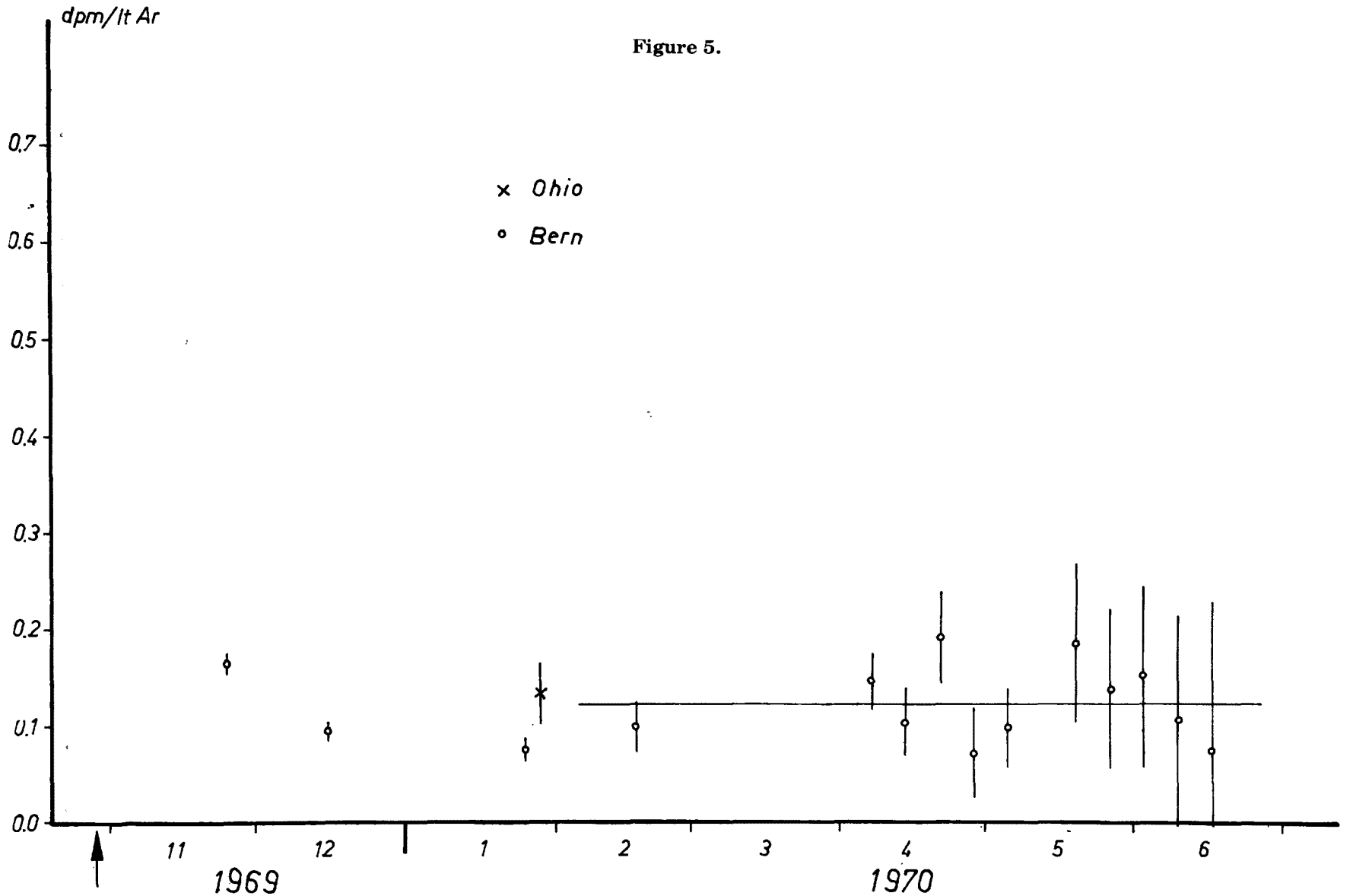

Figures 5 through 8. The activity data (from Figures 1 through 4) are presented after a cosmic ray produced contribution of 0.0025 dpm/l of Ar was subtracted and a correction for radioactive decay to the most probable date of explosion was made. Weighted average values for the excess ^{37}Ar activity in a well-mixed northern troposphere are indicated by a horizontal line.

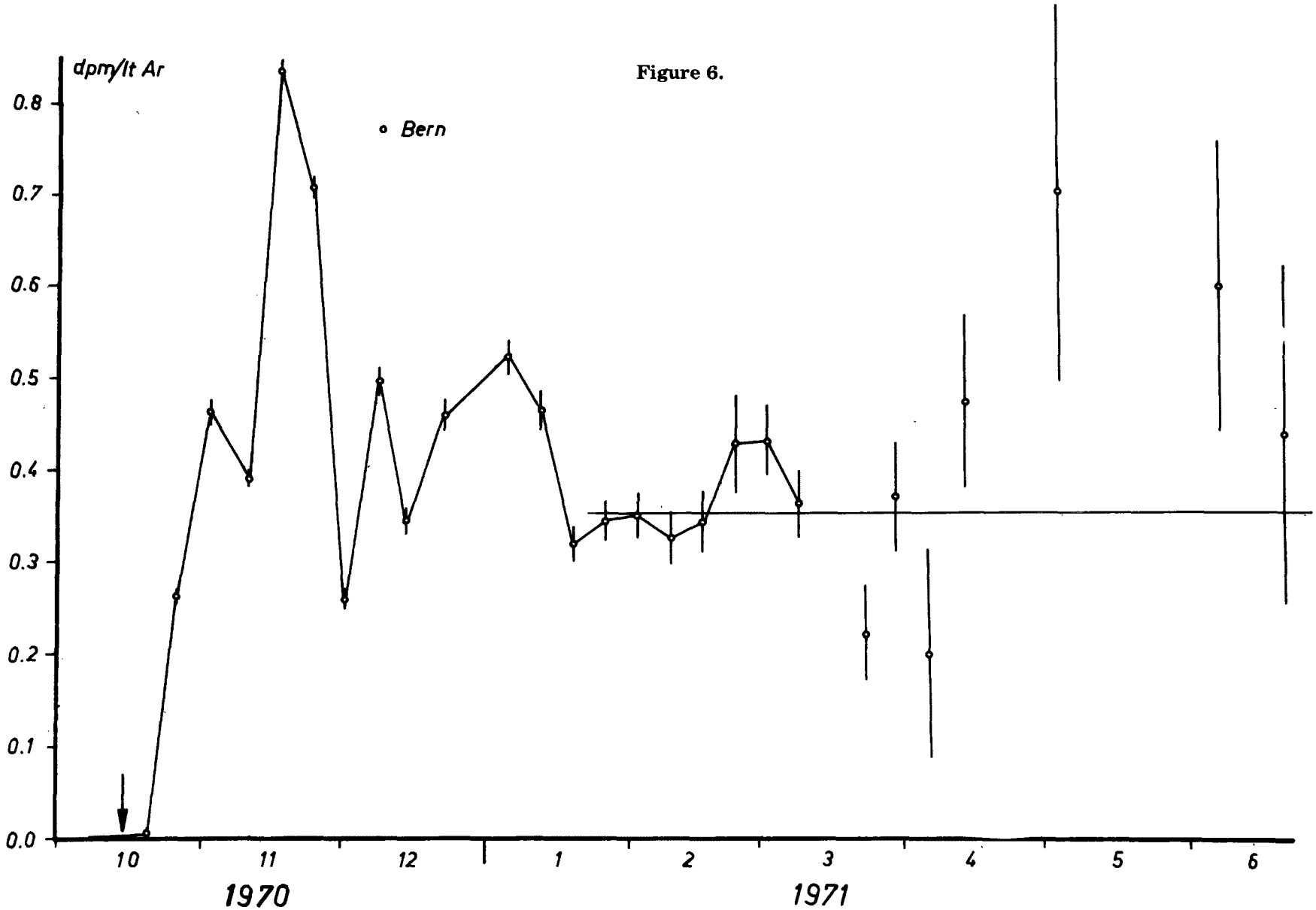

Figure 6.

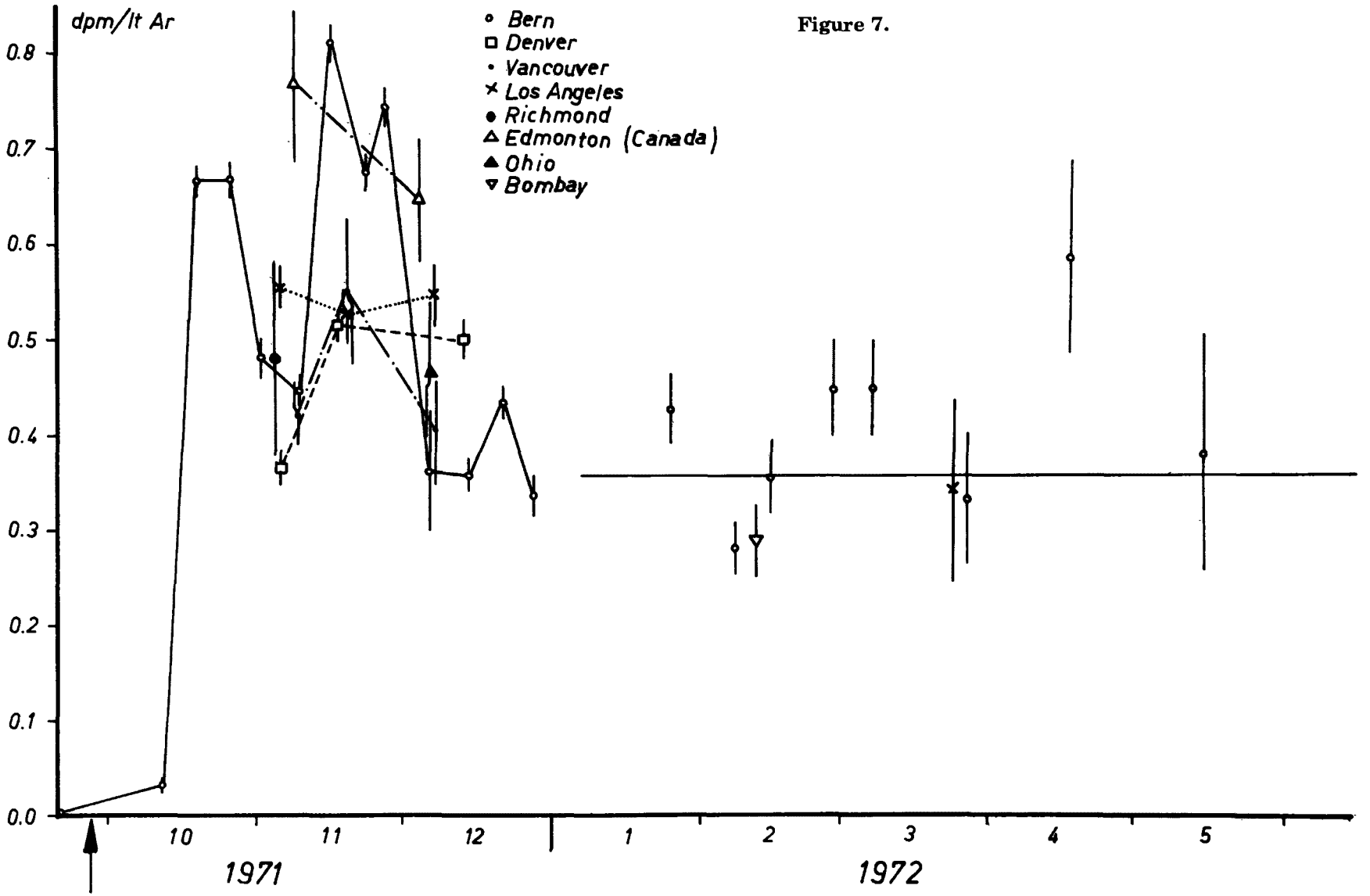
dpm/lt Ar
0.8
0.7
0.6
0.5
0.4
0.3
0.2
0.1
0.0
Bern
Denver
Vancouver
Los Angeles
Richmond
Edmonton (Canada)
Ohio
Bombay
10
11
12
1
2
3
4
5
1971
1972

Figure 7.

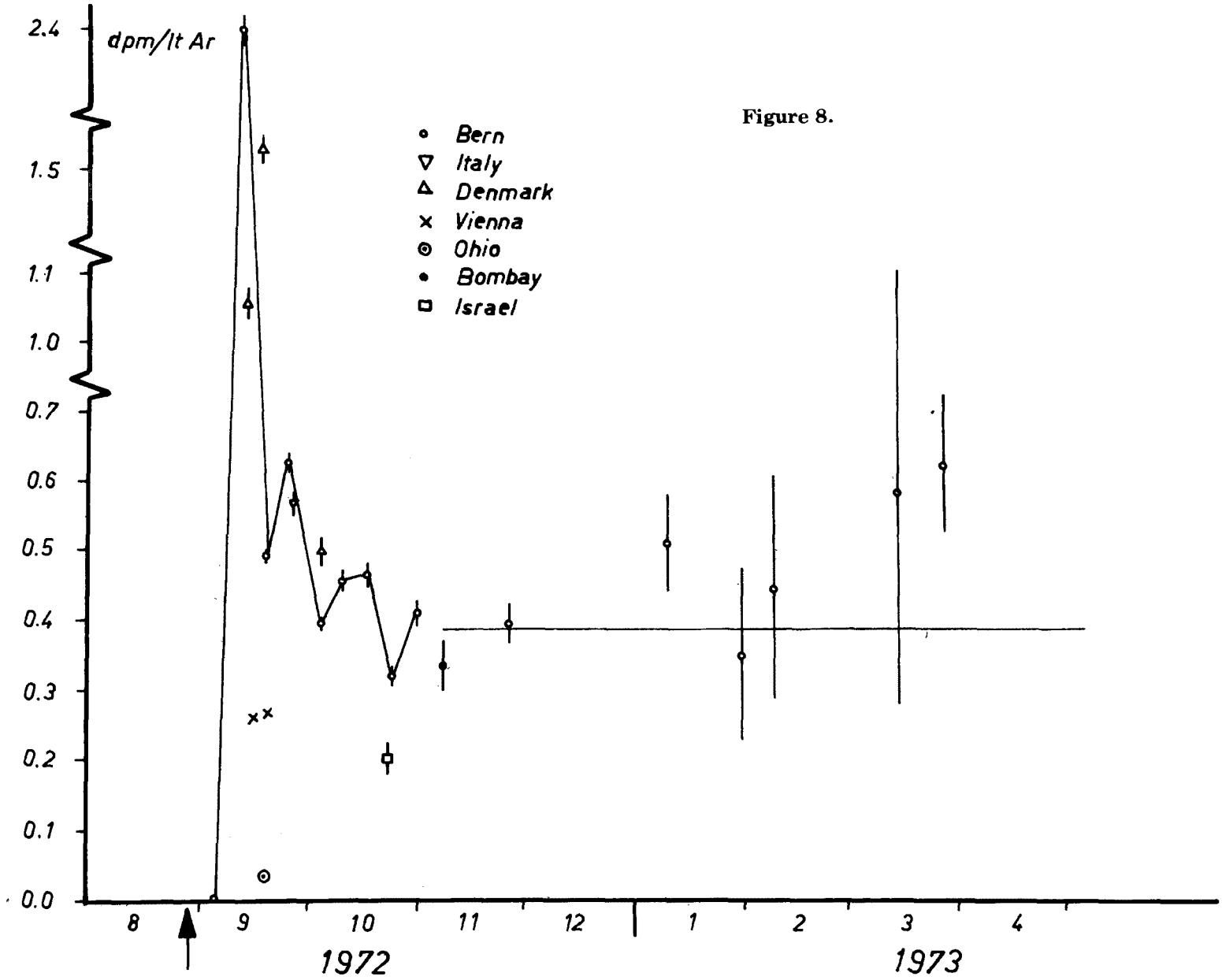
dpm/lt Ar
2.4
1.5
1.1
1.0
0.7
0.6
0.5
0.4
0.3
0.2
0.1
0.0
Bern
Italy
Denmark
Vienna
Ohio
Bombay
Israel
8
9
10
11
12
1
2
3
4
1972
1973

Figure 8.

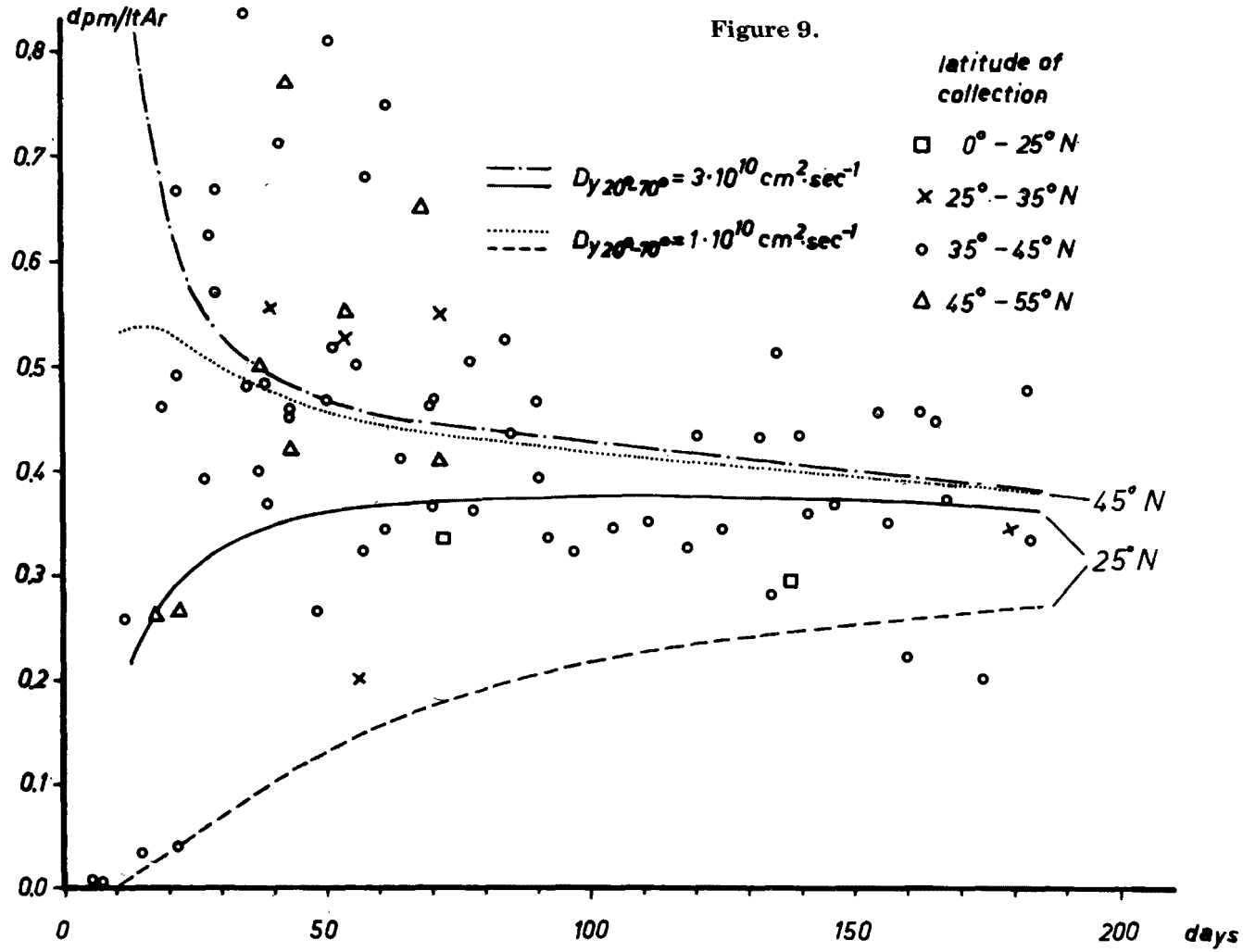

Figure 9. All data given in Figures 6 through 8 are summarized, with different symbols denoting the range in latitude from which the samples are collected. The activity distribution, as a function of time following a 1.6 MCi ^{37}Ar input at 75°N, is shown as obtained by the box-model calculation for two latitudes and two sets of meridional diffusion coefficients (assumed to be constant between 20°N and 70°N). The meridional diffusion coefficients are decreasing from 1 x 10^{10} cm^2s^{-1} at 20°N to 10^8 cm^2s^{-1} at the equator. Vertical diffusion coefficients are between 1 and 5 x 10^5 cm^2s^{-1} in the troposphere, decreasing to a value of 4 x 10^3 cm^2s^{-1} towards the stratosphere. The best fits to the experimental data for the time of 2 months after an explosion are obtained with average meridional diffusion coefficients between 1 and 3 x 10^{10} cm^2s^{-1}.

THE NBS MEASUREMENT SYSTEM FOR NATURAL ARGON-37

L. A. Currie and R. M. Lindstrom
Analytical Chemistry Division
National Bureau of Standards
Washington, D. C. 20234

ACKNOWLEDGEMENTS

Several of the sample purification and counting techniques that we adopted were based upon earlier work of R. Davis, Jr., R. W. Stoenner, J. C. Evans, V. Radeka and L. C. Rogers of Brookhaven National Laboratory. Cooperation in sampling and counting with H. H. Loosli and H. Oeschger of the University of Bern has been continual. We are grateful to L. Machta (National Oceanographic and Atmospheric Agency) for providing stratospheric samples and for numerous helpful discussions. W. Roos and R. Schwind at Mound Laboratory performed the isotopic enrichments, with important contributions from W. Rutherford. The stratospheric sample (Table 2) was purified by D. Martin of Teledyne/Isotopes, Inc. Computer programs were written by J. Travis, J. Wing, P. Shoenfeld, and J. Barkley of NBS. Assistance from J. R. DeVoe, J. Matwey and J. J. Filliben, also of NBS, is appreciated. The fine-ground calcium carbide was kindly provided by G. Porter of Union Carbide. Support by the Advanced Research Project Agency and the Air Force Technical Applications Center of the Department of Defense is gratefully acknowledged.

Abstract

A project to determine the cosmic-ray production rate and the natural levels of 35-day half-life ^{37}Ar in the atmosphere has been underway at the National Bureau of Standards for about the past year. The prime objective of this project is to determine the spatial dependence of ^{37}Ar production in the atmosphere, and the spatial distribution of the naturally-produced ^{37}Ar (observed concentrations). The results of this study are to be used, in cooperation with L. Machta (National Oceanographic and Atmospheric Administration), to derive information about atmospheric mixing. The purpose of this communication, however, is to present a general description of the various components of the measurement system.

As the lowest concentrations of interest are but $\cong 10^{-3}$ dpm (^{37}Ar)/l-Ar, very high sensitivity measurement techniques are required. Among the techniques which we have adopted are: quantitative separation of the noble gases from about 1 m^3 of air, using a CaC_2 reactor; gas chromatographic separation of the argon fraction; isotopic enrichment (by a factor of $\cong$ 100) of purified argon; use of specially selected low-level gas proportional counters together with massive shielding and anticoincidence meson cancellation; and the application of pulse discrimination based upon both amplitude (energy) and pulse shape. Finally, on-line computer techniques are being applied for data acquisition and system control.

INTRODUCTION AND SUMMARY

1. Program Aims and Requirements.

A detailed study of the natural occurrence and production of ^{37}Ar has been undertaken in our laboratory in order to provide experimental data from which atmospheric mixing parameters may be deduced. ^{37}Ar is a most suitable nuclide for the purpose, as it is produced — through the nuclear interactions of cosmic rays with atmospheric argon — with a pronounced vertical gradient; its mean life (50.6 days) is quite appropriate for the study of atmospheric transport phenomena; and its chemical nobility obviates model complications arising from processes such as rainout, fallout, chemical reaction, and exchange among reservoirs. A number of excellent discussions of ^{37}Ar in the atmosphere and its application to the study of air transport — particularly, vertical mixing of the troposphere — may be found in the recent literature (Loosli, *et al.*, 1973; Machta, 1973; Machta, *et al.*, 1970; Oeschger, *et al.*, 1970; Schell, 1970; and Wiest, 1973).

The quantitative connection between cosmic ray production and atmospheric concentrations of ^{37}Ar and stratospheric and tropospheric mixing processes, has been clearly set forth in the steady-state model of Machta (1973). A principal result of the model is that, given the absolute production profile of ^{37}Ar in the atmosphere, one can derive important information about tropospheric mixing from the determination of the ground-level concentration of the nuclide. The sensitivity and accuracy requirements for the determination of this ground-level ^{37}Ar are those to which our measurement facilities must be matched. The approximate magnitude of the naturally-produced, ground-level ^{37}Ar concentration ($\cong$ 0.0025 dpm/l-Ar) may be deduced from the data of Loosli, *et al.*, (1973), based upon experiments which took place during the periods which were relatively free from contamination. (Calculated concentrations may be derived from theoretical ^{37}Ar production rates given by Oeschger, *et al.*, [1970], and by Lal and Peters, [1967].) Although the calculated values are more or less consistent with the experiments, the theoretical production rates include quite large uncertainties. The accuracy with which the ground-level ^{37}Ar concentrations ought to be determined (~10%, relative error) obtains from Machta's (1973) vertical diffusion model. This accuracy requirement follows from the fact that the relative uncertainty of the derived vertical, tropospheric diffusion coefficient will be approximately equal to that of the measured ground-level ^{37}Ar concentration.

The few experimental results which have been included (in order to illustrate our measurement process) touch upon the major facets of our study. The cosmic ray production rate of ^{37}Ar in the atmosphere may be derived from either (1) measured cross sections of the contributing nuclear reactions, or (2) the observed rate of production in a captive or non-mixing sample. The ^{37}Ar sample whose spectrum is shown in Figure 3 arose in our measurement of the $^{40}Ar(p,X)^{37}Ar$ cross section with 200 MeV protons; whereas the measurement of the stratospheric samples (Table 2) may permit us to determine the production rate (at a given point) directly. The other aspect of the study — sampling of tropospheric argon to determine the mixed ^{37}Ar concentrations — led to the sample from Brazil (Figure 8) which was involved in our examination of individual counting events. (Approximate values obtained for the cross section, and the stratospheric and surface ^{37}Ar concentrations were 13 mb, and 0.03 dpm/l -Ar and 0.01 dpm/l -Ar, respectively.)

2. ^{37}Ar Measurement System.

Although our principal concern is with the determination of the absolute cosmic-ray production rate of ^{37}Ar in the atmosphere, as well as the natural concentration variations with altitude, latitude, season and solar activity, the present discussion is limited to the measurement system which was devised to determine those natural concentrations. As noted above, our measurement system should be capable of determining ^{37}Ar at a level of $\sim$ 0.0025 dpm/l Ar with a relative error of $\lesssim$ 10%. A detailed analysis of the sensitivity requirements of the overall measurement process has been prepared by Rutherford, *et al.*, (1974), for a range of counting times and counter backgrounds. It is of interest now to carry out a similar analysis for the existing measurement system at NBS using the above ^{37}Ar radioactive concentration (0.0025 dpm/l-Ar), and assuming a counting period of one week. (More information concerning notation and the evaluation of detection and quantitation limits, is given in Currie [1972].) Using our most sensitive counter (background rate ~ 0.02 cpm), considering only Poisson counting errors, and assuming a delay between sample collection and counting of two weeks, we conclude that for quantitation the effective sample volume ($V_{eff} = [VI]_Q$) must be 16.0 liters. (V here refers to the final argon volume [STP]; I, to the ^{37}Ar isotopic enrichment factor; and the subscript Q, to the fact that the measurement is quantitative — i. e., having a relative standard deviation of 10%.)

The foregoing result may now be examined in the light of the enrichment factors actually obtained for us during the last several months by the Mound Laboratory (Roos, 1973). Typically, I_Q has been approximately 100, and V_Q is therefore ~0.16 l. The final volumes available, however, have ranged as high as 0.75 l, and therefore the minimum required effective volume was well exceeded. Despite the consequent improvement in counting precision, the overall accuracy may not be better than 10%; the relative uncertainty in the enrichment factor, itself, may sometimes be as large as 10%. Assuming ,for example, that V_{eff} =50 l, and combining relative errors from counting, and enrichment in quadrature, we calculate an overall uncertainty of $\sim$11%. It may be noted, in passing, that the volume of the feed material for enrichment by thermal diffusion (pre-enrichment volume) has been typically $\sim$200 liters. For high-level argon samples — those not requiring enrichment — the calculated quantitative determination limit (Σ_Q^o) is found to be 0.044 dpm/l-Ar for our particular measurement system.

In the following text, we discuss the means for separating and purifying atmospheric argon, and the instrumentation and computational methods for determining its ^{37}Ar content. The possibility of measuring the very low, natural concentrations of ground-level ^{37}Ar rests upon two factors: (1) the ability to separate from the atmosphere and isotopically enrich large volumes of argon; and (2) the availability of stable, low-background proportional counters. The counting requirement is being met through the use of specially constructed counters, low-level counting techniques — including pulse-shape analysis, and a stability control scheme involving the use of an on-line computer. A convenient chemical method, based upon reactions with CaC_2, was employed for the separation of argon from moderate quantities of air ($\lesssim$1000 l.). The method, to be described in the next section, is attractive in terms of cost, simplicity, speed, and non-fractionation of the noble gases.

ARGON SEPARATION AND PURIFICATION

The large volumes of argon (some 200 liters) required as feed material for isotopic enrichment are obtained from commercial air rectification plants. Sampling from the crude-argon drawoff from the still, or from intermediate holding tanks (with volumes small compared to the daily production) insures that the sample's date of separation from the tropospheric reservoir is well defined. Samples are air shipped directly to the Mound Laboratory for enrichment.

The enrichment process is described in Rutherford, *et al.*, (1974). A series-parallel cascade of thermal diffusion columns is used, designed for rapid initial transport of the light fraction, and high enrichment factors with little holdup in the product reservoir. Enrichment of ^{37}Ar specific activity by a factor of >70 requires one week, which is acceptably short compared with its half-life.

In some cases, as with stratospheric samples, the separation of argon from air must be done in the laboratory. For this particular case, isotopic enrichment is not necessary, and the sample size required is 10 l of argon, or 1 m^3 of air. We chose to employ chemical rather than physical means for the separation. Calcium

carbide at high temperature has been shown to be an effective reagent for separating noble gases from air on this scale of volume (Fischer and Ringe, 1908). The reactions are

$$N_2 + CaC_2 \rightarrow CaCN_2 + C$$

$$O_2 + 2CaC_2 \rightarrow 2CaO + 4C$$

Both reactions are exothermic. Atmospheric CO_2 is reduced to C, so all major constituents of dry air form nonvolatile solids except for the noble gases.

A diagram of the apparatus is shown in Figure 1. The carbide reactor is constructed of 6-inch (diameter) Inconel tubing welded to an 8-inch (diameter) stainless steel vacuum flange. Most of the rest of the system is made of copper tubing with bellows-sealed brass valves. The circulating pump is a 1/3 hp refrigerator compressor.

Air enters slowly from the sample cylinder through a flow meter and molecular sieve dryer, then flows downward through a bed of finely-divided CaC_2 at 800°C. Effluent gas passes through hot CuO to oxidize H_2 and hydrocarbons. The resulting water is removed downstream with a dry ice trap, beyond which the crude product passes to a 50-liter buffer volume. After all of the sample has passed once through the carbide reactor, the inlet valve is shut off and the gases are circulated through the system by a pump until there are no further changes in pressure.

The processing of a sample of 320 liters of air proceeded as follows:

A charge of 2.5 kg of carbide was degassed with continuous pumping, while heating the reactor to the operating temperature. Large quantities of low molecular weight gas were evolved. After pumping overnight at 800°C the reactor was deemed sufficiently well degassed, and admission of the air sample was begun.

Both major reactions are exothermic, and the rate of at least the nitrogenation reaction increases with temperature. Indeed, in the industrial production of cyanamide, heat is applied only to bring the carbide to ignition temperature (Kastens and McBurney, 1951). In order to minimize local overheating, the reaction is controlled by admitting the sample at a moderate rate. A reaction of 1 liter of air per minute liberates 350 watts; thus, 300 liters of sample was bled into the system over a 4-hour period. Although industrial production of cyanamide employs a flux of CaF_2 or CaC_{12} mixed with the carbide charge, the finely ground carbide employed here (about 13μm surface-equivalent diameter), results in a reaction rate sufficiently high at 800°C with no flux.

The experiment reported here gave a production composition of 84% Ar, 8.6% H_2, 6.3% N_2, and 0.9% O_2. Since the process operates within a closed system, the yield of all the noble gases is quantitative, as was confirmed in the present experiment by measurements of the volumes of product and reactant gases. Earlier, smaller-scale experiments gave purities as high as 99.5% Ar.

The crude noble gas mixture from the carbide system is further purified by contact with titanium cooling from 800°C to room temperature. (Momyer, 1960). Hot titanium forms oxide, nitride and carbide with most reactive gases, while the hydride forms quantitatively on cooling. (This step is also applied to enriched samples, some of which have contained tritium.) The purified mixture of noble gases is then separated by gas chromatography on an activated charcoal column at -30°C to -20°C, using He as the carrier gas.

The pure argon sample from the titanium furnace or the gas chromatograph is collected on a cold trap or with an automatic Toepler pump, methane is added to make a pressure of 0.10 atmosphere in the counter, and the gases are transferred to the evacuated counter for measurement.

MEASUREMENT OF ^{37}Ar

1. Instrumentation and Detectors.

Because of the decay mode of ^{37}Ar (electron capture, releasing the 2.82 keV K-electron-binding energy, and a 35.1 day half-life), and because of its physical state (gaseous), a most effective and sensitive means of measurement is the use of low-level gas proportional counters with anti-coincidence shielding, together with energy and pulse-shape discrimination. As specific activity (rather than total activity) is generally limiting, it is desirable to count as large an effective volume of argon as feasible in as small a counter as feasible. Effective volume increases may be brought about by increased sample pressure (Oeschger, *et al.*, 1970; and Schell, 1970) and/or by means of isotopic enrichment (Rutherford, *et al.*, 1974). Because of these alternatives, we have available counters of various sizes as shown in Table 1.

The two Delrin counters are of a design originated by H. H. Loosli, W. Wiest and H. Oeschger. The 1 cm thickness of the Delrin walls permits operation at a pressure of several atmospheres. Cathodes are of aluminized Mylar foil kindly provided by M. A. Geyh. Degassing of the plastics is not troublesome until a week or more after filling. Calibration is accomplished by external X-ray sources, in the larger counter through a 1 mm thick window machined in the wall. The silica counter, based on designs by R. Davis, Jr., and F. H. Kummer at Brookhaven, consists of a cylinder of 0.025-cm Fe foil in a quartz envelope. This counter is operated at atmospheric pressure. Energy calibration is accomplished by exciting the Fe K-fluorescence X-ray with an external ^{241}Am source. Long-term stability is very good, and the counter may be thoroughly degassed

by baking in a vacuum. The Oeschger counter (Houtermans and Oeschger, 1955) constructed in Bern, is of stainless steel with an aluminized Mylar foil separating the central counting volume from the integral anticoincidence assembly. It is used for large volume unenriched samples.

Four means of discrimination have been employed in order to select ^{37}Ar disintegrations from other types of events due to environmental γ-radiation, penetrating cosmic rays (μ- mesons), radioactive contamination in the counter or sample, and electrical noise. First, we applied the conventional low-level techniques involving anticoincidence counting and massive shielding. Next, proportional counter spectrometry was used to delimit those events whose energy deposition was consistent with the 2.8 keV K-electron binding energy which is released following the (K-) electron capture of ^{37}Ar. Finally, the application of pulse shape discrimination, as described by Davis, *et al.*, (1972) was utilized to distinguish localized events from extended ones within the counter. (See also Culhane and Fabian, 1972).

The effectiveness of pulse shape discrimination in reducing background derives from the fact that, for a given total energy deposition (E) in the counting volume, the initial ion pairs are far more localized when the primary particles (β's photoelectrons, Auger electrons) have low energy than when they possess high energy (high energy β's, muons, Compton electrons) and, therefore, lower ionization density. Secondary electrons from short track length (localized) events tend to approach the anode together and produce a single, very fast avalanche; electrons from extended events, however, drift from different regions of the counting volume, and, therefore, produce a series of avalanches, distributed in time. The system designed by V. Radeka (Brookhaven National Laboratory) discriminates against extended events by using fast electronics to derive a quantity ADP (Amplitude of the Differentiated Pulse) which is proportional to the charge reaching the anode within the first 10 ns. The ratio ADP/E therefore approaches a maximum, relatively independent of energy, for short-range events, because a larger fraction of the total energy is contained in the initial portion of the pulse.

A schematic diagram of the measurement system is shown in Figure 2, where the dashed pulse shape indicates that an extended (γ) event will generally produce a smaller ADP-pulse than a localized (X) event when their E pulses are equal. Certain types of electronic noise may be further distinguished either by unusually large ADP/E or by an early peaking of the E-pulse.

We currently employ three different systems for the analysis of the ADP and E pulses. The first uses an analog divider, whose output is proportional to the ratio ADP/E, in conjunction with a modified single-channel analyzer to route E pulses into one of three quadrants of a 400-channel analyzer for ADP/E below, within, or above the selected window. The fourth quadrant stores the pulses coincident with the guard (μ mesons), as shown in Figure 3. (The spectrum appearing in Figure 3 was actually derived from ^{37}Ar produced by high-energy proton bombardment of gaseous argon. We are undertaking such bombardments in order to measure the nuclear cross sections for the reactions producing ^{37}Ar in the atmosphere.)

The second mode of analysis utilizes a dual-parameter analyzer to accumulate ADP vs E in a two-dimensional array. Calibration is easier with this system; a further procedural advantage is that the (ADP,E) window selected for integration of the ^{37}Ar signal may be chosen in light of calibration spectra both preceding and following a sample spectrum. Very much more analyzer or computer storage space is required, however. Figure 4a shows an Fe-fluorescence X-ray spectrum. As can be seen, the X-rays fall along a narrow band near the diagonal. Figure 4b shows a background spectrum. As can be seen, discrimination is considerable, amounting to a factor of 3 background reduction in this example.

The most recent addition to our counting system makes it possible for us to operate four central counters (plus guard counters) simultaneously. In this sytem, signals (ADP,E) are digitized and transferred directly to a data acquisition computer. Accompanying information includes counter identification, pulse occurrence time, and coincidence data. Figure 5 is a photograph of this system; the row of indicator lights permits the qualitative monitoring of guard and sample counters, and the 4 "write" switches make it possible to test or adjust one or more of the counters while continuing to transmit data from the remaining ones. Besides provided the possibility of counting multiple samples — so important for very lengthy counting of low-level samples — this system gives us the possibility of searching for unanticipated coincidences and time correlations. Also, by means of an associated pulser, it permits the continual monitoring of electronic stability. Counter stability, on the other hand, is assessed periodically by examination of the ADP and E signals from an X-ray calibration source, such as ^{55}Fe.

Data acquisition and computations are performed with the aid of the Analytical Chemistry Division computer utility which comprises an EMR 6135 CPU with 2 M words of disc storage, and a teleprocessor with a digital data bus (serving our laboratory and nine others). Data collected in the multi-channel analyzers are read manually or automatically into the computer; time of year and barometric pressure are recorded, and the spectrum files are stored on archive magnetic tape.

2. Data Presentation and Interpretation.

The partitioning of events in ADP-E space may be seen by referring to Figure 6. A relatively narrow band along the diagonal — set to $\sim 45°$ by means of amplifier gain adjustments — contains localized events (X) such as those due to X-ray or Auger electron emission. Only very occasional pulses, due to electronic noise, are found with higher values of ADP/E. Extended tracks (γ) lead to smaller values of ADP/E, and these fall primarily below the X-ray band. For the measurement of ^{37}Ar we are particularly interested in the intersection of the X-ray band with the appropriate energy region — indicated by dotted lines — for the decay of ^{37}Ar ($\sim$2.8 keV) by K-capture.

Counts (Y_I) accumulated within the intersection region as well as those outside (Y_O), but of proper energy, are of interest in calculating the ^{37}Ar activity. Also of interest are counts above the X-ray band, the total anticoincidence counts and the total coincidence (muon) counts. A typical computer summary for the 1.4-liter counter background is given in Figure 7. The data were obtained with the analog divider - 400 channel analyzer combination operating in the recycle mode. In addition to the various counting data noted above, the summary includes time of year and barometric pressure information as well as the rejection ratio, which is a measure of background reduction due to pulse shape discrimination. For this particular example, it may be noted that E- and ADP- constraints reduce the background by almost a factor of 200 as compared to the gross anticoincidence background. For extended counting periods, which are required for the lowest level samples, replicate measurements plus a systematic control program may be applied for the periodic monitoring of the foregoing counting data and the rejection ratio as a function of time and barometric pressure.

For the estimation of net (^{37}Ar) signals from the two dimensional data, we use three alternative methods of analysis. The first and simplest is based upon the observation of gross counts (Y_I) and background counts (Y_{IB}) in the ADP-E window as indicated in the following:

$$\underline{^{37}Ar \text{ - window}}$$

$$Y_I = S_I + B_I + e_I \qquad (1a)$$

$$Y_{IB} = B_{I/\kappa} + e_{IB} \qquad (1b)$$

$$\hat{S}_I = Y_I - \kappa Y_{IB}; \quad \sigma_{\hat{S}_I} = (Y_I + \kappa^2 Y_{IB})^{1/2}$$

Y, S, and B refer to gross, sample (^{37}Ar) and background counts; e, to a random (Poisson) error; and, κ, the ratio of sample/background counting times. The second method, which offers improved precision, uses also the counts outside the X-ray band (Y_o) as follows:

$$\underline{\text{Rejection Ratio}}$$

$$Y_I = S\alpha_I + B\beta_I + e_I \qquad (2a)$$

$$Y_o = S\alpha_o + B\beta_o + e_o \qquad (2b)$$

The above equations are readily solved for $\hat{S}$ and $\sigma_{\hat{S}}$ but the vectors $\underset{\sim}{\alpha}$ and $\underset{\sim}{\beta}$ must be known. Note that S_I and B_I (Eq. 1a) are equivalent to $S\alpha_I$ and $B\beta_I$ (Eq. 2a), respectively. Solution of the simultaneous equations, including propagation of counting errors yields,

$$\hat{S} = (\beta_o Y_I - \beta_I Y_o)/D$$

$$\sigma_{\hat{S}} = (\beta_o^2 Y_I + \beta_I^2 Y_o)^{1/2}/D$$

where,

$$D = \beta_o \alpha_I - \beta_I \alpha_o$$

$\frac{\beta_o}{\beta_I + \beta_o} = \beta_o$ is just the rejection ratio (fraction of the background counts lying outside the ^{37}Ar window); and

$\frac{\alpha_I}{\alpha_I + \alpha_o} = \alpha_I$ the acceptance ratio (fraction of the ^{37}Ar events lying inside the window). (Note that $\Sigma\alpha$ and $\Sigma\beta$ have been normalized to unity.) Use of this second mode of calculation is attractive, but dangerous. More information is used (Y_o, $\underset{\sim}{\alpha}$ and $\underset{\sim}{\beta}$) and hence, the estimate ($\hat{S}$) is more precise. Also, a separate background measurement is not involved, so measurement time is saved; and the background amplitude (B) is determined in real time — i. e., B refers to the same counting period and counting system as does S. The danger lies in the fact that systematic errors in the basis vectors ($\underset{\sim}{\alpha}, \underset{\sim}{\beta}$) can vitiate results without adequate warning,

as there are no spare degress of freedom. Perhaps the most likely sort of model error is that due to contamination. For example, we recently discovered a small amount of tritium in one of our low-level counters. Under these circumstances, the use of the vector $\underset{\sim}{\beta}$ as above is quite incorrect. In fact, tritium is one of the most severe contaminants for ^{37}Ar counting, because pulse shape discrimination does not distinguish between the low energy tritium β^- pulses and the X-ray pulses. (A few dpm of ^{3}H in our quartz counter required thorough decontamination of the iron cathode, before the counter could be re-used successfully for low-level ^{37}Ar measurements.)

The most general method of analysis, which possesses the advantages of the preceding two, requires least-squares fitting of the entire ADP-E-time surface, using the observations,

$$\underset{\sim}{Y} = S\underset{\sim}{\alpha} + B\underset{\sim}{\beta} + \underset{\sim}{e} \qquad (3)$$

That is, the two-valued (in/out) vectors above are now generalized to cover the entire space of interest. Besides giving maximum precision, this approach provides protection against model errors because of many degrees of freedom which can be used for χ^2-testing, for example. The least-squares analysis is not without difficulties, particularly if the counting rates are very low, but further discussion of such problems will not be given here.

The advantages and limitations of the "^{37}Ar-window" and "rejection ratio" methods may be illustrated by our first measurement of ^{37}Ar from a stratospheric air sample. Measurements of this type of sample are particularly important with respect to our overall objectives, for they can provide basic information about the cosmic-ray production rate of ^{37}Ar. The sample in question was collected on 2 February 1973 at an altitude of 15.5 km over the southwestern United States. Because of delays in transport plus many difficulties with counters and electronics, the sample became a very low-level sample by the time we were able to measure it.

The counting data from the stratospheric sample are given in Table 2, together with deduced ^{37}Ar concentrations and their standard deviations. Look first at the relative precision and counting times required for the two approaches. The rejection-ratio approach yields an improvement in precision which is equivalent to an increase in counting time by a factor of $(0.021/0.017)^2 \sim 1.5$; also, it requires no separate background measurement. If the change in precision is translated into a change in counting time and then combined with the time saved by the elimination of an independent background measurement, one finds that the time required for the rejection ratio approach is smaller by a factor of 3, for a given level of precision. As the first measurement alone took nearly a week (6.9 days), such a saving is quite significant. Other important advantages includes the simultaneity of background and sample measurement, the absence of exact matching requirements for sample (composition, pressure) vs. blank counter fillings, and a less stringent requirement on composition stability with time. The throughput of samples is, of course, also increased by the same factor as in equation (3). These advantages must, however, be weighed against limitations imposed by possible systematic error in the assumed value for the rejection ratio (β_0). Had the value of β_0 (0.93) obtained with an external ^{60}Co source been applied, for example, rather than that (0.86) obtained from a background spectrum, the estimated signal ($\hat{S}$) would have been seriously biased. (Note that the ratio [dpm/ℓ - Ar]/cpm $\sim$ 11.4 due to decay, counting volume and efficiency.)

3. Analysis of Individual Events.

Complete information concerning a counting process can only be obtained by acquiring the data on a pulse-by-pulse basis. Besides information on mean rates and spectrum shapes, such an acquisition process affords a wealth of information on randomness, error distribution, correlation and coincidence, trends, periodicity, and stability in the counting process. (The importance of long-term stability can hardly be over-emphasized for low-level counting.) An illustration of the type of information available is given in Figure 8, where the computer output for our on-line system is given for approximately a three second counting interval. The record of individual events in this figure actually relates to one of our southern hemisphere argon samples (S2) which was collected at ground-level in Sao Paulo on 1 April 1973, and subsequently enriched by more than a factor of 100 at the Mound Laboratory.

The time interval included in Figure 8 was selected because it was particularly rich in different types of events. The first four columns of the figure give the time of occurrence of each central counter pulse to the nearest millisecond; the fifth column gives the interval between pulse pairs to the nearest microsecond, and the seventh column indicates whether counter number-1 (0) or number-2 (1) was the second member of the pair. (The electronics are such that the microsecond clock can only be started by the occurrence of an event in counter number-1.) The next column (labeled ID) tells which of the central counters was discharged. Spectral information appears in columns nine and ten; ADP and E amplitudes are given with 8-bit resolution (equivalent to a 256 x 256 two-parameter analyzer). A one (1) appears in column eleven if a guard coincidence occurs, and in column twelve if a very fast rising pulse (noise or pulser) is detected.

When one considers that Figure 8 represents only about 3 seconds our of a normal counting period of 1 week ($\sim 6 \times 10^5$ seconds), it becomes clear that a vast amount of information may be accumulated, even for quite "low-level" counting. Full utilization of this information will come only after some experience with the system, but it is clear that it may permit still more effective discrimination against unwanted events, and it will certainly permit extremely sensitive means for testing assumed system performance plus the detection of unexpected occurrences.

By way of illustration, we shall conclude with a brief examination of some of the information contained in the record of pulse times for sample S2.

In an ideal counting process, the distribution of counts is Poisson and the distribution of time intervals (between counts) is exponential. Under these circumstances, it can be shown that the estimation of mean rates may be carried out equally well using counts or time intervals (Cox and Lewis, 1966). Using an extended series of observations from the counting of sample S2, we have made a test of the assumed exponential distribution, as shown in Figure 9. In this figure the expected distribution, shown by the solid line, was deduced from the mean rate of the anti-coincidence events in counter number-1 ($\sim$3.6 cpm). A sample of 19 observations (only 10 of which are shown) was then used to construct the probability plot (Filliben, 1973). The mean interval from this plot ($\hat{\tau}$ = 17.2 ± 3.9 s) is in agreement with the expected value (τ = 16.5 s), and the shape is reasonably consistent with that predicted.

A rather more stringent test of the system may be made by examining the time intervals between coincidence and anticoincidence events. Knowing the mean rates for each, an expected interval distribution may again be given (solid line in Figure 10), and the observed intervals may be used to construct the corresponding probability plot. In this case the fit was completely unsatisfactory. In fact, the observed intervals did not even respect the axis boundaries, for negative time intervals were observed! The astute observer, of course, will already have discovered the existence of negative time intervals from Figure 8. This represents a case where the overall system (sample-counters-electronics-computer) was not behaving as assumed; in fact there existed a fault in the operation of the internal computer timer. It is worth emphasizing that this fault, for example, would not have been detected if counts rather than intervals had been recorded, nor was it detected when intervals between anticoincidence events only were examined.

Correcting for the clock error we obtained the second set of points in Figure 10. Although the resulting plot was less discordant with the expected distribution, questions still remain. The estimated mean interval ($\hat{\tau}$ = 0.99±0.28 s) seems somewhat too large; the shapes are not altogether consistent; and one interval (Δt = 5.78 sec) is much too large (prob. $\lesssim$ .1%). Confirmation and understanding the possible discrepancy must await considerably more experimentation. It might be due to chance or to imperfect behavior in either the proportional counting system or the on-line computer. Non-receptive periods, which would tend to lengthen intervals between recorded events, are known to exist in both parts of the system.

The views and conclusions contained in this manuscript are those of the authors and should not be interpreted as necessarily representing the official policies, either express or implied, of the Advanced Research Projects Agency, the Air Force Technical Applications Center, or the U. S. Government.

REFERENCES

Cox, D. R. and P. A. W. Lewis, (1966), *The Statistical Analysis of Series of Events*, (Wiley, New York).

Culhane, J. J. and A. C. Fabian, (1972), *Circuits for Pulse Rise Time Discrimination in Proportional Counters*, IEEE Trans. Nucl. Sci., NS-19, p. 569.

Currie, L. A., (1972), *The Measurement of Environmental Levels of Rare Gas Nuclides and the Treatment of Very Low-Level Counting Data*, IEEE Trans. on Nucl. Sci., NS-19, p. 119.

Davis, R., Jr., J. C. Evans, V. Radeka, and L. C. Rogers, (1972), *Report on the Brookhaven Solar Neutrino Experiment*, BNL Report 16937.

Filliben, J. J., (1973), personal communication and probability plot assistance.

Fischer, F. and O. Ringe, (1908), *Die Darstellung von Argon aus Luft mit Calciumcarbid*, Ber. Deut. Chem. Ges., 41, p. 2017.

Houtermans, F. G. and H. Oeschger, (1955), Helv. Phys. Acta, 28, p. 464.

Kastens, M. L. and W. G. McBurney, (1951), *Calcium Cyanamide*, Ind. Eng. Chem, 43, p. 1020.

Lal, D. and B. Peters, (1967), *Cosmic Ray Produced Radioactivity on the Earth*, Handbuch der Physik, Vol. 46, No. 2 Springer-Verlag, pp. 551-612.

Loosli, H., H. Oeschger, R. Studer, M. Wahlen, and W. Wiest, (1973), *^{37}Ar-Activity in Air Samples and its Atmospheric Mixing*, Noble Gases Symposium, Las Vegas, Nevada.

Machta, L., (1973), *Argon-37 as a Measure of Atmospheric Vertical Mixing*, Noble Gases Symposium, Las Vegas, Nevada.

Machta, L., R. J. List, M. E. Smith, Jr., and H. Oeschger, (1970), *Use of Natural Radioactivities to Estimate Large-Scale Precipitation Scavenging*; Precipitation Scavenging, U. S. Atomic Energy Commission CONF-700601, pp. 465-474.

Momyer, F. F., Jr., (1960), *Radiochemistry of the Rare Gases*, NAS-NS-3025.

Oeschger, H., (1963), *Low Level Counting Methods*; Radioactive Dating (Internation Atomic Energy Agency) Vienna, 13.

Oeschger, H., J. Houtermans, H. Loosli, and M. Wahlen, (1970), *The Constancy of Cosmic Radiation from Isotope Studies in Meteorites and on the Earth*; in Nobel Symposium 12, Radio-carbon Variations and Absolute Chronology I. Olsson, Ed. Almquist and Wiksell, p. 471.

Roos, W., (1973), Monsanto Research Corporation — personal communication.
Rutherford, W., J. Evans, and L. A. Currie, (1974), *The Application of Isotopic Enrichment and Pulse Shape Discrimination to the Measurement of Atmospheric ^{37}Ar* — to be published.
Schell, W. R., (1970), *Investigation and Comparison of Radiogenic Argon, Tritium, and ^{14}C in Atmospheric Reservoirs*, (I. U. Olsson, Edit.), p. 447, Nobel Symposium 12, Almquist and Wiksell (Stockholm).
Wiest, W., (1973), *Messung von Argon-Isotopen in Luftproben und Vergleich mit Modellrechnungen*; Dissertation, Universitat Bern, Switzerland.

Table 1. Low-Level Proportional Counters.

Construction	Sensitive Volume (l)	^{37}Ar Background (cpm) (1 atm, 2 fwhm Δ E)
Small Delrin	0.10	0.02
Quartz, Fe Cathode	0.42	0.05
Large Delrin	1.38	0.05
Stainless Steel Oeschger-Type	1.64	0.4

Table 2. Stratospheric Sample. (15.5 km. 2 Feb. 1973)

Δt (min)	Y_I	Y_o	Y_{IB}
9,905	187	1012	
9,554	-	-	158

^{37}Ar-window (Y_I, Y_{IB}): 0.027 ± 0.021 dpm/l-Ar

Rejection Ratio (Y_I, Y_o): (0.027) + 0.017 dpm/l-Ar(a)

(a)Result for β_o = 0.86. Radioactive concentration (0.027 dpm/l-Ar) was not independently estimated; however, because β_o was not known with sufficient precision (β_o = 0.87 ± 0.01).

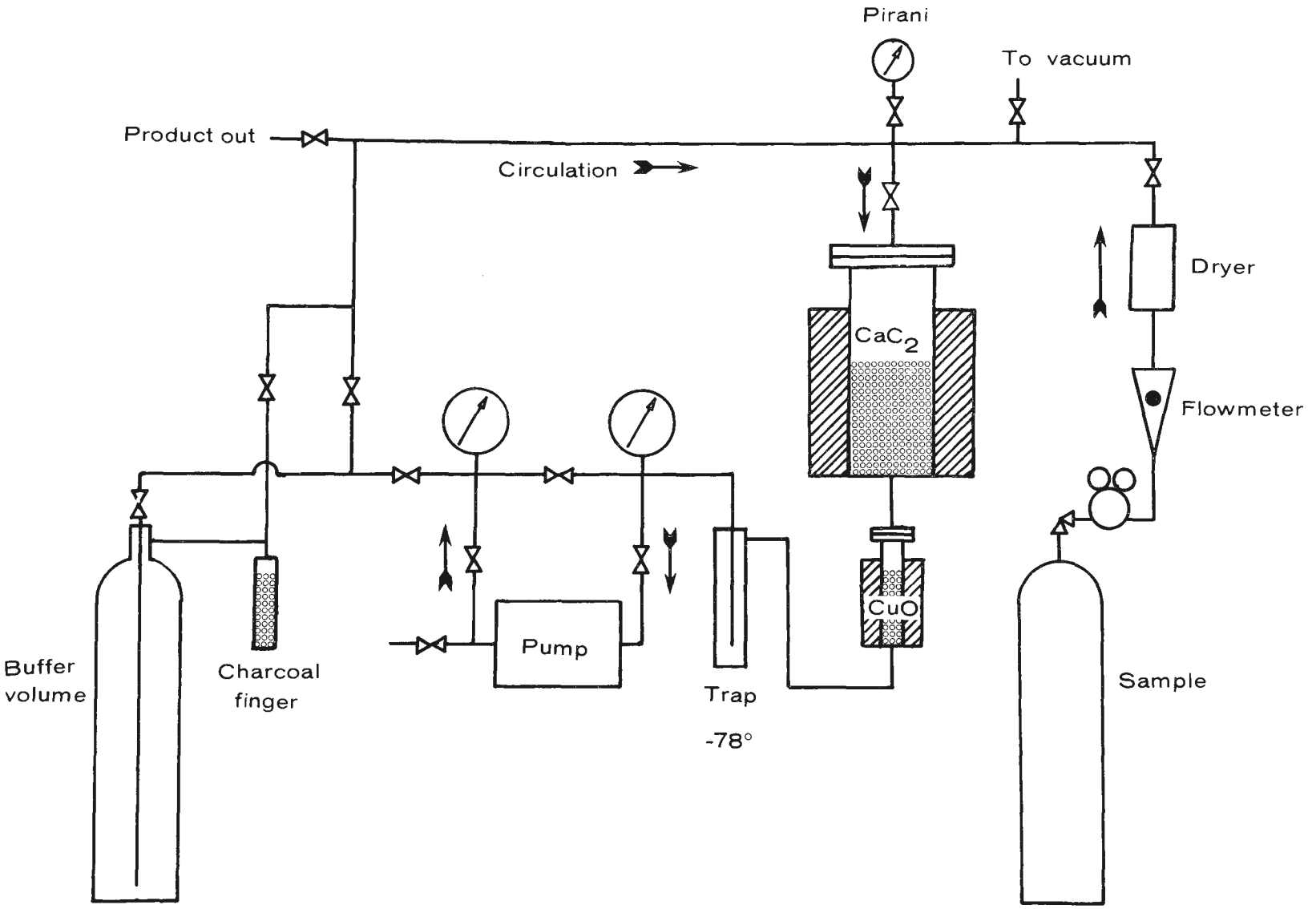

Figure 1. Calcium Carbide System for Argon-Air Separations. (After drying, the whole air sample is pumped through CaC_2 at 800°C to reduce N_2 [to $CaCN_2$] and O_2 [to CaO].)

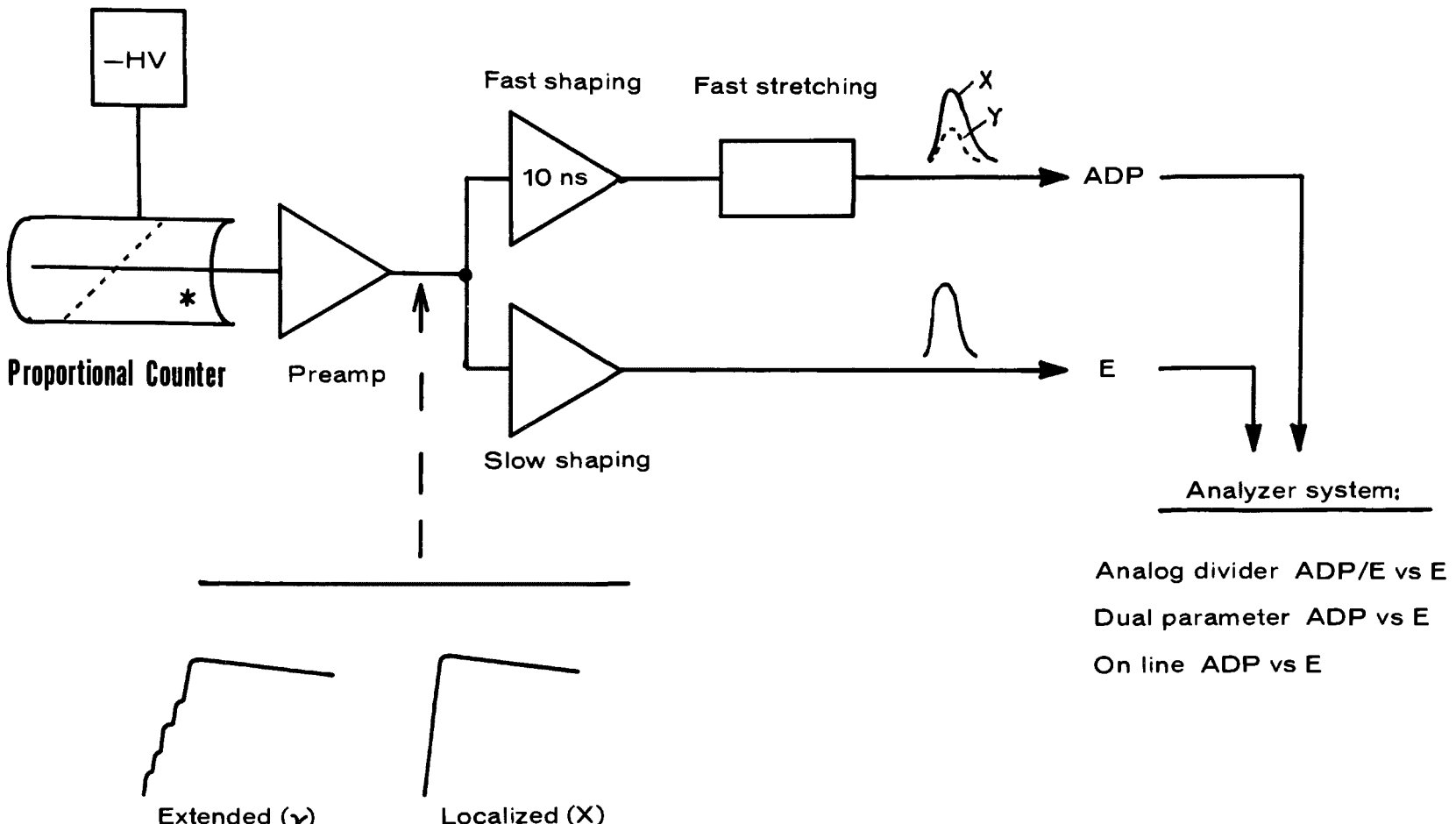

Figure 2. Proportional Counter Spectrometer. (^{37}Ar disintegrations are distinguished by energy [E] and pulse shape [ADP/E].)

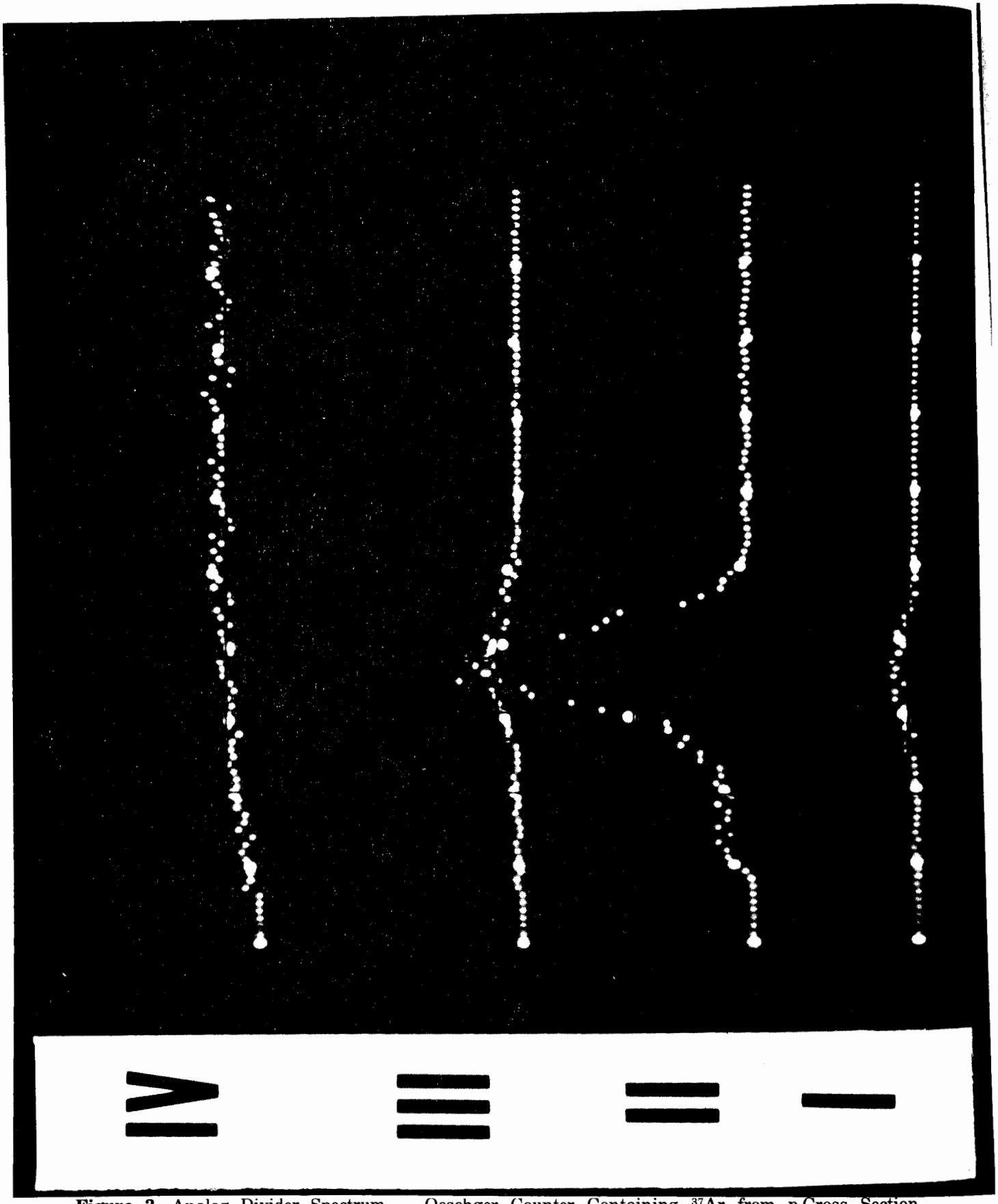

Figure 3. Analog Divider Spectrum — Oeschger Counter Containing ^{37}Ar from p-Cross Section Measurements. (Compton electrons, ^{37}Ar [and X-rays], and electrical noise are directed mostly to quadrants I, II, and III, respectively; the spectrum of coincidence events [muons] is routed to quandrant IV.)

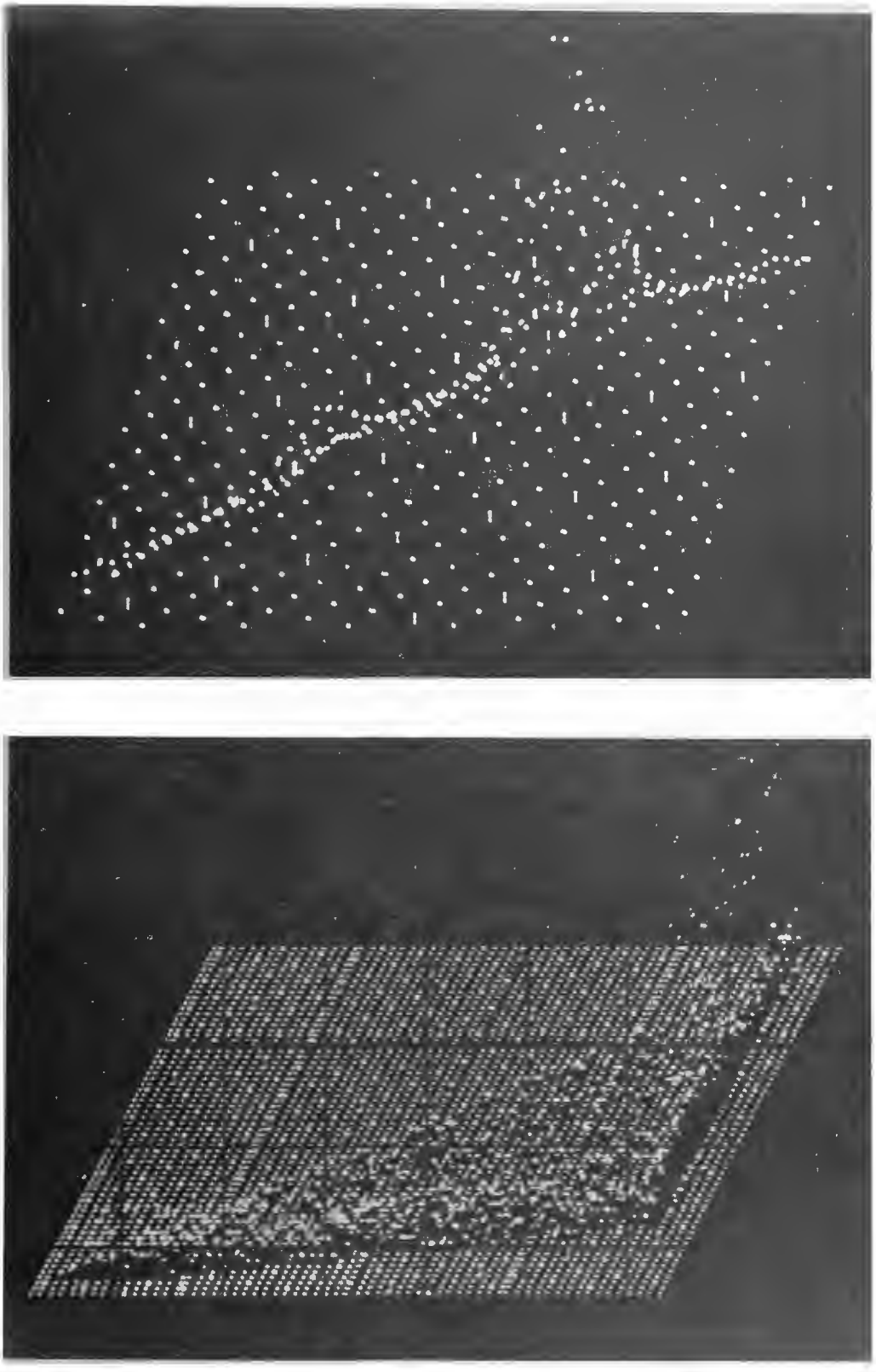

Figure 4. Two-Dimensional Spectra. (Pulses are sorted according to shape [ADP] and energy. The upper spectrum, which is typical of X-rays, is due to ^{241}Am-excited Fe - fluorescence radiation; the lower spectrum, which is due to background, shows a larger proportion of weakly-ionizing radiation.)

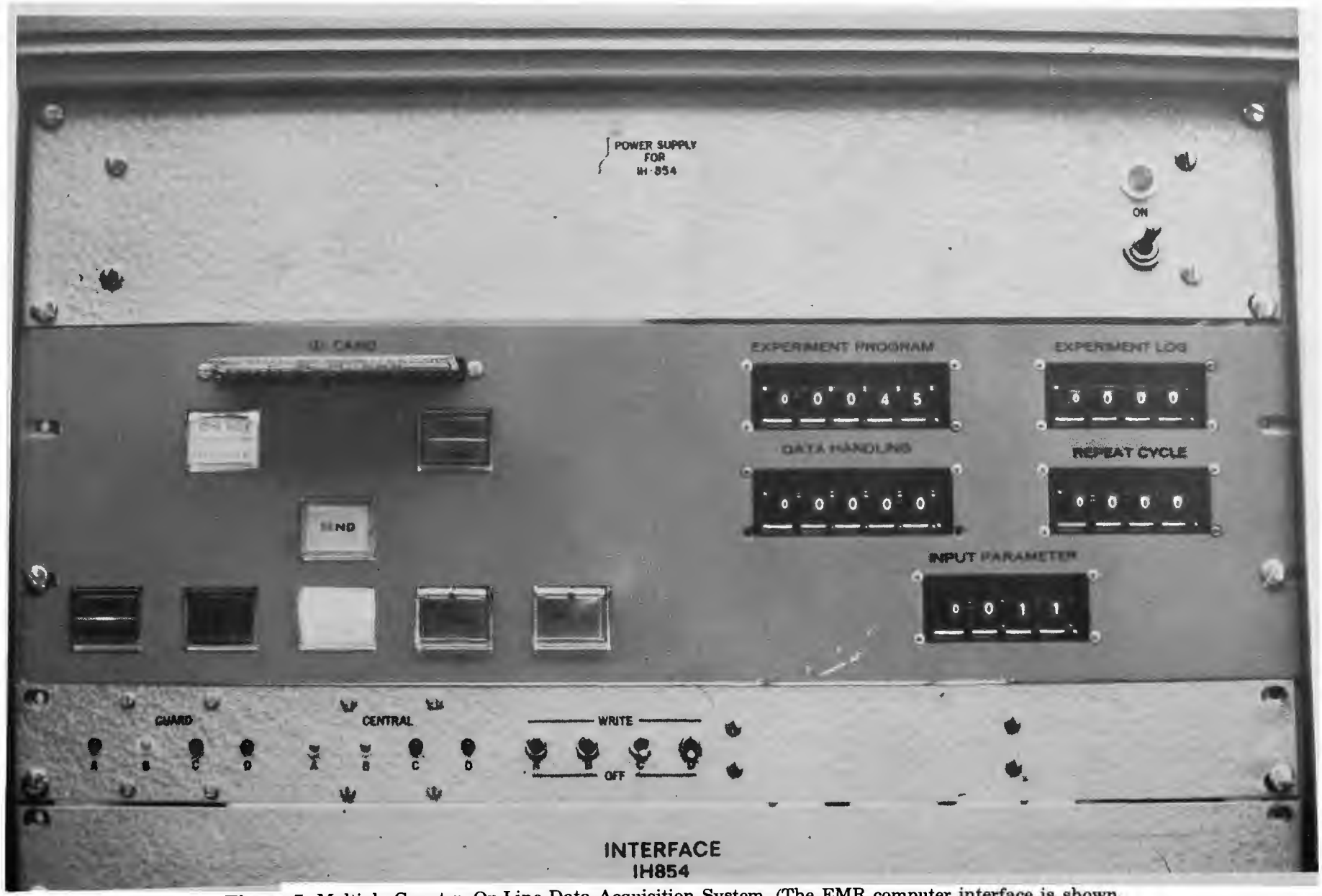

Figure 5. Multiple Counter, On-Line Data Acquisition System. (The EMR computer interface is shown together with pulse display lights for four guard counters [scale of 10] and four central counters [scale of 2].)

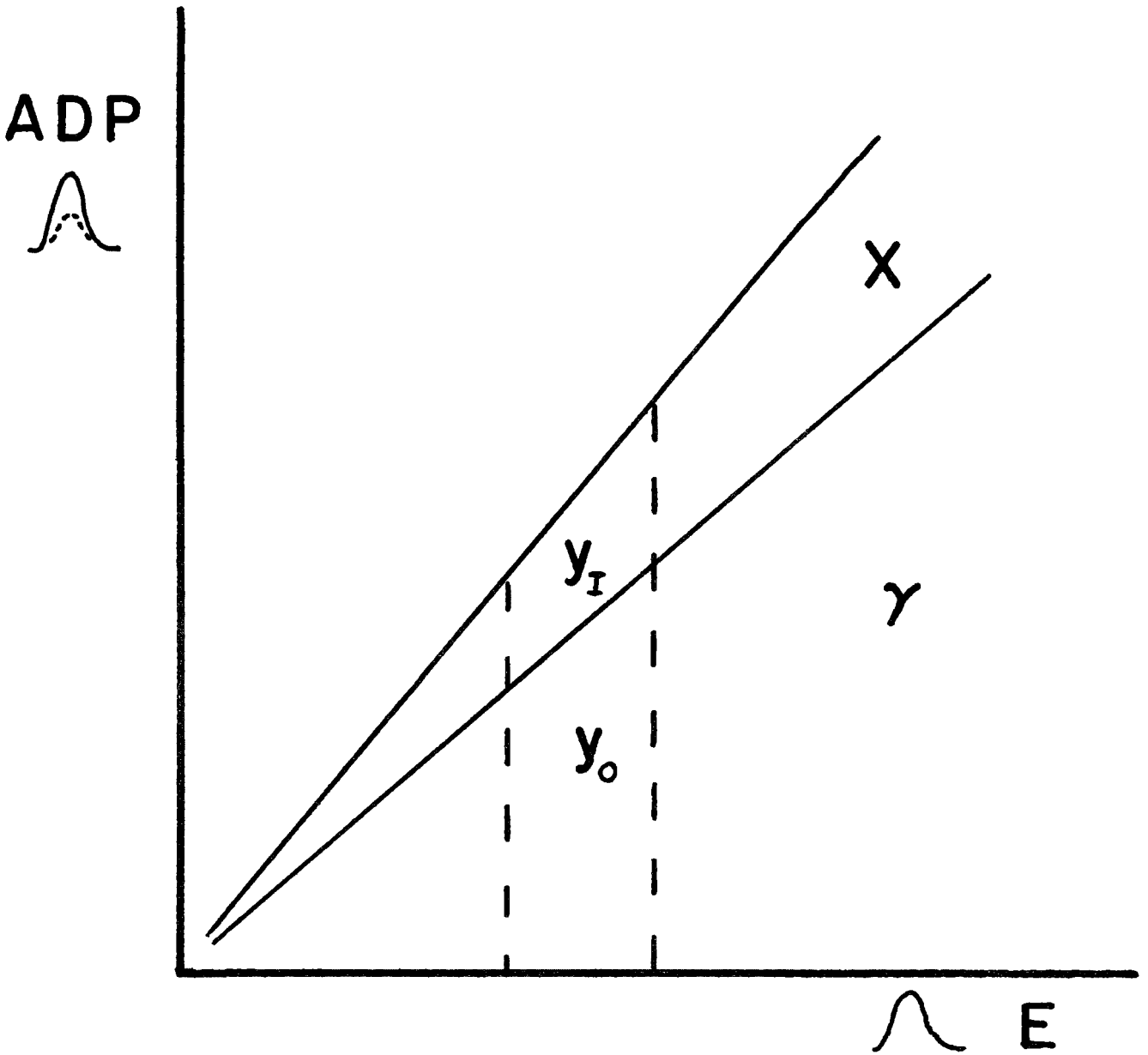

Figure 6. Partitioning of the Two-Dimensional Spectra. (^{37}Ar events lie primarily within the intersection of the X-ray pulse-shape band [X] and the proper energy [Y_I, Y_o] band.)

ATMOSPHERIC ARGON-37 DETECTION

SUM OF LOG NOS. 102 THROUGH 104

SAMPLE NUMBER 0

BACKGROUND

TERMINATED AT 850 ON DAY 89, 1973

A/COINC EVENTS GATED ON ADP/E INTO 3 100 CHN SUBGROUPS OF CTS VS ENERGY.

ENERGY AXIS SEGMENTED BELOW CHN 35 AND ABOVE CHN 44.

ACCUMULATION TIME = 600 MINUTES, NO. CHANNELS = 400

INITL BAROMETER = 753.44 MM(HG) AT 2147 ON DAY 88

FINAL BAROMETER = 752.79 MM(HG) AT 849 ON DAY 89

REJECTION RATIO = .6061 +- .1717

AREAS AND RATES

	IN	OUT	OUT/IN	NOISE	TOTAL A/COINC	TOTAL COINC
AREA	13.0	20.0	1.5	2.0	2465.	88556.
	+- 3.6	+- 4.5	+- .5	+- 1.4	+- 50.	+- 298.
RATE (1/MIN)	.022	.033	1.538	.003	4.1	147.6
	+- .006	+- .007	+- .548	+- .002	+- .1	+- .5

Figure 7. Background Data Summary — 1.4-Liter Counter. (Computer summary of analog divider spectra including rejection ratio, muon rate, barometric pressure, and time of year.)

EVENT RECORD

Sample S2, Brazil

TIME												
hr	m	s	ms	μs			ID	ADP	E	C		
23	42	56	853	0	0	0						
							1	145	171	1	0	0	coincidence (μ)
23	42	56	997	0	0	0						
							2	0	157	0	0	0	
23	42	56	52	0	0	0						
							1	34	53	0	1	0	pulser
23	42	56	587	0	0	0						
							2	0	214	0	0	0	
23	42	57	952	0	0	0						
							2	0	73	0	0	0	
23	42	57	449	0	0	0						
							1	33	53	0	1	0	
23	42	58	888	0	0	0						
							1	19	0	0	0	0	anticoincidence
23	42	58	549	0	0	0						
							2	0	190	0	0	0	
23	42	58	636	0	0	0						
							2	0	248	0	0	0	
23	42	58	754	39	0	1							
							1	94	154	1	0	0	$t_2 - t_1 = 39\mu s$
							2	0	184	0	0	0	
23	42	59	846	0	0	0							
							1	34	53	0	1	0	
23	42	59	474	0	0	0							
							1	50	130	1	0	0	

Figure 8. Event Record. (Computer output, showing times of occurrence [to the nearest ms] plus amplitude, shape, and coincidence information for individual pulses over about a three-second interval [See text for detailed explanation]).

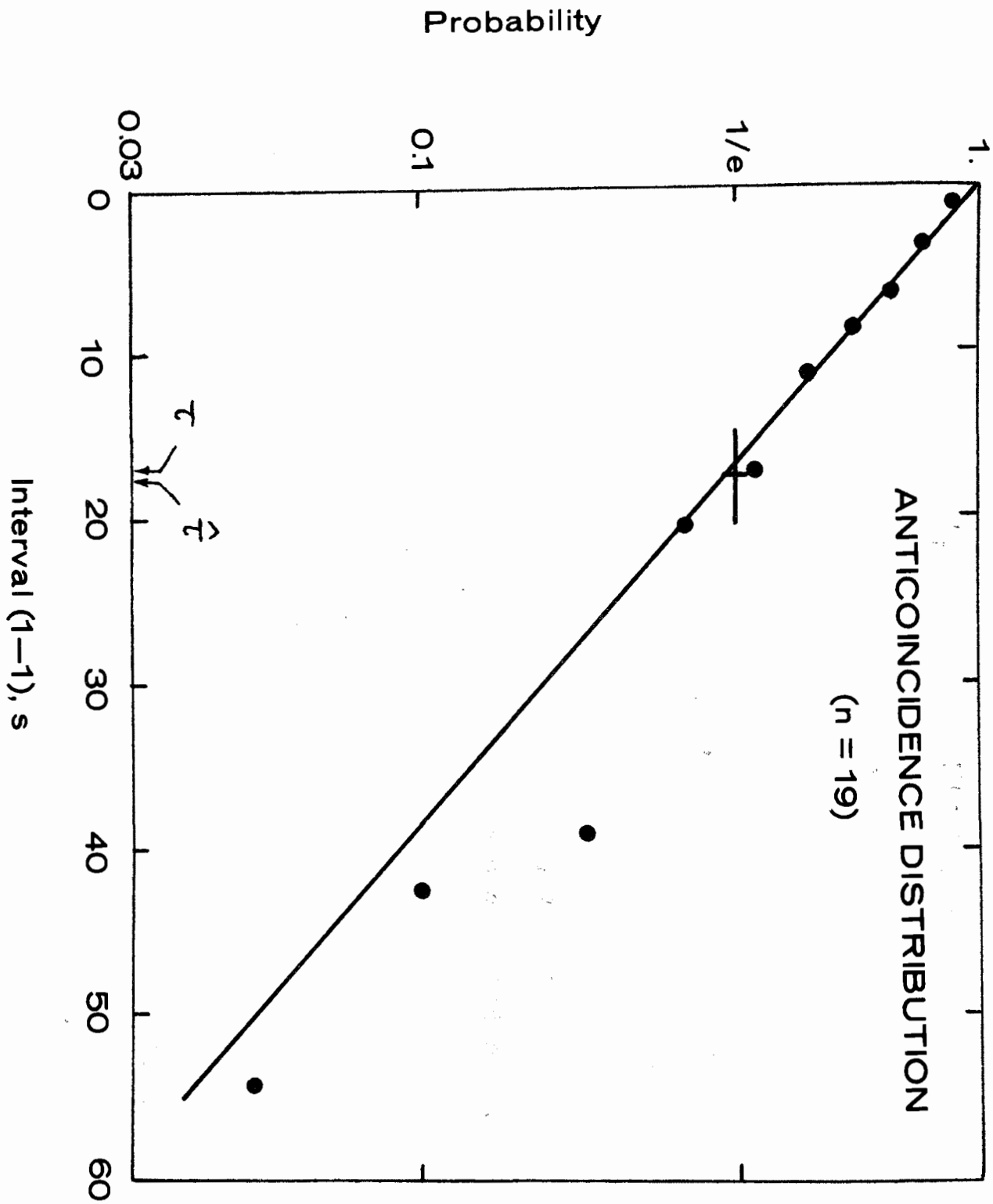

Figure 9. Interval Distribution, Anticoincidence Events. (The solid curve represents the expected exponential distribution [τ = 16.5 s]; points refer to the observed distribution of 19 events.)

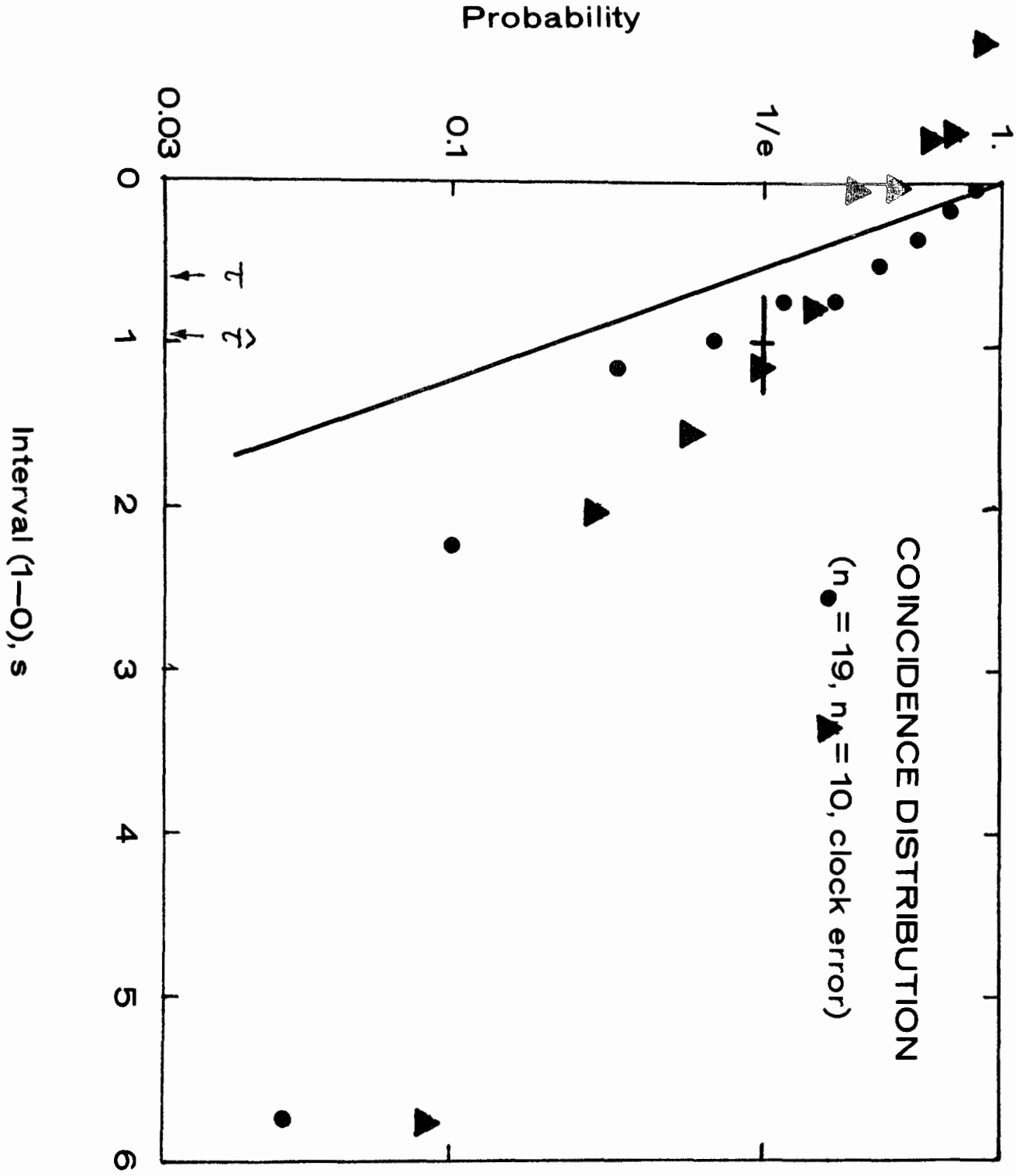

Figure 10. Interval Distribution; Anticoincidence vs Preceding Coincident Events. (The solid curve represents the expected exponential distribution [τ = 0.52 s]. Initial observations [△] fit badly because of a computer clock error; corrected observations [○] fit much better, but they imply too long a mean interval [$\hat{\tau}$].)

ARGON-37 AS A MEASURE OF ATMOSPHERIC VERTICAL MIXING

L. Machta
National Oceanic & Atmospheric Administration
Silver Spring, Md. 20910

ACKNOWLEDGEMENTS

The support of this work by the Advanced Research Projects Agency of the Department of Defense is gratefully acknowledged. Also, the assistance of Mr. W. Hass, of the Air Resources Laboratories, is appreciated.

Abstract

Cosmogenic argon-37 distribution in the atmosphere is determined by its production, decay, and by atmospheric transport. If the first two processes are known, one may use the observed distribution of argon-37 to determine global scale atmospheric transport. The atmospheric transport, as a first approximation, assumes that the flux of argon-37 lies in the direction of its gradient of concentration. The proportionality factor, called the eddy diffusion coefficient, is related to atmospheric turbulence. Using estimates of cosmic ray production of argon-37 given by Rama in Lal and Peters and observations of minimum concentrations (to minimize the likelihood of man-made contamination) given by Oeschger and Loosli, it will be shown that the likely global vertical diffusion coefficient averages about 5 x 10^4 cm^2 sec^{-1}.

INTRODUCTION

Global scale vertical dispersion modeling may be applied to many theoretical and practical problems. For example, our laboratory has already employed an early version of the two-dimensional model of atmospheric transport to predict the fate of long-lived radioisotopes such as krypton-85 over a period of many years for population-dose estimates.

Unfortunately, there are very few substances which can be used as tracers to follow global scale mixing (Machta, 1973). Our most frequently used tracer substances are particulate and, more often than not, the transport is assumed to be known, and the removal rates deduced from the observed distribution. To describe transport and dilution, we need tracers with exactly known sinks. Very few atmospheric tracers can be detected after global scale dilution. Argon-37 (^{37}Ar) is relatively unique in this regard. Atmospheric carbon dioxide can also be followed globally. From the latter, on the average, a coefficient of vertical eddy diffusion was found to be 5 x 10^4 cm^2 sec^{-1} in the troposphere.

It may come as a surprise to the non-meteorologist that there are no direct free-air measurements of the vertical components of the winds which can be used to directly infer the vertical mixing intensity. Virtually all wind measurements reflect the horizontal displacement of a buoyant rising balloon. Efforts to derive vertical wind components from changes in the ascent rate of balloons have rarely been successful. One can understand the difficulty in measuring the vertical wind components, when, in most of the atmosphere, the vertical wind is usually less than 0.1 mph — compared to horizontal winds between about 10 and 100 mph.

But, there is an atmospheric parameter that either controls the vertical component of turbulent motions, or responds to it — the vertical temperature gradient. Most people are familiar with the so-called lid on vertical mixing — the temperature inversion which inhibits vertical mixing through it. Its low altitude and persistence is a problem for the people of Los Angeles. The relationship between vertical mixing and thermal structure is still, at best, a qualitative one.

These introductory remarks are intended to convey the fact that the meteorologist does not, as yet, have a good handle on global scale vertical mixing. The opportunities and limitations presented by ^{37}Ar as a tracer for vertical mixing are described below as an effort to improve the situation. The terms "large scale" or "global scale" imply an averaging process (over many days to weeks) in order to include the motions of high- and low-pressure systems as turbulent components. In principle, this averaging time also demands a comparably long sampling time for tracers; but, in practice, this requirement is not always satisfied.

GENERAL CONCEPT

Argon-37 production by cosmic rays increases rapidly with altitude. Figure 1 illustrates the schematic sharp increase in ^{37}Ar concentration with altitude, in the case of no vertical mixing, the thin solid, curved line, exactly balances radioactive decay production. Note that the ground-level concentration is smaller than those for the other curves on this figure. The vertical heavy line indicates that, with very fast vertical mixing in the troposphere, the concentration per unit mass of air is uniform with height. Assuming for the moment that there is no mixing across the tropopause, then, this value shows the same as the average concentration of the "no vertical mixing curve" in the troposphere. As you can see, the "fast vertical mixing curve" shows the highest ground-level concentration. However, the third curve more nearly represents reality, yielding a ground-level concentration intermediate between the other two.

Qualitatively, then, the observed ground-level concentration lying between the two extremes is related to the intensity of vertical mixing. Several guesses at the intensity of vertical mixing are used to predict ground-level concentration — the best fit to the limited observed data determining the preferred mixing intensity.

PHYSICAL PROCESSES AND A METEOROLOGICAL MODEL

There are three physical processes determining the atmospheric distribution of ^{37}Ar: (1) production, |2) radioactive decay, and (3) atmospheric transport. In this presentation the first two are assumed to be known, allowing the transport to be inferred from the distribution, as discussed in the preceding section.

Meteorologists normally separate transport processes into two categories: (1) organized air movements averaged over some space or time domain, and (2) turbulent movements fluctuating around the average airflow. The west-to-east and east-to-west organized air motions are much larger than the north-to-south and south-to-north organized air movements (by at least 10 to 100) averaged around the globe.

The organized wind motions around circles of latitude, and the attendant wind shear and longitudinal mixing, results in approximate zonal homogeneity within a matter of weeks to months. This fairly rapid approach to zonal homogeneity represents the justification for a two-dimensional model in which no variation in ^{37}Ar concentration around circles of latitude is admitted.

An organized circulation also exists in the meridional plane (north-south and vertical), but it is omitted from the model below for several reasons. The first, and least justifiable, relates to our inability to correctly incorporate the advective process. Unless a very considerable increase in computer time and power is accepted, the inclusion of advection introduces artificial dispersion. (This can seriously confuse the mixing process in the model.) A second reason is the lack of definitive information on the details of the organized meridional circulation. The mixing process, which is used to transport ^{37}Ar vertically and meridionally, must effectively include the contribution of organized circulation as well as turbulent mixing.

The turbulent transfer mechanism used is the classical flux-gradient relationship — where the flux of a conservative property takes place in the direction of the gradient of the property (from high towards low concentration) with the proportionality constant (called the eddy diffusion coefficient, or simply the diffusion coefficient). This flux-gradient statement defines most of the atmospheric physics included in the model. What remains are adjustments for the sphericity of the earth, the decreasing density with altitude, treatment of the boundaries, and the radioactive decay. The boundaries are considered to be perfectly non-absorbing; i.e., no transport takes place through the ground or through the top of the model atmosphere at 50 kilometers.

Figure 2 illustrates the grid spacing; 2 km in the vertical, and 20° latitude in the north-south direction. The inset shows the location of the eddy diffusion coefficients along the walls of each box. The grid points extend throughout the atmosphere — even though some of the lines have been omitted in the figure.

The "horizontal mixing" in the lower stratosphere occurs in a plane, inclined very slightly downwards, towards the poles as suggested by the behavior of nuclear bomb debris.

The rationale for selecting the diffusion coefficients in the model has been described by Machta, 1973. This rationale includes such considerations as the vertical stability of the air (noted earlier), and the fluctuations of the north-south wind components. Mainly, however, these coefficients derive from a trial and error fit in which the model tries to match real atmospheric tracers. Again, since some transport also takes place by organized motions, the above fitting-procedure yields effective eddy diffusion coefficients, which try to include all transfer processes — not only mixing processes.

Both the horizontal and vertical eddy diffusion coefficient vary with time and space, Machta, 1973. The vertical eddy diffusion coefficients in the troposphere, which average about 5×10^4 cm^2 sec^{-1}, are larger in summer (up to 8×10^4 cm^2 sec^{-1}) than in winter, and smaller in the stratosphere (averaging 3×10^3 cm^2 sec^{-1}). They are also smaller near the ground than in the free air. The horizontal diffusion coefficients are generally on the order of 10^{10} cm^2 sec^{-1}.

COSMIC RAY PRODUCTION

The cosmic ray production of ^{37}Ar was taken from Lal, *et al.*, (1967), which was based on estimates by Rama. They attribute an uncertainty factor of 3 to the Rama values. Oeschger, *et al.*, (1970) suggest production values about twice those of Rama. They also assign a large uncertainty, at least a factor of two, to their estimates. During high solar activity, Oeschger, *et al.*, (1970) believe the tropospheric production to be about 20% below the average for the complete solar cycle. Lal, *et al.*, (1962) indicate a 9% range over a typical solar cycle.

The solid lines in Figure 3 (upper section) display the production of ^{37}Ar used in the present analysis in which geographical and geomagnetic latitude are assumed identical. One need only multiply a given value in the figure by the ^{37}Ar decay constant (1.375×10^{-5} min^{-1}) to yield the production of ^{37}Ar in units of atoms (gm^{-1} min^{-1}).

It is evident from the observed history of ^{37}Ar concentration in air (Loosli, *et al.*, 1973), that nuclear detonations also contribute to its concentration. The periods of such interferences are fairly evident from observed ^{37}Ar concentrations, or from other information.

GENERAL RESULTS OF MODEL CALCULATION

The distribution of ^{37}Ar predicted by the transport model, appears as the lower section of Figure 3, and is shown in the same units as the upper section of the figure. The most conspicuous difference between the two sections is the reduced gradients of concentration — especially in the troposphere. Careful inspection of these findings also reveal that the ground-level values rise, from below 0.0001 dpm per liter of ^{37}Ar in the upper section (no transport), to about 20-fold higher values, when transport is admitted. The dotted lines show the difference between the two sets of data.

Figure 4 shows the response of the ground-level concentration in the mid-latitudes (left side of figure) to changes in the intensity of the vertical diffusion coefficients. This figure suggests that there is about the same percentage response in the concentration as with the percentage change in tropospheric (or whole atmosphere) change in the vertical diffusion coefficients. Thus, if the more correct tropospheric vertical diffusion coefficient were say 4×10^4 cm^2 sec^{-1}, rather than 5×10^4 cm^2 sec^{-1} (a 20% decrease), then this figure predicts a corresponding 20% decrease in the ground-level concentration. If all other factors were known exactly, except the ground-level concentration, then one could specify the accuracy of establishing the ground-level concentration for matching the uncertainty in the global scale vertical diffusion coefficient desired by meteorologists. The left hand figure also shows that changing the diffusion coefficient in the stratosphere does not, however, appreciably change the ground-level ^{37}Ar concentration. Thus, the ground-level concentration responds almost entirely to tropospheric meteorology. It is likely that the real transfer process through the tropopause plays more of a role than suggested by this figure, and on rare occasions samples taken at ground-level contain substantial stratospheric air.

The right hand side of this figure shows how the concentration at 20 km in the mid-latitude (although the result applies, more or less, to all latitudes) responds to changes in diffusion rates. The altitude of 20 km was selected because the production of ^{37}Ar per gram of air reaches a maximum at this height. The almost vertical line indicates that the 20 km concentration is very insensitive to the meteorological parameters. It can also be added that about the same concentration is found where there is no mixing of any kind — or if the slantwise mixing is replaced by purely horizontal diffusion. This insensitivity to the meteorology suggests that a measurement of about 20 km may be a good way of determining the stratospheric cosmic ray production of ^{37}Ar.

Figure 5 indicates the seasonal variation of ground-level mid-latitude concentration. The horizontal bar values show that the diffusion coefficients in the mid-latitude troposphere are higher in summer than in winter seasons. This variation produces a parallel increase in ^{37}Ar concentration. (One of the aims of the ^{37}Ar program is the verification of seasonal variations in concentration.)

STRATOSPHERIC RESULTS

Table I compares the predictions of stratospheric concentrations of ^{37}Ar with the few available measurements taken over the southwestern U.S.A. First, the table illustrates that at about 20 km, the several predictions, as well as the "no transport equilibrium calculation," are all virtually the same; the discrepancy between the several predictions is greater at the lower levels.

The observed value at 15.6 km is due to the analysis of Dr. L. Currie (1973), of the National Bureau of Standards, for a sample collected on February 2, 1973. The other two entries were provided by Dr. H. Loosli (1973), of the University of Bern, Switzerland, based on collections obtained on January 16, 1973. The large errors in our samples are, in part, due to decay during shipping delays.

The observed values are consistently higher than those predicted: (For example: The 18.3 km value is about 30% greater than that predicted by the model, and the observed values at lower altitudes are over 50% higher than the model prediction.) It should be noted, however, that the sizeable errors attached to the observed values allow agreement within two standard deviations — this discrepancy may be due solely to the uncertainty in the measurements.

However, the consistency of the bias between the observed and the predicted values suggests that other explanations be examined. Four others come to mind: (1) The samples may have been collected during periods when winds brought air from higher latitudes causing the average concentrations to be higher than expected over the southwestern U.S. (See Figure 3). The examination of weather charts, however, indicates that this type of weather pattern was absent. (2) Bomb-produced ^{37}Ar contaminated the stratospheric samples. Atmospheric tests, last occurring in the summer of 1972, were of small yield in the southern hemisphere. It is unlikely that the ^{37}Ar from these tests could have significantly contributed to the sample concentration. In late August 1972, a large underground nuclear explosion was reported in the Arctic; the data presented by Loosli, *et* al., (1973), suggest that this may have been the source of the abrupt increase in ^{37}Ar concentrations in the northern hemisphere immediately thereafter. Model calculations suggest, however, that the amount of ^{37}Ar in the lower stratosphere from this source is too small to significantly alter its cosmic ray concentrations.

(1) The samples may have been collected during periods when winds brought air from higher latitudes causing the average concentrations to be higher than expected over the southwestern U.S. (See Figure 3). The examination of weather charts, however, indicates that this type of weather pattern was absent.

(2) Bomb-produced ^{37}Ar contaminated the stratospheric samples. Atmospheric tests last occurring in the summer of 1972, were of small yield in the southern hemisphere. It is unlikely that the ^{37}Ar from these tests could have significantly contributed to the sample concentration. In late August 1972, a large underground

nuclear explosion was reported in the Arctic; the data presented by Loosli, *et al.*, (1973) suggest that this may have been the source of the abrupt increase in ^{37}Ar concentrations in the northern hemisphere immediately thereafter. Model calculations suggest, however, that the amount of ^{37}Ar in the lower stratosphere from this source is too small to significantly alter its cosmic ray concentrations.

(3) During January and February 1973, and for some months preceding, solar activity was relatively low. Thus, the correct ^{37}Ar production values used in the model calculations should have been higher (by perhaps a few to ten percent over the average production numbers provided by Rama).

(4) The true ^{37}Ar production due to cosmic rays may be too low — by an amount required to produce agreement — between observation and prediction in the lower stratosphere.

Considering the large uncertainty in the cosmic ray production of ^{37}Ar, the last of the four possible explanations is most likely.

GROUND-LEVEL VERIFICATION

Figure 6 compares predictions of ground-level ^{37}Ar concentrations at about 50° N latitude, during the indicated months, with selected observations in Bern, Switzerland, taken from Loosli, *et al.*, (1973). This figure shows a scatter among the observations — as well as uncertainties attached to the very low concentrations. (The observed values are presumed to be the result of cosmic ray production alone.) These observation periods were selected from the entire record at Bern, Switzerland, because they appear to represent minimum concentrations. Because there are still variations from one reading to the next, the assumption of no man-made contribution is uncertain.

The predictions include, not only the model vertical diffusion parameters, but also doubled- and halved-vertical diffusion coefficients. The model predictions (the solid horizontal bars in Figure 6) appear to fit the general average in July and August, but fall below the average of observations in June and September (see the numbers above the data). It may well be that the meteorology in the latter two months is incorrect, but, at this stage in the program, other possibilities loom equally likely. Thus, the stratospheric samples suggest a higher production rate. If a higher production rate were used in the model, the predictions would be proportionally higher. Such a change would tend to improve the fit in the months of June and September, but not in July and August. Second, there exists a possibility that small amounts of man-made ^{37}Ar have contaminated some of the samples. Contamination of this sort could have produced the discrepancies noted in June and September which are shown in Figure 6.

It seems fair to argue that, as of the present, the model vertical diffusion coefficients, or somewhat higher values, are most likely to be correct.

CONCLUSIONS

Cosmogenic ^{37}Ar appears to offer considerable promise as a tracer to establish the large scale intensity of vertical mixing. Two features currently limit its usefulness. First, the cosmic ray production of ^{37}Ar must be known far more reliably than is now the case. Second, many more measurements of ^{37}Ar need to be obtained. These samples must also be uncontaminated by man-made sources.

The present state of knowledge, in which existing models of large scale atmospheric transport is applied to ^{37}Ar, suggests that the summertime vertical diffusion coefficient in the northern hemisphere troposphere of about 6-8 x 10^4 cm^2 sec^{-1}, or perhaps somewhat higher, fits the observed data. However, the very limited observations in the stratosphere also indicate that the cosmic ray production given by Rama in Lal, *et al.*, (1967), may be low.

REFERENCES

Currie, L., (1973), Personal communication.

Lal, D. and B. Peters, (1962), *Cosmic Ray Produced Isotopes and Their Applications to Problems of Geophysics. Progress in Cosmic Ray and Elementary Particle Physics,* Vol. 6, North-Holland Publishing Co., Amsterdam.

Lal, D. and B. Peters, (1967), *Cosmic Ray Produced Radioactivity on the Earth.* "Handbuch der Physik," Vol. 46, No. 2, Springer-Verlag, pp. 551-612.

Loosli, H., H. Oeschger, R. Studer, M. Wahlen, and W. Wiest, (1973), *^{37}Ar-Activity in Air Samples and Its Atmospheric Mixing.* Noble Gas Symposium, Las Vegas, Nevada, Sept. 24-28, 1973.

Machta, L., (1973), *Global Scale Atmospheric Mixing.* Paper presented at the Second International Union of Theoretical and Applied Mechanics, and International Union of Geodesy and Geophysics Symposium, on Turbulence in Environmental Pollution, Charlottesville, West Virginia, April 8-14, 1973.

Oeschger, H., J. Houtermans, H. Loosli and M. Wahlen, (1970), *The Constancy of Cosmic Radiation from Isotope Studies in Meteorites and on the Earth.* Nobel Symposium 12, "Radiocarbon Variations and Absolute Chronology," Almqvist and Wikesell, pp. 471, 496.

TABLE I. Comparison of Predicted and Observed ^{37}Ar Concentrations in the Lower Stratosphere.

Altitude (km)	Predictions (in dpm/liter ^{37}Ar)				Observed
	K_Z (model) x 2	K_Z (model) (January)	K_Z (model) x 0.5	Equilibrium (No Transport)	
14	0.013	0.014	0.016	0.027	
					(15.2 km) 0.029 ± 0.010
					(15.6 km) 0.030 ± 0.024
16	0.017	0.019	0.020	0.029	
18	0.025	0.027	0.027	0.031	
					(18.3 km) 0.037 ±0.008
20	0.032	0.033	0.034	0.033	

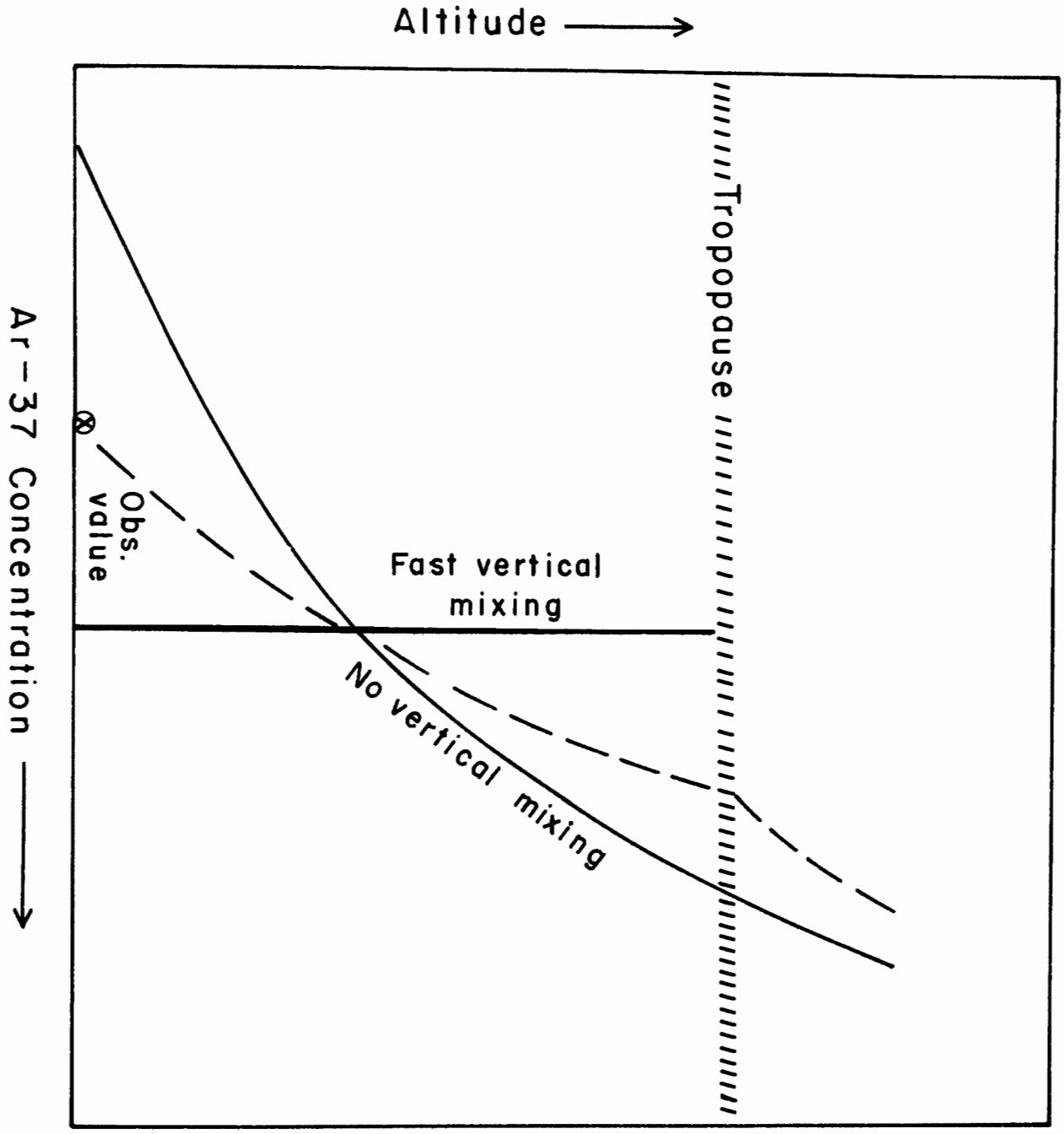

Figure 1. Schematic variation of ^{37}Ar concentration with altitude for extreme conditions of vertical mixing (solid curves), and for realistic conditions (dashed curve).

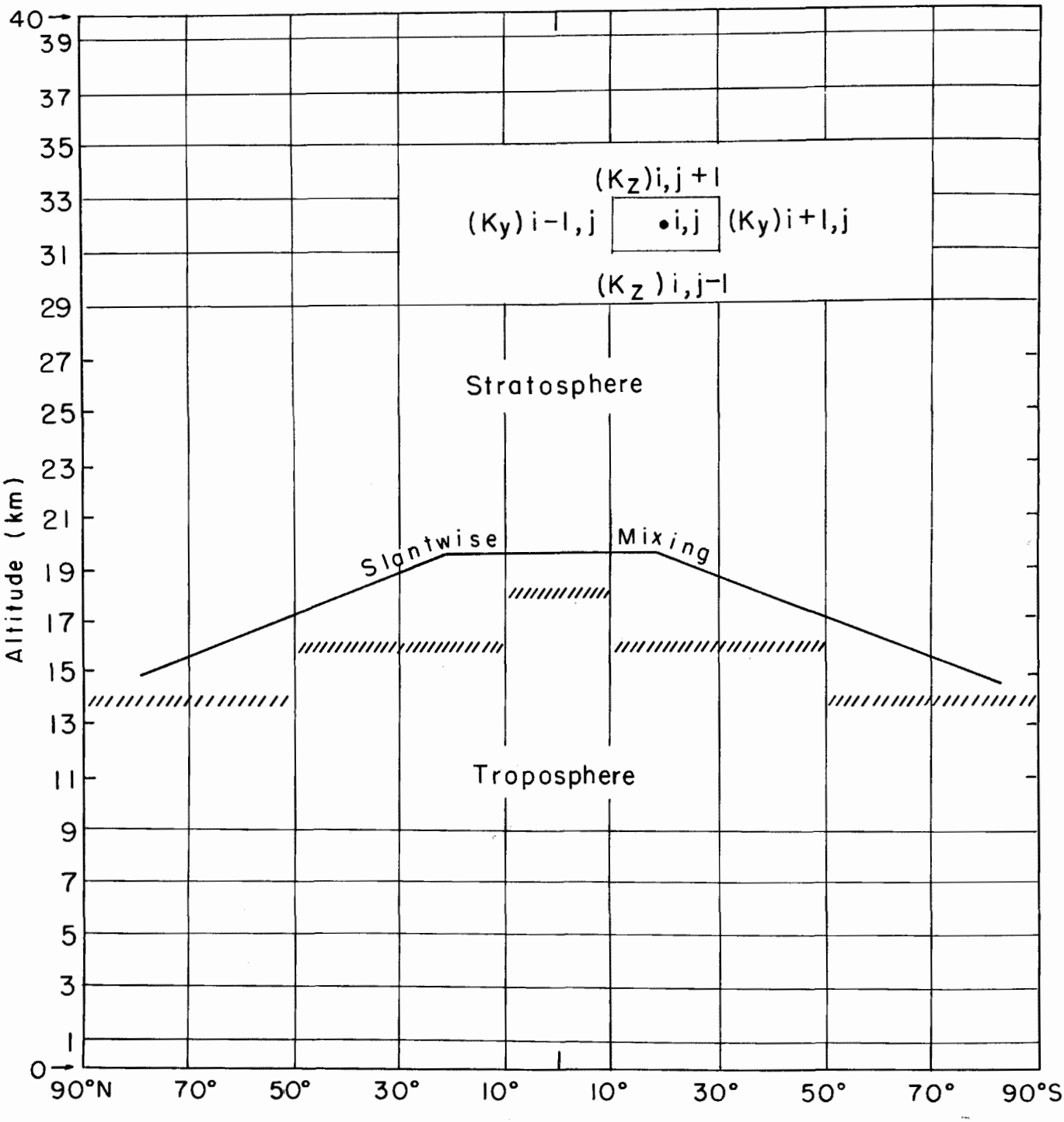

Figure 2. Schematic presentation of the two-dimensional atmospheric diffusion model. The inset shows the vertical (K_z) and horizontal (K_y) eddy diffusion coefficients at the interfaces of each grid box.

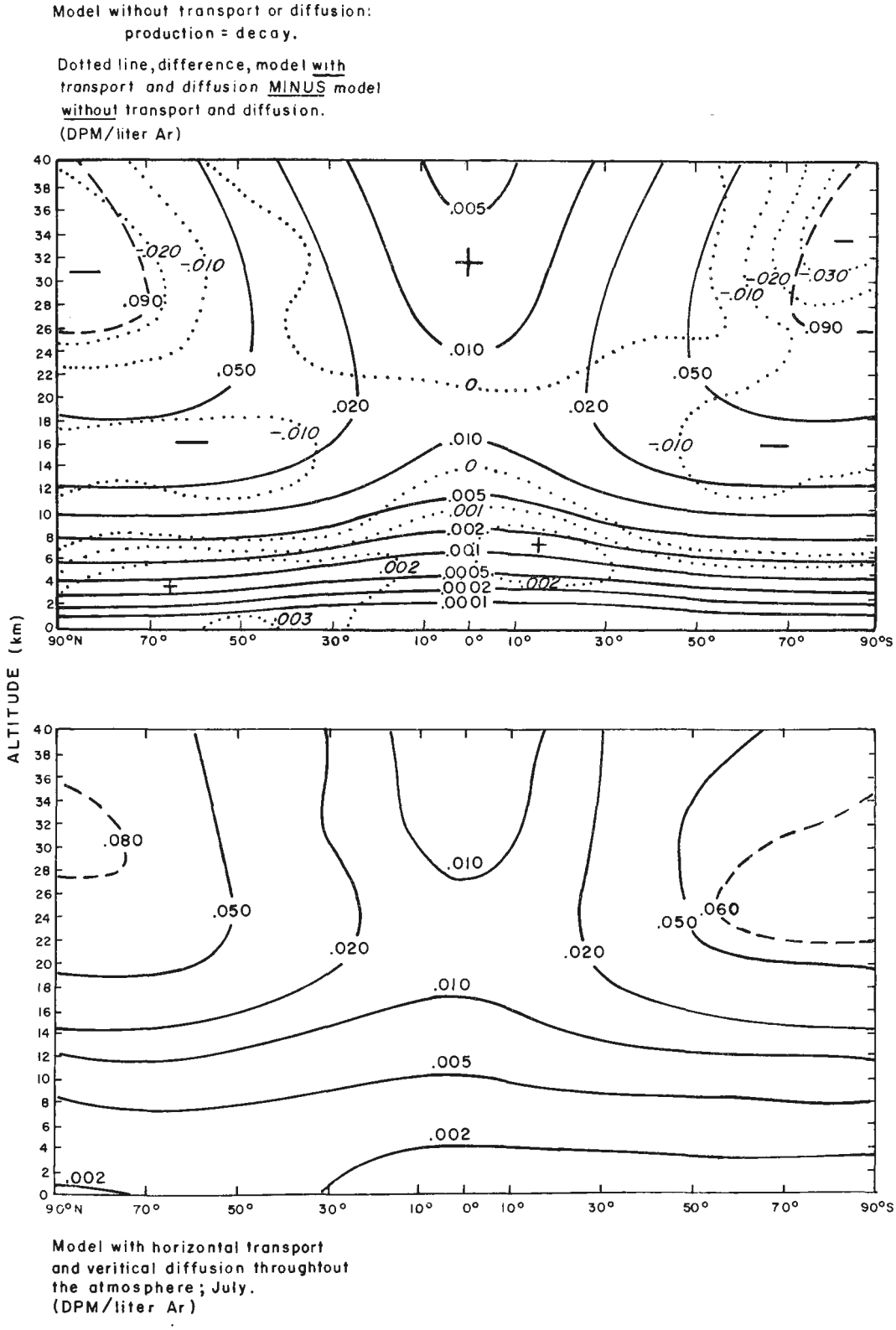

Figure 3. Model results of equilibrium ^{37}Ar distribution, above, with no transport or diffusion (*i.e.*, production equals decay); and, below, with horizontal transport and vertical diffusion throughout the atmosphere.

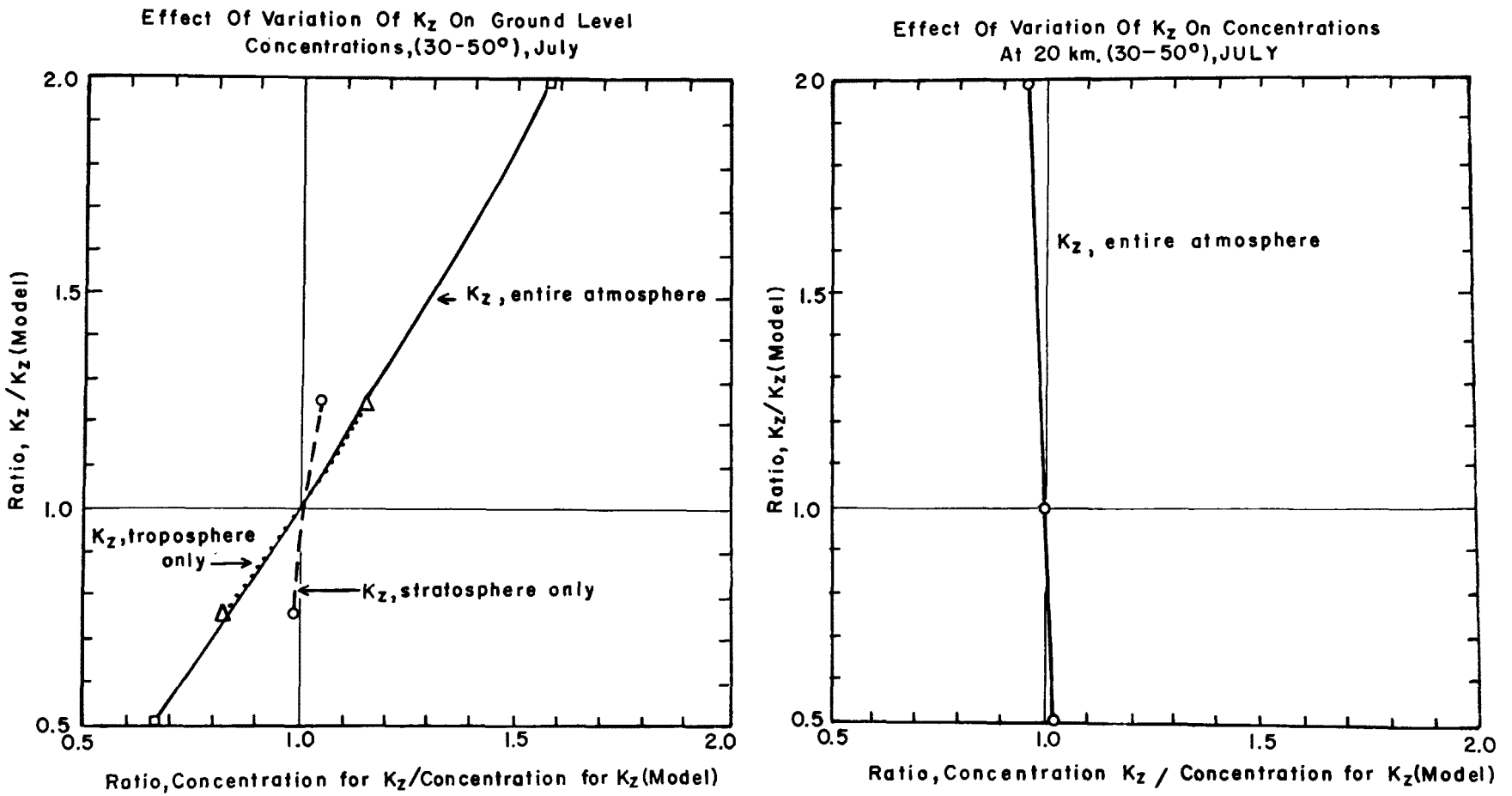

Figure 4. Response to ground-level concentration of ^{37}Ar in mid-latitudes (30-50°N) to changes in the intensity of the vertical diffusion coefficient, K_z.

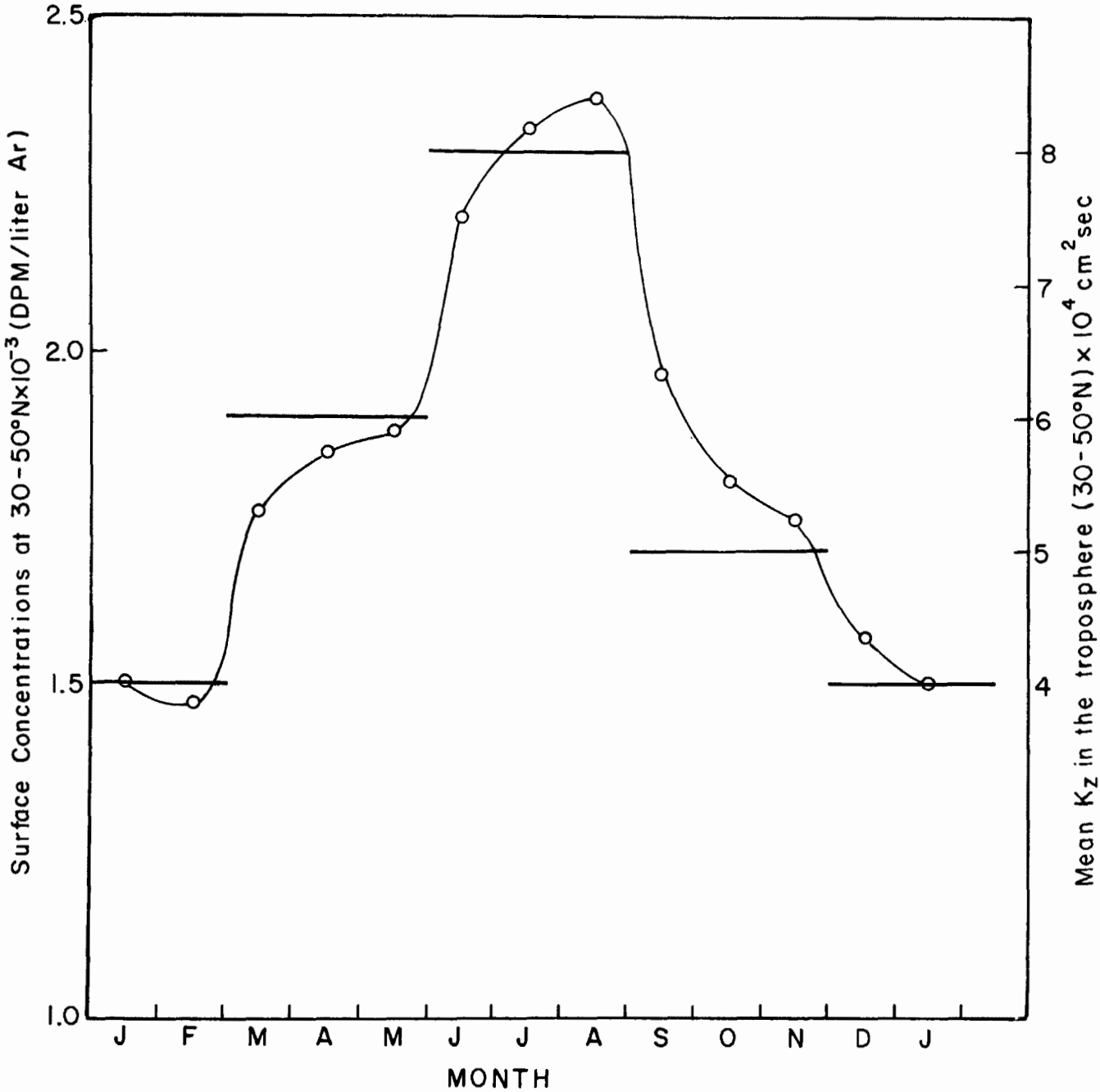

Figure 5. Seasonal variation of ground-level mid-latitude (30-50°N) concentration of ^{37}Ar is shown by the open circles. Mean tropospheric values of the vertical diffusion coefficient (K_z), as used in the model during the indicated quarterly periods, appear as horizontal bars.

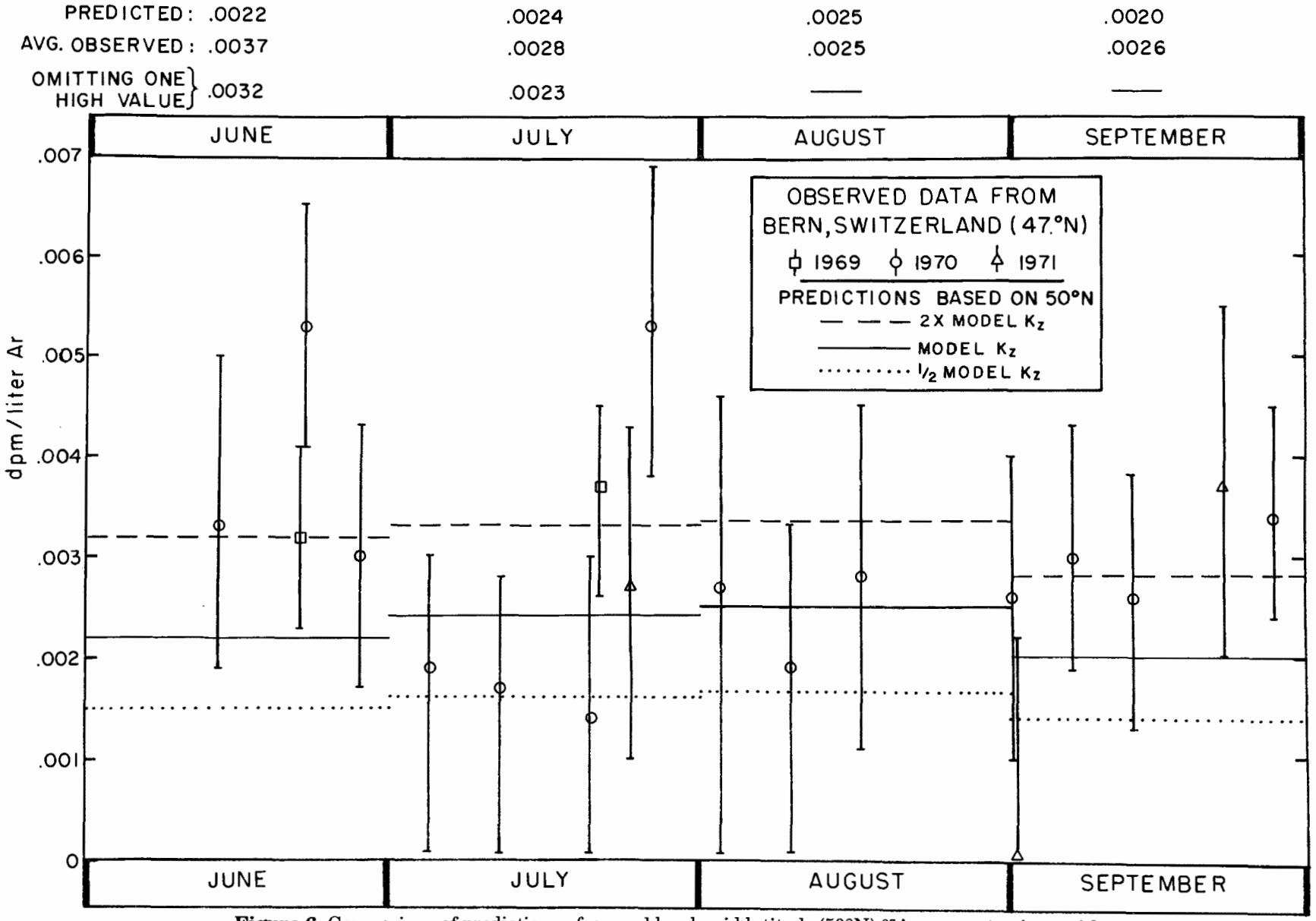

Figure 6. Comparison of predictions of ground-level, mid-latitude (50°N) ^{37}Ar concentrations with selected observations at Bern, Switzerland (47°N), 1969-1971. Predicted values are also indicated for vertical diffusion coefficients (K_z), of twice (dashed lines), and half (dotted lines), those used in the model.

II. Production of Noble Gases

PRODUCTION OF NOBLE GASES BY NUCLEAR FISSION

R.B. Chitwood
Directorate of Licensing
U.S. Atomic Energy Commission
Washington, D.C.

Abstract

The noble gases, krypton and xenon, are produced in significant amounts in operating nuclear reactors. The quantity of noble gas, as well as radioisotopes, produced in the fission process are discussed in relationship to future power requirements. Currently, in light water reactors these gases are released to the earth's atmosphere when the spent fuel is processed to recover plutonium and unused uranium. The impact on the environment of this release from the total industry, along with the state of technology for recovery and retention of these gases, is discussed.

INTRODUCTION

The gaseous effluents from nuclear reactors and spent-fuel reprocessing plants contain significant quantities of both stable and radioactive noble gases. With the continued growth of the nuclear industry in this country and abroad, the magnitude of the effects of the release of these gases to the atmosphere, in comparison with the problems associated with their retention, recovery, and ultimate disposal, are being evaluated by the AEC in observance of the policy that radiation exposures should be maintained "as low as practicable." At least part of the reason for our being at this symposium is to examine in depth the possible problems associated with these effluents, and from the variety of papers presented, obtain a greater insight as to how these problems may best be resolved.

In this paper, which introduces the session on noble gas production, I discuss the production of noble gases by the fission process; relate this production to projected nuclear power requirements and reactor characteristics; point out the potential releases from nuclear reactors and plants reprocessing spent fuels; comment on the impact to the environment as a consequence of noble gas release from the total industry; and, finally, report on the state of technology for the retention and recovery of these gases.

NOBLE GAS PRODUCTION

The principal noble gases produced by nuclear fission are krypton and xenon. The noble gas mixture contains several isotopes of each element. As with all noble gases, the isotopes of krypton and xenon are relatively difficult to confine because they are chemically inert and are relatively insoluble in water.

Table 1 lists the cumulative fission yields for the principal isotopes of Kr and Xe from the fissioning of ^{235}U and ^{239}Pu by thermal and fission spectrum neutrons (Meek, *et al.*, 1972). The fission yields for the Xe isotopes are nearly the same for these two fissionable materials; those for the Kr isotopes show rather large differences.

In the current generation of reactors, about 7.3×10^{-5} moles (1.64 cc at STP) of radioactive krypton and xenon are produced by each megawatt-thermal-day of operation — mainly, ^{85}Kr and ^{133}Xe. In addition to these radioisotopes, the fission process yields four stable isotopes of Kr (i.e., 82, 83, 84, 86), of which 83, 84, and 86 are the most abundant, and seven stable isotopes of Xe (128-132, 134, 136), of which 131, 132, 134, and 136 are the most abundant. After short decay times, the stable isotopes are by far the major part of the total elemental composition — being about 94% for krypton, and greater than 99% for Xe. Negligible amounts of helium (i.e., less than 150 ml/MTU) are produced by the normal burn up in current LWR's and detectible, but insignificant, quantities of ^{41}Ar are found in the off-gas.

The radioisotopes produced in significant quantities, which are of any lasting effect, are ^{85}Kr (with a half-life of 10.76 years) and ^{133}Xe (with a half-life of 5.27 days). For a 1000 MW(e)LWR (approx. 300 MW), at a steady state after three years of operation with 1/3 of the core replaced per year, the accumulated inventory of ^{85}Kr would be about 33 moles (28 scf), which corresponds to an activity of 1.12×10^6 Ci; and about 6.8 moles (5.8 scf) of ^{133}Xe would also accumulate, which corresponds to an activity of 1.65×10^8 Ci. After 150 days of cooling, the ^{85}Kr activity would decrease by only 2%; while the Xe activity would decrease by 5 to 6 orders of magnitude. Total quantities of elemental Kr and Xe would be about 570 and 3200 moles, or 490 and 2730 scf, respectively (Jarry, *et al.*, 1970).

Probably an example more illustrative of noble gas production are the data presented in Table 2 showing the accumulated gas and activity production, at discharge, of typical reactor types. Data are presented for a typical LWR, and a LWR with self-sustaining Pu recycle, an HTGR, and an advanced LMFBR (Bell, 1973 and ORNL 4436, 1970). The elemental activities are also shown — after the anticipated minimum cooling times before reprocessing (i.e., 150, 365, and 90 days for the LWR's, HTGR, and LMFBR, respectively).

Figure 1 shows a typical decay curve after shutdown for xenon and krypton species produced in an LMFBR core (Clark, *et al.*, 1970). The relatively rapid decay of the xenon species, the early leveling out and dominance of krypton (i.e., ^{85}Kr), after about 90 days cooling, are readily apparent.

PROJECTED U.S. NUCLEAR POWER CAPACITY AND NOBLE GAS PRODUCTION

Table 3 is a forecast of the U.S. nuclear electric power generating capacity through the year 2000 (Blomeke, *et al.*, 1973). These data were developed at ORNL as a basis for estimating the quantities of waste generated at spent fuel reprocessing plants. The total capacities predicted at the end of each calendar year are in agreement with those predicted to be most likely in a recent report (WASH-1139, 1972) from the AEC Office of Planning and Analysis. The estimates of the contribution of various reactor types to the total generating capacity are more specific than in the latter report, but within the range considered in developing the material of the report.

The accumulated noble gas quantities and their activities from the reprocessing of spent fuels are shown in Table 4. These data points were calculated using the ORIGEN code (Bell, 1973) and the projected capacities of Table 3. By far, the greatest amount of the radioactivity (5 orders of magnitude) is due to ^{85}Kr. Note that the krypton activities are given in mega-curies while the xenon activities are in curies. The ^{85}Kr is only about 5 to 7% of the total volume of krypton generated; while the total xenon generated is 8 to 9 times greater in volume than the total krypton, but contributes only a very small fraction of the total activity.

POTENTIAL RELEASES FROM NUCLEAR REACTORS

A small fraction (usually very much less than 1%) of the total noble gas fission products generated within a nuclear reactor is released at nuclear power plants as a result of fission of "tramp uranium" on the surfaces of fuel elements and minor leakage from fuel rods. The gaseous effluents contain, among other radionuclides, ^{85}Kr, ^{131m}Xe, ^{133m}Xe, and ^{133}Xe. Since the gamma radiation energy from the short-lived xenon radioisotopes is a significant contributor to the potential whole-body exposure to persons living in the vicinity of a reactor site, a substantial reduction in potential off-site exposure can be obtained by the retention of the noble gases for a sufficient period to allow the short-lived xenon isotopes to decay to insignificant amounts. In pressurized water reactors it has been feasible to provide for the holdup of these gases for one to two months before discharge; after these times, only ^{85}Kr and ^{133}Xe contribute significantly to the radioactivity of the effluent. In boiling water reactors it has been economically difficult, until recently, to provide for gas holdup times greater than about 30 min. due to the leakage of large volumes of gas into the system through the steam condenser; the gaseous effluent from a BWR, therefore, contains short-lived isotopes of xenon and krypton in addition to the ^{85}Kr and ^{133}Xe. Now, a separation process for the removal of noble gases from the reactor effluent using charcoal beds to hold up the gas for decay may be applied to the main condenser off-gas after the normal 30-minute holdup of this stream.

The isotopic compositions of the krypton and xenon mixtures in gaseous effluents are dependent on the irradiation history of the reactor fuel and on the age of the fuel at the time of release. The effect of decay time on the "equilibrium mixture" of noble gases (defined by Smith, 1960) as that present in the fuel after irradiation for a month or longer with all isotopes except 10.76 yr half-life ^{85}Kr in isotopic equilibrium) is shown in Table 5 (Blomeke, *et al.*, 1969).

In the case of PWR's, while there is a small continuous leak of noble gases from the primary system to the steam generator, and thence to the atmosphere, the bulk of the noble gases leaked from the fuel rods is released when the primary coolant is let-down for chemical and volume control. These gases are then collected in decay tanks until they can be released at a controlled rate through HEPA filters to the atmosphere. A typical 1100 MW(e) PWR, using an off-gas decay time of 45 days, has an annual release of 3900 Ci of noble gases — including 970 Ci of ^{85}Kr and 2700 Ci of ^{133}Xe (WASH 1258, 1973). Annual exposures to individuals at the site boundary are estimated at less than 5 mrem (WASH 1258, 1973).

Table 6 lists the predicted quantities of individual radioactive noble gas isotopes that might be released in the absence of a separation or delaying process at the site of a 1100 MW(e) BWR (WASH 1258, 1973). Table 7 shows the predicted total annual amounts of Xe and Kr that would be encountered by a process for separating them from the main condenser exhaust stream of such a reactor (Trevorrow, 1973). The total amounts of Xe and Kr radioisotopes add up to about 9×10^{-3} moles each — rather small quantities in spite of the corresponding large numbers of curies of radioactivity. The concentrations of Xe and Kr in the air stream (assumed to be 20 scfm) are not significantly higher than the normal concentrations of Xe and Kr in air, 0.087 and 1.14 ppm, respectively (Trevorrow). To meet the criteria of "as low as practicable" exposure, and to give annual exposures to individuals at the site boundary of less than 5 mrem, the gaseous effluent from a 1100 MW(e) BWR may have to be put through a charcoal delay system (WASH 1258, 1973).

POTENTIAL RELEASES AND EXPOSURES FROM FUEL REPROCESSING

Currently, all of the noble gas fission products generated within nuclear power reactors are discharged ultimately to the atmosphere, following interim holdup for decay of short-lived radionuclides. The experience has been that greater than 99% of the gases are released when the spent reactor fuel is chopped up and dissolved at a spent fuel reprocessing plant. Since the fuel is stored at least 150 days before reprocessing, however, the only noble gas radionuclide of significance in the effluent is ^{85}Kr.

The radiation exposures resulting from the release of noble gas fission products from reactors and reprocessing plants to the atmosphere have been small as compared with current guidelines for population exposure (AEC, DRO, 1973; Rogers, *et al.*, 1970; and ORNL 4451, 1970). However, in continuing observance of the policy that radiation exposures should be maintained "as low as practicable," the AEC has funded development of systems for minimizing the release of noble gas nuclides to the atmosphere.

Although it may seem that the total curies of ^{85}Kr released in the gaseous effluent from a fuel reprocessing plant is large, the kind of radiation and its energy results in prospective whole-body exposures to persons from ^{85}Kr that is relatively low compared to the radiation from the short-lived xenon radioisotopes present when gases are released from a reactor with short cooling times. Like all the noble gases, ^{85}Kr is chemically inert under normal conditions, and relatively insoluble in normal fluids. Therefore, it does not deposit in the environment, but becomes dispersed in the atmosphere. Because it is predominantly a beta emitter (β max. = 0.67 MeV), exposure requires immersion in the passing plume; the resulting dose is primarily to exposed skin surface. The beta dose to the lens of the eye is filtered by the eye structure to insignificance. The internal exposure to surface lung tissue from ^{85}Kr in the lungs is only about twice the whole-body gamma exposure from 2π immersion. The gonadal dose, which is approximately 2.3% of the surface skin dose, results from the 0.41% of the disintegrations that yield a 0.514 MeV gamma photon. The whole-body dose is about 1.4% of the surface skin dose (Kirk, 1972). The average annual potential whole-body exposure from ^{85}Kr near the site boundary of either the MFRP or the BNFP is expected to be 1% or less of the exposure an individual would receive from natural background radioactivity (AEC Docket 50-268 and 50-332a).

Table 8 shows the exposures to the population in the northern hemisphere that would result from the quantitative release of ^{85}Kr produced in nuclear reactors (Nichols, *et al.*, 1971). The model from which the estimates were made assumes all nuclear power to be generated in the northern hemisphere, that the exposure within relatively short times after release can be described by the Gaussian plume dispersion model, and that later exposures would result from steady circulation of the volume of air in the northern hemisphere.

To put the exposures shown in Table 8 in perspective, Table 9, which was taken from the November 1972 BEIR report, gives a summary of whole-body dose rate estimates for 1970 in the United States (NRC, 1972). It is seen that the average dose rate from all causes is about 182 mrem/yr; annual exposures in millions of man-rems are about 37.4.

RETENTION, RECOVERY AND ULTIMATE DISPOSAL OF NOBLE GASES

Several processes are available or under development for the retention or recovery of noble gases from off-gas streams of nuclear reactors of fuel reprocessing plants. These include adsorption on charcoal at ambient and cryogenic temperatures, cryogenic distillation, selective adsorption in fluorocarbons (chlorofluoromethanes), selective permeation through membranes, and clathrate precipitation (Nichols, *et al.*, 1971). Charcoal adsorption is effective for interim holdup of xenon and krypton. The two most promising processes for recovery are cryogenic distillation and selective adsorption in fluorocarbons. Processes that incorporate adsorption on low temperature charcoal and cryogenic distillation have been demonstrated at the Idaho Chemical Processing Plant (Bendixsen, *et al.*, 1973). A process utilizing selective adsorption in fluorocarbons has been undergoing engineering development for several years at the Oak Ridge Gaseous Diffusion Plant (Stephenson, *et al.*, 1972).

Systems for the hold-up or retention of the noble gases from the reactor's gaseous effluent are not complex because the gaseous effluent is essentially free of chemical impurities. Economically competitive systems for holdup (activated charcoal beds), and for retention (fluorocarbon absorption or cryogenic systems) are currently available for treating the gaseous effluents from nuclear reactors.

The gaseous effluents from fuel reprocessing plants, however, contain chemical constituents such as H_2 H_20, N_20, NO, NO_2, HNO_3, CO, CO_2, I_2. F_2, particulates, and organics. These must be removed before the process off-gas can be safely processed in fluorocarbon or cryogenic systems to remove the noble gases. The recovery of noble gases from an air stream is within the capability of present technology, but the combined unit operations relevant to removal of chemical impurities, recovery of the noble gases, and the packaging and disposal of the recovered noble gases, are not yet adequately demonstrated for application in a fuel reprocessing plant. Early demonstration in a radioactive pilot plant is desirable.

In general, the principal requirement for a commercial krypton removal system is reliability; i.e., a system relatively free of operating and maintenance problems, and concomitant personnel exposure. Otherwise, the desired benefits expected to result from high overall recovery efficiency will not be attained, and the prospective benefit could be offset by: (1) increased exposures to plant employees; and (2) higher exposures to certain population groups — resulting from puff releases which allow the escape to the environs of accumulated ^{85}Kr inventories from the system.

Cryogenic distillation provides an effective, continuous, small-size system for the separation of gases based upon their relative volatility. This type of process is used commercially for the isolation of the components of air, and is being used intermittently to remove radioactive xenon and krypton from a 20-scfm off-gas stream at the Idaho Chemical Processing Plant. This process is capable of recovering krypton and xenon in a relatively pure form suitable for bottling in gas cylinders. In the Idaho operation (during Fiscal 72), while overall recovery efficiencies were less than 50%, recovery efficiencies in the cryogenic portion of the operation approached 100% (Bendixsen, *et al.*, 1973). It should be noted that the process was designed and operated as a production facility, and was not intended as a demonstration of efficient noble gas removal.

Until recently, demonstrations of the fluorocarbon absorption system have been limited to the recovery of noble gases from a relatively pure air stream — such as the gaseous effluents from a reactor. Recent work, however, has been concerned with carrier gases other than air, the effects of noble gas concentrations, and the effects of various impurities such as carbon dioxide, iodine, methyl iodide, and the nitrogen oxides on the absorption process. The data show that the process can be operated efficiently at low- and high-

concentrations of krypton; can remove xenon as effectively as krypton; and can separate the noble gases from carrier gases such as nitrogen, argon, helium and hydrogen (Stephenson, *et al.*, 1972). This process continues to separate krypton efficiently when the feed becomes contaminated with nitrogen oxides and carbon dioxide; and, in fact, has a high tolerance for these impurities. Furthermore, it appears that any iodine and methyl iodide passing into the system are collected in the solvent. Systems for solvent purification and recovery may have to be developed. Additional studies are also needed to investigate irradiation effects, and the long-term cumulative effects of impurities in the fluorocarbon system.

Ultimately, the recovered noble gases will have to be disposed of. Initially, it is probable they will be collected in high pressure gas cylinders. This presents safety issues relating to how and whether these gas bottles can be stored at a plant site, and how to eventually dispose of them. First of all, criteria will have to be developed for assuring acceptable packaging and storage of the bottled ^{85}Kr at a site. Secondly, the pressurized gas containers will have to meet the hypothetical accident standards of 10 CFR Part 71 for shipments of "large quantities" of radioactive gas off-site; specifically, with respect to release limits in the event of severe impact and fire. Thirdly, appropriate facilities for long-term storage of the gas cylinders until the ^{85}Kr has decayed must be designed and built. Alternative methods that have been considered are to place the gas cylinders in deep sections of the ocean for long term decay, or injecting the gas into deep subsurface stratum where it would decay before it migrated to the surface.

There remains the question as to whether the benefits derived from noble gas recovery and disposal on a large scale are worth the costs and risks. The additional exposure entailed by releasing the ^{85}Kr to the atmosphere, even up to the year 2000, would be less than 0.1% of the 125 mrem per year whole-body exposure from natural causes. In addition, the risks of possible exposure of some segments of the population to high levels of radiation from accidental releases of noble gases would appear to be significant. The risks of exposures from accidental releases are present, not only during the recovery operations themselves, but also during the one hundred or more years of storage required for the decay of the ^{85}Kr activity to a negligible level. Moreover, to achieve a significant reduction in exposure from the ^{85}Kr that may accumulate in the atmosphere, it will be necessary to have international agreement that ^{85}Kr will not be released to the atmosphere. Otherwise, by the year 2000, about 6×10^9 Ci of ^{85}Kr will have accumulated in the atmosphere, of which less than one-third will be from the United States. Given the present state-of-the-art, it would appear that we can defer the decision as to whether or not we should require the removal and recovery of ^{85}Kr until a safe and reliable system is developed — and do so without undue risk to the environment. By designing fuel reprocessing plants so that krypton recovery systems could be added, industry is preserving the option to add such systems in the event that a satisfactory system is demonstrated, and the benefits to be gained warrant such an investment (AEC Docket 50-332b).

REFERENCES

Advisory Committee on the Biological Effects of Ionizing Radiations, Report of; Division of Medical Sciences, National Academy of Sciences, National Research Council (NRC), Washington, D.C., (1972), *The Effects on Populations of Exposures to Low Levels of Ionizing Radiation,* p. 19.

Bell, M. J., (1973), *ORIGEN — The ORNL Isotope Generation and Depletion Code,* USAEC Report ORNL-4628.

Bendixsen, C.L., F.O. Geiman and R.R. Hammer, (1973), *1972 Operation of the ICPP Rare Gas Recovery Facility,* ICP-1023, March, 1973.

Blomeke, J.O. and F.E. Harrington, (1969), *Management of Radioactive Wastes at Nuclear Power* Stations, ORNL 4070, February, 1969.

Blomeke, J.O. and J.P. Nichols, (1973), *Commercial High-Level Waste Projections,* USAEC Report ORNL-TM-4224, May, 1973.

Clark, W.E. and R.E. Blanco, (1970), *Encapsulation of Noble Fission Product Gases in Solid Media Prior to Transportation and Storage,* USAEC Report ORNL-4473, February, 1970.

Directorate of Licensing, Fuels and Materials, USAEC, *Safety Analysis Report, Barnwell Nuclear Fuel Plant,* AEC Docket No. 50-332b.

Directorate of Licensing, Fuels and Materials, USAEC, (Allied Gulf Nuclear Services), *Draft Environmental Statement, Barnwell Nuclear Fuel Plant,* AEC Docket No. 50-332a.

Directorate of Licensing, Fuels and Materials, USAEC, (G.E. Co.), *Final Environmental Statement, Midwest Fuel Recovery Plant,* AEC Docket No. 50-268.

Directorate of Regulatory Operations, USAEC, (1973), *Report on Releases of Radioactivity in Effluents and Solid Wastes from Nuclear Power Plants for 1972,* AEC, DRO, August, 1973.

Directorate of Regulatory Standards, USAEC, (1973), Final Environmental Statement concerning *Proposed Rules Making Action: Numerical Guides for Design Objectives and Limiting Conditions for Operation to Meet the Criterion 'As Low As Practicable' for Radioactive Materials in Light-Water-Cooled Nuclear Power Reactor Effluents,* WASH-1258, Vol I, July, 1973.

Forecasting Branch: Office of Planning and Analysis, USAEC, (1972), Nuclear Power 1973-2000, WASH-1139, December, 1972.

Jarry, R.L. and M.J. Steindler calculated (Dec. 1971) from atom yield numbers of Vartaressian, K.A. and L. Burris, (1970), *Fission Product Spectra from Fast and Thermal Fission of ^{235}U and ^{239}Pu,* USAEC Report ANL-7678, March, 1970.

Kirk, W.P., (1972), *Krypton-85, A Review of the Literature and an Analysis of Radiation Hazards,* Environmental Protection Agency, Office of Research and Monitoring, January 1972, p. 18.

Meek, M.E. and B.F. Rider, (1972), *Compilation of Fission Product Yields, Vallecitos Nuclear Center-*1972, NEDO-12154, January, 1972.

Nichols, J.P. and F.T. Binford, (1972), *Status of Noble Gas Removal and Disposal,* USAEC Report ORNL-TM-3515, August, 1971.

ORNL Chem. Tech. Div. Staff, (1970), *Aqueous Processing of LMFBR Fuels — Technical Assessment and Experimental Program Definition,* USAEC Report ORNL 4436, June, 1970.

ORNL Staff, (1970), *Siting of Fuel Reprocessing Plants and Waste Management Facilities,* ORNL-4451, July, 1970.

Rogers, L. and C.C. Gamertsfelder, (1970), *U.S. Regulations for the Control of Releases of Radioactivity to the Environment in Effluents from Nuclear Facilities,* IAEA-SM-146/8, August 10-14, 1970.

Smith, J.M., (1960), *Release of Radioactive Wastes to the Atmosphere,* General Electric Company, San Jose, Calif.

Stephenson, M.J., J.R. Merriman, D.I. Dunthorn and J.N. Pashley, (1972), *Experimental Demonstration of the Selective Absorption Process for Krypton-Xenon Removal,* Proceedings of the 12th AEC Air Cleaning Conference, Oak Ridge, Tenn., August 28-31, 1972, pp.11-25 (KL-6294).

Trevorrow, L.E. and M.J. Steindler, (1973), Personal Communication.

TABLE 1. Cumulative Fission Yields for Krypton and Xenon (Meek, *et al.,* 1972).

Isotope	Half-Life	Fission Yield (% of Total Fissions)			
		Thermal Neutrons		Fission Spectrum Neutrons	
		^{235}U	^{239}Pu	^{235}U	^{239}Pu
Krypton					
83m	1.86 hrs.	0.54	0.29	0.63	0.35
83	Stable	0.54	0.29	0.63	0.35
84	Stable	1.00	0.47	1.03	0.53
85m	4.4 hrs.	1.33	0.60	1.43	0.64
85	10.76 yrs.	0.29	0.14	0.32	0.14
86	Stable	1.94	0.74	1.86	0.84
87	1.3 hrs.	2.37	0.95	2.56	1.11
88	2.8 hrs.	3.64	1.34	3.48	1.37
89	3.2 min.	4.64	1.44	4.57	1.65
90	32 sec.	4.83	1.80	4.57	1.76
Xenon					
131m	12.0 days	0.017	0.023	0.019	0.025
131	Stable	2.77	3.89	3.21	4.20
132	Stable	4.13	5.16	4.51	5.37
133m	2.26 days	0.19	0.19	0.19	0.19
133	5.27 days	6.77	6.84	6.60	6.82
134	Stable	7.19	7.22	6.98	7.26
135m	15.7 min.	1.05	1.06	1.01	1.90
135	9.2 hrs.	6.72	7.22	6.45	7.45
136	Stable	6.12	6.55	5.84	6.83
137	3.8 min.	5.94	6.05	6.14	5.78
138	14.2 min.	6.24	5.14	6.23	3.71
139	40 sec.	4.96	4.36	5.40	5.24

TABLE 2. Effect of Reactor Type on Noble Gas Production.

Reactor	KRYPTON			XENON		
	Elemental Accumulation at Discharge	Elemental At Discharge	Activity After Decay(e)	Elemental Accumulation at Discharge	Elemental At Discharge	Activity After Decay(e)
	scf/MT	Ci/MT	Ci/MT	scf/MT	Ci/MT	Ci/MT
LWR- (a)	3.72	4.49×10^{6}	1.11×10^{4}	35.8	1.01×10^{7}	4.04
LWR W Pu Recycle (b)	3.36	4.35×10^{6}	1.01×10^{5}	35.8	1.00×10^{7}	4.01
HTGR (c)	20.2	1.47×10^{7}	5.97×10^{4}	96.2	1.66×10^{7}	1.95×10^{-5}
LMFBR (d)	7.51	7×10^{7} (f)	2.44×10^{4}	67.6	7×10^{7} (f)	6.49×10^{9}

(a) Fuel (3.19% enriched U); 38 MW/MTU; 33,000 MWD/MTU; 3.79×10^{13}n/Cm^2 sec.
(b) Self-sustaining Pu Recycle; 38 MW/MT (U+Pu); 33,000 MWD/MT (U+Pu); 3.29×10^{13}n/Cm^2 sec.
(c) 64.57 MW/MT (Th+U); 94,271 MWD/MT (Th+U); 7.25×10^{13}n/Cm^2 sec.
(d) 148.15 MW/MT (U+Pu); 80,000 MWD/MT (U+Pu); 5.15×10^{15}n/Cm^2 sec.
(e) Decay Periods: LWR's-150 days; HTGR-365 days; LMFBR-90 days.
(f) Includes short-lived krypton and xenon isotopes (cf. Tables 5 and 6).

TABLE 3. Forecast of U.S. Nuclear Electric Power Generating Capacity, GW(e) (Net) (Blomeke, *et al.*, 1973).

Year	End of Calendar Year	Average in Fiscal Year			
		LWR	HTGR	LMFBR	Total
1970	5.0(a)				
71	8.1(a)	5.2(a)			5.2
72	17	8.2(a)			9.2
73	31	17.5			17.5
74	45	31.2			31.2
75	55	45.3			45.3
76	63	55.1			55.1
77	76	62.9			62.9
78	94	76.0			76.0
79	114	94.4			94.4
1980	134	111.7	2.2		113.9
81	159	129.1	5.3		134.4
82	185	149.9	8.8		158.7
83	213	168.1	16.6		184.7
84	245	187.7	25.0		212.7
85	281	209.8	34.9		244.7
86	318	235.0	45.7		280.7
87	362	260.9	56.8		317.7
88	408	289.6	69.1	3.5	362.2
89	453	318.3	81.4	8.5	408.2
1990	504	344.9	92.8	15.5	453.2
91	559	374.0	105.2	25.0	504.2
92	617	404.1	118.1	37.0	559.2
93	676	432.1	130.0	55.0	617.2
94	740	456.3	140.9	79.0	676.2
95	807	476.2	151.1	113.0	740.3
96	879	490.7	160.7	156.0	807.4
97	955	505.0	170.6	203.0	878.6
98	1,033	519.7	181.1	254.0	954.8
99	1,117	533.1	191.0	309.0	1,033.1
2000	1,201	546.3	201.2	370.0	1,117.5

(a) Operating data from *Nucleonics Week*.

TABLE 4. Accumulated Noble Gases From Reprocessing (a).

Year	KRYPTON Total Elemental Accumulation		KRYPTON Activity (b)(c)	XENON Total Elemental Accumulation		XENON Activity (c) ^{131m}Xe ^{133}Xe	
	moles	scf	mCi	moles	scf	mCi	Ci
1973	6.41×10^2	5.47×10^2	1.52	5.92×10^3	5.05×10^3	13.0	0.01
1975	3.98×10^3	3.39×10^3	9.30	3.68×10^4	3.14×10^4	73.9	0.06
1980	3.68×10^4	3.14×10^4	80	3.43×10^5	2.93×10^5	337	0.3
1985	1.20×10^5	1.02×10^5	241	1.16×10^6	9.89×10^5	734	0.5
1990	2.83×10^5	2.41×10^5	540	2.60×10^6	2.22×10^6	2,820	96
1995	7.75×10^5	4.90×10^5	1,040	4.81×10^6	4.10×10^6	14,600	600
2000	1.01×10^6	8.62×10^5	1,720	7.89×10^6	6.73×10^6	50,100	2,780

(a) The values shown are for the total quantities of noble gas releases over the years to that date with the activities corrected for decay.

(b) All krypton activity is due to ^{85}Kr.

(c) Assuming cooling period of 150, 365 and 90 days for the LWR, HTGR and LMFBR fuels, respectively.

TABLE 5. Effect of Decay Time on the Characteristics of Radioactive Noble Gas Mixtures from ^{235}U Fission.

Isotope	Half-Life	Percent of Total Activity After Indicated Decay Time					
		2 min.	30 min.	2 hrs.	1 day	3 days	60 days
^{90}Kr; ^{139}Xe	32 sec.; 41 sec.	3.0					
^{89}Kr	3.2 min.	8.2	0.1				
^{137}Xe	3.8 min.	11.3	0.1				
^{135m}Xe	15 min.	4.6	2.0	0.1			
^{138}Xe	17 min.	14.1	7.5	0.3			
^{87}Kr	1.3 hrs.	7.3	9.4	5.7			
^{83m}Kr	1.86 hrs.	1.3	1.8	1.4			
^{88}Kr	2.8 hrs.	10.2	14.8	13.5	0.2		
^{85m}Kr	4.4 hrs.	4.2	6.3	6.7	0.5		
^{135}Xe	9.2 hrs.	17.2	27.2	32.2	14.7	0.5	
^{133m}Xe	2.3 days	0.5	0.8	1.0	1.7	1.5	
^{133}Xe	5.27 days	18.0	29.7	30.0	82.1	96.7	2.5
^{131m}Xe	12.0 days	0.1	0.2	0.2	0.5	0.8	1.0
^{85}Kr	10.7 yrs.	0.1	0.1	0.1	0.3	0.5	96.5

TABLE 6. Calculated Annual Releases (a) of Noble Gas Isotopes from a 1100 MW(e) BWR (WASH 1258, 1973).

Isotope	Half-Life	Decay Mode	Ci/yr
^{89}Kr	3.2 min.	β^-	4.8×10^3
^{87}Kr	1.3 hrs.	β^-	3.4×10^5
^{83m}Kr	1.9 hrs.	γ	7.5×10^4
^{88}Kr	2.8 hrs.	β^-	4.3×10^5
^{85m}Kr	4.4 hrs.	0.19γ	1.4×10^5
		$0.81\beta^-$	
^{85}Kr	10.76 yrs.	β^-	7.7×10^2
^{137}Xe	3.8 min.	β^-	1.7×10^4
^{135m}Xe	15.6 min.	γ	2.1×10^5
^{138}Xe	17 min.	β^-	7.4×10^5
^{135}Xe	9.2 hrs.	β^-	7.3×10^5
^{133m}Xe	2.3 days	γ	9.3×10^3
^{133}Xe	5.27 days	β^-	2.6×10^5
^{131m}Xe	11.9 days	γ	6.7×10^2
TOTAL			2.9×10^6

(a) After a 30 min. holdup, experience with smaller BWR's indicate actual releases are much less (Trevorrow, 1973, and AEC, DRO, 1973).

TABLE 7. Estimated Total Amounts of Xenon and Krypton Released Annually from 1100 MW(e) BWR.

Sources	Xenon		Krypton	
	moles	scf	moles	scf
Air leak (a)	1.2	1.0	15	12
Fission Products:				
Radioactive (b)	0.009	0.007	0.009	0.007
Stable	0.9	0.7	0.1	0.08

(a) Based on 20 scfm air flow.

(b) Based on annual emission of 3×10^6 Ci of noble gas isotopes.

TABLE 8. Estimates of Population Doses in the Northern Hemisphere That Would Result From Quantitative Release of ^{85}Kr Produced in Nuclear Reactors.

	1970	1975	1980	1985	1990	1995	2000
Installed Nuclear Capacity:							
U.S., GW(e)	6.1	63	149	281	481	788	1,294
World, GW(e)	24	125	353	827	1,660	2,900	4,500
Percent LMFBR's					7.7	31.5	58.7
Thermal Efficiency	0.325	0.325	0.325	0.325	0.332	0.353	0.378
Average Capacity Factor	0.714	0.754	0.761	0.754	0.742	0.716	0.700
Ci of ^{85}Kr/MWD(Th)	0.342	0.342	0.342	0.342	0.340	0.332	0.323
^{85}Kr Produced Annually:							
U.S., megacuries	1.68	18.3	43.6	81.5	134	194	284
World, megacuries	6.59	36.3	103	240	461	713	988
Total ^{85}Kr Accumulated in Northern Hemisphere, MCi	55	116	339	901	2,070	3,870	6,280
Relative Population	1.0	1.09	1.19	1.30	1.41	1.54	1.68
Population Whole-Body Dose, millions of man-rem	0.003	0.007	0.022	0.062	0.15	0.31	0.53
Average Whole-Body Dose Rate, mrem/yr	0.0008	0.002	0.005	0.013	0.031	0.056	0.09
Average Skin Dose Rate, mrem/yr	0.055	0.13	0.37	0.96	2.2	4.0	6.4

TABLE 9. Summary of Estimates of Annual Whole-Body Dose Rates in the United States (1970).

Sources	Average Dose Rate* (mrem/yr)	Annual Man-Rems (in millions)
Environmental:		
Natural	102	20.91
Global Fallout	4	0.82
Nuclear Power	0.003	0.0007
Subtotal	106	21.73
Medical:		
Diagnostic	72**	14.8
Radiopharmaceuticals	1	0.2
Subtotal	73	15.0
Occupational	0.8	0.16
Miscellaneous	2	0.5
TOTALS	182	37.4

*Note: The numbers shown are average values only. For given segments of the population, dose rates considerably greater than these may be experienced.

** Based on the abdominal dose.

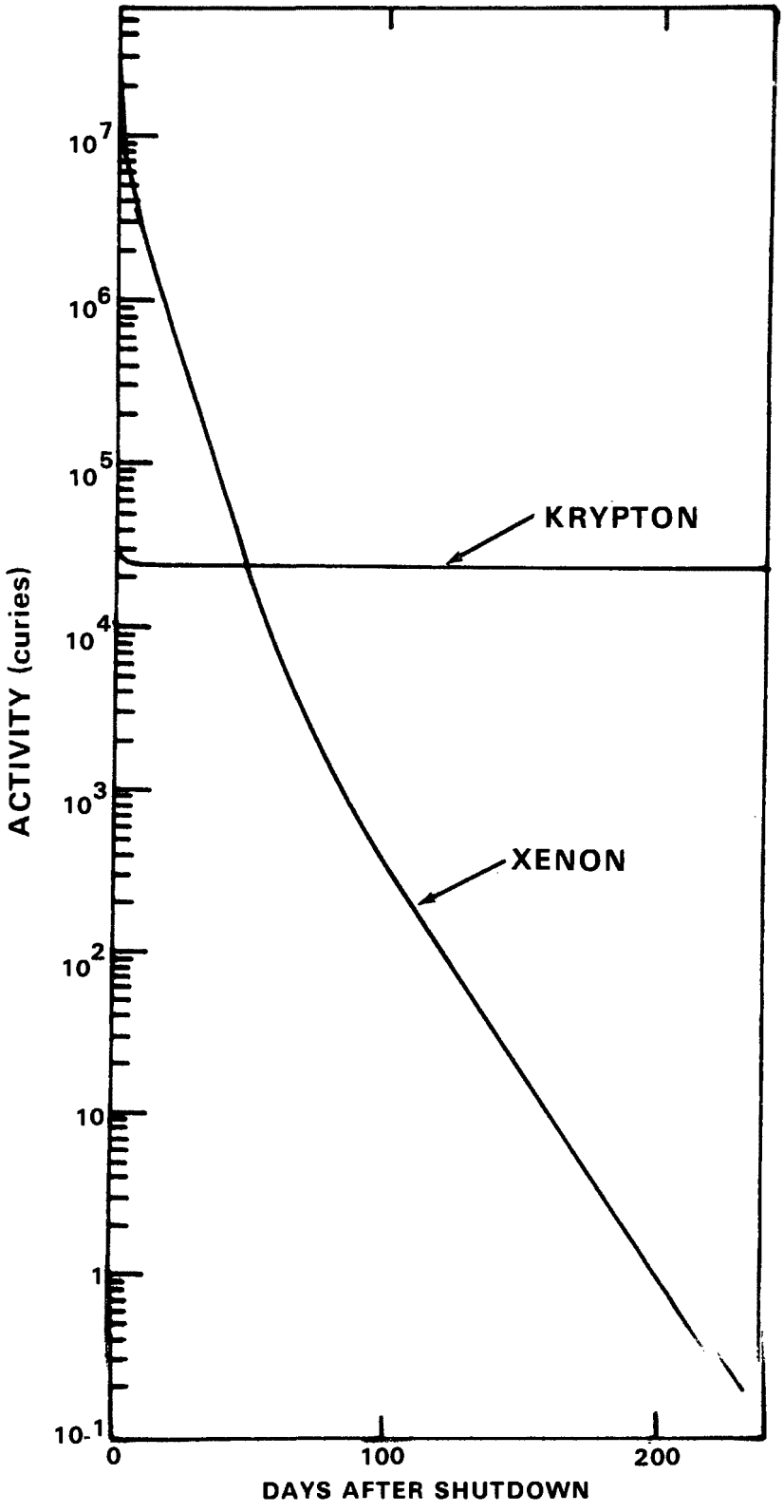

Decay of Xe and Kr After Shutdown (LMFBR Core)

Figure 1.

EXPERIENCE WITH RADIOACTIVE NOBLE GASES FROM BOILING WATER REACTORS

J. M. Smith
Nuclear Energy Division
General Electric Company
San Jose, California 95114

Abstract

Experience with radioactive noble gases associated with the operation of boiling water reactors supplied by the Nuclear Energy Division of the General Electric Company spans a fifteen-year period. This experience has been characterized by minor leakage of fission product radioactive noble gases through fuel cladding defects as the source term to reactor water. In the open cycle boiling water reactor, the radioactive gases transfer quantitatively with the steam flow to the turbine and condenser. The principal removal point of the noble gases from the process is via the main condenser air ejector system for continuous removal of any non-condensable gases. Other minor noble gas pathways from the process include the turbine gland seal system, the condenser mechanical vacuum pump, and any minor leakage of process fluids to ventilated building spaces.

Experience indicates that the fission product radioactive noble gases mixture available in the steam can vary across the spectrum from the equilibrium to the recoil mixture, as a function of the physical characteristics of the fuel cladding defects. Thus the effectiveness of effluent treatment systems can vary due to fuel performance.

On the ejector pathway, most operating boiling water reactors have been provided with a normal thirty-minute decay system prior to discharge to the atmosphere via a stack of a height appropriate with consideration of adjacent structures. The nominal decay provides an activity reduction of a factor of about 25 on the usually observed gas mixture. Experience over the years at operating plants indicates that radioactive noble gas emissions cause an estimated annual dose to nearest neighbors of the order of 1 to 3% of the appropriate permissible dose of 500 mrem per year, and thus in the range of proposed "as low as practicable" dose objectives for radioactive noble gases.

Augmented treatment systems have been developed in recent years to provide a high degree of assurance that doses due to radioactive noble gases emissions will be well below currently proposed "as low as practicable" dose objectives. Achievement of substantial additional decay time by dynamic adsorption in charcoal beds is considered the most applicable approach. Systems currently available are based on the design and operational experience of the adsorption system in service at the KRB Plant in Germany since 1966. Charcoal systems may be operated at ambient or low (~ 0°F) temperatures with an activity reduction capability of a factor of 10^2 to 10^4 compared to a nominal 30-minute decay system. Thus, neighbor dose from the air ejector effluent becomes negligible. Many plants currently in design and operation will employ augmented systems of this type to minimize dose from radioactive noble gas emission.

INTRODUCTION

General Electric Company now has fifteen years of experience with the fission product noble radiogases associated with operation of the direct cycle boiling water power reactors supplied by its Nuclear Energy Division. With the use of the direct cycle, particular attention has been given to the study of noble radiogas behavior in the process system, and the evaluation of the significance of emissions of radioactive noble gases via the several effluent pathways. This review paper summarizes the work of many over this time span, with some indication of the contributors being shown by the authors listed in the references.

Experiences at existing plants with conservative design objectives have indicated a high degree of compliance concerning releases of noble radiogases to the environment. In consequence, off-plant radiation doses have been very small compared to permissible dose or natural background.

The GE objective is to minimize, to the extent practicable, the radioactivity content of effluents. Monitoring the environs of BWR facilities is performed as an audit on effluent controls and to provide data from which dose to the general public may be determined. Augmented systems have been developed, and improved operating methods have been established, to provide assurance for new larger plants that the dose to the public is insignificant compared to both natural background and permissible dose.

THE DIRECT CYCLE BOILING WATER REACTOR SYSTEM

In the single cycle (or direct cycle) BWR system, water is boiled within the reactor vessel to produce saturated steam that passes through internal steam separators and dryers before proceeding directly into the turbine. (The steam enters the high-pressure turbine casing at about 965 psia and 546°F.) Steam leaving the high-pressure casing passes through combined steam reheaters and moisture separator units before admission to the lower pressure casings.

The main condenser provides deaeration and is followed by a demineralizer through which all the condensate passes prior to entering the feed heaters.

The demineralizer system removes the corrosion products produced by the turbine and condenser. It also protects the reactor against condenser tube leaks and removes other sources of impurities which may enter the system in the make-up water.

The power cycle uses a conventional regenerative feedwater system. The feedwater temperature, and the number of feed heaters, are selected in accordance with the normal power plant considerations of power cycle performance and economics.

The required heat transfer is achieved, and the proper steam void content maintained, through the use of external recirculation loops — which have been reduced in number through the use of internal jet pumps. The boiling water reactor system is more fully described in Richards (1967), and Koke, *et al.*, (1972). See also Figure 1 attached.

BWR NOBLE RADIOGAS SOURCES AND PATHWAYS

Water reactor experience has been characterized by minor leakage of fission product noble radiogases through fuel cladding defects as the source term for accumulation in the reactor water. In the direct cycle boiling water reactor, continuous removal occurs as the radiogases transfer quantitatively with the steam flow to the turbine and condenser. The principal removal point of the noble gases from the process is via the main condenser air ejector system for continuous removal of any noncondensible gases. Secondary noble gas pathways from the process include the turbine gland seal system, the condenser mechanical vacuum pump, and any minor leakage of process fluids to ventilated building spaces.

Experience indicates that the noble radiogas mixture available in the steam can vary across the spectrum, from the equilibrium to the recoil mixture, as a function of the physical characteristics of the fuel cladding defects. Thus, the effectiveness of effluent treatment systems can vary due to fuel performance (Williamson, *et* al., 1971; Klepfer, *et al.*, 1972; and Williamson, *et al.*, 1972a,b).

The noble gases initially follow the steam pathways, and then the non-condensible gas pathways after steam condensation. About 99.9% of the reactor steam follows pathways through the turbine and associated equipment to the main condenser. The steam jet air ejector system maintains condenser vacuum and continuously removes non-condensibles, which include hydrogen and oxygen from radiolytic decomposition of reactor water, condenser system air in-leakage, water vapor, and most of the trace quantities of noble gases.

About 0.1% of reactor steam, with associated noble gases, is removed through the turbine gland seal system to a separate condenser. The noncondensible off-gas from this system thus represents a minor, but chronic, emission of noble radiogases. Most BWR plants currently in design will use seal steam from a separate source to minimize radiogas emission.

The presence of radioiodine precursors in process water volumes, such as in liquids being treated for recycling, and in the main condenser during plant shutdowns, generates minor amounts of radioxenons requiring consideration in emission to the atmosphere.

NOBLE RADIOGAS SOURCE TERMS

Definitions of radioactive material source terms are necessary for any power reactor system to provide a basis for design at points in the process, to establish a basis for effluent treatment system design, and for evaluation of the radiological significance of effluents to the environment. For noble radiogases, our early work considered the various mixtures that could be present, and conservatively selected the slowest decaying "equilibrium mixture" as a design basis (Smith, 1960). After several years operation of the first generation BWRs, it was evident that the intermediate "diffusion mixture" was a better representation of actual experience (Smith, *et al.*, 1969). The most recent review (Skarpelos, *et al.*, 1973) indicated that the most appropriate mixture for design and evaluation differed only slightly from the long-used diffusion mixture. The currently established design basis mixture, as shown in Table 1, is representative of operating experience; however, variations in the mixture composition would normally be expected during a typical plant operating history.

The magnitude of the noble radiogas design basis source term was selected by operating experience to be at the level of 100 millicuries per second at the conventionally stated thirty-minute decay time. A design basis value is one which is expected to be approached or exceeded infrequently in plant operation for any extended period. The experience record to date shows that the selected level is reasonably conservative.

DESIGN OBJECTIVE FOR EFFLUENT TREATMENT

In recent years, it has been General Electric's policy and recommendation to use effluent system design which will result in minimal radiation dose to plant neighbors. The design objective is that the increment of dose due to the plant shall be very small compared to either nature of the permissible dose limits; and also small compared to the variations in natural radiation. Based on this, a design objective was selected that no off-site person should receive an additional whole body dose of more than about 5 mrem per year due to the presence of a power plant. This is a design objective, and an operating expectancy, and has been our engineering interpretation of the overall objective of minimizing radiation dose to the extent practicable, as generally recommended by the expert advisory groups (Kent, *et al.*, 1971).

For GE/BWRs currently in operation, the effluent system design objective was that radiation dose to any member of the public should be "well below" the internationally accepted radiation limit of 500 mrem per year to any individual. A specific numerical interpretation of "well below" was not a requirement in any case. The expectancy was that actual performance would be on the order of 5 mrem per year, as averaged over the years of operation.

OPERATING PLANTS EMISSION EXPERIENCE

A number of published reports record the noble radiogas emission experience for all except the most recent years (Blomke, *et al.*, 1968; Kahn, *et al.*, 1970; Kent, *et al.*, 1971; Smith, *et al.*, 1973; and Pelletier, 1973). Table 2 lists actual emissions reported by the plant operators for 1971 and 1972 for all plants except those that just started operation in 1972.

On the principal radiogas removal pathway, the main condenser air ejector off-gas system, most of the operating plants have been provided with a nominal thirty-minute decay system, followed by a HEPA filter and elevated stack release to the atmosphere. The nominal decay period provides an activity reduction of a factor of about 25 on the design basis radiogas mixture as shown in Table 1. Depending on operating conditions, the actual decay time is usually in the range of 30 to 60 minutes. The 1971-72 record shows that the average annual emission for plants with the short-term decay system was about 20 millicuries per second, and that emissions from all plants were less than the design basis source term of 100 millicuries per second. The noble radiogas emissions from pathways other than the air ejector system are estimated to be about one to two percent of the total.

Several of the plants listed provide augmented radiogas decay systems. The Gundremmingen plant has used an ambient temperature charcoal adsorption system since startup (Schrader, *et al.*, 1971; Forster, 1971; Bridenbaugh, *et al.*, 1972). The two plants in Japan initially used storage systems designed to provide about one day decay, and have since changed to ambient temperature charcoal systems. Experience indicates that such systems provide an activity reduction factor of up to about one hundred — compared to the nominal thirty-minute decay system; and thus is an appropriate retrofit for other operating plants to reduce the air ejector emission to the same level as emissions from the other minor pathways.

RELATION OF EMISSION TO DOSE

Estimation of dose from noble radiogases to receptors in the plant environs requires: (1) consideration of the radioisotopes released; (2) the physical properties of the emission plume; (3) the plant site geometry and meteorology; and (4) the location and habits of the receptor. Methods have been developed for dose estimation which show good correlation with actual experience (Stuart, *et al.*, 1967). Proper estimation of effective stack height considers the temperature and flow conditions at the release point. The method includes evaluation of the vertical concentration profile downwind as influenced by atmospheric stability, wind velocity, and wind frequency in each direction, as related to the site size and shape. Dose to a receptor on the ground is estimated by integration of the dose from all levels of the plume under each condition, as dose to a receptor is not directly related to ground-level concentrations.

Estimates are made of the annual average emission rate that would deliver a dose of 500 mrem per year to a receptor at the least favorable location at the site boundary; examples are shown in the "best estimate" column of Table 2. It is noted that the permissible emission rates which are included in plant operating licenses shown in the "Tech Spec" column of Table 2, are conservatively selected in many cases; and therefore, cannot be used directly for "fence-post" exposure estimates. Estimation of dose to any actual neighbor must consider actual location (usually further away and/or in a more favorable direction than the worst "fence-post"), occupancy time, and incidental shielding such as provided by structures. Estimates of the relation of worst "fence-post" exposure to actual neighbor dose for a number of sites show a factor of difference in the range of three to ten. The estimated neighbor doses shown in Table 2 use a factor of difference of five.

Experience over the years shows that, for plants using the nominal thirty minute decay system, estimated neighbor doses are in the order of less than a few percent of the applicable permissible dose of 500 mrem per year; and much less than one mrem per year at plants using charcoal adsorption systems.

AUGMENTED TREATMENT FOR NOBLE RADIOGASES

Augmented treatment systems have been developed in recent years to provide a high degree of assurance that dose due to noble radiogas emissions will be well below currently proposed "as low as practicable" dose objectives. Achievement of substantial additional decay time by dynamic adsorption in charcoal beds is considered the most feasible approach. Systems currently available are based on the design and operational experience of the ambient temperature adsorption system in service at the Gundremmingen plant. Additional research and development work is needed on charcoal adsorption for the air ejector flow for increased retention of radiogases to permit natural radioactive decay prior to release (Smith, *et al.*, 1972; Siegwarth, *et* al., 1972; Michels, *et al.*, 1972; and Head, *et al.*, 1973).

The effective decay time for radiogases in a charcoal system is influenced principally by system flow rate, stream moisture content, and charcoal bed temperature. Work has been in the direction of operating the

adsorber at low temperatures, thereby providing a significant increase in radiogas decay time compared to operating at ambient temperatures.

In a low-temperature charcoal adsorption system, a catalytic recombiner is used to recombine radiolytically dissociated hydrogen and oxygen from the air ejector system. After cooling to approximately 130°F (to strip the condensibles and reduce the volume), the remaining non-condensibles (principally kryptons, xenons, and air) are delayed in a short-term holdup system to permit decay of many of the shorter half-lived gases, and to permit formation of the more important radioactive daughters. The gas is cooled to 45°F and filtered through a high-efficiency filter. The gas is then passed through a desiccant dryer that reduces the dew point to -90°F, and then is chilled to 0°F, to selectively and dynamically adsorb and delay the xenons and kryptons from the bulk carrier gas (principally dry air). See Figure 2 attached.

While the system is designed to produce a gas stream which is below the combustible limit range for hydrogen, gas stream containing-components are designed to be explosion resistant with a basic design pressure of 350 psig. System operating pressure is just above atmospheric, with an input pressure of about 2 psig required for normal system operation.

To provide a high degree of system reliability, and to minimize the effect on plant availability, many system components are provided with redundant equipment. Access for maintenance on the gas stream containing equipment is not a routine requirement. Certain auxiliaries, including the refrigerated glycol system for the chiller, and the closed cycle hot air regeneration system for the desiccant dryer, do require routine maintenance, and are to be located to permit easy accessability.

Assuming the constancy of other parameters affecting holdup time in the charcoal beds, the radiogas delay time due to adsorption will vary inversely as a function of the gas stream flow rate. This flow rate is primarily due to air inleakage to the plant main condensers, and, for a design basis, is taken to be 30 scfm. Plant operation and maintenance which achieves a lesser air inleakage will improve the performance of the charcoal adsorption. Under design basis conditions of flow and temperature, retention times of about two days for kryptons and about six weeks for xenons, are achieved.

Effluent from the charcoal system will vary as a function of the delay times, and also to some extent as a function of variation in the radiogas mixture entering the system. Using the system design basis source term of 100 millicuries per second, and the radiogas mixture shown in Table 1, the effluent under design basis flow conditions would be:

Radiogas	Half-Life	Microcuries per second
^{85m}Kr	4.4 hours	4
^{133m}Xe	5.3 days	34
^{131m}Xe	12.0 days	1
^{85}K	10.7 years	150
	Total	**54**

The other gases listed in Table 1 will have decayed to less than one microcurie per second.

Thus, the low-temperature adsorption system provides an activity reduction factor of about 2000 compared to a nominal thirty-minute holdup system, and a tall stack is no longer essential for this effluent stream. Many plants that will use such a system can safely provide a release point at roof elevation, typically at a height of about 50 meters.

The previously established dose estimation methods have been refined to consider the actual decay scheme of the few radiogases remaining in the effluent. At a typical site, the emission would result in an estimated exposure on the order of 0.05 mrad per year to a site boundary location, and, therefore, an order of 0.01 mrem per year to a neighbor. The dose from long-lived krypton-85 would be only a fraction of this; so there is no technical basis which would require retention. It is noted that the AEC's Environmental Statement on proposed "as low as practicable" regulations, evaluates cases where no ^{85}Kr retention is provided, and concludes that such cases meet the proposed objectives.

Noble radiogas emissions for a modern boiling water reactor are effectively minimized by use of the available technology of charcoal adsorption for the condenser air ejector stream and the separate steam for the turbine equipment sealing system. Residual-leakage-pathway noble radiogas emissions are estimated to produce a neighbor dose of 0.1 to 0.2 mrem per year — below any proposed "as low as practicable" dose objective by an ample margin.

REFERENCES

Blomeke, J. O. and F. E. Harrington, (1968), *Management of Radioactive Wastes at Nuclear Power* Plants, Report ORNL-4070, Oak Ridge National Laboratory.

Bridenbaugh, D. G., R. L. Turner, General Electric Company, and R. Ettemeyer, Kernkraftwerk-RWE-Bayernwerk; (1972), *Five Years of Operation of the Gundremmungen Nuclear Power Plant.* Nuclex 72, Basel, Switzerland, October 1972.

Forster, K., (1971), *Delaying Radioactive Fission Product Inert Gases in Cover Gas and Off-Gas Streams of Reactors by Means of Activated Charcoal Delay Lines.* Kerntechnik 13, Jahrgang No. 5.

Head, R. A., C. W. Miller, and J. E. Oesterle, (1973), *Releases from BWR Radwaste Management* Systems, Report NEDO-10951, General Electric Company, San Jose, California.

Kahn, B., *et al.,* **(1970),** *Radiological Surveillance Studies at a Boiling Water Nuclear Power Reactor,* Report BRH/BER 70-1, U. S. Public Health Service, Washington, D. C.

Kent, C. E., S. Levy and J. M. Smith, General Electric Company, (1971), *Effluent Control for Boiling Water Reactors,* Proceedings of a Symposium, New York, August 10-14, 1970, Environmental Aspects of Nuclear Power Stations, International Atomic Energy Agency, Vienna.

Klepfer, H. H., R. B. Richards, T. Trocki, General Electric Company, (1972), *Fuel Performance in Boiling Water Reactors.* Proceedings of the American Power Conference, Volume 34, Illinois Institute of Technology, Chicago.

Koke, L. C., G. M. Roy, R. E. Brandon, General Electric Company, (1972), *Optimizing the Design of BWR Power Plants.* Proceedings of the American Power Conference, Volume 34, Illinois Institute of Technology, Chicago.

Michels, L. R. and N. R. Horton, General Electric Company, (1972), *Improved BWR Off-Gas* Systems, 12th AEC Air Cleaning Conference.

Pelletier, C. A., (1973), *Results of Independent Measurements of Radioactivity in Process Systems and Effluents at Boiling Water Reactors,* U.S. Atomic Energy Commission, Washington, D.C.

Richards, R. B., General Electric Company, (1967), *Technical Progress in the Design and Construction of Boiling Water Reactors,* XII Nuclear Congress of Rome.

Schroder, H. J., H. Queiser, and W. Rein, *Off-Gas Facility at the Gundremmingen Nuclear Power Plant,* Kerntechnik 13, Jahrgang No. 5.

Siegwarth, D. P. and C. K. Neulander, (1972), *Measurement of Dynamic Adsorption Coefficients for Noble Gases on Activated Carbon,* Report NEDO-12327, General Electric Company, San Jose, California.

Skarpelos, J. M. and R. S. Gilbert, (1973), *Technical Derivation of BWR 1971 Design Basis Radioactive Material Source Terms,* Report NEDO-10871, General Electric Company, San Jose, California.

Smith, J. M., (1960), *Release of Radioactive Wastes to Atmosphere from Boiling Water Reactors,* Report GEAP-3594, General Electric Company, San Jose, California.

Smith, J. M. and W. A. Hartman, Jr., (1969), *Release and Decay of Noble Gases in the Off-Gas System of a Boiling Water Reactor,* Report APED-5663, General Electric Company, San Jose, California.

Smith, J. M. and J. E. Kjemtrup, General Electric Company, (1972), *Developments in Nuclear Plant Effluent Management.* Proceedings of the American Power Conference, Volume 34, Illinois Institute of Technology, Chicago.

Stuart, I. F. and M. J. May, (1967), *Comparison of Calculated and Measured Long Term Gamma Doses from a Stack Effluent of Radioactive Gases,* General Electric Company, San Jose, California.

Williamson, H. E. and D. C. Ditmore, (1972a), *Experience with BWR Fuel Through September 1971,* Report NEDO-10505, General Electric Company, San Jose, California.

Williamson, H. E. and D. C. Ditmore, General Electric Company, (1971), *Current BWR Fuel Design and Experience,* Reactor Technology, Vol. 14, No. 1, Spring 1971.

Williamson, H. E. and D. C. Ditmore, General Electric Company, (1972b), *Experience with BWR* Fuel. Nuclex 72, Basel, Switzerland, October 1972.

TABLE 1. GE-BWR Noble Radiogases Design Basis Source Terms.

Radiogas	Half-Life	Zero Decay*	30-Minute Decay*
^{95}Kr	0.5 sec.	2.1	---
^{143}Xe	1.0 sec.	12.0	---
^{97}Kr	1.0 sec.	0.14	---
^{94}Kr	1.0 sec.	23.0	---
^{142}Xe	1.2 sec.	73.0	---
^{93}Kr	1.3 sec.	99.0	---
^{141}Xe	1.7 sec.	240.0	---
^{92}Kr	1.8 sec.	330.0	---
^{91}Kr	8.6 sec.	330.0	---
^{144}Xe	9.0 sec.	0.56	---
^{140}Xe	13.6 sec.	300.0	---
^{90}Kr	32.3 sec.	280.0	---
^{139}Xe	40.0 sec.	280.0	---
^{89}Kr	3.2 min.	130.0	0.18
^{137}Xe	3.8 min.	150.0	0.67
^{138}Xe	14.2 min.	89.0	21.0
^{135m}Xe	15.7 min.	26.0	6.9
^{87}Kr	76.0 min.	20.0	15.0
^{83m}Kr	1.9 hrs.	3.4	2.9
^{88}Kr	2.8 hrs.	20.0	1.8
^{85m}Kr	4.4 hrs.	6.1	5.6
^{135}Xe	9.2 hrs.	22.0	21.0
^{133m}Xe	2.3 days	0.29	0.29
^{133}Xe	5.3 days	8.2	8.2
^{131m}Xe	12.0 days	0.015	0.015
^{85}Kr	10.7 yrs.	0.015	0.015
	Total	2,500	100

*mCi/sec.

TABLE 2. GE-BWR Noble Radiogases Recent Emission Experience and Estimated Neighbor Dose.

Plant (a)	Best (b) Estimate*	Tech (c) Spec*	Actual Emission* 1971	Actual Emission* 1972	Estimated Neighbor Dose, mrem per yr (d) 1971	Estimated Neighbor Dose, mrem per yr (d) 1972
Dresden 1	700	560	24	31	4	5
Big Rock Point	2,600	1,000	9	8	1	1
Humboldt Bay	125	50	16	14	13	11
Garigliano	1,000	1,000	20	10	2	1
Gundremmingen (e)	1,500	68	1	1	1	1
Tarapur 1 & 2	580	580	67	38	12	7
Oyster Creek	600	300	16	28	3	5
Nine Mile Point	800	800	8	16	1	2
Tsurga (f)	500	50	4	1	1	1
Dresden 2 & 3	1,800	900	18	14	1	1
Millstone Point	820	820	9	23	1	3
Fukushima 1 (g)	500	50	2	4	1	1
Nuclenor	600	600	30	63	5	11
Monticello	480	270	3	24	1	5

Notes:

(a) Plants used a nominal 30-minute holdup system — except as noted.

(b) GE calculation of annual average emission rate that would cause an exposure of 500 mrad per year at the site boundary.

(c) Permissible annual average emission rate in the plant's operating license (as established by licensing authority).

(d) Dose to a location is estimated by direct comparison of an actual emission with the "best estimate" permissible emission in (b); then, the actual dose to any neighbor is estimated to be lower than the exposure at the boundary by a factor of about 5; this is due to the actual location of the neighbor, occupancy time, and incidental shielding by structures.

(e) Gundremmingen has used an ambient temperature charcoal adsorption system since startup.

(f) Tsuruga used one-day tank storage, until the installation of an ambient temperature charcoal adsorption system in June 1971.

(g) Fukushima 1 used one-day tank storage, until the installation of an ambient temperature charcoal adsorption system in December 1972.

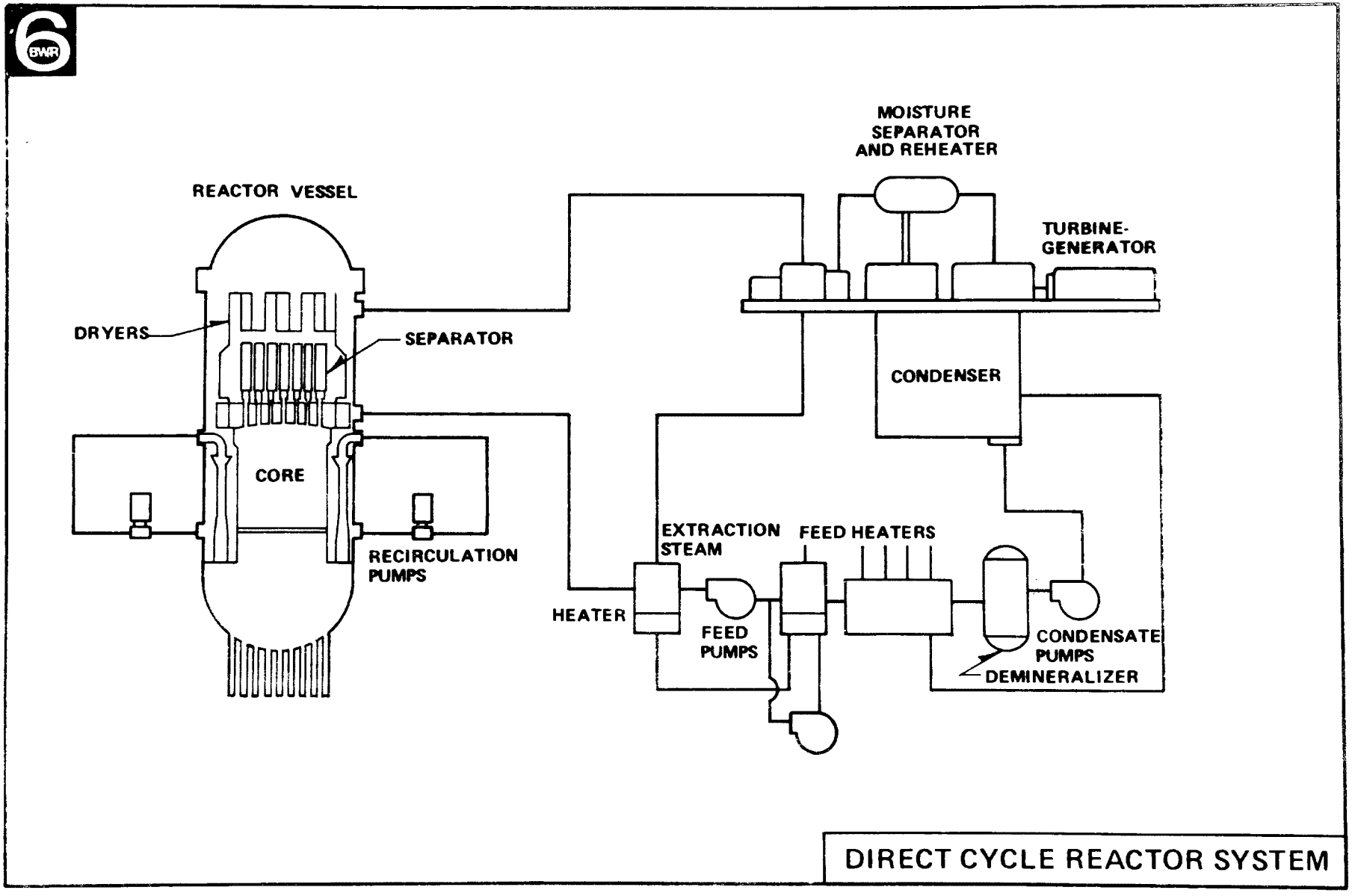
6
BWR
MOISTURE
SEPARATOR
AND REHEATER
REACTOR VESSEL
TURBINE-
GENERATOR
DRYERS
SEPARATOR
CONDENSER
CORE
EXTRACTION
STEAM
FEED HEATERS
RECIRCULATION
PUMPS
HEATER
FEED
PUMPS
CONDENSATE
PUMPS
DEMINERALIZER
DIRECT CYCLE REACTOR SYSTEM

Figure 1.

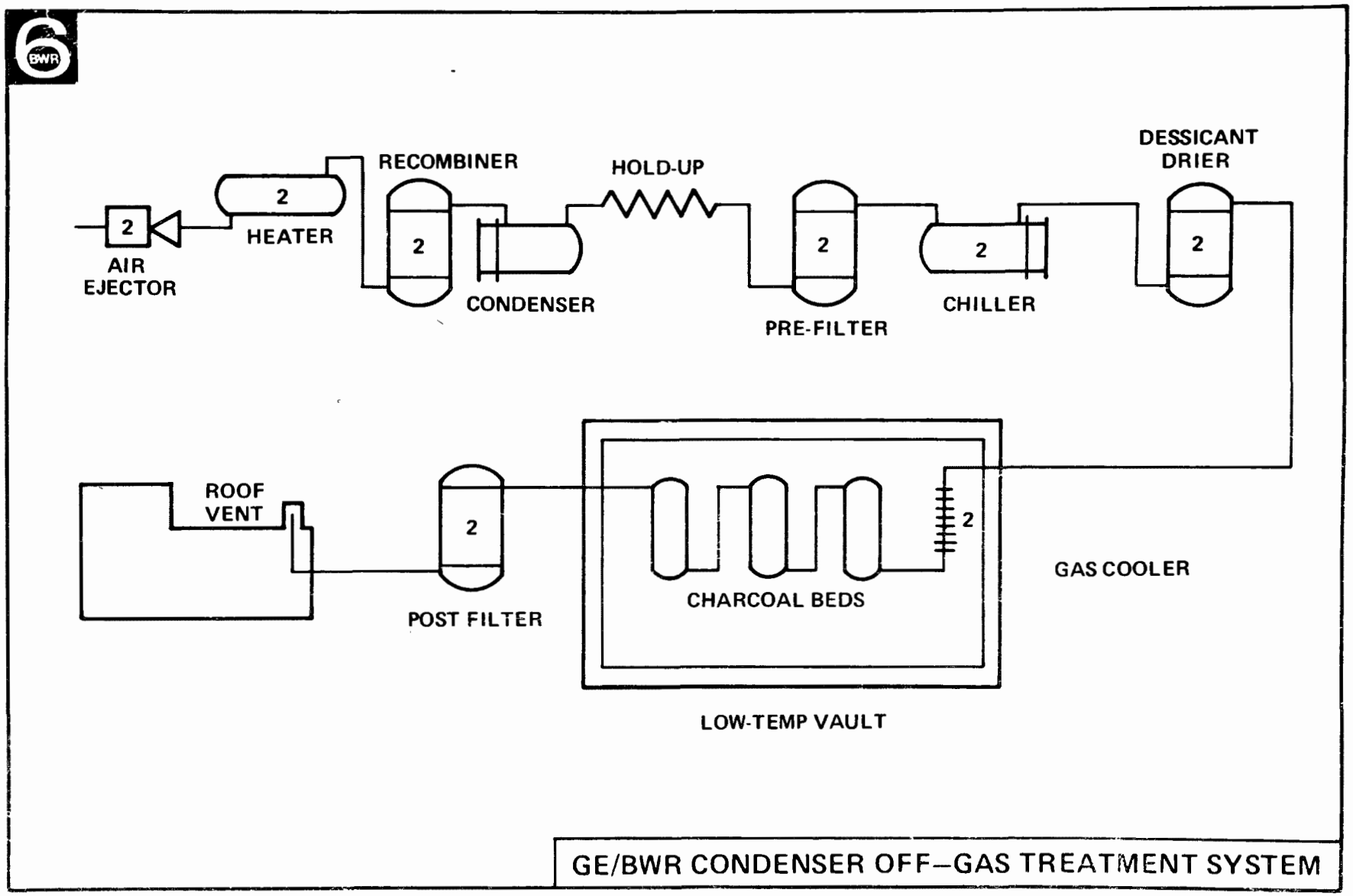
6
BWR
AIR EJECTOR
2
HEATER
2
RECOMBINER
2
CONDENSER
HOLD-UP
2
PRE-FILTER
2
CHILLER
DESSICANT DRIER
2
ROOF VENT
2
POST FILTER
CHARCOAL BEDS
2
GAS COOLER
LOW-TEMP VAULT
GE/BWR CONDENSER OFF–GAS TREATMENT SYSTEM

Figure 2.

COMMERCIAL PRODUCTION OF KRYPTON AND XENON

G. G. Handley
Air Products and Chemicals, Inc.
Allentown, Pennsylvania 18105

Abstract

This paper reviews a cryogenic process for the commercial production of high purity gaseous krypton and xenon by separation from atmospheric air. Process and equipment descriptions, operating procedures, analytical procedures, and safety considerations are discussed. Some current uses for these noble gases are also described.

The production unit was designed and constructed by Air Products and Chemicals, Inc., and installed near Cleveland, Ohio, where it has been operational since 1965.

The semi-continuous process involves three major steps. Step I is the continuous simultaneous upgrading of atmospheric krypton from 1.1 ppm to 3,500 ppm, and atmospheric xenon from 0.086 ppm to 350 ppm, as a byproduct stream from two large commercial cryogenic air separation plants. Step II is additional continuous simultaneous upgrading to 85% krypton and 8.5% xenon, followed by batch withdrawal and storage of these raw products. Step III is a batch process, using the same equipment as in Step II to produce commercially salable high purity product at >99.995% krypton and >99.995% xenon.

INTRODUCTION

Air Products and Chemicals, Inc., produces commercial quantities of high purity gaseous krypton and xenon from its facilities located in Cleveland, Ohio. The production unit was designed and constructed by the Company, and has been operational since 1965. The semi-continuous process involved has three major phases:

(1) Phase I is the continuous simultaneous upgrading of atmospheric krypton from 1.1 ppm to 3,500 ppm, and atmospheric xenon from 0.086 ppm to 350 ppm, as by-products from two large commercial cryogenic air separation plants. The higher boiling points of krypton and xenon, as related to the other major constituents of atmospheric air, makes it possible to take advantage of their tendency to collect in oxygen, rather than in the nitrogen cuts. Refer to Table 1.

(2) Phase II is the additional continuous simultaneous upgrading to 85% krypton and 8.5% xenon, followed by batch withdrawal and storage.

(3) Phase III is a batch distillation, using much of the same equipment as in Phase II, to produce a commercially saleable product — at greater than 99.995% krypton and greater than 99.995% xenon. Refer to Table 2 for a typical analysis.

Design production rates are 7,500 scf per year for krypton and 550 scf per year for xenon. This represents an overall recovery of 25% based on processed air. Actual production rates have exceeded these values.

The following general information covers process conditions, equipment descriptions, analytical procedures, safety considerations, and end uses.

PROCESS CONDITIONS

1. Phase I (Figure 1 is a simplified flow diagram for the Phase I upgrading of krypton and xenon.)

Two identical air separation plants, operating in parallel, perform the initial upgrading of atmospheric krypton and xenon as a by-product from the production of large volumes of oxygen. The air separation plant process is typical of several hundred units operating throughout the world. Each of our Cleveland plants is designed to process atmospheric air as a raw material, and produce 280 tons per day of oxygen, at 99.6% purity, as the primary product. Gaseous oxygen is pipelined to a large nearby steel mill for use in the basic oxygen steel making process. Other by-products recovered from the Cleveland plants include: liquid oxygen, liquid nitrogen, crude liquid argon, and crude gaseous neon.

Each air separation plant processes 1,500,000 scfh of atmospheric air containing 1.1 ppm krypton and 0.086 ppm xenon. The air is drawn through the inlet air filter (A) to remove solid debris, and compressed to 104 psia in the main air compressor (B). The discharge is cooled to 90°F, the condensate is removed, and the flow is split into two streams. One stream, containing 64% of the incoming air, flows directly to the regenerator (C) for carbon dioxide plus moisture removal, and simultaneous cooling to -274°F by cold waste nitrogen.

The second stream, containing 36% of the incoming air, is compressed to 1,850 psia in the booster air compressor (D). The high-pressure discharge is cooled to 40°F in the precooler (E). Condensed water and lubricating oil are trapped and removed. Final traces of moisture and oil are removed in the drier (F). The dry, high-pressure air stream passes through the warm end tube bundle (G) of the main heat exchanger (H), and is cooled to -56°F. External cooling to -99°F is accomplished in the refrigerant evaporator (I), and the stream is returned to the intermediate tube bundle (J) of the main exchanger. High-pressure air leaves the intermediate bundle at -230°F, expands through valve (K) to 815 psia at -234°F, and enters the carbon-dioxide adsorber (L). Air, free of water and carbon dioxide, returns to the cold end tube bundle (M) in the main exchanger, and is

cooled to -247°F. Cooling is accomplished in the main heat exchangers by the counter-current flow of cold waste nitrogen through the shell, plus cold product oxygen in a separate tube circuit.

High-pressure air from the final pass of the main exchanger splits into two streams. Most of the air expands across the valve (N) to 103 psia at -277°F, forming 78% liquid. Additional cooling from waste nitrogen in the regenerator preheater (O) increases the liquid fraction to 83%. This air then joins the low-pressure air stream from the regenerator, along with the second high-pressure air stream, as described below, to provide feed for the high-pressure distillation column (P), at 102 psia, -277°F, and 28% liquid.

The second high-pressure air stream expands across the valve (Q) to 103 psia, and enters the condenser section of the lower crude krypton column (R). The vapor fraction is condensed by reboiling the liquid in the column sump, and returning it to the high-pressure column as additional feed.

High purity nitrogen vapor leaves the top of the high-pressure column, at 100 psia and -283°F, and splits into two streams. One stream liquefies in the condenser section of the upper crude krypton column (S), and reboils the liquid in the column sump. Condensed nitrogen is subcooled to -308°F by waste nitrogen, expands through a valve to 19 psia at -316°F, and provides partial reflux for the low-pressure distillation column (T). The second stream, containing most of the nitrogen vapor, condenses in the main reboiler-condenser (U), and reboils liquid oxygen from the low-pressure column sump.

Condensed nitrogen at -283°F from the main reboiler-condenser splits into two streams. One stream provides reflux for the high-pressure column. The second stream is subcooled to -308°F by waste nitrogen, and expands through the valve (V) to -316°F and 19 psia to provide the remaining reflux for the low-pressure column.

Crude liquid oxygen from the high-pressure column sump passes through the hydrocarbon adsorber (W) at -278°F and 102 psia. Most of the hydrocarbons, except for methane, are removed from the system at this point. The crude liquid oxygen, at 32% purity, along with the krypton-xenon fractions, then expands across the valve (X) to 19 psia, and provides feed for the low-pressure column.

Liquid oxygen, at 99.6% purity, from tray number five in the low-pressure column, is pressurized to 615 psia in the pump (Y). This liquid passes through a tube circuit in the main exchanger, and is vaporized by counter-current incoming air. The resulting product, gaseous oxygen, is pipelined to a steel mill.

Cold waste nitrogen, at -316°F and 19 psia, from the top of the low-pressure column, provides refrigeration to subcool the low-pressure column reflux, and then splits into two streams. One stream provides refrigeration and purge gas for the regenerator, and is vented to the atmosphere. The second stream passes through the shell side of the main exchanger to provide the primary source of refrigeration for incoming air, and is also vented to the atmosphere.

Reboiled oxygen from the main reboiler-condenser, at 99.7% purity, with trace quantities of krypton and xenon, enters the phase separator (Z) at -288°F and 25 psia. The gas phase and excess liquid return to the low-pressure column. A small liquid flow provides reflux for the upper crude krypton column at -288°F and 28 psia. Oxygen vapor from the top of the upper column containing lower concentrations of krypton and xenon, returns to the low-pressure column. Liquid oxygen in the upper column sump contains higher concentrations of krypton and xenon, and is reboiled by condensing nitrogen vapor at -283°F.

A small stream of liquid oxygen from the upper column sump provides reflux for the lower crude krypton column. Oxygen vapor from the top of the lower column contains lower concentrations of krypton and xenon, and returns to the upper column as feed. Liquid oxygen in the lower column sump nominally contains 3,500 ppm krypton, 350 ppm xenon, and 2,500 ppm methane, and is reboiled by condensing air at -277°F.

Liquid oxygen from the lower column is vaporized, and warmed to 70°F in a steam heater (AA), and piped to Phase II processing at 5 scfm, along with a similar stream from the second air separation plant.

2. Phase II. (Figure 2 is a simplified flow diagram for the Phase II upgrading of krypton and xenon.)

A combined gaseous oxygen flow of 10 scfm from two air separation plants, containing 3,500 ppm krypton, 350 ppm xenon, and 2,500 ppm methane at 70°F and 16 psia, is compressed to 85 psia in the oxygen feed compressor (BB). The stream is preheated to 400°F in the recuperative exchanger (CC). Hydrocarbons are burned to water and carbon dioxide at 900-1100°F in an electrically heated catalytic methane burner (DD). The hot stream is cooled to 200°F in the recuperative exchanger, cooled to 90°F in the water cooler (EE), and further cooled to 40°F in the refrigerator (FF) to permit trapping and removal of water. Carbon dioxide and remaining traces of moisture are removed in the adsorber (GG).

The process stream is further cooled to below -200°F by returning oxygen in the exchanger (HH), and provides feed for the krypton distillation column (II). The column is held at 65 psia. Reflux refrigeration is provided by liquid nitrogen coils in the column overhead. Krypton and xenon concentrate in the sump at -250°F. Reboiling is maintained by electric heaters mounted on the column sump. Waste oxygen is discharged from the top of the column at -255°F. This provides refrigeration for the incoming process stream, and then vents to the atmosphere.

At monthly intervals, crude products of 85% krypton and 8.5% xenon, together with trace quantities of carbon dioxide and methane, are removed from the column sump, heated to 70°F in the crude vaporizer (JJ), compressed to 150° psia in the product compressor (KK), and stored in the crude cylinders (LL).

3. Phase III. (Figure 3 is a simplified flow diagram for the Phase III purification of krypton and xenon.)

At 3-4 month intervals, Phase II upgrading is discontinued, and much of the same equipment is used during a batch distillation to produce pure products. This operation takes about one week.

Crude cylinders (LL), containing 2500 scf of krypton and 250 scf of xenon are charged to the system at 45 psia via the recuperative exchanger, and are heated to 400°F. The crude is then heated to 900-1100°F in the catalytic methane burner (DD) to remove trace quantities of hydrocarbons. The hot stream is successively cooled to 40°F in the recuperative exchanger (DD), water cooler (EE), and refrigerator (FF), as in Phase II. Traces of carbon dioxide are removed in the caustic trap (MM), and residual moisture is removed in the crude adsorber (NN).

The crude stream is then cooled to -50°F by cold nitrogen in the exchanger (HH), and provides feed for the krypton distillation column (II). Liquid nitrogen refrigerant is supplied to coils in the column overhead and sump to liquefy the crude at -250°F and maintain 45 psia column pressure. When all of the crude is charged, liquid nitrogen refrigerant flowing to the column sump is discontinued. Electric heaters are activated to cause a total reflux condition at 65 psia.

Gaseous oxygen is slowly vented from the overhead, while the column is maintained at a high . ux rate. When the column stabilizes at -220°F, and krypton appears in the overhead, a pre-cut flow is dire d to the compressor (GG), and stored in pre-cut cylinders for future processing.

When the overhead oxygen concentration drops to 500 ppm, the product krypton flow is directed through the deoxo (OO) to remove traces of oxygen. The krypton stream then flows through the final caustic trap (PP), and the final adsorber (QQ), to remove traces of carbon dioxide and moisture respectively. The resultant product krypton is pressurized to 1,500 psia in the compressor (KK), and stored in previously evacuated pure cylinders (RR). When traces of xenon appear in the product krypton, the compressor discharge is directed to intermediate-cut cylinders for future processing. When the overhead krypton concentration drops to 25 ppm, the product xenon flow is directed to previously evacuated pure cylinders, and is compressed to 540 psia.

Product krypton and xenon cylinders are then shipped to our Specialty Gases Department located at Hometown, Pa., for final analytical certification and repackaging as pure or blended gas to meet customer requirements.

DESCRIPTION OF MAJOR EQUIPMENT

Each piece of equipment is only described once, and is not repeated in subsequent phase listings.

1. Phase I. (Refer to Figure 1.)

Inlet Air Filter (A). The inlet air filter contains a moving 8' by 8' fiber glass blanket backed up by 40 stationary fiber glass sacks. The unit is designed to remove at least 95% of atmospheric dust.

Main Air Compressor (B). The main air compressor is a four stage centrifugal machine, operating at 6,055 rpm, with water cooled intercoolers after each compression stage. It is driven by a 6,000 hp synchronous motor..

Regenerator (C). The regenerator system includes four vertical cylindrical aluminum vessels. Each vessel is 40' high x 8' in diameter, and contains 60 tons of quartz pebbles, which have a high heat capacity. Counter-current warm air, and cold nitrogen, alternately flow through each vessel on a ten minute cycle.

Booster Air Compressor (D). The booster air compressor is a three stage, four cylinder, reciprocating machine, operating at 277 rpm, with water-cooled intercoolers after each compression stage. It is driven by a 3,000 hp synchronous motor.

Precooler (E). The precooler system includes a 100 hp refrigerant cycle to cool an intermediate ethylene glycol-water solution to 30°F. The solution cools the process air stream in a shell and tube heat exchanger.

Drier (F). The drier system includes two vertical cylindrical carbon steel vessels. The vessels are 11' high x 2' in diameter, and contain 1,400 lbs. of activated alumina desiccant. Each vessel is on stream for 12 hours, followed by a 12-hour reactivation period using hot nitrogen.

Main Heat Exchanger (H). The main heat exchanger system includes three vertical cylindrical stainless steel vessels operating in parallel. Each vessel is 22' high x 2' 4" in diameter, and contains spiral wound copper tube bundles for air and oxygen circuits.

Refrigerant Evaporator (I). The refrigerant evaporator is a 12' long x 6' in diameter silica bronze vessel containing Freon 22 refrigerant. Process air is cooled in 1" copper tubes passing through the evaporator. The system uses a compound refrigeration cycle consisting of a single stage low side centrifugal compressor (75 hp), a four stage intermediate centrifugal compressor (200 hp), and two single stage high side reciprocating compressors (100 hp each) in parallel.

Carbon Dioxide Adsorber (L). The carbon dioxide adsorber system includes two vertical cylindrical stainless steel vessels. The vessels are 14' high x 4' in diameter and contain 5,400 lbs. of silica gel adsorbant. Each vessel is on stream for 24 hours, followed by a 24-hour reactivation period using hot nitrogen.

High-Pressure Distillation Column (P). The high-pressure distillation column is a 22' high x 6' 4" in diameter aluminum vessel that contains 30 sieve trays.

Lower Crude Krypton Column (R). The lower crude krypton column is a copper vessel consisting of a distillation section mounted above a reboiler-condenser. The distillation section is 3' high x 10" in diameter,

and contains 10 sieve trays. The reboiler-condenser section is 8' high x 2' in diameter. A spare column is also installed.

Upper Crude Krypton Column (S). The upper crude krypton column is a copper vessel consisting of a distillation section mounted above a reboiler-condenser. The distillation section is 4' high x 1',9" in diameter, and contains 10 bubble cap trays. The reboiler-condenser section is 11' high x 3' in diameter.

Low-Pressure Distillation Column (T). The low-pressure distillation column is a 60' high x 8', 8" in diameter aluminum vessel, and contains 90 sieve trays.

Main Reboiler-Condenser (U). The main reboiler-condenser consists of three aluminum vessels operating in parallel. Each vessel is 17' high x 3', 8" in diameter, and contains 3,414 aluminum tubes.

Hydrocarbon Adsorber (W). The hydrocarbon adsorber system includes two vertical cylindrical stainless steel vessels. The vessels are 13' high x 2', 6" in diameter, and contain 1,520 lbs. of silica gel adsorbant. Each vessel is on stream for 72 hours, followed by a 72-hour reactivation period using hot nitrogen.

Liquid Oxygen Pump (Y). The liquid oxygen pump is a vertical unit with 14 stages of compression, and is driven by a 40 hp motor. A spare pump is also installed.

2. Phase II. (Refer to Figure 2.)

Oxygen Feed Compressor (BB). The oxygen feed compressor is a 25 hp centrifugal machine containing a rotating band of water that acts as the compressant.

Catalytic Methane Burner (DD). The catalytic methane burner is a stainless steel cylinder containing 50 lbs. of platinum-based catalyst. Reaction temperatures are maintained by external electric heaters.

Refrigerator (FF). The refrigerator is a ¼ hp Freon unit.

Adsorber (GG). The adsorber system includes two vertical cylindrical carbon steel vessels. The vessels contain 150 lbs. of molecular sieve. Each vessel is on stream for 12 hours, followed by a 12-hour reactivation period using hot nitrogen.

Exchanger (HH). The exchanger is a 10' high x 4" in diameter vertical stainless steel vessel containing copper tube bundles.

Krypton Distillation Column (II). The krypton distillation column is a 10' high x 3" in diameter stainless steel vessel containing stainless steel packing. The reboiler is a 40-gallon cylindrical tank with external electric heaters and an internal liquid nitrogen coil. The overhead condenser also contains a liquid nitrogen coil.

Product Compressor (KK). The product compressor is a two-stage reciprocating machine with metal diaphrams. It is driven by a 2 hp motor.

3. Phase III. (Refer to Figure 3.)

Caustic Traps (MM & PP). The caustic traps are 3' long x 3" in diameter copper tubes filled with a pelletized form of caustic soda on asbestos. The charge is replaced as needed.

Crude Adsorber and Final Adsorber (NN & QQ). The crude and final adsorbers are 3' long x 4" in diameter copper tubes containing molecular sieve.

ANALYTICAL PROCEDURES AND SAFETY CONSIDERATIONS

Process streams are monitored at critical points to ensure product purity and maintain safe operating conditions.

1. Hydrocarbon Concentrations.

Hydrocarbon concentrations are limited to avoid explosive mixtures with oxygen. Total hydrocarbon concentrations, consisting primarily of methane, are maintained below 500 ppm throughout the process. The only exception to this rule is a 5,000 ppm total hydrocarbon limit in the stream from the lower krypton column (R) to the catalytic methane burner (BB). In all cases, methane concentrations are held well below the 5% lower explosive limit of methane in oxygen. Total hydrocarbons are monitored at the following locations:

(1) Air from the regenerator (C).
(2) Air from the drier (F).
(3) Oxygen from the pump (Y).
(4) Oxygen to the lower crude krypton column (R).
(5) Oxygen from the lower crude krypton column (R).
(6) Oxygen to the oxygen feed compressor (BB).
(7) Oxygen from the catalytic methane burner (DD).
(8) Crude from the sump of the krypton distillation column (II).
(9) Gas from the crude cylinders (LL).

2. Acetylene Concentrations.

Acetylene concentrations are of particular concern because it has a relatively low solubility of 5 ppm in liquid oxygen. If the solubility limit is exceeded, solid acetylene deposits create localized concentrations which are explosive hazards. Accordingly, acetylene concentrations are maintained below 2 ppm, and are monitored at the following locations:

(1) Liquid oxygen from the sump of the low-pressure distillation column (T).

(2) Liquid oxygen from the sump of the lower crude krypton column (R).

3. Other Analytical Procedures.

Continuous analyzers are used to monitor various process streams for carbon dioxide, moisture, nitrogen, oxygen, and argon.

The following instruments are used to analyze for impurities in the products, krypton and xenon:

(1) **Gas chromatograph.** Analyze for helium, hydrogen, nitrogen, oxygen/argon, traces of xenon in krypton, and traces of krypton in xenon.

(2) **Infra-red spectrophotometer.** Analyze for carbon dioxide, carbon monoxide, methane, and nitrous oxide.

(3) **Trace oxygen analyzer.**

(4) **Moisture analyzer.**

(5) **Total hydrocarbon analyzer.**

END USES

In recent years, significant quantities of krypton have been used to fill incandescent light bulbs in the United States. Typically, a krypton-nitrogen mix is used to replace the conventional argon-nitrogen mix. The high molecular weight of krypton reportedly inhibits vaporization of the tungsten filament and increases bulb life. The lower thermal conductivity of krypton also permits smaller bulb configurations without excessive heat loss.

Research projects using krypton and xenon have been under way at numerous industrial, education, and government laboratories. The following additional uses for krypton and xenon are among those reported as actual or proposed:

(1) Krypton in fluorescent lamps.

(2) Xenon in lamps requiring extreme brightness and/or pulsating features such as search lights, navigation lights, movie projection lights, and laser stimulators.

(3) Xenon in electronic tubes.

(4) Xenon in radiation detectors — including bubble chambers.

(5) Krypton and xenon to increase the rate of radiation-induced polymerizations.

(6) Xenon as a general inhalation anesthetic for humans.

(7) Krypton and xenon to reduce radiation damage to human tissue.

(8) Xenon-difluoride to fluorinate aromatic rings.

Table 1. Selected Air Data.

Constituent	Normal Boiling Point (°F)	Molecular Weight	Typical Concentration in Dry Air (Volume Basis)
Helium	- 452	4	5.24 ppm
Hydrogen	- 423	2	Less than 1 ppm
Neon	- 411	20	18.21 ppm
Nitrogen	- 320	28	78.08 %
Argon	- 303	40	0.93 %
Oxygen	- 287	32	20.95 %
Methane	- 259	16	Varies
Krypton	- 244	84	1.139 ppm
Ozone	- 169	48	Varies
Xenon	- 163	131	0.086 ppm
Nitrous Oxide	- 127	44	Varies
Acetylene	- 119	26	Varies
Carbon Dioxide	- 109*	44	0.03 % (Approx.)
Sulfur Dioxide	+ 14	64	Varies
Other Hydrocarbons	--	--	Varies
Water	+ 212	18	Varies

* Sublimation Point

Table 2. Typical Analysis for Research Grade Krypton and Xenon.

	Krypton	Xenon
Purity	> 99.995%	> 99.995%
Impurities (ppm)		
Carbon Dioxide	< 0.5	< 5.0
Carbon Monoxide	< 1.0	< 1.0
Helium and Hydrogen	< 5.0	< 5.0
Methane	< 5.0	< 5.0
Nitrogen	5 - 15	< 10.0
Nitrous Oxide	< 0.1	< 0.1
Oxygen	< 2.0	< 5.0
Total Hydrocarbons	< 5.0	< 5.0
Xenon	< 25.0	--
Krypton	--	< 25.0 ppm
Water	< 1.0	< 1.0

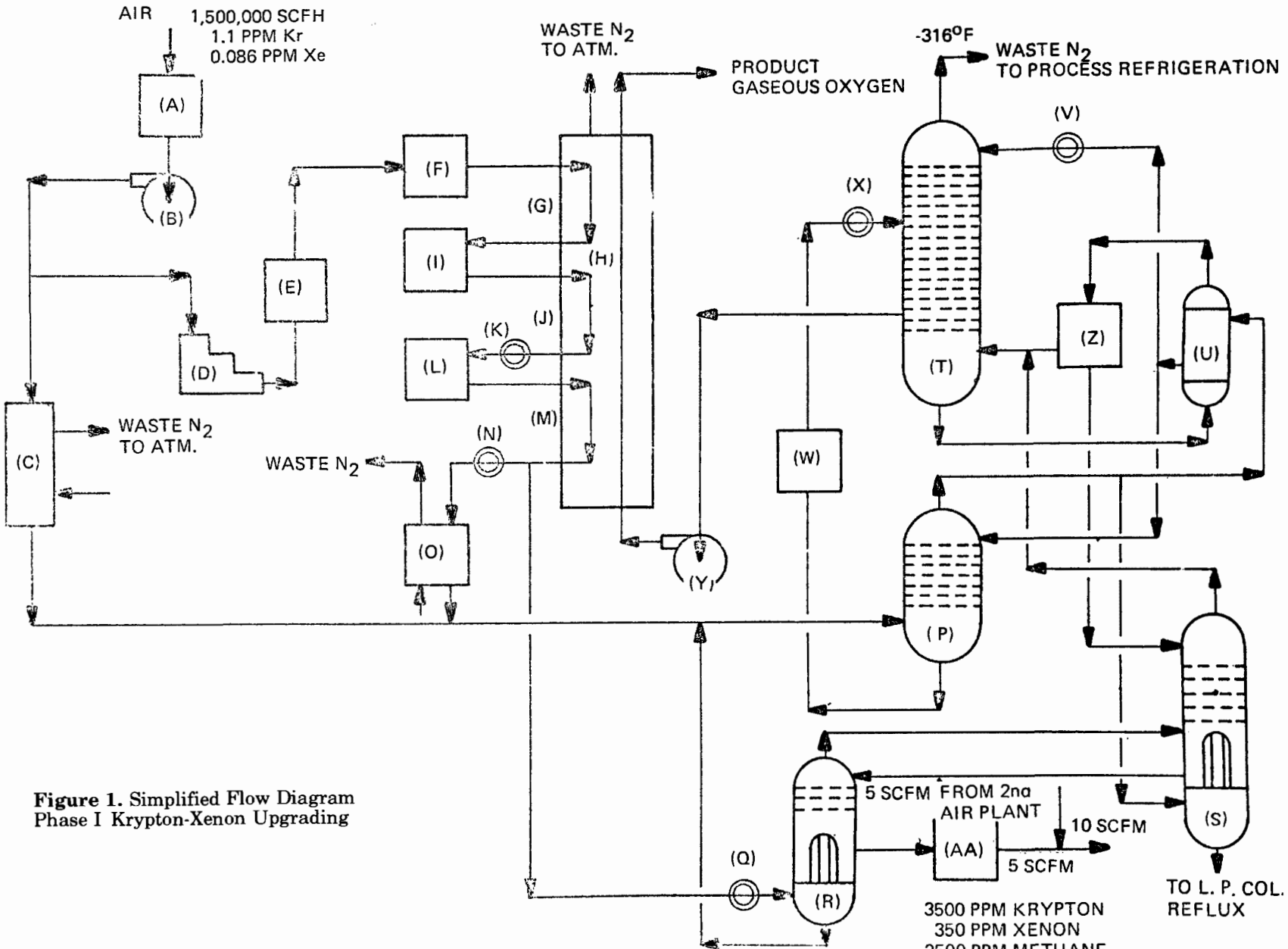

Figure 1. Simplified Flow Diagram
Phase I Krypton-Xenon Upgrading

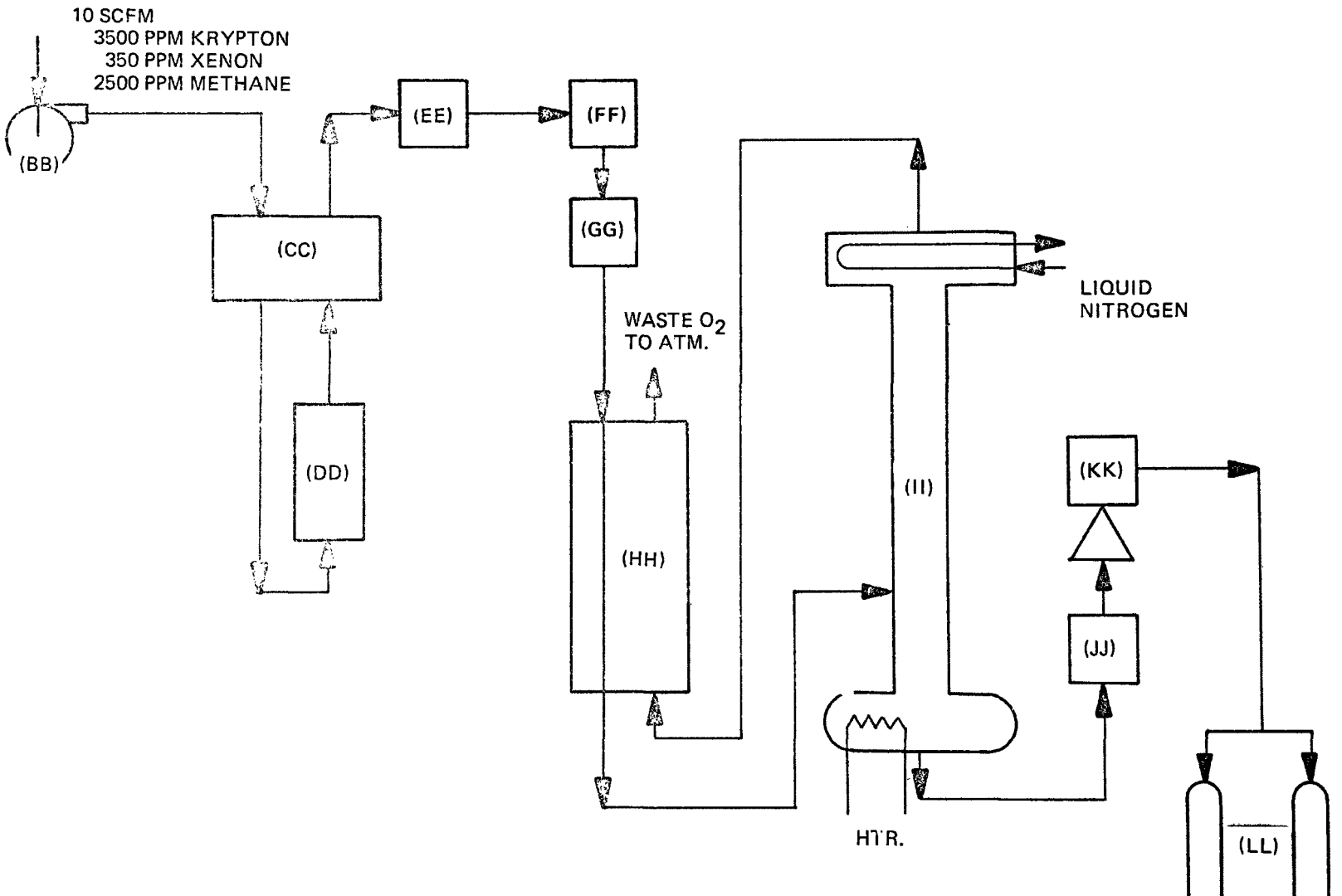

Figure 2. Simplified Flow Diagram
Phase II Krypton-Xenon Upgrading

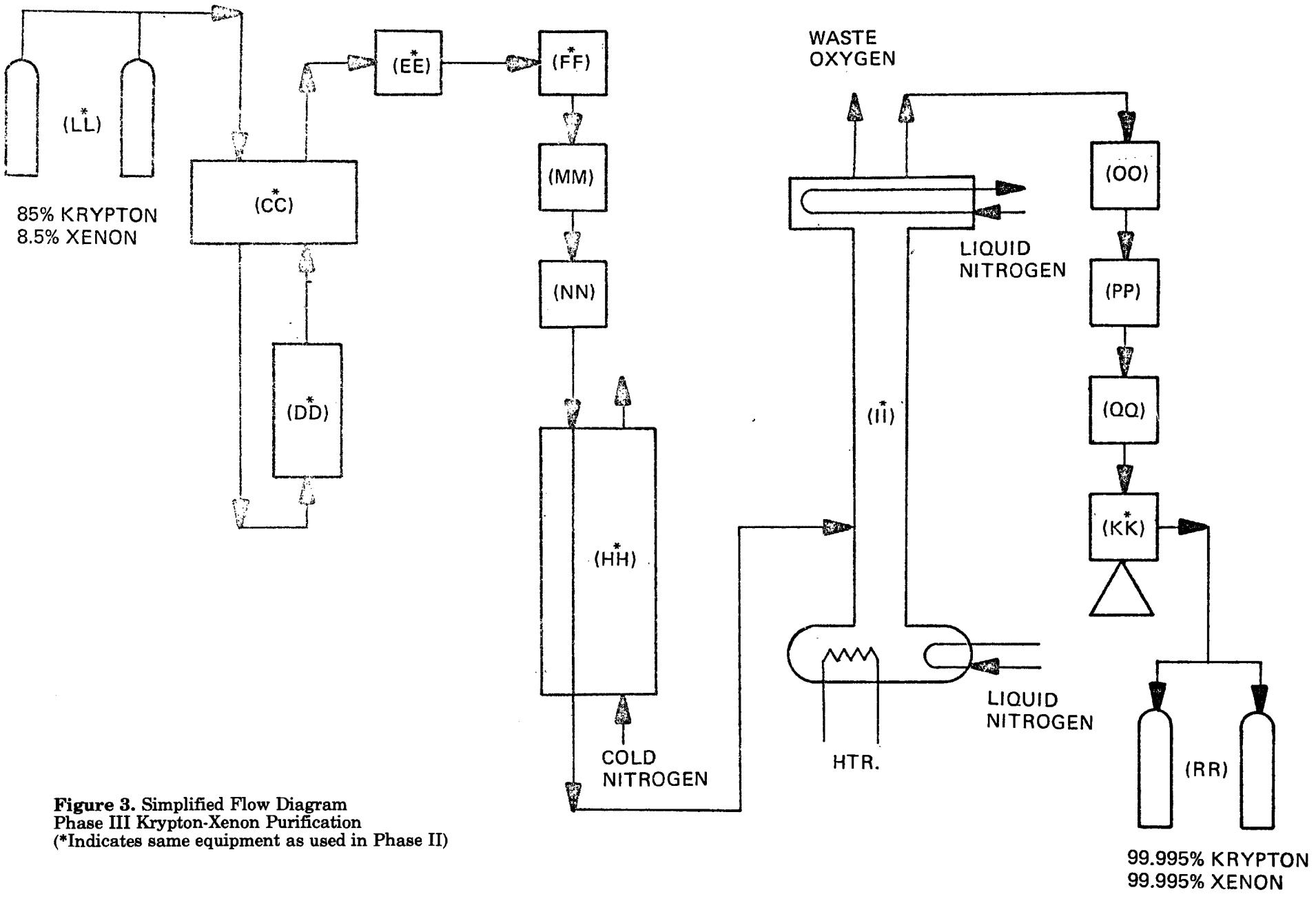

Figure 3. Simplified Flow Diagram
Phase III Krypton-Xenon Purification
(*Indicates same equipment as used in Phase II)

RADIOACTIVE NOBLE GASES IN EFFLUENTS FROM NUCLEAR POWER STATIONS

H. E. Kolde, W. L. Brinck, G. L. Gels, and B. Kahn
Radiochemistry & Nuclear Engineering Laboratory
U. S. Environmental Protection Agency
National Environmental Research Center
Cincinnati, Ohio 45268

Abstract

The discharge rates, isotopic composition, and major in-plant pathways for radioactive krypton and xenon in effluent gases at commercially operated nuclear power stations in the United States are reported. Specific information was obtained in the course of radiological surveillance studies at two BWR and two PWR stations, and periodic average discharge rates are reported by station operators. Techniques for radiochemically analyzing these radioactive gases are described: in-plant samples at relatively high concentrations are analyzed directly by gamma-ray spectrometry; low-level samples, especially those collected in the environment, are first concentrated, and may also be treated to separate krypton and xenon from each other and from other gases. Also discussed is the measurement of radionuclide concentrations in air by radiation dosimetry.

INTRODUCTION

Radioactive noble gases are major waste products of nuclear reactor operations. Krypton and xenon are generated along with many other radionuclides by nuclear fission. Although practically all fission products remain in place within the fuel, a small fraction leaks through minute cladding imperfections into the reactor coolant. Radioactive gases from the coolant, at present, are held for partial radioactive decay, and then are discharged to the atmosphere. Being relatively non-reactive, they remain in the air, and may be measured with very sensitive instruments for some distance downwind of the release point, until atmospheric dispersion processes dilute them to a level difficult to detect. In many cases, detection limits are set by natural background radiation. Local populations are exposed to the radiations emitted by the plume, although such exposures have been small fractions of the annual allowable limits permitted by governmental regulations (Rogers, *et al.*, 1971). Based on this experience, and the concept of lowest practicable population exposure, guidelines are being considered to restrict radioactive reactor effluents to levels that would keep exposure to persons living near stations to five percent or less of average natural background radiation (AEC NR4-30, 1973).

The use of large reactors and multiple reactor sites for commercial electrical power generation has increased significantly during the past decade. To meet needs for more detailed information on reactor-discharged radioactivity and possible environmental effects, studies were begun in 1967 by the U. S. Public Health Service, and are now being continued by the U. S. Environmental Protection Agency. Many of the discharges and environmental measurements at that time were being reported by plants only on a gross activity basis. The studies identify internal plant pathways leading to the discharge of specified radionuclides, determine the degree of dispersion afforded by local meteorology, test the applicability of mathematical models and sampling and analytical techniques, and measure the radiation dose in the environment.

Studies were conducted initially at the Dresden 1 boiling water reactor (BWR) (Kahn, *et al.*, 1970) and Yankee pressurized water reactor (PWR) (Kahn, *et al.*, 1971), and later at the larger Haddam Neck (Connecticut Yankee) PWR (Kahn, *et al.*, UP-a) and Oyster Creek BWR plants (Kahn, *et al.*, UP-b). Dresden 1 and Yankee operate at approximately 200 megawatts-electrical (MW[e]) output; the latter two, at approximately 600 MW[e]. All studies were performed in cooperation with the state health or environmental protection departments, the U. S. Atomic Energy Commission (USAEC), and the station operator. At Oyster Creek, the USAEC also undertook many in-plant measurements.

GASEOUS WASTE HANDLING SYSTEMS

Of the more than 30 krypton and xenon radionuclides produced by fission, most change rapidly within reactor fuel to stable or radioactive nuclides of other elements. The noble gases of potential significance as gaseous wastes are those with longer half-lives, as listed in Table 1 with their fission yield, generation rate, and radioactive progeny. The generation rate, a convenient indication of relative importance, was estimated from fission yield and half-life values for a unit MW[e] (~ 3 megawatt-thermal) power operation. All except ^{85}Kr possess half-lives of less than 5.3 days. Although generated in minor amounts, ^{85}Kr is of interest because its discharge adds to the world-wide inventory of gaseous radionuclides. Fission-produced noble gases are accompanied by such other radioactive noble gases as ^{37}Ar, ^{39}Ar, and ^{41}Ar produced by neutron activation of air in reactors. Other radioactive gases include ^{3}H, ^{13}N, ^{14}C, and radioiodine. The relative abundance of all gaseous radionuclides in reactor effluents depends on reactor type and power level, fuel cladding, waste treatment system, and plant operating practices.

Gaseous waste pathways and treatment are different at BWR and PWR plants due to their distinct coolant systems. In the direct-cycle BWR, air that continuously leaks into reactor coolant water must be removed to

maintain operation. The purged air contains the radioactive gases swept from the reactor with the steam. A PWR reactor primary system is sealed, resulting is gas volumes small enough to be accumulated, stored, and released in batches. The resultant shorter holdup times at BWR's produce higher effluent radioactivity levels than PWR's, as shown in Table 2, due to a preponderance of short-lived radionuclides. Average BWR release rates during 1972 were on the order of 10^4 μCi/sec, based on discharge reports from six stations operating longer than one year. Average releases from seven PWR's operating before 1972 were lower, and more varied, ranging from 6×10^{-1} to 6×10^2 μCi/sec (AEC, UP).

The Oyster Creek gaseous waste disposal system shown in Figure 1 illustrates typical pathways in BWR's built by the General Electric Co. The gases entrained in the reactor-produced steam are removed after passage through the turbines by air ejectors at the steam condensers. The off-gas is passed through a holdup system that normally requires approximately 72 minutes for passage at Oyster Creek (23 minutes at Dresden 1). This achieves reduction of radioactivity through decay of short-lived radionuclides. A particular benefit is the decay of ^{90}Kr before the effluent gas is filtered, so that no significant amounts of its ^{90}Sr daughter can be formed in the environment. The off-gas is passed through high efficiency particulate air (HEPA) filters before entering the stack. The gas is diluted by a factor of about 2000 at the base of the stack by ventilation air exhausted from the turbine, reactor, and occasionally other buildings. A tall 112-meter stack at Oyster Creek (91-meter at Dresden 1) provides additional dilution by atmospheric dispersion before the plume reaches the ground.

Other BWR pathways that contribute in minor ways to effluent radioactivity include: (1) steam leading through turbine gland seals from which gas is evacuated and pumped to the stack through a 2-minute holdup line; (2) leaks from various reactor components, pipes, etc., into building ventilation air; (3) turbine building air exhausted partially through roof vents during warm weather; and (4) radioactive gas emanating from liquids contained in waste tanks.

In the PWR, radioactivity from activation or leaking fission products accumulate in the primary coolant, until adjustments of coolant volume or composition are made, resulting in partial removal of gases. Figure 2 depicts the pathways observed at Haddam Neck (Yankee has similar pathways). Removed gases at Haddam Neck are collected in a sphere where they are held for decay. The gas is discharged 2 to 4 times per year to a 53-meter high vent stack at Haddam Neck (46-meter at Yankee), diluted with building ventilation and outside air by large fans, and discharged to the atmosphere.

Other sources include the contamination of secondary coolant by leakage of the radioactive primary coolant through faulty heat exchanger tubes. Gases in the secondary coolant are removed continuously by air ejectors on the condensers and vented directly to the discharge stack. When the reactor or its vapor container are opened for refueling or major maintenance, gases accumulated in these vessels are purged with large volumes of air and exhausted to the vent stack. Other releases to the stack occur when aliquots of primary coolant are depressurized and collected for analyses, or as gas separates from liquids stored in waste tanks.

These descriptions of gas treatment systems do not include changes being planned to meet the proposed USAEC regulations for "as low as practicable" levels of effluent radioactivity. Most new systems feature increased holdup times by adsorbing gases on charcoal or molecular sieve beds at ambient or lower temperatures. An alternate method is cryogenic distillation of noble gases and storage in gas cylinders. In many cases, the new systems will be incorporated in major radioactivity pathways, and plant discharge of gases by secondary routes may continue at current levels.

MEASUREMENTS IN GASEOUS WASTE HANDLING SYSTEM

Gases within the reactor plant are collected for measurement in sample containers of sizes determined by radioactive concentration and analytical requirements. Gases highest in radioactivity are obtained in sealed glass serum bottles 4 to 15 ml in volume, while those of lower concentration are collected in evacuated metal 2-liter bottles. Gases that emit photons are identified and measured with Ge(Li) or NaI(Tl) detectors coupled to multi-channel analyzers. Aliquots of large samples are transferred for counting to sealed evacuated 200-ml volumetric flasks. Samples are counted for periods ranging from 1 to 1,000 minutes, and counts are repeated at intervals.

Krypton-85, at relatively low concentrations, is processed through a gas separation apparatus developed by the Las Vegas National Environmental Research Laboratory, EPA. Since aliquots are usually of small volume, the apparatus at this laboratory has been modified to incorporate a ^{83m}Kr tracer with each sample to determine separation yield. The Kr fraction is transferred to 25-ml vials, containing approximately 15 ml of 1-mm plastic scintillator spheres, and measured by conventional liquid scintillation counters (Stevenson, *et al.*, 1971).

Results of radionuclide measurements in the internal pathways at the Oyster Creek BWR and Haddam Neck PWR are summarized in Table 3. These data represent annual releases based on average observed concentrations normalized to duration or frequency of various operations per year — such as, number of days of reactor operation, stored gas release volume, how often the reactor is opened for refueling or maintenance, etc. The data confirms that PWR releases tend to be long-lived, mostly ^{133}Xe and ^{85}Kr. BWR effluents contain similar amounts of long-lived radionuclides, but also short-lived radionuclides in much greater amounts. Gaseous effluents other than noble gases are mostly 10-minute ^{13}N at BWR's, and tritium as water vapor at PWR's.

Relative emissions through principal BWR pathways are indicated in Table 4 in terms of ^{133}XE and ^{135}Xe measurements at Oyster Creek. Practically all atmospheric discharge resulted from gas removed by the air ejectors from reactor steam after passing through the turbines. Gas escaping from turbine seals and contaminated ventilation exhaust account for less than one percent.

From observations at Haddam Neck and Yankee, no single PWR pathway appears to predominate. Typical Haddam Neck pathways, and their estimated annual contributions, are given in Table 5; the two most abundant gaseous radionuclides are used as indices. Most of the ^{133}Xe discharge resulted from gas leaking from the reactor into the secondary coolant system and from contaminated ventilation air. Purging the gases accumulated in the reactor vapor container resulted in discharge of much of the longer-lived ^{85}Kr. At the Yankee PWR, most plant discharge, on an annual basis, was long-lived, and resulted from vapor container discharge. The major pathway for short-lived noble gases, although a small fraction of the total, was losses occurring during primary coolant sampling.

MEASUREMENTS IN THE ENVIRONMENT

PWR discharges — mostly the longer-lived radionuclides ^{85}Kr and ^{133}Xe — lead to maximum radiation doses of approximately 1 mrem/year. BWR release rates, usually 100 to 1000 times higher than PWR's, but discharged from tall ($\geq$ 100-meter) stacks, result in maximum doses of about 10 mrem/year. The maximum exposure applies usually to small groups of people living near the reactor exclusion boundary in prevalent downwind directions; whereas most people, residing at greater distances or in less prevalent wind directions, receive much less dose. By comparison, these dose levels are small fractions of the average per capita dose of 130 mrem/year from natural radioactivity in this country, or the 500 mrem/year allowed for operations licensed by the USAEC. The stringent proposed criteria of five percent or less of average natural radiation, however, will require the aforementioned gas treatment in many instances.

Highly accurate and sensitive techniques are needed to measure ambient reactor radioactivity, and to distinguish it from natural background radioactivity, which fluctuates at a relatively low intensity. Often, short-term sampling is conducted only when meteorological, or other conditions, are favorable. Typical environmental concentrations and doses from BWR and PWR releases are given in Table 6. The PWR example applies during release of stored gas — usually the only occasion when its plume is detectable.

To determine the effects of a planned reactor, radiation to populations within 80 km of the site is estimated from expected atmospheric dispersion of effluents, taking into account local wind and atmospheric stability patterns. Environmental studies by this laboratory are made to confirm such dose estimation techniques, and to seek sensitive methods for monitoring exposure.

Plumes in the environment at BWR's can usually be detected readily with 5 x 5-cm NaI(T1) detectors coupled to count-rate meters. The plume at a PWR during a stored gas release was located with a large thin (2-mm thick by 13-cm diameter) NaI(T1) probe developed for the detection of low-energy photons — in this case, the 81 keV gamma ray from ^{133}Xe. Such instruments can provide semi-quantitative exposure rates, if they are calibrated with reference, for example, to an ionization chamber.

Short-term measurements, to test dose estimates from plume gamma radiation, are obtained with a Shonka tissues-equivalent ionization chamber coupled to a sensitive vibrating capacitor electrometer. The instrument can measure an increase of approximately 0.1 μ rad/hr, which corresponds to a steady exposure of 1 mrad/year. Each reading requires 30 seconds to 10 minutes, depending inversely on the radiation intensity. The addition of a chart recorder allows continuous instantaneous readings (Gustafson, *et al.*, 1964).

Long-term exposure monitoring is accomplished with a commercially available, high-pressure ionization chamber and a continuous recorder. Its sensitivity is similar to the Shonka ionization chamber. Simultaneous monitoring at many locations is performed with thermoluminescent dosimeters (TLD's). TLD's must be carefully selected for low intrinsic radioactivity, and, at best, are less sensitive than ionization chambers. Optimum sensitivity of the EG&G Model TL-15 CaF_2(Mn) type, for example, is approximately 10 mrad/year. Taking the TLD reader to the reactor site eliminates the need to account for the sizable dose accumulated in shipping TLD's (Beck, *et al.*, 1972).

Samples for determining ambient concentrations of radioactive gases in the plume are obtained by compressing air into 34-liter metal bottles, with rated capacities of 0.9 m^3 each. Xenon-133 is a useful radionuclide for analysis because its discharge rate is relatively high at both BWR's and PWR's and its half-life is conveniently long. Xenon-133 is concentrated for analysis by passing 100-liter aliquots through a 450-ml bed of charcoal immersed in a dry ice-acetone refrigerant bath. The charcoal is transferred to a sealed 450-ml container, and analyzed by a gamma-ray spectrometer. Minimum detectable concentration, using a 10- x 10-cm NaI(T1) detector, is 400 pCi/m^3 for analysis 5 days after sampling.

Atmospheric dispersion values can sometimes be determined by passing large volumes (> 1 m^3/min) of air through particulate filters for sampling the 17.8-min ^{88}Rb and 32-min ^{138}Cs progeny of noble gases. Their short half-lives, however, require that multichannel analyzers be nearby for immediate counting. Since the concentration varies as the plume shifts, sampling durations must be restricted to less than an hour to minimize errors in decay calculations.

Sampling ground-level air in the environment, as well as stack effluents, is a direct method for determining the effects of local meteorology and topography on plume dispersion. Samples of airborne particles may also give this information, but require rapid analysis and some interpretation of results. The Shonka tissue-

equivalent ionization chamber yields direct readings of exposure rates with high precision, but the instrument must be handled carefully in the field, and is sensitive to adverse weather conditions. The high-pressure ionization chamber is useful for measuring plume radiation in the environment for long periods of times. Simultaneous dose measurements at many locations is obtained economically with low background TLD's, when high sensitivity is not necessary. For long duration measurements, monitoring, to integrate fluctuating natural radiation contributions during the period, must be performed to obtain the net dose from the plume.

REFERENCES

Beck, H., *et al.,* **1972),** *New Perspectives on Low Level Environmental Radiation Monitoring Around Nuclear Facilities,* Nuclear Technology 14, 232-239.

Gustafson, P. F., J. Kastner, and J. Luetzelschwab, (1964), *Environmental Radiation: Measurements of Dose Rates,* Science 145, 44.

Kahn, *et al.,* **(1970),** *Radiological Surveillance Studies at a Boiling Water Nuclear Power Reactor,* U. S. Public Health Services Rept. BRH/DER 70-1.

Kahn, B., *et al.,* **(1971),** *Radiological Surveillance Studies at a Pressurized Water Power Reactor,* U. S. Environmental Protection Agency Rept. RD 71-1.

Kahn, B., *et al.,* **(UP-a),** *Summary Report — Field Trips to Haddam Neck Nuclear Power Station,* U. S. Environmental Protection Agency Rept., to be published.

Kahn, B., *et al.,* **(UP-b),** *Radiological Surveillance Studies at the Oyster Creek Nuclear Generating Station — Progress Report No. 2,* U. S. Environmental Protection Agency, not published.

Martin, M. J., Nuclear Data Project, Oak Ridge National Laboratory. Untitled data, to be published.

Meek, M. E., and B. F. Rider, (1972), *Compilation of Fission Product Yields,* General Electric Co. Rept. NEDO-12154.

Rogers, L., and C. C. Gamertsfelder, (1971), *USA Regulations for the Control of Releases of Radioactivity into the Environment in Effluents from Nuclear Facilities,* Environmental Aspects of Nuclear Power Stations, International Atomic Energy Agency, Vienna, 127-144.

Stevenson, D. L., and F. B. Johns, (1971), *Separation Techniques for the Determination of ^{85}Kr in the Environment,* Rapid Methods for Measuring Radioactivity in the Environment, International Atomic Energy Agency, Vienna, 157-162.

U. S. Atomic Energy Commission, (AEC, UP), *Report on Releases of Radioactivity in Effluents and Solid Waste from Nuclear Power Plants for 1972,* to be published.

U.S. Atomic Energy Commission (1973), News Releases 4, No. 30 (AEC, NR4-30).

TABLE 1. Properties of Fission Produced Noble Gases with Half Lives Greater than 3 Minutes.

Radionuclide	Half-Life*	Fission yield**	Generation rate, Ci/sec-MW(e)	Radioactive progeny
^{83m}Kr	1.86 hrs.	6.3×10^{-3}	1.6×10^{6}	---
^{85m}Kr	4.36 hrs.	1.4×10^{-2}	1.6×10^{6}	---
^{85}Kr	10.7 yrs.	3.2×10^{-3}	1.6×10^{1}	---
^{87}Kr	76.4 min.	2.6×10^{-2}	9.7×10^{6}	^{87}Rb
^{88}Kr	2.80 hrs.	3.5×10^{-2}	6.0×10^{6}	^{88}Rb
^{89}Kr	3.16 min.	4.7×10^{-2}	4.3×10^{8}	^{89}Rb, ^{89}Sr
^{131m}Xe	11.9 days	1.9×10^{-4}	3.2×10^{2}	---
^{133m}Xe	2.20 days	1.9×10^{-3}	1.7×10^{4}	---
^{133}Xe	5.29 days	6.6×10^{-2}	2.5×10^{5}	---
^{135m}Xe	15.6 min.	1.0×10^{-2}	1.9×10^{7}	---
^{135}Xe	9.13 hrs.	6.4×10^{-2}	3.4×10^{6}	^{135}Cs
^{137}Xe	3.84 min.	6.1×10^{-2}	4.6×10^{8}	^{137}Cs, ^{137m}Ba
^{138}Xe	17 min.	6.2×10^{-2}	1.1×10^{8}	^{138}Cs

* Martin, Unpublished.
** Meek, *et al.,* (1972).

TABLE 2. Average Rates of Noble Gas Release at BWR and PWR Stations, 1972 (AEC, UP).

Station	Year of initial operation	Release rate, μCi/sec
BWR		
Dresden 1	1959	2.78×10^4
Dresden 2 & 3	1970-71	1.36×10^4
Millstone	1970	2.51×10^4
Monticello	1971	2.38×10^4
Nine Mile Point	1969	1.64×10^4
Oyster Creek	1969	2.75×10^4
PWR		
Ginna	1969	3.74×10^2
Haddam Neck	1967	2.05×10^1
Indian Point 1	1962	1.72×10^1
Palisades	1971	1.60×10^1
Point Beach 1	1970	8.92×10^1
Robinson 2	1971	No Data
San Onofre	1967	6.06×10^2
Yankee	1960	5.81×10^{-1}

TABLE 3. Annual Releases of Gaseous Radionuclides in Curies from 600-MWe BWR and PWR Stations.

	Oyster Creek BWR*	Haddam Neck PWR**
^{85m}Kr	9×10^4	7
^{85}Kr	1×10^2	1×10^2
^{87}Kr	2×10^5	7
^{88}Kr	2×10^5	1×10^1
^{133m}Xe	7×10^3	2×10^1
^{133}Xe	3×10^5	3×10^3
^{135}Xe	4×10^5	8×10^1
^{138}Xe	7×10^4	3†
Others, half-lives $\leq$ 15 m	7×10^4	4†
Other gases	7×10^2	8×10^1

* Based on an average gross stack release rate of 4.3×10^4 μ Ci/sec from July 1971 to June 1972 and 319 days/yr of reactor operation.

** Based on 330 days/yr of reactor operation and measurements made from July 1970 to May 1971.

† Computed relative to measured ^{85m}Kr for ^{89}Kr; and to ^{133}Xe for ^{135m}Xe, ^{137}Xe, and ^{138}Xe.

TABLE 4. Typical BWR Pathway Contributions to Plant Gaseous Releases in Ci/yr (Based on Annual Releases Estimated for the Oyster Creek Station).

Pathway	^{133}Xe	^{135}Xe
Main condenser air ejectors	2.8×10^5	3.9×10^5
Turbine gland seal air ejector	2.6×10^2	7.2×10^2
Building ventilation exhaust	1.6×10^3	3.9×10^3

TABLE 5. Typical PWR Pathway Contributions to Plant Gaseous Releases in Ci/yr (Based on Annual Releases Estimated for Haddam Neck Plant).

Release Pathway	^{85}Kr	^{133}Xe
Stored gas	2.8×10^{1}	7.0×10^{1}
Secondary steam condenser air ejector	1.2×10^{1}	1.6×10^{3}
Building exhaust	1.0×10^{1}	9.6×10^{2}
Vapor container	7.2×10^{1}	1.7×10^{2}
Coolant sampling	1×10^{-3}	1×10^{-1}
Turbine hall to air	1.8×10^{1}	ND*
Totals	1.4×10^{2}	2.8×10^{3}

* Not detectable

TABLE 6. Typical Reactor Effluent Release Rates and Environmental Measurements.

Reactor type	Noble gas release rate μCi/sec	^{133}Xe stack conc., $\mu Ci/m^3$	Ground-level conc. of ^{133}Xe, $\mu Ci/m^3$	Radiation exposure, $\mu R/hr$
BWR	1.4×10^{5}	2.7×10^{2}	4.6×10^{-2}*	3.1×10^{1}*
PWR	4.8×10^{3} (4-hr release of stored gas)	7.4×10^{1}	2.7×10^{-2}**	1.4×10^{-1}**

* At 1.5-km distance and atmosphere slightly unstable.

** At 0.6-km distance and atmosphere slightly unstable.

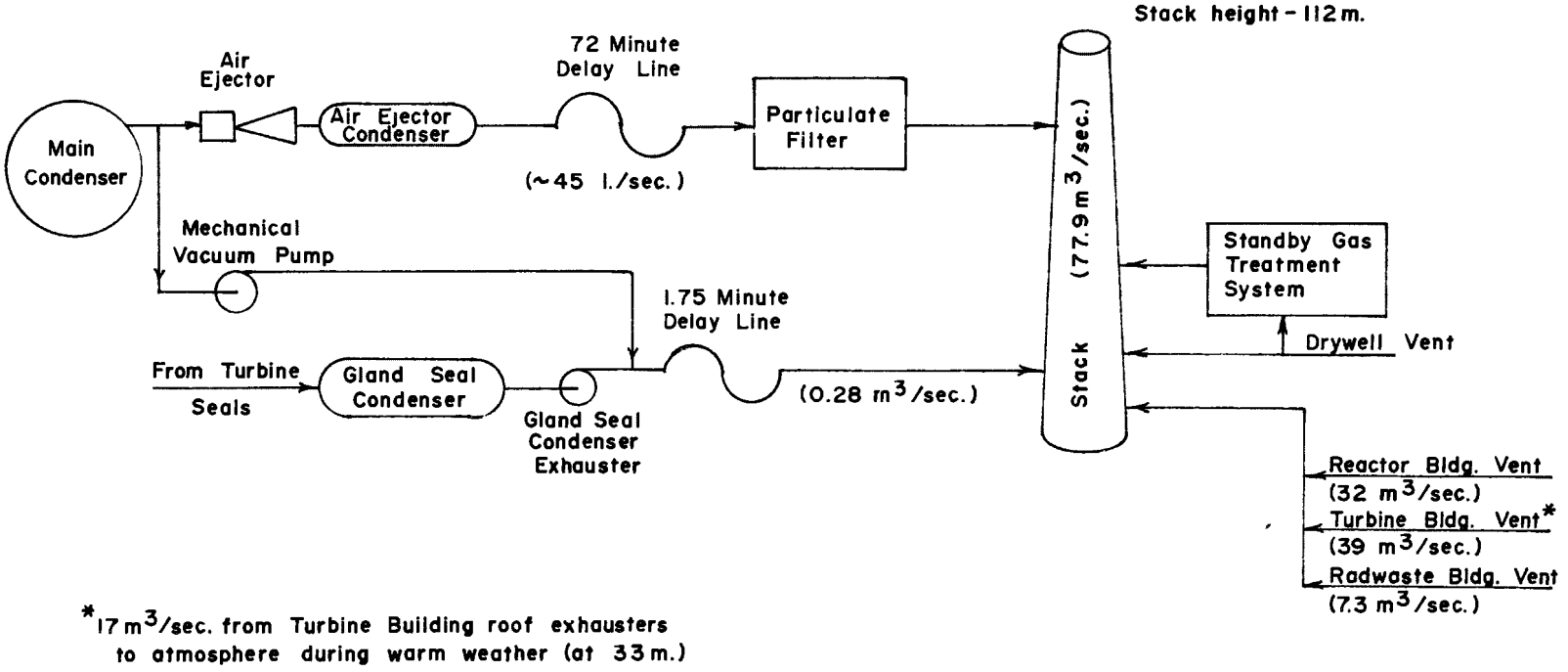

Figure 1. Typical BWR Gaseous Waste System (Oyster Creek).

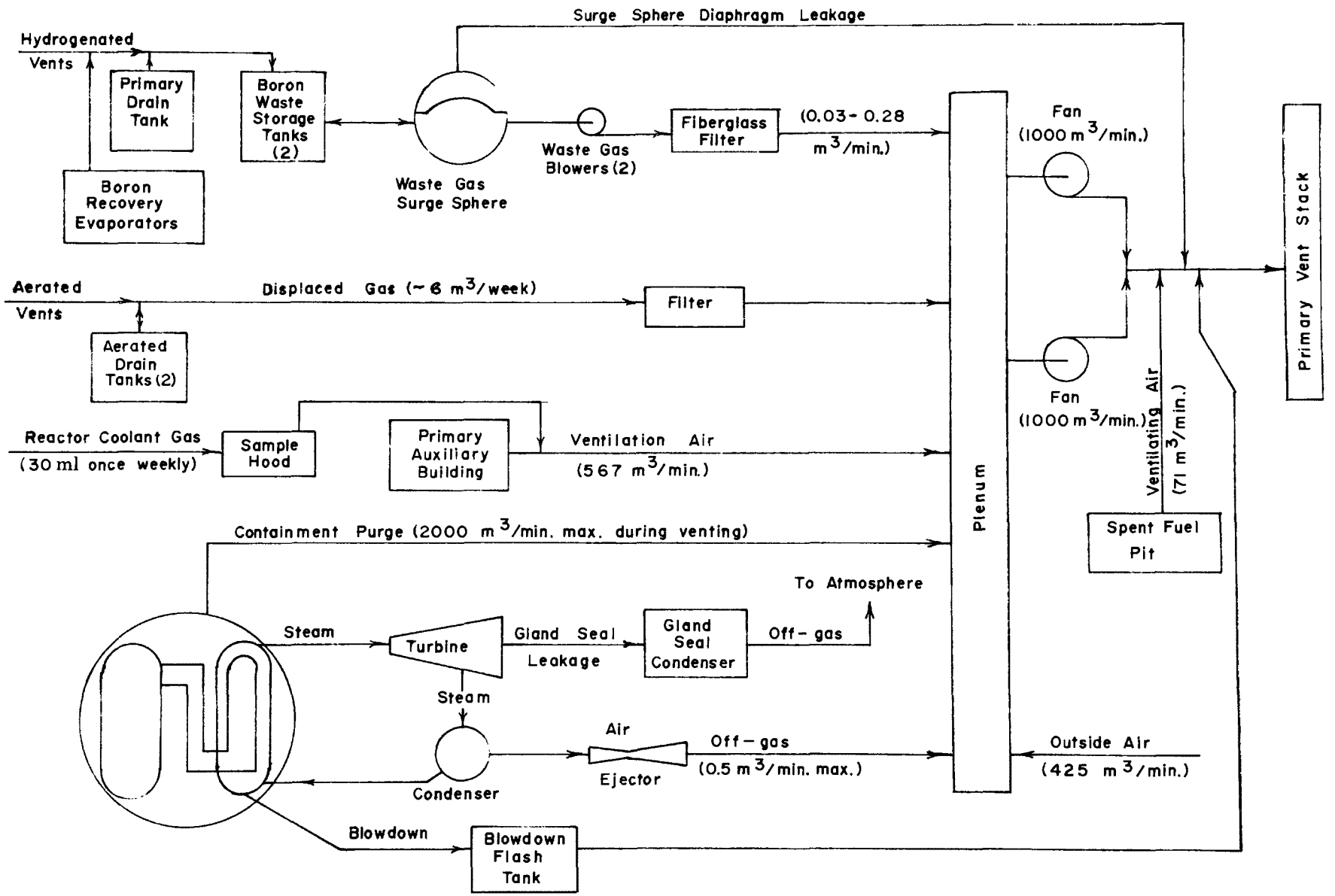

Figure 2. Typical PWR Gaseous Waste System (Haddam Neck).

III. Environmental Radon

ENVIRONMENTAL RADON

J. H. Harley
Health and Safety Laboratory
U.S. Atomic Energy Commission
New York, New York

Abstract

Of all the noble gases, radon has been the one which could be most easily measured in the atmosphere. This may very well be the reason why a bibliography of a thousand references to radon and its daughters can be easily assembled. Taking a more charitable view it may be that concern for the radiation dose to man or the use of radon and its particulate daughters as tracers has brought on this flood of literature.

Radon-222 is the most interesting of the three radon isotopes since its half-life is of the same order as many atmospheric processes. This allows tracing on a global scale and even the development of global inventories.

While radon-222 and its daughters present the highest natural dose to man, we have been much more concerned by certain special cases of exposure. These include the occupational exposure of miners, the use of high radium content materials in housing, and the high radon content of certain local water supplies. These latter will be described briefly along with the more normal distribution of radon levels in the environment.

INTRODUCTION

A number of people have expressed surprise at the recent reports (e.g. Brodzinski, 1972 and Gorenstein, *et al.*, 1973) of finding radon on the moon. I am afraid our real surprise would have come if no radon had been found; and such a finding would certainly require some new theories on the origin of the moon. After all, radon-222 seems to be everywhere on earth — being distributed in the soil, in the ground waters, and in the lower levels of the atmosphere. Its presence in air has been known since the turn of the century when Rutherford observed that the properties of atmospheric radioactivity were consistent with the properties of radon.

In the case of our own laboratory, our first publications involving radon date back more than twenty years, and each time we feel that our radon work is complete, some new problem arises that requires additional study. In preparing this paper, I soon found a large excess of data, and so I was forced into limiting the material to atmospheric radon, with most of the emphasis on radon-222. The approach is to be a broad-brush treatment of where radon comes from, where it is, and where it goes. The documentation and calculations appear at the end of the paper.

SOURCES OF RADON IN THE ATMOSPHERE

Radon-222 is the immediate daughter of radon-226, which is distributed in soil, rocks, ocean water, and ocean sediments. Some reasonable portion of the radon atoms, produced by radium decay on land, enter the soil gases or escape into the atmosphere. The remainder may be trapped inside soil or rock particles, or appear in solution in the various parts of the aquatic environment. Radon produced in ocean sediments can only remain in the sediments or escape into the bottom waters. The first exercise here is an attempt to look at radon production and distribution on a global basis.

The major release of radon to the atmosphere is from soil. Many measurements of the rate of emanation show a value of 1,600 pCi/cm^2 per year to be a reasonable average for soil. If we multiply this by the land area of the world, we come up with a release of 2.4×10^9 curies/year.

The release from the ocean surface is less than from the land, being only about 6 pCi/cm^2 per year. Multiplying by the area of the ocean, we have a total release of 2.3×10^7 curies per year. The ocean evaporation process would be included in this quantity, but the contribution is small.

The burning of natural gas and coal contributes even smaller amounts. Natural gas contains about 10 pCi/liter, and the world consumption of about 8×10^{14} liters per year would yield only 8,000 curies. Coal appears to average about 0.2 pCi of radium per gram. If the radon in equilibrium is released from the world usage of 2.3×10^{15} grams per year, we end up with about 450 curies as the annual production. I do not know of any comparable figures for crude oil, but it is obvious that fuels do not contribute a major part of our global radon.

It is difficult to assess the possible contribution of radon escaping from ground water and that exhaled by plants. We do know that many waters contain thousands of picocuries of radon per liter, and that plants may release several times as much radon per unit of earth's surface as the soil itself. An educated guess is that these sources would not increase the amount of radon entering the atmosphere by 20%. The other possibility, production from airborne radium, is easy to dismiss since concentrations of radon in air are thousands of times greater than the radium.

The greatest pool of ^{226}Ra lies in the deep sediments of the oceans. This maintains the sea water near the bottom at levels of radium a few times that of the surface, but does not contribute to our environmental radon.

RADON IN THE ATMOSPHERE

Our total radon release to the atmosphere of about 2.4×10^9 curies per year is, of course, decaying with a 3.8 day half-life. This means that the equilibrium amount present at any time is 3.6×10^7 curies. This figure can be compared with measured air concentrations, if we can approximate the distribution of radon with altitude.

There are a reasonable number of vertical profiles available, but the data are extremely variable. However, if we want some sort of approximation, an exponential decrease with height, and a half-thickness of 700 meters will do. From this, we would calculate the average surface concentration for radon to be 70 pCi/m^3.

The measured values for radon in surface air over the continents would appear to average between 100 and 200 pCi/m^3 while, over the oceans, the value is probably nearer to 5. Thus the agreement is sufficiently good so that we can accept the general picture from our calculations. A number of measurements of radon gas at the earth's surface are tabulated in Table 1. Similar concentrations derived from daughter measurements are shown in Table 2. These values give some idea of the geographic variability, and are obviously dependent on continental sources.

Indoor radon concentrations will be of the same order as the values measured outdoors when there is reasonable ventilation. There are a number of cases where building materials with high activity have produced elevated radon concentrations, but these are not widespread.

VARIABILITY IN RADON CONCENTRATION

Radon concentrations vary locally with height, with certain meteorological factors, and with time. Since the source of radon is the ground surface, it is not surprising that the concentration falls off with height. This change is more apparent in a stable atmosphere, where diffusion is the controlling process, but disappears in a turbulent atmosphere where mixing destroys the profile.

The activity is not only greater near the ground, but it also tends to fluctuate more with time than at heights of a few meters. Moses, *et al.*, (1970) showed the radon concentration to be 2 to 5 times greater at 2 millimeters than at one meter. Fontan (1966), found the concentration at 30 meters to be about one-half of that below one meter. At greater heights, Bradley, *et al.*, (1970), estimated a half-depth for radon concentration of about 700 meters; while others have found other gradients or found more than one slope. Such values are not universally applicable, since they depend on the degree of mixing in the atmosphere studied.

Machta, *et al.*, (1962), attempted to measure radon in the upper atmosphere. Their average value in the troposphere at 25,000 feet was 7 pCi/m^3. Comparable measurements made at HASL (Hallden, 1962) gave similar results over Alaska, and a range of 4-40 pCi/m^3 in the troposphere over the southwestern United States. Measurements at higher altitudes, by these and other authors, are dubious because of a "blank problem," but the concentration in the stratosphere is apparently very low.

There is reasonable agreement that the meteorological factor showing the greatest affect on radon concentrations is atmospheric stability. All of the other factors only seem to indicate differences in the horizontal distribution of emanating radon. For example, the change in concentration, often found with wind direction, merely shows a change of source. It is true that emanation is lower when the soil is cold or frozen, Pearson, *et al.*, (1965); and it has been shown that the radon concentration drops to about one-half following a rain (Israel, 1966). This again is apparently due to a temporary decrease in emanation.

The diurnal variations reported indicate a morning peak and a sharp drop in the afternoon. These correlate quite well with inversion conditions. High values exist during the inversion in the still air, with a decrease at the time when the inversion vanishes and the turbulent diffusion moves the radon upward into a larger volume. The overall averages tend to show that nighttime concentrations are a few times higher than those existing during the day, once again due to atmospheric stability. Over longer time periods, Lockhart (1962) showed that the concentrations in Washington were lowest in April, and were more than twice as high in December. He attributed this to the preponderance of continental air in winter and oceanic air in the spring.

The variations described are all the resultant of two factors, the emanation rate, and the degree of dilution with air having higher or lower concentrations of radon. These changes can be used to follow atmospheric processes in time scales on the order of days, but the scientist must take account of multiple sources, so that the experiment frequently becomes hopelessly complex.

FATE OF ATMOSPHERIC RADON

A little consideration shows that radon essentially disappears by decay. The oceans and ground waters appear to be sources of radon — rather than sinks — and the amount transferred to the stratosphere seems to be negligible.

The concentration difference over the oceans and over the continents seems at first sight to be too great to be due only to decay. This is not so, if we consider that surface winds probably average about 15 km/hour. At that speed, it would take ^{222}Rn twenty half-lives to go around the earth at our latitude. Thus the concentrations in or over the ocean surface seem reasonable.

The winds at higher altitudes move much more rapidly, therefore, the concentrations at high altitudes over land and over the oceans should differ by smaller factors. While there are only a few vertical profiles over the oceans (BaCuong, *et al.*, 1967), they do show that the concentration does not fall off as rapidly as over the continents.

RADON-DAUGHTERS

The simplicity of measuring the short-lived radon-daughters has been a trap for many authors. The daughters usually become attached to the ambient aerosol and cease to follow gaseous radon; consequently, measurements of activity on filters cannot be automatically converted to radon concentrations.

The degree of equilibrium between radon and its daughters is of considerable dosimetric interest — as well as being important for tracer studies. If radon is in a large confined volume, the daughters will approach equilibrium with a half-life of about 30 minutes. This equilibrium condition is very closely approached in the open air during inversions (Lindeken, 1968). As a specific case, Malakov (1966) found that the average ratio of RaA:RaB:RaC was 1:0.9:0.9. Malakov also showed that the ratios during the emanation maximum got as low as 1:0.05:0.02. The more general condition would seem to be similar to measurements made by our own laboratory of 1:0.7:0.5 (Fisenne, 1973). It is also of dosimetric interest that almost 10% of the RaA in outdoor air exists as unattached ions (Jonassen, *et al.*, 1970).

DOSES FROM RADON AND DAUGHTERS

In considering dose to man, it is fortunate that most of the radon decays outside the biosphere. The ocean sediments, much of the rock and soil, and the air above a few meters, absorb the decay energy, with no consequence to man.

Radon, however, delivers a small dose to the body from the gas that is dissolved in body fluids and fat. This is enhanced by the *in-situ* formation and decay of the solid short-lived daughter products. This has been estimated by the U. N. Scientific Committee as 0.3 mrad/a for their average of 100 pCi $^{222}Rn/m^3$ in air (UNSCEAR, 1966).

The direct inhalation of the daughter products produces the highest localized dose rate to man from natural sources. Using the equilibrium values of 1:0.7:0.5, and a fraction of 0.1 for the free ions or atoms of ^{218}Po, the dose rate will be 15 mrad/a for our calculated air concentration of 70 pCi/m^3 (Harley, 1972). This dose is to basal cells of the tracheobronchial tree. Obviously, from the data of Tables 1 and 2, several areas show exposures several times as high.

THORON IN THE ATMOSPHERE

The global activity of ^{238}U and ^{232}Th are about equal, so it is to be expected that ^{222}Rn and ^{220}Rn will be produced in equal quantities. However, the short half-life of thoron modifies these conditions markedly.

The emanation rates, measured in terms of activity, tend to be much higher for thoron than for radon, since the number of atoms released are comparable, and the thoron half-life is so short. Birot (1971) summarized available data showing radon emanation to be about 50 $aCi/cm^2/s$, while the thoron values averaged a few thousand $aCi/cm^2/s$.

A comparison is possible where concentrations of the parent have been measured in soil, along with the emanation rates. Pearson, *et al.*, (1965) found that soil with 0.64 pCi of ^{226}Ra per gram showed 0.14 $fCi/cm^2/s$ emanation of ^{222}Rn. Guedalia, *et al.*, (1970) found that soil with 0.5 pCi of ^{228}Th per gram showed 7 $fCi/cm^2/s$ of ^{220}Rn. Thus similar parent soil concentrations produced about 50 times as much activity for the emanating thoron.

The possible difference is much greater, since the soil with radium should produce 1.4×10^{-3} fCi/s of ^{220}Rn per gram of soil. The ratio in this case would be several thousand.

Estimated levels of thoron in free air are frequently less than radon by factors of 20 to 200. Israel (1964) has explained this extreme reduction by the fact that thoron is generally measured as Thorium-B (^{212}Pb), which is not in equilibrium. When calculated to equilibrium, Israel believes the activities of the two radons are about equal near the surface.

There are a few direct measurements of the gas. Israel (1966) found thoron levels of roughly 30, 45, and 50 pCi/m^3 at one site in Germany when measuring at 3.5, 2, and 1 meters, respectively. Fontan (1966) found comparable levels at one site in France when measuring at 1.5 meters. Simultaneous measurements of radon at this site were only a few times higher than the thoron. Thus, thoron concentrations at the surface are on the same order as the radon even though they will decrease much more rapidly with height.

The contribution of the oceans to the global thoron is negligible — the thorium is rapidly transferred to sediments, and the time scale of other processes is too great.

CONCLUSIONS

It is possible to account for the global concentrations of radon-222 in the atmosphere using measured values of emanation rate from soil. The oceans, fuel combustion, and miscellaneous sources do not contribute significantly. The distribution of gaseous radon released from emanating areas is controlled by the winds and by vertical turbulence. Radon disappears by decay, with no other apparent sink.

The daughters of radon are fairly close to equilibrium with their parent, and about 10% of the first daughter exists unattached to the ambient aerosol. The calculated global average of 70 pCi/m^3 would give a whole body dose of about 0.2 mrad/year from the radon itself and 15 mrad/year to the tracheobronchial tree from the daughters.

CALCULATIONS

1. Radon Production from Soil.

A number of values for emanation of ^{222}Rn from soil have been reported. Wilkening (1972) reviewed the data and showed an overall mean of 43 $aCi/cm^2/s$. Birot (1971) showed a mean of about fifty (or 1600 $pCi/cm^2/a$), and this round number is used here.

The rate is lower when the ground is cold or frozen, and when the ground is wet following rain. The most marked change is a transient doubling of the emanation rate when the barometric pressure falls 1% as shown

by Kraner, *et al.*, (1964). The reason is that the concentration of radon gas in the soil is perhaps 10^4 to 10^5 times that in the free air above it. It is interesting that a similar ratio holds for the radon in water held in ocean sediments, and the overlaying sea water, Broecker, *et al.*, (1967).

Land Area of the Earth: 1.5×10^{18} cm^2
Average Emanation: 1.6×10^3 pCi/cm^2/y
Production = $(1.6 \times 10^3)(1.5 \times 10^{18})(10^{-12}) = 2.4 \times 10^9$ Ci/a

2. Radon Production from the Oceans.

Emanation from the oceans is estimated indirectly as the deficiency of radon in the upper layers of the oceans compared with the equilibrium amounts expected from the radium concentrations. Hoang, *et al.*, (1972) estimated the flux as being about 50 atoms/m^2/s, which would be 0.3 aCi/cm^2/s (or 9 pCi/cm^2/a), Broecker (1973) has added new data and would prefer a lower value of 6 pCi/cm^2/a.

Evaporation from the ocean surface does not contribute to the emanation. The annual evaporation of 5.6×10^{14}m^3, when multiplied by a surface radon concentration of about 30 pCi/m^3 would only supply 1.7×10^4 Ci/a.

Ocean Area of the Earth: 3.6×10^{18} cm^2
Average Emanation: 6 pCi/cm^2/a
Production = $(6)(3.6 \times 10^{18})(10^{-12}) = 2.3 \times 10^7$ Ci/a

3. Radon Production from Natural Gas.

World Consumption (SCEP, 1970): 8.2×10^{14} 1/a
Average Concentration (Barton, *et al.*, 1973): 10 pCi/1
Production = $(8.2 \times 10^{14})(10)(10^{-12}) = 8200$ Ci/a

4. Radon Production from Coal.

World Consumption (SCEP, 1970): 2.3×10^{15} g/a
Average Concentration: 0.2 pCi/g
Production = $(2.3 \times 10^{15})(0.2)(10^{-12}) = 460$ Ci/a

5. Radon Production from Plants and Ground Water.

Pearson (1967), has shown that the release of radon through the leaves of corn plants was about 3 times greater per unit of land area than bare soil. Also, it is quite possible that significant amounts of radon are released when ground water and sub-surface water carrying dissolved radon become warmed at the surface. These factors are impossible to evaluate at the present time. The best approach is that transpiration and evaporation from the continents totals 1×10^{14} m^3/a of water. Since ground water seems to average about 5,000 pCi/1 (UNSCEAR, 1972), the evaporated and transpired water should release 5×10^8 Ci/a of radon as a maximum.

6. Radon in the Atmosphere.

Annual Emanation: 2.4×10^9 Ci $= 6.6 \times 10^6$ Ci/d
Decay Constant: 0.18 d^{-1}
Equilibrium Amount: $\frac{6.6 \times 10^6}{0.18} = 3.6 \times 10^7$ Ci

7. Radon Concentration in the Atmosphere.

Calculating the average radon concentration at the earth's surface is only an approximation, depending on assumptions of vertical distribution.

Half-depth = 700 m, $\mu = 1 \times 10^{-3}$ m^{-1}
Total Radon: = 3.6×10^{19} pCi
World Area: 5.1×10^{14} m^2
Surface Concentration = $\frac{(3.6 \times 10^{19}/(10^{-3})}{5.1 \times 10^{14}} = 70$ pCi/m^3

The global value can be modified considering that the northern hemisphere has twice the land area of the southern hemisphere. The concentrations would then be about 100 pCi/m^3 in the northern hemisphere, and 50 pCi/m^3 in the southern.

8. Radon Concentrations Indoors.

Haque, *et al.*, (1965) measured the emanation from the walls in several rooms in England and found values ranging from 6 to 100 pCi/m^2/h (or 0.2 to 3 aCi/cm^2/s). If we consider a sealed room 5 meters square and 3 meters high, with walls and ceiling emanating at 30 pCi/m^2/h, the hourly emission would be 2,500 pCi. The equilibrium concentration would be about 4,400 pCi/m^3.

High ventilation rates would reduce the concentration toward the outdoor level; for example, 4 air changes per hour with outside air at 70 pCi/m^3 would drop the room concentration to less than 80 pCi/m^3. This drop is possible because the emanation does not supply radon fast enough to replace the amount removed. Thus, for normal building materials, indoor concentrations of radon are only high in closed or poorly ventilated areas.

REFERENCES

Ba Cuong, N. and G. Lambert, G. Polian, J. Jacquin (1967), *Comparison of the Vertical Distributions of ^{222}Rn from 0 to 4500 m above the Atlantic Ocean, the Antarctica Continent and the Paris Region* "Compt. Rend." 265, Series B. 1065-8.

Barton, C. J., R. E. Moore and P. S. Rohwer (1973), *Contribution of Radon in Natural Gas to the Natural Radioactivity Dose in Homes.* U. S. Atomic Energy Commission Report ORNL-Tm-4154.

Birot, A.(1971), *Contribution a l'etude de la diffusion du radon et des aerosols dans la troposphere.* Thesis, Universite de Toulouse, France.

Bradley, W. E. and J. E. Pearson (1970), *Aircraft Measurements of the Vertical Distribution in Radon in the Lower Atmosphere.* "J.G.R." 75, 5890.

Brodzinski, R. L. (1972), *Radon-222 in the Lunar Atmosphere.* "Nature," Physical Science 238, No. 85, 107-09.

Broecker, W. S., Y. H. Li and J. Cromwell (1967), *Radium-226 and Radon-222: Concentration in Atlantic and Pacific Oceans.* "Science" 158, 1307.

Broecker, W. S. (1973), Private Communication, Lamont-Doherty Geological Observatory.

Fisenne, I. M. (1973), *Measurements of New York City Air,* Health and Safety Laboratory, unpublished.

Fontan, J., A. Birot, D. Blanc, A. Bouville and A. Druilhet(1966) *Measurement of the Diffusion of Radon, Thoron and Their Radioactive Daughter Products in the Lower Layer of the Earth's Atmosphere,* "Tellus" 18, 623.

Glauberman, H. and A. J. Breslin(1957), *Environmental Radon Concentrations,* U.S. Atomic Energy Commission Report NYO-4861.

Gold, S., H. W. Barkhau, B. Schleien and B. Kahn (1964), *Measurement of Naturally Occurring Radionuclides in Air,* "The Natural Radiation Environment," 369, John A. S. Adams and Wayne M. Lowder (Editors), University of Chicago Press.

Golden, J. C. Jr. (1968), *Natural Background Radiation Levels in Florida,* U. S. AEC Report, Sandia Laboratories SC-RR-68-196.

Gorenstein, P. and P. Bjorkolm(1973), *Detection of Radon Emanation from the Crater Aristarchus,* "Science" 179, 792.

Guedalia, D. J. L. Laurent, J. Fontan, D. Blanc and A. Druilhet (1970), *A Study of Radon-220 Emanation from Soils,* "J.G.R." 75, 357-69.

Hallden, N. (1962), *Rn Analyses of Stratospheric Samples,* Health and Safety Laboratory, unpublished.

Haque, A. K., A. J. L. Collinson and C. O. S. Blyth Brooke(1965), *Radon Concentration in Different Environments and the Factors Influencing It,* "Phys. Med. Biol." 10, 505.

Harley, N. and B. S. Pasternack(1972), *Alpha Absorption Measurements Applied to Lung Dose from Radon Daughters,* "Health Physics" 23, 771-782.

Hoang, C. T. and J. Servant (1972) *Le flux de radon de la mer,* "Comptes rendus Acad. Sci." Paris, Serie D, 205.

Israel, H.(1964), *The Radon-220 Content of the Atmosphere,* "The Natural Radiation Environment," 313, John A. S. Adams and Wayne M. Lowder (Editors), University of Chicago Press.

Israel, H., M. Horbert and G. W. Israel (1966a), *Results of Continuous Measurements of Radon and its Decay Products in the Lower Atmosphere,* "Tellus" 18, 638.

Israel, G. W. (1966) 2 Meteorological Influences on the Thoron (^{220}Rn) Content of the Atmosphere, "Tellus" 18, 633-37.

Israelsson, S., E. Knudsen and E. Ungethum(1972), *Radon and Thoron in the Air Near the Ground,* Marsta Observatory, Uppsala, Sweden, Report No. 28.

Jonassen, N. and M. H. Wilkening(1970), *Airborne Measurements of Radon-222 Daughter Ions in the Atmosphere,* "J.G.R." 75, 1745.

Kraner, H. W., G. L. Schroeder, and R. D. Evans(1964), *Measurements of the Effects of Atmospheric Variables on Radon-222 Flux and Soil-Gas Concentrations,* "The Natural Radiation Environment," 191, John A. S. Adams and Wayne M. Lowder (Editors), University of Chicago Press.

Lindeken, C. L. (1968) *Determination of the Degree of Equilibrium Between Radon-222 and its Daughters in the Atmosphere by Means of Alpha-Pulse Spectroscopy,* "J.G.R." 73, 2823.

Lockhart, L. B., Jr. (1962), *Atmospheric Radioactivity at Washington, D. C., 1950-1961,* U. S. Naval Research Laboratory Report NRL 5764.

Lockhart, L. B., Jr.(1964), *Radioactivity of the Radon-222 and Radon-220 Series in the Air at Ground Level,* "The Natural Radiation Environment," 131, John A. S. Adams and Wayne M. Lowder (Editors), University of Chicago Press.

Machta, L., and H. F. Lucas, Jr. (1962), *Radon in the Upper Atmosphere,* "Science" 135, 296.

Malakhov, S. G., *et al.,***(1966),** *Diurnal Variations of Radon and Thoron Decay Product Concentrations in the Surface Layer of the Atmosphere and their Washout by Precipitation,* "Tellus" 18, 643.

Moses, H., A. F. Stehney, and H. F. Lucas, Jr. (1960), *Effect of Meteorological Variables upon the Vertical and Temporal Distributions of Atmospheric Radon,* "J.G.R." 65, 1223.

Pearson, J. E. and G. E. Jones(1965), *Emanation of Radon-222 from Soils and its Use as a Tracer,* "J.G.R." 70, 5279.

Pearson, J. E.(1967), *Natural Environmental Radioactivity from Radon-222,* U. S. Public Health Service Report 999-RH-26.

Report of the United Nations Scientific Committee on the Effect of Atomic Radiation (UNSCEAR 1972), "Ionizing Radiation: Levels and Effects", General Assembly, Official Records, XXVII Session, Supplement No. 25 (A/8725)

Report of the United Nations Scientific Committee on the Effects of Atomic Radiation (UNSCEAR 1966), General Assembly, Official Records, XXI Session, Supplement No. 14 (A/6314).

Servant, J.(1966), *Temporal and Spatial Variations of the Concentration of Short-Lived Decay Products of Radon in the Lower Atmosphere,* "Tellus" 18, 663.

Study of Critical Environmental Problems (SCEP 1970), "Man's Impact on the Global Environment", Assessment and Recommendations for Action, MIT Press, Cambridge, Mass.

Wilkening, M. H.(1959), *Daily and Annual Courses of Natural Atmospheric Radioactivity,* "J.G.R." 64, 521.

Wilkening, M. H., W. E. Clements and D. Stanley (1972), *Radon-222 Flux Measurements in Widely Separated Regions,* Natural Radiation Environment II, In Press.

TABLE 1. Some Measured Radon-222 Concentrations.

Author	Location	Concentration Range (Mean) pCi/m³	
Fontan, *et al.,* (1966)	France	-	(250)
Israelsson, *et al.,* (1972)	Sweden	600 - 5000	-
Moses, *et al.,* (1960)	Illinois	50 - 1000	-
Haque, *et al.,* (1965)	London	10 - 300	(90)
Glauberman, *et al.,* (1957)	N. Y. City	20 - 500	(130)
Wilkening (1959)	New Mexico	-	(240)
Gold, *et al.,* (1964)	Cincinnati	-	(260)
Israel, *et al.,* (1966)	Germany	-	(70)

TABLE 2. Some Radon-222 Concentrations Inferred from Daughter Measurements.

Author	Location	Concentration Range (Mean) pCi/m³	
Servant (1966)	Indian Ocean		(2)
	North Atlantic		(6)
	South Pacific		(2)
	Mediterranean		(100)
Bradley, *et al.,* (1970)	Illinois	70 - 300	-
Malakhov (1966)	Russia	-	(170)
Golden (1968)	Florida	20 - 300	-
Lockhart (1964)	Peru		(42)
	Bolivia		(40)
	Little America		(2.5)
	South Pole		(0.5)
	Washington		(122)
	Japan		(56)

THE SIGNIFICANCE OF RADON AND ITS PROGENY AS NATURAL RADIATION SOURCES IN SWEDEN

J. O Snihs
National Institute of Radiation Protection
Stockholm, Sweden

ACKNOWLEDGEMENT

I should like to acknowledge the substantial assistance provided me in the collection of this material from Mr. H. Ehdwall, Mr. B. Hakansson, and Mr. J. Kulich, in the statistical analysis from Dr. S. Lundquist, and in the preparation of this paper from Mr. C. Wilson.

Abstract

Radon is of current interest from several points of view: as a radiation source in water, buildings, and mines; as a disturbing agent in low-activity measurements; as a tracer element for radium in man; etc. For many years, measurements have been made at the Swedish National Institute of Radiation Protection (NIRP) on radon and its occurrence and behavior in nature. Appropriate sampling and measuring techniques are described for radon in water and air, intended for field as well as laboratory measurements. Some observations on radon concentrations in outdoor air, water, and buildings are reported. Special attention is given to the experience of measurements in mines. The observed concentrations are reported and discussed — as well as the health aspects of the exposure to radon and radon-daughters in mines.

INTRODUCTION

The natural occurrence of radon and its progeny and variations has been studied for many years in many parts of the world. Among radon investigations in Sweden, that carried out by Hultqvist (1956) on the radon content of the air in dwellings deserves particular attention. Hultqvist demonstrated that in some cases the order of magnitude of the natural radon content was such that resultant doses were not insignificant in comparison with the internationally recommended highest permissible radon levels for radiation workers.

Those involved in practical radiation protection work are familiar with the fact that radon can interfer with their measurements. When checking a laboratory for alpha-active surface contamination, the alpha-emitting radon-daughters can influence the measurements. These daughters settle on the surfaces of the room, and if the ventilation is bad, concentrations of radon-daughters can be sufficient to give a direct reading from the surface. Those who use alpha-monitors for the routine measurement of activity on hands should also be aware of the risk of obtaining misleading results. For the same reason, filtration of the ventilation air is employed at many low-level measurement laboratories.

In the routine measurement of airborne activity, the influence of radon can at times appear capricious. For example, when the nuclear-powered ship USS Savannah visited Swedish ports in 1964, one of the precautionary measures was to check on any airborne release of activity from the ship by filter measurements. A barely measurable reading was obtained during the first days, however, late one evening the activity suddenly increased. This was observed both by the safety group on the ship and by the Swedish group ashore. The result was a short, but intensive, spurt of activity on both sides until it was confirmed that the increase was due to radon-daughters. That evening the sea breeze with a low radon content, which had been blowing until then, changed to a land breeze with considerably greater airborne activity.

In this paper, a brief picture is first given of the variations in the radon contents which were observed indoors and outdoors, and their reasons. This is followed by a summary of some observations on the radon contents in drinking water and milk. Finally, the results of radon measurements in Swedish mines will be discussed. The sampling and measuring techniques used will also be described and discussed.

RADON OUTDOORS

Since this airborne activity is due to the diffusion of radon from the ground to the air, its variation is partly a reflection of the variation in the exhalation capacity of the ground. This is reduced by periods of rain, low temperatures, frost, snow cover, and increasing atmospheric pressure (Kraner, *et al.*, 1964 and Tanner, 1964). When the ground is frozen to a depth of 10-20 cm with no snow or ice, for instance, the exhalation may be less than half of that under summer conditions. At the same time the radon concentration in the ground increases during corresponding periods. The relative change in the radon concentration in the ground due to meteorological conditions, however, is a function of the depth below the surface (Kraner, *et al.*, 1964). The nature of the ground and, in particular, its water content influences its ability to diffuse and thus to exhale radon.

The exhalation increases with increasing wind speed. However, increasing wind speed normally results in greater dilution in the lower atmosphere (Israelson, 1968). This is an example of opposing effects which various meteorological conditions often have on the resultant radon content of the air; this makes if difficult to interpret most observations as functions of the weather and the wind.

Other factors which affect the radon concentration in the air, in addition to those influencing the exhalation, are the wind direction, the height above the ground, and the degree of turbulence (Jacobi, 1962). The concentrations in the air of the (short-lived) daughter products of radon (RaA, RaB, and RaC) are also dependent on the height above the ground and the turbulence (Jacobi, 1962). Because of the gradual growth of radon-daughers, there is a lag in the activity concentration in air compared with radon, and with a high degree of turbulence, the equilibrium occurs first at heights of more than 100 m above the ground.

The concentration in air of radon and its daughters shows a diurnal variation which is greatest during the summer and autumn months and least during the winter and spring months (Israelson, 1968). As a rule, a maximum occurs towards the end of the night and a minimum in the afternoon. The reason for this is that the temperature of the lowest layers of the atmosphere reaches a maximum in the afternoon causing a maximum in the turbulent transfer and a minimum in the radon concentration of the air. An interesting comparison can be made between the monthly variations in the natural radioactivity of the air and the concentration in the air of fission products from nuclear weapons tests. Figure 1 shows the monthly variations in 1967 for ^{137}Cs and for radon-daughters in the Stockholm air. It can be seen that a maximum occurs in the ^{137}Cs at approximately the same time as a minimum in the radon-daughter activity and vice versa. The low values for the natural airborne activity during the winter are due to low radon exhalation, and those during the spring and early summer to turbulent dilution. In the autumn the radon exhalation is still high, but the turbulent dilution is less. On the other hand the enhanced turbulence during the spring contributes to the higher ^{137}Cs concentration in ground-level air by increasing the transfer of air between the upper troposphere where there is ^{137}Cs from the reserves in the stratosphere and the ground-level air.

The radon concentration in air over an ocean is low due to dilution and low exhalation from the sea. Thus, the radon concentration in air above ground near the coast can be expected to be low when a sea wind is blowing. In Sweden some determinations of the influence of the wind direction on the radon concentration have been made (Snihs and Wilson, 1968). It was found that the dependence on wind direction was more marked for the west coast (Kristineberg, about 80 km north of Gothenburg) than for the east coast (Stockholm), presumably due the Stockholm archipelago which makes the east coast less well defined than the west. The average radon concentration in air at the west coast was 12 pCi/m^3 (sea wind) and 71 pCi/m^3 (land wind) and at the east coast 38 pCi/m^3 (sea wind) and 82 pCi/m^3 (land wind). The radon and radon-daughter activities were almost identifical in the case of a persistent sea wind, but after a change to a land wind, the radon concentration exceeded that of the daughters. The lowest values for the west coast were lower than the lowest for the east coast. But they were not as low as those which would be expected if the sea wind represented air over the ocean (0.5-2 x pCi/m^3 — Jacobi, 1962). The reason is presumably the contribution made by radon exhalation in Norway or the British Isles.

RADON INDOORS

In Hultqvist's (1956) investigation on gamma radiation and radon levels in some Swedish dwellings built of different building materials, the average values of the radon levels were found at be related to the radium content of the building material, but there was a considerable spread in the radon levels as seen in the summary presented in Table 1.

The highest radon levels in houses built of lightweight concrete are not much higher than in houses of other materials, despite the fact that the radium content of lightweight concrete may be more than an order of magnitude higher than that of other building materials. More important is the ventilation in the houses. With poor ventilation high-radon levels may easily be attained even in houses with a normal radium content in the building materials.

The question of radioactive building materials and its significance for radon levels and especially for gamma radiation indoors, has recently been given renewed attention in Sweden. Some preliminary measurements have been made on radioactivity in building materials and on gamma radiation in houses. The question of how to handle for the future the question of unsuitable building materials causing the unacceptable gamma radiation doses is under discussion. Radon has been measured, but it does not seem to present any problem — probably because of the good ventilation in modern houses.

Radon indoors can present problems in low-activity measurements; e.g. in low-activity whole body gamma measurements and in radon measurements on breath. In the laboratory for whole body measurement at the NIPR, special low-activity building materials were chosen (Lindell, *et al.*, 1964). Before making radon measurements on breath to check, for instance, that the radium burden is well below MPBB, the person has to stay out of doors about half an hour and then breathe aged air from compressed air bottles during the measurement (Snihs, 1973a).

RADON IN DRINKING WATER AND MILK

In connection with a nation-wide investigation made in 1965 on radioactivity in milk due to nuclear weapons testing, it was found that milk from 13 dairies had measurable contents of radon. The highest value (for Vimmerby Dairy) was 0.5 nCi/l. Earlier measurements on the radon content of milk and water (Dobeln, *et al.*, 1964), had indicated that the radon was probably transferred to the milk via radon-rich water drunk by the cows. The relation between the content of radon in milk and the cows' drinking water is such that the concentration in the water can be expected to be about 40 times as high as that found in the milk.

The milk from Vimmerby Dairy came from 458 suppliers and the 0.5 nCi/l thus implied an average of 20 nCi/l in the drinking water at the farms. It was considered improbable that an average value of 20 nCi/l could have been caused by a general occurrence of radon concentrations on that order of magnitude, and there was every reason to suspect that the high average value was caused by a few wells with very high radon concentrations.

By means of sampling and measurement at the farms, and by samples sent to the Stockholm laboratories, the radon concentration was investigated for 135 of the 458 water sources used by the farms supplying milk to Vimmerby Dairy. The selection was made on the basis of the answers to questionnaires sent to all the milk suppliers requesting information on the type of water source and the number of cows. Answers were received from 76% of the farms. The radon measurements gave the results shown in Table 2.

The average value for the 135 water sources investigated was about 2 nCi/l and the highest value found (in a deep bored well) was 63 nCi/l. The results obtained thus gave no explanation for the radon content found in the dairy milk in the 1965 sampling program. More recent radon samples on the milk from Vimmerby Dairy (10 times during 1966 and 1967) have failed to show any measurable radon content. During the spring of 1967, milk was obtained from 26 dairies in the same area every week for four weeks. Only one of these 104 samples had a measurable content of radon. During the spring of 1965, nine of these 26 dairies had radon contents exceeding 35 pCi/l.

The investigation of radon in drinking water continued in 1970 in the form of the measurement of radon in water, mostly from deep-bored wells and with radon contents exceeding 10 nCi/l. The contents of ^{226}Ra, ^{210}Pb, and ^{210}Po were also determined. The data were then compared with earlier data in order to see if there was any correlation between the contents of these nuclides and the geological properties of the infiltration areas of the wells or the depths of the wells (Snihs, 1973b). Some of the conclusions concerning radon were as follows:

(1) Only bored wells, especially those in granite bedrock, had radon contents which exceed 20 nCi/l.

(2) Dug wells had, as a rule, low-radon contents (< 2 nCi/l). Wells on granite bedrock and in till had on the average higher radon contents than other dug wells.

(3) Communal wells (each supplying more than 200 people) are most often dug in sand and gravel and can, therefore, be expected to have low-radon contents.

(4) There was no significant correlation between the radon content and the depths of the wells.

(5) The radiation dose from radon was completely dominant in comparison with the radiation dose caused by the other nuclides examined. In estimating the dose, 100 nCi/l was assumed to correspond to 15 rem/year (Dobeln, *et al.*, 1964).

RADON IN MINES

Since 1970, extensive measurements have been made on radon and radon-daughters in Swedish underground mines. These are ferrous ore mines and non-ferrous ore mines, about 60 altogether. The number of employees working underground is at present (1973) on the order of 4,000. The radon problem in the mines was discovered at the end of the 1960's, and after a rapid survey of the radon and radon-daughter levels in the mines, it was possible to assess the extent of the problem. More detailed measurements resulted in slight re-evaluation of the levels, which are summarized in Table 3.

After the discovery of the serious radon problems in the mines, research and investigative work was quickly initiated, and, with the support of the mining companies and their association, simultaneous studies were started on a broad front. Specifically, identifying and solving the problems associated with radon in the mines required: appropriate sampling and measuring techniques; finding the sources and reasons for the high-radon levels; monitoring the variations in radon levels; developing appropriate countermeasures; discovering the exact nature of the effects on health; etc. It was also considered necessary to print special instructions on protection against radon in mines; these were issued in March 1972. Lung cancer studies were started in 1971, and are still in progress. This extensive work on the radon problem was justified above all by the large number of miners involved, and by the relatively high radon-daughter exposure experienced. A slightly ironical element is that, formally, work in mines is not covered by the Swedish Radiation Protection Act. Thus, more than 1,000 miners were not classified as radiation workers, although they were probably exposed to radiation doses higher than those which were acceptable in radiation work in effect at the same time. The number of overexposed Swedish radiation workers has only been a handful in recent years. However, in practice, the extensive efforts to solve the problems in the mines have naturally not been curtailed by this curious legal situation.

Now, in 1973, the radon situation in the Swedish mines has been improved, but it is not yet satisfactory. There are still 15 mines with about 500 underground miners where the radon-daughter levels are too high. The countermeasures are often complex, and their introduction takes considerable time, but it is expected that the situation will be greatly improved within a year or so. In the meantime, the instructions on radon protection prescribe the maximum permissible exposure corresponding to a radon-daughter concentration of 30 pCi/l as an average over a year. They also prescribe the maximum permissible time before countermeasures must be taken; i. e., the maximum permissible overexposure during the transitional period (KAS, 1972).

1. Sampling and Measuring Techniques.

Measurements in mines are made on radon in air, radon-daughters in air, radon in water, gamma radiation, and the radioactive content of rock samples. A few measurements are also made on ^{212}Pb (ThB) in the air. The principal measurements are those on radon; the others are more or less supplementary.

The object of the radon measurements is to localize the radon sources and to provide guidance for measurements on the radon-daughters. Often radon measurements may also be used directly for the estimation of the radon-daughter levels by using a predetermined ratio ("dose factor") between the concentration of radon-daughters and that of radon. The concentration of radon-daughters is expressed in pCi/l and is equivalent to the WL value times 100.

Potential high radon-daughter levels may also be discovered by means of radon measurements as the method of choice. There are examples of mines where radon-rich air with a relatively low content of radon-daughters is introduced into some part of the mine. During the passage through the drifts, the radon-daughters build up, and may cause unacceptable concentrations at some more remote point in the mine. If the only measurement had been on the daughters, this risk would not have been observed.

The radon sampling is carried out by using commercial 4.8 l propane containers which are evacuated in advance and opened in the mine at the place of interest. These containers are easy to handle. airtight, and sturdy. This last attribute is essential for sampling in mines. The sample may be measured above ground at the mine or at the laboratory of the NIRP in Stockholm. In the latter case, the containers are sent by mail.

The measurement is made in an 18 l ionization chamber which is evacuated before being connected, via a drying agent, to the sample container. The connection is opened three times; prior to opening for the second and third times, the container is filled to atmospheric pressure with aged air from a compressed air cylinder. Using this method, 95% of the sample is transferred to the ionization chamber. The measurement takes, in general, 20 minutes. In the calculation of the radon content of the sample, corrections are made for the contribution to the background from the preceding measurements, the non-equilibrium ratio in the ionization chamber, the calibration factor, the transfer efficiency, and the decay from the time of sampling. The measurement is recorded by a pen-recorder, and the sensitivity is such that a 4.8 l air sample with a radon concentration of 0.13 pCi/l gives a net deflection of 1 mm.

In the early discussions of appropriate sampling and measuring techniques, various different proposals were considered. ZnS-coated bottles, the charcoal filter method, and other methods were discussed. But, the need for sturdiness, commercial availability, moderate price, simplicity, and reliability in use determined the choice of method. The simplicity of the sampling method has made it possible to use untrained persons from the mines to assist in taking samples — a considerable advantage. In the survey measurements of 1969-70, when all the mines were checked twice, all sampling was made by staff from the mines, and the containers were sent by mail to the NIRP for measurement.

The reliability of the sampling and measuring method has been tested on several occasions with excellent results. One test was performed in collaboration with Norwegian colleagues. Evacuated containers were sent from Sweden to Norway and opened in a Norwegian mine. Two samples were taken at each location, one being retained and measured by the Norwegian laboratory staff and the other sent back to Sweden and measured there. Ionization chambers were used in both countries, but the calibrations were made by independent methods. The results are shown in Table 4. The agreement is excellent.

The samples are generally taken in the center of the drift about 1 m above the floor. The exact position of the sampling appears to be of no importance, since no significant differences in radon concentrations in air at different heights from the floor and distances from the walls have been found in ventilated drifts.

Radon-daughters are sampled and measured in the conventional way, using glass-fiber filters, battery-powered air-pumps, air volume meters, and ZnS-detectors. In the evaluation of the radon-daughter concentration, the method of Kusnetz, (JCAE, 1967) is used. Measurements on the glass-fiber filters are generally made above ground.

Gamma measurements in the mine are performed with a ten-liter ionization chamber pressurized to 20 atmospheres. The background of the chamber corresponds to 2 μR/h, and the sensitivity enables detection of gamma levels of less than 5 μR/h.

Finally, water and rock samples are measured by gamma spectrometric methods at the NIRP in Stockholm.

2. Radon Sources.

The reasons for the significant radon levels found in many Swedish mines are: the type of ventilation, radon-rich water, and, to a lesser extent, radioactive minerals.

In many mines the spaces left after mining ore are filled with crushed rock. When the mine gets deeper, the air is admitted via this crushed rock and it becomes contaminated by radon emanating from the crushed rock and from the water in it. However, it is difficult to prove the true significance of this source as any evidence must be indirect.

Nevertheless, it is possible to make rough estimates of the emanation of radon from the rock which would be necessary to account for the radon levels actually found in the air reaching the working places. The following relationship is relevant for the emanation from the rock:

$$v \times p = M \times Ra \times R \times K$$

where

v = ventilation rate (l/s)
p = radon concentration (pCi/l)
M = mass of crushed rock (kg)
Ra = radium content of the mass (pCi/kg)
R = radon production per pCi of radium = 2×10^{-6} pCi/s
K = radon leakage factor; i.e. the proportion of the produced radon which leaks out.

In one mine (Malmberget) the amount of crushed rock above a ventilation shaft (FI) was estimated to be about 1×10^{10} kg and the ventilation rate was 9×10^4 l/s. The radium content cannot be measured, but is probably within the limits 10^{21}-10^4 pCi/kg. The radon concentration was 130 pCi/l.

That gives:

$9 \times 10^4 \times 130 = 10^{10} \times (10^2\text{-}10^4) \times 2 \times 10^{-6} \times K$
i.e., K = 0.06 - 6.

Any values of $K > 1$ is impossible by definition, so that $0.06 \leq K \leq 1$ depending on the radium content. The smaller value of K is most probable, but that implies a radium content on the order of 10 pCi/g which is not normal (Hultqvist, 1956). Furthermore, there may also have been an under or over-estimation of the amount of crushed rock by a factor of 3, which implies a minimum value of K between 0.02 and 0.18. A leakage factor of 0.02 is not impossible, but seems high for an average value for a large amount of crushed rock with pieces varying from grams to tons. Other sources of emanation may be necessary to explain the degree of radon contamination of the inlet air.

By means of continuous radon measurements on return air in a mine (Exportfaltet) it has been possible to follow the effects of ventilation on the radon concentration. When radon is measured in this way, the air has passed operating parts of the mine. Measurements are performed by a continuously running ionization chamber. The results are seen in Figure 2. Until the 47th week in 1970, the ventilation air was taken from older parts of the mine via crushed rock and abandoned spaces. At the 47th week, the ventilation was changed to shaft ventilation and a much lower radon concentration was achieved.

There is a strong need for adequate and reliable ventilation fans. This is probably due to the fact that the natural ventilation through old parts of the mine acts in the opposite direction. Overpressure is thus needed to force the air through the shaft with the new ventilation system. After a ventilation stop, the radon level increases considerably in a rather short time, some hours, and it takes about a day before the radon level has decreased to normal again when the ventilation is restarted.

Radon-rich water is a significant source of radon, either locally in unventilated drifts with a lot of running water or in limited parts of the mine when there is recirculation of the air which has become contaminated by passing radon-rich running water once or several times.

In one mine (Bastkarn) the inlet air to the working levels (140-225 m depth) has a relatively low-radon concentration, but is mixed with air from a very wet part of the mine at 225 m, and is recirculated between the levels 140-225 m. The waterflow is about 4 m^3/min, and the radon content of the water is about 4 nCi/l. This means that at least about 16 μCi of radon is brought into the air per minute, which should cause an average radon concentration in the air of 50 pCi/l, if the air renewal is about 5 m^3/s. The radon concentrations found varied up to about 100 pCi/l.

In unventilated drifts with radon-rich water the radon levels may be very high, sometimes on the order of 10 nCi/l. The gamma radiation in these radon concentrations is not insignificant, about 200 μR/h. The radon content of the water is on the order of 10 nCi/l and the amount of water is on the order of 100 l/min and more in a single drift.

The necessary radon release from the walls in an unventilated drift to cause a radon concentration of 10 pCi/l corresponds to a 100% diffusion depth on the order of mms or less. The radium content of the rock is then assumed to be normal (0.1 10 pCi/g). It is, however, difficult to prove a reasonable 100% diffusion depth if the mine is ventilated and 10 pCi/l produced in the mine is found in the return air of the mine. Local radon sources seem to be necessary, such as radon-rich water or radioactive anomalies in the rock.

In Table 5 the mines are divided with respect to the type of ore and the radon-daughter levels. Twenty-two of the non-ferrous ore mines with less than 30 pCi/l of radon-daughters belong to the same company. Because the lifetime of each of these mines is not very long, new mines are opened from time to time and the collected experience and development work on ventilation systems has been applied by degrees in the mines of this company. These mines also had early problems with silicosis which necessitates good ventilation. Therefore, the skewed distribution in Table 5 is misleading regarding any possible relation between type of ore and radon levels. Nevertheless, it is still possible that there are differences in the geology of the rock in non-ferrous ore mines and ferrous ore mines that may be of significance for the radon levels.

In some mines radioactive minerals (radium content $\gg$ 10 pCi/g) may cause high-radon levels in the mine air. However, this is often a local phenomenon at separated parts of the mine. The significance of the radium content of the rock and the occurrence of especially radioactive minerals is still not fully understood; research is in progress on this problem.

3. The Variation of the Radon Levels.

In the general survey of radon levels in Swedish mines in 1969/1970, it was found that in some mines the radon levels in the summer were much higher than in the winter. This has been examined in more detail in some cases by taking a radon sample every week for a year and more. An example of the results is shown in Figure 3.

The variation illustrated in Figure 3 is one of the extreme cases. On the average for all the mines, the difference between the summer and winter radon levels was a factor of two. The higher radon levels during the summer may be due to the increased emanating power of the crushed rock with higher temperatures, and the absence of ice, decreased ventilation efficiency because of unfavorable temperature gradients, more water, or a combination of these factors.

4. The Radon-Daughters.

Radon-daughter measurements are performed at each mine which is visited by the staff of the NIRP. The object of these measurements is to find the true exposure at working places, and to determine the so-called "dose factor" as defined above. The size of this dose factor is believed to be a measure of the ventilation air renewal in the mine, or in parts of the mine. For later measurements on radon only, the dose factor previously determined has been used to estimate the corresponding radon-daughter level. The accuracy is acceptable provided that the ventilation principle has not been changed.

The increase of the dose factor as a function of time is shown in Figure 4. It was considered to be of interest to demonstrate its applicability to the true situation in a mine atmosphere. It was necessary to have well-defined conditions so an abandoned drift was chosen. At the end of the drift there was a heavy inundation of radon-rich water, about 200 l/s. The radon supply to the air at the dead end of the drift was about 600 nCi/s. The ventilation was arranged by a duct terminating about 25 m from the dead end of the drift. Accordingly, there was a steady air stream along the drift, the length of which was 400 m, and by measurements on radon and radon-daughters along the drift, the increase in the dose factor was studied. There was no significant increase in radon caused by the running water on the floor of the drift, and the radon release from the water was estimated to be less than 20% over a distance of 400 m. The result is shown in Figure 5.

As seen in Figure 5 the experimental values are, with one exception, somewhat higher than the theoretical values. Since radon-daughters may settle on the walls of the drift, lower rather than higher experimental values would be expected. The explanation may be either incomplete ventilation at the dead end of the drift (compare the first point at time zero), or an overestimation of the ventilation rate.

The magnitude of the dose factor may vary in different parts of a mine. In unventilated parts the dose factor may be unity or almost unity. In intake air the dose factor may be very low. By comparison of the dose factor in intake air at working places, and in return air, it is possible to evaluate the overall efficiency of the ventilation of the mine. This is illustrated by an example from one mine (Idkerberget) as shown in Table 6.

The intake air has passed abandoned parts of the mine with crushed rock and has evidently been contaminated with radon during that passage. There is no significant addition of radon in the working areas of the mine, but there is an increase of the radon-daughters.

The intake air has passed abandoned parts of the mine with crushed rock and has evidently been contaminated with radon during that passage. There is no significant addition of radon in the working areas of the mine, but there is an increase of the radon-daughter concentration by a factor of about four. The corresponding increase of the dose factor from 0.15 to 0.65 corresponds to an average transit time for the ventilation air of about one hour.

An interesting correlation between radon and the dose factor was found in one mine (KUJ); the dose factor decreases as the radon concentration increases, see Figure 6. As a consequence, the radon-daughter concentration was always less than 30 pCi/l. The reason for this favorable correlation may be that the higher radon levels are caused by local sources such as water. As the air progresses further, the radon-daughter activity increases; i. e., the dose factor increases. When air passes along a drift, it may also mix with air with a relatively low content of radon and radon-daughters from shafts or other drifts. The concentrations will then decrease, but the dose factor is unchanged and continues to increase.

5. Health Aspects.

Epidemiological studies on uranium miners indicate a significant excess of lung cancer in connection with high radon-daughter exposures. The most thorough study on the lung cancer rate among uranium miners was made by Lundin, *et al.*, (1971). They have also been able to correlate the excess of lung cancer to the radon-daughter exposure. Lung cancer studies on non-uranium miners have also been made; e. g., Newfoundland fluorspar miners (Royal Commission, 1969) and British underground iron miners (Boyd, *et al.*, 1970). Even among these miners an excess of lung cancer was found, and an association with the radon-daughter exposures found in the mines cannot be excluded.

In Sweden, lung cancer studies on miners started in 1971. The first results were reported in October 1972 by Renard, *et al.*, (1972) and refer to the years 1961-1968. The lung cancer rate among men other than miners in the mining districts was not higher than expected (99 observed, 125 expected) and that was also the case for

above-ground miners (7 observed, 6 expected). But, among underground miners, there was a significant excess (26 observed, 6 expected). These figures relate to lung cancer among men aged 20-64 years and for the miners, to those which appeared and caused death within 5 years of cessation of employment at the mine. Twenty-one of twenty-six cases were observed among miners who had worked more than 10 years underground.

In an attempt to correlate the lung cancer rate with the radon-daughter exposure in the mines, the corresponding miners were divided into two groups: (a) those experiencing radon-daughter levels of less than 30 pCi/l, and (b) those experiencing more than 30 pCi/l respectively, according to the measurements since 1969. The results are shown in Table 7, where the numbers refer to the years 1961-1971 in very recent follow-up studies.

As can be seen from Table 7, there are about four times as many lung cancer deaths among the miners experiencing radon-daughter levels exceeding 30 pCi/l than among the other miners, if the number of deaths is normalized to the same number of employees. The true radon-daughter exposure of the miners before 1969 is not known because no measurements were made. However, there is reason to believe that the radon-daughter levels found in the measurements since 1969 are representative for the recent past. The ventilation has been improved with time, and it is reasonable to assume that this would cause the radon levels to decrease with time. On the other hand, the mines are continually being deepened, and that will increase the amount of crushed rock and also make the ventilation more difficult; i.e., the radon levels would increase with time if no other factors were involved. The resulting effect may quite possibly be a relatively constant radon situation over the last few decades.

On this assumption it is possible to divide the numbers of lung cancer deaths into different exposure groups; this is done in Table 8.

The exposure ranges in Table 8 are caused by the radon-daughter ranges 1-10, 10-30, 30-100, and 100-300 pCi/l, respectively, and the range of employment time for the deceased workers. The last column of Table 8 is plotted in an exposure-effect diagram in Figure 7 together with the results of the lung cancer studies in the USA among uranium miners. The agreement appears to be excellent. Considering the numerous statistical errors, and the uncertainty of the exposures, it is, however, not possible to draw any conclusion about the dose-effect relation in the region of the low exposures around 100 WLM.

The average exposure is estimated to be 163 WLM (range 90-275 WLM corresponding to the radon-daughter ranges mentioned above) assuming an average employment time of 30 years. If 1 WLM corresponds to 2 rads, it follows that the rate of excess lung cancer is 1.7 cases per year per rad per million miners. The studies on uranium miners in the USA gave 0.9, on Newfoundland fluorspar miners 1.1, and on British underground iron miners 3.0 (Lundin, *et al.*, 1971).

REFERENCES

Boyd, J. T., R. Doll, J. S. Faulds, and J. Leiper, (1970), *Cancer of the Lung in Iron Ore (Heamatite) Miners,* Brit. J. Industr. Med. 27:97-105

Dobeln, W. von and B. Lindell, (1964), *Some Aspects of Radon Concentration Following Ingestion.* Arkiv for fysik, Band 27, No 32, 531-572.

Hearings on Radiation Exposure of Uranium Miners before the Subcommittee on Research, Development, and Radiation of the Joint Committee on Atomic Energy, Part 2 (1967), Washington, D.C.; Government Printing Office.

Hultquist, B. (1956), *Studies on Naturally Occurring Ionizing Radiations with Special Reference to Radiation Doses in Swedish Houses of Various Types.* Kungl. Svenska Vetenskapsakademiens Handlingar, Vol. 6, Ser. 4, No 3.

Israelson, S. (1968), *On the Variation of the Natural Radioactivity in the Air Near the Ground.* Reports No 5, Meteorologiska Institutionen, Uppsala.

Jacobi, W., (1962), *Die naturliche Radioaktivitat der Atmosphare und ihre Bedeutung fur die Strahlenbelastung des Menschen.* Report HMI-B21, Hahn-Meitner-Institut fur Kernforschung, Berlin.

Kungl. Arbetarskyddsstyrelsens (KAS) anvisningar, (1972), No 82, B1 4426, Svenska Reproduktions Aktiebolag, Vallingby, Sweden.

Kraner, H. W., G. L. Schroeder, and R. D. Evans, (1964), *Measurements of the Effects of Atmospheric Variables on Radon-222 Flux and Soil-Gas Concentrations.* The Natural Radiation Environment by J. A. S. Adams and W. M. Lowder, 191-215. The University of Chicago Press.

Lindell, B., and P. Reizenstein, (1964), *A Swedish Building Material for Low-Radioactivity Laboratories.* Arkiv for fysik, Band 26, No 5, 65-74.

Lundin, F. E., J. K. Wagoner, and V. E. Archer (1971), *Radon-Daughter Exposure and Respiratory Cancer, Quantitative and Temporal Aspects.* National Technical Information Service, U. S. Department of Commerce, Springfield, Virginia.

Renard, K. G. S:t, *et al.*, **(1972),** *Gruvforskningen Serie B,* No 167. Svenska Gruvforeningen, Stockholm.

Royal Commission, (1969), *Report Respecting Radiation, Compensation and Safety at the Fluorspar Mines,* St. Lawrence, Newfoundland, Canada, pp.104.

Snihs, J. O. and C. Wilson, (1968), *Some Measurements on Natural Radioactivity at Kristineberg Zoological Station.* Report SSI 1968-010. National Institute of Radiation Protection, Stockholm.

Snihs, J. O. (1973a), unpublished data.
Snihs, J. O., (1973b), *The content of Some Radioactive Elements, Especially ^{222}Rn, in Some Potable Waters in Sweden.* To be published in Nordic Hydrology.
Tanner, A. B., (1964), *Radon Migration in the Ground: A Reveiw.* The Natural Radiation Environment by Adams, J. A. S. and W. M. Lowder, 161-190. The University of Chicago Press.

TABLE 1. Radon Levels in Houses with Different Building Materials, Data from Hultquist (1956).

Building material	Average radon concentration, pCi/l	Extreme radon concentrations, pCi/l
Wood	0.5	0.2-1
Brick	1	0.2-4
Lightweight concrete	2	0.3-6

TABLE 2. Radon Concentration in Drinking Water in the Vimmerby District of Sweden.

Radon concentration (nCi/l)	Number of bored wells	Number of other wells
All wells measured	45	90
More than 2	32	17
More than 10	14	0
More than 20	9	0
More than 30	3	0
More than 50	1	0

TABLE 3. Number of Mines and Miners in Different Radon-Daughter Exposure Groups in 1970.

Radon-daughter concentration, pCi/l	Number of mines	Number of miners
<10	26	1,388
10-30	12	2,003
30-100	16	696
100-300	6	615
>300	1	21

TABLE 4. A Comparison Between Norwegian and Swedish Results of Measurements on Radon Samples from a Norwegian Mine. The Samples Sent to Sweden by Mail were Measured 9 Days after Sampling.

Norwegian results, pCi/l	Swedish results, pCi/l
30	34
32	32
16	17
80	72

TABLE 5. The Mines Divided into Ferrous Ore Mines and Non-Ferrous Ore Mines and Radon-Daughter Levels as Found in 1969/70.

Radon-daughter levels	<30 pCi/l	>30 pCi/l
Number of ferrous ore mines	13	20
Number of non-ferrous ore mines	25	3

TABLE 6. The Average Radon Levels and Dose Factors (the Ratio Between the Radon-Daughter Concentration Expressed in WL x 100 pCi/l and the Radon Concentration, pCi/l) in Intake Air, at Working Places, and in Return Air.

Idkerberget Mine	Intake air	At working places	Return air
Average radon level (pCi/l)	164	144	172
Average dose factor	0.15	0.50	0.65

TABLE 7. Observed Numbers of Lung Cancer Deaths During the Years 1961-1971 Among Miners Who have Worked More than 10 Years Underground. All but Two of the Miners Aged 20-64 Died within 5 Years of Cessation of Employment at the Mine. (30 pCi/l is Equivalent to 0.3 WL.)

Radon-daughter concentration	Number of lung cancer deaths: age at death			Number of mines	Number of miners in 1966
	20-64	65-79	20-79		
≤30 pCi/l	9	7	16	9	2.760
>30 pCi/l	27	23	50	11	2.099

TABLE 8. Lung Cancer Deaths for 1961-1971 Among Miners Aged 20-64 Years. All the Deceased Worked More than 10 Years Underground, and all Except Two died within 5 Years after Cessation of Employment.

Estimated cumulative WLM:		Employees underground (average)	Expected number of lung cancer deaths	Observed number of lung cancer deaths	Calculated annual mortality per 10^4 miners from lung cancer:	
Range	Average				Expected	Observed
2-36	15	1,001	1.25	2	1.1	1.8
13-112	48	1,852	2.31	7	1.1	3.4
48-528	218	1,488	1.85	15	1.1	9.2
170-1,512	696	525	0.66	12	1.1	21.0

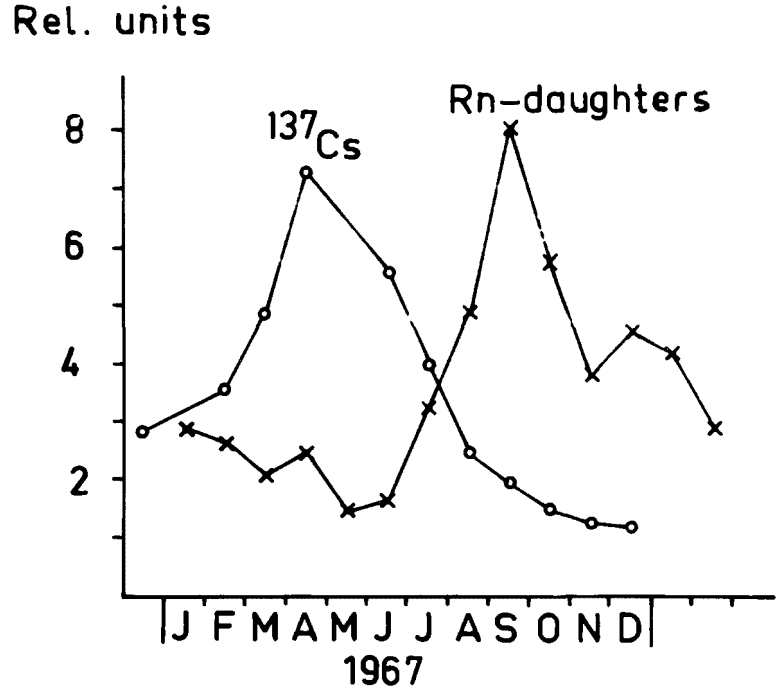

Figure 1. Relative monthly values in 1967 for ^{137}Cs and for radon-daughters in Stockholm air.

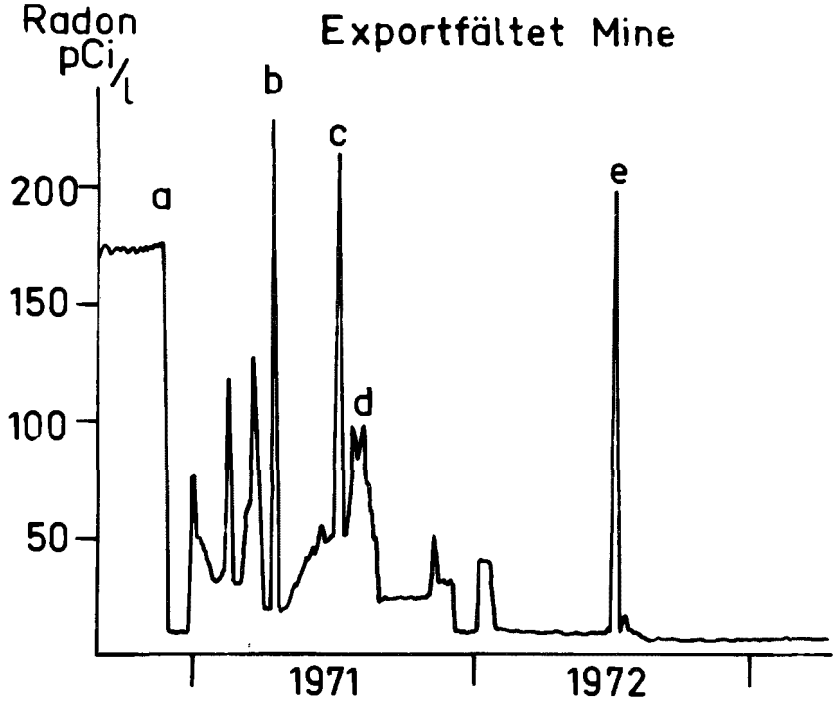

Figure 2. Radon concentration in the return air of Exportfaltet Mine measured by a continously running ionization chamber. (a = Dec. 1970, change to shaft ventilation; b = ventilation shut-down, 4.5 days during Easter break [Equilibrium was reached after 1-2 days]; c = ventilation breakdown, summer 1971; d = fans under repair during holiday period; and e = major water inundation in the mine.)

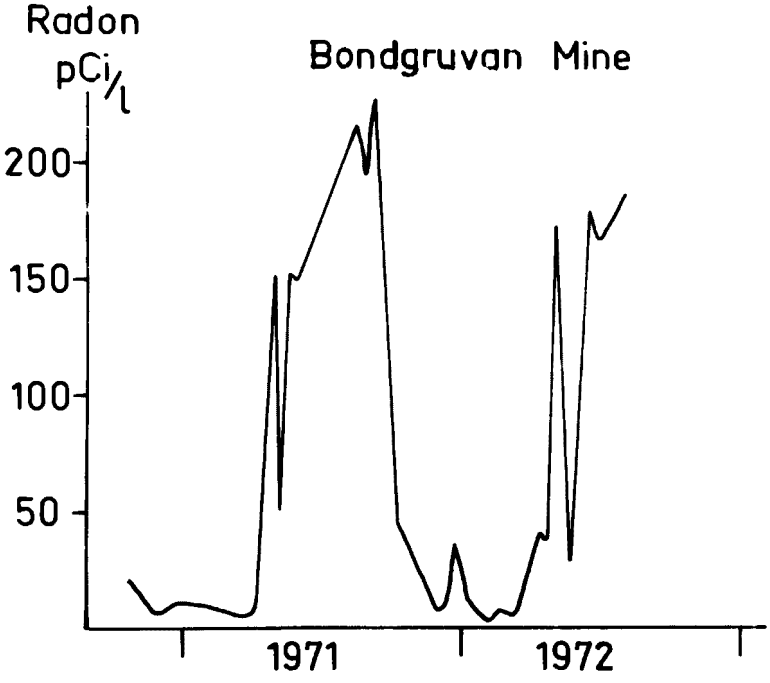

Figure 3. The radon concentration in the return air of the Bondgruvan Mine was measured once a week.

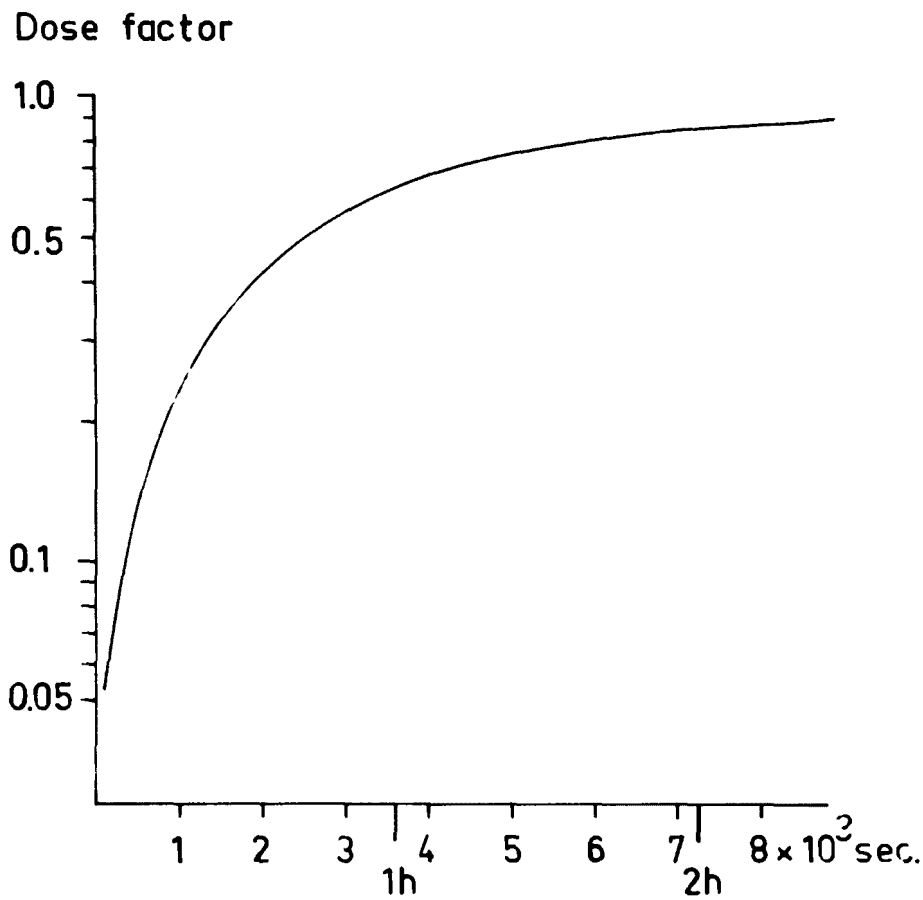

Figure 4. The theoretical increase of the "dose factor" as a function of time.

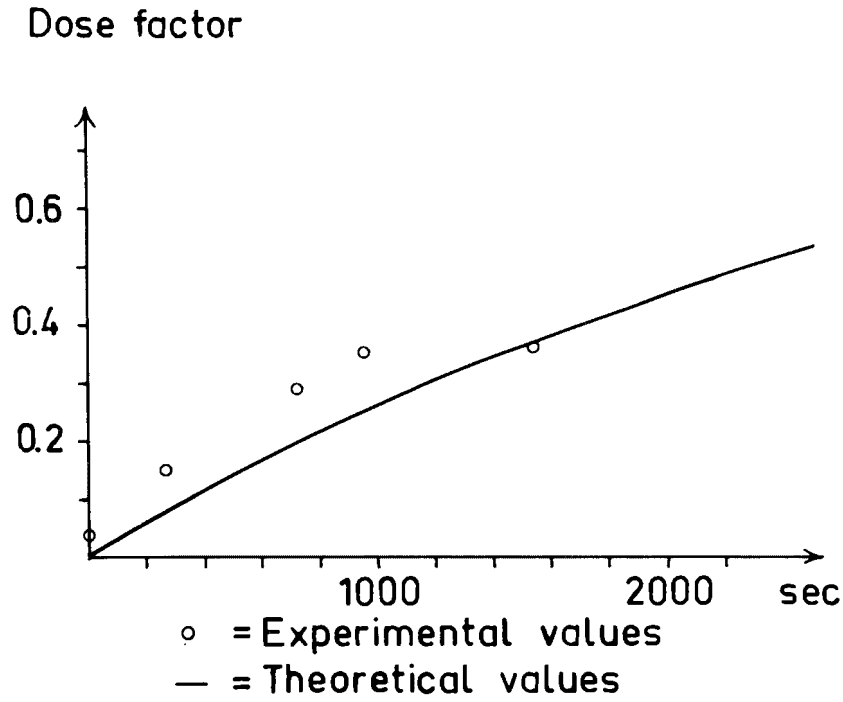

Figure 5. Measured dose factor (circles) as compared with theoretical dose factor (continuous line) as a function of time as studied in a 400 m long drift with the radon source (water) at the dead end of the drift. The ventilation air speed was 0.28 m/s and was directed outwards from the dead end of the drift.

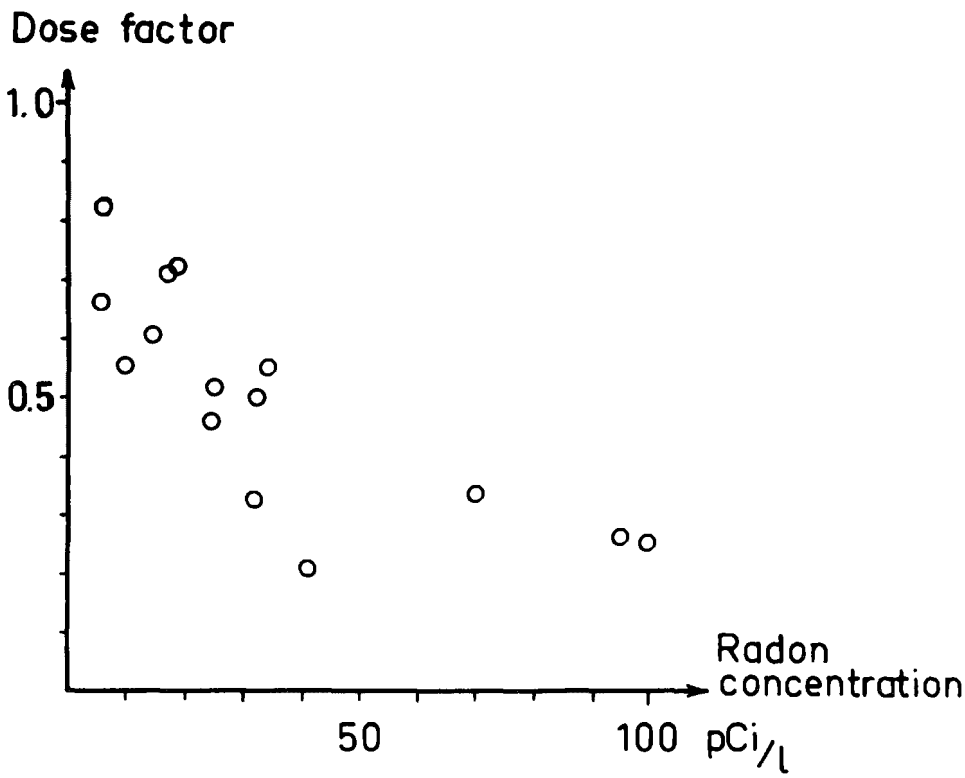

Figure 6. Correlation between radon concentration and dose factor as found in the mine KUJ.

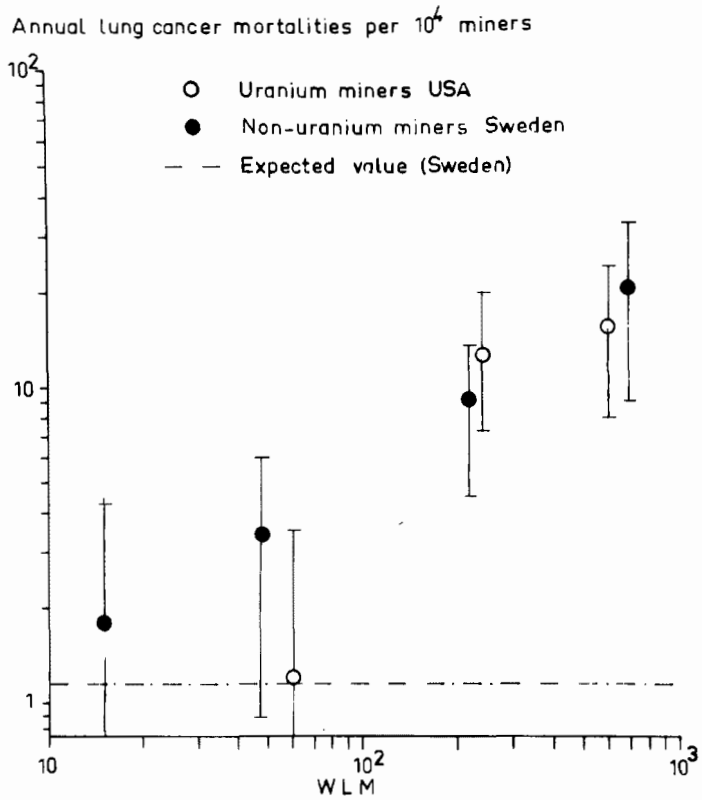

Figure 7. Comparison between the lung cancer mortalities for American uranium miners and Swedish non-uranium miners as a function of the radon-daughter exposure. 95% confidence limits are shown for the mortality values.

MONITORING RADON CONCENTRATIONS IN RESPIRABLE AIR *

F. Wachsmann and J. David
Gesellschaft fur Strahlen- und Umweltforschung m.b.H.
Institut fur Strahlenschutz
Munchen - Neuherberg
Federal Republic of Germany

Abstract

The radon-daughters present in air were collected on filters for different length periods. The determinations of separate alpha activities were done by using a silicon semiconductor detector and by the etch-foil technique. The differences between these techniques, including their feasibility and calibration, are described. Finally, some measurement results are discussed.

INTRODUCTION

In addition to the great interest given to radiation workers who inhale radon and radon-daughters in uranium and fluorspar mines, German authorities have begun to take an interest in the radiation doses received by the general public by desiring to measure the concentrations of radon and radon-daughters in the air of their dwellings.

The aim of this work is to prepare simple and inexpensive instruments for routinely measuring exposures to radon-daughters.

We decided to collect radon-daughters on diaphragm filters because they are inexpensive, can be used at a high-speed, and allow for the continuous measurement of alpha activities. A simple maintenance-free diaphragm pump is used to produce a constant air flux. The sampling period must be long, due to the relatively long half-lives of the radon-daughters, in order to get a stable ratio effect on the filter measurements. We used a silicon semiconductor detector and the etch-foil technique to measure the alpha activities of the radon-daughters.

SILICON SEMICONDUCTOR DETECTOR

The silicon semiconductor detector, or surface barrier detector, we used counted impulses with a single-channel analyzer. The lower and upper trigger-levels were set to exclude beta and gamma radiation — as well as pulses due to ThC' alpha particles. We were able to keep the bias from thorium-daughters at a negligible level.

The detector we used has a sensitive surface of 400 mm^2, which is covered by a protective foil. The distance between the filter and the detector surface we used was 5.2 mm. With this geometry, the counting efficiency is about 0.20 without allowing for the self-adsorption in the filter. A constant air flux of 1265 1/hr was used for continuous monitoring.

The potential alpha energy concentration was measured in units of MeV/1, or in WL, as the potential alpha energy concentration is very important for the estimation of dose.

Due to ventilation, variable aerosol concentration, and plate-out on the wall surfaces, there is no radioactive equilibrium in closed rooms. Therefore, disequilibrium factors must be taken into account while measuring potential alpha energy concentrations of single decay products by count rate in room air. In practice, the proportionality between counting rate and energy concentration is sufficient (Jacobi, 1972).

A sensitivity of 28 Imp/hr for 1 MeV/1, or 37.2 x 10^5 Imp/hr for 1 WL, results for the counting apparatus when filter efficiency, detector efficiency, and the activity distribution in the air and on the filter is taken into consideration.

Accordingly, the definition of the working level has the same counting rate as in the case of radioactive equilibrium and 100 pCi/1. The high sensitivity of this measuring system allows the measurement of daily variations of alpha energies in the room atmosphere to be made in only two minutes.

Figure 2 shows the course (curve) of the potential alpha energy concentrations in a living room over 24 hours. On this day, there had been warm and sunny weather.

Figure 3 demonstrates the course (curve) of this same room on a rainy day. These examples show the big influence weather has on energy concentrations in a room.

The measuring range of the mentioned air flux is 10^{-5} -10 WL. Higher concentrations can be secured by restricting the air flux; however, they cannot be expected to be in the applicable range. With an integrated indication of the pulse counter, which is equal to a prolongation of the measuring time from 2 minutes up to the measuring time in question, the radon-daughters exposure can be read.

**This research was financed by the Federal authority "Bundesministerium des Innern" within the research-project "Statistical Measurings."*

The semiconductor method can easily be employed for continuous and long-term measurements. Unfortunately, the silicon semiconductor detector is too expensive for routine wide-scale use — as is a requirement in our work. Purchasing several of these detectors, which would be needed by the surveyor teams, would be prohibitive.

ETCH-FOIL TECHNIQUE

After we decided the silicon semiconductor detector was not feasible economically for our purposes, we experimented with an etch-foil technique using a plastic foil. With this technique only a small diaphragm pump with variable air flux was needed together with a gas counter and a filter-foil holder. These items are all inexpensive to purchase or fabricate.

After reaching the stable (stationary) state during the time of interest, the alpha activities collected on the diaphragm-filter are measured by counting the tracks produced on the foil. The result is the time integral of the potential alpha energy concentration. In order to get an average (or mean value) for the whole day, a 24-hour measurement is taken.

Cellulose-nitrate is a good detector foil because of its high sensitivity to alpha particles. Since the necessary thickness of 15 micrometers for this plastic foil is not available in Germany, it must be produced by centrifuge as recommended by Paretzke (1972).

Even though an accurate visual counting of the tracks can be done by microscope, the analysis is made by the spark-counter. The spark-counter allows the routine use of this method.

The measurement sensitivity of this system using a detector surface of 850 mm^2, a filter, and an air flux of one 1/hr equals 0.8 tracks per MeV/1 x hrs., or 10^5 tracks per WL x hrs. This sensitivity results when the detector foil and filter are 5 mm apart and a 20 micrometers thick absorption foil is used.

SURVEY MEASUREMENT RESULTS

Preliminary results show alpha energy concentrations in living rooms have the same temporal variation as outdoors. This means that the concentration inside is directly affected by the concentration outside. Very low values were found in rooms like concrete cellars, which are relatively independant of outdoors. Apparently there is no correlation between building materials and alpha energy concentrations, for no significant differences were found in buildings made of concrete, brick, or gypsum. The only exception to this that we found was in the case of granite and new uraniferrous red sandstone buildings where the measurements showed somewhat higher concentrations of alpha energies.

REFERENCES

Evans, D. (1969), *Engineers' Guide to the Elementary Behaviour of Radon-Daughters*, Health Phys. 17, 229-252.

Gross, W. G. and L. Tommasino (1969), *A Rapid Reading Technique for Nuclear Particle Damage Tracks in Thin Foils*, Proc. Int. Conf. Nuclear Registration in Insulating Solids.

Haider, B. and W. Jacobi (1972), *Entwicklung von Verfahren und Geraten zur Langzeitigen Radonuberwachung im Bergbau*, BFBW, Forschungsbericht K 72-14.

Jacobi, W. (1972), *Acitivity and Potential α-energy of ^{222}Radon- and ^{220}Radon-daughters in Different Air Atmospheres*, Health Phys. 22, 441-450.

Paretzke, H. G. (1971), *Kernspuren in Kunststoffen*, Ges. F. Strahlen- und Umweltforschung Bericht S-138.

Paretzke, H. G. (1972), *Entwicklung und Einsatz eines Funkenzahlers*, zur schnellen Auswertung von Kernspurdetektoren BMVg-FBWT 72-34.

Semiconductor System:	$28 \frac{Imp}{h}$ for $1 \frac{MeV}{l}$
	$37 \times 10^5 \frac{Imp}{h}$ for 1 WL
Solid State Track Det. System:	0,8 tracks for $1 \frac{MeV \cdot h}{l}$
	10^5 tracks for 1 WL·h

Figure 1. Sensitivity of the Filter Method.

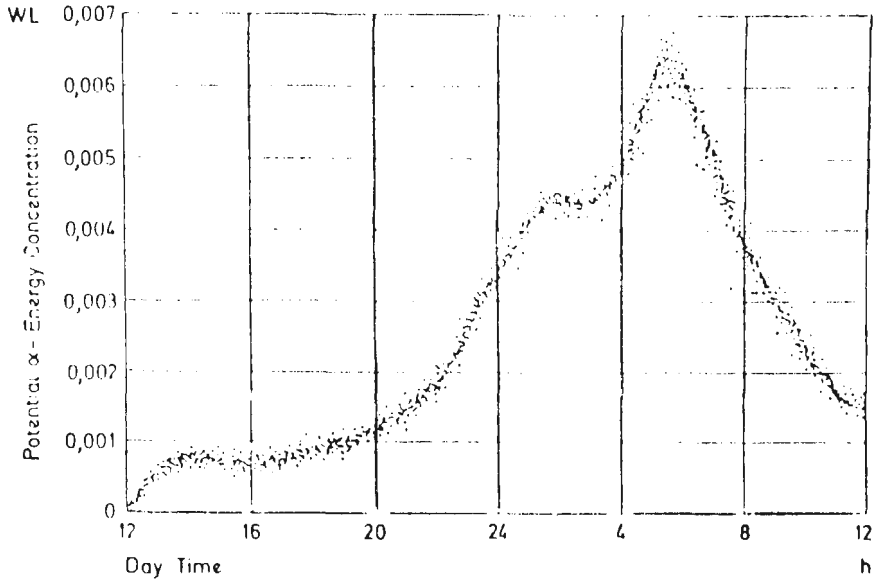

Figure 2. Daily variation of the potential a-energy concentration during 24 h (warm and sunny weather).

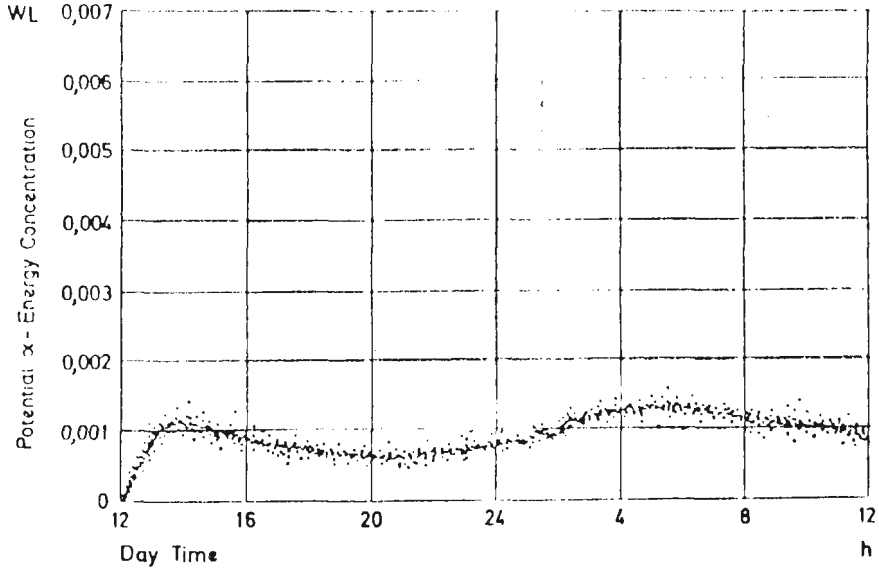

Figure 3. Daily variation of the potential a-energy concentration during 24 h (rainy weather).

CONTRIBUTION OF RADON IN NATURAL GAS TO THE DOSE FROM AIRBORNE RADON-DAUGHTERS IN HOMES*

C.J. Barton, R.E. Moore, and P.S. Rohwer
Environmental Sciences Division
Oak Ridge National Laboratory
Oak Ridge, Tennessee 37830

ACKNOWLEDGMENTS

The authors thank a number of individuals and organizations for their help in gathering data on the radon concentration at points of use: Texas Eastern Transmission Company, Transcontinental Gas Pipeline Corporation, Natural Gas Pipeline Company of America, Colorado Interstate Gas Company, and El Paso Natural Gas Company for furnishing samples; and A. J. Breslin and A.C. George, Atomic Energy Commission, New York Health and Safety Laboratory; H. F. Lucas, Jr., Argonne National Laboratory; K. J. Schiager, Colorado State University; and M. H. Wilkening and W. E. Clements of New Mexico Tech for measurements of radon concentration in natural gas samples.

Abstract

Data have been obtained on the radon concentration in natural gas supplied to several metropolitan areas in the United States. The average value of 20 pCi/l was selected to estimate the contribution of this source of natural radioactivity to doses from radon-daughters received by individuals in homes. Radon-daughter concentrations in the home atmosphere were calculated by use of computer programs for an 8000 ft³ house in which 27 ft³ of gas per day was used for cooking in an unvented kitchen range. The total estimated dose to the bronchial epithelium included contributions from radon plus daughters in the outside ventilation air, each of which was assumed to be present at a concentration of 0.13 pCi/l, and from the radon plus daughters in the natural gas. The latter contribution averaged approximately 3% of the total dose. There was a 3.5% decrease in the estimated total dose when the air change rate increased from 0.25 to 2.0 per hour. We conclude that radon and radon-daughters entering the home with natural gas produce a negligible fraction of the total dose to the respiratory system of home occupants from airborne radon-daughters.

INTRODUCTION

The presence of radioactivity in natural gas was noted early in this century (Satterly, *et al.*, 1904), and measurements of the radon content of gas were first reported in 1919 (Satterly, *et al.*, 1918-1919). Since that time, many determinations of the radon content of natural gas at the wellhead have been reported, but little information has become available on the concentration of this radioactive rare gas in the natural gas entering homes. Also, little effort has been devoted to evaluation of doses that gas users receive from this natural source of radioactivity. We devised a three-part program to supply the missing information. The first part consisted of gathering data on the radon content of natural gas being supplied to several metropolitan areas in the United States. The second part involved the calculation of radon-daughter concentrations in homes produced by use of natural gas in an unvented home appliance. The last phase combined data from the first two parts of the program with the average of published estimates of the dose conversion factor for radon-daughters deposited in the human respiratory system to provide dose estimates for exposure to this source of natural radioactivity. To put these doses in perspective, we made a comparison with the dose received from radon-daughters produced by decay of radon in the atmosphere. A literature survey (Barton, 1971) pointed to the need for this investigation; a preliminary report has been published (Barton, *et al.*, 1973a).

RADON AND RADON-DAUGHTER CONCENTRATIONS IN NATURAL GAS AT POINTS OF USE

Several possible methods of obtaining data on the radon content of natural gas points of use were considered; sampling of a large fraction of the gas supplied to several large metropolitan areas was selected. Table 1 shows the organization of this part of the program which extended over approximately 1 year in search for possible seasonal variations. Table 2 summarizes the results obtained, while individual values (or monthly averages where more than one sample was analyzed) are plotted in Figure 1. In addition to monthly pipeline samples in the New York area, daily samples were analyzed at the U. S. Atomic Energy Commission's New York Health and Safety Laboratory. Monthly averages of these data are included in Table 2. The average value for all sampling locations is 17 pCi/liter, and we selected the rounded figure of 20 pCi/liter for dose calculations.

No data are available on radon-daughter concentrations in pipeline gas. Two efforts to detect daughter products in New York City gas (Breslin, 1972) and in Colorado (Schiager, 1973) were unsuccessful. The New

*Research sponsored by the U. S. Atomic Energy Commission under contract with the Union Carbide Corporation.

York City test was handicapped by the low radon concentration in the gas (~1 pCi/liter). The radon concentration in the gas used in the Colorado test was higher, and a minimum detectable level of 0.06 working levels at the 95% confidence limit was reported. Since one working level is defined as the concentration of daughters in equilibrium with 100 pCi/liter of radon (or as any combination of short-lived daughters that will result in the ultimate emission of 1.3×10^5 MeV of alpha energy per liter of air), the above detectable level corresponds to the daughters in equilibrium with 6 pCi/liter of radon.

It was also reported (Breslin, 1972) that the particle count in New York City pipeline gas was quite low. This would partially account for the failure to detect daughters, since they are charged ions when formed. Unless there are gasborne particles to which they can become attached, they would be expected to migrate quickly to the pipeline wall.

RADON AND RADON-DAUGHTER CONCENTRATIONS IN VENTILATION AIR

Results of numerous studies of radon concentration in the atmosphere have been reported in the literature. They are summarized, in part, in literature surveys (Barton, 1971 and United Nations, 1972). The ^{222}Rn concentration in air ranges from approximately 0.001 to 1.0 pCi/liter, while the ^{220}Rn (thoron) concentration is approximately a factor of 100 lower. We have neglected the thoron content of the air in our dose calculations; it is not present in natural gas at points of use because of its short half-life (54.4 s). Determinations of the concentration of individual radon-daughters in air have been made much less frequently than radon measurements, and data on simultaneous measurements of radon and its daughters are relatively scarce.

For our average or representative radon concentration in air, we have averaged the results of a compilation of published data on measurements in the United States (Lowder, *et al.*, 1971). The resulting value (0.13 pCi/liter) is below the middle of the range mentioned above, but, if values as low as 0.001 to 0.003 pCi/liter observed in coastal areas and islands (Blifford, *et al.*, 1956) were included in the compilation, the average would be even lower than 0.13 pCi/liter.

Because of the above-mentioned scarcity of data on radon-daughter concentrations relative to radon in the atmosphere, we have adopted the reference radioactive atmosphere used by Altshuler, *et al.*, (1964) which was used earlier by the Public Health Service (Holaday, *et al.*, 1957) in recommending the working level. Although this ratio was based primarily on measurements made in mine atmospheres, it appears to be reasonably consistent with the scarce data on the atmospheric radon-daughter ratio; that is, both higher and lower values have been observed for the different daughters.

EXPOSURE MODEL

The exposure situations considered in this study assume, as in earlier studies of doses from tritium in gas (Barton, *et al.*, 1973b), that 0.765 m^3 of gas is consumed per day in an unvented kitchen range located in 226.6-m^3 (92.9 m^2 floor area) house. We further assume that the gas combustion products are uniformly dispersed in the home atmosphere. The above-mentioned value for daily range consumption is an average value for gas usage in this appliance in the United States (Segeler, 1966).

In the earlier studies, we assumed an average air turnover or ventilation rate of one per hour. In this investigation, our calculations covered air change rates of 0.25 to 2.0 per hour because we lacked definitive information on the average air change rate in houses having gas ranges.

As was mentioned in the section on radon and its daughter concentrations at points of use, we do not know how much, if any, radon-daughters are in the natural gas when it enters homes. Because of this lack of data, we calculated doses for the limiting case in which the daughters are in equilibrium with the radon on leaving the pipeline, and compared the results with those for gas containing no daughters. We also estimated doses, with and without the assumed presence of radon and its daughters, in the ventilation air. The different cases for which we estimated doses are described below.

Case 1. Natural gas containing radon at a concentration of 20 pCi/liter, but with no daughter activity, is used. This provides the lower dose limit. Ventilation air is assumed to contain no radon or radon-daughters. Although this case is not a practical situation, it permits calculation of the dose effect of radionuclides resulting from radon in the gas without the complication of ventilation air activity.

Case 2. The exposure conditions are identical to those for case 1 — except that the natural gas is assumed to also contain radon-daughters (RaA, RaB, and RaC) at their equilibrium concentrations (20 pCi/liter). This case provides an upper limit value for the dose from natural radioactivity in the natural gas for the specific conditions considered.

Case 3. The exposure conditions are identical to those for Case 1 — except that the ventilation air is assumed to contain radon and its daughter radionuclides (RaA, RaB, and RaC) each at a concentration of 0.13 pCi/liter. This case provides the lowest dose limit for the effect of radon in natural gas when the ventilation air also contains radionuclides.

Case 4. The exposure conditions are identical to those for Case 1 with two exceptions: (1) the natural gas is assumed to also contain radon-daughters at their equilibrium concentrations; and (2) the ventilation air is assumed to contain radon and its daughter radionuclides each at a concentration of 0.13 pCi/liter. This case provides an upper dose limit for the conditions under which Case 3 gives the lower limit.

Case 5. The exposure conditions are identical to those in case 3 — except that the daughters are assumed to have the distribution of the reference atmosphere of Altshuler, *et al.*, (1964) rather than being in equilibrium with radon. Since it appears probable that little, if any, daughter activity is in the gas when it enters homes, and that the daughter activity in the atmosphere is not generally in equilibrium with radon, this case is the most realistic of the five cases considered in regard to assumptions.

CALCULATION OF RADON-DAUGHTER CONCENTRATIONS IN HOMES

Radon decays according to the following scheme:

$$^{222}\mathrm{Rn} \xrightarrow[3.823\ \mathrm{days}]{5.49\ \mathrm{MeV}\ \alpha} {}^{218}\mathrm{Po(RaA)} \quad \xrightarrow[3.05\ \mathrm{min}]{6.00\ \mathrm{MeV}\ \alpha} {}^{214}\mathrm{Pb(RaB)} \quad \xrightarrow[26.8\ \mathrm{min}]{0.7\ \mathrm{MeV}\ \beta} {}^{214}\mathrm{Bi(RaC)}$$

$$\xrightarrow[19.7\ \mathrm{min}]{3.3\ \mathrm{MeV}\ \beta} {}^{214}\mathrm{Po(RaC')} \quad \xrightarrow[164\ \mu\mathrm{s}]{7.687\ \mathrm{MeV}\ \alpha} {}^{210}\mathrm{Pb(RaD)} \quad \xrightarrow[21\ \mathrm{year}]{0.02\ \mathrm{MeV}\ \beta} {}^{210}\mathrm{Bi(RaE)}$$

Only the first three daughter products (RaA, RaB, RaC) need to be considered in making dose calculations, but the energy contribution of RaC', an alpha emitter, is attributed to RaC, because it has such a short half-life that its decay immediately follows that of its parent radionuclide (^{214}Bi RaC). Although RaB is a β-emitter and does not contribute significantly to the total dose, our dose calculations take into consideration its decay to RaC'. The very long half-life of RaD, in addition to its soft beta emissions, makes it unimportant from the radiation dose standpoint.

When the range is turned on, radon in the gas combustion products is dispersed in the home and the concentration of radon-daughters from this activity source begins to build up. At the same time, the daughters are removed by radioactive decay and by ventilation. A computer program was written to handle the calculation of radon-daughter concentrations in this dynamic situation. Mathematical analysis has demonstrated that the average 24-hour concentration of radionuclides is not affected by range-use schedule. In other words, it makes no difference whether the gas is used in three 1-hour periods during the day or all in one 3-hour period during the day. The important variables are the volume of gas used, the radon concentration in the gas, and the home ventilation rate. Our computer model assumes that the total average daily consumption of gas is burned in the range at a constant rate in one hour. The program calculates the number of atoms of radon, and each of the three daughters, for each second of a 24-hour period, and the results at each 60-s interval are included in the computer printout, as well as the cumulative average number of atoms of each species for a given radon input and ventilation rate.

For the even more complex situation, in which radon-daughters are present in the natural gas and/or in the ventilation air, another computer program, while less exact mathematically than the above-mentioned program, was developed that gives results which agree with the other program within 1 or 2%.

The average 24-hour values for the number of atoms of each radon-daughter are converted to concentrations by assuming that the gas combustion products are dispersed uniformly in the 226.6-m^3 house. They are then converted to working levels, as defined previously, by use of the known decay constants and decay energies for the individual daughters.

DOSIMETRY

The calculated concentrations of radon and radon-daughters in the home atmosphere were converted to estimates of radiation dose by using a dose conversion factor selected on the basis of a literature survey. Because of the complexity and specialization of radon-daughter dosimetry in the respiratory system, we concluded that our current interests do not justify independent development of the necessary factor. Data from the survey are summarized in Table 3. The dose conversion factors (rads/year) in the table are for an assumed continuous inhalation of radon-daughters at a concentration of one working level (WL). Discarding the highest and lowest factors in Table 3, the average value of the five remaining factors is 85 rads/year. Walsh (1970) reviewed the literature regarding radiation dose to the respiratory tract of uranium miners from inhalation of radon-daughters, and concluded that the average dose to the bronchial epithelium of the tracheobronchial tree from an exposure to radon-daughters at 1 WL for one year is not larger than 50 to 100 rads, and that the dose to the basal cells may be less than 50 rads. He pointed out, however, that localization of activity (e.g., at bifurcations) could produce much higher doses. In a report from the epidemiological study of United States uranium miners, Lundin, *et al.*, (1971) concluded that one year of continuous exposure to radon-daughters at 1 WL is equivalent to approximately 103 rads averaged over the tracheobronchial epithelium. Evans (1967) has concluded from the work of Altshuler, *et al.*, (1964) and Jacobi (1964) that the dose conversion factor for inhalation of radon-daughters ranges from approximately 25 to 160 rads per year of continuous exposure at 1 WL. The dose conversion factor selected for use in this report is 100 rads to the bronchial epithelium per year of continuous exposure to radon-daughters at a concentration of 1 WL. The basal cells of the bronchial epithelium are assumed to be the critical tissue. An estimate of the corresponding dose to the total lung mass is given by Holleman (1968); based on uniform deposition of the alpha energy in a 1,000-g lung, the organ dose is approximately an order of magnitude less than the dose estimated for the bronchial epithelium.

Additional considerations in our treatment of the problem should be noted. These considerations, which may influence the reader's interpretation of the dose estimates presented, are:

(1)Use of the WL concept implies that the relative concentrations of RaA, RaB, and RaC in the inhaled air are not of major importance for dose calculation — in spite of the difference in the alpha decay energy of RaA and that of RaC' to which all three daughters decay. However, there are differing opinions on this point. For example, Lundin, *et al.*,(1971) state that the relative concentrations of RaA, RaB, and RaC are not of major importance for dose calculations; while Harley, *et al.*,(1972) state that the alpha dose for 1 WL may be widely different depending on the ratios of the radon-daughters.

(2) The dose contributions from inhaled radon, and from the decay of radon, or its daughters, absorbed in tissue have been ignored. Work reported by Holleman (1968) indicates that the absorbed radon and radon-daughter dose component adds only a small (0.5%) dose. For the exposure conditions specified in this report, the radiation dose is primarily due to inhaled radon-daughters (Shapiro, 1954).

(3) We adopted a quality factor (QF) of 10 for alpha particles in converting our dose estimates from rads to rems — following the current recommendations of the International Commission on Radiological Protection (1966). Some investigators adopt other values for QF. For example, Lundin, *et al.*, (1971) selected a QF of 3; however, most investigators express their results only in rads because of the lack of agreement on the appropriate QF for alpha particles.

RESULTS AND DISCUSSION

Estimated doses to the bronchial epithelium as a function of ventilation rate for Cases 1 and 2 are shown in Figure 2, while similar data for Cases 3 and 5 are displayed in Figure 3. The data for Case 4 are too close to those shown for Case 3 to make it practical to include them in the graph.

It is quite clear from Figure 2 that doses from radon, or radon plus daughters, introduced in gas vary quite markedly with ventilation rate. The assumed presence of daughters in the entering gas does increase the dose appreciably, but comparison of Figures 2 and 3 shows that the dose contribution from radionuclides in natural gas is small compared to that from ventilation air. The small variation in estimated dose with ventilation rate observed for Case 3 in Figure 3 is due to the radon-daughters from radon in natural gas. Since the daughters in ventilation air in this case are assumed to be in equilibrium with radon, changes in ventilation rate would not change the dose from this source, but daughters from radon in the gas will increase with decreasing ventilation rate. The relatively large effect of ventilation rate on total dose for Case 5 (Figure 3) is due to the assumed nonequilibrium daughter concentrations in this case. If the ventilation rate were zero, the daughter activities would soon be equal to the radon activity (0.13 pCi/liter).

Inspection of the data in Table 2 shows that, although the average of all the values is close to the 20-pCi/liter figure used in our dose calculations, the total range of radon concentrations at points of use is approximately 1 to 100. Doses in this range can be scaled directly from the values in Figure 2. Considering only the ventilation rate of one air change per hour, the above radon concentration range corresponds to doses varying from 0.75 to 75 millirems per year for Case and 1.4 to 141 millrems per year for Case 2. The maximum values are 6 to 11%, respectively, of the Case 3 and 4 values. Although the maximum doses are not insignificant, they are considered to be small as compared to probable variations in dose from radon and its daughters in air.

We have not previously mentioned a third source of airborne radioactivity in the home: radon and thoron from home construction materials. Reported measurements surveyed by Barton (1971) and others (United Nations, 1972) show that values vary widely with type of construction material and ventilation rate, so that it is difficult to arrive at an average or typical value. The mean of measurement in 324 dwelling places in Europe and the United States (United Nations, 1972, Table 13) is 0.52 pCi/liter, and values as high as 10 pCi/liter were reported in Europe and 4.8 pCi/liter (Lowder, *et al.*, 1971) in the United States. The mean of all measurements of outdoor radon concentrations made in connection with the indoor measurements quoted above is 0.084 pCi/liter. It appears, therefore, that the radon concentration in homes is likely to be much higher than the value assumed in our calculation (0.13 pCi/liter), which ignores the contribution of home construction materials, further reducing the significance of the contribution of natural gas activity to the total airborne natural radioactivity in homes. We conclude that other factors such as home construction material and ventilation rate are more important than the radon concentration in natural gas in determining the level of airborne natural radioactivity in homes.

REFERENCES

Altshuler, B., N. Nelson, and M. Kuschner, (1964), *Estimation of Lung Tissue Dose from the Inhalation of Radon and Daughters,* Health Physics 10, 1137-1161.

Barton, C.J., (1971), *Radon in Air, Natural Gas, and Houses: A Preliminary Survey and Evaluation,* ORNL-CF-71-5-48.

Barton, C.J., R.E. Moore, and P.S. Rohwer, (1973a), *Contribution of Radon in Natural Gas to the Natural Radioactivity Dose in Homes,* ORNL-TM 4154.

Barton, C.J., R.E. Moore, and S.R. Hanna, (1973b), *Radiation Doses from Hypothetical Exposures to Rulison Gas,* Nuclear Technology (in press).

Blifford, I.H., Jr., H. Friedman, L.B. Lockhard, and R.A. Baus, (1956), *Geographical and Time Distribution of Radioactivity in the Air,* J. Atmospheric Terres. Phys. 9, 1-17.

Bresline, A.J., (1972), New York Health and Safety Laboratory, U.S. Atomic Energy Commission, private communication with C.J. Barton, Oak Ridge National Laboratory.

Chamberlain, A.C., and E.D. Dyson, (1956), *The Dose to the Trachea and Bronchi from the Decay Products of Radon and Thoron,* Brit. J. Radiol. 29, 317-325.

Evans, R.D., (1967), *Carcinogenity of Inhaled Radon Decay Products in Man (CORD)* in *Radiation Exposure of Uranium Miners, Hearings before the Joint Committee on Atomic Energy,* 90th Congress, Part 2, U.S. Government Printing Office, Washington, D.C., p. 1188-1207.

Harley, N.H. and B.S. Pasternack, (1972), *Alpha Absorption Measurements Applied to Lung Dose from Radon Daughters,* Health Physics 23, 771-782.

Haque, A.K.M.M., and A.J.L. Collinson, (1967), *Radiation Dose to the Respiratory System Due to Radon and Its Daughter Products,* Health Physics 13, 431-443.

Holaday, D.A., D. Rushing, R. Coleman, P. Woolrich, H. Kusnetz, and W. Bale, (1957), *Control of Radon and Daughters in Uranium Mines and Calculations on Biologic Effects,* Public Health Service Publication No. 494, Washington, D.C.

Holleman, D.F., (1968), *Radiation Dosimetry for the Respiratory Tract of Uranium Miners,* Colorado State University Report C00-1500-12.

International Commission on Radiological Protection, (1966), *Recommendations of the International Commission on Radiological Protection* (adopted September 17, 1965), ICRP Publ. 9, Pergamon Press, London.

Jacobi, W., (1964), *The Dose to the Human Respiratory Tract by Inhalation of Short-Lived* ^{222}*Rn- and* ^{220}*Rn-Decay Products,* Health Physics 10, 1163-1174.

Lowder, W.M., A.C. George, C.V. Gogolak, and A. Blay, (1971), *Indoor Radon Daughter and Radiation Measurements in East Tennessee and Florida,* Health and Safety Laboratory, USAEC, HASL-TM-71-8.

Lundin, F.E., Jr., J.K. Wagoner, and V.E. Archer, (1971), *Radon Daughter Exposure and Respiratory Cancer Quantitative and Temporal Aspects,* National Institute for Occupational Safety and Health, National Institute of Environmental Health Sciences, Joint Monograph No. 1, PB-204871 (NIOSH-M-71-1).

Satterly, J. and R.L. Elworthy, Canadian Bureau of Mines, Bulletin No. 16, Parts I and II.

Satterly, J. and J.C. McIennan, (1918-1919), *The Radioactivity of the Natural Gases of Canada,* Trans, Royal Soc. Canada, Sec. III, 12, 153-160.

Schiager, K.J., (1973), Colorado State University, private communication with C.J. Barton, Oak Ridge National Laboratory.

Segeler, C.G., editor, (1966), *Gas Engineers Handbook,* The Industrial Press, New York, p. 12/344.

Shapiro, J., (1954), *An Evaluation of the Pulmonary Radiation Dosage from Radon and Its Daughter* Products, Report 298, University of Rochester, Rochester, New York.

United Nations, General Assembly, (1972), *A Report of the United Nations Scientific Committee on the Effects of Atomic Radiation, Vol. 1: Levels,* New York.

Walsh, P.J., (1970), *Radiation Dose to the Respiratory Tract of Uranium Miners — A Review of the Literature,* Environmental Research 3, 14-36.

Table 1. Sampling and Analyses of Natural Gas.

Area	Pipeline Company	Organizations That Made Analyses	Organizations Bearing Analytical Costs
New York	Texas Eastern Transmission Company (TET)	AEC-New York Health and Safety Laboratory	AEC-New York Health and Safety Laboratory
New York	Transcontinental Gas Pipeline Corporation (TRANSCO)	AEC-New York Health and Safety Laboratory	AEC-New York Health and Safety Laboratory
Chicago	Natural Gas Pipeline Company of America (NGPL)	Argonne National Laboratory	Natural Gas Pipeline Company of America
Denver	Colorado Interstate Gas Company (CIG)	Colorado State University	Colorado Interstate Gas Company
Southwest and West Coast	El Paso Natural Gas Company (EPNG)	New Mexico Technical Research Foundation	El Paso Natural Gas Company

Table 2. Summary of Radon Measurements in Natural Gas Samples.

Area Served	Identification	Number of Samples	^{222}Rn Analysis (pCi/liter) Average	Range
Chicago	Amarillo	12	24.6	19.3 - 31.3
Chicago	Gulf Coast	12	3.2	2.3 - 4.4
New York City	TET	10	1.8	0.6 - 3.5
New York City	TRANSCO	8	1.4	0.6 - 1.6
New York City	TRANSCO-HASL	85	1.4	0.5 - 7.4
Denver	Wyoming	15(a)	5.8(a)	1.2 - 8.2
Denver	Kansas	8	91	15.3(b) - 118.8
Denver	Ft. Morgan (storage)	1	9.3	
El Paso	El Paso	2	17	
West Coast	Topock	--	19(c)	
West Coast	Blythe	--	9(c)	

(a) Includes examples taken at Ault and Aurora.

(b) Value excluded from average — sample taken during period of low gas usage.

(c) Values corrected for mixing and decay to the listed distribution point from analyses of samples taken at upstream sampling points. There would be further decrease of approximately 1 to 2 pCi/liter before the gas reached the Los Angeles market.

Table 3. Summary of Dose Conversion Factors for Radon and Radon-Daughters.

Isotopes Included	Critical Tissue	Calculated Dose (rads/year)(a)	Reference
Radon + daughters	Tertiary bronchioles	30	Shapiro (1954)
Radon + RaA	Main bronchi	20	Chamberlain, *et al.*,(1956)
Radon + daughters	Bronchial tissue	120	Holaday, *et al.*,(1956)
Radon-daughters	Segmented bronchi	150	Altshuler, *et al.*,(1957)
Radon-daughters	Secondary-quarternary bronchioles	150	Jacobi (1964)
Radon-daughters	Segmented bronchi	620	Hague, *et al.*,(1967)
Radon-daughters	Tertiary bronchioles	40	Holleman (1968)
Radon-daughters	Segmented bronchioles	12	Harley, *et al.*,(1972)

(a)The dose is calculated in rads per year for continuous exposure to radionuclides in a concentration equivalent to one "working level," defined as any combination of short-lived radon-daughters that will result in the ultimate emission of 1.3×10^5 MeV of alpha energy per liter of air.

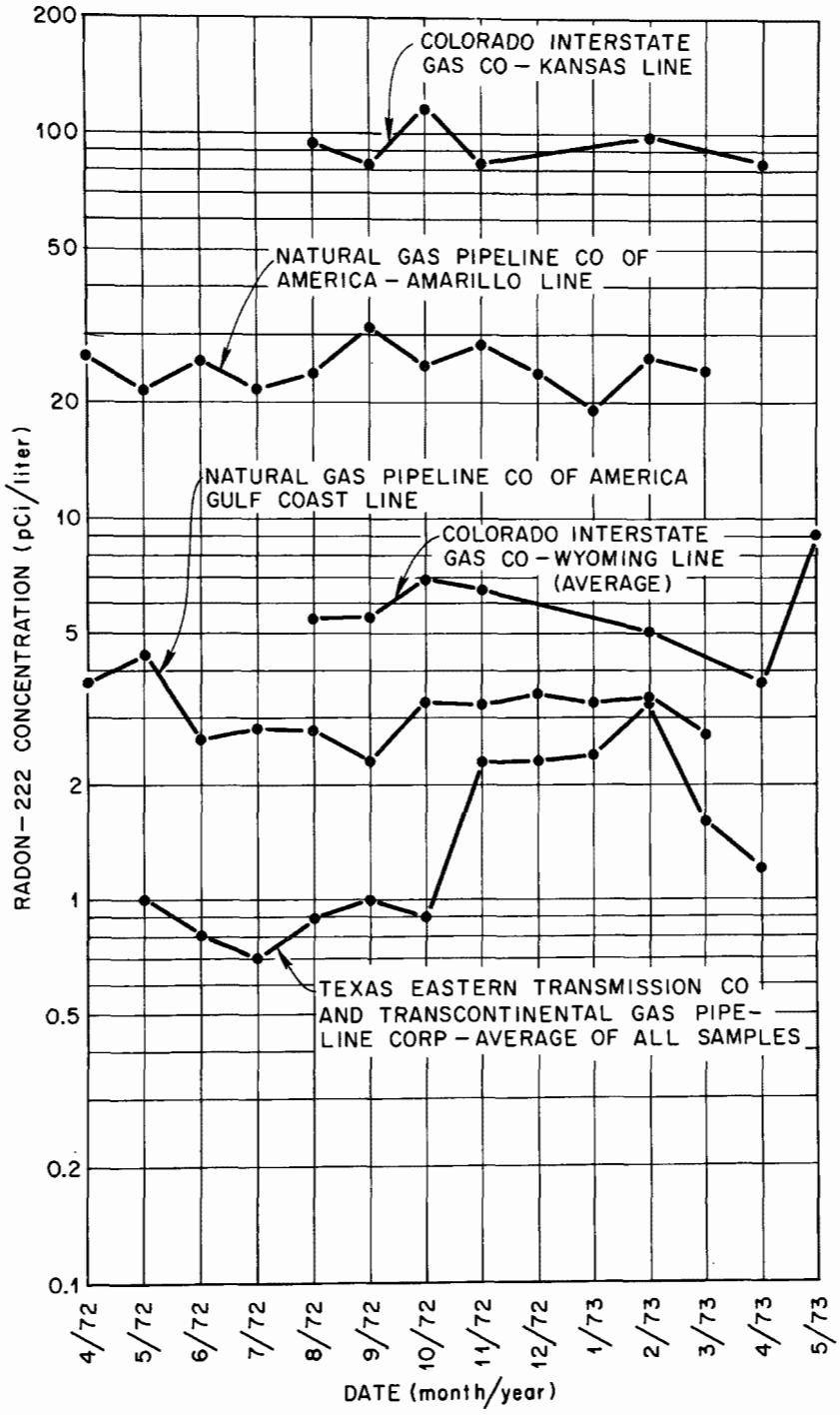

Observed Concentrations of Radon in Pipeline Gas Samples.

Figure 1.

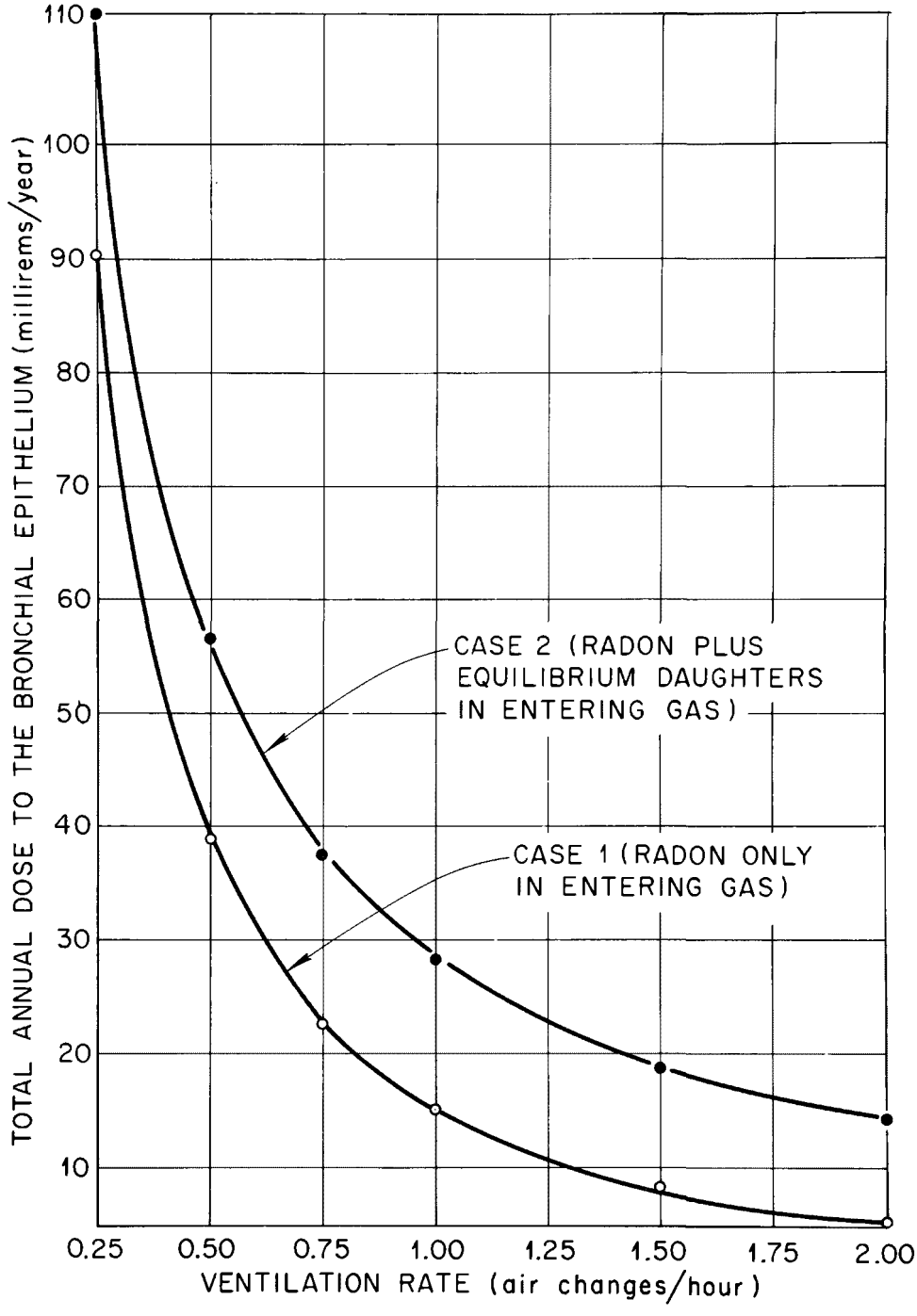

Effect of Ventilation Rate on Dose from Radon Daughters Assuming No Activity in Ventilation Air.

Figure 2.

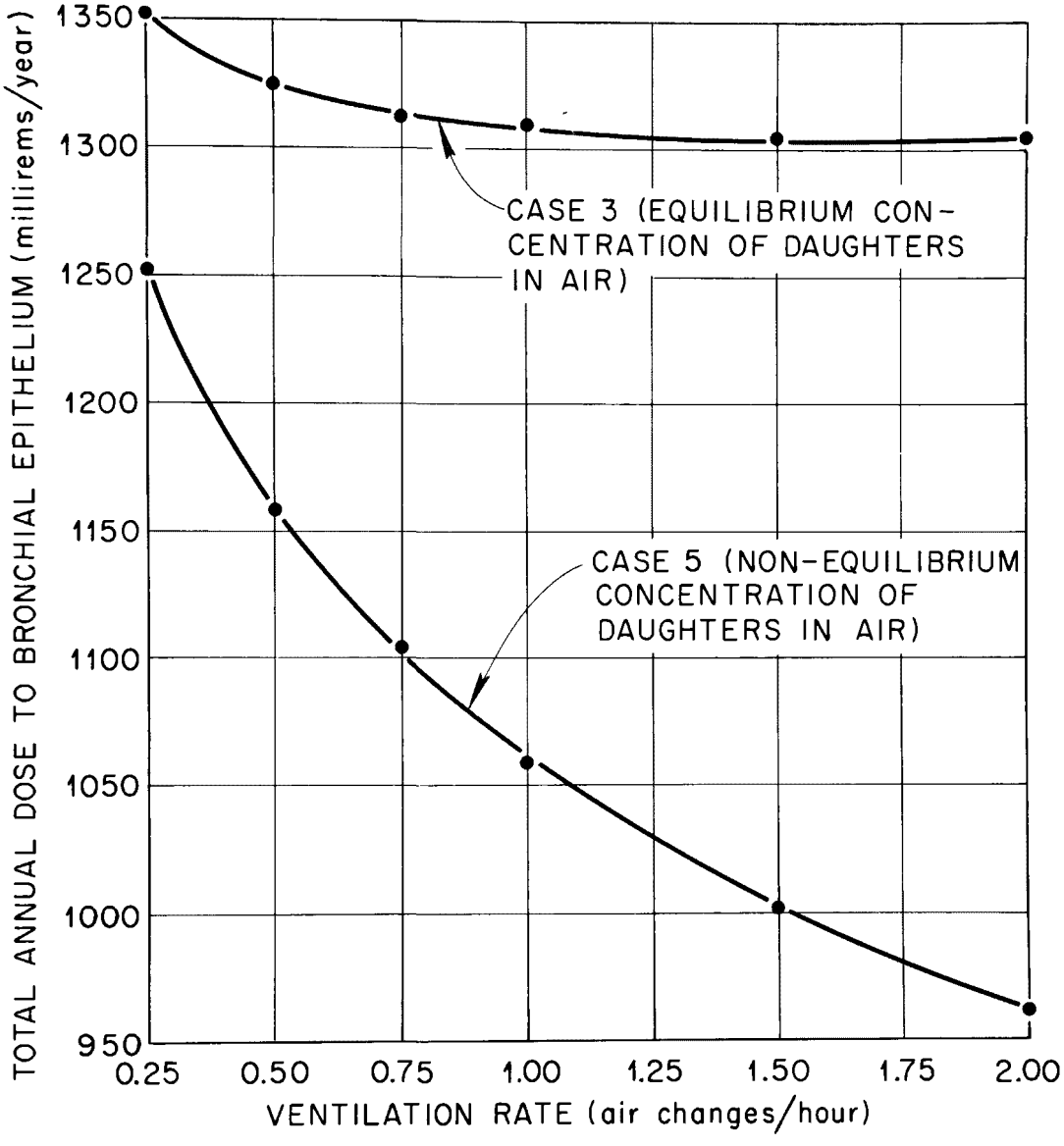

Effect of Ventilation Rate on Dose from Radon Daughters from Natural Gas and Air.

Figure 3.

IV. Detection and Measurement of Noble Gases

RADIOACTIVITY STANDARDS OF THE NOBLE GASES

W. B. Mann, F. J. Schima and M. P. Unterweger
Center for Radiation Research
National Bureau of Standards
Washington, D.C. 20234

Abstract

The National Bureau of Standards gas-counting equipment is described. This consists of matched, length-compensated copper and stainless steel internal gas counters, which can be used in the proportional or Geiger-Mueller regions. The data acquisition and processing is by means of a computer-based multichannel analyzer. Methods for preparing relative standards based on measurements with ion chambers and fixed-geometry solid-state detectors are discussed. Noble-gas standards for argon-37, krypton-85, xenon-131m, and xenon-133 have so far been prepared, the last involving purification on the NBS isotope separator.

INTRODUCTION

The measurement techniques to be described, and much of the work to be discussed in this paper have, been quite fully discussed in a recent publication (Garfinkel, *et al.*, 1973). We, therefore, have limited this paper to those aspects of our work that have not previously appeared in the published literature.

The chief interest of those who are participating in this Symposium lies in the measurement of the increasing burden of radioactive noble gases in the atmosphere, arising from either fission or activation as a byproduct in the production of nuclear power. These radioactive noble gases range from the highly active, but short-lived argon-41, to the much less active, but long-lived krypton-85.

By way of introduction, it is both interesting and instructive to examine two forecasts of krypton-85 world burdens made by the then Division of Radiological Health (DRH) in 1966 (Coleman, *et al.*, 1966), and by the Environmental Protection Agency (EPA) in 1972 (Klement, *et al.*, 1972).

Figure 1 shows the EPA forecast which gives predicted levels between the years 1960 and 2000, based on the assumptions of both uniform world mixing and a 75-percent preponderance in the northern hemisphere.

Figure 2 shows the DRH predicted world burdens between the years 1965 and 2060. Measured values are shown as triangles between about 1958 and 1963, and the EPA 1972 predictions (for uniform world mixing), have been superimposed, by way of comparison, as large circular discs for the years 1960, 1970, 1980, 1990, and 2000. This comparison shows that the two forecasts are not greatly discrepant. Both also tend to follow the somewhat gloomy Club-of-Rome type of forecast, with no feedback due to the balance that arises due to modification of demand, cost of supply, or the simple commonsense reaction of trapping the gas. The departure from a continuing exponential growth, in both these forecasts, must arise from the 11-year half-life of krypton-85, which would tend to impose an equilibrium upper limit, if the krypton-85 were being supplied at a constant rate. Obviously, however, the demand for power is also assumed to be an increasing function.

At the moment, with the occasional exception of the fuel element processing facility at Idaho Falls, krypton-85 is essentially not being trapped, so it is important for us to provide the measurements capabilities to determine its increasing levels.

This may not seem to be of too great importance now, but in 2060 we, or, rather our grand-children and great-grandchildren, may be approaching closely (as we see from Figure 3, which is based on the predictions of Figure 2) to the maximum permissible annual dose of 170 mrad for krypton-85 alone, in the absence of any other radioactive insults.

GAS COUNTING EQUIPMENT

The NBS gaseous radioactivity standards are normally calibrated in length-compensated internal gas counters, generally in the proportional region, and sometimes in the Geiger region (Mann, *et al.*, 1960 and 1961). A set of three such counters is shown in Figure 4. These are three stainless-steel counters, having equal diameters, but different lengths, with as nearly as possible, identical end supports for the central anode wire. Using such counters we can compensate, by taking the difference in count rate for a given difference in volume, for the decrease in electric field strength at the ends of the counters, and also for events occurring in these regions and penetrating into the inner region of normal electric field.

This counter system, using both copper and stainless-steel counters, and the principle of compensation and method of operation, have been discussed in detail (Garfinkel, *et al.*, 1973).

The count-rate data for all six counters, three of copper and three of stainless steel, are fed simultaneously into an on-line computer used as a multi-channel analyzer. The detailed specifications and modes of operation of this computer are discussed by Schima (1973).

ANALYTICAL CORRECTIONS

A typical pulse-height spectrum from a single counter in the assay of argon-37, with the K- and L-capture peaks well resolved is shown in Figure 5. In this assay a correction on the order of one percent was made for M-capture events that would clearly be lost in the amplifier noise.

Previously, before use of a computer, discrimination curves of integral count versus discriminator bias were plotted and extrapolated to zero discriminator bias to eliminate "low-energy" noise. In our present method of

operation, the computer is programmed to make a similar extrapolation by summing counts above chosen equal intervals from "low-energy" channels. The zero channel is determined by using a precision pulser with linear characteristics. This is referenced to the output response of the gas counting system using the K- and L-capture peaks of argon-37.

Appropriate dead-time corrections are made for the data from each counter, and the difference count rates are then obtained from the summed counts over all channels for each counter, corrected for dead-time, background, and noise.

With a long-lived radioactive gas such as krypton-85, the background count rate is determined by recording the count-rate data for each counter, filled with a gas mixture identical with that used, but with the radioactive gas replaced by an equal proportion of inactive carrier gas of the same element, and at the same gas pressures.

In the case of a short-lived radioactive gas, such as xenon-133, a least-squares fitting procedure is used to determine both the net activity at any chosen zero reference time, t_0 (usually the mid-point of the data-acquisition period), and the average background. The internal count rate, corrected for dead-time and low-energy amplifier noise, for a given counter difference and given pressure, are fitted to the expression

$$N = N_0 e^{-\lambda (t - t_0)} + B,$$

Where N is the observed count-rate for the count period starting at time t, and N_0 is the count rate at the chosen reference time t_0. The accuracy of this method is, of course, dependent on the accuracy with which the half-life, λ, is known, the number of half-lives over which the data are taken, and on the background being low and stable.

The results must finally be corrected for efficiency and wall effects by an extrapolation of the plot of activity per gram molecule of the sample gas versus reciprocal pressure to zero reciprocal pressure (infinite pressure), where 100% efficiency for the counters is assumed.

CALIBRATION METHODS AND STANDARDS

Point-source standards of krypton-85 implanted in aluminum, at 30 kilovolts in Oak Ridge, have also been prepared. Discs of aluminum foil about 5 mm in diameter are sealed between plate-glass discs using optical epoxy resin. The gamma-ray emission rate was determined by comparison with point sources of strontium-85 calibrated by x-γ coincidence counting. The same 514-keV gamma ray of rubidium-85 is involved in the decay of both krypton-85 and strontium-85.

After a radioactive gas has been directly calibrated by internal gas counting, the calibration is preserved by either calibrating an ionization chamber with an auxiliary vibrating-reed electrometer; or, in the case of gamma-ray emitting radionuclides, by calibrating, in fixed geometry, a NaI(Tl), GE(Li), or Si(Li) detector. These latter solid-state detector calibrations are carried out with both extended gas samples, in say, approximately 5-ml ampoules, or with the gas condensed by means of liquid nitrogen into the tip of the ampoule, thus obtaining a source that subtends a smaller solid angle to the detector.

Table 1 is a list of the radioactivity standards of rare gases, available from the National Bureau of Standards. These include noble-gas standards for argon-37, krypton-85, xenon-131m, and xenon-133. As the source material for the xenon-133 standards is fission off-gas, it has been found necessary to use the NBS isotope separator to prepare xenon-133 standard essentially free of xenon-131m. Figures 6 and 7 are photographs of the isotope separator collector foils for krypton and xenon respectively. The mass dispersion is readily seen. High specific activity samples of extreme isotopic purity are available by physically cutting out the appropriate portion of the collector foil, and evaporating off the noble gas. Measurements of the isotopic enhancement factor have been made at this laboratory (Landgrebe, *et al.*, 1970) for mass 142, using the radioisotope praseodymium-142. Figure 8 is a plot of the mass dispersion of praseodymium-142 as obtained with the NBS isotope separator. The tail of the mass 142 isotope at the mass 141 position is seen to be more than three orders of magnitude less than the peak intensity. From this, the isotopic enhancement factor for xenon-133 over xenon-131m can be estimated to be on the order of 10^6. In the xenon-133 samples prepared to date, no evidence of xenon-131m activity has been found.

REFERENCES

Coleman, J.R. and R. Liberace, (1966), *Nuclear Power Production and Estimated Krypton-85 Levels,* Radiological Health Data and Reports, 7, p. 615.

Garfinkel, S.B., W.B. Mann, F.J. Schima and M.P. Unterweger, (1973), *Present Status in the Field of Internal Gas Counting,* Nuclear Instruments and Methods (in press).

Klement, A.W., Jr., C.R. Miller, R.P. Minx and B. Shleien, (1972), *Estimates of Ionizing Radiations in the United States 1960-2000,* ORP/CSD 72-1, p. 49, unpublished.

Landgrebe, A.R., W.B. Mann and F.J. Schima, (1970), *The Distribution of 70-kV Praseodymium Ions in Iron Foil and a Technique for Removing Thin Layers of Iron,* Int. J. Appl. Rad. Isotopes, 21, 169.

Mann, W.B., H.H. Seliger, W.F. Marlow and R.W. Medlock, (1960), *Recalibration of the NBS Carbon-14 Standard by Geiger-Mueller and Proportional Gas Counting,* Rev. Sc. Instr. 31, 690.

Mann, W.B., W.F. Marlow and E.E. Hughes, (1961), *The Half-Life of Carbon-14,* Int. J. Appl. Rad. Isotopes, 11, 57.

Schima, F.J., (1973), *A Computer System Used for Pulse Height Analysis,* (to be published).

TABLE 1. National Bureau of Standards Rare Gas Radioactivity Standards.

Radionuclide	Transition	Radiation Counted
Hydrogen-3	Beta	Beta
Carbon-14	Beta	Beta
Argon-37	Electron Capture	Auger Electrons, X-Rays
Krypton-85	Beta	Beta
Xenon-131m	Gamma	Conversion Electrons
Xenon-133	Beta	Beta
Radon-222(a)	Alpha	Alpha

(a) In Equilibrium with Radium-226.

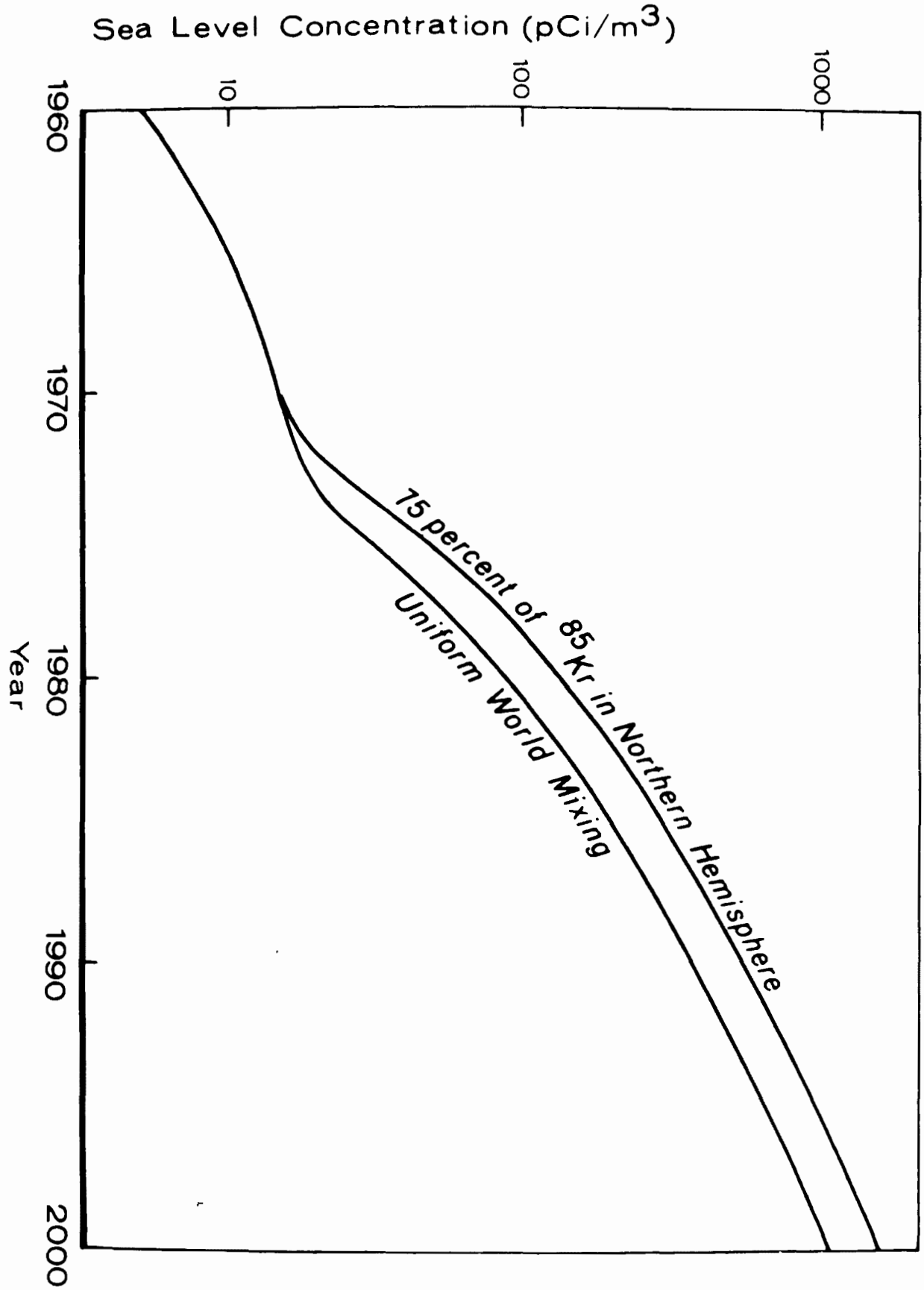

Figure 1. Estimated krypton-85 concentration in the Northern Hemisphere from nuclear electric power production.

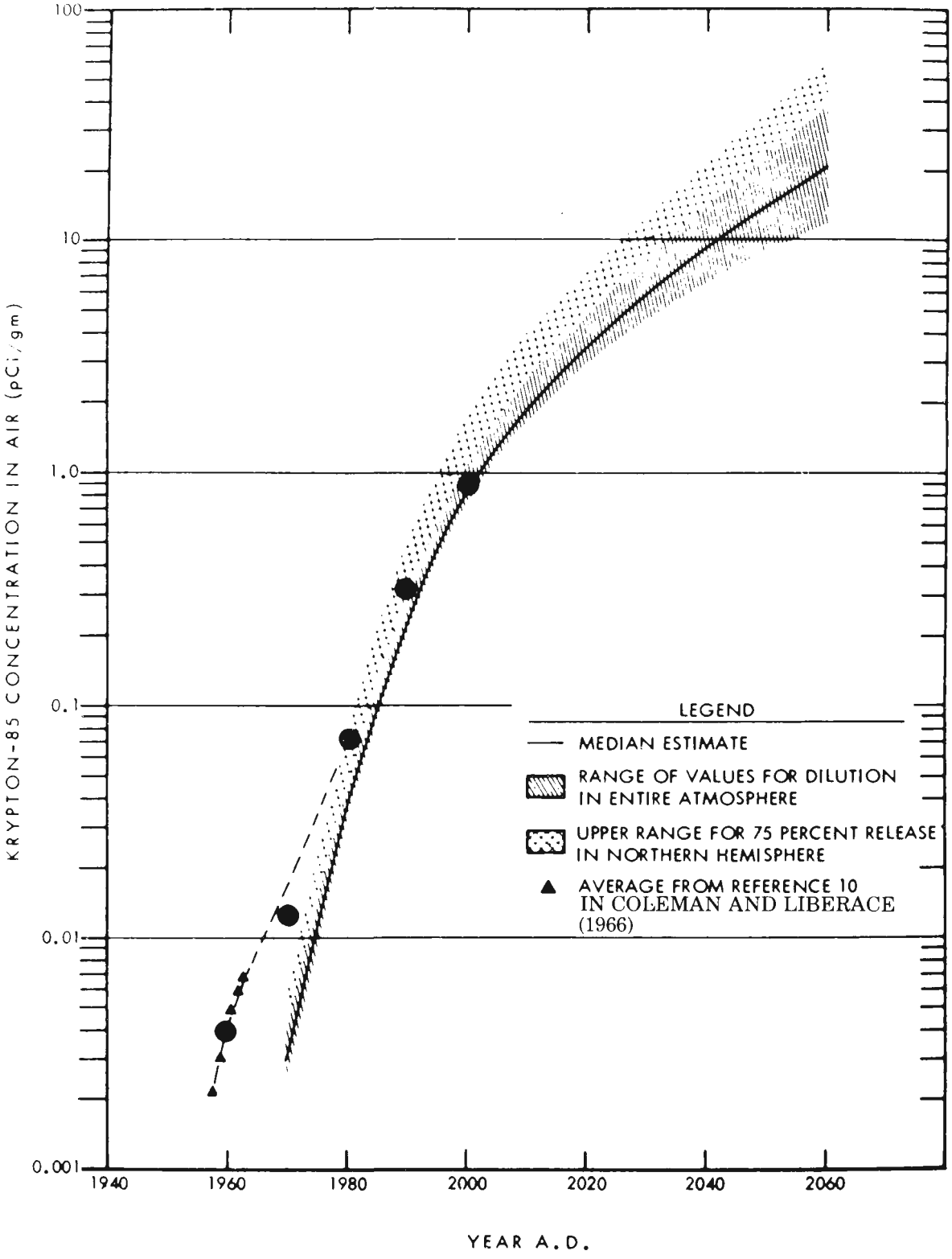

Figure 2. Estimated krypton-85 concentration in the air 1970-2060.

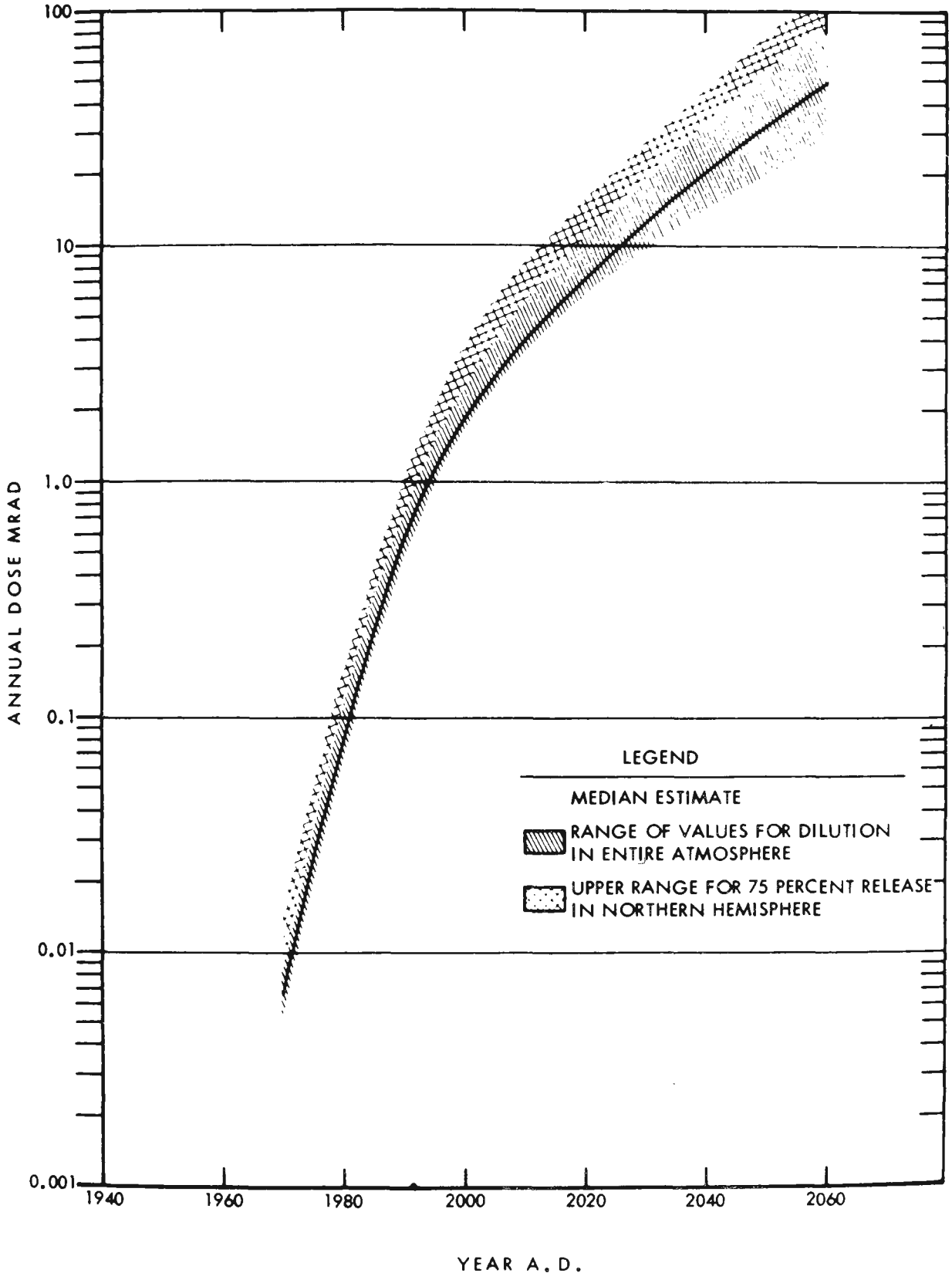

Figure 3. Estimated annual dose arising from exposure to atmospheric krypton-85 for the years 1970-2060.

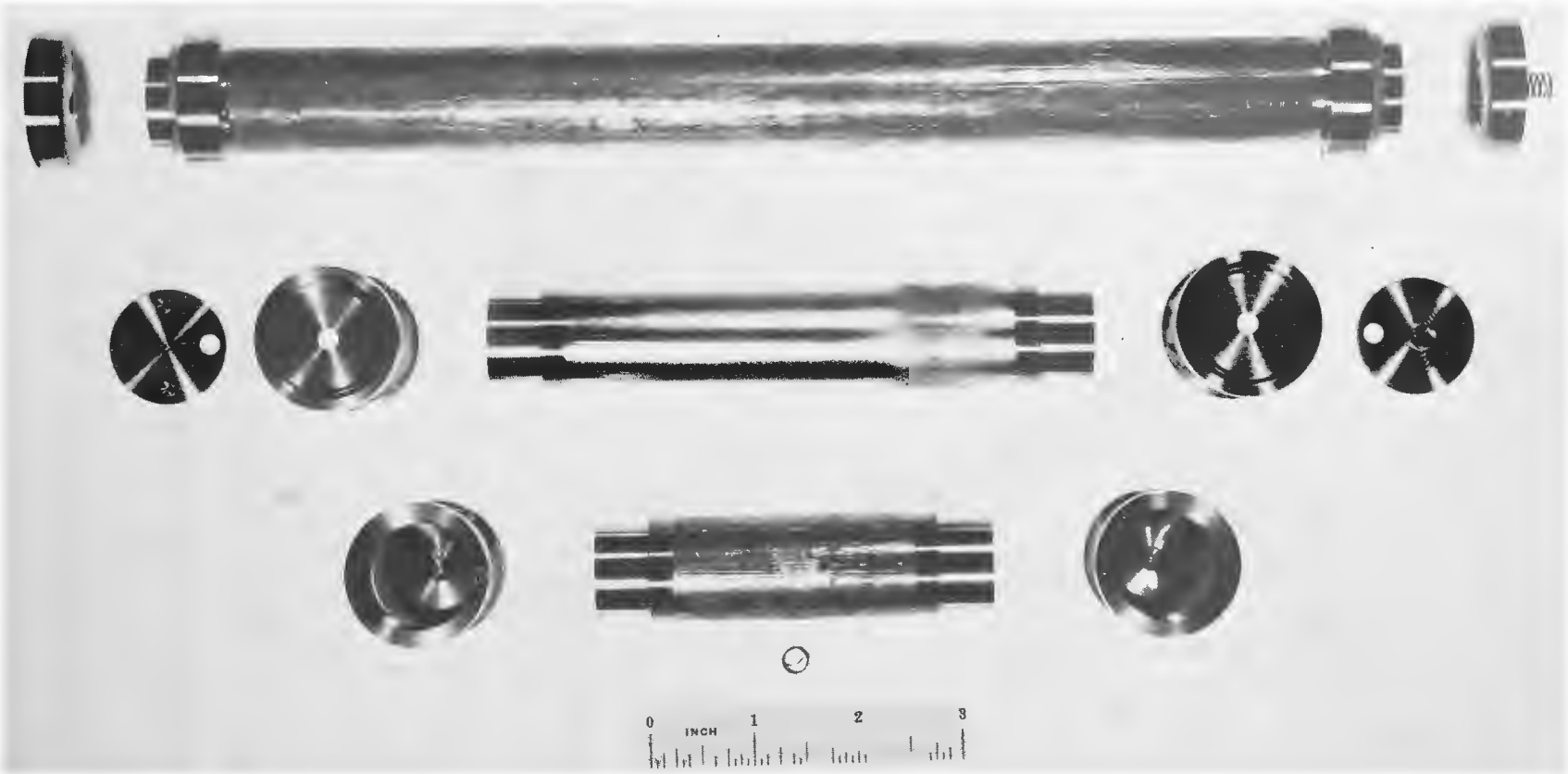

Figure 4. Set of stainless-steel gas counters, made from one piece of tube, and with as nearly as possible identical end supports for the anode wires.

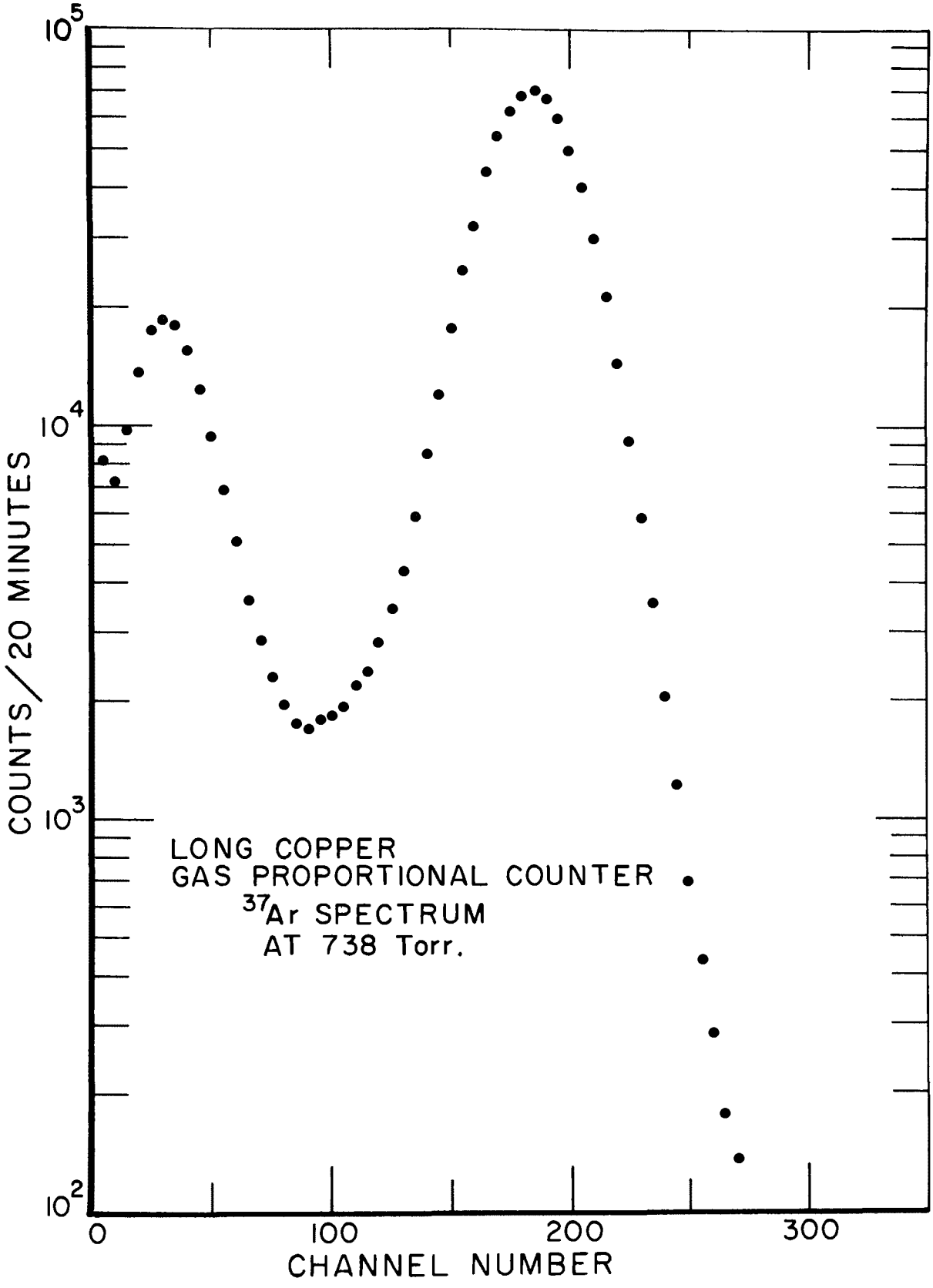

Figure 5. The pulse-height spectrum of argon-37. The K and L capture peaks are clearly resolved. Each peak represents the binding energy of the appropriate shell less the average outer shell ionization energy.

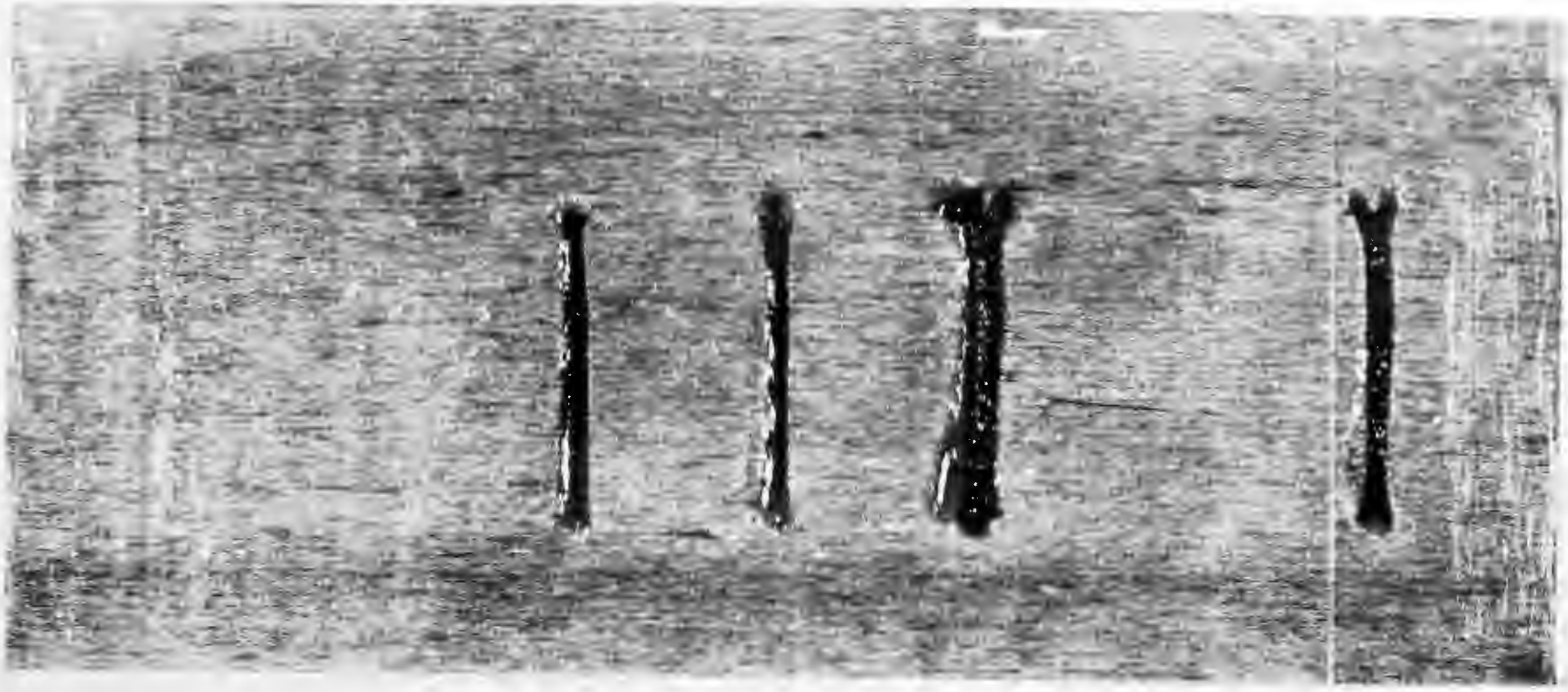

Figure 6. Aluminum target foil implanted with the isotopes of natural krypton. The major isotopic constituents are identified by the respective mass number.

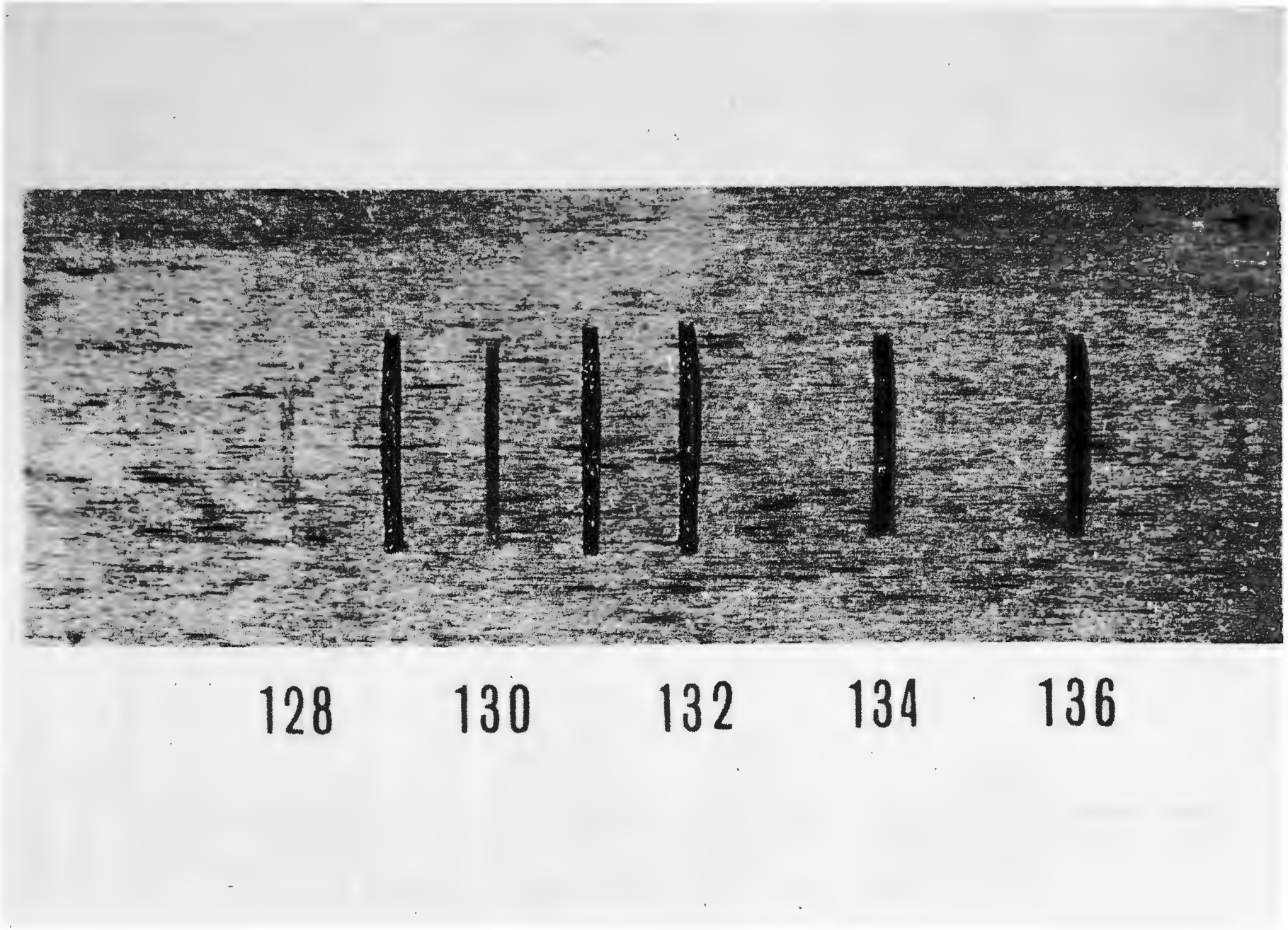

Figure 7. Aluminum target foil implanted with the isotopes of natural xenon, similar to Figure 6.

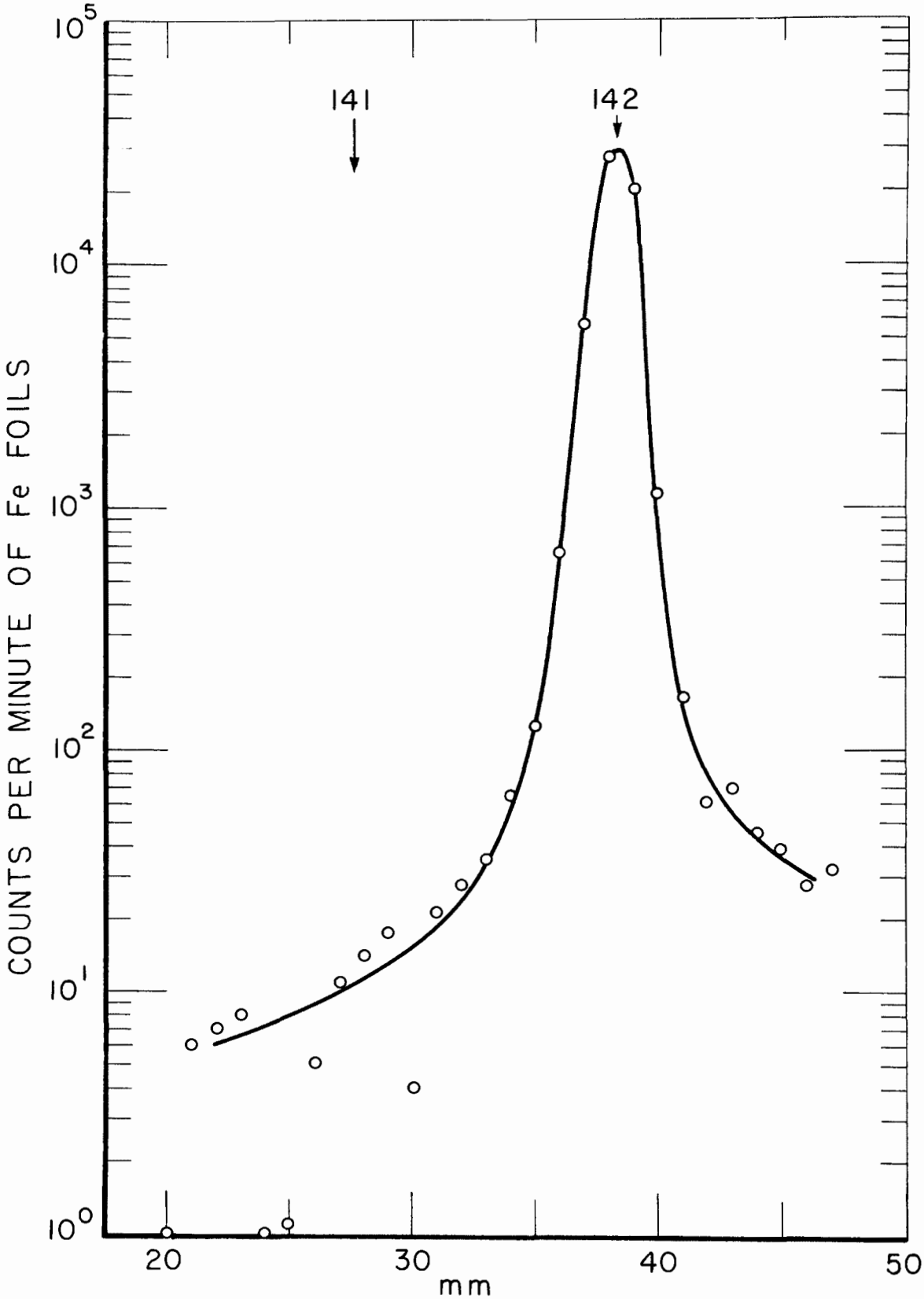

Figure 8. A dispersion plot of mass 142 as determined from the radioactivity of praseodymium-142 implanted into iron foils arranged in steps.

CALIBRATION OF DETECTORS FOR ARGON-41

H. E. DeSpain and S. B. Garfinkel*
Center for Radiation Research
National Bureau of Standards

Abstract

Most nuclear reactors produce argon-41 during their operation. For many, it is the largest single gaseous radioisotope released outside the reactor. It is essential, therefore, to know the concentration of this gas — both in working areas for the protection of reactor personnel and in reactor effluents for environmental protection. For this reason, it was important to develop a rapid and easy method to precisely measure the concentration of argon-41, wherever it may be found.

The radioactivity of an irradiated sample of argon was assayed by comparing it to an NBS Standard Reference Material of sodium (^{22}Na). The argon-41 was then transferred to an ionization chamber, and an accurate calibration of the response of the ion chamber was made. This chamber was subsequently used to calibrate other detectors, including the stack monitor for the NBS 10 MW heavy-water research reactor. The method used does not require an accurate knowledge of the neutron flux density, cross section, nor volume of gas irradiated for the calibrating samples. Also, the activated argon does not have to be transferred to another container before assaying. Furthermore, this method allows for quick and repeated recalibrations and measurements whenever required. The results to date have been excellent.

INTRODUCTION

One of the critical problems of today is the question of radioactive releases into the environment because of the potentially significant impact on the health and safety of the public. This problem is accentuated by the rapid growth of nuclear power plants and facilities coupled by newly instituted AEC Regulations limiting all radioactive releases to "as low as practicable". For these reasons, it has become essential to know, accurately, the magnitude of such releases, even for previously ignored small amounts. In order to measure the amount of radioactive material released into the environment, accurately calibrated monitors are needed. In this connection, a new technique has been developed which provides a simple, fast, and accurate method for the calibration of these monitors. While the technique has a wide range of application, it is being initially tested for one of the most prevalent gaseous effluents, argon-41, which has a half-life of 110 minutes. Most reactors produce argon-41 during their operation, and, for many, it is the largest single gaseous radioisotope released to the environment.

The general method for producing a known amount of argon-41 is to irradiate a known mass of argon (99.6% argon-40) in a known thermal neutron flux for a given time (Meck, 1969). Then, by using the thermal activation cross section and decay constant, one can calculate the amount of argon-41 produced. It is obvious that several variables will have to be known accurately in order to obtain a meaningful number on the amount of argon-41 produced during the irradiation.

A program was started to determine an alternate method to generate a known amount of argon-41 for use in calibrating detectors. The technique developed here eliminates many of these problems.

EXPERIMENTAL

It was decided to assay the radioactive argon after production by comparing it to a calibrated source. Sodium-22 was chosen because of its single gamma ray of 1,274.5 keV (Adams, *et al.*, 1969), which is near the argon-41 gamma of 1,293.6 (Adams, *et al.*, 1969), and is readily available from the National Bureau of Standards (NBS, 1973). This known amount of ^{41}Ar was injected into an ionization chamber (IC), and measurements were made of the detector's response as a function of time. The half-life of the ^{41}Ar was checked, and the response of the detector was calculated. This calibrated detector may then be used to sample systems containing ^{41}Ar or may be used to calibrate other detectors.

The first technique tried was to place the ^{22}Na source in a cylindrical IC which could be taken apart. The source was placed at various points inside the cylinder and counts were taken with a NaI detector at 40 cm. This proved to be a long, tedious procedure and was abandoned rather quickly. The next method involved counting a sample of irradiated argon (in plastic tubing) in the same geometry as the ^{22}Na source (40 cm from the NaI detector), then placing the tubing in a glass finger attached to an evacuated detector. The finger was opened to the chamber and heated until the plastic tubing melted and released the ^{41}Ar. Although this method worked satisfactorily for calibrating a G.M. detector system, the hydrocarbons evolved during the heating decreased the efficiency of an ionization chamber by about 10%, so the present method was developed.

Figure 1 shows the general scheme employed. A ^{22}Na Standard Reference Material (SRM) obtained from the NBS was used to determine the efficiency of a NaI detector for 1,274.5 keV gamma rays. This detector was then used to assay a sample of ^{41}Ar in the same geometry.

The γ-ray efficiency of the detector for ^{41}Ar was determined by a straight line interpolation of the efficiency for the 1,274.5 keV γ-ray of ^{22}Na and the 1,332.4 keV (Adams, *et al.*, 1969) γ-ray of ^{60}Co. This was done by

**Deceased*

recording the spectrum for each radionuclide on a 400 channel analyzer (MCA) and evaluating by Hutchinson's method (Hutchinson, *et al.*, 1967). Once E (the ratio of ^{22}Na to ^{41}Ar γ-detector efficiency) was determined, it was found that one could achieve satisfactory results with a single channel analyzer (SCA) instead of the MCA by adjusting a single channel analyzer window to cover the photopeak pulses from both radionuclides.

A section of polyethylene tubing (3.17 mm 1D x 3.99 mm OD) was flushed with pure argon gas at atmospheric pressure, then heat sealed at the open end. Next, several samples were prepared by heat sealing the tubing in 2-3 cm long sections until a sufficient number of samples were sealed. At this time, the sealed samples were cut from the tubing and checked for leakage by submersion in water. After drying, a sample was irradiated in a thermal neutron flux density of about 10^{13} n/cm^2/s for a period of 30 seconds, producing approximately 2μCi of argon-41. The sample was then positioned at 40 cm from the surface of the previously calibrated NaI detector. A preliminary count was taken to check for the presence of impurities. Another count was started, and after counting long enough to accumulate the desired counts, the sample was placed inside a modified syringe which was then attached to an evacuated detector.

A 20 ml syringe was modified in order to permit filling the detector with various gases without using a dry box. This was done by adapting a 1/4" OD glass tubing to the wall of the syringe at about the 15ml line (Figure 2). A number 21 scalpel blade was sheared off at each end and top to form a cutting edge of 5 mm x 17 mm. This blade was epoxied to a 17 mm diameter washer with a sharp edge up. The washer and blade were then placed in the bottom of the syringe, and the plunger was coated with vacuum grease. A magnesium perchlorate filter was used to remove the water vapor while filling the detector through the syringe. The valve between the detector and syringe was opened, causing the pistol to press the source against the blade severing the polyethylene tubing and releasing the argon-41 into the detector. Next, the detector inlet valve was closed and the piston was pulled out far enough to allow room air from the filter to enter into the syringe, then the plunger was inserted until the opening to the filter was closed. After a short time, the detector inlet valve was opened again to allow the argon-41 air mixture in the syringe to enter the detector. This process was repeated several times to ensure that all the argon-41 was injected into the detector, then both valves were opened, and the detector was allowed to come to atmospheric pressure.

To provide a check on possible leakage of the radioactivity during the expansion, the detector was brought to atmospheric pressure through another detector, and this second detector indicated that a negligible amount of radioactivity had escaped during the expansion. The syringe was removed intact and recounting with the NaI detector indicated that less than 1/2 of 1% of the original activity remained in the syringe. Leakage through the polyethylene tubing was checked by counting an intact sample at various times, and comparing the observed count rate to the theoretical count rate, allowing for decay of the sample. This leakage average$\approx$0.1% per minute. Since the time lapse from counting until the sample was placed into the syringe was on the order of 30 seconds, the loss due to leakage was 0.1% or less. The detector used was a one liter spherical ionization chamber (IC). The volume of the chamber was determined by weighing before and after filling with water. The vibrating reed electrometer (VRE) was used in the constant voltage mode, whereby the voltage produced across a 10^{12} ohm resistor by the current from the IC is measured by the VRE and indicated on a digital voltmeter (DVM). The DVM has an accuracy of 0.1%$\pm$one digit. The combination of the $10^{12}\Omega$ resistor-VRE-DVM was checked by introducing a current from a calibrated picoampere source and found to be accurate within 0.6%. The IC was checked for saturation by use of an external ^{60}Co source, and it was found that a potential of 270 volts was sufficient to ensure saturation for the currents produced by a nominal sample (8×10^{-12} A). A further check was made by extrapolating the indicated voltage after a period of decay back to the time of the transfer and initial voltage measurement. If these voltages did not closely agree, the process was repeated for a later measurement, until it was determined that the IC was saturated. From this point on, the decay time after γ-counting and the indicated voltage was recorded at intervals of 10-30 minutes, until at least ten measurements were made. These data were used in an exponential least squares fitting program to calculate the decay constant and the voltage the sample would have produced at T = 0. By calculating the total activity by reference to the ^{22}Na source, one could calibrate the detector as described in Appendix 1. The accuracy of the calibration was primarily dependent upon the uncertainties of the sources used in the ^{41}Ar detection efficiency and the counting statistics of the ^{41}Ar sample. The overall uncertainties of the ^{22}Na and ^{60}Co sources, respectively, were 1.5% and 1.2%; i. e., the linear sum of 0.1%, which is the 99% confidence limit, and the estimated systematic errors. A calibration accuracy estimated to be within $\pm$5% was attained easily. The precision achieved in eight calibrations of the same detector was a standard deviation of the mean of 0.8%. The observed mean half-life was 109.6 minutes with a standard deviation of 0.3%. The sample activities ranged from about 2 to 4 μCi; all were γ-counted for four minutes at 40 cm from the crystal surface.

This technique has also been used to calibrate a pair of 14.6-liter ionization chambers which are used to sample the stack exhaust of the NBS 10 MW heavy-water reactor.

APPENDIX I

Calibration of the Detector

$$CF_{41} = \frac{S_{22}.R_{41}.E}{Vml.V_o.Ar_{41}} \cdot \frac{76}{P} \cdot \frac{273+T}{T}$$

where CF_{41} = Calibration factor in $\frac{Ci}{ml\ volt}$ for ^{41}Ar @ STP

S_{22} =Sensitivity of γ-detector for ^{22}Na in $\frac{Ci}{\text{counts per minute}}$

R_{41} =Count rate of γ-detector for ^{41}Ar @ time = 0

E =Ratio of efficiency of γ-detector for ^{22}Na versus ^{41}Ar

P =Pressure in mm of Hg

T =Temperature in °C

V_{ml} =Volume of detector in ml

V_o = Voltage indicated by VRE @ time = 0

AR_{41} = Abundance of argon-41 gamma ray (0.992)

REFERENCES

Adams, F. and R. Dams, (1969), *Compilation of Gamma Transition Energies*, Journal of Radioanalytical Chemistry, 3, 99-125.

Hutchinson, J. M. R. and D. H. Walker, (1967), *A Simple and Accurate Method of Calibration by Photopeak Efficiencies*, Int. J. Appl. Rad. Isotopes, 18, 86-89.

Meck, R. A., (1971), *Measurement of Argon-41 Effluent from University-Size Reactors*, Proceedings, Health Physics Society Symposium (1969), pp 1029-1042. C. A. Willis, ed., Gordon and Breach, pub.

NBS Radioactivity Standard Reference Materials, (1973), Office of Standard Reference Materials, National Bureau of Standards, Washington, D. C. 20234.

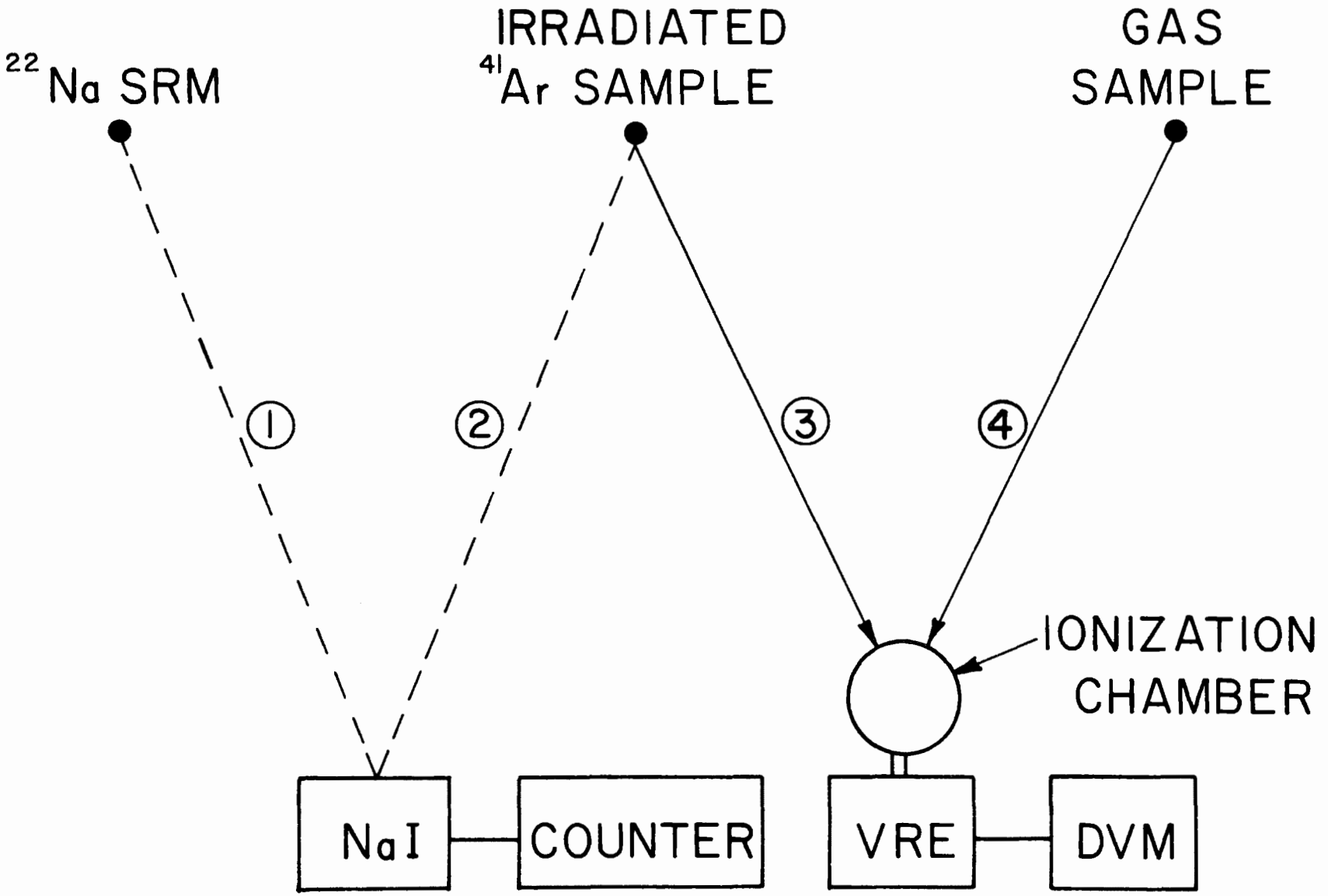

Figure 1. Calibration Scheme.

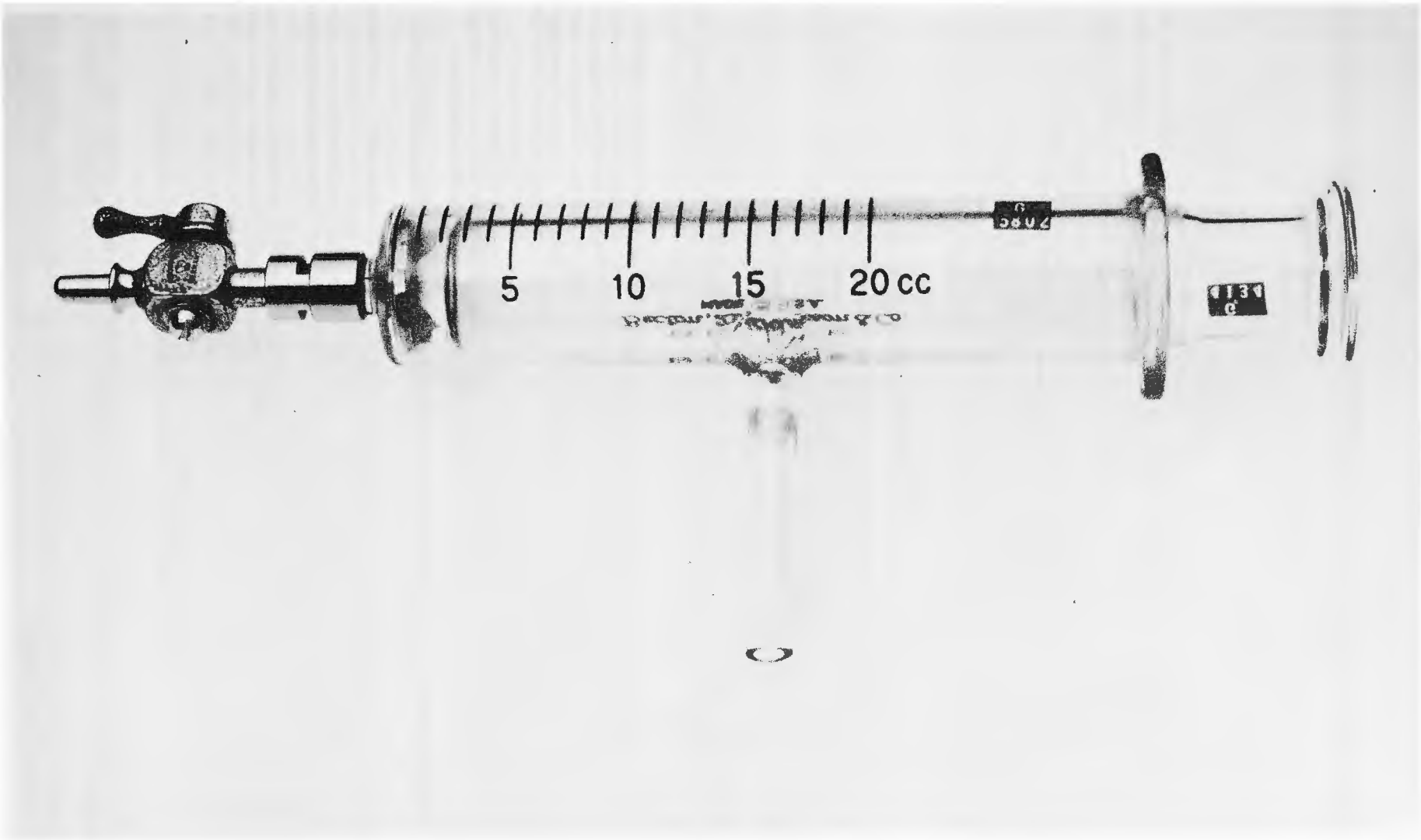

Figure 2. Modified Syringe.

SEPARATION OF NEON-21 FROM NATURAL NEON BY THERMAL DIFFUSION

W. M. Rutherford, G. E. Stuber, Jr., and R. A. Schwind
Monsanto Research Corporation
Mound Laboratory*
Miamisburg, Ohio

Abstract

The rare stable isotope neon-21 comprises 0.27% of natural atmospheric neon. In earlier work, separation of neon-21 in high purity was accomplished by thermal diffusion with the aid of deuterated methane as an auxiliary gas. The separation is now being accomplished by thermal diffusion without the use of an auxiliary gas. In the latter process a two-stage, multiple column, thermal diffusion system is employed. The most abundant isotope, neon-20, is removed in the first stage, leaving a binary mixture of neon-21 and neon-22. The binary mixture is further separated in the second stage of the process, yielding high purity neon-21. It was found that the performance of the separation apparatus in both the transient and steady-state modes could be accurately predicted from thermal diffusion column and cascade theory.

The thermal diffusion separation technique can be used for the separation of a wide variety of gas mixtures, including isotopic separations of stable and radioactive nuclides. Recent examples include separation of argon-37 and argon-39 from atmospheric argon and the enrichment of krypton-85 and xenon-136 from nuclear reactor fission gas.

INTRODUCTION

The rare stable isotope ^{21}Ne comprises 0.27% of atmospheric neon. The separation of this material from the much more abundant isotopes, ^{20}Ne and ^{22}Ne, is of interest for many applications to physical research problems. The separation is a difficult one involving the extraction of a small quantity of the desired isotope from large quantities of material of both higher and lower atomic mass.

A small quantity of ^{21}Ne of very high enrichment (99.6%) was separated by using the thermal diffusion column and an auxiliary gas technique (Clusius, *et al.*, 1956). The auxiliary gas (deuterated methane) was used to displace the end components of the ternary mixture, and was later separated by conventional physical techniques from the ^{21}Ne product. This rather tedious batch technique has also been used by the authors to prepare small quantities of ^{21}Ne of a somewhat lower concentration. The work to be described in this paper, however, involved the successful continuous separation of ^{21}Ne at high-enrichment without the aid of an auxiliary gas.

The thermal diffusion column, invented by Clusius and Dickel (1938), is an especially effective tool for separating small quantities of isotopes in the gas phase, and a number of such separations were accomplished by Clusius and co-workers using batch techniques (Grove, *et al.*, 1968). An extensive and unique facility has been developed at the Mound Laboratory for the continuous separation by thermal diffusion of many of the isotopes of the noble gases. This paper describes the continuous separation of ^{21}Ne in a two-stage thermal diffusion process, wherein the ternary mixture is converted essentially to a binary mixture in the first stage and the binary is separated in the second stage.

Operation of the dual cascade system afforded a useful experimental test of the theory of multicomponent isotope separation cascades and of the associated computational techniques for solving the system of nonlinear partial differential equations which describes the transient behavior of such cascades.

THEORETICAL BASIS OF ISOTOPE SEPARATION BY THERMAL DIFFUSION

The theoretical aspects of the problem of separating ^{21}Ne fall into three categories: (1) the theory of the individual separation unit or column; (2) the theory of multiple column units, or cascades; and (3) design techniques for arriving at optimum configurations of cascade systems for multicomponent separations. Portions of these topics have been treated separately in the literature. This section contains a summary of the information pertinent to the particular problem at hand.

The theory of the thermal diffusion column was developed originally by Jones, *et al.*, (1946) for the heavy isotope case. It was later extended by Rutherford (1970) to mixtures of light isotopes and to non-isotopic mixtures. In the theory, the behavior of the column is described by a system of transport equations which give the net rate at which the various components of a mixture are transported toward the ends of the column. Thus,

$$T_i = H_o w_i \left(d_i - \sum_{j=1}^{m} w_j d_j\right) - (K_o + K_d)\frac{dw_i}{dz} + \sigma w_i , \qquad (1)$$

where T_i is the net rate of transport in mass per unit time of component i, the w_i are the mass fractions of the components, the d_i are molecular or atomic mass differences relative to an arbitrarily chosen component

**Mound Laboratory is operated by Monsanto Research Corporation for the U. S. Atomic Energy Commission under Contract AT-33-1-GEN-53.*

called the key component, σ is the net mass flow rate through the column, and z is the vertical coordinate. The coefficients, H_o, K_c, and K_d are the reduced initial transport coefficient, the convective remixing coefficient, and the diffusive remixing coefficient, respectively.

The three coefficients are functions of the geometry and operating conditions of the thermal diffusion column and of the physical properties of the fluid. Generally, they must be evaluated by a series of numerical integrations of the corresponding theoretical expressions. Recent work (Rutherford and Kaminski, 1967; Rutherford, *et al.*, 1969; and Roos and Rutherford, 1969 and 1970) has shown that in carefully constructed columns the experimentally determined column coefficients agree quite well with those predicted from theory, provided that the physical properties of the gas mixture are accurately known.

As will subsequently be demonstrated, the transient performance of a thermal diffusion column is frequently of more interest than the steady-state behavior. Under transient conditions, Equation (1) becomes

$$\frac{\partial T_i}{\partial z} = -\mu \frac{\partial w_i}{\partial t}, \tag{2}$$

where μ is the mass holdup per unit length in the column and t is the time. Equations (1) and (2) comprise a system of nonlinear partial differential equations which must be solved by finite difference techniques.

A straightforward approach to the solution of (2) involves the step-by-step evaluation of the following finite difference approximations to Equation (2):

$$w_{i,m,k+1} = w_{i,m,k} + \frac{(T_{i,m+1,k} - T_{i,m,k})\Delta t}{\mu_m (z_m - z_{m-1})} \tag{3}$$

where the subscript i refers to the component, the subscript m to the location along the cascade in the z direction, and the subscript k refers to the time step. Although this is a workable scheme, the calculation is stable only for unrealistically small time intervals, and excessive amounts of computer time are required to obtain solutions for moderately complex problems.

At the expense of additional complexity a much more efficient method has been developed for solving the transient problem. In the new method, the transport of component i during the kth time period is taken to be the average of the transport at the beginning of the time interval, and the transport at the end of the interval; thus,

$$w_{i,m,k+1} = w_{i,m,k} + \frac{\Delta t}{\mu_m \Delta z}\left[\frac{(T_{i,m,k} + T_{i,m,k+1}) - (T_{i,m-1,k} + T_{i,m-1,k+1})}{2}\right] \tag{4}$$

These equations cannot be used for the direct calculation of the new concentrations at the end of k + 1 time intervals because the quantities $T_{i,m,k+1}$ are also explicit functions of the new concentrations. The system of equations, however, can be reduced to a set of tridiagonal equations for each component, so that

$$A_m w_{i,m-1,k+1} + B_m w_{i,m,k+1} + C_m w_{i,m+1,k+1} = D_{i,m}. \tag{5}$$

The $D_{i,m}$, contain the new concentrations in the form of the non-linear part of Equation (4). If the $D_{i,m}$, are initially assumed constant during a time step, a first approximation to the new concentrations can be obtained by solving the resulting linear set. The first approximations can be used to calculate new values of the $D_{i,m}$, and so forth until convergence is obtained within the desired accuracy.

The implicit scheme is quite stable, and can be used with a time step on the order of 100 times that of the more direct method. The amount of computation, however, is roughly a factor of 10 greater so that the net gain in speed of operation is reduced to a factor of 10.

The steady-state solution of Equation (1) can be more difficult and sometimes more time consuming than the solution of the transient problem. The typical problem involves processing feed material of a specified composition to yield two or more product streams for which the flow rates are specified. The transport equations can be integrated in a straightforward way (Runge-Kutta, for instance), but the composition of the mixture is not known *a priori* at any point in the cascade. The boundary conditions, then, are the material balances for each component. One must assume the composition at some base point in the cascade, calculate the corresponding concentration profiles for each component, then iterate upon the assumed composition to satisfy the material balances. Newton's method is a satisfactory iteration technique, but some artifice must be adopted in the choice of the way in which the base point composition variables are used in the iteration. It was found that fewer failures were encountered, and more rapid convergence was obtained, by a transformation of the compositions such that the iteration was performed on the quantities R_i where

$$R_i = \ln[f_i/(1-f_i)] \tag{6}$$

and

$$f_i = w_{ib} P_b / w_{iF} F \tag{7}$$

The quantities w_{ib} and w_{if} are the mass fractions at the base point, and in the feed, respectively; P_b is the product flow at the base point and F is the feed rate. Equation (6) restricts f_i to the region between 0 and +1; thus, according to (7) the amount of any one component in the product stream cannot exceed the amount in the feed.

Most of the literature on the design of cascades for the separation of multicomponent isotope mixtures was summarized by Tucker (1963). The basic design method is that of the "key weight" of M* cascade described by De la Garza (1962). The M* cascade can be interpreted as a cascade in which the abundance ratio (ratio of concentrations) of two fictitious components are equal in all of the streams which come together within the cascade. The average of the molecular weights of these two components is equal to M*. The M* cascade has the property that those components whose molecular weights are less than M* are preferentially enriched above the feed point, and those components which are heavier than M* are preferentially enriched at the bottom of the cascade. Because of this property, it is possible to enrich a middle isotope (neither the lightest nor heaviest isotope in the feed) to any desired purity by using two M* cascades. The M* design method can also be used to design a single cascade to enrich a middle isotope to any desired purity; however, the use of a single cascade seems to be less efficient than the dual cascade system.

EXPERIMENTAL SEPARATION SYSTEM

The dual cascade system for the separation of ^{21}Ne (Figure 1) is comprised of eight thermal diffusion columns. In a primary cascade of four columns, feed of natural abundance was separated into three streams containing respectively, neon-20, neon-22, and a "binary" partially enriched mixture of neon-21 in neon-22. The latter mixture was used as feed to the secondary cascade of four columns. The neon-21 product, and a byproduct stream of neon-22, were obtained from the second cascade.

The separation system deviated somewhat from the concept described in the previous section primarily because of limitations imposed by the number, type, and physical locations of the available columns. The four columns of the primary cascade were separately located, and were of a different type than the columns of the secondary cascade; therefore, it was not practical to consider configurations involving a 5-3 or a 6-2 split for the two cascades. The M* or key weight concept could not be used in the design of the system because of the small number of separation units available for the job; however, one might consider the two cascades to be something like squared-off M* cascades with $20 < M^* < 21$ in the primary cascade, and $21 < M^* < 22$ in the secondary cascade.

The side stream in the first cascade is also a departure from the basic design principle. The side stream was an expedient which was adopted to get around the unfavorable characteristics of a "square" primary cascade. (A square cascade is one in which the number of columns are parallel along the entire series length of the cascade.) Specifically, the use of the side stream greatly reduced the time required before usable product could be delivered to the secondary cascade. In addition, an intermediate product of a higher ^{21}Ne concentration could be obtained with no sacrifice in the rate of transport of ^{21}Ne. These advantages of side stream operation would be unlikely to be encountered in a large cascade which could be arranged in an optimum series-parallel combination of columns.

The columns of the primary cascade were of a standard Mound Laboratory design described by Rutherford, *et al.*, (1968). The columns, which were mounted in individual cooling water jackets, were heated by tubular electric heaters having an active hot-length of 4.88 m. They were connected in a series by circulating gas from the bottom of one column through the top of the next with sealed, magnetically-driven circulating pumps. High-purity neon gas was fed to the system through a two-stage metal diaphragm pressure regulator. The top, bottom, and side streams were allowed to flow from the cascade through variable leaks into lines at reduced pressure. Gas from the top and bottom of the cascade was pumped into storage bottles with sealed refrigerator compressors. The gas from the side stream was allowed to accumulate in an evacuated tank. It was periodically pumped by means of a peristaltic pump into a 300 ml bottle filled with activated coconut charcoal at liquid nitrogen temperature. There were two 300-ml bottles. One was used to feed the secondary cascade while the other was being filled from the primary cascade.

The secondary cascade consisted of four hot wire columns of an older Mound Laboratory design. They were equipped in a configuration very similar to the columns of the primary cascade. The top product was removed through two solenoid valves operated alternately by a timer. The product was then stored in the head space of a refrigerator compressor. The bottom product was removed through a very fine metering valve into a line also evacuated by a refrigerator compressor.

Operating pressures of the two cascades, which were 9.7 and 1.0 atm, respectively, were chosen on the basis of column coefficients calculated from theory. The theoretical calculations were done in a way similar to that reported by Rutherford and Kaminski (1967) for neon columns operated under similar conditions. The primary cascade was operated at a high pressure relative to the maximum in the relationship between the static (total reflux) separation and pressure. This was done in order to gain as high a transport of neon-21 as possible at the feed point. A higher pressure could have been effectively used, but the maximum working pressure of the circulating pumps was on the order of 10 atm. The secondary cascade, for which a high transport was not required, was operated at a pressure equal to that of the maximum static separation factor. It was desirable to operate at lower pressures in the secondary cascade because the extent of separation per unit of neon-21 holdup became more favorable as the pressure was reduced.

The dimensions and operating parameters of the columns of the two cascades are summarized in Table 1. Also given in Table 1 are the theoretical values of the column coefficients, and the calculated electrical power requirements for the column heaters and wires.

SEPARATION OF NEON-21

Exploratory calculations of the behavior of the two cascades showed that neon-21 of 90% or greater enrichment could be produced from the secondary cascade if it were fed a "pseudo-binary" mixture containing several percent neon-21 in neon-22. It was necessary that the neon-20 content of the mixture be no more than 5 to 7% of the neon-21 content, and perferably very much less than 5%. Calculations of the transient behavior of the primary cascade showed that the desired mixture could be produced as a side stream after a startup period of some 90 days. During the startup period, neon-20 and neon-22 would be separated from the feed mixture, and neon-21 would be allowed to accumulate in the cascade until the desired operating holdup of neon-21 was acquired.

The decision was made *a priori* to recover approximately two-thirds of the neon-21 in the feed gas; therefore, operation of the cascade was designed so that the byproduct neon-20 and neon-22 streams contained 0.1% neon-21. Later, it became apparent that a more favorable distribution of concentrations would result in the primary cascade if the neon-22 stream were allowed to drop to 0.05% neon-21, and this was done shortly before product withdrawal was started.

As shown in Figure 2, the predicted behavior of the primary cascade was closely matched by the experimental results. This included a sharp transient maximum in the neon-21 concentration at the bottom of the cascade just prior to the commencement of neon-22 withdrawal at 7 days of operation. In calculating the behavior from theory, the column coefficients were adjusted somewhat on the basis of previous operating experience with similar columns. Specifically, the initial transport coefficient was taken to be 85% of the value given in Table 1, and the convective remixing coefficient was taken to be 115% of that given in Table 1.

A period of reasonably stable operation was encountered after the start of a side stream product withdrawal. Accordingly, average flow rates and product compositions were calculated from the data for a period representing approximately 30 days of operation. These results and the material balances constructed therefrom are given in Table 2 along with the corresponding values derived from the theoretical calculations. The agreement of the side stream compositions is not especially striking, but it should be recognized that the side stream composition is critically sensitive to the positioning of the neon-21 concentration peak in the cascade. The location of the neon-21 peak can be manipulated within a very short period of time by adjustment of the neon-22 withdrawal rate at the bottom of the cascade.

When a quantity of approximately 6 STP l of side stream product had been accumulated, feed was started to the secondary cascade. The secondary cascade contained an initial inventory of neon-21 as the result of previous separation experiments outside the scope of this report. Thus, the starting concentration of neon-21 at the top (product) end of the cascade was 39%. During a start-up period of 76 days, the neon-22 byproduct was removed from the bottom of the secondary cascade, and the neon-21 concentration was allowed to increase at the top to the desired value of 90%. Progress of the concentration as a function of time is shown in Figure 3. Theoretical calculations of the transient behavior of the secondary cascade were not made; however, it was recognized that the capacity of the secondary cascade exceeded the ability of the primary cascade to deliver material. Figure 3 represents the behavior during the operating time when feed material was available, and does not include periods of shutdown. Following the startup period, the cascade was operated for a period of 92 days to produce a total of 257 ml of neon averaging 90 to 92% neon-21.

DISCUSSION

The successful operation of a dual cascade has resulted in the separation of a significant quantity of enriched neon-21 for subsequent application in physical research. In addition, it was shown that, for a relatively complex system, the behavior of thermal diffusion cascades can be predicted with confidence. This is of particular significance in relation to isotope separation problems involving the rare gases, because thermal diffusion is one of the few available separation methods which can be applied to these materials on a small scale.

The thermal diffusion technique was recently applied by one of the authors (Rutherford) to the calibrated, quantitative transient enrichment of argon-37 in the atmosphere. The techniques and theoretical calculations associated with this work are to be described in a forthcoming publication. Similar methods can be applied to other noble gas isotopes of sufficiently long half-lives, e.g., krypton-84 and -85 and argon-39. Argon depleted in argon-39, and krypton depleted in krypton-85, have also been separated at Mound Laboratory.

REFERENCES

Clusius, K. and G. Dickel, (1938), *New Process for Separation of Gas Mixtures and Isotopes*, Naturwiss, 26, 546.

Clusius, K., M. Huber and H. Hurzeler, (1956), *The Separation Tube. XVII. Preparation of the Rare Isotope Neon-21 at 99.6% Purity.*, Z. Naturforsch 11a, 702-9.

De la Garza, A., (1962), *A Generalization of the Matched Abundance Ratio Cascade for Multicomponent Isotope Separation*, Oak Ridge Gaseous Diffusion Plant Report K-1527, Union Carbide Nuclear Co., Oak Ridge, Tennessee.

Grove, G. R., (1959), *Thermal Diffusion: A Bibliography*, Mound Laboratory Report MLM-1088.

Jones, R. C. and W. H. Furry, (1946), *The Separation of Isotopes by Thermal Diffusion*, Rev. Mod. Phys. 18, 151-224.

Roos, W. J. and W. M. Rutherford, (1969), *Experimental Verification, with Krypton of the Theory of the Thermal Diffusion Column for Multicomponent Systems*, J. Chem. Phys. 50, 424-9.

Roos, W. J. and W. M. Rutherford, (1970), *Separation of Xenon Isotopes in the Thermal Diffusion Column*, J. Chem. Phys. 52, 1684-7.

Rutherford, W. M. and K. J. Kaminski, (1967), *Experimental Verification of the Theory of the Thermal Diffusion Column*, J. Chem. Phys. 47, 5427-32.

Rutherford, W. M., (1970), *Separation of Light Isotopic Mixtures in the Thermal Diffusion Column*, J. Chem. Phys. 53, 4319-24.

Rutherford, W. M., W. J. Roos and K. J. Kaminski, (1969), *Experimental Verification of the Thermal Diffusion Column Theory as Applied to the Separation of Isotopically Substituted Oxygen*, J. Chem. Phys. 50, 5359-65.

Rutherford, W. M., F. W. Weyler and C. F. Eck, (1969), *Apparatus for the Thermal Diffusion Separation of Stable Gaseous Isotopes*, Rev. Sci. Instr. 39, 94-100.

Tucker, T. C., (1963), *An Investigation of Some Problems Involved in the Separation of Multicomponent Mixtures Having Small Separation Factors*, Oak Ridge Gaseous Diffusion Plant Report KOA-1160. Union Carbide Nuclear Co., Oak Ridge, Tennessee.

TABLE 1. Dimensions and Other Parameters of Thermal Diffusion Columns Used for Neon-21 Separation.

	Primary Cascade	Secondary Cascade
Length, m	4.88	7.32
Cold wall diameter, cm	1.75	1.91
Hot wall diameter, cm	0.8	0.16
Cold wall temperature, °K	303	303
Hot wall temperature, °K	973	1,023
H_0, initial transport coefficient for 1 mass unit, g/s	6.36×10^{-5}	2.07×10^{-5}
K_c, convective remixing coefficient, g-cm/s	3.04×10^{-3}	1.41×10^{-3}
K_d, diffusive remixing coefficient, g-cm/s	6.57×10^{-4}	1.66×10^{-3}
Calculated power input, W	4,850	2,670

TABLE 2. Compositions and Flow Rates in the Primary Cascade During Steady Operation.

		Flow Rate, STP ml/hr	Composition mole percent: Neon-21	Neon-22
Top stream	exptl.	300	0.11	0.12
	theory	299	0.10	0.077
Side stream	exptl.	8.3	5.3	94.6
	theory	9.0	7.9	91.9
Bottom stream	exptl.	23.7	0.048	99.95
	theory	22.3	0.052	99.95

Neon-21 balance:		
	Feed	0.90 ml/h
	Top	0.33
	Side	0.44
	Bottom	0.01
	Net accumulation	0.12 ml/h

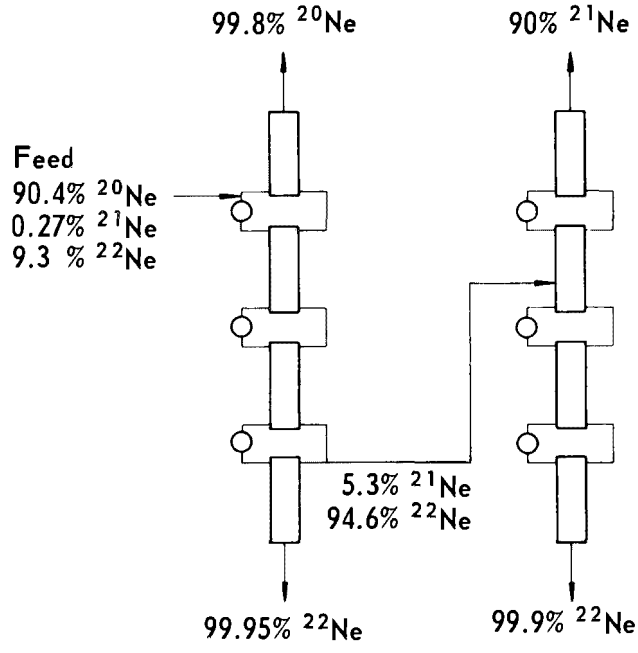

Figure 1. Two cascade system for separating neon-21. The rectangles represent thermal diffusion columns and the circles, interstage circulating pumps.

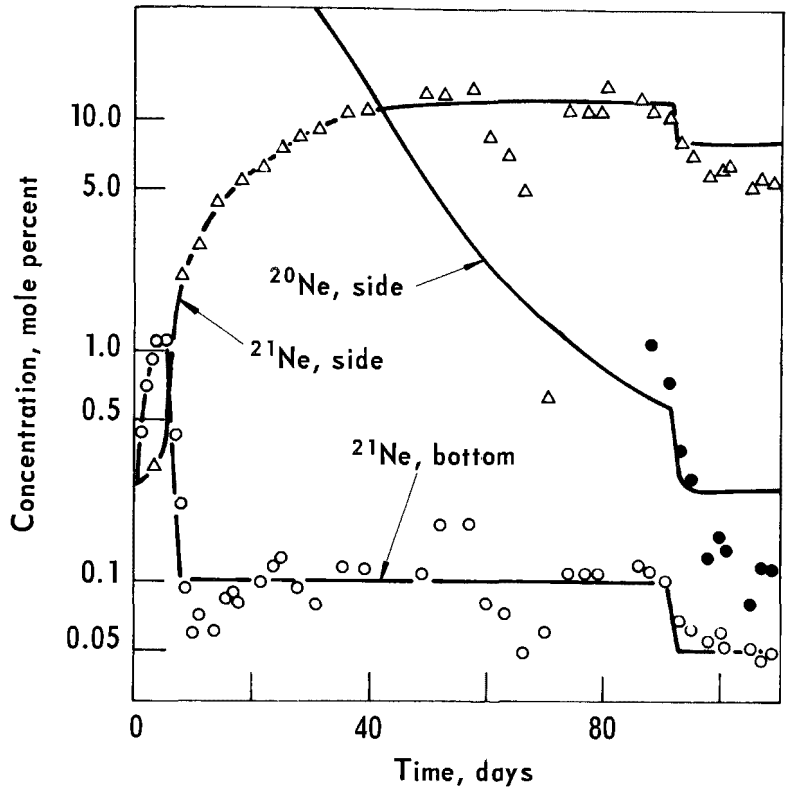

Figure 2. Concentrations in the primary cascade as a function of time. The solid lines are calculated from theory.

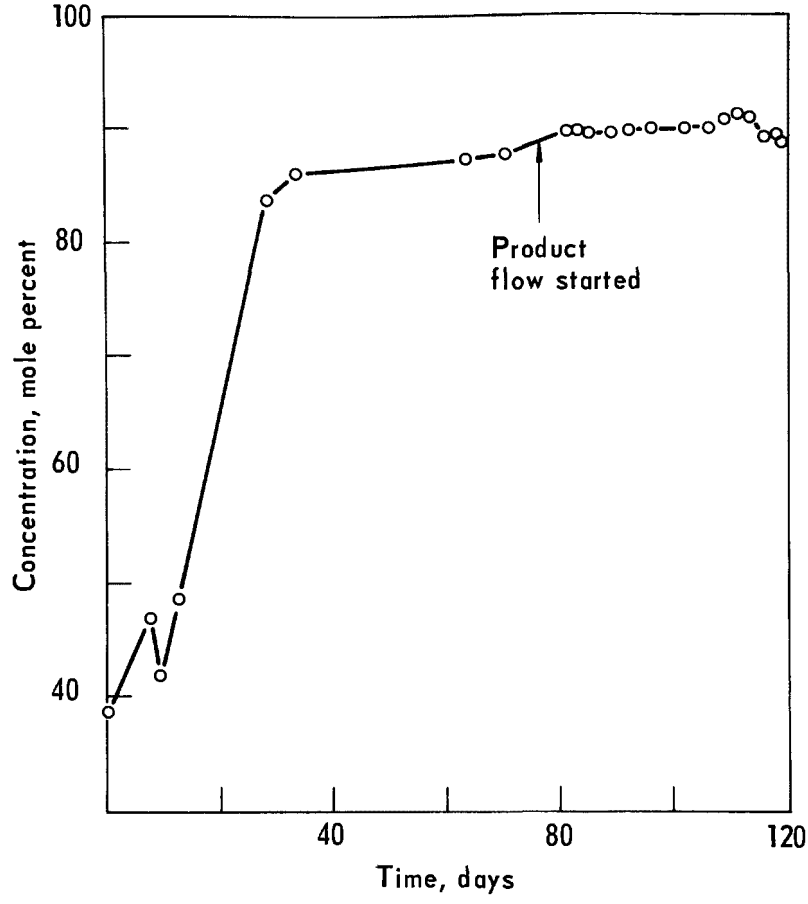

Figure 3. Concentration of neon-21 in the secondary cascade as a function of time.

SURVEY OF ANALYTICAL METHODS FOR ENVIRONMENTAL MONITORING OF KRYPTON-85

R. E. Jaquish and A. A. Moghissi*
National Environmental Research Center
Office of Research and Development
U. S. Environmental Protection Agency
Las Vegas, Nevada

Abstract

Numerous methods have been developed for measuring krypton-85 in air as krypton ultimately accumulates in air once it is released into the environment. However, krypton-85 can be present in other media such as natural gas from wells stimulated with nuclear devices or in water when krypton-85 is used for aeration studies.

Methods for the measurement of ambient levels of krypton-85 require a concentration of krypton from a large air sample of one m^3 or more. If elevated levels are to be measured, carrier krypton may be used provided the contamination of atmospheric krypton with krypton-85 does not interfere with the measurement. In certain cases, such as in the vicinity of nuclear fuel processing plants, direct measurement techniques may be used.

A variety of techniques are employed for krypton-85 counting. At low levels, internal gas counting or organic scintillation is used to measure the beta emission of this radionuclide. At higher levels the gamma emission of krypton-85 may be measured using scintillation or solid state gamma spectroscopic methods.

Techniques for collection of the sample, concentration of krypton, and radioactivity measurement of krypton-85 are discussed and various processes are critically evaluated and compared.

INTRODUCTION

Numerous analytical methods have been developed for measuring krypton-85 in air and other media. The method of choice for a particular application depends on the concentration to be measured, the interfering radionuclides, and the accuracy and precision required. Krypton-85 decays by beta emission having a maximum beta energy of 0.67 MeV and a frequency of 99.6%. The gamma photon is 0.514 MeV with a branching ratio of 0.41%.

Most analytical methods are based on measuring the beta emission because the gamma emission has such a low branching ratio. When high levels of krypton-85 are encountered, gamma measurement can be used. Table 1 gives a comparison of the levels of krypton-85 that might be encountered in monitoring situations.

ANALYTICAL METHODS

1. Direct Measurements.

Direct measurement of the beta emissions from krypton-85 is the simplest, least expensive method of monitoring this radionuclide in air; numerous instruments have been developed for this purpose. There are several limitations, however, to utilizing this technique. The sensitivity of direct measurements is low, being in the order of 10^{-7} to 10^{-8} μCi/ml depending on the particular system. The sensitivity is influenced by background radiation and gamma fields. At the lower levels of detection, the radon in air creates interferences, particularly with flow-through counters. Because of the short range of the 0.67 MeV beta particles, thin window or flow-through detectors are used. Another consideration is that direct beta measurements are not specific for krypton-85. Other radioactive gases that may be present, such as xenon-133/135 or krypton-85m/88, will be readily detected and not differentiated from krypton-85.

Shapiro, *et al.*, (1963) reviewed the sensitivities of various detectors for measuring krypton-85. They presented the calculations for the efficiencies of idealized ionization chambers and other detectors. Data were also presented on the laboratory testing of the detectors as well as test data utilizing an ionization chamber in a reactor stack. A summary of their calculated lowest concentrations of krypton-85 that can be measured by various detectors is given in Table 2. These sensitivities are based on an external radiation background of 0.02 mR/hr.

Smith, *et al.*, (1967a,b) reviewed the various techniques for monitoring krypton-85, and reported sensitivity by direct measurement of 1.5×10^{-7} μCi/ml for a G-M tube in an annular one liter chamber. Theoretically, an internal G-M or proportional counter with a one-liter volume and a 50% counting efficiency could detect 5×10^{-9} μCi/ml. To attain lower sensitivities, concentration techniques are required.

Smith, *et al.*, (1970) laboratory tested a variety of detectors for environmental krypton-85 monitoring applications. They found that the detectors had a linear response over the range of 1×10^{-7} to 5×10^{-5} μ Ci/ml. A comparison of the calibration curves for G-M tubes with a thin plastic scintillator showed the most efficient G-M tube (double-windowed pancake G-M) to be 2.3 times more sensitive than the plastic scintillator. For a maximum counting time of 4 hours and a 30-minute background count, concentrations as low as 7×10^{-9} μCi/ml were detected in the laboratory. The G-M tubes and ionization chambers were field tested at the

Now with the Georgia Institute of Technology, Atlanta, Georgia.

Nuclear Fuel Service reprocessing plant. All detectors tested provided adequate sensitivity; however, under field conditions the ruggedness of the detector was an important factor. The thicker-walled tubes, though slightly less sensitive, were more durable. A one-liter ion chamber was successfully tested to measure the krypton-85 concentration in the plant stack. This ion chamber was no more sensitive than conventional stack monitors consisting of G-M plastic scintillation detectors, and did not offer the rapid response, ease of replacement, or insensitivity to humidity.

G-M detectors were used by Ludwick, *et al.*, (1968) to study atmospheric transport and diffusion using krypton-85 as a tracer. The detectors were similar to those described previously, however, they used more sophisticated electronics for data acquisition. A series of 64 G-M detectors was assembled to relay data into a 4096 channel address memory. Information was accumulated in groups of 64 time channels, and these groups were automatically stepped by a programmer. The system could make quantitative measurements of transport and diffusion for both continuous and puff-type radioactive gas releases on a real time basis.

Special on-line monitors have been developed to measure krypton-85 in the presence of tritiated methane produced by nuclear stimulated gas wells. Bowman, *et al.*, (1973) describes a flow-through proportional counter that can detect as low as 10^{-8} μCi/ml of krypton-85 in natural gas.

2. Separation and Concentration Techniques.

To measure concentrations of krypton-85 at lower levels than those attained by direct measurement, and to remove interfering radionuclides, requires separation and concentration techniques. Numerous techniques, based on the physical properties of krypton, have been developed to monitor krypton-85 at low concentrations. A summary of the physical properties of krypton-85 is given in Table 3.

Mechanisms which possibly could be utilized for concentrating krypton-85 include:

(1) Distillation of liquefied gases.
(2) Electrostatic diffusion.
(3) Molecular diffusion.
(4) Thermal diffusion.
(5) Extraction by oils or solvents.
(6) Chemical removal of other components of the sample.
(7) Formation of chemical compounds with fluoride.
(8) Formation of clathrates.
(9) Pressurization of gas.
(10) Adsorption on molecular sieves.
(11) Adsorption on activated carbon.
(12) Gas chromatography.

Not all of these methods are suitable for monitoring applications, even though they may be applicable for large scale separation systems, or special qualitative and quantitative analyses of noble gas mixtures. When measuring krypton-85 concentrations in air, one is faced with the problem of separating the krypton, which is present at a concentration of 1.14 ppm, from a large volume of oxygen and nitrogen and lesser amounts of argon, neon, methane, and xenon. The amount of krypton recovered must be sufficient to determine the radioactivity of the krypton-85 by a counting technique. A relatively pure fraction of krypton must be recovered for this purpose. A volume of 0.5-2 ml is normally used. Numerous qualitative and quantitative methods for the analysis of noble gases have been developed (Cook, 1961). These techniques are not directly applicable for krypton-85 monitoring because a suitable krypton fraction for counting is not produced. The general techniques for separation, however, are applicable. In general, the methods used for monitoring employ some combinations of adsorption onto activated charcoal or molecular sieve at low temperatures, low-temperature chromatography, and chemical removal of components of the sample.

When measuring krypton-85 in air, stable krypton can be used as a carrier, or analysis can be performed by carrier-free techniques utilizing the 1.14 ppm of krypton gas in the atmosphere as a carrier. It should be noted, however, that commercially available krypton is contaminated with krypton-85, and the current level of this radionuclide in krypton recovered from the atmosphere is approximately 14 pCi/ml krypton (Schroder, *et al.*, 1971). In some applications, this level of contamination would not create a problem. Where small sample sizes are used, the use of a carrier gas is essential.

The sensitivities of the analytical techniques vary, but, in general, all techniques of this type can measure concentrations of ambient krypton-85 in air, which is currently about 17 pCi/m^3 air. The sensitivity of a method is greatly influenced by the technique used to count the radioactivity from the separated krypton fraction. The counting techniques are described in Section 3.

Several analytical techniques employ chemical methods to remove oxygen and nitrogen from the sample, usually as a final cleanup of the krypton fraction before counting. Oxygen and nitrogen can be removed quantitatively by reacting the gas stream with a titanium sponge at 1,000 - 1,100°C. Calcium can be used to remove nitrogen at 400 500°C; however, the reaction diminishes with the formation of surface films. Clean uranium turnings at 800°C will react with nitrogen and oxygen. Oxygen can readily be removed with copper turnings at about 350°C. Zirconium-titanium alloy at 500°C has been used to remove oxygen and nitrogen. Cook (1961) describes the metal-gas reactions for purification of noble gases.

ANALYTICAL TECHNIQUES

1. Separation and Concentration Techniques.

Glueckauf, *et al.*, (1956) developed a very accurate and sensitive technique for measuring the content of krypton and xenon in atmospheric air. The purpose of the measurements was to determine the content of these stable gases; however, the technique could be used to determine krypton-85. The technique consisted of metering 300 liters of dry air into a distillation column at liquid nitrogen temperature (cooled by evaporation). A measured quantity of krypton-85 was added. Nitrogen, argon, helium, neon, and hydrogen were quantitatively removed by distillation under reflux. Oxygen was partially removed by distillation, and a check of the effluent was made for radioactivity to determine when krypton began to be lost. The final liter of oxygen was removed by passage over heated copper turnings. Separation of krypton from xenon was achieved by low-temperature gas chromatographic separation by passage through a cool charcoal column using hydrogen as a carrier, and monitoring the column effluent for krypton-85 activity. A final cleanup of the krypton fraction consisted of passage over copper oxide to combust the hydrogen and passage over heated titanium sponge and pyrophoric uranium before a direct pressure measurement was made to determine the quantity of the krypton gas recovered. This was followed by mass spectrographic analysis and krypton-85 analysis of the final fraction. By this technique they determined that the content of krypton in air was $1.139 \pm 0.01 \times 10^{-6}$ by volume. The standard deviation of nine analyses was $\pm 0.7\%$ with a total spread of 2.5%. The time required for one analysis was three days. It is of interest to note that this technique is very similar to the techniques used subsequently by other laboratories for atmospheric krypton-85 analyses.

In a detailed study of the transport and global distribution of krypton-85, Pannetier (1968) used a concentration technique utilizing the adsorption of krypton onto molecular sieve. Four columns of 5A molecular sieve were used. About four meters of air were passed through the first column containing two kilograms of sieve at ambient temperature to remove carbon dioxide and water vapor. The air was adsorbed onto a second trap of 1.5 kg of sieve at liquid oxygen temperature. This retained about 140 liters of air and all of the rare gases except helium. The second column was desorbed at 300°C, and transferred with dry nitrogen to a third column containing 0.5 kg of sieve at liquid oxygen temperature. This operation was repeated, and the air transferred to a fourth column which was the same as column three. The desorption from the fourth column yielded 2 to 3 ml of krypton in several liters of air. The yield for the recovery of krypton through this operation, as determined by mass spectroscopy, ranged from 30-80%. The final purification of the krypton was performed by passing the air through a furnace containing zirconium-titanium alloy at 500°C. Krypton was collected in a small U-tube containing activated charcoal for transfer of the gas to a proportional counter. The activity of krypton in France in 1964 was measured to be about 15 dpm/ml of krypton utilizing this technique.

Reist, *et al.*, (1968) investigated methods of increasing the sensitivity of krypton-85 monitoring by concentrating the krypton onto an activated charcoal cannister at -78.5°C. The cannister contained 590 ml of charcoal. The gas in the cannister was desorbed and passed through a 2.8-liter ion chamber. It was found that the method produced an average concentration factor of 12.9 for the gas desorbed from the cannister as compared to the concentration of the input air. A sensitivity of about 10^{-8} μCi/ml could be made using a 2.8-liter ion chamber directly, and with this concentration process a sensitivity of about 10^{-9} μCi/ml could be attained.

Sax, *et al.*, (1969) measured the concentration of krypton-85 in air at several locations in New York State over the period 1967-1968. Their analytical technique consisted of the collection of up to three cubic meters of air in plastic bags, or directly into a 5A molecular sieve trap immersed in liquid nitrogen. The sample was transferred to a charcoal trap cooled with liquid nitrogen. The sample was fractionally desorbed from the charcoal trap with all but the last 100 ml of sample being discarded. This step resulted in less than one percent loss of the krypton-85 in the sample. Oxygen was added to subsequently combust the traces of methane in the sample; the carbon dioxide and water was removed from the gas stream with a liquid nitrogen trap. Excess oxygen was removed with a hot copper furnace, and nitrogen was removed with liquid lithium at 300°C. The final gas fraction consisted of 2-3 ml of gas containing more than 90% pure krypton. Their measurements indicated that the concentration of air in New York was about 11 pCi/ml^3 of air.

Stevenson, *et al.*, (1971) developed a technique to analyze krypton-85 in air that did not require high-temperature gas-metal reactions. Their procedure utilized an air sample of one cubic meter which was transferred to a charcoal trap at liquid nitrogen temperature after passage through a trap of 13X molecular sieve to remove carbon dioxide and water. A pressure differential of one-half atmosphere was maintained across the charcoal trap to remove oxygen and nitrogen, and thus prevent the condensation of liquid air in the trap that could create a potential explosion hazard. The temperature of the charcoal trap was raised with a dry ice acetone bath, and the trap was purged with helium to remove most of the oxygen and nitrogen. The effluent from the trap was monitored with a thermal conductivity cell. The remaining gas from the trap was transferred to a 150-cm long column containing 5A molecular sieve at liquid nitrogen temperature. A flow of helium was established through the column, and the temperature of the column raised to -15°C, the effluent being monitored by a thermal conductivity cell. The first fraction to be eluted was the remaining portion of oxygen and argon which was discarded. Krypton was the next fraction to appear and was transferred to a second 150-cm molecular sieve column. The krypton fraction was followed closely by the nitrogen and methane fractions, which were discarded. Elution from the second column was performed in the same manner

with the final traces of oxygen, nitrogen, and methane being discarded. After transfer of the krypton to a miniature charcoal trap, the krypton was expanded into a known volume where pressure measurements were made to determine the volume of krypton gas recovered. The yield determination was made based on the recovery of the 1.14 ppm of krypton in the atmospheric air sample. Sample analysis up to the point of counting requires about three hours.

Cummings, *et al.*, (1971) utilized a similar technique to that of Stevenson's. The major difference in this technique was the use of krypton-83m as an internal standard. Krypton-83m is produced by a krypton-83m generator which has been described by Moghissi, *et al.*, (1971). Krypton-83m, which has a 1.86-hour half-life, is a daughter product of rubidium-84. A known amount of krypton-83m was added to the air sample, and the yield determined by measuring the krypton-83m activity in the final fraction. After decay of the krypton-83m, the krypton-85 activity was measured. This procedure provides a yield determination on each sample without requiring an accurate volume measurement of the final fraction or knowing the purity of the final fraction. Their technique utilized one 345-cm column of 5A molecular sieve for chromatographic separation of the gas fractions, and combined a furnace containing titanium sponge to remove the final traces of nitrogen. Yields of 80-90% were attained by this technique.

The analytical methods described above consist of similar combinations of concentration and purification techniques which can quantitatively measure krypton-85 in air. Basically, the techniques utilize a 1-3 m^3 sample of air with a recovery of krypton of approximately 50-90% which will produce 0.5-2 ml of krypton gas that can subsequently be counted in a low-level counting device. Other similar analytical techniques have been developed. The ones described here give a cross-section of the analytical techniques that have been and are being used for measuring krypton-85 and other krypton isotopes in air.

3. Counting Techniques.

a. External Gas Counting.

Gas envelope G-M tubes can be used for counting krypton-85 at higher activity levels. These provide a fixed geometry so that the activity of the krypton-85 gas can be accurately measured. Tubes of this type are commercially available, and consist of a central glass walled G-M tube with a thickness of 30 mg/cm^2. This is surrounded by a glass envelope with a volume of 3-10 cm^3, and provides a counting efficiency of 5-20%. With these counting tubes, activities of 100-200 dpm per ml STP can be accurately measured.

b. Internal Gas Counting.

For low-level counting, internal gas counters have been extensively used for counting krypton-85 as well as other radionuclides such as tritium and carbon-14 in gaseous form. For a detailed description of such counting systems, one is referred to standard texts on radiation counting. Counters utilizing both Geiger and proportional regions have been utilized. Proportional counters seem to be used more often since lower backgrounds can be obtained by discriminating against pulses produced by interferences of both high- and low-energy. For low-level work such counters utilize an anti-coincidence guard counter. Schroder, *et al.*, (1971) used a proportional counter with a sensitive volume of 11 cm^3 surrounded by a lead shield 10 cm thick, and a plastic scintillator for an anti-coincidence counter. Pannetier (1968) used a proportional tube with a volume of 1175 cm/m^3 surrounded by 36 G-M tubes as an anti-coincidence guard. Large volume tubes are not needed since the volume of gas to be counted is usually only a few milliliters. The shield consisted of 8,000 kg of lead brick and 60 kg of mercury. The filling gas was a mixture of argon and methane. This counting system had a background of 3.9 cpm and an efficiency of 78.5 percent. With the proper selection of counting gases, electronic circuitry and shielding, high-efficiency low-background gas counters can be constructed to meet krypton-85 counting requirements.

c. Scintillation.

Scintillation counting has been a popular method for counting krypton-85. The size of the sample to be counted is usually small. The efficiency and background considerations of these counters are good, sample preparation is simple, and samples can be stored for a sufficient period for recounts. Horrocks (1964) studied the application of liquid scintillation counting of krypton-85 and other gases. He used a toluene base liquid scintillator in which noble gases have a high solubility. Various containers and pressures were investigated to determine quenching effects and efficiencies. Curtis, *et al.*, (1966) reported a method which utilized a commercially available liquid scintillation spectrometer with polyethylene counting vials and a toluene based cocktail. The technique utilized counting vials sealed with rubber serum stoppers. This limited the amount of gas that could be added to about one ml at STP, and also allowed some krypton to escape from the scintillation solution thus reducing precision. Schuping, *et al.*, (1969) developed a technique that utilized a toluene base, liquid scintillation solution; however, the apparatus used for preparing and counting the samples was different from those described previously. Luer fittings were fused to 25-ml counting vials constructed of borosilicate glass. After filling the vials to 400-600-mm pressure, with the stopcock attached, de-aerated scintillation liquid was added with a 50-ml luer-type syringe with stopcock attached. After the entire vial was filled, it was capped. The luer fittings and plastic valves provided an excellent vacuum seal. A

counting efficiency of 92%, and a background of 25 cpm, could be obtained with a commercially available scintillation counter. Cohen, *et al.*, (1968) used liquid scintillation for measuring krypton-85 and tritiated water in studies of re-aeration rates in streams. The krypton-85 dissolved in water was measured utilizing the dioxine base scintillation solution. A counting efficiency of approximately 56% for krypton was obtained when counting tritium and krypton-85 simultaneously with a 2-ml sample size. Sax, *et al.*, (1968) used plastic scintillator shavings contained in a glass-type vial to measure krypton-85 activity. Vials were made from 12-mm borosilicate glass approximately 40-mm long, sealed at both ends with neoprene septums, and containing 20-40 mesh scintillation plastic shavings. The void volume of the vials was about 1.5 ml, and the counting efficiency about 94%. This counting technique, with associated separation technique, enabled the investigators to measure krypton activity down to one pCi/m^3 air.

SUMMARY

In summary, numerous methods have been developed to measure krypton-85. Instruments are available to measure high concentrations by direct counting, and ambient levels can be measured by a variety of separation, concentration, and counting techniques.

REFERENCES

Bowman, C. R., E. W. Chew, and A. E. Dales,(1973), *On-Line Monitor for Natural Gas from Nuclear Stimulation*, Tritium, Messenger Graphics, Las Vegas, p 548, CONF-710809.

Cochran, J. A., D. G. Smith, P. J. Magno and B. Shleien, (1970), *An Investigation of Airborne Radioactive Effluent from an Operating Nuclear Fuel Reprocessing Plant*, U. S. Dept. of HEW, Public Health Service, Bureau of Radiological Health, BRH/NERHL 70-3.

Cohen, J. J., J. L. Setser, W. D. Kelley and S. D. Shearer, Jr.,(1968), *Analytical Determination of Tritium and Krypton-85 in Aqueous Samples by Liquid Scintillation Techniques.* TLNTA, Vol. 15, p 233.

Cook, G. A.(1961). *Argon, Helium and the Rare Gases*, Interscience Publishers.

Cummings, S. L., R. L. Shearin, and C. R. Porter(1971), *A Rapid Method for Determining Krypton-85 in Environmental Air Samples.* Proceedings of the International Symposium on Rapid Methods for Measurement of Radioactivity in the Environment, IAEA.

Curtis, M. L., S. L. Ness and L. L. Bentz,(1966), *Simple Technique for Rapid Analysis of Radioactive Gases by Liquid Scintillation Counting.* Anal. Chem., Vol. 38, p 636.

Curtis, M. L. and H. L. Rook(1964), *Improved Techniques for Routinely Counting Low-Levels of Tritium and Krypton-85.* Anal. Chem., Vol. 36, p 2047.

Glueckauf, E. and G. P. Kitt(1956), *The Krypton and Xenon Contents of Atmospheric Air.* Proceedings of the Royal Society of London, p 234, p 557.

Horrocks, D. L. and M. H. Studier,(1964), *Determination of Radioactive Noble Gases with a Liquid Scintillator.* Anal. Chem., Vol. 36, p 2077.

Johns, F. B. and R. E. Jaquish,(1970), *Gas Analysis Capabilities of the Southwestern Radiological Health Laboratory.* Southwestern Radiological Health Laboratory, SWRHL-91.

Ludwick, J. D., J. J. Lushock, R. E. Conally and P. W. Nickola,(1968). *Automatic Real Time Air Monitoring of Krypton-85 Utilizing the 4096 Memory of a Multiparameter Analyzer.* Review of Scientific Instruments, Vol. 39, p 853.

Moghissi, A. A. and H. B. Hupf(1971), *A Krypton-83m Generator.* Int. J. Appl. Radiat. Isotope., Vol 22, p 218.

Momyer, Jr.(1960), *The Radiochemistry of the Rare Gases.* National Academy of Sciences, NAS-NS 3025.

Pannetier, R.,(1968), *Distribution, Atmospheric Transfer and Balance of Krypton-85* (Thesis) CEA-R-3591, translated by E. R. Appleby, Battelle Northwest, BNWL-TR-34.

Reist, P. C. and D. G. Smith(1968), *Low Level Monitoring of Krypton-85 in Air.* USAEC Report NYO-841-13.

Sax, N. I., J. D. Denny and R. R. Reeves, (1968), *Modified Scintillation Counting Technique for Determination of Low-Level Krypton-85.* Anal. Chem., Vol. 40, p 1915.

Sax, N. I., R. R. Reeves and J. D. Denny(1969), *Surveillance for Krypton-85 in the Atmosphere.* Radiol. Health Data Rep., Vol. 10, p 99.

Schroder, J., K. O. Munnick and D. H. Ehhalt(1971), *Krypton-85 in the Troposphere.* Nature, Vol. 233, p 614.

Shapiro, J., R. E. Yoder and L. Silverman(1963), *Limits of Sensitivity in the Monitoring of Radioactive Gases with Particular Reference to Krypton-85.* Proceedings of the 8th AEC Air Cleaning Conference, USAEC Report TD-7677, pp 317-329.

Shuping, R. E., C. R. Phillips and A. A. Moghissi,(1969), *Low Level Counting of Environmental Krypton-85 by Liquid Scintillation.* Anal. Chem., Vol. 41, p 2082.

Smith, D. G., J. A. Cochran, and B. Shleien(1970), *Calibration and Initial Field Testing of Krypton-85 Detectors for Environmental Monitoring.* U. S. Dept. of HEW, Public Health Service, Bureau of Radiological Health, BRH/NERHL-70-4.

Smith, D. G., P. C. Reist and L. Silverman(1967a), *A Review of Detection Sensitivity for Monitoring of Krypton-85.* USAEC Report NYO-841-5.

Smith, D. G., P. C. Reist and L. Silverman,(1967b), *Increased Detection Sensitivity for Krypton-85.* Proceedings of the 9th AEC Air Cleaning Conference, USAEC Report CONF-600904, 2: pp 781-798.

Stevenson, D. L. and F. B. Johns(1971), *A Separation Technique for the Determination of Krypton-85 in the Environment.* Proceedings of the International Symposium on Rapid Methods for Measurement of Radioactivity in the Environment, IAEA.

TABLE 1. Comparative Krypton-85 Levels.

	μCi/ml
Ambient Air (Northern Hemisphere, 1973)	2×10^{-11}
Fuel Reprocessing Plant (several km from plant following fuel dissolution)	10^{-7}
Effluent of Fuel Reprocessing Plant (during fuel dissolution)	10^{-3}
Natural Gas (Project Rulison)	10^{-4}
Radioactivity Concentration Guide (10 CFR20 Table II)	3×10^{-7}

TABLE 2. Lowest Concentration of Krypton-85 Which Can Be Monitored by Various Detectors (From Shapiro, *et al.*, 1963).

Detector	Level (μCi/ml)
2.8-liter ion chamber, current reading	2.5×10^{-7}
2.8-liter ion chamber, rate of charge	1.3×10^{-7}
Kanne chamber, current reading	2.0×10^{-7}
Pressurized ion chamber, current reading	0.6×10^{-7}
Pressurized ion chamber, rate of charge	0.3×10^{-7}
Cylindrical G-M tube, in infinite volume	0.5×10^{-7}
Solid state or thin scintillation detector, with cosmic-ray guard counter	0.1×10^{-7}

TABLE 3. Physical Properties of Krypton.

Atmospheric abundance (volume %)	1.14×10^{-4}
Boiling Point (°C)	-153
Melting Point (°C)	-157
Atomic diameter in crystal (angstroms)	3.94

INTEGRATED ENVIRONMENTAL MODELING SYSTEM FOR NOBLE GAS RELEASES AT THE SAVANNAH RIVER PLANT*

R. E. Cooper
Environmental Analysis and Planning
Savannah River Laboratory
E. I. du Pont de Nemours & Co.
Aiken, South Carolina 29801

Abstract

The Savannah River Plant (SRP) is a large nuclear complex engaged in varied activities and is the AEC's major site for the production of weapons material. As a result of these activities, there are continuous and intermittent releases of radioactive gases to the atmosphere. Of these releases, the noble gases constitute about 11% of the total man-rem exposure to the population out to a distance of 100 km.

Although SRP has an extensive radiological monitoring program, an environmental modeling system is necessary for adequately estimating effects on the environment. The integrated environmental modeling system in use at SRP consists of a series of computer programs that generate and use a library of environmental effects data as a function of azimuth and distance. Annual average atmospheric dispersion and azimuthal distribution of material assumed to be released as unit sources is estimated from a 2-year meteorological data base — assuming an arbitrary point of origin. The basic library of data consists of: (1) ground-level concentrations according to isotope, and (2) whole body gamma dose calculations that account for the total spatial distribution at discrete energy levels. These data are normalized to tritium measurements, and are subsequently used to generate similar library data that pertain to specific source locations, but always with respect to the same population grid. Thus, the total additive effects from all source points, both on- and off-site, can be estimated.

The final program uses the library data to estimate population exposures for specified releases and source points for the nuclides of interest (including noble gases). Multiple source points are considered within a single pass to obtain the integrated effects from all sources.

The total man-rem exposure to the local population out to 100 km resulting from SRP operation is about 0.4% of that received from natural activity. The noble gases contribute about 11% of this fraction. Current efforts at SRP are directed toward improving the above methods, and toward applied research to develop, verify, and use techniques reliable out to several 100 km and beyond.

SITE DESCRIPTION

The Savannah River Plant (SRP) is a large nuclear complex located in the southeastern United States near Aiken, S. C. (Figure 1). The plant occupies an area (roughly circular in shape) of about 300 square miles and is the major producer of weapons material for the U. S Atomic Energy Commission. Activities at SRP are varied (Figure 2). Nuclear materials are produced by the transmutation of elements in large nuclear reactors that are moderated and cooled by heavy water. Support operations include heavy water extraction, nuclear fuel and target fabrication, separation of nuclear products from radioactive byproducts, and waste management.

The SRP site is shown in more detail in Figure 3. The major nuclear operations are performed at facilities located well within plant boundaries, thus providing large exclusion distances (>8 km) between these operations and the plant boundary. In addition to SRP operations, there are two planned commerical nuclear operations immediately adjacent to the plant site. The Barnwell Nuclear Fuel Plant to the east of SRP is being built on a site of about 2,500 acres that was originally part of SRP, and was subsequently deeded to Barnwell County. The Vogtle Nuclear Power Plant on the southwest boundary across the Savannah River from SRP is to be built by Georgia Power Co. The Barnwell Plant will have the capability of processing 1,500 metric tons of fuel per year, and the Vogtle Plant will have twin units each having a generating capacity of 1,100 MW(e). Each of these facilities is expected to have potential releases that will be significant with respect to SRP releases. Therefore, an assessment of total man-rem exposure to the local population from nuclear operations needs to account for these and possibly other facilities.

ATMOSPHERIC RELEASES

Radioactive atmospheric releases from SRP operations are shown in Table 1 as a percent of total curies released on an annual basis. Noble gases are about 51.7% of the total source term, and tritium makes up about 48.3%. There is much less than 1% to be distributed among the remaining isotopes. The actual contribution to man-rem dose is very different from this distribution as is shown later.

**The information contained in this article was developed during the course of work under Contract AT(07-2)-1 with the U.S. Atomic Energy Commission.*

ENVIRONMENTAL MONITORING

Environmental monitoring has been an integral part of plant operations since the very beginning of activities at SRP. Extensive monitoring was performed before any plant activities that resulted in radioactivity releases and has continued and increased in scope and efficiency over the years. Monitoring activities were necessary before plant operations to gain knowledge of the environment that would enable subsequent estimates of the effects of SRP operations. Continued monitoring efforts on- and off-site are designed to assure that the amounts of radioactivity released to the environs are such that guideline values of concentrations are not exceeded. That assurance becomes more important when it is applied to a shared nuclear environment, as the region containing SRP is rapidly becoming. This point is made clear by observing the various nuclear installations indicated in Figure 4 that will be contributing radioactivity in the general area.

MODELING REQUIREMENT

Although SRP does have an extensive radiological monitoring program, assessment of the total environmental effect of radioactive releases is difficult for two reasons: (1) a monitoring network designed to adequately define the exposures to populations as a function of azimuth and distance out to 100 to 150 km would be prohibitively expensive, and (2) much of the SRP contribution to environmental radioactivity would be below background, and probably below the threshold of detectability. Therefore, total environmental effect must be based on a knowledge of what is being released and the subsequent dispersion to the environs. The environmental model currently in use at SRP was designed to provide this capacity.

MODELING SYSTEM OVERVIEW

The SRP environmental model is shown diagrammatically as Figure 5. The first objective in the model was to obtain a library of data that represented annually averaged azimuthal and radial distributions of released material. Atmospheric releases at SRP are generally such that they may be treated as continuous releases when performing annual dose calculations.

Two kinds of distributions were obtained, air concentrations at ground-level for each isotope considered and whole body dose estimates for discrete gamma energies resulting from spatially distributed sources.

The meteorological data (Cooper and Rusche, 1968) were obtained from measurements on a tower located approximately 30 km from the geometric center of the SRP area. For modeling purposes the data obtained are assumed to apply to any release point of interest within the general area, including off-site release points. The first phase of library construction leaves the emission point undefined. The second phase relates calculated distributions to specific emission points.

Annually averaged air concentrations are estimated individually for each isotope by processing the meteorological data, assuming a unit release (1 Ci) for each data period (15 minute averages), and a release height of 70 m, corresponding to the height of most SRP radioactive releases. Ground-level concentrations are accumulated as a function of azimuth and radial distance out to about 300 km from an arbitrary origin. The azimuth was divided into 16 equal sectors of 22.5° each. After all the meteorological data for the two-year period are processed, the accumulated concentrations at each point are divided by the total number of data periods represented. The result is a quantity to be associated with each grid point that represents a yearly integrated concentration, assuming a unit curie release over the year. These quantities are corrected for decay according to isotope and the measured meteorology for each data period.

Whole body dose calculations are performed by processing the meteorological data in a similar manner. However, the calculations are significantly more complex because the gamma dose to a receptor may be strongly dependent on the total spatial distribution of the emitting material about the receptor, and not necessarily related to ground-level concentration. To minimize computations, and at the same time to have a library of data covering the normally encountered spectrum of gamma energies, parameters for discrete gamma energies were calculated instead of those for individual isotopes. Also, multiple energies from individual isotopes can be efficiently utilized in later calculations. Since the gamma calculations are isotope-independent, the library data are uncorrected for decay, but a correction is made when the data are utilized as is later described. The gamma calculations are performed with the aid of EGAD (Cooper, 1972) a computer code developed at SRP for that purpose. As before, the calculations are normalized to a unit curie release of discrete gamma energies of 0.01 through 5.0 MeV.

At this point the library consists of isotope and gamma energy data, assuming an arbitrary point of origin. The data are also calculated for a much coarser grid than that of Figure 6 because distances out to 300 km are represented. To facilitate man-rem calculations, the library data are reprocessed to relate the data to a specific population grid. In this processing, each source that is to be treated separately is assumed to be the origin of material distributions, and a fixed population grid (Figure 6) is exposed. Thus, a new library is constructed that contains annually averaged data that are source specific, but always with respect to the same fixed population grid.

Man-rem calculations are performed by processing the library data for each source point and release magnitude. Multiple source points may be considered within a single pass to estimate total man-rem exposure

from sources that may be separated by large distances. In addition, multiple gamma energies may be input for individual isotopic species. At this point, decay corrections are applied to the gamma calculations. Some of the isotopes being considered from each source point, particularly tritium and ^{85}Kr, can be assumed to have infinite half-lives over the time intervals of interest; i.e., transport times out to a distance of a few 100 km. For any particular isotopic species whose decay is significant, a decay correction for each grid point is simply determined as the ratio of ground-level concentrations with respect to a long-lived isotope from the same source.

The SRP program considers many atmospheric pathways to man as indicated by Figure 7. All pathways have dose conversion factors that allow all dose calculations except whole body gamma doses to be relative to estimated ground-level concentrations as contained in the library data. The dose conversion factors represent lifetime (70-year) dose commitments from annual releases to each pathway. Therefore, all dose rates given in this report imply annual total dose commitment rates.

A summary of the basic features of the SRP environmental model are given in Table 2.

CALCULATIONAL PROCEDURES

Library data were obtained by processing meteorological data, assuming a unit release (1 curie) for each data interval. The meteorological data assumptions were: (1) the data were site independent; i.e., they could be applied equally to sites widely spaced within a radius of 100 to 200 km about the point of measurement; (2) directional persistance was assumed for a time period sufficient to transport the material to the extremities of the calculational grid; and (3) no precipitation scavenging was assumed. Although precipitation scavenging is not included in the model, it is empirically treated for iodine by adjusting the dose conversion factor of iodine in milk based on measured air-to-milk concentration ratios (Marter, 1963).

1. Ground-Level Air Concentrations.

All ground-level air concentration calculations are based on a sector-averaged Gaussian plume model with a finite mixing depth imposed.

$$X/Q = \frac{2N}{(2\pi)^{3/2}\sigma_z \bar{u}\, x} \sum_{m=o}^{\infty} \left\{ \exp\left[-\left(\frac{2mH+h}{\sqrt{2}\,\sigma_z}\right)^2\right] + \exp\left[-\left(\frac{2mH-h}{\sqrt{2}\,\sigma_z}\right)^2\right]\right\} \quad (1)$$

where N = number of azimuthal subdivisions or sectors
σ_z = standard deviation of material distribution in the vertical, m
H = mixing depth, m
h = release height, m
X/Q = concentration per unit source, m^3/s
x = downwind distance
u = effective wind speed, m/s

An average mixing depth of 300 m was used in all these calculations. This value of the mixing depth provides good agreement between calculations and experimental tritium concentration measurements over 12 years, but does not imply the actual existence of an average mixing depth of 300 m. If gravitational settling is assumed, there are no ground reflections, and the plume is assumed to be tilted downward from the horizontal according to settling velocity.

$$X/Q = \left(\frac{N}{(2\pi)^{3/2}\sigma_z \bar{u}\, x}\right)\left\{\exp\left(-\frac{(h-xV_g/u)^2}{2\sigma_z^2}\right) + \exp\left(-\frac{(2H-h+xV_g/u)^2}{2\sigma_z^2}\right)\right\} \quad (2)$$

where Vg = gravitational settling velocity, m/s

Where chemical dry deposition is assumed, as for iodines, Equation 1 must be modified to account for depletion. Chemical dry deposition is generally assumed to result in plume depletion in a manner that leaves the remaining material distribution unaltered. Thus, Equation 1 must be multiplied by a fraction representing the material remaining in the plume as a function of distance. This can be accomplished by integrating total deposition out to the distance of interest to obtain the ratio of the material remaining to that from the original source. Due to the form of the integral expression, it has to be evaluated by numerical means for each new calculation. Rather than devoting a large amount of computational time in this manner, a simple approach was taken that depleted the source by radial increments. At each radial grid point of the sector, the estimated concentration is assumed to apply over an area represented by that point. The source term for each point is then determined as

$$Q'(x_i) = Q(0) - V_d \sum_{j=1}^{i-1} Q'(x_j)\, A_j, \quad i \geq 2 \tag{3}$$

where A_j = area represented by grid point j in m^2 and
$Q(0)$ = the original source which applies at the first (i=1) radial increment in each sector.

2. Whole Body Gamma Calculations.

Calculations involving gamma photon emissions are complicated by the fact that a receptor need not be near the material to receive exposure. For an elevated source under stable meteorological conditions, significant exposure (at downwind distances of several kilometers) may be received from material passing overhead. A computer program, EGAD, was developed for the specific purpose of accounting for the spatial distribution of gamma photon emissions in the geometry required for this application. The expression solved in EGAD is

$$D = \frac{Q_\gamma}{2\pi} \int_{z=0}^{H} f(z) \cdot \int_{y=0}^{\infty} \frac{G(\mu a)}{a}\, dydz \tag{4}$$

where D is related to the total integrated dose from $Q\gamma$ photons. The first integral expression represents the spatial distribution with ground and inversion reflections. The second expression, which is an analytical integration with respect to x, accounts for attenuation and buildup in air where

μ = linear attenuation coefficient for air, m^{-1}
a = distance from spatial point to receptor $= \sqrt{x^2 + y^2}$, m

This program was used to generate the gamma library for incremental gamma energies from 0.01 to 5 MeV.

3. Library Data Translation.

The initial library data as compiled by sector and radial distance are not specific to any location as indicated earlier. The population distribution (Figure 6) has as its origin the geometric center of SRP. The operations at SRP that are responsible for the most significant emissions are located sufficiently near this population distribution origin to assume coincidence with a resulting small error from geometry effects in population exposure estimates. Therefore, only the distance has to be interpolated so that the initial library data can be applied to the population grid, and the SRP contribution to population exposure can be determined. However, for other emission sites, both distance and azimuthal angle must be interpolated. For reasonable accuracy, each sector was further subdivided according to Figure 8. A translator computer program requires only two parameters, r and θ, as input, where r is the distance from emission site to population grid origin, and θ is the angular direction. Population data for each subregion of the population grid were included in the translator program to collapse the calculations at each radial distance on the population grid into a single value

$$C_{ij} = \sum_{k=1}^{N} C_{i,j,k}\, P_{i,j,k} \tag{5}$$

where $C_{i,j,k}$ are the calculated results after data translation for sectors i, radial increments j, and azimuthal subdivisions k at the j_{th} radial distance. The $P_{i,j,k}$ are the corresponding populations. This procedure reduces the number of subsequent calculations required for man-rem estimates.

The translation procedure generates a set of library data (ground-level concentrations and gamma calculations) that are specific to the site being considered. The data are coded by site, isotope, sector, and radial increment for ground-level concentrations and by site, gamma energy, sector, and radial increment for gamma calculations.

4. Man-Rem Calculations.

Population exposures are estimated by processing the library data generated above with respect to specified emission data. The data are processed by a computer program that requires as input the isotope code number, yearly emission rate in curies, the associated gamma energies, and the fractional yields of each energy.Because no distinction is made with respect to site — except in the isotope code number, the program can treat multiple sites. The program also has the population data built in to maintain simple input requirements. The population distribution within each subdivision of Figure 6 is assumed to be homogeneous, and dose rates estimated at the center point of each subdivision are assumed to apply over the entire region.

Output from the code is under option control with the exception of input information and two summary sheets. The available output is tabulated in Table 3. The first summary sheet (Table 4) provides man-rem estimates cumulative by isotope, sector, and radius, so that the dose estimates presented for the maximum distance represent the total exposure out to that distance. The second summary sheet (Table 5) provides estimates of population dose and individual dose rates according to isotope and totals for all isotopes.

5. Man-Rem Estimates.

Although many interesting results are obtained from the above calculational procedures, only the most significant are presented here for discussion. All dose estimates presented pertain only to SRP operations. Man-rem estimates based on the population distribution out to 100 km (Figure 6) are given in Table 6. These values are cumulative by sector and radius, and, therefore, represent the total SRP annual contribution to population dose — assuming 1972 releases to be representative. Critical organ doses are given where there was any appreciable difference from the total body dose. These doses reflect significant contributions to organ doses in excess of total body dose by particular isotope groups as listed. Only about 7% of the total thyroid exposure results from iodines. Noble gases and tritium account for the remainder.

A more-detailed listing of releases by isotope group is given in Table 7, which compares source and dose contribution on a percentage basis. The noble gases, which consist of 51.7% of the release inventory in curies, yield almost 100% of the whole body gamma exposure and only 10.8% of total body exposure. Tritium is the major total body exposure contributor, with 89.2% of the total.

Noble gas releases are presented in more detail in Table 8. Although ^{85}Kr constitutes about 71.8% of the noble gas source term, the contribution to whole body gamma dose within 100 km is less than 2% of the total.

The estimated dose rates resulting from annual releases from SRP operations are shown in Table 9. The maximum plant perimeter dose rate in any sector is 2.25 mrem with an average of 1.62 mrem. At a distance of 100 km, the dose drops to 0.22 mrem. These values are compared to background estimates as shown. At the maximum plant perimeter dose (2.25 mrem), the SRP contribution is about 1.9% of total annual natural background, and about 1.0% of total background — including medical and weapons fallout contributions. The overall average within the 100-km radius (0.49 mrem) is about 0.42% of natural activity.

CONTINUING PROGRAM

Efforts to properly evaluate population exposures caused by SRP operations are being continuously updated. Although the results presented here assume validity of the calculational techniques out to distances of 100 km and beyond, such an assumption is based on convenience instead of experimental verification. An extensive program directed by T. V. Crawford is currently in progress that is aimed at improving the methods of estimating environmental effects. This program will also seek to extend applications out to several hundred kilometers through applied research in model development and verification.

REFERENCES

Cooper, R. E. (1972), *EGAD — A Computer Program to Compute Dose Integrals from External Gamma Emitters.* USAEC Report DP-1304, E. I. du Pont de Nemours & Co., Savannah River Laboratory, Aiken, S. C.

Cooper, R. E. and B. C. Rusche (1968), *The SRL Meteorological Program and Off-Site Dose Calculations.* USAEC Report DP-1163, E. I. du Pont de Nemours & Co., Savannah River Laboratory, Aiken, S. C.

Marter, W. L. (1963), *Radioiodine Release Incident at the Savannah River Plant.* Health Physics 9, 1105.

TABLE 1. Annual Radioactive Releases to Atmosphere from SRP Operations.

Isotope Group	Curies Released	% of Total Curies
Tritium	7.8×10^5	48.3
Halogens	2.7	$\ll 1$
Noble Gases	8.4×10^5	51.7
Particulates	8.0	$\ll 1$

TABLE 2. Summary of Environmental Modeling Features.

1. Modular structure
2. Dual data libraries
   (a) Site independent
   (b) Site dependent
3. Library data translator
4. Isotope-independent gamma library
5. Multiple site representation

TABLE 3. Output Available from Environmental Model.

1. Population distribution
2. Tabulation of input data
3. Optional isotopic data for all pathways for 20 radial increments out to 100 km
   (a) By individual sector and radial increment
   (b) By individual sector and cumulative by radial increment
   (c) Cumulative by both sector and radial increment
4. Summary I — Population doses cumulative for all isotopes
5. Summary II — Cumulative 100-km population doses by individual isotopes and dose rates at selected distances
6. Dose rates for selected pathways by sector and radial increment cumulative over all isotopes

TABLE 4. Doses Accumulative by Isotope, Sector, and Radial Increment, man-rem.[a] (Totals for All Isotopes)

Distance, km	Whole Body Gamma Dose	Total Skin Dose	Total Body Dose	Critical Organ Dose					
				Bone	Lung	Thyroid	Kidney	Liver	GI Tract
5	0.0	0.0	0.0	0.0	0.0	0.0	0.0	0.0	0.0
10	0.0	0.0	0.0	0.0	0.0	0.0	0.0	0.0	0.0
15	0.0	0.0	0.0	0.0	0.0	0.0	0.0	0.0	0.0
20	2.2619E 00	1.2801E 01	9.8921E 00	1.0316E 01	8.8062E 00	1.0847E 01	9.8921E 00	9.8921E 00	9.8921E 00
25	3.9639E 00	2.3753E 01	1.8348E 01	1.9060E 01	1.8371E 01	2.0100E 01	1.8348E 01	1.8348E 01	1.8348E 01
30	6.6060E 00	4.3419E 01	3.3514E 01	3.4680E 01	3.3553E 01	3.6660E 01	3.3514E 01	3.3514E 01	3.3514E 01
35	9.1074E 00	6.4613E 01	4.9869E 01	5.1519E 01	4.9924E 01	5.4447E 01	4.9869E 01	4.9869E 01	4.9869E 01
40	1.2680E 01	9.8484E 01	7.6023E 01	7.8411E 01	7.6102E 01	8.2778E 01	7.6023E 01	7.6023E 01	7.6023E 01
45	1.7921E 01	1.5557E 02	1.2009E 02	1.2361E 02	1.2021E 02	1.3037E 02	1.2009E 02	1.2009E 02	1.2009E 02
50	2.1437E 01	1.9854E 02	1.5329E 02	1.5761E 02	1.5343E 02	1.6610E 02	1.5329E 02	1.5329E 02	1.5329E 02
55	2.2925E 01	2.1874E 02	1.6889E 02	1.7355E 02	1.6905E 02	1.8285E 02	1.6889E 02	1.6889E 02	1.6889E 02
60	2.3990E 01	2.3480E 02	1.8130E 02	1.8618E 02	1.8147E 02	1.9615E 02	1.8130E 02	1.8130E 02	1.8130E 02
65	2.4665E 01	2.4564E 02	1.8969E 02	1.9472E 02	1.8986E 02	2.0511E 02	1.8969E 02	1.8969E 02	1.8969E 02
70	2.5465E 01	2.5984E 02	2.0068E 02	2.0590E 02	2.0086E 02	2.1681E 02	2.0068E 02	2.0068E 02	2.0068E 02
75	2.6061E 01	2.7161E 02	2.0979E 02	2.1515E 02	2.0997E 02	2.2649E 02	2.0979E 02	2.0979E 02	2.0979E 02
80	2.6837E 01	2.8814E 02	2.2259E 02	2.2813E 02	2.2277E 02	2.4005E 02	2.2259E 02	2.2259E 02	2.2259E 02
85	2.7349E 01	3.0010E 02	2.3186E 02	2.3753E 02	2.3205E 02	2.4985E 02	2.3186E 02	2.3186E 02	2.3186E 02
90	2.7993E 01	2.1702E 02	2.4497E 02	2.5082E 02	2.4517E 02	2.6366E 02	2.4497E 02	2.4497E 02	2.4497E 02
95	2.8506E 01	3.3173E 02	2.5639E 02	2.6238E 02	2.5658E 02	2.7565E 02	2.5639E 02	2.5639E 02	2.5639E 02
100	2.9278E 01	3.5483E 02	2.7430E 02	2.8052E 02	2.7451E 02	2.9447E 02	2.7430E 02	2.7430E 02	2.7430E 02

(a) Where E followed by a positive or negative number is the power of ten by which the number in front of E is to be multiplied.

TABLE 5. Individual and Population Dose by Isotope.[a] (Summary Data by Isotope)

	Population Dose, man-rem	Individual Whole Body Dose, mrem			Average Organ Dose At Plant Perimeter, mrem					
		Plant Perimeter		100 km						
		Average	Maximum	Average	Bone	Lung	Thyroid	Kidney	Liver	GI Tract
^{3}H	2.448E 02	1.261E 00	1.707E 00	2.123E-01	1.261E 00	1.261E 00	1.261E 00	1.261E 00	1.261E 00	1.261E 00
^{131}I	5.977E-02	4.641E-04	6.616E-04	3.296E-05	4.641E-04	4.641E-04	1.570E-01	4.641E-04	4.461E-04	4.641E-04
^{131m}Xe	3.325E-09	1.884E-11	2.613E-11	2.573E-12	1.884E-11	1.884E-11	1.884E-11	1.884E-11	1.884E-11	1.884E-11
^{131m}Xe	2.443E-02	1.449E-04	2.055E-04	1.894E-05	1.449E-04	1.449E-04	1.448E-04	1.449E-04	1.449E-04	1.449E-04
^{135}Xe	1.046E 00	8.097E-03	1.172E-02	6.007E-04	8.097E-03	8.097E-03	8.097E-03	8.097E-03	8.097E-03	8.097E-03
^{41}Ar	2.415E 01	3.131E-01	4.806E-01	6.492E-03	3.131E-01	3.131E-01	3.131E-01	3.131E-01	3.131E-01	3.131E-01
^{85m}Kr	3.094E-01	2.855E-03	4.216E-03	1.412E-04	2.855E-03	2.855E-03	2.855E-03	2.855E-03	2.855E-03	2.855E-03
^{85}Kr	4.798E-01	2.123E-03	2.952E-03	4.585E-04	2.123E-03	2.123E-03	2.123E-03	2.123E-03	2.123E-03	2.123E-03
^{88}Kr	1.660E 00	1.772E-02	2.664E-02	6.082E-04	1.772E-02	1.772E-02	1.772E-02	1.772E-02	1.772E-02	1.772E-02
^{133}Xe	1.611E 00	9.811E-03	1.393E-02	1.215E-03	9.811E-03	9.811E-03	9.811E-03	9.811E-03	9.811E-03	9.811E-03
^{90}Sr	6.856E-03	6.695E-05	8.936E-05	2.976E-06	6.188E-04	6.695E-05	6.695E-05	6.695E-05	6.695E-05	6.695E-05
^{95}Zr	1.043E-04	1.019E-06	1.360E-06	4.529E-08	1.019E-06	1.290E-05	1.019E-06	1.019E-06	1.019E-06	1.019E-06
^{103}Ru	1.235E-04	1.206E-06	1.609E-06	5.360E-08	1.206E-06	1.152E-04	1.206E-06	1.206E-06	1.206E-06	1.206E-06
^{106}Ru	4.260E-04	4.160E-06	5.552E-06	1.849E-07	4.160E-06	1.609E-03	4.160E-06	4.160E-06	4.160E-06	4.160E-06
^{137}Cs	3.359E-05	3.280E-07	4.378E-07	1.458E-08	3.280E-07	4.539E-06	3.280E-07	3.280E-07	3.280E-07	3.280E-07
Natural Uranium	3.802E-04	3.713E-06	4.955E-06	1.650E-07	3.713E-06	1.531E-04	3.713E-06	3.713E-06	3.713E-06	3.713E-06
^{239}Pu	1.855E-01	1.811E-03	2.417E-03	8.051E-05	6.180E-02	1.811E-03	1.811E-03	1.811E-03	1.811E-03	1.811E-03
^{144}Ce	8.989E-04	8.778E-06	1.172E-05	3.902E-07	8.778E-06	1.395E-04	8.778E-06	8.778E-06	8.778E-06	8.778E-06
^{60}Co	1.790E-06	1.748E-08	2.333E-08	7.770E-10	1.748E-08	1.748E-08	1.748E-08	1.748E-08	1.748E-08	2.953E-08
^{95}Nb	3.825E-05	3.735E-07	4.985E-07	1.660E-08	3.735E-07	5.467E-06	3.735E-07	3.735E-07	3.735E-07	3.735E-07
^{134}Cs	4.636E-06	4.528E-08	6.043E-08	2.013E-09	4.528E-08	4.754E-07	4.528E-08	4.528E-08	4.528E-08	4.528E-08
^{141}Ce	9.041E-07	8.829E-09	1.178E-08	3.925E-10	8.829E-09	2.222E-07	8.829E-09	8.829E-09	8.829E-09	8.829E-09
^{244}Cm	1.008E-03	9.848E-06	1.314E-05	4.378E-07	1.779E-04	9.848E-06	9.848E-06	9.848E-06	9.848E-06	9.848E-06
^{87}Cr	2.530E-04	3.382E-06	5.225E-06	6.100E-08	3.382E-06	3.382E-06	3.382E-06	3.382E-06	3.382E-06	3.382E-06
Totals	2.743E 02	1.617E 00	2.250E 00	2.219E-01	1.677E 00	1.619E 00	1.773E 00	1.617E 00	1.617E 00	1.617E 00

(a) Where E followed by a positive or negative number is the power of ten by which the number in front of E is to be multiplied.

TABLE 6. Cumulative Man-Rem Per Year Dose (1972) at 100 km by Isotope Group.

Isotope Group	Whole Body Gamma	Total Body	Critical Organ Dose in Excess of Total Body Dose			
			Skin	Bone	Lung	Thyroid
Tritium	0	244.8	0	0	0	0
Iodine-131	1	0.06	0	0	0	20.2
Noble Gases	29.3	29.3	80.4	0	0	0
Particulates	1	0.2	0	6.2	0.2	0
Total	29.3	274.3	80.4	6.2	0.2	20.2

TABLE 7. Distribution of Cumulative Man-Rem Dose Per Year (1972) at 100 km by Isotope Group.

Isotope Group	Source, % of Total Ci	%Distribution		
		Whole Body Gamma	Skin	Total Body
Tritium	48.3	0	69.0	89.2
Iodine-131	$\ll 1$	$\ll 1$	$\ll 1$	0.02
Noble Gases	51.7	100	31.0	10.8
Particulates	$\ll 1$	$\ll 1$	$\ll 1$	0.07

TABLE 8. Cumulative Man-Rem Per Year Dose (1972) from Noble Gases Out to 100 km.

Isotope	Noble Gas Source, % of Total Ci	Whole Body Gamma, %
^{41}Ar	20.35	82.48
^{85m}Kr	0.87	1.06
^{85}Kr	71.83	1.64
^{87}Kr	0.30	0.00
^{88}Kr	0.50	5.67
^{131m}Xe	0.03	0.08
^{133}Xe	4.67	5.50
^{135}Xe	1.44	3.57

TABLE 9. Annual Average Dose Rate from SRP Operations.

	Annual Dose Rate, mrem	% of Natural Activity	% of Total Background
Average at Plant Perimeter	1.62	1.4	0.7
Maximum at Plant Perimeter	2.25	1.9	1.0
100 km Radius	0.22	0.2	0.1
Overall Weighted Average	0.49	0.4	0.2

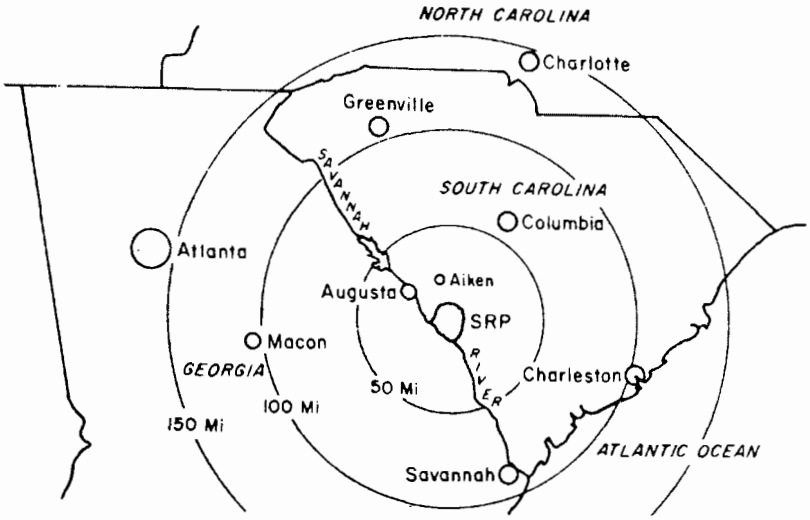

Figure 1. Location of SRP Relative to Surrounding Population Centers.

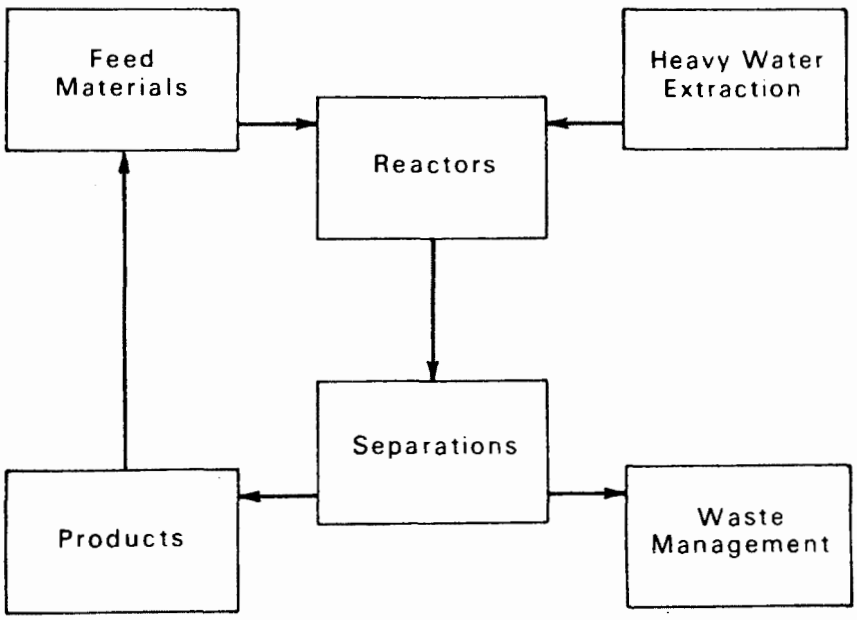

Figure 2. The Savannah River Production Complex.

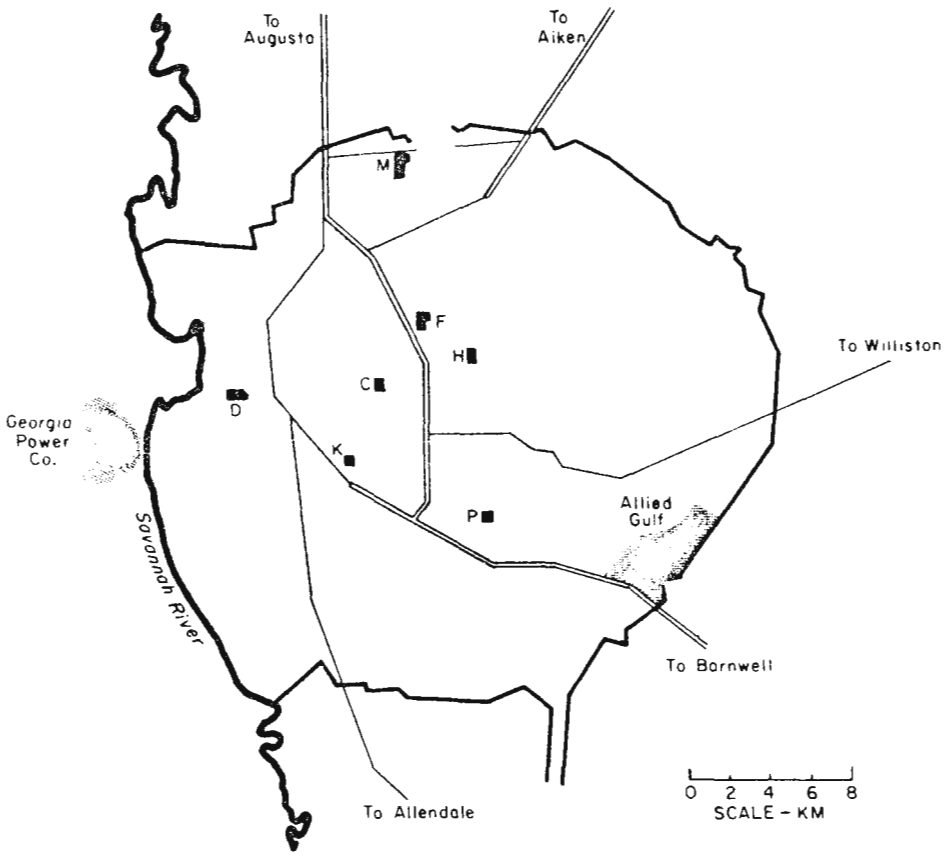

Figure 3. The Savannah River Plant Site.

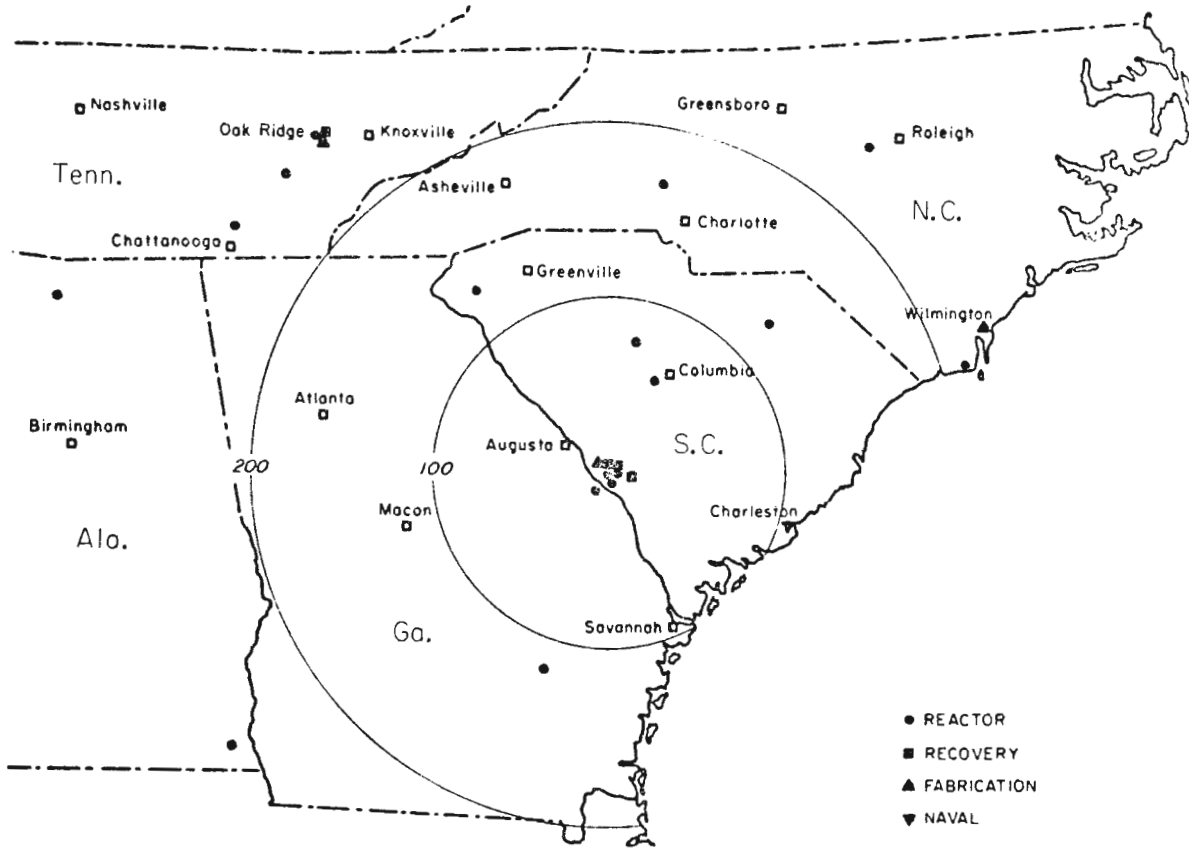

Figure 4. Southeast Nuclear Industry.

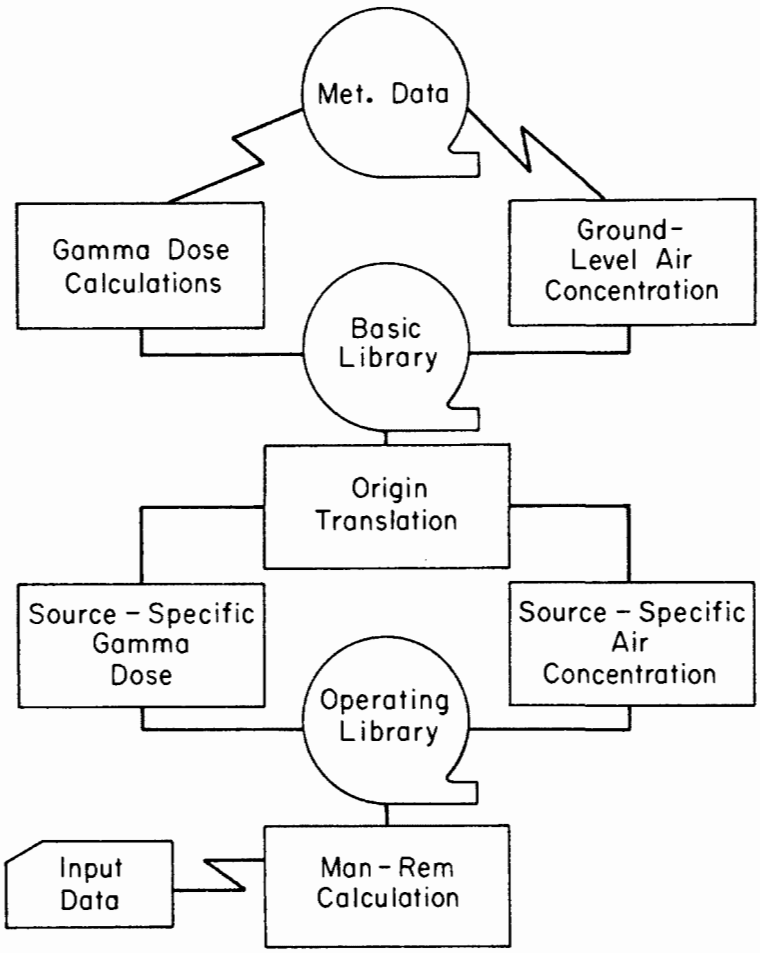

Figure 5. Man-Rem Calculation Procedures.

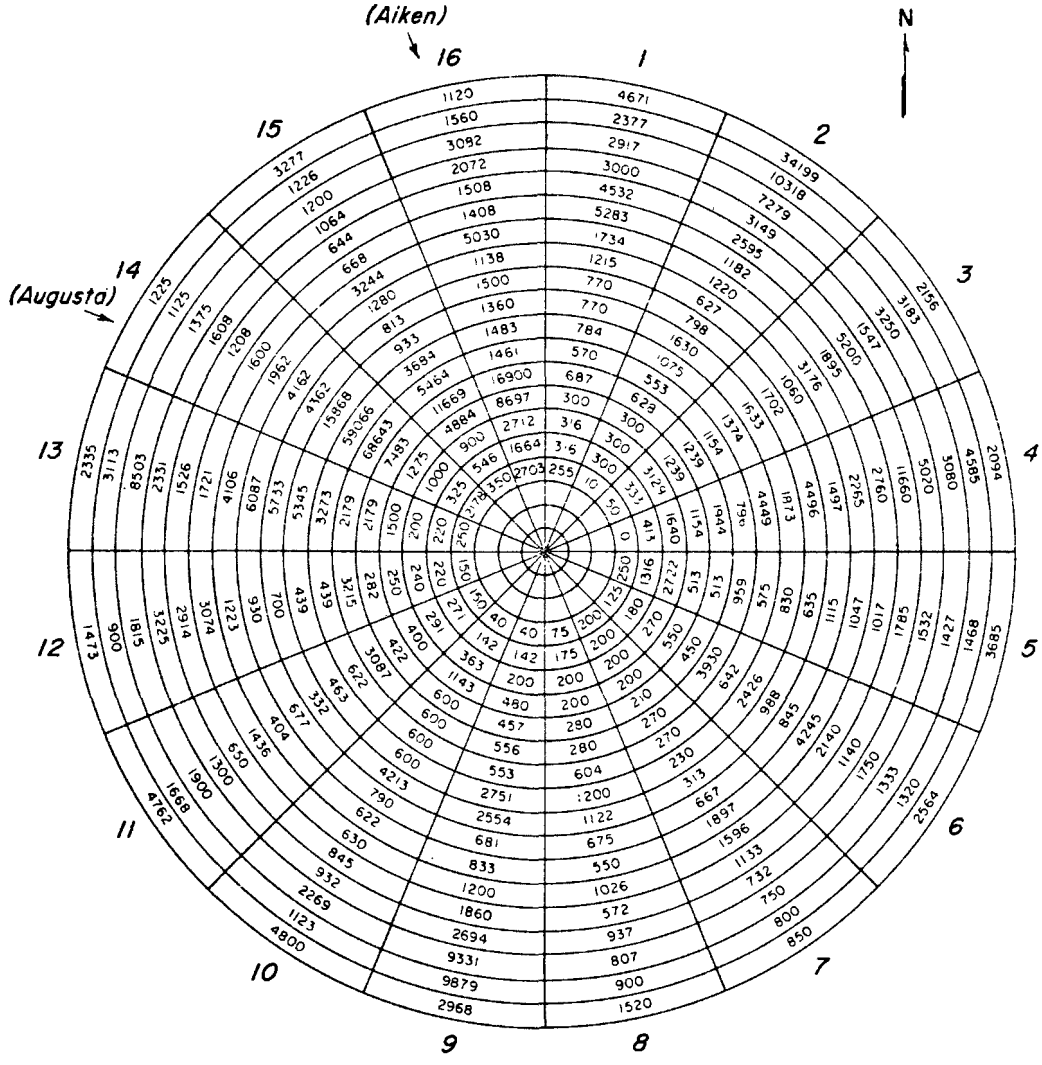

Figure 6. Distribution of Population in Region Surrounding the Plant (Radial Increments = 5 km, 22.5° Sector) 1970 Census.

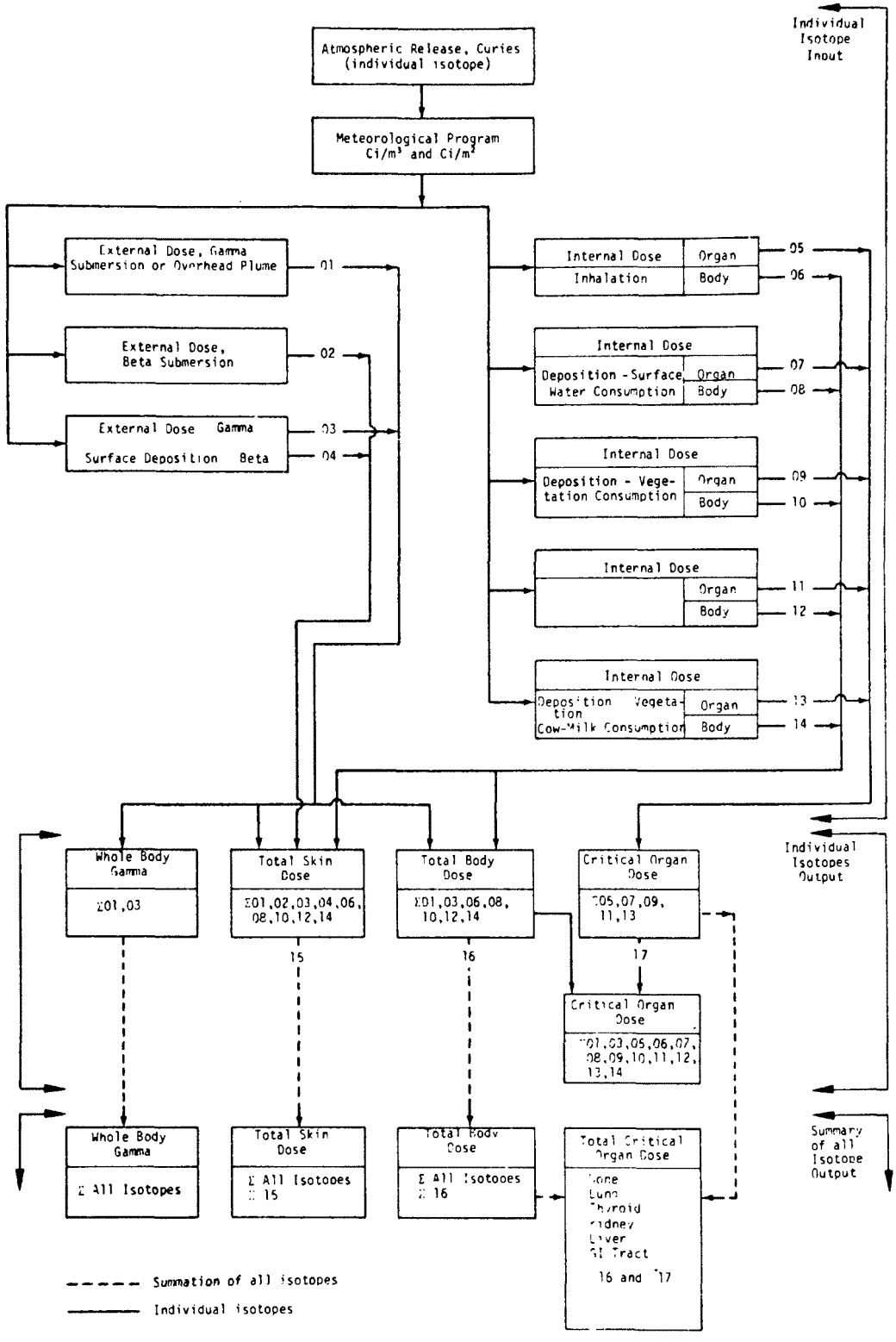

Figure 7. Pathways to Man From Atmospheric Releases.

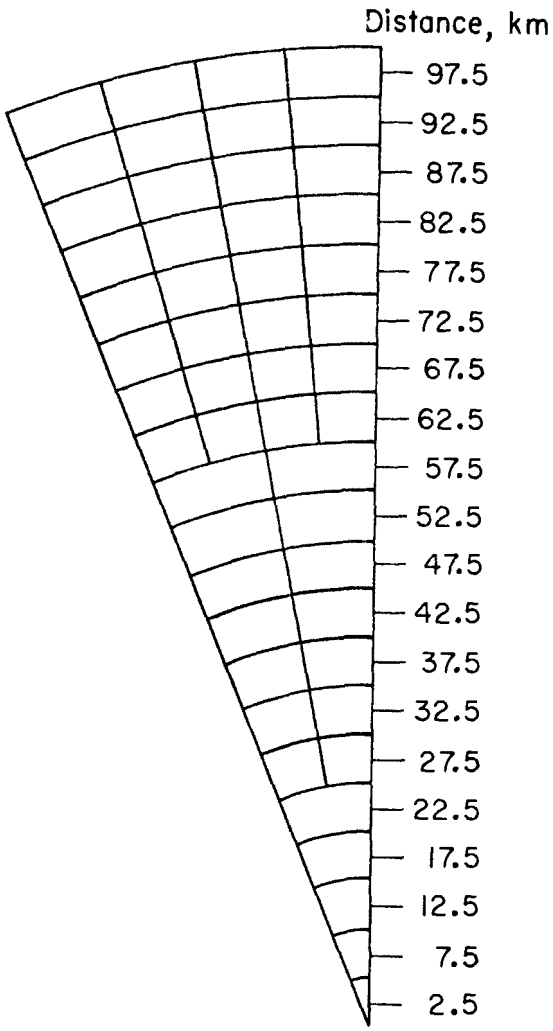

Figure 8. Sector Subdivisions Used in Man-Rem Estimates.

KRYPTON-85: A REVIEW OF INSTRUMENTATION FOR ENVIRONMENTAL MONITORING

R. J. Budnitz
Lawrence Berkeley Laboratory
University of California
Berkeley, California 94720

ACKNOWLEDGEMENTS

The constant support and encouragement of D.A. Mack and R.M. Graven is gratefully acknowledged, as is the generous advice and review of G. A. Morton.

This research was conducted in conjunction with a "Survey of Instrumentation for Environmental Monitoring" (Env. Inst. Group, 1973), which was funded under Grant No. AG-271 from Research Applied to National Needs, National Science Foundation, and performed at the University of California, Lawrence Berkeley Laboratory, in facilities provided by the U.S. Atomic Energy Commission.

The mention of commercial products, their source or their use in connection with material reported herein is not to be construed as either an actual or implied endorsement of such products. The opinions expressed herein do not necessarily express the opinion of the National Science Foundation, the Atomic Energy Commission, or the University of California.

Abstract

The aim of this review is to provide an overview of the techniques which have been developed for measuring krypton-85 in various media. The main emphasis is on measurements for surveillance and protection in environmental situations, especially around nuclear reactors and nuclear fuel reprocessing plants. Measurements in specialized research applications are not treated in detail. Overviews are first provided of the physical characteristics of krypton-85; of the sources of and typical levels of concentrations in the environment; and of the radiation protection guides. The various measurement techniques are then discussed, including both laboratory-type and field-type instrumentation.

INTRODUCTION

Krypton-85 is one of the main radioactive fission products normally released to the atmosphere in the reprocessing of nuclear reactor fuels. In fuel ready for reprocessing (150 days of cool-down) it is present in the amount of about 11,200 curies/metric ton of fuel (ORNL, 1971). In all reprocessing plants presently operating or under construction, the entire ^{85}Kr content of the fuel is released to the atmosphere. Since these plants operate at a through-put of from one to six tons per day, ^{85}Kr is a potential environmental pollutant, requiring measurement both in the plant stack during release and in the environment after dispersion. With the rise in nuclear power production the worldwide ^{85}Kr inventory is expected to increase dramatically. One projection from ORNL (1971) is shown in Figure 1.

A recent study (Diethorn, *et al.*, 1972) indicates that the present worldwide dose to man averages about 10^{-3} mrad/year to the bare skin, and about 10^{-4} mrad/year to the whole body. Figure 1 can be used to determine approximately how these doses might increase in the next few decades.

Krypton is a noble gas, chemically inert, which is present (as stable krypton-78, 80, 82, 84, 86) in normal air at a concentration of 1.14 ppm = 1.14 ml/m^3 (Sax, *et al.*, 1968). The radioactive decay of ^{85}Kr has a half-life of 10.76 years. The principle decay mode is β - emission, with a maximum beta energy of 672 keV. The beta has a broad energy spectrum shown in Figure 2 (Mantel, 1972). The range for the maximum-energy beta is 0.3 g/cm^2 (3 mm in water, 250 cm in air). A small (0.41%) branching ratio also exists for the emission of a 514-keV gamma.

RADIATION PROTECTION GUIDES

For 168-hour occupational exposures, the International Commission on Radiological Protection (ICRP, 1959) has established a maximum permissible concentration in air, (MPC)a. This occupational limit is 3×10^6 picocuries per cubic meter (pCi/m^3). For individuals in the general public, the applicable MPC values are a factor of 10 smaller (300,000 pCi/m^3); for exposure to a suitably large sample of the general public, another factor of 3 smaller still (100,000 pCi/m^3) applies. The U.S. Atomic Energy Commission's MPC values agree exactly with the ICRP MPC's just quoted (USAEC, 1973). Throughout this discussion, the MPC will be taken as 300,000 pCi/m^3, since exposure to a few individuals in the general public at the 300,000 level is undoubtedly more likely than to a larger population at the 100,000 level.

This MPC is equivalent to fractional krypton-85 atomic concentrations of 2.0×10^{-7} (^{85}Kr/total Kr) or 2.3×10^{-11} (^{85}Kr/total air). At the fence around a typical fuel reprocessing plant, concentrations of a few percent of MPC are expected to occur periodically.

MEASUREMENT CONSIDERATIONS

In environmental samples, the measurement of ^{85}Kr is essentially always based upon detecting the decay β^-, with any of a number of detectors sensitive to ionization energy loss. Several detection systems exist, including liquid scintillators, plastic scintillators, Geiger-Mueller counters, and ionization chambers. Each of the methods has its advantages and disadvantages; the discussion below is intended to point out some of the factors involved.

We shall concentrate upon measurements in the air around nuclear reactors and their fuel-reprocessing plants. Here the principle beta emitter besides ^{85}Kr is tritium (^3H); however, the tritium β- has such a low energy (E_{max} = 18.6 keV), that its interference in the ^{85}Kr measurement is usually not significant. (The reverse is not true.)

There are two quite different classes of ^{85}Kr measurement systems: those which operate in the field, designed to run unattended except for periodic maintenance; and those which require laboratory procedures. The latter are invariably the more sensitive, and the more precise. We shall discuss these two classes separately.

1. Laboratory Techniques.

There are a number of ^{85}Kr techniques which have been developed for use in the laboratory. They involve one substantial handicap, namely, that the volume of gas which can be sampled at some remote location, and then transported to the laboratory for analysis, is not large. This disadvantage limits sensitivity, but is counterbalanced by the ability to concentrate the krypton before counting, and to perform other analytical procedures which are impossible to carry out in the field.

The two most common laboratory techniques use plastic-scintillator shavings contained within a gas-tight vial, and liquid scintillator as a solvent for the ^{85}Kr-containing gas.

a. Plastic Scintillator.

We shall discuss the technique of Sax, Denny, and Reeves (Sax, *et al.*, 1968), which is typical of the plastic scintillator methods.

Plastic scintillator shavings of 20-40 mesh (an inexpensive by-product from any of several scintillator manufacturers) are encased in a glass vial of volume about 4 ml. A sample of pure krypton gas is prepared using vacuum-cryogenic techniques. The vial is evacuated and then filled to a known pressure (near 600 torr) with the krypton samples. A scintillation counter then measures the pulse-height spectrum.

Calibration of the counting efficiency (the fraction of the β spectrum above the counting threshold) is determined using a known ^{85}Kr standard acquired from NBS (NBS, 1962). The counting efficiency is about 95%. Given about 0.5 ml of nearly pure krypton (equivalent to that present in about 0.5 m^3 of air), measurements can be made of normal ^{85}Kr background levels in the 10 pCi/m^3 range to about $\pm$10% (Sax, *et al.*, 1968). The limit of detection is about 1 pCi/m^3 of air sample, with a 100-minute counting time, at the two-standard-deviation level above background.

b. Liquid Scintillator.

Here we shall discuss that aspect of liquid-scintillation counting which is unique to or particularly relevant to ^{85}Kr.

The liquid scintillator method relies upon the high solubility of krypton in many of the commonly used liquid scintillators. Krypton is soluble (Linke, *et al.*, 1965 and Shuping, *et al.*, 1969) in aromatic solvents to $\cong$1 ml Kr/ml solvent.

The earliest descriptions of liquid scintillators used for ^{85}Kr counting are those of Horrocks, *et al.*, (1964), and Curtis, *et al.*, (1966). These early methods suffered from a limit on the amount of krypton which could be introduced into the solution.

Shuping, Phillips, and Moghissi have reported a method in which about 25 ml of toluene-based liquid scintillator acts as solvent for about 10 ml of gas (Shuping, *et al.*, 1969). The gas is introduced into an evacuated glass vial, filled with de-aerated scintillation solution. "If the ^{85}Kr concentration in air is sufficiently high, the sample may be introduced directly into the solution and successfully counted" (Shuping, *et al.*, 1969). More commonly, krypton is concentrated cryogenically. A rate of 1 cpm above background corresponds to 0.025 pCi $^{85}Kr/m^3$ of air, so that levels of that order of magnitude are detectable with the method. Accuracies in the $\pm$4% range are achieved, when ^{85}Kr activities of $\cong$10 pCi/m^3 of air are present.

One of the more difficult problems in the procedure just described is the separation of krypton gas from the main air sample. To overcome this problem, a separation system for krypton, by Cummings, Shearin, and Porter employs ^{83m}Kr as a spike in the air sample, in order to determine directly the ^{85}Kr yield after a complicated separation procedure involving "charcoal and molecular sieve cold traps, calcium sulfate, ascarite, and a titanium furnace (900°C) for the removal and separation of other air constituents from krypton" (Cummings, *et al.*, 1971). A description of a method for generating ^{83m}Kr (2-hour half-life) from ^{83}Rb in the laboratory has been given by Moghissi, *et al.*, (1971).

Another ^{85}Kr system, described by Stevenson and Johns, uses a battery-operated air compressor to collect 1 m^3 of air in the field. After a series of cryogenic absorptions and elutions in the lab, the krypton is dissolved and counted in a liquid scintillator. The krypton recovery ranges from 50 to 70%, measured volumetrically. These workers report a minimum detectable sensitivity (three standard deviations above background) of about 2 pCi $^{85}Kr/m^3$ of air, with a 4-hour counting time (Stevenson, *et al.*, 1971).

2. Field Instruments.

For measurements in the field, the ideal goal is an instrument which can record continuously, with reasonably short time-integration periods, at sensitivity levels well below the current average background of about 10 pCi/m^3 of air The ideal instrument must also be rugged enough to withstand temperature and humidity extremes and shock; and should require little maintenance.

A study (Smith, *et al.*, 1970) of several possible field instruments was carried out in 1969 by the Northeastern Radiological Health Laboratory, U.S. Public Health Service. Four ionization chambers and four Geiger-Mueller counters were studied. Calibrations were performed in the laboratory, followed by determinations of the minimum detectable concentrations. Some of the instruments were then used in the field around a fuel-reprocessing plant, to determine performances under actual field conditions.

None of the field instruments came close to the sensitivity required for background measurements in the pCi/m^3 range. However, all were sensitive enough to measure fractions of the MPC for individuals in the general public (300,000 pCi/m^3).

a. Flow-Through Ionization Chambers.

Four flow-through ionization chambers were tested in the laboratory using dry, radon-free air. They ranged in size from 0.5 to 4.3 liters in volume. After calibration against an NBS standard (NBS, 1972), the minimum detectable concentrations (MDC, defined as twice the standard deviation in counting) were determined; they ranged from 130,000 to 40,000 pCi/m^3. The calibrations were performed with errors (2σ) in the $\pm 7\%$ to $\pm 17\%$ range. These ionization chambers have several undesirable properties:

(1) They must be used downstream of a radon holdup trap and filter (or equivalent).

(2) Because of the use of the radon trap, the averaging time is in the 30-minute range, which is much longer than the few-minute time for a significant change in ^{85}Kr concentration when a fuel-reprocessing-plant plume passes directly overhead.

(3) It is necessary to make appropriate measurements of pressure, temperature, humidity, and external background variation to obtain reasonable accuracy.

(4) Maintenance requirements are high.

To quote from Smith, *et al.*, (1970):

"It should be noted that although the ionization chamber systems can be made to operate in the field, the degree of care, number of precautions, and amount of operator training required to obtain usable data for environmental levels, and the questionable nature of the data obtained when the field levels passing the instrument are fluctuating rapidly, all weigh heavily in favor of using simpler systems for this purpose."

b. Geiger-Mueller Counters.

Several Geiger-Mueller (G-M) tubes were also studied by Smith, *et al.*, (1970). These were calibrated against the flow-through ionization chambers described above, and then minimum detectable concentrations were determined. The calibration errors (2σ) were in the $\pm$ 13% region for all of the G-M detectors. The most sensitive G-M detector was found to be the Eon 8008H, a double end-window pancake detector, of 2" diameter with 3.5 mg/cm^2 mica windows. It had a MDC of 12,000 pCi/m^3 with a counting time of 10 minutes (sample) and 10 minutes (background). Unfortunately, this detector was so fragile that its use in the field was precluded.

The other G-M detectors all had MDC's in the region of about 25,000 pCi/m^3. These instruments were Amperex 18546 and an Eon 8001T (both one-window pancake detectors of 2" diameter); and an LND 719 and an Eon 5108E (both cylindrical probes were 5-1/2" long, 0.6" in diameter, and with 30 mg/cm^2 wall thicknesses). These cylindrical instruments were found to be durable against mild shock and rain in the field; the single-window detectors were less durable against shock. However, all performed in the field with sensitivities nearly identical to those measured in the laboratory. The conclusion can be taken directly from Smith, *et al.*, (1970):

"Long-term (weeks to months) environmental monitoring would demand the most sensitive detectors and systems that could endure the environment with a minimum of attention. The choice at present is between the single windowed pancake tube (Amperex 18546) and the thicker walled (30 mg/cm^2) cylindrical probes (Eon 5108E or LND 719) which, though slightly less sensitive, are certainly the most durable of the detectors evaluated."

3. New Technological Developments.

There are a few technological developments on the horizon which will provide some increased sensitivity. The most important of these is the recent development of substantially better photomultiplier tubes (Leskovar, *et al.,* 1972). These tubes have higher quantum efficiency, lower noise, and generally superior operating characteristics. This will improve the scintillation counting method considerably.

The incorporation of integrated circuit electronics into the G-M detector systems will also be important, helping to increase the ruggedness and reliability of the technique. Also, read-out systems are being developed which will enable the data to be collected, recorded, and analyzed remotely, bypassing the strip-chart-recorder step entirely.

SUMMARY AND CONCLUSIONS

Two important numbers determine the sensitivity required of instruments for measuring ^{85}Kr in environmental air:

(1) The maximum permissible concentration for individuals in the general public is 300,000 pCi/m^3 (ICRP, 1959; USAEC, 1973).

(2) The typical "background" level of ^{85}Kr in air today is in the range of 10 to 15 pCi/m^3 (Sax, *et al.,* 1968).

The ideal instrument is one capable of measuring the background level to a small fractional accuracy; several of the laboratory techniques described have this sensitivity. These techniques, which use liquid or plastic scintillation counting, all suffer from a common problem: a complicated series of laboratory steps is required to concentrate the krypton from the original gas sample.

In contrast, the field monitoring instruments (Smith, *et al.,* 1970) are all several orders of magnitude less sensitive, with MDC's ranging from 12,000 to 28,000 pCi/m^3 for the G-M detectors and from 39,000 to 190,000 for the ion chambers. All of these instruments are thus capable of detecting ^{85}Kr at levels well below the 300,000 pCi/m^3 for individuals in the general public, but cannot measure ^{85}Kr in "background" samples.

At present, there does not exist (to our knowledge) a commercially available "Krypton-85 Monitor" which can be purchased off-the-shelf. The G-M detectors described by Smith, *et al.,* (1970) are worthy of commercial development to meet the need for monitoring in the field around fuel-reprocessing plants and nuclear power reactors. Any commercial instrument would have to satisfy several requirements besides sensitivity:

(1) Rugged construction.

(2) Insensitivity to changes in temperature and humidity.

(3) Some method of continuously recording the data (at least a strip-recorder, or preferably a direct magnetic-tape record).

(4) Some method of calibration (perhaps a frequent, rapid check with a high-energy source, and a less-frequent check in a controlled chamber of known ^{85}Kr concentration).

For the more sensitive measurements of levels below the natural background of a few pCi/m^3, field instruments are presently out of the question. Some kind of cryogenic concentration method is required to increase the specific activity to the point where reasonable counting times ($\lesssim$ a few hours) are possible.

One key problem here is with the accuracy and reproducibility of the concentration mechanism. Accurate determinations of the fractional yield through a multi-stage sequence are notoriously difficult. This is true especially if a known volume of "ordinary" krypton is introduced as a carrier, since all krypton today unfortunately contains ^{85}Kr at levels in the ppm region. One solution is the use of ^{83m}Kr as a tracer to determine the yield.

Finally, it should be noted that some of the instruments designed to measure tritium in gaseous environmental samples are also capable (or adaptable) for the ^{85}Kr problem, with some modifications and changes in procedure.

REFERENCES

Cummings, S.L., R. L. Shearin, and C.R. Porter, (1971), "A Rapid Method for Determining ^{85}Kr in Environmental Air Samples," p. 163 of *Rapid Methods for Measuring Radioactivity in the Environment, Proceeding of a Conference, 5-9 July 1971,* (International Atomic Energy Agency:Vienna).

Curtis, M.L., S.L. Ness, and L.L. Bentz, (1966), Anal. Chem. 38, 636.

Diethorn, W.S., and W.L. Stockho, (1972), Health Phys. 23, 653.

Environmental Instrumentation Group, (1973), Lawrence Berkeley Laboratory, *"Survey of Instrumentation for Environmental Monitoring",* Report LBL-1, Lawrence Berkeley Laboratory, Berkeley, CA 94720, unpublished.

Horrocks, D.L., and M.H. Studier, (1964), Anal. Chem. 36, 2077.

International Commission on Radiological Protection (ICRP), (1959), ICRP Publication 2, (Pergamon Press:New York).

Leskovar, B. and C.C. Lo, (1972), IEEE Trans. Nucl. Science, NS-19 (3), 50.

Linke, W.F. and A. Seidell, (1965), *"Solubilities of Inorganic and Metal Organic Compounds,"* Vol. II, 4th ed., American Chemical Society, Washington, DC, p. 342.

Mantel, J., (1972), Int. J. Appl. Radiat. Isotopes 23, 407.

Moghissi, A.A. and H.B. Hupf, (1971), Int. J. Appl. Radiat. Isotopes 22, 218.

National Bureau of Standards, (NBS), (1962), NBS Standard #204, 10-9-62, $60.8X10^6$ dps/gram-mole.

Oak Ridge National Laboratory, (1971), *Siting of Fuel Reprocessing and Waste Management* Facilities, Report ORNL-4451, Oak Ridge, TN 37830, unpublished.

Sax, N.I., J.D. Denny, and B.R. Reeves, (1968), Anal. Chem. 40, 1915.

Shuping, R.E., C.R. Phillips, and A.A. Moghissi, (1969), Anal. Chem. 41, 2081.

Smith, D.G., J.A. Cochran, and B. Shlaien, (1970), *Calibration and Initial Field Testing of ^{85}Kr Detectors for Environmental Monitoring,* Report BRH/NERHL 70-4, U.S. Public Health Service, Northeastern Radiological Health Laboratory, 109 Holton Street, Winchester, MA01890, unpublished.

Stevenson, D.L., and F.B. Johns, (1971), *Separation Technique for the Determination of ^{85}Kr in the Environment,* p. 157 of *Rapid Methods for Measuring Radioactivity in the Environment, Proceedings of a Conference 5-9 July 1971,* (International Atomic Energy Agency: Vienna).

U.S. Atomic Energy Commission, (USAEC), (1973), Code of Federal Regulations, Title 10, Part 20, 10CFR20.

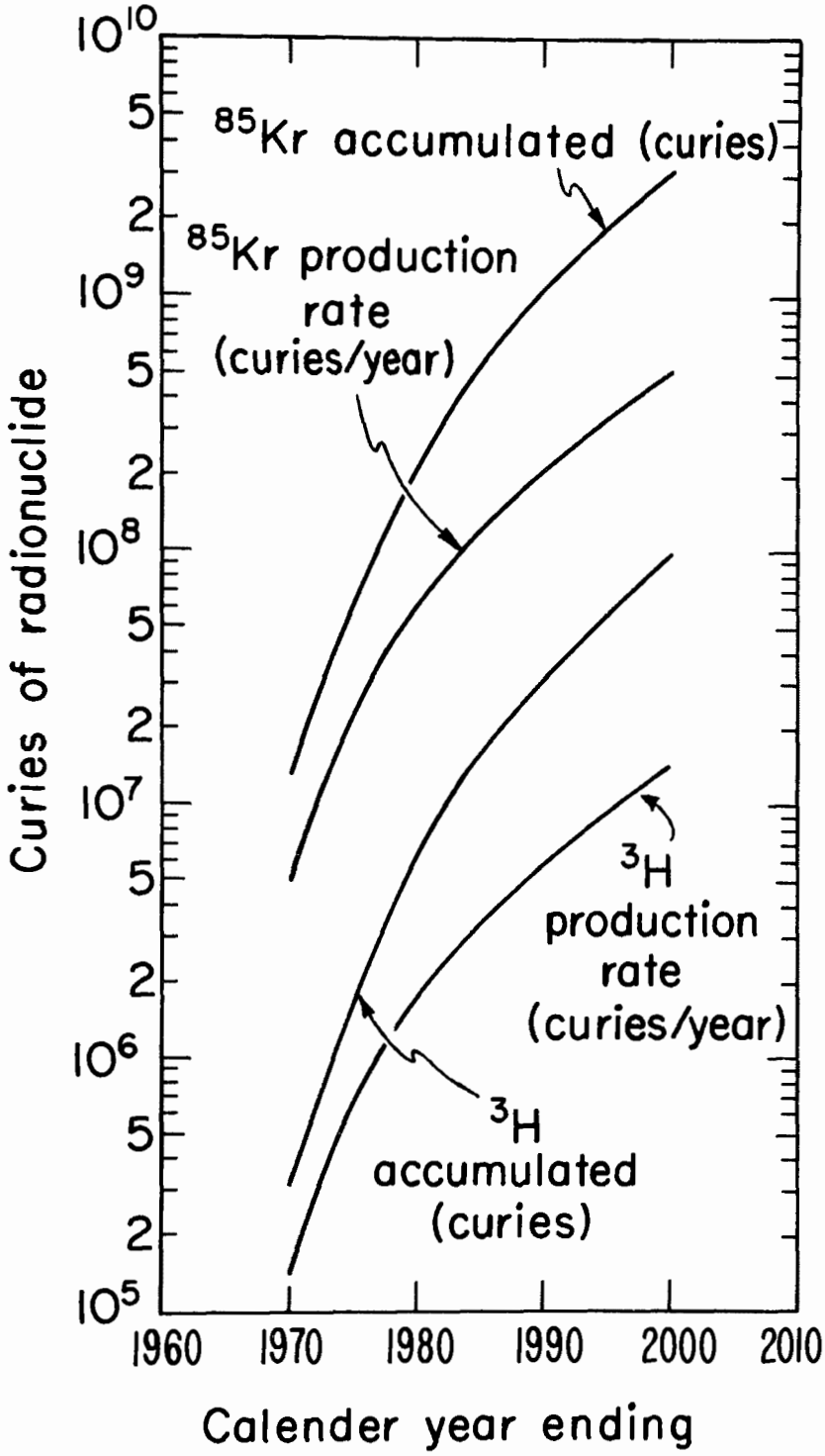
10^{10}
5
2
10^9
5
2
10^8
5
2
10^7
5
2
10^6
5
2
10^5
1960
1970
1980
1990
2000
2010
Curies of radionuclide
Calender year ending
^{85}Kr accumulated (curies)
^{85}Kr production rate (curies/year)
^{3}H production rate (curies/year)
^{3}H accumulated (curies)

Figure 1.

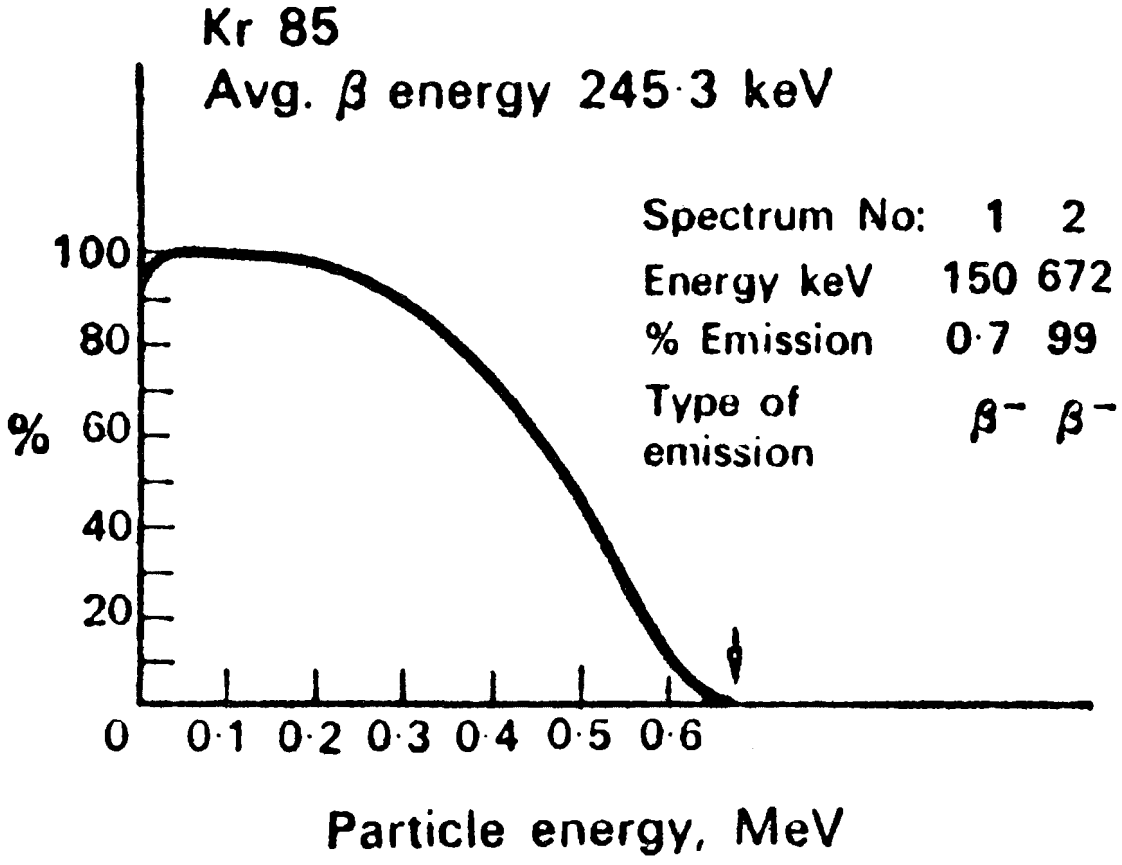
Kr 85
Avg. β energy 245·3 keV
Spectrum No: 1 2
Energy keV 150 672
% Emission 0·7 99
Type of emission β⁻ β⁻
100
80
%
60
40
20
0
0·1
0·2
0·3
0·4
0·5
0·6
Particle energy, MeV

Figure 2.

MEASUREMENT OF RADIOACTIVE NOBLE GASES BY LIQUID SCINTILLATION TECHNIQUES

D. L. Horrocks
Beckman Instruments, Inc.
Scientific Instrument Division
Fullerton, CA 92634

Abstract

The solubility of noble gases in aromatic solvents is sufficient enough to allow for measurement of radionuclides of the noble gases in liquid scintillator systems. This paper will discuss some techniques for sample preparation. The counting data will be discussed and related to the individual radionuclide decay scheme. The environmental monitoring aspects will be presented.

INTRODUCTION

It was known for many years that the heavier noble gases were appreciably soluable in aromatic hydrocarbons such as toluene and xylene (Clever, *et al.,* 1957; Clever, 1957; Saylor and Battino, 1958; and Steveberg and Manowitz, 1959). It was a logical conclusion that liquid scintillator solutions which use these same aromatic hydrocarbons as solvents could be used to measure radioactive isotopes of the soluble noble gases (Horrocks and Studier, 1964). Liquid scintillators had been used for the measurement of radioactivity for many years prior to this application (Birks, 1964 and Horrocks, 1966).

Horrocks and Studier (1964) first showed that it was indeed possible to measure radioactive noble gases in liquid scintillator systems. By choosing conditions which favored the incorporation of the noble gases into a toluene liquid scintillator solution, the radionuclides could not only be counted, but their pulse height distributions could be used to identify and separate the pulse spectra produced by different radionuclides in the same liquid scintillator sample. This is possible because liquid scintillator solutions have different responses for different energy particles (Flynn, *et al.,* 1964 and Horrocks, 1964a and b).

Since this initial investigation, several others have applied liquid scintillator systems to the measurement of radioactive noble gases (Curtis, *et al.,* 1966; Sax, *et al.,* 1968; Cohen, *et al.,* 1968; Shuping, *et al.,* 1969; Smith, *et al.,* 1970; and Iorgulescu, 1971). In many of these studies the radioactive gas sample was added to a counting vial by the use of gas transfer techniques. The gas was transferred to either an evacuated or a scintillator filled counting vial by the use of syringes and hypodermic needles. In those cases where evacuated counting vials were used, the scintillator solution was subsequently added through hypodermic needles until the pressure inside the vial equalled that outside (atmospheric). In most cases, the counting rates were more reproducible, and less variant with time, when the counting vial was filled as full as possible with the scintillator solution. The reduced air space above the solution forced more of the gas into the liquid phase by the mass action principle.

In other experiments, the amount of a radioactive isotope of a noble gas (usually ^{85}Kr) in aqueous solutions (water or blood) was measured by dissolving the aqueous sample in a liquid scintillator solution. The scintillator solution usually contained dioxane as the solvent or an emulsifier and toluene as the solvent. Transfer of the aqueous solution was critical in obtaining reproducible results. During the pipetting, the noble gases can be lost from the solution. It was also observed that the measured count rate of the sample varied less with time when the vial was nearly completely filled with scintillator solution.

Many of the studies were performed without the use of air-tight seals on the counting vial. This always lead to the subsequent loss of the noble gas through diffusion through and around the screw-on or snap-on caps. Sometimes these losses could be minimized for about 24 hours by the use of special cap liners such as polyethylene liners or self-sealing rubber serum stoppers. In all these types of studies, the losses were always present. Depending on the accuracy of the results required, this loss could lead to serious errors when corrections were not made for the effect upon the measured count rate.

SOLUBILITY IN AROMATIC SOLVENTS

The ability to measure a radioactive isotope of one of the noble gases in a liquid scintillator is the result of its solubility in the solvents used in the liquid scintillators. The solubility of noble gases in aromatic hydrocarbons was at one time considered as the basis for a technique for trapping off-gas releases from reactors and nuclear fuel recovery plants (Steinberg and Manowitz, 1959). The off-gases would be passed through a scrubbing tower containing aromatic hydrocarbons. It was demonstrated that certain kerosene base solvent systems would remove almost all of the noble gases (especially Kr and Xe) and most of the halogens. Table 1 lists some of the solubility data reported by Steinberg and Manowitz (1959) for xenon and krypton in several solvents. Noble gas solubilities in toluene were also measured by Horrocks and Studier (1964) by using radioactive isotopic tracers and a toluene base scintillator solution. A small capillary tube was used to connect a reservoir and a fixed volume of the toluene scintillator solution. The volume of the gas reservoir was decreased step-wise. After each reduction the equilibrium was obtained between the amount of noble gas in the gas reservoir and the amount dissolved in the toluene. The measured count rate was

proportional to the amount of noble gas dissolved in the toluene. The capillary tube prevented the excitation of the scintillator solution by particle emissions from the radionuclides above the solution. The equilibrium was altered by a change in temperature, and the new count rate was measured. The results are shown in Table 2. They are essentially the same as reported in Table 1.

TYPES OF COUNTING EQUIPMENT

Usually the counting was done in commercially available liquid scintillation systems. These are coincidence systems which use two multiplier phototubes (MPT's) viewing the sample in a counting vial located between the two MPT's. A true scintillation event is recorded only when both MPT's simultaneously (within 20-30 nanoseconds) detect a photon burst from the scintillator solution. This type of system is necessary when measuring small amounts of radioactivity and/or low energy events, because often other events occur which have similar pulse heights to true pulses from the scintillator solution. These events are usually generated in the MPT, and, thus, do not produce a simultaneous response in the other MPT. Thus, the coincidence circuit will reject these tube generated events. The tube generated events are usually the result of the spontaneous emission of electrons from surfaces (photocathode and/or dynodes) within the MPT and are commonly called tube "noise".

In one study (Horrocks and Studier, 1964), a home-made single MPT system was used. This system was used primarily to study the pulse height spectra produced by different radionuclides, different types of particles, and particles of different energy. The isotropic scintillation burst produced many photons (depending upon the energy of the exciting particle) and the optical system reflected all of them upon the face of the single MPT. This type of system gave a good response to the scintillation event and provided for the best resolution between different energy events (Horrocks, 1964a and b; Curtis, *et al.*, 1966; Sax, *et al.*, 1968; Cohen, *et al.*, 1968; Shuping, *et al.*, 1969; Smith, *et al.*, 1970; Iorgulescu, 1971; and Horrocks, 1966).

COUNTING ^{222}Rn

There are no stable isotopes of radon. The longest lived isotope of radon is ^{222}Rn, and this has been used as a tracer for radon studies. ^{222}Rn has a half-life of 3.82 days. This radionuclide is important because it is the daughter of ^{226}Ra, and is released whenever radium solutions are vented to the atmosphere. ^{222}Rn is an alpha-emitter, but several other radionuclides (daughters) rapidly appear in any sample of ^{222}Rn. Some of the daughters are alpha-emitters also, and others are beta-emitters. Some of these radionuclides also emit gamma rays. Often ^{222}Rn is determined by measurement of these gamma rays with a NaI(Tl) crystal scintillation detector.

When the ^{222}Rn is dissolved in a liquid scintillator solution the alpha particles are counted with 100% efficiency (Horrocks and Studier, 1958 and Wright, *et al.*, 1961). Using a single MPT system (Horrocks and Studier, 1964) and a multichannel analyzer (MCA) to sort pulses by pulse height (energy), it is possible to distinguish between the pulses produced by the alpha particles from ^{222}Rn (5.49 MeV) and the alpha emitting daughters ^{218}Po (6.00 MeV) and ^{214}Po (7.68 MeV). Figure 1 shows the pulse height spectrum obtained for a sample of ^{222}Rn dissolved in 0.25 ml of a toluene liquid scintillator solution. The three alpha energy groups gave responses which are easily distinguished. The response for alpha particles from ^{214}Po gives a peak which is somewhat broader due to the partial deposition of the ^{214}Po on the walls of the counting vial before the isotope has decayed. This does not occur with ^{218}Po because of its short half-life, which does not allow enough time for the ^{218}Po to diffuse through the solution and deposit on the vial walls. The continuum of pulses, ranging from zero pulse height to pulse heights above the 7.68 MeV alpha particle pulse heights, are produced by the beta particles from the beta-emitting daughters. Because of the small volume and low stopping power of the scintillator solution, there is very little efficiency for measuring a response to any gamma rays.

The decay rate of the ^{222}Rn is equal to the number of pulses in the peak corresponding to 5.49 MeV alpha particles (given by the area under the peak) divided by the time of the data accumulation, since the alpha particles are counted with 100% efficiency. A correction is made for the number of beta particle produced pulses, which give the same pulse height values as the 5.49 MeV alpha particles. The number of beta pulses is obtained by a simple interpolation of the smooth beta continuum. At equilibrium, the area under the 6.00 MeV alpha particle produced peak (corrected for beta particles) is the same as that for the 5.49 MeV alpha particle produced pulses. Equilibrium between the ^{222}Rn and the ^{218}Po is re-established about 30 minutes after separation of the ^{222}Rn from its daughters. Except for the wall effect, the area under the peak produced by the 7.68 MeV alpha particles would also be equal (at equilibrium) to the area under each peak due to the 5.49 MeV or the 6.00 MeV alpha particles.

COUNTING RADIONUCLIDES OF XENON

Several isotopes of xenon are usable as a tracer for stable xenon. All of the radionuclides can be efficiently counted in liquid scintillator solutions. Two xenon isotopes, which are often required to be measured because they are fission products, are ^{131m}Xe and ^{133}Xe. The ^{133}Xe decays by beta emission to an 80 keV excited energy level of ^{133}Cs, which gives rise to conversion electron in 63% of the decays and an 80 keV gamma ray in 37% of the decays. The conversion electrons are coincident with the beta particle which preceeded it, giving rise to a displaced beta spectrum. Internal conversion in the K shell followed by escape of the K x-ray (31 keV) gives rise to the beta pulses displaced by 49 keV. Conversion in the L shell or the K shell without the escape of an x-ray (Auger electron release) gives rise to beta pulses displaced by 80 keV.

The ^{131m}Xe decays by isometric transition to the ground-state of ^{131}Xe (stable). The energy transition releases 164 keV in the form of a 164 keV gamma ray in only 3% of the decays. In the other 97% of the decays, the energy release is in the form of internal conversion. Internal conversion in the K shell followed by escape of the 30 keV x-ray gives rise to a 134 keV electron. Internal conversion in either the K or L shells, not followed by capture of the x-rays, produces a response equivalent to a 164 keV electron.

Often samples with both of these Xe isotopes present are required to be measured, and the determination of each is desired. They decay by different modes and by different half-lives. The half-life of ^{133}Xe is 5.3 days, while the half-life of ^{131m}Xe is 11.9 days. Both of these differences have been utilized for such measurements. Xenon produced during the fission process for ^{235}U leads to a ratio of ^{133}Xe in excess of 500:1. Thus, "fresh" fission product xenon gives a pulse height spectrum similar to that for pure ^{133}Xe, as shown in Figure 2. The three peaks at the low energy end of the pulse height spectrum correspond to the beta continuum coincident with the gamma ray (no extra energy), coincident with the 50 keV conversion electron and coincident with the 80 keV conversion electron (or equivalent). Only a slight indication is seen that any ^{131m}Xe might be present in the sample.

After allowing the sample to stand for about one month, the pulse height spectrum looked like that shown in Figure 3. Superimposed on the beta pulse height spectrum from ^{133}Xe is the conversion electron spectrum from the ^{131m}Xe. Due to the difference in the half-lives of the two radionuclides, there appears to be almost equal amounts of each in the sample even though the total number of counts has decreased drastically.

Finally, the sample was re-counted after about four months; the pulse height spectrum obtained is shown in Figure 4. Essentially all of the ^{133}Xe has decayed away leaving only the remaining ^{131m}Xe. The pulse height spectrum shows both the 134 and 164 keV conversion electron events. The resolution of this sample using a one-MPT counting system was sufficient to resolve the two conversion electron groups.

Utilizing the differences in decay schemes and half-lives, it is possible to determine the relative activity of each of the xenon isotopes in the same sample. This information can be used to determine the source of the xenon; if it is mainly ^{133}Xe this would indicate a recent release from an operating reactor, while if it is mainly ^{131m}Xe, this would indicate a release from a processing plant (stored fuel rods), or a release which occurred several months prior to sample collection.

COUNTING OF KRYPTON RADIONUCLIDES

There are two radioactive isotopes of krypton which are commonly used as tracers for krypton; ^{81}Kr (100% E.C., half-life of 2.1 x 10^5years) and ^{85}Kr (100% beta, E_{max} of 672 keV, half-life of 10.76 years). Of these two, ^{85}Kr is the more important because large amounts of it are produced and released during the operation of reactors and fuel reprocessing plants. When ^{85}Kr is dissolved in a toluene scintillator solution, the pulse height spectrum obtained is shown in Figure 5. The relatively high maximum beta energy (672 keV) causes the observed pulse height distribution to be dependent upon the volume of the scintillator solution. When the solution volume is small (0.25 ml), many of the energetic beta particles strike the walls of the counting vial before all of the beta energy is released in the solution. Those beta particles give a pulse height response equivalent to a beta particle with less energy which was stopped in the solution. This is called a "wall effect". The pulse height spectrum is distorted toward the low energy pulse heights, as shown in curve (a) of Figure 5. When the solution volume is 5 ml, even the most energetic beta particles are stopped in the solution. The measured pulse height spectrum is essentially as expected from the known beta particle energy distribution.

COUNTING RADIONUCLIDES OF ARGON

Several isotopes of argon can be used as a tracer for argon gas samples. However, argon has a very limited solubility in toluene. Also, argon is much harder to handle by conventional vacuum line techniques. Its boiling point is much lower than krypton, xenon, and radon. The isotope ^{37}Ar is often used because of its high specific activity. It has a very low energy release per decay; only 2.8 keV for electron capture in the K shell. Even when ^{37}Ar is dissolved in a toluene scintillator solution, the counting efficiency is low and any quenching drastically reduces the counting efficiency.

CONCLUSIONS

The liquid scintillator solutions are very useful for the counting of radioactive isotopes of the noble gases. When the noble gas sample is dissolved in the solution, the counting efficiencies that are obtained are close to 100% in many cases, depending upon the mode of decay of the radionuclide. Many techniques which do not use air-tight seals are useful only over a limited time span before the gas sample begins to escape.

REFERENCES

Birks, J. B., (1964), *Theory and Practice of Scintillation Counting*, Pergamon Press, Oxford.

Clever, H. L., (1957), *The Solubility of Argon and Krypton in p-Xylene and p-Xylene-p-Dihalobenzene Mixtures at 30×C*, J. Chem. Phys. 61, 1082.

Clever, H. L., R. Battino, J. H. Saylor, and P. M. Gross, (1957), *The Solubility of Helium, Neon, and Krypton in Some Hydrocarbon Solvents*, J. Chem. Phys. 61, 1078.

Cohen, J. B., J. L. Setser, W. D. Kelley, and S. D. Shearer, Jr., (1968), *Determination of ^{3}H and ^{85}Kr in Aqueous Samples by Liquid Scintillation Techniques*, Talanta 15, 233.

Curtis, M. L., S. L. Ness, and L. L. Bentz, (1966), *Simple Technique for the Rapid Analysis of Radioactive Gases by Liquid Scintillation Counting*, Anal. Chem. 38, 636.

Flynn, K. F., L. E. Glendenin, E. P. Steinberg, and P. M. Wright, (1964), *Pulse Height-Energy Relations for Electrons and Alpha Particles in a Liquid Scintillator*, Nucl. Instr. Meth. 27, 13.

Horrocks, D. L., (1966), *Low-Level Alpha Disintegration Rate Determinations with a One-Multipler Phototube Liquid Scintillation Spectrometer*, Intern. J. Appl. Radiat. Isotopes 17, 441.

Horrocks, D. L., (1966), *Liquid Scintillator Solutions in Nuclear Physics and Nuclear Chemistry*, in Progress in Nuclear Energy Series IX, Analytical Chemistry, Volume 7, H. A. Elion and D. C. Stewart, eds., Pergamon Press, Oxford, pp 21-110.

Horrocks, D. L., (1964a), *Alpha Particle Energy Resolution in a Liquid Scintillator*, Rev. Sci. Instr. 35, 334.

Horrocks, D. L., (1964b), *Pulse Height-Energy Relationships of a Liquid Scintillator for Electrons of Energy Less Than 100 keV*, Nucl. Instr. Meth. 30, 157.

Horrocks, D. L. and M. H. Studier, (1964), *Determination of Radioactive Noble Gases with a Liquid Scintillator*, Anal. Chem. 36, 2077.

Horrocks, D. L. and M. H. Studier, (1958), *Low-Level Plutonium-241 Analysis by Liquid Scintillation Techniques*, Anal. Chem. 30, 1747.

Iorgulescu, A., (1971), *Study of ^{37}Ar Decay with Various Types of Organic Scintillators*, Stud. Cercet. Fiz. (Rumania) 23, 359.

Sax, N. I., J. D. Denny, and R. R. Reeves, (1968), *Modified Scintillation Counting Technique for Determination of Low-Level Krypton-85*, Anal. Chem. 40, 1915.

Saylor, J. H. and R. Battino, (1958), *The Solubilities of the Rare Gases in Some Simple Benzene Derivatives*, J. Chem. Phys. 62, 1334.

Shuping, R. E., C. R. Phillips, and A. A. Moghissi, (1969), *Low-Level Counting of Environmental Krypton-85 by Liquid Scintillation*, Anal. Chem. 41, 2082.

Smith, A. L., J. W. Thomas, and H. Wollman, (1970), *Determination of the Concentration of Volatile Isotopes in Blood by Liquid Scintillation Counting*, Intern. J. Appl. Radiat. Isotopes 21, 171.

Steinberg, M. and B. Manowitz, (1959), *Recovery of Fission Product Noble Gases*, Ind. Eng. Chem. 51, 47.

Wright, P. M., E. P. Steinberg, and L. E. Glendenin, (1961), *Half-Life of Samarium-147'*, Phys. Rev. 123, 205.

TABLE 1. Solubilities of Xenon and Krypton in Various Solvents (Steinberg and Manowitz, 1959).

Solvent	Xenon Solubility Temp., °C	Xenon Solubility ml/ml*	Krypton Solubility Temp., °C	Krypton Solubility ml/ml*
Water	32	0.10	30	0.05
Xylene (Tech.)	32	1.46	—	—
p-Xylene	29	2.95	30	0.72
	0	3.28		
Toluene	24	3.17	—	—

*Volume of gas (corrected to 15°C and 1 atmosphere) absorbed under total system pressure of 1 atm. per unit volume of solvent (corrected to 15°C).

TABLE 2. Solubilities of Some Radionuclides of the Noble Gases in a Toluene Liquid Scintillator Solution (Horrocks and Studier, 1964).

$$K = a_s/a_g$$

Noble Gas	T=-15°C	T=27°C
Krypton (^{85}Kr)	0.9	----
Xenon (^{131m}Xe)	5.0	3.0
Radon (^{222}Rn)	32.0	-----

a_s is the specific activity of the liquid scintillator solution; counts per minute/ml of solution.

a_g is the specific activity of the gas reservoir; counts per minute/ml of gas.

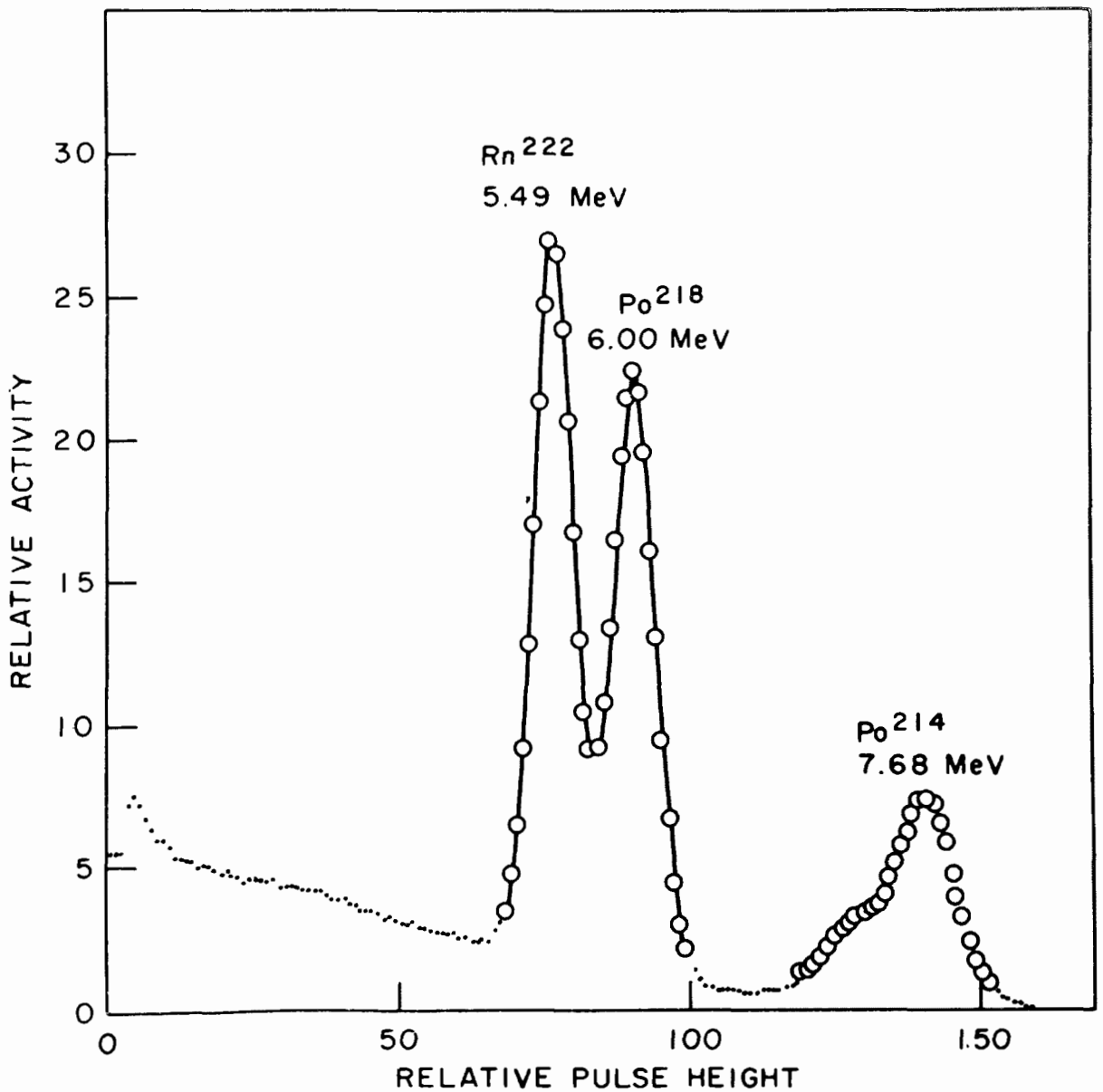

Figure 1. Differential pulse height spectrum for a sample of ^{222}Rn and daughters dissolved in 0.25 ml of a toluene liquid scintillator solution.

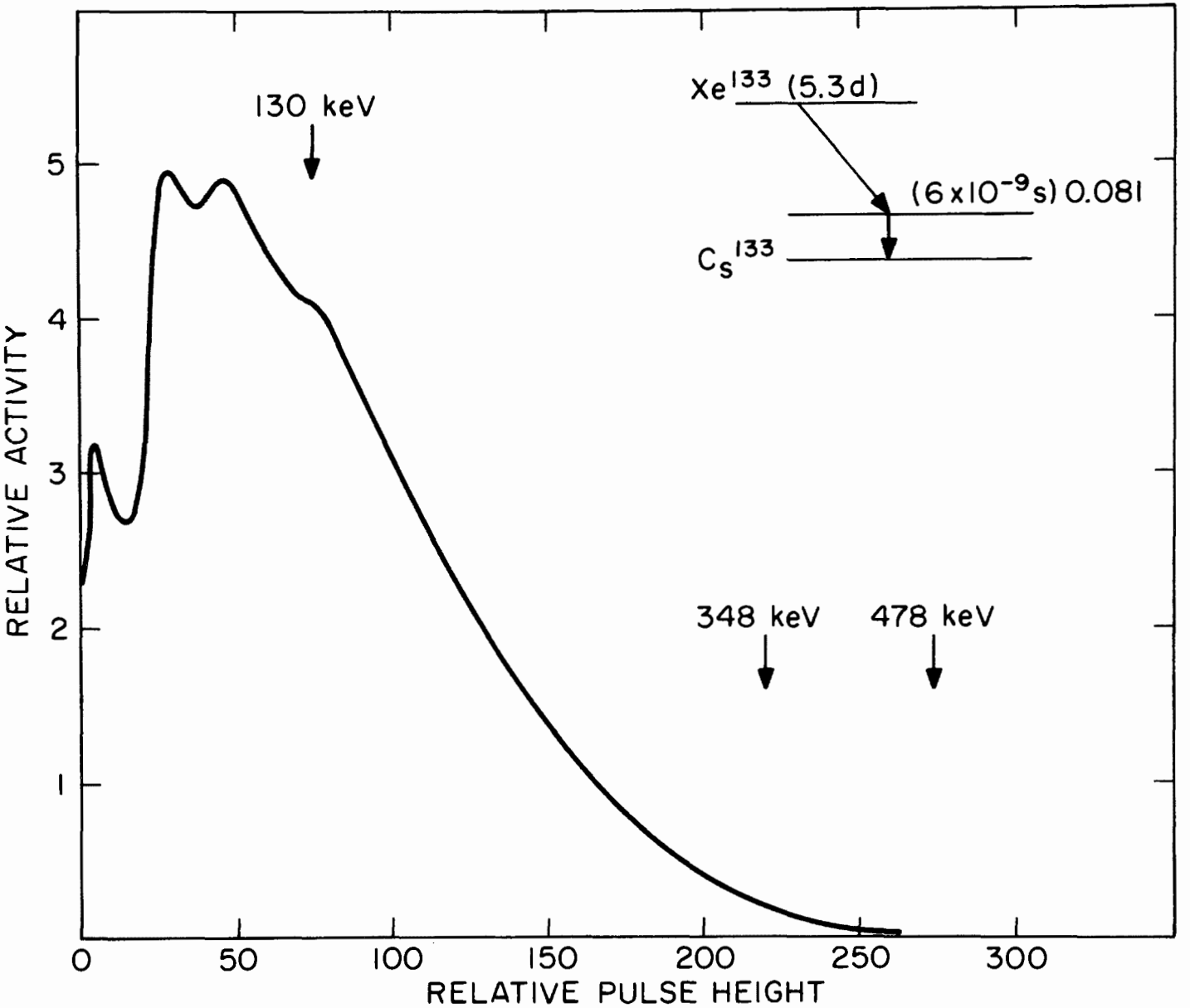

Figure 2. Differential pulse height spectrum for a sample of xenon gas from a "fresh" fuel rod from a reactor which contains both ^{133}Xe and ^{131m}Xe. The specific activity of the ^{133}Xe is many times greater than that of the ^{131m}Xe.

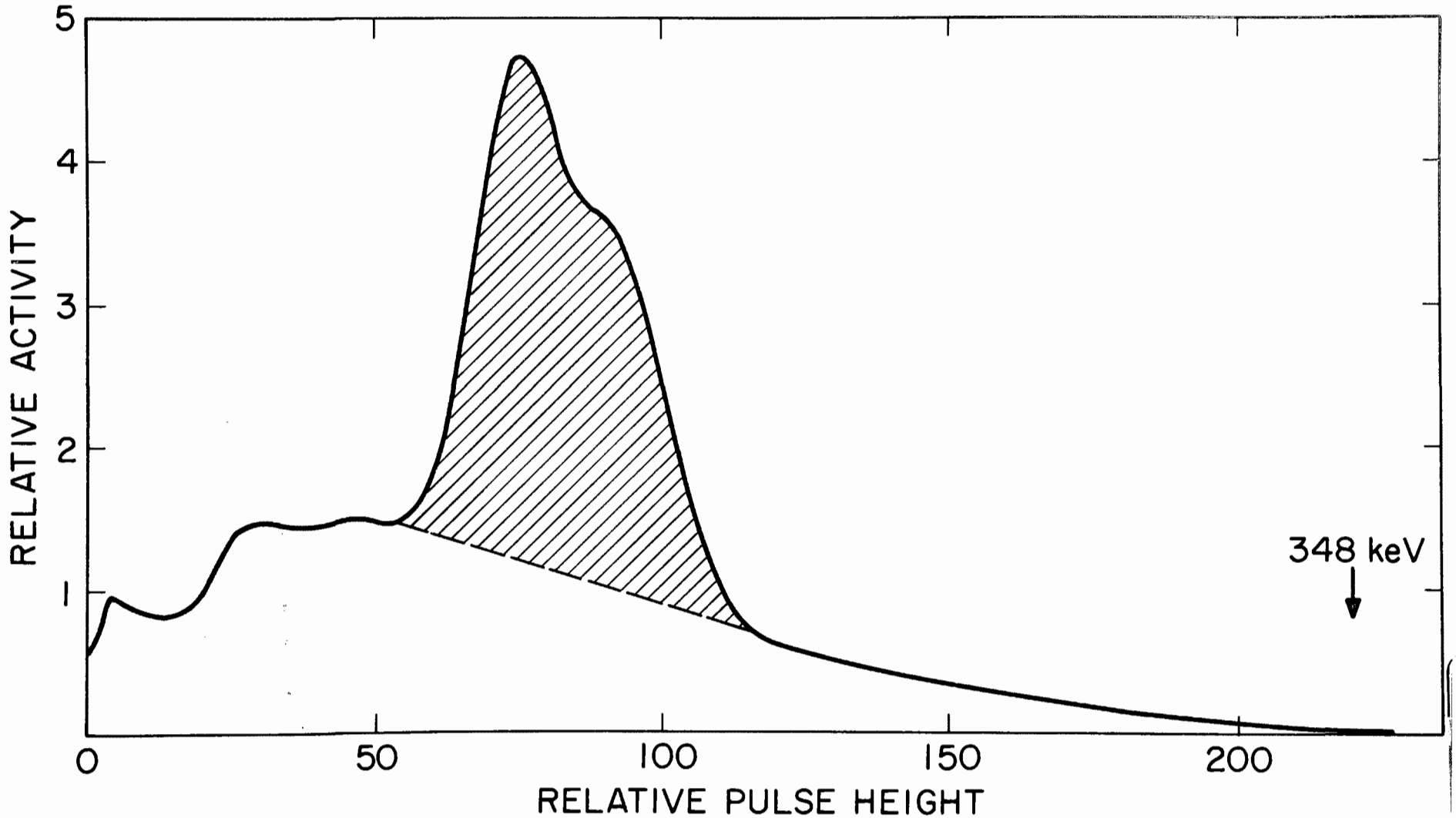

Figure 3. Differential pulse height spectrum for the same sample as counted in Figure 2 after one month time elapsed. The specific activities of the two radionuclides is such that both the ^{133}Xe beta spectrum and the ^{131m}Xe conversion electron spectrum can be measured.

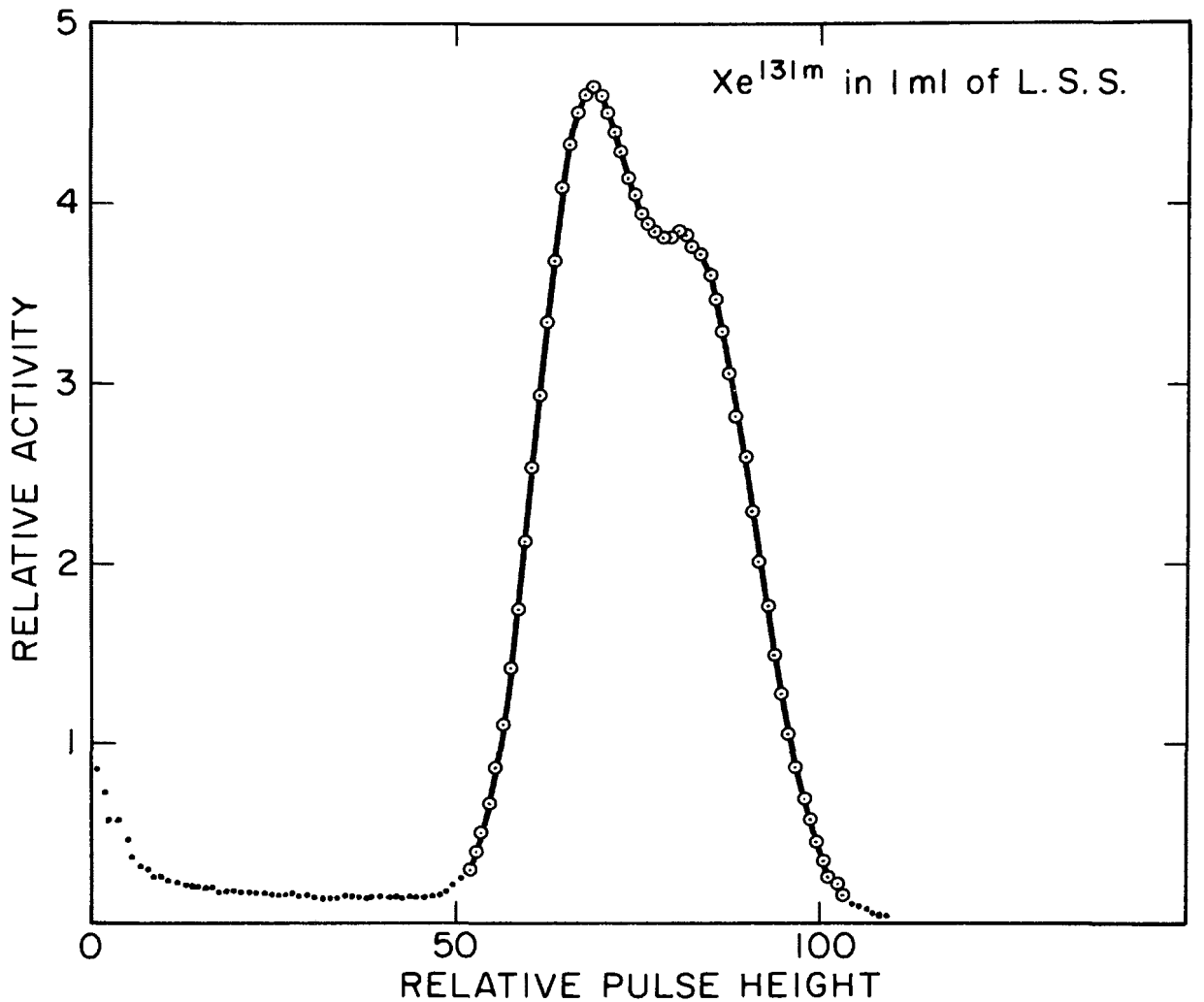

Figure 4. Differential pulse height spectrum of the same sample as counted in Figures 2 and 3 after four-month time elapse. Essentially all of the remaining activity is due to the conversion electrons from ^{131m}Xe.

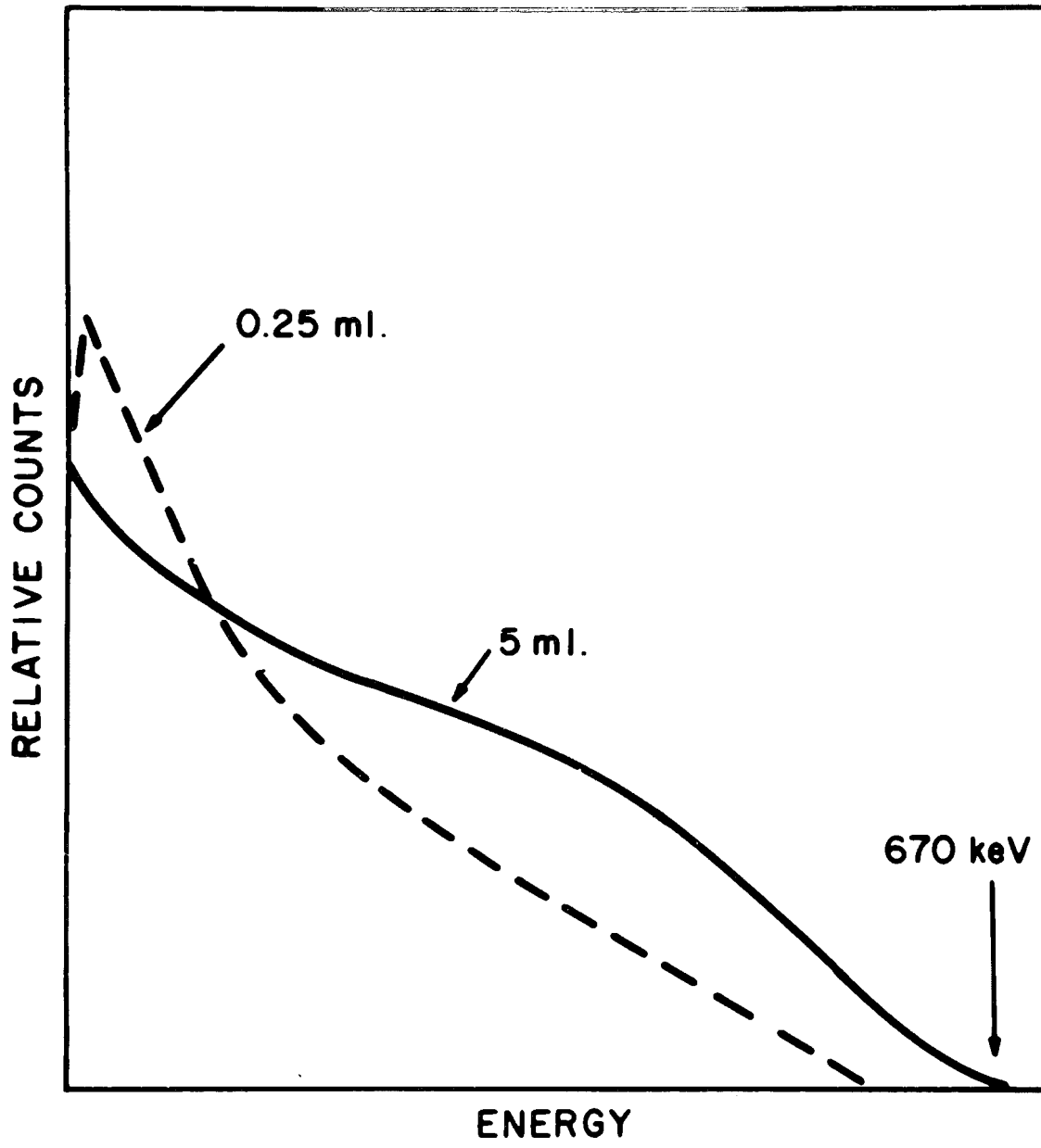

Figure 5. The differential pulse height spectrum of a sample of ^{85}Kr dissolved in (a) 0.25 ml and (b) 5.0 ml of toluene scintillator solution. This difference is due to the wall effect of the higher energy beta particles (672 keV) in the small volume of scintillator.

SEPARATION TECHNIQUES FOR REACTOR-PRODUCED NOBLE GASES*

C. O. Kunz
Radiological Sciences Laboratory
Division of Laboratories and Research
New York State Department of Health
Albany, New York 12201

Abstract

Procedures for separating the permanent gases have been developed as part of a study to characterize the gaseous radioactive effluents released from nuclear facilities. The gases being separated for internal gas-proportional counting include Ar, Kr, Xe, H_2, CH_4, and CO_2. Water vapor is cryogenically separated for liquid scintillation counting. Samples taken for processing within each facility range from 0.1 ml to several liters in volume. Sample volumes less than 10 ml are separated directly by chromatographic methods. Larger samples are processed using cryogenic-adsorption techniques for rough separation followed by chromatographic purification. Procedures for preventing cross-contamination from sample to sample, and between different radioactive gases within a sample, are considered. Processing requirements imposed by gas composition are also discussed.

INTRODUCTION

The Radiological Sciences Laboratory of the New York State Department of Health is studying the gaseous radioactive effluents from nuclear facilities (Matuszek, *et al.*, 1973). Samples have been obtained from two pressurized water reactors (PWR), a boiling water reactor (BWR), a high-temperature gas-cooled reactor (HTGR), and a pressurized heavy-water-moderated research reactor. The samples, taken from a variety of locations at each reactor, include primary strip gas, cover gas, decay-tank gas, containment air from the PWRs, and stack gas from the BWR.

Procedures for separating the noble gases, in addition to other permanent gases, have been developed as part of this study. The gases currently being routinely separated include Ar, Kr, Xe, H_2, CH_4, and CO_2. The activity is measured using internal gas-proportional beta-spectrometry (Paperiello, 1973). Water vapor is cryogenically separated for liquid scintillation counting.

The range of specific activity from sample to sample has been greater than five orders of magnitude, depending on the reactor and sampling locations. We have measured activities of various nuclides in individual samples that differ in activity by approximately seven orders of magnitude. Consequently precautions have been taken to prevent cross-contamination from sample to sample, and between different radioactive gases within a sample. Sample aliquots from about 0.1 ml to several liters have been processed, depending on the activity of the gases being analyzed.

Sample volumes less than 10 ml are separated directly by chromatographic methods. Larger samples are processed using cryogenic-adsorption techniques for rough separation followed by chromatographic purification.

SAMPLE COLLECTION AND MASS SPECTROMETRIC ANALYSIS

Samples are collected in a variety of vessels ranging in volume from 14 ml to 16 liters. Since vessels with septum caps tend to leak, those with stopcocks or valves are preferable.

Upon receipt of a sample, an aliquot is counted on a Ge(Li) spectrometry system to measure the activity of gamma-emitting gaseous radionuclides. These results are used as an aid in determining the subsequent separation procedures, and are compared with the results obtained by proportional counting.

An aliquot of the sample is also taken for mass spectrometric analysis to determine the composition of the gas. A few examples of such analyses of gases sampled from various locations in various types of reactors are shown in Table 1. The composition, which can vary considerably from sample, to sample, influences the choice of a separation procedure. In addition, species such as hydrocarbons that may contain ^{14}C or tritium can be identified and subsequently measured for possible activity. Finally, it is necessary to determine whether a significant amount of any of the gases being separated is present in the sample. The concentrations of most of the radioactive gases in the sample are far too low for the normal methods of chemical analysis, and measured amounts of carriers for the gases being separated are added. The radiochemical recovery of the separated gas finally loaded into a proportional tube for counting is determined from the total amount of gas present before separation.

GENERAL SEPARATION PROCEDURE

Figure 1 indicates the general procedure for processing the samples. If a sample (such as cover gas or decay-tank gas) is relatively high in total specific activity, and if the concentration of the lowest-activity gas fraction

**Supported in part by USAEC contract AT(11-1)2222 and USEPA contracts 68-01-0522 and 68-01-LA-0505.*

is higher than approximately 5 pCi/ml of sample, less than 10 ml of sample is processed. The sample is mixed with carriers and injected directly into a chromatograph for high-activity samples. The separated fractions are trapped, and those relatively high in activity are measured for percent yield, and loaded into proportional tubes for counting. The trapped gases that are relatively low in activity (in general, $< 10^{-4}$ μCi in the separated fraction) are sent through a separate chromatograph for further purification and decontamination. The gases trapped from this intermediate-level chromatograph are measured for chemical recovery, and loaded into gas-proportional counting tubes using a gas-handling rack reserved for the intermediate- to low-activity fractions. This separation of systems is necessary to minimize cross-contamination.

Samples (such as containment air) that are relatively low in specific activity and contain gas fractions with activity less than approximately 5 pCi/ml must be processed in aliquots of one or more liters. These undergo rough separation prior to chromatographic purification. Because of the volume reduction following this rough separation from such large sample volumes, some fractions have high specific activity, while others are relatively low. The high-activity fractions and the intermediate- to low-activity fractions are chromatographically purified on separate systems prior to being loaded for counting as described above.

HIGH-ACTIVITY SAMPLES

Figure 2 is a schematic drawing of the gas-handling vacuum rack used for processing samples of less than about 10 ml of gas having relatively high specific activity. The sample is measured and mixed with measured amounts of carriers for Ar, Kr, Xe, H_2, CH_4, and CO_2. About 0.5-1.5 ml of each carrier is a convenient amount to process. The sample and carriers are then transferred to a molecular sieve U-trap connected to a gas injection valve on the chromatograph. The gases are transferred from section to section using molecular sieve fingers and U-traps. The molecular sieve is cooled with liquid nitrogen to adsorb the gases, and heated with a nichrome wire wrap to desorb the gases. Using helium carrier gas, the sample is passed through the chromatograph. As the various gases are eluted (as observed with a thermal conductivity detector), the gases of interest are trapped on molecular sieve U-traps cooled with liquid nitrogen. The helium carrier is pumped off the cooled traps. The trapped gases that are relatively high in activity are volume-measured for chemical recovery and then loaded into gas-proportional counting tubes. The low-activity gases are transferred to a separate system used only for intermediate- to low-level gases. There they are further purified through the intermediate-activity chromatograph, volume-measured, and loaded into tubes.

Figure 3 is a more detailed drawing of the type of volume-measure and tube-load systems used. The gas to be measured is transferred to the molecular sieve finger. Stopcocks A and B are then closed, and the finger is heated to desorb the gas off the molecular sieve. When no more gas is being desorbed, stopcock C is closed, and the pressure of the gas contained between stopcocks A, B, and C is measured. The volume contained between these stopcocks has previously been determined, and from these data the amount of gas present is calculated. If the gas is to be loaded into a proportional-counting tube, it is expanded into the evacuated tube, which is then filled with counting gas to slightly more than atmospheric pressure.

Figure 4 shows typical chromatograms obtained with the high-activity and intermediate-activity chromatographs. The high-activity chromatograph has a column of 10' x 1/4" molecular sieve 5A, 40-60 mesh, with helium carrier flowing at 60 ml/min. Normally the column is run at room temperature until the CH_4 fraction is off, and then is heated to 300°C to drive off the xenon and CO_2 fractions. There is very little separation between the krypton and CH_4 on the high-level chromatograph. However, on the intermediate-level chromatograph, which has a column of 20' x 1/4" molecular sieve 5A, 40-60 mesh, the separation is very good.

Very often the krypton in a sample has a much higher activity than the ^{14}C or tritium in methane. To determine the decontamination factor between krypton and CH_4, a ^{85}Kr source was mixed with the carriers, and as the krypton and CH_4 were eluted from the high-level chromatograph, the gases were trapped separately, and subsequently counted without further purification. The initial activity of the krypton was 3.5 x 10^{-3} μCi; the activity of krypton in the CH_4 fraction was 2.0 x 10^{-5} μCi. The decontamination factor for krypton in the CH_4 fraction was thus 175.

The same experiment was repeated with the intermediate-level chromatograph. In this case, to avoid possible contamination of the system, only 1.4 x 10^{-4} μCi of krypton was mixed with the carriers prior to injection. No measurable activity could be seen for krypton in the CH_4 fraction, and a value of less than 8.2 x 10^{-7} μCi was obtained, resulting in a decontamination factor greater than 170. There is over 10 minutes of baseline separation between these peaks, and the decontamination factor is certainly much higher than indicated from the low activity of krypton used. In the normal processing of a sample, the CH_4 fraction trapped off the high-level chromatograph would be sent through the intermediate-level chromatograph prior to counting, with a combined decontamination of krypton considerably greater than 3 x 10^4. This example illustrates the high decontamination factors obtainable with multiple GC purification.

Cross contamination is normally limited not by GC separation, but by system contamination. The problem of system contamination varies from gas to gas, and is most severe with tritium — either as gas or water vapor. To measure activities differing by more than six orders of magnitude, a separation of gas-handling systems and chromatographs as described above is required. In addition, system and proportional-tube blanks must be run between samples to determine possible residual activities.

INTERMEDIATE-ACTIVITY SAMPLES

The separation system used for liter-size, intermediate-activity samples is shown schematically in Figure 5. With this system, the volume of each separated fraction is reduced to several milliliters for subsequent chromatographic purification. The procedure involves adsorption followed by elution with helium carrier, similar to the methods described by Momyer (1960) for krypton and xenon. The sample is mixed with carriers, bled at a rate of approximately 40 ml/min through two cold traps, and then adsorbed on a 4' x 1/2" glass coil of activated charcoal cooled with liquid nitrogen. The trap cooled with dry ice-acetone collects the water vapor; the trap cooled with liquid nitrogen collects the xenon and CO_2.

After the sample has been adsorbed onto the charcoal, which is maintained in a liquid nitrogen bath, a helium flow is initiated at about 500 ml/min, passing through the charcoal and molecular sieve coils and out through a mercury stick manometer. The molecular sieve coil is about 4' x 1/2". After the helium flow is established, a small fraction of the helium stream coming off the molecular sieve coil is continuously sampled with an Aero Vac 610 mass spectrometer. Various other methods, such as a thermal conductivity cell, could be used to monitor the gases eluted from the adsorbents.

Once the retention times for the gases of interest have been determined, sampling is not necessary. When dry ice-acetone slurries are placed around both the charcoal and molecular sieve coils, the hydrogen, argon, oxygen and nitrogen are rapidly eluted from the charcoal, while the krypton and CH_4 are retained. The hydrogen is observed coming off the molecular sieve coil about 5 minutes after both coils have been cooled with dry ice-acetone, and it is entirely off approximately 3 minutes later. It is trapped in a molecular sieve U-trap cooled with liquid nitrogen. Approximately 5 minutes after the hydrogen is off, argon and oxygen are observed coming off the molecular sieve coil. These gases are trapped together on a separate U-trap. At dry-ice temperature, the nitrogen is retained on the molecular sieve coil, while the argon and oxygen are eluted and trapped. The coil is then warmed to room temperature to elut the nitrogen. When the nitrogen is off, both coils are warmed to about 100°C to accelerate the elution of the krypton and CH_4, which are trapped together on the third molecular sieve U-trap. The argon and oxygen, which are not easily separated by chromatographic methods, are transferred to a furnace containing copper turnings which is heated to approximately 400°C to remove the oxygen by reduction to CuO.

All the separated fractions, which are now reduced in volume to several milliliters, are chromatographically purified as described for small-volume samples.

Between samples all the adsorbents used in separation of the gases are heated to 400°C while being purged with helium, or evacuated, in order to remove any residual gases and to reactivate the adsorbents for subsequent processing cycles.

SUMMARY

Methods of separation for Ar, Kr, Xe, H_2, CH_4, and CO_2 in reactor gas effluent samples up to several liters in size have been described. These general separation procedures are being extended to include other gases of interest, such as CO, C_2H_6, C_3H_8, SO_2, I_2, and CH_3I.

The counting techniques and interpretation of the effects of noble gas levels are described in the accompanying papers.

REFERENCES

Matuszek, J.M., C.J. Paperiello and C.O. Kunz, (1973), *Reactor Contributions to Atmospheric Noble-Gas Radioactivity Levels,* Proceedings of the Noble Gas Symposium, Las Vegas, Nevada, September 24-28, 1973.

Momyer, F.F., (1960), *The Radiochemistry of the Rare Gases,* Report NAS-NS 3025 (National Academy of Sciences, National Research Council).

Paperiello, C.J., (1973), *Internal Gas-Proportional Beta-Spectrometry for Measurement of Radioactive Noble Gases in Reactor Effluents,* Proceedings of the Noble Gas Symposium, Las Vegas, Nevada, September 24-28, 1973.

TABLE 1. The Gas Compositions of Samples from Various Reactors (Vol %).

Gas	BWR stack gas	PWR (I) decay tank	PWR (II) decay tank	PWR (II) containment air	HTGR decay tank	Heavy-water research reactor cover gas
N_2	68.79	7.61	79.14	78.83	10.88	0.22
O_2	21.41	0.17	0.04	20.09	1.10	0.02
Ar	0.80	0.08	0.17	0.92	0.14	----
CO_2	0.11	0.04	0.11	0.20	0.12	----
H_2	8.89	91.82	18.76	----	0.07	----
He	----	----	----	----	87.69	99.76
CH_4	----	0.14	0.19	----	----	----
C_2H_6	----	ID	0.02	----	----	----
C_3H_8	----	ID	----	----	----	----
H_2O	----	0.07	0.87	----	----	----

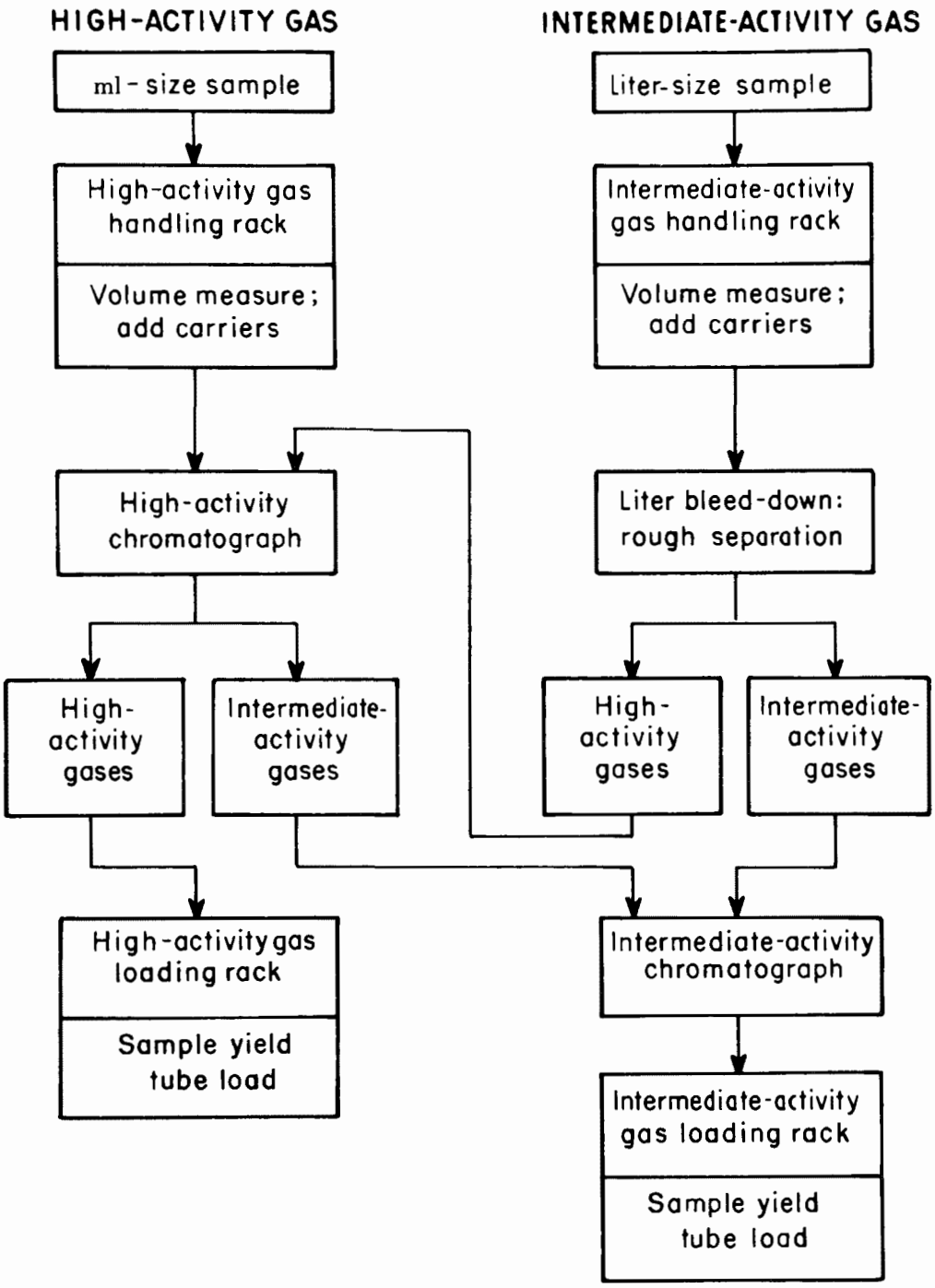

Figure 1. Processing procedure for high-activity and intermediate-activity gas samples.

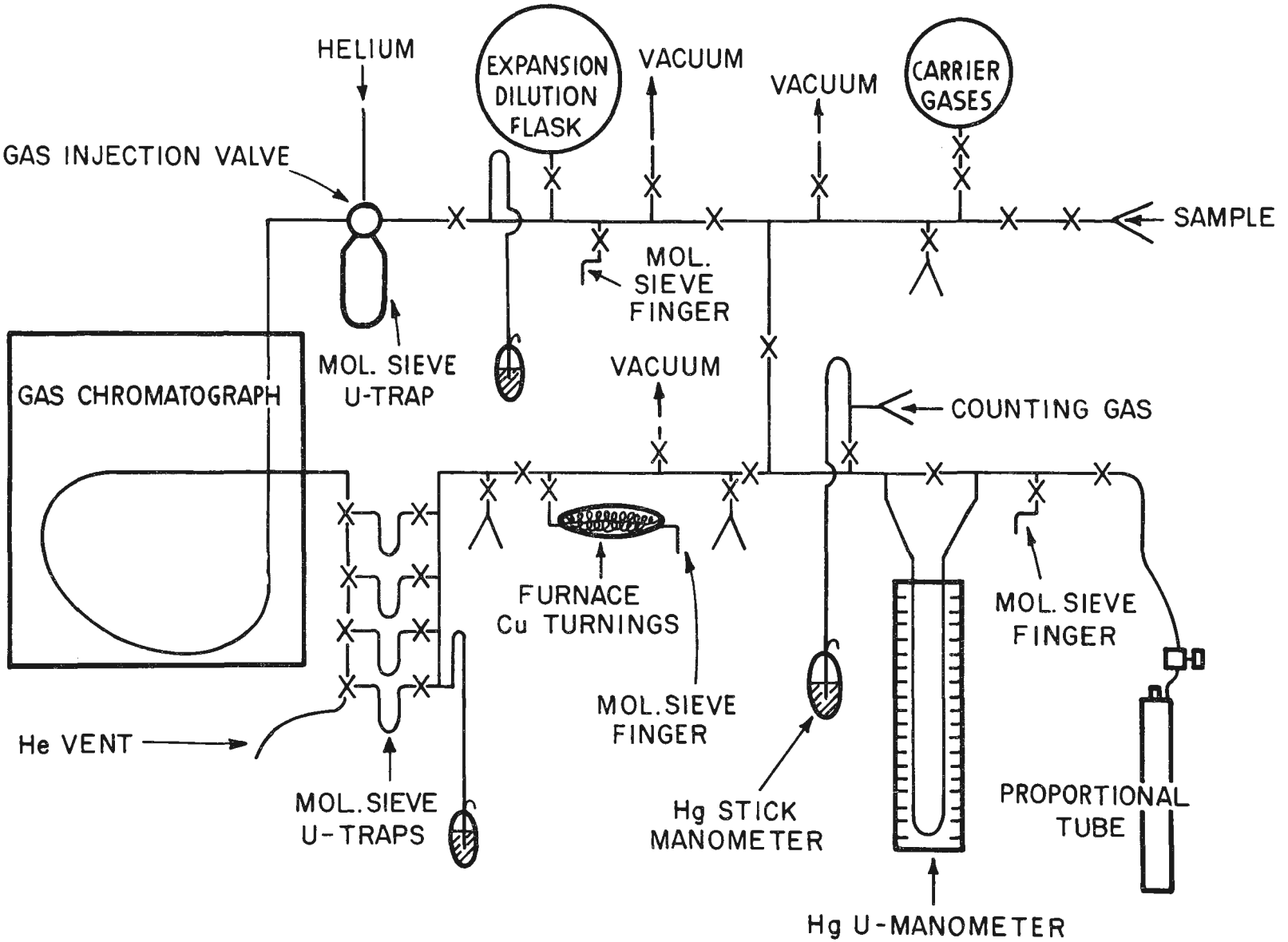

Figure 2. Schematic diagram of the high-activity gas separation system.

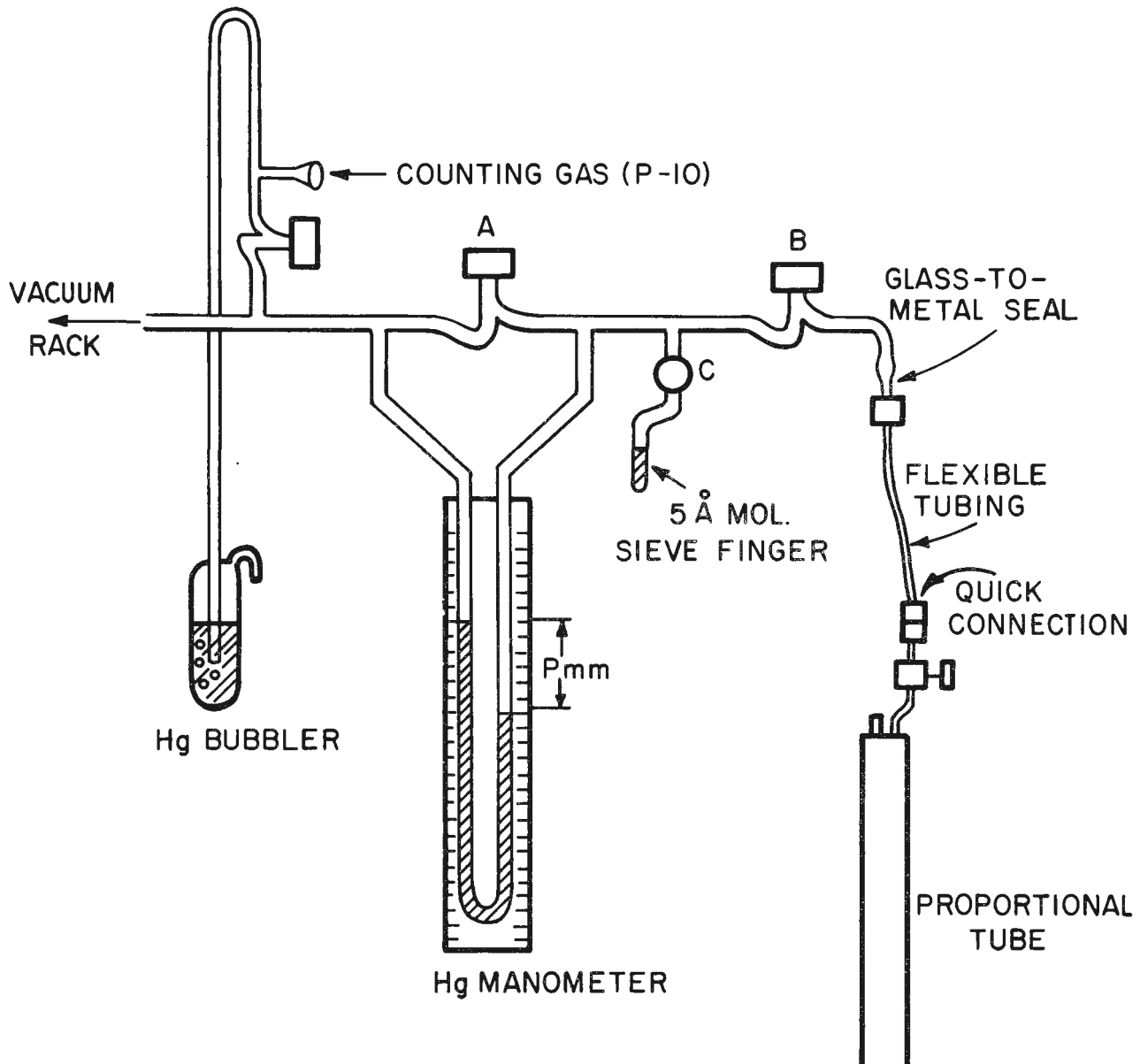

Figure 3. Volume-measure and tube-load sections of separation system.

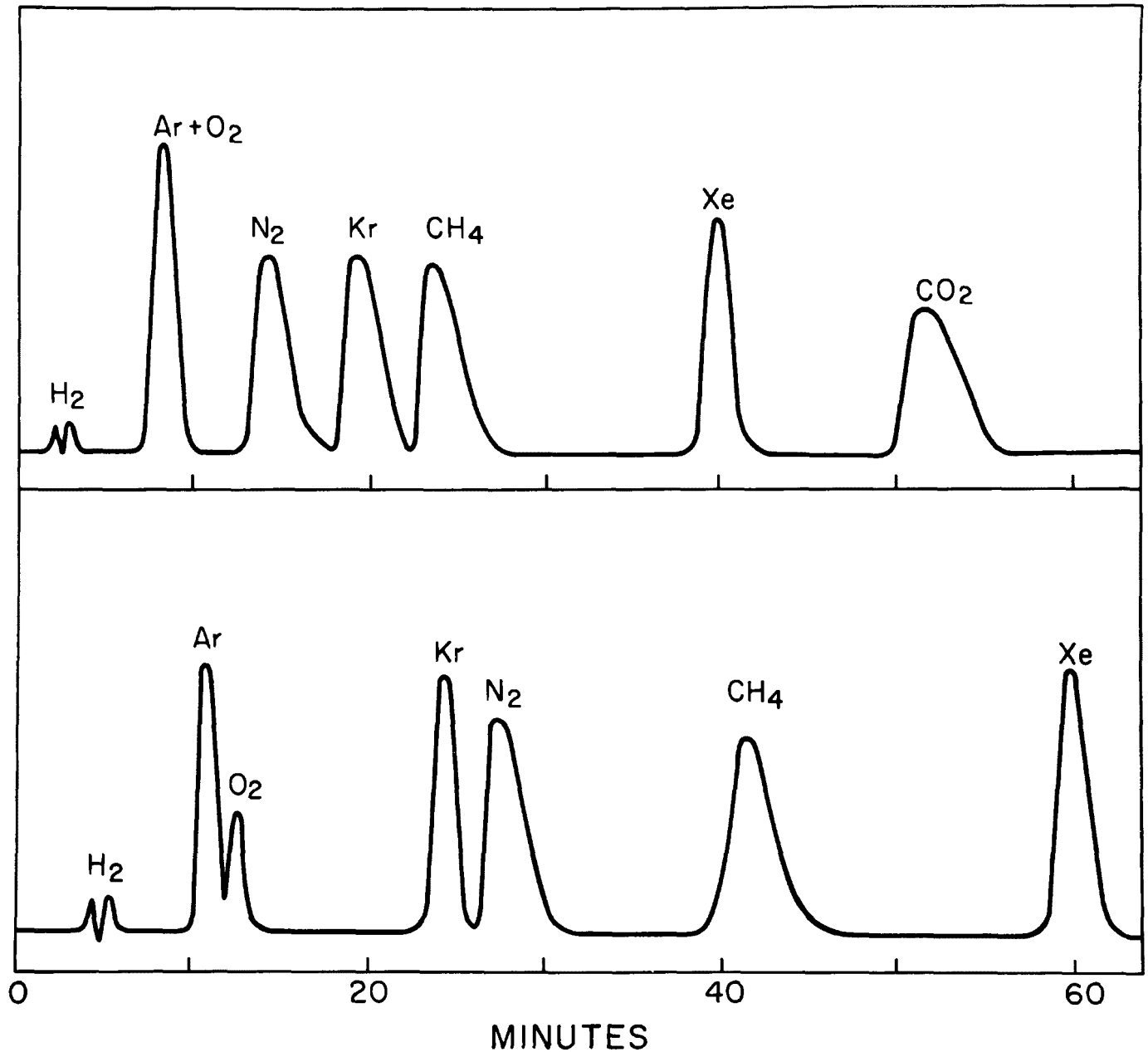

Figure 4. Chromatograms for permanent gases on molecular sieve 5A, 40-60 mesh; helium flow 60 ml/min. (Top: High-activity column; 10' x 1/4". Bottom: Intermediate-activity column; 20' x 1/4".)

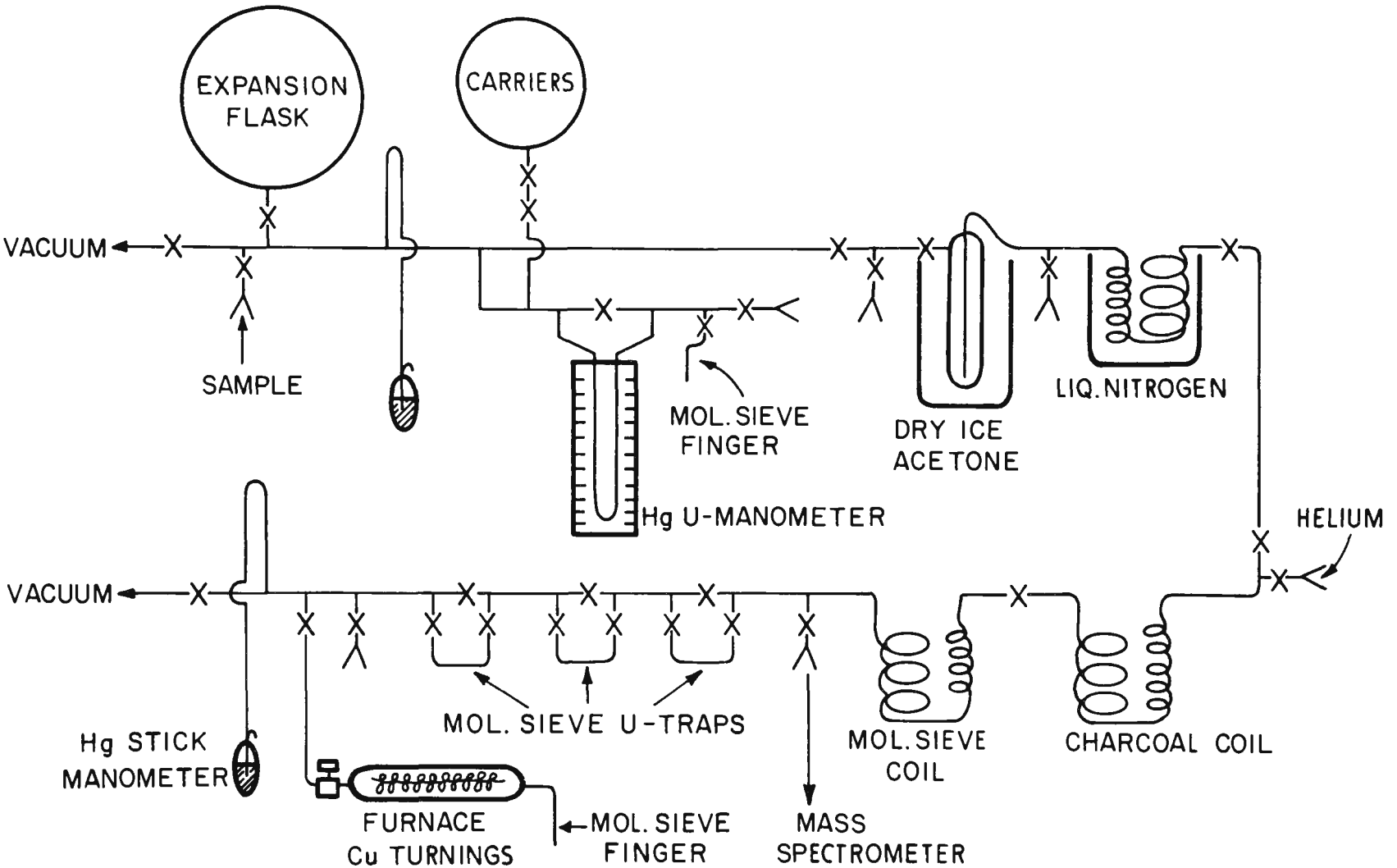

Figure 5. Bleed-down system for liter-size samples.

DETERMINATION OF TRACE NOBLE GASES IN AIR AND NATURAL GAS*

J. C. Newton, F. B. Stephens, R. K. Stump
Lawrence Livermore Laboratory,
University of California
Livermore, California 94550

Abstract

A method was developed for the analysis of air and natural gas samples containing trace amounts of noble gases. The gas samples are preconcentrated by reaction with calcium at 900-1,000°C and analyzed by mass spectrometry on an automated instrument. Methods of relating the concentrated sample to the original sample and the preparation of gas standards are given. The accuracy of the technique at the 25 ppm level was determined. The precision of the method and requirements for improving the technique are also discussed.

ACKNOWLEDGEMENTS

Special thanks go to Richard Crawford for the routines he wrote for the PDP-7 computer and for assisting with the mass spectrometer. The support of the Chemistry Mechanical Technician Division is gratefully acknowledged, especially the work of Tony Echeverria, LeRoy Schrawyer, and Jim Pastrone. Harold Crampton efficiently performed the glass blowing. The coordination of electronic support and design of the electronic control panel by Arnie Kirkewoog was especially appreciated.

INTRODUCTION

In the underground testing of nuclear devices at the Nevada Test Site (NTS), He, Kr, and Xe gases are added as tracers or are generated during the detonation. Gases, consisting principally of air, are pumped from the cavity to the surface and are sampled. For the last few years we have routinely analyzed these cavity gases to determine the noble gas concentrations at the ppm level (Cady and Cady, 1945).

More recently we had a need to determine noble gases at the sub-ppm level in natural gas. This work resulted from the Lawrence Livermore Laboratory's effort to stimulate natural gas production with nuclear explosives. In the Rio Blanco event three nuclear devices were detonated simultaneously. Cylinders of Kr, Xe, and Ne were emplaced with the lower, middle, and upper devices, respectively. We had to determine the background of noble gases in gas samples from gas wells prior to the detonation and then analyze the post-shot gas samples quantitatively for the noble gas concentrations. From this data the Laboratory hoped to assess the extent of gas communication between the three cavities.

Ordinarily an analytical mass spectrometer can detect about 100 ppm of a component in a gas mixture. The most common method of lowering this detection limit in the case of samples containing noble gases is to remove the active gases by gettering them with hot calcium (Cady, *et al.*,1945).[1]This method also eliminates interference from mass peaks due to the presence of active gases. Horton (1973) has used the gettering of air samples with a titanium sponge to lower the detection limit. We have used both methods and found gettering with Ca faster than pumping with a titanium sublimation pump (TSP). H_2, CO_2, and hydrocarbons are pumped rather slowly by hot titanium. In the case of NTS samples, gettering with Ca provides a 100-fold increase in the concentration of the noble gases. With natural gas samples the method typically gives a 10^4-fold increase in their concentration.

To calculate final results in ppm or ppb, the concentration factor[2] must be determined. For the NTS samples this is done using PVT measurements before and after removing the active gases from an aliquot with a TSP. In the case of natural gas samples, the percent of total gas pressue due to noble gases is found by analyzing the original sample before concentration on the mass spectrometer.

To calibrate the mass spectrometer, gas standards are prepared from normal air which has been gettered with Ca. The composition of normal air is obtained from literature values (Eck, 1969). Pure gases are also used as standards.

[1]These cavity samples are referred to as Nevada Test Site (NTS) samples throughout this paper to distinguish them from normal (atmospheric) air samples.

[2]$$\text{Concentration factor} = \frac{\text{ppm total noble gases after gettering}}{\text{ppm total noble gases before gettering}}$$

**This work was performed under the auspices of the U. S. Atomic Energy Commission.*

APPARATUS AND PROCEDURE

1. Analysis of NTS Samples.

The three steps in the analysis are:

(a) determining the percent of noble gases in the original sample with a TSP using a small aliquot;

(b) concentrating the noble gases from about 800ml STP of sample gas by gettering active gases with hot calcium: and

(c) analyzing the concentrated sample by mass spectrometry.

The percent noble gases in the original NTS sample is determined with the apparatus shown in Figure 1. The pressure transducer is a CGS/Datametrics 10-torr Barocel.[3] The TSP with Ti-Mo filaments has a Varian Model No. 922-0032 power supply. The TSP was built at LLL to minimize the volume. It is cooled by water circulating in coils around the circumference of the pump. The sample bulbs are constructed of stainless steel and have a volume of approximately 800 ml. Fifteen grams of CA shot are loaded into the bulb. A Nupro 8BK valve is attached to the sample bulb with Cajon 8VCR fittings.

The entire system, exclusive of the sample cylinder, is evacuated to about 10^{-6} torr. The sample bulb is filled to a pressure of about 1 atm. with sample gas and removed from the manifold. The determination of the percent of noble gases is made with the gas remaining in the vacuum cross. About 100 millitorr of gas is admitted to the manifold and 3-liter volume with the TSP valve closed. This initial pressure is recorded. Then the gas in the manifold and 3-liter volume is introduced into the TSP. The TSP filament is operated at 42 amps for one minute or less if a steady pressure value is attained. The final pressure is recorded, and the percent of total noble gases in the sample is calculated from the known volume ratio of the manifold and manifold plus TSP. The gas in the sample bulb is then gettered for 15 minutes at 900 to 1,000°C with a resistance furnace of our design. The sample bulb is cooled and transferred to the mass spectrometry laboratory.

The mass spectrometer used for the gas analysis is a CEC Model 21-103C with a multiple, automated gas inlet system, which can be operated under time-share control of a PDP-7 computer. To achieve a high sensitivity the ionizing current (electron collector current) is set to 70 microamps — rather than the usual 30 microamps. Also, we use a sample pressure of about 300 millitorr in the expansion reservoir compared to about 50 millitorr used for routine gas analysis. The ion signal is detected with a Keithley Model 640 Vibrating Capacitor Electrometer with an input resistor of 2×10^{10} ohms. Then the signal is filtered with a 0.2 Hz active filter and amplified with a Hewlett-Packard Model 2470A Data Amplifier. A gain of 100 gives a good signal-to-noise ratio. The effect of these operating conditions is to increase the mass spectrometer sensitivity (recorder divisions/millitorr) by a factor of about 200 over the usual sensitivity. At the same time the detection limit is lowered to about 1 ppm.

Samples are run on a routine basis in duplicate. Typically, a batch consists of two air standards and four air samples in duplicate. Calculation of the results is performed with a program for the CDC-6600 computer. A typical computer output is shown in Table 1. Note that the difference between the observed and calculated pressures is listed to serve as an internal consistency test.

2. Natural Gas Analysis.

The apparatus used to concentrate the natural gas samples is shown in Figure 2. Because the total concentration of noble gases may be only about 100 ppm, several aliquots (about 1,500 torr-liter each) of gas must be concentrated before sufficient sample is available for analysis by the mass spectrometer. These aliquots are transferred from the concentrating chamber to the sample bulb by the English transfer pump and the Toepler pump. It is also possible to transfer samples which have been partially concentrated from the sample bulb back to the concentrating chamber for a final quantitative gettering.

It is very important to have the system free of vacuum leaks for this work. Of course, any atmospheric leak will contain 1% Ar. However, there is an internal check available to establish if vacuum leaks have occurred. The ratio of $^{40}Ar/^{36}Ar$ for the natural gas samples differs from the same ratio for air; an examination of the consistency of these ratios is a valuable check on the integrity of the vacuum system.

While gettering the natural gas samples, the pressure is monitored with the pressure transducer. When the pressure reaches a constant minimum value, the oven is removed and the concentrator is allowed to cool to room temperature. This cooling is necessary in order to prevent the dissociation of the various Ca compounds into Ca and the respective gases. For example, if the concentrator is not sufficiently cooled before the gas is transferred with the Toepler pump, large amounts of H_2 are observed.

After several aliquots of natural gas have been concentrated and transferred, the pressure in the sample bulb can be observed. It is seen from Figure 2 that the pressure transducer can be used to measure the pressure in almost any part of the system. This is very useful for leak checking, too. Volumes throughout the system have been minimized.

Results for the noble gas content in two different samples of natural gas are given in Table 2.

[3]Reference to a company or product name does not imply approval or recommendation of the product by the University of California or the U.S. Atomic Energy Commission to the exclusion of others that may be suitable.

3. Detection Limits, Precision and Accuracy.

The detection limits for the noble gases as a function of their original concentration are listed in Table 3. The second line corresponds to values for air samples; the third line represents a typical value for natural gas. Note that the first three lines are based on a sample pressure of 300 millitorr in the expansion reservoir, and the fourth line refers to a pressure of about 30 millitorr. By concentrating more aliquots of the natural gas sample the detection limits are lowered as shown in Table 4.

The relative standard deviation (r.s.d.) for total noble gas concentration is less than ±1% of air standards gettered with a TSP. Four batches with a total of 18 normal air samples were gettered with hot calcium to evaluate the overall precision of this method; i.e., the precision value includes random errors due to the concentration and analysis steps. The r.s.d. values for the noble gases are listed in Table 5. This precision has been confirmed by over four years of experience in determining trace amounts of noble gases by this method. We routinely check the precision and reliability of our measurements by analyzing two air standards with each batch of samples. One air standard is assumed to be an "unknown" and its noble gas concentrations are calculated based on the other air standard.

The possible existence of systematic errors in the method was investigated by determining mass spectrometer sensitivities with pure noble gases and with the concentrated air standards. The sensitivities, so determined, typically agree to within ±1%, i.e., are within the precision of the method. In another accuracy check two mixtures of ^3He in argon were prepared and analyzed. The results are shown in Table 6. The agreement between calculated and experimental results was very good.

A check on the internal consistency of the mass spectrometric analysis is the agreement between the measured sample pressure in the expansion reservoir and the sum of the calculated partial pressures as shown in Table 2 on the computer printout. Typically, this pressure closure is within ±1%.

4. Method Improvement.

Attempts to getter air samples on-line with the mass spectrometer were not successful because of insufficient cooling of the hot bulbs. This lack of rapid quenching resulted in N_2, O_2, and H_2 being dissociated from their respective compounds. Also, the ratio of the Kr/He peaks was not constant. However, a horizontally movable oven which can be quickly removed from the hot bulb, and which is also amenable to remote operation, has now been built.

Because the mass spectrometer is under computer control, it should be possible to automate the entire analysis. The additional time required for temperature equilibration could be gained by overnight runs. A program has already been written that automatically analyzes the concentrated gas samples. The determination of the percent of noble gases present could be accomplished by analyzing a sample of the original gas on the mass spectrometer rather than using the TSP. A synthetic mixture of noble gases could serve as a standard. Several bulbs could be heated by moving the furnace between them in the course of the analysis of several samples. An enlarged memory core on the time-shared computer should make possible the on-line calculation of the sample compositions.

REFERENCES

Cady, G. H., and H. P. Cady., (1945), Ind. and Eng. Chem., Anal. Ed. 17, 760.

Eck, C. F., (1969), J. Chem. Ed., 46, 706.

Horton, J. C., (1973), *Mass Spectrometric Analysis of Krypton and Xenon in Low Concentrations,* Oak Ridge Gaseous Diffusion Plant, Rept. No. K-1843.

TABLE 1. Computer Output Format.

This is Sample No. 3
Pot 32-A (31813)

M/E	PPM Based on Air Std	PPM Due to Air
^{3}He	.0005	
^{4}He	5.2163	5.0330
Ne	17.6313	17.4905
Ar	8974.3960	8997.6963
Kr	3.7884	1.0950
Xe	.0787	.0836
TXe	.0831	.0836

PPM AR Calc by Diff -	8970.98		
PPM Inerts by TSP ---	8997.70		
PPM AR calc on 36 PH is	8974.40		
Sample Pressure is	316.90	and Calc Pressure is	317.02
Closure for Sample is	-.12		

TABLE 2. Results for Noble Gas Concentrations in Natural Gas.

	Local Natural Gas (PPM)	Fawn Creek #1 Well (PPM)
^{4}He	440	80
Ne	---	< .015
Ar	100	11
Kr	.006	.001
Xe	.005	.001

TABLE 3. PPB Detectable as a Function of Total PPM of Noble Gases.

Total Inerts (PPM)	Conc. Factor	PPB Detectable He	Ne	Ar	Kr	Xe
10^6(Gross)	10^0	5,000	30,000	600	800	1,000
10^4	10^2	50	30	6.0	8.0	10.0
10^2	10^4	0.5	3.0	0.6	.08	0.1
	Based on a 300 μ sample pressure					
10^2	10^4	5	30	0.6	0.8	1.0
	Based on a 30 μ sample pressure					

TABLE 4. PPB Detectable Krypton vs. No. of Aliquots Concentrated.

Aliquot No.	PPM Total Inerts	Sample Pressure Mass Spec (Millitorr)	Kr-Detectability in PPB
1	90	22	.50
2	"	44	.25
3	"	66	.16
4	"	88	.13
5	"	110	.10
6	"	132	.08

TABLE 5. Relative Standard Deviation Based on Analysis of Concentrated Air Samples.

	Relative Std. Dev.	Level in Air (PPM)*
He	± 2%	5.24
Ne	± 2%	18.21
Ar	±1%	9340.
Kr	±1%	1.14
Xe	±15%	.087

*Literature Value

TABLE 6. Accuracy of ^{3}He at 350 and 25 PPM levels.

	Std. A	Std. B
Calculated PPM ^{3}He	350.	25.3
PPM Determined - Conc. Air Std.	352.	35.4
PPM Determined - Pure Gas Std.	346.	25.0

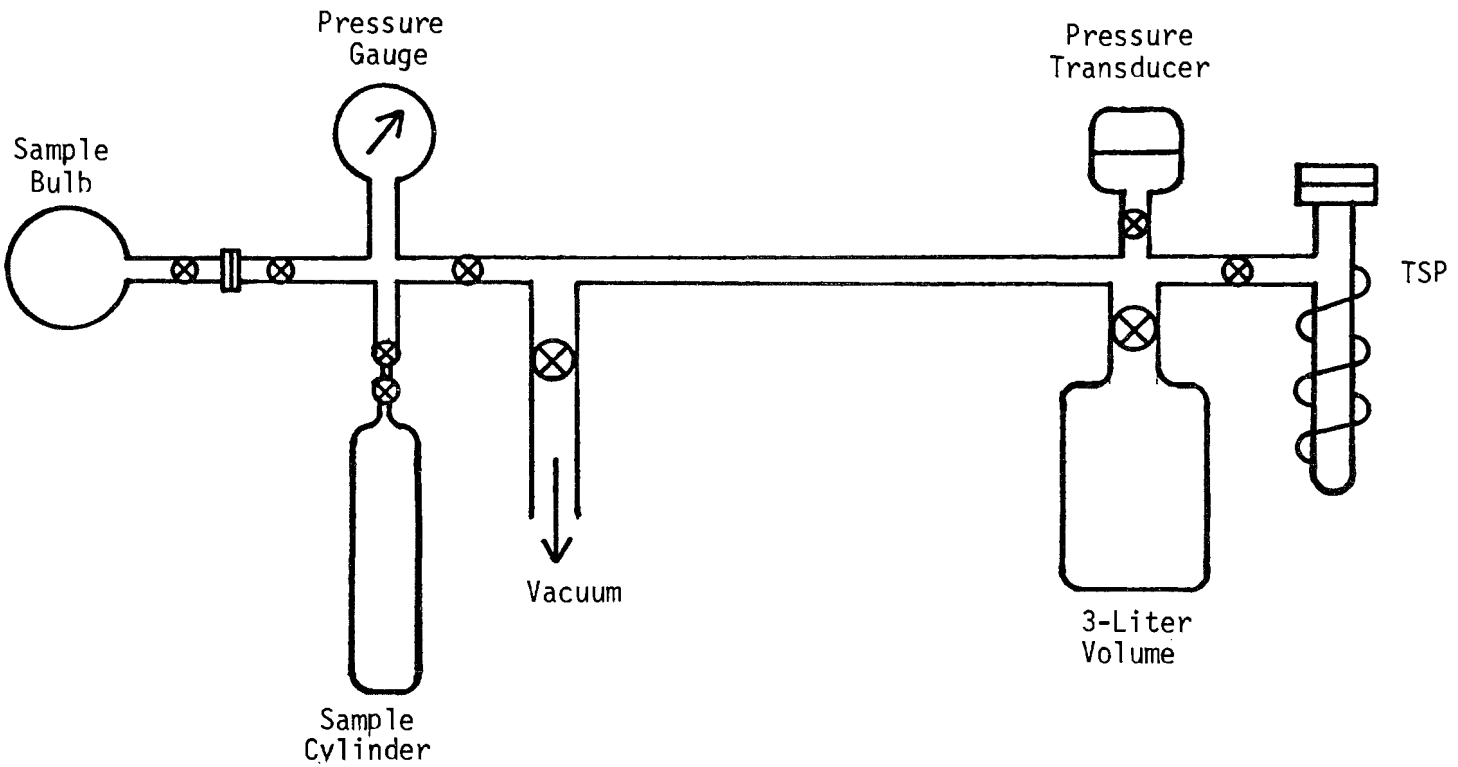

Figure 1. Apparatus to Determine Percent of Noble Gases in Sample.

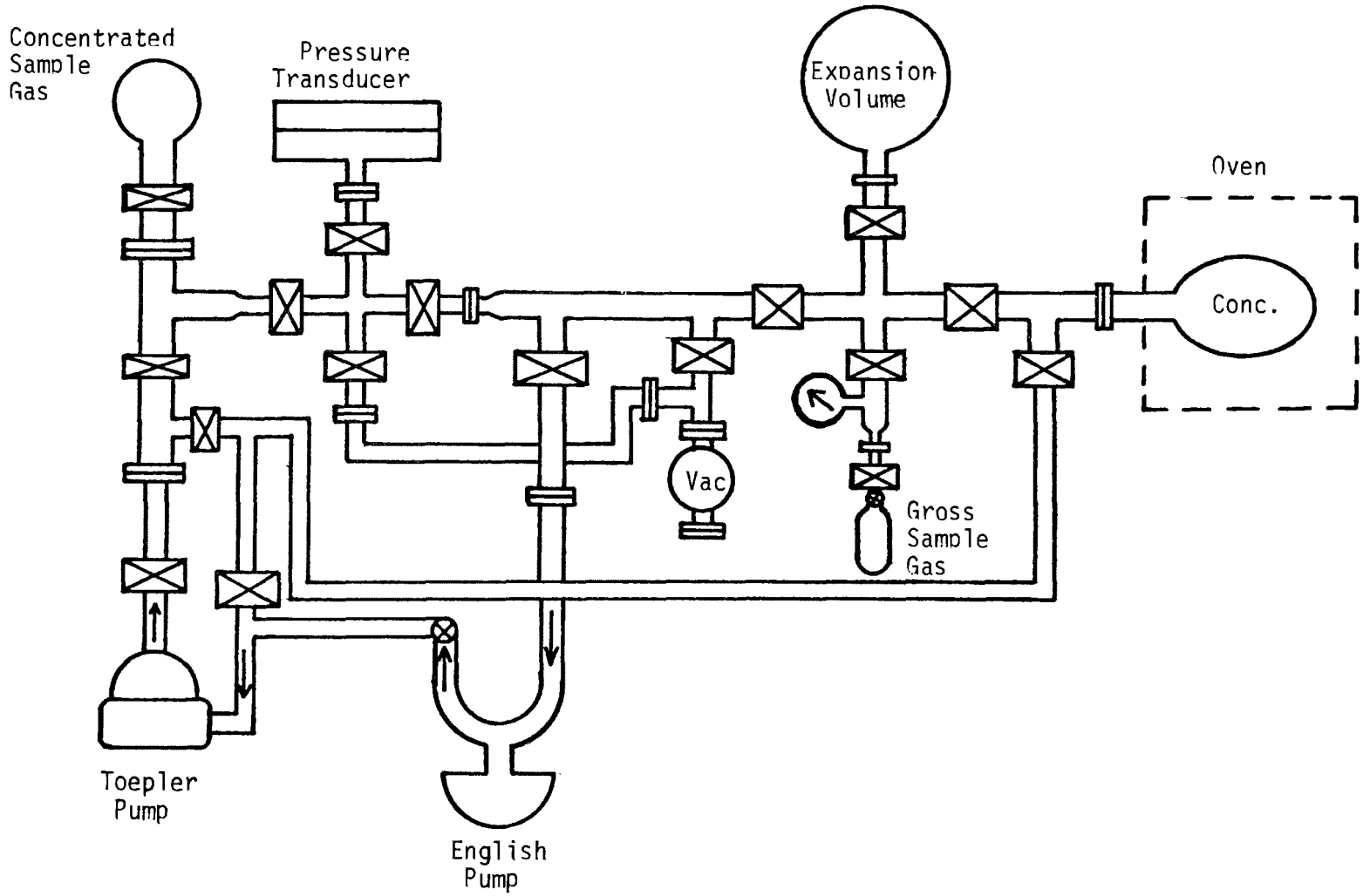

Figure 2. Vacuum Line to Concentrate Natural Gas.

PORTABLE APPARATUS AND PROCEDURE FOR THE SEPARATION OF KRYPTON, XENON, AND METHANE IN AIR

F. B. Johns
National Environmental Research Center-Las Vegas
U.S. Environmental Protection Agency
Las Vegas, Nevada

Abstract

A portable apparatus and procedures are described for the rapid separation, collection, and counting of radio-krypton, -xenon, and -methane in atmospheric air. The apparatus consists of a series of adsorbing and chromatographic columns. Subsequent elution of the krypton, xenon, and methane at various temperatures provide the separation.

The detection of the various gases is accomplished with the use of a unique thermistor detector circuit. After volume determination, the krypton, xenon, and methane are dissolved in a degassed toluene-base, liquid scintillation solution, and counted in a small commercial liquid scintillation counter.

With this apparatus and separation method, the krypton, xenon, and methane from a one-m^3 air sample can be separated in 2 to 2.5 hours, a short enough time that the 76-minute, 2.8-hour, and 4.4-hour half-life krypton isotopes can be detected with a lower detection limit of 10 pCi/m^3. Krypton-85, xenon-133, xenon-135, and methane can be detected at the 2 pCi/m^3 level.

INTRODUCTION

The construction and use of a portable apparatus for the separation of krypton, xenon, and methane from atmospheric samples is described. The apparatus, and its associated counting system, can be readily transported to any site where electricity is available or can be provided. The need for this device became apparent in 1971 with the proposal to do on-site investigations of nuclear power reactors. The radioactive noble gases, with the exception of krypton-85, have short half-lives, and it follows that the time for transporting the samples to a laboratory for analysis will inhibit the collection of the necessary data concerning these isotopes. With the system described below, half-lives of two hours may be easily quantitated. Detectable limits of 2 pCi/m^3 are attained for krypton-85, xenon-133 or 135, and tritiated methane, with recoveries of 85% of krypton, 70% of xenon, and 40% of methane. This system is a portable version of the separation system described by Stevenson and Johns (1971) using the counting method described by Shuping, *et al.*, (1969).

APPARATUS

The apparatus consists basically of three gas chromatographs adapted to accept the large sample. Photograph 1 portrays the system as it is presently being used, and Figure 1 is a flow diagram of the system. The cabinet can be disassembled into two portions. The lower portion contains the mechanical vacuum pump (133 liter/min at 0.1 micrometer) and storage. A filter is attached to the discharge of the pump to collect oil fumes. A shelf is provided to support the helium carrier bottle.

The upper portion contains the separation section, the collection system, and the electronic controls and recorder, as described below.

1. The Separation Section.

This section consists of three portions: a sample introduction-noble gas collection portion, and two chromatographic separation systems. Toggle-operated vacuum valves (Nupro 4B K-T) are used throughout the apparatus. The sample introduction-noble gas collection system consists of a molecular sieve trap (200 grams of one-eighth x three-sixteenth inch, 13X pellets), a pre-cooler, a charcoal trap (100 grams, 16-20 mesh activated charcoal), a vacuum gauge (0-760 mm of Hg), and a thermistor detector. The traps are all glass as illustrated in Figures 2 and 3, and are attached to the metal system with metal ball joints. These ball joints havehad an O-ring groove added, and are silver-soldered to a short length of flexible metal tubing (Figure 4). The O-ring eliminates the use of lubricant on these connections. The flow rate of the sample is controlled by maintaining a pressure of 350 mm of mercury on the system, using the control valve on the sample bottle, and a vacuum on the outlet of the charcoal trap. The thermistor detector is used to indicate the final elution of the gases from the charcoal trap. A source of helium carrier gas is provided through a flow meter as indicated in Figure 1.

The two chromatographic separation systems consist of two molecular sieve columns, (100 gm 30-60 mesh 5A molecular sieve), thermistor detectors on the outlet of each of the columns, and a helium flow meter.

2. The Collection System.

The collection system consists of a mini-trap (C-2) (6 in. of 1/8" copper tubing packed with 0.3 grams of chromatograph-grade 30-60 mesh charcoal), a liquid scintillation vial with luer fitting (Figure 5), and a digital manometer (0-100 mm of Hg). A special valve (Figure 6) is used to direct the flow from the second molecular sieve trap either to vent or to the mini-trap. The total volume of the system is kept as small as possible.

3. The Electronic System.

Figure 7 shows the schematic wiring diagram of the system. Two types of thermistor cell blocks are used; one, on the outlet of the first charcoal trap, is a two-thermistor cell, reference, and detector; and the other, a three-cell block, is located on the outlet of the first and second molecular sieve trap. It consists of three thermistors, one reference, and two separate detectors. Figure 8 shows the plumbing of these two cells. During operation of the system a current of 150 mA is maintained on the cell being used by means of an adjustable potentiometer (R-2). By switching (S-1) to the proper cell position the flow through the cell may be monitored. The output is fed into a 1 mV recorder through the attenuating switch (S-2).

4. Counting Apparatus.

The liquid scintillation counter used with this apparatus is a Beckman Beta Mate II. This is a single sample, single channel, manually-operated counter. Now permanently mounted on a little red wagon (Photograph 2), the counter has been modified for easier transport and use. The lead shield bricks have been bolted in place and additional shielding added to cover the pre-amps. The instrument, as received, has a five-digit printout which was modified to add a sixth digit. A time-of-day clock was added; also the original timing circuit was changed to increase counting time capabilities. Prior to transport, the preamps and photo tubes are removed in total darkness, and shock mounted in a separate case.

PROCEDURE

1. Principle of the Method.

This method describes a procedure for the separation of various gaseous radionuclides from gross air samples. The air samples are received either as a "grab" sample, a "cryogenic" sample, or an "integrated" sample. The grab sample represents approximately 10 cubic feet of air collected at a flow of 15 cubic feet per minute. The cryogenic sample represents an integrated sample collected at a flow of 3 to 4 cubic feet per minute for one hour. The integrated sample represents a continuous sample of approximately five cubic meters collected at a single sampling point for one week. The sample is transferred to the gas analysis apparatus. Water and carbon dioxide are removed in a molecular sieve trap. The krypton, xenon, and methane are separated by elution through a molecular sieve column at various temperatures. The volumes of the separated gases are measured for yield determination, and transferred to appropriate counting chambers.

Reagents:
- Alcohol bath, -32°C
- Charcoal, 16-20 mesh
- Molecular sieve 5A, 30-60 mesh
- Molecular sieve 13X, 1/8" x 3/16" pellets
- Liquid Nitrogen
- Liquid scintillation cocktail, 0.6g POPOP, 10.0 gPPO, 2,000 ml scintillation grade toluene
- Dry ice
- Acetone
- Helium
- Xenon carrier
- Krypton carrier

a. Initial Preparation.
All traps are degassed at 350°C and evacuated until a pressure of $< 10^4$ mm of mercury is obtained. The traps are then filled with helium; the thermistor cells are zeroed with a flow of helium. The pre-cooler, C-1, MS-1, and MS-2 are cooled with liquid nitrogen (LN).

b. Sample Transfer.
Because of the different types of samples, the transfer of the sample will be treated separately:

(1) Grab.
Record weight and pressure of the sample bottle. Connect bottle to the sample inlet port and place in a heating mantle. Using a vacuum pump on exit from C-1, and suitable valving, establish sample flow through the molecular sieve trap, pre-cooler, and C-1 of about 15 liters per minute and 35 cm pressure. (Reduced pressure is necessary to avoid condensation of liquid air in system.) Continue bleeding sample until the pressure drops to less than 10 mm of mercury. Shut off sampling inlet port and add the carriers.

(2) Cryogenic.

Remove the sampler from the 25-liter liquid nitrogen dewar, and place in a furnace capable of reaching 350°C in 45 minutes; attach helium line to inlet of sampler and outlet to sample inlet port. Check for leaks. With suitable valving, use needle valve on helium inlet to establish flow through pre-cooler and C-1 of 15 to 20 liters/minute at 35 cm helium pressure with roughing pump. Continue adding sample until the molecular sieve sampler is at 350°C; hold for 30 minutes, shut helium valve and sample inlet port, and add carriers.

(3) Integrated.

Record weight and pressure of the sample bottle. Connect the sample bottle to the sample inlet port. Using the vacuum pump on the exit from C-1, and suitable valving, establish sample flow through molecular sieve, pre-cooler, and C-1 of about 15 liters per minute and 35 cm absolute pressure. Continue bleeding sample into C-1 until the pressure drops to less than 10 mm of mercury. Shut off sampling inlet port. As the sample has had 1 ml stable xenon carrier added before sampling, and the one cubic meter of air contains 1.14 ml stable krypton and 1 ml methane, no further carriers need be added.

c. Water Removal and Recovery.

The water and carbon dioxide are collected in the molecular sieve trap and may be recovered by heating.

d. Air Removal from C-1.

Close valves C and B, open valve D with C-1 in LN; establish helium flow (600-800 ml/min) through C-1, thermistor 1, vent. Remove LN from C-1, and replace with dry ice acetone (DIA) slush. Continue this flow until all of the air is removed — as evidenced by a return of the pen recorder to the baseline (approximately 55 minutes). Shut vent valve and helium flow.

e. Removal of Krypton, Xenon, and Methane from C-1.

(1) Leave DIA on C-1 and re-establish helium flow C-1, thermistor 1, MS-1, Vent 2. MS-1 and MS-2 are in LN when flow is stabilized. Remove DIA from C-1 and replace with electric furnace and start heating.

(2) Continue heating until a temperature of 350°C is reached, or until all of the gases are transferred to MS-1. This is indicated by a return to baseline by recorder (a shift in baseline is usually noted at this point, due to the higher temperature of the gases entering the thermistor block, and also by a decrease in flow rate).

(3) Shut Vent 2 and turn off helium flow. Open high vacuum valve to C-1, and continue heating until a temperature of 350°C is reached, and a vacuum of $< 10^{-4}$ mm of mercury is obtained. (C-1 is then ready for another run.)

f. Separation of Krypton, Xenon, and Methane from MS-1.

(1) With LN on MS-1 and MS-2, establish helium flow to (200-300 ml/min) MS-1, thermistor 2, vent 2.

(2) Remove LN from MS-1 and replace with a -23°C alcohol bath. After approximately two minutes, a sharp increase is noted on the recorder. This is the argon and oxygen. Continue helium flow until the pen returns to near the baseline (4 to 5 minutes). (Leave a small amount of oxygen.)

(3) Quickly rearrange helium flow, MS-1 to MS-2 to vent-3. (The oxygen transferred to MS-2 is used as an indication in the elution of krypton from MS-2.) Continue flow until the krypton is eluted from MS-2, approximately 12 to 14 minutes.

(4) Quickly rearrange flow MS-1 to vent-2 (MS-2 and vent-3 closed). Replace the alcohol on MS-1 with cold water (20°C), and elute the nitrogen to vent. Watch the elution of nitrogen carefully and, by rearranging the flow MS-1 to MS-2 to vent-2, transfer the last of the nitrogen peak to MS-2 (this is mostly methane).

(5) Place immersion heater in the cold bath, and heat until the carbon monoxide and xenon are all transferred to MS-2, (10 to 12 minutes). Remove boiling water from MS-1.

g. Separation and Collection of Krypton, Methane, and Xenon from MS-2.

(1) Prepare C-2 by heating with a heat gun. Place a clean liquid scintillation vial and valve (P*) in position. Evacuate to 0.0 mm on the manometer. Place LN on C-2.

(a) Arrange helium flow MS-1, MS-2, thermistor 3, vent 3. Remove LN from MS-2 and replace with -23°C alcohol bath. The small oxygen peak which will be noted in two minutes is vented, (this indicates the normal operation of the system). When the krypton peak appears, immediately close vent 3 and open valve M. Collect the krypton in C-2 until the pen on the recorder returns to baseline. Close valve M, open vent 3 and allow helium to continue to flow.

(b) Remove the helium in C-2 by pumping until a pressure of < 0.1 mm of mercury is attained. Close vacuum valve (N), and heat C-2 to transfer the krypton to the vial. When pressure has stabilized, record pressure and temperature. Close valve P. See following procedure (2).

(c) Repeat preceding procedure (1) for the methane separation.

(d) Flow should still be MS-1, MS-2, thermistor 3, vent 3. Replace alcohol bath with cold water (20°C). A small peak of nitrogen should be noted on the recorder. When the methane peak appears, immediately close vent 3 and open valve M. Collect the methane in C-2 until the recorder returns to the baseline. Close valve M, open vent 3 and allow helium to continue to flow.

(e) Transfer the methane to the vial as in Section b.

(f) Repeat preceding procedure (1) for the xenon separation.

**P is a Luer Teflon plug valve.*

(g) Flow should be MS-1, MS-2, thermistor 3, vent 3. Heat, with immersion heat, MS-2. Allow the carbon monoxide peak to vent, and immediately close vent 3; open valve M. Collect the xenon in C-2 as in procedure (a).

(h) Transfer the xenon to vial as in Section b.

(2) Fill each scintillation vial with degassed toluene-base, liquid scintillation cocktail as illustrated in Photograph 3, and place in liquid scintillation spectrometer for determination of radioactivity.

2. Calculations.

$$V_1 \quad 1.14 \times \frac{\text{sample wt.}}{1293}$$

$$V_3 \quad 1.0 \times \frac{\text{sample wt.}}{1293}$$

where V_1 volume krypton in sample

V_3 volume methane in sample

1.14 vol concentration of krypton normally found in air

1293 gm air per cubic meter

1.0 vol concentration of methane normally found in air

$$V_{Kr}, V_{Xe}, \text{ or } V_{CH_4} \quad v \times \frac{p}{760} \times \frac{273°}{t+273°} \quad \text{volume recovered}$$

where v vial volume + volume of C-2 and transfer line

p pressure in vial

$$\frac{V_{Kr}}{V_1} \times 100 \quad \% \text{ Kr recovered}$$

$$\frac{V_{Xe}}{V_2} \times 100 \quad \% \text{ Xe recovered}$$

$$\frac{V_{CH_4}}{V_3} \times 100 \quad \% \text{ } CH_4 \text{ recovered}$$

where V_2 volume Xe carrier added to sample

$$pCi/m^3 = \frac{cpm}{\{\text{Counting Efficiency}\} \text{ volume gas in vial } \% \text{ recovery}}$$

REFERENCES

Shuping, R. E., C. R. Phillips and A. A. Moghissi, (1969), *Low Level Counting of Environmental Krypton-85 by Liquid Scintillation*, Analytical Chemistry.

Stevenson, D. L. and F. B. Johns, (1971), *Separation Techniques for the Determination of ^{85}Kr in the Environment*, International Atomic Energy Agency, Vienna, pp 157-162.

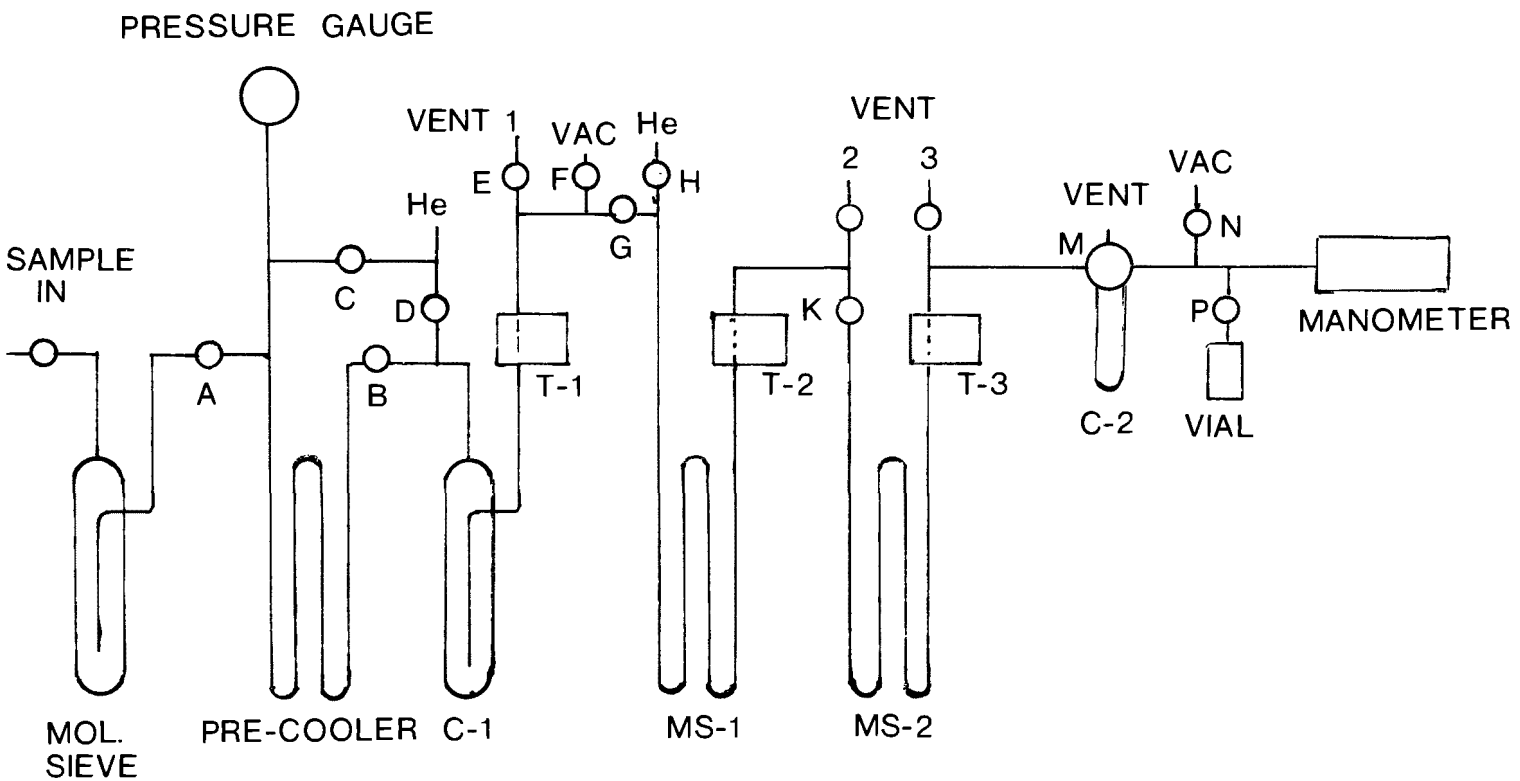

FLOW DIAGRAM FOR SEPARATION OF METHANE, KRYPTON, AND XENON

Figure 1.

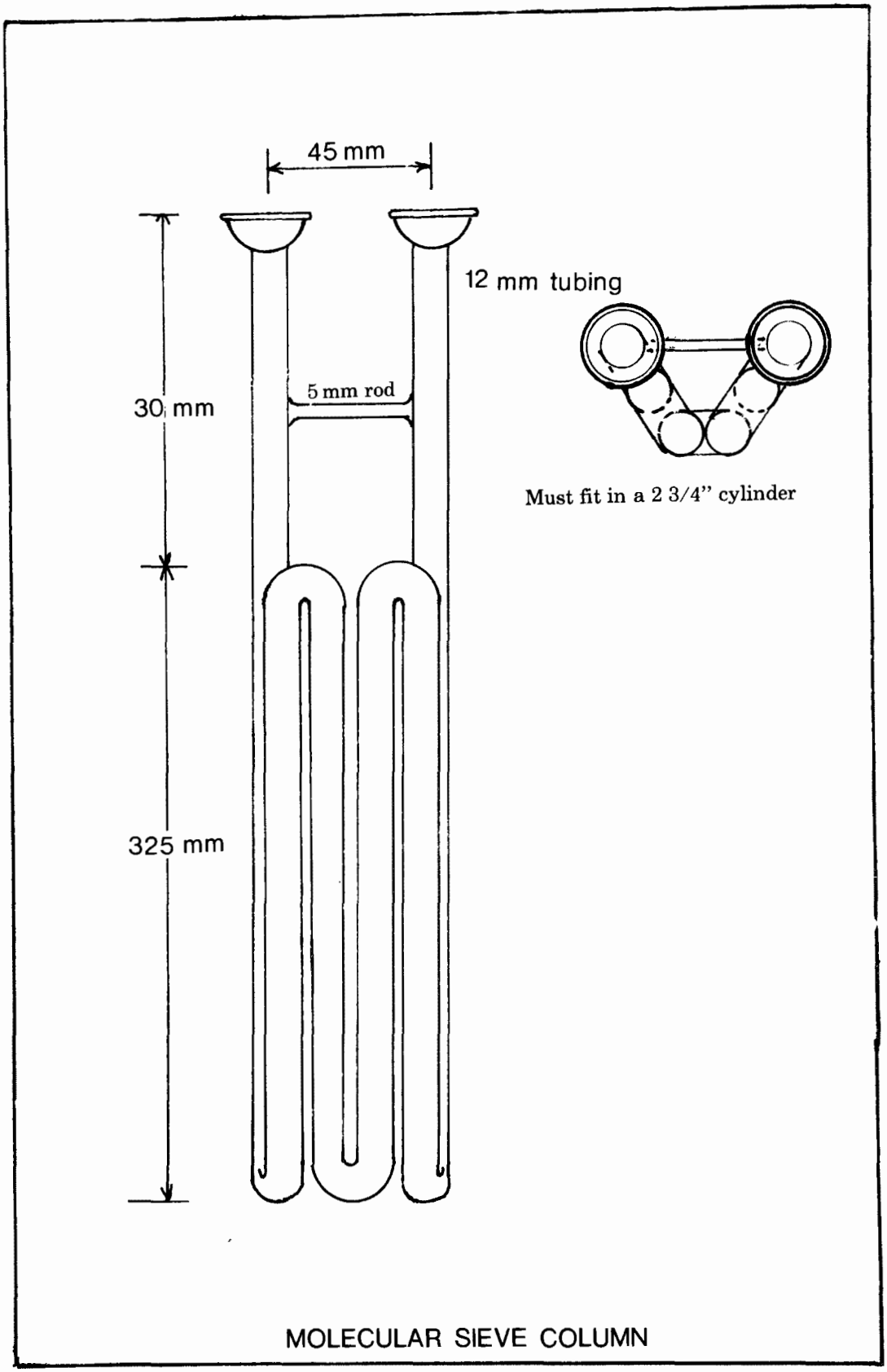
45 mm
12 mm tubing
5 mm rod
30 mm
325 mm
Must fit in a 2 3/4" cylinder
MOLECULAR SIEVE COLUMN

Figure 2.

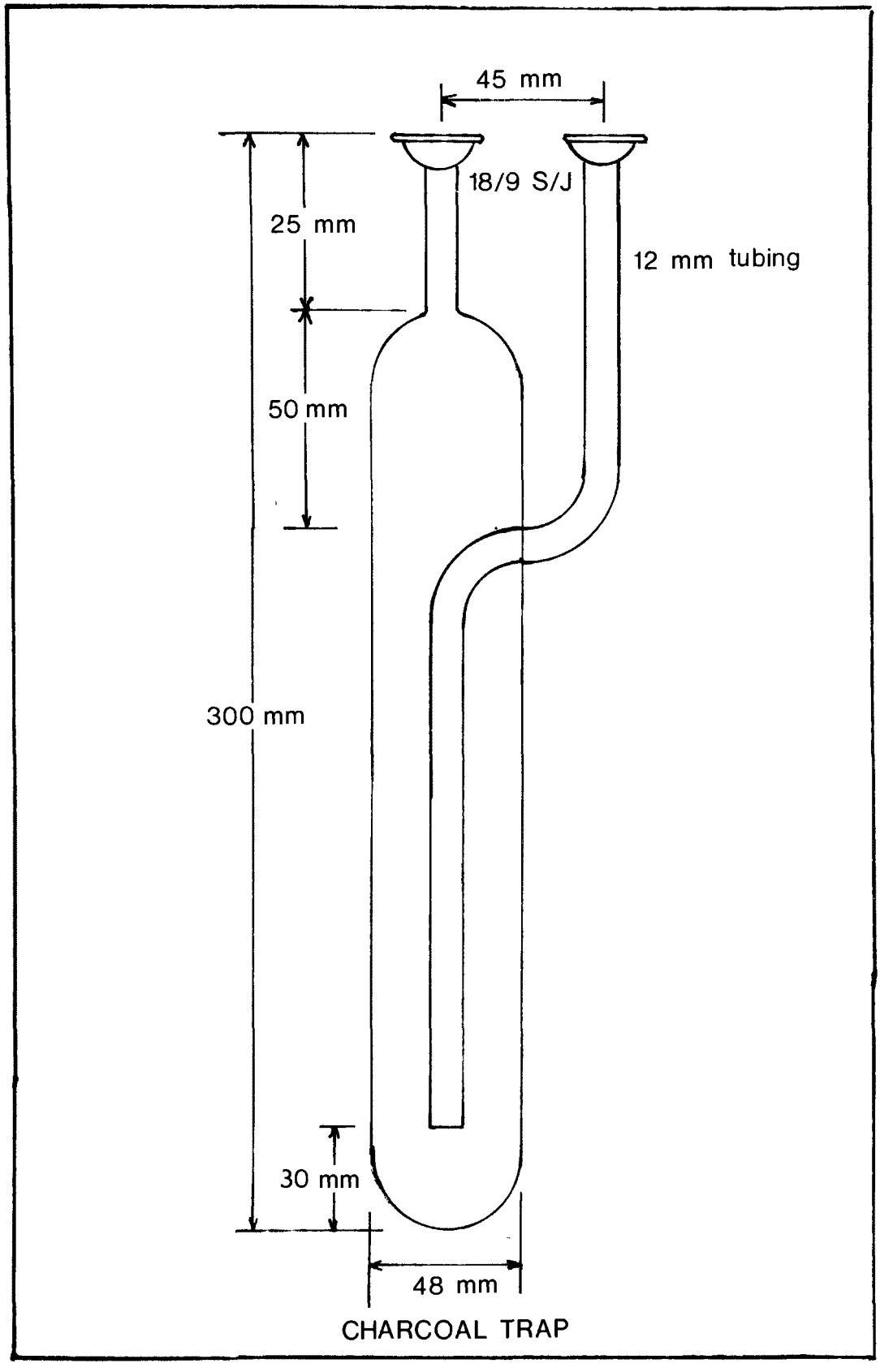
45 mm
18/9 S/J
25 mm
12 mm tubing
50 mm
300 mm
30 mm
48 mm
CHARCOAL TRAP

Figure 3.

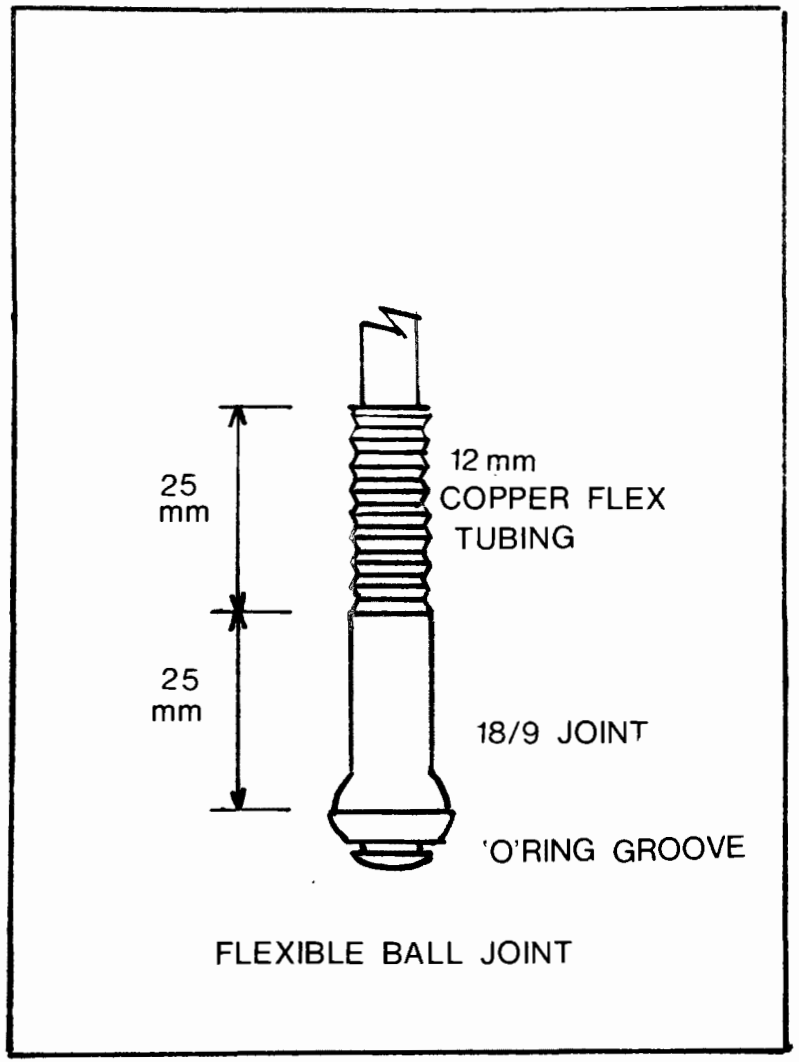

Figure 4.

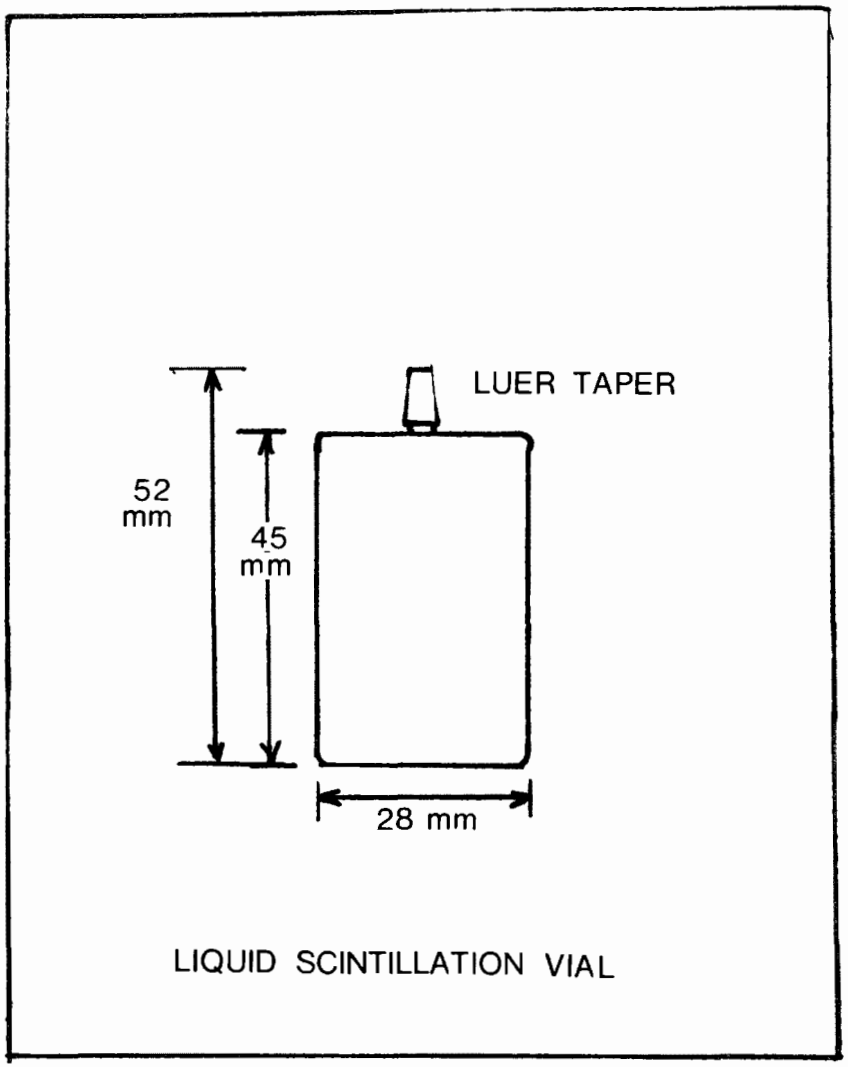

Figure 5.

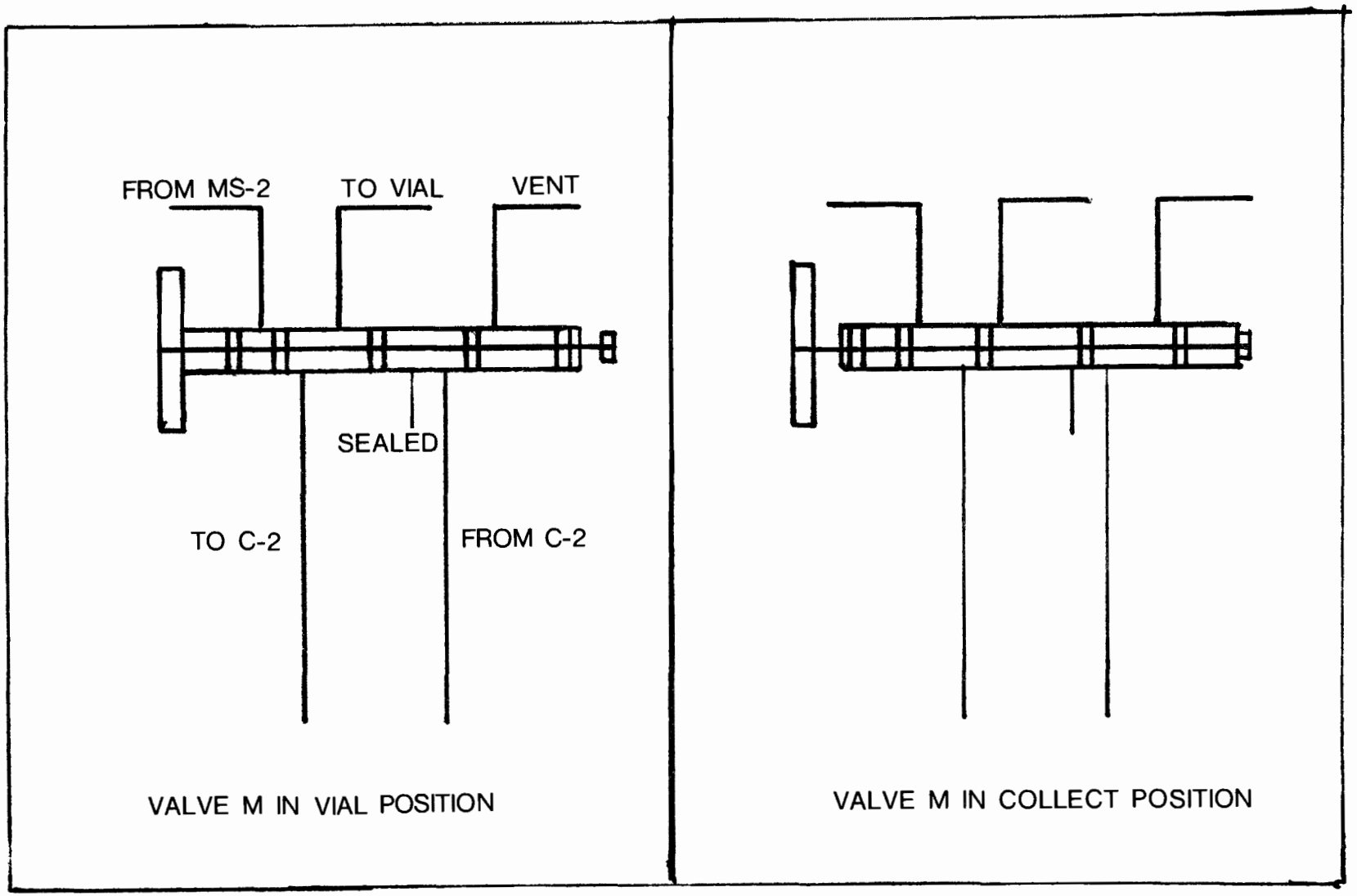
FROM MS-2
TO VIAL
VENT
SEALED
TO C-2
FROM C-2
VALVE M IN VIAL POSITION
VALVE M IN COLLECT POSITION

Figure 6.

Figure 7. Schematic Wiring Diagram.

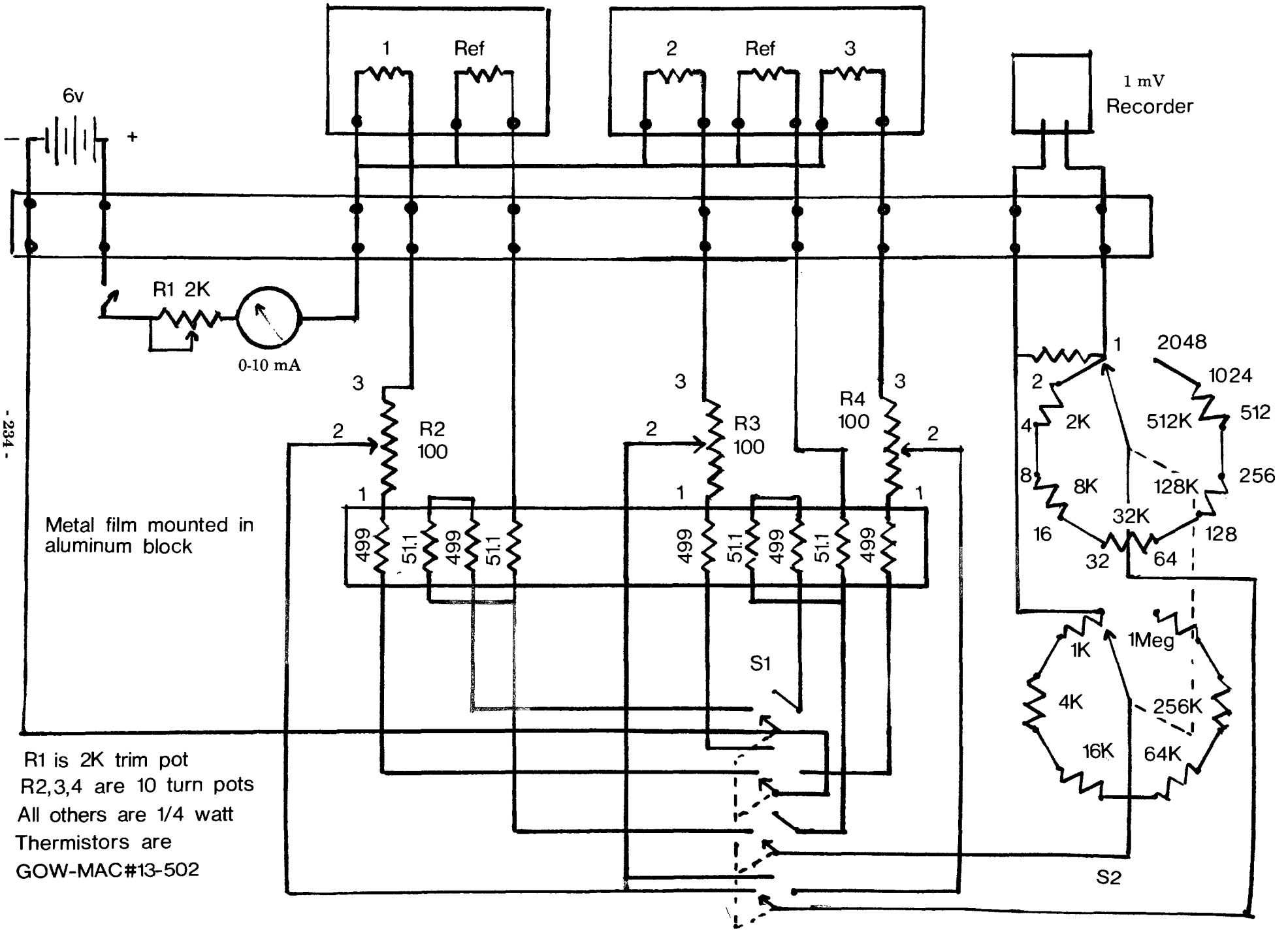

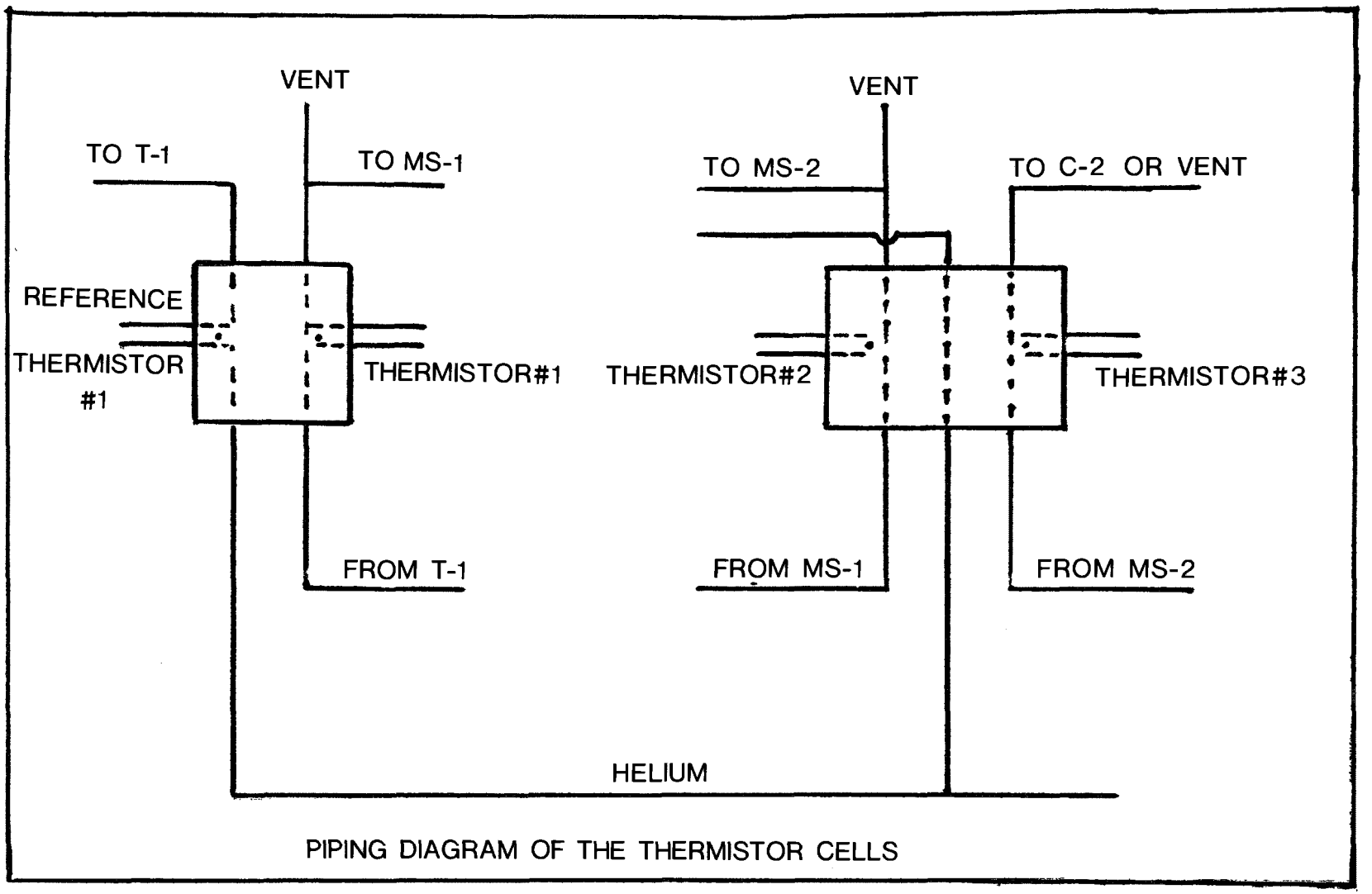
VENT
TO T-1
TO MS-1
REFERENCE
THERMISTOR
#1
THERMISTOR#1
FROM T-1
VENT
TO MS-2
TO C-2 OR VENT
THERMISTOR#2
THERMISTOR#3
FROM MS-1
FROM MS-2
HELIUM
PIPING DIAGRAM OF THE THERMISTOR CELLS

Figure 8.

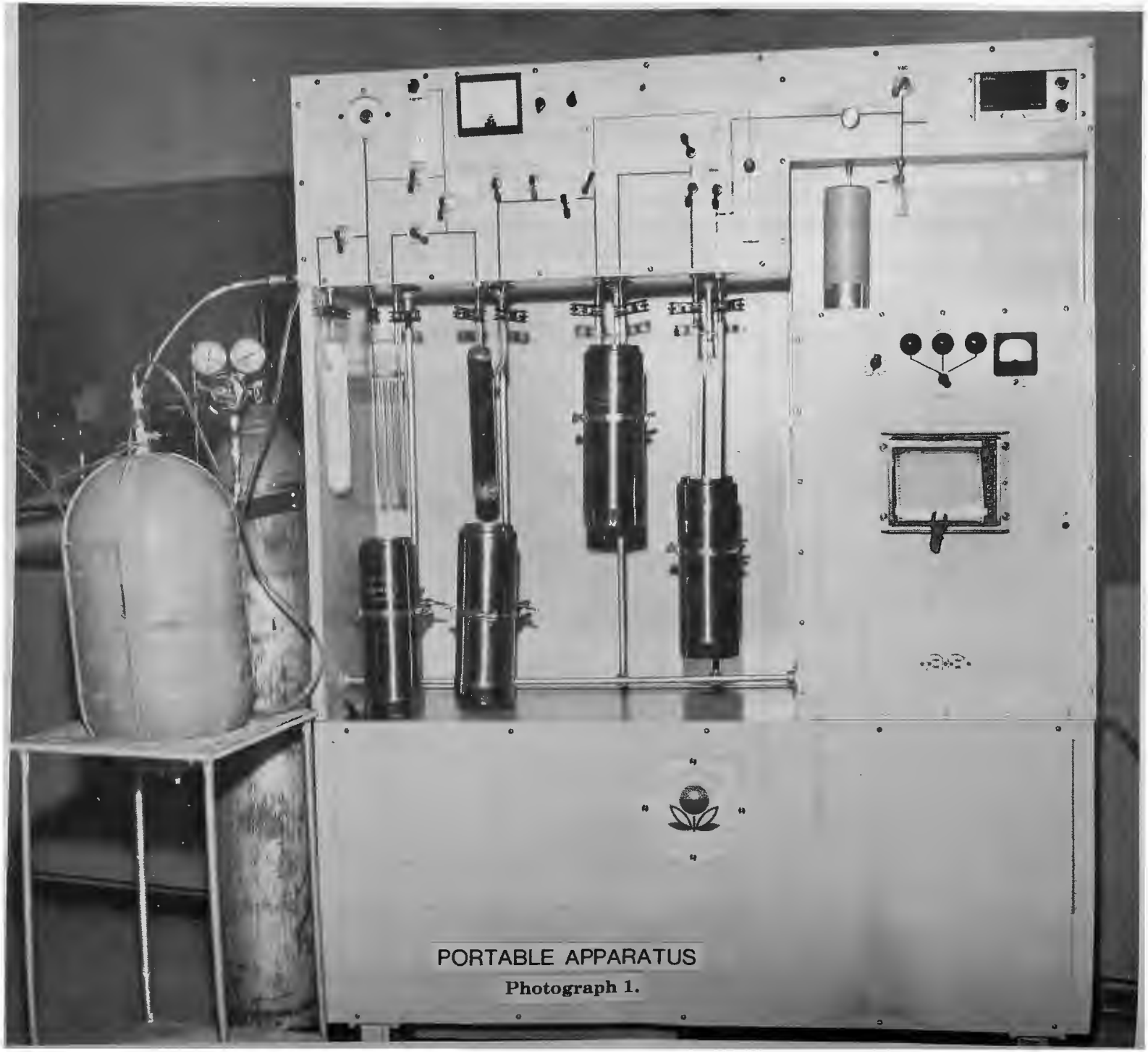

PORTABLE APPARATUS

Photograph 1.

LIQUID SCINTILLATION COUNTER

Photograph 2.

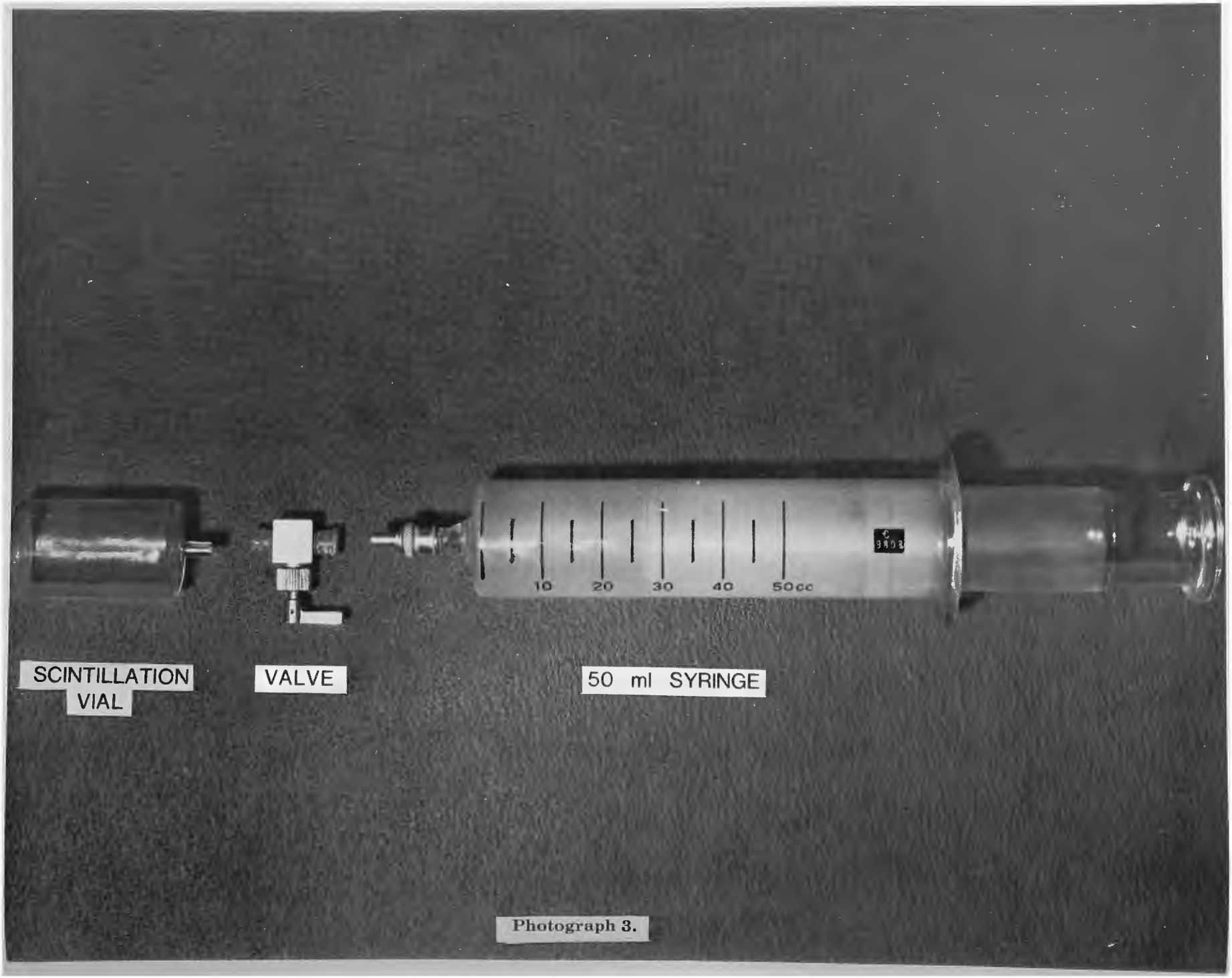

Photograph 3.

INTERNAL GAS-PROPORTIONAL BETA-SPECTROMETRY FOR MEASUREMENT OF RADIOACTIVE NOBLE GASES IN REACTOR EFFLUENTS*

C.J. Paperiello
Radiological Sciences Laboratory
Division of Laboratories and Research
New York State Department of Health
Albany, New York 12201

Abstract

At the Radiological Sciences Laboratory of the New York State Department of Health, gas fractions separated by gas chromatography are analyzed by internal gas-proportional spectrometry systems. These systems include gas-proportional detectors, plastic anticoincidence detectors, multichannel analyzers, and associated electronics. Detector systems are enclosed in 6-inch thick steel shields.

Internal proportional counting with multichannel analysis offers several advantages, particularly improved sensitivity and specificity. Gas counting efficiencies are greater than 60% for ^{37}Ar and 90% for ^{85}Kr. Detector background with 100-ml copper proportional tubes and plastic anticoincidence guards is on the order of 0.3 cpm for ^{37}Ar and 1.5 cpm for ^{85}Kr. Shielded and guarded steel tubes have backgrounds approximately four times higher, but are acceptable for high-level reactor samples.

By examining the spectra with a multichannel analyzer, the figure of merit for low-energy beta-emitters is greatly improved over integral bias counting. The purity of the sample following chromatographic separation can also be checked. Within certain abundance ratios, the levels of ^{3}H and ^{14}C in hydrocarbon fractions can be determined without combustion. Similarly, direct ^{37}Ar and ^{39}Ar measurements are possible.

The application of spectrometric techniques for analysis of several types of reactor gas effluents is discussed.

INTRODUCTION

At the Radiological Sciences Laboratory of the New York State Department of Health, reactor gas effluents are analyzed by Ge(Li) gamma-ray spectroscopy and internal gas-proportional spectrometric systems. Although gamma-ray spectroscopy is the simpler procedure, low-background beta-proportional counting offers greater sensitivity for all gaseous radioactive fission products, and for those which decay with little or no gamma emission it is an absolute necessity. Although one might expect the activity of reactor samples to be so high a low-background system is not needed, this is not the case. The range of activity ratios for a given sample may be 10^7 between nuclides, and the range of activity may be greater than 10^5 between samples, resulting in an overall range of about 10^{12} in activity in these studies.

The use of multichannel analyzers for counting proportional tube output offers several advantages as compared to integral bias counting. These include improvement in the figure of merit for some beta-emitters, a check on the purity of the sample after chromatographic separation, and simultaneous analysis of certain isotopic mixtures found in reactor gas effluents after chromatographic separation. These mixtures include $^{37}Ar/^{39}Ar$ in the radioargon fraction, $^{14}C/^{3}H$ in methane, and other hydrocarbon fractions.

The gases routinely measured in reactor effluents by internal gas-proportional counting include the noble gases ^{85}Kr, ^{131m}Xe, ^{133}Xe, ^{37}Ar, and ^{39}Ar and the permanent gases $^{3}H_2$, $^{14}CO_2$, and CH_4 (^{14}C and ^{3}H). The latter group is important in noble gas measurements because during chromatographic separation, contamination of the argon fraction with $^{3}H_2$, the methane fraction with ^{85}Kr, and the CO_2 fraction with the ^{133}Xe can occur.

SPECTROMETER SYSTEM

The spectrometer system is similar to those described by Curran (1958). The proportional tubes used in the reactor sample measurements are commercial 100-ml stainless-steel proportional tubes manufactured by LND, Inc. The active region of these tubes is a cylinder 2.3 cm in diameter and 24 cm long. For background reduction, plastic scintillator anticoincidence guard detectors are used, and the entire detection system is enclosed in a 14.4-cm thick steel shield. Figure 1 shows two of the 100-ml proportional tubes along with a 1-liter tube and two of the guard detectors. The smaller guard will accept the 100-ml tubes, while the larger guard will accept tubes as large as the 2.6-liter tube manufactured by LND, Inc. A typical 100-ml tube with a P-10 (90% argon, 10% methane) fill has a plateau 250 volts long, beginning at 1,750 volts with a slope of less than 1% per 100 volts.

A block diagram of the system is shown in Figure 2. Pulses from the proportional tube are amplified and shaped before passing through a linear gate to the multichannel analyzer. If an event occurs in the guard detector, the linear gate is for 10 μsec. The system dead-time, due to guard events closing the linear gate, is less than 0.1%. All of the units shown in Figure 2, with the exception of the plastic guard detector, are commercial products. With new multichannel analyzers, one can use the built-in linear gate in the anticoincidence mode, thereby avoiding the cost of an external gate.

**Supported in part by USAEC contract AT(11-1)2222 and USEPA contracts 68-01-0522 and 68-01-LA-0505.*

OPERATION AND CHARACTERISTICS OF SPECTROMETER SYSTEM

Spectra of ^{3}H, ^{14}C, and ^{85}Kr obtained with this spectrometer system are shown in Figure 3. Using the x-ray fluorescence produced in the steel walls of the proportional tube with an external ^{125}I source, the gain of the system was set at 0.83 keV/channel. At this fixed gain, there are clear differences in end points and shapes for these three isotopes.

Background spectra at a system gain of 0.42 keV/channel are shown in Figure 4. The integrated backgrounds were: for the bare stainless-steel detector, 104 cpm; for the detector shielded by 14.4 cm of steel, 53 cpm; and for the detector shielded by the steel and an anticoincidence guard, 4.9 cpm. With a 100-ml copper tube, not presently used for these reactor samples, an integrated background as low as 1.25 cpm has been achieved with a background of 0.3 cpm under the ^{37}Ar peak.

Argon spectra are analyzed for both ^{37}Ar (from the Auger peak) and ^{39}Ar (from the continuous spectrum). In order to avoid possible pulse pileup from ^{37}Ar, only the spectral region about 6 keV is used for ^{39}Ar analysis. The system has been calibrated for ^{37}Ar efficiency using a standard obtained from the National Bureau of Standards, and a value of 0.63 cpm/dpm has been obtained for the Auger peak efficiency.

A major advantage of spectral analysis is shown by comparing the spectra of an NBS ^{37}Ar standard, a contaminated argon fraction after two passes through a gas chromatograph, and the same sample after an additional pass (Figure 5). The contaminated sample contains a very small amount of ^{3}H, which would not affect the ^{37}Ar value, but could have a serious effect on the ^{39}Ar value. Integral bias counting would not show this contamination. Gross contamination can occur even with double chromatographic separation because of the large range of isotopic abundances in reactor gas effluents. The chromatographic separation sequence leads to decontamination factors of 10^3 to 10^4 (Kunz, 1973). One may occasionally observe ^{3}H interferences in argon, ^{85}Kr in methane, and ^{133}Xe and ^{131m}Xe in CO and CO_2 fractions. If great care is not taken in cleaning the separation system after a particularly high activity sample, ^{3}H can show up anywhere.

For sample spectra such as ^{85}Kr, ^{3}H, $^{14}CO_2$, and ^{14}CO, the spectral shape and end point are first examined for radiochemical purity. The spectrum is then summed; the background is subtracted; and the net counting rate is corrected for counting efficiency, sample size, chemical recovery, and radioactive decay. In the cases of ^{131m}Xe and ^{133}Xe, this procedure is repeated for several counts, and the data are fitted by a least squares method to a two-component decay curve.

At the present time, ^{37}Ar and ^{85}Kr are the only gas standards available from NBS. For ^{133}Xe the method of beta-gamma coincidence counting (Allen, 1965) was used to determine efficiency. While this procedure gave a value of 0.86 cpm/dpm, which seems consistent with other measured efficiency values, the presence of a conversion electron branch in ^{133}Xe has been ignored. The result should be a somewhat greater value for this factor. The same factor is used for ^{131m}Xe. Since ^{39}Ar has a beta spectrum similar to ^{85}Kr, the ^{85}Kr efficiency factor for that spectral region is used for ^{39}Ar. In many reactor gas samples ^{85}Kr and ^{133}Xe are present in a sufficient concentration to permit analysis by Ge(Li) gamma counting of the sample in the sampling vessel. The ^{133}Xe proportional-counter efficiency from coincidence calibration provides good agreement with the Ge(Li) diode measurements.

One of the more interesting gases present in reactor effluents is methane. It may be composed of ^{3}H or ^{14}C, or both, and beta-spectrometry permits the simultaneous analysis of both nuclides. In Figure 6 the spectrum of the methane fraction from a heavy-water-moderated reactor is presented. The spectrum is run at a system gain of 0.42 keV/channel. The regions from channels 1 to 39, and from 40 to 255, are summed, and the background subtracted. The net counts in region 1 and 2, N_1 and N_2 are given by:

$$N_1 = f_1(T)N_T + f_1(C)N_C \qquad (1)$$

$$N_2 = f_2(T)N_T + f_2(C)N_C \qquad (2)$$

where $f_1(T)$ = fraction of ^{3}H spectrum in region 1,

$f_1(C)$ = fraction of ^{14}C spectrum in region 1,

$f_2(T)$ = fraction of ^{3}H spectrum in region 2,

$f_2(C)$ = fraction of ^{14}C spectrum in region 2,

N_T = net ^{3}H count in spectral region,

N_C = net ^{14}C count in spectral region.

For our tubes and gain range these equations are:

$$N_1 = 0.985\,N_T + 0.575\,N_C \qquad (3)$$

$$N_2 = 0.015\,N_T + 0.425\,N_C \qquad (4)$$

Since N_1 and N_2 have been measured, these equations can be solved for N_T and N_C and the activities determined without combustion of the sample. By counting a series of twelve ^{14}C methane samples, it has been determined that the gain can be set with ^{125}I with sufficient reproducibility that the errors in the constant terms in Equations (3) and (4) are restricted to the third significant figure. The major drawback of this method is that the ^{3}H sensitivity is limited by the amount of ^{14}C present. If the ^{14}C activity is one order of magnitude or more above the background, the detectable limit for ^{3}H is about 7% of the ^{14}C activity. In Figure 7 the decomposition of the methane fraction into ^{3}H and ^{14}C components is shown. A summary of system performance appears in Table 1.

The detectable limit is reduced by poor chemical recovery and, for short-lived nuclides, long delays between collection and counting. It is enhanced by processing larger samples. Samples as large as 2 liters have been processed in our laboratory. The major uncertainty in our work at the present time is the accuracy of the efficiency factors. Those given in Table 1 for ^{39}Ar, ^{3}H, and ^{14}C are estimates for ^{85}Kr and ^{37}Ar, and that for ^{133}Xe has been determined by a method which is somewhat lacking in technical justification.

Standards for these and other gases will presumably become available in the future. Proportional tube efficiency, however, unlike that of most other radiation detectors, varies slowly over a wide range of energies. Extrapolation of detector efficiency for beta-emitting isotopes is not especially difficult, but isotopes which decay by electron capture or by decay of metastable states present problems which require direct comparison to standards.

REFERENCES

Allen, R.A., (1965), *Measurement of Source Strength, In Alpha-, Beta- and Gamma-Ray Spectroscopy* Vol. 1, K. Siegbahn, Ed., p. 425, (Amsterdam, North-Holland).

Curran, S.C., (1958), *The Proportional Counter as Detector and Spectrometer,* in Handbuch der Physik, Vol. 45, 174 (Berlin:Springer).

Kunz, C.O., (1973), *Separation Techniques for Reactor-Produced Noble Gases,* Proceedings of the Noble Gas Symposium, Las Vegas, Nevada, Sept. 24-28, 1973.

TABLE 1. Spectrometer Performance.

Isotope	Gain keV/channel	Channels used	Gas detector efficiency (cpm/dpm)	Ave bkgd (cpm)	Detectable limit 1-ml sample 1,000-min count (μCi/ml)
^{85}Kr	0.83	1-255	0.90	5.0	1.1×10^{-7}
^{37}Ar	0.21	10-19	0.63	0.8	6.0×10^{-8}
^{39}Ar	0.21	32-255	0.45	1.5	1.2×10^{-7}
^{133}Xe	0.83	1-255	0.86	5.0	1.1×10^{-7}
^{3}H	0.42	1-39	0.75	5.0	1.3×10^{-7}
^{14}C	0.42	1-255	0.85	5.0	1.1×10^{-7}
^{14}C	0.42	40-255	0.36	0.13	4.0×10^{-8}

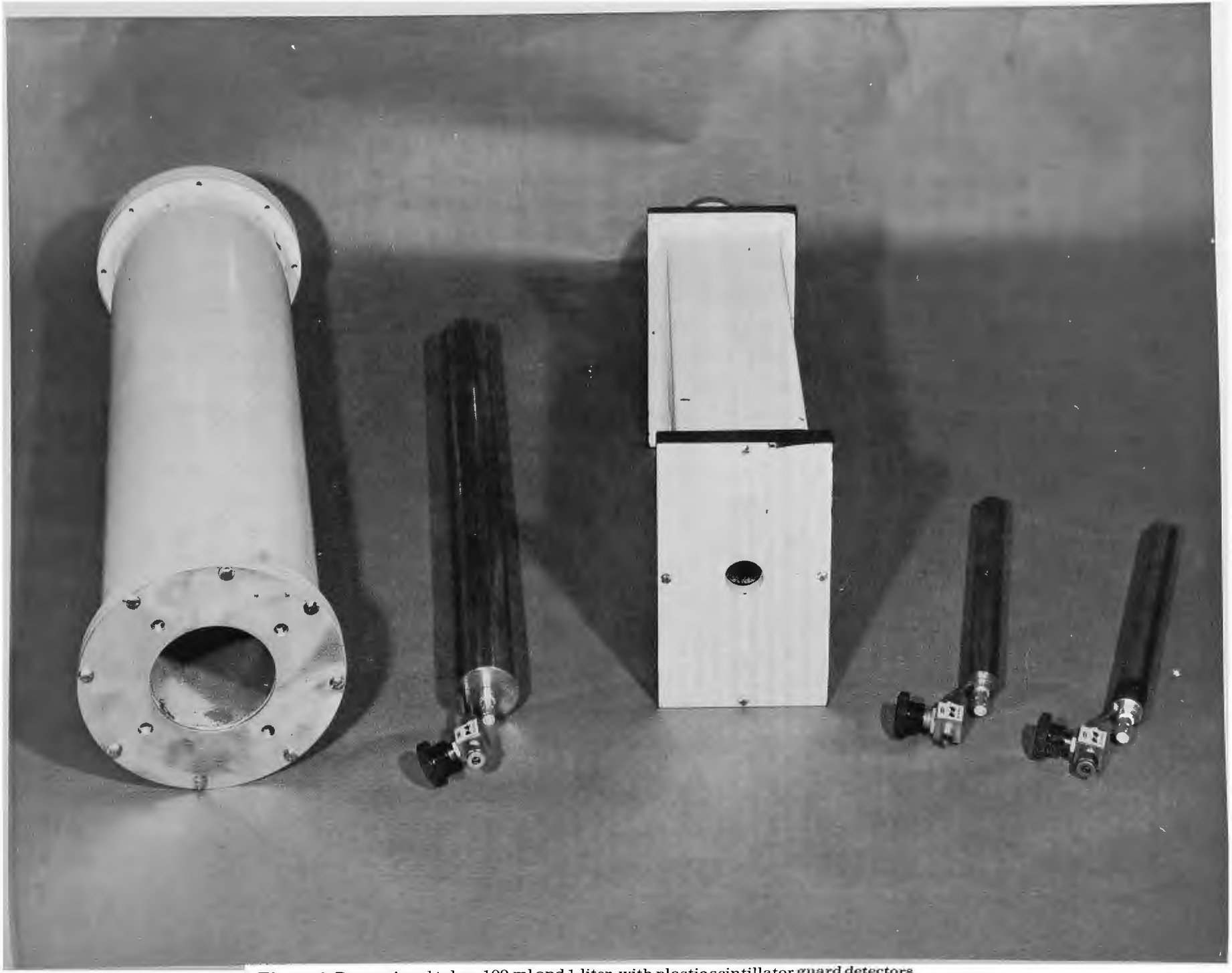

Figure 1. Proportional tubes, 100-ml and 1-liter, with plastic scintillator guard detectors.

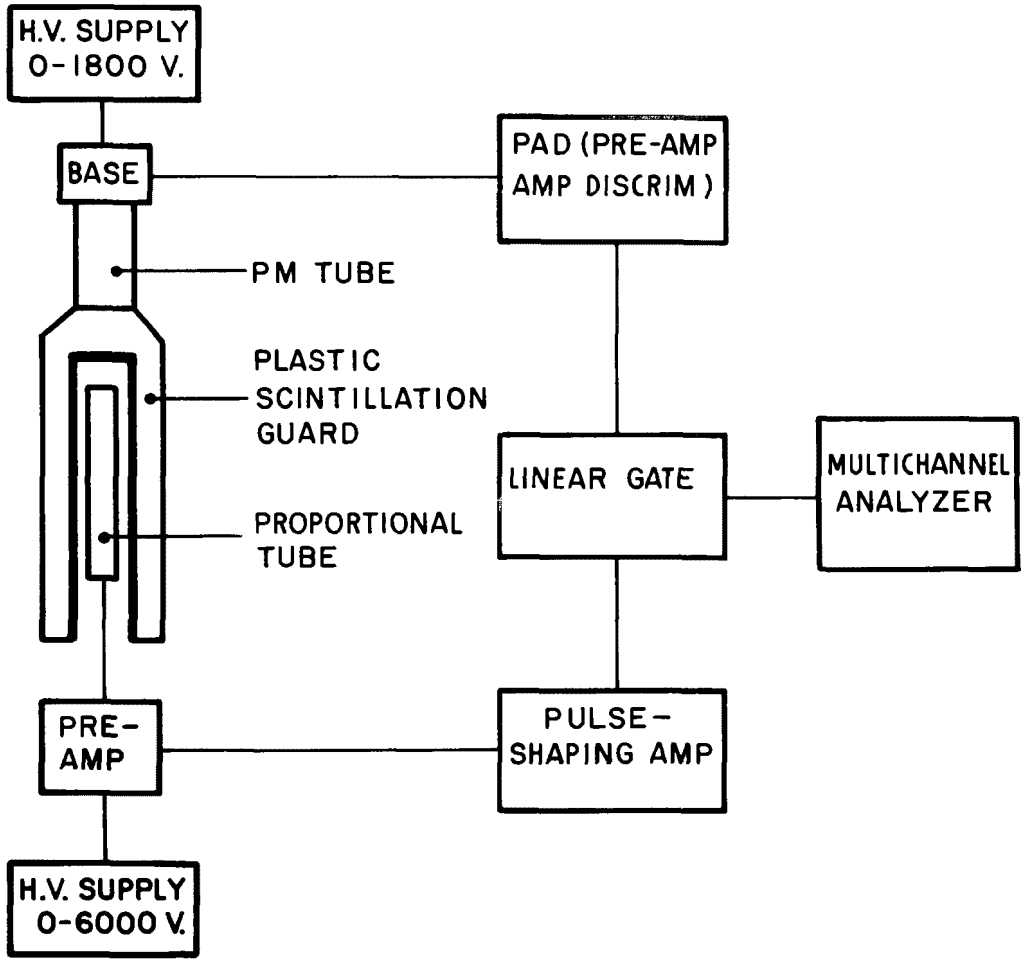

Figure 2. Block diagram of internal gas-proportional beta-spectrometer system.

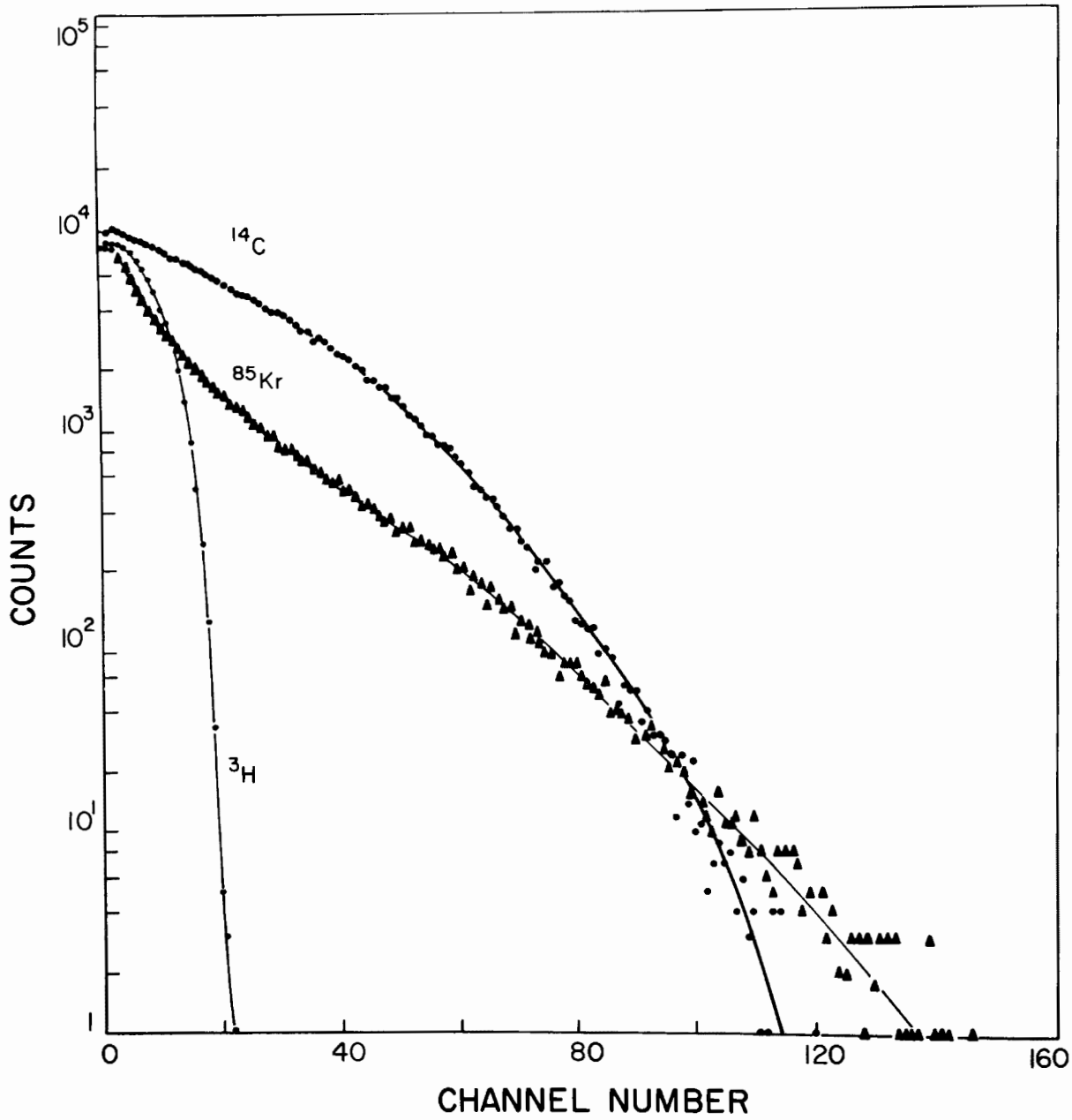

Figure 3. Spectra of ^{3}H, ^{14}C, and ^{85}Kr. (Gain 0.83 keV/channel.)

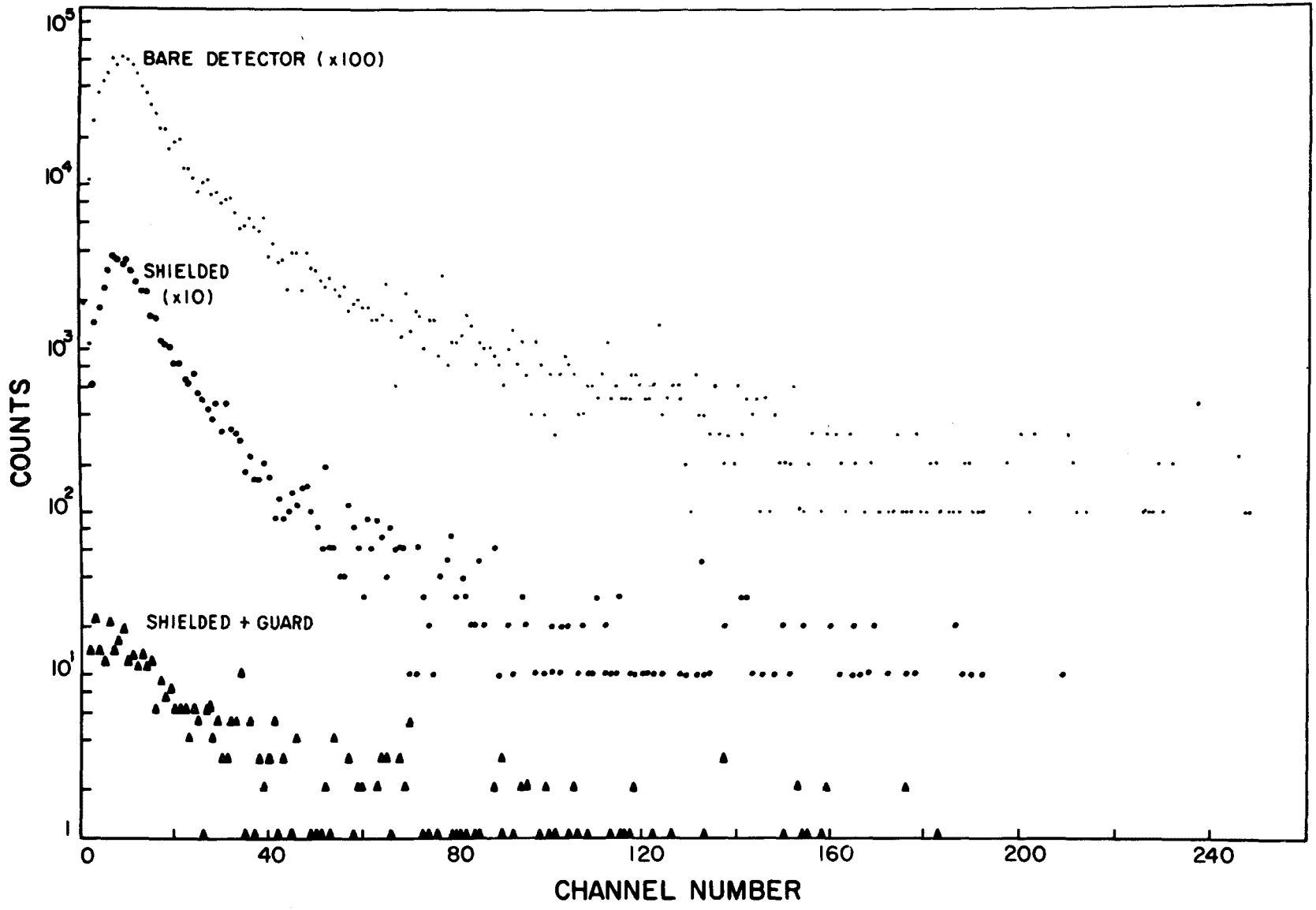

Figure 4. Background spectra for a 100-ml steel proportional tube. The spectra of the shielded and bare detectors have been shifted upward by factors of 10 and 100, respectively. (Gain 0.42 keV/channel.)

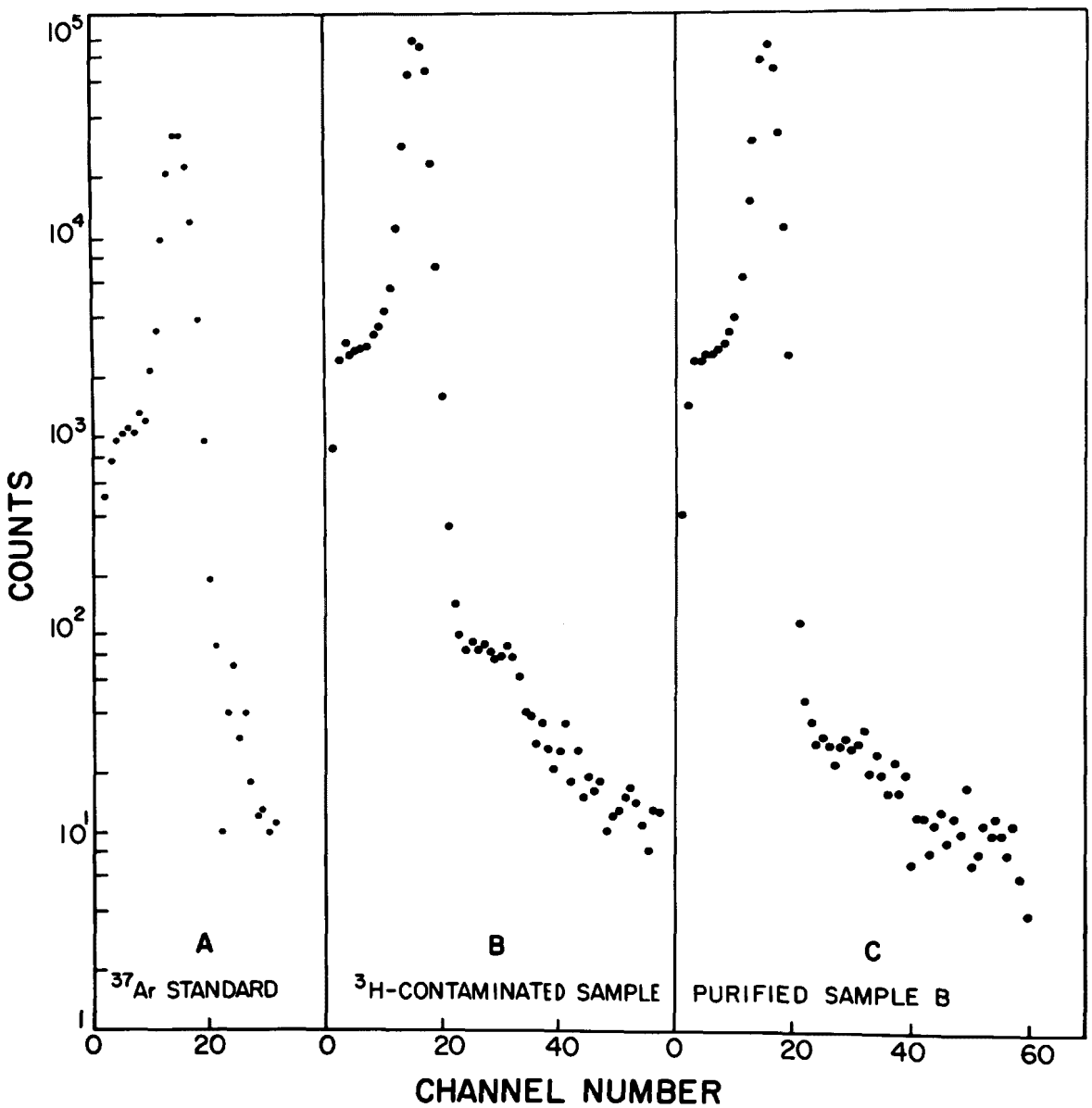

Figure 5. Argon spectra: A. NBS ^{37}Ar standard; B. Argon fraction with ^{3}H contamination; and C. Fraction shown in B with an extra purification step. (Gain 0.21 keV/channel.)

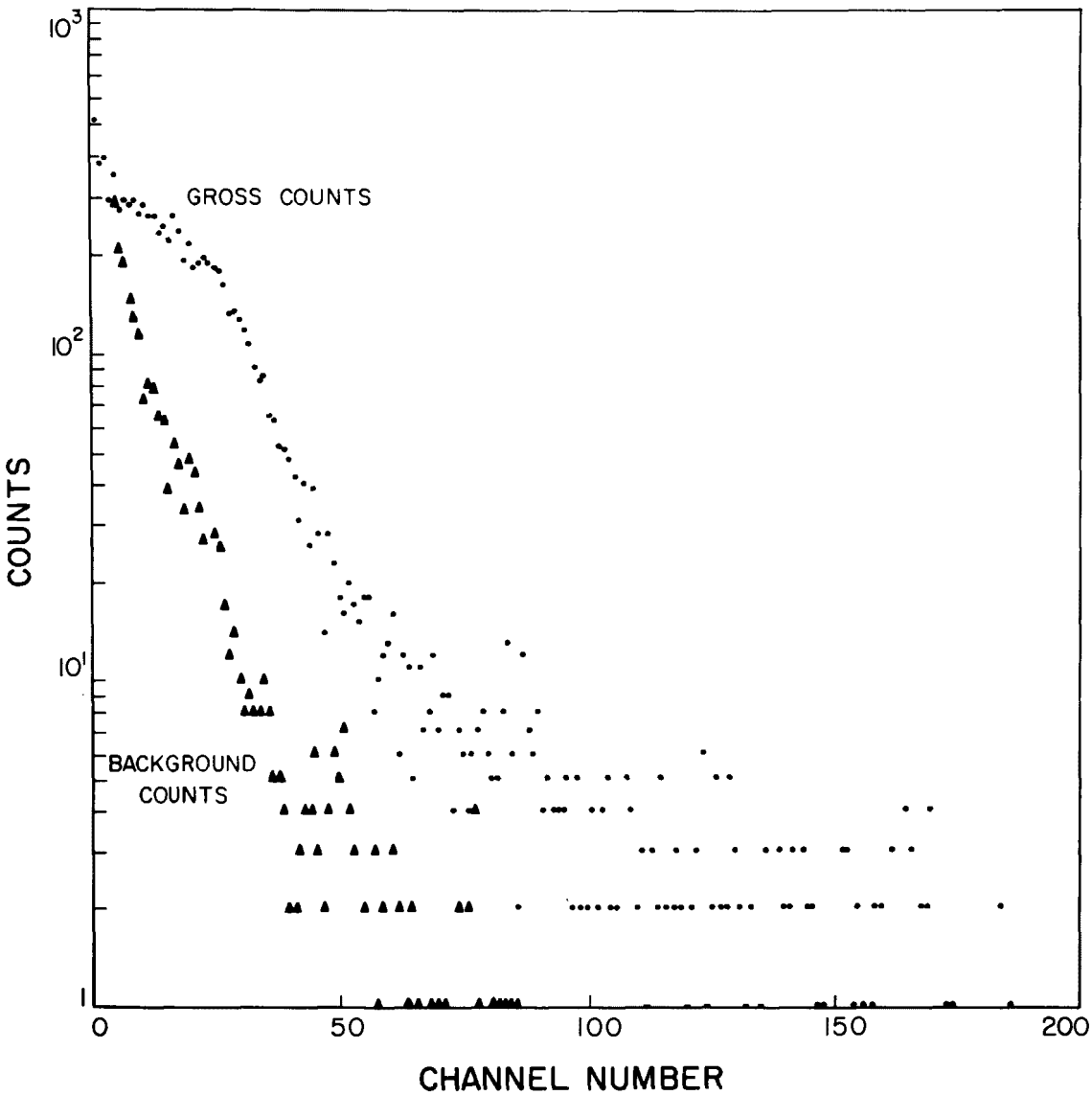

Figure 6. Gross spectrum of a methane fraction showing the presence of ^3H and ^{14}C compared with background. (Gain 0.42 keV/channel.)

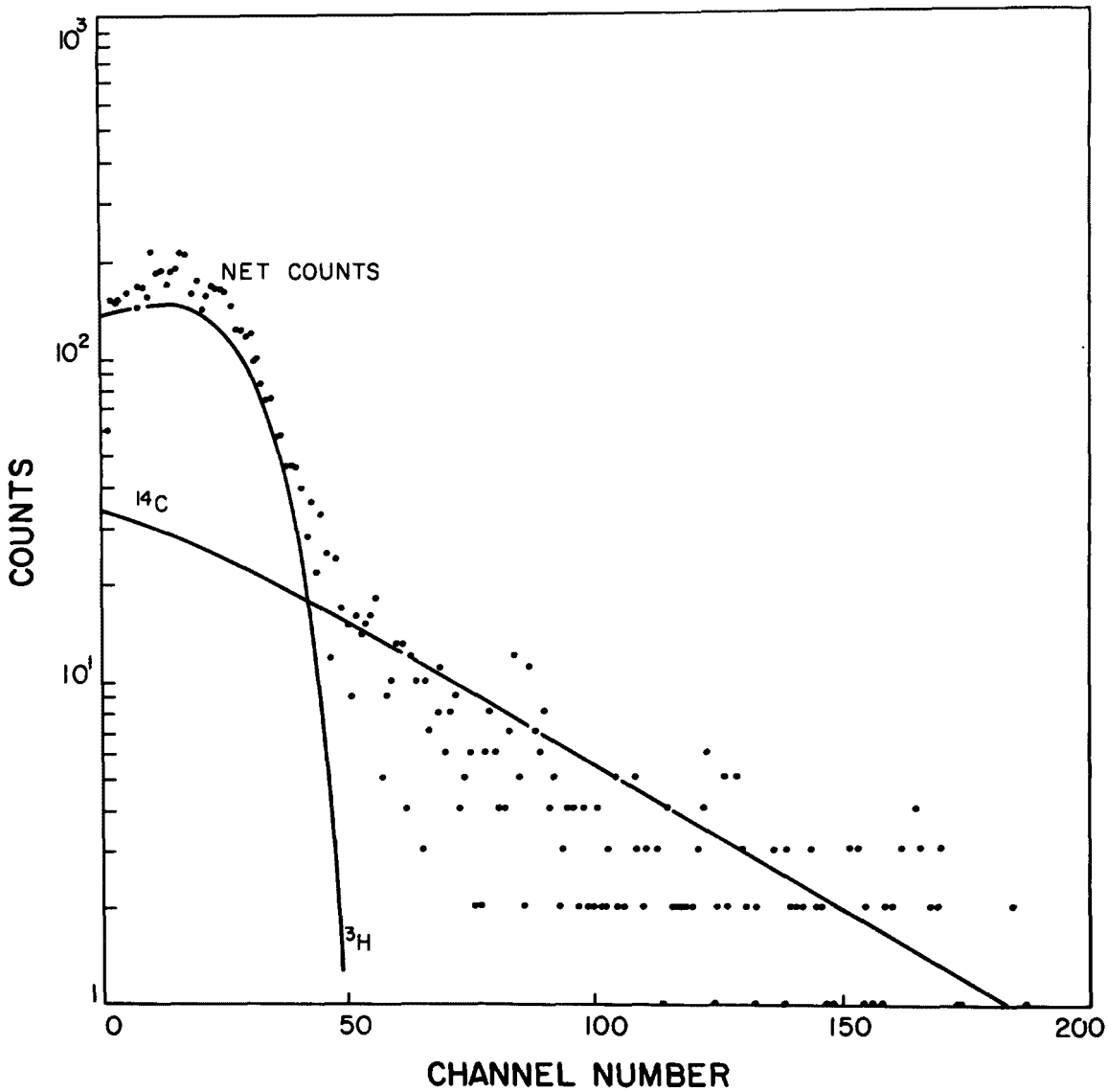

Figure 7. Spectrum of the methane fraction shown in Figure 6 with background subtracted. The ^{3}H and ^{14}C components are indicated. (Gain 0.42 keV/channel.)

ENVIRONMENTAL MONITORING FOR KRYPTON-85*

D. E. Barber
School of Public Health
University of Minnesota
Minneapolis, Minnesota 55455

Abstract

^{85}Kr presents unique environmental monitoring problems because it does not react with other elements and compounds at normal ambient temperatures and pressures. However, elaborate means are available to manage the ^{85}Kr problem, but a simpler, inexpensive approach is required if monitoring is to be accomplished at many sampling locations. This work shows that environmental monitoring for ^{85}Kr is possible by collecting air samples in thin plastic bags, and counting the bags for beta particle activity. The direct counting of contained samples of this type makes it possible to detect concentrations less than the public MPC for ^{85}Kr. The bagged-sample technique is readily adaptable to any environmental monitoring station with power to run a low-volume air pump. The idea of counting the bagged-sample directly is a new, low-cost, approach to environmental gas monitoring which may have application in environmental, clinical, and industrial situations.

INTRODUCTION

^{85}Kr is a fission product which escapes or is released to the environment primarily as a byproduct of reprocessing nuclear fuel. In fuel reprocessing, ^{85}Kr, ^{131}I, ^{129}I, ^{133m}Xe, ^{133}Xe, and ^{3}H are released, but only ^{85}Kr and ^{3}H are released in sufficient quantities, and have long enough half-lives, to produce significant concentrations in extensive environmental air volumes (Kirk, 1972). The present atmospheric inventory of ^{85}Kr is estimated to be 60 MCi — more than twice the inventory in 1962 (Kirk, 1972). If projections with respect to population, demand for electric power, use of nuclear power plants, and release of ^{85}Kr to the environment are correct, concentrations of ^{85}Kr in the atmosphere may reach 3×10^{-7} μCi/ml (the public MPC) about the year 2050 (Holland, 1969; Cowser and Morgan, 1967; and Coleman and Liberace, 1966). Treatment of effluents to remove up to 98 percent of the noble gases from fuel reprocessing is possible, and methods have been tested on a pilot plant scale (Slansky, 1971). The cost of treating the effluent has been estimated at about 1 percent of the total reprocessing cost (Slansky, *et al.*, 1969), and treatment will probably be used extensively in the near future. Consequently, present projections with respect to anticipated atmospheric concentrations in the 21st century are probably much too high. However, effluent treatment or not, ^{85}Kr releases to the atmosphere will require environmental monitoring for the gas because:

(1) A removal efficiency of 98 percent reduces released concentrations to only 0.02 times their original values.

(2) The atmosphere cannot be used exclusively for ^{85}Kr dilution.

(3) It will be necessary to assure compliance with regulatory standards.

Although this paper addresses itself to the problems of monitoring ^{85}Kr, the results are more generally useful. There are situations which arise when one would like to know the response to be expected from ordinary radiation detectors when they are presented to clouds of beta particles or low-energy gamma ray emitters with dimensions less than those of infinite volume.

There are a number of possibilities for monitoring ^{85}Kr in the atmosphere given unlimited financial resources. Any of the methods for removal of noble gases on a large scale from fuel reprocessing effluents might be used on a smaller scale; but, these methods involve elaborate pretreatment of the intake gases and/or cryogenic temperatures (Slansky, 1971). When adsorbing media such as molecular sieves or charcoal beds are used, the operating temperature must be matched to the sampling rate and sample size (Kirk, 1972). In liquid scintillation counting, the lowest concentration of ^{85}Kr that can be analyzed without preconcentration is about 3 pCi/ml, and the poor solubility of air in liquid scintillation cocktails presents a problem for sampling air mixtures of gases (Kirk, 1972). So, sophisticated sampling for ^{85}Kr in the environment presents severe practical limitations for both technical and financial reasons, especially in those situations where numerous monitoring stations may be involved. Simple, inexpensive methods must be found.

Direct counting of gas samples in vinylidene chloride (Saran) is the approach taken here. The sampling approach is similar to one already reported for ^{222}Rn (Sill, 1969). But, the idea of counting beta particle emitters directly, without removing the sample from the bag for the purpose of gas monitoring, is believed to be new. It has been noted recently that ^{133}Xe contamination in the air should probably be done by counting the air sample directly rather than attempting to collect the Xe in aqueous solution (LeBlanc, 1972). LeBlanc points out that there is a misunderstanding concerning the best methods to monitor for ^{133}Xe because of erroneous solubilities for ^{133}Xe given by the Hbk. of Chm. and Phys. (1966). Similar uncertainties may also apply to krypton.

**The data on ^{85}Kr reported here resulted from work completed in the Faculty Research Participation Program of Associated Western Universities at the Health Services Laboratory, USAEC, Idaho Falls, Idaho. The author also gratefully acknowledges the cooperation of Aerojet Nuclear Company.*

PROPERTIES OF ^{85}Kr AND INTERFERENCE PROBLEMS

Some properties of ^{85}Kr are given in Table 1. ^{85}Kr is nearly a pure beta emitter from the dosimetry viewpoint, but the gamma ray is useful for calibration purposes for activities greater than $10^{-2}\mu$Ci. Monitoring for ^{85}Kr by gamma ray spectrometry can be accomplished provided the concentration is high enough, and is sustained for a period of time at least equal to the measurement period. At concentrations approaching the maximum permissible concentrations, however, the branching ratio (0.004) of gamma ray disintegration to beta particle disintegration makes beta particle measurements far more attractive.

Iodine impregnated, activated charcoal can be used to eliminate interference from iodine-131. Silica gel can be used to keep the sample dry. Storage can be used to eliminate interference from radon-daughter product activity, and filters can be used to reduce interference from particulate activity. There remain, then, ^{133}Xe and ^{133m}Xe. The technique might be biased against these nuclides by storage, careful selection of detector window thickness, and detector design. Interference from ^{133}Xe is not expected to be significant at present because the ratio of ^{133}Xe to ^{85}Kr activity for aged nuclear fuel is typically less than 10^{-4} percent (Smith, *et al.*, 1970). However, as use of nuclear fuels increases, the used fuel will be less and less aged before reprocessing, in which case it will be necessary to cope with the ^{133}Xe problem. This should be relatively easy to do because of the large differences in modes of decay, and beta energies between those for ^{133}Xe and ^{85}Kr.

If ^{133}Xe is produced as a fission product, ^{133m}Xe will also be present (Martin and Blichert-Toft, 1970). The ^{133m}Xe could present severe beta particle detection interference problems if fuel is stored for less than 10 days prior to reprocessing. The conversion electron energies from ^{133m}Xe are only slightly lower than the average energy of beta particles from ^{85}Kr. However, advantage might be taken of the 0.233 MeV gamma ray from ^{133m}Xe to distinguish it from both ^{85}Kr and ^{133}Xe.

METHODS

1. ^{85}Kr Chamber.

A chamber approximating an infinite volume of air for ^{85}Kr beta particles was constructed of 4' x 8' x 3/4" plywood on a 2" x 4" wood superstructure. The resultant chamber was an 8' cube equipped with feed-throughs provided for power, sampling inlets, outlets, and a G.M. detector lead. The chamber was kept outside at ambient temperature and pressure.

Chamber concentrations were measured and monitored by a 30 mg/cm^2 metal-walled Amperex G.M. tube (1/2" dia. x 7" long) operated at 960 volts. Pulses from this detector were counted with a Baird-Atomic Mod. 530 scaler.

Serial dilutions from ^{85}Kr stock to glass vials, to the chamber, and ultimately to polyethylene and Saran bags, were made to produce various concentrations of ^{85}Kr ranging from $2 \times 10^{-8}\mu$Ci/ml to $7 \times 10^{-4}\mu$Ci/ml.

2. Calibrations.

Unfortunately, the detection limit by gamma ray spectrometry for ^{85}Kr is on the order of $10^{-2}\mu$Ci. As a result, chamber concentrations could not be confirmed by this method over the range of concentrations of interest. To enable measurements of concentration in the chamber over the entire range of interest, the G.M. tube in the chamber was calibrated as follows. A sample from ^{85}Kr stock was counted on a 65 ml GeLi detector in the standard geometry. The GeLi detector was calibrated with a ^{85}Kr source from the National Bureau of Standards. The sample was then transferred to a 4.2-liter Saran bag to calibrate an 8" x 4" NaI detector for this geometry. A 4.2-liter sample taken from the chamber was then counted on the same crystal yielding the true concentration in the chamber, $1.05 \pm 0.15 \times 10^{-4}\mu$Ci/ml. This concentration provided the primary calibration factor, $3.82 \times 10^{-9}\mu$Ci/ml per cpm, for the chamber G.M. tube. The G.M. tube count rate was then used as the reference for the concentration in all samples taken from the chamber. The G.M. tube calibration factor agrees well with the $2.1 \times 10^{-9}\mu$Ci/ml per cpm previously reported for a similar, but longer, G.M. tube (Smith, *et al.*, 1970).

The rotameter was calibrated with a wet-test meter, and was found to be in calibration within ± 20 percent. The uncertainties in visually setting the rotameter are large. Consequently, the rotameter reading was taken to be the true flow rate at ambient temperature and pressure.

3. Sampling and Instrumentation.

A diagram of the dilution and sampling system is given in Figure 1. The sampling line was prepared as it might be used in the field to pretreat samples taken from the chamber. Components of the sampling line were connected with plastic tubing ranging from 1/4 to 3/8 inch inside diameter. The input to the rotameter from the chamber was at ambient pressure, and consisted of 3/8 inch plastic tubing suspended at the center of the ^{85}Kr chamber close to the G.M. tube. Samples were collected at various flow rates and various sampling times as indicated in the results.

Except for a few measurements with the 5-liter Saran bag filled to capacity, bags were filled to less than capacity to minimize leakage, if any should occur, and to provide a flexible bag geometry. In this way, it was possible to achieve 2π counting geometry when samples were placed on the detectors, and to reduce the error which might be introduced as a result of pressure build-up in the bag.

The instruments used to analyze the bagged-samples were as follows:

(1) Ludlum Instrument Co., Model 14A Gieger Counter with LND Inc. G.M. tube, 30 mg/cm^2 metal wall.

(2) Eberline Instrument Co., Model HP-210 G.M. probe with LND 731-1 G.M. tube, 2" diameter thin window, connected to Baird-Atomic, Model 530 scaler, operated at 800 V.

(3) A sheet of plastic scintillator, 4.1" diameter by 0.19" thick, attached with Dow Corning QC-2-0057 silicone compound to a DuMont 6364 photomultiplier tube (5" diameter face). The scintillator was covered with two layers of doubly aluminized Mylar to make a total window thickness of 2.06 mg/cm^2. The detector signal was fed through a preamplifier into a Baird-Atomic, Model 530 scaler with input sensitivity set at approximately 50 mV. The high-voltage to the detector was 1,000 V.

The first and second instruments were used outside, immediately adjacent to the chamber, to examine their response to samples taken from the chamber. The third detector was used inside a vault with 10" thick steel walls.

Measurements with the first two instruments were made in the presence of radon-daughter product activity. Measurements with the third instrument were made on samples stored overnight.

4. Sample Containers.

Two types of plastic bags were used to collect, store, and count samples. One bag was Saran type 18-100 (manufactured by Analytical Specialties, Inc., and distributed by the Anspec Co., Ann Arbor, Michigan). This Saran has a density thickness of 8.0 mg/cm^2. Saran is known to contain ^{222}Rn with losses of less than 0.12 percent per day up to at least 14 days (Percival, 1971). It, therefore, seemed a suitable choice for ^{85}Kr. Saran of this thickness is also very durable and easy to handle.

The second type of plastic bag used in this work was a simple polyethylene bag. The bag was 20" square with a wall thickness of 4.7 mg/cm^2. The open end of the bag was heat-sealed, and the center of one side was cut out to a diameter of about 7" to accommodate a thin Saran window. The Saran used for this window was the ordinary household type. Its thickness was 2.2 mg/cm^2. The Saran window was attached to the bag with a translucent silicone rubber adhesive sealant (RTV-108, General Electric Co., Waterford, New York). This made a satisfactory seal for the purpose of this experiment, but it does not provide a permanent seal. Further, polyethylene is generally known to be permeable to many compounds, including water vapor, and probably is unsuitable for ^{85}Kr containment for more than a few days. The purpose in using these homemade bags was to provide a large-volume container with a very thin window to provide maximum beta particle transmission with essentially a 2π geometry when placed on the plastic scintillation detector.

RESULTS

1. ^{85}Kr Chamber.

With the chamber containing 3×10^{-4} μCi/ml of ^{85}Kr, the count rate of the chamber G.M. tube dropped from 7.43×10^4 cpm to 7.30×10^4 cpm over a 150-minute period. This amounts to a leakage rate of 0.8 percent per hour at the highest concentrations used in the chamber.

Rate meter measurements showed that the gas dispersed in the chamber within two seconds, and remained dispersed even without the benefit of the fans in the chamber. No significant reduction in chamber concentration occurred which could not be explained on the basis of the chamber leakage rate. The chamber concentrations were remarkably stable and reproducible. With the access door fully open, and with the fans running as usual in the chamber, it required 2 to 3 minutes to reduce the chamber concentration to 1/2 of its original value.

2. Chamber G.M. Tube.

The count rate of the ^{85}Kr chamber G.M. tube as a function of ^{85}Kr concentration is given in Figure 2 for both input to the scaler and to the Ludlum rate meter. Each observation involved a 3-minute count. The first observation was made at the lowest concentration. Two subsequent additions of ^{85}Kr provided the three concentrations in the figure. The tube was used bare, and was supported with its coaxial cable at the center of the chamber. The practical lower limit of detection for the Ludlum rate meter with the chamber G.M. tube is about 6×10^{-7} μCi/ml; this provides a net meter reading of 0.04 mR/h in an infinite cloud. When the tube is connected to a scaler, the lower limit of sensitivity is a function of the background and counting time. For the conditions of Figure 2, the limit for detecting ^{85}Kr with the scaler is much lower than with the rate meter.

3. Ludlum G.M. Survey Meter.

With a chamber concentration of 7.0×10^{-4} μCi/ml samples were taken in the 5-liter Saran bag for time intervals ranging from 5 to 25 seconds at 12.5 lpm. When the Ludlum probe, with beta shield open, was laid on each sample the response was found to be linear with respect to activity — irrespective of bag geometry (see Figure 3).

The lowest activity was distributed in a volume of only 1 liter, but the highest activity was distributed in 5 liters. There are large uncertainties in reading this meter, but the linear relation over a factor of five change in volume is clear.

The minimum reliable net reading for the Ludlum survey meter is 0.04 mR/hr. This corresponds to about 0.05 μCi which, according to the figure, might be distributed in as much as 5 liters. Hence, the minimum detectable concentration for this meter under these conditions of measurement becomes 10^{-5} μCi/ml. This is much too high for environmental monitoring purposes.

4. Eberline G.M. Probe.

This probe was used to measure ^{85}Kr activity in the 5-liter Saran bag containing various volumes of gas at a constant concentration of 6.3×10^{-4} μCi/ml. The results are shown in Figure 4. The statistical counting errors are large; but, again the linear relation between activity and different geometries is obvious. One observation was made at low-activity (therefore, low-volume) by rolling the bag to about 1/4 of its maximum volume to show the importance of widely different geometries.

In this case the minimum detectable activity appears to be about 0.5 μCi. When expanded to 5 liters, this yields a minimum detectable concentration of 10^{-4} μCi/ml. But, measurements at maximum volume and various concentrations show the minimum detectable concentration to be much lower than this (See Figure 5).

When 5 liters of ^{85}Kr are taken from the chamber in the 5-liter Saran bag, the response of the probe is as indicated in Figure 5. The probe was lightly pressed against the side of the sample bag for each measurement. The highest concentration was measured first. Subsequent lower concentrations were produced by opening the chamber between samples. All counts were for three minutes.

The figure shows that this detector is capable of detecting as low as 3×10^{-7} μCi/ml of ^{85}Kr under the condition of measurement. But, it is not likely to detect 3×10^{-8} μCi/ml even for long counting times. A more sensitive detector is require.

5. Plastic Scintillation Detector.

Samples were taken from the chamber, diluted to the desired concentration with ambient air through the sampling chain into the polyethylene bags, and stored overnight to permit the decay of radon-daughter product activity. The ^{85}Kr concentration for all these samples was 2×10^{-7} μCi/ml. Ambient air samples taken through the sampling chain also were found to contain activity. This activity had an effective half-life of 33 minutes, which is typical for radon-daughter product activity. The filters do not eliminate interference from radon-daughter products at these low ^{85}Kr concentrations.

When stored samples of ^{85}Kr are counted, Figure 6 shows that it is possible to detect concentrations less than 3×10^{-8} μCi/ml using the polyethylene bags containing 23 liters of sample. Two 13-liter samples in commercial Saran bags showed that it may be possible to measure these low-concentrations in a lesser volume and in a more durable bag than provided by the polyethylene.

DISCUSSION

^{85}Kr has been measured at a variety of concentrations, in several different sample volumes, and with several different sample containers. In this work, the best combination was a 23-liter sample, stored overnight in a polyethylene bag with a 2.2 mg/cm^2 Saran window, and counted on a plastic scintillation counter. This combination provides minimum detectable concentrations of less than 3×10^{-8} μCi/ml for ^{85}Kr. The method is suitable for environmental monitoring provided pretreatment of the sample removes other beta emitters, such as ^{131}I, which would interfer with the analysis, and provided the sample container used in the field is reasonably durable and impermeable to ^{85}Kr.

The commercially available, 8.0 mg/cm^2 density thickness Saran bag, in the size advertised as 12 liters, is a good possibility for field sampling. One of the difficulties will be finding a metering pump with a low enough flow rate, and sufficient flow rate stability, to accurately pump a 12-liter volume into the bag over a long period of time. A much larger sample may be necessary for the sake of obtaining an accurately known volume of sample.

Common G.M. rate meters can detect ^{85}Kr in bagged, 5-liter samples containing concentrations as low as 10^{-4} to 10^{-5} μCi/ml. Common G.M. probes connected to scalers can detect ^{85}Kr in bagged, 5-liter samples containing concentrations as low as 3×10^{-7} μCi/ml — without benefit of shielding and in the presence of radon-daughter product activity. Under the conditions of an infinite cloud, bare G.M. detectors connected to scalers are capable of detecting concentrations below 3×10^{-8} μCi/ml, depending upon counting time. Detecting these low-concentrations with 12- or 23-liter bagged-samples requires a well-shielded, large area plastic scintillation counter or its equivalent. If the background count of the plastic scintillator doubled, and if the true concentrations in the samples were twice those reported here, it should still be possible to measure ^{85}Kr concentrations as small as 3×10^{-8} μCi/ml using the technique described here with slight modifications.

The variations in data points for bagged-samples are due primarily to inaccuracies in reproducing rotameter settings. Construction variations in polyethylene bags also contribute to the variation in observations where these bags were used. Observations in Figures 2 through 5 were made immediately after the samples were taken. Variations in radon-daughter product activity over short periods of time contribute to the variation in observation for these samples.

With the detector on the sample bag, the geometry is essentially constant at 2 π. So, the detector response is expected to be linear with increasing volume (therefore activity) for a fixed concentration in the sample as shown in Figures 3 and 4. This should be true for volumes and geometries for which self-absorption in the sample is negligible. So, if one is on the edge of a cloud, detector response will be proportional to the total activity in the cloud, irrespective of cloud dimensions within broad geometric limits. The linear relation must begin to level off and reach saturation as the dimensions of the cloud approach those of an infinite volume. Figure 4 yields an efficiency of 0.003 cpm/dpm at all different volumes and geometries at a fixed concentration of $6.3 \times 10^{-4} \mu$Ci/ml.

There is some variation in counting efficiency with concentration of activity at a fixed volume. Figure 5 has a slope of 1.04, and shows an efficiency of 0.003 cpm/dpm at $10^{-6} \mu$Ci/ml and 0.004 cpm/dpm at 6.3×10^{-4} μCi/ml (the concentration used in Figure 4). An increase in efficiency accompanying an increase in concentration is to be expected because of the larger number of maximum energy beta particles contained in the samples at higher concentrations. This increase in efficiency with increases in concentration is not apparent at concentrations on the order of $10^{-7} \mu$Ci/ml as Figure 6 shows. The slope shown in Figure 6 is 1.00.

Figure 6 yields an efficiency of 0.014 cpm/dpm for 23-liter samples, and 0.024 cpm/dpm for 13-liter samples. The smaller, thicker bag yields higher efficiency probably because it keeps more activity in the solid angle of the detector. The 23-liter bags drooped somewhat below the 2 π solid angle of the scintillation detector. The optimum geometry is probably a hemisphere with its flat plane centered on the detector surface. The optimum geometry and volume of the sample for this technique is still open to question and deserves additional study. Careful attention to this question would probably reduce further the minimum detectable concentration for ^{85}Kr.

Bagged-samples provide several advantages over *"in situ"* measurements of ^{85}Kr.

(1) When multiple sampling stations are required, *"in situ"* measurements require multiple detectors and recorders or a telemetering system. This approach is considerably more expensive.

(2) *"In situ"* measurements must also include pretreatment of the air to eliminate interference from other beta particle emitters. Accumulation of activity in the sampling chain may interfer with detection sensitivity to ^{85}Kr beta particles.

(3) Both sample geometry and detector geometry are always known, and are reproducible with bagged-samples.

(4) Provided sufficient activity is collected, the average concentration during the sampling period will be measured with bagged-samples, irrespective of either the dimensions or the concentrations of the contaminated air. This may yield a sensitivity greater than that provided by *"in situ"* measurements.

The disadvantages of bagged-samples are:

(1) They are incapable of identifying either the time or the magnitude of changes in air concentrations, and are not suitable for an alarm system.

(2) In large volumes they are awkward to handle, and require that precautions against leakage be taken.

SUMMARY AND CONCLUSIONS

An inexpensive method to monitor atmospheric ^{85}Kr at or below $3 \times 10^{-8} \mu$Ci/ml (0.1 MPC), with minor modifications to existing environmental air sampling stations, has been described. But the method needs further development and testing with mixtures of radioactive gases and aerosols likely to be found where ^{85}Kr is emitted. The method does not require volumes which are infinite with respect to the beta particle energy of ^{85}Kr. Neither does it require concentrations of activity which are stable with respect to time. Therefore, it is a realistic method from the viewpoint of conditions likely to be experienced in the field. One rarely encounters a truely infinite cloud sustained over a period of time long enough to make infinite cloud measurements realistic.

The ultimate test of the technique should involve mixtures of ^{131}I, ^{133}Xe, ^{3}H, and ^{85}Kr in concentrations likely to be encountered in the environment of reactors and fuel reprocessing plants. If the technique should fail this test of mixtures, it may still be useful as a screening technique for radioactive gases released to the environment by man.

REFERENCES

Berger, M. J., (1971), J. of Nucl. Med., Sup. No. 5, Vol, 12.

Code of Federal Regulations (1965), Title 10, Part 20.

Coleman, J. R., and R. Liberace, (1966), Radiolog. Health Data Reports, 7, 615.

Cowser, K. E., and K. Z. Morgan, (1967), *Health Physics Division Annual Report,* ORNL-4168, 39-45.

Handbook of Chemistry and Physics, (1966), Cleveland: The Chemical Rubber Company.

Holland, J. A., (1969), *Proceedings of the AEC Symposium, Biological Implications of the Nuclear Age,* USAEC Division of Technical Information.

Kirk, W. P., (1972), Environmental Protection Agency, Office of Research and Monitoring, Washington, D.C.: U.S. Government Printing Office, 484-482/46.

LeBlanc, A. D., (1972), Phys. Med. Biol., 17, 585-589.

Lederer, C. M., J. M. Hollander, and I. Perlman, (1967), *Table of Isotopes,* 6th Ed. (New York: John Wiley and Sons, Inc.).

Martin, M. J. and P. H. Blichert-Toft, (1970), *Nuclear Data Tables,* 8A, 108.

Percival, D. R., (1971), Personal Communication, Analytical Chemistry Branch, Health Services Laboratory, USAEC, Idaho Falls, Idaho.
Radiological Health Handbook, (1970), Washington: Public Health Service.
Sill, C. W., (1969), Health Physics, 16, 371-377.
Slansky, C. M., (1971), Atomic Energy Review, 9, 423-440.
Slansky, C. M., H. K. Peterson, and V. G. Johnson, (1969), Environmental Science and Technology, 3, 446-451.
Smith, D. G., J. A. Cochran, and B. Shleien, (1970), PHS, BRH/NERHL 70-4, Rockville, Maryland.
Voilleque, P. G., D. R. Adams, and J. B. Echo, (1970), Health Physics, 19, 835.

TABLE 1. Properties of ^{85}Kr.

Property	^{85}Kr	Reference
Density, mg/ml	3.74	Hbk. of Chem. & Phys., (1966)
Density/Density Air	2.9	Hbk. of Chem. & Phys., (1966)
Maximum Beta Energy, MeV and Abundancy (%)	0.67 (99.6) 0.160 (0.4)	Lederer, *et al.*, (1967); Rad. Health Hbk., (1970); and Martin and Blichert-Toft, (1970)
Average Beta Energy, MeV	0.2464	Berger (1971)
Range of Maximum Energy Beta in: Aluminum, mg/cm^2	235	Rad. Health Hbk. (1970)
Air, cm	182	Rad. Health Hbk. (1970)
Range of Average Energy Beta in: Aluminum, mg/cm^2	59	Rad. Health Hbk. (1970)
Air, cm	46	Rad. Health Hbk. (1970)
Specific Gamma Ray Constant, $\frac{R}{Ci\text{-}hr}$ at 1 meter	2.34×10^{-4}	The Author
Deposition Velocity on Grass, cm/sec	2.3×10^{-11}	Voilleque, *et al.*, (1970)
Max. Permissible Concentrations, μCi/ml;		
Occupational	1×10^{-5}	10 CFR20 (1965)
Public	3×10^{-7}	10 CFR20 (1965)
Half-life, years	10.76	Rad. Health Hbk. (1970)
Gamma-Ray Energy, MeV and Abundancy (%)	0.517 (0.4)	Martin and Blichert-Toft (1970)

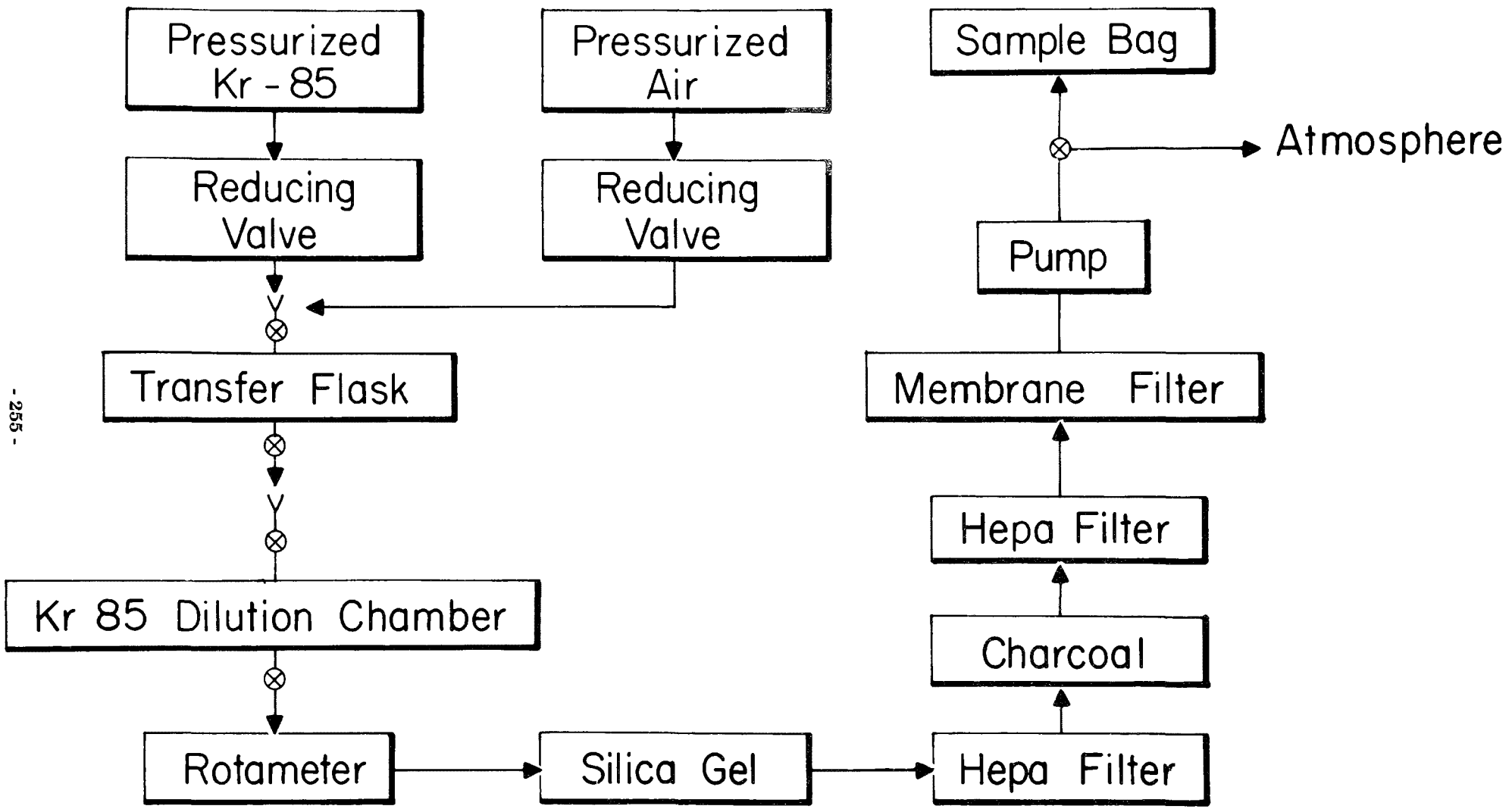

Figure 1. Krypton dilution and sampling system.

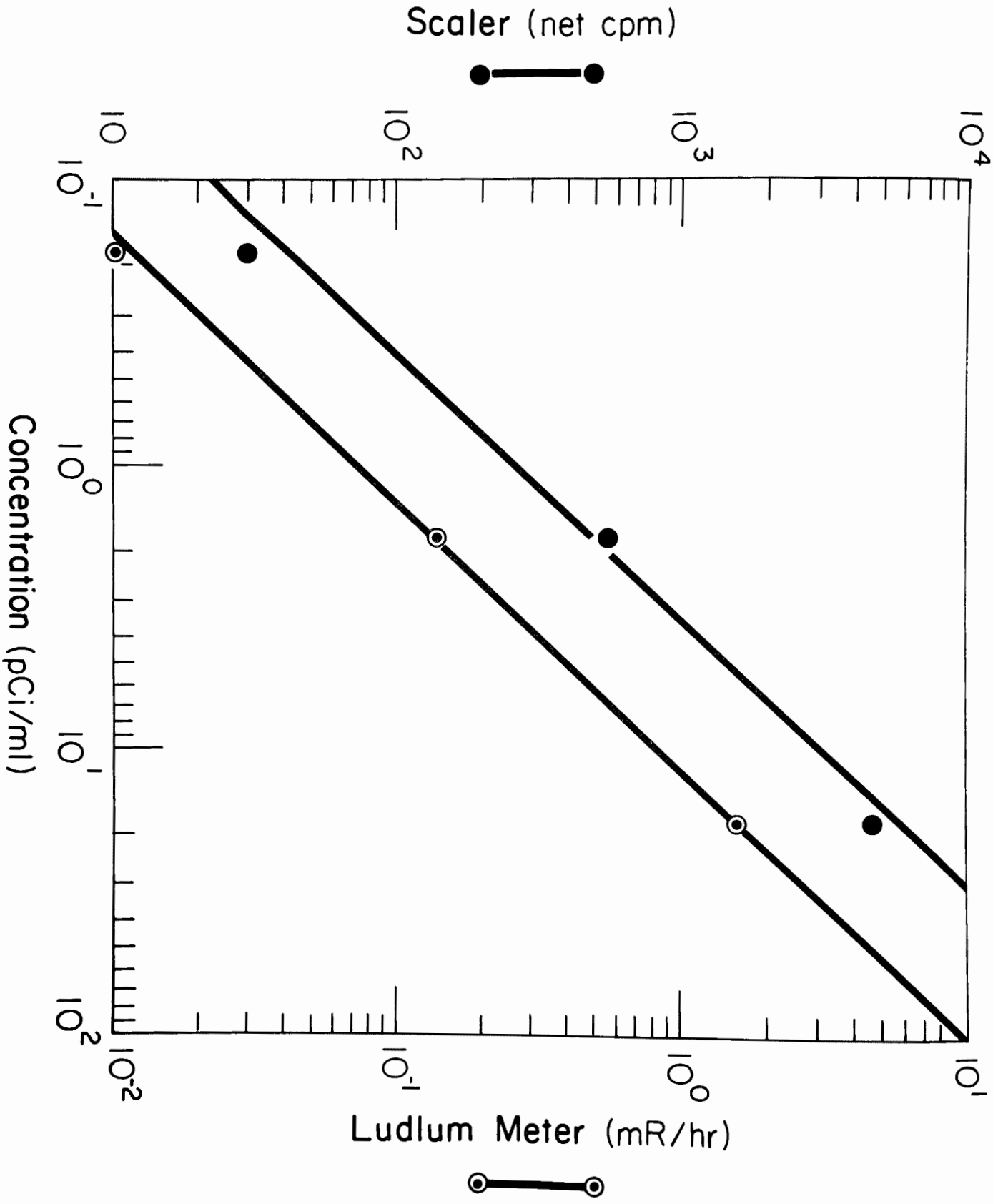

Figure 2. Response of the Amperex G.M. tube in the exposure chamber as a function of ^{85}Kr concentration. (The counting time for each observation with the scaler was 3 minutes.)

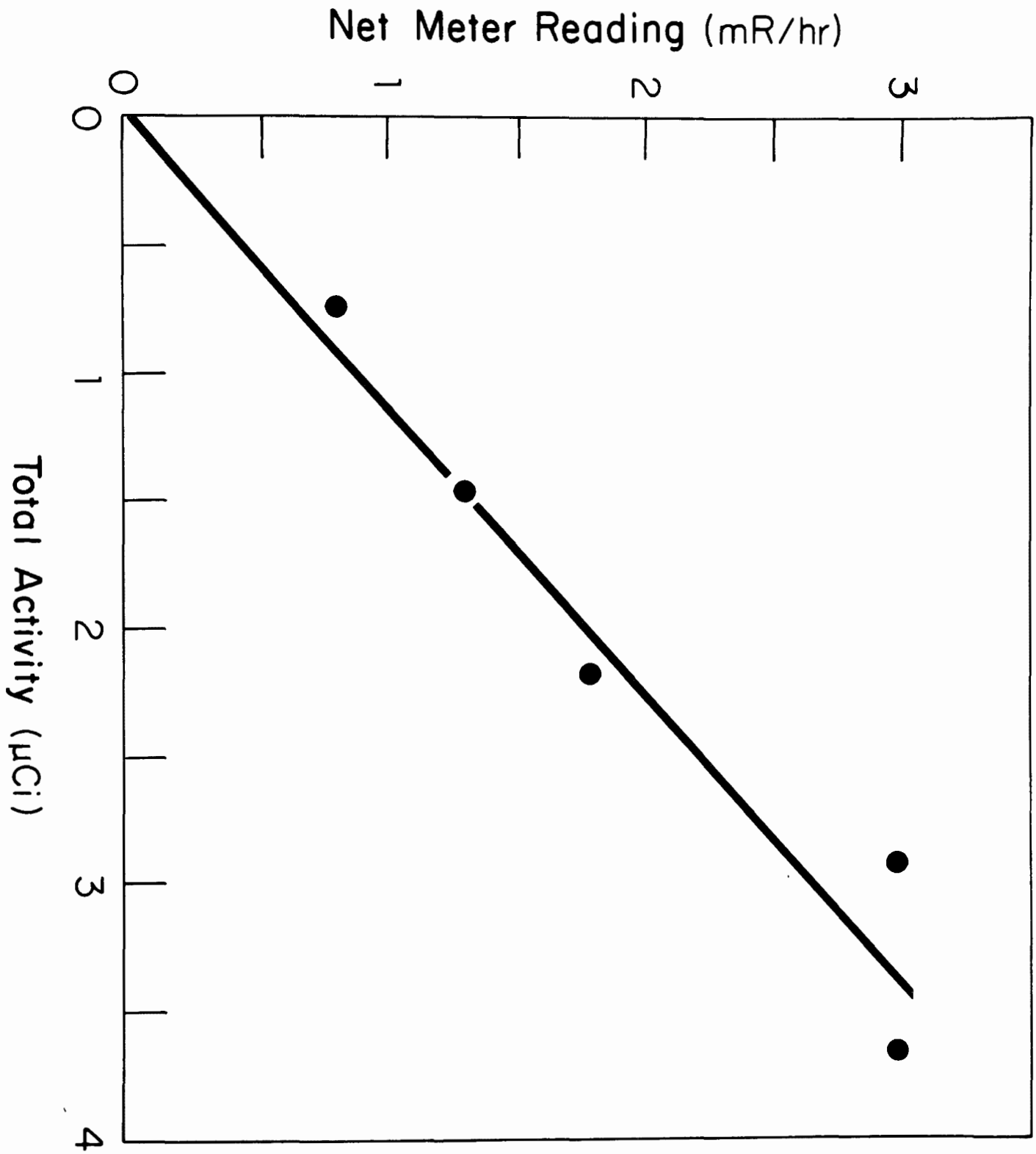

Figure 3. Ludlum G.M. survey meter response to a fixed concentration of ^{85}Kr in a 5-liter Saran bag at different volumes.

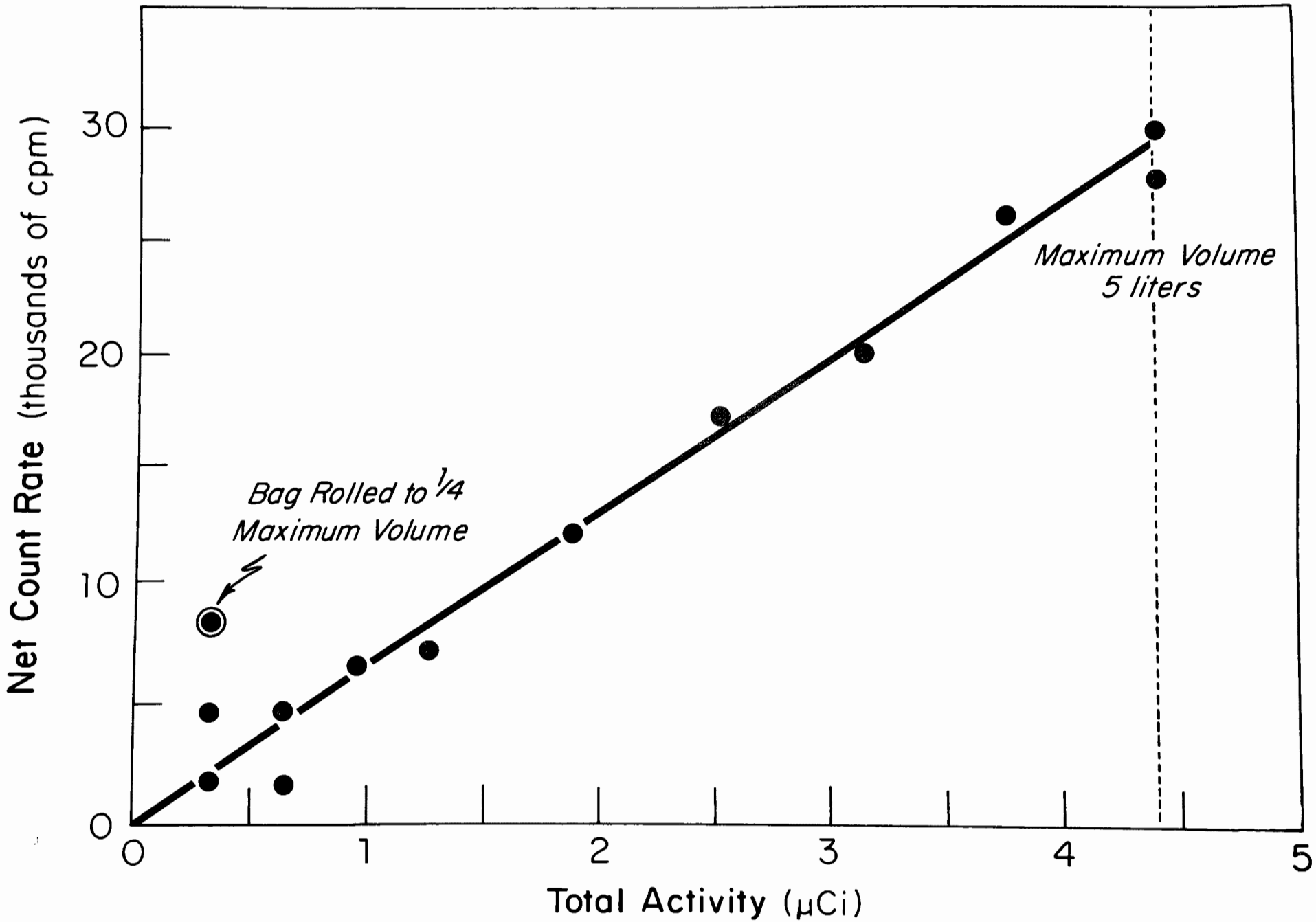

Figure 4. Response of the Eberline HP-210 G.M. probe to a fixed concentration of ^{85}Kr in a 5-liter Saran at different volumes. (The counting time for each observation was 1 minute.)

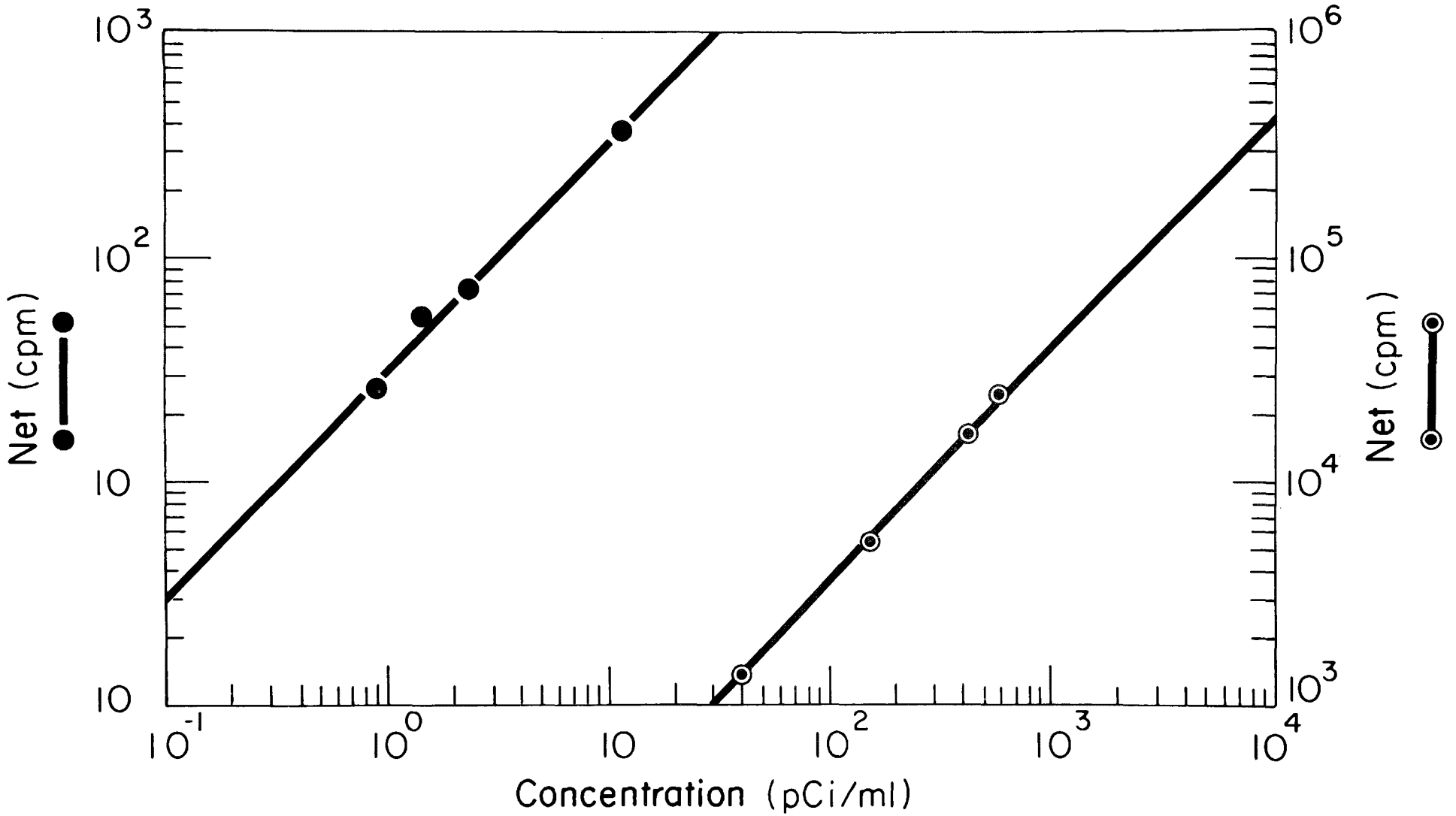

Figure 5. Response of the Eberline HP-210 G.M. probe to 5 liters of ^{85}Kr in the 5-liter Saran bag containing various concentrations. (The counting time for each observation was 3 minutes.)

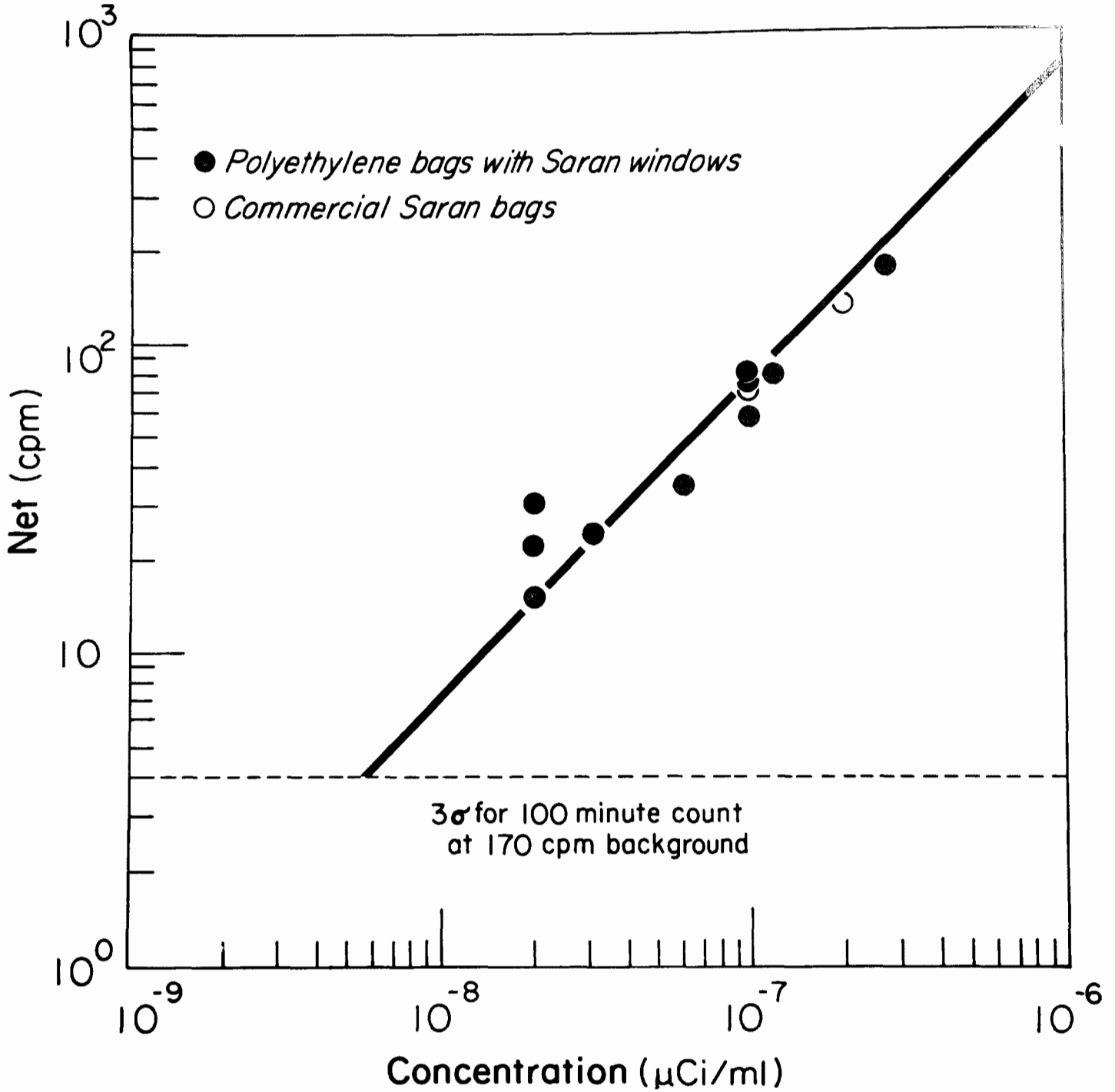

Figure 6. Response of plastic scintillation detector to 23-liter samples of ^{85}Kr in polyethylene bags with Saran windows and 13-liter samples in commercial Saran bags. (All samples were stored overnight and counted to yield a 3σ error of 3% or 100 minutes counting time, whichever occurred first.)

ENVIRONMENTAL RADIATION MONITORING WITH THERMOLUMINESCENT DOSIMETERS

E. L. Geiger and E. A. Sanchez
Eberline Instrument Corporation
Santa Fe, New Mexico 87502

Abstract

Thermoluminescent dosimetry (TLD) provides one method of documenting environmental radiation dose rates near nuclear facilities. Factors that affect the accuracy and precision of TLD measurements have been evaluated using badges with five solid lithium fluoride dosimeters sealed in plastic. Data obtained from 1968 to date (July 1973) indicate that careful attention to annealing and reading can provide an accurate and precise documentation of background radiation dose rates. In-transit exposure was found to be the largest variable, and this error can be eliminated by local annealing and reading. With the TLD program described, a change at the site perimeter as small as 10 mrem/year can be measured, but the problem is to identify the reason for the change. Changes in background radiation dose rates due to snow cover, soil moisture, and various other natural phenomena, and natural differences in dose rates at various locations near a nuclear power station complicate the interpretation of TLD data. For best results, the monitoring program should be designed to compare "indicator" and "reference" station measurements as well as "pre-operational" and "operational" measurements.

INTRODUCTION

The "as low as practicable" (ALAP) concept for the control of radiation exposures has caused some changes in methods for environmental radioactivity surveillance around nuclear power plants. Regulatory guides, technical specifications, and design objectives require sensitivities for some measurements that are one or more orders of magnitude lower than previously considered necessary. For example, the method now used by Eberline Instrument Corporation for ^{131}I in milk has a sensitivity of 0.2 pCi/1, whereas a year ago 10 pCi/1 was adequate.

The measurement of radiation dose from noble gases released to the atmosphere at the design objective of 10 mrem/year is even more difficult than the measurement of ^{131}I in milk at the level specified in AEC Regulatory Guide 1.42. In an attempt to measure this small dose attributable to the nuclear power plant in the presence of a much larger and variable dose attributable to natural background, integrating dosimeters are placed at sites around the nuclear facility. The dosimeters must accurately measure dose for a wide range of photon energies. Thermoluminescent dosimeters (TLD) have been used by Eberline for environmental monitoring since 1968, but the need to measure changes as low as 10 mrem/year has only recently been emphasized. Precision and accuracy of measurement have become increasingly important with the emphasis on reducing exposures to the ALAP design objective.

The U.S. Environmental Protection Agency review of natural radiation exposure in the United States (EPA, 1972a) provides an indication of the magnitude of variations in background radiation. Variations due to cosmic radiation at a specified site location and altitude are less than 10%, but variations due to terrestrial radiation are frequently larger than 10%. Natural ^{40}K and the decay chains of uranium-238 and thorium-232 account for most of man's exposure from natural terrestrial radiation.

Spatial variations at a site are due primarily to terrestrial radioactivity. The results in Figure 1 illustrate the magnitude of variations due to terrestrial radioactivity that have been measured within ten miles of a proposed site. These data are based on 12,581 usable spectra from *in-situ* gamma spectrometry within a ten-mile radius of the Allen's Creek site in Austin, County, Texas. A helicopter was used to make the survey for Houston Lighting and Power Company. Terrestrial radiation dose rates at this site varied from 1 to 8 μrem/hr. Total dose rates (terrestrial plus cosmic) at 25 TLD locations were estimated based on this one-day survey of terrestrial dose rates, assuming 33 mrem/year from cosmic radiation at the altitude and latitude of the site. These estimated total dose rates are compared in Table 1 with integrated dose (TLD) measurements over a period of two calendar quarters. The estimated total dose rates based on *in-situ* gamma spectrometry measurements are lower than the TLD measurements. This may be attributed to soil moisture at the time of the survey (water standing in some areas), which causes a negative bias in the *in-situ* gamma spectrometry data, and in-transit exposure of the TLD badges, which causes a positive bias in the TLD data.

Time variations of radiation exposure at a site are due primarily to soil moisture (and snow cover at some sites), migration of radon gas from the ground to the atmosphere, and subsequent deposition of the radon-daughters on the surface of the ground. Order of magnitude changes have been observed in the dose rate from the uranium-238 decay series due to migration of radon from the ground and subsequent deposition of radon-daughters (Adams, 1972). Short-term dose rate measurements are subject to more variation than long-term integrated dose measurements. Even so, integrated month-to-month variations as large as 10% have been measured (Burke, 1972), and monthly variations as high as 25% can be expected (EPA, 1972a).

These natural fluctuations complicate the measurement of 10 mrem/year attributable to operation of a nuclear power plant, and indicate a need for a series of monthly or quarterly integrated dose measurements at "indicator" and "reference" stations verified by annually integrated dose measurements. The purpose of this paper is to discuss some of the factors that affect the accuracy of this type of measurement, present some of the results obtained from 1968 to date, and discuss the design of an environmental monitoring program for measuring external radiation dose.

METHOD

Lithium fluoride was selected as the dosimeter material because its response to gamma is relatively independent of energy and it has a similar response/rad for penetrating beta radiation. Solid lithium fluoride (TLD-100) chips, ⅛" by ⅛" by 0.035", were 100% selected for uniform response to gamma irradiation. They were annealed at 400°C for one hour, and then overnight (16 hours) at 80°C, immediately prior to use. (For best results, Eberline now anneals the dosimeters twice, immediately before each use period.) Each TLD badge contained five dosimeters sealed in black plastic to protect the dosimeters from direct exposure to sunlight, and then in clear plastic to further protect the dosimeter from weather. The total thickness of the plastic has ranged from 20/mg/cm^2 to 50/mg/cm^2. The 50 mg/cm^2 thickness has been found to be the most satisfactory because the badges are more durable. Some evaluation data were also obtained using additional aluminum shielding so that the total thickness was 300 mg/cm^2. The dosimeters were read as soon as possible after exposure with an Eberline Model TLR-5 thermoluminescent dosimeter reader. The reader was set to integrate only the light output at temperatures between 150°C and 250°C. Using this method, Eberline has not been able to detect any fading of dosimeters when exposed to radiation and then to extreme weather conditions over extended periods of time, up to 15 months.

RESPONSE VS. RADIATION ENERGY

The radiation emitted from steam lines or tanks on-site, a semi-infinite cloud of gas, radioactivity in the earth, cosmic scatter in the atmosphere, and other sources are scattered, absorbed, and reduced in energy so that the environmental TLD must measure dose from a continuous spectrum of photon energies, ranging from 0 to the maximum energy of the emitted radiation. For a BWR, the gamma energy may be as high as 7 MeV. Some of the low-energy radiation will not penetrate the skin or covering over the lens of the eye and does not contribute significant dose to lens of the eye, gonads, other critical organs, or whole body. This non-penetrating component is difficult to measure and its measurement is of doubtful value since the major concern for large population groups is genetic and whole body dose (NCRP, 1971). Photons above 20 keV contribute most of the whole body and genetic dose.

Some of the most sensitive TLD materials, *e.g.,* $CaSO_4$:Tm, CaF_2:Mn, and CaF_2 :Dy, have responses that are very energy dependent below 200 keV. The response of one glass encapsulated CaF_2 :Mn system used extensively for environmental monitoring is discussed in reference (EPA, 1972b), and shows an over response as high as a factor of ten to energies below 200 keV unless an energy compensating shield is used. This is typical of the data that can be expected from CaF_2 and $CaSO_4$ dosimetry systems. The major disadvantage of the shielded CaF_2 or $CaSO_4$ systems is that the response is very sharply reduced or eliminated below 70 keV. Above 70 keV, the error due to energy dependence can be reduced to less than ± 10% with an energy compensating shield. This is the major reason LiF is preferred to CaF_2 or $CaSO_4$ for this application.

The response vs energy for solid LiF dosimeters, 0.125" x 0.125" x 0.035", is shown in Table 2 for dosimeters shielded with 50 mg/cm^2 (plastic) and 300 mg/cm^2 (aluminum and plastic). Prior to 1973, the TLD badges supplied by Eberline for environmental monitoring were provided in plastic bags with no additional aluminum shielding. If no attempt is made to measure non-penetrating skin dose, the total thickness of material covering the LiF dosimeters should be 300 mg/cm^2, which is the approximate thickness of the covering over the lens of the eyes.

IN-TRANSIT EXPOSURE

Shipment of badges by mail or commercial carrier may result in some radiation exposure in transit. The variations due to in-transit exposure are indicated by the data in Table 3 for badges that were shipped by air from Santa Fe, New Mexico, to Cedar Rapids, Iowa, and then returned immediately to Santa Fe for reading. Results for eight out of eleven shipments were within a 2 to 6 mrem range which can be attributed to natural background. Three of the shipments were 10 mrem or higher, indicating some exposure above normal background. Thus, in-transit exposure is an unpredicatable variable that causes a positive bias in some of the results. To minimize in-transit exposure, Eberline has established three regional service facilities and encourages in-plant annealing and reading for plants not located near one of these service facilities.

PRECISION OF MEASUREMENT

Each environmental TLD badge contains five dosimeters. The average reading for the five dosimeters is considered the dose for the period from time of annealing to time of reading. The precision of measurement at the 95% confidence level is indicated by the error term in Table 2. At a dose level of 100 mrem, the precision (95% confidence) is 3% to 5% for energetic gamma radiation, and approximately 10% for lower energy x-rays.

MONTHLY VARIATIONS

Data from an extensive program of pre-operational environmental radiation monitoring at the Duane Arnold Energy Center (DAEC) near Cedar Rapids, Iowa, are summarized in Table 4. These data provide an indication of the magnitude of monthly variations in natural background readings. Time dependent variations are primarily a function of weather conditions (snow, rain, and barometric pressure); however, the data in Table 4 includes some variation due to annealing and reading which cannot be identified separately. A total of 48 stations were monitored for one complete year. Results were grouped by reference stations (those greater than five miles from the site), on-site stations, perimeter stations, and stations located one to three miles from the site. The ranges of average dose rates in mrem per week for these four groups were 1.03 to 1.73, 1.26 to 2.24, 1.06 to 1.85, and 1.10 to 1.89, respectively. The low-reading for each group occurred in mid-winter (December, 1972), and the high-reading occurred in the fall (September, 1972). This is consistent with published information about the effects of snow cover and soil moisture on natural background dose rates.

The magnitude of these monthly variations indicates the potential error associated with making background dose measurements over a period of one month or less, and extrapolating that to an annual dose rate. These data indicate the need for pre-operations TLD measurements at carefully selected locations over a period of at least two years.

CONFIRMATION OF MONTHLY READINGS WITH ANNUALLY EXCHANGED BADGES

The data in Table 4 may be used also to compare the annual average dose rate based on badges exchanged monthly with others exchanged annually. The badges that were read monthly were annealed and read on-site to avoid intransit exposure. One set of annual badges was annealed and read on-site and another set was annealed and read in Santa Fe, New Mexico. Assuming that the DAEC annual badges provide the best indication of the annual average dose rate, the results for annual badges read in Santa Fe seem to be biased high by 3% to 5%. This is excellent agreement, but even this small bias may be due to in-transit exposure. The annual average dose rates based on badges exchanged monthly seem to be high by about 25%. This may be associated with the very low readings (near the sensitivity of LiF) obtained after only a month. TLD badges exchanged quarterly and annually may provide better documentation than badges exchanged monthly and annually.

COMPARISON OF INDICATOR AND REFERENCE STATIONS

Data were obtained in 1970 at the Dresden Nuclear Power Station to compare TLD and ion chamber results at "indicator" and "reference" stations near an operating nuclear power station (EPA, 1972c). The data in Table 5 and 6 were obtained by annealing and reading the TLD badges in Santa Fe, New Mexico; therefore, the readings may include some in-transit exposure as previously discussed. Ion chamber readings should not be considered absolute values because they are affected by energy response, temperature, atmospheric pressure, humidity, calibration method, charge leakage, and readout error. The Dresden badges were placed in a locked metal enclosure which also contained the air sampling equipment. This equipment causes some shielding and also produces secondary electron scatter from metal surfaces. Even with known errors, the TLD and ion chamber results indicate that on-site and site perimeter readings are significantly higher than more distant off-site readings. Environmental TLD badges would be expected to provide the most usable data with local read-out and a program that is designed to compare dose at "reference" (background) locations with dose at "indicator" locations to distinguish changes due to natural causes from changes attributable to operation of the nuclear power plant.

RECOMMENDATIONS

One of the most difficult ALAP measurements to make is 10 mrem per year of environmental radiation dose attributable to the operation of a nuclear power plant. For this purpose, the following TLD program is recommended using solid LiF dosimeters and the Eberline TLR-5 method of reading:

(a) Use local annealing and reading to avoid unpredictable in-transit exposure during shipments by mail or commercial carrier.

(b) Anneal the dosimeters just before they are placed out in the environment, and read them within one or two days after they are removed from the location being monitored.

(c) Use two sets of badges, exchanged quarterly and annually.

(d) Design the program to include reference stations located five to ten miles from the site, indicator stations located on the site perimeter, and indicator stations located within three miles of the site perimeter. The number of stations in each group depends on the site. Use of TLD is very economical in comparison to other environmental measurements, and a large number of stations should be included in the monitoring program. Averages for each group should be compared to help identify changes attributable to the nuclear power plant.

(e) Use pre-operational measurements to establish the relative average background dose rates for groups of reference and indicator stations.

REFERENCES

Adams, J.A.S., (1972), Rice University, Department of Geology, personal communication.

Burke, G.P., (1972), *Thermoluminescent Dosimeter Measurements of Perturbations of the Natural Radiation Environment,* paper presented at the Second International Symposium on the Natural Radiation Environment, Houston, Texas.

Environmental Protection Agency, (1972a), *Natural Radiation Exposure in the United States,* Document ORP/SID 72-1.

Environmental Protection Agency, (1972b), *Radiation Data and Reports,* Vol. 13, No. 10, October 1972, p. 539.

Environmental Protection Agency, (1972c), *Radiation Data and Reports,* Vol. 13, No. 11, November 1972, p. 601.

National Council on Radiation Protection and Measurement, (1971), *Basic Radiation Protection* Criteria, NCRP Report No. 39, January 1971.

TABLE 1. Variations in Terrestrial and Total Background Dose Rates at Different Locations Near the Allens Creek Site.

	Dose Rates (mrem/week*)			
Station Number	**In-Situ Terrestrial**	**Estimated Total**	**TLD 1st Qtr.**	**TLD 2nd Qtr.**
1	0.62	1.3	1.4	1.5
2	0.47	1.1	1.4	1.1
3	0.50	1.2	1.2	1.2
4	0.45	1.1	1.2	1.4
6	0.50	1.2	1.3	1.2
7	0.37	1.0	1.2	1.2
8	0.39	1.0	1.4	1.3
9	0.62	1.3	1.6	-
10	0.76	1.4	1.6	1.6
11	-	-	1.3	-
12	0.54	1.2	1.5	1.4
13	0.40	1.0	1.2	1.0
14	0.35	1.0	1.0	1.2
15	0.76	1.4	2.0	1.8
16	0.25	0.9	1.3	-
17	0.47	1.1	1.5	1.0
18	0.55	1.2	1.4	1.2
19	0.47	1.1	1.1	0.9
20	0.32	1.0	1.1	0.8
21	0.37	1.0	1.0	1.5
22		-	1.1	
23	-	-		1.2
24	0.42	1.1	1.3	1.2
25	-			1.3

*Terrestrial dose rates were measured by *in-situ* gamma spectrometry. The cosmic-ray dose rate at the site was estimated to be 33 mrem/year. The "estimated total" dose rates were obtained by adding the measured terrestrial component to the estimated cosmic component. TLD results are based on annealing and reading in Santa Fe without any correction for in-transit exposure, and is the total reading for the period divided by number of weeks from annealing to reading. Each *in-situ* measurement was made on one day over a large area, whereas the TLD integrates over a period of three months for a smaller area.

Table 2. Energy Calibration of LiF TLD Area Badges*
(All Badges Exposed in Air to 100 mR).

Photon Energy and Source	Average of Ten Badges ± 2 σ	
	50 mg/cm²	300 mg/cm²
23.7 keV, K-Fluorescence	121±10	76±6
58 keV, K-Fluorescence	117±7	119±8
120 keV, Filtered X-Ray	94±10	99±9
662 keV, ^{137}Cs Gamma	100±5	100±5
1250 keV, ^{60}Co Gamma	108±3	98±3

*The TLD badge used for routine environmental monitoring has a total plastic thickness of 50 mg/cm² covering the dosimeters. If only penetrating whole body dose is to be measured, an aluminum shield should be used to increase the total absorber thickness to 300 mg/cm².

Table 3. In-Transit Exposure Via Air
(Santa Fe, New Mexico to Cedar Rapids, Iowa and Return*).

Date Annealed	Date Read	Readings Obtained (mrem ±2 σ)			
06-28-71	07-02-71	2±1	2±1	2±1	1±1
07-26-71	07-30-71	10±1	10±1		
08-30-71	09-03-71	2±1	1±0		
09-27-71	10-04-71	4±1	4±1		
11-29-71	12-06-71	4±1	4±1		
02-28-72	03-06-72	6±1			
03-27-72	04-03-72	3±1	3±1		
04-24-72	05-10-72	6±1	6±2	6±1	
05-30-72	06-07-72	18±2	14±1		
07-31-72	08-16-72	2±1	5±1		
03-16-73	04-09-73	10±1			

**Normal route via Denver or Chicago.*

Table 4. Monthly Variations in Dose Rates Measured with LiF TLD (Duane Arnold Energy Center).

Period of Exposure	Average mrem/week*			
	Reference Stations ≥5 Miles from Plant	On-Site Stations	Perimeter Stations	Stations 1 to 3 Miles from Plant
Apr. 1972	1.51	1.58	1.52	1.57
May 1972	1.52	1.58	1.62	1.67
June 1972	1.52	1.61	1.65	1.75
July 1972	1.55	1.85	1.70	1.77
Aug. 1972	1.50	1.93	1.71	1.89
Sep. 1972	1.73	2.24	1.85	1.89
Oct. 1972	1.48	1.81	1.55	1.62
Nov. 1972	1.29	1.44	1.33	1.36
Dec. 1972	1.03	1.26	1.06	1.10
Jan. 1973	1.42	1.67	1.56	1.60
Feb. 1973	1.47	1.38	1.58	1.61
Mar. 1973	1.23	1.30	1.34	1.41
12-Month Average	1.44	1.63	1.53	1.61
Annual Badges:				
On-Site Annealing and Reading	1.27	1.31	1.33	1.32
Santa Fe Annealing and Reading	1.31	1.44	1.37	1.46

*Data are for the pre-operational period. Any differences noted are not due to plant operation.

TABLE 5. Comparison of TLD Data for Reference Stations and Indicator Stations (Dresden Nuclear Power Station, 1970).

Reading Location	Distance from Stack (miles)	Net Dose* Ion-chamber (mrem/yr)	Net Dose* TLD (mrem/yr)
On-Site:			
#1	NW	33	37
#2	NE	69	77
#3	S	24	33
Perimeter:			
Bennet	1 NE	26	32
Breen		32	27
Hansel	1.5 NNW	27	29
Off-Site:			
Lorenzo	2.1 SSE	9	2
Clay Product	2.5 S	9	16
McCabe	2.9 WSW	6	11
Channanon	4.2 NE	6	9
Minooka	4.4 NNE	5	5
Coal City	8.0 S	7	3
Morris	8.0 SW	4	5
Elwood	8.2 E	14	7
Wilmington	8.6 SE	5	8
Lisbon	12.3 NW	5	4
Joliet	12.7 NE	9	0
Plainfield	15.7 NNE	3	5
Summary:			
On-Site		42	49
Perimeter		28	29
Off-Site		7	6

*Net dose is actual readings in 1970 with natural background subtracted based on 4th quarter of 1969 when the Dresden Station was not operating. For details, see reference (EPA, 1972c).

TABLE 6. Comparison of Data for Indicator and Reference Stations.

Location	Net Dose (mrem/a) Ion Chamber	Net Dose (mrem/a) TLD
On-Site 1	33	37
On-Site 2	69	77
On-Site 3	24	33
Average On-Site	42	49
Perimeter 1	26	32
Perimeter 2	32	27
Perimeter 3	27	29
Average Perimeter	28	29
Average of 12 Off-Site Stations > 2 miles	7	6

Figure 1.

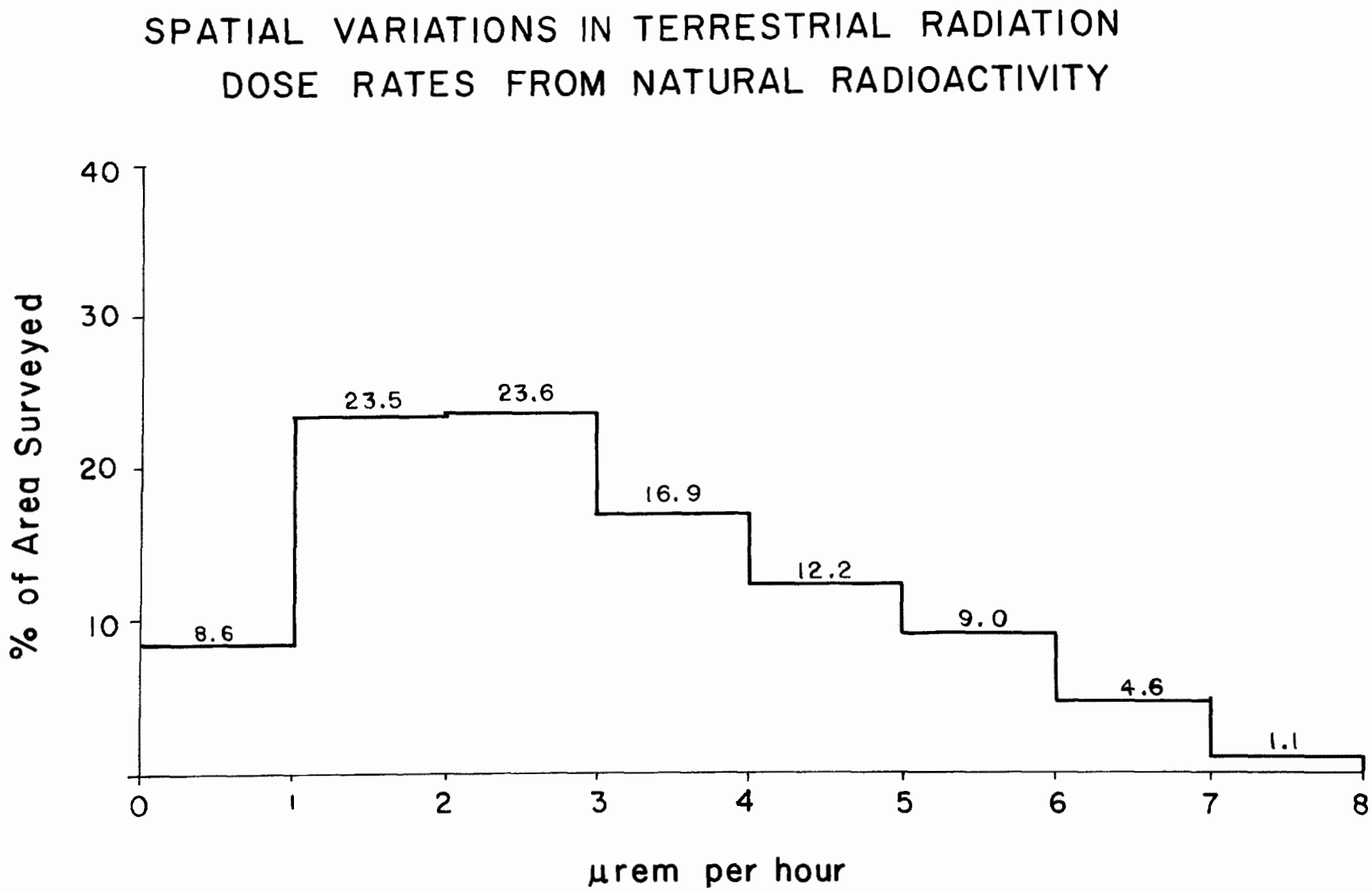
SPATIAL VARIATIONS IN TERRESTRIAL RADIATION
DOSE RATES FROM NATURAL RADIOACTIVITY
% of Area Surveyed
40
30
20
10
8.6
23.5
23.6
16.9
12.2
9.0
4.6
1.1
0
1
2
3
4
5
6
7
8
µrem per hour

RADON EMANATION FROM URANIUM MILL TAILINGS USED AS BACKFILL IN MINES

M. Raghavayya and A. H. Khan
Health Physics Division
Bhabha Atomic Research Center
Bombay-400085, India

ACKNOWLEDGEMENTS

The authors are grateful to Dr. A. K. Ganguly, Director, Chemical Group, Bhabha Atomic Research Center and Mr. S. D. Soman, Head, Health Physics Division, Bhabha Atomic Research Center for guidance. Appreciation is expressed for the assistance received from Mr. P. M. Markose, Mr. K. P. Eappen, and other colleagues.

Abstract

As a standard practice, uranium mill tailings are returned to the mine as backfill to stabilize stoped out areas. The tailings returned to the mine are the coarser fraction as separated by hydrocyclones. These "sands" still contain significant quantities of radium. Being in a finely divided form, the sands offer a much larger area for the emanation of radon as compared to the unbroken ore. The emanation of radon from the backfill is, therefore, expected to be much higher than from the ore body itself.

This paper describes a method for estimating the radon emanation from mill tailings used as backfill. The effect of increased emanation rates on ventilation requirements is discussed.

INTRODUCTION

The process of mining ore leaves voids underground which can be hazardous if not stabilized. A standard practice in uranium mines, as elsewhere, is to use the tailings left over after extracting the useful minerals from the ore as backfill. For this purpose, the tailings are separated into two parts with hydrocyclones of which the coarser "sands" are used for backfill.

At Jaduguda in India, where the work being described was carried out, nearly 50 percent of the uranium mill tailings was used as the backfill material. The sand slurry was pumped to the worked out stopes. The water percolated through, and the sand settles under gravity. The sands are made up predominantly of particles above 74 μm in size.

While aiding in the stabilization of the ground, the mill tailings used for this purpose create certain problems. Although uranium itself has been extracted, the tailings are still left with significant quantities of radium, which give rise to radon. Being in a finely divided form, the sands offer a much larger surface area for radon to emanate through. The sands, even after settling down to a consolidated mass, are still highly porous as compared to the original ore. All these factors may combine to eventually increase the rate of radon emanation into the mine atmosphere, and thereby raise the ambient levels of radon and daughter products.

This work deals with a laboratory method devised to study the rate of emanation of radon from the sands. Emanation studies carried out under actual field conditions are also described.

EXPERIMENTAL DETAILS

1. Laboratory Setup.

The apparatus we built is shown in Figure 1. It consists of a chamber C1 with a B-55 standard joint at one end and a tightly stretched thick polyster filter cloth at the other. The filter end can be sealed off completely if necessary.

The sand sample normally occupies almost the entire volume of C1, as shown in the figure. A second chamber C2 which is open at both ends fits into the open end of C1. The other end of C2 is connected to a third chamber C3 with a wide collapsible rubber tube. The other end of C3 is closed with a single-hole rubber stopper provided with a stopcock. The air space in the upper chambers C2 and C3 serves as the accumulation volume for the radon gas emanating from the sample of the sand placed in the lower chamber C1.

Sands are collected in chamber C1 in the form of a slurry from the tailings fraction sent to the mines for backfilling. The slurry is generally filled up to the brim of the chamber. The water is allowed to drain completely through the filter cloth by gravity. As the water drains, the sands get consolidated to a certain level somewhat below the brim. The lower end is then sealed off and the chamber C1 is connected to the remaining part of the emanation setup after flushing the space in C1 above the sands with air to remove all radon already present.

Radon emanates through the sand surface and accumulates in the air space in the system. After a known interval 't' (usually on the order of a few hours), the passage between chamber C2 and C3 is pinched off with a pinch cock. Next, an evacuated scintillation flask is connected to the stopcock and a sample of air from chamber C3 is drawn into the scintillation flask. The purpose of pinching the passage between C2 and C3 is to ensure that the partial vacuum created in the system during sampling does not enhance emanation from the

sands. The stopcocks are closed and the scintillation flask is then detached from the system. The pressure in the chamber C3 is equalized with the outside by introducing the required amount of radon-free air into it. The pinch cock is then released. Sampling is repeated several times.

2. Field Setup.

Six sets of experiments were carried out under actual field conditions in some of the stopes in the mine, where sand stowing was in progress. The apparatus consisted of a drum about 25 liters in capacity and with a cross sectional area of about 600 cm^2. It was open at one end and a stopcock was attached to the other end which was otherwise closed. The drum was buried in the sand to a depth of about 20 cm, open end downwards. Radon collected in the drum was measured twice, once immediately after inserting it in the sand, and again after a time lapse varying between 7 and 65 hours.

THEORETICAL CONSIDERATIONS

Throughout this treatment the following notations are used:

1. Laboratory Experiment.

- V = total volume wherein radon from the sand sample accumulates (liter)
- V_1 = volume of chamber C3 plus half the volume of the passage between C2 and C3 (liter)
- V_2 = volume of the scintillation flask (liter)
- A = area of cross section of chamber C1 which is also the area of the surface through which radon emanates, (cm^2)
- r_i = concentration of radon measured from the ith air sample from each sand specimen, (Ci/liter), i = 1, 2, 3, ...n
- R_i = total radon activity in the system just before the collection of the ith sample, (Ci)
- t = time interval between any two sampling instants
- λ = decay constant of radon
- J = radon emanation rate during any interval 't', (Ci/cm^2.s)

Let $\left(\frac{V_1 + V_2}{V_1}\right) V = (P)$

and $(P) - V_2 = (Q)$

It can be shown that, $R_i = (P) r_i$

The sampling depletes the system of a part of the accumulated radon. The radon activity so removed is $V_2 r_i$, so that the total radon activity remaining in the system immediately after the ith sample has been drawn is given by,

$$R_i = (Q) r_i \qquad (2)$$

The $(i + 1)^{th}$ sample is collected after a lapse of time 't'. During this interval, two simultaneous processes may be imagined to be taking place within the emanation system, finally resulting in a total radon activity in the system equal to R_{i+1}.

(1) Activity of radon already present decays to a value $\exp^{-\lambda t}$ times the original activity.

(2) Due to emanation from the sand; fresh radon is introduced into the free space in the system, thereby tending to increase the radon activity. The activity of radon introduced by the second process can be expressed as,

$$R'' = \frac{A \times J}{2.097 \times 10^{-6}} \left(1 - \exp^{-\lambda t}\right) \qquad (3)$$

where 2.097×10^{-6} is the decay constant of radon expressed in s^{-1}

$$\text{Now, } R_{i+1} = R_i' \exp^{-\lambda t} + R''$$

$$\text{so, } (p)\, r_{i+1} = (Q)\, r_i \exp^{-\lambda t} + \frac{A\, J}{2.097 \times 10^{-6}} \left(1 - \exp^{-\lambda t}\right) \qquad (4)$$

$$\text{and hence } J = \frac{2.097 \times 10^{-6}}{A\,(1-\exp^{-\lambda t})} \left[(P)\, r_{i+1} - (Q)\, r_i \exp^{-\lambda t}\right] \qquad (5)$$

2. Field Experiments.

In the field experiments, only two samples were collected in each case, the first at the commencement of experiment and the second after a time t. The emanation rate in this case can be calculated from

$$J = \frac{2.097 \times 10^{-6}}{A\ (1-\exp^{-\lambda t})} \quad (R_2 - R_1' \exp^{-\lambda t})$$

In this case $V_1 = V$, so from (1) and (2)

$$R_2 = (V + V_2)\ r_2, \text{ and } R_1' = Vr_1$$

$$\text{therefore, } J = \frac{2.097 \times 10^{-6}}{A\ (1-\exp^{-\lambda t})} \cdot \left[(V + V_2)\ r_2 - Vr_1 \exp^{-\lambda t}\right] \qquad (6)$$

RESULTS

Table 1 presents the emanation rates obtained from the different sand specimens in the laboratory, and Table 2 presents the emanation rate in the mine stopes. In the case of laboratory experiments, the 'J' values were determined several times for each sand specimen. The mean of the several determinations is given. The corresponding radium contents of the sand specimens are also given.

DISCUSSION

Table 1 shows that the emanation rates and the radium content of the different sand specimens are of the same order, and we are, therefore, justified in calculating the mean values (Table 2). The emanation rate in the stopes was about 4.5 times more than the corresponding value obtained in the laboratory. The reason is that the sand mass in the stopes was very large compared to the small quantity of the sands used in the laboratory experiments.

It may be concluded that the rate of radon emanation from the sands used as backfill at Jaduguda is $(27.2 \pm 9.5) \times 10^{-16}$ Ci/cm^2.s on the average. A gram of Jaduguda ore contains about 200 pCi of radium while the radium content of the tailings sands is only a third of this value. Khan and Raghavayy (1972) have shown that a representative radon emanation rate from the ore body itself is only 0.41×10^{-16} Ci/cm^2.s despite the higher radium content. The ratio of radon emanation rates of the sands to that of the ore, when radium content is normalized, is 217. This is understandable in view of the higher porosity of the sand, and the increased surface area as a result of the fractionation of the ore. The porosity of the sand is about 50% while that of the ore was found to be about 0.5%. The increase in surface area was found to be about 470 times. The porous sands are affected by changes in barometric pressure in the mine which is also likely to affect the emanation of radon from the sands more than that from the ore.

At Jaduguda, it was observed that the radon concentrations in stopes where tailings sands were used as backfill were more than the radon concentrations in other stopes. The average concentration of radon in filled stopes was 120 ± 15pCi/l while in other stopes it was 45 ± 12 pCi/l, denoting an increase of radon concentration by a factor of 2.7. To compensate for the elevated radon levels, ventilation in these stopes was correspondingly increased.

It can be concluded that the use of uranium mill tailings as backfill in worked out stopes increases the ambient radon concentrations as a result of an elevated emanation rate. The increase in emanation rate is so large that the emanation from the ore body itself becomes negligible when compared to that from the sands. Ventilation has to be increased in these stopes to cope with the increased radon emanation. The actual increase must be worked out in each case.

REFERENCE

Kahn, A. H. and M. Raghavayya (1973), *Radon Emanation Studies in Jaduguda Uranium Mine*, paper presented at the Third International Congress of the International Radiation Protection Association, Washington, D.C.

TABLE 1. Radon Emanation Rates from Sand Samples (Laboratory Experiments).

Sample No.	Emanation rate ($x10^{-16}$ Ci/cm^2.s)	Radium content (pCi/g)
S1	5.1	68.4
S2	5.2	92.3
S3	2.9	83.0
S4	6.7	69.4
S5	12.5	67.3
S6	4.8	66.9
S7	8.7	57.2
S8	4.5	45.9
S9	6.5	67.3
S10	9.2	58.7
S11	7.8	53.6
S12	7.5	75.3
S13	5.0	78.3
S14	1.9	41.3
S15	2.1	44.2
Mean	6.0 ±1.3	64.6 ±6.6

TABLE 2. Radon Emanation Rates in Mines Stopes (Field Experiments).

Sample No.	Emanation rate ($x10^{-16}$Ci/cm^2.s)	Radium content (pCi/g)
U1	26.7	72.6
U2	27.2	69.3
U3	38.9	-
U4	13.3	51.5
U5	41.4	56.6
U6	53.1	
Mean	27.2 ± 9.5	60.6 ± 9.4

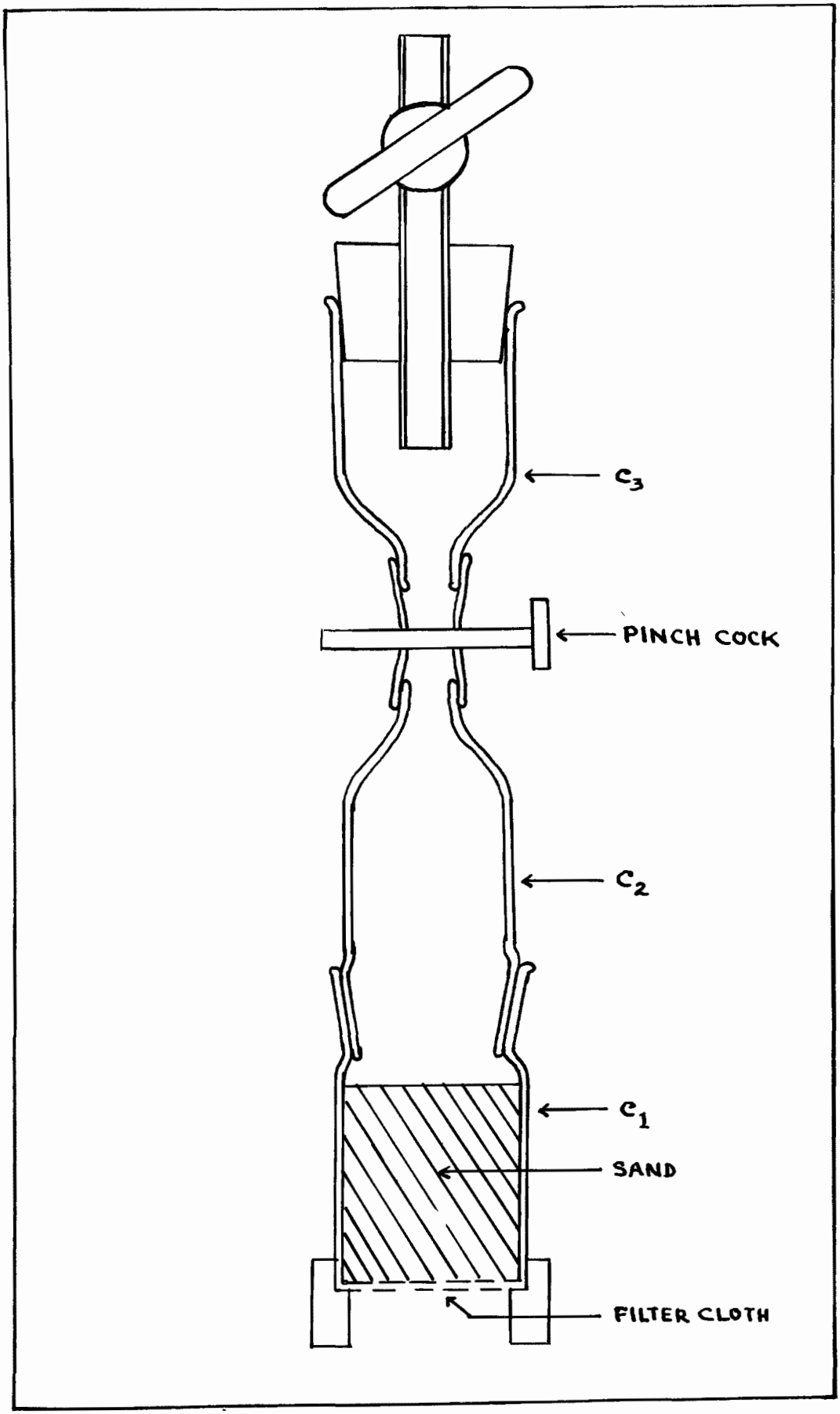

Figure 1. Emanation Set-Up.

FISSION PRODUCT NOBLE GASES IN NUCLEAR POWER STATION OPERATION

P. Abraham and S. D. Soman
Health Physics Division
Bhabha Atomic Research Center
Bombay 400085, India

Abstract

This paper presents the experience with radioactive noble gases during the operation of the 400 MWe twin Boiling Water Reactor station at Tarapur. The design measures to minimize, control, and monitor the discharge of noble gases from the station into the environment are described. The limits prescribed for the gaseous effluents from the station are given along with the assumptions used to derive them. Actual environmental releases during the four years of station operation are tabulated. Gamma spectra and decay curves of typical off-gas samples are presented and analyzed.

The effects of fuel defects on the isotopic composition of the gaseous releases during operation and the problems encountered in operating the reactors with defective fuel are discussed.

INTRODUCTION

India's first atomic power station (TAPS Report, 1969) is at Tarapur, on the west coast, about 100 km north of Bombay. The power station has two dual-cycle boiling water reactors (BWR's), each of 210 MWe capacity. The station started commercial operation in October 1969. At the end of July 1973, the station had generated 6,748 million kWh of electricity for the two states of Maharashtra and Gujarat.

The second station (RAPS Report, 1971), consisting of two identical units of 200 MWe each of the CANDU type, is located on the Rana Pratap Sagar Lake, 67 km from Kota in Rajasthan State. One of these units attained criticality in August 1972 and is now operating at about 100 MWe. The other unit is under construction.

DESCRIPTION OF SYSTEMS

At Tarapur, the fuel is in the form of sintered UO_2 pellets, stacked in the Zircaloy-2 tubes forming the fuel rods. Thirty-six such fuel rods are arranged in a six-by-six array to form a fuel bundle. The Rajasthan reactor also uses sintered UO_2 in Zircaloy-2 tubes. Each fuel bundle has 19 elements.

By far the largest amount of radioactivity in any reactor is produced by fission which is mostly contained within the fuel itself. Gaseous and volatile fission products, which diffuse out of the fuel, are trapped by the cladding and collect in the gas plenum provided in the fuel. Gaseous radioactivity can come out of the fuel if the cladding is defective or develops defects during operation. Tramp uranium in the cladding also contributes to fission product activity in the reactor water.

Removal of radioactivity from the reactor coolant takes place by several processes; namely, (1) radioactive decay, (2) deposition on surfaces and accumulation in recesses as crud, (3) removal in the cleanup filter and demineralizer, and (4) carry-over with the steam to the turbine and condenser (in the case of BWR's). It is the last process which contributes mainly to the release of gaseous wastes to the environment during the normal operation of the Tarapur Reactors. The different streams of gaseous radioactive effluents reaching the Tarapur stack are shown in Figure 1. At Tarapur the radionuclides carried over to the turbine-condenser in the steam phase are mostly xenon, krypton, nitrogen-16, and nitrogen-13. Nitrogen-16 decays rapidly in the condenser due to its short half-life (7.3 seconds), and is almost completely removed from the waste steam before it reaches the environment. Nitrogen-13 (half-life of 10 minutes) is the only activation product [$^{16}O(p,\alpha)\,^{13}N$] worth considering among the gaseous wastes released to the environment. In fact, it is the most important gaseous radioactive waste during the initial phase of reactor operation, when fuel defects are at a minimum. However, with increased irradiation of the reactor cores, the fission gases have overshadowed the release of nitrogen-13. BWR type reactors are not provided with on-load refueling facilities and, as such, they operate with failed-fuel. Hence, the fission product noble gas release rate increases during the fuel cycle.

The Rajasthan reactors are designed for on-load fueling, so that defective fuel bundles can be replaced immediately after detection with fresh ones. As such, fission product noble gases in the exhaust stream can be minimized by careful operation. However, the use of heavy water as the moderator and coolant causes the presence of tritiated water vapor in the exhaust. In addition, the use of air for cooling certain reactor components contributes to the presence of argon-41 in the effluent stream.

Radioactivity from the Tarapur condenser is continuously removed along with other non-condensable gases by the air ejectors. More than 99% of the gases in the steam go to the air ejector system. This stream flows at the rate of about 20 liters per second from the condenser and is allowed to decay for about 30 minutes in a holdup line of volume 60 m^3, thereby almost completely eliminating short-lived radionuclides like ^{16}N, ^{89}Kr, ^{90}Kr, ^{91}Kr, ^{97}Kr, ^{137}Xe, ^{139}Xe, and ^{140}Xe. Before the gases are released to the base of the 100 m stack, they are filtered using a high-efficiency particulate air (HEPA) filter. Gaseous wastes released to the stack are diluted by ventilation air which flows at the rate of 55 m^3/s. Less than 1% of the process gases escaping through the turbine gland seals is separated from the steam by the gland seal condenser and is exhausted through a

holdup line providing a delay of about 100 seconds. Some of the gases circulate in the primary reactor water. This is indicated by the fact that any primary system leak is accompanied by the release of noble gases, which are readily detectable by the presence of their particulate daughters. Airborne contamination in the occupied areas of the station is almost always caused by such leaks and is due to noble gases and their short-lived daughter products, especially ^{88}Rb and ^{138}Cs. In addition, argon-41 has been detected in the operational areas at Rajasthan probably due to inadequate ventilation.

EXPERIMENTAL RESULTS

Gamma spectra of the off-gas sample from Tarapur Station 30 minutes and 6 hours after collection are given in Figures 2 and 3. Figure 3 shows that ^{133}Xe, ^{85m}Kr, and ^{135}Xe are the only isotopes present after a few hours of decay. The radioactive decay curve of the off-gas sample (Figure 4) indicates that about 3 days after collection the entire activity is due only to ^{133}Xe.

RELEASE LIMITS

ICRP has recommended that populations in the neighborhood of nuclear installations should not receive radiation doses in excess of 500 mrems annually from all sources of radiation. To allow for environmental dose from other routes, 50% of the ICRP limit is apportioned to the air route. Based on meteorological studies at the two sites, release limits are specified for the two stations. The annual average continuous release limit for noble gases works out to 246 mCi/s (21,250 curies/day) for Tarapur Station (Abraham, *et al.,* 1973). At RAPS, the limits (Sah and Subbaratnam, 1973) are as follows:

Noble gases	—	2,500 Ci/day
Tritium	—	29,500 Ci/day

Actual release rates at Tarapur during operation were well within the permissible limits, as is evident from Table 1.

However, these releases were higher than the values expected by design due to defects in the fuel. It was expected that, after refueling, the off-gas releases would be reduced. However, off-gas releases were not significantly lower after refueling. The small relative difference in the radioactivity content of the samples taken from the fuel bundles for identification of the defective bundles made the job very difficult. It should be noted that operation with failed-fuel increases not only the gaseous effluent releases, but also the liquid effluents and the in-plant radiation levels. In order to keep the radiation exposures to station personnel and liquid wastes as low as possible, it is advisable to remove defective fuel as quickly as possible after identification. When defective fuel is present in the core, any reactor transient (increase or decrease in reactor power) causes the activity (in reactor water as well as in the off-gas) to increase and then to level off. This is probably due to the thermal stresses caused by the transients. To overcome this problem for the environment, some BWR's like the KRB nuclear power station (Eickelpasch, 1972) in Germany are using augmented off-gas facilities for the past several years to enable operation of the station without off-gas affecting station output. The KRB facility reduces the releases from the station by a factor of about 1,000. The radioactive gases undergo adsorption and desorption processes and are, therefore, transported through the charcoal beds more slowly than the accompanying air, thus giving the gaseous radioactive nuclides more time to decay during their passage through the delay line. It is reported that it is possible to achieve a delay time of 14 days for xenon. At present, proposals are being examined for the augmentation of the off-gas system at Tarapur by additional holdup capacity to reduce the environmental releases. This is being done as a part of the efforts to reduce environmental radiation levels to as low a level as practicable. Systems which have been proposed include catalytic recombiners followed by low-temperature or cryogenic adsorption on charcoal, gas storage under pressure, or cryogenic distillation. Operational experiences on these systems are not readily available.

DISCUSSION

The off-gas composition at the Dresden BWR is reported (Blomeke and Harrington, 1968) to be 40% hydrogen, 20% oxygen, and 36% air. This means that at least 96% of the gas passing through the delay line is non-radioactive, and in the company of the non-radioactive component, the radioactive gases are speeded through the delay line into the environment. Effective removal of the accompanying gases by using a recombiner (catalytic combustion of the hydrogen and oxygen with the aid of a palladium catalyst or other techniques) can increase the delay time by a factor of 25 or more. The present delay line, which causes a delay of 30 minutes with a flow of 20 l/s, will be able to provide a delay of 12.5 hours if the non-radioactive gases are removed. Perusal of the decay curve would show that 12.5 hours delay will reduce the concentration by a factor of about ten, and the off-site dose (Martin, *et al.,* 1973) by a factor of about 25. This would be enough to reduce the annual environs dose from stack effluents at Tarapur to less than ten millirems even for the periods when the off-gas generation rate is as high as 500 mCi/s. During normal operation, the generation rates in BWR's are considerably lower, and, hence, the dose rates will be less. In other words, the provision of facilities to remove the non-radioactive gases from the stream reaching the delay line would be adequate to reduce the environmental release rates from BWR stations so as to achieve the "as low as practicable" limits currently

under consideration throughout the world. Further increases in holdup may not be necessary to achieve this objective. Martin, *et al.*, (1973), have reported that the discharge of processed effluents after 25-30 days holdup would reduce the off-site dose by a factor of 5,000 at a substantial increment of cost.

Argon-41 concentrations are constant when the power level is not varied. Isolating the exhaust from areas where D_2O leakage is possible, and condensing the moisture from it, can substantially reduce environmental releases from CANDU-type stations in addition to recovering the heavy water if on-load fueling is adopted scrupulously to remove defective fuel immediately after detection.

REFERENCES

Abraham, P., D. Pattnaik, and S. D. Soman, (1973), *Safety Experience in the Operation of a BWR Station in India.* Paper presented at the IAEA Symposium on Principles and Standards of Reactor Safety. IAEA-SM/169-26.

Bloemke, J. O. and F. E. Harrington (1968), *Management of Radioactive Wastes at Nuclear Power Stations.* ORNL-4070.

Design and Analysis Report of the Tarapur Atomic Power Station, Tarapur, India (1969).

Eickelpasch, N. (1972), Personal communication.

Martin, J. E., F. L. Galpin, and T. W Fowler (1973), *Technology Assessment of Risk Reduction Effectiveness of Waste Treatment Systems for Light Water Reactors.* Radiation Data and Reports 14, 1.

Safety Report: Rajasthan Atomic Power Station (1971).

Sah, B. M. L. and T. Subbaratnam (1973), *The Calculation of DWL and ARE Values for the Rajasthan Atomic Power Station.* Paper presented at the Nuclear Science and Engineering Symposium, Bombay.

TABLE 1. Gaseous Radioactivity Releases from Tarapur.

Year	Release rate, mCi/s
1969	3.0
1970	19.2
1971	67.2
1972	38.7
1973 (up to June)	55.2

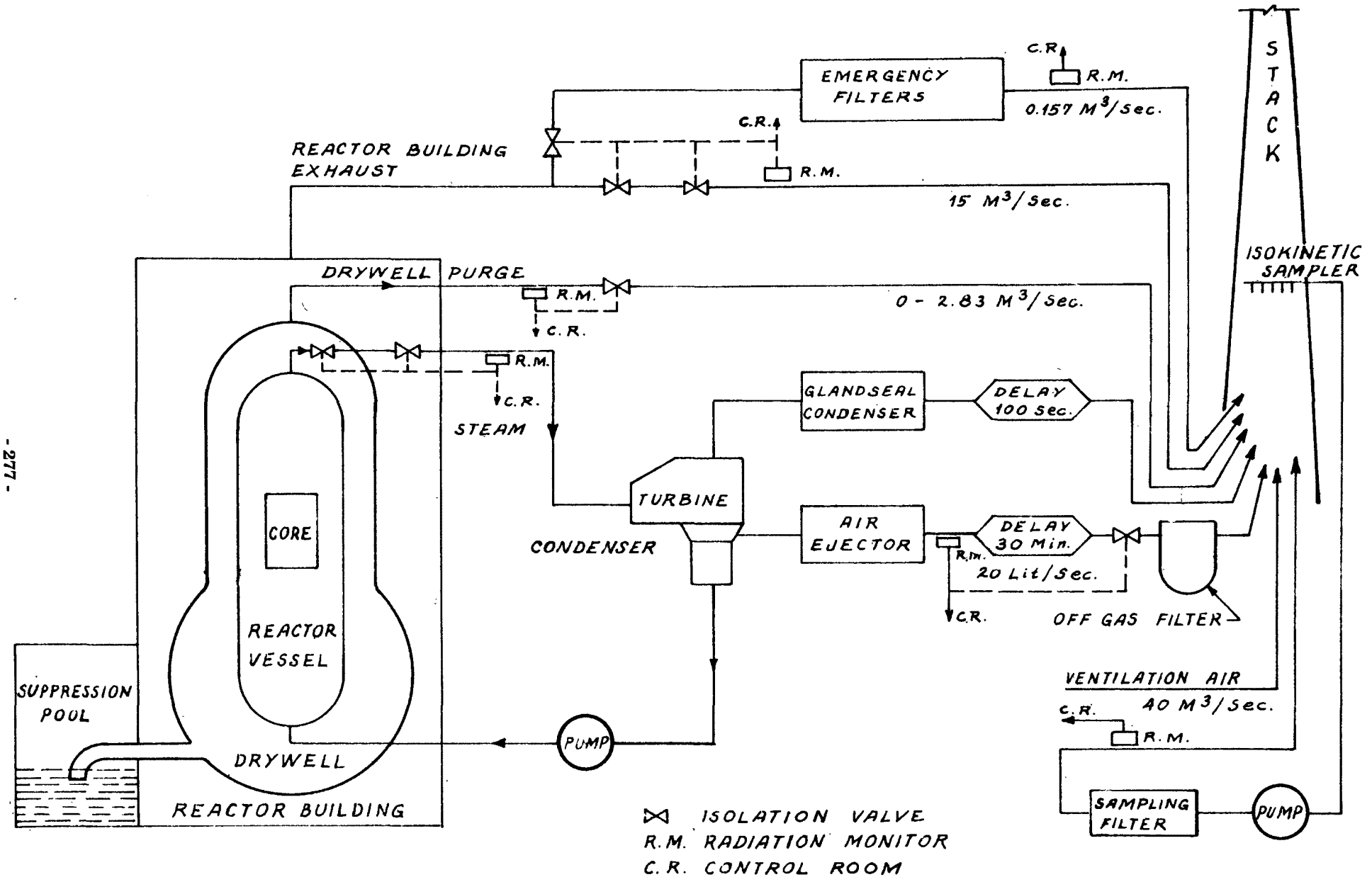

Figure 1. Gaseous Effluent Streams at Tarapur.

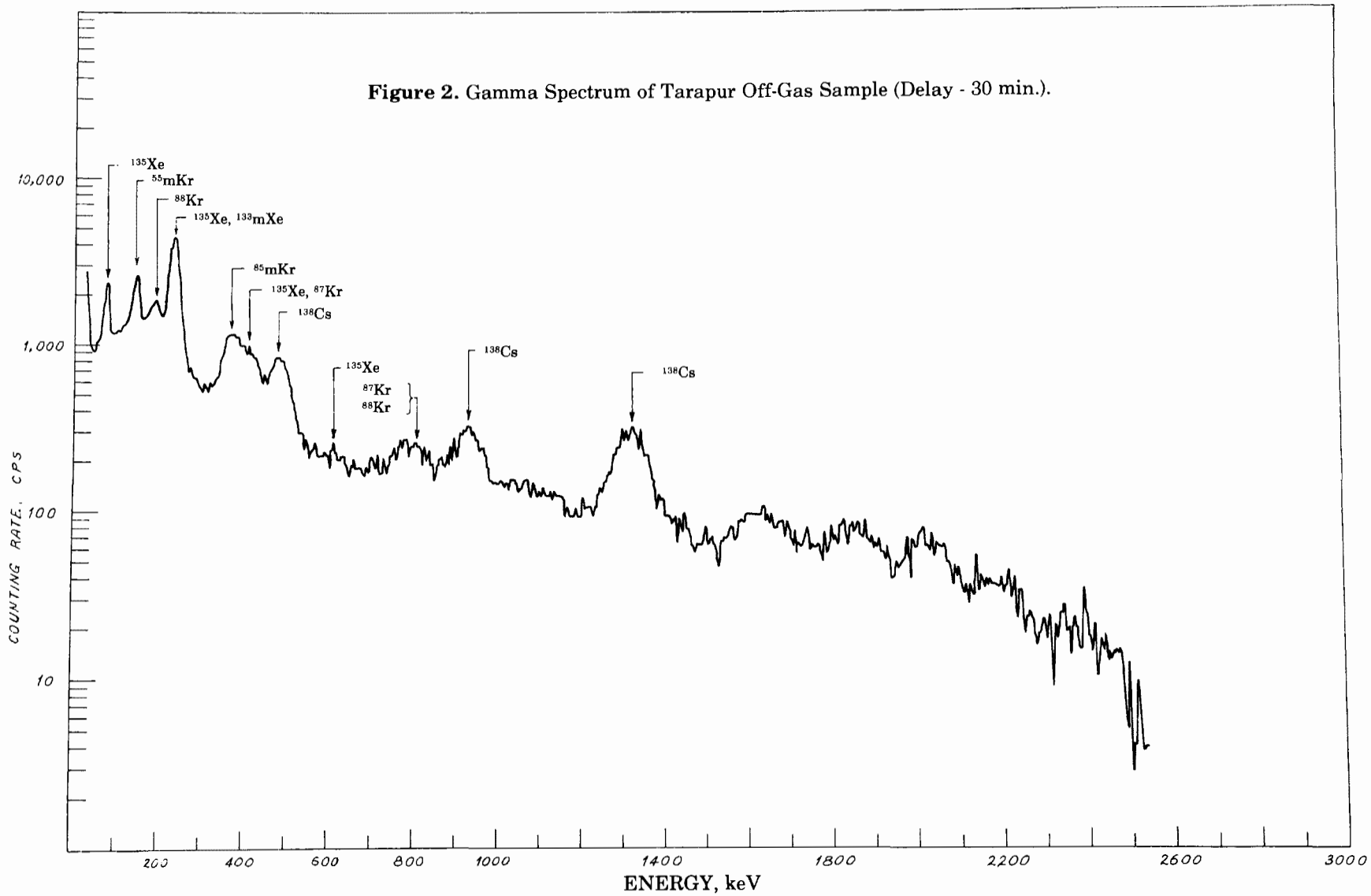

Figure 2. Gamma Spectrum of Tarapur Off-Gas Sample (Delay - 30 min.).

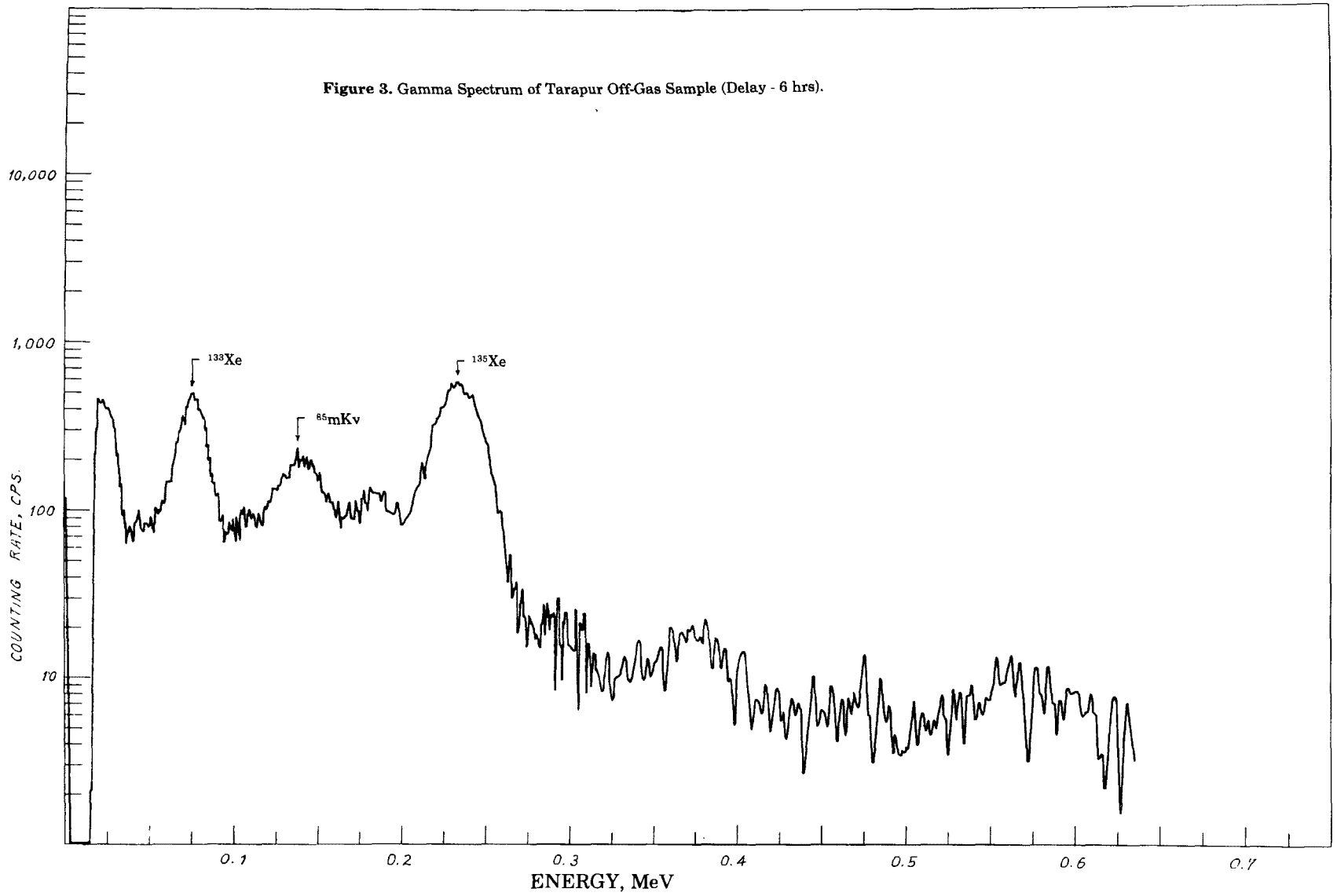

Figure 3. Gamma Spectrum of Tarapur Off-Gas Sample (Delay - 6 hrs).

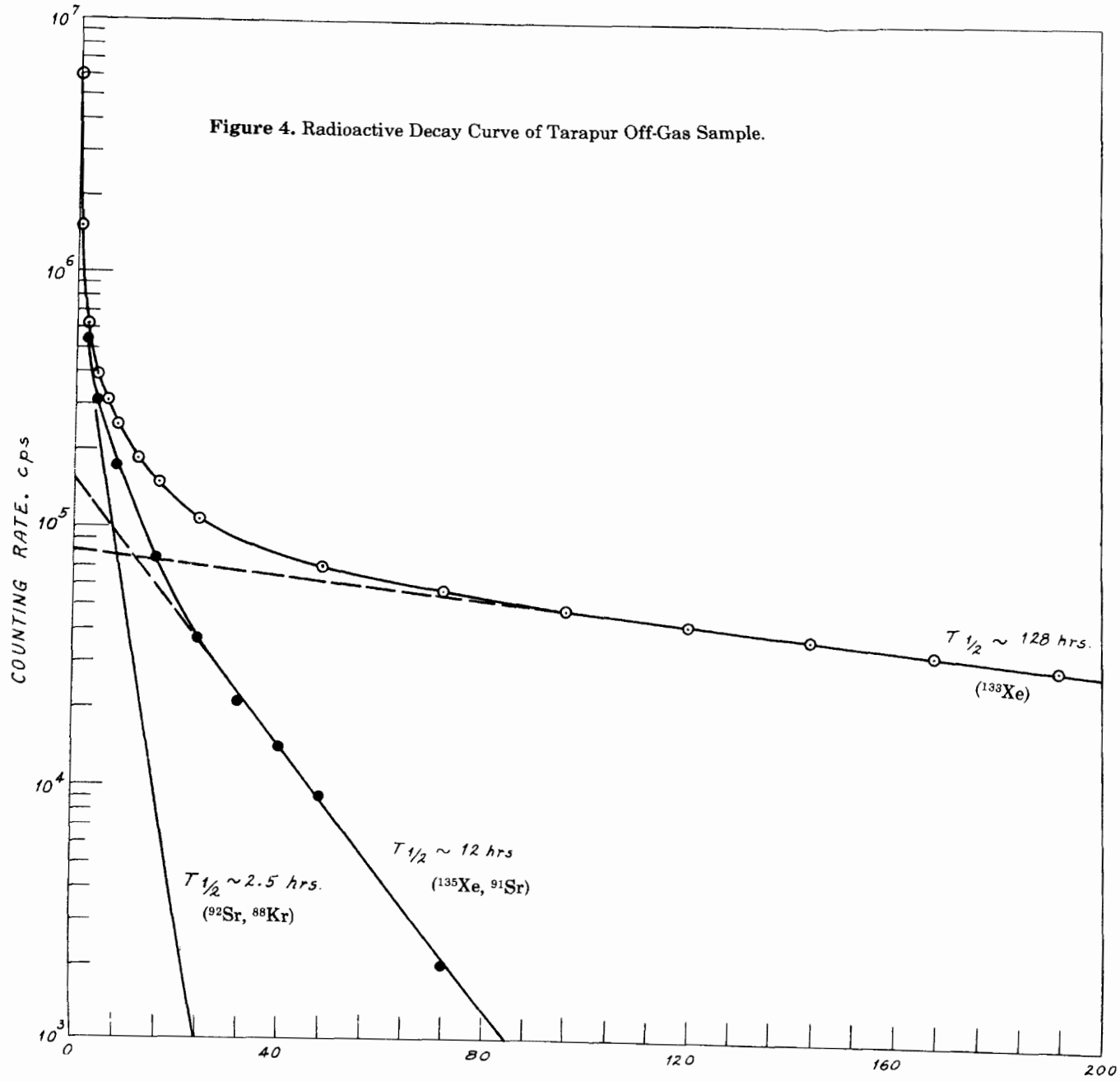

Figure 4. Radioactive Decay Curve of Tarapur Off-Gas Sample.

NOBLE GAS SURVEILLANCE NETWORK, APRIL 1972 THROUGH MARCH 1973*

V.E. Andrews and D.T. Wruble
Monitoring Operations Division
National Environmental Research Center
U.S. Environmental Protection Agency
Las Vegas, Nevada

Abstract

In April 1972, the National Environmental Research Center-Las Vegas initiated a ten-station network of continuous air samplers to monitor noble gas radioactivity on and around the nuclear explosive testing ground (Nevada Test Site). The network uses compressed air samplers designed and built by the Center. The samplers are described and operating experience and sample results are reported. After one year of operation, the network has shown its ability to document ambient levels of krypton-85 and to detect the occasional low-level releases of xenon-133 at the Nevada Test Site. Analysis of the data shows a small, but significant, higher level of krypton-85 concentrations measured at on-site locations compared to off-site. Average concentrations over the year were 15.7 ± 2.4 pCi/m³ off-site and 16.2 ± 2.4 pCi/m³ on-site. A systematic variation in krypton-85 levels at off-site stations was similar to that found in weekly grab samples collected off-site in Las Vegas during the preceding year.

INTRODUCTION

Since 1958, the National Environmental Research Center-Las Vegas (NERC-LV) has operated a system of surveillance networks to monitor the nuclear testing activities at the Nevada Test Site (NTS). The purpose was to document the sources and magnitude of radiation exposure to the off-site population. Prior to 1971, these networks monitored external gamma radiation, and routinely collected air, water, and milk samples which were analyzed for various radioisotopes. For the types of radioactive releases normally occurring at NTS, these networks successfully documented the significant sources of exposure.

The sole transport medium for radioactivity to the off-NTS area is the atmosphere. Accordingly, an extensive air sampling program was conducted throughout the continental United States west of the Mississippi River. (EPA, 1972). Until September 1973, integrated 24-hour samples were collected daily and mailed to NERC-LV for analysis. Three 48- to 72-hour samples are now collected each week. All stations collect airborne particulates on glass fiber filters. Selected stations routinely use activated charcoal cartridges after the filter for the collection of gaseous radioiodine. These cartridges are also used at the other stations whenever needed.

For the past several years, the underground testing program has experienced a high degree of success in preventing accidental releases of radioactivity to the atmosphere at detonation time. However, at least two pathways exist for releases of small amounts of radioactive noble gases. First, some gases may be released during post-detonation drilling for the collection of samples for radio-chemical analysis. Second, slow seepage of gases to the surface may allow some additional noble gas radioactivity to leave NTS.

Beginning in 1970, NERC-LV began collecting a weekly 20-minute compressed air grab sample at two locations on NTS and one at NERC-LV. These samples were analyzed for ^{85}Kr and radioxenon. In 1971, the Center was requested by the AEC-Nevada Operations Office to establish a network for continuously monitoring radioactive noble gases and atmospheric ^{3}H at ten locations on- and off- NTS. The weekly grab sample collection was continued until the ten-station continuous sampling network was put into operation in April 1972. (Figure 1 shows the station locations.) This report covers the first full year of continuous monitoring at these stations.

NETWORK REQUIREMENTS

Results of the weekly grab samples collected at NTS demonstrated that any radiation exposures off-site would be very low. In order to adequately monitor the impact of any small releases of noble gases on the off-site populated areas, a monitoring system capable of detecting any change in ambient levels was desired. The Technical Services Division at NERC-LV had recently completed development of a new gas analysis system capable of detecting 2 pCi/m³ of radioxenon or radiokrypton in a 1-m³ sample of air (Stevenson, *et al.*, 1971). Atmospheric krypton samples analyzed at NERC-LV and at the Eastern Environmental Research Laboratory, Montgomery, Alabama (Shearin, *et al.*, 1971 and Jaquish, *et al.*, 1973), showed that current ambient levels of ^{85}Kr are approximately 16±2pCi/m³. Theoretically, the normal background for ^{133}Xe and ^{135}Xe should be zero, because of infrequent releases and short half-lives.

The design concept, then, was to provide a sampler capable of taking advantage of the high-sensitivity capability of the laboratory for radioxenon, and to be able to detect changes in the ^{85}Kr concentration. Since

**This surveillance performed under a Memorandum of Understanding (No. AT(20-1)-539) for the U.S. Atomic Energy Commission.*

the samples would be compressed air, it would be necessary to have them collected at regular intervals by NERC-LV personnel to eliminate shipping problems. The logistics of sample collection from the 10,000 square mile area, plus analytical time required in the laboratory, dictated a weekly collection schedule. Final design considerations were that the sample should be unfractioned air, it should be collected at a constant rate over the 1-week period, the system should be as reliable as possible, and the entire operation must be economically feasible.

SAMPLER DESIGN

The basic design was similar to a sampler in use by Isotopes, Inc. (now Teledyne Isotopes). A schematic of the sampler is shown in Figure 2, and a photograph of a typical station is shown in Figure 3. An aquarium aerator pump draws air at 3 cm^3/sec through a glass fiber filter, and pumps it into a 38-l low-pressure tank. A pressure-actuated switch activates a solenoid, starting a high-pressure compressor. The compressor pumps air from the low-pressure tank, and through a manifold, to two 38-l high-pressure storage tanks connected in parallel. When pressure in the low-pressure tank drops to 1.5 mm Hg, a second pressure-actuated switch deactivates the solenoid, stopping the compressor. Sample pressure in the high-pressure tank is about 2.8 MPa (400 psig).

The high-pressure tanks are collected weekly, and replaced with evacuated tanks containing one ml of carrier xenon. One tank is analyzed in the laboratory, while the second serves as a backup for analysis in case the sample in the first tank is destroyed, lost during analysis, or exhibits unusually high concentrations. The actual standard sample volume in a pressure tank is determined by weighing the full tank as it enters the laboratory, and subtracting the tank tare weight. A normal volume is approximately one m^3. A separate sampler was designed for collection of atmospheric moisture, and H_2 for ^3H analysis, the satisfy the requirements of the Atomic Energy Commission. Methane gas collected by the compressed air sampler is also analyzed for ^3H as CH_3T. The operation and results of the ^3H sampling network will be described in a later paper.

NETWORK EXPERIENCE

After 1 year of operation, the noble gas surveillance network can be termed successful. It has demonstrated the ability to satisfactorily meet most design requirements, although design changes are being studied to improve sampler operational reliability. The network produced successful sample results 85 percent of the time. Although most of the lost samples were due to sampler failure, some resulted from loss of sample during laboratory analysis. Because of the sample work load in the laboratory, duplicate analysis was not performed on the few samples lost in analysis — unless results of other stations indicated the possible presence of elevated levels over the network. Table 1 shows the success rate by month. The improved performance during the final 5 months of the period was due, primarily, to replacement of sub-standard components, which were responsible for the high failure rate experienced during the first few months. Based on ^{85}Kr results, the total collection and analytical process has proved to be as accurate as any technique currently available. As shown in the following section, the network is capable of documenting small changes in ^{85}Kr concentrations. As expected, most radioxenon concentrations have been below the 2 pCi/m^3 detectable level; however, several samples have contained measureable ^{133}Xe.

Table 2 summarizes the results of ^{85}Kr analyses for the ten stations for the period April 1972 through March 1973. It can be seen that the average concentrations measured are very near the 16 pCi/m^3 determined from other studies. The ranges observed, and number of results at the extremes, are consistent with statistical predictions based on counting data.

The total annual cost of the noble gas sampling network is about $31,000. The average cost per sample, assuming a 100 percent success rate, is about $60, including approximately $10 for collection and $50 for analysis. The actual cost attributed to operation of the network is greater than the incremental cost incurred by NERC-LV; this is because some of the personnel and equipment used to operate the network were also necessary to provide the basic capability for off-site surveillance and noble gas analysis of event-related activities. Since the network includes an atmospheric ^3H sampling system, the field collection costs must be shared by that system, as well. Therefore, the actual cost of operating the noble gas sampling network at NERC-LV is somewhat less than it would be if a ^3H sampling network was not operated in conjunction with it.

DATA ANALYSIS

Several questions arise from the operation of a new network such as this:

(1) Do differences exist between on-site and off-site stations, or between off-site stations in different sectors?

(2) Do releases of radioactive noble gases occur which are detectable at off-site locations?

(3) Are the background concentrations of radioactive noble gases constant and predictable?

(4) If the background is constant or predictable, what increase above background can be considered detectable for a single sample?

(5) What sources of random variation are associated with sampling, analysis, and background fluctuations?

(6) Is there a time-dependent, or seasonal, variation in the background concentration of ^{85}Kr?

(7) What effects of meteorology are reflected in on-site and off-site station comparisons, and between stations ?

An attempt has been made to answer these questions, although additional data will be required to satisfactorily answer all of them. A superficial examination of the data in Table 2 shows that the average concentration on-site is greater than the average concentration off-site, with the greatest average at BJY. This was expected, as BJY was selected on the basis of terrain, location, and meteorology to reflect the higher on-site concentrations. Other areas on-site may have higher concentrations, but are not as accessible or do not have power available. The data were subject to X^2 tests to determine if they were drawn from a population having a normal distribution. At the 5% level of significance, the sample distributions are consistent with the hypothesis that the population distribution is normal. In Table 3 are listed the average monthly concentrations for off-site stations and on-site stations. In eight cases the on-site concentrations are greater than off-site, and in one case they were equal. An analysis of runs (Crow, *et al.*, 1960) was performed which showed that at the 5% level of significance the two samples have the same distribution. A t-test on the data (Crow, *et al.*, 1960) in Table 3, to determine if there is a significant difference in the means, showed the means to be different at the 10% significance level, but not at the 5% level. A similar analysis was performed on the weekly averages. In this case, 31 out of 48 on-site averages were greater than off-site. A comparison of weekly averages, to determine if a significant difference exists between on-site and off-site means, shows a significant difference at the 5% (and 1%) level of significance. An analysis of variance, performed on the weekly on-site and off-site averages, showed the mean difference to be significant at the 10% level of significance, but not at the 5% level. Since these analyses indicated significantly higher concentrations on-site than off-site, it can be stated that releases of ^{85}Kr occur which are detectable at on-site locations.

Prevailing winds at NTS are generally from the south to south-west during the summer months, and from the north during the winter months. If the prevailing winds carry noble gases from NTS to the off-site areas, comparison of stations north of NTS to stations south of NTS would be expected to demonstrate any resultant effects.

Weekly and monthly average concentrations of stations to the north of NTS were compared to those to the south. The northern stations are Diablo Maintenance Station, Hiko, and Tonopah. Those to the south are Death Valley Junction, Desert Rock, Beatty, and Las Vegas. The monthly averages are summarized in Table 4. For 9 months out of 12, the northern stations averaged higher than the southern. An analysis of runs shows that at the 5% significance level, both samples are from the same distribution. A comparison of monthly averages, to determine if any difference exists between the means, showed no difference at the 5% level of significance.

Twenty-nine weekly averages were higher for the northern stations compared to 19 for the southern stations. An analysis of runs indicates that, at the 5% level of significance, the two samples were taken from the same distribution. A t-test of the hypothesis that the difference in the means is zero could not be rejected at the 5% level of significance. An analysis of variance was performed to compare northern to southern stations for two periods of time — April through September, and October through March. In neither case could the hypothesis that the means are equal be rejected at the 5% level of significance. All tests for both monthly and weekly averages indicate that the ^{85}Kr concentrations measured to the north of NTS were not significantly different from those to the south.

From the data generated to date, it is not possible to state what increase in ^{85}Kr above background can be considered detectable from a single sample; nor can the background be stated with great precision. Jaquish, *et al.*, (1973) found that ^{85}Kr in grab samples collected in Las Vegas from April 1971 to March 1972 followed a second degree polynomial curve of $Y = 0.0386X - 0.00006X^2 + 10.9$; where Y = concentration in pCi/m^3 and X = days after January 1, 1971. The equation was found to be significant at the 5% level of significance, but not at the 1% level. Concentrations of ^{85}Kr, measured with the continuous sampling network from April 1972 to March 1973 at Las Vegas, and averaged over the off-site stations, followed a similar curve. However, since two years of data collected by the same technique are necessary to accurately determine any cyclic or periodic variations in the background, no attempt has been made at this time to do so. No ready explanation is available to account for such a variation since the observed annual maximum (if there really is one) occurs in September, rather than in the late spring as with the peak of particulate radioactivity from stratospheric fallout. This phenomenon will be investigated further after another year has passed.

Both the data presented by Jaquish and Johns, and that shown in Table 3, indicate that the annual variation in ^{85}Kr concentration may be as much as 3 pCi/m^3. It is, therefore, important to establish this variation as accurately as possible. Some determination must also be made as to the relative contributions to the total error from counting and analytical errors. Since June 1973, a duplicate analysis has been performed each week on one sample selected at random, using the spare high-pressure cylinder. It will take approximately a year to collect enough data to assess the probable analytical error. If, and when, an annual variation can be described, and the counting and analytical errors can be assessed, it will be possible to establish a background, and a detectable level above background, for a single sample.

The problem is much simpler for radioxenon. As stated earlier, the theoretical background for ^{133}Xe and ^{135}Xe should be zero. With a detection limit of 2 pCi/m^3 for radioxenon, essentially any increase above background can be considered detectable. Table 5 lists those few samples, out of the 287 collected, which

contained measurable ^{133}Xe. In most cases, they are well above the detectable level. Positive ^{133}Xe results are not well correlated with higher ^{85}Kr results in the same samples. Several of the higher ^{133}Xe concentrations were associated with higher concentrations of ^{85}Kr, but others were associated with average or below average ^{85}Kr concentrations.

CONCLUSIONS

One year of operation of the continuous noble gas sampling network has demonstrated success in producing a workable sampling system, and in measuring ambient concentrations of ^{85}Kr and ^{133}Xe. The failure of several sampler components to meet specifications resulted in a large number of sampler malfunctions during the first few months. Replacement with suitable parts resulted in greatly improved reliability.

Although insufficient data is available to predict background concentrations of ^{85}Kr as a function of time of year, and minimum detectable increase above background for a single sample, it is anticipated that such information will be available after another year of operation. Statistical analysis of the ^{85}Kr data indicates that although no individual samples could be said to be above background, average concentrations on the NTS were above those off-site. Average concentrations north of the NTS were not significantly different than those to the south for the entire year or for summer and winter seasons. The conclusion is that low-level releases of ^{85}Kr occur at NTS which are detectable on-site, but which do not result in measureably increased concentrations in the off-site area.

Measurable concentrations of ^{133}Xe were collected at off-site stations five times during the year. The maximum concentration of ^{133}Xe measured off-site was less than 1 percent of the radioactivity concentration guide (AEC, 1963) for exposure to a suitable sample of the population.

REFERENCES

Crow, E. L., F. A. Davis, and M. W. Maxfield, (1960), *Statistics Manual,* New York, N. Y., Dover Publications, Inc. p 56, 60-62, 101-102.

Environmental Protection Agency, (1972), *Radiation Data and Reports,* Volume 13, Number 2 (Feb. 1972) p 88-92.

Jaquish, R. E., and F. B. Johns, (1973), *Concentrations of Krypton-85 in Air,* (To be published).

Shearin, R. L., C. R. Porter, and S. L. Cummings, (1971), *Study of the Feasibility of Measuring ^{85}Kr Through a National Surveillance System,* IAEA-SM-148/ 64.

Stevenson, D. L. and F. B. Johns, (1971), *A Separation Technique for the Determination of Krypton-85 in the Environment.* Proceedings of Symposium on Rapid Methods for Measuring Radioactivity in the Environment, IAEA-SM-148/68, p 157-162.

U. S. Atomic Energy Commission, (1963), AEC Manual, Chapter 0524; *Standards for Radiation Protection.*

TABLE 1. Total Sampling Success Rate by Month April 1972 through March 1973.

Month	Percent Successful Samples
April	75
May	78.5
June	68
July	88.5
August	71.5
September	74
October	75
November	89
December	77
January	96.5
February	86
March	93

TABLE 2. Mean Annual ^{85}Kr Concentration by Station April 1972 through March 1973.

Station	Location	Mean Annual Concentration (pCi/m³)	Standard Deviation (pCi/m³)	Range (pCi/m³)
Area 12	On-Site	15.8	2.6	11-23
BJY	On-Site	17.2	2.9	12-25
Gate 700	On-Site	15.7	1.9	13-23
Average	On-Site	16.2	2.5	11-25
Beatty	Off-Site	15.8	2.4	12-22
Diablo	Off-Site	16.0	2.2	12-22
Death Valley Junction	Off-Site	15.0	3.5	10-25
Desert Rock	Off-Site	15.7	2.6	12-25
Hiko	Off-Site	15.6	1.6	12-19
Las Vegas	Off-Site	15.5	1.9	10-18
Tonopah	Off-Site	15.9	2.0	12-21
Average	Off-Site	15.7	2.4	10-25
Average	All	15.8	2.4	10-25

TABLE 3. Mean Monthly ^{85}Kr Concentrations On-Site and Off-Site Locations April 1972 through March 1973.

	On-Site Average		Off-Site Average	
Month	Concentration (pCi/m³)	Standard Deviation (pCi/m³)	Concentration (pCi/m³)	Standard Deviation (pCi/m³)
April	16.5	1.9	16.1	1.5
May	17.4	2.1	15.8	1.6
June	14.7	1.5	15.2	1.9
July	16.6	3.1	16.5	2.2
August	16.3	2.6	16.9	2.8
September	18.0	3.5	18.0	3.0
October	15.6	2.2	15.1	2.0
November	15.1	2.2	15.3	2.1
December	15.5	2.2	15.1	2.2
January	17.9	2.6	15.7	1.5
February	17.2	3.1	15.0	1.0
March	15.0	1.5	14.6	1.6

TABLE 4. Mean Monthly ^{85}Kr Concentrations North and South Off-Site Stations April 1972 through March 1973.

Month	^{85}Kr Average Concentrations, pCi/m^3 North (a)	South (b)
April	15.8	16.2
May	16.3	15.5
June	15.5	14.9
July	17.0	16.2
August	16.2	17.4
September	17.6	19.0
October	15.7	14.7
November	15.7	15.1
December	15.2	15.0
January	15.5	15.1
February	15.5	14.6
March	15.1	14.3

(a) Diablo Maintenance Station, Hiko, Tonopah.
(b) Beatty, Death Valley Junction, Desert Rock, Las Vegas.

TABLE 5. Positive ^{133}Xe Results April 1972 through March 1973.

Collection Period	Station	Concentration, (pCi/m^3)
3/22-3/29/72	Area 12	14
5/4-5/10/72	Diablo Maintenance Station	33
5/8-5/15/72	Desert Rock	30
5/15-5/22/72	BJY	380
5/22-5/30/72	BJY	530
5/23-5/31/72	Beatty	17
5/24-6/1/72	Hiko	570
6/12-6/19/72	BJY	430
6/14-6/21/72	Hiko	230
7/24-7/31/72	BJY	9.9
7/24-7/31/72	Area 12	4.6

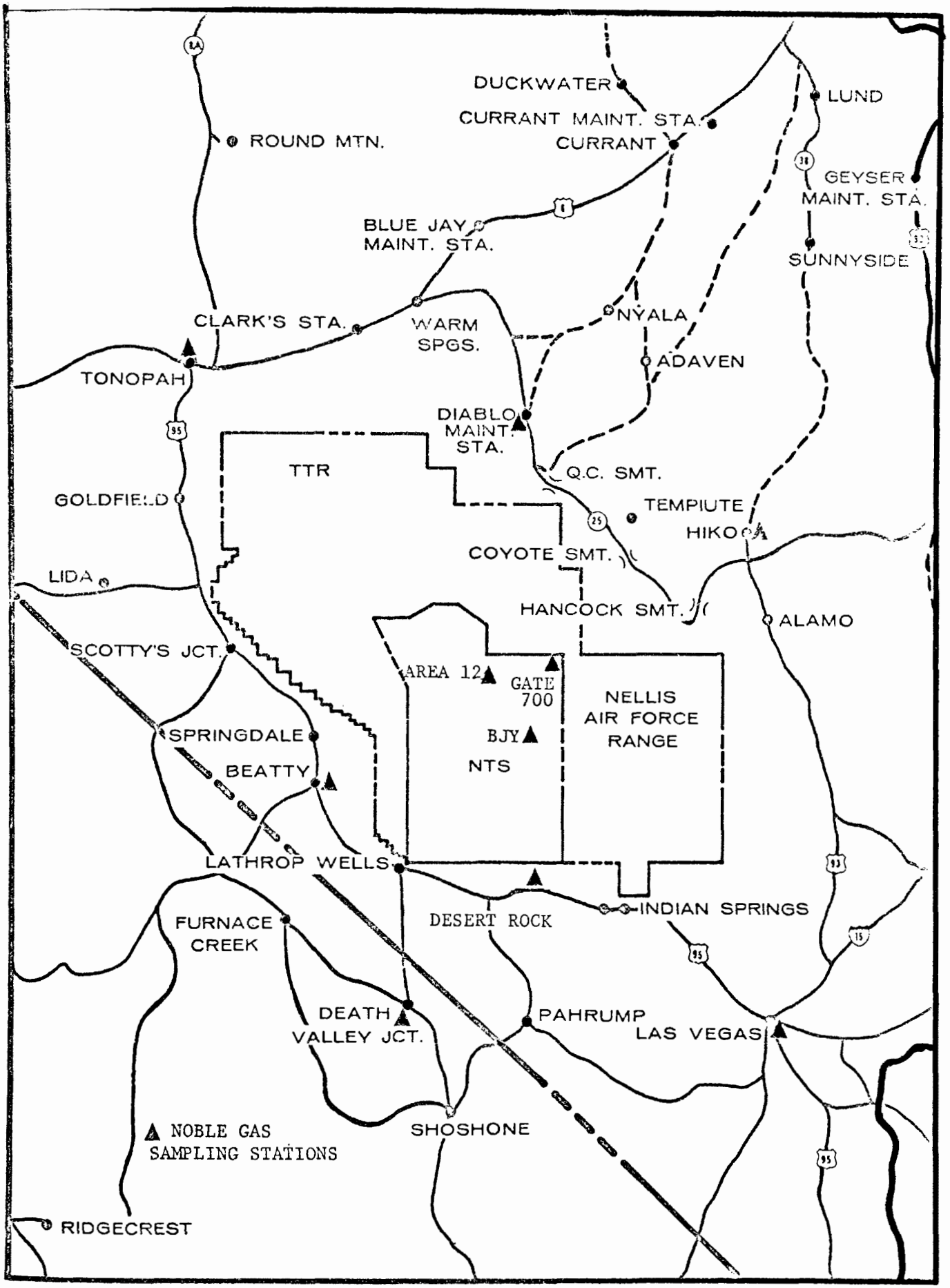

Figure 1. Noble Gas Sampling Station Locations

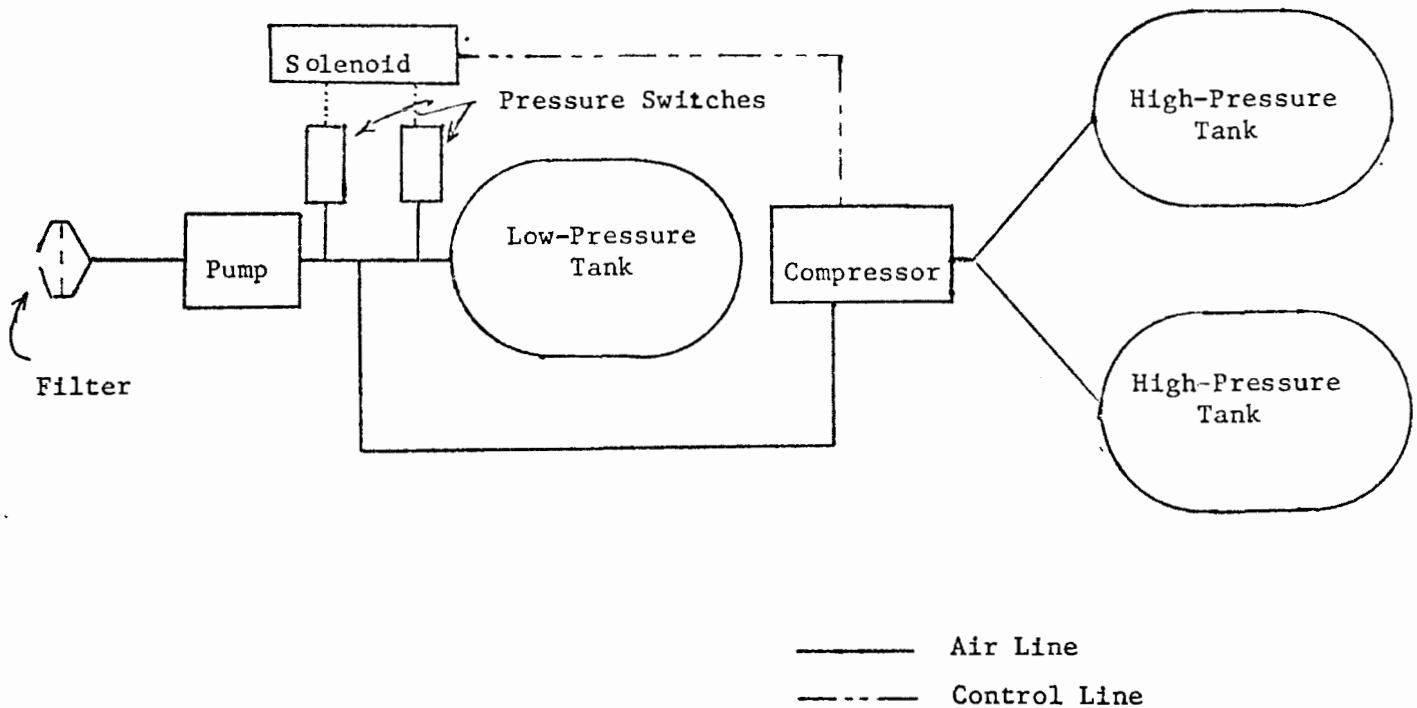

Figure 2. Schematic of Noble Gas Sampler

Figure 3. Typical Noble Gas Sampling Station

V. Separation and Containment of Noble Gases

GENERAL SURVEY OF TECHNIQUES FOR SEPARATION AND CONTAINMENT OF NOBLE GASES FROM NUCLEAR FACILITIES

C. L. Bendixsen and J. A. Buckham
Allied Chemical Corporation
Idaho Falls, Idaho

Abstract

Radioactive noble gases produced during uranium fission constitute a waste material requiring special treatment and handling techniques if releases to the environment are to be reduced or minimized. To date, treatment has been confined to short-term holdup of reactor off-gases to allow short half-life fission products to decay. Although the required degree of noble gas separation and containment is not yet defined, considerable development effort has been expended on a variety of separation processes. With some separation processes, the technology is sufficiently advanced that commercial separation units are now being offered for sale. Early installations of these will be mainly at reactors where their prime advantage is a reduction in size of the holdup system required and an increase in the holdup time for radioactive decay. Eventually, separation processes may be installed at fuel processing plants to collect the long-lived krypton-85. The separation processes potentially applicable to removing noble gas fission products from off-gas streams include absorption in liquids (liquid air, carbon dioxide, or fluorocarbons), adsorption on charcoal and other solids, thermal diffusion, electrostatic diffusion, and diffusion through a selective membrane. These processes are at a variety of technological levels and each has its own particular advantage or disadvantage. A cryogenic liquid-air absorption process has been operated intermittently at the Idaho Chemical Processing Plant for many years to recover krypton-85 for a variety of uses, but total recovery has never been attempted. High pressure storage in steel cylinders presently appears to be the most practical means of ultimate disposal of the krypton-85. However, inclusion of the krypton-85 into glasses, resins, clathrates, molecular sieves, and metals offer ways of reducing the effective vapor pressure in a cylinder. Long-term disposal means that have been considered including placement of the cylinders into an engineered storage facility, dumping of cylinders into the sea, and direct discharge of the krypton-85 into an appropriate geologic formation.

INTRODUCTION

Radioactive noble gases produced during uranium fission constitute a waste material requiring special treatment and handling techniques if releases to the environment are to be reduced or minimized. To date treatment has been confined to the short-term holdup of nuclear reactor off-gases to allow for the decay of short half-life fission products. Although the required degree or efficiency of noble gas separation and containment is not yet determined, considerable development effort has been expended on a variety of separation processes. With some separation processes, the technology has advanced sufficiently for commercial separation units to be offered for sale. Early installations of these units will mainly be at reactors where their prime advantage is a reduction in the size of the holdup system required and an increase in the holdup time for radiolytic decay. Eventually, separation processes may have to be installed at nuclear fuel reprocessing facilities to collect the long-lived krypton-85.

NOBLE GAS SEPARATION

The separation processes (Nichols, *et al.*, 1971; Dunster, *et al.*, 1970; Kovah, 1970; Slansky, *et al.*, 1969; Slansky, 1969; and Swieger, 1973) potentially applicable to removing fission-product noble gases from the off-gas streams include absorption in liquids (liquid air, carbon dioxide, or fluorocarbons), adsorption on charcoal or other solids, and diffusion through a selective membrane. These processes are at a variety of technological levels, and each has its own particular advantage or disadvantage (summarized in Table 1) with respect to the recovery efficiency, purity and the ultimate containment requirements of the noble gases. The technological level, advantages, and disadvantages of each process are discussed individually as follows:

1. Cryogenic Distillation.

The major advantage of the cryogenic distillation process for absorption of noble gases is its present high technological level. Liquid air plants have been in existence for decades and, thus, considerable knowledge has been assembled on materials of construction, valves, compressors, distillation column design, modes of operation, and reliability. Specific cryogenic processes recovering natural krypton from air have also been operated for some time. Because of this projected capital and operating costs for a fission-product noble-gas removal system are well defined. In addition, the cryogenic distillation process is the only process to have operated on a significant scale at a fuel reprocessing facility for the recovery of production quantities of krypton-85 (AIRCO, 1958; and Bendixsen, *et al.*, 1968, 1971, and 1973). A number of U.S. companies are offering similar units for use at nuclear facilities with projected krypton-85 recovery efficiencies typically in excess of 99 percent. A significant disadvantage of the cryogenic process is the explosion hazards associated

with the radiolytic formation and the concentration of ozone. Methods to minimize this specific explosion hazard include either total removal of oxygen from the process gas (Davis, *et al.*, 1973) or dilution of an ozone-bearing stream through periodic flushing or dilution (Bendixsen, 1973) using appropriate operating parameters. Adequate control of krypton-85 leakage rates to achieve high recovery efficiencies has not been demonstrated yet, but appears achievable. A high degree of process gas cleanup is required, and product purity is relatively high.

2. Absorption in Fluorocarbons.

A significant decrease in refrigeration costs can be achieved by using a fluorocarbon (Stephenson, *et al.* 1970) such as Freon-11 or 12, to absorb the fission-product noble gases at temperatures of -30 to -90°F and at pressures up to 400 psig. Process system size, mode of operation, and capital costs are comparable to the cryogenic distillation process, although the quantity of mechanical cooling equipment is higher. The high pressure required for the process increases the possibility of gas leaks and product losses. The fluorocarbon process has been extensively pilot-plant tested at ORNL, but additional information on the effect of process gas contaminants is desirable. The solvent cost is relatively low, but solvent losses through volatilization and radiation degradation need more definition. Explosion hazards with ozone or xenon-tetrafluoride are estimated to be very low. No plant-scale tests at a power reactor or a reprocessing facility have been performed.

3. Absorption in Carbon Dioxide.

Absorption of the noble gases in distillation processes using liquid carbon dioxide appears possible for gas streams rich in carbon dioxide, such as those coming from reprocessing of graphite fuels (Glass, *et al.*, 1972a, b and Wheatley, 1973). Scoping tests of the process have occurred at ORNL and are continuing in order to obtain basic carbon dioxide absorption data of the noble gases. Refrigeration needs, operating pressures, process equipment, mode of operation, and temperatures are similar to the fluorocarbon process. No explosion hazards from ozone or other radiolytic products have been identified, and a ready supply of solvent is available in the process gases. The process is specific for gas streams with high carbon dioxide concentration and is not applicable to other gas streams.

4. Ambient-Temperature Charcoal Adsorption.

Adsorption of fission-product noble gases on charcoal beds at ambient temperatures has been used for delaying the release of radioactive off-gases from nuclear power reactors (Dunster, *et al.*, 1970 and Keilholtz, 1971). No attempt has been made to use the ambient-temperature adsorption process specifically as a recovery system for fission-product noble gases. The quantity of charcoal required for a typical nuclear facility is in the tens-of-tons range; thus, process equipment would be large and bulky, although operation could be relatively simple. A distinct fire hazard exists, although fires are easily extinguished by shutting off the flow of oxygen-containing gases. Use of adsorbent material other than charcoal cannot be considered because of increased bed volume and high unit costs. Due to the quantities of charcoal required, such a recovery process may be limited to small scale, batch processes.

5. Low-Temperature Charcoal Adsorption.

By reducing the temperature of the charcoal bed, the adsorption capacity is increased, thus reducing the bed volume required (Dunster, *et al.*, 1970 and Keilholtz, 1971) by 50 to 80%. Although a slightly more concentrated product then is possible, the other disadvantages with charcoal beds remain relatively unchanged. A cryogenic temperature adsorption system was used extensively at ICPP at one time, but proved to be unreliable, and refrigeration costs were prohibitive. The use of dual adsorptive beds of relatively small capacity in conjunction with a small cryogenic distillation system to achieve a high-purity product has been suggested.

6. Perm-Selective Membranes.

Differences in permeability of gases through a special membrane is the bases of a perm-selective membrane separation process. Using this difference at high pressures (150 psi) with a silicon rubber membrane, krypton and xenon gases can be separated from the bulk off-gases, as shown in tests at ORNL (ORNL-4572, 1970 and ORNL-4522, 1971). Large membrane surface areas and high pressures are required, and this results directly in high capital and power costs with a high mechanical ratio. Long-term radiation and chemical effects on the membrane are not known, and the membranes are particularly sensitive to ozone and NO_x damage. The system also can be damaged by thermal and pressure shock. The concentration factors are in the range of 10-500 ppm at the reported decontamination factor of 10^4. The system appears economical for low decontamination factors only.

NOBLE GAS CONTAINMENT

High-pressure storage of the recovered noble gases in steel cylinders presently appears to be the leading means for practical ultimate disposal. However, the inclusion or encapsulation of krypton-85 into glasses, resins, clathrates, molecular sieves, and metal offer ways of reducing the effective vapor pressure in a cylinder and may provide primary containment for the radioactive gases. Long-term disposal means that have been considered include placing the cylinders into an engineered storage facility, dumping cylinders into the sea, and directly discharging krypton-85 into an appropriate geologic formation. Commercial uses (Nuc. Ind., 1971 and Kir, 1972) will not utilize significant quantities of the recovered krypton-85. However, a demanding market for the recovered xenon is envisioned. A comparison of the various containment techniques is given in Table 2.

1. Low-Pressure Storage.

Storage of recovered krypton-85 within steel cylinders at ambient pressure and temperature conditions has been studied. The storage volume required has been studied. The storage volume required has been predicted to be similar to the volume of medium-level liquid wastes presently stored at nuclear facilities. With such storage conditions, rupture of a single tank is considered to be controllable and very improbable. Ozone removal is considered necessary; the stored gas must also be free of either oxygen, nitrogen, or both to prevent formation of corrosive products through radiolysis. Although storage at ambient conditions appears possible, considerable economic evaluation appears necessary before considering use at reprocessing facilities.

2. High-Pressure Storage.

High-pressure storage (Blomeke, *et al.*, 1969) appears to be practical and economical, and has extensive technical development obtained during many decades of use in a wide variety of systems. In addition, some experience with high-pressure storage and shipping has been obtained at ICPP during shipment of their product to ORNL. A well-engineered facility could provide a double containment design and minimize such things as leak probability, actual krypton-85 release if a leak occurs, and corrosive radiolytic products. The double-containment concept is deemed necessary because an instantaneous release of one high-pressure storage cylinder may produce unacceptable radiation doses. Further study into overall costs of the complex facility and the long-term effect of possible corrosion of storage cylinder walls by radiolytic products is required. High-pressure storage may require high-purity noble gases. to prevent formation of corrosive, oxidizing products through radiolysis.

3. Storage Through Adsorption or Encapsulation.

Inclusion or encapsulation (Slansky, 1969; Clark, *et al.*, 1970; Breck, 1964; Carden, 1969; Iso. Rad. Tech., 1967; and Reist, 1967) of the krypton-85 into molecular sieves, clathrates, resins, glasses, and metals may offer a means to provide primary containment within a steel cylinder, and also reduce the effective vapor pressure within the cylinders. Cost, safety, and environmental adequacy of any of these inclusion methods are dependent upon storage capacity, temperature restrictions, and radiation damage of the materials. Present information is available only on a lab-scale basis. Storage capabilities of molecular sieves are fairly well-known, but are limited at ambient or elevated temperatures. Use of molecular sieves at low or cryogenic temperatures is not desirable since any loss-of-cooling accident would cause high storage-cylinder pressures which would increase the probability of massive, uncontrollable leaks. All of the encapsulation materials require extensive investigation to determine their storage capacities, and the long-term effects of radiation, possible radiolytic corrosion products, and elevated temperatures. Possible engineering difficulties in constructing a truly effective (and efficient inclusion facility need considerable study. The proposed encapsulation methods are technically difficult, require very high pressures to achieve significant storage capacity, and require complicated and expensive equipment. At best, encapsulation is presently a laboratory possibility and requires lengthy investigation.

4. Long-Term Disposal/Containment.

Eventually, all recovered cylinders containing krypton-85 must be transported to an AEC facility for long-term disposal or containment. Long-term disposal methods may include placement of the cylinders into an engineered storage facility, dumping of cylinders into the sea, and even direct discharge of the krypton-85 into deep or shallow wells leading into a geologic formation (Reist, 1967; Tadmor, *et al.*, 1967; Jacobs, 1967; Mudra, *et al.*, 1965; and Schmaltz, 1969). An engineered facility could be specifically designed to monitor and protect the storage cylinders from the environment (storm, earthquake, etc.), and also provide secondary containment or recovery of gases should initial releases occur. Dumping of storage cylinders into a deep-sea trench might be technically feasible and acceptable, but public acceptance would be difficult to predict. Disposal into deep geological formations (Reist, 1967 and Tadmor, *et al.*, 1967) is in the same category. Very high pressures are required which create a high leak potential and the required detailed knowledge of the deep geologic formation is difficult and expensive to obtain. In the public's eye, there is alwasy the fear of the "undiscovered crack"

which could release the radioactive gases into one's backyard. Some investigation and testing has been done on shallow-well disposal of krypton-85 (Jacobs, 1967; Mudra, *et al.*, 1965; and Schmaltz, 1969). Such a disposal means does not involve high pressures and does not depend on an impermeable geologic formation, but assumes the soil will adsorb the noble gases and release them slowly over a period of decades. Such a method would require large volumes of loosely packed rock and relatively large ground surface areas. However, the concept suffers from the disadvantage of a constant, highly visible-to-the-public, release of krypton-85 to the atmosphere, however small. Well-engineered facilities for high-pressure storage of the radioactive gases still appear to have an important technological and experience advantage over other methods.

REFERENCES

Bendixsen, C. L. and F. O. German, (1971), *Operation of the ICPP Rare Gas Recovery Facility During Fiscal Year 1970,* ICP-1001.

Bendixsen, C. L., F. O. German and R. R. Hammer, (1973), *1972 Operation of the ICPP Rare Gas Recovery Facility,* ICP-1023.

Bendixsen, C. L. and G. F. Offutt, (1968), *Rare Gas Recovery Facility at the Idaho Chemical Processing* Plant, IN-1221.

Blomeke, J. O. and J. J. Perona, (1969), *Management of Noble-Gas Fission Product Wastes from Reprocessed Spent Fuelds,* ORNL-TM-2677.

Breck, D. W., (1964), *Crystalline Molecular Sieves,* Journal of Chemical Education, Vol. 41, No. 12, pp. 678-689.

Carden, J. E., (1969), *Radio-Release in Review with Emphasis on ^{85}Kr Clathrates and Kryptonates,* ORNL-IIC-18.

Chemical Technology Division Annual Progress Report for Period Ending May 31, 1970, (1970), ORNL-4572, p. 106-107.

Clark, W. E. and R. E. Blanco, (1970), *Encapsulation of Noble Fission Product Gases in Solid Media Prior to Transportation and Storage,* ORNL-4473.

Davis, J. S. and J. R. Martin, (1973), *A Cryogenic Approach to Fuel Reprocessing Gaseous Rad Waste* Treatment, presented at the ANS National meeting in Chicago, Illinois, during June 1973, Linde Division of Union Carbide Corporation.

Dunster, H. J. and B. F. Warner, (1970), *The Disposal of Noble Gas Fission Products from the Reprocessing of Nuclear Fuel,* AHSB(RP) R-101, Harwell, U.K.

Final Report on Development of Dissolver Off-Gas Unit, (1958), AIRCO-C-214-6).

Glass, R. W., *et al.*, (1972a), *HTGR Head-End Processing: A Preliminary Evaluation of Processes for Decontaminating Burner Off-Gas,* ORNL-TM-3527.

Glass, R. W., *et al.*, (1972b), *Removal of Krypton from the HTGR Fuel Reprocessing Off-Gases,* ANS Transactions, Vol. 15, No. 1, p. 95.

Jacobs, D. G., (1967), *Behavior of Radioactive Gases Discharged into the Ground,* Nuclear Safety, 2, pp. 175-178.

Kr and Xe as Reactor By-Products, (1972), Nuclear Industry, pp. 45-46.

Keilholtz, G. W., (1971), *Krypton-Xenon Removal Systems,* Nuclear Safety, Vol. 12, No. 6, pp. 591-599.

Kirk, W. P., (1972), *Krypton-85, A Review of the Literature and an Analysis of Radiation Hazards,* PB-207-079, Environmental Protection Agency.

Kovach, J. L., (1970), *Review of Radioactive Noble Gas Collection Processes,* North American Carbon, Inc., NACAR010007.

Krypton-85 Clathrates, (1967-68), Isotopes and Radiation Technology, Vol. 5, No. 2, pp. 108-111.

Merriman, J. R., M. J. Stephenson and D. I. Dunthorn, (1972), *Recent Developments in Controlling Release of Noble Gases by Absorption in Fluorocarbons,* ANS Transactions, Vol. 15, No. 1, p. 95.

Mudra, P. J. and B. L. Schmaltz, (1965), *An Appraisal of Gaseous Waste Disposal into the Lithosphere at the NRTS,* Id., IDO 12024.

Nichols, J. P. and F. T. Binford, (1972), *Status of Noble Gas Removal and Disposal,* ORNL-TM-3515.

Noble Liquid Forms a Radiation Detector, (1972), Industrial Research, p. 29.

Rainey, R. H. and S. Blunkin, (1972), *Completion Report — Evaluation of the Use of Perm-Selective Membranes in the Nuclear Industry for Removing Radioactive Xenon and Krypton From Various Off-Gas* Streams, ORNL-4522.

Reist, P. C., (1967), *The Disposal of Waste Radioactive Gases in Porous Underground Media,* Nuclear Applications, 3, pp. 474-80.

Schmaltz, B. L., (1969), *Injection of Gas Into the Lithosphere at the NRTS,* Id., IDO 12069.

Schwieger, R. C., (1973), *Controlling Radioactive Discharges from Water-Cooled Reactors,* Power, pp. 21-28.

Slansky, C. M., (1969), *Separation Processes for Noble Gas Fission Products From the Off-Gas of Fuel Reprocessing Plants,* presented at the Consultant's Meeting on Safety Analysis of Radioactive Noble Gas Releases from Reprocessing Plants, organized by the International Atomic Energy Agency at Centre d'etudes nucleaires de Saclay, France.

Slansky, C. M., H. K. Peterson and V. G. Johnson, (1969), *Nuclear Power Growth Spurs Interest in Fuel Plant Wastes,* Environmental Science and Technology, Vol. 3, pp. 446-451.

Stephenson, M. J., J. R. Merriman and D. I. Dunthorn, (1970), *Experimental Investigation of the Removal of Krypton and Xenon From Contaminated Gas Streams by Selective Absorption in Fluorocarbon Solvents: Phase I Completion Reports,* K-1780.

Tadmor, J. and K. E. Cowser, (1967), *Underground Disposal of ^{85}Kr From Nuclear Fuel Reprocessing* Plants, Nuclear Eng. and Design, 6, pp. 243-250.

Wheatley, M. F., (1973), *Calculations on the Performance of the KALC Process,* ORNL-4859.

TABLE 1. Comparison of Krypton-85 Separation Processes for Nuclear Facilities.

Process	Development Status	Advantages	Disadvantages
Cryogenic Distillation	Developed and operated on a significant scale; commercial units for nuclear reactors have been sold.	Low capital costs well defined; product purity relatively high; high technical background gives high reliability.	Ozone explosions potential must be controlled, high-efficiency gas cleanup required.
Fluorocarbon Adsorption	Developed and tested in pilot plant; no demonstration or operating experience at nuclear facility.	Low refrigeration costs; low solvent costs; very low explosions hazards; reduced process gas pre-treatment.	High-pressure (300-400 psig) with high leak potential; low product purity with corrosion hazards.
Absorption in Liquid Carbon Dioxide	Pilot-plant scoping tests performed and continuing; feasibility studies completed.	Zero solvent costs; low refrigeration costs; no explosion hazards identified.	High-pressure with high leak potential; low product purity; restricted to HTGR nuclear fuels.
Ambient Temperature Charcoal Adsorption	Laboratory tests completed; presently used in delayed release facilities.	Simple operation; adequate technical background to assure reliability.	Large-volume beds; fire and explosion hazard.
Low-Temperature Charcoal Adsorption	Developed and operated on a significant scale.	Smaller volume beds.	Fire hazard and explosion; high refrigeration costs; reliability unproven.
Perm-Selective Membranes	Bench scale tests; no pilot-plant tests.	Room temperature operation.	High capital costs; high pressures; high power costs; membranes sensitive to oxidizing chemicals.

TABLE 2. Comparison of Krypton-85 Containment Techniques.

Technique	Development Status	Advantages	Disadvantages
Low-Pressure Tanks	Feasibility studies performed; no field tests.	Low pressures with low leak probability.	Very large storage volume; ozone removal required; radiolytic product corrosion unknown.
High-Pressure Cylinders	Used for shipment at ICPP; no long-term tests.	Low storage volumes; long technical background.	Long-term corrosion unknown; high pressures increase probability of massive release; secondary containment required.
Adsorption on Charcoal	Development data completed; short-term operation.	Reduces vapor pressures of containers.	Large storage volume; fire and explosion hazard.
Encapsulation	Laboratory studies only partly completed containers; provides primary containment.	Reduces vapor pressures of containers.	Effects of radiation, temperature, and corrosion need extensive study; process technically difficult.
Engineered Storage Facility	Cost and feasibility studies continuing; no field experience.	Protection from environment, earthquakes, and gas leaks, secondary containment and recovery of leaked gases.	High capital cost perhaps high operating cost.
Deep Sea Disposal	Feasibility studies limited; field experience on related chemicals.	Long storage time; isolated from public; simple concept.	Public opinion; reliability not 100% assured.
Deep Geologic Formation	Feasibility studies performed.	Long-term storage.	Public opinion; very high pressures; complicated site investigation required.
Shallow Geologic Formation	Field tests performed.	Unaffected by earthquake; long-term reliability; low cost.	Public opinion.

A CRYOGENIC SYSTEM FOR COLLECTING NOBLE GASES FROM BOILING WATER REACTOR OFF-GAS

G. E. Schmauch
Air Products and Chemicals, Inc.
Allentown, Pennsylvania 18105

Abstract

Industrial gas processing and cryogenic air separation technology provides an effective and reliable means for control and limitation of the environmental release of radioactive noble gases from nuclear power reactors. In boiling water reactors, noncondensible gases are expelled from the main condenser. This off-gas stream is composed largely of radiolytic hydrogen and oxygen, air in-leakage, and traces of fission product krypton and xenon.

In the Air Products' treatment system, the stoichiometric hydrogen and oxygen are reacted to form water in a catalytic recombiner. The design of the catalytic recombiner is an extension of industrial gas technology developed for purification of argon and helium. The off-gas after the recombiner is processed by cryogenic air-separation technology. The gas is compressed, passed into a reversing heat exchanger where water vapor and carbon dioxide are frozen out, further cooled, and expanded into a distillation column where refrigeration is provided by addition of liquid nitrogen.

More than 99.99% of the krypton and essentially 100% of the xenon entering the column are accumulated in the column bottoms. Every three to six months, the noble-gas concentrate accumulated in the column bottom is removed as liquid, vaporized, diluted with steam, mixed with hydrogen in slight excess of oxygen content, and fed to a small recombiner where all the oxygen reacts to form water. The resulting gas stream, containing from 20 to 40% noble gases, is compressed into small storage cylinders for indefinite retention or for decay of all fission gases except krypton-85, followed by subsequent release under controlled conditions and favorable meteorology.

This treatment system is based on proven technology that is practiced throughout the industrial gas industry. Only the presence of radioactive materials in the process stream and the application in a nuclear power plant environment are new. Adaptations to meet these new conditions can be made without sacrificing performance, reliability, or safety.

INTRODUCTION

In recent months, we have heard a lot of discussion about treating gaseous radioactive waste from nuclear power plants. One of the major problems for light water reactor nuclear power stations is the environmental release of radioactive gases. In the design and construction of nuclear power stations, the utilities and their architects and engineers are confronted with the goal of limiting releases of radioactive gases to an "acceptable level" for licensing. When selecting a process and equipment to achieve this objective, special emphasis is placed upon the following factors:

(1) System Performance. The system must perform the required duty effectively and efficiently.

(2) Reliability. The system must perform continuously for extended periods of time with little or no maintenance or operator attention.

(3) Safety. The system must not present any hazard with respect to the plant personnel nor to the plant itself.

(4) Cost. The system must meet these criteria with a minimum of capital and operating costs.

These criteria are applicable to all light water reactors, but this paper considers the problem with respect to boiling water reactors (BWR's).

A typical off-gas stream composition is shown in Table 1 for a nominal 1000 MWe BWR.

The non-condensable gas from the main condenser consists of a mixture of approximately 150 scfm of hydrogen and 75 scfm of oxygen produced by the radiolysis of water within the reactor. The off-gas includes from 30 to 60 scfm of ambient air resulting from in-leakage at the condenser. This mixture contains trace quantities of the fission products krypton and xenon from fuel element leakage, and is generally saturated with water vapor. This stream is highly radioactive as a result of the gaseous fission products and activation products formed in the reactor. The problem is to reduce the radioactivity to a level which is compatible with the plant environment and ensures licensability.

A variety of systems have been offered to solve this problem. These include short delay pipes to allow some decay prior to release, long delay pipes, and pressurized delay tanks to increase the period of delay, and extended delay by charcoal beds prior to release. All of these techniques provide some reduction in radioactivity prior to release, but their overall effectiveness is limited either by size or cost.

Air Products and Chemicals, Inc. (APCI) proposes a more effective and versatile solution to the problem. A solution which would provide activity reduction factors in the range of 10,000 as compared to the more conventional factors in the range of 50 to 500 with respect to the 30-minute decay reference.

This solution, based upon the application of industrial gas and cryogenic processing technology, is widely practiced in industry, and has proven to be highly reliable, safe, and economically competitive in the gas processing market.

APCI'S GASEOUS RADWASTE TREATMENT SYSTEM

The APCI's Gaseous Radwaste Treatment System for BWR off-gas consists of two major sections. The first is a recombiner section for the removal of the radiolytic hydrogen and oxygen. This section provides a significant off-gas volume reduction by a factor of 3 to 6, and also removes the hydrogen explosion hazard. The second is a cryogenic section for the removal and collection of fission product gases from the residual off-gas stream after the recombiner, with subsequent release of an essentially radiation free effluent to the atmosphere. The removal and collection of the fission product krypton and xenon is accomplished by cryogenic distillation, since the residual off-gas after the recombiner, is air contaminated by the fission products.

Examination of the normal boiling points of the components of this residual off-gas stream as shown in Table 2 illustrates that cryogenic distillation is an attractive technique for further volume reduction and collection of the fission product gases.

The major components nitrogen, argon, and oxygen are all significantly more volatile than the krypton and xenon. This approach utilizes standard air separation technology for the concentration of the gaseous fission products, but certain other contaminants must also be considered. Water vapor and carbon dioxide must be removed to prevent freeze-up. Methane and ozone must be removed and controlled to eliminate any safety problem. These factors are discussed further in the description of the process.

The overall system is described with the aid of the flowsheet shown in Figure 1. The off-gas from the nuclear power plant is expelled from the main condenser steam jet air rejectors, and is mixed with the diluent steam to produce a mixture which has a hydrogen concentration of 4% by volume on a wet basis, and is at 280°F with about 60°F superheat. This stream enters the catalytic recombiner which uses a pelletized catalyst (noble metal on ceramic base) called NIXOX(TM) where 99.99% or better of the hydrogen is reacted with oxygen to form water. The water is subsequently removed in the cooler condenser. This radioactive water is returned to the plant water system.

The remaining uncondensed stream consisting of air in-leakage, trace fission gases, and about 200 ppmV residual hydrogen is compressed from 14.7 psia to 115 psia in a water-sealed compressor. The compressor discharge is cooled in an aftercooler which condenses additional water, and subsequently is passed through a short delay line to permit decay of most of the krypton isotopes greater than atomic weight 138, and most of the nitrogen-17, nitrogen-16, and oxygen-19. The compressed air stream enters the cryogenic section through a series of timed switch valves, which control the flow to a reversing heat exchanger. At approximately 10 minute intervals, the flow passages for the warming (low-pressure) side, and cooling (high-pressure) side, are interchanged. The water and carbon dioxide, which is frozen out of the high-pressure stream, is evaporated from the exchanger surface into the outgoing low-pressure off gas stream, and, hence, to the atmosphere. Since the high-pressure passages will be filled with compressed air containing radioactive noble gases, the passages are first purged back to the compressor suction before venting the passages to the atmosphere. By careful selection of design flows, pressures, and temperatures, this scheme, which is common to most modern tonnage air plants, provides quantitative removal of water and carbon dioxide without allowing noble gases to escape to the atmosphere. The process stream, which is cooled in the freeze-out heat exchanger to about -275°F, is further cooled and expanded into the distillation column. The boil-up from the column reboiler is provided by using warm nitrogen and radiolytic heat. Reflux in the column can be provided by either the direct or indirect addition of liquid nitrogen. More than 99.99% of the krypton, and essentially 100% of the xenon, entering the column is accumulated in the column bottoms.

Light hydrocarbons, primarily methane, are present in the air in concentrations comparable to the noble gases. These hydrocarbons accumulate in the column bottoms at a rate comparable to the noble gases; and after prolonged operation, there could be sufficient quantities to be hazardous in the presence of liquid oxygen. However, the buildup of hydrocarbons is readily prevented by the continuous withdrawal of a small stream from the column bottom liquid, passage through a hydrocarbon oxidation chamber, and recycle to the suction of the feed compressor. This continuous hydrocarbon removal system has the additional capability of thermal decomposition of any ozone which might be formed by irradiation of the liquid oxygen.

As noble gases are accumulated in the column bottom, the krypton-xenon enriched liquid oxygen is periodically removed and further concentrated on a batch basis by removing the oxygen. At 1% fuel-leakage and 40 scfm air in leakage, *periodically* means about 4 times a year. This infrequent batch operation for secondary concentration of the fission gases is accomplished in about 24 hours. The liquid withdrawal from the column bottom for hydrocarbon and ozone control is shunted to the secondary concentrator at about 2 scfm. This small flow is diluted with steam, mixed with hydrogen in slight excess of oxygen content, and passed through a small recombiner to effect oxygen removal. Hydrogen requirements range from 3 to 4 scfm over a 24-hour period for each batch transfer. This is insignificant compared to the continuous hydrogen addition concept. The diluent steam is removed in a condenser, and the residual gas is compressed to 500 psia and stored in cylinders. The composition of the stored gas is approximately 20% krypton and xenon, 5% hydrogen, 37% nitrogen, and 38% argon. The stored gas can be held indefinitely or held until all fission gases except ^{85}Kr are decayed, and subsequently released under controlled conditions and favorable meteorology. One major advantage of this system is its versatility. For example, the residual gas from the secondary concentrator can be further concentrated in a small cryogenic adsorber to yield a product which is 70 to 80% noble gases if storage volume is at a premium.

A major criticism of the cryogenic collection system is the accumulation of large quantities of radioactive gases. In our opinion, both the quantity of collected gases, and the radiation levels associated with the collected gas, are reasonable and manageable. For example, at 40 scfm air in-leakage and a 100 mCi/s activity release level referenced to 30 minutes delay, the total quantity of krypton and xenon collected per year is about 25 standard cubic feet. At 20% purity, the total volume of stored gas is about 125 standard cubic feet per year. If stored at 500 psia, about 3 or 4 standard gas cylinders per year are required.

The data in Table 3 are presented to illustrate the accumulation of radioactivity in the distillation column sump during operation of the system and the subsequent decay after transfer to storage. These data are based upon a design level feed gas activity of 100 mCi/s after 30 minutes, and show the maximum buildup of radioactivity in the sump during operation. Time intervals of 7, 14, 30, 90, and 180 days are used to illustrate the buildup. This table also shows the activity accumulation in the sump after continuous operation at the design level for these time periods. The data are shown graphically in Figure 2.

The inventory builds up rapidly during the first seven days, but soon levels off to a near steady-state level after 30 days. At this point, the accumulation rate is almost completely off-set by the decay rate except for the ^{85}Kr. The maximum accumulation in the sump for the design conditions reachs a steady-state level slightly in excess of 8,000 curies. This level increases by about 50 curies per month due to the continuous accumulation of ^{85}Kr.

Table 3 also contains data to illustrate the decay of the accumulated radioactive material after shutdown or transfer to storage. Data are presented for operation during periods of 90 days and 180 days prior to transfer. These data are also shown graphically in Figure 2. After shutdown or transfer, the accumulation rate becomes zero, and decay occurs rapidly. Within 7 days, the inventory has decayed to about 1/3 the original inventory. Within 90 days, the only undecayed activity is due to ^{85}Kr. After operation for 90 days, the ^{85}Kr residual is 152 curies,; while after 180 days, the ^{85}Kr residual is about 302 curies.

These data show that the annual accumulation of ^{85}Kr for the design conditions is about 600 curies. Since ^{85}Kr is the only gaseous fission product that is accumulated over the long term, the increase in inventory over and above the steady-state level of 8,000 curies is about 600 curies per year. Therefore, the inventory difference between a delay system and a collection system is only 600 curies per year. Both types of system will contain up to 8,000 curies as inventory during normal operation.

The system provides the added benefit that it can be operated as a delay system or as a collection and storage system. The collected radioactive gases can be stored indefinitely with no significant long-term accumulation of activity (600 curies per year of ^{85}Kr), or it can be released at a controlled rate when meteorological conditions are appropriate. Even when operated as a delay system, this APCI system allows the operator to select the period of delay. For example, when release rates are below design levels, the delay period can be short, but when release rates approach the design level, added delay may be desirable. Most competitive systems do not provide this flexibility. This versatility also provides insurance for the future when more stringent restrictions on release levels may be imposed.

SUMMARY

The APCI Gaseous Radwaste Treatment System does not incur the accumulation of higher levels of radioactive gases when operated as a delay system then do competitive systems. When operated without release of ^{85}Kr, this APCI system accumulates, at the design condition, a maximum of 600 curies per year of ^{85}Kr — over and above the steady-state inventory of 8,000 curies required of all delay systems.

The performance of this cryogenic system can be summarized as follows:

(1) Activity Reduction Factor of 10,000. This is based upon a plant release rate of 100 mCi/s after thirty minutes delay to yield a total release of 10 μCi/s.

(2) Automatic and Safe Operation.

(3) High reliability is achieved by using some redundancy on mechanical equipment.

(4) Low Operating Costs. This is possible because liquid nitrogen costs are less than $1,000 per month, and compressor power requirements are about 40 kW.

This APCI system design is based upon many years of industrial operating experience in such fields as hydrogen-oxygen recombination units for high-purity argon and helium production, on-site industrial gas generation plants, portable oxygen generators for military use, and shipboard oxygen generators for the U. S. Navy. The design is supported by research and development programs which provided phase equilibria data for the distillation column design, krypton-xenon solubility data, catalyst performance data, and catalyst poisoning data. The design is also supported by laboratory demonstrations of recombiner performance using diluent steam, and hydrocarbon and ozone control systems.

In conclusion, this off-gas treatment system is based upon proven technology that is practiced throughout the industrial gas industry. Only the presence of radioactive materials in the process stream and the application in a nuclear power plant environment are new. Adaptations to meet these new conditions can be made without sacrificing performance, reliability, or safety.

TABLE 1. Typical Off-Gas Stream (1,000 MWe BWR).

150 scfm Hydrogen	-Water Radiolysis
75 scfm Oxygen	-Water Radiolysis
30 to 60 scfm Air	-Condenser Leakage
Fission Product Krypton and Xenon	-Fuel Element Leakage
Water Vapor	-Reactor Steam

TABLE 2. Physical Properties.

Component	Normal Boiling Point, °F
Hydrogen	-423
Neon	-411
Nitrogen	-320
Argon	-302
Oxygen	-297
Methane	-258
Krypton	-244
Ozone	-169
Xenon	-163
Carbon Dioxide	-109*
Water	212

*Sublimation Point

TABLE 3. Sump Inventory Accumulation During Operation.

Time of Operation, Days	Activity in Sump, Curies
0	0
7	5,410
14	6,871
30	7,815
90	8,071
180	8,223

Inventory Decay After Shutdown or Transfer to Storage
(After 90 Days Operation)

Time After Transfer, Days	Activity in Storage, Curies
0	8,071
7	2,672
14	1,224
30	307
90	152
180	150

(After 180 Days Operation)

Time After Transfer, Days	Activity in Storage, Curies
0	8,223
7	2,825
14	2,376
30	458
90	302
180	297

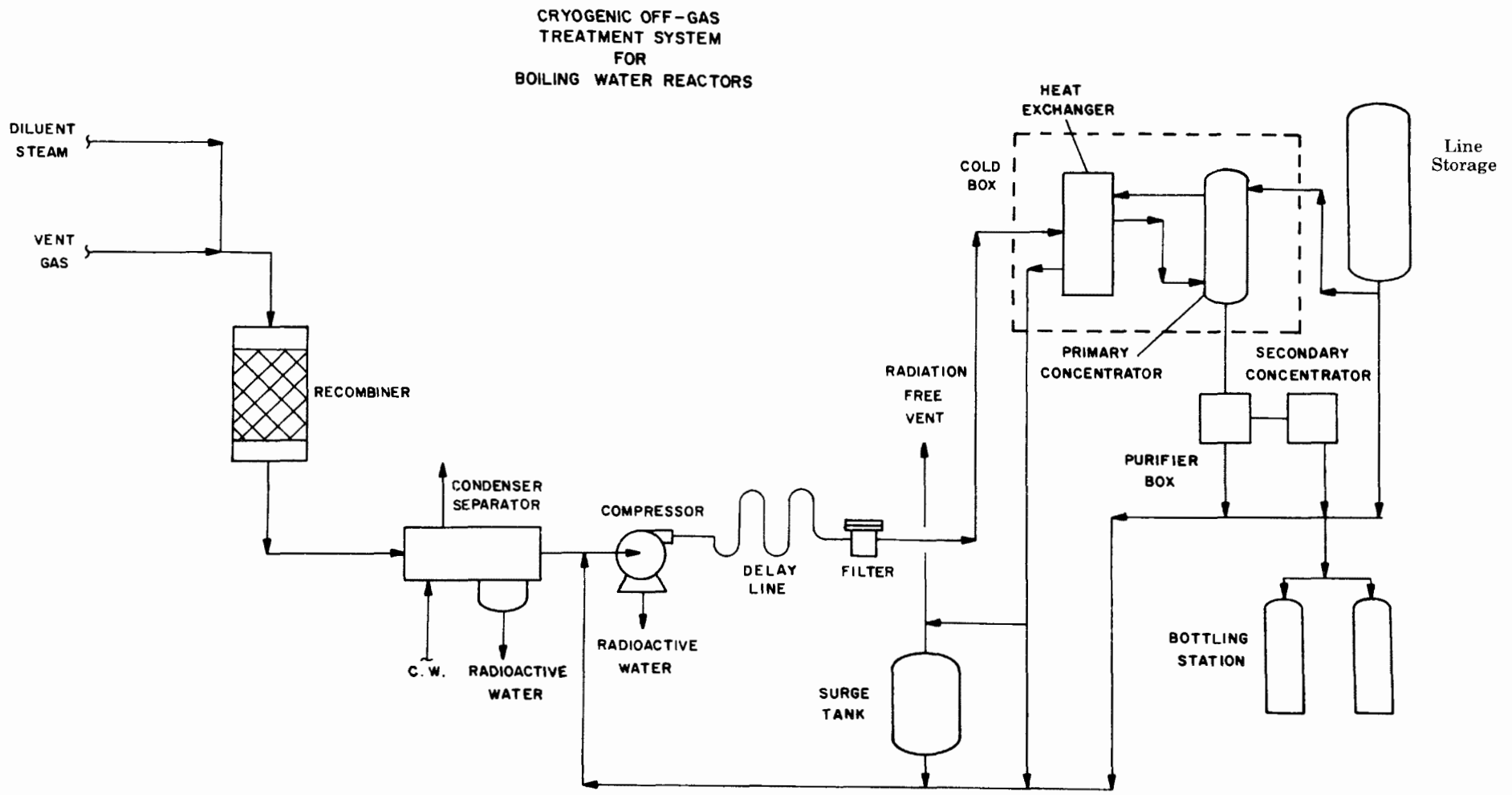
CRYOGENIC OFF-GAS
TREATMENT SYSTEM
FOR
BOILING WATER REACTORS
DILUENT
STEAM
VENT
GAS
RECOMBINER
CONDENSER
SEPARATOR
C. W.
RADIOACTIVE
WATER
COMPRESSOR
RADIOACTIVE
WATER
DELAY
LINE
FILTER
RADIATION
FREE
VENT
SURGE
TANK
COLD
BOX
HEAT
EXCHANGER
PRIMARY
CONCENTRATOR
SECONDARY
CONCENTRATOR
PURIFIER
BOX
Line
Storage
BOTTLING
STATION

Figure 1.

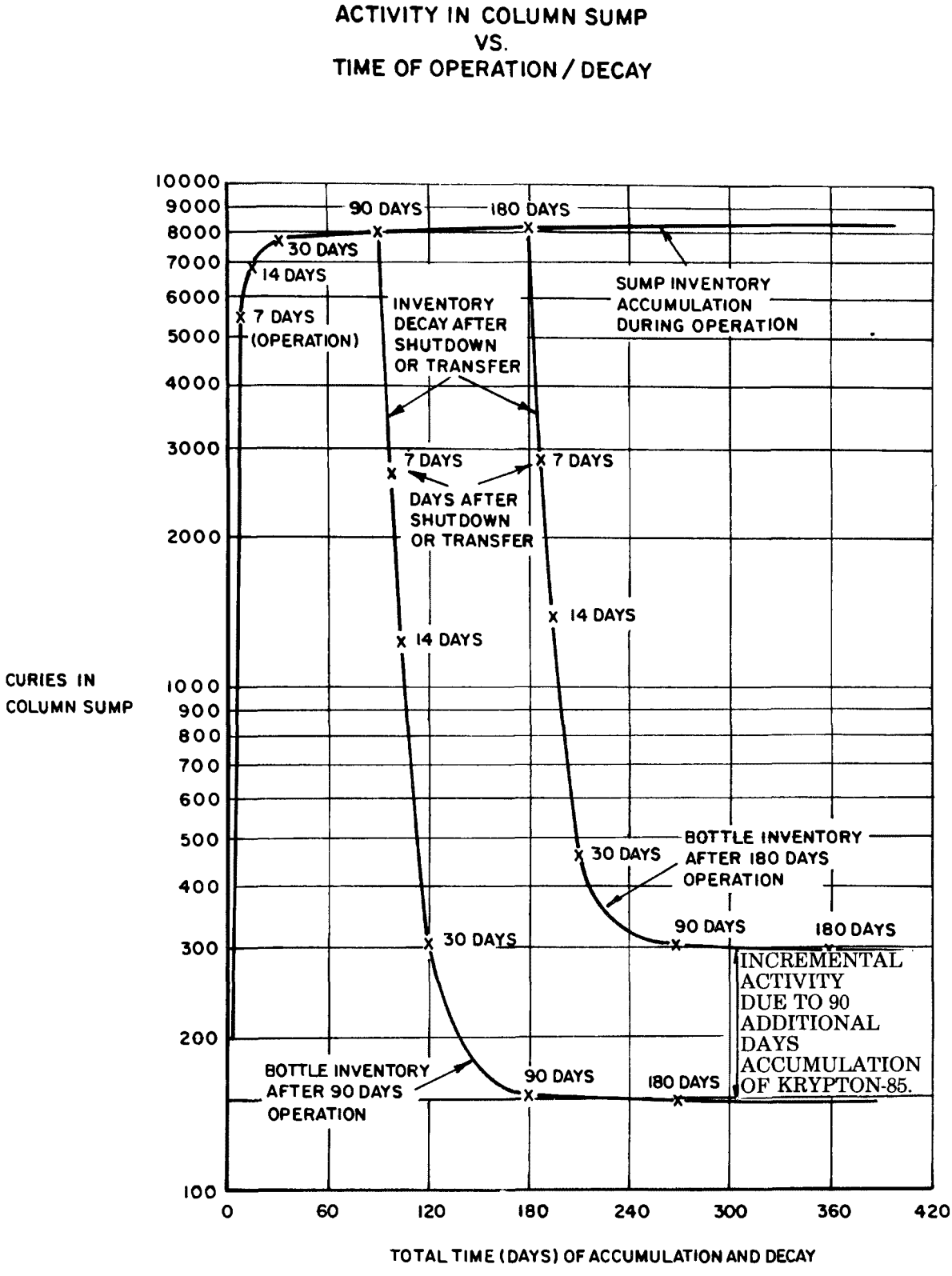
ACTIVITY IN COLUMN SUMP
VS.
TIME OF OPERATION / DECAY
CURIES IN COLUMN SUMP
10000
9000
8000
7000
6000
5000
4000
3000
2000
1000
900
800
700
600
500
400
300
200
100
0
60
120
180
240
300
360
420
TOTAL TIME (DAYS) OF ACCUMULATION AND DECAY
90 DAYS
180 DAYS
30 DAYS
14 DAYS
7 DAYS (OPERATION)
INVENTORY DECAY AFTER SHUTDOWN OR TRANSFER
SUMP INVENTORY ACCUMULATION DURING OPERATION
7 DAYS
7 DAYS
DAYS AFTER SHUTDOWN OR TRANSFER
14 DAYS
14 DAYS
30 DAYS
BOTTLE INVENTORY AFTER 180 DAYS OPERATION
90 DAYS
180 DAYS
30 DAYS
INCREMENTAL ACTIVITY DUE TO 90 ADDITIONAL DAYS ACCUMULATION OF KRYPTON-85.
BOTTLE INVENTORY AFTER 90 DAYS OPERATION
90 DAYS
180 DAYS

Figure 2.

A CRYOGENIC APPROACH TO FUEL REPROCESSING GASEOUS RADIOACTIVE WASTE TREATMENT

J. S. Davis and J. R. Martin
Union Carbide Corporation
Linde Division
Tonawanda, New York

Abstract

The coupling of industrial gas processing and cryogenic technology yields an approach for the efficient and reliable recovery of the radioactive fission product noble gases (especially ^{85}Kr) from the off-gas of LWR and LMFBR fuel reprocessing plants. The fundamental processing step that is employed to separate the noble gases is the cryogenic or low-temperature liquefaction and distillation of the off-gas. The residual gas after the removal of the noble gases is rejected to the atmosphere through the plant stack as a decontaminated waste stream. System krypton recovery factors of greater than 99.9% can be achieved while minimizing the required krypton storage. All elements of the process design utilize proven technology which has been commercially demonstrated.

INTRODUCTION

Today, the United States and the world stands on the verge of an era of increasing industrial growth and energy consumption. To meet these new demands, it is expected that a phenomenal growth of the utilization of nuclear power will occur in the next decades. Coupled with this growth will be the continued expansion of ancillary services such as fuel reprocessing facilities.

The purpose of this paper is to describe a cryogenic approach for the efficient and reliable recovery of the radioactive fission product noble gases (especially ^{85}Kr) from the off-gas of LWR and LMFBR fuel reprocessing plants. The particular off-gas treatment system discussed in this paper is adapted for fuel reprocessing facilities utilizing a nitric acid dissolution process. This system can be easily designed to handle similar applications such as the hydrofluoric acid dissolution of zirconium fuels by minor modifications to the preliminary contaminant removal steps.

Current experience in the utilization of a cryogenic system for this particular application area has until now been limited to operations at the Idaho Chemical Processing Plant (Bendixsen, *et al.,* 1969 and 1971). A cryogenic system has been in use at this facility for the primary purpose of removing a portion of the krypton and xenon for isotopic utilization. The system was not designed to operate continuously or function as a high-efficiency recovery unit. Modernization is currently being contemplated for this unit to assure continuous, reliable, and efficient operation.

This paper is intended to clarify misunderstandings which apparently exist on the status of krypton removal systems.

OFF-GAS CONSTITUENTS

Of primary importance to a discussion of gaseous radioactive waste systems is the identification of all constituents in the influent off-gas stream. These off-gases contain significant quantities of the oxides of nitrogen formed from the nitric acid dissolution process. As illustrated in Table 1, the oxides of nitrogen, fission product gases, and an air stream comprise the off-gas from the reprocessing plant. Air flow rates (10-75 scfm) and compositions were examined in the design for typical fuel reprocessing plants as represented by the Midwest Recovery Facility (USAEC, 1972 and Martin, 1971).

The fundamental processing step that is employed to separate the noble gases is the cryogenic liquefaction and distillation of the off-gas. The manner in which any off-gas constituent hampers or in any way reduces this objective must be recognized and handled in the system design.

DESIGN CRITERIA

The fundamental criteria for the design of the off-gas treatment facility is the safe, reliable, and efficient recovery of the fission product noble gases. Design considerations must include a fail-safe approach to the handling of interim hazards, a minimization of operator required interaction, and a feasible system for long-term krypton storage. With due regard for a safe and reliable operational system, the design presented utilizes the concept of complete oxygen removal from the off-gas prior to cryogenic processing. Thus, several potential problems associated with the operation of the cryogenic equipment are eliminated; these include:

(1) Nitrogen Dioxide Formation.
  a. Radiolysis of Nitrogen-Oxygen Mixtures.
  b. Trace Reaction of Nitric Oxide With Either Oxygen or Ozone.
(2) Ozone Formation.
  a. Cryogenic Radiolysis of Oxygen Mixtures.
(3) Processing of Hydrocarbon-Oxygen Mixtures.

Of major importance in delineating the design criteria is the requirement that the potential presence of nitrogen dioxide (NO_2) be eliminated in the low-temperature processing equipment. Nitrogen dioxide exhibits a high freezing point temperature. In the off-gas treatment system, precautions must be included to maintain NO_2, xenon, and other contaminants below their solubility limits in the various cryogenic fluid mixtures to prevent solids formation. Solid oxides of nitrogen have been a contributing factor to destructive explosions in industrial air separation plants. In addition to this aspect, the solid nitrogen dioxide represents a fouling problem in all cryogenic equipment.

Nitric oxide exhibits a high reactivity with either oxygen or ozone to form nitrogen dioxide. Thus, it is virtually impossible to prevent this conversion from occurring in the presence of these oxides. Therefore, the removal of nitric oxide to the parts per million range is unacceptable if this trace quantity exists in conjunction with significant quantities of oxygen.

An additional consideration in the elimination of the oxides of nitrogen in the cryogenic equipment is their potential formation from the radiolysis of nitrogen-oxygen mixtures.

During normal operating conditions with an oxygen-rich environment, these products would be formed by the radiolysis of the liquid oxygen-nitrogen mixtures residing on the distillation trays near the feed point. The reaction occurs mainly in the cryogenic foam with a negligible contribution due to the gas phase formation in the intertray space. Although the nitrogen dioxide formation rate is much less than that of ozone, it is important due to the extremely low solubilities exhibited by the oxides of nitrogen in the various cryogenic fluid mixtures.

The removal of oxygen also eliminates the danger inherent in cryogenic processing of a stream that contains large quantities of hydrocarbons. Although the hydrocarbons are catalytically converted to carbon dioxide, there is still a significant portion of the methane that is unconverted in the effluent from the hydrocarbon conversion. This methane presents no potential explosion problems in a cryogenic system in the absence of oxygen.

Catalytic oxidation of the hydrocarbons is employed with the design concept of complete oxygen removal as a secondary safety design factor, and to aid in the minimization of krypton storage requirements. Methane has the characteristic nature of krypton in terms of its volatility or separation capability by distillation. If unremoved, the methane tends to accumulate with the krypton fraction and acts as a diluent in the krypton product.

In the system design, the formation of ozone by the irradiation of oxygen must be considered. At cryogenic temperatures, thermal decomposition of ozone is negligible. Though in theory the ozone could be controlled below generally accepted safe concentrations by recycle, several incidents of apparent ozone explosions in cryogenic equipment under a radiation field have been reported in the literature. Due to the high reactivity of ozone, and the general lack of a complete understanding of its interactions with other molecules, it cannot be claimed that an off-gas system with an oxygen-rich environment is completely free from any explosion hazards.

Ozone is similar to xenon in terms of its volatility or separation capability by distillation. Where commercial utilization of the xenon is contemplated, ozone from an oxygen-rich processing environment would be concentrated with the xenon product and would represent a significant oxygen impurity at ambient conditions.

A second consideration in the radioactive waste system design is the elimination of the presence of high freezing point constituents in the cryogenic equipment. Coupled with this requirement is the necessity for proper system design to eliminate those potential operational modes in which certain constituent mixtures exhibit limited solubility behavior. Several components, notably water and carbon dioxide, exhibit freezing points at substantially higher temperatures than those encountered in the cryogenic equipment. These components are prevented from entering the cryogenic equipment to eliminate potential solids formation with subsequent blockage of the equipment. Methods that have been extensively employed in the industrial air separation industry are available for the pretreatment and removal of these contaminants.

In the second separation column of the off-gas treatment system, a krypton-rich product and a high-purity xenon fraction are produced. Below 25 psia, saturated liquid krypton-xenon mixtures form a solid third phase over a portion of the xenon concentration range. For this particular design, as illustrated in Figure 1, the operation of this column at a pressure exceeding 50 psia eliminates any problem associated with a freezeup. This approach is based upon the strong pressure functionality of the liquid-vapor thermodynamic equilibrium relationships as compared with the extreme insensitivity of the mixture freezing point to this parameter. Consideration must be given in the system design to eliminate this and other solubility problems due either to the presence of trace contaminants or the effects of operational conditions on thermodynamic equilibrium.

The third major processing objective is the assurance that the unit design incorporates all steps necessary to achieve krypton recovery factors of greater than 99.9% while minimizing the required krypton storage. The design approach must provide for safe, and reliable system performance under any foreseeable modes of operation. Inherent to this concept, the off-gas system must be designed to minimize or eliminate any potential for the environmental release of the system's radioactive inventory during a component outage or the loss of a support system.

The design philosophy is for the continuous, automatic, and unattended operation of the equipment under the supervision of an operator in the main control room. Alarms are provided to both alarm and indicate the source of the problem. Instrumentation and valving are selected for fail-safe operation. Reliability is a major consideration in the functional specfication of equipment, and redundancy is employed where necessary to assure continuous service. The safety of the system is enhanced by utilizing proven technology previously demonstrated on a commercial scale.

Dependent upon the fissile fuel employed, typical fission yield ratios of xenon to krypton vary between ten and twenty on a volume basis. Therefore, due to the long-term storage requirements for a ^{85}Kr rich product, it was deemed necessary to separate the krypton and xenon to reduce the ultimate storage volume requirements. All fission product xenon isotopes have half-lives so short (12 days max.) that no detectable xenon radioactivity will exist one year after the fuel is removed from the reactor. This high-purity xenon product is thus available for commercial utilization.

The proper application of radiation technology shares an equal role with cryogenic technology in the design of a safe, reliable off-gas treatment system. Radiation considerations are important in the areas of material selection and stability, dose rate calculations to determine access and maintenance problem areas, radiation chemistry effects in terms of contaminant formation rates, and fission yield calculations to determine the off-gas system's influent concentrations of radioactive and non-radioactive fission product gases.

PROCESS DESCRIPTION

The process incorporates complete oxygen removal from the off-gas of the fuel reprocessing facility. The hazards associated with concentrating radioactive xenon and krypton in the presence of oxygen (e. g., ozone and the higher oxides of nitrogen) are eliminated. At the start of the process, the feed gas and a krypton-rich recycle stream from the product column are combined prior to entrance into a dual stage catalytic system. Recycling of the krypton-rich stream serves the primary function of maintaining the desired krypton product purity at a minimum of 75%. This stream is taken from the overhead of the second column to remove methane and nitric oxide from the krypton product. Thus, residual contaminant traces from the catalytic equipment are controlled at safe concentration levels in the cryogenic distillation system.

Following preheating, the feed gas enters the first stage of the catalytic equipment where the hydrocarbons are oxidized (95% efficiency) to carbon dioxide and water.

The effluent from the hydrocarbon conversion unit next passes through a catalytic recombiner where the oxygen is converted to water. Prior to entering the recombiner, a recycle stream around the catalytic unit is added to the process stream to dilute the oxygen concentration in the recombiner inlet stream. The temperature rise in the recombiner is a combined function of the influent preheating, oxygen concentration, and known heats of reaction. The influent reheating is accomplished by countercurrent heat exchange of the recycle stream with the catalytic unit hot effluent. The amount of preheat is controlled by the fraction of the catalytic unit effluent stream bypassing the preheater. Control of the outlet temperature is the means of minimizing the undesirable side reaction involving the methanation of small quantities of carbon dioxide to methane.

Hydrogen, in excess of the stoichometric requirements, is added to the combined process-recycle before entrance into the catalytic recombiner. Two methods of hydrogen generation have been evaluated for utilization with this system. These consist of hydrogen generation by either the electrolysis of water or the thermal dissociation of ammonia. Final determination of the method for hydrogen generation is a function of the system's operational requirements in relation to a cost evaluation. The generator operates automatically and is designed to control hydrogen production in accordance with consumption.

In the recombiner, the oxides of nitrogen are reduced by hydrogen to yield gaseous nitrogen and water, while the oxygen is eliminated from the process stream by the chemical reaction with hydrogen to form water. The effluent stream contains 150-200 ppm of nitric oxide and less than 0.1 ppm of oxygen. The heat of reaction and product water are removed in an aftercooler condenser. A small quantity of steam ejection is utilized to provide the motive power for recycling around the catalytic unit.

The off-gas from the recombiner is essentially deoxidized air saturated with water; containing 2-4% residual H_2 with the fission products xenon and krypton. After compression, carbon dioxide and water are removed from the off-gas prior to cryogenic processing. To minimize potential fission product losses and provide maximum reliability, either an adsorption (prepurifier) or a caustic wash-dryer unit may be utilized. The paramount importance of assuring the minimization of potential system losses during this processing step due either to co-adsoprtion effects or equipment malfunction warrants a fuller discussion of the alternative methods of carbon dioxide-water removal in a later section.

From this prepurification process, the off-gas enters the primary heat exchanger of the cold box and is cooled to within several degrees of its saturation temperature. The gas enters the cryogenic separation equipment consisting of two distillation columns. In the first column, the feed vapor joins the vapor from the lower section of this column and has all traces of krypton, xenon, methane, nitric oxide, oxygen, and other gases less volatile than argon removed from the vapor by a liquid nitrogen flow downward in the column. This decontaminated vapor stream passes from the top of the column and is later utilized in a heat exchange function temperature by countercurrent heat exchange with the influent feed stream in the primary heat exchanger. Liquid nitrogen addition is utilized as a refrigeration source for both columns.

The liquid levels at the bottom of the recovery and product columns are controlled by the electrical energy input to the heaters. The heaters also function to provide the boil-up requirments in the column. A fixed L/V is maintained at the top of the recovery column by measuring the feed to the column and the reflux through a "flow cup." Liquid from the bottom of the primary recovery column, containing mainly xenon and krypton, is continuously withdrawn for processing in the product column.

The second distillation column separates a high-purity xenon product from the krypton fraction. The high-purity xenon product is withdrawn on a scheduled basis. The vapors overhead pass from the top of the column and are heat exchanged against the cold nitrogen gas. A fixed L/V is maintained at the top of the product column by measuring the reflux flowing through a "flow cup" and controlling the temperature of the cold

nitrogen gas entering the heat exchanger. The krypton-rich vapor, which consists of the krypton recycle and product streams, is warmed to ambient temperature. The recycle krypton stream is exhausted into the feed gas prior to the hydrocarbon catalytic conversion unit preheater. The krypton product stream (containing 75% krypton) is periodically withdrawn and is available at 50 psig for further compression into shielded storage cylinders. Separately, the krypton and xenon are compressed for ultimate storage. Due to the short-life nature of the xenon radioactivity, disposal through commercial sale is feasible.

ALTERNATIVE METHODS OF CO_2-WATER REMOVAL

The carbon dioxide-water removal procedure could represent a potentially significant area of process losses under normal operating conditions. Of the various processes currently employed in cryogenic applications, two approaches were evaluated as satisfactory for this application. As illustrated in Figure 3, the first approach embodies the concept of the adsorption of these contaminants by molecular sieves. Feed gas after compression is introduced into the prepurifier for carbon dioxide and water removal. A prepurifier back purge is required to recycle any xenon and krypton co-adsorbed in the prepurifier during the CO_2 and water adsorption. This assures the complete absence of any loss of the noble gases with water and carbon dioxide during the regeneration step.

The portion of the decontaminated off-gas from the cryogenic unit that is not utilized as a prepurifier purge recycle is used to regenerate the adsorption beds in the prepurifier. The gas is heated to strip the CO_2 and water off the molecular sieve adsorbent. The off-gas is then vented to the atmosphere. To virtually eliminate the possibility of feed gas "short-circuiting" the adsorption system to the atmosphere, the prepurifier controller is designed to positively sequence the valves and prevent the opening of the wrong valves through various system interlockings. In addition, major modes of operation are checked and alarmed to prevent improper operation of the prepurifier.

The caustic wash-dryer system, the second approach, represents a major step in the absolute minimization of fission product losses in an off-gas system. Prior to compression, the carbon dioxide in the feed gas is removed by the aqueous, caustic-solution scrubbing in the packed tower through the process of absorption and irreversible chemical reaction. A liquid recycle pump is utilized to maintain the proper liquid to vapor flow ratio in the packed tower. After compression, the effluent from the caustic wash tower enters the two-bed dryer unit. Water and residual carbon dioxide are adsorbed on the molecular sieve of the dryer bed. This application utilizes a portion of the dryer effluent gas for regeneration of the unit. The dryer recycle function is to provide a closed-loop circuit for regeneration of the adsorption beds while recycling any of the co-adsorbed fission gases. At no time, during the regeneration cycle, is any of the regeneration gas vented to the atmosphere. Water rejected from the dryer during the regeneration step is ultimately removed in the compressor's water separator, while the residual carbon dioxide is rejected in the caustic wash system.

LONG-TERM STORAGE

Due to the long life nature of the krypton-85 isotope, it is important that the radioactive waste system design incorporate a feasible solution for the problems associated with the handling and storage of the concentrated krypton product. The off-gas system design is not dependent upon the adaptation of a particular method of krypton product storage and disposal. Consideration must be given in the implementation of product storage design to the ease of handling and transportation, long-term storage integrity, storage volume minimization, and the elimination of potential sources of environmental releases. Table 2 illustrates typical influent noble gas conditions for the radioactive waste system.

Due to the extensive commercial experience for high-pressure gas storage, it has been adopted for the product storage system. The approach involves the utilization of non-vented gas cylinders, designed with a complete sealing procedure after their initial filling. This is coupled with the separation in the cryogenic distillation equipment of the krypton and xenon to reduce the ultimate krypton storage volume. The process is capable of krypton product purities in excess of 75%. Typical storage requirements are presented in Table 3.

The system is designed for the automatic bottling of the krypton product. The product cylinders require only air cooling through convective and radioactive heat transfer mechanisms. The storage pressure is reduced significantly from the design pressure to enhance its safety characteristics — especially with respect to accidents involving incendiaries. It is envisioned that the cylinders would be shipped in a light cask, providing transportation protection and personnel shielding functions. The xenon product is compressed into commercial gas cylinders and held for a short delay period prior to commercial utilization.

Commercial gas cylinder shipments number in the millions annually. It is common industrial practice to ship toxic gases such as phosgene in similar non-venting (absence of pressure relief device) cylinders. The bulk of commercial cylinder rejections are due to the detection of fabrication flaws or field induced defects by non-destructive testing procedures. Therefore, through the application of proven fabrication procedures, proper material selection and design, the utilization of high-pressure gas storage provides a viable answer to the krypton radioactive waste storage problems.

EQUIPMENT DESCRIPTION

To enhance overall system reliability and safety, all elements of the process design utilize proven technology which has been commercally demonstrated. Similar applications for the catalytic equipment exist

industry-wide — especially in nitric acid tail gas treatment. The contaminant pretreatment and cryogenic processing steps are representative of industrial gas processing technology.

The major items of equipment supplied to accomplish the operations of catalyzed chemical reaction, compression, adsorption, and cryogenic distillation can be packaged very compactly as illustrated by the preliminary arrangement diagram shown in Figure 5.

The equipment is provided skid-mounted with the exception of the free-standing cold box, liquid nitrogen tank, hydrogen generation system, and a control panel to allow for unattended operation.

The cold box equipment contains the cryogenic distillation equipment and the necessary heat exchangers to cool the feed to cryogenic operating temperatures. The liquid nitrogen from the storage tank is directly added into the cold box to supply sufficient refrigeration to both cook the feed and provide the motive force for the distillation step. The xenon and krypton are not only separated from the off-gas in the cold box, but are also separated from each other by a distillation step within the cold box. This latter step thus allows the xenon and krypton to be ultimately disposed of in a separate fashion.

The cold box pressure casing is designed to hold the equivalent of the distillation system's liquid inventory at ambient temperature. This pressure casing ensures that no portion of the radioactive inventory is released to the environment in the event of an internal equipment failure.

SYSTEM MODIFICATIONS

The off-gas treatment system can be designed to handle similar applications such as the hydrofluoric acid dissolution of zirconium fuels by minor modifications to the preliminary contaminant removal steps. Currently, a few reprocessing facilities operate at air in-leakage rates much higher than those examined in this paper. The adaptation of a cryogenic radioactive waste system to these situations must include a complete evaluation of the effects of possible system modications as compared to front-end reprocessing equipment modification in terms of the overall system economics, while retaining the design criteria guidelines.

SUMMARY OF PERFORMANCE

The following presents the performance highlights for the off-gas treatment system:

(1) Design Conditions.

	Air Leakage(a) (scfm)	H_2 Addition (scfm)	Liquid Nitrogen(b) Usage (gpd)	Product Storage Requirements (acf)(c)
5 TPD Reprocessing Capacity	60	28	500-800	150

(2) Utility Requirements (5 Metric tpd Capacity).

Electrical(d)	250-310 kW
Steam	150-250 lb/hr
Cooling Water	90 gpm
Liquid Nitrogen Requirements	500-800 gpd

(a) All flows on a dry basis at 60°F, 14.696 psia.
(b) LN_2 requirements include:
1. Column wash requirements (10^{6+} krypton D.F.).
2. Cold box heat leak.
(c) Product storage requirements at 655 psig, 200°F.
(d) Includes electrolytic H_2 generation unit.

FREON ABSORPTION SYSTEM

Recent literature has indicated an increased interest in the possible utilization of the Freon Absorption System for fuel reprocessing off-gas treatment. Therefore, a brief review highlighting a comparison of the system with the cryogenic distillation system for this application is presented in Table 4.

REFERENCES

Bendixsen, Offutt, and Wheeler (1969), *Rare Gas Recovery Facility at the Idaho Chemical Processing Plant*, presented at the 1969 Winter Meeting of the American Nuclear Society.

Bendixsen, *et al.*, **(1971),** *Cryogenic Rare Gas Recovery in Nuclear Fuel Reprocessing*, Chem. Eng. p. 55-57.

Gillespie, Boyum, and Collins (1971), *Catalytic Purification of Tail Gas*, presented at the 64th Annual Meeting of the AIChE.

Hardison (1970), *Techniques for Controlling the Oxides of Nitrogen*, AFCA Journal 20(6) 377-382.
Martin (1971), *Cryogenic Noble Gas Recovery System as Applied to Nuclear Fuel Recovery Plants.* Material prepared for verbal presentation at the Illinois Pollution Control Board; Reference — Midwest Fuel Recovery Plant.
Rohrmann (1971), *Fission Product Xenon and Krypton — An Opportunity for Large Scale Utilization*, Isotopes and Radiation Technology 8(3) 253-260.
USAEC (1972), *Final Environmental Statement Related to the Operation of the Midwest Fuel Recovery Plant.* Docket No. 50-268.

TABLE 1. Influent Off-Gas Constituents

	Normal Boiling Point	Freezing Point
Air		
Nitrogen	-320.4°F	-346.0°F
Argon	-302.6	-308.9
Oxygen	-297.3	-361.8
Methane	-258.7	-296.4
Carbon Dioxide		69.9
Water	212.0	32.0
Oxides of Nitrogen		
Nitrous Oxide	-127.2	-131.6
Nitric Oxide	-241.0	-263.6
Nitrogen Dioxide	70.1	11.7
Noble Gases		
Krypton	-244.0	-250.9
Xenon	-162.6	-169.1

TABLE 2a. Influent Noble Gases (5 t/d Facility)

	Total Flow (scfd)	Radiation Level (μCi/s)	Half-Life
Krypton	14.5		
^{85}Kr		400,000	10.73 yr.
Xenon	144		
^{133}Xe		100	5.29 days

TABLE 2b. Isotopic Composition (Rohrman, 1971).

Xenon			Krypton		
Isotope	Natural atm%	Fission Product atm% (approx.)	Isotope	Natural atm%	Fission Product atm%(approx.)
124	0.096	-	78	0.354	-
126	0.090	-	80	2.27	-
128	1.92		82	11.56	0.2
129	26.44	0.15	83	11.55	11
130	4.08		84	56.90	31
131	21.18	8	85	-	6
132	26.89	22	86	17.37	52
134	10.44	29			
136	8.87	41			

TABLE 3. Annual Storage Requirements.

Plant Capacity -	Specialty Gas Cylinder (24" D x 94" H) (Design P = 1800 psig)
1 Ton/Day -	<2 Cylinders (Storage P = 655 psig)
5 Ton/Day	8 Cylinders (Storage P = 655 psig)

TABLE 4. Comparison Highlights.

(1) Freon Adsorption System cannot provide for the fractionation of the krypton from xenon, thus, the low krypton product purity (3-6%).

(2) To provide refrigeration requirements, the utilization of a mechanical system with reciprocating machinery is necessitated in the Freon system.

(3) The adsorption system has higher operating pressure (300-500 psia).

(4) Even with the addition of peripheral solvent recovery steps, solvent makeup remains a major utility requirement.

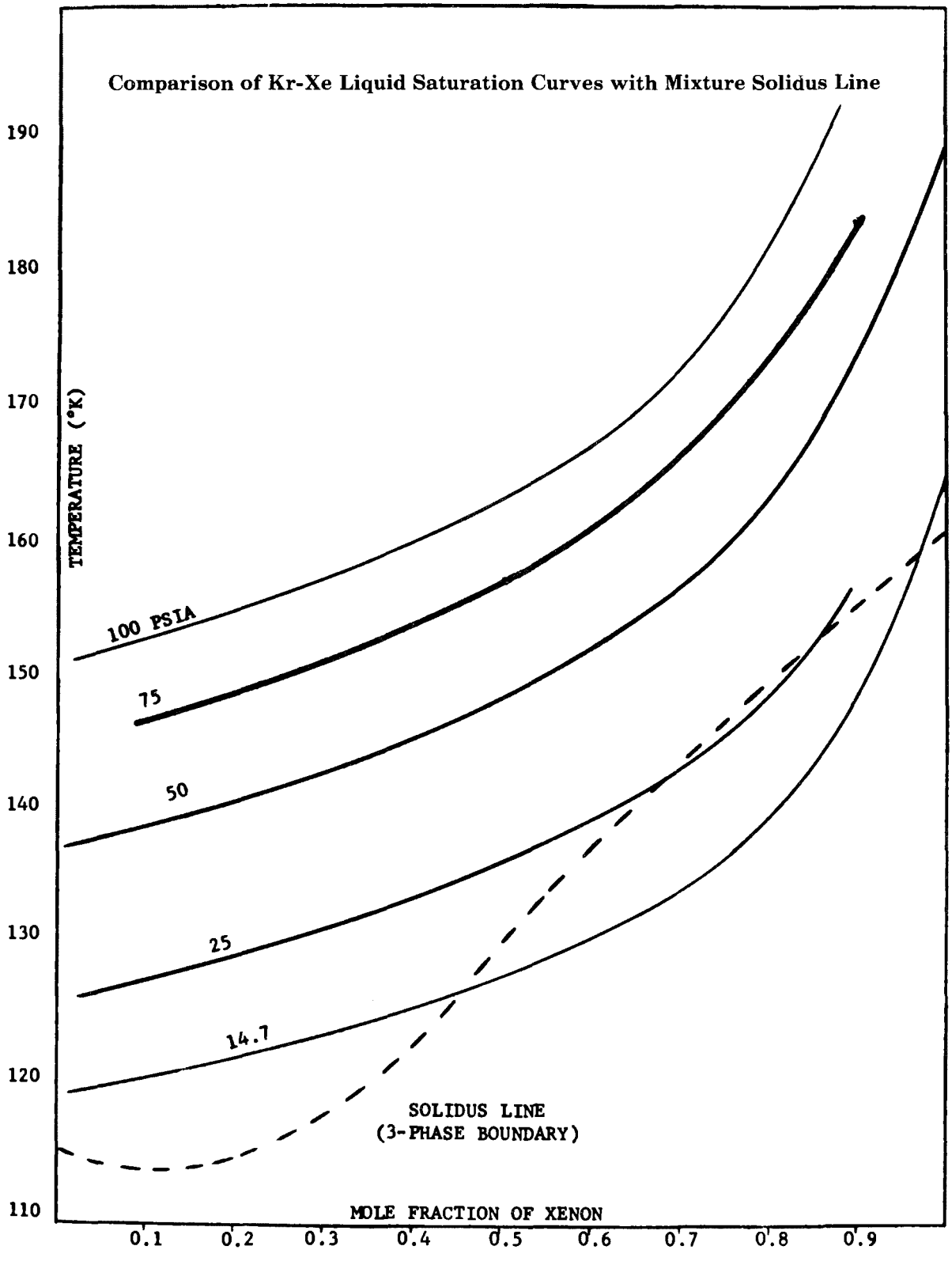
Comparison of Kr-Xe Liquid Saturation Curves with Mixture Solidus Line
TEMPERATURE (°K)
190
180
170
160
150
140
130
120
110
100 PSIA
75
50
25
14.7
SOLIDUS LINE
(3-PHASE BOUNDARY)
MOLE FRACTION OF XENON
0.1
0.2
0.3
0.4
0.5
0.6
0.7
0.8
0.9

Figure 1.

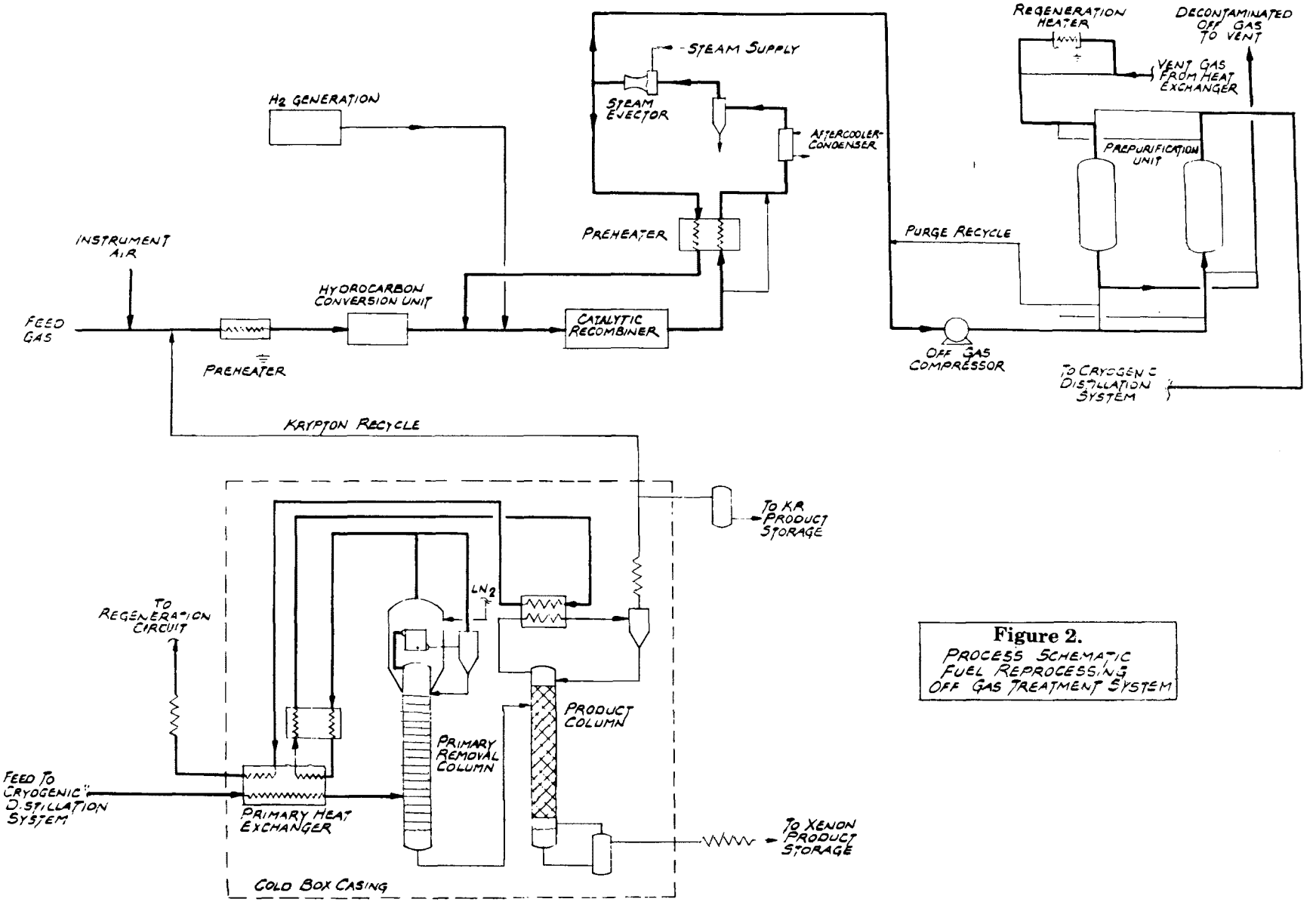

Figure 2.
PROCESS SCHEMATIC
FUEL REPROCESSING
OFF GAS TREATMENT SYSTEM

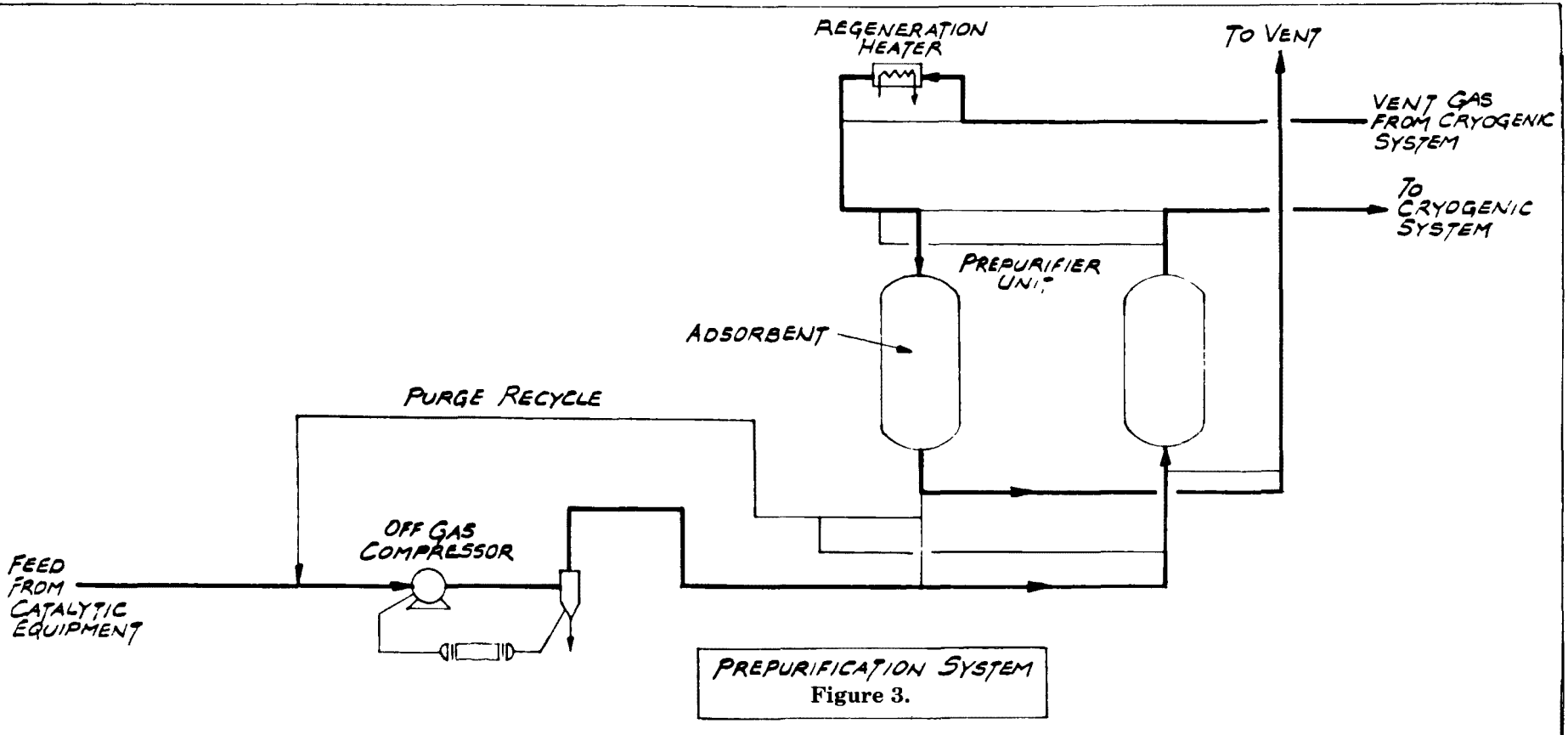

PREPURIFICATION SYSTEM
Figure 3.

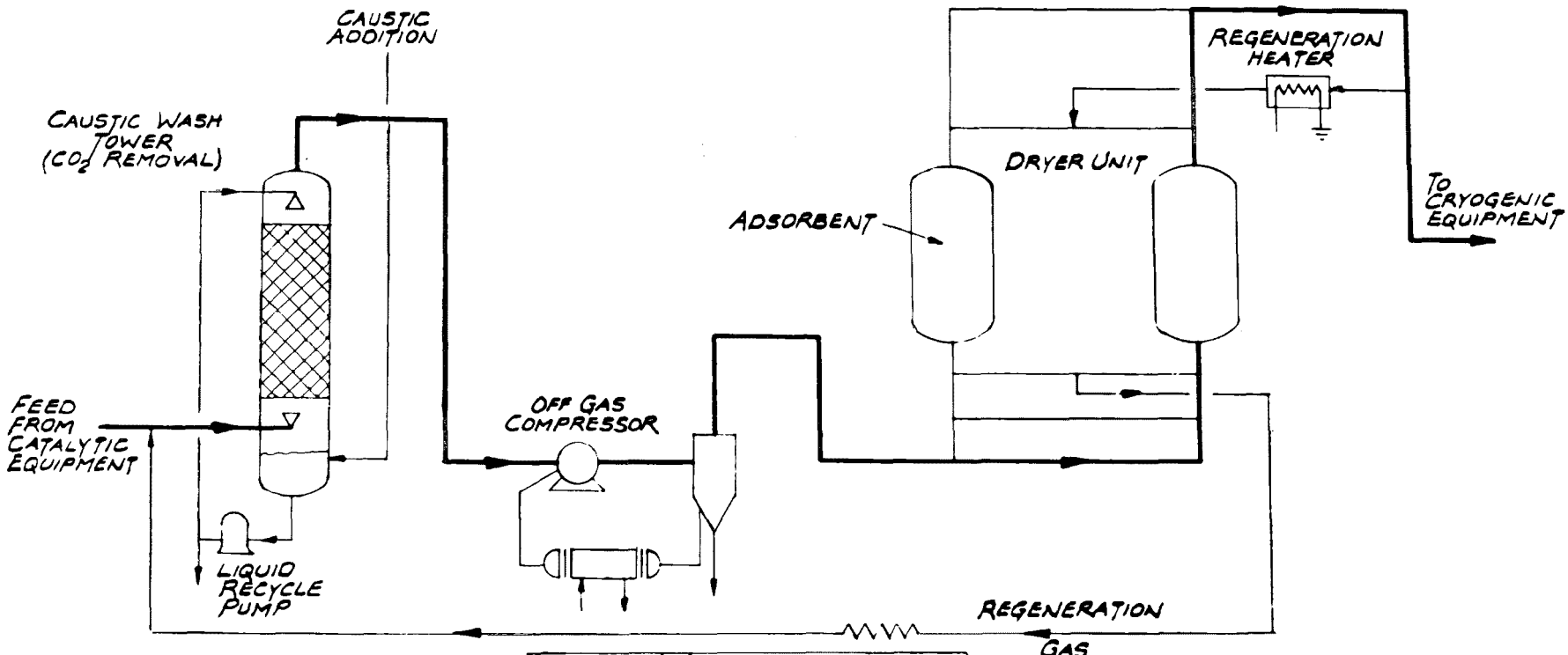

CAUSTIC WASH-DRYER SYSTEM
Figure 4.

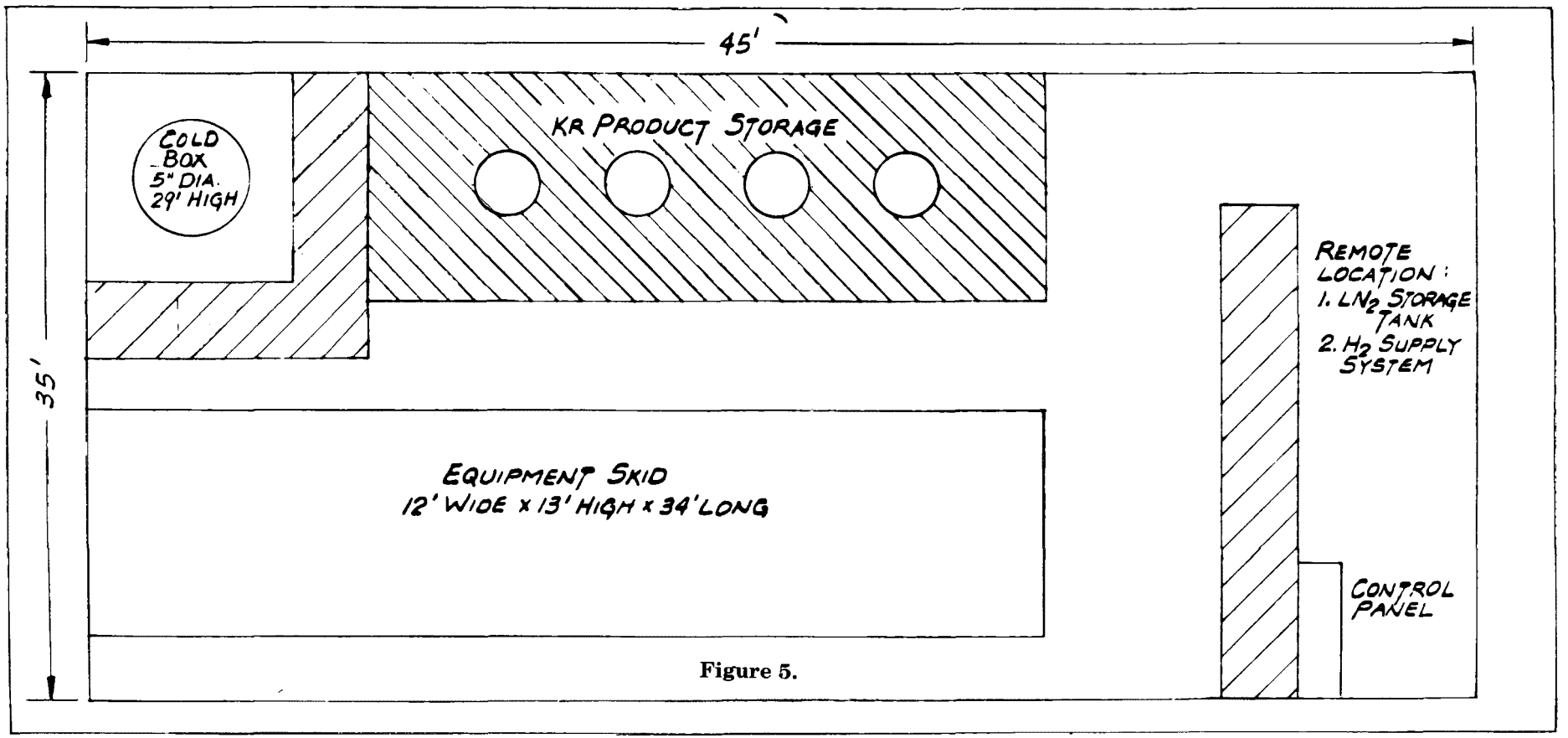
45'
35'
COLD BOX
5" DIA.
29' HIGH
KR PRODUCT STORAGE
REMOTE LOCATION:
1. LN_2 STORAGE TANK
2. H_2 SUPPLY SYSTEM
EQUIPMENT SKID
12' WIDE x 13' HIGH x 34' LONG
CONTROL PANEL

Figure 5.

EFFECTS OF CONTROL TECHNOLOGY ON THE PROJECTED KRYPTON-85 ENVIRONMENTAL INVENTORY

E. E. Oscarson
Office of Radiation Programs
U. S. Environmental Protection Agency
Washington, D. C. 20460

Abstract

Growth projections for the USA nuclear power industry may be used to make projections of future radioactive material inventories available for potential release to the environment. Since krypton-85 is produced in reactors, the potential routes of release to the environment are at the reactors or the fuel reprocessing plants.

The present generation of reactors and fuel reprocessing plants do not use any systems to limit the release of krypton-85 into the biosphere. Clean-up systems are currently being designed and could be introduced when necessary. The cumulative inventory of krypton-85 in the environment is dependent upon the time of introduction of these clean-up systems and their efficiencies, in addition to the total quantity produced.

Annual and cumulative inventories of krypton-85 are projected to increase dramatically over the next 50 years. If controls are assumed to be initiated at various years, a series of graphs of different cumulative environmental inventories and the associated doses and health effects are drawn. Varying the year of introduction and the efficiency of these systems allows one to speculate as to the optimum time for control implementation.

INTRODUCTION

Population growth and increased per capita energy consumption are expected to continue into the foreseeable future. The combination of these factors leads to projections of energy needs which influence utility decisions on the construction of new electric generating capacity.

With continued depletion of fossil fuel resources, and more stringent restrictions on air pollution produced from fossil fuel combustion, the utility industry is expected to increase their commitment to nuclear generated electric power. This projected proliferation of nuclear power implies significantly greater quantities of reactor produced radioactive waste products. One of the consequences of this rapidly expanding waste inventory, is the potential for long-term environmental buildup of certain radionuclides. Under normal operating conditions, a nuclear reactor presents very little potential for significant releases of radioactive material; however, when spent reactor fuel is reprocessed, the release probability increases.

Up to the present time, both commercial and government fuel reprocessing facilities have not attempted to prevent the release of noble gases, and have, in most cases, tried to release them as quickly as possible to reduce the in-plant exposure. Of the noble gases, only krypton-85, with a 10.7-year half-life, is considered an important long-term environmental contaminant.

Recent concern over long-term buildup of krypton-85 in the biosphere has prompted companies committed to commercial fuel reprocessing to examine potential noble gas removal systems (NEDO 14504-2, 1971). The removal efficiencies, costs, and feasibility of various processes are currently being investigated by potential vendors of such equipment. Data developed by these suppliers will help to determine the optimum time for the introduction of control measures.

This paper explores nuclear power projections, the introduction of krypton removal systems, and how they relate to the release to the atmosphere through the year 2020. Also considered are the doses and health effects to the world's population from the uncontrolled release of krypton.

NUCLEAR POWER CAPACITY PROJECTIONS

Projections of electrical power demand have traditionally been a controversial subject. Since energy consumption depends on population and per capita consumption, variations in one or both of these factors can significantly affect long-term power requirements.

The Federal Power Commission (FPC) annually compiles the current U. S. installed electrical capacity, and, considering previous years capacities, predicts future power demands. The U. S. Atomic Energy Commission (AEC) and their contractors have often related the growth of nuclear power to these FPC projections. One study, published in 1970 by Oak Ridge National Laboratory on the siting of fuel reprocessing plants (ORNL-4451, 1970), contains nuclear power capacity projections by FPC regions up to the year 2020. Also included are the projected spent fuel discharges, from which krypton-85 releases can be calculated. Another source of nuclear power projections comes from the Forecasting Branch of the AEC (WASH-1139, 1972). Their forecasts give a range of installed capacity which includes high, low, and most likely estimates. Figure 1 compares these two particular forecasts, as well as one compiled by the Office of Radiation Programs of the EPA (EPA-S2019-73-003D, 1973). Of these three estimates, the EPA forecast falls between the other two, and will be used in this paper for making krypton-85 projections. Examination of Figure 1 reveals a probable

increase in U. S. nuclear generation capacity of 1,000% from 1975 to 1990, and 7,000% between 1975 and the year 2020. The nuclear capacity over the total 50 year period from 1970 to 2020 is expected to increase by a factor of 10^3 (100,000%) from 2.6 to 2,700 gigawatts electric.

FUEL DISCHARGE, REPROCESSING, AND KRYPTON-85 RELEASES

The isotopic composition of fissile materials in nuclear fuels is expected to change significantly over the next 50 years. Thermal reactors, presently designed to use low enrichment uranium fuel, will probably utilize recycled plutonium; and breeder reactors, fueled with plutonium, will produce more fuel than they consume. Knowledge of the relative numbers of each reactor type are important primarily for the determination of the total quantities of actinides produced per unit of electric power generation. In the case of krypton-85, the amount produced per megawatt day is approximately the same for both thermal and fast reactors. Therefore, the annual inventory of krypton-85 is calculated from the total fuel discharged annually for reprocessing and is displayed in Table 1 and Figure 2.

Since much of the fuel presently discharged from reactors has not been and will not be reprocessed in the near future, there may be a delay in the release of krypton-85 to the environment. This may cause fluctuations in annual discharges but should have little effect on the cumulative environmental inventory.

CUMULATIVE ENVIRONMENTAL INVENTORY OF KRYPTON-85

For purposes of calculating krypton-85 buildup in the biosphere, the projected annual releases, depicted in Figure 2, were used in conjunction with equation (1).

$$C = \sum_i A_i e^{-\lambda t_i} \qquad (1)$$

Where C = cumulative environmental inventory of krypton-85 (curies),

A_i = annual release of krypton-85 in year i (curies),

λ = decay constant for krypton-85 (6.45×10^{-2} years^{-1}),

and t_i = decay time for krypton-85 introduced into the biosphere in year i (years).

The cumulative inventories calculated for the years 1970 through 2020 are listed in Table 2 and are displayed in Figures 3 and 4.

EFFECTS OF CONTROL TECHNOLOGY

Concern over long-term environmental buildup of krypton-85 has prompted government agencies, companies committed to operating fuel reprocessing facilities, suppliers of noble gas removal equipment, and citizen action groups to evaluate the practicality and desirability of reducing krypton emissions. Several vendors have indicated that they can supply systems to reduce krypton emissions by factors of 10^2 to 10^3 (NEDO 14504-2, 1971). For this paper, we will consider that such systems can be built and installed when they are considered necessary.

Determining the optimum time for the introduction of control measures depends on many factors including: costs of systems, decontamination factors, achievable growth of the reprocessing industry, health effects, and others. In this instance, only decontamination factors and cumulative fuel inventories are used as bases for suggesting optimum implementation times, although health effects will be considered later.

If control systems with a decontamination factor of 10^2 were required to be installed on all reprocessing facilities at different years, and assuming the fuel inventories listed in Table 2, the series of curves in Figure 3 represent the probable environmental inventories. With the additional assumption that the power supplied by nuclear fission levels off at the year 2020, it is apparent that the steady state cumulative krypton-85 inventories would approach asymptotic values. Such values for the controlled and uncontrolled cases are also displayed in Figure 3. A similar analysis, carried out for controls with a 10^3 decontamination factor, produced the results plotted in Figure 4.

If a lower constant environmental level is used as a criterion for krypton controls, and a decontamination factor of 10^2 is postulated, the most opportune date for control implementation appears to be 1980. Following the same line of reasoning, if a decontamination factor of 10^3 is assumed, the best year for control implementation might be 1974 or 1975.

HEALTH EFFECTS

Although the primary purpose of this paper is to illustrate the probable effects of controls on the atmospheric levels of krypton-85, some discussion of potential health effects is appropriate. For purposes of evaluating potential health effects, the recommendations of the Advisory Committee on the Biological Effects of Ionizing Radiation (BEIR Committee) of the National Academy of Sciences, National Research Council (BEIR, 1972) are used.

Given information on the cumulative environmental inventory of krypton-85, its atmospheric concentration may be estimated by diluting it into the total atmosphere. The total atmosphere is assumed to contain 5.14×10^{21} grams of air (Coleman, *et al.*, 1966) with a sea level density of 1.29×10^{-3} grams /cm^3. The calculated values for sea level concentration are presented in Table 2 and Figure 5.

Conversion of atmospheric concentration to integrated population doses requires population projections and appropriate dose conversion factors. The media-dose conversion factor used in this analysis is 1.5×10^{-8} (rem/y)/(pCi/m^{3}air), and represents the conversion from atmospheric concentration to average whole body dose based on external photon exposures (EPA-52019-73-003D, 1973). Conversion factors for genetic, lung, and skin doses are also available; however, the whole body dose appears to yield the highest number of health effects, and is used for this analysis. Population projections must be based on past information with the additional assumption that no dramatic changes in fertility rates will be experienced over the projection period. Beginning with the United Nations world population estimate of 3.632 billion for the year 1970 (UNSO, 1971), and using an average growth rate of 1.9= per year (UNSO, 1966), gives a projected world population of 9.3 billion by the year 2020; i.e., over 150% increase in fifty years. The integrated population dose in any year is, therefore, a product of the air concentration of krypton-85, the total world population, and the dose conversion factor. The resultant population doses, in person-rem, are plotted in Figure 6 and listed in Table 2.

The transition from population dose to health effects also requires a number of assumptions. Consistent with the recommendations made in the BEIR report (BEIR, 1972), the health risks presented are based on the assumption that there is a linear relationship between dose and biological effect, and that any increased risk is in addition to that produced by background radiation (i.e., no threshold). For a given dose equivalent, the BEIR report estimates a range for the health impact per million exposed persons. Since these risk estimates neglect repair mechanisms, the range of mortality given by the BEIR Committee is probably an upper limit. The cancer mortality risk (including leukemia mortality) listed as "most likely" by the Committee, for whole body radiation, is about 200 deaths per year for 10^6 person-rem annual exposure. Cancer mortality is not a measure of the total cancer risk, which the Committee states is about twice the yearly mortality (i.e., 400 health effects per 10^6 person-rem) (EPA 52019-73-003D, 1973). These estimates are for a population with the characteristics of the U. S. or Northern European countries, and would not necessarily be representative of the total world population. However, with the assumption that the rest of the world will attain the present U. S. vital statistics by the year 2020, these risk numbers may be reasonably applied.

Computation of health effects from continuous exposure to the population doses listed in Table 2 indicates that there will be approximately 110 total cancers caused per year, including 55 excess deaths per year, for the year 2020 from the U. S. nuclear industry. These health effects would be for the total world population with only about 5% occurring in the United States. By applying controls with a decontamination factor of 10^2, the health effects and excess deaths are reduced to 1 and .5 per year, respectively. Consequently, installing controls by 1980 would keep the yearly health effects from U. S. produced krypton-85 below these levels.

It must be understood that the U. S. nuclear industry will produce only a portion of the total world inventory of krypton-85, and our unilateral implementation of controls will reduce only that contribution. The U. S. contribution to the total world inventory is estimated to be about 50% by 2020. Since 110 total cancers per year would result from uncontrolled U. S. discharges, the total world cancer rate would be approximately 220 per year, if all krypton-85 from projected worldwide nuclear power production is discharged.

SUMMARY AND CONCLUSIONS

The above discussion of the effects of krypton-85 controls is intended to suggest some of the factors and approaches which may be used to evaluate the desirability and possible timing of control implementation. The question of whether or not krypton-85 releases should be controlled is one of wide interest concerning the nuclear industry, government standard setting and regulatory agencies, and citizen action groups. Consequently, final decisions as to the necessity of controls, their required efficiency, and the timing of their installation will probably not be made solely on technical grounds, but will consider the prevailing political and societal forces.

REFERENCES

Advisory Committee on the Biological Effects of Ionizing Radiation (BEIR Committee), (1972), *The Effects of Populations of Exposure to Low Levels of Ionizing Radiation.* National Academy of Sciences — National Research Council.

Coleman, Jr. and R. Liberace, (1966), *Nuclear Power Production and Estimated Krypton-85 Levels.* Rad Health Data and Reports 7:11.

General Electric Company, (1971), *Applicants Environmental Report-Suppliment 1,* Midwest Fuel Recovery Plant, NEDO 14504-2.

Oak Ridge National Laboratory, (1970), *Siting of Fuel Reprocessing Plants and Waste Management* Facilities, ORNL-4451. Oak Ridge National Laboratory, Oak Ridge, Tennessee.

Office of Radiation Programs — U.S.EPA, (1973), *Environmental Analysis of the Uranium Fuel Cycle: Part III — Nuclear Fuel Reprocessing,* EPA-520/9-73-003D. U.S. Environmental Protection Agency.

U. S. Atomic Energy Commission, (1972), *Nuclear Power 1973-2000,* WASH-1139 (1972). U.S. Government Printing Office, Washington, D.C.

United Nations Statistical Office (UNSO), (1971), *Demographic Yearbook.* Publishing Service United Nations, New York.

United Nations Statistical Office (UNSO), (1966), *World Population Prospects as Assessed in 1963,* Population Studies No. 41 United Nations, New York.

TABLE 1

ESTIMATED U.S. NUCLEAR INDUSTRY AND ANNUAL INVENTORIES OF KRYPTON–85 EPA-52019-73-003D (1973).

YEAR	NUCLEAR ELECTRIC GENERATION: GW(e)	TONNES OF FUEL DISCHARGED ANNUALLY *					ANNUAL INVENTORY OF KRYPTON–85 (CURIES)
		LWR–U	LWR–PU	LMFBR	HTGR	TOTAL	
1970	2.6	25	0	0	0	25	2.6×10^5
1975	40	700	90	0	0	790	8.3×10^6
1980	110	1900	500	1	1	2,400	2.5×10^7
1985	220	2700	2600	0	100	5,400	5.7×10^7
1990	420	3700	3800	480	2,420	10,400	1.1×10^8
1995	650	4100	4100	2,600	6,600	17,400	1.8×10^8
2000	1000	3700	3800	11,500	7,800	26,800	2.8×10^8
2005	1360	3700	3700	20,600	10,000	38,000	4.0×10^8
2010	1780	4300	4400	32,800	10,000	51,500	5.4×10^8
2015	2220	5300	5400	43,800	10,000	64,500	6.8×10^8
2020	2700	6100	6100	58,000	8,800	79,000	8.3×10^8

* BURNUP: 33 GWd(t)/ TONNE AND 0.35 THERMAL EFFICIENCY.

TABLE 2

ESTIMATED KRYPTON–85 CONTRIBUTIONS TO WORLD POPULATION DOSE

YEAR	KRYPTON–85 CUMULATIVE INVENTORY (CURIES)	SEA LEVEL CONCENTRATION (pCi/m^3)	WHOLE BODY DOSE CONVERSION FACTOR * (REM/YEAR)/(pCi/m^3)	WORLD ** POPULATION $\times 10^9$	INTEGRATED WORLD POPULATION DOSE (PERSON–REM)
1970	2.6×10^5	6.63×10^{-2}	1.5×10^{-8}	3.632	3.6
1975	1.8×10^7	4.59×10^0	1.5×10^{-8}	3.990	275
1980	9.3×10^7	2.36×10^1	1.5×10^{-8}	4.384	1555
1985	2.6×10^8	6.63×10^1	1.5×10^{-8}	4.817	4790
1990	5.8×10^8	1.49×10^2	1.5×10^{-8}	5.292	11,821
1995	1.1×10^9	2.81×10^2	1.5×10^{-8}	5.814	24,462
2000	1.9×10^9	4.77×10^2	1.5×10^{-8}	6.388	45,692
2005	2.9×10^9	7.40×10^2	1.5×10^{-8}	7.018	77,847
2010	4.2×10^9	1.08×10^3	1.5×10^{-8}	7.711	125,057
2015	5.8×10^9	1.49×10^3	1.5×10^{-8}	8.472	189,248
2020	7.6×10^9	1.95×10^3	1.5×10^{-8}	9.308	272,259

*(EPA-52019-73-003D, 1973)
**(UNSO, 1966 and 1971)

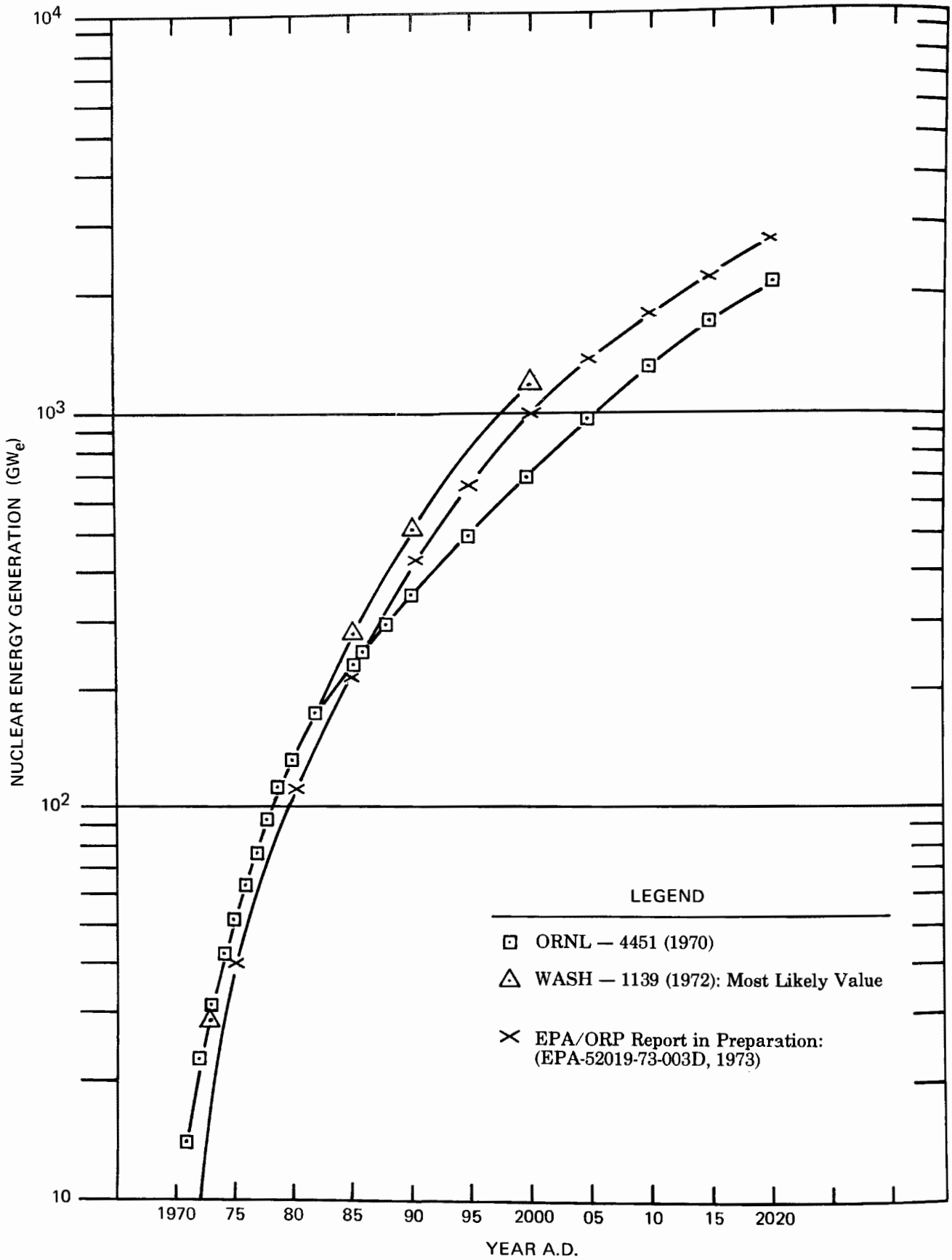

FIGURE 1. PROJECTIONS OF NUCLEAR ELECTRIC GENERATION 1970 – 2020

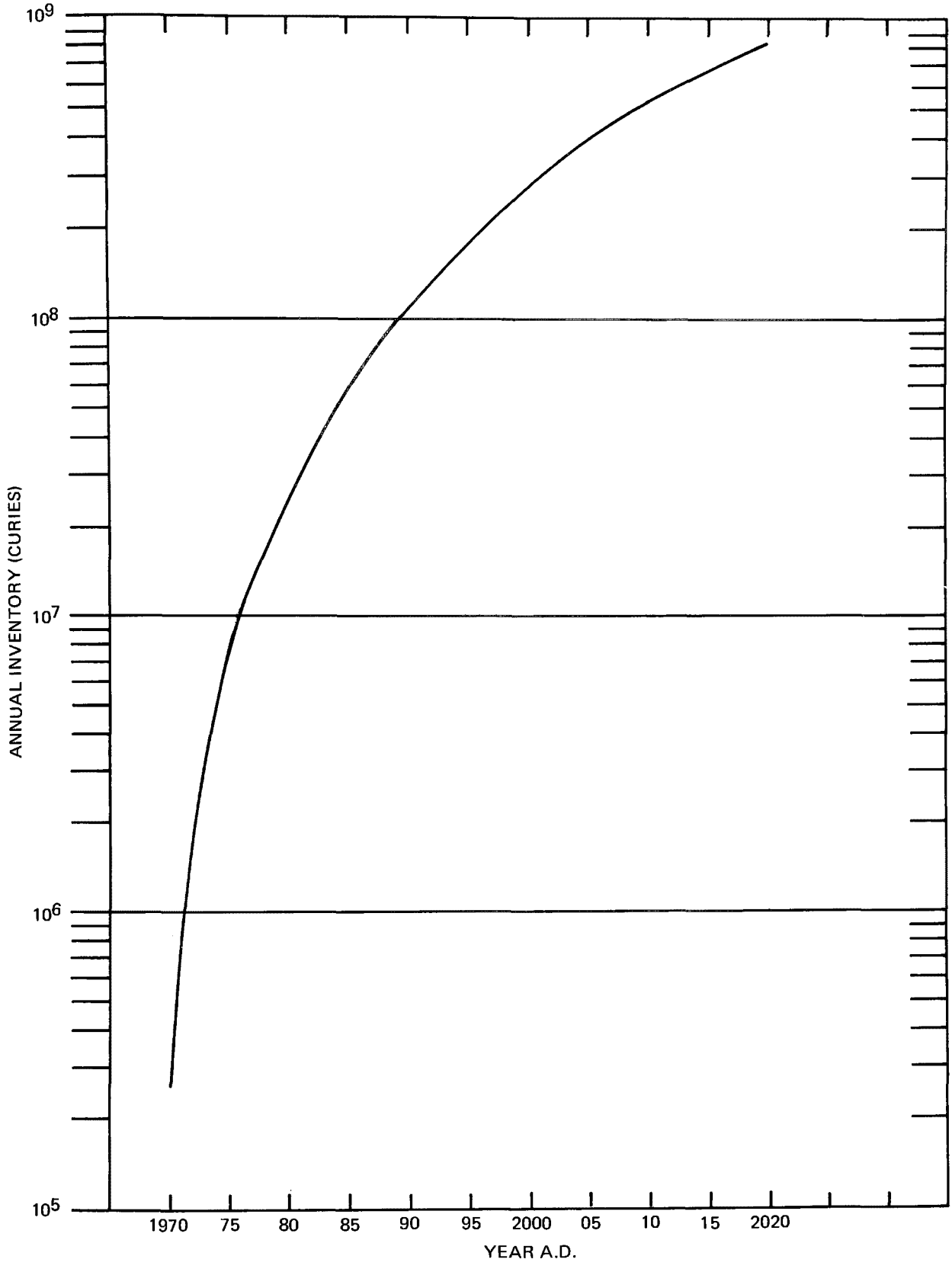

FIGURE 2. ESTIMATED KRYPTON–85 RELEASES TO THE ENVIRONMENT 1970 – 2020

(ADAPTED FROM TABLE 1)

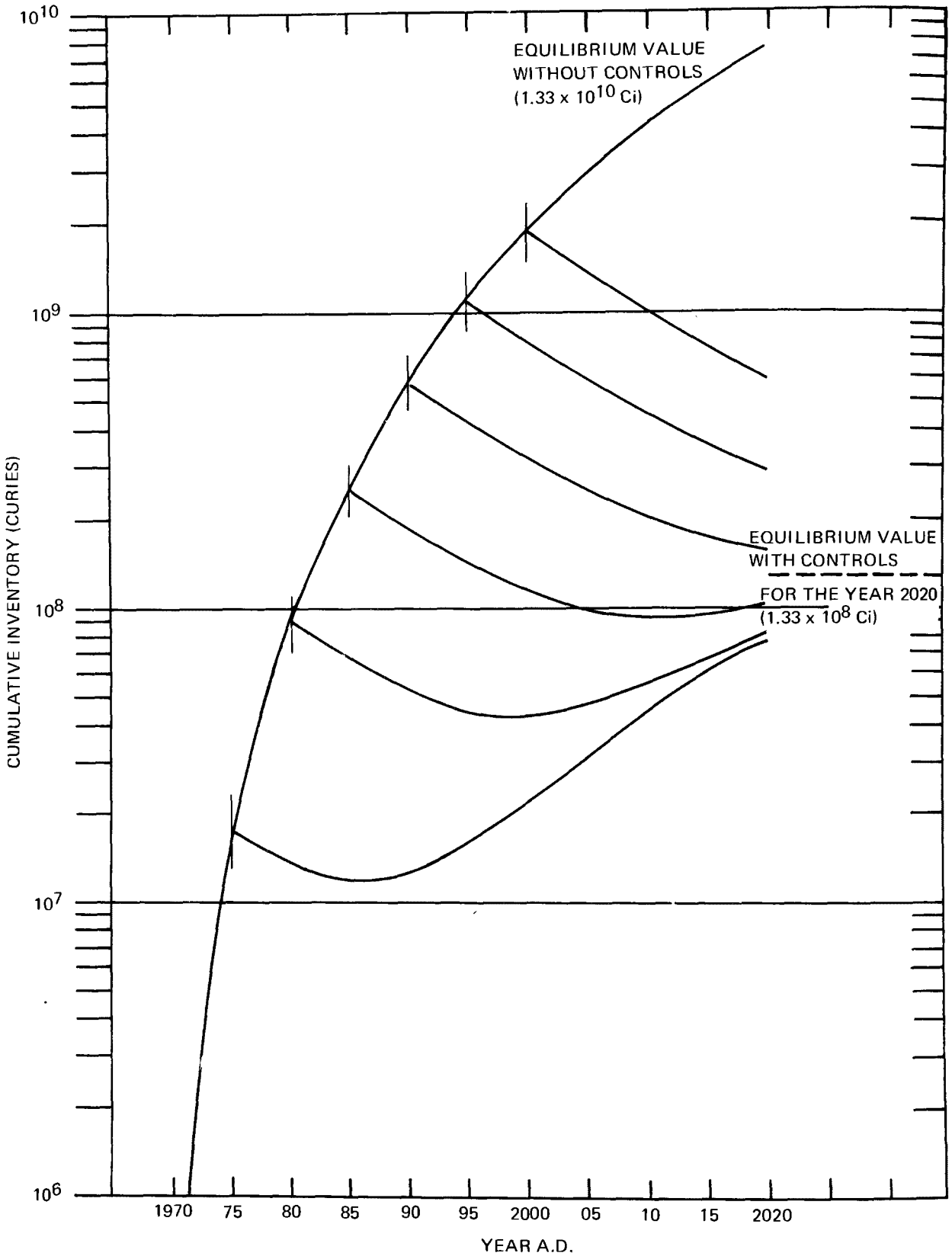

FIGURE 3. ESTIMATED KRYPTON–85 INVENTORY IN THE ENVIRONMENT FOR CONTROLS INITIATED IN VARIOUS YEARS (DECONTAMINATION FACTOR = 100)

1970 – 2020

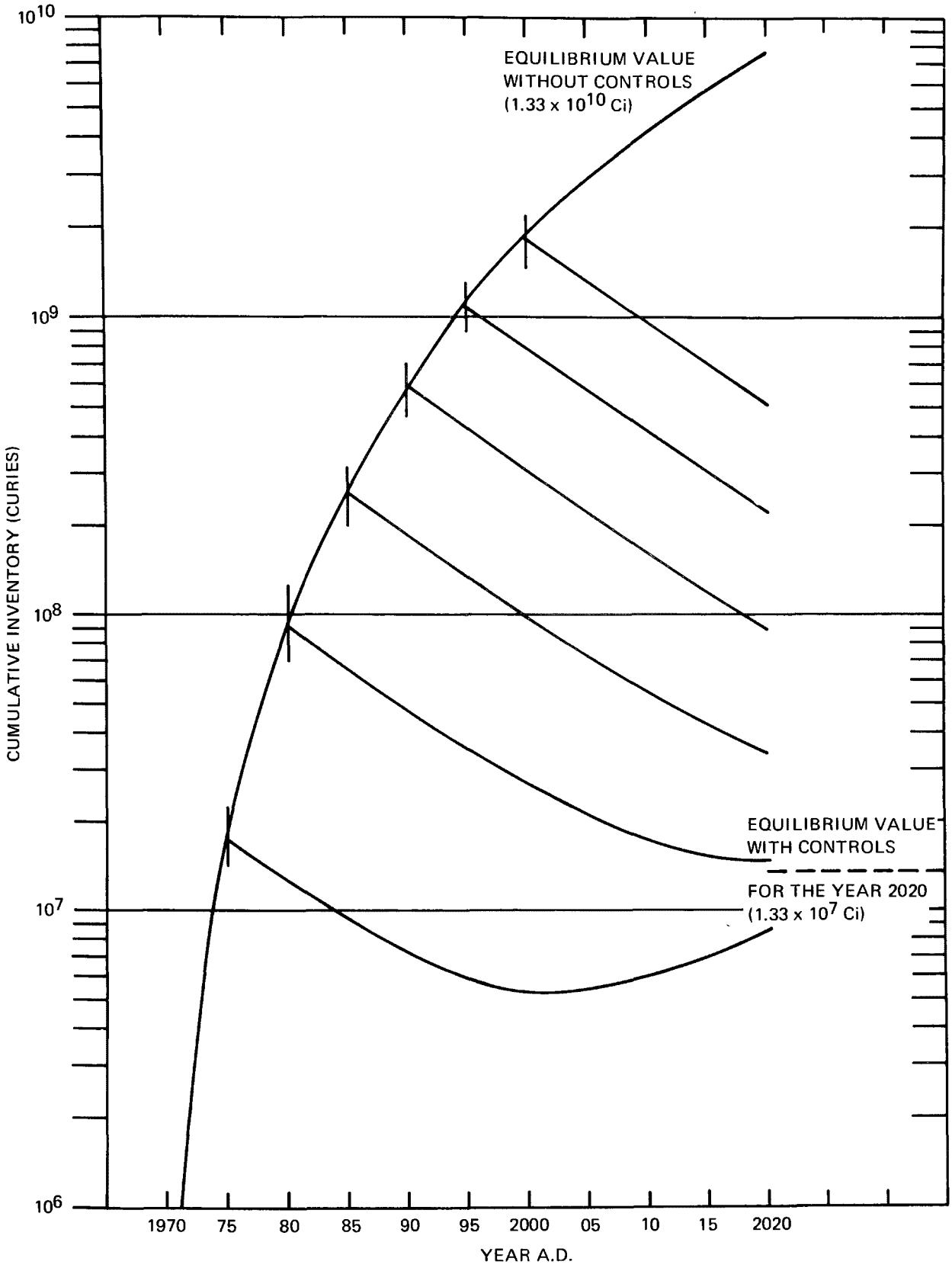

FIGURE 4. ESTIMATED KRYPTON–85 INVENTORY IN THE ENVIRONMENT FOR CONTROLS INITIATED IN VARIOUS YEARS (DECONTAMINATION FACTOR = 1000)

1970 – 2020

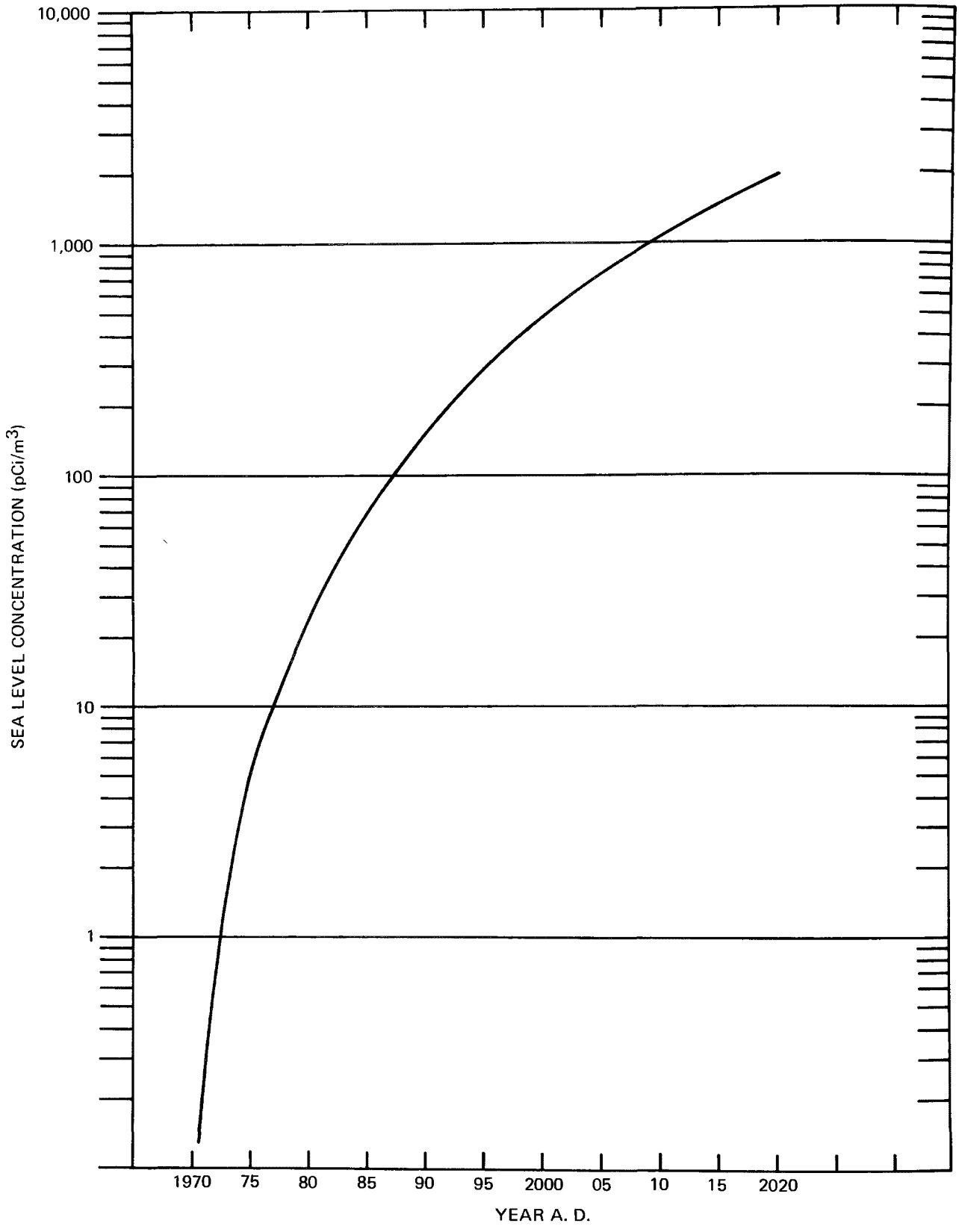

FIGURE 5. ESTIMATED KRYPTON–85 CONCENTRATION IN THE WORLDS ATMOSPHERE FROM U.S. NUCLEAR ELECTRIC POWER PRODUCTION

1970 – 2020

(ADAPTED FROM TABLE 2)

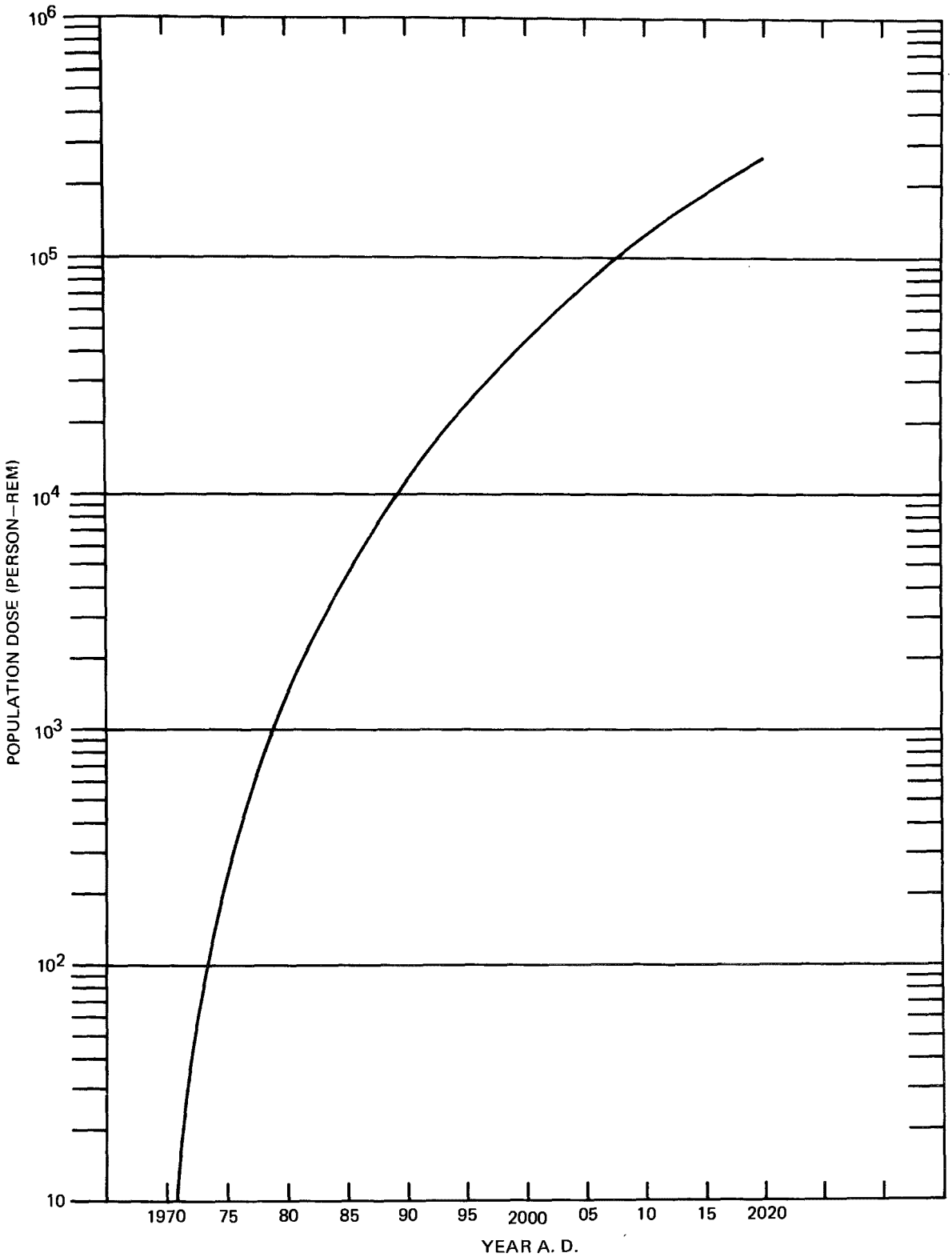

FIGURE 6. ESTIMATED ANNUAL INTEGRATED WORLD POPULATION DOSE TO THE WHOLE BODY FROM KRYPTON–85 GENERATED BY THE U.S. NUCLEAR POWER INDUSTRY

1970 – 2020

(ADAPTED FROM TABLE 2)

CRYOGENIC ADSORPTION SYSTEMS FOR NOBLE GAS REMOVAL

A. R. Smith
Cryogenic Technology, Inc.,
Waltham, Massachusetts 02154

E. L. Field
Arthur D. Little, Inc.
Cambridge, Massachusetts 02140

R. L. O'Mara
Stone & Webster Engineering Corp.
Boston, Massachusetts 02107

Abstract

Because of the continuing emphasis on decreasing or eliminating noble gas emissions from nuclear power reactors, systems for the delay and retention of noble gases have been developed. Several of these systems rely on adsorption, either under ambient or refrigerated conditions. The usual adsorbents are activated charcoal or synthetic zeolites (molecular sieves).

This paper discusses the design of such noble gas treatment systems. As an example, a description of the noble gas recovery system installed at the Wisconsin-Michigan Power Company's Point Beach Nuclear Plant will be presented, including the design philosophy, data upon which the design was based, and some test results on the final system.

INTRODUCTION

The continuing concern of utilities with the release of radioactive materials from nuclear power plants resulting in possible exposure to the public and to plant personnel has led to the development of many systems to limit these releases. Of major concern is the release of radioactive gases which leak from pinholes or cracks in reactor fuel rods, and find their way into the steam in a boiling water reactor (BWR) or into the reactor coolant system of a pressurized water reactor (PWR).

In a PWR, which is continuously maintained at high-power levels, the noble gas concentration in the reactor coolant system slowly increases unless these gases are removed. As the noble gas concentration increases, the possibility of accidental leakage resulting in a hazard to the public and operating personnel increases because of the increased concentration of longer-lived noble gas isotopes, particularly krypton-85. A leak from the primary coolant system to the secondary system of as much as 500 gallons of water per day for each reactor has been postulated. This would provide a leak path to the atmosphere via the main condenser air ejectors. It is, therefore, desirable to continuously remove the noble gases from the coolant system to reduce the potential hazard.

In the Fall of 1970 the owners (Wisconsin-Michigan and Wisconsin Electric Power Companies) of the Point Beach Nuclear Plant, a plant with two 500 MW(e) PWR's. asked Stone & Webster Engineering Corporation to provide waste treatment improvements at the plant consistent with the state of the art. In particular, the reduction of krypton-85 releases to the "as low as practicable" amount was specified.

PROJECT DESCRIPTION

It was determined that the most effective means of reducing the long-lived noble gas specific activity in the coolant systems of the two reactors was to continuously strip these gases from the coolant water. This was to be accomplished by passing the maximum expected let-down flow through a gas stripper. The noble gases contained in this gas stream would then be separated in a new gas treatment system, and the hydrogen, which is the major component of the stream, would be returned to the primary system.

The stripper design was based on the fact that short-lived isotope concentrations in the coolant system are limited primarily by decay as opposed to other forms of removal; e.g., a minimum decay period of only one hour would be sufficient to reduce the short-lived isotopes in the air ejector releases to a ^{133}Xe equivalent value approaching 1 percent of that specified by 10 CFR Part 20. The long-lived noble gases content would then be reduced by continuous stripping and subsequent decay or storage.

In addition, another source of gaseous radwaste releases was recognized — that of boron recovery tank cover gas being displaced by tank filling operations with small leaks through nitrogen gas regulators. This gas would be delayed in storage tanks and periodically vented to the atmosphere through the gas treatment system.

The basic design criteria for the gas treatment facilities involved two main tasks:

(1) delay of noble gases to decay short-lived isotopes, with subsequent removal of longer-lived isotopes from the hydrogen gas, which is continuously stripped from the reactor coolant and recycled; and,

(2) removal of noble gases from the decayed cover gas prior to release to the environment.

Typical characteristics for these two gas streams are as follows:

	Stripper Overhead Gas	Cover Gas
Flow	0.8 scfm	600 scf per month
Inlet Conditions		
Temperature, °F	120	120
Pressure, psig	1	120 down to 30
Composition (Note: Streams will be saturated with water.)		
(mole fraction dry basis)		
hydrogen	9.39	.494
nitrogen	.060	.501
oxygen	.003	.0046
argon	7.1×10^{-4}	8.0×10^{-5}
carbon dioxide	---	8.0×10^{-5}
stable krypton	3.7×10^{-6}	2.5×10^{-5}
stable xenon	18.9×10^{-6}	8.0×10^{-6}
radio krypton	1.9×10^{-7}	2.8×10^{-8}
radio xenon	2.1×10^{-7}	7.5×10^{-9}

EXPERIMENTAL PROGRAM

In response to an inquiry, Cryogenic Technology, Inc., (CTI) proposed to Stone & Webster and Wisconsin Electric Power Company that the simplest, safest, most reliable method of concentrating and collecting noble gases is adsorption on charcoal at cryogenic temperatures because of:

(1) the selectivity that charcoal exhibits for krypton;

(2) the dramatic increase in the adsorption effectiveness of the charcoal at -315°F (capacity of charcoal for krypton per unit volume is about 1,500 times that at 80°F);

(3) the high decontamination factors that can be achieved (in excess of 1,000).

CTI proposed that a study program be initiated in conjunction with Arthur D. Little, Inc. (ADL) to develop theoretical predictions concerning the adsorption of noble gases at cryogenic temperatures, and to establish the design parameters for the gas treatment system. Work was begun on the study program with the following specific goals:

(1) preparation of a theoretical analysis of the multi-component adsorption in the beds;
(2) building of a laboratory-scale test apparatus and conducting of a test program to verify the analysis; and
(3) preparation of a preliminary process and mechanical design for the noble gas removal system.

An experimental apparatus simulating the cryogenic section of the proposed design was built, and tests were conducted at the ADL laboratories. A flow schematic of the test system is shown in Figure 1.

The test apparatus was designed so that the gas can flow forward through the adsorber beds for normal operation or backwards through the beds for regeneration. The system can be cooled with liquid nitrogen or heated with hot nitrogen for regeneration. Six sample taps are provided so that the relative krypton concentration at various points in the system can be monitored with radiation counting equipment. Two evacuated sample receivers are provided to collect the adsorbed gases as they are evolved during warm-up. One cylinder is connected to the first adsorption beds and the other is connected to the last bed. A shut-off valve can be closed to isolate the last bed from the rest of the system, thus providing the capability of sampling this bed separately.

During normal operation, the hydrogen gas and the radioactive gas mixture flow from storage cylinders to Flowmeters 1 and 2, respectively, where they are then combined and flow through a heat exchanger, a filter, and the three adsorption beds, all of which are contained in an insulated dewar. Pressure on the system is maintained at the desired level by a back pressure regulator located downstream of the beds. Cooling of the beds (to -315°F) is accomplished by flowing liquid nitrogen through the cooling/heating loop which is in contact with the adsorber beds. A small portion of the process gas is continuously bled through one of the six sample taps, through Flowmeter 3, to the radiation counting equipment. The counts were fed to both a count rate meter and an automatic scaler for measurement.

The radioactive counting apparatus consists of a modified windowless flow counter. A window of 1/4 mil aluminized mylar was used to separate the hemispherical counting chamber from the sample chamber, through which a flow of gas from any given sample point was maintained. Somewhat less than half of the beta particles emitted during decay of the ^{85}Kr in the sample chamber passed upward, through the mylar window, into the counting chamber where they were recorded as pulses (counts) per second.

Warm-up and collection of the adsorbed gases involves shutting off the flow of process gas, isolating Bed No. 3 from the rest of the system, opening the valves to the sample receivers, and stopping the flow of liquid nitrogen. The beds are then heated to 300°F by heat exchange with hot gas. As the beds warm up the pressure rise is noted to determine the quantity of gas evolved from the beds, and the gas is collected in the sample receivers for analysis.

The pressure, temperature, and gas composition used in the test apparatus were essentially the same as would be expected in processing the gas from the stripper except that 22.6 ppm of Kr with ^{85}Kr tracer was substituted for 18.9 ppm Xe and 3.7 ppm Kr, making the results conservative by a factor of approximately 1.1. A higher level of radioactivity in the actual plant could result in somewhat reduced capacity because of radiation heating, but a check on the magnitude of this effect at the expected radiation levels predicts that it will be negligible (Glueckauf, 1959). The charcoal used was the same as that used in the full scale plant.

The apparatus contained three 0.31 in. I.D. beds in series; the first two were 2.5 inches long, and the third was 11.5 inches long. The first two were intended to provide equilibrium and rate data while the third was intended to provide decontamination factor (D.F.) data as well as a back-up source of information if performance estimates were drastically in error. Because the data on the first beds were in close agreement with performance estimates, it was not necessary to run the last bed to breakthrough.

After a number of familiarization test runs, three runs were made of duration 21 hours, 46.2 hours, and 50.8 hours, respectively. The breakthrough data for these runs are as shown in Table 1. Additional tests have subsequently been run wherein varying temperatures, gas compositions, sorbents, flow rates, regeneration conditions, etc., were explored. The data from these additional tests were consistent with the results shown in Table 1.

The breakthrough times for Runs 2 and 3 (which were duplicated with respect to flow) are also shown as the experimental points on Figure 2; the correlating curves shown were based on matching with the theoretical plots of breakthrough given in Hougen and Marshall, (1961) as extended by Burnette, *et al.*, (1961).

The radioisotope level was increased on the third run to provide a more sensitive measurement of the decontamination factor. The inlet stream produced 2,200 counts per second. The background level was 1.3 ± 0.1 counts per second so that it would have been possible to detect 0.2 c/s change in the background. Prior to breakthrough on both Beds 1 and 2, there was no difference between the sample stream and the background which could be detected; this indicated that the decontamination factor was $2{,}200/0.2 = 10^4$ or better.

The results of the experimental program showed that for a charcoal bed operated at -315°F and 120 psig with a 22.6 ppm Kr inlet concentration:

(1) the equilibrium capacity for Kr was 60 scc/gm vs. a value of 120 scc/gm which had been predicted by theory. The dynamic adsorption coefficient for Kr was thus $60/(22.6 \times 10^{-6}) = 2.6 \times 10^6$ scc of bulk gas/gm at a pressure of 120 psig;

(2) the test bed number of transfer units (NTU) was 14 per inch vs. an expected value of 105; and

(3) decontamination factors of 10^4 or better are possible with adsorption systems.

Although the departures from theoretical estimates were significant, the agreement is adequate to provide assurance that the projected design would function as expected. The difference in the equilibrium capacity can be accounted for by slight differences in the literature values of pure component adsorption isotherms for N_2 and Xe on charcoal. The differences in the dynamic transfer processes can be accounted for by other possible effects such as pore diffusion limitations or channeling, but are unimportant as long as a system has on the order of hundreds of transfer units.

SYSTEM DESIGN

With the completion of the experimental program, attention was then focused on the specific design requirements of the full scale noble gas removal system. Some of these requirements were:

(1) the ability to achieve a D.F. of at least 1,000 in processing both the gas from the stripper and the cover gas;

(2) the ability to operate for 180 days on one adsorber before noble gas breakthrough;

(3) the ability to retain the adsorbed noble gases for subsequent transfer to an evacuated noble gas storage tank;

(4) the ability to regenerate the adsorption bed after transfer of the noble gas in such a way as to remove all of the residual noble gases and to permit a D.F. of at least 1,000 when the bed was put back on stream;

(5) design for safety, simplicity, and reliability with particular attention being given to leak-tight, rupture-proof construction; and

(6) design of a compact system to fit into the limited space available at the plant.

The unit subsequently built is shown schematically in Figure 3.

The plant provides two independent systems for processing the gas including compression, water knockout, oxygen removal, gas drying, and cryogenic separation of the noble gases from the hydrogen-nitrogen streams. The plant is capable of processing stripper gas (normal continuous operation) through either flow path while at the same time processing cover gas (intermittent operation) through the other flow path. Each cryosorber module and dryer circuit is capable of regeneration independent of the other.

The equipment is arranged as shown in Figure 4 with all the components located on one 9 ft. x 4 ft. skid with the exception of the compressors, the ambient charcoal delay bed, and the cryosorber modules. These components are located behind concrete shield walls for operator protection.

During normal operation the stripper gas is compressed to 150 psig by a diaphragm compressor, and then passed through a chiller/water separator operating at 35°F for bulk removal of moisture and attainment of a low relative humidity for effective utilization of the ambient charcoal delay bed. The gas then goes to the ambient temperature charcoal bed which delays the noble gases for several hours to permit the shorter-lived isotopes to decay, thus reducing the radioactivity level at the main skid for operator protection. The gas stream then goes to a catalytic oxygen removal system to remove trace quantities of oxygen and ozone so as to preclude the collection and/or formation of ozone on the cryogenic adsorption bed. The oxygen removal system consists of a preheater, an iodine preadsorber, and a precious metal catalytic hydrogen/oxygen recombiner.The iodine adsorber protects the recombiner catalyst from iodine, the only possible contaminant in the stream which would retard its oxygen conversion activity. The gas is then passed through another chiller/water separator and a molecular-sieve dryer. The dryer, containing adequate 5-A molecular sieve for 180 days operation before regeneration, reduces the dew point of the gas to about -100°F before it enters the cryogenic heat exchanger. This high performance moisture removal is necessary to prevent frost plugging in the counterflow cryogenic heat exchanger where the gas is cooled to about -300°F. The cold gas then passes through the charcoal adsorption bed.

The adsorption bed was designed using information obtained during the experimental program which showed that a bed containing 0.25 cubic feet of charcoal, 2 inches in diameter by about 140 inches long, operating at -315°F would be adequate for processing stripper gas for 180 days (plus 3,500 scf of cover gas) with a safety factor of 2. This bed would liberate approximately 38 scf of adsorbed gas during each regeneration. Since two regenerations per year were planned, the 525 cubic foot evacuated vessel in which the desorbed gas would be stored should be adequate for the storage of at least seven years regeneration gas without exceeding one atmosphere.

Each heat exchanger and its adsorption bed is contained in a separate perlite-insulated vessel. They have remotely operated valves on the inlet and outlet piping which will automatically close in the event of high temperatures in the adsorber or high radiation downstream of the adsorber, thus preventing the release of any radioactive material. The heat exchanger vessel is oversized to act as a surge volume to reduce the pressure rise, which would occur if the vessels were to warm to the ambient temperature. These components are also designed to withstand the stresses associated with this pressure rise. The bed is maintained at -315°F by a continuous flow of liquid nitrogen.

After passing through the adsorption bed, the clean hydrogen passes out through the heat exchanger and a back pressure regulator which maintains the operating pressure at 150 psig. The gas is then monitored for radiation and routed back to a volume control tank for reuse.

The system is designed to operate for 180 days on one processing stream. Flow will then be switched to the other stream, the off-stream adsorber will be warmed and the adsorbed noble gases will be collected and stored; then the system will be regenerated by flowing clean, dry effluent gas from the on-stream system backwards through the adsorber and dryer. The regeneration gas will be routed to the volume control tank via the closed loop system and there will be no radioactive material vented to the atmosphere. After regeneration is complete, this processing stream will then be placed on standby until the 180-day cycle on the other stream is complete.

When the nitrogen-rich cover gas is processed, the operation of the system is essentially the same except that the ambient temperature charcoal delay beds are bypassed, and the system is operated at one atmosphere to avoid nitrogen condensation in the cryogenic part of the system. This cleaned cover gas is vented to the atmosphere after passing through a radiation monitor rather than being recycled.

The equipment and components used in the system were selected with safety and reliability as a main concern. Leak-tightness is assured by the use of diaphragm compressors, bellows seal valves, and all-welded piping construction whenever possible. The entire system was helium-mass-spectrometer leak checked after assembly. Vessels were built in accordance with Section III of the ASME code. The electrical equipment was designed for use in hazardous locations in accordance with the Class II, Division 1, Group B requirements of the National Electrical Code.

To prevent the inadvertent release of radioactive materials, sample streams and relief valve vents are routed back to the process stream. Radiation monitors which will automatically close the system outlet valves and contain the adsorbed gases in the adsorbers are installed in the system effluent piping. Regeneration is a closed loop process with no release of gases to the atmosphere.

Process variables such as temperature, pressure, and process stream oxygen content are continuously monitored and displayed on a local control panel. Critical variables are alarmed at this local panel and on the main reactor control panel. The system can be started and operated from the local control panel with a low radiation exposure hazard, because the components containing highly radioactive materials, the compressors, the ambient delay beds, and the adsorbers are isolated behind shield walls. This arrangement also results in a low radiation level at the main equipment skid and permits routine inspection and maintenance to be performed with the system in operation.

PRESENT STATUS

Before the unit was shipped, a full scale radioactive ^{85}Kr tracer test was conducted under design flow conditions. Gas mixtures approximating both the stripper overhead gas and the cover gas were processed through the unit for several days. All functions of the system were verified, including water removal, oxygen removal, and noble gas adsorption. The system demonstrated a D.F. of 5,000 during a four-day continuous run at a flow rate of 1 scfm.

The system was installed at the Point Beach plant and is in the final stages of checkout. The installed equipment is shown in Figure 5. The operating data from the plant will form the basis for future reports on the performance of the system.

Construction and operation of the Point Beach system and a similar system installed by the CVI Corporation, at the Southern California Edison Company's San Onofre plant, to remove noble gases from an intermittent flow of cover gas, have proven the practicality of cryogenic adsorption systems. Other charcoal or molecular sieve delay beds have since been designed by CTI both for low PWR off-gas flow rates and for the higher flow rates from BWR's and fuel processing plants. Adsorption systems for noble gas delay operating at higher temperatures have also been designed for use in lower performance systems. However, cryogenic adsorption has been shown to be appropriate and practical where noble gas removal or highly effective delay with an extremely high D.F. is required.

REFERENCES

Burnette, R.D., W.W. Graham and D.C. Morse, (1961), GA 2395, (unclassified).

Glueckauf, E., (1959), *The Movement of Highly Radioactive Gases in Adsorption Tubes*, Annals of N.Y. Acad. Sci., 72, 562.

Myers, A.L. and J. M. Prausnitz, (1965), AIChE Journal 11, 121, 127.

TABLE 1. Kr Breakthrough Times at 80°K from Experimental Gas Mixture.

		Mass Velocity	Times to Indicated Breakthrough Ratio (hrs)							
1	8.6 atm	3.0 times	-	-	17.7	(b)	-	-	-	-
2	9.3	4.6	-	-	14.1	18.6		-	34.5	(b)
3	9.3	4.6	7.5	9.8	12.9	16.6	21.8	27.0	31.5	41.7

(a) Plant nominal mass velocity = 18.5 lb/ (hr-ft^2)
(b) Run terminated prior to reaching this breakthrough.

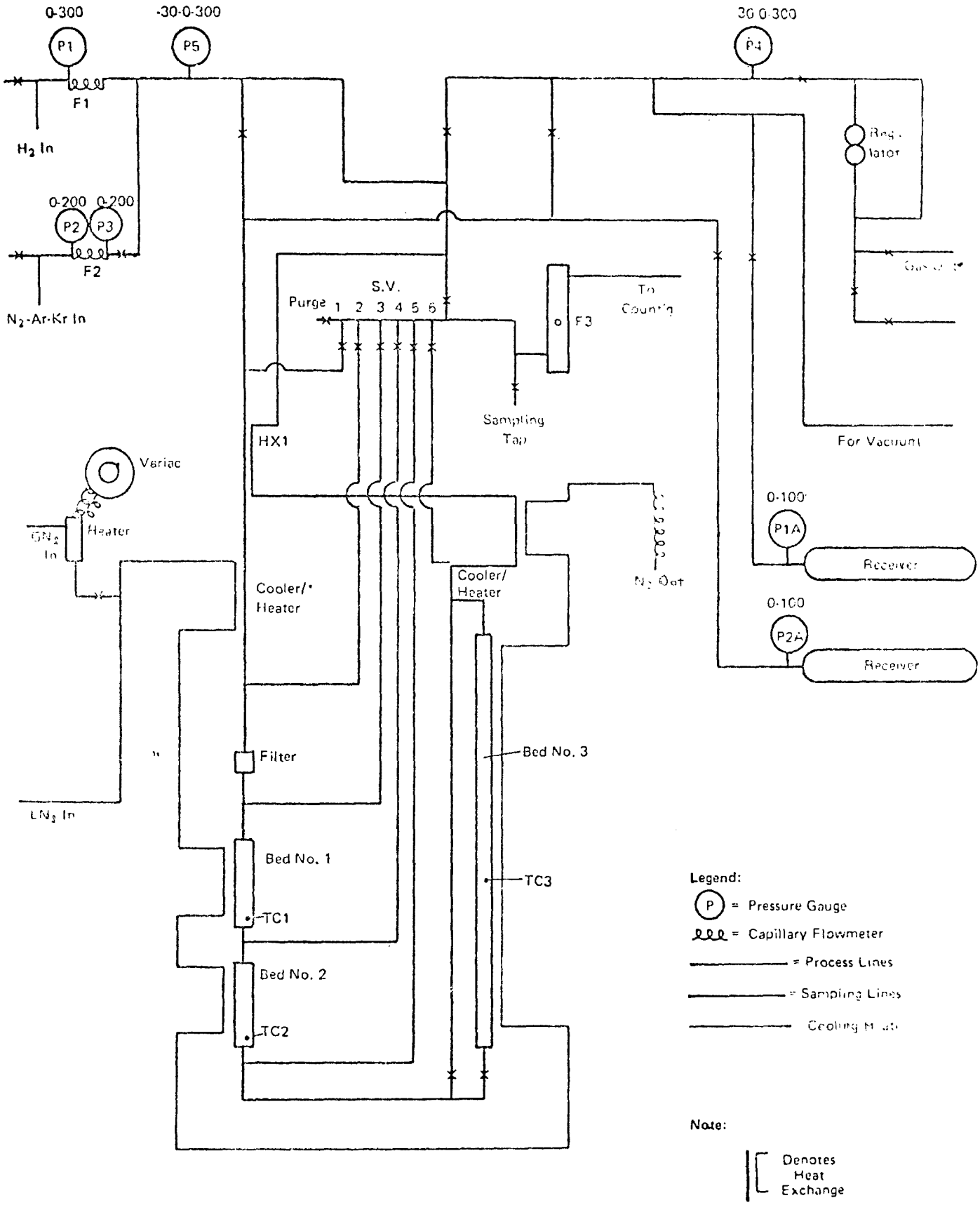

Figure 1. Test Rig Schmetic.

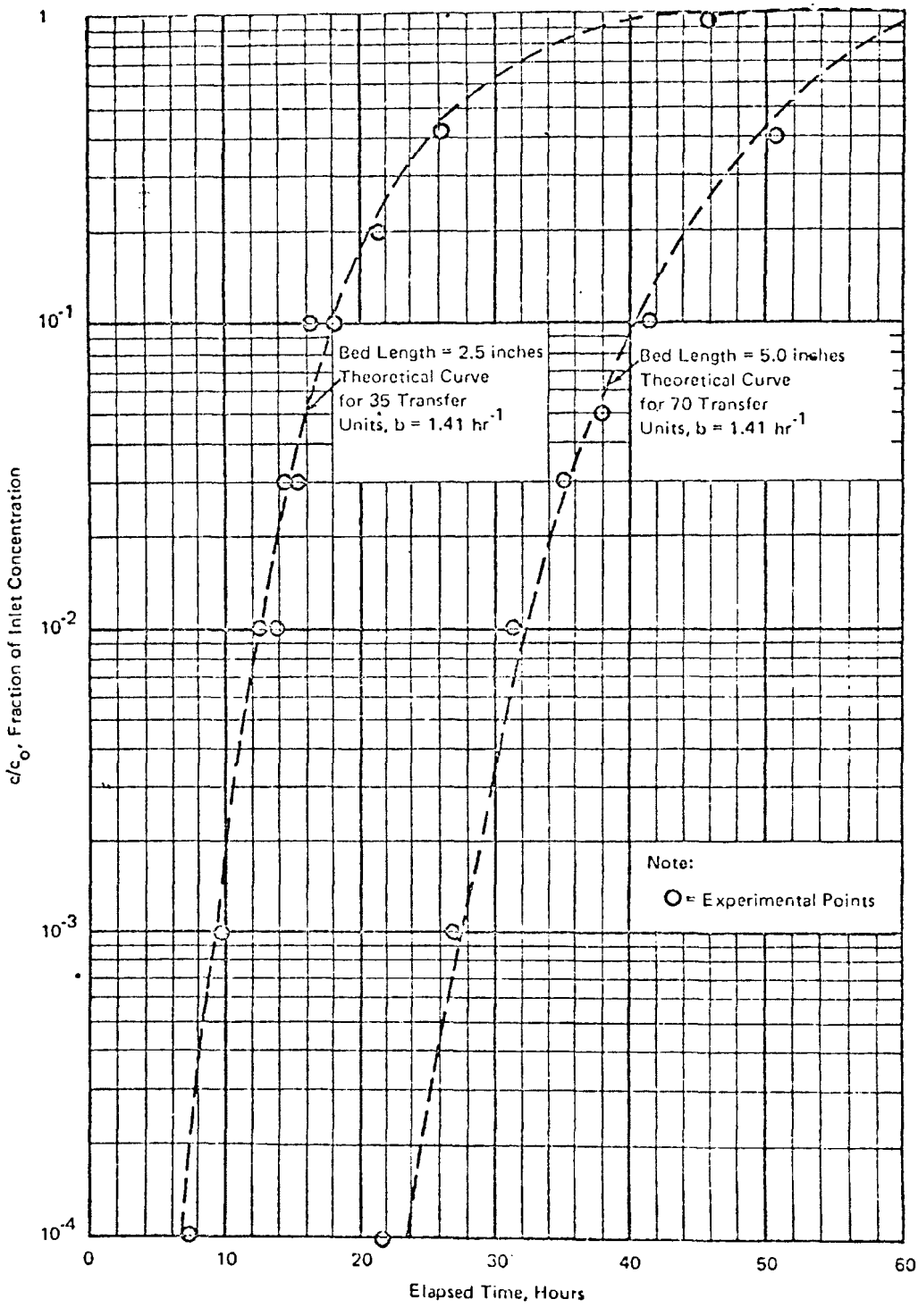

Figure 2. Breakthrough Performance for 2.5-inch and 5.0-inch bed length.

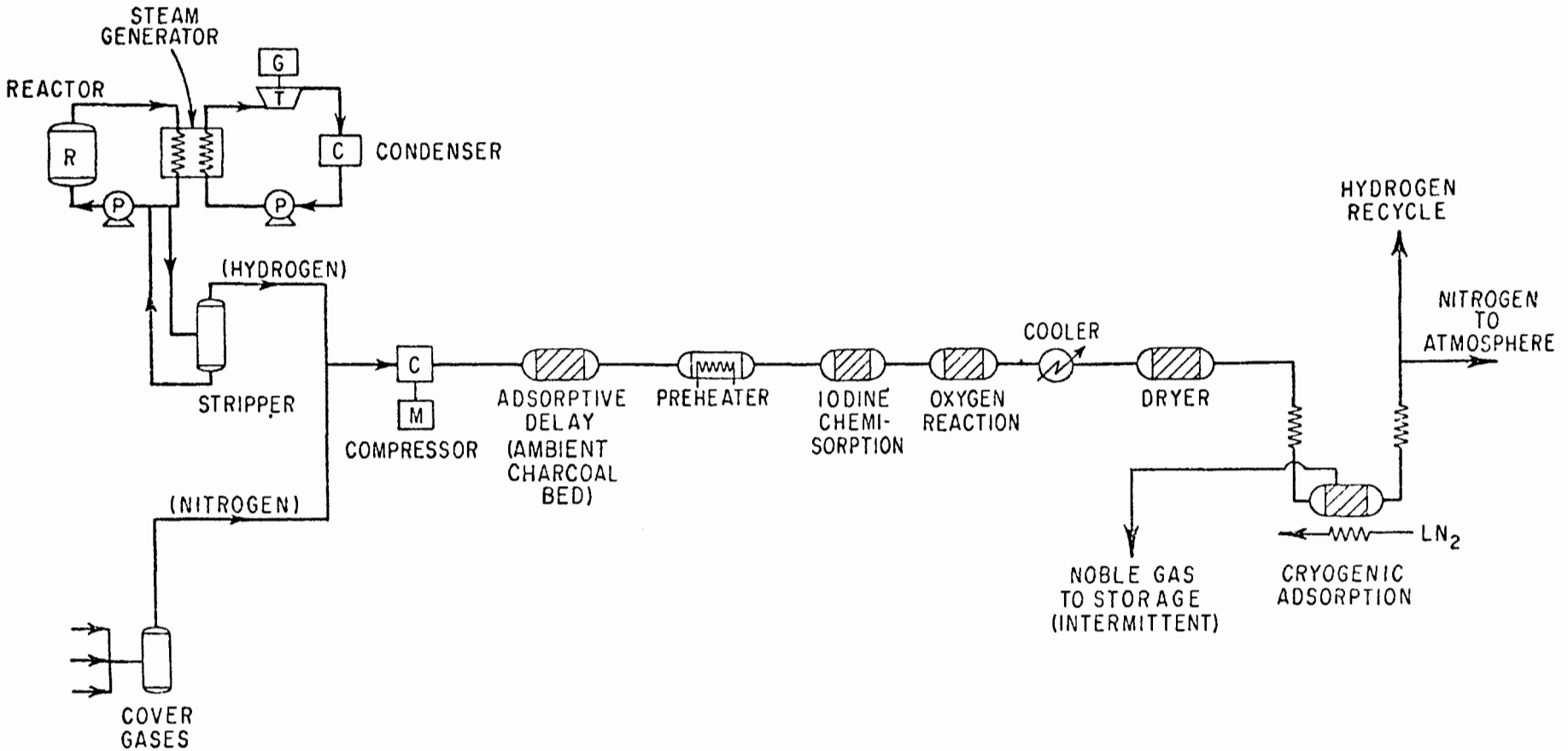

Figure 3. Noble Gas Separation by Selective Adsorption (PWR).

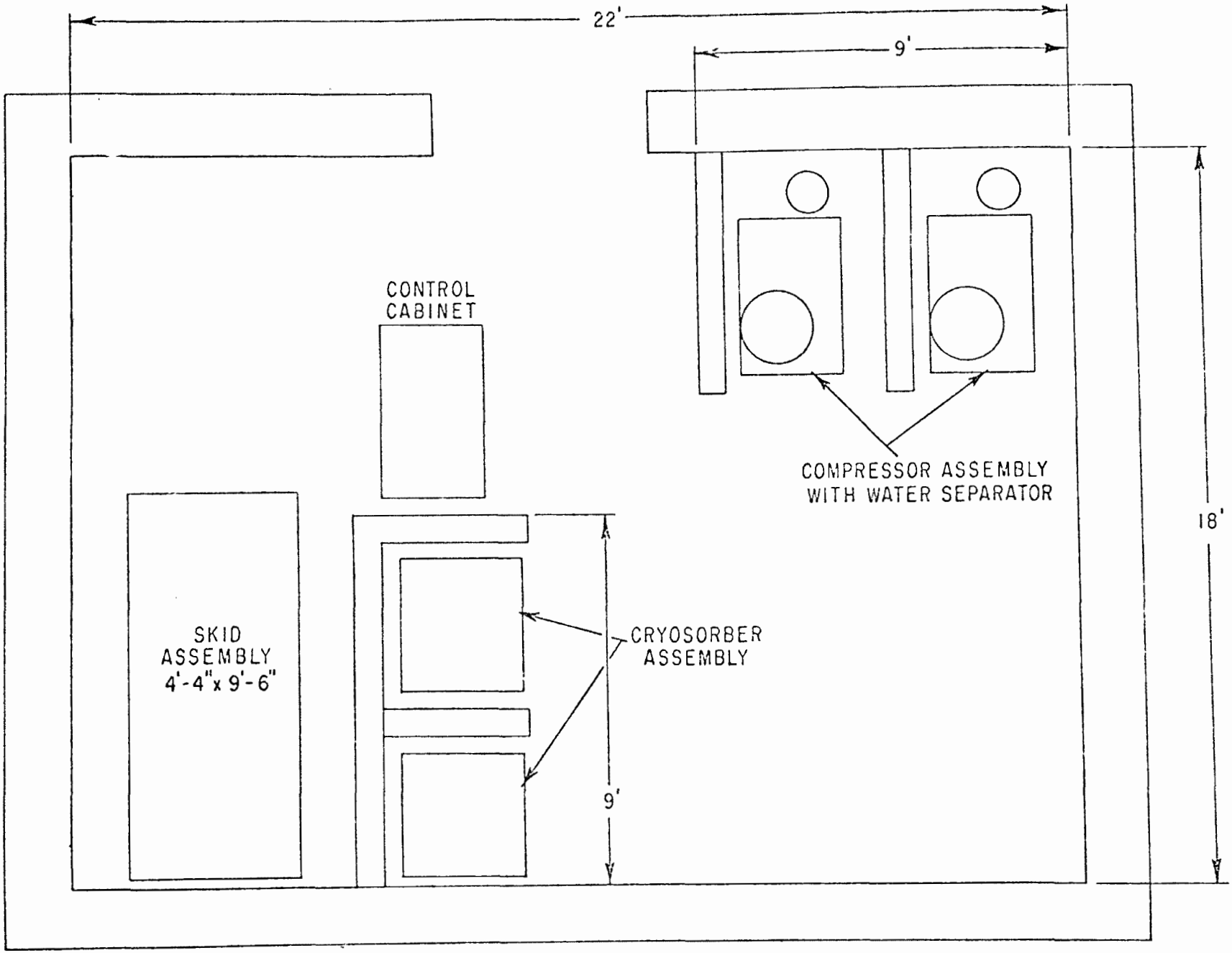

Figure 4. Equipment Arrangement.

Figure 5. Noble Gas Removal System at Point Beach Station.

RECENT ADVANCES IN THE ADSORPTION OF NOBLE GASES

D.W. Underhill and A.S. Goldin
Harvard University
School of Public Health
Department of Environmental Health Sciences
Boston, Massachusetts 02115

Abstract

The Harvard Air Cleaning Laboratory has had an active role in the design of krypton and xenon adsorption beds for the FFTF reactor. We describe an inexpensive laboratory system for measuring fission gas adsorption on various charcoals, and present results of an extensive series of tests of adsorption of krypton from an argon carrier gas on Pittsburgh PCB charcoal. The effects of decay heat, as well as the release of fission gases from the rupture of a pressurized bed, are also discussed.

INTRODUCTION

From 1969 to 1973, basic research for the design of fission gas adsorption beds for the FFTF nuclear reactor was carried out at the Harvard Air Cleaning Laboratory. We summarize here some of the more interesting results of this work.

MEASUREMENT OF ADSORPTION COEFFICIENTS OF KRYPTON AND XENON

At the time this study began, some data (Collins, *et al.*, 1967; Trofimov, *et al.*, 1968; Barilli, *et al.*, 1969; and Forster, 1971) were available for the adsorption of krypton and xenon from the argon carrier gas to be used as the FFTF cover gas, but there was little information available from studies in which the specific charcoal used was domestic. In order to make a preliminary design there was a pressing need for such data over a wide range of temperatures and pressures. We found that an experimental test system could be assembled rapidly from commercially available equipment (see Figures 1 and 2), using as the constant temperature chamber a foamed plastic picnic basket cooled by an internal liquid nitrogen spray. Ordinary copper refrigerator tubing was used to pre-cool the gases in the chamber before passing through the small iron pipe used to contain the charcoal adsorbent. Argon carrier gas was supplied from a commercial compressed gas cylinder, and liquid nitrogen coolant was obtained from a 160-liter cryogenic tank which had to be replaced once or twice a week. The fission gas isotopes, ^{85}Kr and ^{133}Xe, dissolved in isotonic saline, were obtained commercially. In this form, these fission gases are often used for medical studies of blood-gas interaction in the lung. For our purposes, we would withdraw $\cong$0.1 to 1.0 mCi of fission gas into a syringe, shake the liquid with a small amount of argon to bring the fission gas into the gaseous carrier, and inject the argon-fission gas into the carrier gas system entering the cryogenic chamber. The concentration of fission gas, and the quantity of carrier gas passing through the bed, were measured by an ionization chamber and a wet test meter, respectively. From these data, the dynamic adsorption coefficient can easily be calculated.

There are three points that we would now like to make about this system:

(1) It was quite inexpensive to construct.

(2) The experimental data we otained on small samples of charcoal appear to be in good agreement with much larger scale (10^3 to 10^4 times larger) tests run more recently by Kabele, 1973, *et al.*

(3) We found a surprising variability between commercially available charcoals in their ability to retain fission gases.

The variability between charcoals is illustrated in Figure 3 which shows a plot of relative adsorptive capacity vs. relative surface area (as stated by the manufacturer). The correlation between these two parameters is quite small, showing the need for the experimental testing of charcoals before their use in fission gas adsorption beds.

CALCULATION OF ADSORPTION COEFFICIENTS FROM BREAKTHROUGH DATA

The use of moment analysis to calculate adsorption coefficients from breakthrough curve data has the two advantages of: (1) using all the data of the breakthrough curve for the analysis (rather than depending heavily on a few of the experimental points); and (2) being independent of the mechanisms of mass transfer that occur within the bed. The theory behind this analysis has been reported elsewhere (Underhill, 1970a); here we show how it can be applied to the analysis of experimental data.

The moments of the breakthrough curve produced from a pulse input of a fission gas isotope into the bed, are calculated as:

$$M_N = \int_0^\infty t^N e^{\lambda t} c(t)\,dt \Big/ \int_0^\infty e^{\lambda t} c(t)\,dt$$

where t = time following injection of fission gas,

$c(t)$ = concentration of fission gas in effluent at time, t, $\mu Ci/cm^3$

λ = decay constant for the fission gas isotope, s^{-1}.

From the first two moments, we can make some simple, but useful, calculations.

The mean holdup time is equal to M_1 and the dynamic adsorption coefficient, k, is

$$k = \frac{M_1 V_t}{m}$$

where k = dynamic adsorption coefficient, cm^3/gm

V_t = flow of carrier gas, cm^3/s

m = mass of adsorbent, gm

M_1 = mean holdup time, s.

The mass transfer in fission gas adsorption beds can be characterized by the number of theoretical plates, N, calculated as

$$N = M_1^2/(M_2 - M_1^2).$$

If it is desired to calculate the efficiency of the bed for the removal of a noble gas isotope, then the ratio of effluent to input concentration, at steady state, following a constant input of fission gas is

$$R = \int_0^\infty e^{-(\lambda_2 - \lambda)t} c(t)\,dt \Big/ \int_0^\infty e^{\lambda t} c(t)\,dt$$

where λ = decay constant of isotope used in pulse test, s^{-1}

λ_2 = decay constant of the fission gas isotope under consideration, s^{-1}.

The generality of this procedure is illustrated by applying it to current theories of mass transfer in fission gas adsorption beds. These same results are obtained when applied to breakthrough curves calculated from film controlled mass transfer (Young, 1958), interparticle diffusion (Madey, *et al.*, 1962), intraparticle diffusion (Underhill, 1970a), and from the theoretical chamber model (Underhill, 1970b).

As a computer exercise we calculated a breakthrough curve for which N = 20, M_1 = 10 days, input = 70 Ci, λ = 0.148/day, and the mechanism of mass transfer was interparticle diffusion. Then we tried the inverse calculation. Starting with the value for λ, and the breakthrough curve data, the values for N, M_1, and the input were correctly calculated using the above procedure. In making this calculation, no knowledge was needed of the mechanism of mass transfer within the bed.

DECAY HEAT EFFECTS

Good adsorbents — porous granular materials — are not good conductors of heat. Consequently, at steady state operation, a constant release of a relatively small quantity of decay heat can result in a rather large temperature increase.

There is, at present, no complete mathematical solution available for the calculation of the temperature rise in a fission gas holdup bed. The basic difficulty is the nonlinear effect of the temperature on the adsorption coefficient. Glueckauf (1959) did find an analytic solution for a non-linear radial distribution of fission gas resulting from the radial temperature distribution, but this solution neglects other factors — including the channeling of hot gases through the center of the bed, making it less useful than would first appear.

The analysis given here assumed initially that the temperature rise is small. On this assumption, a linear partial differential equation can be written describing heat transfer. By integrating this equation to meet the boundary condition of an initially ambient temperature for the entering gases, the average temperature and the centerline temperature can then be calculated. If the effective adsorption coefficient used for design purposes is based on this latter temperature, the design will be conservative. If the calculated temperature increase is large, it may be possible to redesign the bed to lessen the thermal effects, and in doing so to permit this analytic analysis to be valid for the final design.

This analysis began with the following differential equation (First, *et al.*, 1970) which gives the effects of radial and axial heat conduction, convection, and radioactive decay on the average bed temperature at a distance, x, from the inlet.

$$k\frac{\partial^2 t_I}{\partial x^2} - \gamma\frac{\partial t_I}{\partial x} - \beta t_I + q_I e^{-\alpha_I x} = \rho C_k \frac{\partial t_I}{\partial \tau}$$

where C_k = heat capacity of charcoal, where cal/gm-°C

C_p = heat capacity of carrier gas at constant pressure, cal/cm^3-°C

k = thermal conductivity of the charcoal, cal/cm-s-°C

K = adsorption coefficient for fission gas, cm^3/gm

q_I = production of decay heat per unit volume of bed from the Ith isotope at the inlet, cal/cm^3-s

t_I = average temperature increase resulting from the decay of the Ith isotope, °C

V_s = superficial carrier gas velocity, cm/s

x = distance from inlet of bed, cm

α_I = linear decay coefficient for the Ith isotope, cm^{-1}

$= \lambda\rho K/V_s$

β = coefficient for radial heat loss, cal/cm^3-s-°C

(For an infinite cylinder, $\beta = 2k/r^2$.

γ = convection coefficient, cal/cm^2-s-°C

$= C_p \cdot V_s$

λ = isotopic decay coefficient, s^{-1}

ρ = bulk density of charcoal, gm/cm^3

τ = time, s.

Assuming that the temperature rise is small, the adsorption coefficient will remain constant across the bed. At steady state, $\frac{\partial t}{\partial \tau}$ I=o, and the above differential equation can be integrated to give

$$t_I = \frac{q_I}{\beta - \alpha_I\gamma - \{\alpha_I\}^2 k}\left\{e^{-\alpha_I x} - e^{-\left(\sqrt{\gamma^2 + 4\beta k} - \gamma\right) x/2k}\right\}$$

The average temperature increase at a point, x, from the inlet is

$$\Delta t_{av} = \sum_N t_I .$$

Furthermore, a particular isotope, t_I produces a maximum temperature at a distance x_{max}, found where

$$\frac{dt_I}{dx} = 0.$$

From the equation for t_I, at steady state

$$x_{max} = \frac{\ln[\alpha_I] - \ln\left\{\left(\sqrt{\gamma^2 + 4\beta k} - \gamma\right)/2k\right\}}{\alpha_I - \left(\sqrt{\gamma^2 + 4\beta k} - \gamma\right)/2k}.$$

A general solution to the problem of decay heat can be obtained by numerical analysis with a digital computer. At present, we have only a one dimension model with a constant adsorption coefficient; i.e., a numerical equivalent of the analytical solution we have just described. These computer calculations replace the differential equation with the following difference equation for $t_I(x)$, the temperature increase resulting from decay of the Ith isotope at a distance, x, from the inlet.

$$k\,\{t_I(x-\Delta x) + t_I^*(x-\Delta x) - 2t_I(x) - 2t_I^*(x) + t_I(x+\Delta x) + t_I^*(x+\Delta x)\}/2\Delta x^2 - \gamma\,\{t_I(x+\Delta x) + t_I^*(x+\Delta x) - t_I(x-\Delta x) - t_I^*(x-\Delta x)\}/4\Delta x - b\,\{t_I(x) + t_I^*(x)\}/2 + q_I e^{-\alpha_I x} = \rho C_k\{t^*(x) - t(x)\}/\Delta\tau$$

where Δx = incremental distance, cm
$\Delta\tau$ = incremental time, sec
$t_I^*(x) = t_I(x)$ at time $\tau + \Delta\tau$

The set of simultaneous equations describing the temperature increase across the bed is then solved by use of the tridiagonal matrix procedure described by Westlake (1968). We assumed, in making these computer calculations, that both the inlet and effluent gas temperatures were controlled by coming into contact with cold walls; in contrast, the analytical model discussed earlier assumed a semi-infinite adsorption bed with only one cold end. Figure 4 shows the heating in an adsorption bed following a steady state input of a fission gas mixture in an argon carrier gas starting at time $\tau = 0$. The numerical values used in this calculation are listed in Table 1. The important observation is that a significant temperature rise can result from a fairly small — but constant — input of fission gas. Table 2 gives a comparison between the steady state numerical and analytical solution. Where the difference in boundary conditions can be ignored, the agreement is quite close.

It would be useful to extend this numerical analysis to a more general analysis which can take into account the difference in the adsorption coefficient brought about by radial and axial heating, and this will be the subject of future work. A particularly interesting result would be to extend this model to the point where it can be used to follow the affect of a sudden release of a large number of curies of fission gas isotopes into an adsorption bed.

EFFECT OF DEPRESSURIZATION OR OF COOLANT LOSS

A theoretical equation for the fission gas release due to a sudden loss of pressure has been compared with experimental measurements of the same phenomenon (Underhill, 1972). The theory predicted that the loss of fission gas would be considerably less than the loss of carrier gas, but the experimental results showed an even smaller release than that predicted theoretically. We attributed this effect to the noticeable cooling of the bed which occurred as a result of the rapid desorption of the carrier gas.

More recently, in work unrelated to FFTF design, we have examined theoretically the loss of fission gas from a bed undergoing an increase in temperature. As the bed warms up, some of the desorbed carrier gas will carry out some of the fission gases. This effect is closely related to the loss of fission gases during the rapid cooling and subsequent warming of a bed, which we found taking place during the loss of pressure accident, and we think that it will not be very difficult to develop equations which will prove to be more accurate than those developed earlier to describe this type of accident. As future work, we plan to test such results experimentally.

ADSORPTION OF CARRIER AND FISSION GASES

In the course of our work, we made a number of measurements of the dynamic adsorption coefficients of krypton and xenon, as well as of the adsorption coefficient of the argon carrier gas. We are presently preparing a report on the results of these measurements. As a summary of what was found, the following two figures are quite useful . The first (Figure 5) is a Polanyi plot of the adsorption of the argon carrier gas. In this plot the y axis gives the volume of liquid argon adsorbed per 100 grams of charcoal, and the x axis is proportional to the free energy required to compress argon to form a unit volume of the liquid phase. This plot represents, nearly as a straight line, results from a wide range of test conditions. The final figure (Figure 6) shows krypton adsorption as influenced by the adsorption of the argon carrier gas. The points which correspond to zero carrier gas adsorption were obtained using helium as the carrier gas. This figure shows clearly the strong effect of the carrier gas in reducing the adsorption of the fission gas; and, indeed, it was the accurate measurement of this effect that was one of the main goals of this research.

REFERENCES

Barilli, L., L. Bruzzi, and J. C. Shorrock (1969), *Fission Product Removal from a Vented Fuel FBR,* Report RT/ING (70)7 of Conf 691104-5, Paper presented at the International Congress on the Diffusion of Fission Products, Saclay, France, November 1969.

Collins, D. A., R. Taylor and L. R. Taylor (1967), *The Adsorption of Krypton and Xenon from Argon by Activated Charcoal,* TRG Report 1578 (W) Draft, September 1967.

First, M. W., *et al.*, (1970), *Semiannual Progress Report of the Harvard Air Cleaning Laboratory,* NYO-841-22, April 1970.

Forster, K. (1971), *Delaying Radioactive Fission Product Inert Gases in Cover Gas and Off-Gas Streams of Reactors by Means of Activated Charcoal Delay Lines,* Kerntechnik, 13, 214-19.

Glueckauf, E. (1959), *The Movement of Highly Radioactive Gases in Adsorber Tubes,* Annals New York Academy of Sciences, 72, 562.

Kabele, T. J., J. L. McElroy, E. O. Badgett and A. P. Bohringer (1973), *FFTF Fission Gas Delay Beds: Engineering Scale Test Report,* HEDL-TME-73-26, May 1973.

Madey, R., R. A. Fiore, E. Pflumm, and T. E. Stephenson (1962), *Transmission of a Pulse of Gas Through an Adsorber Bed,* Trans. Am. Nuc. Soc., 5, 465-66.

Trofimov, A. M. and A. M. Pankov (1968), *Influence of the Gas Macrocomponent of the Distribution of ^{85}Kr and ^{133}Xe Between the Gas Phase and the Solid Carbon Sorbent,* Soviet Radiochemistry, 7, 293-98.

Underhill, D. W. (1970a), *An Experimental Analysis of Fission Gas Holdup Beds,* Nuclear Applications and Technology, 8, 255-60.

Underhill, D. W. (1970b), *Commentary on the Theoretical Chamber Model for Fission Gas Holdup Beds,* Nuclear Safety, 11, 321-22.

Underhill, D. W. (1972), *Effect of Rupture in a Pressurized Noble Gas Adsorption Bed,* Nuclear Safety, 13, 478-81.

Westlake, J. R. (1968), *A Handbook of Numerical Matrix Inversion and Solution of Linear Equations,* J. Wiley and Sons.

Young, J. F. (1958), *A Derivation of the Equation for Elution Chromatography Assuming Linear Rate Constants,* in Gas Chromatography, Coates, V. J., Ed., pp. 15-23, Academic Press.

Table 1. Values Used to Calculate Temperature Increase in a Fission Gas Adsorption Bed.

Bed Length = 310 cm

Bed Diameter = 90 cm

Thermal conductivity of Argon + Charcoal = 0.00021 cal/cm-s-°C

Heat Capacity (per unit volume)

of Charcoal 0.085 cal/cm^3-°C
of Argon 0.000194 cal/cm^3-°C

Adsorption Coefficient (volume/volume)

for Krypton 14 ml/ml
for Xenon 250 ml/ml

Flow of Argon 1,610 ml/s

Fission Gas Data:

Isotope	Curies Released per day	Initial Volume production of decay heat, q_I cal/ml-s x 10^{-8}	Linear decay constant α_I cm^{-1} x 10^{-4}
^{131m}Xe	1.392	0.055	66.8
^{133m}Xe	.03369	1.9	34.8
^{133}Xe	676.50	29	15.1
^{135}Xe	3,420.	481	20.90
^{83m}Kr	235.86	0.27	118
^{85m}Kr	391.50	5.2	50
^{85}Kr	.026	0.000183	0.0023
^{87}Kr	679.20	46	160
^{88}Kr	824.40	53	78.5

Incremental distance = 1 cm

Incremental time = 15,000 s

Table 2. Comparison of Numeric and Analytic Solutions for the Average Increase Resulting from Decay Heat.

Note: For numeric analysis $\Delta x = 1$ cm and $\Delta\tau = 15{,}000$ s (See text for boundary conditions.)

Distance from Inlet, cm	Calculated Temperature Increase °C	
	Numeric	Analytic
0	0.0	0.0
1	11.52	11.52
2	22.78	22.79
10	104.79	104.80
100	462.22	462.39
200	453.67	458.39
300	353.74	389.93
309	81.16	383.34
310	0.0	382.61

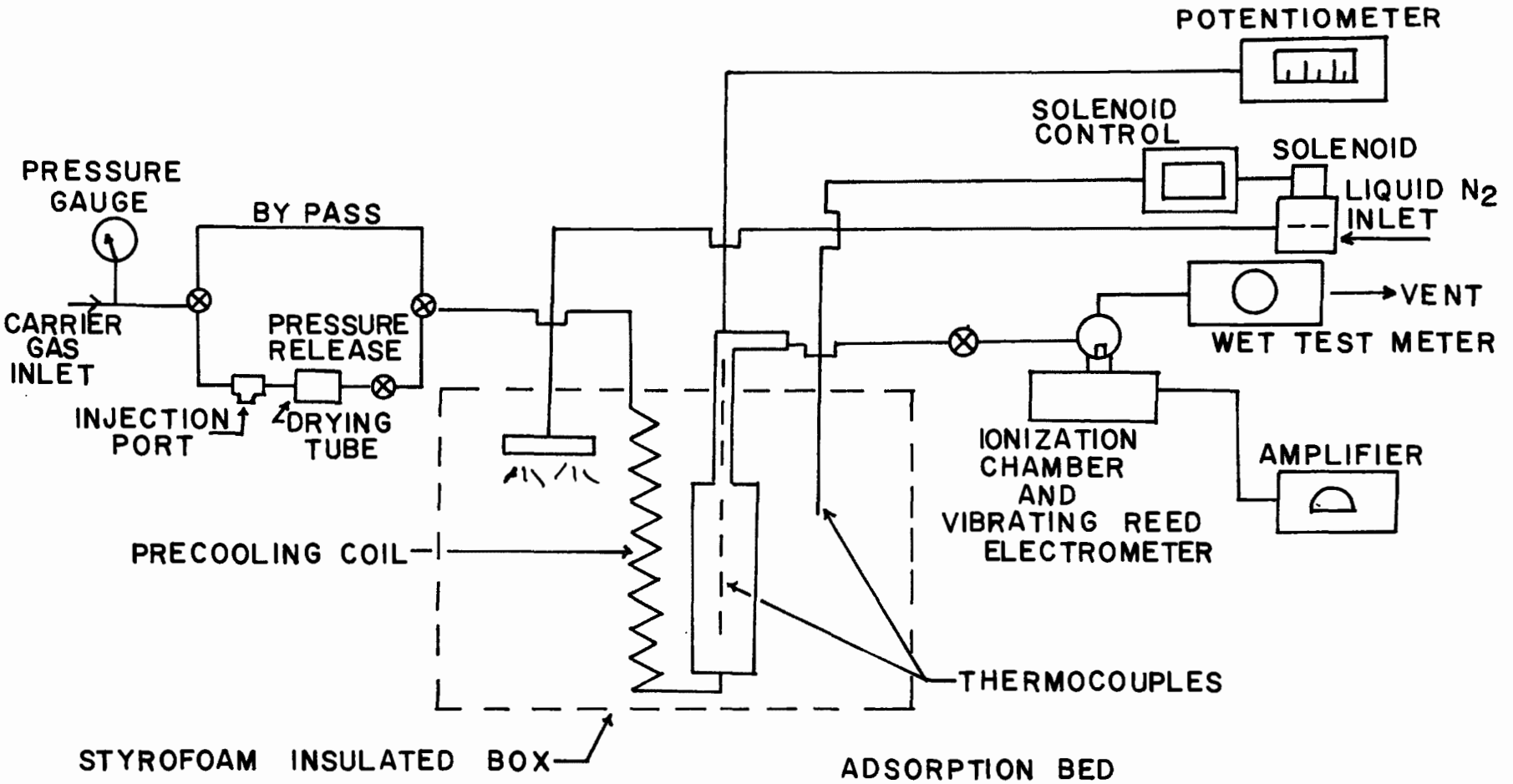

Figure 1. Diagram of test apparatus.

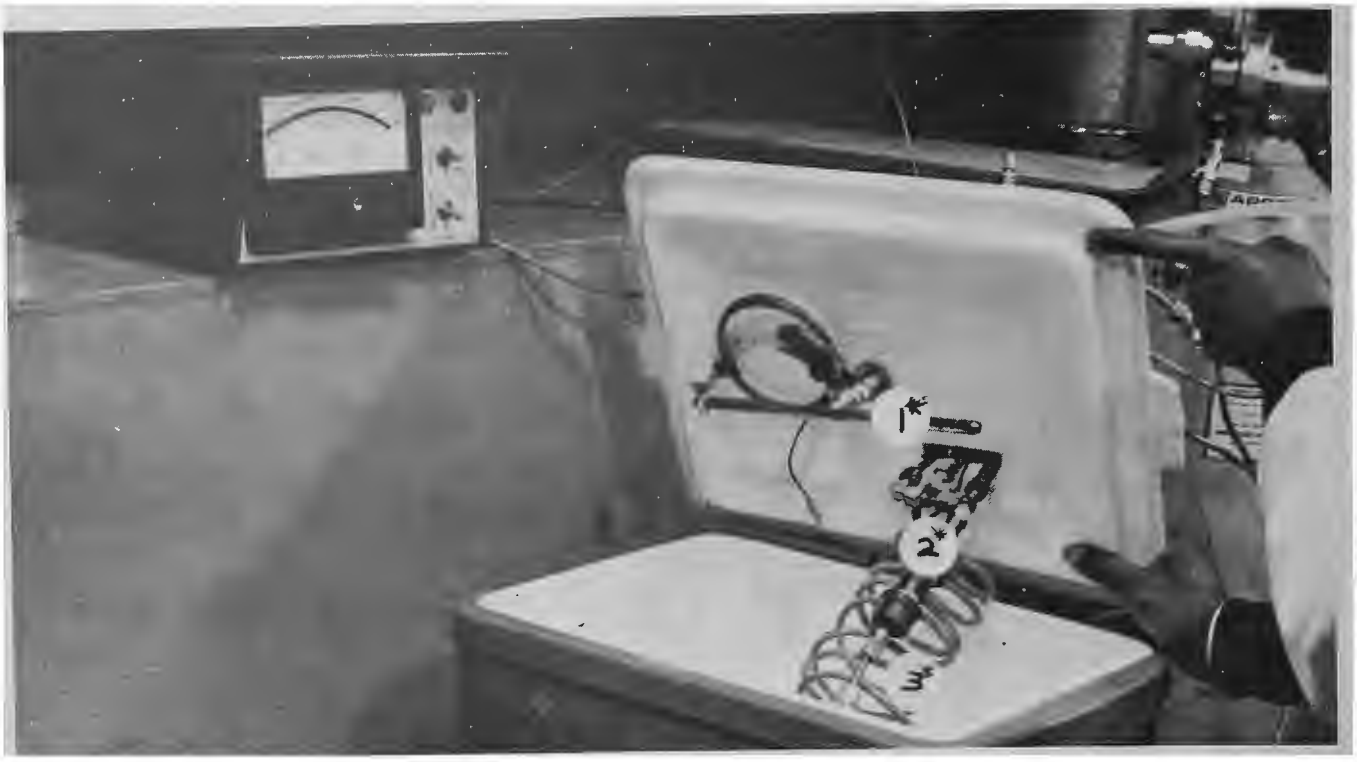

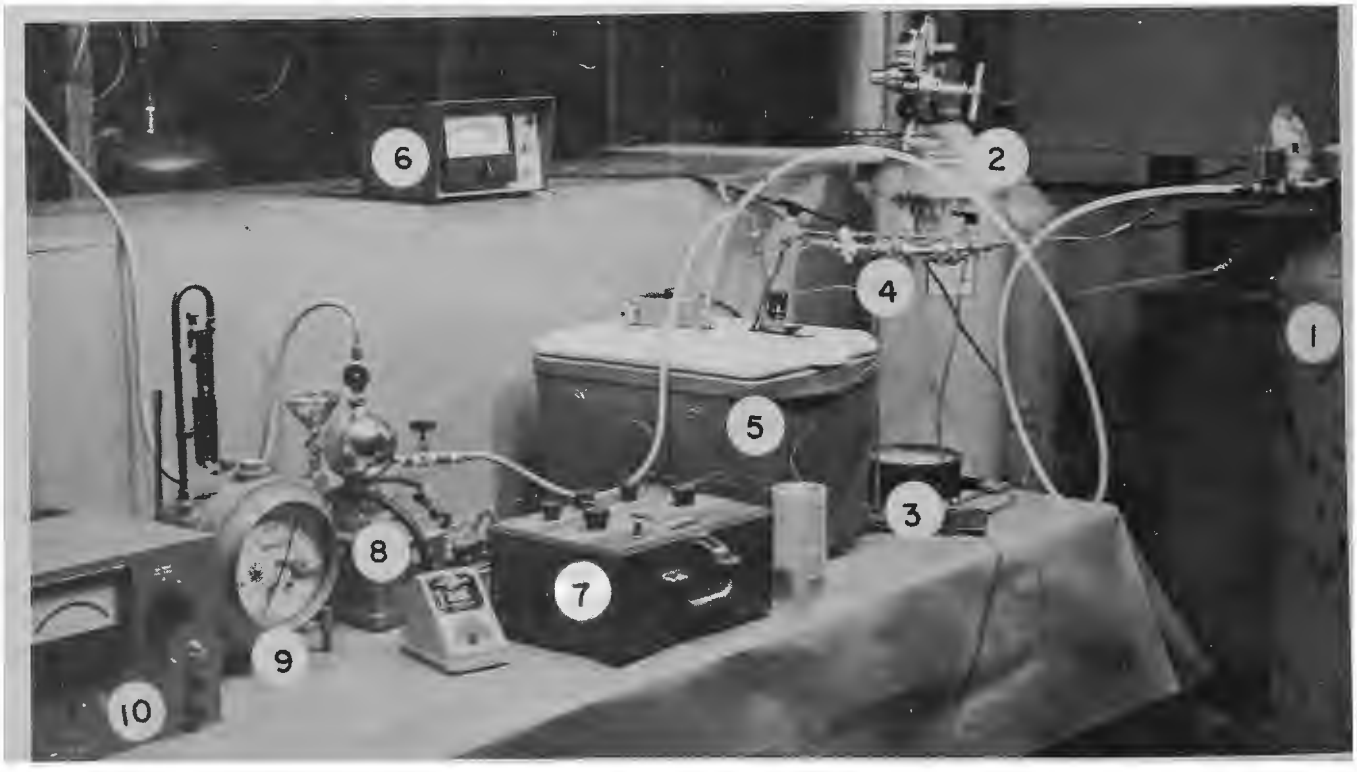

Figure 2. Apparatus for determining adsorption coefficients at elevated pressures and reduced temperatures. *1-nitrogen spray head; *2-adsorption column; *3-carrier gas precooling coil; — 1-liquid nitrogen source; 2- carrier gas source; 3-pressure gauge; 4-injection system; 5-low temperature chamber; 6-low temperature controller; 7-potentiometer for column thermocouple; 8-ionization chamber; 9-west test gas meter; 10-electrometer for ionization chamber.

*Close up view.

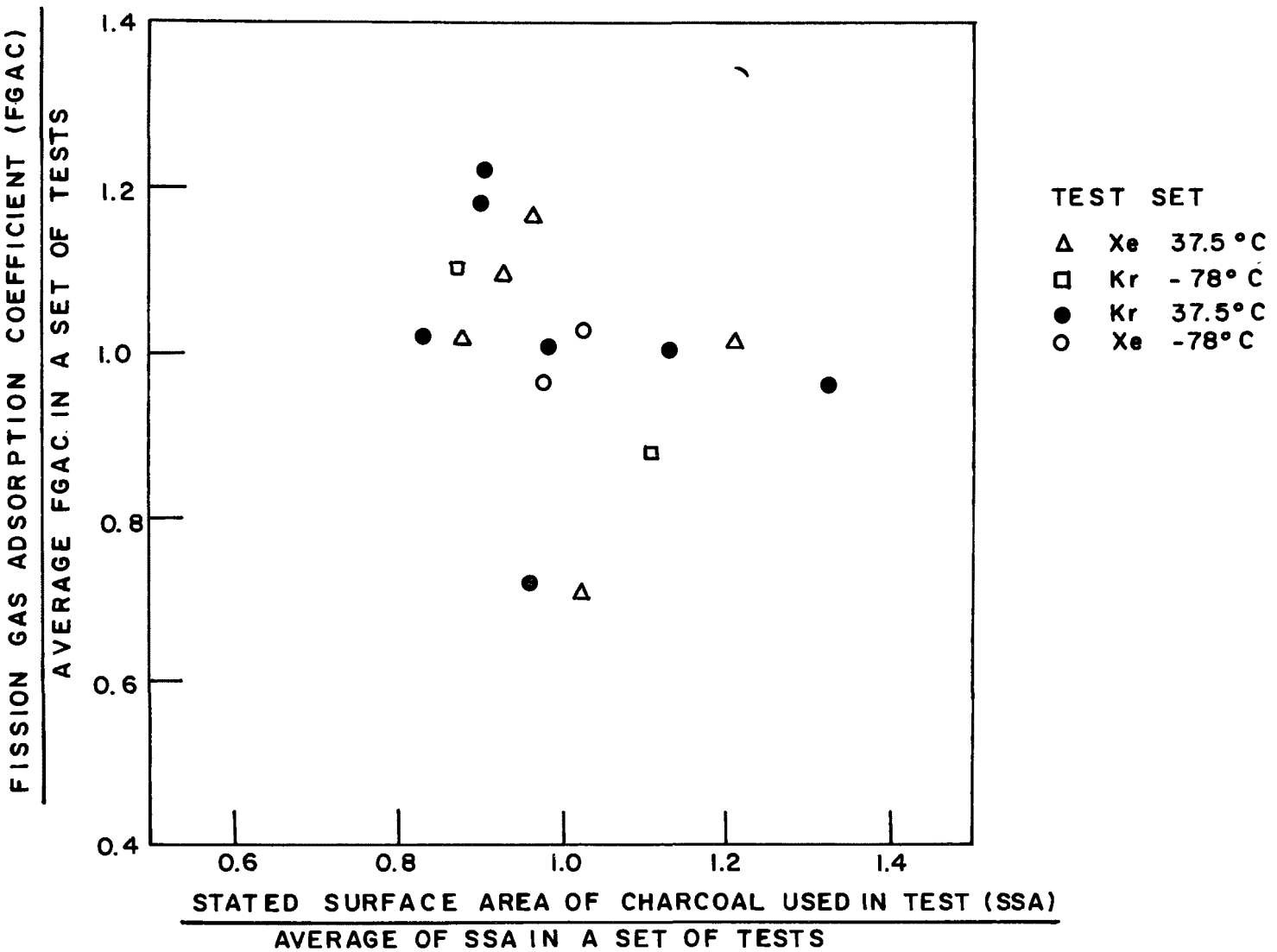

Figure 3. Correlation of fission gas adsorption coefficient with stated surface area of charcoal.

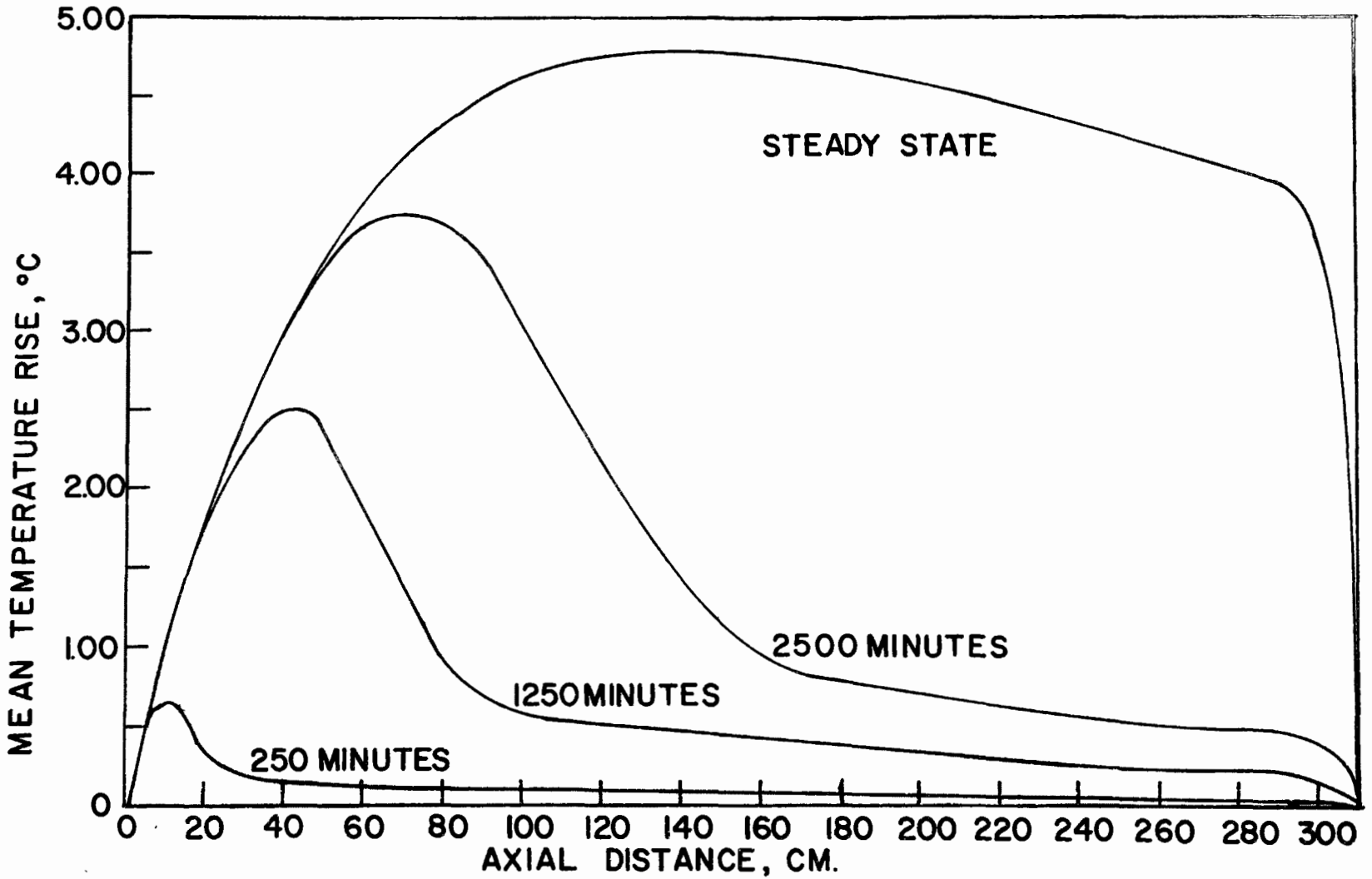

Figure 4. Calculated temperature increase from fission gas input as a function of time and axial distance.

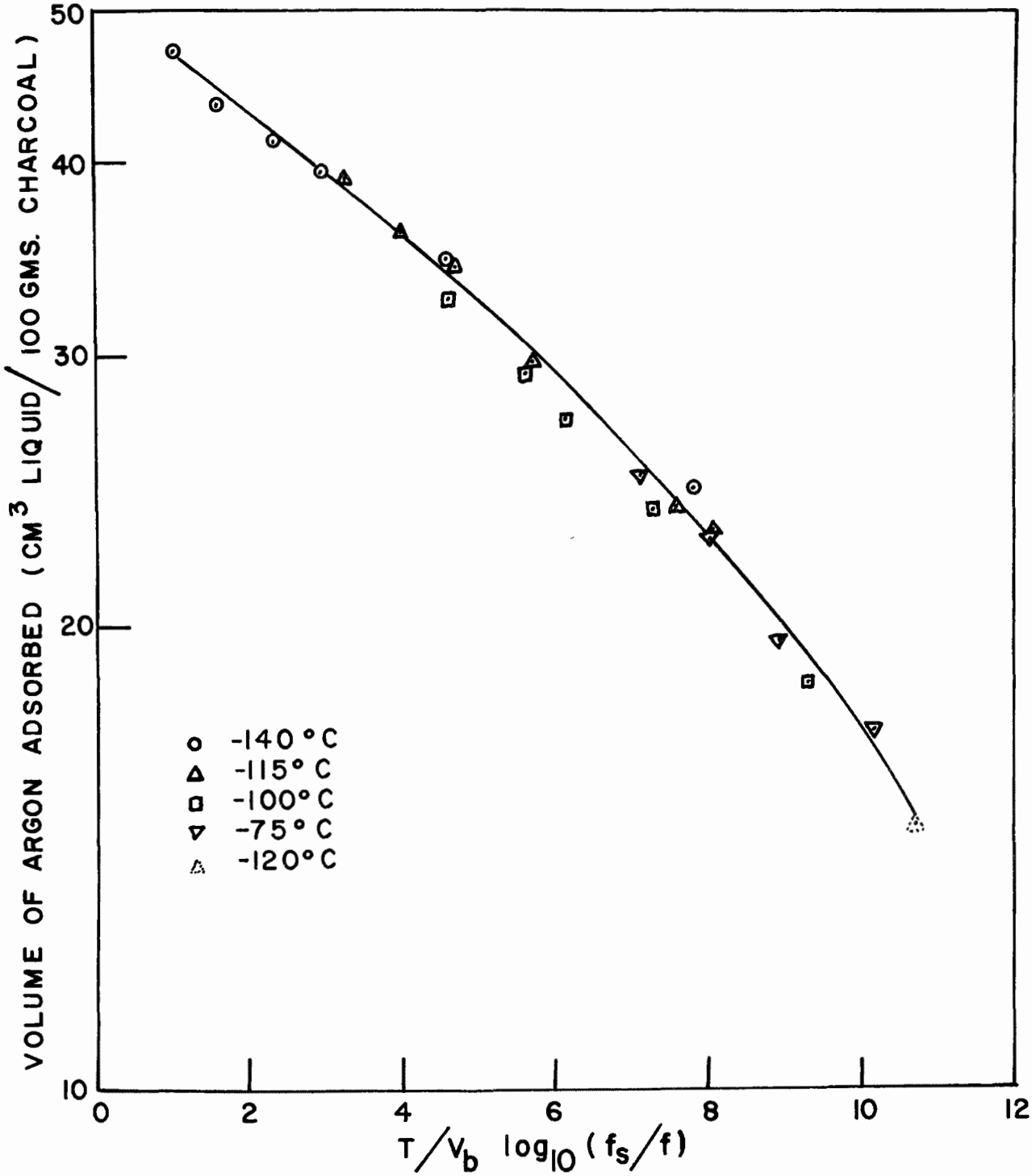

Figure 5. Polanyi plot of argon adsorption on Pittsburgh PCB charcoal.

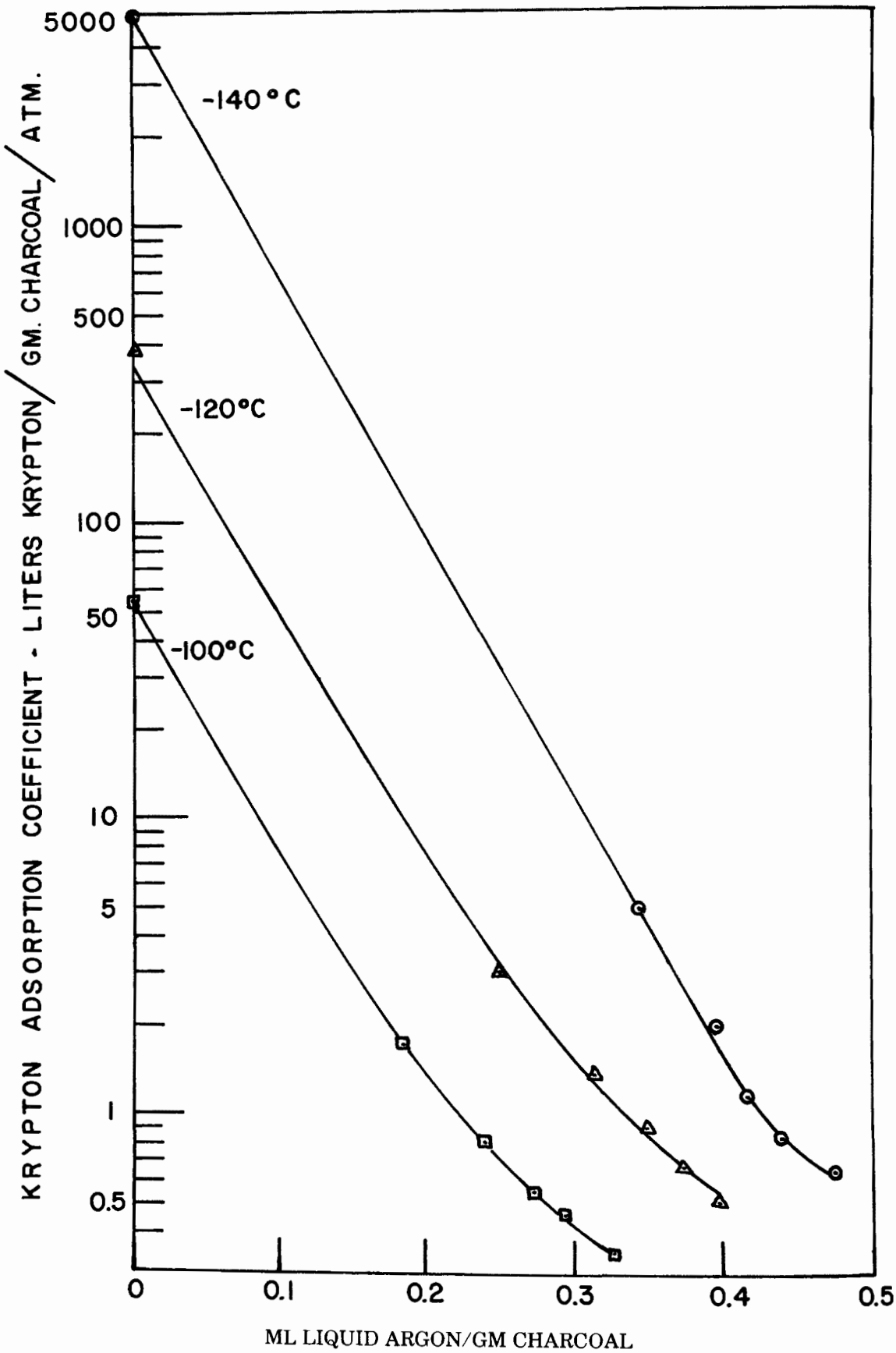

Figure 6. Effect of adsorbed argon on the krypton adsorption coefficient.

ADSORPTION OF RADIOKRYPTON ON ACTIVATED CHARCOAL IN THE PRESENCE OF HYDROGEN*

B. B. Fisher, A. E. Norris, and D. G. Rose
Los Alamos Scientific Laboratory
University of California
Los Alamos, New Mexico

Abstract

Tests in 1972 of the Nuclear Furnace-1 reactor at the Nuclear Rocket Development Station in Nevada marked the first time that fission product radioactivity in the effluent from a nuclear rocket engine development experiment was removed before the effluent was exhausted to the atmosphere. The final component in the effluent clean-up system was a stationary bed containing 1,565 kg of activated charcoal to remove radiokrypton and radioxenon from the effluent stream.

Experiments with the charcoal trap operating at a different temperature during each of three reactor tests were conducted to measure the velocities of the krypton adsorption front, moving through the charcoal under operating conditions. Results from measurements of radioactivity associated with krypton-85m, krypton-88, and krypton-89 are presented. At a charcoal temperature of 186°K, the measured adsorption coefficient agrees with that reported in the literature, but at 161°K and 172°K the coefficients are significantly lower than the literature values. Most likely the differences arise from interference by the major component of the effluent, hydrogen, with the adsorption of radiokrypton on the activated charcoal.

INTRODUCTION

The Nuclear Furnace-1 (NF-1) was a small test reactor which was devised to provide an inexpensive means of testing nuclear rocket fuel elements and other core components. The various runs, called Experimental Plans, which took place in the period between May 24 and July 27, 1973 were the first occasions in which the hydrogen propellant flow from a reactor rocket engine was scrubbed clean of all radioactivity before being liberated to the atmosphere by burning it in a flare stack. The last component of the NF-1 Effluent Cleanup System (ECS) was a fixed-bed activated charcoal trap operated at low temperatures to remove radiokrypton and radioxenon from the effluent gases. Experiments were performed to measure the velocity of the krypton adsorption-front through the charcoal trap by measuring the amounts of radiokrypton upstream, downstream, and in two locations within the charcoal trap.

The following results were obtained:

(1) When operated at the proper temperature, the NF-1 charcoal trap removed the radiokrypton and radioxenon from the effluent stream.

(2) The dynamic adsorption coefficients of krypton upon activated charcoal derived from these experiments are less than those in the literature for krypton adsorbed from helium. This effect can probably be ascribed to the fact that the hydrogen in the effluent is interfering with krypton adsorption.

(3) The number of ^{89}Kr atoms entering the charcoal trap as measured by these experiments is in fair agreement with the measurements made by Nuclear Rocket Test Operations, and both agree with the computations of the amount of ^{89}Kr released by the elements.

THEORY

Hydrogen effluent exiting the reactor at ≅ 2440°K was cooled by the injection of water into the effluent stream. Passing through a series of heat exchangers and water separators, the effluent was then cooled further and condensed; the added water was removed with a large fraction of nuclides that were in particulate form or were solubile in water. After this, the effluent passed through a fixed-bed silica gel drier, and a cryogenically cooled fixed-bed activated charcoal trap to remove the noble gas fission products, krypton and xenon.

Xenon is adsorbed much more strongly upon activated charcoal than is krypton. Therefore, any trap designed to remove krypton from a gas stream is more effective for xenon. This discussion is limited to the case of the adsorption of krypton on activated charcoal, particularly North American G-212, 8 x 16 mesh — the type used in the charcoal trap.

When the effluent stream from the reactor reaches the inlet to the charcoal trap, the effluent consists primarily of hydrogen gas, but contains gaseous impurities that result from fuel-element corrosion, and from the reaction of those corrosion products with the water added to cook the reactor effluent. It may also contain some particulate matter, which need not be considered here. Table 1 lists a predicted composition of the effluent stream from NF-1 at the inlet to the charcoal trap.

Although such impurities as CH_4 and carbon monoxide can reduce the amount of krypton adsorbed upon charcoal, an examination of the literature (Burnette and Lofing, 1967) indicated that, in the concentrations found in the NF-1 effluent stream, they do not affect krypton adsorption. Water vapor is so strongly adsorbed

**Work performed under the auspices of the U.S. Atomic Energy Commission.*

upon charcoal as to completely prevent the adsorption of krypton or xenon, but the amount of water carried to the trap by the effluent is so low that it poisons only the first few millimeters of charcoal, and effectively shortens the trap by that short length. Hydrogen is adsorbed upon activated charcoal less strongly than either krypton or xenon. However, the amount of gas adsorbed on charcoal at any temperature will increase as the pressure of that gas is increased. What effect the hydrogen in the effluent, which is at $\cong 4 \times 10^5$ Pa, would have upon the adsorption of krypton, which is at a partial pressure of only 5.45×10^{-7} Pa, was unknown before the NF-1 tests, and this was one of the facts to be determined by the experiments.

Table 2 and Figure 1 present the dynamic adsorption coefficient of krypton upon activated charcoal versus the temperature for low concentrations of krypton in helium (Burnette, *et al.*, 1961; Burnette and Lofing, 1967; and Kovatch, 1970). These values were measured in the absence of gases that would interfere with the adsorption of the krypton.

When krypton is added at some definite time to a hydrogen stream flowing through a fixed charcoal bed, the krypton travels through the bed as a concentration-front which moves from the inlet to the outlet of the trap. Because the escape of fission products from the fuel elements is a very steep function of temperature, the krypton does appear in the effluent stream suddenly as the fuel elements reach their operating temperature. This front moves through the bed at a velocity that is a fraction of the velocity of the carrier hydrogen, depending upon the value of the dynamic adsorption coefficient. As the krypton concentration-front moves through the charcoal bed, the krypton becomes diffuse because of mass-transfer effects and diffusion. Burnette, *et al.*, (1961) presents an expression that allows the concentration of the krypton in a hydrogen stream flowing through an activated charcoal bed to be calculated as a function of bed conditions, time of flow, and distance through the charcoal bed (this expression includes the effect of decay if the krypton is radioactive):

$$\frac{c}{c_o} = e^{-\alpha x r/(1+r)} \left[1 - \left(\frac{1}{1+r}\right) e^{-\beta\tau(1+r)} \int_0^{\alpha x} e^{-t/(1+r)} \, I_o \left(2\sqrt{\beta\tau t}\right) dt \right],$$

$$\alpha = \frac{1}{H}, \quad \beta = \frac{LV}{kHM},$$

where

c_o = concentration in gas stream entering bed, moles/m^3

V = volume flow rate of gas, m^3/s

H = height of mass-transfer unit, m

H can be estimated from the following expression:

$$H = \frac{0.168}{a} \left[\frac{D_p G}{\mu}\right]^{0.51} \left[\frac{\mu}{\rho D_v}\right]^{2/3}$$

where

a = superficial area of bed particles per unit volume, m^2/m^3

D_p = average particle diameter, m

G = flow rate per unit area, kg/m^{2}s

μ = viscosity, kg/ms

ρ = carrier gas density, kg/m^3

D_v = diffusivity of adsorbate in carrier gas, m^2/s

c = concentration of adsorbate in gas stream, mole/m^3

t = time, s

x = distance along adsorber bed, m

M = total mass of adsorbent in bed, kg

F = void fraction in adsorber bed

L = total length of bed, m

λ = radioactive decay constant, s^{-1}

r = λ/β

I_0 = modified Bessel function of the first kind and zero order.

They found good agreement with this expression in experiments investigating the adsorption of krypton on activated charcoal from a helium stream.

The experiments carried out on the NF-1 effluent cleanup system charcoal trap involved the use of activated charcoal sampling traps, cooled to liquid-nitrogen temperatures, which sampled the effluent upstream, downstream, and at two positions within the large charcoal trap. The sampling traps, operating at much lower temperatures than the large trap, are much more efficient and are able to remove all the krypton and xenon from the effluent. These traps integrate the concentration of ^{89}Sr, ^{88}Kr, and ^{85m}Kr in the effluent over the time of the reactor run. For comparison with the experimental results the integral of c/c_0 was computed for each sampling trap in each experimental plan. The computations were done by using the proper operating temperature for the large charcoal trap and length of run for each experimental plan. In addition, because the effect of hydrogen upon the adsorption of krypton is uncertain, the computation was performed by using a dynamic adsorption coefficient equal to 1, 1/2, 1/3, 1/5, 1/7, and 1/10 the literature value for krypton adsorption upon charcoal. The results of these computations as well as the experimental results are discussed in the following section.

EXPERIMENTAL

The charcoal trap of the NF-1 Effluent Cleanup System has a diameter of 1.52 m, and is filled to a depth of 1.8 m with 1565 kg of North American Type G-212 activated charcoal of 2 x 16 mesh particle size.

The experiments were planned to measure the velocity of the krypton concentration-front through the fixed charcoal trap by sampling the effluent in the charcoal trap at four locations. To do this, four bypass lines were installed in and around the large charcoal trap to lead small fractions of the effluent flow to the sampling traps. Figure 2 presents a schematic of the sampling system. The identifications and locations of the sampling positions are given below:

(1) TRAP 20 — immediately upstream from the large trap.
(2) TRAP 30 — 0.152 m below the charcoal inlet surface.
(3) TRAP 40 — 0.762 m below the charcoal inlet surface.
(4) TRAP 50 — at outlet from charcoal trap; this is equivalent to 1.8 m below the charcoal inlet surface.

The effluent sampling head placed in the charcoal trap itself consisted of 0.5-inch stainless-steel tubing, which was capped at the end and had holes of ≅ 9.5 mm diameter drilled into the sides of the tube at such positions that gas flow was taken from 0.152, 0.244 and 0.337 m from the centerline of the charcoal trap. The holes were covered with 20-mesh wire screen to exclude charcoal from the bypass lines. The samples upstream and downstream of the charcoal trap were taken through 1.0-inch pipes which led from the main effluent piping. The effluent flow through each of the sampling traps, amounting to 6.3×10^{-4} m^3/s, was led directly to the flare-stack header. The effluent flow to be analyzed was taken from the bypass and put through the sampling traps which collected the radiokrypton. The flow in the bypass line and in the lines leading to the sampling traps were adjusted so that the time of flow from the large charcoal trap to the small sampling traps would all be equal and less than 30 s.

Each sampling line was associated with the following hardware:
(1) a solenoid valve to allow the sampling flow to be saturated and stopped at a definite time;
(2) a heater to warm the cold effluent;
(3) a manual valve for flow control;
(4) a floating ball-type flow meter;
(5) a cooling coil to cool the effluent before it entered the sampling traps;
(6) the sampling traps;
(7) a heater to warm the cold effluent; and
(8) a check valve to prevent accidental backflow through the sampling traps.

Each sampling trap consisted of two sections in a series. The upstream section (called FRONT) and the downstream section (called REAR) were of the same shape and size, a right circular cylinder 0.203 m in diameter by 0.146 m deep. They each contained 2.132 kg charcoal.

The bypass and sampling system without the flow meters was first operated during EP-II, but so little radioactivity was found in the sampling traps that there was doubt that any flow had taken place through the sampling system. To ensure bypass flow through the sampling traps for EP-III and succeeding runs, the following changes were made:

(1) the 0.250-inch tubing in the liquid-nitrogen bath, immediately ahead of each sampling trap, was changed to 0.5 inch tubing to help prevent formation of ice blockage should any water enter the system;

(2) the flow meters shown in Figure 2 were installed in the outlet line from each trap, just upstream from the check valve; a television camera was used to view the flow meters during the reactor runs;

(3) a wet test meter was used to calibrate the flow meter before EP-III and EP-V, but not before EP-IV. Helium had to be used for the calibrations, the response of the flow meters to hydrogen flow had to be calculated. This computation was performed by NRTO. The calibration data were combined with the flow meter readings observed during each reactor run to obtain the rates of flow for each sampling trap during each experimental plan. The results are shown in Table 3.

Of necessity, the flow calibrations were carried out rather crudely in the field, which leads one to expect that the largest source of error in the results of the measurements arises from uncertainties in the flow measurements. Before each reactor run, the small traps were filled with North American Carbon Type G-212 activated charcoal 8 x 16-mesh, sealed, pressure-tested, and the charcoal was regenerated by a flow of hot N2 for 86.4 ks. During installation of the traps, care was taken to minimize the atmospheric water that could enter the piping.

On the day following each reactor run, the sampling traps were removed from Test Cell C to the core sample building at the Nevada Test Site, where the charcoal in each trap was thoroughly mixed and aliquots taken. One aliquot was used for γ-ray spectrometric measurements, and the other was sent to LASL for radiochemical analysis of ^{89}Sr. The γ-ray spectroscopy measurements were made with a 16 x 10^3 mm^3 Ge(Li) detector at NRDS.

RESULTS AND CONCLUSIONS

Only the final ratios of activities in the various traps are presented below.

1. Gamma Ray Spectroscopy.

Table 4 gives the ratios of the activities of ^{85m}Kr and ^{88}Kr in Traps 30, 40, and 50 to that found in Trap 20, as measured by γ-spectroscopy. The specific γ-ray peaks that were integrated for these results are the 151.1-keV peak for ^{85m}Kr, and the 196.1-keV peak for ^{88}Kr. The data have been corrected for radioactive decay, for branching ratios, for sample mass, and for detector efficiency. The detector efficiency was measured with an I.A.E.A. calibrated ^{22}Na source imbedded in an appropriate mass of inactive charcoal. Inaccuracies in the absolute measurement of the detector efficiency cancel in the ratios.

A potentially important source of error in these γ-ray measurements results from the gradual desorption of krypton from charcoal at room temperature while the samples are being counted. One indication that krypton was being lost from the samples during the process of γ-ray counting comes from measurements taken on Trap 30 from EP-IV. Triplicate aliquots of charcoal from the front cannister of Trap 30 were taken to measure the uniformity of sampling. The activity of each sample, corrected for mass and radioactive decay, monotonically decreased with the order in which the samples were counted. The same three aliquots were analyzed for ^{89}Sr, and no such monotonic decrease in activity was observed. The plastic bottles that served as containers for the charcoal during γ-ray counting were not gas-tight. In Table 4 only the data from the qliquot that was counted first are shown.

In all cases except for EP-V, the quantities of ^{135}Xe, which was measured in the small traps, was higher in the downstream portion of the traps than in the upstream portion. In addition, the complete absence of ^{135}Xe in EP-III Trap 30, and its presence in Traps 20, 40, and 50 indicated that the ^{135}Xe might be entering the traps other than in the normal way. Also, in EP-III the Trap-40 and Trap-50 data indicated significant quantities of ^{85m}Kr and ^{88}Kr in the downstream portions of these traps. The probability that the data from Trap 40 and Trap 50 were compromised by extraneous effects is sufficiently high that no further use are made of these data. The check valve in each bypass line was replaced before EP-IV, and the situation seemed to improve. The check valves were replaced again before EP-V, and further improvement was noticed — although the ^{135}Xe detected in EP-V Trap 50 indicated that some small problem remained.

2. ^{89}Sr Analysis.

The results of the ^{89}Sr measurements are shown in Table 5. The principal source of error is likely to be uncertainties in the actual flow of H2 through each of the sampling traps, and the problem of back-flow in the traps. The ratios shown in parentheses for EP-III were derived by considering only the activities in the upstream portion of the sampling trap; all other ratios are formed by summing the activities in the upstream and downstream portion of each sampling trap.

Sampling trap activities as calculated and as measured are compared in Tables 6 through 12. From such a comparison an estimate of the effective velocity of travel of the concentration-front or, alternatively, the effective dynamic adsorption coefficient can be obtained. Table 13 gives the estimates of the velocity factors thus obtained. Note that the ^{88}Kr and ^{85m}Kr results, although suspect, do not disagree seriously with the ^{89}Sr data.

The dynamic adsorption coefficients obtained from these ratios are plotted in Figure 1. They fell below the measured line for the adsorption of krypton from helium onto activated charcoal. This decreased dynamic adsorption coefficient may be caused by the hydrogen in the effluent, decreasing the amount of krypton adsorbed.

Independent measurements of the amount of ^{89}Kr entering and leaving the large charcoal trap were made during EP-IV and EP-V by NRTO under the technical direction of SNSO-N. In Table 14, the values labelled NRTO were obtained by the analysis of gas samples taken upstream and downstream of the charcoal trap during EP-IV and EP-V. The values labelled LASL were measured by adsorption of the ^{89}Kr in cooled charcoal traps as described above. All values were corrected for aliquots taken, counter efficiencies, flow inequalities, and decay from the time of shutdown of each EP.

Although the number of ^{89}Kr atoms in and out of the trap in EPs-IV and -V, as measured by the two methods, are in fair agreement, differing only by at most a factor of 4; there is an anomaly in the NRTO data. Their measurements show the same amount of ^{89}Kr release by the trap in both experimental plans, and this makes the calculated throughput less for EP-V than for EP-IV. Because the charcoal trap was operated during EP-V at a higher temperature and for a longer time, this result is most probable. Perhaps the NRTO data were compromised by a sneak source of activity as some of the LASL data were.

REFERENCES

Burnette, R. D., W. W. Graham III, and D. G. Morse, (1961), *The Removal of Radioactive Krypton and Xenon from a Flowing Helium Stream by Fixed-Bed Adsorption*, Report Ga-2395.

Burnette, R. D. and D. R. Lofing, (1967), *Low-Temperature Adsorption Studies for the PSC Reactor*, Report GA-7932.

Kovatch, J. L., (1970), *Krypton-Xenon Adsorption Studies on Nacar Carbons*, Report NACAR-10004.

TABLE 1. Estimated NF-1 Effluent Composition.

Constituent	Mole Fraction	Partial Pressure, Pa
H_2	1.0	4.14×10^{5}
H_2O	7.09×10^{-7}	4.89×10^{-3}
CH_4	2.78×10^{-6}	1.92×10^{-2}
CO	8.44×10^{-7}	5.82×10^{-3}
Xe	1.54×10^{-7}	1.06×10^{-6}
Kr	7.91×10^{-11}	5.45×10^{-7}

TABLE 2. Dynamic Adsorption Coefficients, K_D, For Krypton on Charcoal.

$1000/T\ (K^{-1})$	$K_D\ (m^3/kg)$	Reference
3.55	0.103	(a)
3.62	0.127	(c)
3.62	0.152	(c)
4.0	0.229	(a)
4.0	0.275	(b)
4.35	0.488	(b)
4.45	0.700	(a)
4.60	1.195	(b)
5.25	5.230	(b)
5.65	18.150	(b)
5.95	135.	(b)
6.60	305.	(b)
7.00	940.	(b)
7.50	1953.	(b)

(a) Kovatch (1970).
(b) Burnette, *et al.*, (1961).
(c) Burnette and Lofing (1967).

TABLE 3. Hydrogen Flow Data.

	TRAP 20	TRAP 30	TRAP 40	TRAP 50
Hydrogen flow rate computed, from wet test meter results before EP-III	4.18×10^{-4} m³/s	4.2×10^{-4} m³/s	4.18×10^{-4} m³/s	3.85×10^{-4} m³/s
Flow gage level computed for H_2(a)	0.35	0.305	15.6	0.24
EP-III observed flow gage level(a)	0.30	0.30	25.0	0.2
Computed H_2 flow rate	3.58×10^{-4} m³/s	4.13×10^{-4} m³/s	6.69×10^{-4} m³/s	3.21×10^{-4} m³/s
Normalization factor	1.000	0.866	0.535	1.115
EP-IV observed flow gage level(a)	0.3	0.2	10.0	0.10
Computed H_2 flow rate	3.58×10^{-4} m³/s	2.75×10^{-4} m³/s	2.68×10^{-4} m³/s	1.60×10^{-4} m³/s
Normalization factor	1.000	1.300	1.337	2.232
Hydrogen flow rate computed from wet test meter results before EP-V	4.18×10^{-4} m³/s	4.1×10^{-4} m³/s	3.88×10^{-4} m³/s	2.28×10^{-4} m³/s
Flow gage level computed for H_2(a)	0.38	0.32	16.0	0.25
EP-V observed flow gage level(a)	0.47	0.33	15.0	0.19
Computed H_2 flow rate	5.17×10^{-4} m³/s	4.23×10^{-4} m³/s	3.64×10^{-4} m³/s	1.73×10^{-4} m³/s
Normalization factor	1.000	1.224	1.421	2.990

(a) Arbitrary scale.

TABLE 4. Gamma-Ray Spectroscopy Results.

	EP-III		EP-IV		EP-V	
	^{85m}Kr	^{88}Kr	^{85m}Kr	^{88}Kr	^{85m}Kr	^{88}Kr
TRAP 30/TRAP 20	4.1×10^{-2}	6.27×10^{-2}	6.5×10^{-1}	7.57×10^{-1}	8.34×10^{-1}	8.37×10^{-1}
TRAP 40/TRAP 20	--	--	9.86×10^{-6}	--	5.96×10^{-1}	5.57×10^{-1}
TRAP 50/TRAP 20	--	--	--	--	4.24×10^{-1}	4.27×10^{-1}

TABLE 5. ^{89}Sr Analysis Results.

	EP-III	EP-IV	EP-V
TRAP 30/TRAP 20	5.27×10^{-2}	3.26×10^{-1}	3.18×10^{-1}
TRAP 40/TRAP 20	1.06×10^{-3}(1.1×10^{-4})	4.42×10^{-5}	4.82×10^{-2}
TRAP 50/TRAP 20	2.7×10^{-3}(6.5×10^{-4})	7.73×10^{-5}	1.31×10^{-3}

TABLE 6. Comparison of Computed and Measured Sampling Trap Activity Ratios of ^{89}Sr for EP-III.

Trap Pair	Velocity Factor 1	2	3	5	7	10	Measured Ratio
730/720	10^{-5}	0.001	0.006	0.053	0.146	0.296	0.053
740/720	10^{-3}	10^{-25}	10^{-22}	10^{-18}	10^{-13}	10^{-9}	---
750/720	10^{-76}	10^{-68}	10^{-63}	10^{-54}	10^{-47}	10^{-40}	---

TABLE 7. Comparison of Computed and Measured Sampling Trap Activity Ratios of ^{89}Sr for EP-IV.

Trap Pair	Velocity Factor 1	2	3	5	7	10	Measured Ratio
730/720	10^{-4}	0.004	0.016	0.133	0.233	0.326	
740/720	10^{-22}	10^{-16}	10^{-12}	10^{-7}	10^{-9}	10^{-4}	10^{-5}
750/720	10^{-58}	10^{-50}	10^{-42}	10^{-30}	10^{-40}	10^{-14}	10^{-4}

TABLE 8. Comparison of Computed and Measured Sampling Trap Activity Ratios of ^{89}Sr for EP-V.

Trap Pair	Velocity Factor 1	2	3	5	7	10	Measured Ratio
730/720	0.208	0.450	0.580	0.709	0.773	0.826	0.318
740/720	10^{-4}	0.016	0.061	0.182	0.302	0.443	0.048
750/720	10^{-13}	10^{-5}	0.001	0.016	0.053	0.131	0.001

TABLE 9. Comparison of Computed and Measured Sampling Trap Activity Ratios of ^{88}Kr for EP-III.

Trap Pair	Velocity Factor 1	2	3	5	7	10	Measured Ratio
730/720	10^{-4}	0.002	0.012	0.089	0.233	0.435	0.063
740/720	10^{-29}	10^{-25}	10^{-22}	10^{-17}	10^{-13}	10^{-9}	--
750/720	10^{-76}	10^{-68}	10^{-62}	10^{-53}	10^{-47}	10^{-40}	--

TABLE 10. Comparison of Computed and Measured Sampling Trap Activity Ratios of ^{88}Kr for EP-IV.

Trap Pair	Velocity Factor 1	2	3	5	7	10	Measured Ratio
730/720	0.021	0.212	0.427	0.644	0.743	0.819	0.757
740/720	10^{-20}	10^{-13}	10^{-8}	10^{-4}	0.014	0.170	--
750/720	10^{-58}	10^{-46}	10^{-38}	10^{-26}	10^{-19}	10^{-10}	--

TABLE 11. Comparison of Computed and Measured Sampling Trap Activity Ratios of ^{88}Kr for EP-V.

Trap Pair	Velocity Factor 1	2	3	5	7	10	Measured Ratio
730/720	0.838	0.939	0.956	0.960	0.961	0.963	0.837
740/720	0.258	0.604	0.729	0.828	0.888	0.951	0.557
750/720	10^{-8}	0.131	0.389	0.616	0.720	0.819	0.427

TABLE 12. Comparison of Computed and Measured Sampling Trap Activity Ratios of ^{85m}Kr for EP-V.

Trap Pair	Velocity Factor 1	2	3	5	7	10	Measured Ratio
730/720	0.847	0.944	0.959	0.962	0.963	0.964	0.834
740/720	0.271	0.621	0.742	0.837	0.895	0.956	0.596
750/720	10^{-8}	0.140	0.406	0.632	0.733	0.830	0.424

TABLE 13. Charcoal Trap Velocity Factors for Various Isotopes.

Temperature, °K	Velocity Factor for Isotope[a] ^{89}Sr	^{88}Kr	^{85m}Kr
161 (EP-IV)	~14	7.2	5
172 (EP-III)	5	4	4
186 (EP-V)	1.6	1	0.95
	2.5	1.6	1.6
	3.0	3.2	3.2

[a]The velocity factor is the ratio of the Krypton-front velocity found in this work divided by the velocity reported in Burnette, *et al.*, (1961).

TABLE 14. ^{89}Kr Atoms in and out of Charcoal Trap.

	EP-IV (2628 s)			EP-V (3078 s)		
Source	In	Out	Tractional Throughput	In	Out	Fractional Throughput
NRTO	2.22×10^{19}	1.9×10^{16}	0.00086	3.22×10^{19}	1.9×10^{16}	0.00059
LASL	8.25×10^{19}	1.421×10^{16}	0.00017	1.476×10^{20}	5.77×10^{17}	0.0039

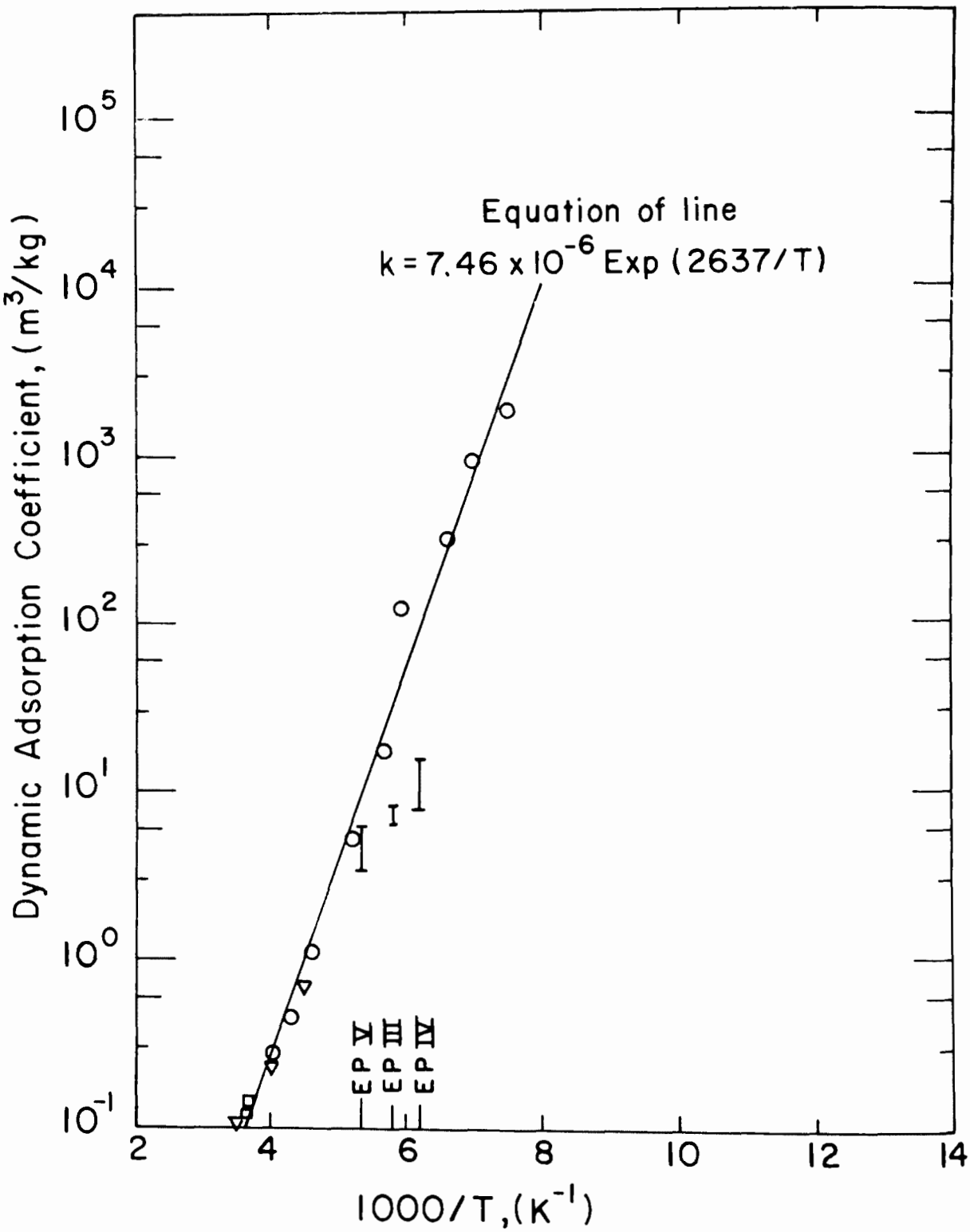

Figure 1. Dynamic Adsorption Coefficients of Krypton on Charcoal.

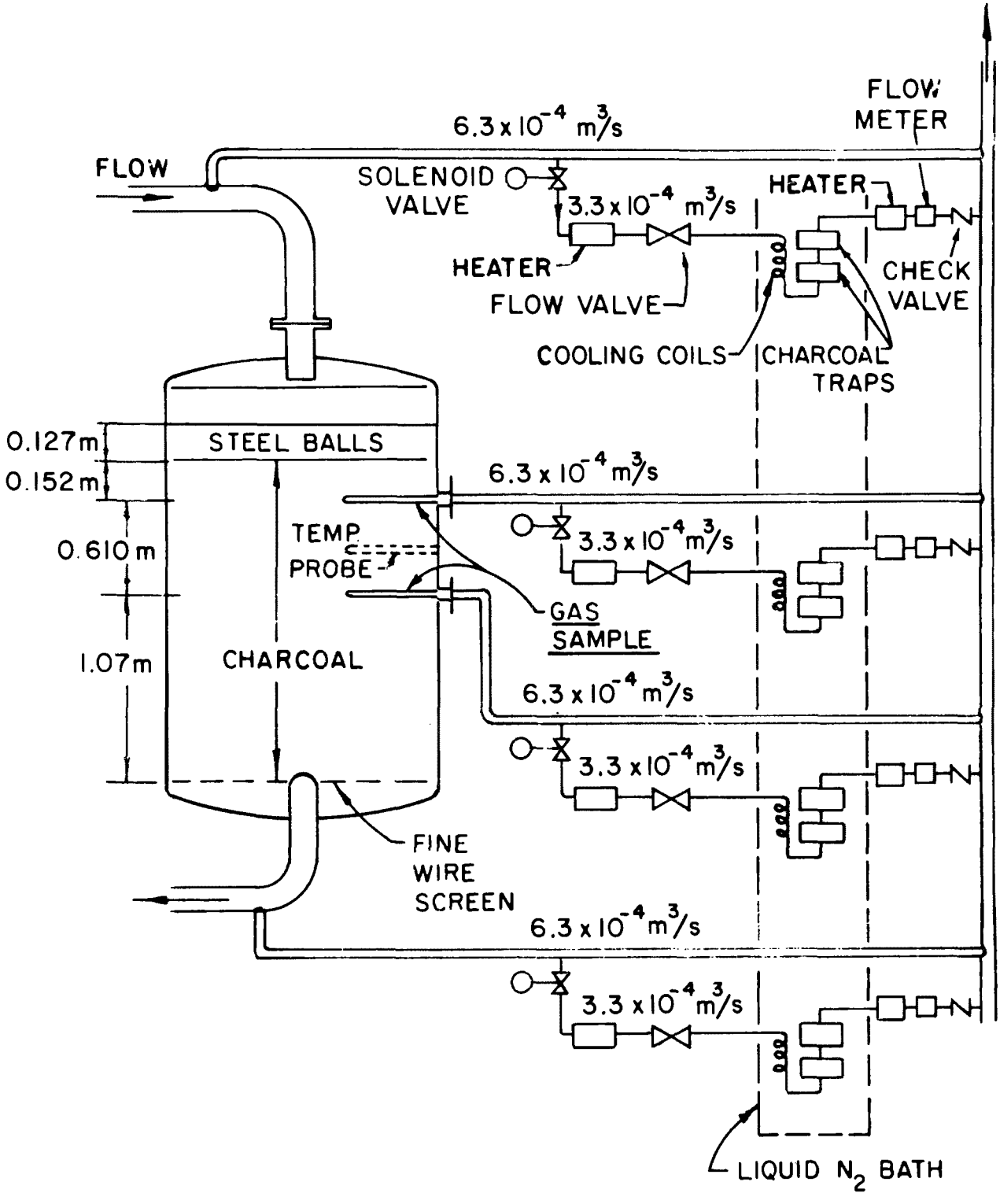

Figure 2. NF-1 Charcoal Trap Sampling System.

REACTOR CONTRIBUTIONS TO ATMOSPHERIC NOBLE GAS RADIOACTIVITY LEVELS*

J. M. Matuszek, C. J. Paperiello, and C. O. Kunz
Radiological Sciences Laboratory
Division of Laboratories and Research
New York State Department of Health
Albany, New York 12201

Abstract

Nuclear power reactors produce copious quantities of several species of radioactive gases. Samples of these gaseous effluents were analyzed from two pressurized-water power reactors (PWR), one boiling water power reactor (BWR), one high-temperature gas-cooled power reactor (HTGR), and a heavy-water-moderated pressurized-water research reactor (HWPWR). Several noble gas activities were quantitatively identified; these included ^{37}, ^{39}Ar, ^{85}Kr, and ^{131}m, ^{133}m, ^{133}Xe. Direct stack sampling in the case of the BWR ensured representative samples of actual releases. A variety of in-plant samples were collected from the other reactors in order to derive characteristic patterns for release levels.

Gamma-emitting gaseous species were identified by spectral resolution using a Ge(Li) detector and associated electronics. The beta-emitters were identified by chromatographic separation on a series of molecular sieve columns, followed by spectral analysis using internal gas-proportional counting tubes and associated multichannel analyzer systems.

The Laboratory's experiences in sample collection, handling, and analysis are summarized. Estimates of relative release rates and of total annual releases of the several species are provided for each type of reactor.

INTRODUCTION

Noble gas releases from nuclear facilities are usually monitored routinely by the facility operator to ensure against an excessive external (submersion) dose to the population living in the environs affected by the facility. Facility measurement systems are, therefore, designed to measure gamma-emitting radiogases. Some facilities also collect water vapor from the gas stream in order to measure releases of tritiated water.

The Radiological Sciences Laboratory of the New York State Department of Health is conducting a study of the gaseous effluents from various types of reactors, searching particularly for radiogases which were not measured by the plant effluent monitors, but which might contribute to the total off-site dose.

Certain noble and permanent gases, particularly ^{37}Ar and tritium, have found increasing use as atmospheric tracers (Lal and Peters, 1967; Loosli and Oeschger, 1969; Agerter, *et al.*, 1967). A number of these gases are released by certain reactors in sufficient quantities to influence atmospheric measurements, particularly if the collection locations are near the release sites.

This paper presents the activity ratios of the long-lived noble gas effluents, the estimated annual release levels of the several nuclides of interest, and projections of potential release levels for larger reactors. Unfortunately, no commercial fuel-reprocessing facilities were operating during the period of this study, so only reactor effluents are discussed.

EXPERIMENTAL PROGRAM

1. Sample Collection.

Several samples have been collected from three light-water reactors: a boiling water power reactor (BWR) and two pressurized-water power reactors (PWR). Samples were collected directly from the stack of the BWR. The PWR samples, collected from a variety of locations, included pressure-tank (cover gas), dissolved gas in the primary coolant (strip gas), and decay-tank gas (containment air).

Samples received from a high-temperature gas-cooled power reactor (HTGR) have consisted of the off-gas from the regeneration of two cryogenic charcoal beds used to purify the helium primary coolant.

A set of samples has also been collected from the pressure vessel of a heavy-water-moderated pressurized-water research reactor (HWPWR). This reactor is probably of sufficient size to provide clues toward heavy-water power reactor performance.

Sample containers in this ongoing study vary according to the collection facilities available at each reactor. If flow-through samples can be collected, conventional gas-sampling containers of 30 ml, 125 ml, and 1,000 ml were filled to pressures of from one to three atmospheres. Otherwise, rubber-capped septum vials are filled through a hypodermic needle, as is conventionally done at most power reactor facilities. Containment air is collected in a 16-liter stainless-steel container. The largest gas volume possible is collected; i. e., the highest level the facility operator will allow off-site.

*Supported in part by USAEC contract AT(11-1)2222 and USEPA contracts 68-01-0522 and 68-01-LA-0505.

2. Chemical Processing.

Immediately on receipt of samples at the Laboratory, gamma-emitting nuclides are measured on a Ge(Li) detector. Subsequent separations and purifications of specific radiogas species are conducted as many times as necessary to assure consistently reproducible data. A krypton fraction is separated from each aliquot to provide a reference point for all other nuclides separated from that aliquot. Thus, leakage of air through the rubber septum caps does not cause analytical errors. Details of the chemical processing technique are described in an associated paper (Kunz, 1973).

3. Measurements.

Separated fractions are counted in 100 ml stainless-steel gas-proportional counting tubes, using a plastic anticoincidence guard for nuclides in very low abundance. Details of the measurement techniques are provided by Paperiello (1973).

RESULTS AND DISCUSSION

Transit time to the Laboratory for most samples is at least 3 hours from time of collection. The first gamma-spectral measurements are normally made after 30 hours have passed, so data for noble gases with half-lives of less than 10 hours are limited. The following results are, therefore, confined primarily to those nuclides with half-lives of greater than 1 day.

Noble gas activities on each sample are normalized on ^{85}Kr, then averaged for presentation in Table 1. In general, the consistency of ratios for repeated analysis of a given sample is better than $\pm$10% when counting statistics permit that precision. The consistency of ratios for a specific nuclide in multiple samples of the same type from a given reactor is $\pm$ 20% if counting statistics are adequate. Fission gas ratios are consistent with decay times for each type of reactor.

The ^{37}Ar ratios for samples from the HTGR and HWPWR are startlingly high and consistent to $\pm$20%. The ^{39}Ar activity ratios, on the other hand, are very low for all reactors, so measurements are possible only on large samples, limiting any attempts at evaluating the consistency of ^{39}Ar results.

In Table 1, the first column under each nuclide reports the ratio for the sample at collection time. The second column reports the values corrected as necessary for decay from time of sample collection to the average time of release.

The amount of each noble gas released annually (Table 2) is estimated by multiplying the normalized activity ratio by the published release levels of ^{85}Kr or "total noble gas" for the two PWR's and the HTGR. Since ^{85}Kr is not measured by the BWR operator and the total noble gas includes many short-lived activities, release estimates were made from reported ^{133}Xe levels. The HWPWR reports only the amount of HTO released annually, so all noble gas release estimates were calculated from the operator's estimates of total pressure-vessel volume released and from the radionuclide concentrations measured at the Laboratory.

Reported values for BWR fission gas releases normally include ^{133}Xe as the longest-lived noble gas constituent. The data in Table 2 indicate that the other fission gases discussed here do not contribute significantly to the local submersion dose. In particular, the calculated amounts of ^{85}Kr released appear low when compared to the values for other reactors. Radioargon releases from the BWR are lower than those from the other reactors with the exception of PWR(I). The maximum release rate of ^{37}Ar from the BWR could be as high as 1μCi/s at a concentration of 0.01 pCi/ml. Since the total release rate can vary downward from the maximum values as much as one order of magnitude at any specific time, BWR releases are not continuous in the strictest sense. The mean release rate for ^{37}Ar is 0.3μCi/s.

Long-lived noble gas releases from PWR(I) are also low. Radioargon releases are lower than those for any other reactor studied. The maximum release rate of ^{37}Ar could be as high as 2μCi/s at a concentration of 0.005 pCi/ml. Sample volumes were too small to obtain a real value for ^{39}Ar releases.

Release estimates for PWR(II) must be considered in two data groups. Core elements used in 1970, 1971, and 1972 were of a type found to suffer densification and leakage (Gillette, 1972). Fission gas releases were high during these years, and releases of ^{85}Kr were higher than those from the other light-water reactors studied. Installation of pressurized fuel elements appears to have reduced the amount of fission gases released in 1973 by factors of 30 and 50 for ^{85}Kr and ^{133}Xe, respectively. The 1973 values are extrapolations of reactor performance using data for the first six months of operation with the new core.

Releases of ^{37}Ar from PWR(II), however, remain the highest from the light-water reactors. The change in fuel element design has not significantly reduced them, indicating the ^{37}Ar production likely occurs outside the fuel elements. Although these releases are too low to contribute to the submersion dose, they may be sufficiently large to affect atmospheric ^{37}Ar measurements. At a PWR of this type ^{37}Ar activity could be released for a few hours at a rate of 12μCi/s and a concentration of about 0.2 pCi/ml with a periodicity of 4 to 8 weeks, depending on operating conditions. Puffs could, therefore, appear periodically at locations where atmospheric ^{37}Ar samples are being collected.

Long-lived fission gas releases from the HTGR appear limited to ^{85}Kr and are similar in magnitude to the light-water reactors. The plant itself has approximately one-tenth the thermal power level of the light-water reactors. It will be interesting to follow the trend of ^{85}Kr release as larger HTGR's become operational. The ^{133}Xe releases were not measurable because of the small size of the sample and its age when processed. A second set of samples has been collected, but the data are not available at the time of this writing.

If the measurements from the one sample obtained to date are representative, the release of ^{37}Ar from the HTGR is doubly significant. Though ^{85}Kr is the dose-limiting nuclide during release, ^{37}Ar contributes a 20% additional submersion dose. It may also have a pronounced affect on atmospheric studies. Not only are copious quantities of ^{37}Ar released annually, but the releases occur as puffs of a few hours duration every 3 to 4 weeks. The release rate, calculated from the highest annual release level in Table 2, could be 4 mCi/s at a concentration up to 500 pCi/s. Furthermore, the ^{85}Kr release limit in the plant's technical specifications is 6 mCi/s. The corresponding ^{37}Ar release level could be as high as 300 mCi/s at a concentration of 30 nCi/ml.

Fission gas releases from the HWPWR are also low and appear to consist predominantly of ^{133}Xe. The ^{37}Ar release levels appear quite high; puff releases of approximately 1-hour durations would occur monthly at the rate of approximately 5 μCi/s and with concentrations of 0.5 pCi/ml. However, only a single sample has been analyzed to date, and this research reactor has a 4-week operating cycle, so buildup factors may be more sensitively related to the time of sampling within the cycle. Until more samples are processed, the HWPWR data must be considered somewhat tenuous. Plans have been made to collect a series of samples at different times during the operating cycle in order to better define the noble gas releases from this reactor.

The highest annual release values (Table 2) are not necessarily the maximum possible release rates. For PWR(I) and PWR(II), the values represent only about 60% of the plant operating capacity. Unfortunately, we have no estimate of plant capacity for the HTGR, but it seems reasonable to assume that these values represent 60% to 70% of the operating capacity for this reactor as well. As plant capacity improves with new reactor designs, scaling factors for noble gas releases might exhibit an increase greater than that based on thermal power levels alone.

The mechanism for production of ^{37}Ar and ^{39}Ar in reactors is a matter of conjecture. Activity ratios for $^{37}Ar/^{39}Ar$ for the light-water reactor effluents are reasonable similar (Table 3), but they are different from the air activation ratio calculated for each duty cycle. A likely source of ^{37}Ar, particularly in the case of the HTGR, would be via the $^{40}Ca\ (n,\alpha)^{37}Ar$ reaction from calcium impurities in reactor materials such as the carbon moderator. The lack of ^{41}Ar data for these samples limits the comparison to the one ratio.

A $^{37}Ar^{39}Ar$ ratio lower than the calculated for air activation could be due to an inadequate accounting of ^{37}Ar decay. Except for the PWR(II)'s new core and the NWPWR, the calculations were made for continuous irradiation over the annual operating cycle. The power reactors actually made brief, periodic shutdowns, permitting some ^{37}Ar decay; but, to explain the low ratio in this way, one would have to postulate approximately 100 days of shutdown each year which seems unreasonably long. A more likely explanation in the light-water reactors is that the reaction $^{39}K(n, p)^{39}Ar$ leads to a greater abundance of ^{39}Ar, thus decreasing the value of the ratio below that for air activation.

The $^{37}Ar/^{39}Ar$ ratio for HTGR effluents is greater than the air activation value by a factor of approximately 1,000. Such a high ratio must come from calcium activation. The ratio for the HWPWR effluents is also markedly different from the air activation ratio. One the other hand, the $^{41}Ar/^{37}Ar$ ratio for the HWPWR is quite similar to the air activation value, leaving some question of the interpretation of the data. In general, the radioargon ratios indicate that air activation is a minor source of ^{37}Ar radioactivity in reactor effluents.

The ^{37}Ar reactor release levels have an important relationship to atmospheric studies being conducted by several speakers at this Symposium. Lal and Peters (1967) estimated that the average tropospheric specific activity of ^{37}Ar would be 2.1×10^{-2} dpm per kg of air, which is equal to 2×10^{-3} dpm per liter of argon or 1×10^{-14} μCi/ml of air.

Using the atmospheric dispersion coefficients suggested by the U. S. Atomic Energy Commission in recently published regulatory guides (USAEC, 1973a and b), the ^{37}Ar concentrations at 100 and 1,000 km from the stack can be estimated (Table 4).

It is apparent that the BWR and PWR(I) would have only a nominal effect, if any, on measurements such as those being carried out at approximately $10^{-14}\mu$Ci/ml (Loosli and Oeschger, 1969). The short-term puffs from PWR(II) could contribute to such low-level measurements, particularly where most samples are collected within 150 km of a reactor identical in design to the PWR(II).

The HTGR would apparently contribute significantly to atmospheric ^{37}Ar measurements at distances up to a few thousand kilometers. Furthermore, if ^{37}Ar is released at the technical specification limit, an 80-fold increase would result for the HTGR concentrations in Table 4. Since the HTGR is about 110 km from the National Bureau of Standards laboratory which is conducting atmospheric ^{37}Ar measurements, its impact there must be considered. The HTGR is relatively small compared to other gas-cooled reactors. A number of carbon-moderated, gas-cooled reactors in Europe, particularly in France (total of 2,700 MWt), and the United Kingdom (total of 8,000 MWt), could contribute large quantities of ^{37}Ar to the global inventory and have a significant impact on atmospheric ^{37}Ar studies being performed at Bern. The newest U.S. HTGR, due to start operations soon, may contribute up to 44 kCi/year of ^{37}Ar. Four HTGR's now on order in the U.S. could each release up to 130 kCi/year of ^{37}Ar when finally operational.

The influence of the HWPWR on any of the atmospheric studies' laboratories is less pronounced. To our knowledge, no samples of atmospheric ^{37}Ar are being collected near the facility in which this reactor is located. What influence other research reactors of similar design might have is a matter of conjecture. The 40-MWt power level of this HWPWR is also very small compared to approximately 2,800 MWt of heavy-water power reactors distributed globally. The influence of these reactors on the global inventory of ^{37}Ar should also be examined.

Extrapolation of noble gas releases for reactors of different design — or even for different reactors of the same design — cannot be quantitatively exact. It seems fair to expect, however, that within a scaling factor of approximately 100 for total thermal power, there is a significant probability of perturbations on atmospheric ^{37}Ar levels by the several HTGR's currently operating and especially by those being constructed.

SUMMARY

Noble gas releases from several types of reactor have been measured, and annual releases of the long-lived constituents have been estimated. Of serious import to the atmospheric physicists are the copious quantities of ^{37}Ar produced in some of the reactors, particularly the HTGR. For those involved in atmospheric research, the important concern is the even greater unmeasured releases from many larger gas-cooled reactors.

REFERENCES

Aegerter, S. K., H. H. Loosli, and H. Oeschger, (1967) *Variations in the Production of Cosmogenic Radionuclides*, Symposium on Radioactive Dating and Methods at Low-Level Counting. International Aomic Energy Agency, Vienna, pp 49-51.

Gillette, R., (1972) *Nuclear Safety: Damaged Fuel Ignites a New Debate in AEC*, Science 177, 330.

Kunz, C. O., (1973) *Separation Techniques for Reactor-Produced Noble Gases*, this Symposium.

Lal, D. and B. Peters, (1967) *Cosmic Ray Produced Radioactivity on the Earth*, Handbuch der Physik XLVI/2, 551.

Loosli, H. H. and H. Oeschger, (1969) *^{37}Ar and ^{81}Kr in the Atmosphere*, Earth and Planetary Science Letters 7, 67.

Paperiello, C. J., (1973) *Internal Gas-Proportional Beta-Spectrometry for Measurement of Radioactive Noble Gases in Reactor Effluents*, this Symposium.

U. S. Atomic Energy Commission, (1973a) Regulatory Guide 1.3, *Assumption Used for Evaluating the Potential Radiological Consequences of a Loss of Coolant Accident for Pressurized Water Reactors.*

U.S. Atomic Energy Commission, (1973b) Regulatory Guide 1.4, *Assumption Used for Evaluating the Potential Radiological Consequences of a Loss of Coolant Accident for Boiling Water Reactors.*

TABLE 1. Average Activity Ratios for Long-Lived Noble Gas Reactor Effluents at Time of Measurement and Time of Release.

Reactor Type	^{37}Ar		^{39}Ar	^{85}Kr	^{131m}Xe		^{133m}Xe		^{133}Xe	
	Meas.	Rel.	Meas. Rel.	Meas. Rel.	Meas.	Rel.	Meas.	Rel.	Meas.	Rel.
BWR	8.5×10^{-2}	8.5×10^{-2}	1.1×10^{-4}	1.0	9	9	95	95	2,100	2,100
PWR (I)	3.2×10^{-3}	3.1×10^{-3}	$<4\times10^{-6}$	1.0	4×10^{-1}	4×10^{-1}	2	1	42	32
PWR (II)(a)	3.9×10^{-3}	3.1×10^{-3}	$<1\times10^{-6}$	1.0					30	6
PWR (II)(b)	1.0×10^{-1}	8×10^{-2}	6×10^{-5}	1.0	1.4×10^{-1}	8×10^{-2}	2.9×10^{-1}	1.1×10^{-2}	17	5
HTGR	49	49	4×10^{-6}	1.0					$<3\times10^{-2}$	$<3\times10^{-2}$
HWPWR	19,000	19,000	17	1.0					14,000	14,000

Notes:

(a) Old core.

(b) New core.

Table 2. Highest Annual Releases of Long-Lived Noble Gases.

Reactor	Power Level (MWt)	Year	Estimated Releases (Ci)					
			^{37}Ar	^{39}Ar	^{85}Kr	^{131m}Xe	^{133m}Xe	^{133}Xe
BWR	1,538	1972	3	$3x10^{-3}$	31	260	2,900	65,000
PWR (I)	615	1970	$1.7x10^{-1}$	$<2x10^{-4}$	53	20	50	1,700
PWR (II)(a)	1,300	1971	12	$<4x10^{-3}$	3,700			23,000
PWR (II)(b)		1973	7	$5x10^{-3}$	90	7	1	450
HTGR	116	1971	6,000	$5x10^{-4}$	122			<4
HWPWR	40		$1.9x10^{-1}$	$2x10^{-4}$	$9x10^{-6}$			$1.4x10^{-1}$

Notes:

(a) Old core.

(b) Based on first six months of operation with new core.

TABLE 3. Comparison of Radioargon Production Ratios to Air Activation Ratios.

Source	$^{37}Ar/^{39}Ar$	$^{41}Ar/^{37}Ar$
Annual duty cycle:		
Air activation	$1.5x10^4$	
BWR	$9x10^2$	
PWR(I)	$>1.6x10^3$	
PWR (II)(a)	$> 8x10^3$	
HTGR	$8x10^7$	
Monthly duty cycle:		
Air activation	$9x10^4$	58
HWPWR	$1.1x10^3$	50
PWR (II)(b)	$1.7x10^3$	

Notes:

(a) Old core.

(b) New core; sample collected one month after start-up.

TABLE 4. ^{37}Ar Concentrations (μCi/ml) at 100 and 1,000 km from the Stack.

Reactor	Release period	at Stack	100 km distant	1,000 km distant
BWR	Continuous	1×10^{-8}	2×10^{-16}	2×10^{-17}
PWR (I)	≅ 1 week	5×10^{-9}	1×10^{-16}	1×10^{-17}
PWR (II)	≅ 8 hours	2×10^{-7}	1×10^{-12}	1×10^{-13}
HTGR	≅ 8 hours	5×10^{-4}	3×10^{-10}	3×10^{-11}
HWPWR	1 hour	5×10^{-7}	1×10^{-12}	1×10^{-13}

EFFECT OF HEAT PRODUCED BY RADIOACTIVE DECAY ON THE ADSORPTION CHARACTERISTICS OF CHARCOAL BEDS*

G. G. Curzio[1] and A. F. Gentili[2]
[1]Instituto Impianti Nucleari
University of Pisa
Pisa, Italy

[2]Servizio di Fisica Sanitaria
Camen, S. Piero a Grado
Pisa, Italy

Abstract

The effects of radioactive decay heat from the fission-produced noble gases on the characteristics of an activated charcoal holdup bed, and related problems, were studied.

A computer code currently being developed for the evaluation of the radioactive decay heat effects; distortions in elution curves under various conditions; the formation of hot spots; the appearance of preferential paths; and risks of ignition is mentioned.

An experimental facility was set up to test the behavior of a small charcoal bed. The facility and the adopted method are briefly described and the experimental results are reported.

A preliminary comparison is made between the experimental results and the theoretical ones.

INTRODUCTION

The dynamic characteristics of an activated charcoal bed for use in the delay and retention of the radioactive noble gases, i.e., using the adsorption coefficient and the parameters of the Van Deemter equation for the evaluation of the reduced height of theoretical plates, can easily be evaluated in ideal work conditions (Underhill, 1967; Kovach, 1970; and Curzio and Gentili, 1972a and b).

However, many factors can modify the ideal behavior of an activated charcoal bed; such as, the presence of moisture or other impurities in the carrier gas, irregular packing of the charcoal, vibrations, transient hydrodynamic and/or thermal conditions, and radioactive decay heat, (Kovach 1970; Curzio and Gentili, 1972b; and Romberg 1964).

Radioactive decay heat can be of considerable interest in beds of a small size designed to treat high activities of noble gases: In the literature there are several theoretical approaches to this problem (Kovach, 1970; Underhill, *et al.*, 1971; Glueckauf, 1958; and Shields and Davis, 1970). But, as far as we know, no direct systematic experimental approach exists. This is probably due to the practical difficulties involved in obtaining measurable variations of temperature from decay heat; this requires the use of hundreds of curies or more of radioactive gas, which creates substantial safety problems.

The only experimental data (Kovach, 1970 and Glueckauf, 1958) were obtained by injection of a 10 W pulse of ^{85}Kr into a charcoal bed the size of a gas chromatographic column; a drastic reduction was obtained in the delay time as well as an increase in the number of the theoretical plates of the bed. No quantitative theoretical correlation was attempted to obtain the relevant parameters of the phenomenon. This method can meet with considerable difficulties, however, not only in the setting up of a test, but also in the interpretation of the results if the high inlet activities are due to such quantities of radioactive noble gas that the linearity limits of the adsorption isotherm are surpassed, and/or the adsorption heat becomes no longer negligible.

In the normal work conditions of a delay bed, adsorption heat can be ignored, but its effects can become predominant if a strong concentration gradient should move through a filter.

We can make an approximate quantitative comparison between the thermal effects of decay heat and adsorption heat produced by a bell shaped pulse of 1 Ci of ^{85}Kr moving through a 1 cm^2 cross section charcoal bed.

Figures 1 and 2 illustrate the problem. The distribution of ^{85}Kr along the bed is

$$n(z,t) = (n^*/\sqrt{2\pi}\,\sigma)\exp\left[-(z - vt)^2/2\sigma^2\right]$$

where v = 1 cm/s and σ = 1 cm.

The decay heat source is roughly a Gaussian distribution (with a standard deviation slightly larger than one sigma due to the range of the beta particles from ^{85}Kr) and moves forward together with the ^{85}Kr pulse.

The adsorption heat production per unit of volume and time is $Q_A = q_A\,(dn/dt)$, where q_A is the molar adsorption heat (assuming q_A = 5,000 cal/mole (Kitani and Takada, 1965); at the front of the pulse there is a heat source, and at the tail a sink. The resulting temperature profiles, as can be easily calculated without considering conduction and convection, are shown in Figures 1 and 2 (bulk density is assumed to be 0.5 g/cm^3 and specific heat 0.12 cal/°C g). It can be seen that the effect of the adsorption heat source near the krypton peak is by far the predominant one.

**This work was supported by CNR contract No. 72.00749.07.*

This fact suggests that it is possible to employ the heat production by adsorption for determining the parameters that characterize a charcoal bed designed for highly radioactive noble gases.

Qualitatively we can expect that the krypton at the maximum of the pulse will pass through the bed faster than the krypton at the front and tail of the peak: therefore, the mean delay time will be shorter and the peak will assume an asymmetric shape.

EXPERIMENTAL

The feasibility of the suggested method was tested using the experimental setup shown in Figure 3; this consisted of a cylindrical bed, 155 mm long and 20 mm in diameter, using 83-90 mesh activated charcoal and dry air as the carrier gas. The thermostatic bath used ice.

The tests were made by injecting krypton pulses into the bed and analyzing the elution curves. Comparisons were made between tests performed with small amounts of stable krypton ($\cong 4 \times 10^{-3}$ cm^3 (s.t.p.) traced with ^{85}Kr ($\cong$ 70 mCi/cm^3), and those performed with up to 60 cm^3 (s.t.p.) of stable krypton with a specific activity (down to 1 μCi/cm^3). The upper limit of the amount of krypton was selected in such a way that the linearity limit of the adsorption isotherm of the krypton on the charcoal was not surpassed (Kitani and Takada, 1965).

RESULTS

Figure 4 shows two elution curves obtained at the same temperature and carrier gas flow rate; it can be seen that the test performed with the macroscopic amount of krypton has a delay time considerably shorter than the test done with krypton in the tracer quantity, and the elution curve appears very asymmetric. From the value of the time Tmax corresponding to the maximum of the elution curve, an effective adsorption coefficient K' can be calculated.

The results of the preliminary tests are summarized in Figures 5 to 7. In the first two figures, the ratio between K' and the true adsorption coefficient at O° C (K_o) is shown first as a function of the inlet amount of krypton at constant carrier gas flow rate, and then as a function of the flow rate at a constant inlet amount of krypton. In the third figure, an increase in asymmetry is clearly due to an increase in the amount of inlet krypton.

DISCUSSION AND CONCLUSIONS

For a correct interpretation of the reported results, we plan to employ an IBM 360/67 FORTRAN code, which is about nearly completed. At present, it can be said that the code was successfully tested only in simple situations where either a comparison with analytical solutions was possible (e. g., the determination of the temperature profile due to a moving heat source with a known and constant shape, [Wilson, 1904]) or where drastic approximations were made.

In the near future, the code will be completed, and on the basis of the predictions that will be obtained, we shall be able to plan further tests under meaningfully different experimental conditions. It would then be possible to assure a feasible extension of the results from our laboratory scale to a full-scale charcoal bed.

At any rate, the experimental results are already in satisfactory agreement with those calculated. The delay time can presently be calculated by the computer code with an approximation better than 20%. In Figure 8, for example, an experimental elution curve is compared with a calculated curve, which was obtained by neglecting all the heat transfer mechanisms; the calculated delay time is about 15% less than the measured one, and the calculated curve profile is sharper than the experimental one.

The introduction of the conduction mechanisms in the model of calculation will have as an effect the decrease of the maximum temperature rise (and, therefore, an increase of the calculated delay time), and the smoothing of the temperature profile (and therefore, of the elution curve).

NOTATIONS

K_o — adsorption coefficient (at O°C)
K' — effective adsorption coefficient
n — molar density of krypton
n^* — number of injected moles
q_A — molar adsorption heat
Q_A — adsorption heat production per unit of time and volume
Q_D — decay heat production per unit of time and volume
t — time
T_{max} — time corresponding to the maximum of the elution curve
v — velocity
z — axial coordinate

ΔT_1 — time necessary for outlet concentration to rise from the first half maximum value of the elution curve to the maximum
ΔT_2 — time necessary for outlet concentration to decrease from the maximum of the elution curve to the second half maximum value
$\Delta 9$ — temperature rise
σ — standard deviation

REFERENCES

Curzio, G. G. and A. F. Gentili, (1972a), *Noble Gas Adsorption Characteristics of Charcoal Beds: Van Deemter's Coefficient Evaluation*, Anal. Chem. 44, 8, 1544-45.

Curzio, G. G. and A. F. Gentili, (1972b), *Liberation de gas nobles par les centres nucleaires: quelques remarques sur le fonctionnement des filtres de charbon de bois*, VI Congres International, Societe Francaise de Radioprotection, Bordeaux 27-30 March 1972.

Glueckauf, E., (1958), *Gas Chromatography*, pp 69-89.

Kitani, S. and J. Takada, (1965), *Adsorption of Krypton and Xenon on Various Adsorbents*, J. Nucl. Sci. Technol., 2(2)51-56.

Kovach, J. L., (1970), *Review of Krypton-Xenon Adsorber Design*, Part I, North American Carbon, NACAR 010005.

Romberg, E., (1964), *The Effect of Moisture on the Adsorption of Krypton on Charcoal*, Dragon Project Report (D.P.R.) 276.

Shields, R. P. and R. J. Davis, (1970), *Ignition of Charcoal Adsorbers by Fission-Product Decay Heat*, ORNL-TM-3122, Oak Ridge National Laboratory, Oak Ridge, Tenn.

Underhill, D. W., (1967), *Dynamic Adsorption of Fission-Product Noble Gases on Activated Charcoal*, NYO-841-8, New York University, New York, N.Y.

Underhill, D. W., H. Yusa and O. Grubner, (1971), *Design of Fission Gas Holdup Systems*, USAEC Contract-AT(30-1) 841, New York University, New York, N.Y.

Wilson, H. A., (1904), *On Convection of Heat*, Proc. Ceb. Phil. Soc. 12, 406-423.

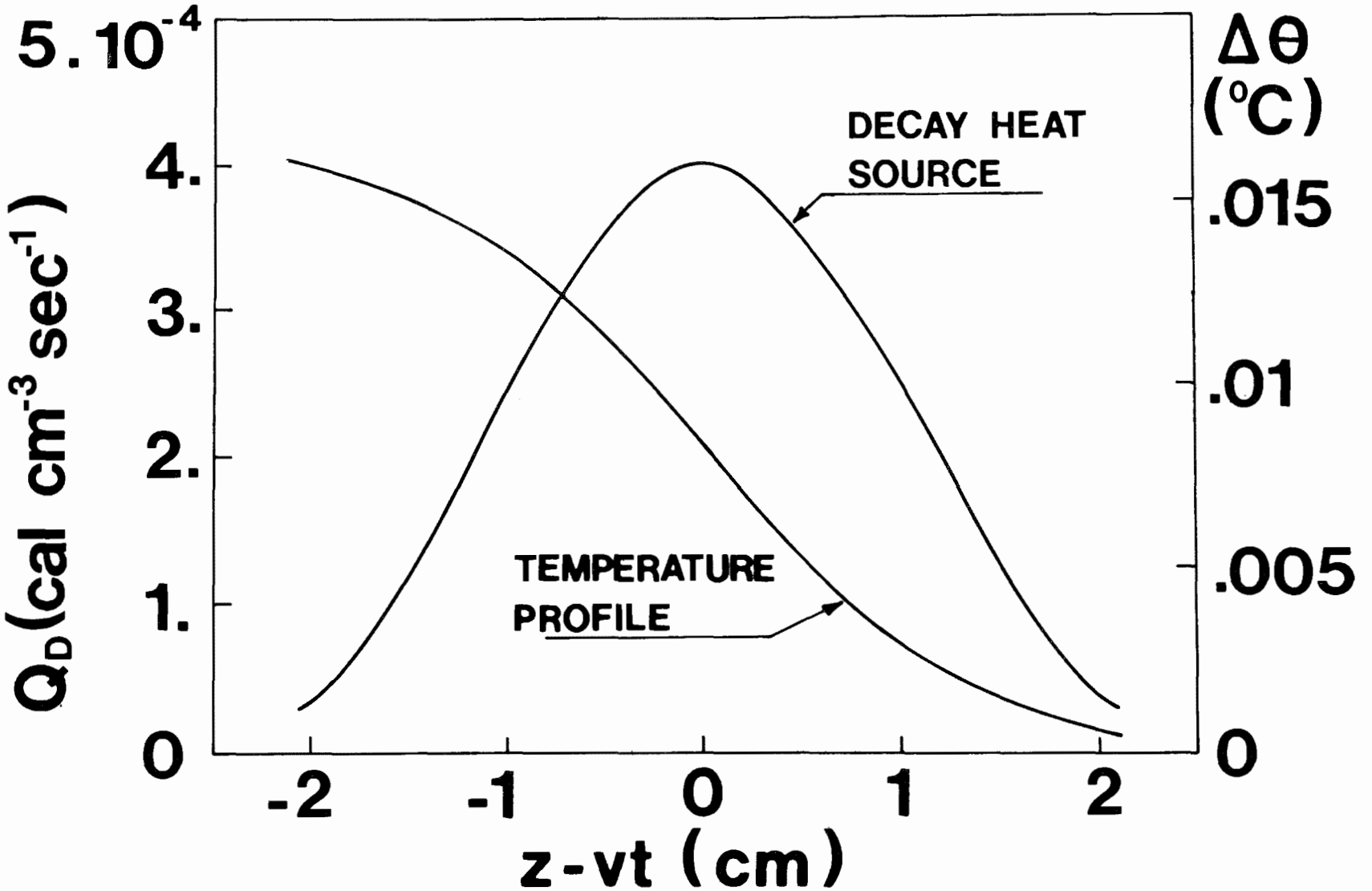

Figure 1. Decay heat source and related temperature profile.

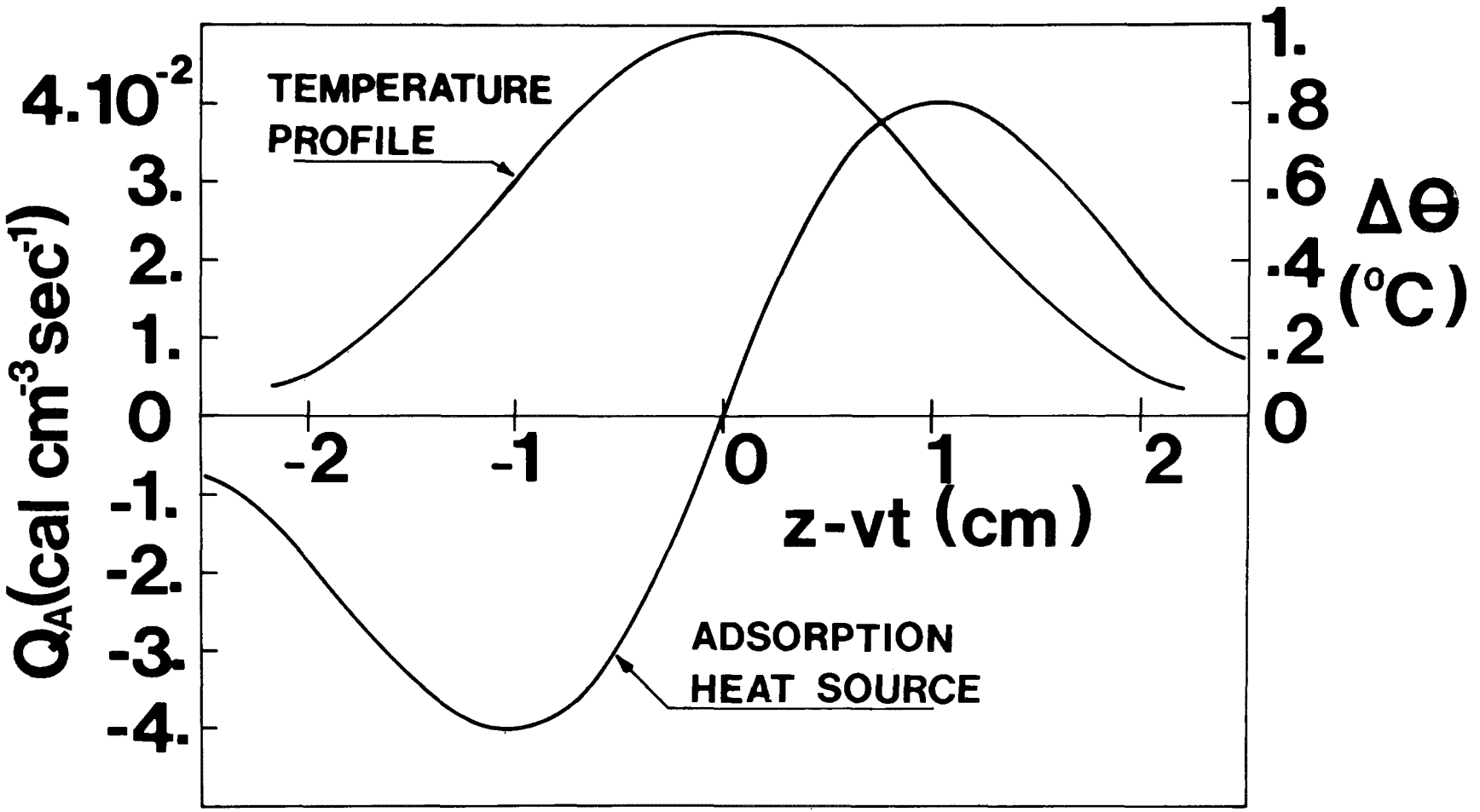

Figure 2. Adsorption heat source and related temperature profile.

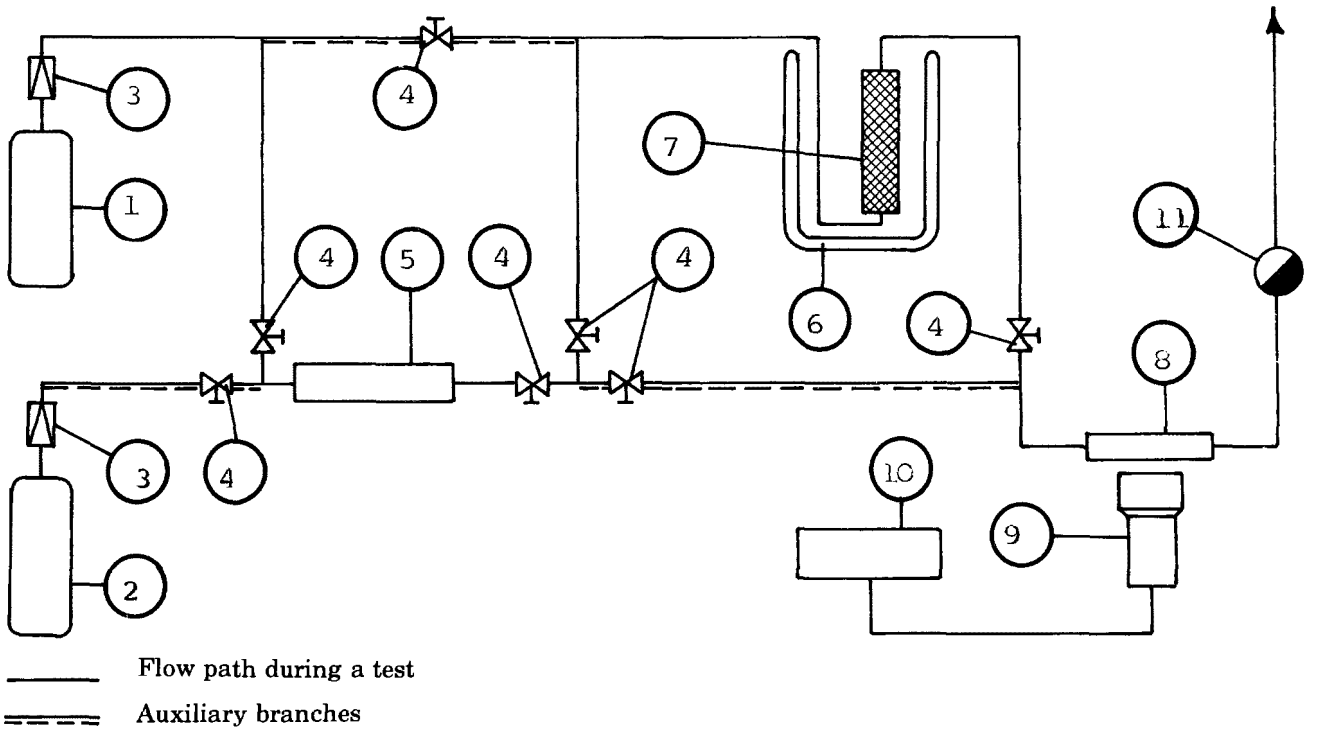

Figure 3. Test circuit flow-sheet.

1 - Dry air container
2 - Stable krypton container
3 - Regulation valve
4 - Intercept valve
5 - ^{85}Kr introduction device
6 - Thermostatic bath
7 - Charcoal bed
8 - Measuring box
9 - 3" x 3" NaI (Tl) scintillator
10 - Analyzer
11 - Flowmeter

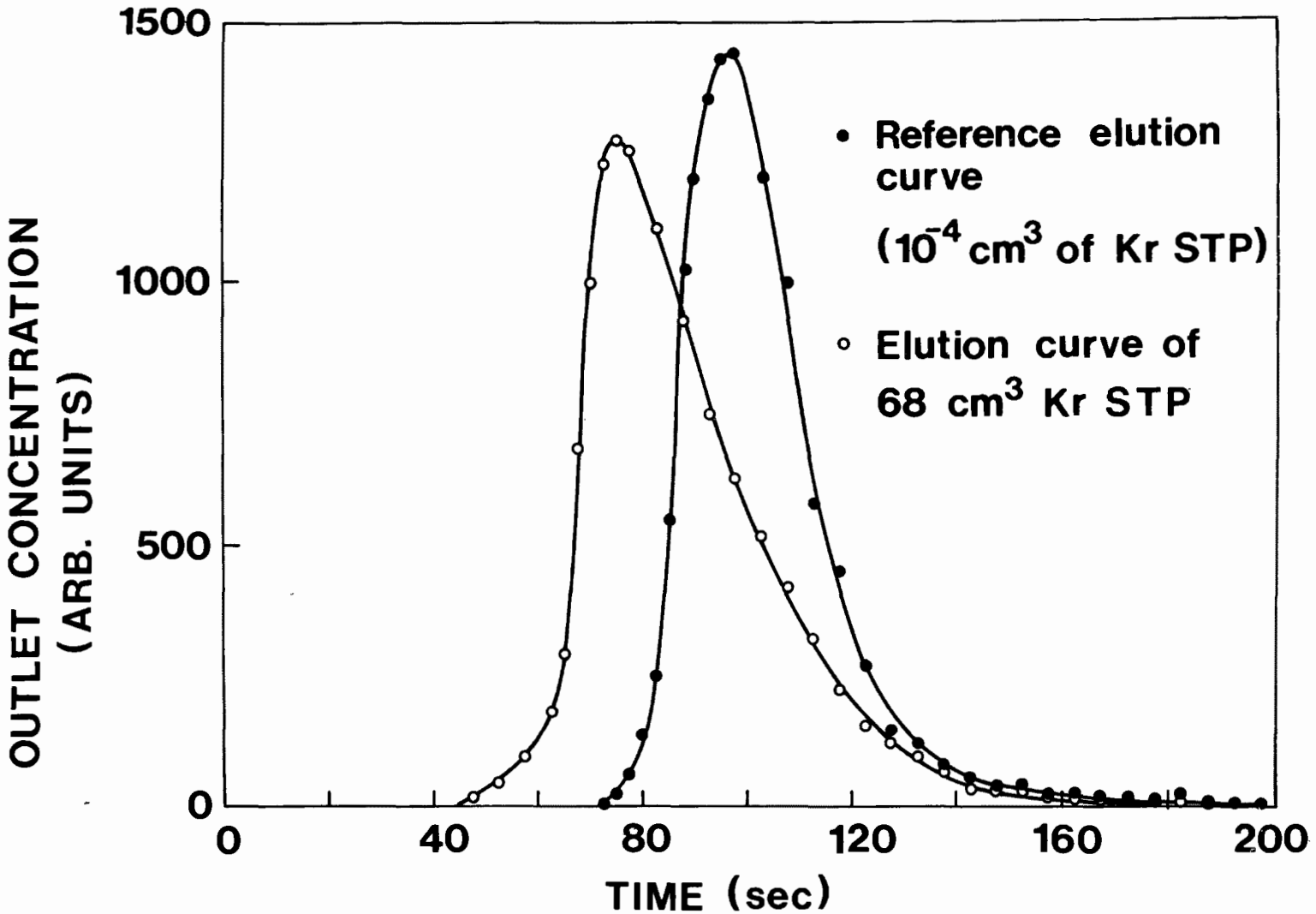

Figure 4. Comparison between two elution curves.

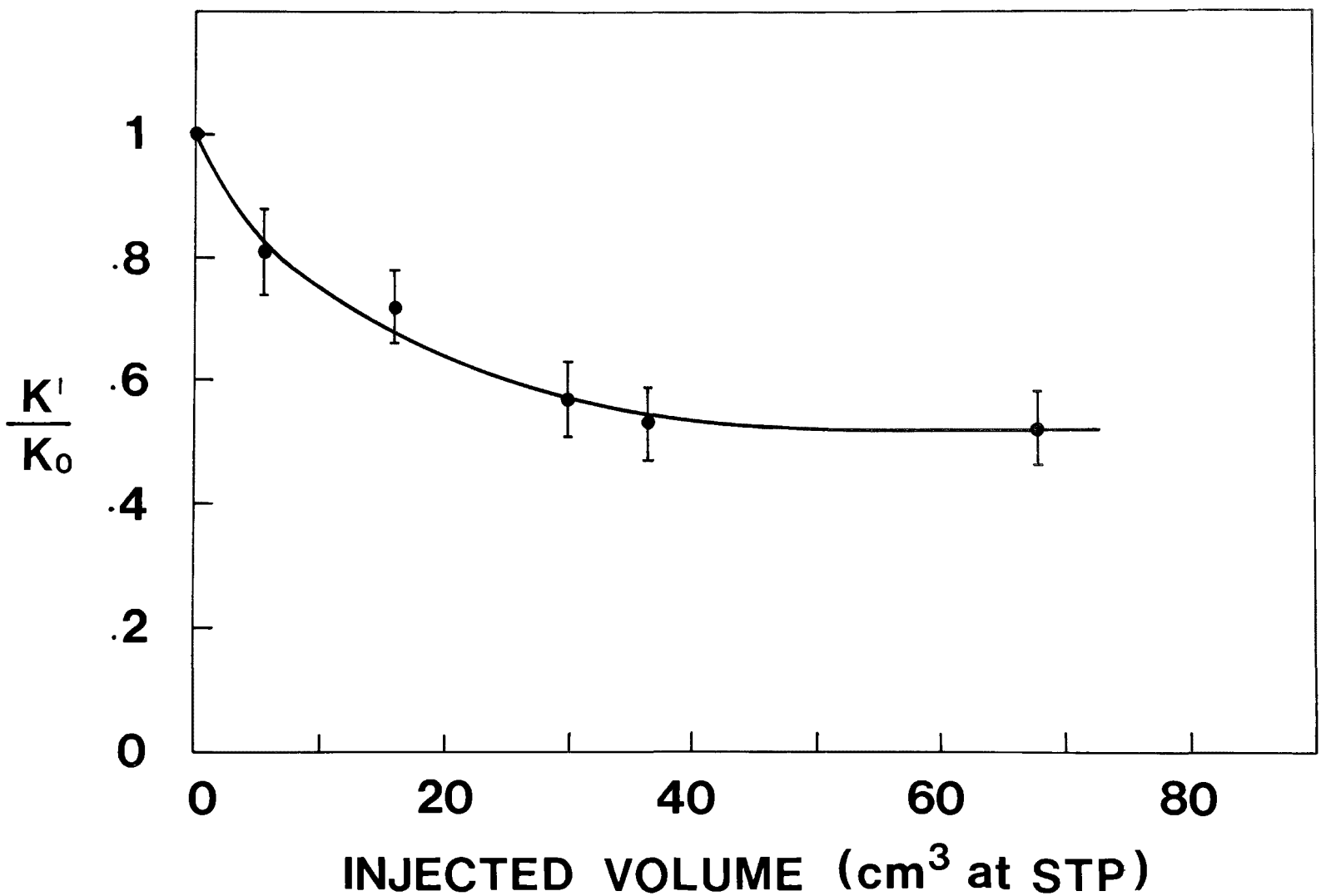

Figure 5. Apparent adsorption coefficient as a function of the injected krypton volume.

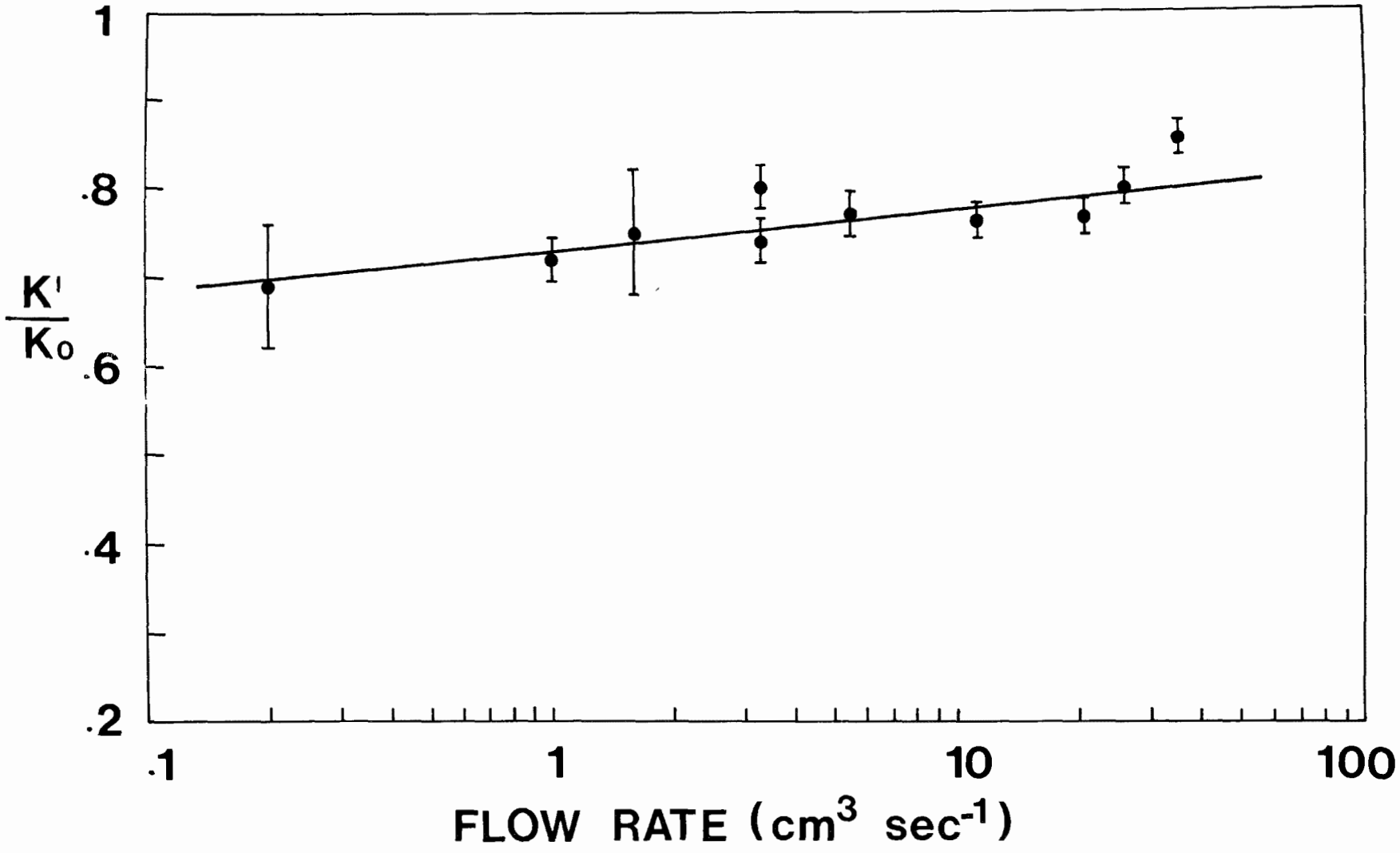

Figure 6. Apparent adsorption coefficient as a function of the flow rate.

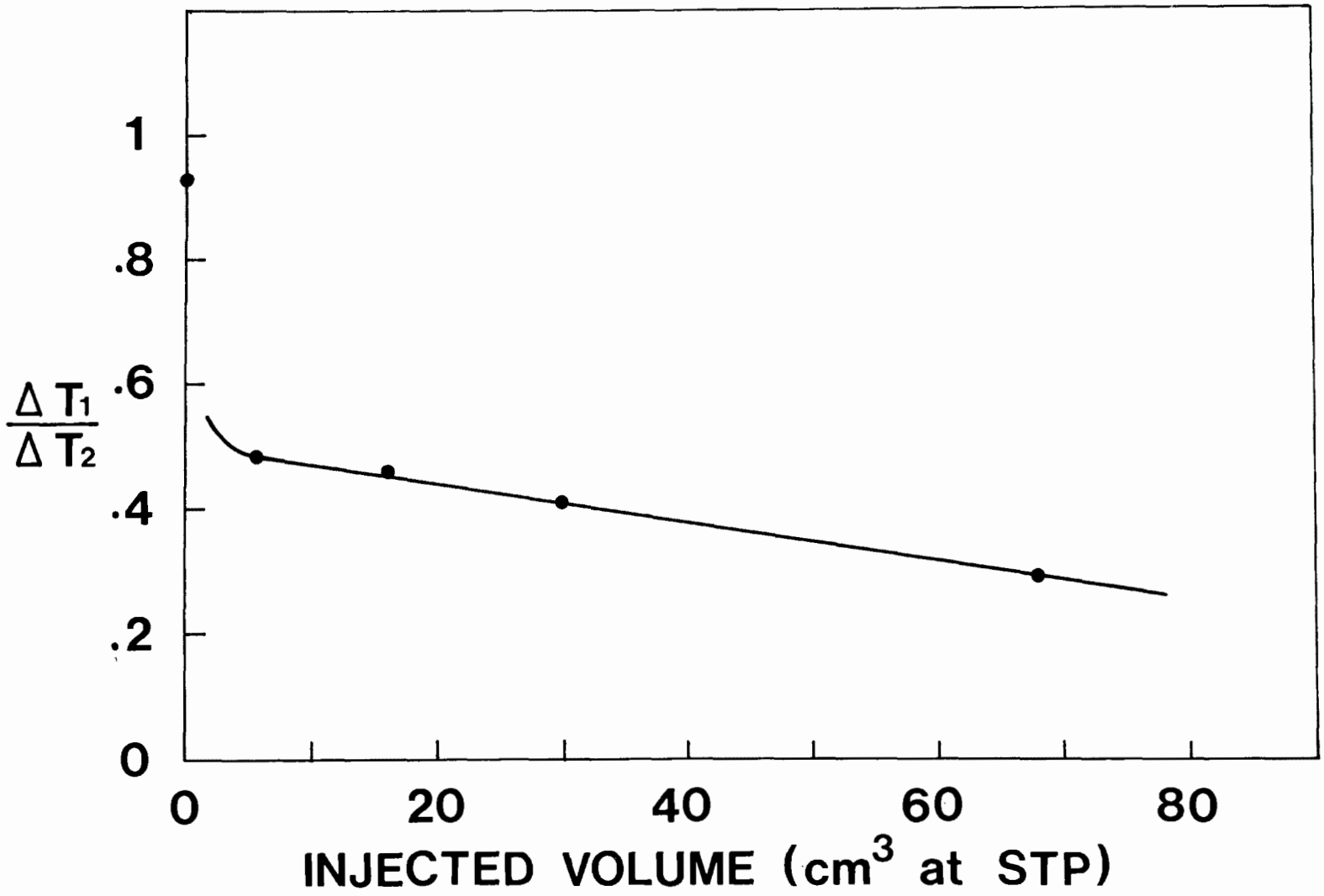

Figure 7. Asymmetry coefficient as a function of the injected krypton volume.

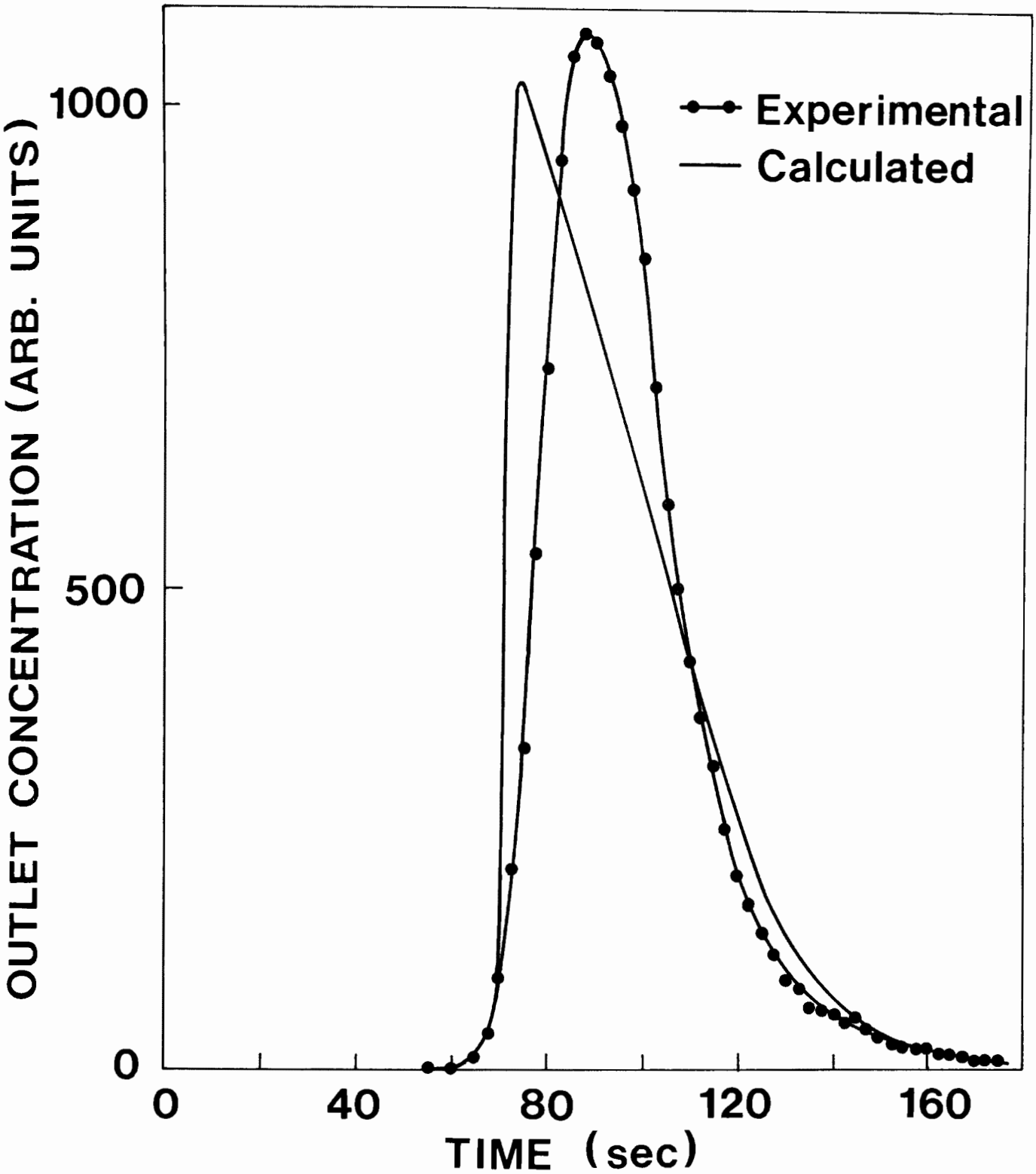

Figure 8. Comparison between experimental and calculated elution curves.

VI. Chemistry of Noble Gases

CHEMICAL METHODS FOR REMOVING XENON AND RADON FROM CONTAMINATED ATMOSPHERES*

L. Stein
Argonne National Laboratory
Chemistry Division
Argonne, Ill. 60439

Abstract

A number of solid reagents have been shown to react spontaneously with radon and xenon at 25°C to form nonvolatile compounds. These appear very promising for such purposes as purifying uranium mine atmospheres, reducing emissions of xenon radioisotopes from nuclear power plants and fuel reprocessing plants, detecting failed fuel elements, and analyzing radon and xenon isotopes in air. Radon can be collected with halogen fluoride-metal fluoride complexes, such as ClF_2SbF_6, BrF_2SbF_6, $BrF_4Sb_2F_{11}$, and $IF_4(SbF_6)_3$; with the dioxygenyl salt O_2SbF_6; and with the fluoronitrogen salts N_2FSbF_6 and $N_2F_3Sb_2F_{11}$. Xenon can also be collected with O_2SbF_6 and N_2FSbF_6. All of these compounds are decomposed by water vapor; therefore, they must be used in conjunction with desiccants, such as Drierite, silica gel, or molecular sieve. Methods of preparation of the compounds and reactions of the compounds with radon and xenon will be described. Chemical separations of krypton and xenon and laboratory-scale decontamination experiments with samples of air containing radon-222 and xenon-133 will also be described. The possibility of finding solid oxidants for krypton (antimony salts, for example, that would be capable of forming the complex $KrF^+Sb_2F_{11}^-$ and liquid oxidants for radon, xenon, and krypton that would be suitable for use in spray towers) are discussed.

INTRODUCTION

A number of physical methods for controlling noble gas emissions from nuclear power plants and fuel reprocessing plants have been tested in recent years. These include cryogenic distillation (Bendixsen and German 1971; Bendixsen, *et al.*, 1971; and Wilson and Taylor, 1958), charcoal adsorption (Wirsing, *et al.*, 1970; and Burnette, *et al.*, 1962; Browning, *et al.*, 1959 and 1960; Mecca, *et al.*, 1971; and Slavsky, 1971), solvent extraction (Stephenson, *et al.*, 1972 and Merriman, *et al.*, 1968), and permselective-membrane diffusion (Rainey, *et al.*, 1968 and 1971). However, very little attention has been directed to the possibility of using chemical methods to trap noble gases. This is clearly an oversight, inasmuch as compounds of the heavy gases (krypton, xenon, and radon) have been known for more than 10 years, and isotopes of these gases are involved in several environmental problems. For example, krypton-85, xenon-133, and xenon-135 are the chief fission gases released by boiling-water reactors, and radon-222, a member of the uranium-238 decay chain, is a major atmospheric contaminant in underground uranium mines. Xenon forms many chemical compounds, including halides, oxides, oxyfluorides, perxenate salts, and complex fluorides with alkali metal and transition metal fluorides (Bartlett, 1962; Hyman, 1970; and Malm and Appelman, 1969). Krypton and radon, however, appear to form only a small number of simple and complex fluorides (Hyman, 1970; Malm and Appelman, 1969; Turner and Pimentel, 1963; Streng, *et al.*, 1963; Selig and Peacock, 1964; Frlec and Holloway, 1973; Gillespie and Schrobilgen, Unpub.; Prusakov and Sokolov, 1971; Fields, *et al.*, 1962; and Stein, 1969, 1970a,b, 1972, and 1973a,b). Research on radon chemistry is somewhat limited by the fact that no stable isotopes of radon are known; therefore, most research on the chemistry of this element has been performed by tracer methods, with microcurie and millicurie amounts of radon-222. In this paper, some initial tests of laboratory-scale scrubbing units containing liquid bromine trifluoride, solid complexes of halogen fluorides and metal fluorides, and the dioxygenyl salt O_2SbF_6 are described. These tests have shown that radon can be removed from air efficiently by oxidation with bromine trifluoride and solid complexes containing the cations ClF_2, BrF_2, BrF_4, and IF_6, and that radon and xenon can both be removed efficiently by oxidation with O_2SbF_6.

Bromine trifluoride reacts spontaneously with radon at 23-25°C to form solutions of nonvolatile radon fluoride (Stein, 1969). The oxidized radon is present as a positive ion in these solutions, since it migrates to the cathode in a D. C. field (Stein, 1970a). The oxidation and the interaction with the solvent are believed to occur as follows:

$$Rn + BrF_3 \quad \text{(large excess)} \rightarrow \text{solution of} \quad RnF_2 + BrF$$

$$RnF_2 + BrF_3 \rightleftharpoons RnF^+ + BrF_4$$

$$RnF^+ + BrF_3 \rightleftharpoons Rn^{2+} + BrF_4^-$$

Work performed under the auspices of the U. S. Atomic Energy Commission.

Once it is oxidized, radon behaves very much like a metallic element. The solutions can be exposed to the atmosphere, can be poured from one container to another, and can be distilled to dryness under vacuum without loss of radon. (In the last instance, a deposit of solid radon fluoride is obtained.) This behavior is somewhat analogous to that of hydrogen, since hydrogen is also very volatile in its elemental state, but only slightly volatile in its oxidized state (i.e., as a solvated proton in aqueous solutions).

Figure 1 shows the first scrubber unit that was tested with liquid bromine trifluoride and samples of air containing 2.4 to 4.5 mCi/l of radon-222 (Stein, 1972). The contaminated air was passing through two Kel-F test tubes in series, each containing 4.0 ml of bromine trifluoride at 23-25°C, and through a trap which was cooled with liquid nitrogen to condense any unreacted radon. Flow rates of 2.9 to 3.0 ml/min were used, and the air was dispersed as very fine bubbles by a stainless steel frit in the down-leg of each tube. At the conclusion of each test, the distribution of radon was determined by measuring the γ -emission of its daughters (lead-214 and bismuth-214) after several hours, when radon and its daughters were known to be in radioactive equilibrium. All of the radon was found in the first test tube each time; none was found in the second tube or in the cold trap.

Since the concentrations of radon were very high and the flow rates were very low in these tests, further tests were carried out with samples of ordinary air (not artificially contaminated with radon) with the apparatus shown in Figure 2 (Stein, 1973a). This was slightly more complicated than the first apparatus because a much more sensitive scintillation counting method was used. The air was passed through Ascarite, Drierite, and two tubes of bromine trifluoride, through a trap at -80°C and a bed of soda lime, to remove BrF_3, BrF, and Br_2 vapors, and through a trap at -195°C to condense any remaining radon. The radon was then vacuum-distilled into an ampoule containing frozen scintillator solution (together with xenon carrier gas), and the ampoule was sealed and counted in a low-background scintillation counter. Figure 3 shows the type of α-particle pulse-height spectrum that was obtained for radon-222 and its short-lived daughters, polonium-218 and polonium-214.

It was found that bromine trifluoride removed 76-95% of the radon from ambient air at flow rates of 130-740 ml/min — the highest percentage removal being observed at the lowest flow rate. The concentration of radon in the ambient air (measured by a condensation-scintillation counting method) ranged from 0.098 to 0.189 pCi/l during the course of these experiments, whereas the concentration in the scrubbed air ranged from 0.009 to 0.025 pCi/l.

The results of the two series of tests indicate that radon can be removed from air efficiently by the oxidation process over a wide range of concentrations — pCi/l to mCi/l. It is only necessary for the air to be well dispersed in the liquid phase, and to remain in contact with the liquid long enough for oxidation to occur.

Bromine trifluoride reacts violently with water and organic materials, and may, therefore, be too hazardous a reagent for large-scale use; other types of oxidants may be more acceptable from the standpoint of safety. Solutions of complex metal ions in unusually high valence states appear very promising for further study, as these are frequently nonvolatile and reactive. It has been shown that radon can be oxidized by solutions of K_2NiF_6 in liquid HF, for example, but liquid HF is unsatisfactory as a solvent because of its high vapor pressure and toxicity. If suitable nonaqueous solvents can be found, it may be possible to oxidize radon safely and conveniently with solutions of K_2NiF_6, K_3NiF_6, Cs_2CoF_6, K_3CuF_6. $CsAgF_4$, Cs_2AgF_6, and similar fluoro-salts.

Figure 4 shows one type of system that could be developed in the future for purifying and recirculating the air in a section of a uranium mine, such as a working stope, where the radon radiation problem is generally most acute. This would include the following components: dust filter, blower, air drier, radon absorption tower, vapor trap, and liquid circulating pump. Radon-daughters suspended in the air on particulate matter would be chiefly removed by the dust filter, and radon would be removed by oxidation in the absorption tower (spray tower). Some lead or concrete shielding might be needed around the absorption tower, because radon and its daughters would build up to high concentrations in the recirculating liquid. One of the major problems would be that of adequately drying the air to prevent hydrolysis of the radon oxidant. (All of the oxidants that are known at present are easily hydrolyzed). This is not an insurmountable problem, however; refrigeration- or desiccant-type drying units similar to those now used by some chemical industries could probably be developed for this purpose. It has been estimated that this air-purification system should have a flow capacity of at least 5,000 cfm to appreciably lower the radon concentration in a single stope and that it should have a greater capacity, 15,000 cfm or more, to lower the concentration in several stopes.

Table 1 lists a number of solid complexes of halogen fluorides and metal fluorides and also some simple fluorides that have been tested as oxidants for radon (Stein, 1972). The solid complexes are of two types: those formed by alkali metal fluorides, KF, RbF, and CsF; and those formed by Group (V) metal fluorides, SbF_5, TaF_5, and BiF_5. The latter are better oxidants for radon than the former, since they contain halogen fluoride cations, BrF_2, ClF_2, BrF_4, and IF_6, which can react with radon as follows:

$$Rn + BrF_2^+SbF_6^- \rightleftharpoons RnF^+SbF_6^- + BrF$$

$$Rn + ClF_2^+SbF_6^- \rightleftharpoons RnF^+SbF_6^- + ClF$$

$$Rn + BrF_4^+Sb\,F_{11}^- \rightleftharpoons RnF^+SbF_6^- + BrF_2^+SbF_6^-$$

$$Rn + IF_6^+Sb_3F_{16}^- \rightleftharpoons RnF^+SbF_6^- + IF_4^+Sb_2F_{11}^-$$

The solid complexes are less hazardous to handle than liquid halogen fluorides, and can be used conveniently in packed bed reactors to remove radon from air. However, the air must still be dried, because the complexes are easily hydrolyzed by water vapor.

None of the halogen fluorides or solid complexes listed in Table 1 have sufficient oxidizing power to react with xenon at 23-25°C. However, dioxygenyl hexafluoroantimonate (O_2SbF_6) — a very unusual salt containing the O_2 cation — has been found to react with both radon and xenon at 25°C (Stein, 1973a). Raman spectral analyses have shown that the xenon product is XeF Sb_2F_{11}, a 1:2 xenon difluoride (antimony pentafluoride complex). Mass spectrometric analyses have also shown that two molecules of oxygen are released for each atom of xenon absorbed as follows:

$$Xe + 2\,O_2^{+}SbF_6^{-} \rightarrow XeF^{+}Sb_2F_{11}^{-} + 2O_2$$

No spectral or analytical data have been obtained for the trace amounts of radon product, but radon probably forms an analogous 1:2 radon difluoride — antimony pentafluoride complex as follows:

$$Rn + 2O_2^{+}SbF_6^{-} \rightarrow RnF^{+}Sb_2F_{11}^{-} + 2O_2$$

The dioxygenyl salt can be prepared by several methods. At Argonne, it has been prepared by the photochemical reaction of oxygen, fluorine, and antimony pentafluoride, which was first reported by Shamir and Binenboym (1968). At the research laboratory of the Ozark-Mahoning Company, Tulsa, Oklahoma, it has been prepared by a high-pressure bomb reaction of oxygen, fluorine, and antimony pentafluoride (Beal, *et al.*, 1969). And at Bell Laboratories, Murray Hill, New Jersey, it has been prepared by a similar bomb reaction of oxygen, fluorine, and antimony metal (Edwards, *et al.*, 1973). All three products appear to be identical. An intermediate product, $O_2Sb_2F_{11}$, has been obtained in some instances, but it has been shown that this can be converted to O_2SbF_6 by further reaction with oxygen and fluorine. (O_2SbF_6 cannot be distinguished from $O_2Sb_2F_{11}$ by appearance; both compounds are white powders at 25°C. However, the compounds can be distinguished by their characteristic Raman spectra (Bartlett and McKee, 1973).

O_2SbF_6 has been shown to remove xenon-133 and radon-222 from contaiminated air very efficiently in laboratory-scale experiments (Stein, 1973b). These were performed with metal and glass vacuum lines similar to the one shown in Figure 1. In each experiment, a noble gas-air mixture was passed through a glass U-tube packed with O_2SbF_6 powder at 23-25°C then through a trap cooled with liquid nitrogen to condense any unreacted radioisotope. The distribution of the radioisotope was afterwards determined by measuring the γ- emission of the U-tube and the cold trap. (The distribution of xenon-133 was determined immediately; the distribution of radon-222 was determined after 3 hours, when radon-222 and its daughters (lead-214 and bismuth-214) were known to be in radioactive equilibrium). In 5 experiments with the xenon isotope and with a bed of powder 6.5 cm long and 5.5 mm in diameter, 67-100% of the xenon was removed. In three experiments with the radon isotope and with a bed of powder 5.0 cm long and 6.3 mm in diameter, all of the radon was removed. The initial concentrations of radioisotopes ranged from 2.0 to 9.8 mCi/l (xenon-133), and 13 to 24 mCi/l (radon-222); flow rates ranged from 12 to 15 ml/min.

Because it has negligible vapor pressure at 25°C and produces oxygen as the gaseous product, O_2SbF_6 appears to be a very "clean" reagent for air-purification purposes. It is less corrosive than halogen fluoride and metal fluoride complexes, and can be stored for long periods in glass or fluorinated plastic containers. Very little decomposition has been noted, for example in samples that have been stored for 6 to 9 months in Pyrex bulbs and Kel-F test tubes. Some corrosion of Kel-F has been observed, however, by products formed in the reaction with xenon — probably excited xenon, oxygen, or ozone species. The dioxygenyl compound is decomposed by moisture; in treatment of wet gases, it must, therefore, be used in conjunction with a desiccant, such as silica gel or a molecular sieve.

O_2SbF_6 and other solid oxidants can probably be used for such purposes as removing xenon isotopes from reactor and reprocessing plant off-gases; reducing radon concentrations in uranium mines (Argonne Study, Ongoing); separating xenon from lighter noble gases; and analyzing xenon and radon isotopes in air. In one of the methods that has been developed to control emissions from boiling-water reactors, large beds of charcoal are used as chromatographic columns. Waste gases are passed through the beds at ambient temperature, and the noble gases are retained long enough for short-lived isotopes to decay. Xenon isotopes may be held for 20 days, for example, and krypton isotopes for about a day. Small beds of O_2SbF_6 can probably be substituted for the large (25-50 ton) beds of charcoal to remove xenon isotopes from the off-gases completely).

Following a suggestion of Liebman (1973) two fluoronitrogen salts, $N_2F_3Sb_2F_{11}$ and N_2FSbF_6, have been prepared by thermal reactions of antimony pentafluoride with tetrafluorohydrazine (Ruff, 1965 and 1966), and difluorodiazine (Ruff, 1966; Roesky, *et al.*, 1966; and Pankrator and Savenkova, 1968), respectively, and have been tested as oxidants for radon, xenon, and krypton. The first reacts only with radon, whereas the second reacts with both xenon and radon at 25-100°C. Mass spectrometric analyses have shown that in the second reaction, one molecule of nitrogen is liberated for each atom of xenon absorbed as follows:

$$Xe + N_2F^{+}SbF_6^{-} \rightarrow XeF^{+}SbF_6^{-} + N_2$$

Because nitrogen is liberated rather than oxygen, this reaction may not be as suitable for air-purification purposes as the reaction of xenon with O_2SbF_6.

Thus, far, no solid or liquid reagent with sufficient oxidizing power to capture krypton has been found. However, krypton is known to form a stable complex fluoride, $KrF^+ Sb_2F_{11}^-$, in the reaction of krypton difluoride with antimony pentafluoride (Selig and Peacock, 1964). (The krypton difluoride must first be prepared by an excitation method, such as the reaction of krypton and fluorine in an electric discharge at low-temperature (Streng, *et al.*, 1963).) By substituting cations of very great oxidizing power for O_2^+ and N_2F^+ in the complex antimony salts, it may be possible to prepare reagents which will combine directly with krypton to form $KrF^+Sb_2F_{11}^-$. If so, these should be useful for capturing krypton-85.

REFERENCES

Bartlett, N., (1962), *Xenon Hexafluoroplatinate (V), e PtF6,* Proc. Chem. Soc., 218.

Bartlett, N., and D. E. McKee, (1973), private communication.

Beal, J. B., Jr., C. Pupp and W. E. White, (1969), *The Reaction of Oxygen Difluoride with Some Lewis Acids: The Preparation of Dioxygenyl Salts,* Inorg. Chem., 8, 828.

Bendixsen, C. L. and F. O. German (1971), *Operation of the ICPP Rare Gas Recovery Facility During Fiscal Year 1970,* USAEC Report ICP-1001, Allied Chemical Corporation, Oct 1971.

Bendixsen, C. L., G. F. Offutt and B. R. Wheeler, (1971), *Cryogenic Rare Gas Recovery in Nuclear Fuel Reprocessing,* Chem. Eng., New York, Oct. 4, 1971, pp. 55-57.

Browning, W. E., Jr., R. E. Adams and R. D. Ackley, (1960), *Removal of Volatile Fission Products from Gases,* USAEC Report TID-7610, Oct. 1960, pp. 44-57.

Browning, W. E., Jr., R. E. Adams and R. D. Ackley, (1959), *Removal of Fission Product Gases from Reactor Off-Streams by Adsorption,* USAEC Report CF59-6-47.

Burnette, R. D., W. W. Graham III and D. C. Morse, (1961), *The Removal of Radioactive Krypton and Xenon from a Flowing Helium Stream by Fixed-Bed Adsorption,* Proc. Second Conf. Nucl. Reactor Chem., Gatlinburg, Tenn., Oct. 10-12, 1961, USAEC Report TID-7622, (1962), pp. 218-235.

Edwards, A. J., W. E. Falconer, J. E. Griffiths and W. A. Sunder, (1973), *Dioxygenyl Salts,* paper No. I-29, 7th Int. Symp. on Fluorine Chem., Santa Cruz, Calif., July 15-20, 1973.

Fields, P. R., L. Stein and M. H. Zirin, (1962), *Radon Fluoride,* J. Amer. Chem. Soc., 84, 4164.

Frlec, B. and J. H. Holloway, (1973), *New Krypton Difluoride Adducts,* J. Chem. Soc., Chem. Commun., 370.

Gillespie, R. J. and G. J. Schrobilgen, unpublished studies of krypton difluoride complexes.

Hyman, H. H., (1970), *Rare Gas Compounds,* in Physical Chemistry, Vol. 5, H. Eyring, D. Henderson, and W. Jost, editors, Academic Press, New York, 1970, pp. 589-662.

Liebman, J. R., (1973), *Oxidant for Trapping Atmospheric Radiokrypton,* Nature, 244, 84.

Malm, J. G. and E. H. Appelman, (1969), *The Chemical Compounds of Xenon and Other Noble Gases,* At. Energ. Rev. 7, 3.

Mecca, J. E., J. D. Ludwick and E. L. Etheridge, (1971), *Noble Gas Confinement Study.,* Vol. II. Cryogenic Porous Media Bed. Final Report, FY-1970, USAEC Report DUN-7221, Vol. 2, Feb. 1971.

Merriman, J. R., J. H. Pashley, K. E. Habiger, M. J. Stephenson and L. W. Anderson, (1968), *Concentration and Collection of Krypton and Xenon by Selective Absorption in Fluorocarbon Solvents,* in Treatment of Airborne Radioactive Wastes, Int. At. Energ. Agency, Vienna, 1968, pp. 303-313.

Pankratov, A. V. and N. J. Savenkova, (1968), *Fluorodiazonium Compounds,* Zh. Neorg, Khim., 13, 2610.

Prusakov, V. N. and V. B. Sokolov, (1971), *The Krypton Difluoride-Bromine Pentafluoride Binary* System, Zh. Fiz. Khim., 45, 2950.

Rainey, R. H., W. L. Carter, S. Blumkin and D. E. Fain, (1968), *Separation of Radioactive Xenon and Krypton from other Gases by the Use of Permselective Membranes,* in Treatment of Airborne Radioactive Wastes, Int. At. Energ. Agency, Vienna, 1968, pp. 323-342.

Rainey, R. H., W. L. Carter and S. Blumkin, (1971), *Completion Report: Evaluation of the Use of Permselective Membranes in the Nuclear Industry for Removing Radioactive Xenon and Krypton from Various Off-Gas Streams,* USAEC Report ORNL-4522, April 1971.

Roesky, H. W., O. Glemser and D. Bormann, (1966), *On the Preparation and Some Reactions of* Difluorodiazine, Chem. Ber., 99, 1589.

Ruff, J. K., (1965), *The Reaction of Antimony (V) Fluoride with Tetrafluorohydrazine,* J. Amer. Chem. Soc., 87, 1140.

Ruff, J. K., (1966), *The Reaction of Antimony (V) Fluoride with Tetrafluorohydrazine and* Difluorodiazine, Inorg. Chem., 5, 1791.

Selig, H. and R. D. Peacock, (1964), *A Krypton Difluoride-Antimony Pentrafluoride Complex,* J. Amer. Chem. Soc., 86, 3895.

Shamir, J. and J. Binenboym, (1968), *Photochemical Synthesis of Dioxygenyl Salts,* Inorg. Chem. Acta, 2, 37.

Slansky, C. M., (1971), *Separation Processes for Noble Gas Fission Products from the Off-Gas of Fuel-Reprocessing Plants,* At. Energ. Rev., 423

Stein, L., (1969), *Oxidized Radon in Halogen Fluoride Solutions,* J. Amer. Chem. Soc. 91, 5396.

Stein, L., (1970a), *Ionic Radon Solutions,* Science, 168, 362.

Stein, L., (1970b), *Chemical Properties of Radon,* Yale Scientific Magazine, 44, 2.

Stein, L., (1972), *Chemical Methods for Removing Radon and Radon-Daughters From Air,* Science, 175, 1463.

Stein, L., (1973a), *Removal of Radon from Air by Oxidation with Bromine Trifluoride,* J. Inorg. Nucl. Chem., 35, 39.

Stein, L., (1973b), *Removal of Xenon and Radon from Contaminated Atmospheres with Dioxygenyl Hexafluoroantimonate, O_2SbF_6,* Nature, 243, 30.

Stephenson, M. J., J. R. Merriman and D. I. Dunthorn, (1972), *Recent Developments in Controlling the Release of Noble Gases by Absorption in Fluorocarbons,* USAEC Report K-L-6292, June 1972.

Streng, A. G., A. D. Kirshenbaum, L. V. Streng and A. V. Grosse, (1963), *Preparation of Rare-Gas Fluorides and Oxyfluorides by the Electric Discharge Method,* in Noble Gas Compounds, H. H. Hyman, editor, The University of Chicago Press, Chicago, 1963, pp. 73-80.

The safety and efficiency of O_2SbF_6 for use as a radon oxidant in mines is currently being investigated at Argonne under U. S. Bureau of Mines contract HO230018 (Argonne Study, ongoing).

Turner, J. J. and G. C. Pimentel, (1963), *Preparation of Inert-Gas Compounds by Matrix Isolation: Krypton Difluoride,* in Noble Gas Compounds, H. H. Hyman, editor, The University of Chicago Press, Chicago, pp. 101-105.

Wilson, E. J. and K. J. Taylor, (1958), *The Separation and Purification of Krypton-85 at the Multi-Curie* Level, UKAEA Report AEREI/R-2693.

Wirsing, E., Jr., L. P. Hatch and B. F. Dodge, (1970), *Low-Temperature Adsorption of Krypton on Solid Adsorbents,* USAEC Report BNL50254 (T-586), June 1970.

TABLE 1. Some Complex Fluorides and Simple Fluorides That Have Been Tested as Oxidants for Radon.

Compound	Radon Retention (%)
$KBrF_4$	28
$CsBrF_6$	7
$KClF_4$	19
$RbClF_4$	16
ClF_2SbF_6	100
BrF_2SbF_6	100
$BrF_4Sb_2F_{11}$	100
$IF_6Sb_3F_{16}$	100
BrF_2BiF_6	100
BrF_2TaF_6	27
IF_4SbF_6	76
$NOSbF_6$	0
AgF_2	0
CoF_3	0

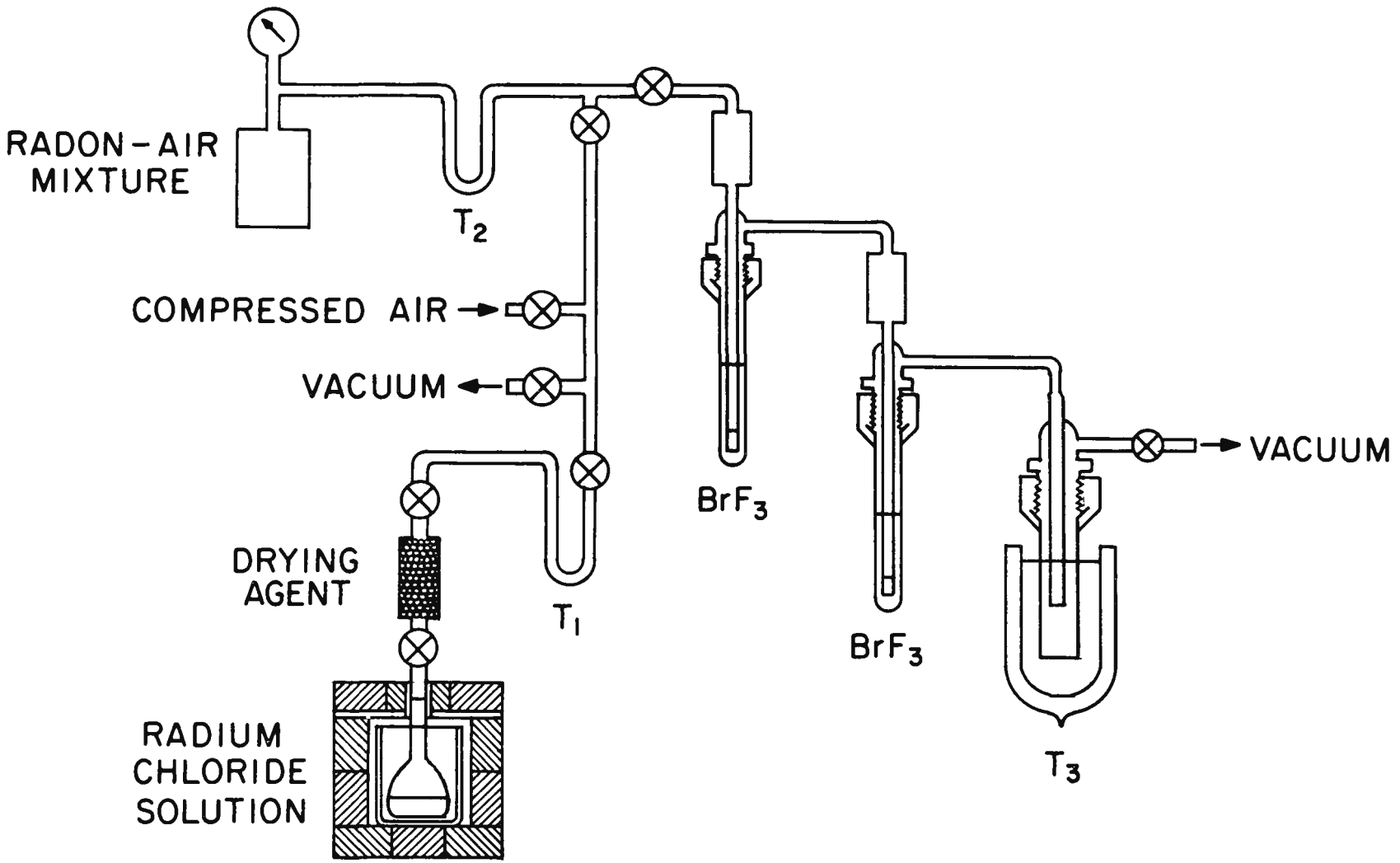

Figure 1. Two-Stage Bromine Trifluoride Scrubber.

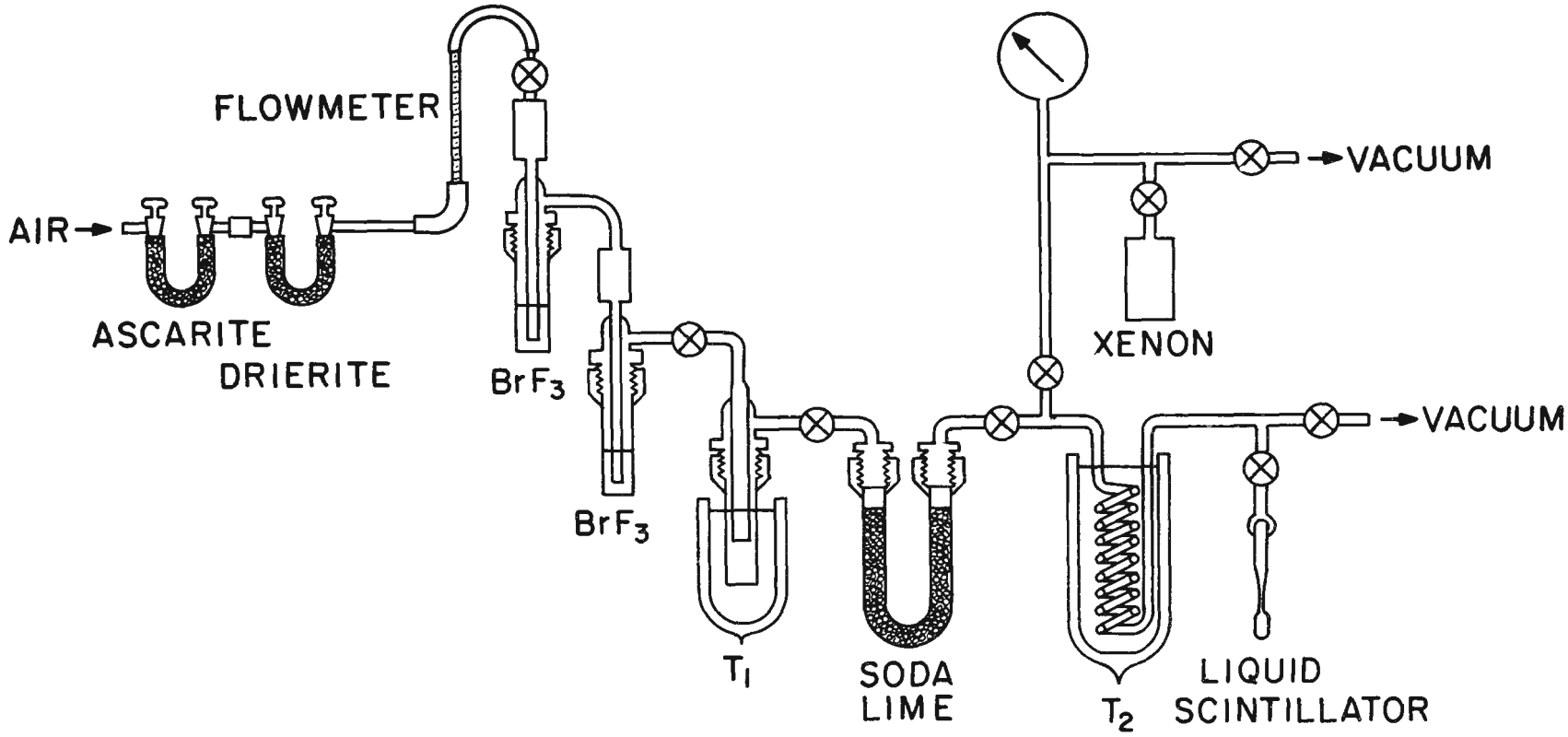

Figure 2. Two-Stage Bromine Trifluoride Scrubber and Radon Condenser.

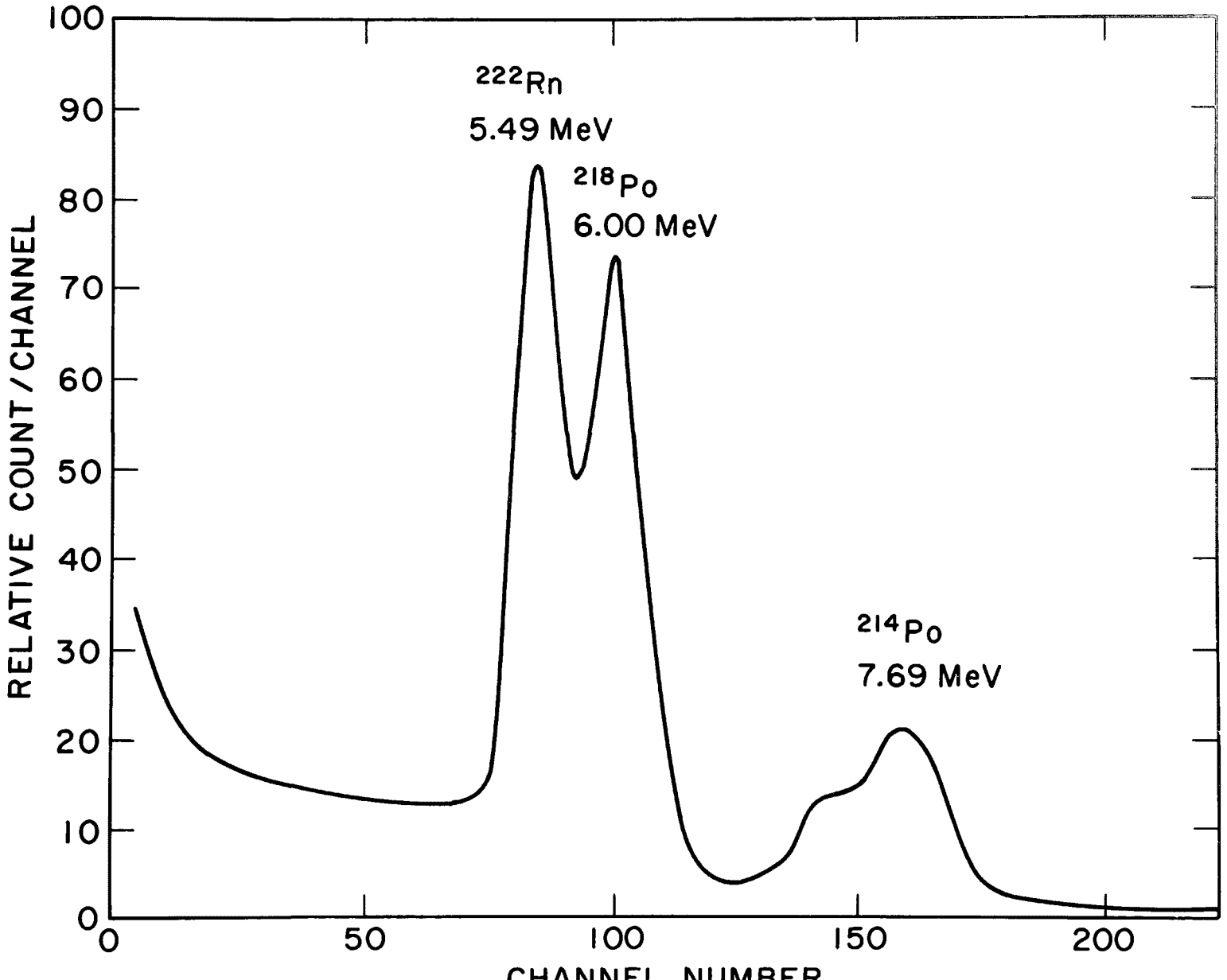

Figure 3. Pulse-Height Spectrum of Radon-222 and Daughters in Scintillating Solution.

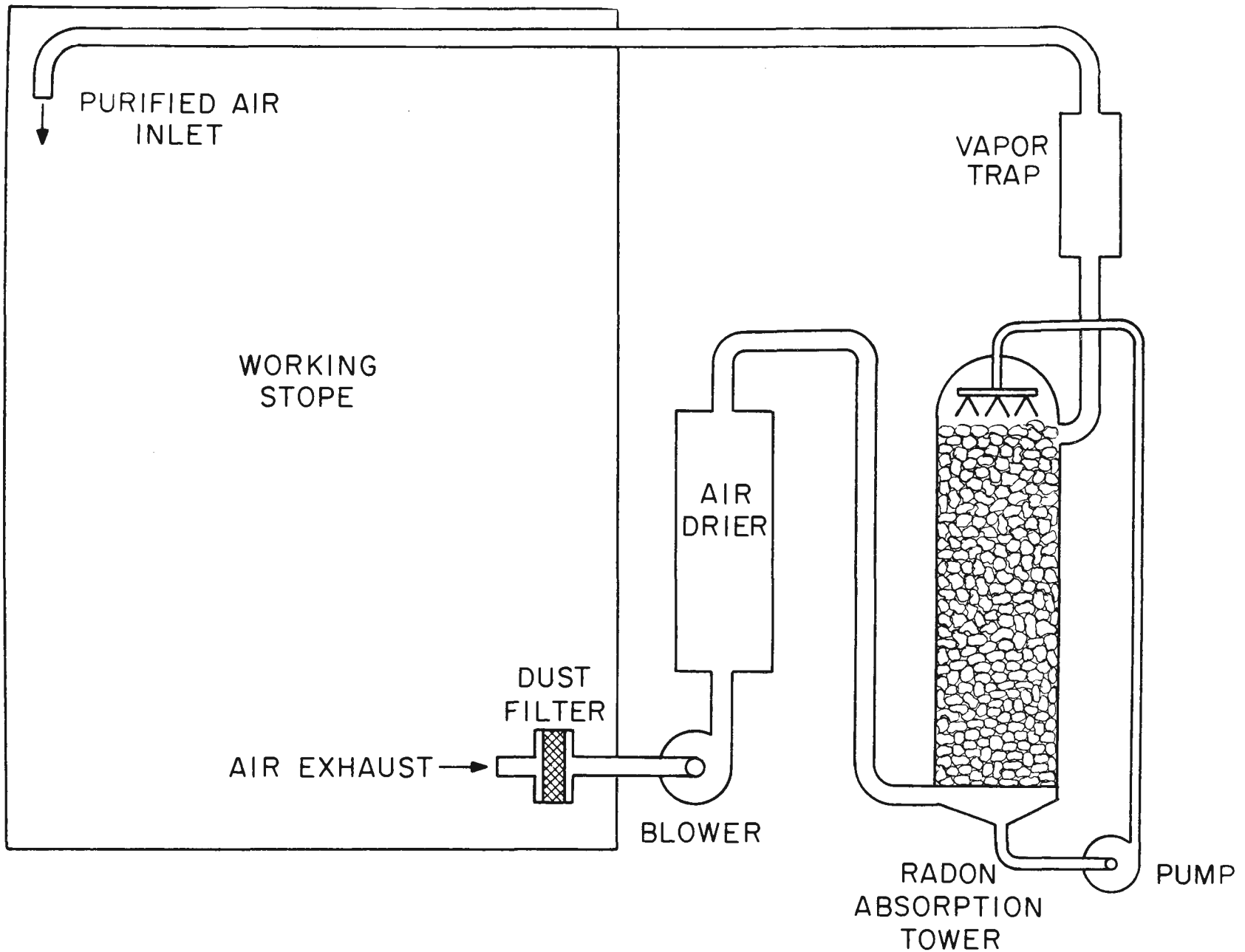

Figure 4. Proposed Air-Purification System For Use in a Uranium Mine.

STRUCTURAL CONSIDERATIONS IN THE CHEMISTRY OF NOBLE GASES

W.E. Falconer
Bell Laboratories
Murray Hill, New Jersey 07974

Abstract

The structures of noble gas compounds provide insight into the bonding between noble gas atoms and various ligands and into the electronic environment of the bound noble gas atoms. Structural knowledge of the free molecules is thus important in advancing theories of chemical bonding. Structures inferred from infrared, raman, visible, and ultraviolet spectroscopy, microwave spectroscopy, electron diffraction, Mossbauer measurements, nuclear magnetic resonance, x-ray and neutron diffraction, electric deflection, and thermodynamic measurements are compared for self-consistency and with theoretical calculations and predictions. The structure of XeF_6 has proved particularly elusive. Most physical measurements indicate that XeF_6 is not octahedral and that the F-Xe-F bond angles are not 90°. However, electric and magnetic deflection of molecular beams of XeF_6 have shown the absence of a static dipole moment and of significant electronic paramagnetism. Weakly bound noble gas molecules have been formed in hypersonic nozzles and examined using the molecular beam electric deflection techniques.

INTRODUCTION

From the inception of noble gas chemistry, physical measurements have played an indispensible role, partly in simply identifying species under study, but more importantly, in characterizing their properties. We may think of structure in the broadest terms as encompassing the spatial arrangement of atoms and the electronic environment surrounding these atoms responsible for the spatial array. In this paper, we direct attention to physical measurements which bear on the geometrical structures, emphasizing the technique of deflection of molecular beams by inhomogeneous electric fields, and using the structures of simple fluorides as examples.

Early speculations suggested that new concepts of bonding or compound formation might be required for noble gas molecules. Experience quickly showed, however, that the properties of these molecules could be correlated qualitatively by either valence bond or semiempirical molecular orbital methods (Malm, *et al.*, 1965). The electron pair repulsion theory has in fact proved very useful in describing the geometries of the known compounds (Gillespie, 1963 and Yamada, 1963).

Many structures of the simple molecules have been well established experimentally. For XeF_2, the band shape of the gas phase infrared active antisymmetric stretching motion, $\nu 3$, at 560 cm^{-1}, tells us the molecule is $D_{\infty h}$, linear and symmetric (Smith, 1963a and Reichman, *et al.*, 1969). The linear structure is confirmed by x-ray (Siegel, *et al.*, 1963) and neutron diffraction (Levy, *et al.*, 1963) studies of XeF_2. XeF_4 was shown by electron diffraction (Bohn, *et al.*, 1963) to be square planar, D_{4h}, consistent with gas phase infrared spectra (Claassen, *et al.*, 1963a), Raman spectra of the solid (Claassen, *et al.*, 1963a), neutron diffraction (Burns, *et al.*, 1963), and X-ray diffraction (Siegel, *et al.*, 1963; Ibers, *et al.*, 1963; and Templeton, *et al.*, 1963) measurements. The structure of KrF_2 is known to be analogous to that of XeF_2 from spectroscopic (Murchison, *et al.*, 1968) and electron diffraction (Harshbarger, 1967) measurements. The arrangement of linear molecules in the tetragonal cell has been shown by X-ray diffraction (Burbank, *et al.*, 1972). For $XeOF_4$, the microwave spectrum (Martins, *et al.*, 1964 and 1968), the vapor phase infrared spectrum (Smith, 1963b and Claassen, *et al.*, 1963b), the liquid phase Raman spectrum (Smith, 1963b and Claassen, *et al.*, 1963b), and high resolution nuclear magnetic resonance (Brown, *et al.*, 1963), all indicate C_{4v} symmetry for this molecule, with the xenon atom close to the plane of the fluorine atoms and the oxygen at the apex of the square pyramid. These geometries of the binary fluorides are predicted by semiemipirical molecular orbital treatments (Bordreaux, 1963; Lohr, *et al.*, 1963, and Jortner, *et al.*, 1963) as well as by the electron pair repulsion theory (Gillespie, 1963 and Yamada, 1963) which also predicts the geometry of $XeOF_4$.

The situation is less straightforward for XeF_6. XeF_6 has been subjected to three electron diffraction studies in the gas phase (Harshbarger, *et al.*, 1967; Gavin, *et al.*, 1968; and Hedberg, *et al.*, 1966) and intensive study by infrared, Raman, and other spectroscopy in all phases (Smith, 1963b; Claassen, *et al.*, 1972; and Kim, *et al.*, 1968). These experimental studies are not consistent with a simple static structure for XeF_6, and much thought has led to the conclusion that a dynamical description is needed for the actual configuration. The distortion may be viewed as a result of the role of the nonbonding electron pair in XeF_6. The valence shell of XeF_6 contains 14 electrons, only 12 of which are involved in Xe-F bonds. The electron pair would behave as a seventh ligand. In any of the structures in Figure 1, six of the black dots representing ligands would be fluorine atoms, the seventh would be the nonbonding pair. No matter which of these structures resulted, there would be a considerable distortion from octahedral O_h symmetry and a contradiction of the predictions of the simplest semiemipirical molecular orbital theory.

One might hope that an X-ray study of the XeF_6 molecule isolated in the solid state at a low temperature would resolve the structural question. However, the solid is a complex system, with four polymorphs (Jones, *et al.*, 1970): a cubic form stable from 90°K to the melting point, and an interconverting and coexisting series of two monoclinic and one orthorhombic modifications. XeF_6 exists either as hexameric rings or tetrameric rings

in the crystals (Jones, *et al.*, 1970; Burbank, *et al.*, 1971 and 1973; and Agron, *et al.*, 1965). No simple molecules have been observed. The rings are fluorine bridged, and the molecular units are far from being simple octahedra.

Because of the extensive intermolecular interaction, solid-state measurements are unlikely to provide a clean-cut molecular structure for XeF_6. Similarly, structural studies in the liquid are likely to be complicated by intermolecular interactions, especially since Raman (Gasner, *et al.*, 1967) and heat capacity (Schreiner, *et* al., 1969) data show that the liquid is associated. Therefore, we must rely on gas phase measurements of unperturbed molecules.

We have studied the behavior of molecular beams of XeF_6 and related molecules in an inhomogeneous electric field (Falconer, *et al.*, 1969). For those species where sophisticated spectroscopic techniques cannot be applied, or fail to provide an unambiguous interpretation, simply knowing whether or not a molecule possesses a permanent electric dipole can considerably narrow the range of possible structures. The electric deflection method is sensitive to dipole moments of around 0.01D for near symmetric tops, and can detect those of ClO_3F(0.02D) and CH_3D(0.005) unambiguously.

A schematic of the apparatus is shown in Figure 2. Molecules effuse from the source, O, and are detected by a high efficiency electron impact ionizer, mass spectrometer, and electron multiplier, MS. The direct line of sight between the source and the detector can be blocked by a stop wire S, and a large electric field can be imposed by the quadrupoles A and B. For polar molecules the signal is increased with applied electric field; for nonpolar molecules, a decrease is observed.

We have performed separate mass spectrometric measurements to show that XeF_6 is monomeric in the gas phase under the effusion source conditions. The electric deflection experiments show a decrease in signal, or defocusing for XeF_2, XeF_4, and XeF_6. An increase in signal or focusing is observed for $XeOF_4$. The results for XeF_2, XeF_4, and $XeOF_4$ are consistent with their known structures, discussed above. However, these observations argue against any static polar distortion in XeF_6. An analysis shows, equally, that the results argue against centrosymmetric inversions of polar structures, analogous to that in the ammonia molecule.

The electric deflection experiments do not define a structure for XeF_6. However, they do set interesting restrictions on allowable structures. Models consistent with these measurements have been proposed by *Burbank, et al.*, (1969), and by Bartell, *et al.*, (1968), who have independently hypothesized a dynamic molecular structure for XeF_6. The dynamic molecular structure for XeF_6. The dynamic structural concept is being further developed by Pitzer, *et al.*, (1973).

An alternate model to describe the observed physical properties of XeF_6 has been proposed by Goodman (1972). It suggests that XeF_6 vapor is a mixture of molecular isomers differing in electronic state and nuclear geometry. Some of these states are triplets and should be paramagnetic. However, neither magnetic susceptibility measurements on the solid or liquid (Selig, *et al.*, 1966), nor magnetic deflection experiments on molecular beams (Code, *et al.*, 1967), similar to the electric deflection measurements described above, were able to detect paramagnetic components in XeF_6. Thus, it is unlikely that electronic isomerism satisfactorily explains the structure of XeF_6. The dynamic structural approach appears more promising.

We have also used electric deflection and mass spectroscopy to examine noble gas molecules which are held together by a weak Van der Waals interaction. The experiments enable us to determine whether given systems are stable or nonstable, polar or nonpolar. We have expanded mixtures of noble gas atoms, fluorine atoms, and fluorine molecules together through hypersonic nozzles (Harris, *et al.*, 1973). Under the conditions of the experiment, the diatomics Xe_2, Kr_2, and Ar_2 were readily formed. With a room temperature source (no fluorine atoms), we observed the weakly bound systems Xe . . . F_2, Kr . . . F_2, and Ar . . . F_2. The mass spectral cracking pattern of Xe . . . F_2 was distinctly different from XeF_2 (chemically bound). Similar experiments using FCl have provided the molecules Ar . . . Cl -F and Kr . . . Cl -F. A diatomic molecule of Kr and F has also been observed. These experiments have enabled us to study thermodynamically stable, but physically unstable, species. They provide insight into potential functions and important experimental comparisons with sophisticated calculations. These experiments which are continuing will resolve questions of the stability of these species and will provide estimates of the amount of charge transfer involved in the weak bonds.

The above examples demonstrate that physical structural measurements of free molecules continue to advance our understanding of the chemistry of the noble gases which has excited the imaginations of scientists since the work of Cavendish, Ramsey, and Rayleigh.

REFERENCES

Agron, P. A., C. K. Johnson and H. A. Levy, (1965), Inorg, Nucl. Chem. Letters 1, 145.

Bartell, L. S. and R. M. Gavin, Jr., (1968), J. Chem. Phys. 48, 2466.

Bartell, L. S., (1967), J. Chem. Phys. 46, 4530.

Bohn, R. K., K. Katada, J. V. Martinez and S. H. Bauer, (1963), *Noble Gas Compounds,* H. H. Hyman, Ed. (U. of Chicago Press, Chicago, Ill., 1963), p. 238.

Bordreaux, E. A., (1963), *Noble Gas Compounds,* H. H. Hyman, Ed. (U. of Chicago Press, Chicago, Ill., 1963), p. 354.

Brown, T. H., E. B. Whipple and P. H. Verdier, (1963), J. Chem. Phys. 38, 3029.

Burbank, R. D. and N. Bartlett, (1968), Chem. Comm. 645.

Burbank, R. D. and G. R. Jones, (1970), Science 168, 248.

Burbank, R. D. and G. R. Jones, (1971), Science 171, 485.

Burbank, R. D. and G. R. Jones, (1973), J. Amer. Chem. Soc. in press.
Burbank, R. D., W. E. Falconer and W. A. Sunder, (1972), Science 178, 1285.
Burns, J.H., P.A. Agron and H.A. Levy, (1972), Science 139, 1208.
Cavin, R. M., Jr., and L. S. Bartell, (1968), J. Chem. Phys. 48, 2460.
Claassen, H. H., G. L. Goodman and H. Kim, (1972), J. Chem. Phys. 56, 5042.
Claassen, H. H., C. L. Chernick and J. G. Malm, (1963a), J. Amer. Chem. Soc. 85, 1927.
Claassen, H. H., C. L. Chernick and J. G. Malm, (1963b), *Noble Gas Compounds,* H. H. Hyman, Ed. (U. of Chicago Press, Chicago, Ill., 1963b), p. 287.
Code, R. F., W. E. Falconer, W. Klemperer and I. Ozier, (1967), J. Chem. Phys. 47, 4955.
Falconer, W. E., A. Buchler, J. L. Stauffer and W. Klemperer, (1968), J. Chem. Phys. 48, 312.
Gasner, E. L. and H. H. Claassen, (1967), Inorg. Chem. 6, 1937.
Gillespie, R. J., (1963), *Noble Gas Compounds,* H. H. Hyman, Ed. (U. of Chicago Press Chicago, Ill., 1963), p. 333.
Goodman, G. L., (1972), J. Chem. Phys. 56, 5038.
Harris, S. J., S. E. Novick, W. Klemperer and W. E. Falconer, (1973), Unpublished results.
Harshbarger, W., R. K. Bohn and S. H. Bauer, (1967), J. Amer. Chem. Soc. 89, 6466.
Hedberg, K., S. H. Peterson, R. R. Ryan and B. Weinstock, (1966), J. Chem. Phys. 44, 1726.
Ibers, J. A. and W. C. Hamilton, (1963), Science 139, 106.
Jones, G. R., R. D. Burbank and W. E. Falconer, (1970), J. Chem. Phys. 53, 6450 (1970); 53, 1605 (1970).
Jortner, J., E. G. Wilson and S. A. Rice, (1963), *Noble Gas Compounds,* H. H. Hyman, Ed. (U. of Chicago Press, Chicago, Ill., 1963).
Kim, H., H. H. Claassen and E. Pearson, (1968), Inorg. Chem. 7, 616.
Levy, H. A. and P. A. Agron, (1963), J. Amer. Chem. Soc. 85, 241.
Lohr, L. L., Jr. and W. N. Lipscomb, (1963), *Noble Gas Compounds,* H. H. Hyman, Ed. (U. of Chicago Press, Chicago, Ill., 1963), p. 347.
Malm, J. G., H. Selig, J. Jortner and S. A. Rice, (1965), Chem. Rev. 65, 199.
Martins, J. and E. B. Wilson, Jr., (1964), J. Chem. Phys. 41, 570.
Martins, J. and E. B. Wilson, Jr., (1968), J. Mol. Spectroscopy 26, 410.
Murchison, C., S. Reichman, D. Anderson, J. Overend and F. Schreiner, (1968), J. Amer. Chem. Soc. 90, 5690.
Pitzer, K. S. and L. Bernstein, (1973), personal discussion.
Reichman, S. and F. Schreiner, (1969), J. Chem. Phys. 51, 2355.
Schreiner, F., D. W. Osborne, J. G. Malm and G. N. McDonald., (1969), J. Chem. Phys. 51, 4838.
Selig, H. and F. Schreiner, (1966), J.Chem. Phys. 45, 4755.
Sieged, D. and E. Gebert, (1963), J. Amer. Chem. Soc., 85, 240.
Smith, D. F., (1963a), J. Chem. Phys. 38, 270.
Smith, D. F., (1963b), *Noble Gas Compounds,* H. H. Hyman, Ed. (U. of Chicago Press, Chicago, Ill., 1963b), p. 295.
Templeton, D. H., A. Zalkin, J. D. Forrester and S. M. Williamson, (1963), J. Amer. Chem. Soc. 85, 242.
Yamada, S., (1963), Rev. Phys. Chem. Japan 33, 39.

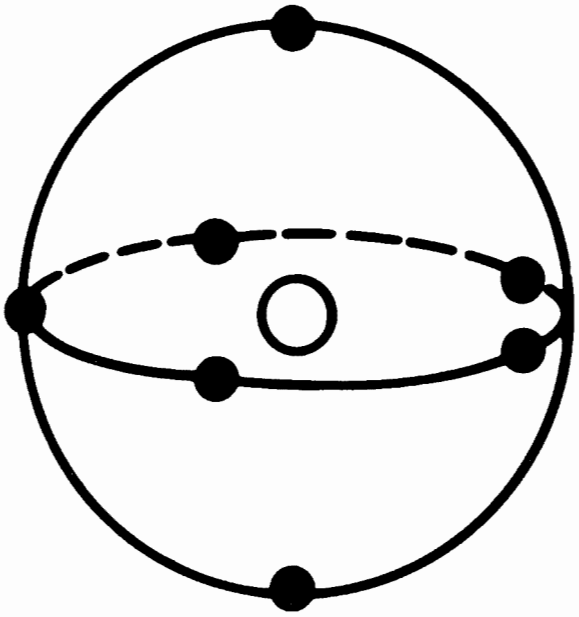

D_{5h}

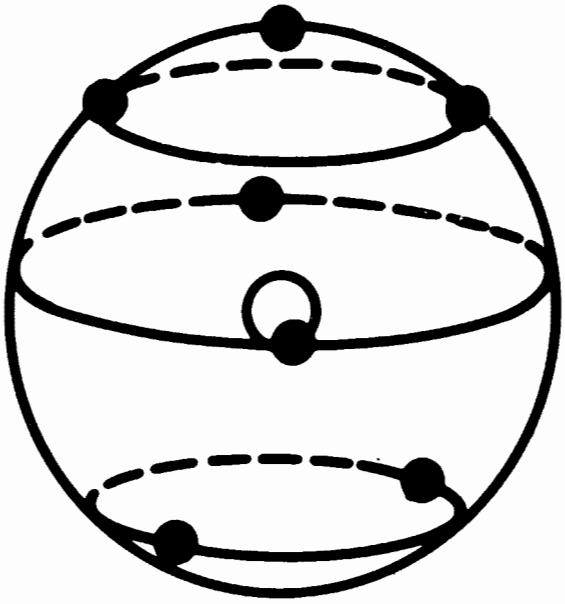

C_2

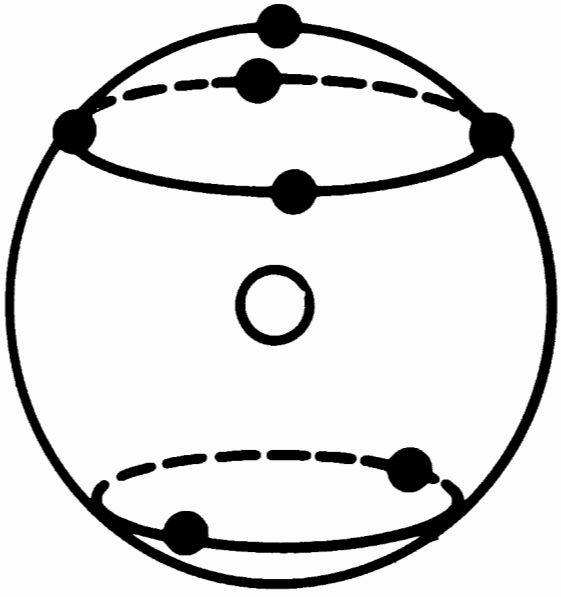

C_{2v}

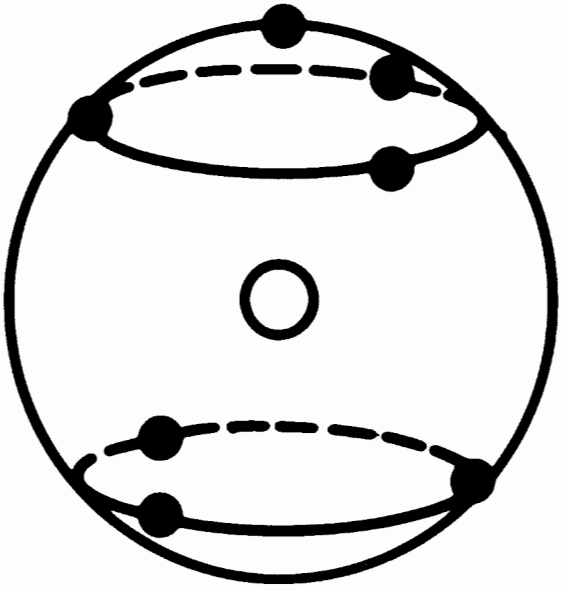

C_{3v}

Figure 1. Possible distorted structures for XeF_6.

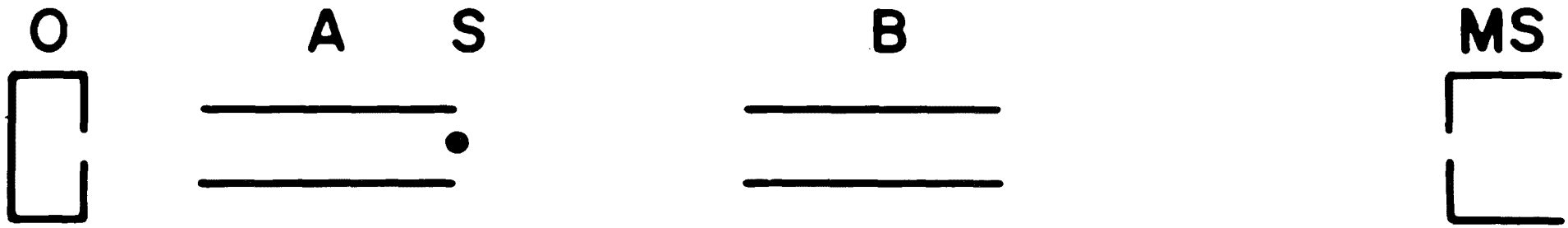

Figure 2. Schematic diagram of the electric deflection apparatus.

AN OVERVIEW OF THE PHYSICAL-CHEMICAL PROPERTIES OF THE NOBLE GASES

C. McKinley
Air Products and Chemicals, Inc.,
Allentown, Pennsylvania

Abstract

This paper lists the concentrations of noble gases in the atmosphere and the relative abundance of the stable isotopes. Selected physical properties are tabulated; solubilities of noble gases in water and other liquids, and liquid-vapor equilibria data for binary systems containing a noble gas are presented. Adsorption data are tabulated for illustrative conventional adsorbents and are also presented by a Polanyi correlation. Clathration, biochemical effects, and chemical reactivity are highlighted. Analytical procedures are briefly described. Other relatively non-reactive gases present in the atmosphere in trace quantitites are mentioned: methane, carbon tetrafluoride, and sulfur hexafluoride.

CONCENTRATION OF NOBLE GASES IN THE ATMOSPHERE

The five stable noble elements, which share a complete lack of activity towards many chemical reagents, range in atmospheric concentration from 9,340 ppm for argon to 0.086 ppm for xenon. The noble element concentration sequence, as seen in Table 1, is Ar > Ne > He > Kr > Xe > Ra. Radon, which has no stable isotopes, is present at an average concentration of about 6×10^{-14} ppm, but is quite variable in concentration, being exhaled from the earth's land masses (Junge, 1963).

The concentrations of neon, krypton, and xenon in the atmosphere should be quite constant with time while the concentrations of helium and argon may be changing. Helium, 5.24 ppm, is composed of two isotopes, ^{3}He and ^{4}He, which appear in the atmosphere in the ratio of about 1.2×10^{-6} (Junge, 1963; Mamyrin, *et al.*, 1970). ^{4}He is produced in almost equal parts by the decay of ^{238}U and ^{232}Th, and about 2% is due to decay of ^{235}U. ^{3}He is produced by cosmic-ray spallation reactions with ^{14}N in the atmosphere and by reactions with lithium and other elements in the lithosphere. Thus, helium is entering the atmosphere. It appears, however, that sufficient helium reaches escape velocity to somewhat stabilize the atmospheric content of helium for both isotopes. Atmospheric argon has been estimated (Moody, *et al.*, 1964) to increase through the decay of $^{40}_{19}K$ to $^{40}_{18}Ar$, the rate being such that the Ar concentration would rise about 1 ppm each 700,000 years.

Radon isotopes arise from decay of uranium and thorium. $^{222}_{86}Rn$, arising from uranium-238 (radium), is the dominant radon isotope in the atmosphere as its half-life of 3.8 days is significantly longer than that of the 59 second half-life of $^{220}_{86}Rn$ derived from the decay of thorium-232. The concentration of radon over land has been noted to be 2 orders of magnitude higher than over the ocean. Actual concentrations vary substantially with height and atmospheric condition. The recording in a noble gases concentration table of an average value for radon, thus, is an enormous simplification of the actual concentration distribution at any one time.

Naturally occurring isotopic concentration ratios are listed in Table 2.

PHYSICAL PROPERTIES OF THE NOBLE GASES

The noble gases are colorless, odorless, tasteless, monatomic, and non-reactive with all the usual chemical reagents. Perfect spherical symmetry results from the monatomic molecular structure and accounts for some of the interesting physical properties. The vapor pressures of the noble gases at the triple point are high, ranging from 0.4273 atm for Ne to 0.806 atm for Xe. The helium isotopes, indeed, cannot be frozen under their own vapor pressure; an external higher pressure must be supplied. Selected physical properties are listed in Table 3 (Kirk-Othmer, 1966 and Comprehensive Inorganic Chemistry, 1973).

The principle of corresponding states (Leland, *et al.*, 1968) is illustrated in excellent fashion by Ar, Kr, and Xe. The classical corresponding states principle (CSP), in which reduced parameters are obtained by dividing the particular temperature, pressure, and density by the corresponding critical values, is well-suited to the heavier noble gases. An illustration of this empirical CSP is shown in Figure 1, in which the reduced vapor pressures of the various gases are plotted as a function of the reciprocal of the reduced temperature. The experimental points for krypton and xenon are seen to fit the line obtained for the extensively studied gas, argon, quite well. The fit of the Rn data is not much better than for Ne, however, these data are quite old (1909), and the temperature scale is possibly the cause for the poor correlation. The deviation from the argon line is apparent for neon, is substantial for ^{4}He, and becomes greatest for the lightest element in the group, ^{3}He. To include these lighter noble gases, it is best to use theoretically based molecular parameters to obtain reduced variables. This allows the introduction of an additional parameter to account for the deviations from the classical behavior caused by quantum effects. P-V-T transport properties and other similar data can be obtained for Xe, Kr, and especially Rn from the extensively determined properties of Ar using CSP.

This useful tool should allow the establishment of radon properties which are difficult to measure because of its scarcity and radioactivity. Neon to some extent exhibits anomalous behavior at low temperatues caused by Quantum-mechanical effects; the two helium isotopes exhibit substantial anomalies. Critical point and normal boiling point properties for ^{3}He and ^{4}He differ substantially (see Table 3); these two isotopes have been

much studied because of their unique low temperature properties. (Helium is the only matter in the universe existing as a liquid below the triple point of hydrogen.)

Figure 2 illustrates trends in several noble gas properties as a function of atomic number. The critical properties, pressure, temperature, and density increase with increasing atomic number; however, ionization potential and minimum exitation energy decrease. He and Ne are seen to depart from the smooth curves, which fit the four larger molecules.

The Ar-Kr pressure-temperature projection, shown in Figure 3, is typical of a binary system which forms solid solutions in that the S-L-V locus is a smooth continuous curve connecting the respective triple points. Figure 4 is an isothermal section for this system at the temperature of the peak in the S-L-V curve. This pressure-composition diagram indicates the compositions of the various phases including the solubility or triple point composition. Such data are of theoretical interest because of the simplicity of the molecules, and are of practical use in the cryogenic separation of these gases.

ADSORPTION OF THE NOBLE GASES

Adsorption processes are used both in the production of noble gases and in the removal of trace quantities of radioactive noble gases from nuclear power plant vent gases. For activated carbon, silica gel, 5A and 13X zeolites, the affinity of the adsorbent for the noble gases increases with increasing molecular weight. This is shown in Table 4 which gives data for the adsorption of all of the noble gases except radon on activated carbon and 13X zeolite. (Silica gel and 5A zeolite capacities are similar to those for 13X.) Because of the limited amount of available data, there is some variation in temperature and pressure, but the trend of increasing capacity with molecular weight can be seen. As can be seen from the table, the helium and neon adsorption capacities are about two orders of magnitude lower than the capacities for argon, krypton, and xenon. Also, the capacity of the 13X zeolite for the noble gases is lower than that of activated carbon. In the case of the 4A zeolite, the krypton and xenon are excluded because of their size, while the argon capacity is reduced at temperatures below -165°C apparently because of a slight pore contraction. Argon, xenon, and krypton are excluded from 3A zeolite. Adsorption data for radon are not readily available. A review of the adsorption of noble gases is given by Cook (1961).

Figure 5 gives a correlation of adsorption data for krypton on activated carbon using the Polanyi technique.

Examples of the use of adsorption in the production of the noble gases are: the separation of helium-neon mixtures by neon adsorption on activated carbon, removal of oxygen from crude argon by adsorption on 4A zeolite, and separation of krypton-xenon mixtures using activated carbon. A description of these processes is given by Barron (1966). Activated carbon adsorbers are also being considered to remove or reduce trace radioactive krypton and xenon impurities from nuclear power plant vent gases. A review of this work is given by Kovach (1970).

CLATHRATION

The noble gases, as "guest" molecules, may be trapped in crystalline cages formed by "host" molecules. Water, hydroquinone, and phenol have been found to be such "hosts' for clathration of the noble gases. Examples of several such crystalline structures are given in Table 5 along with some of the observed properties. The heat of formation of the clathrates is relatively low. If one subtracts from the heat of formation of the Kr and Xe hydrates an approximated 8.3 kcal, representing crystallization of 5.75 gm moles of H_2O, one obtains 5.6 and 8.4 kcal, respectively, per gm atom of noble gas, which values correspond approximately to the heats of adsorption of the same gases. The forces which hold the noble gas in the hydrate are seen to be of the same order as Van der Waals bonding forces (Cook, 1961).

Bartlett, *et al.*, (1973) provide an excellent summary of the noble gas clathrates.

SOLUBILITY

The solubility of the noble gases in water is shown in Figure 5 for the temperature range 0 to 70°C and at atmospheric pressure. The solubility increases with increasing atomic number. The two smallest molecules, helium and neon, exhibit a minimum solubility in the temperature range illustrated.

PHYSIOLOGICAL AND BIOCHEMICAL EFFECTS

The noble gases, although chemically inert, do affect living systems when present in sufficient concentrations. The effects upon living systems increase with increasing molecular weight for several of the phenomena. Narcosis is sufficiently strong with xenon that surgery has been conducted at atmospheric pressure using 80%Xe:20%O_2 as the anesthetic. The depth of anesthesia obtained with xenon is intermediate between nitrous oxide and ethylene. Krypton exhibits slight narcosis at atmospheric pressure; several atmospheres partial pressure of krypton would probably be required to induce deep anesthesia and even higher pressures with argon. Helium has been used to replace nitrogen in breathing atmospheres for work at several hundred feet depth in the ocean with no narcotic effects, these depths being such that nitrogen narcosis would have been a severe problem.

Helium-oxygen mixtures for breathing have found utility also in medicine, in aviation, and in other operations under pressure.

Members of the noble gas family have been studied, in addition to their applications in breathing mixtures and in medicine, for effects upon metabolism, upon responses to stimuli and upon oxygen-dependent sensitivity to radiation. Cook (1961) provides an excellent historical summary of noble gas related biological research.

CHEMICAL REACTIONS

Bartlett (1962) reported the interaction of xenon with platinum hexafluoride to form a red solid of composition $Xe(PtF_6)_x$. Interest in noble gas compounds spread very rapidly; shortly a large number of brief communications appeared in the literature followed by several excellent reviews: Hyman (1963), Moody (1964), Holloway (1969), Horn (1970), Jha (1970), Geovold (1972), and Bartlett (1972). Many compounds containing xenon have been prepared and their properties measured; only a few containing krypton and radon have been made. Moody's (1964) summary listed 24 compounds containing xenon, 2 containing krypton, and 1 containing radon.

ANALYTICAL PROCEDURES

Frequently noble gas samples contain one or more of the noble gases in very low concentration and, as a consequence, extraordinary precaution must be taken to ensure that the sample is initially collected in a fashion to be truly representative. Further, care must be taken that adsorption and/or absorption do not bring about composition changes. With appropriate handling care one can select an analytical procedure to fit the specific requirement. Gas chromatography is very useful, allowing separation of all the noble gases and their determination to very low concentration levels; mass spectrometry is particularly effective in stream monitoring for specific masses and for determination of isotope ratios; emission spectroscopy is valuable in stream monitoring of a high-purity inert gas for the presence of a trace of an impurity (Cook, 1961 and Schmauch, 1971). Radioactivity measurements are useful to supplement analysis by chromatography or mass spectrometry when radioactive isotopes are present. It is necessary to ensure that the radiation being counted is uniquely from the isotope of interest. Gibbs (1973) describes a portable radon monitoring instrument, and the techniques for avoiding background radiation and radiation from radon-daughters.

OTHER RELATIVELY NON-REACTIVE GASES IN THE ATMOSPHERE

Man's activities have resulted in the introduction into the atmosphere of some gases which will have a relatively long life in the atmosphere. Sulfur hexafluoride is an interesting example. Clemens (1968), based on production and consumption data provided by manufacturers and users, has estimated that the worldwide average concentration of SF_6 should be at least 10^{-7} ppb. He found that a number of samples of air taken in and around Cincinnati, Ohio ranged from 0.04 to 0.20×10^{-3} ppb, and that no sample taken was free of SF_6. SF_6 lends itself to use in meterological tracing because of its chemical inertness. SF_6 concentration in air can be measured down to a sensitivity of 1×10^{-5} ppb by a gas chromatography procedure using an electron capture detector. The SF_6 content of the air sample is concentrated by adsorption onto charcoal at a low temperature, and then is desorbed for introduction to the chromatograph. The technique has been used to trace air movements over distances of 75 miles with a release rate of SF_6 of about one pound per minute for an hour.

Methane, although an unusually stable hydrocarbon, in contrast to sulfur hexafluoride, has a relatively short atmospheric life estimated to be in the range of 10 to 20 years (Ehhalt, 1967 and Wofsy, 1972). A very large fraction of the methane entering the atmosphere is from decomposition of organic material at the earth's surface. The sinks for methane are not well understood. Electrical discharges, photolysis of methane and bacterial action may be involved. The generation rate is of the order of 3×10^{14} grams per year. Whatever the sinks are, they effectively reduce the methane concentration in the atmosphere to the relatively constant average of about 1.2 to 1.6 ppm (Cavanagh, *et al.*, 1969). The generation rate, with no sinks, would increase the atmospheric concentration of methane about 0.1 ppm per year.

Carbon tetrafluoride, a very stable molecule, is present in the atmosphere at very low concentrations. CF_4 has entered the atmosphere through its production and use, and probably also to a significant extent through the venting of fluorine to the atmosphere through carbon beds. The concentration of CF_4 in the atmosphere can be estimated from its appearance during commercial production of krypton and xenon. CF_4 boils between Kr and Xe, the normal boiling points being Kr 119.8°K, CF_4 145.1°K, and Xe 165°K. Hence, in the fractionation process CF_4 is concentrated in the intermediate fraction between the pure Kr and pure Xe. From a material balance around the entire distillation process, it is possible to calculate the CF_4 concentration in the air feed to the air separation plant. In the spring of 1966, the air feed to the separation plant described in G. G. Handley's paper at this Symposium was found to contain about 2.3×10^{-5} ppm by volume of CF_4. A few months later, in the early fall, the concentration of CF_4 in the air feed was calculated from material balances around the krypton-xenon recovery unit to be 2.7×10^{-5} ppm. CF_4 has also been found in krypton and in xenon produced in other parts of the world. One must conclude that it is distributed throughout the atmosphere, although we do not have information on its concentration variability.

REFERENCES

Barron, R., (1966), Cryogenic Systems, pp. 243-255, McGraw Hill Book Company.

Bartlett, N., (1962), Proc. Chem. Soc., 218.

Bartlett, H. and F. O. Sladky, (1973), *The Chemistry of Krypton, Xenon, and Radon,* Pergamon Press, Chapter 6.

Brunaur, S., (1945), *The Desorption of Gases and Vapors,* 1, p. 58, Princeton Univ. Press.

Cavanagh, L. A., C. F. Schadt, and E. Robinson, (1969), (Stanford Research Institute, Menlo Park, California). Envir. Sc. Tech. 3 (3) 251-7. *Atmospheric Hydrocarbon and Carbon Monoxide Measurements at Point Barrow, Alaska.*

Clemens, C.A., A. I. Coleman and B. E. Seltzman, (1968), (National Center for Air Pollution Control, Public Health Service, Cincinnati, Ohio). Envir Sc. Tech. 1968, 2 (7), 551-6 (Eng.), (C. A. Volume 69, p. 3618, 38525 n).

Cockett, A. H. and K. C. Smith, (1973), *The Monatomic Gases: Physical Properties and Production.* Comprehensive Inroganic Chemistry. Pergamon Press, Chapter 5.

Cook, G. A., (1961), *Argon, Helium and The Rare Gases.* Interscience Publishers, New York (394 pages in Volume I; 395-818 pages in Volume II).

Ehhalt, D. H., (1967), *Methane in the Atmosphere.* J. Air Pollution Control Assoc. 17 (No. 8) 518-9.

Fastovskii, V. G., *et al.*, (1958), Zhur. Prklad. Khim., 31, (1) pp. 5-13.

Geodvold, J. G., (1972), *Noble Gases and Their Compounds,* Chem. Tech. (Amsterdam) 1972, 27 (4), 89-92 (Neth.) (C. A. 76 (1972), 161706u).

Gibbs, H. L. and J. H. Bilbrey, Jr., (1973), *Development of a Portable Radon Detector,* Bureau of Mines Report of Investigations 7741.

Grant, R. and M. Manes, (1964), M. I & EC Fund, 3, p. 221.

Gray, R. W., and W. J. Ramsay, (1909), J. Chem. Soc. 95: 1073.

Heastie, R., (1955), Nature 176: 747-8.

Holloway, J. H., (1968), Methuen: London), *Noble-Gas Chemistry,* 213 pp. (C. A. 70 (1969) p. 294, 102658 h).

Horn, H. G., (1971), (Gmelin-Inst. Max-Planck-Gess., Frankfurt/Main., Ger.), Chem.-Ztg., Chem. App. (1970, 94 (16), 600-7 (Ger). (C. A. 74 p. 9133, 9119 F).

Hyman, H. H., (1963), *Noble Gas Compounds,* The University of Chicago Press, Chicago, 404 pages.

Jha, N. K., (1970), (Dep. Chem., Indian Inst. Technol. New Delhi, India). *Chemistry of Noble Gas* Compounds, Proc. Chem. Symp., 1st 23-26 Sep. 1969, 1, 165-71 (Eng).

Junge, C. E., (1963), *Air Chemistry and Radioactivity,* Academic Press, New York, 382 pages.

Kirk-Othmer, (1966), *Encyclopedia of Chemical Technology,* Second Ed. Volume 10, p. 862-894.

Kovach, J. L., (1970), *North American Carbon R&D Report No. 010005.*

Leland, T. W. and P. J. Chappelear, (1968), Ind. Eng. Chem. 60 (7): 15-43.

Loosli, H. H., H. Oeschger, and W. Wiest, (1970), (Phys. Inst., Univ. Bern, Bern, Switz.). J. Geophys. Res. 1970, 75 (15), 2895-900 (Eng). *Argon-37, Argon-39, and Krypton-81 in the Atmosphere and Tracer Studies Based on These Isotopes.*

Mamyrin, B. A., G. S. Anufriev, I. L. Kamenskii, and I. N. Tolstikhin, (1970), (Phys. Tech. Inst., Leningrad, USSR). Geokhimiya 1970 (6) 721-30 (Russ).

Moody, G. J. and J. D. R. Thomas (1964), *Noble Gases and Their Compounds,* The MacMillan Company, New York, 62 pages.

Penchev, N. P., (1970), (Institute of General and Inorganic Chemistry, Bulgarian Academy of Sciences, Sofia, Bulgaria). Izv. Otd. Khim. Nauki, Bulg. Akad. Nauk. 1970, 2 (3), 607-18 (Eng). *Contribution to the Analysis and the Geochemistry of the Noble Gases.*

Schmauch, G., (1971), *Encyclopedia of Industrial Chemical Analysis,* Volume 13, pages 286-309, Gases, Noble.

Sherman, R. H., S. G. Sydoviak, and T. R. Roberts (1964), J. Res. NBJ, 68A (6): 579-588.

Stein, S. A., *et al.*, (1962), Arnold Engineering Development Center, USAF, TDR-62-200.

Von Antropoff, A., *et al.*, (1952), Kollid;Zeitschrift, 129, pp. 1-10.

Wagner, W., (1973), Cryogenics 13 (8): 470.

Wofsy, S. C., J. C. McConnell, and M. B. McElroy, (1972), (Smithsonian Astrophys. Obs., Cambridge, Mass.). J. Geophys. Res., 77 (24), 4477-93 (Eng). *Atmospheric Methane, Carbon Monoxide, and Carbon Dioxide.*

TABLE 1. Concentration of Noble Gases in the Atmosphere (Kirk-Othmer, 1966).

Element	Symbol	Atomic Number	Atmospheric Concentration ppm by Volume (Dry Air)
Helium	He	2	5.24
Neon	Ne	10	18.18
Argon	Ar	18	9,340
Krypton	Kr	36	1.14
Xenon	Xe	54	0.086
Radon	Rn	86	6×10^{-14}

TABLE 2. Naturally Occurring Isotopic Abundance of the Noble Gas Elements (Schmauch, 1971).

Element	Atomic Number	Mass Number	Abundance, Atom %
He	2	3	0.00013
		4	99.9999
Ne	10	20	90.92
		21	0.257
		22	8.82
Ar	18	36	0.337
		38	0.063
		40	99.600
Kr	36	78	0.354
		80	2.27
		82	11.56
		83	11.55
		84	56.90
		86	17.37
Xe	54	124	0.096
		126	0.090
		128	1.919
		129	26.44
		130	4.08
		131	21.18
		132	26.89
		134	10.44
		136	8.87
Rn	86		no stable isotopes

TABLE 3. Physical Properties of the Noble Gases (a) (Kirk-Othmer, 1966).

Property	Units	Elements						
		^{3}He	^{4}He	Ne	Ar	Kr	Xe	Rn
Atomic number	^{12}C=12	2	2	10	18	36	54	86
Atomic weight	^{12}C=12	3.0160	4.0026	20.183	39.948	83.80	131.30	222
Critical Point:								
temperature	°K	3.324	5.199	44.40	150.86	209.4	289.74	378
pressure	atm	1.149	2.261	26.19	48.34	54.3	57.64	62
density	g/ml	0.0413	0.0693	0.483	0.536	0.908	1.100	
Normal boiling point (nbp)	°K	3.1905	4.215	27.09	87.28	119.80	165.04	211
Triple point (tp):								
temperature	°K	no tp	no tp	24.54	83.81	115.77	161.38	202
pressure	atm	no tp	no tp	0.4273	0.6800	0.7220	0.806	(0.7)
Densitv:								
gas, 1 atm, 273.15°K	g/liter	0.1347	0.17850	0.90002	1.78380	3.7493	5.8971	9.73
gas, nbp	g/liter	23.64	16.714	9.552	5.763	8.6	11	
liquid, nbp	g/ml	0.0589	0.1249	1.206	1.3936	2.415	3.057	4.4
liquid, tp	g/ml	no tp	no tp	1.247	1.418	2.451	3.076	
solid, tp	g/ml	no tp	no tp	1.444	1.623	2.826	3.540	
Gas/liquid vol ratio (b)		437.4	700	1,340	781	644	518	452
Heat of vaporization at nbp	cal/g-mole	6.09	19.4	429	1,550	2,154	3,020	4,325
Heat of fusion at tp	cal/g-mole	no tp	no tp	80.1	283	392	548.5	776
Heat capacity at constant pressure:								
gas, 1 atm, 25°C	cal/g-mole)(°K)	(4.968	4.968	4.969	5.969	5.008	5.022	(5)
liquid, nbp (c)	cal/g-mole)(°K)	4.0	4.33	8.9	10.9	10.6	10.65	
Sonic velocity:								
gas, 1 atm, 0°C	m/sec	(1,122)	974	433	307.8	213	168	
Thermal conductivity:								
gas, 1 atm, 0°C	cal/(sec)(cm^2)(°K/cm)	(391)	339.0	110.1	40.5	20.9	12.1	
liquid, nbp	cal/(sec)(cm^2)(°K/cm)	51	75	310	290	211	175	
Viscosity:								
gas, 1 atm, 25°C	μP	(172)	198.5	317.3	226.4	253	231.0	233.2
liquid, nbp	mP	0.0161	0.030	1.24	2.75	4.31	5.28	
First ionization potential	eV		24.586	21.563	15.759	13.999	12.129	10.747
Min excitation energy	eV		19.818	16.618	11.548	9.915	8.315	6.772

(a) Numbers in parenthesis are estimated.
(b) Volume of gas at 1 atm and 273.15°K (O°C) equivalent to unit volume liquid at nbp.
(c) Heat capacity of saturated liquid.

TABLE 4. A Comparison of Adsorption Capacities of Noble Gases on Activated Carbon and Zeolite Type 13X.

	Activated Carbon			Zeolite		
Gas	**Temp °C**	**Press mmHg**	**Capacity ml*/g**	**Temp °C**	**Press mmHg**	**Capacity ml*/g**
He	-190	100.00	0.28 (a)	-250	0.5	5.6 (c)
Ne	-195	1.0	1.14 (a)		**	
Ar	-196	1.0	224 (b)	-183	0.8	80 (a)
Kr	-170	0.8	242 (a)	-183	0.018	47 (a)
Xe	-170	0.03	230 (a)	-183	0.09	84 (a)

* ml of gas at O°C and 1 atm pressure per gram of adsorbent.
**No data were found for neon adsorption on zeolites.
(a) (Cook, 1961)
(b) (Grant, *et al.*, 1964)
(c) (Stein, *et al.*, 1962)

TABLE 5. Noble Gas Clathrates With Water, Hydroquinone and Phenol (d)(e).

Formula		Noble Gas, wt %		Heat of Formation kcal mole^{-1}	Decomposition Temp, °C at one atm. press.	Dissociation Pressure, atm., at 0°C
Theoretical	Observed	Theoretical	Observed			
$8Ar.46H_2O$	$Ar.6H_2O$	27.8	~27		-42.8	105
$8Kr.46H_2O$	$Kr.6H_2O$	44.7	~44	13.9 (a)	-27.8	14.5
$8Xe.46H_2O$	$Xe.6H_2O$	56.0	~53	16.7 (a)	- 3.4	1.5
$8Rn.46H_2O$		68.2				
$Ar.3C_6H_4(OH)_2$	$0.8Ar.3C_6H_4(OH)_2$	10.8	8.8	5.1 (b)		
$Kr.3C_6H_4(OH)_2$	$0.74Kr.3C_6H_4(OH)_2$	20.3	15.8			
$Xe.3C_6H_4(OH)_2$	$0.88Xe.3C_6H_4(OH)_2$	28.5	26.0			
$4Ar.12C_6H_5OH$	$2.92Ar.12C_6H_5OH$	12.4	9.4	9.85 (c)		33
$4Kr.12C_6H_5OH$	$2.92Kr.12C_6H_5OH$	22.9	18.0	8.97 (c)		6
$4Xe.12C_6H_5OH$	$4Xe.12C_6H_5OH$	31.8	31.8	8.8 (c)		1

(a) Heat of formation based on composition ratio of (one atom noble gas) (5.75 H_2O).
(b) Heat of formation based on composition ratio of (one atom noble gas) ($3C_6H_4(OH)_2$).
(c) Heat of formation in the range of 0° to 40°C, kcal per gm atom of inert gas absorbed.
(d) (Cook, 1961).
(e) (Kirk-Othmer, 1966).

Figure 1.

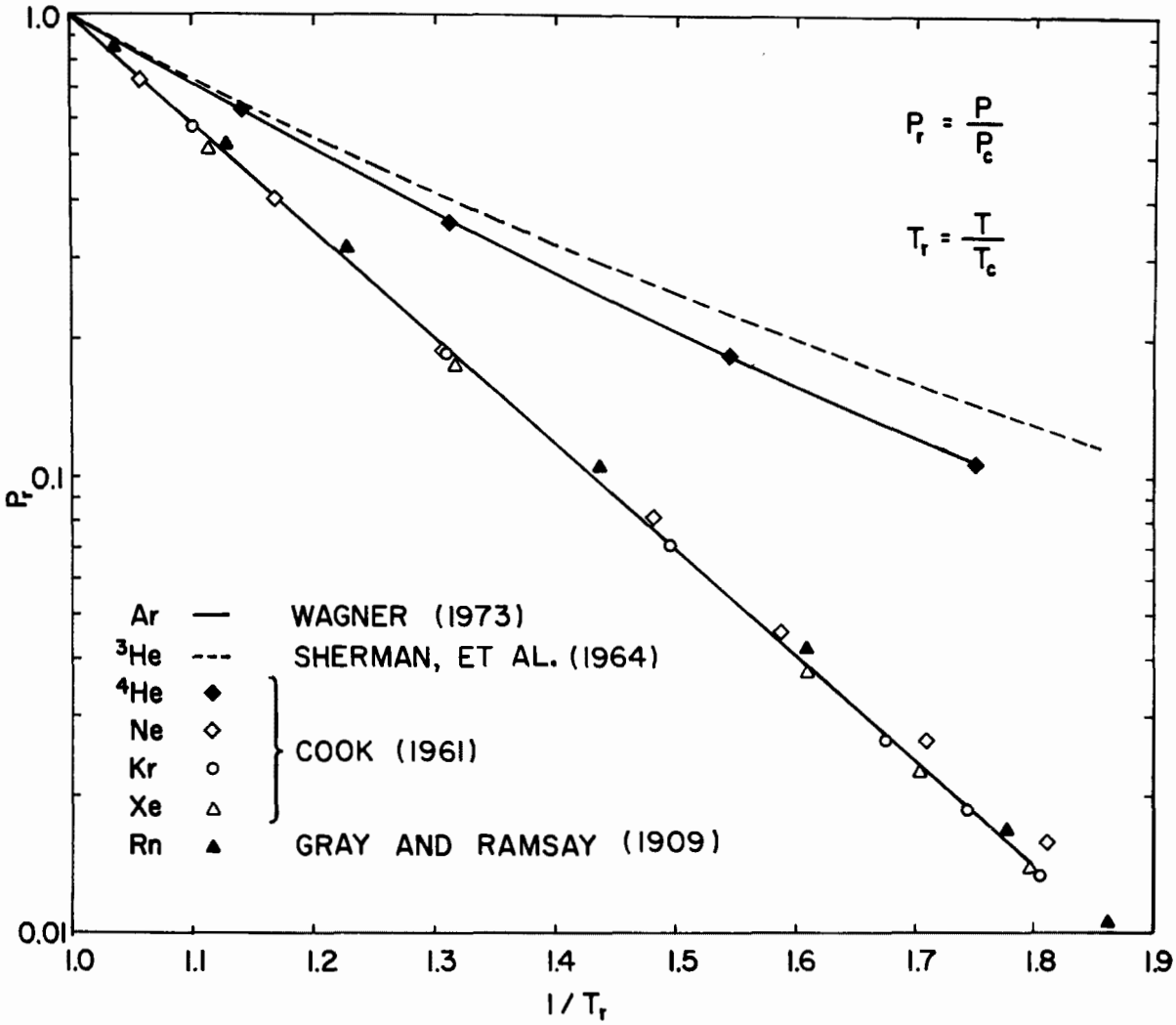

REDUCED VAPOR PRESSURE CURVES
OF THE NOBLE GASES

Figure 2.

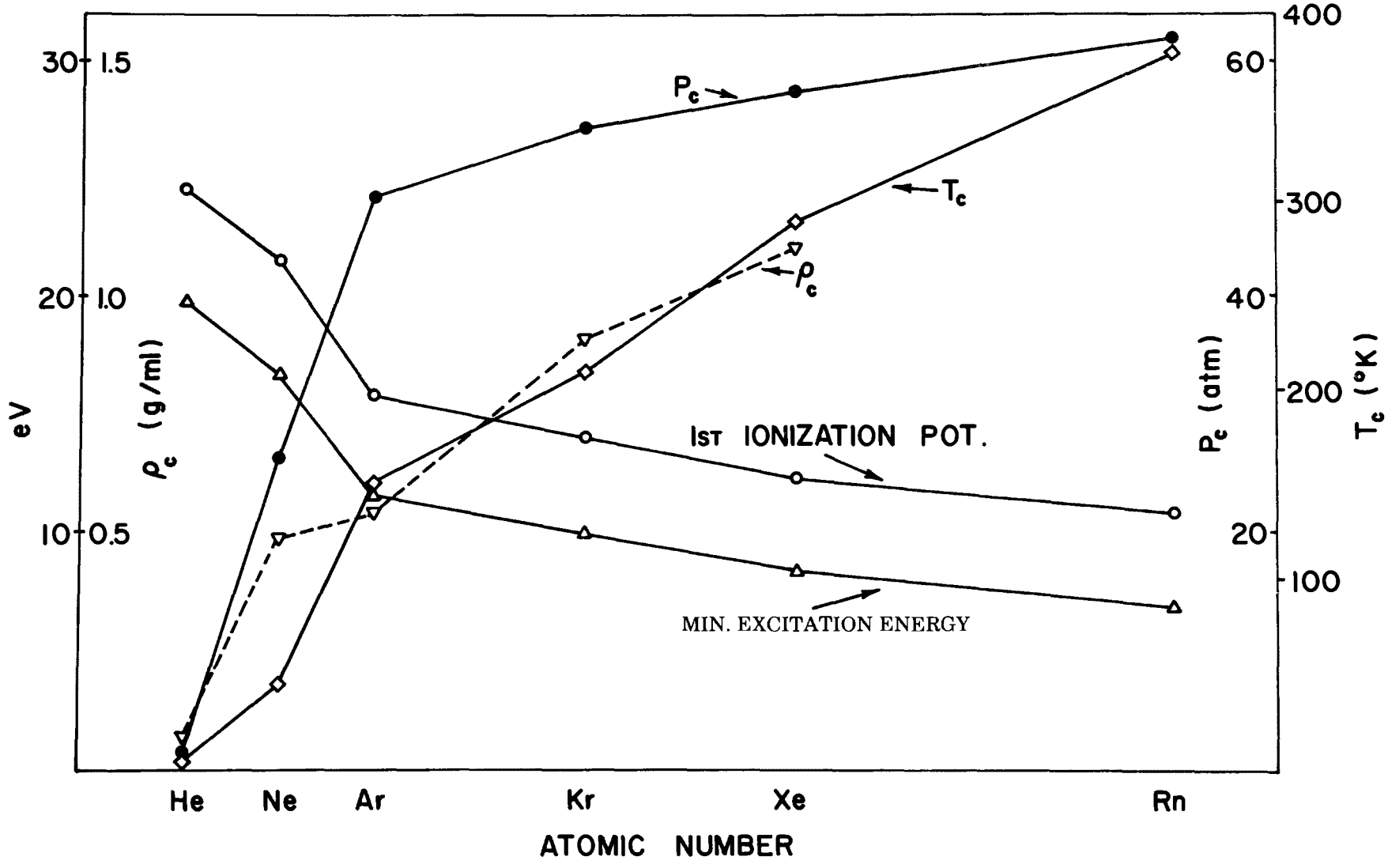

TRENDS IN SELECTED NOBLE GAS PROPERTIES

Figure 3.

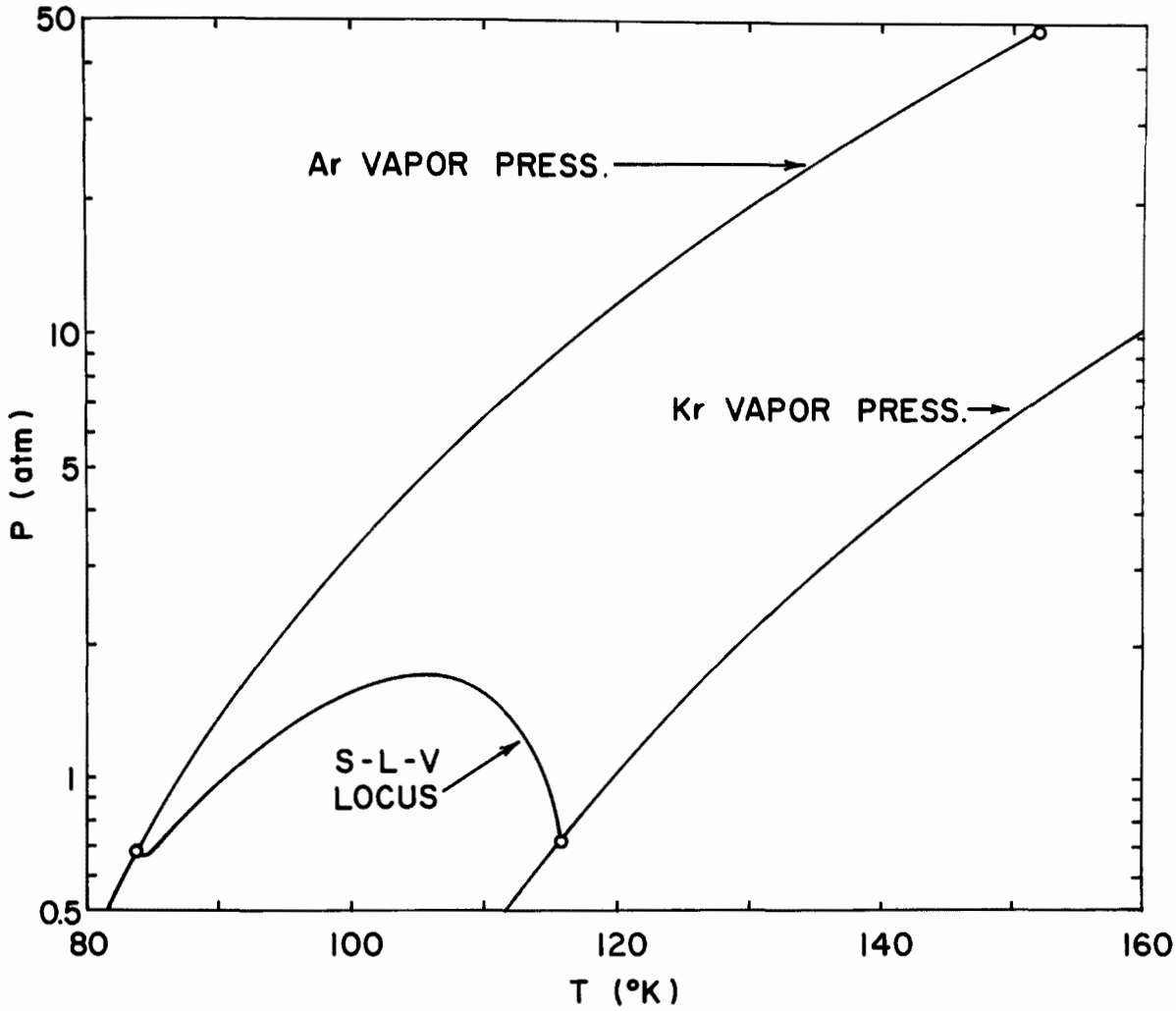

SIMPLIFIED PRESSURE-TEMPERATURE PROJECTION
FOR THE Ar-Kr SYSTEM

Figure 4.

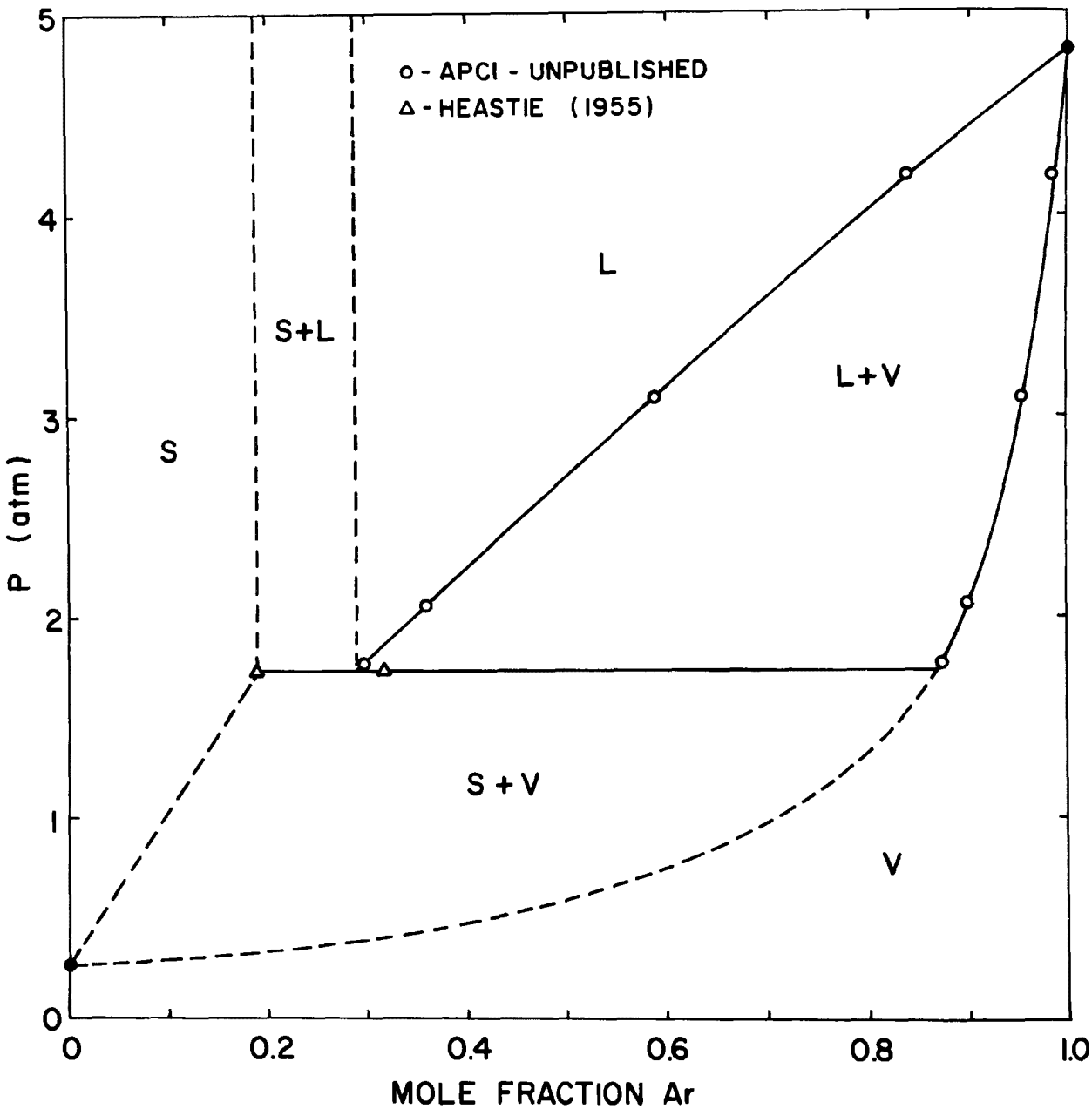

ISOTHERMAL SECTION FOR THE Ar-Kr BINARY AT 105.3 °K

Figure 5.

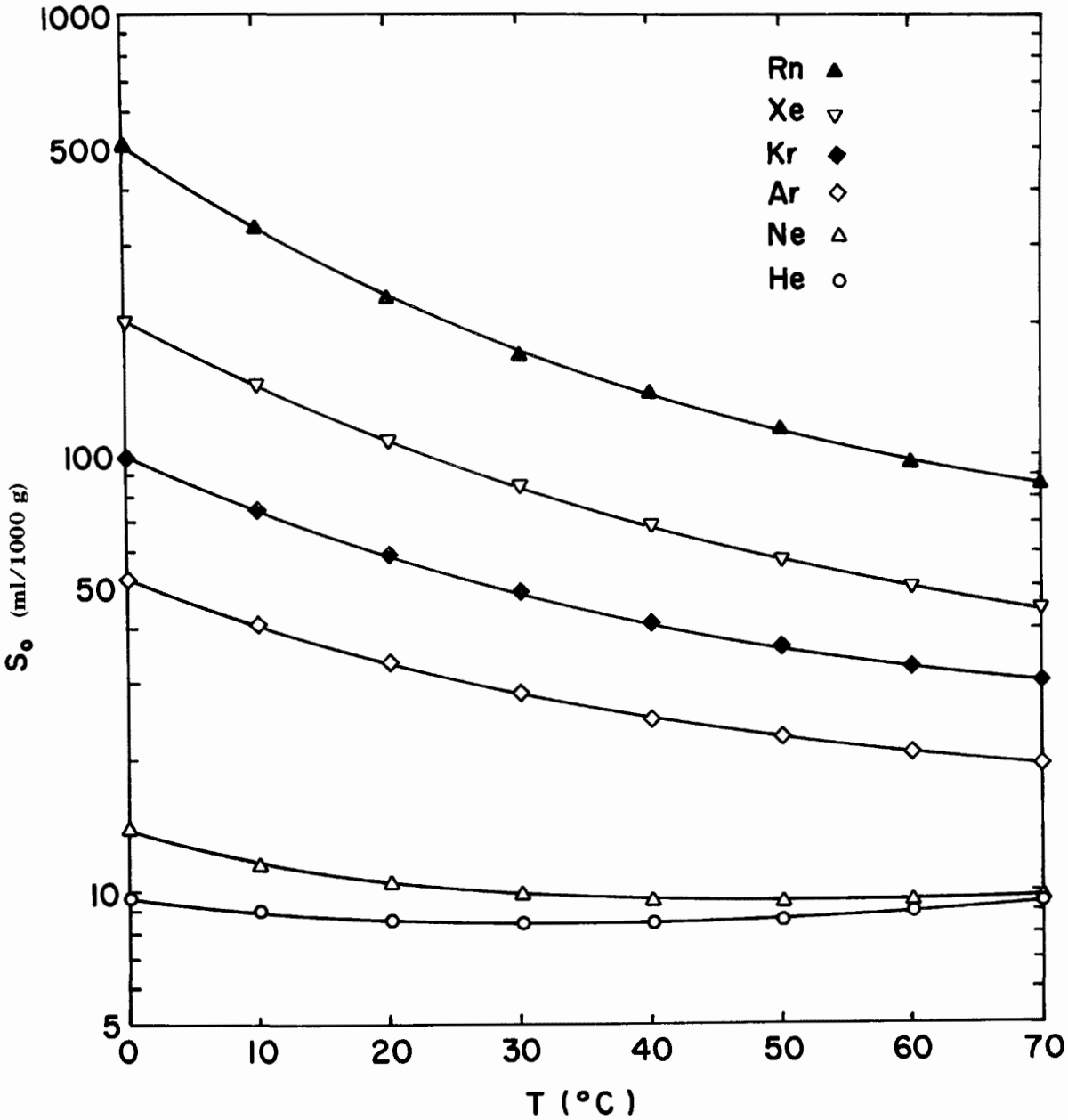

SOLUBILITY OF NOBLE GASES IN WATER

Figure 6.

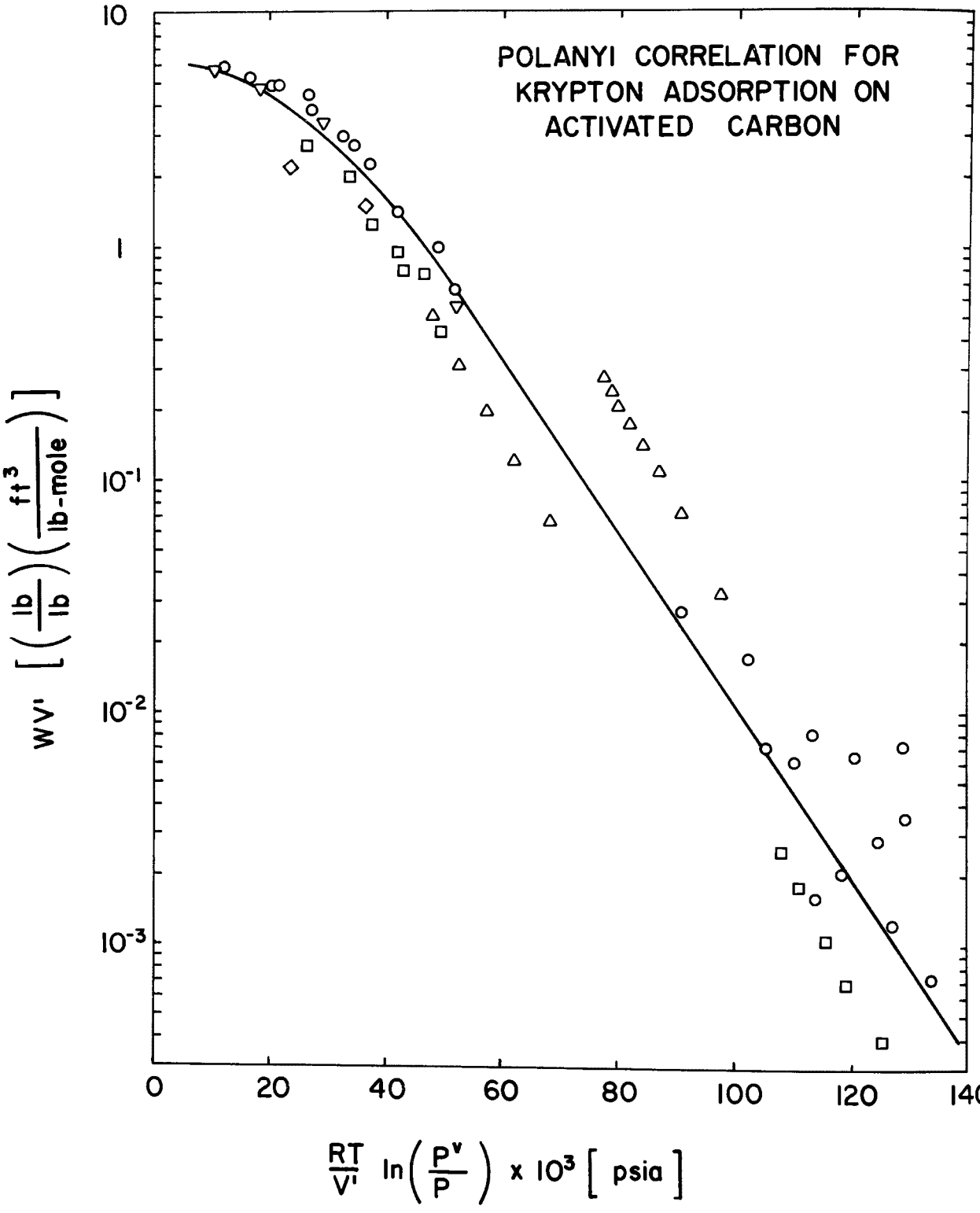
POLANYI CORRELATION FOR
KRYPTON ADSORPTION ON
ACTIVATED CARBON
10
1
10^{-1}
10^{-2}
10^{-3}
$WV' \left[\left(\frac{lb}{lb}\right)\left(\frac{ft^3}{lb\text{-}mole}\right)\right]$
0
20
40
60
80
100
120
140
$\frac{RT}{V'} \ln\left(\frac{P^v}{P}\right) \times 10^3 \left[\text{psia}\right]$

A TEST OF INTERMOLECULAR POTENTIALS FOR THE NOBLE GASES BY COMPARISON WITH EXPERIMENTAL THERMAL DIFFUSION FACTORS

W. L. Taylor
Monsanto Research Corporation
Mound Laboratory*
Miamisburg, Ohio 45342

Abstract

The description of the equilibrium and transport properties of dilute gases follows from a knowledge of the pair interaction energy of the gas particles. We have used a second order effect, the thermal diffusion factor, which is extremely sensitive to the intermolecular potential, as a test of various potentials which have been proposed for the noble gases. Measurements of the thermal diffusion factor were made over a wide range of temperatures in a trennschaukel; and these results, along with other values reported in the literature, were fitted to empirical equations within the experimental uncertainties. Many proposed intermolecular potentials, including some recently obtained from solid state properties and molecular beam scattering, were used to calculate transport collision integrals and thence theoretical thermal diffusion factors which were compared to the empirical equations. In the case of helium, quantum mechanical calculations were made. The "best" potentials for each noble gas were then used to evaluate other macroscopic properties of the homologues.

INTRODUCTION

Knowledge of the intermolecular forces between atoms and molecules can be obtained from both experimental observations and theoretical considerations. However, the successful determination of the interaction forces from empirical data requires the existence of an accurate theoretical description of the physical property, and further requires that the measurements be made in a temperature (or relative kinetic energy) region which is "sensitive" to the intermolecular potential. Traditionally, the properties of dilute gases or those of the crystal lattice have been employed because of the existence of rigorous theoretical treatments. More recently, primarily due to improved experimental techniques, the powerful method of molecular beam scattering to obtain total and differential scattering cross sections has been added to the list. From the practical point of view, once the intermolecular potential has been accurately determined by whatever method, other properties required, for example in engineering applications, can generally be calculated without the need for extensive experimental measurements.

In the present work, we have used one of the transport properties of the dilute gas, the thermal diffusion factor, as the empirical test. Thermal diffusion is especially well suited for this task because transport properties of monatomic dilute gases are very adequately described by the rigorous kinetic theory of Chapman and Enskog, plus the fact that thermal diffusion, being a second-order effect, is the most sensitive to the interaction.

The major drawback to measuring thermal diffusion factors lies in the fact that the effect is very small, particularly for isotopes; and, in fact, was predicted theoretically before it was observed experimentally. Essentially, the measurement consists of determining the isotopic separation in a temperature gradient. There are three basically different methods or types of apparatus that can be used for making the experimental measurement: (a) the thermogravitational column; (b) "two-bulb" apparatus; and (c) the trennschaukel or "swing separator". In the first method the separations are large, a great advantage, but it is difficult to operate a column over an extended temperature range; and theoretical treatment of the column behavior is complicated because of the convective flow caused by the horizontal temperature gradient. The "two-bulb" apparatus suffers from the fact that the separation is very small. We have chosen the trennschaukel, developed by Clusius and Huber (1955), as the preferred method for the present work because it cascades the single stage separation of the "two-bulb"; and a rigorous theoretical treatment of its operation has been given by van der Waerden (1957).

Of the noble gases, far more experimental determinations have been conducted on helium and neon than on argon, krypton, or xenon. Unfortunately, much of the data are widely scattered; and in some cases it is felt that systematic experimental errors are present. We have measured the temperature dependence of the isotopic thermal diffusion factor of the noble gases from approximately 200 to 900°K, and in the case of helium the temperature range was extended down to 5°K. In addition, a wide variety of proposed intermolecular potentials were selected for evaluation. The transport collision integrals were evaluated and used to compute theoretical thermal diffusion factors which were compared to the experimental data. Quantum mechanical calculations were used for helium at low temperatures and classical theory for the heavier gases.

**Mound Laboratory is operated by Monsanto Research Corporation for the U.S. Atomic Energy Commission under Contract No. AT-33-1-GEN-53.*

EXPERIMENTAL

The experimental appartus utilized for the present work is shown schematically in Figure 1. The trennschaukel (C) consists of 20 Inconel tubes heliarc welded into two massive nickel blocks of toroidal shape with each tube connected top to bottom with an Inconel capillary. The top end of the first tube and the bottom end of the twentieth tube are connected to either end of a microbellows pump mounted on the upper block. This assembly is mounted in an environmental chamber (B). The top block and microbellows pump are held at the temperature of the chamber, T_H ; and the bottom block, which is insulated (insulation not shown), is maintained at temperature T_C by passing either air or liquid nitrogen from source (F) through passages in the lower block. The temperature gradient, ΔT, is sustained in the exposed middle one-third of the tubes. During an experiment, the gas is swung back and forth by means of the bellows pump (A). At the end of an experiment the gases from the two sides of the bellows pump are sampled in the sampling manifold (D). The lines are first purged, and then duplicate samples are withdrawn from the bellows.

The expression for the thermal diffusion factor in terms of the experimental quantities is obtained from the mass flux equation for a binary mixture in a one-dimensional temperature gradient. The resulting expression for α_T is

$$\alpha_T = \ln q / \ln (T_H/T_C)$$

where q is the separation factor in a single tube defined by the ratio of concentration ratios (x^1/x^2) at T_H to (x^1/x^2) at T_C . Three corrections must be applied to the measured concentrations to compensate for the operating characteristics of a trennschaukel. These are derived in the theory by van der Waerden (1957). After some minor manipulation, the expression for the experimental thermal diffusion factor from the trennschaukel is obtained.

$$[\alpha_T]_{expt1} = \ln Q \Big/ \frac{n}{k} \sum_{i=1}^{k} \ln \left(1 + \frac{\Delta T_i}{T_c}\right)$$

Here Q is the overall separation with corrected compositions, n is the number of trennschaukel tubes, and k is the number of stations (in this case four) at which the temperature gradient is monitored by differential thermocouples.

Feed gas mixtures were obtained for helium, neon, and argon by mixing equimolar amounts of $^3He/^4He$, ^{20}Ne, and $^{36}Ar/^{40}Ar$, which are available from Mound Laboratory's stable isotope inventory. Special mixtures containing approximately equal amounts ($\cong$5%) of the end isotopes of krypton ($^{78}Kr/^{85}Kr$) and xenon ($^{124}Xe/^{136}Xe$) were produced in Mound's thermal diffusion systems. The isotopic composition of the samples was measured by repetitively scanning the peaks of the desired mass numbers on a mass spectrometer and averaging the isotope ratios obtained.

THEORETICAL

The theoretical expression for α_T is most readily expressed in Chapman's determinant notation,

$$[\alpha_T]_m = \frac{5}{2} \lim_{m \to \infty} (X_1 \quad X_2 A_{oo}^{(m)})^{-1} \left\{ X_1 A_{o1}^{(m)} \left[(M_1 + M_2)/2M_1 \right]^{1/2} + X_2 A_{o-1}^{(m)} \left[(M_1 + M_2)/2M_2 \right]^{1/2} \right\}.$$

The quantities $A_{ij}^{(m)}$ are determinants obtained from a master determinant $A^{(m)}$ of order 2m + 1 by striking out row i and column j. Here X is the mole fraction, M is the molecular weight and m is the order of the approximation. The elements of $A^{(m)}$, which are complicated functions of the transport collision integrals, molecular diameters, and molecular weights, have been given for up to the third order, $[\alpha_T]_3$, by Mason (1957). The theoretical values computed herein are $[\alpha_T]_3$, except where otherwise noted.

In the event the gas has several isotopes, it is sometimes convenient to remove the mass dependence, or convert to another mass pair, by use of a reduced thermal diffusion factor

$$\alpha_0 = \left[(M_i + M_j) / (M_i - M_j) \right] \alpha_T .$$

Where the necessary values of α_T reported by previous workers have been converted to be directly comparable to our measured values.

The collision integrals for the Lennard-Jones (12-6) and certain integral values of α for the modified Buckingham (exp-6) potentials are given in Hirschfelder, *et al.*, (1954). Classical collision integrals for the Parson, *et al.*,(1972) and Barker, *et al.*, (1971) potentials were calculated by Neufeld and Aziz (1973). Since only lower order collision integrals were reported by Neufeld, the additional integrals required for the second Chapman-Enskog approximation, $[\alpha_T]_2$, were generated from the recursion relations using Lagrangian interpolation for the derivative. This was necessary because from previous calculations we have determined that $[\alpha_T]$ may be off as much as 5 or 6%, but $[\alpha_T]_2$ generally converges to $[\alpha_T]_3$ to within a few tenths of a per cent. Collision integrals for the remaining potentials, including non-integral values of α for the (exp-6) potential, were calculated using a method developed by Keller and Taylor (1969). The parameters for the Parson, *et al.*, (1972) potential for the noble gases other than argon were obtained from Lee (1973). The parameters for the Barker, *et al.*, (1971) potential for the gases other than argon were obtained from Rutherford (1973), and adjusted for the slight difference in parameters.

RESULTS AND DISCUSSION

The experimental and theoretical results of xenon are shown in Figure 2. For several years it has been suspected that the values for the isotopic thermal diffusion factor for xenon, which were reported by Paul, *et al.*, (1965b), were in error. Ross and Rutherford (1970) studied the separation of xenon isotopes in a thermal diffusion column and obtained experimental values for the column coefficients H_o', K_c', and K_d. They also evaluated these coefficients theoretically using the best available transport property data. The values of the two remixing coefficients, K_c', and K_d, which are not dependent upon the thermal diffusion factor, were found to be in good agreement with their experimental values. The values of H_o', the initial transport coefficient, were calculated using the data of Paul and were in poor agreement with experimental results. Roos then proceeded to make a corresponding states plot of α_o(the reduced thermal diffusion factor) for all of the noble gases (except helium) and noted that this plot indicated values for α_o lower than those Paul reported. Using the corresponding states predictions, they were able to reconcile the difference between their experimental and theoretical values of H_o'. Recently, Rutherford (1973) made additional separation measurements on xenon isotopes in a precisely constructed thermal column and extracted values of α_T from the column performance which were approximately 40% lower than Paul's data. We have performed the measurements from an average temperature of 250 to 850°K and substantiate the predictions of Roos and Rutherford. Furthermore, the theoretical calculations of α_T using either the Parson, *et al.*, (1972) or the Barker, *et al.*, (1971) potentials agree with the present results within the experimental uncertainty.

The results for krypton are shown in Figure 3. There are no major disagreements among the experimental data except at low temperatures. Below 300°K the present results are higher by a factor of two over those of Paul and Watson (1966). The higher value was predicted by Rutherford (1973) and is also substantiated by a semi-empirical method due to Weissman and DuBro (1970) using isotopic diffusion data. Once again, the potentials of Parson, *et al.*, (1972) and Barker, *et al.*, (1971) represent the data best. The M.B. (exp-6) potential with parameters by Mason (1960) fails at low temperatures where it falls well below the new values.

Most of the experimental data for argon are in agreement within the mutual experimental uncertainty with the exception of de Vries and Laranjeira (1960) and van der Valk and de Vries (1963). Surprisingly, none of the potentials investigated represents the data particularly well. The Parson, *et al.*, (1972) and Barker, *et al.*, (1971) potentials accurately predict the behavior of α_T at low temperatures, but fall considerably lower than the data above approximately 500°K. The M.B. (exp-6) potential with parameters by Mason and Rice (1954b) is excessively high at intermediate temperatures, and the Lennard-Jones potential derived from second virial coefficient data is inadequate as in the previous cases.

A considerable number of workers have reported experimental results for neon which are shown in Figure 5. The temperature range of the data spans 1,100°K which provides a rigorous test of the potential. Unfortunately, much of the data scatter widely; and without some selective process very little information can be obtained concerning the intermolecular forces. The present data pass roughly through the median results of other workers, and since the Mound Laboratory data have appeared to be accurate for the other noble gases, behavior of the theoretical curves is compared to the present measurements. The experimental thermal diffusion factor appears to reach a plateau between 0.026 and 0.027 at high temperatures. The Parson, *et al.*, (1972) and Barker, *et al.*, (1971) potentials never approach this level and fall off markedly at the higher temperatures. The Lennard-Jones potential predicts values which are too high over the entire range. The potential due to Mason and Rice (1954b) is probably the best choice, but approximates the data well only in the intermediate temperature range. We find no really satisfactory potential for neon.

The results of helium, which have been reported elsewhere by Taylor and Weissman (1971) and Taylor (1973), are given in Figure 6 for the sake of completeness. The Mound Laboratory data, which span 900°K are in good agreement with other workers, except at very low temperatures, where it is felt that the data of van der Valk (1963) are erroneously high (see Taylor, 1973). The potentials given by Beck (1969) and Bruch and McGee (1967) represent the data quite well, but from a comparison with other transport properties by Taylor and Keller (1971), we have a slight preference for Beck's potential. The Lennard-Jones and (exp-6) potentials are entirely inadequate for helium.

CONCLUSIONS

We have measured the isotopic thermal diffusion factors for the noble gases over an extended temperature range and have computed theoretical thermal diffusion factors from a variety of intermolecular potentials. Because thermal diffusion is a property which is relatively sensitive to the nature of the intermolecular forces, we have compared the theoretical values to the experimental data in order to test the validity of various potentials. The Lennard-Jones and (exp-6) potentials are generally inadequate. We found that potentials proposed by Parson, *et al.*, (1972) and Barker, *et al.*, (1971) quite accurately predict α_T for xenon and krypton, but fail at high temperatures for argon and neon. This leads us to the conclusion that these workers have, for the noble gases, characterized the well of the potential quite well, but have failed to obtain an accurate representation of the repulsive region of the potential. This follows from the successively poorer behavior of their potentials at higher reduced temperatures. Helium is somewhat of a separate problem, and for this gas we prefer Beck's potential.

REFERENCES

Barker, J. A., R. A. Fisher, and R. O. Watts, (1971), *Liquid Argon: Monte Carlo and Molecular Dynamics Calculations*, Mol. Phys. 21, 657.

Beattie, J. A., R. J. Barriault, and J. S. Brierley, (1951), *Compressibility of Gaseous Xenon. II. The Virial Coefficients and Potential Parameters of Xenon*, J. Chem. Phys. 19, 1222.

Beck, D. E., (1969), *Interatomic Potentials for Helium and Molecules of Helium Isotopes*, J. Chem. Phys. 50, 541.

de Boer, J. and A. Michels, (1938), *The Quantum-Mechanical Theory of the Equation of State and the Law of Corresponding States. Determination of the Law of Force of Helium*, Physica 5, 945.

Bruch, L. W. and I. J. McGee, (1967), *Semi-Empirical Potential and Bound State of Helium-4 Diatom*, J. Chem. Phys. 46, 2959.

Buckingham, R. A., (1938), *The Classical Equation of State of Gaseous Helium, Neon and Argon*, Proc. Roy. Soc. (London) A168, 264.

Clusius, K. and M. Huber, (1955), *Die Trennschaukel Thermodiffusion-Faktoren in System Co^2/H^2*, Z. Naturforsch 10a, 230.

Cunha, M. A. and M. F. Laranjeira, (1972), *High-Temperature Isotopic Thermal Diffusion of Neon*, Physica 57, 306.

Di Pippo, R. and J. Kestin, (1968), Proceedings of the Fourth Symposium on Thermophysical Properties (American Society of Mechanical Engineers, New York) 304.

Fischer, A., (1959), *Messung Wahrer Thermodiffusionsfaktoren mit der Trennschaukel*, Doctorial Thesis (Zurich).

Grew, K. E. and J. N Mundy, (1961), *Thermal Diffusion in Some Mixtures of Inert Gases*, Phys. Fluids 4, 1325.

Hirschfelder, J. O., C. F. Curtiss, and R. B. Bird, (1954), *Molecular Theory of Gases and Liquids*, John Wiley and Sons, New York.

Keller, J. M. and W. L. Taylor, (1969), *Evaluation of Transport Properties of Gases: The Bruch-McGee Potential of Helium*, J. Chem. Phys. 51, 4829.

Laranjeira, M. F. and J. Kistemaker, (1960), *Elementary Theory of Thermal and Pressure Diffusion in Gaseous Binary and Complex Mixtures. III. Ternary Mixtures*, Physica 26, 431.

Laranjeira, M. F. and M. A. Cunha, (1966), *Isotopic Thermal Diffusion in Neon*, Port. Phys. 4, 281.

Lee, Y. T., (1973), *Intermolecular Potentials*, Proceedings of the 1973 Conference on Gas Kinetics, 27-8.

Mason, E. A. and W. E. Rice, (1954a), *Intermolecular Potentials of Helium and Hydrogen*, J. Chem. Phys. 22, 522.

Mason, E. A. and W. E. Rice, (1954b), *Intermolecular Potentials of Some Simple Nonpolar Molecules*, J. Chem. Phys. 22, 843.

Mason, E. A., (1957), *Higher Approximations for the Transport Properties of Binary Gas Mixtures. I. General Formulas*, J. Chem. Phys. 27, 75.

Mason, E. A., (1960), *Redetermination of the Intermolecular Potential for Krypton*, J. Chem. Phys. 32, 1832.

McInteer, B. B., L. T. Aldrich, and A. O. Nier, (1947), *The Thermal Diffusion Constant of Helium and the Separation of ^3He by Thermal Diffusion*, Phys. Rev. 72, 510.

Michels, A. and H. Wijker, (1949), *Isotherms of Argon Between 0× and 150× and Pressures Up to 2900 Atmospheres*, Physica 15, 627.

Moran, T. E. and W. W. Watson, (1958), *Thermal Diffusion Factor for the Noble Gases*, Phys. Rev. 109, 1184.

Neufeld, P. D. and R. A. Aziz, (1973), *Tables of Collision Integrals for the Barker-Pompe, Barker-Fisher-Watts, and Parson-Siska-Lee Inert Gas Potentials*, J. Chem. Phys. 58, 1877.

Nier, A. O., (1940), *Coefficient of Thermal Diffusion of Neon and Its Variation with Temperature*, Phys. Rev. 57, 338.

Parson, J. M., P. E. Siska, and Y. T. Lee, (1972), *Intermolecular Potentials from Cross-Beam Differential Elastic Scattering Measurements. IV. Ar+Ar*, J. Chem. Phys. 56, 1511.

Paul, R., A. J. Howard, and W. W. Watson, (1963), *Isotopic Thermal Diffusion Factor of Argon*, J. Chem. Phys. 39, 3053.

Paul, R., A. J. Howard, and W. W. Watson, (1965a), *Concentration Dependence of the Thermal Diffusion Factor for ^3He-^4He and H^2-D^2*, J. Chem. Phys. 43, 1622.

Paul, R., A. J. Howard, and W. W. Watson, (1965b), *Isotopic Thermal Diffusion Factor for Xenon*, J. Chem. Phys. 43, 1890.

Paul, R. and W. W. Watson, (1966), *Isotopic Thermal Diffusion Factor for Krypton*, J. Chem. Phys. 45, 4132.

Raman, S., S. M. Dave, and T. K. S. Narayanan, (1965), *Thermal Diffusion Factor of Neon from Column Measurements*, Phys. Fluids 8, 1964.

Roos, W. J. and W. M. Rutherford, (1970), *Separation of Xenon Isotopes in the Thermal Diffusion Column*, J. Chem Phys. 52, 1684.

Rutherford, W. M., (1973), *Isotopic Thermal Diffusion Factors of Ne, Ar, Kr, and Xe from Column Measurements*, J. Chem. Phys. 58, 1613.

Saxena, S. C., J. G. Kelly, and W. W. Watson, (1961), *Temperature Dependence of the Thermal Diffusion Factor for Helium, Neon, and Argon,* Phys. Fluids 4, 1216.
Stevens, G. A. and A. E. de Vries, (1968), *The Influence of the Distribution of Atomic Masses Within the Molecule of Thermal Diffusion, Isotopic Methane, and Methane/Argon Mixtures,* Physica 39, 346.
Stier, L. G., (1942), *The Coefficients of Thermal Diffusion of Neon, Argon, and Their Variation with Temperature,* Phys. Rev. 62, 548.
Taylor, W. L. and S. Weissman, (1971), *Thermal Diffusion Factors and the ^4He-^3He System,* J. Chem. Phys. 55, 4000.
Taylor, W. L. and J. M. Keller, (1971), *Transport Properties of Helium Using Beck's Potential,* J. Chem. Phys. 54, 647.
Taylor, W. L., (1973), *Thermal Diffusion Factor for the ^3He-^4He System in the Quantum Region,* J. Chem. Phys. 58, 834.
van der Valk, F., (1963), *Thermal Diffusion in Ternary Gas Mixtures,* Doctoral Thesis (Amsterdam).
van der Valk, F. and A. E. de Vries, (1963), *Thermal Diffusion in Ternary Mixtures. II. Experiments,* Physica 29, 427.
de Vries, A. E. and M. F. Laranjeira, (1960), *Thermal Diffusion of Ternary Mixtures,* J. Chem. Phys. 32, 1714.
van der Waerden, B. L., (1957), *Theorie der Trennschaukel,* Z. Naturforsch 12a, 583.1 **Watson, W. W., A. J. Howard, N. E. Miller, and R. M. Shiffrin, (1963),** *Isotopic Thermal Diffusion Factors for Helium and Neon at Low Temperatures,* Z. Naturforsch 18a, 242.
Weissman, S., (1965), *Thermal Diffusion Factors for ^4He-^3He at Low Temperatures,* Phys. Fluids 12, 2237.
Weissman, S. and G. DuBro, (1970), *Self-Diffusion Coefficients for Krypton,* Phys. Fluids 13, 2689.

TABLE 1. Intermolecular Potential Parameters for the Noble gases.

Gas	Source	ϵ/k	a	r_m	Reference
Xenon	2nd Virial	221.	4.100	--	Beattie, *et al.*, (1951)
	Thermal Diff.	257.	--	3.963	Paul, *et al.*, (1965a and b)
	Mol. Beam	282.5	--	4.43	Parson, *et al.*, (1972)
	Liquid Data	280.3	--	4.358	Barker, *et al.*,(1971)
Krypton	2nd Virial	172.7	3.591	--	Beattie, *et al.*, (1951)
	Transport Prop.	200.0	--	4.036	Mason (1960
	Mol. Beam	201.5	--	4.100	Parson, *et al.*, (1972)
	Liquid Data	199.7	--	4.007	Barker, *et al.*, (1971)
Argon	2nd Virial	119.8	3.405	--	Michels and Wijker (1949)
	Transport Prop.	123.2	--	3.866	Mason and Rice (1954b)
	Liquid Data	142.1	--	3.761	Barker, *et al.*, (1971)
Neon	2nd Virial	35.60	2.749	--	Buckingham (1938)
	Transport Prop.	38.0	--	3.147	Mason, *et al.*, (1954b)
	Mol. Beam	37.15	--	3.17	Parson, *et al.*, (1972)
	Liquid Data	36.82	--	3.142	Barker, *et al.*, (1971
Helium	2nd Virial	10.22	2.556	--	deBoer and Michels (1938)
	Viscosity	86.20	2.158	--	DiPippo and Kestin (1968)
	Transport Prop.	9.16	--	3.135	Mason and Rice (1954a)
	Viscosity	36.1	--	2.725	DiPippo and Kestin (1968)
	2nd Virial	10.38	--	2.96	Beck (1969)
	Transport Prop.	12.13	--	2.975	Bruch and McGee (1967

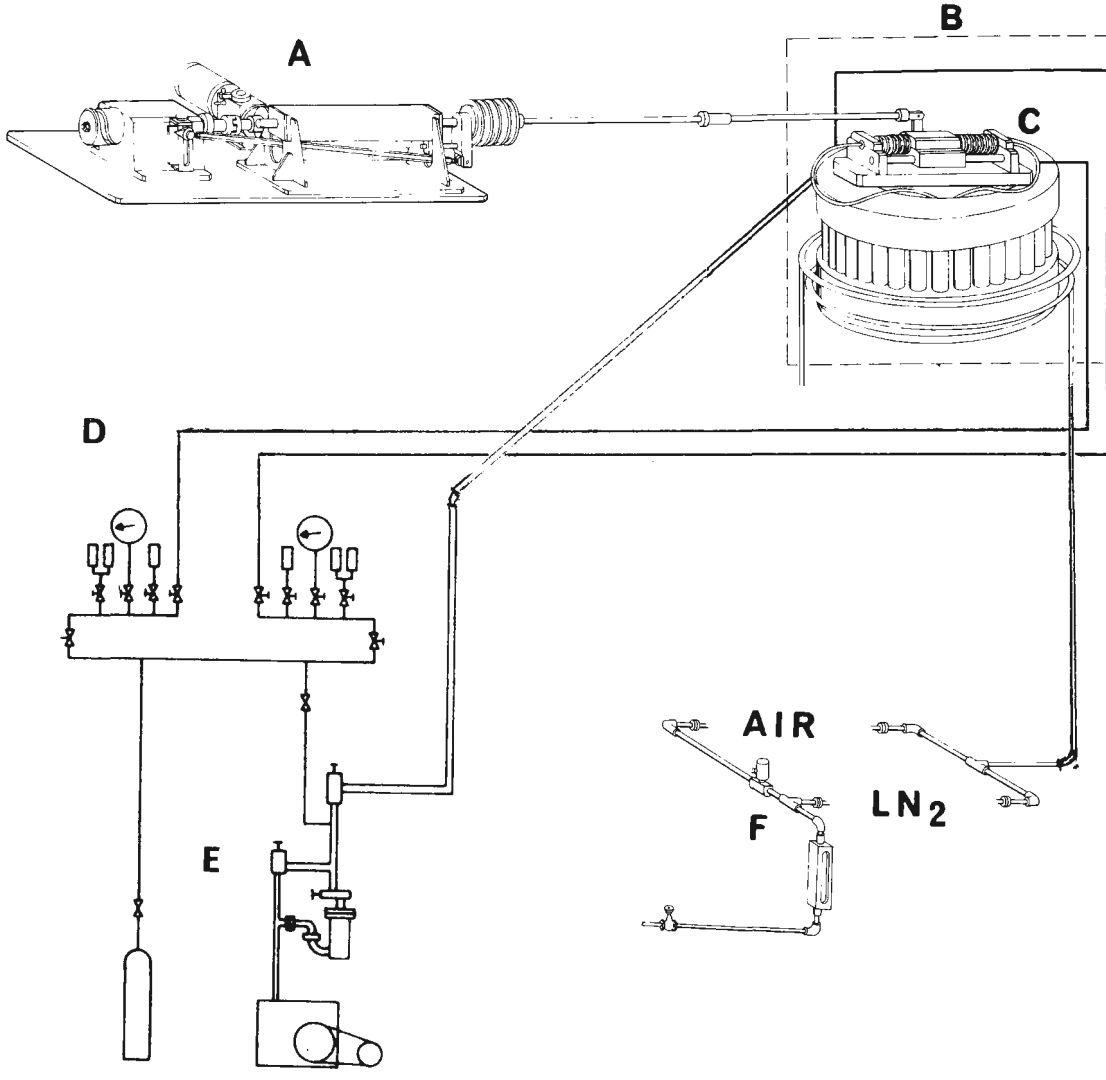

Figure 1. Schematic diagram of apparatus. A, pump drive; B, environmental chamber; C, bellows pump and trennschaukel; D, gas sampling manifold; E, feed gas supply and evacuation system; F, air or liquid nitrogen supply to adjust T_c .

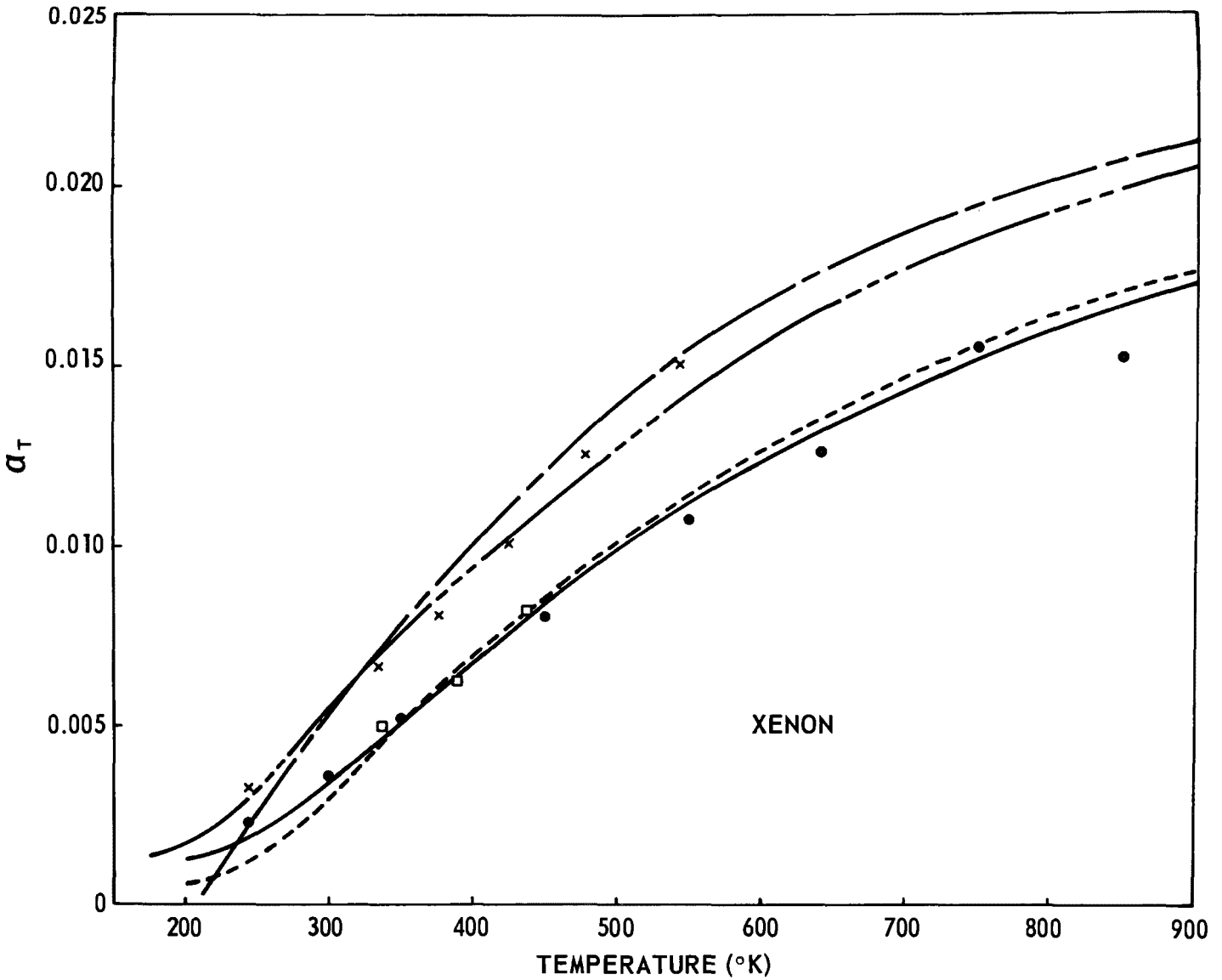

Figure 2. Thermal diffusion factor ^{134}Xe-^{136}Xe. The experimental points are: ●, present data; X, Paul, *et al.*, (1965b); and □, Rutherford (1973). The theoretical curves are: ——— Parson, *et al.*, (1972); ——— - Beattie, *et al.*, (1951); — - - - Paul, *et al.*, (1965a); and - - - - - -, Barker, *et al.*, (1971).

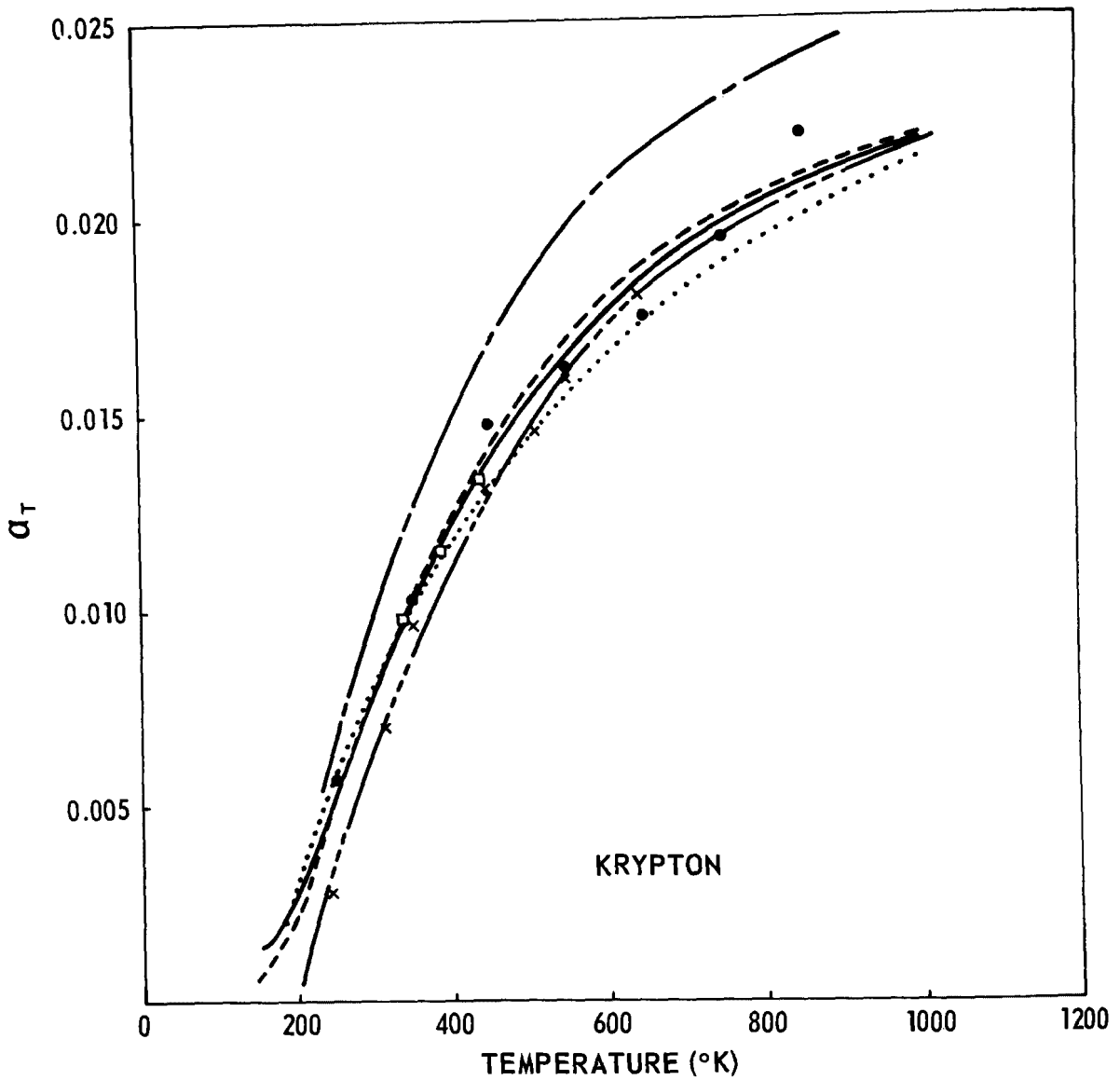

Figure 3. Thermal diffusion factor for ^{78}Kr-^{86}Kr. The experimental points are: ●, present data; X, Paul and Watson (1966); and □, Rutherford (1973). The dotted line represents the semi-empirical values of α_T obtained by Weissman and Dubro (1970) from isotopic diffusion data. The theoretical curves are: ———, Parson, *et al.*, (1972); —— -, Beattie, *et al.*, (1951); — ---, Mason (1960); and ------, Barker, *et al.*, (1971).

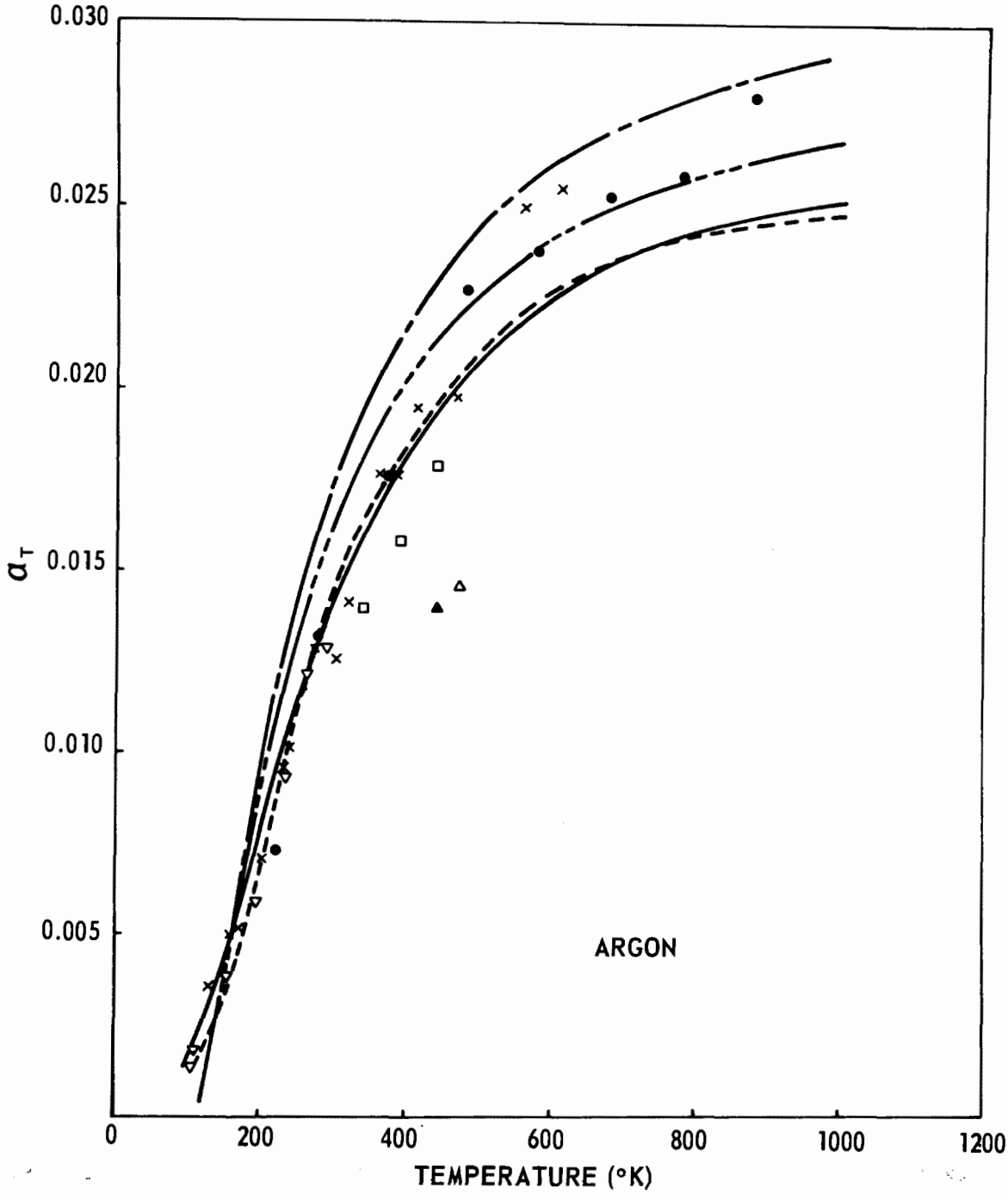

Figure 4. Thermal diffusion factor for ^{36}Ar-^{40}Ar. The experimental points are: ●, present data; X, Paul, *et al.*, (1963); □, Rutherford (1973); ▽, Stevens and de Vries (1968); ▲, van der Valk and de Vries (1963); and △, de Vries and Laranjeira (1960). The theoretical curves are: ———, Parson, *et al.*, (1972); -------, Barker, *et al.*, (1971); — ----, Michels and Wijker (1949); and—— ---, Mason and Rice (1954a and b).

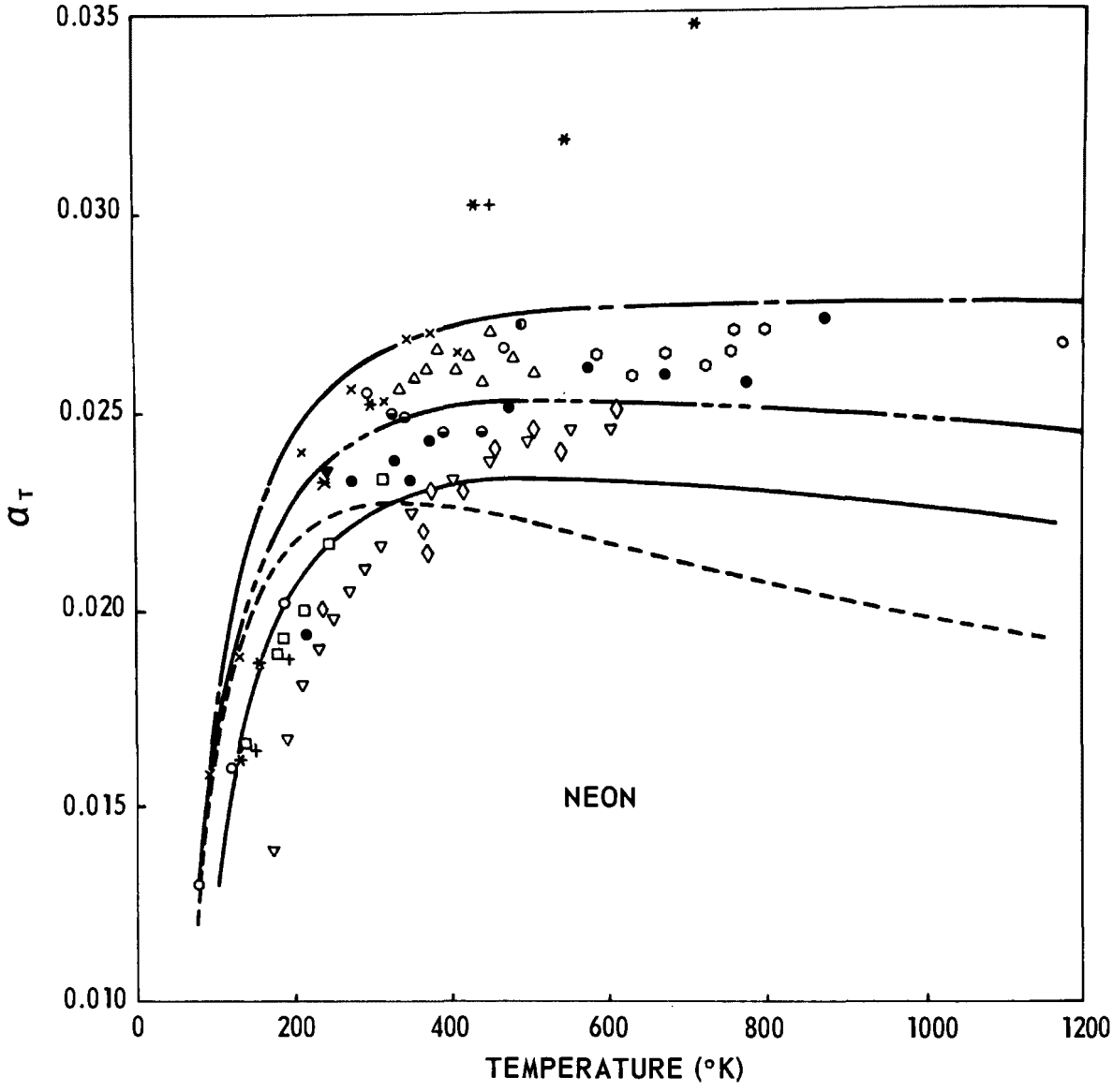

Figure 5. Thermal diffusion factor for ^{20}Ne-^{22}Ne. The experimental points are: ●, present data; ▽, Saxena, *et al.*, (1961); +, Nier (1940); ✱, Stier (1942); ◊, Moran and Watson (1958); X, Fischer (1959); ◐, Laranjeira and Kistemaker (1960); ○, Grew and Mundy (1961); □, Watson, *et al.*, (1963); △, Laranjeira and Cunha (1966); ⬭, Cunha and Laranjeira (1972); ⊖, Rutherford (1973); and ▼, Raman, *et al.*, (1965). The theoretical curves are: ———, Parson, *et al.*, (1972); — — —, Barker, *et al.*, (1971); ——— -, Mason and Rice (1954b); and —— – , Buckingham (1938).

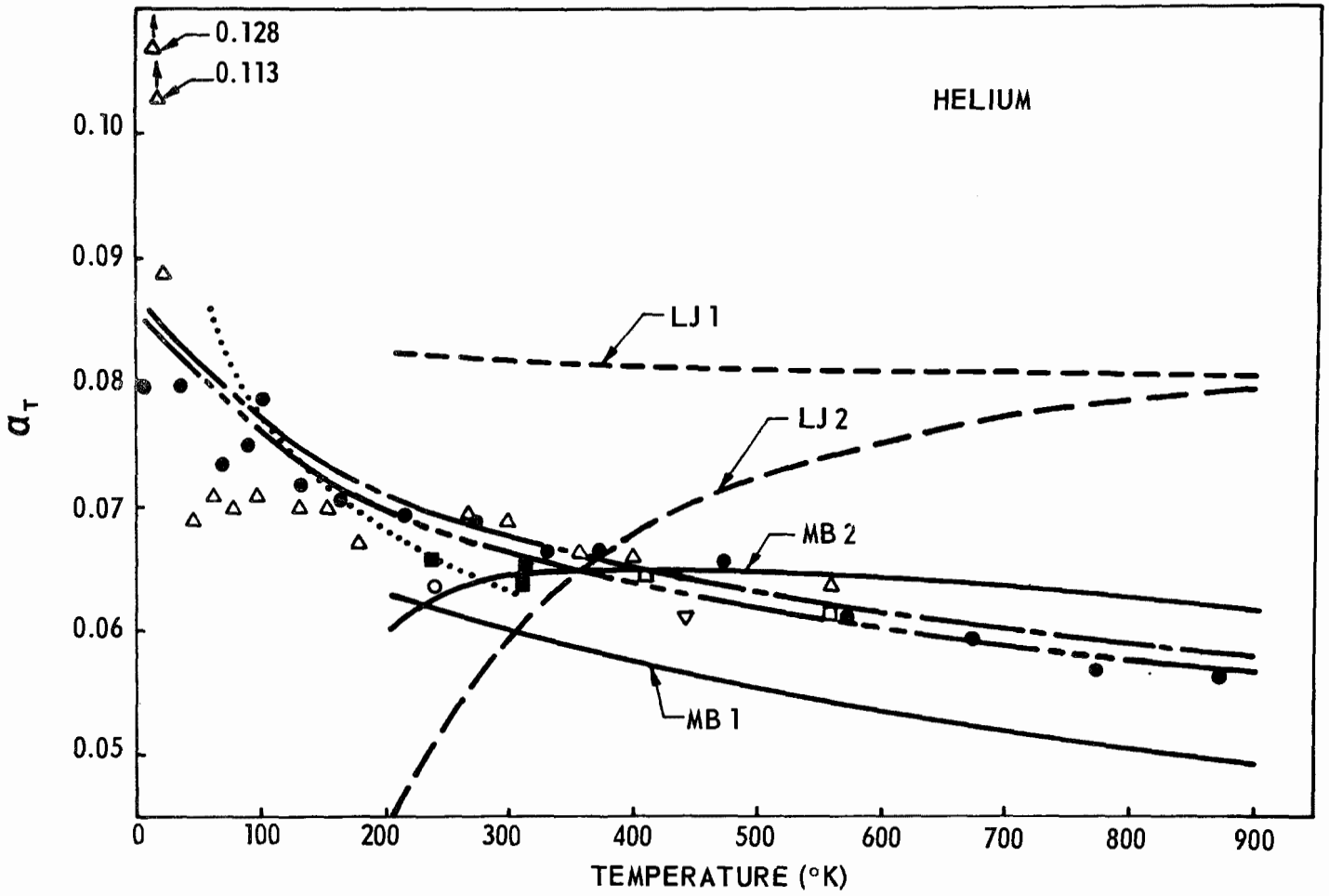

Figure 6. Thermal diffusion factor for ^3He-^4He. The experimental points are: ●, present data; △, van der Valk (1963); ■, Watson, *et al.*, (1963); □, Paul, *et al.*, (1965a); ○, Saxena, *et al.*, (1961); ▽, McInteer, *et al.*, (1947); and . . . ., the smoothed data of Weissman (1969). The theoretical curves are: LJ1, de Boer and Michels (1938); LJ2, Di Pippo and Kestin (1968); MB1, Mason and Rice (1954a); MB2, Di Pippo and Kestin (1968); —— —, Beck (1969); and ---- , Bruch and McGee (1967).

VII. Biological Effects of Noble Gases

PHYSIOLOGY OF THE NOBLE GASES

R. M. Featherstone,*
W. Settle, and H. Althouse
Department of Pharmacology
University of California
San Francisco, California

Abstract

The noble gas series of elements, for many years considered "inert" in a chemical sense, are known to have biologic activities that must be considered in any attempt to assess the possible hazards of having radioactive isotopes of these elements liberated in our environment. Although most is known about the biology of xenon, reports of effects from low concentrations of helium have been made. The anesthetic properties of xenon will be reviewed in some detail including the possible biologic implications of xenon's binding at very specific internal sites of proteins and the effects of this binding on the affinity of heme proteins. The surprising observations that helium substituted for nitrogen at ordinary pressures reduced the baseline heart rate and the concentration of endogenous plasma catecholamines of dogs will also be discussed. Possible mechanisms by which these gases might be altering normal biologic responses will be presented. Biologic effects of neon, argon, and krypton are less well-documented, but the theoretical aspects of their possible associations in biological systems are discussed.

INTRODUCTION

One of the important questions to be addressed during this symposium concerns the biological effects of the noble gases. Are there such effects? If so, what are they? And what are the implications of these effects, particularly when some of these gases may be at times represented in our environments by some of their radioactive isotopes?

We shall describe briefly the relatively little that is known about the physiology or biology of these gases without specific reference to the factor of radioactivity, which will be considered by others.

It is not surprising that we know most about the two ends of our scale — helium and xenon. (Radon will receive special attention later in this symposium). During this presentation we shall mention briefly the scope of the studies on the whole series of gases, then describe some specific studies with xenon and helium, and conclude with comments on the dilemma confronting us with respect to neon, argon, and krypton.

As tools to probe some of the complexities of molecular mechanisms in biology, the noble gases are ideal for focusing on the smaller binding forces among molecules — the non-covalent, non-ionic, and non-hydrogen bonding forces. Also, with these noble gas elements there is never the necessity of considering the possibility of a metabolite whose identity has escaped detection.

Studies have shown that, over a range of pressures appropriate for the relative size of the noble gas atoms, and the sensitivity of the test situation, that the activities of a number of enzymes, including tyrosinase, lipoxidase, acetyl-cholinesterase, alpha-chymotrypsin, leucine amino peptidase, (Powell, 1973) and ATPase (Trevor, *et al.*, 1969) are all affected by the noble gases. On the whole cell level, *Neurospora crassa* growth, (Powell, 1973) cell division of HeLa cells growing in culture (Powell, 1973) and the growth of some *Escherichia coli* strains (Hegeman, 1973) are all inhibited by the noble gases at appropriate pressures.

Physiological effects on nervous activity have been studied in several situations. Gottlieb and others have shown a reversible inhibition of nerve conduction by 200 psi xenon and 950 psi krypton (Gottlieb, *et al.*, 1968). Xenon anesthesia in man has been known and studied extensively for over 20 years (Featherstone, *et al.*, 1963). More recently, the tremors and convulsions of the "high pressure neurological syndrome," caused apparently by helium in environments simulating greater than 600 feet of sea water, has elicited considerable attention (Bennett, *et al.*, 1971).

The first question, then, of the presence of altered physiology in the presence of supernormal amounts of at least some of these noble gases has to be answered affirmatively.

XENON EFFECTS

Let us consider xenon first in some detail. The fact that it can produce anesthesia in man at 0.8 atm., with room for adequate oxygen, and in other organisms at higher pressures (monkeys at 2 atm., dogs at 3 atm., rats at 5 or 6 atm., etc.) has been the subject of studies in our laboratory and others for over 20 years. Early in this period we used radioactive xenon (the first produced by neutron bombardment) to learn that xenon was taken up by equal rates by the cerebral cortex, the caudate nucleus, the thalamus, the hypothalamus, and the medulla oblongata of the brain, as well as by the kidneys. The adrenal gland, for some unknown reason, absorbed xenon to a much greater extent than did the brain, and other tissues absorbed it more slowly and to lesser degrees, depending more or less on vascularity (Featherstone, *et al.*, 1952; Pittinger, *et al.*, 1954). We also learned that blood carries almost half of the xenon bound to hemoglobin.

**On sabbatical during 73-74 in Geneva. Department of Physiology, University of Geneva, Switzerland.*

We shall summarize briefly what we have learned about the nature of the association of xenon with some macromolecules of known biological importance — a system that is serving us well as a model for still unknown systems that are possibly even more important. Comparisons can be made of the size of xenon with other anesthetic molecules and with the gases that make up our normal environment. Xenon is about the size of nitrous oxide and ethylene; it is much smaller than chloroform, ether, or halothane; and larger than hydrogen, oxygen, nitrogen, and carbon dioxide. The only mechanism seemingly possible is the attraction of the electrons of xenon to a dipole, thereby having a dipole induced in the xenon, which, in turn, can attract other electrically neutral molecules, inducing in them also a dipole moment. Both the size and polarizability of these molecules are important and are closely related.

Interactions of anesthetics like xenon with proteins can now be explored at a molecular level. Myoglobin, a small protein whose three dimensional structure is known almost completely, is a compact unit with little empty space inside. Xenon, a tiny molecule by comparison with myoglobin, combines with some specific sites with myoglobin. Two xenon binding sites have been identified by x-ray diffraction studies (Settle, 1973). The first binding site is nearly equidistant between the proximal histidine and the heme. The binding energy of this site approximates 10 kcal/mole (roughly equivalent to two ionic bonds), but composed of over 30 small additive forces. The second site is nearer the surface but still completely within the protein molecule — between the AB and GH corners. In hemoglobin, which is made up of four units similar to myoglobin, binding of xenon has been observed in the second region. In the alpha chain of hemoglobin, the binding site is nearer the GH corner; in the beta chain the site is nearer the AB corner. These sites are inside and near the surface, and are composed essentially of the same non-polar amino acid side chains as those of the myoglobin sites. They compose in each case a small lipid-like pocket.

Studies with lysozyme, another protein whose structure is almost completely known, have shown that xenon does not associate with this protein — there are no suitable environments in it. Our preliminary experiences with some other proteins indicate that some proteins do associate specifically with xenon.

Myoglobin combines with oxygen and carbon monoxide on the side of the heme opposite the first xenon site. When xenon is present, the binding of carbon monoxide is altered. Binding constants of xenon to deoxy and carboxy myglobin indicate that xenon in the site near the heme causes a small increase (10%) in CO affinity; and xenon in the site near the AB and GH corners (see Figure 1.) causes a much larger increase in CO binding (90%)(Settle, 1973). Another site is known to exist in some forms of myoglobin, but it has not yet been identified, although the xenon in it is known to decrease CO affinity.

The diagramatic representation Perutz has recently published on the movement of a hemoglobin subunit upon ligand binding (Perutz, 1970) can be considered in relation to xenon and carbon monoxide binding. Remember that the primary xenon site is near the heme and histidine of the F helix, and that the secondary site is near the GH corner. Upon ligand binding the heme becomes planar, and the distance between the heme and the F helix decreases by 0.9 Å. This causes a movement of the F helix 2 Å toward the G helix, with the F helix pivoting at the FG corner and middle of the E helix, thus producing movements of several angstroms in the region of the secondary xenon site between the AB and GH corners. One can postulate that xenon, when present, can alter the affinity of a ligand (like carbon monixide) by perhaps holding the hemoglobin in a more favorable state for liganding to occur or to be maintained. It is interesting to note that xenon alone, however, does not change the structure of hemoglobin merely by its presence.

This postulate about the mechanisms by which xenon causes increased liganding of carbon monoxide is supported by recent observations (Stewart, *et al.,* 1972) that methylene chloride (dichloromethane) breathed for two hours in low concentrations (probably equivalent to the exposure received from using the compound to remove paint from a small piece of furniture) will cause a tenfold increase in the carboxyhemoglobin level, and that Benno Schoenborn (Pifarre, *et al.,* 1970), of Brookhaven National Laboratory, has shown that this compound, which is only slightly larger than xenon, combines with heme proteins in the "xenon" sites.

HELIUM EFFECTS

Let us turn now to some biological consequences of the presence of helium in a biological system. Here, the observations are mainly phenomenological at this stage. Five examples are cited briefly.

(1) In diving gas mixtures, the use of helium has led to an avoidance of nitrogen narcosis allowing man to descend to far greater depths, although not without limit, as will be indicated later. No depressant effects have been observed on the respiratory centers for up to 19 atmospheres of helium (Powell, 1973). However, it must be remembered that these centers are among the last to be affected in the CNS by foreign substances like anesthetic molecules. Consequently, such a measure is not ideal if one is looking for some effects of helium — more sensitive systems are necessary.

(2)A series of three papers, published since 1968, describe the effects of helium. In the work described in the first two papers (Pifarre, *et al.,* 1970) ventricular fibrillation was induced in a series of dogs by acute occlusion of the left circumflex artery. The surprising observation was made that the presence of 20% helium was sufficient to block these ventricular fibrillations. The data do not show clearly that more oxygen was not also necessary, but the implication of helium seems probable. The authors propose that helium (perhaps coupled with more oxygen) promoted in some way the development of coronary collateral circulation so that more blood was available to the ischemic area and the infarcted area was smaller. Work reported in the third paper (Raymond, *et al.,* 1972) was with dogs not subject to circumflex ligation. The sensitivity of blood pressure, heart rate, and extrasystoles to experimental epinephrine IV was not altered by helium. However, helium (75%) did reduce baseline heart rate (112/119) and concentration of endogenous catechol amines. These

authors concluded that the antiarrhythmic effect of helium may be mediated by changes in symphathetic activity.

These studies are of probable clinical importance in reducing the liklihood of ventricular arrhythmias in persons having myocardial infarctions, but for purposes of this symposium these effects illustrate a clear example of a biological effect from as little as 20% helium in the inspired gases.

(3) Hamilton and Schreiner (Hamilton, *et al.,* 1970 a and b) and their colleagues have studied the biochemical and metabolic effects of a six-month exposure of small animals to helium-oxygen mixtures. In rats and two generations of mice they found no changes except for greater food and water uptake by the mice, possibly due primarily to the differing heat transfer properties of helium. In rabbits they also observed decreases in hemoglobin and red cell levels in blood.

(4) Another example of helium effects is that studied by a group working in Geneva and Lausanne (Sauter, *et al.,* 1973). They are stimulating the isolated cervical sympathetic ganglion of rats preganglionically at 6/second and measuring the electrophysiological answer on the postganglionic nerve. Stimulation is maintained for 30 minutes followed by 30 minutes of rest. The control responses in 95% O_2 and 5% CO_2 at 1 atm. are that the height of the action potential falls at once to 70% of the initial value and then, during the stimulation period, increases to 85% of the initial value. After the stimulus is stopped, there is a hyperexcitability lasting for 30 minutes where the action potential is above the initial value. When 6 atm. of helium are added, with PO_2 and PCO_2 corrected to control levels, the same fall in action potential at the beginning of the stimulus period is observed, but the recuperation does not occur, and the height of the action potential remains below the initial value for at least 30 minutes after stimulation is stopped. This work is still in its preliminary stages. Pressure alone has not been eliminated as a possible cause of the effects, but these experiments may constitute another example of helium effects.

(5) The last example of helium effects to be cited today is the "high pressure neurological syndrome" noted in divers at simulated depths below 600 feet of sea water (Bennett, *et al.,* 1971). This syndrome is characterized chiefly by tremors and convulsions. Its existence probably has little significance for the topic of this symposium, but it, like the other examples cited, helps raise questions about the molecular mechanisms by which helium and xenon can cause changes in physiology.

CONCLUSIONS

Now, having described in some detail the molecular mechanisms by which xenon can alter physiology, and having mentioned some examples of effects by helium, the question arises as to whether the other members of this series, neon, argon, and krypton, cause changes in physiology, and if so, do they all do so by the type of interaction shown for xenon, although, of course, through interactions with different sized receptive environments at the submolecular level.

At present we are left with the guess that all members of this series can interact to some degree with proteins and other biologically important molecules, and that such interactions are involved in any changes that occur. Those changes with helium and xenon are most noticeable — these two are farthest away from nitrogen in size and other properties, and nitrogen is the gas with which we are always living unless we replace it or remove it. It is not surprising that neon, like helium, can be used in diving to avoid nitrogen narcosis. It is also not surprising to find that krypton, at pressures higher than xenon, produces some degree of anesthesia. The data on Neurospora and HeLa cells help predict these events. Perhaps argon is so close to nitrogen in size and properties that it will be shown to have almost no unique biological properties in complex multicellular organisms like man. Schatte (Schatte, *et al.,* 1972) has indicated that argon substituted for nitrogen would require a 10% decrease in oxygen tension to keep the P-arterial tension of oxygen equal to that in air. Likewise, he predicts a 5.6% increase of oxygen would be necessary if helium was used instead of nitrogen, concluding that argon and helium may significantly alter arterial oxygen tension.

In any event, the demonstrated effects of the gases in this series, both progressive effects with size in the studies with whole cells, and the more pronounced effects of helium and xenon, suggest that members of this series do combine, in the chemically subtle ways of which they are capable, with biologically important molecules and may change physiological functions — for better or worse — depending perhaps on their deviation from nitrogen and, of course, on their concentrations in some key biological sites.

Actually, relatively little is known about the physiology of these noble gases. If one adds a concern about the association of radioactivity with them, it seems apparent that all the members of this series need much further study, with appropriate support from government agencies and industries associated with any of these fascinating noble gases.

REFERENCES

Bennett, P. B. and E. J. Towse, (1971), *The High Pressure Nervous Syndrome During A Simulated Oxygen-Helium Dive to 1500 feet.* Electroenceph. Clin. Neurophysiol. 31, 383-393.

Featherstone, R. M., W. Steinfield, E. G. Gross, and C. B. Pittinger, (1952), *Distribution of the Anesthetic Gas Xenon in Dog Tissues as Determined with radioactive Xenon.* J. Pharmacol. and Exper. Therap. 106, 468.

Featherstone, R. M. and C. A. Muehlbaecher, (1963), *The Current Role of Inert Gases in the Search for Anesthesia Mechanisms.* Pharmacol. Reviews. 15, 97.

Gottlieb, S. F., A. Cymeran, and A. V. Metz, Jr., (1968), *Effect of Xenon, Krypton, and Nitrous Oxide on Sodium Active Transport through Frog Skin with Additional Observations on Sciatic Nerve Conduction.* Aerospace Med., 39, 449-453.

Hamilton, R. W., *et al.,* **(1970),** *Biochemical and Metabolic Effects of a 6 months Exposure of Small Animals to a Helium-Oxygen Atmosphere.* Space Life Sci., 2, 57.

Hamilton, R. W., *et al.,* (1970), *Biological Evaluation of Various Spacecraft Cabin Atmospheres.* Space Life Sci., 2, 307 and 407.

Hegeman, S. L., (1973), *Use of Genetic Variants in Molecular Pharmacology,* Chapter in Part II of A Guide to Molecular Pharmacology-Toxicoloty, 561-582.

Perutz, M. F., (1970), *Stereochemistry of Cooperative Effects in Hemoglobin.* Nature 228, 726-734.

Pifarre, R., *et al.,* **(1970),** *The Influence of Oxygen and Helium Upon Ventricular Fibrillation.* J. Thoracic and Cardiovascular Surgery, 55, 535-537, 1968, and 60, 648-652, 1970.

Pittinger, C. B., R. M. Featherstone, E. G. Gross, E. E. Stickley, and L. Levy, (1954), *Xenon Concentration changes in Brain and Other Body Tissues of the Dog During the Inhalation of the Gas.* Pharmacol. and Exper. Therap., 110, 458.

Powell, M. R., (1973), *The Role of the Noble Gases in Molecular Pharmacology,* Chapter in Part II of A Guide to Molecular Pharmacology-Toxicology., pp. 495-518.

Raymond., L., *et al.,* **(1972),** *Possible Mechanism for the Anti-Arrhythmic Effect of Helium in Anesthetized Dogs.* Science, 176, 1250-1252.

Sauter, F., M. Dolivo, and J. M. Posternak, (1973), University of Lausanne and University of Geneva. Personal communication.

Schatte, C. L., *et al.,* (1972), *Predictability of PaO2 in Different Inert Gas-Oxygen Environments.* Space Life Sci., 3, 206.

Settle, W., (1973), *Function of the Myoglobin Molecule as Influenced by Anesthetic Molecules.* Chapter in Part II of A Guide to Molecular Pharmacology-Toxicology. pp. 477-494.

Stewart, R. D., *et al.,* **(1972),** *Carboxyhemoglobin Elevation After Exposure to Dichlormethane.* Science, 176, 295-296.

Trevor, A. J. and J. T. Cummins, (1969), *Properties of NA and K Activated ATPases of Rat Brain — Effect of Cyclopropane and Other Agents Modifying Enzyme Acitivity.* Biochem. Pharmacol. 18, 1157-1167.

Note: Inasmuch as a number of the references are included in the chapers of a recently published book edited by one of the auothors of this article (RMF), these chapters are cited in an effort to bring to the interested reader a far greater bibliography than can be reproduced here.

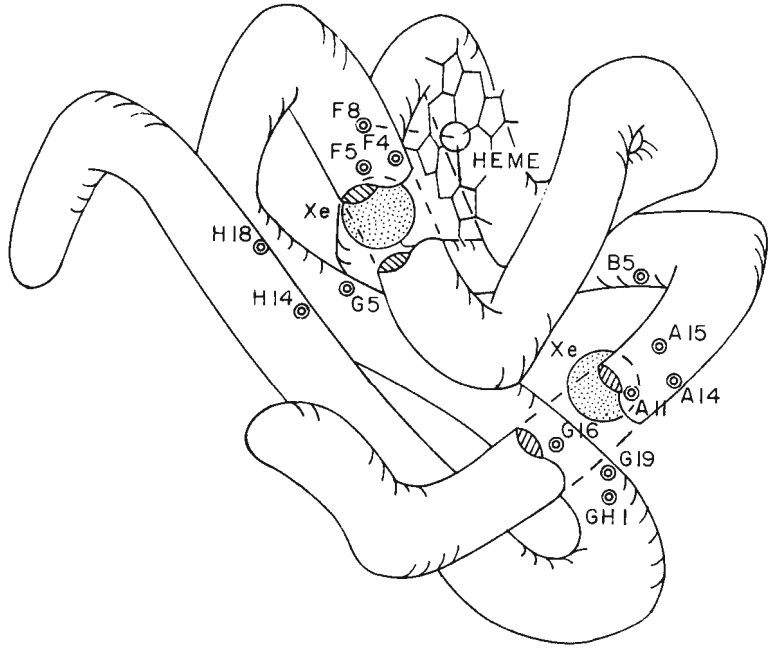

Figure 1. Diagrammatic sketch of sperm whale myoglobin showing the course of the polypeptide chain from the same view as the photograph of a model shown by Settle, 1973. The amino acid residues noted in the sketch are those which have side chains within the van der Waals contact of the xenon atoms. (Reprinted by permission of Marcel Dekker, Inc., New York, from A guide to Molecular Pharmacology-Toxicology, edited by R. M. Featherstone, 1973.)

CALCULATIONS OF THE ABSORBED DOSE TO A MAN IMMERSED IN AN INFINITE CLOUD OF KRYPTON-85*

W. S. Snyder, L. T. Dillman, M. R. Ford, and J. W. Poston
Health Physics Division
Oak Ridge National Laboratory
Oak Ridge, Tennessee 37830

Abstract

A person exposed to an infinite cloud of krypton-85 is exposed to at least seven sources of radiation: (1) photons emitted in air, (2) beta particles emitted in air, (3) photons and beta particles emitted by krypton-85 present in the air passages of the lungs, (4) photons and beta particles emitted by krypton-85 present in body tissues, (5) bremsstrahlung produced in air, (6) bremsstrahlung produced by beta particles incident on the body, (7) bremsstrahlung produced within the body. The energy spectra of scattered photons are calculated by the method of Dillman and half these spectra are taken as incident on the body, producing doses to body organs as in MIRD Pamphlet No. 5. Doses to various organs, e.g., red bone marrow, gonads, etc., from sources (1) and (5) above are calculated by interpolation from these results. Dose to skin from source (2) is calculated by integration of Berger's point kernel (MIRD Pamphlet No. 7) in air. Doses from sources (3), (4), (6), and (7) are calculated by methods developed by the authors of internal sources of photons and beta particles. If the intensity in the cloud is 1 $\mu Ci/m^3$, a dose to skin at a depth of 7 mg/cm^2 is ~1.8 rad/a; to the lungs, 32 mrad/a; ovaries, 6.2 mrad/a; and testes, 16 mrad/a.

INTRODUCTION

The calculations of absorbed dose to a person exposed to ^{85}Kr is at once simple and complicated. It is simple if one is willing to ignore all but the highest dose (i. e., the dose from beta particles incident on the skin), but if one asks for genetic dose, particularly the dose to the ovaries, it is quite another matter. In the latter only the calculation of the absorbed dose for a person exposed to a large cloud of ^{85}Kr, which is assumed to be uniformly distributed in air, is considered. The methods to be described, however, are general and also apply to exposures to infinite clouds of other noble gases. The problem of exposure to a finite cloud or "plume" of ^{85}Kr is not considered here, and will likely demand some different techniques.

The decay scheme as usually shown is given in Figure 1, which is taken from MIRD Pamphlet No. 6. Note that there is only one photon given with an intensity of only 0.41% per disintegration. The Internal conversion is less than 1% of this, and hence is not shown. Only two betas are emitted and these have endpoint energies of 0.67 MeV and 0.16 MeV. The range of the 0.67 MeV beta in tissue is about 0.14 cm.

In all, six sources of radiation need to be considered:

(1) photons and beta particles emitted directly from the ^{85}Kr present in the air;
(2) bremsstrahlung radiation emitted in the air;
(3) bremsstrahlung radiation emitted by the beta particles as they penetrate the skin;
(4) photons and beta particles emitted by ^{85}Kr present in the air passages of the lungs;
(5) photons and beta particles emitted by ^{85}Kr present in the body; and
(6) bremsstrahlung radiation from beta particles emitted from ^{85}Kr present in the body.

Calculations are based on an anthropomorphic phantom which exists as a mathematical object defined by inequalities and equations programmed into the computer's memory. The most complete description of the phantom and of the calculational techniques is that given in MIRD Pamphlet No. 5. A schematic diagram of the outer surface of the phantom and a cutaway view showing some of the principal organs are given in Figure 2. The attempt here is to give a gross representation of the geometry of the human body without attempting a detailed representation. The phantom, however, is composed of three types of tissue:

(1) skeletal tissue (bone plus marrow) with specific gravity of 1.5;
(2) general soft tissue with a specific gravity near 1; and
(3) lung tissue with a specific gravity of 0.3.

The elemental composition of these tissues approximates that of the averages for such tissues and is given in Berger, (1971).

Several changes have been made in the phantom since MIRD Pamphlet No. 5 was published. Those of particular importance for this study are mentioned briefly here.

(a) Regions of bone have been defined in which the active marrow of an adult is largely present, thus enabling dose estimation for the active bone marrow.

(b) The legs have been separated to place the male gonads near the surface of the body as is shown in Figure 3.

(c) The top of the head has been rounded to remove the excess of soft tissue which would provide unwanted shielding for the red marrow present in the skull.

**Research sponsored by the U. S. Atomic Energy Commission under contract with Union Carbide Corporation.*

DOSE FROM PHOTONS PRODUCED IN AN INFINITE CLOUD

The primary photons are scattered by the air, producing a continuum of photons of lower energies. The energy spectrum of these photons may be calculated as has been shown by Dillman (1970b). Since the cloud is infinite and the primary photons are distributed isotropically in angle, all subsequent generations of photons will likewise be distributed isotropically. Thus it suffices to compute this energy spectrum of scattered photons in energy space. This calculation has been performed for twelve monoenergetic photon sources. The energy spectrum for 0.5 MeV photons is shown in Figure 4 (this is the spectrum emitted from each volume element of the infinite cloud and is very nearly the energy of the photon emitted by ^{85}Kr). The photons from each of these twelve energy and angular spectra were used as a source on the phantom. The orginal monoenergetic source energies extended from 0.01 MeV to 4 MeV. (Doses for photons of other energies are obtained by linear interpolation.) The results for each of the twelve sources have been scrutinized, and when the coefficient of variation of an estimate exceeds 30%, the estimate is rejected, and a value estimated on the basis of the depth-dose profiles is substituted. The technique used and the data are in course of publication (Poston, *et al.*, 1973).

For most practical purposes, one is concerned with a person on the surface of the ground, and thus a ground effect must be considered. For an energetic photon (i. e., one having a mean-free path in air which is many times the diameter of the body), the presence of the man on the earth's surface means that essentially half the source in air to which he is exposed (half the infinite cloud) is missing. This assumes there are no surface deposits of ^{85}Kr, as these would be expected to be negligible in view of the chemical characteristics of ^{85}Kr as one of the noble gases. There is some backscattering of photons from the earth, but direct measurement of ^{60}Co sources in air indicates this ground effect is perhaps a correction of some 10-20% or less (Haywood, 1964; Berger, 1957). Of course, the measurements are for essentially a point source, but summation of such sources indicates an increase of dose of this order due to scattering from the ground. Thus one may use half the intensity of the energy spectrum for photons without greatly falsifying the dose received. This argument depends on the fact that even at energies of 10 keV, the mean-free path of photons in air is comparable to the body height, and hence essentially half the source is missing for irradiation of the lower portions of the body, and about 25% is excluded by the ground by irradiation of the upper portions of the body. For higher energies, the ground interface essentially excludes half the source.

The dose to the various body organs from photons emitted by ^{85}Kr in air is shown in the top line of Table 1. A concentration of 1 μCi/m^3 (STP) is assumed, and the dose is shown per day of the person's presence in the infinite cloud. The dose to the skin from photons is an average for a thickness of 0.2 cm extending over the entire body. These doses are determined by a Monte Carlo-type calculation using the source described earlier.

DOSE FROM BREMSSTRAHLUNG PRODUCED IN AIR, IN TISSUE, OR IN SKIN

Bremsstrahlung is emitted whenever an electron is produced or whenever the electron passes through a medium. In fact, the so-called internal bremsstrahlung is emitted from the atom of ^{85}Kr, and the external bremsstrahlung is emitted as the beta particle passes through air or tissue. The energy spectra of these five sources of bremsstrahlung all lie within the shaded area shown in Figure 5; that emitted in skeleton (bone plus marrow) being highest and adipose tissue lowest. The internal bremsstrahlung is combined with the external for all the media; in each medium the units are per disintegration of ^{85}Kr. Note that there is not great difference between the spectra of the bremsstrahlung produced in air and in tissue, but that produced in skeleton and fat varies considerably. The dose from this bremsstrahlung has been obtained by interpolation on doses computed for the twelve monoenergetic sources of photons mentioned earlier for estimation of dose from a semi-infinite cloud. These doses are shown in the second line of Table 1.

Electrons incident on skin produce bremsstrahlung as they move through skin, but in this case the electron only expends a portion of its energy in the skin, and the energy spectrum is computed taking this into account. The values shown in Figure 6 are for the total number of photons produced in the remaining portion of the electron's range after it has entered the skin, and the number shown is opposite the median of the corresponding energy interval. Note that the units here are necessarily quite different than those in Figure 5. The dose distribution for these photons was obtained by interpolation on the doses due to twelve monoenergetic sources originating in the skin of the phantom (i. e., in a layer of thickness of 0.2 cm.). Thus the calculation involves the assumption that these photons are uniformly distributed in angle and in depth, neither of which is strictly true, but this should not matter greatly for estimation of dose. These doses are shown in the third line of Table 1.

DOSE FROM ^{85}Kr IN THE BODY

A person immersed in an atmosphere of ^{85}Kr at 1 μCi/m^3 would quickly come into equilibrium with it. The concentration in the body tissues would be the concentration in air multiplied by Ostwald's coefficient — namely,

$$\text{(tissue concentration) } \mu\text{Ci/cm}^3 = 10^{-6} \times \tau \times \text{(concentration in air) } \mu\text{Ci/m}^3$$

where τ is Ostwald's coefficient. In applying this, one should not consider the air passages of the lung as part of the lung; thus it is equivalent to

$$\text{(tissue concentration) } \mu\text{Ci/g} = 10^{-6} \tau \times \text{(air concentration in } \frac{\mu\text{Ci}}{\text{m}^3}\text{)}.$$

Only a few measurements on bone have been reported, and these have been, for the most part, on whole bone plus marrow. Since the value of τ for fat is approximately an order of magnitude in excess of its value for other tissues, it is likely that the measurements reflect largely the uptake of ^{85}Kr into the marrow.

Some authors (Kirk, 1972; Yeh, *et al.*, 1964) have used a formula

$$\tau_{tissue} = \tau_{fat} \times f_{fat} + \tau_{blood} \times (1 - f_{fat})$$

where f_{fat} is the fractional content of fat in the tissue. This procedure is followed here. The total body can be considered as composed of two tissues — fatty tissue and nonfatty tissue. On the basis of a few measurements and in vitro studies, the Ostwald coefficient for these two types of tissue is about

$$\tau_{fat} = 0.45 \quad \text{and} \quad \tau_{nonfat} = 0.07.$$

The tissues considered are shown in Table 2 together with the fat content, the estimated Ostwald coefficient, and a few measured values. The basis of these values is discussed below in detail. On this basis an average coefficient for the body is obtained. Actually, however, the concentration is not uniform for the concentrations in adipose tissue are almost an order of magnitude higher than in most tissues.

Bremsstrahlung is produced in the body by the beta particles emitted from ^{85}Kr present in body tissues. Because of the greater concentration of ^{85}Kr in fatty tissues, there is a greater source of bremsstrahlung in these tissues, and the production of bremsstrahlung is taken here as proportional to the concentration (i. e., the fact that some portion of the range of the beta particles is outside the organ or tissue of origin is ignored). Likewise, bremsstrahlung is produced in the skeleton to a greater extent than in soft tissues because of the higher charge number of many of the constituents of bone. The spectra produced in adipose tissue, soft tissue, and bone all lie within the shaded area of Figure 5. These have been normalized to the bremsstrahlung produced by one disintegration in the tissue.

The body is considered as composed of fat and a nonfat tissue with the values cited for the Ostwald coefficient. According to Tipton (1973), the reference body contains about 15 kg of adipose tissue of which 12.5 kg is separable, i. e., occurring in easily distinguishable masses of adipose tissue such as the subcutaneous fatty layer, fat about the kidneys, etc. Of this mass, some 10 kg is fat. Using the formula cited earlier, one finds:

$$\tau_{ad} = 0.8 \times 0.45 + 0.2 \times 0.07 = 0.36 + 0.014 = 0.374.$$

This adipose tissue is distributed rather generally throughout the body, and hence is assumed here to be contained in the total body minus the totality of specified organs as defined in the phantom used in MIRD Pamphlet 5.

The skeleton, which here consists of bone plus marrow plus connective tissues, etc., contains a total of 1900 g of fat, most of which is distributed among 1500 g of yellow marrow. Thus

$$\tau_{skel} = \frac{1900 \times 0.45 + 8100 \times 0.07}{10{,}000} = 0.0855 + 0.0567 = 0.142.$$

The Ostwald coefficient is essentially a ratio of concentrations per ml of the substances, and hence a correction for average density of the skeleton (including marrow, etc.) is in order. Thus

$$\tau_{skel}/1.5 = 0.142 \times \frac{2}{3} = 0.0948.$$

The soft tissues are not devoid of fat. In addition to interstitial fat, there is a lipid constituent of most tissues which includes the essential fat. In the remainder of the body (i. e., total body minus separable adipose tissue minus skeleton), there is about 1.5 kg of essential fat out of a total tissue mass of 47.5 kg. Accordingly, the Ostwald coefficient is given by

$$\tau_{skel} = \frac{1.5 \times 0.45 + 46 \times 0.07}{47.5} = 0.0820.$$

Assuming a concentration in air of 1 $\mu Ci/m^3 = 10^{-6}$, one has, at equilibrium, concentrations of 0.37×10^{-6} g of separable adipose tissue, 0.095×10^{-6} $\mu Ci/g$ of skeleton, and 0.082×10^{-6} $\mu Ci/g$ of soft tissue. As mentioned above, the concentration in the soft tissue is for the "other tissues" of the body that remain after skeleton and separable adipose tissue are subtracted. This is equivalent to putting:

$0.082 \times 10^{-6} \times 70{,}000 = 5.7 \times 10^{-3}$ μCi in the total body;
$(0.095 - 0.082) \times 10^{-6} \times 10^{4} = 1.3 \times 10^{-4}$ μCi in the skeleton
(in addition to the activity already there as part of the total body activity); and
$(0.37 - 0.082) \times 10^{-6} \times 12{,}500 = 3.6 \times 10^{-3}$ μCi in the "other tissues" compartment
(in addition to those already there as part of the total body activity).

When this is done, the photon, beta, and bremsstrahlung doses due to ^{85}Kr absorbed in these tissues, and

present there at this equilibrium level, are found to be the values given in lines 4, 5, and 6, respectively, of Table 1. Actually, the calculation of the dose from the bremsstrahlung is slightly more complicated in that it is not merely the total source strength that must be subtracted, as above, but also the spectrum of the soft tissue dose with the proper weighting factor (i. e., [0.095 x spectrum of skeleton - 0.082 x spectrum of soft tissue] x 10^{-6} x 10^{4}) must be used to allow for the difference in spectra of these two media. A similar remark applies for separable adipose tissue.

BETA PARTICLES IN AN INFINITE CLOUD

The depth dose in skin and subcutaneous tissue from beta particles in an infinite cloud was produced by integration of the point kernel given by Berger (1971). There is a slight interface effect due to the differences of density and composition of air and skin at the interface. However, because of the near equivalent of the average Z of these materials, it is not expected to be more than a few percent of the total dose. This is presently under investigation by Berger. A graph of the depth dose is shown in Figure 7.

The skin will be considered here as consisting of an epidermal layer (of which the first 10%, on the average, consists of dead tissue), and a deeper layer, the dermis. Values for the thicknesses of these layers have been given by several authors for a variety of regions of the body (Southwood, 1955; Whitton, 1973). For example, a recent series of measurements by Whitton (1973) would indicate values of 30 to 80 μm for the epidermis on various regions of the body, exclusive of hands and feet, with a mean thickness of perhaps 50 μm. This would indicate a value of $\sim$5 μm for the stratum corneum. Thus an average dose to skin ($\sim$5 μm) is about 1.8 (rads/yr)/(μCi/m^3) with a maximum dose of 2(rads/yr)/(μCi/m^3).

The lenses of the eyes would be at a depth of $\sim$3-4 mm and hence would receive essentially no irradiation from the betas emitted in air. This value is expected to be much the same as for the average dose to the skin.

DOSE FROM ^{85}Kr IN THE AIRWAYS OF THE LUNGS

A certain activity of ^{85}Kr would be present in the air passages of the lungs. The volume of these air passages varies considerably as the person breathes, but an average value would be about 4 liters, where the functional residual capacity is 3.5 liters and the tidal volume is about 0.5 liters for an individual in the resting state (Morrow, *et al.*, 1966). Assuming that the air in these passages is at the same concentration as the outside air, the activity present in the lung air is 4 x 0.001 = 0.004 μCi. At equilibrium the person would have a daily dose to lungs of

$$51 \times 0.004 \times 2.45 \times 10^{-4} = 5.0 \times 10^{-5} \text{ rad/day.}$$

This is essentially the dose from the beta-like radiation. The daily dose to lungs from the gamma radiation would be approximately 3 orders of magnitude less than this. The daily doses to the ovaries and testes from this source in lung are 2.4 x 10^{-10}/rad/day and 4.1 x 10^{-11} rad/day, respectively. The red bone marrow dose would be about 1.6 x 10^{-9}/rad/day. These daily doses are in addition to those given in Table 1.

SUMMARY OF DOSES

Table 3 summarizes the total dose to various body organs in terms of (rads/yr)/(μCi/m^3).

REFERENCES

Berger, M. J., (1957), *Calculation of Energy Dissipation by Gamma Radiation at the Interface Between Two Media*, J. Appl. Phys. 28, 1502.

Berger, M. J., (1971), *Distribution of Absorbed Dose around Point Sources of Electrons and Beta Particles in Water and Other Media*, J. Nuclear Med. Suppl. No. 5; 12, 7.

Dillman, L. T., (1969), *Radionuclide Decay Schemes and Nuclear Parameters for Use in Radiation-Dose Estimation*, J. Nuclear Med. Suppl. No. 2; 10, 5.

Dillman, L. T., (1970, 1970a), *Radionuclide Decay Schemes and Nuclear Parameters for Use in Radiation-Dose Estimation*, J. Nuclear Med. Suppl. No. 4; 5, 5.

Dillman, L. T., (1970b), *Scattered Energy Spectrum for a Monoenergetic Gamma Emitter Uniformly Distributed in an Infinite Cloud*, Health Physics Division Annual Progress Report for Period Ending July 31, 1970, ORNL-4584, p. 216.

Haywood, F. F., J. A. Auxier, and E. T. Loy, (1964), *An Experimental Investigation of the Spatial Distribution of Dose in an Air-Over-Ground Geometry*, USAEC Report CEX-62.14.

Kirk, W. P., (1972), *Krypton 85, A Reveiw of the Literature and an Analysis of Radiation Hazards*, (Environmental Protection Agency, USGPO.

Lederer, C. M., *et al., Table of Isotopes*, 6th edition.

Morrow, P. E., *et al.,* **(1966),** *Deposition and Retention Models for Internal Dosimetry of the Human Respiratory Tract*, Health Phys. 12, 173.

Poston, J. W., and W. S. Snyder, (1973), *A Model for Exposure to a Semi-Infinite Cloud of a Photon Emitter*, submitted to Health Physics Journal.

Snyder, W. S., H. L. Fisher, Jr., M. R. Ford, and G. G. Warner, *Estimates of Absorbed Fractions for Monoenergetic Photon Sources Uniformly Distributed in Various Organs of a Meterogeneous Phantom*, J. Nuclear Med. Suppl. No. 3; 10, 5.

Southwood, W. F. W., (1955), *The Thickness of the Skin*, Plastic Reconst. Surgery 15, 423.

Tipton, H., *Gross and Elemental Content of Reference Man*, Report of ICRP Task Group on Reference Man (in preparation), Chap. II.

Whitton, J. T., (1973), *New Values for Epidermal Thickness and Their Importance*, Health Phys. 24, 1.

Yeh, S. Y., and R. F. Peterson, (1965), *Solubility of Krypton and Xenon in Blood, Protein Solutions and Tissue Homogenates*, J. Appl. Physiol. 20, 1041.

TABLE 1. Dose to Body Organs from an Infinite Cloud of ^{85}Kr (rads/day/ $\mu Ci/m^3$ of air).

Source \ Organ	Skin	Adipose Tissue	Lungs	Red Bone Marrow	Skeleton	Ovaries	Testes	Total Body
Photons in air	4.1×10^{-5}	3.2×10^{-5}	3.1×10^{-5}	3.8×10^{-5}	4.1×10^{-5}	1.3×10^{-5}	3.7×10^{-5}	3.3×10^{-5}
Bremsstrahlung in air	8.7×10^{-6}	5.7×10^{-6}	5.2×10^{-6}	9.9×10^{-6}	1.1×10^{-5}	3.1×10^{-6}	6.9×10^{-6}	6.4×10^{-6}
Bremsstrahlung in skin	1.6×10^{-7}	1.9×10^{-8}	1.1×10^{-8}	1.0×10^{-8}	2.9×10^{-8}	5.8×10^{-9}	2.7×10^{-8}	2.5×10^{-8}
Photons in the body	3.8×10^{-9}	6.2×10^{-9}	6.0×10^{-9}	6.7×10^{-9}	6.3×10^{-9}	7.6×10^{-9}	8.5×10^{-9}	6.2×10^{-9}
Betas in the body	1.0×10^{-6}	3.1×10^{-6}	1.0×10^{-6}	2.1×10^{-6}	1.0×10^{-6}	1.0×10^{-6}	1.0×10^{-6}	2.0×10^{-6}
Bremsstrahlung in the body	1.1×10^{-9}	2.1×10^{-9}	1.9×10^{-9}	3.0×10^{-9}	2.5×10^{-9}	2.1×10^{-9}	2.5×10^{-9}	2.1×10^{-9}

TABLE 2. Percentage of Separable Adipose Tissue and Nonfat Tissues and the Ostwald Coefficient for Subdivisions of the Human Body.

	Separable adipose tissue	Skeleton (bone plus marrow)	Other soft tissues
Total Mass (kg)	12.5	10	47.5
Fat Content (kg)	10	2	1.5
Ostwald Coefficient	0.374	0.142	0.082
$\frac{\mu Ci/g \text{ tissue}}{\mu Ci/ml \text{ air}}$	0.374	0.0948	0.082
Tissue Content (μCi) for 1 μCi/m in air	4.68×10^3	9.48×10^2	3.90×10^3

TABLE 3. Total Dose Rate to Organs of the Body (rads/yr)/($\mu Ci/m^3$).

Organ	Dose Rate
Skin	1.8
Adipose tissue	1.5×10^{-2}
Lungs	3.2×10^{-2}
Red bone marrow	1.8×10^{-2}
Skeleton	1.9×10^{-2}
Ovaries	6.2×10^{-3}
Testes	1.6×10^{-2}
Lenses of the eyes	1.8×10^{-2}

INPUT DATA

Radiation	%/disintegration	Transition energy (MeV)	Other nuclear parameters
Beta-1	0.4	0.16 *	Allowed
Beta-2	99.6	0.67 *	First forbidden unique
Gamma-1	0.41	0.514	M2, $\alpha_K = 0.007$, K/L = 12

Ref.: Lederer, C. M. *et al*, *Table of Isotopes*, 6th ed.
* Endpoint energy (MeV).

OUTPUT DATA

Radiation (i)	Mean number/disintegration (n_i)	Mean energy (MeV) ($\bar{E}_i$)	Δ_i $\left(\frac{\text{g-rad}}{\mu\text{Ci-h}}\right)$
Beta-1	0.0040	0.0437	0.0004
Beta-2	0.9960	0.2455	0.5218
Gamma-1	0.0041	0.5140	0.0045

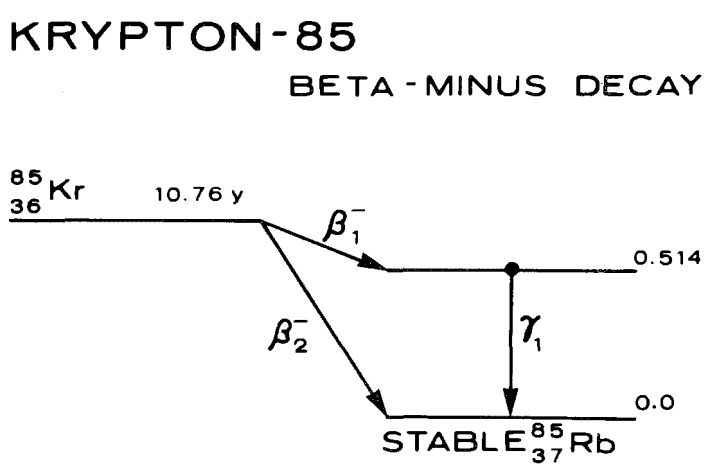

Figure 1.

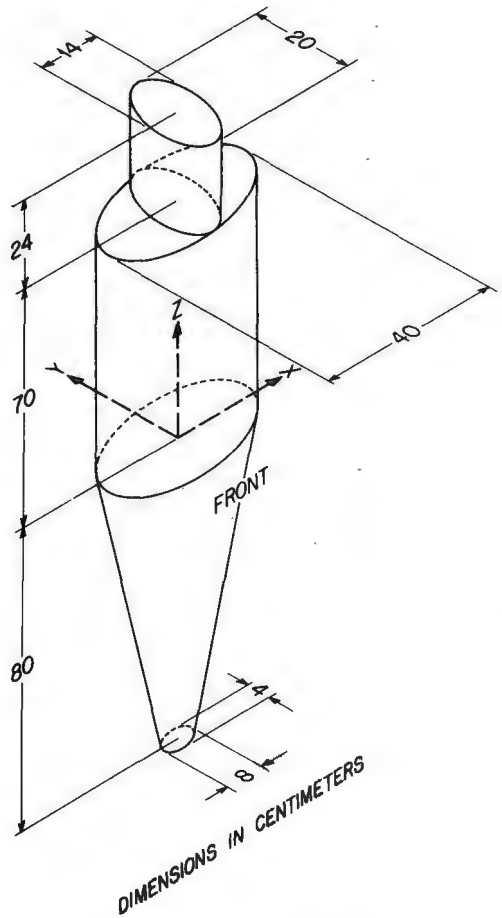

The Adult Human Phantom.

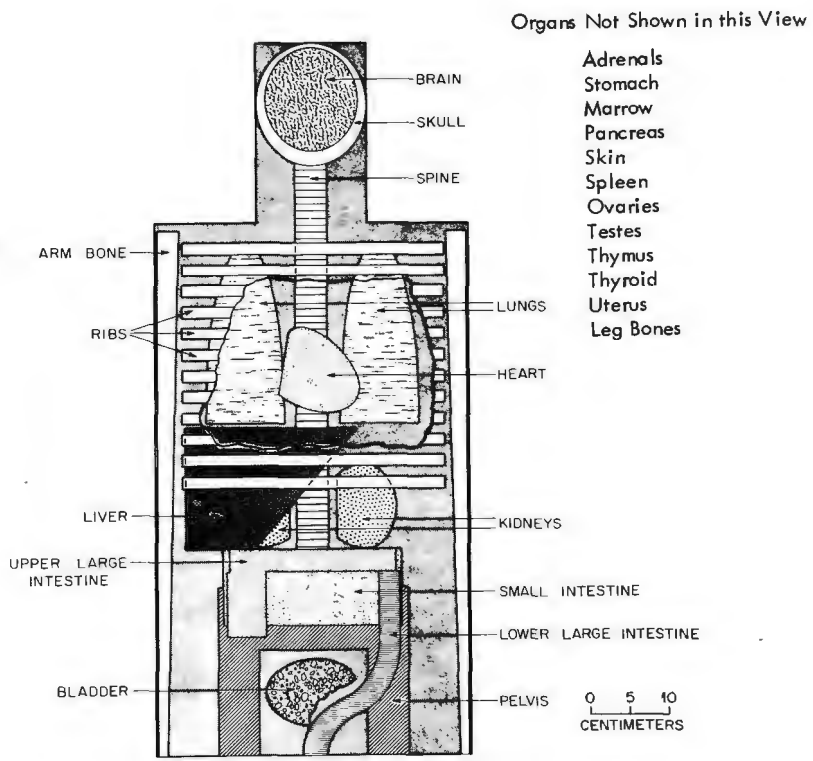

ANTERIOR VIEW OF THE PRINCIPAL ORGANS IN THE HEAD AND TRUNK OF THE PHANTOM

Figure 2.

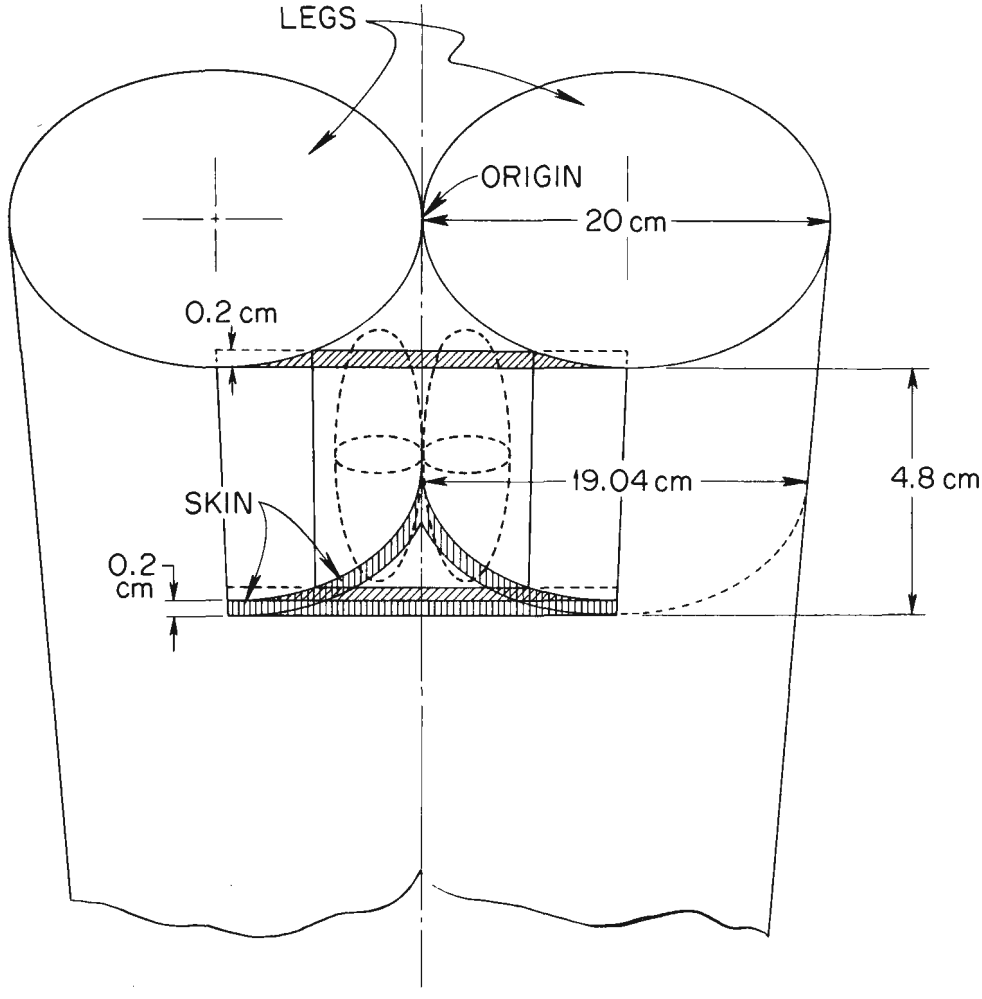

Legs and Male Genitalia of Phantom.

Figure 3.

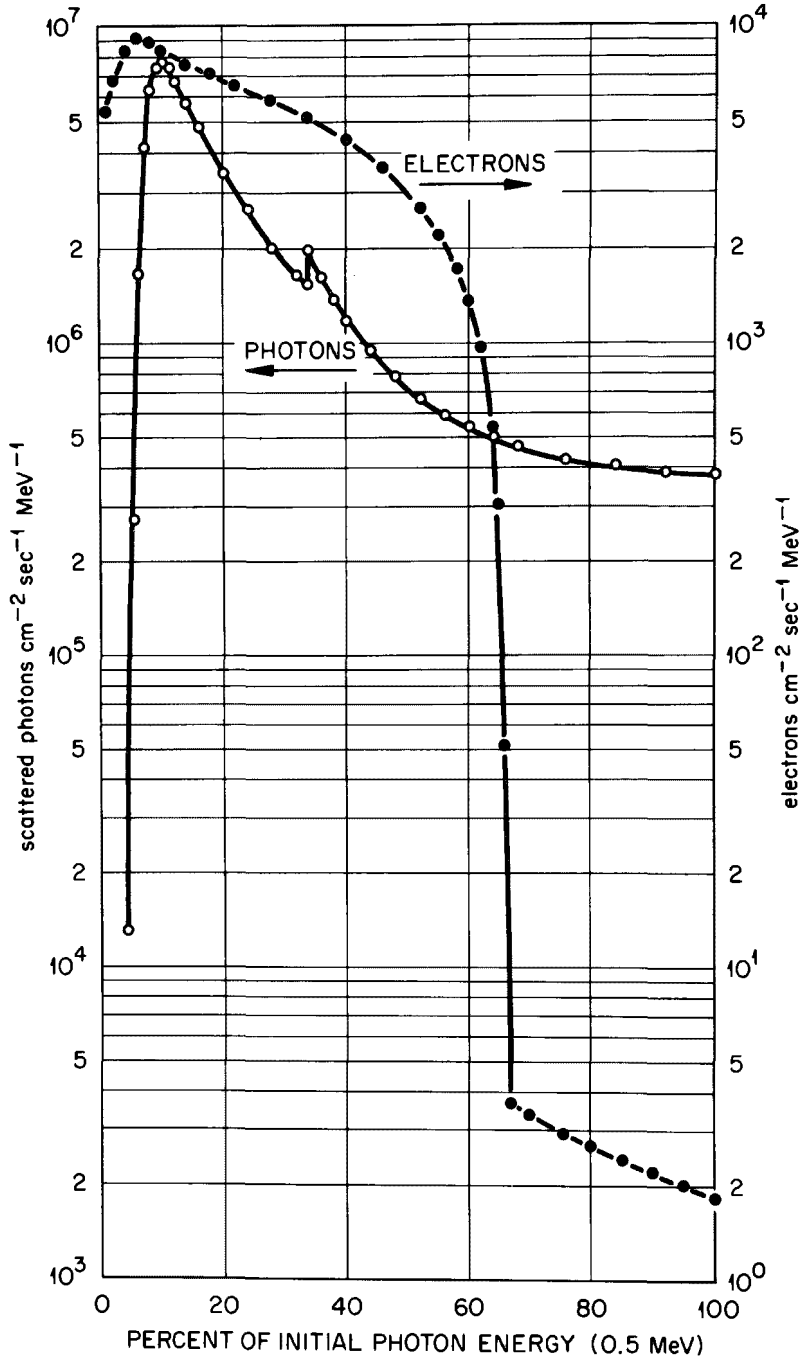
ELECTRONS
PHOTONS
scattered photons cm^{-2} sec^{-1} MeV^{-1}
electrons cm^{-2} sec^{-1} MeV^{-1}
PERCENT OF INITIAL PHOTON ENERGY (0.5 MeV)
0
20
40
60
80
100
10^7
10^6
10^5
10^4
10^3
10^4
10^3
10^2
10^1
10^0

Figure 4.

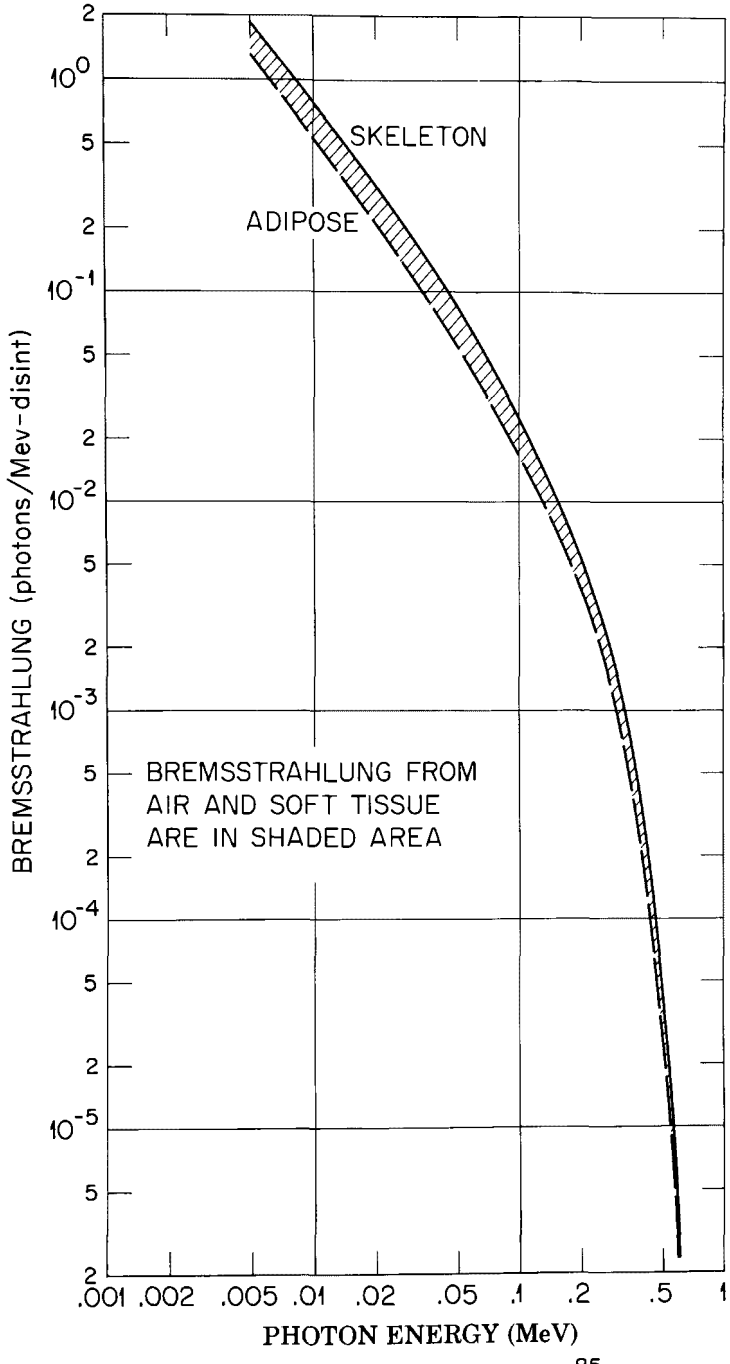

Energy Spectrum of Bremsstrahlung from ^{85}Kr Emitted in Skeleton and in Adipose Tissue.

Figure 5.

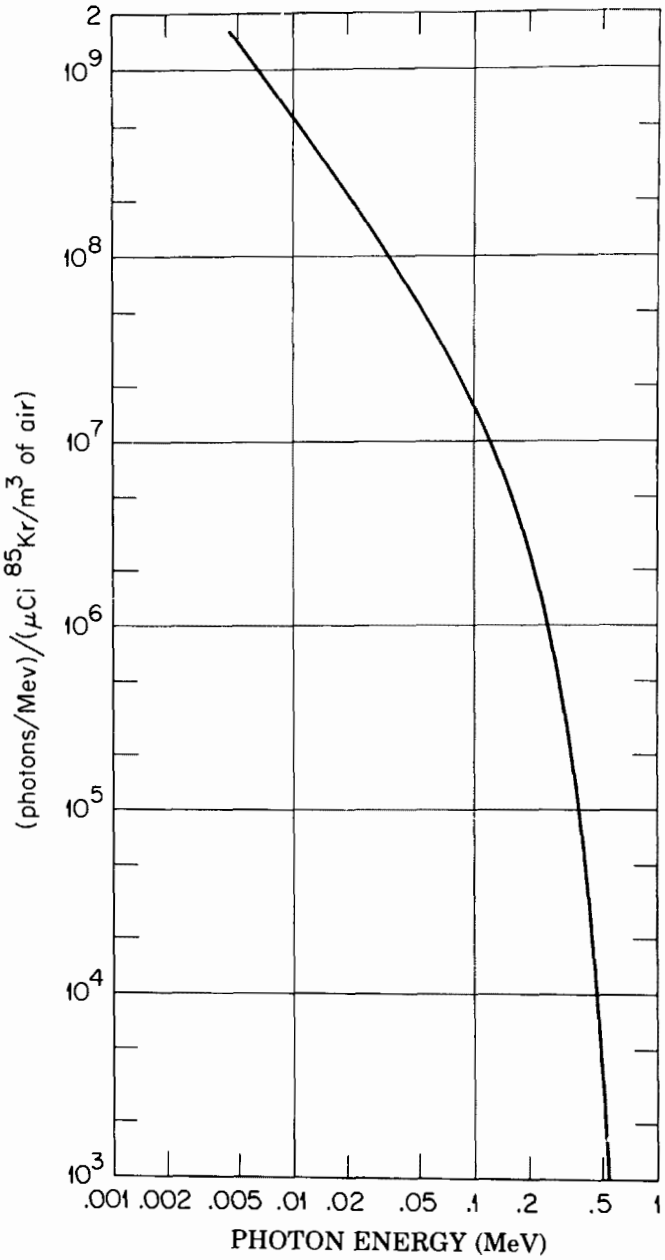

Bremsstrahlung Photons per day as a Function of Energy Produced in the Skin of Reference Man due to a Cloud of ^{85}Kr in Air.

Figure 6.

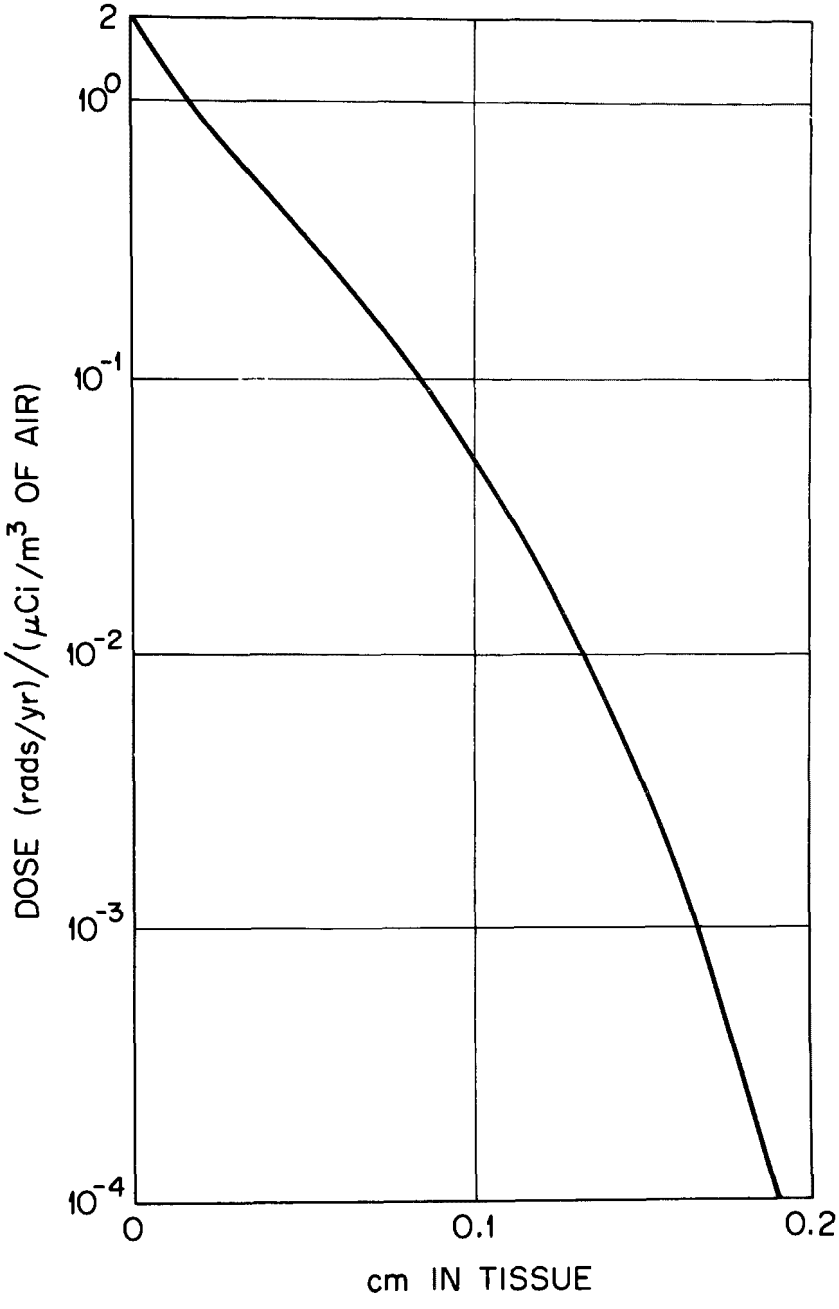

Depth Dose in Tissue from Beta Radiation (Infinite Cloud of ^{85}Kr, 1 μCi/m^3).

Figure 7.

DOSIMETRY FOR RADIOACTIVE NOBLE GASES*

J. K. Soldat, P. E. Bramson and H. M. Parker
Battelle
Pacific Northwest Laboratory
Richland, Washington 99352

Abstract

This is a survey of conventional methods and results in the dosimetry of the noble gases, with special reference to the environmental considerations relating to nuclear energy applications. Radon problems will be excluded, as will all issues specific to medical applications of the gases. (Physiological input data from medical work is, of course, an important part of the required dosimetry information.)

Among the dosimetry methods is the well-known Monte Carlo method of W. Snyder, et al., at ORNL. This will be briefly put in perspective, as a relevant paper by the ORNL group is included in this volume.

The normally low and variable concentrations of the mixed noble gases in the environment lead to problems both in "calculational dosimetry" and in field measurements. The phases selected for comment will mainly relate to reasonable perspective in accounting for such secondary and tertiary intake pathways as the drinking of water containing dissolved noble gases.

INTRODUCTION

The dosimetry of the radioactive noble gases is of widespread interest. Naturally occurring radioactive noble gases are limited to isotopes of radon, but they are important contributors to the internal doses received by uranium mine workers. Radioisotopes of argon are formed by the neutron activation of stable argon. Radioisotopes by krypton and xenon are produced as fission products resulting primarily from the fissioning of uranium of plutonium fuels in nuclear reactors. They are generally retained within the fuel elements until the fuel is chemically reprocessed. Small amounts of fission products, however, are released from reactor facilities as a result of fuel element leaks.

The dosimetry of ^{85}Kr was discussed in detail by Dr. W. S. Snyder. It is my intent to extend the dosimetry discussion to several other artificially created radioactive noble gases.

GENERAL DOSIMETRY CONSIDERATIONS AND CALCULATIONS

As Dr. Snyder has demonstrated, the complete dosimetry of the noble gases requires the calculation of several factors; such as, (1) external dose to the skin from both beta and gamma radiations; (2) external dose to the total body, gonads, and internal organs; (3) dose to the lung from inhaled radioisotopes; and (4) dose to body from noble gases dissolved in the bloodstream, and then absorbed in the various tissues.

Doses from the ingestion of noble gases are generally not addressed in the literature since noble gases have low solubility in water. Although noble gas solubility is higher in pressurized water systems, the release of the pressure results in escape of the gas. Hence, the ingestion of unusually high concentrations of noble gas in water is unlikely. The concentration of the noble gases in the water at the time of ingestion would be difficult to estimate. Adding to the uncertainty in such an estimation is the fact that xenon may be retained in the water to some degree when organic material is present.

It has been aptly demonstrated by several workers (including Dr. Snyder) that the dose from noble gases absorbed in tissue is generally small compared to the dose from direct external radiation, and from inhalation (Hendrickson, 1970; Kirk, 1972; Snyder, *et al.*, 1973; and Whitton, 1968). These internal doses are, however, the ones to consider for medical applications of these nuclides. In subsequent sections some of these results are tabulated and compared with each other, and with external and inhalation doses.

External doses resulting from submersion in a large plume of radioactive gas can be easily calculated if the concentration of the material in the air is relatively uniform. Doses can be determined on the assumption that the plume is "infinite" in volume relative to the range of the emitted radiations. Under this assumption, the energy absorbed per gram of material is equivalent to the energy emitted per gram. All that is required then is to convert the average energy per disintegration to dose, and to correct for differences in energy absorption between air and tissue, and for the physical geometry of each specific exposure situation.

Frequently the airborne concentration surrounding a person is very non-uniform; for example, when he is standing close to a tall stack. For this situation the radiation from the overhead plume must be taken into consideration when evaluating the external dose. Several computer programs have been developed for treating the required numerical integration of the contribution from each finite cloud element (Strenge, *et al.*, 1973). Such specialized situations were not included in the present work, but the calculations are manageable once the geometry has been defined.

The dose from submersion in air is an external dose to either the skin only, or the skin and the total body, depending upon the penetrating power of the radiation emitted from the airborne radioisotope.

All of the noble gases considered in this paper emit only beta and gamma radiation. For the present work, we have converted rad to rem using a quality factor of 1; however, a quality factor (QF) of 1.7 was used for beta particles and electrons with maximum energies equal to or less than 30 keV (ICRP, 1959). It has been reported by H. J. Dunster that the ICRP is seriously considering the use of a QF of 1.0 for all beta and electron energies (Dunster, 1969).

In addition, we have chosen to calculate the skin dose at a depth of 7×10^{-3} cm (7 mg/cm^2) and the total-body dose at a depth of 5 cm as originally suggested by the NCRP (NBS, 1964). Recent measurements indicate that 4 or 5 mg/cm^2 might be more appropriate than 7 mg/cm^2 (Whitton, 1973). The dose to the male gonads was calculated at a depth of 1 cm in tissue. No separate dose calculation was made, however, for the female gonads. (The total-body dose can be used as an upper limit to the female gonad dose from external radiation.)

The ratio of surface to depth dose was estimated for each maximum beta energy by methods given by Loevinger, *et al.*, (1956) and summed by nuclide. Gamma radiation dose at each of the 3 depths in tissue was determined from the values of absorption coefficients for muscle and the ratio of stopping power for muscle and air tabulated by the National Bureau of Standards (NBS, 1964). The decay schemes for the nuclides were taken from (the tables on pages 73 and 285 from) Lederer, *et al.*, (1967).

For a person standing on the ground surrounded by a very large hemisphere of radioactive gas, the geometry for gamma radiation is obviously 2π. For beta radiation with its shorter range in air, the physical arrangement approaches the infinite volume (4π geometry). However, since the beta is of limited penetrating power, it will irradiate the skin from only one side and again the geometry will be 2π. (Minor exceptions can occur in thin membranes, such as a protruding ear, which could receive beta radiation from both sides, approaching a 4π geometry.)

(1) **Equation 1.** The resulting equation for calculation of the dose from air submersion is (Soldat, 1971):

$$(D.F.)_{air\ sub} = 0.887\,(\bar{E}_\beta + \bar{E}_\gamma)$$

where $(D.F.)_{air\ sub}$ is the dose factor in units of mrem/h per μCi/m^3, $\bar{E}_\beta$, $\bar{E}_\gamma$ are the effective energies of the beta and gamma radiations, respectively, calculated at the depth of interest (7×10^{-1} or 5 cm) and corrected for relative stopping power.

The constant takes into account the density of air (1.2×10^{-3} g/ml @20°C), the conversion from MeV to mrem and the factor of 1/2 for 2π geometry.

(2) **Equation 2.** The dose to the lung from the air within it can be calculated from the following equation:

$$(D.F.)_{inhalation} = 2.13\, V_L \mathcal{E}/m \text{ mrem/h per } \mu\text{Ci/m}^3$$

where V_L is the volume of air within the lung, 4 liters, (Snyder, *et al.*, 1973)

$\mathcal{E}$ is the effective energy deposited in the lung, MeV per disintegration,

m is the mass of the lung, 100 g. (ICRP, 1959)

The concentration of the noble gas in the air within the lung is taken to be the same as that in the inspired air. The effective energy, $\mathcal{E}$, is calculated from the formula of the ICRP (1959) using an effective radius of 10 cm for the lung.

The results obtained from applying Equation 1 to calculation of the external dose rates to skin, testes, and total body from 14 radioactive noble gases are summarized in Table 1. Also included in Table 1 are the dose rates to lung tissue from inhalation of these noble gases, as well as the combined dose to the lung from both inhalation and external gamma irradiation.

Two important daughter radionuclides, ^{88}Rb and ^{138}Cs, have been included in Table 1. These two nuclides make significant contributions to the dose rates from their parent activities. Rubidium-88 (18-minute half-life) is nearly always present at equilibrium with its parent ^{88}Kr (2.8-hour half-life). The total dose rate from the parent-daughter combination is from 30% to 300% higher than from the parent alone, depending upon tissue depth.

Both ^{138}Xe and ^{138}Cs have relatively short half-lives, 14 minutes and 32 minutes, respectively, and the daughter contributes a varying amount to the total dose from the ^{138}Xe, depending upon the time since release of the noble gas to the atmosphere. The dose rate per unit concentration of ^{138}Cs is 150% to 200% of that from its parent ^{138}Xe, but its longer half-life may reduce its relative contribution slightly.

Precise lung dosimetry would require that these two daughter radionuclides be treated as attached to particles. As such there would be a buildup in the lung with an attendant increase in the dose calculated. On the practical level, this buildup may be disregarded because of the short radioactive half-lives of the daughters.

DOSE TO THE SKIN AND TESTES

The detailed results for the beta and gamma contributions to the dose to the skin and testes are given in Table 2 (A and B), where they are compared to similar data presented by Schaeffer (1973) at the recent IRPA Congress in Washington, D.C. Dr. Schaeffer calculated the beta dose at a point 'P' in tissue by integrating the contribution from all of the beta particles which were able to reach that point. All of the beta particles were assumed to travel in a straight line through air and tissue. There is excellent agreement between Dr. Schaeffer's results and those obtained with the empirical formula of Loevinger for all nuclides, except perhaps ^{87}Kr, where our values are 30% higher.

Dr. Schaeffer's calculations indicated that no beta rays from any of the noble gases were energetic enough to penetrate through the 1 cm of tissue assumed to be over the male gonads (Schaeffer, 1973). The Loevinger formula, however, implies a small beta contribution to the doses to the testes, especially for the ^{88}Rb daughter of ^{88}Kr, and for ^{87}Kr and ^{137}Xe (Loevinger, *et al.*, 1956).

TOTAL-BODY DOSIMETRY

Table 2 (C) lists the results obtained by us for the total-body dose rate and compares them with those of Schaeffer (1973) and Russell, *etal.,* (1972). The latter authors employed the reciprocity theorem (Loevinger, *et al.,* 1956) for their calculation wherein:

"the internal gamma (total-body dose from an external cloud equals the dose to the cloud from the radioactivity in the body if the concentrations are equal. .... This dose is then the difference between the dose to a point in an infinite medium with uniform source distribution and the dose absorbed in the body from a uniform source in the body with the same concentration as in the infinite media."

This method of calculation yields an average dose over the entire body — rather than a dose at a single depth in tissue. Nevertheless, the results obtained by Russell, *et al.,* (1972) are in reasonable agreement with those obtained by Dr. Schaeffer (1973) and in the present work utilizing the half-infinite cloud calculation.

Dr. Schaeffer's values do not include a correction for attentuation in the first few centimeters of tissue. The attenuation becomes important for the very low energy radiation such as the bremsstrahlung from ^{85}Kr. For this nuclide the dose calculated in the present work is 2/3 of that calculated by Dr. Schaeffer. Neither of these two sets of calculations, however, include a "build-up factor" which could compensate somewhat for the omission of the attenuation corrections in Dr. Schaeffer's calculations. In addition to the results shown in the table, Dr. Snyder has reported values of 1.6×10^{-3} for ^{85}Kr (Snyder, *et al.,* 1973) and 0.020 for ^{133}Xe (Hilyer, *et al.,* 1972).

INTERNAL DOSE TO THE LUNGS

The calculated internal dose to the lungs from inhalation of noble gases is summarized in Table 3 along with the values calculated by Russell and Galpin. The latter authors assumed a lung volume of 5.6 liters — rather than the 4 liters employed in the present work. As a result our values are generally, but not always, lower then those of Russell and Galpin. The two exceptions are ^{88}Kr and ^{135}Xe.

Table 3 also tabulates internal doses to lung and other tissues calculated by Mrs. Whitton (1968) for ^{85}Kr and ^{133}Xe. The value used by Mrs. Whitton for the lung volume was not stated, but her calculated values for lung dose agree well with ours. As can be seen in the table, the doses from noble gases absorbed in tissue are significantly lower than those from external gamma radiation.

INTERNAL AND EXTERNAL DOSES FROM KRYPTON-85

Table 4 lists the results obtained by several workers for internal and external doses from ^{85}Kr. The assumptions used by the various authors were not always the same. This is especially true of the depth at which the "skin" dose was calculated, and the lung volume. The value for the lung dose attributed to Dr. Schaeffer was not actually given in his paper, but was estimated by us from the value of the $(MPC)_a$ which he calculated for lung as the critical organ. As such the value of 5.8×10^{-3} probably includes the contribution from external radiation.

CONCLUSIONS

When the variations in assumptions are taken into account, there is reasonable agreement among the values obtained by the different authors. It is also obvious that the internal doses are insignificant compared to the external total-body and skin doses. For noble gas nuclides with relatively little penetrating radiation, the critical organ is the skin — even considering its less restrictive dose standard. For the other noble gases, the total body is the critical organ.

If one were the calculate the $(MPC)_a$ values for these noble gases based upon the dose rates presented in this paper, the values obtained would be much less restrictive than the ICRP values currently accepted. For example, the ICRP $(MPC)_a$ for 168-hour occupational exposure to ^{85}Kr is 3 μCi/m^3. Dr. Schaeffer calculated corresponding values of 20, 170, and 290 for skin, total body, and lung (internal and external), respectively, as critical organs. As a result, one should always rely on first principles when calculating radiation doses, rather than to simply multiply fractional MPC by the dose standard.

REFERENCES

Dunster, H., (1969), *Progress Report from ICRP,* Health Physics, 17:389.

Hendrickson, M.M., (1970), *The Dose from ^{85}Kr Released to the Earth's Atmosphere,* USAEC Report BNWL-SA-3233, Pacific Northwest Laboratory, Richland, Washington.

Hilyer, M.M. and W.S. Snyder, (1972), *Estimates of Dose from ^{133}Xe to Infants and Children for Immersion in an Infinite Cloud and for Medical Uses,* paper presented at the Mid-Year Health Physics Society Symposium in Puerto Rico, December 1972 (to be published in the conference proceedings).

International Commission on Radiological Protection, (1959), *Report on ICRP Committee II on Permissible Dose for Internal Radiation,* ICRP Publication 2, Pergamon Press, New York.

Kirk, W.P., (1972), *Krypton-85, A Review of the Literature and an Analysis of the Radiation Hazards,* Environmental Protection Agency, Office of Research and Monitoring, Washington, D.C. 20460.

Lederer, C.M., J.M. Hollander and I. Pearlman, (1967), *Table of Isotopes,* 6th Ed., John Wiley and Sons, Inc., New York.

Loevinger, R., E.M. Japha, and G.L. Brownell, (1956), *Discrete Radioisotope Sources,* Chapter 16 in *Radiation Dosimetry,* Academic Press, Inc., New York, NY.

National Bureau of Standards, (1964), *Physical Aspects of Irradiation (Recommendations of the ICRU Report 10b, 1962),* NBS-Handbook 85, U.S. Dept. of Commerce, U.S. Government Printing Office, Washington, D.C.

National Committee on Radiation Protection, (1954), *Permissible Dose From External Sources of Ionizing Radiation,* National Bureau of Standards Handbook 59, Superintendent of Documents, Washington, D.C.

Russell, J.L., and F.L. Galpin, (1972), *Comparison of Techniques for Calculating Doses to the Whole Body and to the Lungs from Radioactive Noble Gases,* pp 286-308 in *Radiation Protection Standards: Quo Vadis* (W.P. Howell and J.P. Corley compilers), Proceedings of the Sixth Annual Health Physics Society Topical Symposium, Columbia Chapter, Health Physics Society, Richland, Washington, February 1972.

Schaeffer, R., (1973), *Calculs de Dose en Irradiation Extreme Par lex Gaz Ranes,* paper presented at the International Radiation Protection Association 3rd Congress, September 9-14, 1973, Washington, D.C.

Snyder, W.S., *et al.*, (1973), *Dosimetry for a Man Immersed in an Infinite Cloud of ^{85}Kr,* paper presented at the Noble Gases Symposium, Las Vegas, Nevada, September 24-28, 1973.

Soldat, J.K., (1971), *Modeling of Environmental Pathways and Radiation Doses from Nuclear Facilities,* USAEC Report BNWL-SA-3939, Pacific Northwest Laboratory, Richland, Washington.

Strenge, D.L., and E.C. Watson, (1973), *KRONIC A Computer Program for Calculating Annual Average External Doses from Chronic Atmospheric Releases of Radionuclides,* USAEC Report BNWL-B-264, Pacific Northwest Laboratory, Richland, Washington.

Whitton, J.T., (1968), *Dose Arising from Inhalation of Noble Gases,* CEGB Report RD/B/N-1274, Central Electricity Generating Board, Berkeley Nuclear Laboratories, Berkeley, Glos.

Whitton, J.T., (1973), *New Values for Epidermal Thicknesses and Their Importance,* Health Physics, 24:1-8.

Table 1. Dose Rates to Selected Tissues from a Semi-Infinite Cloud of Noble Gases (mrem/h per $\mu Ci/m^3$)(a).

	External			Internal	
Nuclide	Skin(b)	Testes(c)	Total Body(d)	Lungs(e)	Total Lungs
^{39}Ar	0.12	0.00043	0.00033	0.0016	0.0019
^{41}Ar	1.6	1.1	1.1	0.0067	1.1
^{83m}Kr	0.00076	0.0	0.0	0.00037	0.00037
^{85m}Kr	0.32	0.13	0.13	0.0024	0.13
^{85}Kr	0.16	0.0022	0.0022	0.0019	0.0041
^{87}Kr	2.7	1.3	1.3	0.013	1.3
^{88}Kr	2.0	1.5	1.5	0.0067	1.5
(^{88}Rb)	(2.7)	(0.93)	(0.56)	(0.019)	(0.58)
^{131m}Xe	0.048	0.0028	0.0028	0.0012	0.0040
^{133m}Xe	0.060	0.027	0.027	0.0015	0.028
^{133}Xe	0.069	0.025	0.025	0.0012	0.027
^{135m}Xe	0.50	0.35	0.35	0.0019	0.035
^{135}Xe	0.49	0.21	0.21	0.0033	0.21
^{137}Xe	1.8	0.22	0.12	0.015	0.14
^{138}Xe	1.7	1.2	1.2	0.0066	1.2
(^{138}Cs)	(3.1)	(1.8)	(1.8)	(0.012)	(1.8)

(a) No credit taken for attenuation by clothing.
(b) At a tissue depth of 7×10^{-3} cm.
(c) At a tissue depth of 1 cm.
(d) At a tissue depth of 5 cm.
(e) Assuming a lung volume of 4 liters.

Table 2. Comparison of External Dose Rates to Selected Tissues from a Semi-Infinite Cloud of Noble Gases (mrem/h per $\mu Ci/m^3$).

A. Skin

		This Paper		
Nuclide	Schaeffer (1973) Beta	Beta(a)	Gamma(b)	Total
^{39}Ar	----	0.12	4.5×10^{-4}	0.12
^{41}Ar	0.37	0.40	1.2	1.6
^{83m}Kr	----	0	7.6×10^{-4}	7.6×10^{-4}
^{85m}Kr	0.17	0.18	0.14	0.32
^{85}Kr	0.17	0.16(0.21)(c)	2.8×10^{-3}(2.1×10^{-3})(c)	0.16(0.21)(c)
^{87}Kr	0.83	1.1	1.6	2.7
^{88}Kr	----	0.32	1.70	2.0
(^{88}Rb)	(----)	(2.1)	(0.64)	(2.7)
^{131m}Xe	----	0.045	3.2×10^{-3}	0.048
^{133m}Xe	----	0.028	0.032	0.060
^{133}Xe	0.040	0.040(0.0075)(d)	0.029(0.026)(d)	0.069(0.034)(d)
^{135m}Xe	----	0.029	0.41	0.50
^{135}Xe	0.23	0.25	0.24	0.49
^{137}Xe	----	1.6	0.17	1.8
^{138}Xe	----	0.38	1.36	1.7
(^{138}Cs)	(----)	(1.0)	(2.1)	(3.1)

(a) Including conversion electrons.
(b) Including Bremsstrah lung.
(c) Values reported by Dr. Snyder, *et al.*, (1973).
(d) Values reported by Dr. Snyder (Hilyer, *et al.*, 1972).

Table 2 (Contd). Comparison of External Dose Rates to Selected Tissues from a Semi-Infinite Cloud of Noble Gases. (mrem/h per $\mu Ci/m^3$).

B. Testes

Nuclide	Schaeffer (1973) Beta	This Paper: Beta(a)	This Paper: Gamma(b)	This Paper: Total
^{39}Ar	----	0	4.3×10^{-4}	4.3×10^{-4}
^{41}Ar	0	2×10^{-4}	1.1	1.1
^{83m}Kr	----	0	0	0
^{85m}Kr	0	0	0.13	0.13
^{85}Kr	0	0	2.2×10^{-3}(1.8×10^{-3})(c)	2.2×10^{-3}(1.8×10^{-3})(c)
^{87}Kr	0	0.047	1.3	1.3
^{88}Kr	----	2×10^{-3}	1.5	1.5
(^{88}Rb)	(----)	(0.37)	(0.56)	(0.93)
^{131m}Xe	----	0	2.8×10^{-3}	2.8×10^{-3}
^{133m}Xe	----	0	0.027	0.027
^{133}Xe	0	0	0.025(0.020)(d)	0.025(0.020)(d)
^{135m}Xe	----	0	0.35	0.35
^{135}Xe	0	0	0.21	0.21
^{137}Xe	----	0.10	0.12	0.22
^{138}Xe	----	9×10^{-4}	1.2	1.2
(^{138}Cs)	(----)	(0.012)	(1.8)	(1.8)

(a) Including conversion electrons.
(b) Including Bremsstrahlung.
(c) Values reported by Dr. Snyder, *et al.*, (1973).
(d) Values reported by Dr. Snyder (Hilyer, *et al.*, 1972).

C. Total Body

Nuclide	Schaeffer (1973)	Russell, *et al.*, (1972)	(Snyder, *et al.*, 1973 Hilyer, *et al.*, 1972)	This Paper
^{39}Ar	----	----	----	3.3×10^{-4}
^{41}Ar	1.16	----	----	1.1
^{83m}Kr	----	----	----	0
^{85m}Kr	0.15	0.076	----	0.13
^{85}Kr	3.3×10^{-3}	1.2×10^{-3}	1.6×10^{-3}	2.2×10^{-3}
^{87}Kr	0.90	0.90	----	1.3
^{88}Kr	----	0.88	----	1.5
(^{88}Rb)	(----)	(----)	(----)	(0.56)
^{89}Kr	----	4.2	----	----
^{131m}Xe	----	6.8×10^{-3}	----	2.8×10^{-3}
^{133m}Xe	----	0.030	----	0.027
^{133}Xe	0.074	0.030	0.020	0.025
^{135m}Xe	----	0.24	----	0.35
^{135}Xe	0.24	0.14	----	0.21
^{137}Xe	----	0.090	----	0.12
^{138}Xe	----	1.7	----	1.2
(^{138}Cs)	(----)	(----)	(----)	(1.8)

(a) 1. The authors used the reciprocity theorem (Loevinger, *et al*, 1956) to calculate total body dose.
2. The values presented here do not include the contribution from beta radiation as did those presented in the original paper.

Table 3. Comparison of Internal Dose Rates from Inhaled Noble Gases (units of 10^{-3} mrem/h per $\mu Ci/m^3$).

	Russell and Galpin (1972)		Whitton (1968) (b)				This Paper
Nuclide	Lungs(a)	Total Body(b)	Lungs(c)	Adipose Tissue	Remaining Tissue(b)	Testes(c)	Lungs(d)
^{39}Ar	----	----	----	----	----	----	1.6
^{41}Ar	----	----	----	----	----	----	6.7
^{83m}Kr	----	----	----	----	----	----	0.37
^{85m}Kr	3.0	0.14	----	----	----	----	2.4
^{85}Kr	3.0	0.11	1.6(2.1)(e)	0.24(0.13)(e)	0.030(0.02-0.09)(e)	0.030(0.042)(e)	1.9
^{87}Kr	17	0.80	----	----	----	----	13
^{88}Kr	5.2	0.52	----	----	----	----	6.7
(^{88}Rb)	20	1.6	----	----	----	----	----
^{131m}Xe							
^{133m}Xe	1.8	0.21	----	----	----	----	1.2
^{133}Xe	2.2	0.27	----	----	----	----	1.5
^{135m}Xe	1.7	0.20	1.0(1.1)(f)	0.53(0.48)(f)	0.095(0.062-0.075)(f)	0.059(0.063)(f)	1.2
^{135}Xe	4.0	0.33	----	----	----	----	1.9
^{137}Xe	1.5	0.54	----	----	----	----	3.3
^{138}Xe	18	2.1	----	----	----	----	15
(^{138}Cs)	13	2.4	----	----	----	----	6.6

(a) Based on a lung volume of 5.6 liters.
(b) Used an average value of Ostwald coefficient for entire body.
(c) Lung volume not stated.
(d) Based on a lung volume of 4 liters.
(e) Values of Dr. Snyder, *et al.*, (1973).
(f) Values of Dr. Snyder (Hilyer, *et al.*, 1972).

Table 4. Comparison of Radiation Doses to Various Tissues from a Semi-Infinite Cloud of ^{85}Kr (mrem/h per $\mu Ci/m^3$).

Pathway	Snyder, *et al.*,(1973)	Russell, *et al.*, (1972)	Whitton (1968)	Schaeffer (1973)	Kirk (1972)	Hendrickson (1970)	This Paper
External — Skin	0.21(a)	1.6×10^{-3}(c)	0.19	0.17(d)	0.24(e)	0.11(d)	0.16(d)
Beta	2.1×10^{-3}(b)	----	----	----	1.9×10^{-3}	2.7×10^{-3}	2.8×10^{-3}
Gamma Bremsstrahlung	----	----	0.19	0.17	0.24	0.11	0.16
Total	1.6×10^{-3}	1.2×10^{-3}(f)	2.3×10^{-3}	3.3×10^{-3}	1.5×10^{-3}	2.7×10^{-3}	2.2×10^{-3}
External — Total Body	1.8×10^{-3}	1.2×10^{-3}(f)	2.3×10^{-3}	3.3×10^{-3}	1.5×10^{-3}	2.7×10^{-3}	2.2×10^{-3}
Gonads	2.1×10^{-3}(g)	3.0×10^{-3}(h)	1.6×10^{-3}(i)	5.8×10^{-3}(k)	----	1.9×10^{-3}(j)	1.9×10^{-3}(g)
Inhalation — Lungs	8.4×10^{-5}	1.1×10^{-4}	----	----	8.7×10^{-5}	----	----
Total Body	1.3×10^{-4}	----	2.4×10^{-4}	----	----	----	----
Adipose Tissue	$(2\text{-}9) \times 10^{-5}$	----	3×10^{-5}	----	----	----	----
Remaining Tissue	4.2×10^{-5}	----	3×10^{-5}	----	----	----	----
Gonads							

(a) Average dose to skin layer 5×10^{-3} cm thick (maximum is ~10% higher).
(b) Average dose to a layer 0.2 cm thick.
(c) Assumed skin depth of 0.1 cm.
(d) Assumed skin depth of 0.007 cm
(e) Assumed skin depth of 0.0 cm.
(f) Based upon reciprocity theorem.
(g) Assumed lung volume of 4 liters.
(h) Assumed lung volume of 5.6 liters.
(i) Lung volume not specified.
(j) Assumed lung volume of 3.5 liters.
(k) Estimated from Dr. Schaeffer's calculated values of $(MPC)_a$ for lung and probably includes the contribution of external radiation.

BEHAVIOR OF KRYPTON-85 IN ANIMALS

W. P. Kirk
Experimental Biology Laboratory
National Environmental Research Center
U.S. Environmental Protection Agency
Research Triangle Park, North Carolina 27711

Abstract

The in vivo behavior of ^{85}Kr can usually be predicted if the protein/water/fat composition of a body or tissue and its blood perfusion characteristics are known. The amount of isotope taken up by the tissue is the weighted sum of component tissue: air partition coefficients multiplied by the concentration of ^{85}Kr in alveolar air, while the rates of saturation or desaturation are determined by perfusion.

Equations describing postulated kinetic behavior of noble gases are presented and compared with ^{85}Kr data reported for individual organs and tissues from several species in the literature, and data obtained with whole guinea pigs and rats.

Partition coefficients are discussed and theoretical values compared with in vitro data from this laboratory and the literature, and with in vivo data for blood and 22 other organs/tissues obtained with guinea pigs in current work.

Equilibrium beta radiation doses to various organs/tissues from a contained isotope in guinea pigs breathing ^{85}Kr at present MPC_a are given.

INTRODUCTION

For several years the author has been investigating the physiological behavior and radiation effects of ^{85}Kr to provide the EPA with *in vivo* bioeffects data upon which various standards for ^{85}Kr can be based. Included in these investigations have been determinations of the saturation and desaturation kinetics of ^{85}Kr in unanesthetized guinea pigs and rats, and determinations of *in vivo* partition coefficients into guinea pig blood and tissues.

The literature search associated with these studies yielded a substantial amount of information on the behavior of Kr in an assortment of organs/tissues in several species. A dichotomy of purpose exists, however. The investigators were usually interested in evaluating blood flow, with the details of kinetic behavior being somewhat incidental, while the reverse is true in the present studies. Reports giving details of kinetic behavior or partition coefficient determinations are mostly those concerned with development of methods using ^{85}Kr to determine organ blood flow with modifications of the Fick principle. Some "use" papers also report kinetic data for control animals. Most investigations have been concerned with one organ, or part of an organ, and have used animals in an abnormal physiological state due to anesthesia, surgical trauma, restraint, or use of circulatory control drugs.

This review discusses the behavior of ^{85}Kr in animals primarily from the empirical viewpoint — what has been seen *in vivo* — rather than trying to present or support any elaborate mathematical model. The author's interests and the scope of this paper have been largely limited to understanding what happens internally when an animal is placed in an ^{85}Kr atmosphere.

THEORY

The saturation or desaturation of ^{85}Kr, and other presumably metabolically inert gases in the body have almost always been describable as an exponential or sum of exponential functions. Kety (1951) has discussed the various possibilities in detail. The simplest of the models presented is derived from the Fick principle, which Kety states as "The amount of inert gas taken up by the tissue per unit of time is equal to the quantity brought to the tissue by the arterial blood minus the quantity carried away in the venous blood." The derivation, as given by Kety (1951), for a single homogenously perfused tissue is:[1]

(1) $$\frac{dQ_i}{dt} = F_i (C_a - C_v)$$

assuming:

arterial inflow = venous outflow = F_i,

C_a = concentration in arterial blood,

C_v = concentration in venous blood,

Q_i = quantity in tissue i having volume V_i (including contained blood).

(2) $$\frac{dC_i}{dt} = \frac{1}{V_i} \frac{dQ_i}{dt} = \frac{F_i}{V_i} (C_a - C_v)$$

[1]The symbol λ, which Kety used for partition coefficients has been replaced with L, (used for the Ostwald solubility coefficient) to avoid confusion with radiation decay constants.

Assuming that venous blood from a tissue is in equilibrium with the tissue itself with respect to the inert gas:

(3) $C_i = L_i C_v$ where L_i = tissue: blood partition coefficient

then (4) $\frac{dC_i}{dt} = \frac{F_i}{L_i}(C_i - L_i C_a)$

and in saturation:

(5) $C_i = L_i C_a (L - e^{-k_i t})$ where: $k_i = \frac{F_i}{L_i V_i}$

(6) $Q = C_a \sum V_i L_i (1 - e^{-k_i t})$ where Q = total quantity in system.

or in saturation:

(7) $C_i = C_1^0 e^{-k_i t}$ where C_i^0 = concentration at t = 0.

(8) $Q = \sum Q_i^0 e^{-k_i t}$

However, for an animal breathing the gas, $C_a = CL$ where C = concentration in air and L = the blood: air partition coefficient if: (1) the gas being considered has a very low solubility in blood; (2) alveolar and arterial concentrations remain constant; and (3) gas is introduced abruptly at its final concentration into alveolar spaces (or the exposure continues long enough for complete equilibrium to occur).

Kety also presents several more complicated models which account for the ambient air-alveolar air equilibrium functions, various flow perturbations in the body, etc.

The partition coefficient is central to any analysis based on the foregoing equations. Usage has not been standard in regard to the units used for partition coefficients. Some investigators have expressed their results in terms of the weight of the receiving medium and others have used the volume. A variety of symbology is also encountered. In this review, albeit arbitrarily, the following symbols/units are used:

(1) $L_{2:1} = \frac{\text{concentration in (receiving) medium 2 } (\mu Ci/cm^3)}{\text{concentration in (source) medium 1 } (\mu Ci/cm^3)}$

as $L_{blood:air}$ or $L_{tissue:blood}$

when the source medium is air, L = the Ostwald solubility coefficient for the receiving medium.

(Note: $L_{3:1} = L_{3:2} \times L_{2:1}$ Example: $L_{tissue:air} = L_{tissue:blood} \times L_{blood:air}$)

(2) $L_{w2:1} = \frac{\text{concentration in (receiving) medium 2 } (\mu Ci/g)}{\text{concentration in (source) medium 1 } (\mu Ci/cm^3}$

$L_{w2:1} = L_{2:1}/P_1$ and

$L_{w3:1} = L_{w3:2} \times P_2 \; L_{w2:1} = L_{w3:2} \times L_{2:1}$

Except for the direct determinations of L_w tissue:air reported elsewhere (Kirk, 1973) use of L_w has been as L_w tissue:blood. In most cases, $L_{blood:air}$ has not been needed for the determinations.

It has been demonstrated *in vitro* that the Ostwald coefficient (L) of blood, saline solutions of beef brain, or rabbit muscle homogenates are the weighted sum of the fat, protein, and water (saline) solubilities for the solution (Yeh, *et al.*, 1965); (*i.e.*, $L_{solution:air} = \sum f_i L_i$ where f_i = fraction of solution made up of component i and L_i is the Ostwald solubility coefficient for fraction i). With blood, hemoglobin, which has a much higher coefficient than other protein, must be treated separately; similarily in brains, non-neutral fat is separately accounted for because its coefficient is lower than that of neutral fat.

The variation in solubility of noble gases in solvents with temperature has been investigated (Hardewig, *et al.*, 1960 ; Markham, *et al.*, 1941; Morrison, *et al.*, 1954; and Yeh, *et al.*, 1963, 1964, 1965) and shown to follow the Clapeyron relationship in organic solvents, and the Valentiner equation in aqueous solutions. The Clapeyron relationship can be expressed as: Log L = A + B/T where

L = Ostwald solubility coefficient
A, B = constants for system
T = temperature (^{0}K)

The Valentiner equation is usually written:

$\log L = a/T + b\log T + c$, where a, b, c, are constants for the system.

Most of the blood flow studies considered have used the Fick derived model presented earlier, and none of the ^{85}Kr data presented herein is sufficiently detailed to justify considering any of the more complicated analyses.

The key to blood flow determination with the Fick relationship is evaluating the exponential coefficient k used in equations (5) through (8). As stated, $k_i = F_i/V_iL_i$. (or $k_i = F_i/W_iL_{wi}$). By defining a specific flow F = ml/g/min and using k = .693/ T 1/2 where T 1/2 = half-time of saturation or desaturation, the flow can be determined by:

$F = L_wk_i = (L_w \times .693)/ T\ 1/2_i = (L_i \times .693)/(P_i \times T\ 1/2_i)$

If the tissue has a constant, uniform flow and uniform partition coefficient, T 1/2 can be easily evaluated graphically from a semi-logarithmic plot of $(C_v - C_a)$ vs time, or a comparable plot of radioactivity in the tissue, as measured externally by an appropriate detector, vs time[2].

Most organs, however, possess neither uniform perfusion nor uniform partition coefficients, and the curves obtained from them are multi-exponential in form. Accurate determination of blood flow by the Fick method in this case requires the determination of an average value[3] for k. Two approaches that have been used extensively are:

(1) Determine the T 1/2 and corresponding k for a monoexponential curve tangential to the combined semilogarithmic plot at t = O. If the partition coefficients involved are closely similar, and the initial concentrations in the compartments are equal, the initial slope will represent the total flow in the organ. Many protocols have been used with varying success in fulfilling the latter condition.

(2) Follow saturation or desaturation (preferred) long enough to accurately resolve the multi-exponential curve into its components, and determine the respective half-times and relative magnitude (extrapolate to equilibrium), and determine a weighted exponential constant or half-time to use in the equations. Best accuracy also requires some notion of the partition coefficients for the compartments.

The author feels more comfortable with results obtained by the second method; but, when multiple determinations are required, as in a clinical situation, the initial slope method is much faster and has been more extensively used.

The method of ^{85}Kr administration has been ignored so far because it has not been material to the mathematical discussions. It will obviously affect the degree to which the experiment conforms to the assumptions stated in the method of analysis. ^{85}Kr has been administered by:

(1) Inhalation from a closed circuit system, or constant concentration source; and analysis of: (a) the disappearance of ^{85}Kr from the exposure system, (b) $(C_c - C_a)$ determined in either saturation or desaturation by assay of simultaneous arterial and venous blood samples; and (c) the quantity of isotope in the organ — as determined by external counting of the radiation emitted, vs time, in saturation or desaturation.

(2) Continuous infusion of ^{85}Kr in solution (saline, dextran, etc.) into the arterial supply to the organ, and analysis of saturation or desaturation curves obtained by plotting $(C_v\ \ C_a)$, or emitted radiation vs time in phase.

(3) Fast injection of a bolus of ^{85}Kr, in a small volume of solution, into the arterial supply to the organ, and evaluation of the desaturation curves obtained by plotting either $(C_v - C_a)$, or externally detected activity vs time.

(4) Direct injection of ^{85}Kr into the organ or tissue (usually in saline), and analysis of desaturation curves obtained by plotting externally detected activity vs time.

The clearest kinetic data in most organs, regardless of the mode of administration, has been obtained by external counting of either the beta (0.672 MeV) or gamma (0.514 MeV) radiation emitted from the organ. The morphological characteristics of the organ, and the characteristics of the radiation vis-a-vis the detector, must be clearly understood, however, to correctly interpret the data.

LITERATURE

The pertinent literature can be broadly divided as follows:

(1) Determinations of blood flow in various organs and tissues, for a variety of clinical reasons; and, incidental to that purpose, study of the fine structure of saturation/desaturation curves and tissue:blood partition coefficients.

(2) *In vivo* whole body fat determinations.

(3) Studies of whole-body kinetic behavior and partition coefficients in small animals.

(4) Determination of Ostwald solubility coefficients or tissue:air partition coefficients for blood, various biological solutions, and whole animal organs.

[2]With any radioactive gas selected for experimental use, one criterion is that its radioactive half-life be long with respect to the duration of the experiment, so that radioactive decay will not significantly affect the slopes of the curves obtained.

[3]Another method is to determine the total quantity of isotope entering or leaving the tissue by integrating the area under the curve.

In the first category, only those papers presenting information on Kr behavior in normal or control subjects, albeit anesthetized or surgically traumatized, are included. Data given in terms of blood flow was back calculated to half-times or exponential coefficients, whenever the original method of calculation was clear. Information from sick animals, or those treated with vasoactive drugs to alter their physiology, has been omitted — although control values from those papers were included if information was needed for that organ and species.

Only information pertaining to partition coefficients and compartmental analysis is covered. No claims are made regarding completeness of literature coverage or crediting of firsts.

1. Blood Flow Determinations.

a. Brain.

Lassen, *et al.*, (1955) pioneered use of ^{85}Kr in the Fick principle circulatory studies with a modification of the Kety, *et al.*, (1948) nitrous oxide method of determining cerebral blood flow. They determined blood flow for the whole brain using (C_v - C_a) from simultaneous samples from the femoral artery and the jugular vein, taken while the subject (cats, dogs, rabbits) breathed ^{85}Kr from a closed system for 14 minutes. Blood radioactivity was assayed by counting the blood in mica-windowed cuvettes with an array of GM detectors.[4] No useful kinetic data were reported, however. L_W brain:blood for the whole brain was determined to be 1.06 (S.E. = .0075) at a hematocrit of 50. L_W was found to vary with hematocrit, and a relationship given to relate the two.

In a similar study, Albert, *et al.*, (1960) used a two-minute saturation time, and plotted (C_v - C_a) in desaturation for the first four minutes after the end of exposure, to determine a cerebral blood flow of 0.37 - 0.642 ml/g/min (t 1/2 = 1.08 - 1.86 min) in human patients who had no overt evidence of cerebral dysfunction. The ^{85}Kr in blood was eluted and assayed in a gas flow counter.

Lassen, *et al.*, (1961) infused ^{85}Kr in saline for six minutes into the common carotid artery of an anesthetized cat, and followed desaturation by counting the beta radiation emitted from the cortex, exposed by craniotomy, with a collimated end-window GM detector. Desaturation was reported to be essentially complete within 15-20 minutes. The curves were clearly multi-exponential. The CBF was calculated, using the initial slope method, and a previously determined, but unpublished, L_W cortex:blood of 0.9, to be 0.4 - 1.6 ml/g/min (T 1/2 = 0.43 - 1.73 min). In a subsequent investigation, using the same technique, Ingvar, *et al.*, (1961) found CBF of 0.65 ml/g/min (T 1/2 = 1.07 min) in dogs and 0.51 - 0.53 ml/g/min in a human brain tumor patient (T 1/2 = 1.31 - 1.36 min).

Cerebral blood flow determinations on anesthetized dogs were reported by Glass, *et al.*, (1961) and Harper, *et al.*, (1961) who used the Lassen and Ingvar methods and partition coefficient. They held anesthesia, blood pressure, temperature, and pCO_2 constant during the experiments, and found an average CBF of about 1 ml/g/min (T 1/2 ~ 0.7 min), using the initial slope of clearly multi-exponential desaturation curves.

In an amplification of their method, Ingvar, *et al.*, (1962) improved the accuracy of CBF determinations by correcting for unequal compartment saturation. Their semi-logarithmic curves were graphically resolved into two components, and the components were extrapolated to equilibrium. An average exponent, weighted by compartment size, was then used to calculate CBF. The fastest component was assumed to be cortical gray matter, and the slower to be white matter. An autoradiographic technique was used to determine the ratio of ^{85}Kr in gray matter to that in white matter with slices of brain from a cat that had been fully saturated *in vivo* with ^{85}Kr. The ratio (0.73), the previously determined L_W brain:blood of 1.06, and an estimated 60:40 gray:white matter weight ratio was used to estimate L_W cortex:blood and L_W white matter:blood of 0.92 and 1.26, respectively, at a hematocrit of 50. The variation of L_W cortex:blood with hematocrit was reported to be:

$$L_W \text{ cortex:blood} = 0.92 \frac{.843}{(H/100) + .685[1 - (H/100)]} \qquad \text{where H = hematocrit}$$

The improved method was used on dogs, cats, and rabbits to determine CBF, but no compartmental breakdowns were given.

Glass, *et al.*, (1962), using a double isotope technique, found an *in vivo* partition coefficient for the cortex in anesthetized dogs of 0.91 ± 6% at a hematocrit of 50. The coefficient reported was neither L or L_W, since they used the ratio of beta counts from the brain, and a beta-infinite layer of blood in their calculations. Since the beta range is mass dependent, the units of their coefficient would be (μCi/g cortex)/(μCi/g blood), and, assuming a blood specific gravity of 1.05, the coefficient would be about 5% higher than L_W.

Lassen, *et al.*, (1963) determined CBF in unanesthetized humans by counting the gamma radiation emitted from the cranium with a collimated NaI detector after injection of ^{85}Kr into the carotid artery. Two-compartment exponential curves were assumed and CBF calculated using a weighted exponent. The CBF was reported to be 0.6 ml/g/min (S.D. = .13) (T 1/2 = 0.8 - 2.0 min), but no specific information was given on curve breakdown.

[1]For benefit of those who do not routinely deal with radioactivity, the abbreviation GM stands for Geiger-Mueller and NaI for sodium iodide. GM detectors primarily register beta radiation; NaI detectors are used for gamma radiation.

Alexander, *et al.*, (1964), using the Lassen, *et al.*, (1955) technique, found half-times for the whole brain of anesthetized human volunteers to be in the range of three to six minutes. In a subsequent paper (Wollman, *et al.*, 1965) with two-compartment analysis of similar CBF data, from both anesthetized and unanesthetized subjects, was reported as shown in Table 1.

McHenry (1964) used a modification of the Lassen, *et al.*, (1955) technique, and the counting techniques of Albert, *et al.*, (1960), to determine CBF in 25 normal males by analysis of desaturation curves. The CBF reported was 0.565 ml/g/min (S.D. = .077) (T 1/2 = 0.96 - 2.3 min).

Lassen (1965), using his GM detector over exposed brain technique, reported average half-times of 0.27 and 1.4 minutes for the two components resolved from four cat brain desaturation curves.

The most elaborate studies of the kinetic behavior of ^{85}Kr in brain appear to be those reported by Haggendal, *et al.*, (1965b), and, less extensively, by Nilsson (1965). They used anesthetized, curarized dogs, and made concurrent recordings with a NaI detector positioned over the skull, and an end-window GM detector over a craniotomy. ^{85}Kr was administered by fast injection into either the vertebral or external carotid artery, or by direct injection (1-5 μ l) into the brain, using a fine needle inserted through a craniotomy adjacent to the one with the counter. In the latter case, dye was injected with the ^{85}Kr so that the point of injection could be located morphologically in histological sections of the brain. Desaturation was followed until the longest component, on a semi-logarithmic plot, was flat enough to ensure good resolution in curve stripping. (The major problem was reported to be counting statistics.) Their results indicated that the total brain desaturation curve consists of four components as follows:

(1) A very fast component with a half-time of about 0.10-0.20 min, which was identified by auxiliary experiments as arterial blood. This component was only resolvable with the fast intra-arterial injections and was usually associated with low total blood flow.

(2) Another fast component, attributed to gray matter, with half-times of 0.35-1.9 min (wide variations of CBF and pCO_2).

(3) A slower component, associated with white matter, with half-times of 1.5-11.6 min (also under varying conditions).

(4) A component with half-times of 14-20 min, which was identified as originating in extra cranial tissue (scalp muscle, neck muscle, connective tissue, etc.)

The NaI and GM curves agreed well and indicate that, in dogs, the GM detector records beta radiation from white matter, as well as from the gray matter, unless the cortex is thicker than usual (in one large dog, whose cortex was 3 mm thick, the GM curve was mono-exponential). Clearance curves from the injections were mono-exponential if the injection was entirely in either gray or white matter. The curves from cortex injections matched component 2 from the NaI or GM curves obtained with the same animal with intra-arterial injections while injection into white matter resulted in curves that matched component 3. If injection was on the border of the gray and white matter, both components 2 and 3 were seen.

In an investigation of blood flow autoregulation, Haggendal, *et al.*, (1965a) injected ^{85}Kr into the vertebral artery of anesthetized curarized dogs, and recorded desaturation curves from the brain by external gamma scintillation. The semi-logarithmic curves were resolved into two components, and the faster assumed to be gray matter. The half-times found with the fast component, with varying blood pressures, ranged from 0.74 - 2.3 min. Using the same techniques, Haggendal (1965) investigated the effects of vaso-active drugs on cerebral circulation in anesthetized dogs. The fast component obtained from normotensive controls had half-times of 0.47 - 1.31 min.

b. Heart.

The Lassen, *et al.*, (1955) technique was applied to the heart by Hansen, *et al.*, (1962) who had anesthetized dogs breathe an ^{85}Kr-air mixture for 14 minutes. After the 14-minute saturation, they took arterial and coronary sinus blood samples to establish initial (saturated) levels, and shifted the animal to breathing air. Five pairs of A-V samples were taken during the first 10-18 minutes of desaturation. Blood radioactivity was assayed by GM counting in thin-windowed cuvettes, and (C_V - C_a) plotted semi-logarithmically to determine the half-time. A partition coefficient of 1 was assumed and coronary blood flow calculated to be 0.48 - 1.33 ml/g/min (T 1/2 = 0.52 - 1.44 min). No original data were given. The curves were assumed to be mono-exponential.

Herd, *et al.*, (1962) injected ^{85}Kr in saline into the left anterior descending coronary artery through chronically implanted catheters in three unanesthetized dogs, and recorded the washout (desaturation) curve with a NaI detector over the precordium. The slope of the first two minutes of the semi-logarithmic plot was used to calculate coronary blood flow. The curves were obviously not mono-exponential, but the authors claimed that the deviation was due to isotope recirculation. This does not appear probable since a reduction in blood concentration by a factor of about 500 would be expected before the isotope returned to the heart (dilution x 25 in the right heart and 95% removed on the way through the lungs). The half-time on the long component from the one curve shown was about 7 minutes.

Ross, *et al.*, (1964) determined coronary blood flow in anesthetized dogs using ^{85}Kr and ^{133}Xe clearance, and calibrated the method against direct measurements. They cannulated either the left, or all three coronary arteries, and supplied blood to the coronary arteries from the carotid artery through a rotometer. ^{85}Kr, in saline, was injected into this arterial supply and washout followed with a NaI detector positioned over the heart. They used a direct-fit initial slope from the semi-logarithmic desaturation curve to calculate blood flow. The initial half-times were 0.4 - 1.07 minutes.

Cohen, *et al.*, (1964) determined (C_v - C_a) by injecting ^{85}Kr in saline into the left ventricles of 11 unanesthetized humans and nine anesthetized dogs, taking five pairs of consecutive 30-second (6 ml) samples of arterial and coronary sinus blood starting 45 seconds post-injection, and then assaying the blood by gamma-counting in a NaI well detector, and analyzing semi-logarithmic desaturation curves. Mono-exponential curves were claimed. Those shown, however, seem to have some deviation at latter times. Blood flow was varied with drugs and the data were not separated by species. The total range of coronary blood flow was 0.30-1.99 ml/g/min (T 1/2 x 32-2.3 min) with a mean of 1.12 ml/g/min (T 1/2 = 0.57 min). The curve from one human control had a half-time of 0.65 minutes.

Johansson, *et al.*, (1964) reported two-component washout curves in dogs with artificial coronary occulsions. The main component had a half-time of 0.44 - 1.2 minutes, and the second component had a half-time of about 30 minutes, as determined by analysis of semi-logarithmic desaturation curves taken after injection of ^{85}Kr into the coronary artery (external NaI detector). The long component was attributed to collateral circulation in the artificially ischemic area.

Subsequently, Linder (1966) reported on a detailed investigation of coronary blood flow measurements in anesthetized dogs (artificial ventilation). ^{85}Kr was injected into the coronary artery; desaturation followed and was monitored with a collimated NaI detector. On semi-logarithmic plots, a very fast component (T 1/2 of 5-15 seconds) was seen followed by the main phase, with a half-time of 0.38-1.08 minutes; and, when 5-20% of the peak activity remained, by a slower component with a half-time of 5 or more minutes. This slow component was attributed to a combination of: (1) recirculation of the isotope due to bad ventilation in parts of the lung (slight effects); (2) connective and fatty tissues in the ventricular walls and along the coronary vessels (main cause); and (3) isotope in the coronary veins (shown to be negligible).

c. Kidney.

A very complete study of ^{85}Kr desaturation in the kidney was reported by Thorburn, *et al.*, (1963) who injected ^{85}Kr in saline into chronically cannulated renal arteries of unanesthetized dogs, and followed washout with an external NaI detector. The data were plotted semi-logarithmically and resolved graphically. The components were associated with various parts of the kidney by sequential radiography. Their results are given in Table 3.

Bell, *et al.*, (1965) determined an *in vivo* partition coefficient for dog kidney cortex of $0.96 \pm .054$, using the ratio of GM (beta) counts from the cortex of ^{85}Kr saturated kidney, and the corresponding count from a cuvette containing arterial (renal) blood. The same comments made on the Glass, *et al.*, (1962) determination of brain partition coefficient apply. These authors also reported mono-exponential washout curves from kidney cortex, determined by GM counting at the exposed cortical surface, after a one-minute infusion of ^{85}Kr in saline into the renal artery. Half-times of 0.2-0.24 minutes were found in 30 anesthetized dogs.

In a similar study, Cosgrove (1965) reported average half-times of 0.23 minutes for mono-exponential half-times of 0.18 - 0.39 minutes in normotensive control dogs (anesthetized, curarized, ventilated).

Carriere (1970) monitored ^{85}Kr washout with a NaI detector over the kidneys of anesthetized dogs after fast injection into the renal artery. He found four components, as reported by Thorburn, *et al.*, (1963), but only reported values for the fastest two. Their half-times and percent of activity were 0.11 min/83% and 0.51 min/13%, respectively. A subsequent report from the same laboratory (Lockhart, *et al.*, 1972) reported half-times of 0.1-0.16 minutes and 0.825-0.9 minutes for the fastest two components.

d. Liver.

Blood flow in livers of anesthetized and unanesthetized dogs was investigated by Hollenberg, *et al.*, (1966). They did two series of animals. In an acute series, catheters were placed in the portal vein and hepatic artery of anesthetized dogs, and clearance curves were recorded externally with a NaI detector after injection into either vessel. In the chronic animals, only the portal vein was used (previously cannulated), and the animals were awake. $L_{liver:blood}$ was determined to be 1.056 ± 0.56 and the specific gravity of liver found to be 1.02. With either type of injection, they found either one or two component exponential curves in the same animal at about the same total flow. Washout by HA injection was found to be about 75% of the PV washout. The half-times from the chronic unanesthetized dogs were reported to be from 0.34-0.46 minutes. Clearance in the anesthetized dogs was considerably slower. One complete desaturation curve was given which had two components with half-times of 0.37 and 17.3 minutes.

The most complete study of ^{85}Kr clearance from liver (dog) was reported by Birtch, *et al.*, (1967), who used fast injections into either the hepatic artery, portal vein, or both simultaneously, followed by monitoring of the emitted gamma radiation with a NaI detector coupled to a digital printer. The data were plotted semi-logarithmically and resolved graphically. The partition coefficient and specific gravity reported by Hollenberg, *et al.*, (1966) were used. Most dogs were anesthetized but four were awake and had chronically implanted catheters in both vessels. Four compartment desaturation curves were found — the longest half-time of which was 19-26 minutes. Their data (converted from blood flow to half-times) are summarized in Table 4. These data and sequential radiographs show that component 1 is from a vascular bed perfused only by the portal vein, component 3 is from a bed perfused only by the hepatic artery, component 2 is from a bed perfused by both supplies, and component 4 is from extra-hepatic tissues and intra-hepatic fat.

e. Stomach.

Jansson, *et al.*, (1966) administered ^{85}Kr by intra-arterial injection to anesthetized cats, and followed desaturation with a NaI detector placed over the stomach. Three-component semi-logarithmic desaturation curves were found. The half-times of the two faster compartments, believed to be gastric mucosa and muscularis, were 0.5-1.2 minutes and 3.5-5.8 minutes, respectively. The half-time of the third component, identified as being tissues outside the stomach wall, was not given.

Bell, *et al.*, (1967a) reported mono-exponential desaturation curves, with half-times of 0.68 minutes (S.D. = 0.09 min), from gastric mucosa of anesthetized control dogs in an investigation of the effects of pCO_2 on gastric mucosal flow. The stomach was opened and an end-window GM detector placed adjacent to the mucosa. ^{85}Kr was given by intra-arterial injection. L gastric mucosa:blood was determined to be 0.84 (S.E. = 0.04). The same control data were reported by Bell, *et al.*, (1967) in an investigation of histamine effects on gastric mucosal flow. In another series from the same laboratory, half-times of 0.44-0.48 minutes were reported for the gastric mucosa of control dogs (Bell, *et al.*, 1969).

f. Intestine.

The behavior of ^{85}Kr in the small intestine of anesthetized, atropinized cats, with the splanchnic nerve severed, was investigated by injecting it into the superior mesenteric artery, and recording the washout curves with an external NaI detector coupled to a ratemeter and recorder (Lundgren, *et al.*, 1966; and Kampp, *et al.*, 1968 a,b). The semi-logarithmic curves were resolved graphically into four components. The total flow was regulated and measured by a regulating flow-meter in the mesenteric vein. In most experiments, the GI tract, except for the 20-50 gram of the test segment, was removed to avoid interference. The temperature of the test segment was controlled. Readings from a lead-shielded end-window GM detector placed close to the serosal surface, and another GM detector in the gut lumen, were used to help identify the morphological origin of the different curve components. Local injection of ^{85}Kr in dye, and autoradiography with antipyrine ^{14}C, were also used for localization. The data obtained are summarized in Table 5.

g. Eyes.

The retinas of anesthetized cats were reported to have four-component ^{85}Kr clearance curves, as determined by counting with a GM detector in contact with the posterior aspect of the sclera, after intra-arterial injection (carotid)(Friedman, *et al.*, 1964; and Friedman, *et al.*, 1965). Their data for cats are summarized in Table 6. Dogs and monkeys were reported to have similar curves. Rabbits had three-component curves with one component having a half-time of 2.5-5 seconds and the other two having half-times of 1.5-30 minutes when measured with the GM detector. When a more sensitive solid-state probe attached to the eye was used, and the ^{85}Kr was injected into a branch of the ciliary artery, all species had four-component desaturation curves.

h. Testis.

Setchell, *et al.*, (1966) investigated blood flow in ram testes by analysis of washout curves obtained after injection of ^{85}Kr, via a chronic implant, into the testicular artery. The animals were usually awake. The scrotum was held in a temperature-controlled harness and a 5 cm NaI detector, coupled to a ratemeter and recorder, was used to record the desaturation curve. Several experiments were done with direct injection of ^{85}Kr into the testis. $L_{W\ testis:blood}$ was determined to be 0.85 (S.E. = .03) by infusing ^{85}Kr in saline into the heart for 75 minutes, determining equilibrium by counting blood taken from the abdominal aorta every 15 minutes, killing the animal, removing and weighing the testes, sealing the testes in parafin in a soldered-top can, assaying the contained radioactivity by gamma counting, and comparing the testis specific activity with the blood activity. The desaturation curves were mono-exponential with half-times of 4.46-16.4 minutes for conscious rams (66 determinations), and 7.65-10.8 minutes for anesthetized rams (16 determinations).

i. Skin.

Mono-exponential clearance from dog skin following femoral artery infusion (4 min) was reported by Bell, *et al.*, (1964). The curves were recorded over the leg with a GM detector. Half-times of 10.97-27.4 minutes were found.

^{85}Kr clearance from rabbit skin after intra-arterial bolus injection was found to be bi-exponential with half-times of 3-4 minutes and 17.3-23.1 minutes, respectively, as measured by a GM detector. (Casey, *et al.*, 1965; and Thorburn, *et al.*, 1966).

The results of extensive investigation of skin blood flow in humans, using ^{133}Xe and ^{85}Kr, were reviewed by Sejrsen (1971) who summarized several of his earlier publications. He concluded that the parallel competitive exponential model used in other blood flow studies does not hold with human skin because: (1) ^{85}Kr or ^{133}Xe is removed from the cutaneous blood supply preferentially in subcutaneous tissue, which has a high fat content, and then is released slowly; (2) some of the isotope is cleared by sweating; and (3) the isotope migrates between cutaneous and subcutaneous tissue by diffusion. The curves recorded from human skin were, therefore, not simple functions of blood flow. The only consistent exponential component reported had an average half-time of 168 minutes (S.D. = 41 min), and was attributed to subcutaneous tissue.

j. Limbs.

Tobias, *et al.*, (1949), in an investigation of the causes of the bends in aviators, had unanesthetized volunteers breathe $^{79-81}Kr$ from a closed-circuit system for three hours while counting gamma radiation, emitted from one hand and one knee, using very heavily collimated GM detectors. After three hours the subjects breathed room air while counting continued for 12 more hours. Three-component exponential curves were found for both hands and knees. The fastest component was negligible for the knee, however. Exercise or heating of the hand caused faster clearance; vasoconstrictive drugs caused slower exchange. The kinetic information reported is given in Table 7. It was also found that radiokrypton was readily absorbed from the intestinal tract, especially the doudenum.

Holzman, *et al.*, (1964) injected ^{85}Kr in saline into forearm muscle in human volunteers and followed washout with an external NaI detector. The curves obtained were multi-exponential with a great deal of variation. Blood flow was determined using the initial slope. The first half-time was reported to be 17.8 minutes (S.D. = 8.2 min).

2. Whole-Body Fat Determinations.

The uptake of Kr from a closed system (with CO_2 scrubbing, and O_2 replacement) has been used by several investigators to estimate body fat content. Lesser, *et al.*, (1963) used inert Kr and reported that equilibrium was not complete in 6-7 hours with human subjects. (Their system had a water spirometer which may have permitted leakage of Kr.) In their discussion, they propose a model for uptake of metabolically inert gases, consisting of blood in equilibrium with the gas in lungs, and three parallel competitive compartments in contact with blood. The compartments proposed, in order of their speed of saturation/desaturation, were: (1) rapidly perfused lean tissue (as heart, brain, kidney); (2) more slowly perfused lean tissue (as resting muscle, skin); and (3) adipose tissue. This model was used by the reviewer to make some predictions about whole body behavior of ^{85}Kr in man (Kirk, 1972) which were subsequently found to be too simple (Kirk, 1973).

Whole body fat determinations were made in another laboratory (Hytten, 1964; and Hytten, *et al.*, 1966) using a similar closed system with a neoprene bellows spirometer replacing the water spirometer, which they felt was the cause of Lesser and Zak subjects not reaching equilibrium. Equilibrium was claimed in 90-120 minutes for normal human subjects, and by 180 minutes for obese subjects. Radioactivity was monitored with a radiation counter coupled to a ratemeter and recorder; equilibrium was considered complete when the recorder trace was flat for ten minutes. Desaturation was found to be much slower than saturation, and a component with a half-time of about 18 hours was reported. From his own experience with other animals, this reviewer believes that the criteria for saturation were not adequate, and saturation was not complete in the time stated.

3.Studies of Whole-Body Kinetic Behavior and Partition Coefficients.

The author has investigated the whole-body kinetic behavior of ^{85}Kr in guinea pigs and, superficially, in rats (Kirk, 1972; Kirk, *et al.*, 1972; Kirk, 1973; and Kirk, *et al.*, 1973). Saturation and desaturation curves in unanesthetized guinea pigs breathing ^{85}Kr in a closed system were found to be three- or four-component exponentials as measured externally with a heavily collimated NaI detector. Half-times of 0.25-2.2 minutes, 6-11.8 minutes, 21.5-41.7 minutes, and 88-178 minutes were found. Of the eight animals studied, one did not have the fastest component, and one did not have the slowest. The desaturation curves (semi-logarithmic) for eight guinea pigs are shown in Figure 1. Figure 2 shows the saturation and desaturation data for one guinea pig plotted on the same graph as a smooth curve generated with kinetic parameters determined by graphic resolution of the desaturation phase. The saturation phase usually agreed fairly well with the desaturation phase for the same animal. However, substantial variation was noted between animals. L_W whole-body:air (fur-free) was found to be 0.1444 (S.D.=.0148). Females had a slightly higher L_W than males, but the difference was not significant. The mean hairless weight of these animals was 840.1 grams (S.D. = 33.9).

The kinetic behavior of ^{85}Kr in 250-gram female Rochester Wistar rats was investigated in preliminary experiments. Three or four rats were saturated with ^{85}Kr for either 12 or 33 hours in an exposure chamber, and then repetitively counted in a large NaI well detector until preexposure background was reached. Counting did not begin until 3-6 minutes after the animals were removed from the ^{85}Kr atmosphere. In the 12-hour experiment, desaturation curves had three components with half-times of 3.87-4.6 minutes, 20-23 minutes, and 81-143 minutes. After the 33-hour exposure, two-component curves were found with half-times of 7.6-15.7 minutes and 41.8-85 minutes. Three of the four animals in the 33-hour exposure had also been used in the 12-hour exposure. The change in curve fine structure is believed to be due to increased stress in the longer exposure, including higher radiation dose, and the fact that counting did not begin until 5-6 minutes after the animals were removed from the chamber — which would obviate seeing any very short half-time component. Figures 3 and 4 show the desaturation curves from one animal for both exposures. The average $L_{W\ rat:air}$ was determined to be 0.092 (S.D. = 0.019) (seven determinations).

4. Tissue:Air Partition Coefficients.

Tissue:air partition coefficients, both L and L_W, have been determined for a number of biological solutions and tissues.

Hardewig, *et al.*, (1960) studied solubility of ^{85}Kr in human blood at 37° C and found $L_{plasma:air}$ to be 0.051 (S.D. = .001) and $L_{blood:air}$ = .05199 + .0001573 H where H = hematocrit.

Mellemgard, *et al.*, (1962) reported $L_{blood:air}$ to be 0.0635 at 37°C and a hematocrit of 40.

Lassen (1964) reported that $L_{blood:air}$ was about 0.06.

Yeh and Peterson's elaborate series of determinations of Kr solubility in lipids, aqueous solutions, blood, albumin, and hemoglobin have been mentioned previously. Figure 5 is a plot of their data fitted to Clapeyron and/or Valentiner curves. These equations were used in the predictive model discussed later.

The Bunsen coefficient for ^{85}Kr was reported to be 0.420 for pooled human fat, and .414 for abdominal fat by Masson, *et al.*, (1967).

Kitani (1972) reported on determinations of ^{85}Kr solubility in human plasma, RBC, and whole blood. The values were reported were: $L_{plasma:air}$ = 0.0499; $L_{RBC:air}$ = 0.0718 and $L_{blood:air}$ = 0.0002223H + .04961 where H = hematocrit. The solubility of Kr in human liver was related to triglyceride content (*in vitro*) and the Ostwald coefficient found to be equal to 0.004072L + 0.04924 where L = lipid concentration (tripalmitin as % wet weight) ((Kitani, *et al.*, 1972).

In vitro partition coefficients ($L_{W\ tissue:air}$) were determined for blood (guinea pig, dog, cat, Chinese hamster), guinea pig brain homogenate, normal saline, and EDTA solution (Kirk, 1973; and Kirk, *et al.*, 1973). These data are given in Table 8. *In vivo* determinations of $L_{W\ tissue:air}$ were made in guinea pigs for blood and 22 other tissues using a dual-isotope technique which permits simultaneous determination of L_W for whole tissue and bloodless tissue. This data are summarized graphically in Figure 5.

DISCUSSION AND CONCLUSIONS

The compartmental half-times already presented are summarized graphically in Figure 6. If one looks closely, with a prejudiced eye, it appears that some grouping, reminiscent of the Lesser and Zak hypothesis, may be present. The half-times for dogs only are shown in Figure 7. Here, grouping of compartmental half-times seems to be fairly clear (0.1-0.4 min, 0.4-1.5 min, 1.5-13 min, and over 13 min). *A priori*, one would hardly expect the multitude of differently perfused tissues in the body to group themselves so conveniently. That this is the case appears to be confirmed by the rat and guinea pig whole-body data. It is also abundantly clear that, on both the organ or whole-body level, "compartmental" composition and rate constants will change with changes in physiological state, and an externally observed compartment will very likely have no firm morphological or physiological meaning. There does seem to be a trend toward slower saturation or desaturation with larger animals. The whole-body clearance of guinea pigs was slower than that of rats, and man seems to have some compartments with substantially longer half-times than any of the smaller animals.

Fortunately, if one is assessing hazards associated with environmental exposure to ^{85}Kr, the rates of saturation and desaturation will usually be of minimal import. Most exposures will be long with respect to saturation times, and the equilibrium concentrations in tissue; the resulting dose will be determined almost entirely by the partition coefficients.

It would be very convenient to be able to calculate partition coefficients from organ composition, using a model such as that proposed by Yeh, *et al.*, (1965). If this can be done, direct determination of partition coefficients would not be necessary if the fat-protein-water composition of the organ or tissue, and the fraction of the fat that is non-neutral, were known.

The Yeh and Peterson values were incorporated into a predictive program for the Hewlett-Packard 9810 calculator (Kirk, 1973). This program calculates $L_{W\ tissue:air}$ when given temperature (°C), the percentage of fat, protein, and water in the tissue, and the non-neutral fat fraction. This program has been used, with limited organ composition data from the literature, to predict the partition coefficients corresponding to a number of experimentally determined values. In several cases, tissue:blood partition coefficients were converted to tissue:air coefficients by using appropriate average blood:air coefficients. The experimental and predicted values are summarized in Table 9. Comparisons for some guinea pig tissues are shown in Figures 8 through 13. The predicted partition coefficients are plotted against the experimental coefficients in Figure 14. A least squares regression reveals good correlation — despite the fact that directly determined tissue composition was available in only a few cases and considerable variation existed in a few tissues. The most notable deviation was noted with the guinea pig brain. The experimental L_W is much lower, both *in vivo* and *in vitro*, than the predicted — even when a 50% non-neutral fat correction is made. The reason for this has not been determined, but may be due to inappropriate tissue composition data. It is felt, however, that this model can be used without major inaccuracy in determining equilibrium levels of ^{85}Kr in the body, if the exposure concentration and tissue composition are reasonably well defined.

The beta dose to guinea pig tissues resulting from exposure to ^{85}Kr at the $(MPC)_a$ levels are given in Table 10. These doses form only a part of the total internal dose resulting from this exposure, and contributions from gamma and Bremsstrahlung radiation arising both within and outside the body must be added.

REFERENCES

Albert, S. N., C. A. Albert and J. F. Faxekas(1960), *A Rapid and Simple Method for Measuring the Rate of Cerebral Blood Flow in Humans with Krypton-85.*, J. Lab. Clin. Med. 56:473.

Alexander, S. C., H. Wollman, P. J. Cohen, P. E. Chase, E. Melman and M. Behar(1964), *Krypton-85 and Nitrous Oxide Uptake of the Human Brain During Anesthesia.*, Anesthesiology 25:37.

Bell, G. and A. M. Harper (1964), *Measurement of Regional Blood Flow Through the Skin from the Clearance of Krypton-85.*, Nature (London) 202:704.

Bell, G. and A. M. Harper(1965), *Measurement of Local Blood Flow in the Renal Cortex from the Clearance of Krypton-85.*, J. Surg. Res. 5:382.

Bell, P. R. F. and A. C. Battersby(1967a), *The Effect of Arterial pCO_2 on Gastric Mucosal Blood Flow by Clearance of Krypton-85.* Surgery 62:468.

Bell, P. R. F. and C. Battersby(1969), *Effect of Vasopressin (Pitressin) on Gastric Mucosal Blood Flow Measured by Clearance of Krypton-85.* Surgery 66:510.

Bell, P. R. F., C. Battersby and A. M. Harper(1967b), *Gastric Mucosal Blood Flow in the Dog Measured by Clearance of Krypton-85 - the Response to Histamine.* Brit. J. Surg. 54:1003.

Betz, E., D. H. Ingvar, N. A. Lassen and F. W. Schmahl(1966), *Regional Blood Flow in the Cerebral Cortex Measured Simultaneously by Heat and Inert Gas Clearance.* Acta. Physiol Scand. 67:1.

Birtch, A. G., B. H. Casey and R. M. Zakheim(1967), *Hepatic Blood Flow Measured by the Krypton-85 Clearance Technique.* Surgery 62:174.

Brock, M. D. H. Ingvar and C. W. Sem-Jacobsen(1967), *Regional Blood Flow in Deep Structures of the Brain Measured in Acute Cat Experiments by Means of a New Beta-Sensitive Semiconductor Needle Detector.* Exp. Brain Res. 4:126.

Casey, B. H. and C. D. Thorburn,(1965), *Distribution of Blood Flow in the Skin Using Radioactive Krypton-85 Clearance Techniques.* In: Biology of the Skin and Hair Growth, A. G. Lyne and B. F. Short, Ed. (Sidney: Angus and Robertson, Ltd.) 603.

Caster, W. O., J. Poncelet, A. B. Simon and W. D. Armstrong,(1956) *Tissue Weights of the Rat. I. Normal Values Determined by Dissection and Chemical Methods.* Proc. Soc. Exp. Biol. Med. 91:122.

Cohen, L. S., W. C. Elliott and R. Gorlin(1964), *Measurement of Myocardial Blood Flow Using Krypton-85.* Amer. J. Physiol. 206:997.

Carriere, S.(1970), *A Comparison of the Disappearance curves of ^{133}Xe and ^{85}Kr for the Measurement of the Intrarenal Distribution of Blood Flow.* Can. J. Physiol. Pharmacol. 48:834.

Cosgrove, M. D.(1965), *The Effect of Arterial Hypoxia on the Blood Flow Through the Renal Cortex.* Brit. J. Surg. 52:613.

Friedman, E., H. H. Kopald and T. R. Smith(1964), *Retinal and Choroidal Blood Flow Determined with Krypton-85 in Anesthetized Animals.* Invest. Ophthalmol. 3:539.

Friedman, E. and T. R. Smith(1965), *Estimation of Retinal Blood Flow in Animals.* Invest. Ophthalmol. 4:1122.

Glass, H. I. and A. M. Harper(1962), *The Measurement of the Partition Coefficient of Krypton Between the Brain Cortex and Blood by a Double Isotope Method.* Phys. Med. Biol. 7:335.

Glass, H. I., A. M. Harper and M. M. Glover,(1961), *The Measurement of Local Cortical Blood Flow in the Brain by the Analysis of the Clearance Curve of Krypton-85.* Phys. Med. Biol. 6:65.

Haggendal, E.(1965), *Effects of Some Vasoactive Drugs on the Vessels of Cerebral Grey Matter in the Dog.* Acta. Physiol. Scand. 66:Suppl. 258.55.

Haggendal, E. and B. Johansson,(1965a), *Effects of Arterial Carbon Dioxide Tension and Oxygen Tension on Cerebral Blood Flow Autoregulation in Dogs.* Acta. Physiol. Scand. 66:Suppl. 258.27.

Haggendal, E., N. J. Nilsson and B. Norback(1965b), *On the Components of ^{85}Kr Clearance Curves from the Brain of the Dog.* Acta. Physiol. Scand. 66:Suppl. 258.5.

Hansen, A. T., B. F. Haxholdt, E. Husfeldt, N. A. Lassen, O. Munck, H. R. Sorensen and K. Windkler(1956), *Measurement of Coronary Blood Flow and Cardiac Efficiency in Hypothermia by Use of Radioactive Krypton-85.* Scand. J. Clin. Lab. Invest. 8:182.

Hardewig, A., D. F. Rochester and W. A. Briscoe,(1960), *Measurement of Solubility of Krypton in Water, Plasma, and Human Blood, Using Radioactive ^{85}Kr.* J. Appl. Physiol. 15:723.

Harper, A. M., H. I. Glass and M. M. Glover(1961), *Measurement of Blood Flow in the Cerebral Cortex of Dogs by the Clearance of Krypton-85.* Scott. Med. J. 6:12.

Herd, J. A., M. Hollenberg, G. D. Thorburn, H. H. Kopald and A. C. Barger(1962), *Myocardial Blood Flow Determined with Krypton-85 in Unanesthetized Dogs.* Amer. J. Physiol. 203:122.

Hollenberg, M. and J. Dougherty(1966), *Liver Blood Flow Measured by Portal Venous and Hepatic Arterial Routes with ^{85}Kr.* Amer. J. Physiol. 210:926.

Holzman, G. B., H. N. Wagner, M. Iio, D. Rabinowitz and K. I. Zierler(1964), *Measurement of Muscle Blood Flow in the Human Forearm with Radioactive Krypton and Xenon.* Circulation 30:27.

Hytten, F. E.(1964), *Measurement of the Total Body Fat in Man with Krypton-85.* Proc. Nutr. Soc. 23:21.

Hytten, F. E., K. Taylor and N. Taggart(1966), *Measurement of Total Body Fat in Man by Absorption of ^{85}Kr.* Clin. Sci. 31:111.

Ingvar, D. H. and N. A. Lassen(1961), *Quantitative Determination of Regional Cerebral Blood Flow in Man.* Lancet 2:806.

Jansson, G., M. Kampp, O. Lundgren and J. Martinson (1966), *Studies on the Circulation of the Stomach.* Acta. Physiol. Scand. 68:Suppl. 277:91.

Johansson, B., E. Linder and T. Seeman (1964), *Collateral Blood Flow in the Myocardium of Dogs Measured with Krypton-85.* Acta. Physiol. Scand. 62:263.

Kampp, M., O. Lundgren and J. Sjostrand (1968a). *On the Components of the ^{85}Kr Washout Curves from the Small Intestine of the Cat.* Acta. Physiol. Scand. 72:257.

Kampp, M. and O. Lundgren (1968b), *Blood Flow and Flow Distribution in the Small Intestine of the Cat as Analyzed by the ^{85}Kr Washout Technique.* Acta. Physiol. Scand. 72:282.

Kety, S. S. (1951), *The Theory and Applications of the Exchange of Inert Gas at the Lungs and Tissues.* Pharmacol. Rev. 3:1.

Kety, S. S. and C. F. Schmidt (1948), *The Nitrous Oxide Method for the Quantitative Determination of Cerebral Blood Flow in Man: Theory, Procedure and Normal Values.* J. Clin. Invest. 27:476.

Kirk, W. P. (1972), *Krypton-85, A Review of the Literature and an Analysis of Radiation Hazards.* Office of Research and Monitoring Report (Washington: U. S. Environmental Protection Agency).

Kirk, W. P. (1973). *In Vivo Behavior and Effects of Krypton-85 in Guinea Pigs.* Ph.D. thesis, University of Rochester, Rochester, New York.

Kirk, W. P. and D. A. Morken (1972). *In Vivo Kinetic Behavior of ^{85}Kr in the Whole Guinea Pig.* Paper 63, 17th. Annual Meeting, Health Physics Society, June 11-15, 1972.

Kirk, W. P. and D. A. Morken (1973), *Physiological Behavior and Radiation Effects of ^{85}Kr Administered to Guinea Pigs via the Respiratory System.* (In review.)

Kitani, K. (1972), *Solubility Coefficients of ^{85}Kr and ^{133}Xe in Water, Lipids, and Blood.* Scand. J. Clin. Lab. Invest. 29:167.

Kitani, K. and K. Winkler (1972), *In Vitro Determination of Solubility of ^{133}Xe and ^{85}Kr in Human Liver Tissue with Varying Triglyceride Content.* Scand. J. Clin. Lab. Invest. 29:173.

Lassen, N. A. (1965), *Blood Flow of the Cerebral Cortex Calculated from ^{85}Kr Beta-Clearance Recorded over the Exposed Surface; Evidence of Inhomogeneity of Flow.* Acta. Neurol. Scand. 41:Suppl. 14:24.

Lassen, N. A., K. Hoedt-Rasmussen, S. C. Sorensen, E. Skinhoj, S. Cronquist, B. Bodforss and D. H. Ingvar (1963), *Regional Cerebral Blood Flow in Man Determined by Krypton-85.* Neurology 13:719.

Lassen, N. A. and D. H. Ingvar (1961), *The Blood Flow of the Cerebral Cortex Determined by Radioactive Krypton.* Experientia 17:42.

Lassen, N. A. and O. Munck (1955), *The Cerebral Flow in Man Determined by the use of Radioactive Krypton.* Acta. Physiol. Scand. 33:30.

Lesser, G. T. and G. Zak (1963), *Measurement of Total Body Fat in Man by the Simultaneous Absorption of Two Inert Gases.* Ann. N. Y. Acad. Sci. 110-40.

Linder, E. (1966), *Measurements of Normal and Collateral Coronary Blood Flow by Close-Arterial and Intramyocardial Injection of Krypton-85 and Xenon-133.* Acta. Physiol. Scand. 68:Suppl. 272:5.

Lockhart, E. A., J. H. Dirks and S. Carriere (1972), *Effects of Triflocin on Renal Tubular Reabsorption and Blood Flow Distribution.* Amer. J. Physiol. 223:89.

Lundgren, O. and N. Kampp (1966), *The Washout of Intra-Arterially Injected Krypton-85 from the Intestine of the Cat.* Experientia 22:268.

MacDonald, A. G. (1969), *The Effect of Halothane on Renal Cortical Blood Flow in Normotensive and Hypotensive Dogs.* Brit. J. Anaesth. 41:644.

McHenry, L. C. Jr. (1964), *Quantitative Cerebral Blood Flow Determination. Application of a Krypton-85 Desaturation Technique in Man.* Neurology 14:785.

Masson, M. B. R. and K. Taylor (1967), *Solubility of Krypton-85 in Olive Oil and Human Fat.* Phys. Med. Biol. 12:93.

Mellemgaard, K., N. A. Lassen and J. Georg (1962), *Right-to-Left Shunt in Normal Man Determined by the Use of Tritium and Krypton-85.* J. Appl. Physiol. 17:778.

Michenfelder, J. D., J. M. Messick and R. A. Theye (1968), *Simultaneous Cerebral Flow Measured by Direct and Indirect Methods.* J. Surg. Res. 8:475.

TABLE 1. Compartmental Analysis from Cerebral Blood Flow Determinations in Human Subjects from Wollman, *et al.*, (1965).

Subject Condition	Compartment	Average % of Brain	T 1/2 (min)
Awake	Slow	50.8	4.36
	Fast	49.2	1.07
Hypoxic	Slow	31.5	2.26
	Fast	68.5	.80
Anesthetized (pCO_2=40)	Slow	47.2	4.85
	Fast	52.8	1.35
Anesth. (pCO_2=10-20)	Slow	68.6	5.63
	Fast	31.4	1.34

TABLE 2. Analysis of ^{85}Kr Desaturation from Cat Brain with GM and Semi-Conductor Detectors from Brock, *et al.*, (1967).

	Fast Component		Slow Component	
Detector	T 1/2 (min)	% of Act.	T 1/2 (min)	% of Act.
GM	0.48	44.7	2.48	55.3
Semi-conductor over cortex	0.63	44.1	3.01	48.7
Semi-conductor over artery	0.42	48.7	2.39	51.3

TABLE 3. Analysis of ^{85}Kr Desaturation in Dog Kidney from Thorburn, *et al.*, (1963).

Component		T 1/2 (min)	% of Total Act.
I	Outer cortex	0.16	80
II	Inner cortex and outer medula	0.65	16
III	Inner medula	5.5	2
IV	Perirenal and hilar fat	44.2	2

TABLE 4. Analysis of ^{85}Kr Desaturation in Dog Livers from Birtch, *at al.*, (1967).

Experiment	Type Injection	Component 1 T 1/2 (min)	Component 1 % Act.	Component 2 T 1/2 (min)	Component 2 % Act.	Component 3 T 1/2 (min)	Component 3 % Act.
Acute-(anesth.)	HA	-----	-----	.38 .8	55	1.13 - 2.3	45
	PV	.25 .38	83.5	.55 2.8	16.5	---------	--
	Both	.26 .39	15.9	.55 - .75	34.6	1.33 - 2.2	49.5
Chronic-(awake)	HA	-----	-----	.45 - .55	55	1.63 2.8	45
	PV	.33 .45	77	.74 - 1.7	23	---------	--
	Both	.22 .42	38.5	.51 - .82	37	1.33 - 3.3	24.5
One chronic dog	HA	-----	-----	.53	--	2.4	--
	PV	.38	-----	1.3	--	---------	--

TABLE 5. Analysis of ^{85}Kr Desaturation in Cat Small Intestine from Lundgren, *et al.*, (1966); and Kampp, *et al.*, (1968a).

Component No.	Identified As	T 1/2 (σ) (min)	% orig. act. (σ)
I	Counter-current exchange in in mucosal vascular loops	0.104 ((.04)	39.9 (10.1)
II	Mucosa	1.55 (.48)	32.1 (10.5)
III	Muscularis and serosa about equally	5.29 (1.93)	28 (12.3)
IV	Perivascular fat, mesentery, delayed recovery from vascular loops of villi	61.8 (44)	Not given and not counted in%

TABLE 6. Analysis of ^{85}Kr Desaturation in Cat Retina from Friedman, *et al.*, (1964).

Component	Identified As	T 1/2 (min)
I	Blood flow in choroid	.050 - .083
II	Retinal vessels	.25 - .78
III	Sclera, choroidal stroma, vitreous, tapetum, etc.	1.5 3.0 9 44

TABLE 7. ^{79}- ^{81}Kr Kinetic Parameters in Human Hands and Knees from Tobias, *et al.*, (1949).

Component	Average Hand T 1/2 (min)	Average Fract. Act.	Knee T 1/2 (min)	Average Fract. Act.
I	4.3	.11	-----	-----
II	35.9	.55	55	.34
III	188	.33	402	.67

TABLE 8. *In Vitro* **Ostwald Coefficients (L) for ^{85}Kr into Selected Biological Solutions (a)**

Solution	Temperature (°C)	Number of Determinations	L	σ
Guinea Pig Blood	39	6	.0513	.0041
	37	8	.0538	.0033
	36	16	.0546	.0076
Guinea Pig Brain (b)	37	12	.0494	.0179
Dog Blood (c)	35.5	8	.0691	.0054
Cat Blood	36	7	.0595	.0065
	39	8	.0559	.0040
Chinese Hamster Blood	37	10(d)	.0822	.0014
0.9% NaCl Solution	37	4	.0472	.0012
10% EDTA Solution	37	8	.0406	.0028

(a) Assuming 760 mm Hg total pressure.

(b) Solubility was determined for a 20% brain homogenate in normal saline and the coefficient for brain calculated from that value.

(c) Dogs were fed 30-60 minutes prior to bleeding.

(d) Five determinations were made on each of 2 pooled samples (Each sample represented 20 animals.)

TABLE 9. Comparison of Predicted and Measured Partition Coefficients for ^{85}Kr.

Species	Organ or Tissue	Calculated Coefficient	Measured Coefficient	Ref. for Measured Coeff.
Cow	Brain Homogenate	.0488(b) (c)	.0454(b) (j)	Yeh, *et al.,* (1965)
Cat	Brain Whole	.0544(a) (d)	.0625(a) (f) (i)	Lassen, *et al.,* (1955)
Dog	Liver Whole	.0544(a) (d)	.0625(a) (f) (i)	Hollenberg, *et al.,* (1966)
Rabbit	Muscle Homogenate	.0442(b) (c)	.0439(b) (j)	Yeh, *et al.,* (1965)
Man	Blood	.0433(b) (c)	.0455(b) (j)	Ibid.
Rat	Whole Body	.076(a) (g)	.0921(a) (i)	Kirk (unpublished data)
Guinea Pig	Whole Body	.1482(a) (e)	.1444(a) (i)	Kirk (1973)
	Omental fat	.4254(a) (e)	.4213(a) (i)	Ibid.
	Subcutaneous fat	.4254(a) (e)	.4054(a) (i)	Ibid.
	Adrenal	.1067(a) (e)	.1017(a) (i)	Ibid.
	Liver	.0524(a) (e)	.0768(a) (i)	Ibid.
	Muscle	.0752(a) (e)	.0396(a) (i)	Ibid.
	Bone Marrow	.0863(a) (d)	.1342(a) (i)	Ibid.
	Brain	.0744(a) (d)) (h)	.0405(a) (i)	Ibid.
	Brain	Ibid.		

(a) $L_{w\ tissue:\ air}$.

(b) $L_{tissue:air}$.

(c) Direct determination of tissue composition.

(d) Tissue composition from *Handbook of Biological Data,* Spector (1956).

(e) Tissue composition from Pace, *et al.,* (1945).

(f) Calculated from reported tissue:blood coefficient using $L_{blood:air} = {}^{0.059}$.

(g) Tissue composition from Caster, *et al.,* (1956).

(h) 50% non-neutral fat correction used.

(i) Determined *in vivo.*

(j) Determined *in vitro.*

TABLE 10. Annual Dose (a) to Guinea Pig Tissues and Organs from Respiratory Exposure to ^{85}Kr at Current $(MPC)_a$ Levels.

Tissue	Occupational (b) rad/year	σ	Unrestricted (c) rad/year	σ
Omental fat	4,460	681	586	90
Subcutaneous fat	4,290	957	564	126
Thymus	2,740	1,390	360	183
Lymph nodes	1,460	794	191	104
Bone marrow	1,420	1,260	187	165
Adrenal	1,080	404	141	53
Thyroid	877	395	115	52
Liver	813	298	107	39
Large intestine	788	765	104	59
Small intestine	764	414	100	54
Testes	613	160	81	22
Ovaries	608	145	80	19
Kidneys	455	199	60	26
Uterus	442	134	58	18
Stomach	439	218	58	29
Brain	429	177	56	23
Eyes	425	136	56	18
Muscle	419	183	55	24
Seminal vesicles	391	72	51	10
Spleen	386	96	51	13
Heart	317	157	42	41

(a) μrad/year beta dose to organ/tissue from contained ^{85}Kr. Values are for bloodless tissue; dose from isotope outside the tissue is not considered.

(b) 2,000 hours at 10^{-5} $\mu Ci/cm^3$.

(c) 24 hours/day, 365 days at 3×10^{-7} $\mu Ci/cm^3$.

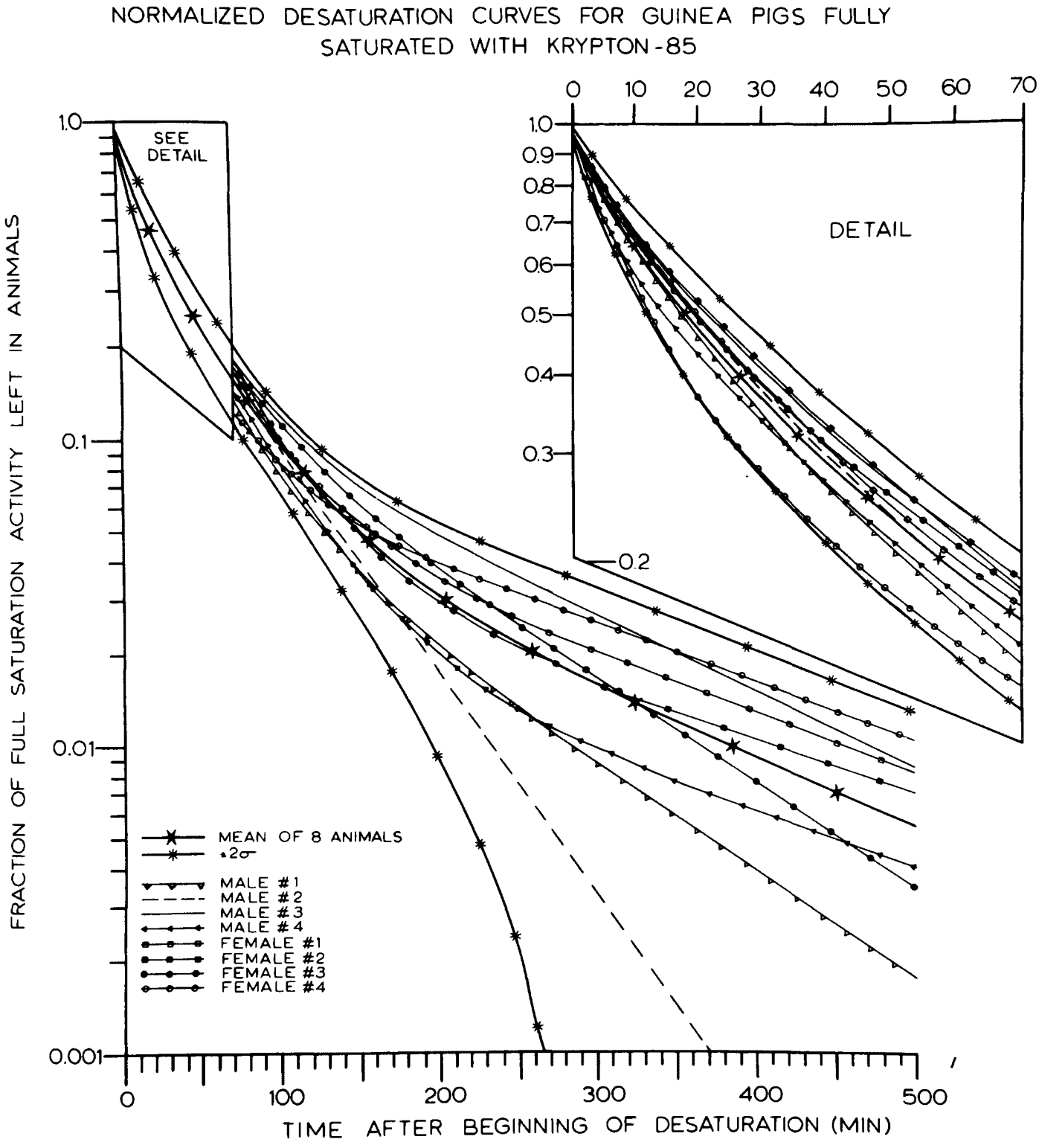
NORMALIZED DESATURATION CURVES FOR GUINEA PIGS FULLY SATURATED WITH KRYPTON-85
SEE DETAIL
DETAIL
FRACTION OF FULL SATURATION ACTIVITY LEFT IN ANIMALS
TIME AFTER BEGINNING OF DESATURATION (MIN)
MEAN OF 8 ANIMALS
±2σ
MALE #1
MALE #2
MALE #3
MALE #4
FEMALE #1
FEMALE #2
FEMALE #3
FEMALE #4

Figure 1.

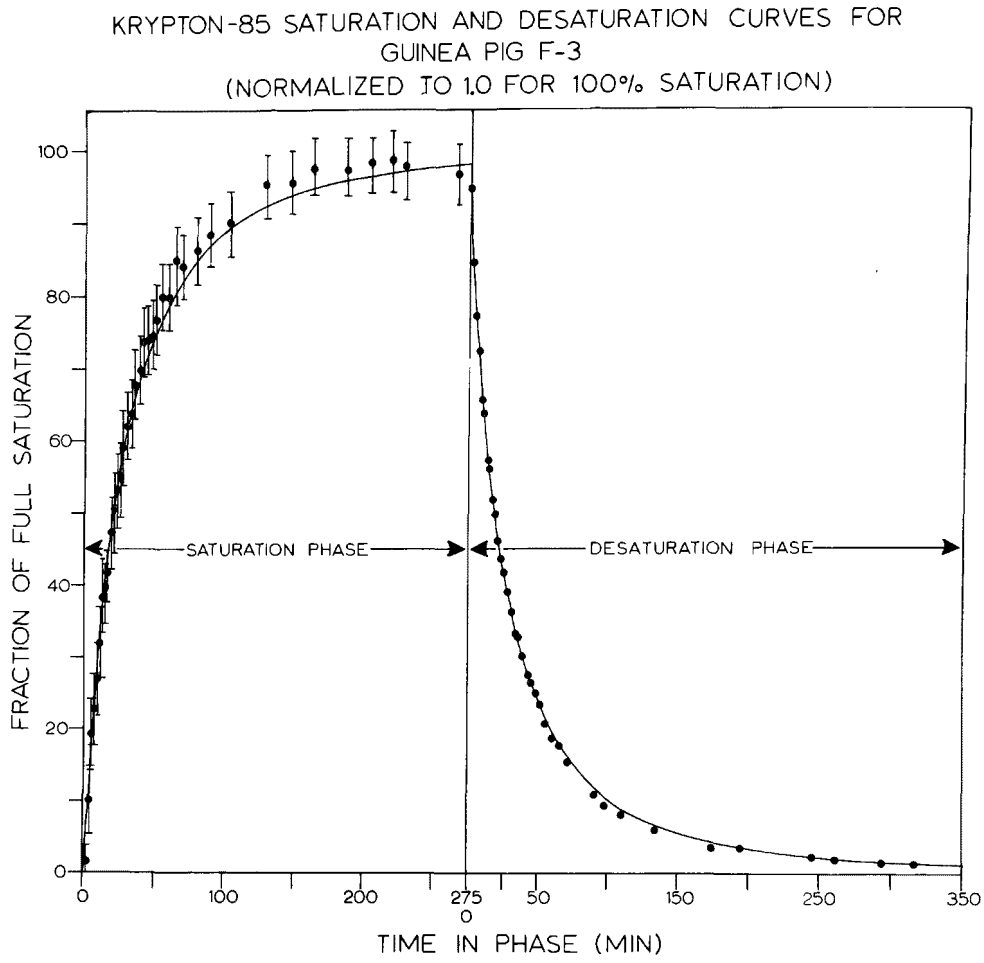
KRYPTON-85 SATURATION AND DESATURATION CURVES FOR
GUINEA PIG F-3
(NORMALIZED TO 1.0 FOR 100% SATURATION)
FRACTION OF FULL SATURATION
100
80
60
40
20
0
SATURATION PHASE
DESATURATION PHASE
0
100
200
275
0
50
150
250
350
TIME IN PHASE (MIN)

Figure 2.

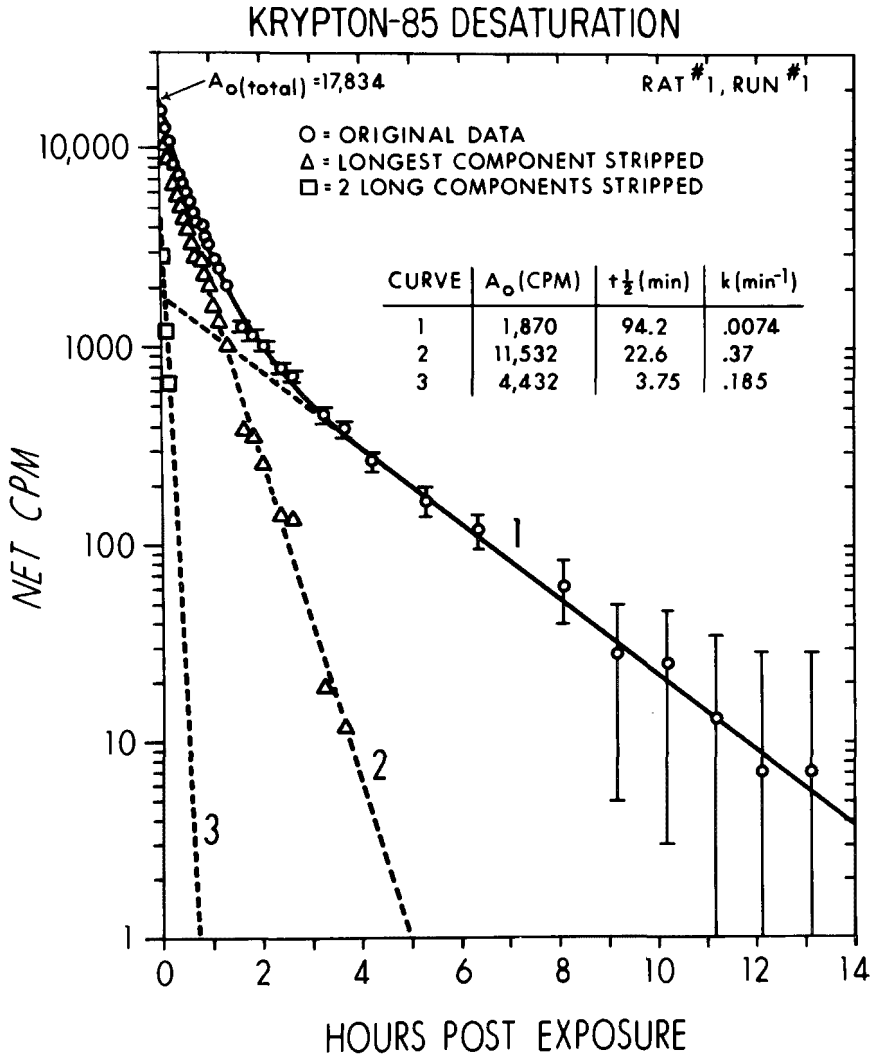

Figure 3. Experimental ^{85}Kr desaturation curves in rat (short exposure).

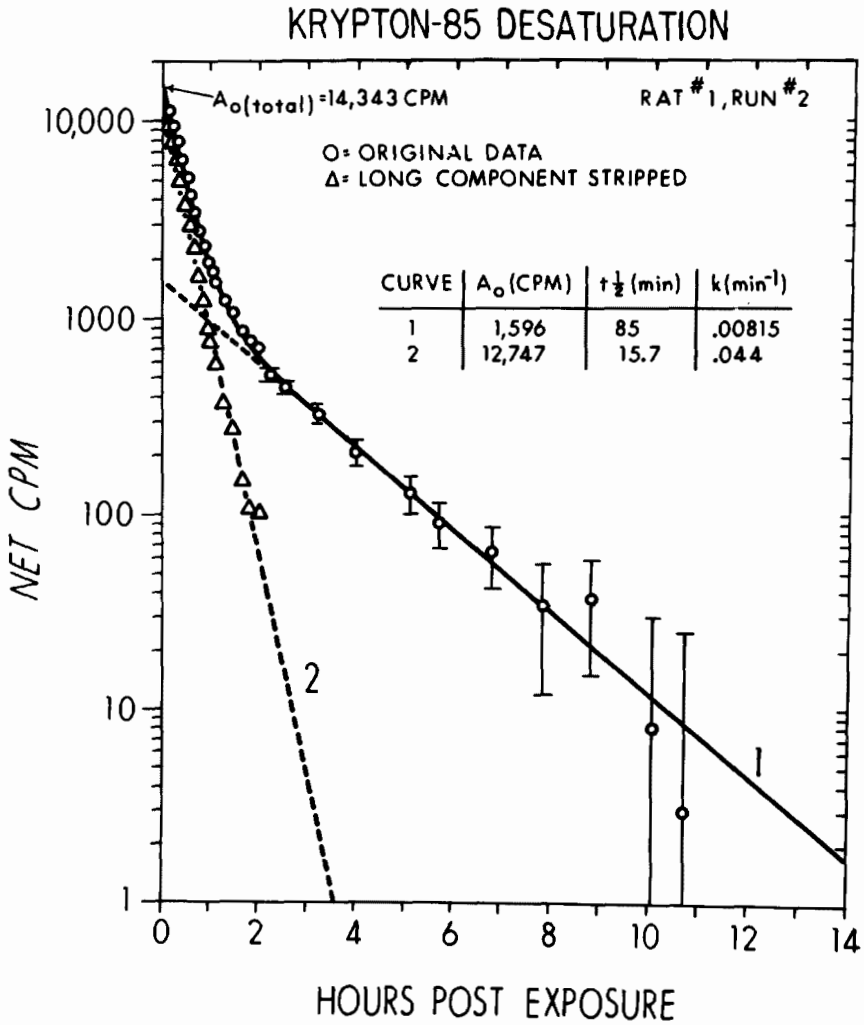

Figure 4. Experimental ^{85}Kr desaturation curves in rat (long exposure).

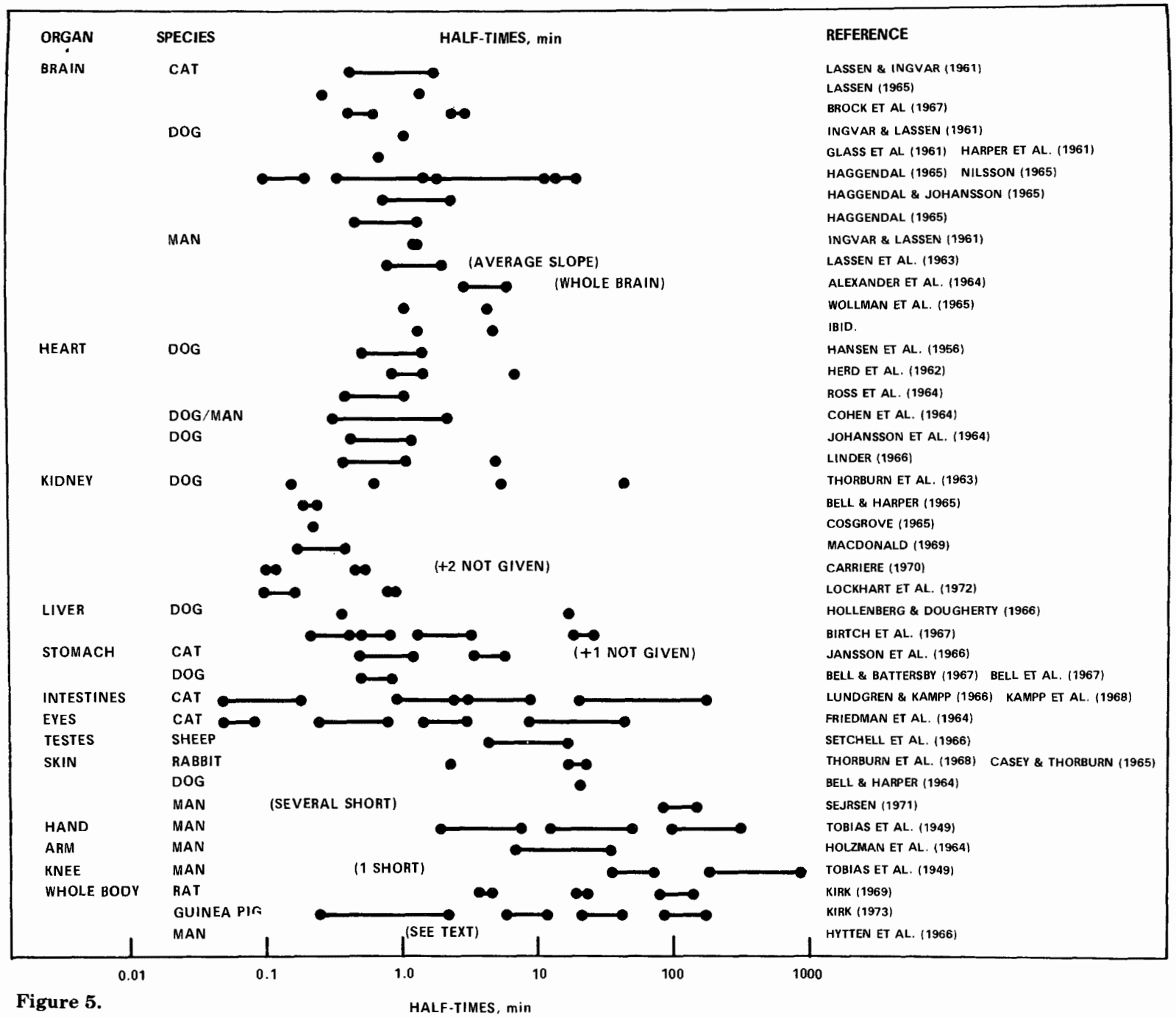
COMPARTMENT HALF-TIMES FROM LITERATURE
ORGAN
SPECIES
HALF-TIMES, min
REFERENCE
BRAIN
CAT
DOG
MAN
(AVERAGE SLOPE)
(WHOLE BRAIN)
HEART
DOG
DOG/MAN
DOG
KIDNEY
DOG
(+2 NOT GIVEN)
LIVER
DOG
STOMACH
CAT
DOG
(+1 NOT GIVEN)
INTESTINES
CAT
EYES
CAT
TESTES
SHEEP
SKIN
RABBIT
DOG
MAN
(SEVERAL SHORT)
HAND
MAN
ARM
MAN
KNEE
MAN
(1 SHORT)
WHOLE BODY
RAT
GUINEA PIG
MAN
(SEE TEXT)
LASSEN & INGVAR (1961)
LASSEN (1965)
BROCK ET AL (1967)
INGVAR & LASSEN (1961)
GLASS ET AL (1961) HARPER ET AL. (1961)
HAGGENDAL (1965) NILSSON (1965)
HAGGENDAL & JOHANSSON (1965)
HAGGENDAL (1965)
INGVAR & LASSEN (1961)
LASSEN ET AL. (1963)
ALEXANDER ET AL. (1964)
WOLLMAN ET AL. (1965)
IBID.
HANSEN ET AL. (1956)
HERD ET AL. (1962)
ROSS ET AL. (1964)
COHEN ET AL. (1964)
JOHANSSON ET AL. (1964)
LINDER (1966)
THORBURN ET AL. (1963)
BELL & HARPER (1965)
COSGROVE (1965)
MACDONALD (1969)
CARRIERE (1970)
LOCKHART ET AL. (1972)
HOLLENBERG & DOUGHERTY (1966)
BIRTCH ET AL. (1967)
JANSSON ET AL. (1966)
BELL & BATTERSBY (1967) BELL ET AL. (1967)
LUNDGREN & KAMPP (1966) KAMPP ET AL. (1968)
FRIEDMAN ET AL. (1964)
SETCHELL ET AL. (1966)
THORBURN ET AL. (1968) CASEY & THORBURN (1965)
BELL & HARPER (1964)
SEJRSEN (1971)
TOBIAS ET AL. (1949)
HOLZMAN ET AL. (1964)
TOBIAS ET AL. (1949)
KIRK (1969)
KIRK (1973)
HYTTEN ET AL. (1966)
0.01
0.1
1.0
10
100
1000
HALF-TIMES, min

Figure 5.

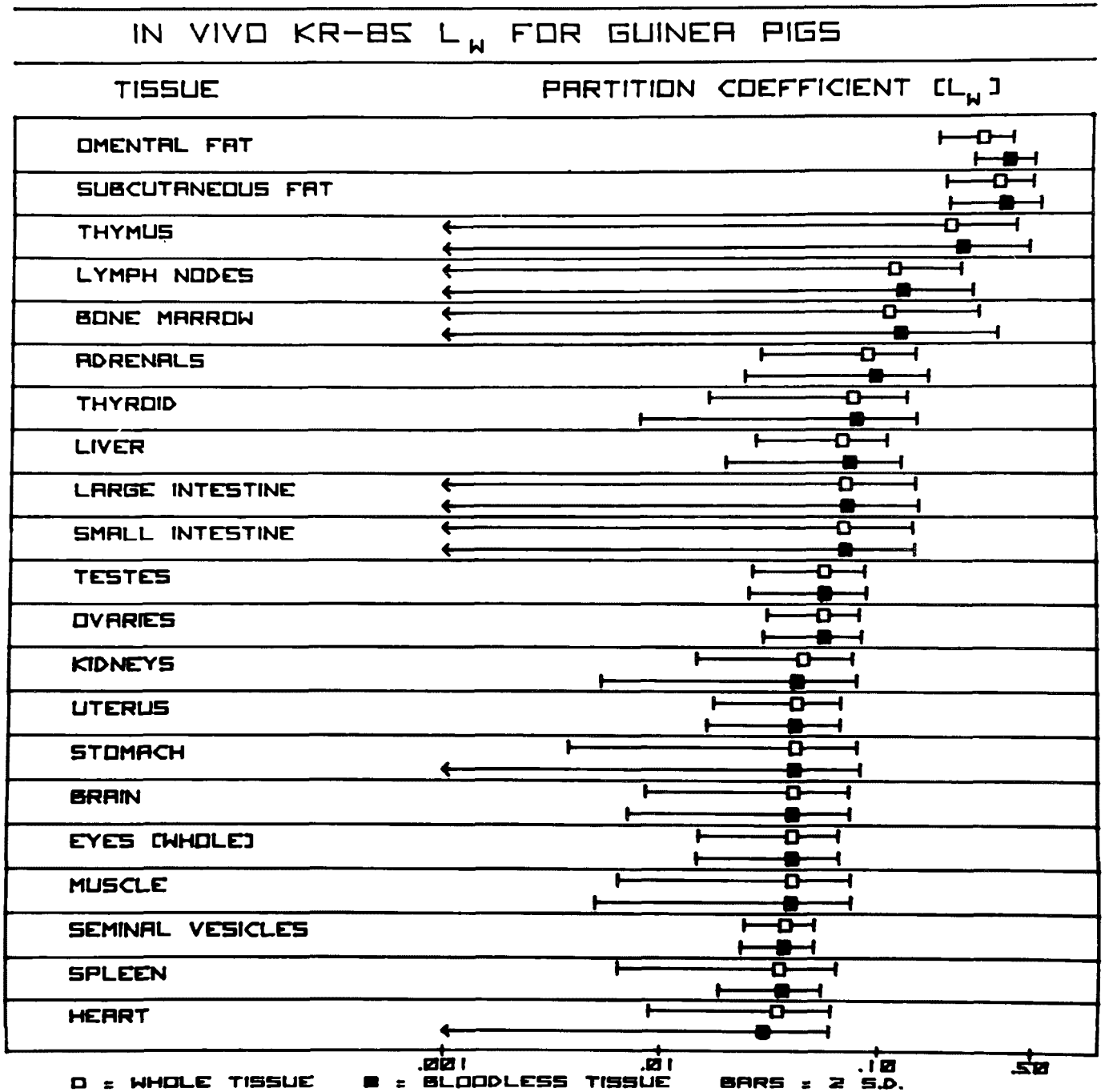
IN VIVO KR-85 L_W FOR GUINEA PIGS
TISSUE
PARTITION COEFFICIENT [L_W]
OMENTAL FAT
SUBCUTANEOUS FAT
THYMUS
LYMPH NODES
BONE MARROW
ADRENALS
THYROID
LIVER
LARGE INTESTINE
SMALL INTESTINE
TESTES
OVARIES
KIDNEYS
UTERUS
STOMACH
BRAIN
EYES [WHOLE]
MUSCLE
SEMINAL VESICLES
SPLEEN
HEART
.001
.01
.10
.50
□ = WHOLE TISSUE
■ = BLOODLESS TISSUE
BARS = 2 S.D.

Figure 6.

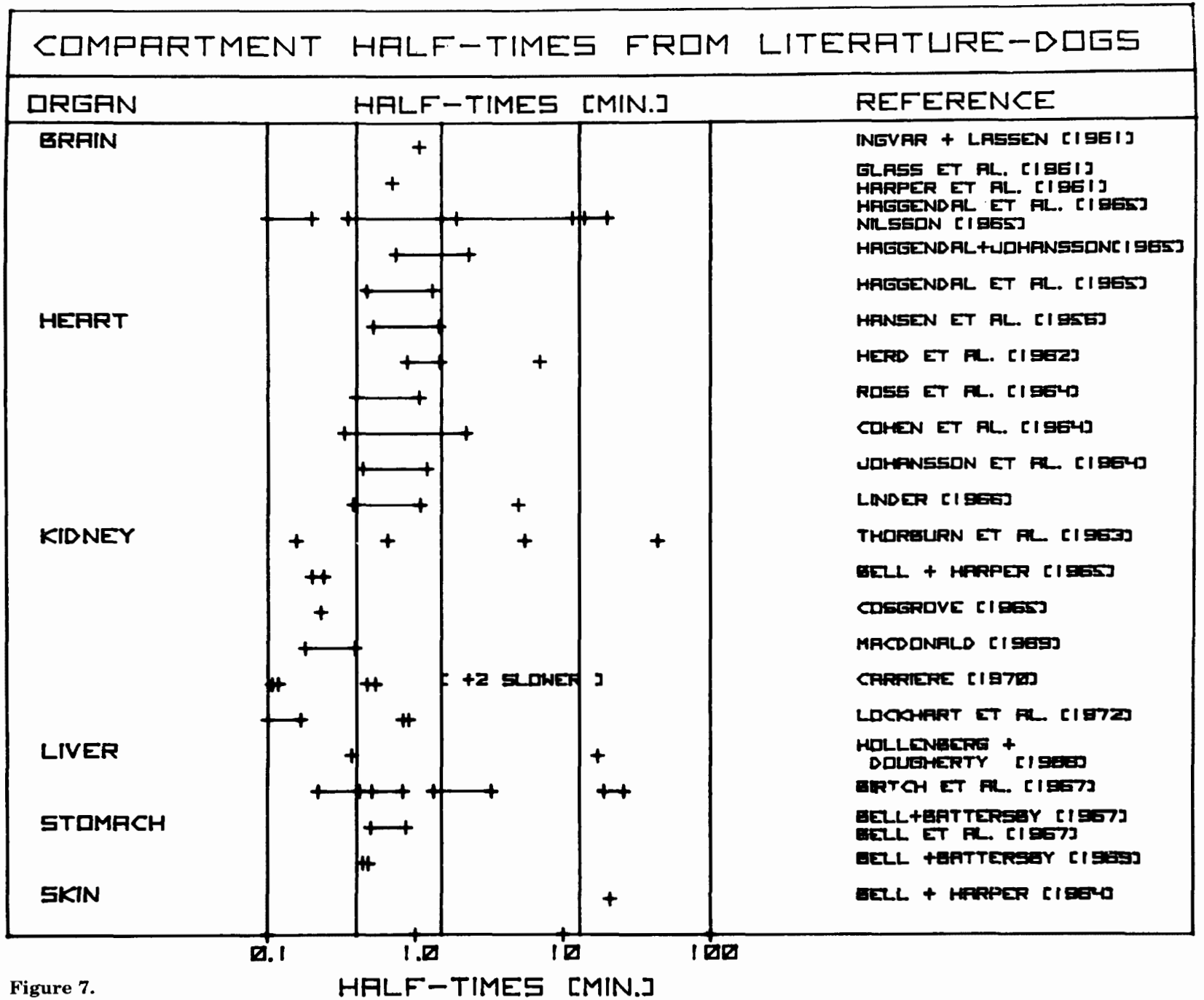
COMPARTMENT HALF-TIMES FROM LITERATURE-DOGS
ORGAN
HALF-TIMES [MIN.]
REFERENCE
BRAIN
HEART
KIDNEY
LIVER
STOMACH
SKIN
[+2 SLOWER]
INGVAR + LASSEN [1961]
GLASS ET AL. [1961]
HARPER ET AL. [1961]
HAGGENDAL ET AL. [1965]
NILSSON [1965]
HAGGENDAL+JOHANSSON[1965]
HAGGENDAL ET AL. [1965]
HANSEN ET AL. [1956]
HERD ET AL. [1962]
ROSS ET AL. [1964]
COHEN ET AL. [1964]
JOHANSSON ET AL. [1964]
LINDER [1966]
THORBURN ET AL. [1963]
BELL + HARPER [1965]
COSGROVE [1965]
MACDONALD [1969]
CARRIERE [1970]
LOCKHART ET AL. [1972]
HOLLENBERG + DOUGHERTY [1968]
BIRCH ET AL. [1967]
BELL+BATTERSBY [1967]
BELL ET AL. [1967]
BELL +BATTERSBY [1969]
BELL + HARPER [1964]
0.1
1.0
10
100
HALF-TIMES [MIN.]

Figure 7.

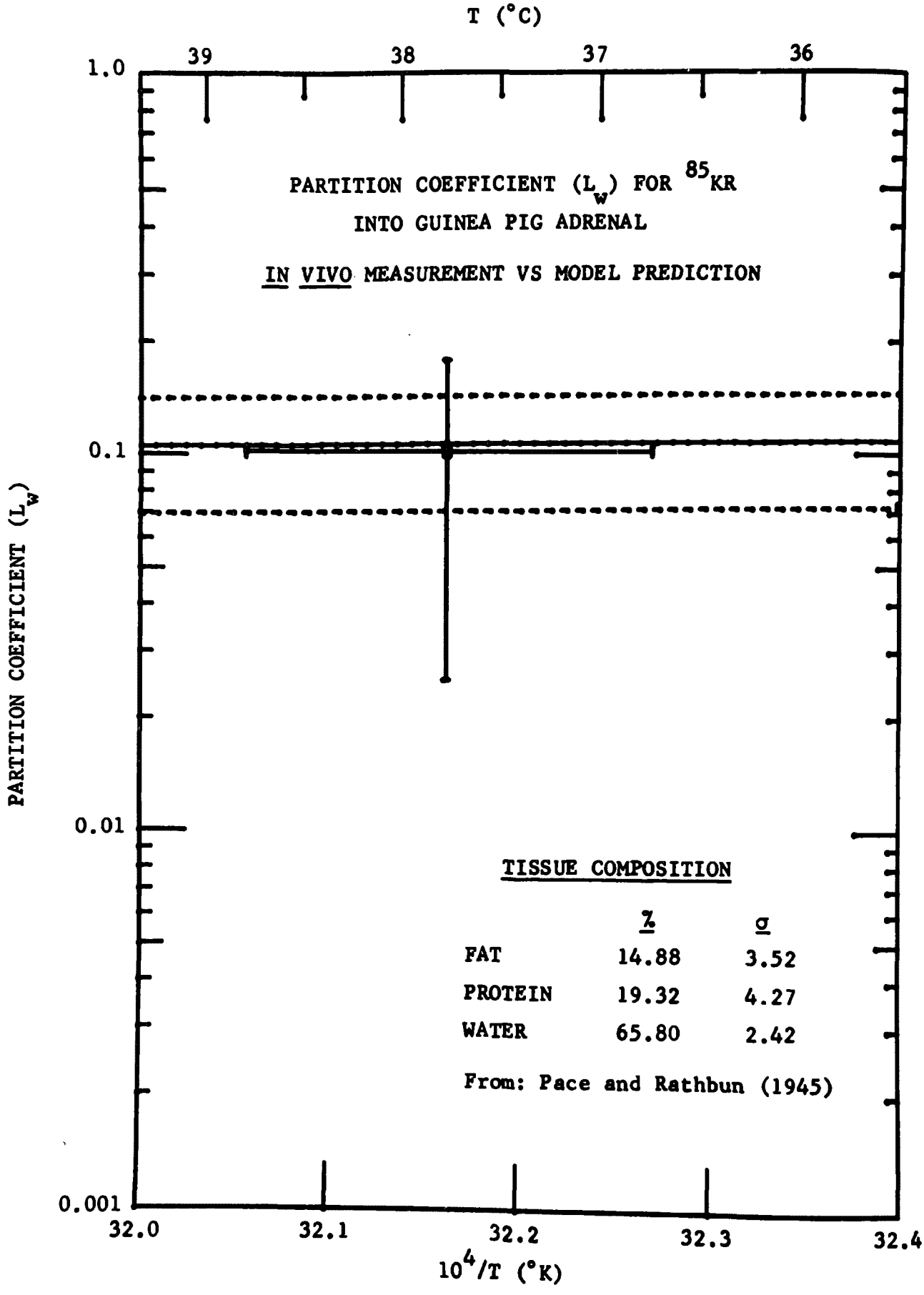
T (°C)
39
38
37
36
1.0
0.1
0.01
0.001
PARTITION COEFFICIENT (L_w)
PARTITION COEFFICIENT (L_w) FOR ^{85}KR
INTO GUINEA PIG ADRENAL
IN VIVO MEASUREMENT VS MODEL PREDICTION
TISSUE COMPOSITION
% g
FAT 14.88 3.52
PROTEIN 19.32 4.27
WATER 65.80 2.42
From: Pace and Rathbun (1945)
32.0
32.1
32.2
32.3
32.4
10^4/T (°K)

Figure 8.

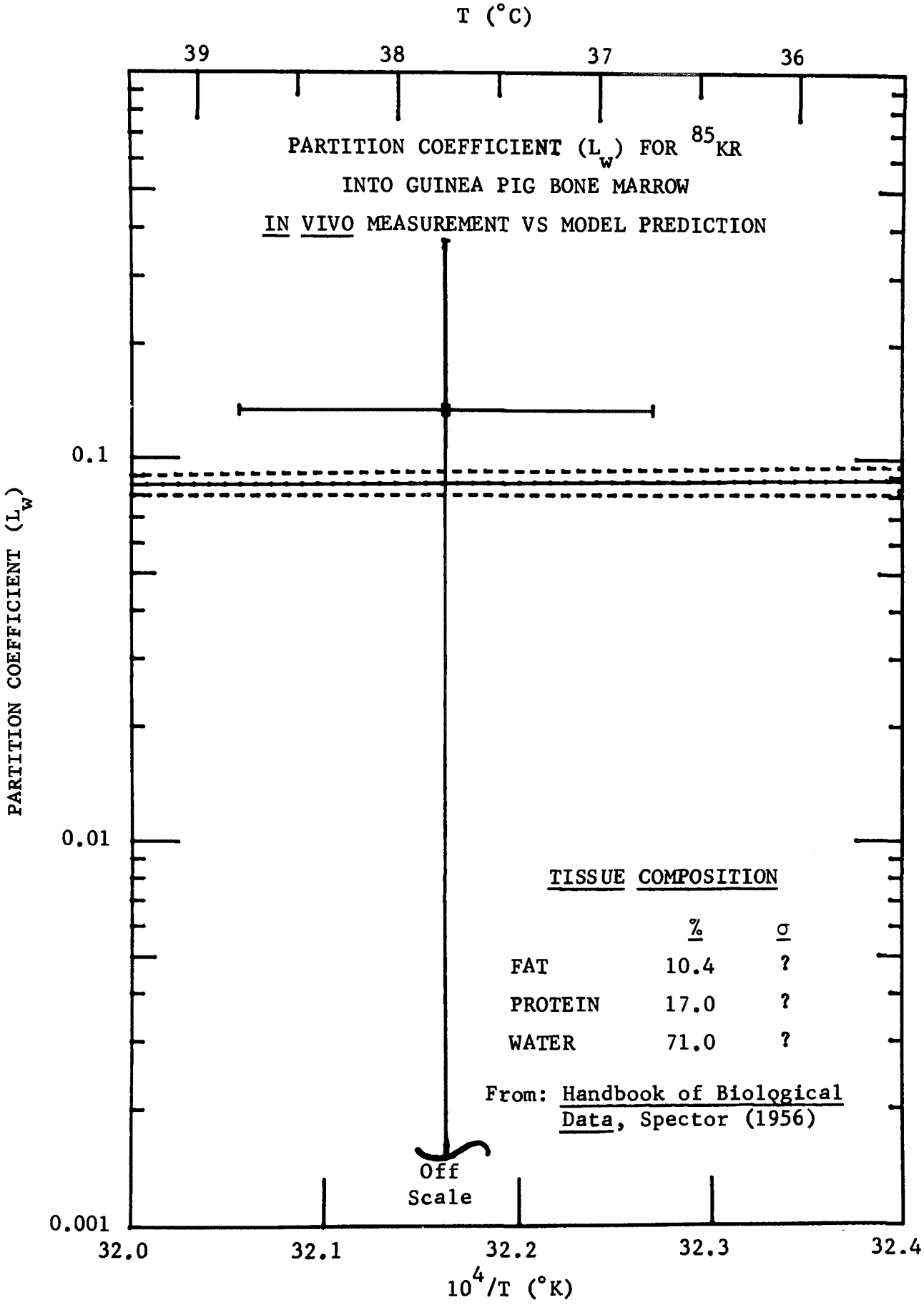
T (°C)
39
38
37
36
PARTITION COEFFICIENT (L_w) FOR ^{85}KR
INTO GUINEA PIG BONE MARROW
IN VIVO MEASUREMENT VS MODEL PREDICTION
0.1
0.01
0.001
PARTITION COEFFICIENT (L_w)
TISSUE COMPOSITION
% σ
FAT 10.4 ?
PROTEIN 17.0 ?
WATER 71.0 ?
From: Handbook of Biological Data, Spector (1956)
Off Scale
32.0
32.1
32.2
32.3
32.4
$10^4/T$ (°K)

Figure 9.

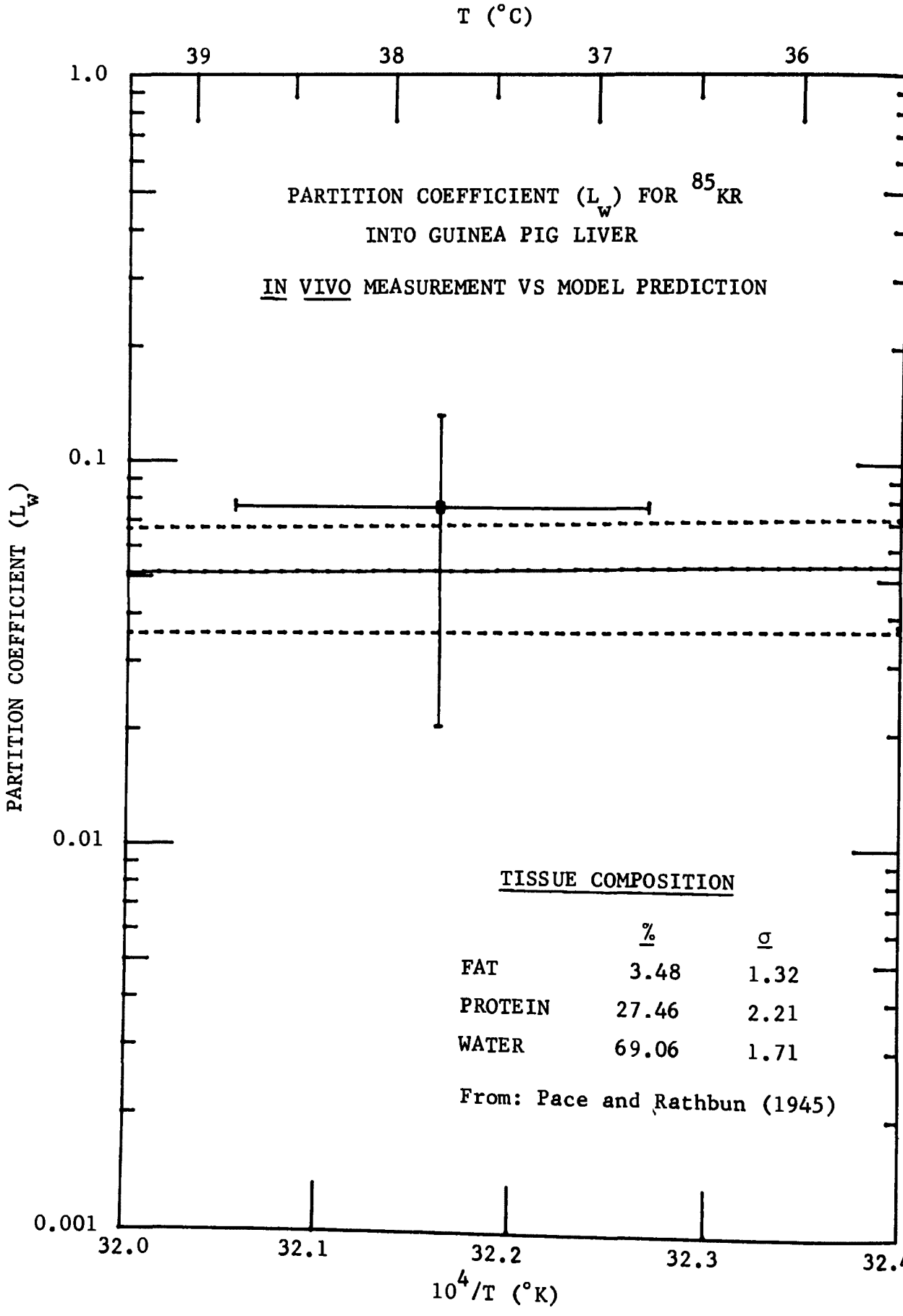
T (°C)
39
38
37
36
1.0
0.1
0.01
0.001
PARTITION COEFFICIENT (L_w)
PARTITION COEFFICIENT (L_w) FOR ^{85}KR
INTO GUINEA PIG LIVER
IN VIVO MEASUREMENT VS MODEL PREDICTION
TISSUE COMPOSITION
% σ
FAT 3.48 1.32
PROTEIN 27.46 2.21
WATER 69.06 1.71
From: Pace and Rathbun (1945)
32.0
32.1
32.2
32.3
32.4
10^4/T (°K)

Figure 10.

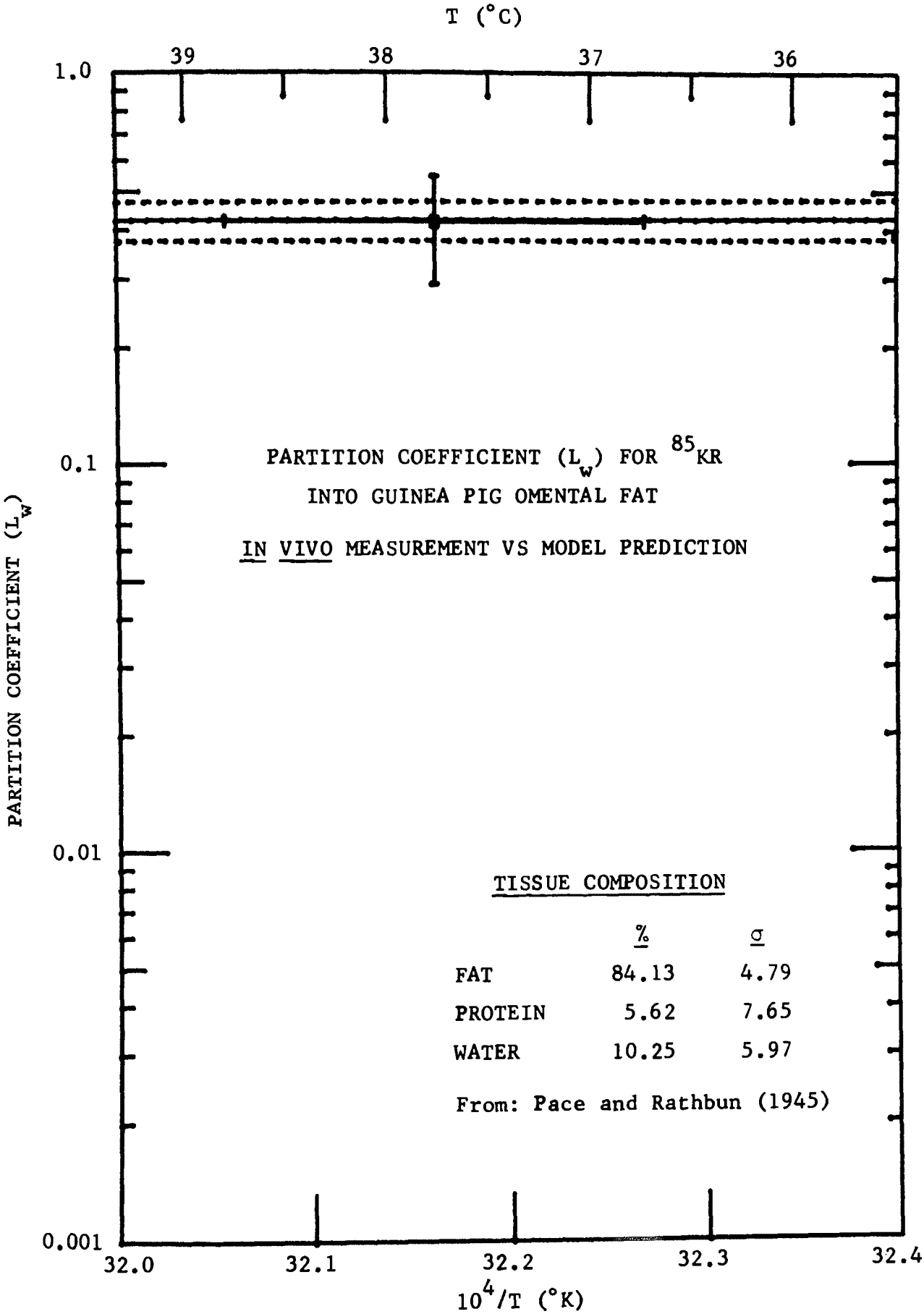
T (°C)
39
38
37
36
1.0
0.1
0.01
0.001
PARTITION COEFFICIENT (L_w)
PARTITION COEFFICIENT (L_w) FOR ^{85}KR
INTO GUINEA PIG OMENTAL FAT
IN VIVO MEASUREMENT VS MODEL PREDICTION
TISSUE COMPOSITION
% σ
FAT 84.13 4.79
PROTEIN 5.62 7.65
WATER 10.25 5.97
From: Pace and Rathbun (1945)
32.0
32.1
32.2
32.3
32.4
10^4/T (°K)

Figure 11.

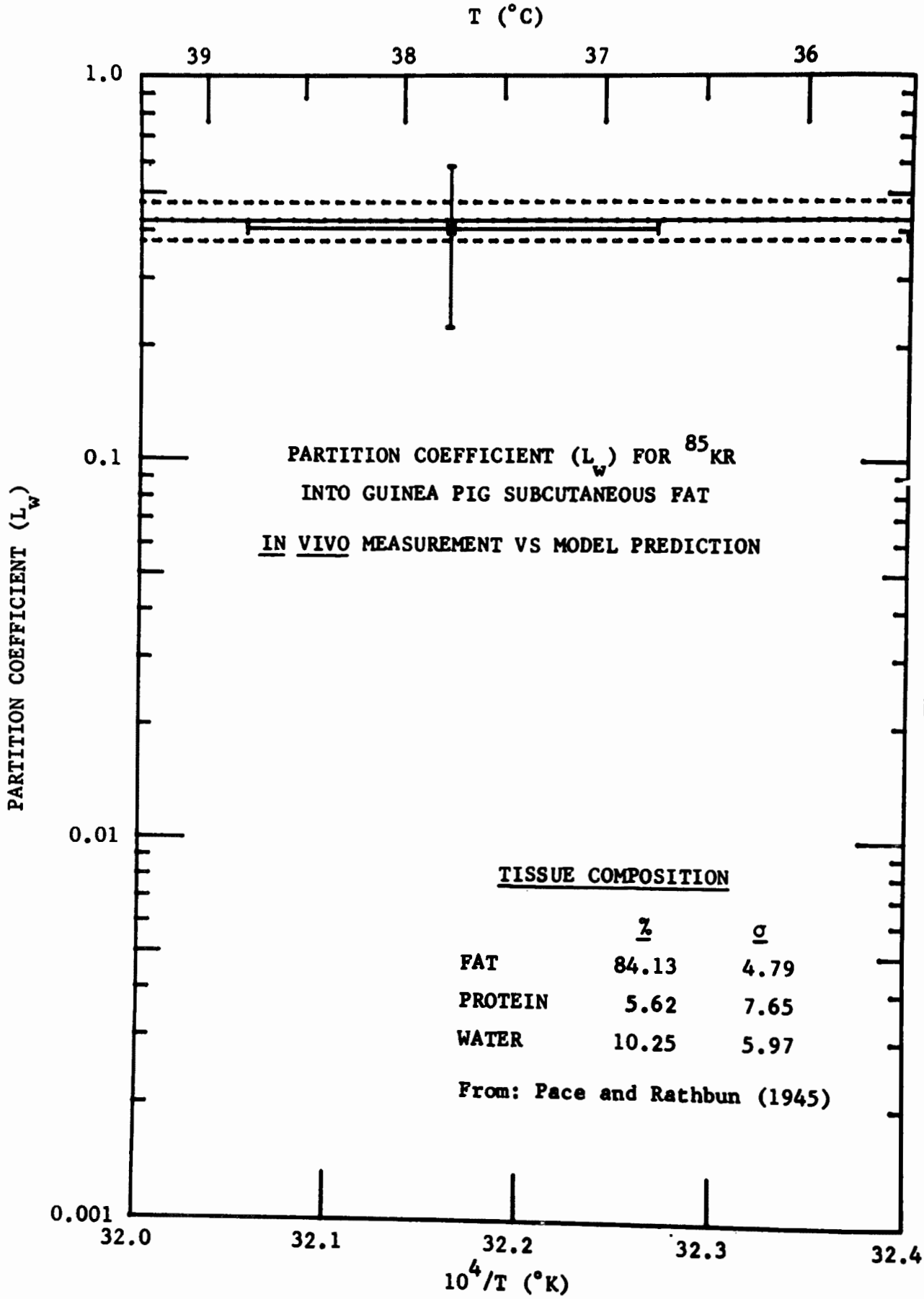
T (°C)
39
38
37
36
1.0
0.1
0.01
0.001
PARTITION COEFFICIENT (L_w)
PARTITION COEFFICIENT (L_w) FOR ^{85}KR
INTO GUINEA PIG SUBCUTANEOUS FAT
IN VIVO MEASUREMENT VS MODEL PREDICTION
TISSUE COMPOSITION
% σ
FAT 84.13 4.79
PROTEIN 5.62 7.65
WATER 10.25 5.97
From: Pace and Rathbun (1945)
32.0
32.1
32.2
32.3
32.4
10^4/T (°K)

Figure 12.

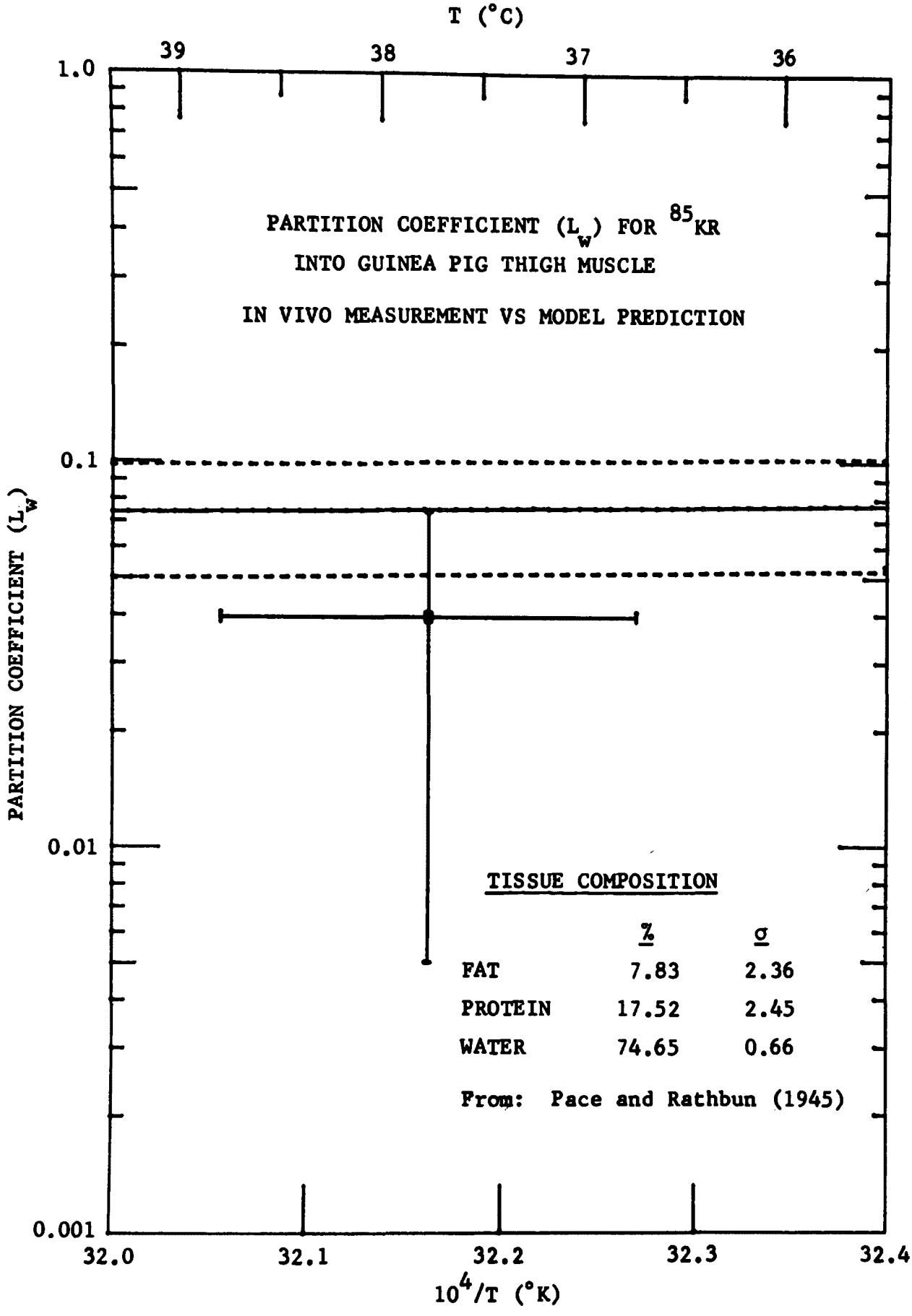
T (°C)
39
38
37
36
1.0
0.1
0.01
0.001
PARTITION COEFFICIENT (L_w)
PARTITION COEFFICIENT (L_w) FOR ^{85}KR
INTO GUINEA PIG THIGH MUSCLE
IN VIVO MEASUREMENT VS MODEL PREDICTION
TISSUE COMPOSITION
% σ
FAT 7.83 2.36
PROTEIN 17.52 2.45
WATER 74.65 0.66
From: Pace and Rathbun (1945)
32.0
32.1
32.2
32.3
32.4
$10^4/T$ (°K)

Figure 13.

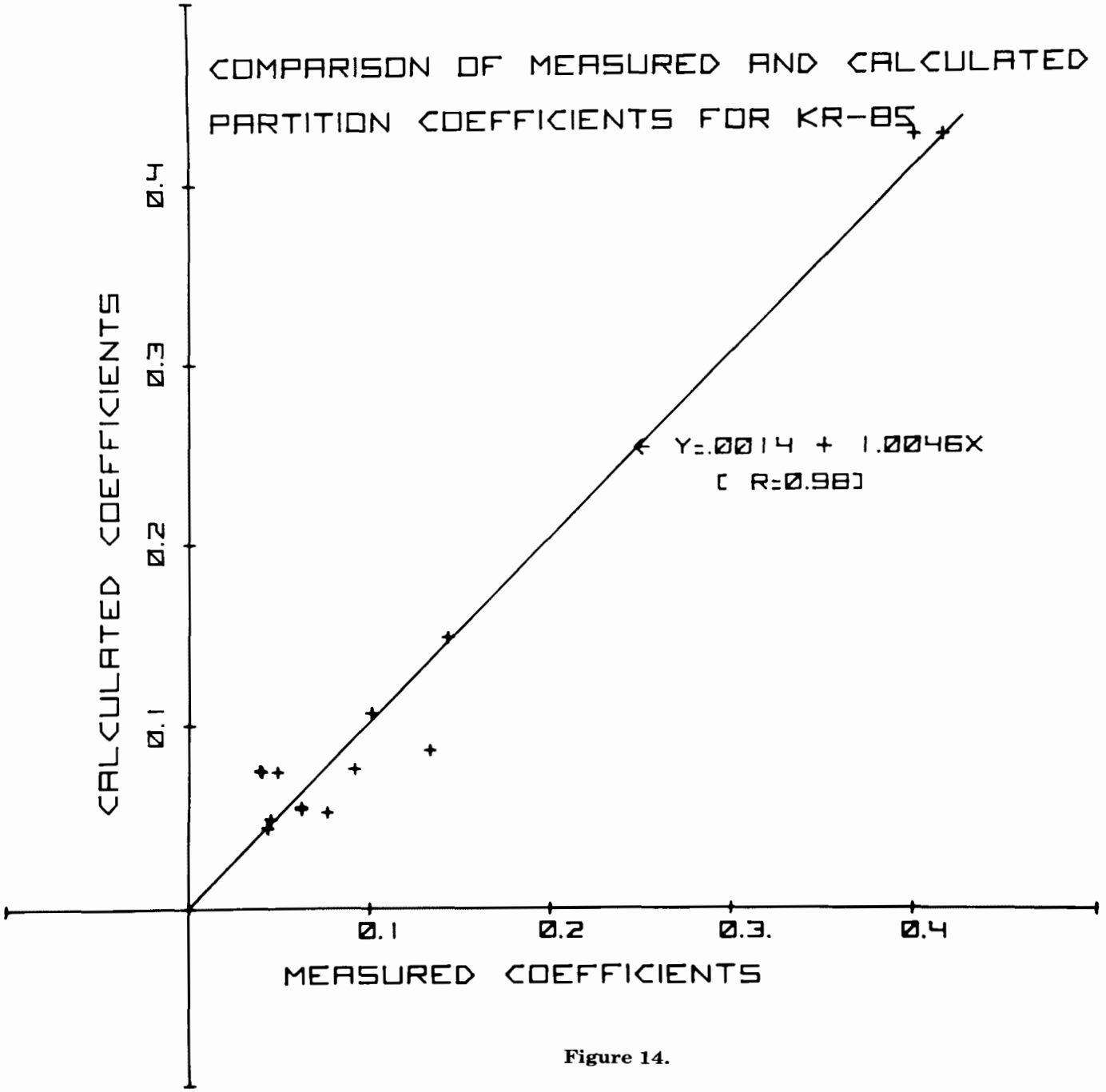
COMPARISON OF MEASURED AND CALCULATED
PARTITION COEFFICIENTS FOR KR-85
Y=.0014 + 1.0046X
[R=0.98]
CALCULATED COEFFICIENTS
0.1
0.2
0.3
0.4
MEASURED COEFFICIENTS
0.1
0.2
0.3.
0.4

Figure 14.

THE BIOLOGICAL EFFECTS OF THE RADIOACTIVE NOBLE GASES*

D. A. Morken
University of Rochester
Rochester, New York 14642

Abstract

The biological effects of the noble gases depend on the physical properties of these gases, since they are non-reactive chemically under physiological conditions. A property of interest for the non-radioactive gases is their solubility in the various body tissues and fluids.

Some of these noble gases have the additional property of radioactivity. The combination of radioactivity and solubility permits the identification of a critical organ according to established procedures. The pathological response is not always greatest, or even of singular importance, in the organ so identified by calculation. Biological responses are desired for a prudent evaluation of the biological effect, but the choice of response and the mode of irradiation pose a large problem.

The radioactive gases decay schemes include the emission of alpha particles, beta particles, positrons, and electron capture; and this decay is sometimes accompanied by gamma radiation. The resulting daughter products may be foreign or natural to the body; whether stable or radioactive, all are reactive chemically. The effects due to the radiation, however, probably exceed those chemical effects which may result.

Radon has no stable isotope. The radon isotopes decay primarily through the emission of alpha particles. The biological effects from radon may arise in greater measure from its daughter products, which include alpha particle, beta particle, and gamma ray emitters, than from the parent radon.

The consequences of these properties are discussed with particular reference to krypton-85 and radon-222.

INTRODUCTION

A prudent evaluation of biological responses to the noble gases can only be obtained by direct experimentation, but such experimentation has not been the general rule for the noble gas series of elements. Only radon has been studied in depth, but a beginning has been made on the effects of inhaled krypton.

Biological studies with radioactive argon, xenon, neon, and helium are difficult to perform in animal systems bacause of their very short half-lives. These elements, except for radon, are beta emitters; their solubility in tissues is a physical property dependent on their molecular weight. Due to these similarities information about one of these gases should be applicable in evaluating the others. Recent experiments with radon suggest that the chemical properties may be more important than radiation in producing long-term effects. It is also necessary to consider the role played by the daughter products.

The isotopes of helium decay either to hydrogen, a natural constituent of the body, or to lithium. Neon decays to either sodium or fluorine, and argon decays to either potassium or chlorine — all of which are normal constituents of the body. Krypton decays to either rubidium or bromine; and xenon decays to either cesium or iodine. Radon decays to polonium, and thence through a series of elements which includes lead and bismuth. The decay of radon and its daughter products is accompanied by alpha, beta, and gamma radiation.

A proper study of the biological effects of these radioactive gases should include the effects of the daughter products which, in general, are stable isotopes. External irradiation by these radioactive gases does not involve the stable daughters, but inhalation of these gases includes the stable daughters. Thus, the age of the radioactive gas may not be the most important factor in evaluating biological effects when the effects are due to chemical properties and not to radiation alone.

The isotopes of greatest environmental interest are krypton-85, which produces rubidium-85 (stable) by beta emission; xenon-133, which produces cesium-133 (stable) by beta emission; and radon, which decays by alpha emission to a series of short-lived elements that are alpha, beta, and gamma emitters. The 5.3-day half-life of xenon-133 limits its usefullness in biological experiments. The 10.6-year half-life of krypton-85 makes it a particularly useful isotope for biological experimentation. Krypton is also of environmental concern because of its relatively long half-life, and its release from nuclear reactor and fuel processing plants.

Because these gases are not accompanied by large amounts of chemically reactive materials, they offer a purity of radiation invaluable for studies involving internal emitters which is not available outside the series of noble gas elements. The purity of the radiation, or lack of chemically active materials, may approach that of x- or gamma radiation for all practical purposes. The comparatively uniform distribution of these gases in the body tissues, as determined by solubility studies, results in a relatively uniform dose distribution with no great differences in effect from similar doses of x- or gamma radiation.

*This paper is based on work performed under contract with the U. S. Atomic Energy Commission at the University of Rochester Atomic Energy Project and has been assigned Report No. UR-3490-383.

BIOLOGICAL EFFECTS

The acute lethality by inhalation (30-day LD-50) for krypton-85 in guinea pigs has been reported by Kirk (1973). The experimental arrangement Kirk used minimized the external exposure. The LD-50 dose required about 12 hours at a concentration of 375μCi/cm^3. The whole body absorbed dose calculated from this air dose amounted to 340 rads — which is within the range of x- and gamma ray doses reported for the guinea pig. Kirk also described the appearance of beta burns on the nose, and epilation around the nose and eyes, but skin healing and hair regrowth were complete in 4 to 10 weeks. He concluded that deaths which occurred before the 30 days were due to a hematopoietic syndrome, whereas those which occurred later were due to lung injury. The lung dose at the LD-50 level was estimated to have been 8,000 rads.

Kirk's report constitutes essentially all that is known about the internal distribution, dose estimates, and the biological responses for inhaled krypton-85. Radon has been studied more extensively in terms of biological effects.

Inhaled radon presents the body with three different kinds of exposure. Exposures from radon alone could be compared to krypton exposures — if it could be obtained alone. Radon, however, is accompanied by a series of short-lived radioactive decay products; consequently exposures with radon must always account for these additional radioactivities and distributions of the decay products. These products are produced within the animal from the inhaled radon. Thus a second kind of exposure, from the isotopes of polonium, lead, and bismuth, delivers a radiation dose to the entire animal. The distribution of this dose is essentially non-uniform because the isotopes are treated independently by the body tissues — within the confines of the short half-lives. It is possible with injection techniques to produce whole body exposures to these decay products alone (Hollcroft, *et al.*, 1951), and the histopathology and acute toxicity following such injections have been reported (Hollcroft, *et al.*, 1955).

The third kind of exposure is to the inhalation of these short-lived radon decay products present in the inhaled atmospheric air. These products are attached to dust particles which may be deposited in the lung when inhaled. Because of their short half-lives (3 to 30 minutes), these products accumulate and decay within the lung structure, since the clearance mechanisms which operate on dust in the lungs are thought to be ineffective in such short times. This method of exposure might deliver large doses to lung alone, and is believed to be the kind of exposure which results in the bronchial cancer found in uranium miners. In the absence of other information, the large physical dose which can be delivered to the lung by this airborne radioactivity is considered sufficient reason to designate the lung as the critical organ for exposure to radon by inhalation.

The radon experiments in this paper consider only the inhalation of radon and its subsequent decay within the animal body. The effects of the inhalation of the daughter products are described in another paper in this symposium (Morken, 1973).

These experiments were conducted with a closed respiration system in which mice (CAF_1 strain) could be exposed to a radon-222 concentration of 0.22 mCi per liter for periods of up to 40 hours. The contained air was kept free from the decay products of radon by air filtering and a rapid air turnover rate.

In this system, mice exposed from 5 to 40 hours showed a 30-day LD-50 near 7.5 mCi-hours/liter (Morken, 1955). This amounted to about 400 rad, when converted to an internal dose, and fell within the range of the x-ray doses required for the same effect. On an energy basis, this is not different from the LD-50 found with krypton-85. Emaciation, reddening of the ears, and dullness of the eyes were the first signs of tissue damage. The mice, which died within a few days after exposure, exhibited the pseudoparalysis which has been reported. The fur generally became bristly, even for the low doses. Deaths which fell within the 30-day period occurred in the first two weeks; no further deaths occurred until after 60 days. The limited pathology information describes changes similar to those following whole-body exposures to x-rays. The changes in the circulating cell numbers were not as great as with an equivalent x-ray exposure. A definite, but not pronounced, anemia occurred. More profound effects were found following x-ray exposures.

The histopathology in mice exposed to radon at the sub-acute level (one-half the LD-50) has been reported (Scott, 1955). Of the internal organs, the spleen evidenced the greatest early damage — and also evidenced rapid repair. Late injury was found in the kidney. The estimated dose to the kidney, due principally to the cumulation of the decay products, was 288 rad, compared to a whole-body dose of 255 rad (Morken, 1959). The lung and trachea showed no lesions, during the early period following exposure, that could be attributed to the radon. Changes in the epithelial lining of the small bronchi appeared at 2 and 5 months, and were fairly clear at 7 months. The changes consisted mainly in an irregularity of the cells, some loss of polarity, and the presence of a number of large cells containing large hyperchromatic nuclei (in many of which were large deeply-staining clumps of chromatin).

Mortality, growth, and the hemogram were studied in mice which received single exposures to radon. The doses ranged from 50 to 150 rad average dose to the whole body (Morken, 1961). Lifespan was shortened in proportion to dose, but the major effect appeared to be an early effect for a small part of the population, and little or no effect on the remainder.

The blood cell picture following single doses was essentially that seen after other kinds of irradiation — except for the erythrocyte count, which became depressed in the normal manner, but showed no recovery. This red cell depression remained at the depressed level for nearly one year after exposure, after which it merged and decreased with the control data. The amount of the depression was fixed at about 15 percent, independent of dose.

Growth of mice following single doses was stopped within a few weeks after exposure. After this initial phase, growth resumed and appeared to follow the normal pattern, but the control values were not attained. Stunted growth appeared to be an early and permanent effect.

Of these changes none appeared to result from the late effects of irradiation, since the initial change in each occurred early in the period following exposure. Only the weights of the mice remained different from those of the controls during the late period of life.

These same parameters were followed in mice which received doses from radon in one or several exposures, with average whole body cumulated dose ranging from 150 to 600 rad (Morken, 1964). Lifespan was shortened in proportion to total dose, whether given in one or several exposures. The mortality data suggested a bimodal response composed of one group which died early after the exposure or group of exposures, and another group which died later. As the total dose was made larger, a greater fraction of the population was transferred from the late to the early deaths group. The probability of a radon-induced kidney lesion was found to have no significance on mortality in these experiments.

The injury which produced lifespan shortening was found to be repaired by 50% over a two-week interval, and the irreparable fraction of total injury was the same whether the injury was produced by single or multiple doses.

Growth of mice was stopped immediately after exposure. After this initial phase, growth resumed in an apparently normal pattern, but with a permanent decrement in body weight. The decrease was proportional to total dose, whether delivered in one or several exposures, although the initial rate of loss of weight was proportional to the individual doses.

The hemogram, following either single or multiple exposures to radon, was essentially the same as that found after exposure to other kinds of radiation. Multiple doses produced immediate injury proportional to the individual dose, but recovery processes were more influenced by the total accumulated dose. An exception to this general picture was the erythrocyte count, which was depressed by 15% following the first exposure, from which no recovery was evident, and was not further changed by additional exposures.

Of these parameters, lifespan and body weight were affected in proportion to total dose, whether fractionated or not, thereby allowing the conclusion that the injury due to the alpha dose delivered from radon is repaired to the same extent of 50% in each case. The effect on the red cell illustrates that permanent, but delimited, injury can be produced by alpha irradiation. The remainder of the blood cells suggest that some injuries from alpha radiation can be completely repaired.

From these experiments with radon we obtain a general conclusion that because of the relationship of effect to cumulated dose, the early effects found here with short exposures would not be evident in experiments with continual exposure to radon at lesser concentrations, or with long-lived internal alpha emitters.

SUMMARY

The effects of inhaled krypton-85, a beta emitter, and radon-222, an alpha emitter, are similar at the acute lethal level to each other and to those from external x- or gamma irradiation. Work with krypton has just begun. Radon has been studied more extensively in terms of mortality, body weight, and the hemogram. In general, the effects are not different from those found with x- or gamma radiation.

Radon produces a few specific differences from x- or gamma irradiation. Red cell forming tissue is only slightly injured, although the other blood cell forming tissues respond in the expected manner. The growth pattern is altered with permanent stunting a result. These specific effects may be a result of a special kind of injury which the alpha particle can produce. Similar experiments with beta particles from krypton-85 may resolve this difference and may lead to a better understanding of the nature of these effects.

REFERENCES

Hollcroft, J. W. and E. Lorenz (1951), *The 30-day LD-50 of Two Radiations of Different Ion Density. J. Natl. Cancer Inst.* 12:533.

Hollcroft, J. W., E. Lorenz, M. Mastthews, and C. G. Congdon(1955), *Long-Term Survival Following X-Irradiation and the Irradiation of the Alpha Particles from Radon and its Decay Products. J. Natl. Cancer Inst.* 15:1059.

Kirk, W. P. II(1973), *In Vivo Behavior and Effects of Krypton-85 in Guinea Pigs.* Dissertation, University of Rochester, Department of Radiation Biology and Biophysics, Rochester, New York.

Morken, D. A.(1955), *The Acute Toxicity of Radon.* AMA Arch. Ind. Health 12:435.

Morken, D. A.(1959), *The Radiation Dose to the Kidney of the Rat from Inhaled Radon.* AMA Arch. Ind. Health 20:505.

Morken, D. A.(1961), *The Effect of Inhaled Radon on the Survival, Body Weight, and Hemogram of the Mouse Following Single Exposures.* University of Rochester, Atomic Energy Project, Report No. UR-593.

Morken, D. A.(1964), *The Effect of Inhaled Radon on the Survival, Body Weight, and Hemogram Following Multiple Exposures.* University of Rochester, Atomic Energy Project, Report UR-624.

Morken, D. A.(1973), *The Biological Effects of Inhaled Radon.* This Symposium.

Scott, J. K.(1955), *The Histopathology of Mice Exposed to Radon.* University of Rochester, Atomic Energy Project, Report UR-411.

KINETICS AND DISTRIBUTION OF XENON-133 AND KRYPTON-85 IN THE HUMAN BODY

A. D. Turkin and Yu. I. Moskalev
Institute of Biophysics
Ministry of Health
Moscow, USSR

Abstract

The kinetics of ^{85}Kr and ^{133}Xe metabolism were studied in experiments on 15 male human beings whose ages ranged from 25 to 50 years. The half-life of ^{133}Xe in the lungs varied from 18 to 42 seconds, with an average half-life of 30 seconds. The elimination of ^{133}Xe from the blood is nearly the same as that for the lungs. The half-lives of ^{133}Xe in the muscle and fat tissues ranged from 0, 1 to 0, 42 and 4.6 to 7.4 hours, respectively. The ^{133}Xe uptake by the skin does not exceed 0.4 per cent.

The elimination of ^{85}Kr from the human body is well described by the sum of exponents. The average half-life of ^{85}Kr in the blood and lung is the same as those for ^{133}Xe, however, in the fat tissue it ranged from 1.8 to 3.7 hours, with an average half-life of 2.7 hours, and in the muscle tissue it ranged from 4 to 11 minutes.

INTRODUCTION

In connection with a broad program of nuclear energy development throughout the world, much attention should be given to the problem of controlling radioactivity releases into the atmosphere. Besides the problem of protecting small groups of people living in the vicinity of the release source, there are problems connected with the global contamination of the atmosphere.

In order to estimate the degree of risk of environmental contamination with the noble gases, one should know the factors which influence tissue doses within the human body.

Internal radiation tissue doses can be predicted only on the basis of data concerning the accumulation, distribution, and elimination of these gases from the human body.

There is limited data at present on the behavior of the radioactive noble gases within the human and animal bodies. According to Kalantarov, *et al.*, (1966), the kinetics of ^{133}Xe elimination from the human body after an intravenous injection is described by four exponents. The half-lives ranged from 0.3 to 30 minutes. The retention of ^{133}Xe in respiratory organs after a one-hour exposure equals 4 percent and after ten hours 0.5 percent of the total activity (Osanov, *et al.*, 1970). This paper presents experimental data on the kinetics of ^{85}Kr and ^{133}Xe metabolism in the body.

METHODS

Experiments on the kinetics of ^{85}Kr and ^{133}Xe metabolism were carried out on 15 male volunteers with ages ranging from 25 to 50 years. These experiments were performed in cooperation with E. S. Trukhmanova and S. V. Levinsky.

In order to ensure contact with radioactive gas, the subject was placed into a hermetic exposure chamber with a volume of 3.1 m^3. The duration of the exposure ranged from 0.5 to 66 hours. After each timed exposure the subject was again enclosed in the chamber for periodic measurements, until all the accumulated gas was eliminated. These experiments showed that noble gases are eliminated from the body almost completely during a period of 10-30 hours. Figure 1 gives a typical picture of the change in the radioactive gas concentrations in the air of the measuring chamber at the various intervals. From this data the noble gas elimination rate can be calculated by means of differentiating the curves Q = f(t) since

$$C_t = V_k \frac{dQ}{dt} = \frac{d\,A_k}{dt}$$

where V_k is volume of the measuring chamber and A_k is gas activity in the chamber.

In the case where the concentration was measured only once before the subject left the measuring chamber, the average value of the elimination rate was found by dividing the gas activity (A_k) by the time "t" of the subject's residence time in the measuring chamber, which in this case is

$$\bar{C}_t = \frac{A_k}{t}\,.$$

Figure 2 gives data characterizing a change in the ^{85}Kr elimination rate from the body of a subject. The kinetics of ^{85}Kr and ^{133}Xe accumulation were obtained by a numerical integration of experimentally obtained functions of the elimination rates.

In addition to determining the activity of the gas by its release into a closed volume, we also studied its distribution within the body by means of a whole body scintillation counter (NaI crystal 40 x 40 mm and PEM-13) coupled with a pulse height analyzer. The background was reduced by a lead screen 30 mm thick, which also served as a collimator. The counting rate was measured at the back, the chest, the abdomen, and the buttocks. Measurements were carried out as predetermined intervals when the subject left the measuring chamber. Thus, the dynamics of ^{133}Xe elimination from the various parts of the body were determined.

The ^{133}Xe concentrations in blood and urine were measured for gamma radiation with a scintillator calibrated using an aqueous solution of ^{133}Xe of a known activity. Urine samples were placed in polyethylene containers each having a volume of 250 ml. Blood samples were taken from the elbow vein into 10 ml glass syringes when the subjects were in the exposure chamber. This was accomplished when the subject's hand was stretched out of the transmission hatch of the chamber. The minimum values of ^{133}Xe concentrations that could be measured in blood and urine were 15 and 2 pCi/ml, respectively. The ^{85}Kr concentration in blood and urine was measured by its beta radiation with a cylindrical counter of the CTC-6 type. The samples were injected into the counter through rubber plugs using a syringe. In order to reduce the background radiation, the counter was placed in a lead housing furnished with a anticoincidence shield.

When the uptake of ^{85}Kr and ^{133}Xe through the skin was being studied, the respiratory organs were isolated with a helmet and "clean" air was fed into the space under the mask. In these studies the ^{85}Kr and ^{133}Xe concentrations in the air of the exposure camber were 0.5 to 5 μCi/1, while in the experiments related to uptake by the respiratory organs, concentrations used ranged from 0.05 to 5 μCi/1.

When the experiments were carried out in a hermetic exposure chamber, comfortable living conditions were provided. The temperature within the chamber was maintained at 20-23° C with a relative humidity of 48-64 percent and a CO_2 content not higher than 0.7 percent. The oxygen content used was kept within 24-27 percent which is slightly higher than ambient concentrations.

RESULTS

1. Experiments with ^{133}Xe.

The accumulation of ^{133}Xe within the human body was found to increase for a period of about 20 hours exposure; after which period, even with the continuing intake of the gas, its content in the body changes insignificantly (see Figure 3 and Table 1).

The numerical values which summarize the activity of ^{133}Xe within the body of the subjects as related to its concentration in the air of the exposure chamber A/Q_e, 1, are given in Table 1. The activity of ^{133}Xe uptake was found to be proportional to the subjects weight and the amount of body fat. Thus, for example, in the case of a man weighing 100 kg of which weight 28 kg is fat (the subject was M.P.), the value of A/Q_e at saturation is 54, while in the case of a 65 kg subject with 9 kg of fat (the subject was A. Shch.) A/Q_e is only 24.

Figure 4 gives typical curves for the accumulation and elimination of ^{133}Xe from the lungs of a subject when he is in a resting state. The accumulation of ^{133}Xe via breathing results in an equilibrium state being reached within 3-5 minutes. After intake of ^{133}Xe ends the activity in the lungs is reduced by 70 percent within 3-5 minutes, after which the rate of elimination decreases. An analysis of the curves of ^{133}Xe accumulation and elimination from the lungs of nine subjects showed that the kinetics of ^{133}Xe metabolism in the lungs is well described by the exponential law.

Table 2 shows that the effective ^{133}Xe half-life in the lungs of nine subjects at the time of exposure and after exposures range from 18 to 42 seconds — with an average value of 30 seconds. Studying the dynamics of ^{133}Xe uptake in human blood shows that after an exposure of 3 to 40 hours, t concentration of ^{133}Xe in blood remains practically constant (see Table 3).

This data indicate that the saturation of blood with ^{133}Xe occurs quickly. Due to a large contact surface with blood, the process of accumulation and elimination of ^{133}Xe proceeds at practically the same speed at which it exchanges in the lungs. This supposition is confirmed by the fact that no ^{133}Xe activity could be measured in blood samples taken from a subject 3 to 10 minutes after the end of the exposure.

The half-lives of ^{133}Xe in the lung, blood, muscle, and fat tissues, as well as the corresponding values of A/Q_e at saturation (that is, in the case of an infinite exposure to a ^{133}Xe atmosphere), are given in Table 4. The data show that the average ^{133}Xe half-lives in the lung and blood are 30 seconds, while in the muscle and fat tissues they are 0.7 $\pm$ 0.42 and 6.2 $\pm$ 1.8 hours, respectively.

The experiment to study the absorbtion of ^{133}Xe through the skin was carried out on three volunteers. The exposure time was three hours and the ^{133}Xe concentration in the air of the exposure chamber was 1 μCi/1.

As one can see from Table 4, the amount of ^{133}Xe absorbed through the skin is not greater than 0.4 percent of its combined intake by inhalation and through the skin. This small penetration through the skin as compared to uptake by the lungs may be explained by the difference in the surface area of the skin (1.8 m^2) and that of respiratory organs (70 m^2). Furthermore, when explaining the difference in the penetration rate of ^{133}Xe through the skin as compared to the alveolar epithelium of the lungs, one should take into account the much greater thickness of the skin barrier. This requires a much longer time to be penetrated than in the case of diffusion through the alveolar epithelium of the lungs, which causes practically an immediate saturation of blood with Xenon and other gases. We were unable to detect any elimination of ^{133}Xe from the body of the subject through the skin.

2. Experiments with ^{85}Kr.

Our experiments with ^{85}Kr show that human uptake is much quicker for smaller, leaner people than for heavier, fatter people. For example; the subjects A. Shch and V. G. (who had a normal amount of fat) reached their saturation level of ^{85}Kr activity in the body within three hours, while the subject E. D., having a higher amount of fat, reached his saturation level within nine hours (see Figure 5 and Table 6).

The elimination of ^{85}Kr from the human body is described by the sum of several exponents (see Table 7 and Figure 6). Due to the fact that the processes of Kr and Xe interaction with the human body are identical, the same half-life was used for ^{85}Kr in lungs and blood (equal to 30 seconds) as was determined experimentally for ^{133}Xe. Analysis of the data given in Table 7 shows that the average values of the ^{85}Kr half-lives in the fat tissue of the subjects ranged from 1.8 to 3.7 hours. The ^{85}Kr half-life in the fat tissue is proportional to the amount of fat within the body. The rate of ^{85}Kr elimination from the fat tissue decreases after a prolonged exposure. Thus, the subject A. Shch. exhibited an ^{85}Kr half-life in the fat tissue equal to 0.8 hours with a short exposure of 0.5 to 0.7 hours, while at exposure durations equal to 9 to 40 hours the ^{85}Kr half-life increased to from 2.2 to 2.8 hours.

Average values for the ^{85}Kr half-life in the muscle and other tissues ranged from 4 to 11 minutes. The exposure time has little effect on the ^{85}Kr half-life in the muscle and other tissues (see Table 7).

SUMMARY

The main parameters characterizing the accumulation, distribution, and elimination of Kr and Xe from the human body are shown in Table 8.

It is evident that the rate of accumulation of the noble gases within the human body exceeds the rate of their elimination. This phenomenon is especially well traced in experiments with ^{85}Kr, where the accumulation in the fat tissue of people reaches a saturation point in 4-5 hours, while its elimination takes 8-9 hours. The higher rate of noble gases accumulation within the body may probably be explained by a dissimilar gradient of inert gases concentration in the blood and the tissues that are being saturated.

During the intake of the inert gases into the body, the gradient of the concentrations is always higher than during their elimination. This may be explained by the fact that at the beginning of the contact, the concentration of the gas in the tissue that is being saturated is close to zero, while in the blood it reaches an equilibirum state in several minutes due to an intensive gas exchange within the lungs. In the process of elimination however, after the gas has been accumulated in the saturated tissues, the gradient between the concentrations is negligible due to the continuous transit of the gas from the tissue to the blood.

REFERENCES

Conn, H. L. (1961), *Equilibrium Distribution of Radioxenon in Tissue: Xenon-Hemoglobin Association Curve.* J. Appl. Physiol., 16, 1065-1070.

Kalantarov, K. D., Yu. M. Varentsov, and F. M. Liass (1966), *Intergral Doses Created by the Intravenous Injection of ^{133}Xe.* Meditsinskaya Radiologia, 8, 19-24.

Osanov, D. P., I. A. Lichtarev, G. B. Radzievsky (1970), *Radiation Dosimetry of Incorporated Radioactive Substances.* M., Atomizdat.

TABLE 1. The Value of A/Q_e, 1 (a) of ^{133}Xe in the Body of the Subject Man for Different Durations of Exposure.

The Subject Man	Durations of exposure, hours				
	3	9	20	40	66
A. Shch.	10	19	23	24	29
N.S.	14	21	24	23	20
A.T.	23	21	41	39	--
M.P.	14	41	--	54	--

(a)
A = Summary activity of ^{133}Xe in the body.
Q_e = Concentration of ^{133}Xe activity in the exposure chamber.

TABLE 2. Effective Half-Lives (T_e) of ^{133}Xe in the Lungs of Nine Male Volunteers, Seconds.

Numbers	T_e	
	At the time of exposure	After exposure
1	42	30
2	18	42
3	18	30
4	36	24
5	30	24
6	30	34
7	18	30
8	48	30
9	30	20

TABLE 3. Factor of ^{133}Xe Distribution in Human Blood, ml/g.

Subject man	Duration of exposure, hours			
	3	9	20	40
A.Shch.	0.17	0.17	0.19	0.16
N.S.	0.17	0.19	---	0.18
A.T.	---	0.15	---	0.13
M.P.	0.1	0.15	---	0.26

TABLE 4. Parameters Characterizing ^{133}Xe Elimination from the Human Body.

The subject man	Lungs and blood		Muscles and other tissues		Fat tissue	
	$(\frac{A_i}{Q_e})$ 1	$\overline{T}$ Seconds	$(\frac{A_i}{Q_e})$ 1	$\overline{T}$ hours	$(\frac{A_i}{Q_e})$ 1	$\overline{T}$ hours
A.Shch.	4	30	6	0.9 ± 2	14	6.0 ± 0.6
N.S.	4	30	5	0.7 ± 0.4	15	4.6 ± 0.45
A.T.	4	30	8	0.9 ± 0.27	28	7.4 ± 2
M.P.	4	30	4	0.4 ± 0.1	46	6.8 ± 0.9
Average Data	--	30	--	0.7 ± 0.42	--	6.2 ± 1.8

Note:
A_i = content of ^{133}Xe activity in the human body at the moment of saturation.
Q_e = concentration of ^{133}Xe activity in the exposure chamber.
$\overline{T}$ = half-life.

TABLE 5. Intake of ^{133}Xe into the Body of the Subject Men Through the Skin After a Three-Hour Exposure.

The subject man	$A/Q_e,1$		Per cent of activity entering through the skin
	Skin	skin and respiratory organs	
M.P.	0.08	23	0.35
A.S.	0.04	10	0.4
V.V.	0.04	10	0.4

Note:
A = ^{133}Xe content in the human body.
Q_e = ^{133}Xe concentration in the air.

TABLE 6. The Values of $A/Q_e,1$ for Different Durations of Exposure (T_e) in an Atmosphere of ^{85}Kr.

The subject man	T_e, hours				
	0.5	3	9	20	40
A.Shch.	6	10.4	10.4	9.3	10.2
V.G.	5.5	13.1	11.5	11.8	11.9
V.P.	4.6	7.8	13.9	13.6	15.3
A.D.	7.1	10.8	13.2	13.5	13.4
E.D.	7.7	14.3	21.2	18.3	19.6
B.V.	2.5	9.8	14.3	13.3	13.2

TABLE 7. Half-Lives of ^{85}Kr (T) in the Body of the Subject Men After Their Exposures and the Corresponding Values of A/Q_e,1.

The subject man	Tissue or organ	Duration of exposure, hours: 0,5-0,7		3		9		20		40		Mean values	
		$\frac{A}{Q_e}$	T	$\frac{A}{Q_e}$	T	$\frac{A}{Q_e}$	T	$\frac{A}{Q_e}$	T	$\frac{A}{Q_e}$	T	$\frac{A}{Q_e}$	T
A.Shch.	1	2.3	0.8 h	3.7	0.75 h	6.4	2.2 h	7.4	2.2 h	5.4	2.8 h	6.4 ± 0.7	1.8 ± 0.8 h
	2	0.6	15 min	2.1	7.8 min	1.9	8.4 min	1.9	1.8 min	1.8	18 min	1.7 ± 0.02	10.2 ± 5.0 min
	3	3	30 s	4.1	30 s	2	30 s	---	---	---	---	3.0 ± 0.7	30 ± 6.0 s
V.G.	1	2.2	1.3 h	6.3	2.2 h	7.6	2 h	7.0	2.4 h	6.3	2.7 h	7.0 ± 0.5	2.1 ± 0.3 h
	2	1.4	4.2 min	2.4	3 min	1.7	3.6 min	1.5	4.2 min	2.1	3 min	1.9 ± 0.3	3.6 ± 0.5 min
	3	1.8	30 s	4.2	30 s	1.0	30 s	3.3	30 s	3.0	30 s	2.7 ± 1.2	30 ± 6.0 s
A.D.	1	3.6	1.4 h	2.8	2.6 h	6	3 h	5.6	3 h	5.6	1.9 h	5.7 ± 0.7	2.4 ± 0.6 h
	2	1.5	4.2 min	2.7	6 min	1.6	10.2 min	2.6	4.8 min	1.8	3.6 min	2.0 ± 0.5	6.0 ± 2.0 min
	3	2	30 s	5.3	30 s	5.5	30 s	5.3	30 s	6	30 s	4.8 ± 0.7	30 ± 6.0 s
V.P.	1	1.6	1.1h	5.4	2.2 h	9.6	3.2 h	11.2	4.5 h	10.2	4.3 h	10.3 ± 1.7	3.1 ± 1.1 h
	2	1.6	6.3 min	0.7	18 min	2.5	22.2 min	1.8	3.6 min	1.7	6 min	1.7 ± 0.7	10.8 ± 7.0 min
	3	1.4	30 s	1.7	30 s	1.7	30 s	0.56	30 s	3.4	30 s	1.8 ± 0.7	30 ± 6.0 s
B.V.	1	1.0	2.2 h	6.9	2.4 h	10.4	3 h	10.4	5 h	10.4	5.7 h	10.4 ± 2.0	3.7 ± 1.4 h
	2	1.1	13.8 min	2.4	12 min	1.6	7.2 min	1.3	7.2 min	2.9	7.8 min	1.9 ± 0.6	9.6 ± 2.6 min
	3	0.4	30 s	0.6	30 s	0.6	30 s	0.1	30s	0.1	30 s	0.4 ± 0.2	30 ± 6.0 s
E.D.	1	1.8	1.7 h	8	2.8 h	16.4	4.2 h	13.8	4.5 h	12	3.3 h	14 ± 2.6	3.3 1.0 h
	2	3.0	3.6 min	2.6	9 min	3.3	3 min	1.4	3.6min	1.4	18 min	2.3 ± 2.0	7.2 ± 5.2 min
	3	2.9	30 s	3.7	30 s	1.5	30 s	3.1	30 s	6.2	30 s	3.5 ± 1.2	30 ± 6.0 s

Note:

A = Content of activity within the body; Q_e = concentration of actvity of ^{85}Kr in the exposure chamber.

T = Half-life.

1 = Fat tissue; 2 = muscles and other tissues; 3 = lungs and blood.

TABLE 8. Main Parameters Characterizing the Accumulation, Distribution, and Elimination of the Radionuclides of Krypton and Xenon from the Human Body.

Organ or tissue	Krypton radionuclides			Xenon radionuclides		
	R, 1k/g	T_e^b	T^b	R, 1/kg	T_e^b	T^b
Fat tissue	0.46	1.4 h	2.7 h	1.4	5 h	6.3 h
Muscles (and other tissues)	0.047	8 min	8 min	0.13	0.4 h	0.7 h
Blood	0.046	30 s	30 s	0.17	30 s	30 s
Lungs	2	30 s	30 s	2	30 s	30 s

Note:
T_e^b = Biological half-life when the subject man is in contact with the gas.
T^b = Biological half-life after the subject man's contact with the gas has ended.
R - Distribution factor.

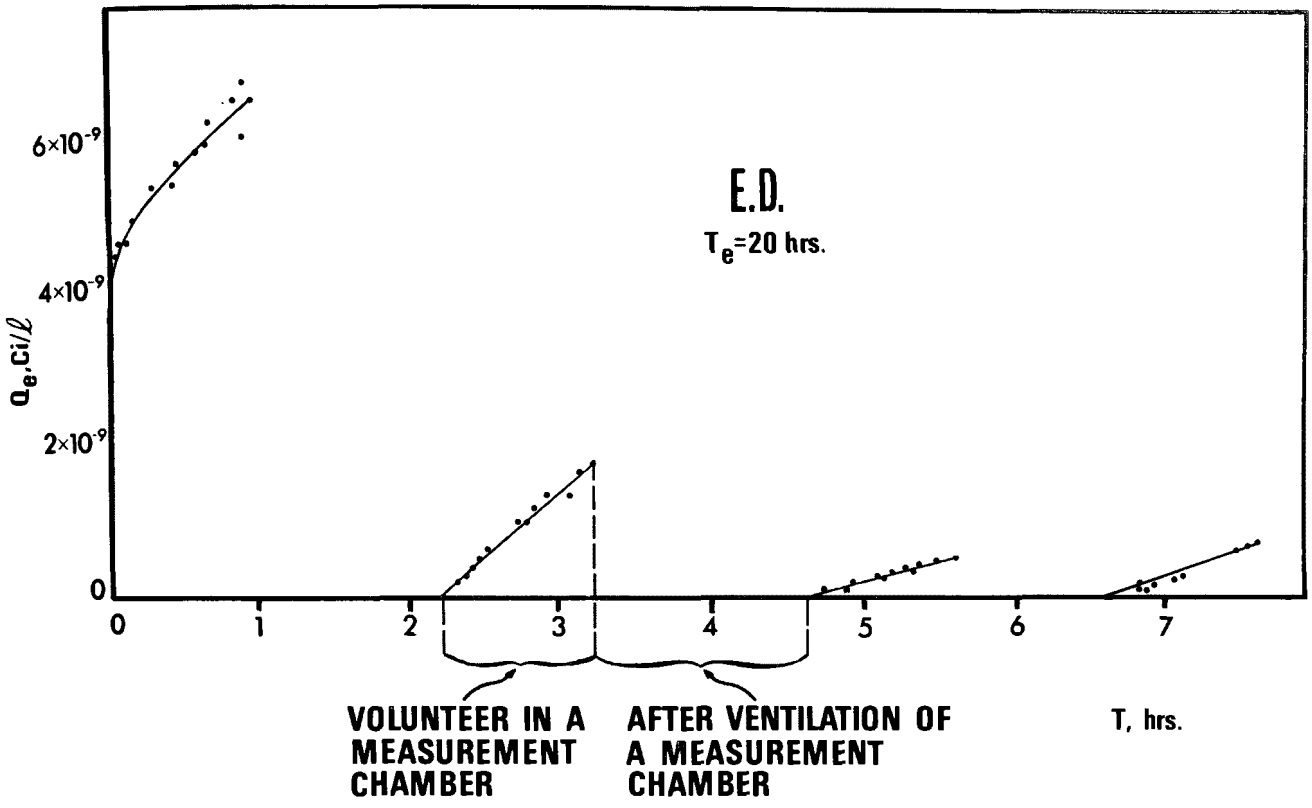

Figure 1. Changes in the ^{85}Kr concentration in the air of the measuring chamber.

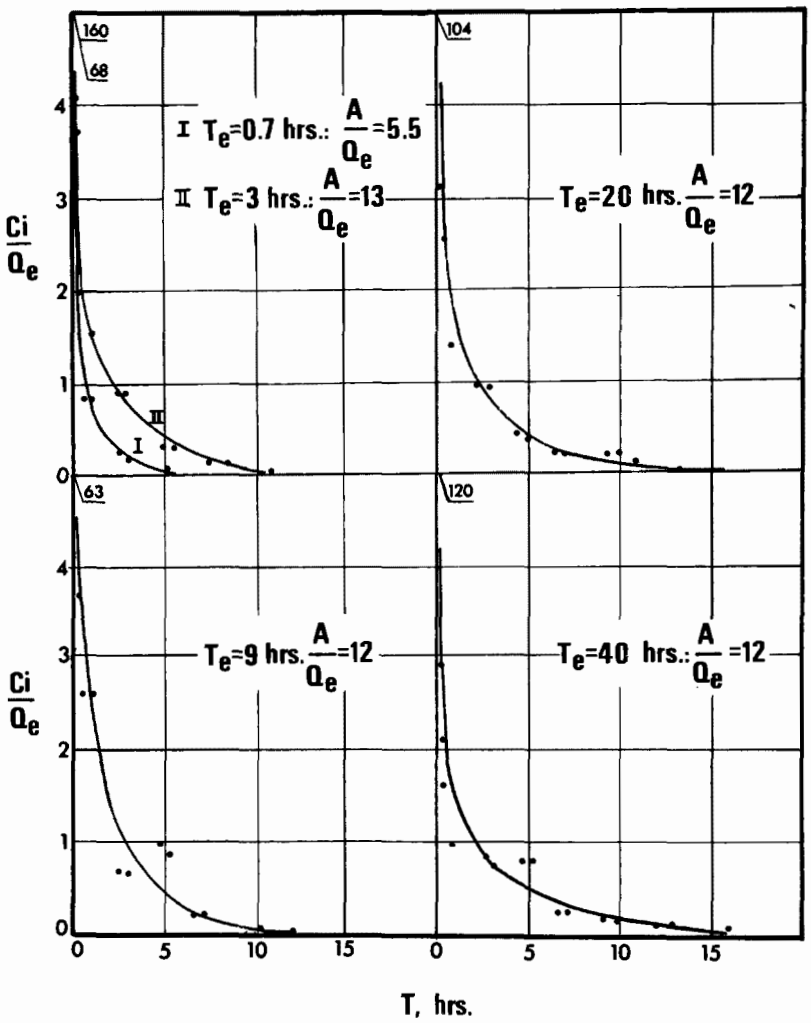

Figure 2. Changes in the rate of ^{85}Kr and ^{133}Xe elimination from the body of one of the volunteers.
t_e = exposure time in the atmosphere of a radionuclide;
Q_e = radionuclide concentration in the air of the exposure chamber; and
A = summary activity of ^{85}Kr and ^{133}Xe in the body.)

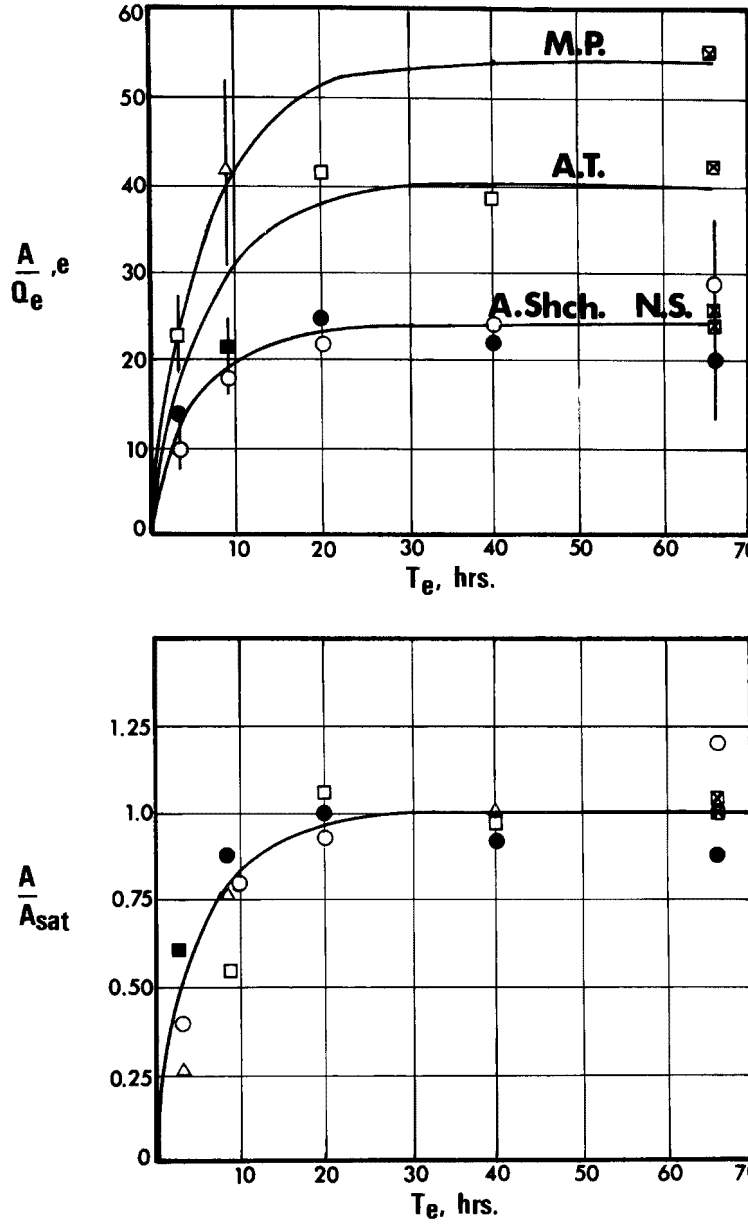

Figure 3. Kinetics of ^{133}Xe accumulation within the human body; ⊠ calculated from the data on distribution (Conn, 1961).

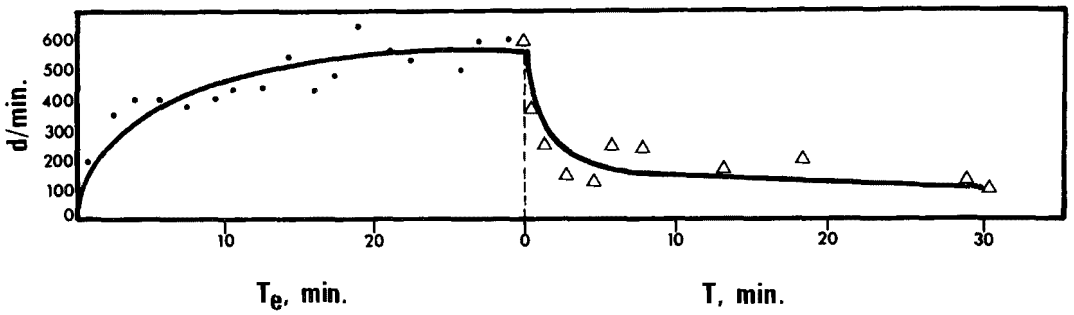

Figure 4. Kinetics of ^{133}Xe accumulation and elimination from the lungs of a man at rest.

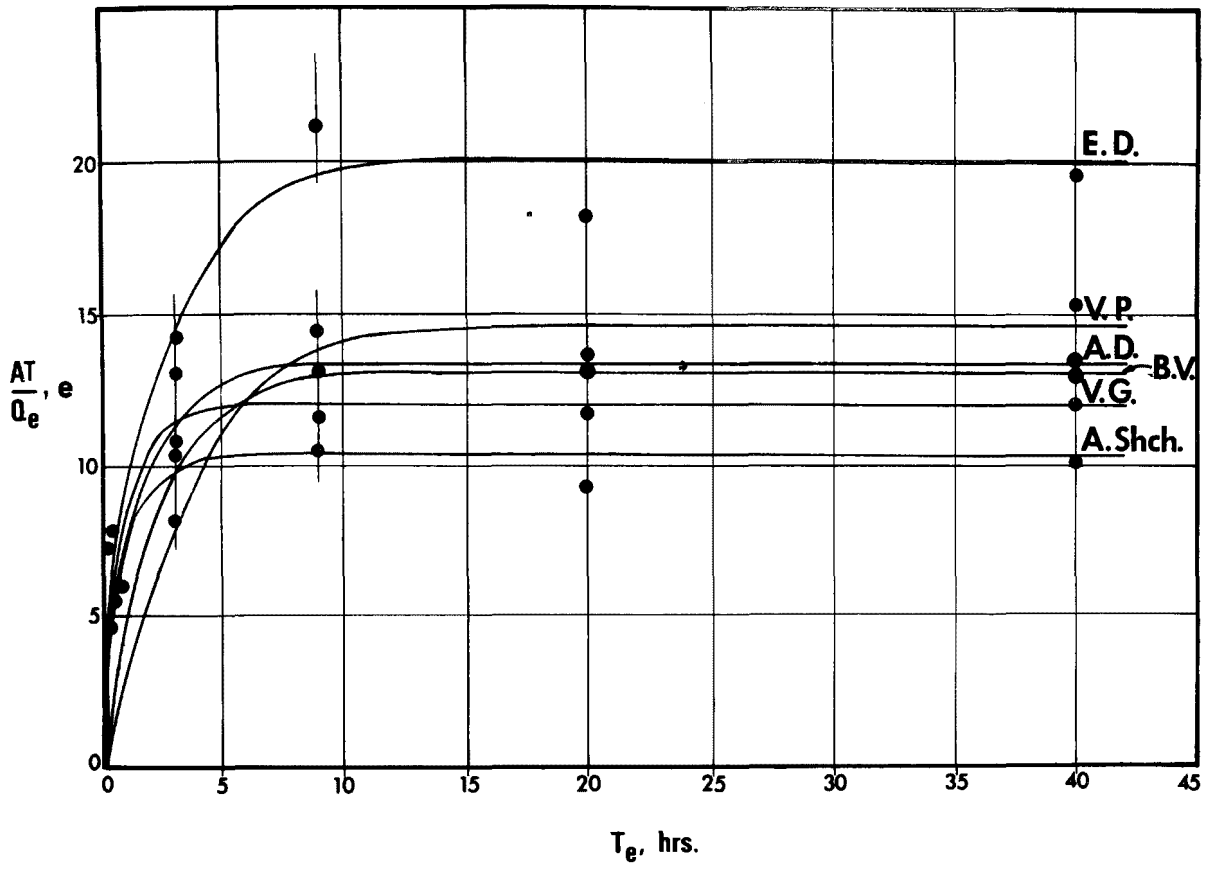

Figure 5. Kinetics of ^{85}Kr accumulation in the human body.

TRANSFER OF AIRBORNE KRYPTON-85 TO VEGETATION

P. G. Voilleque and J. J. Fix
Health Services Laboratory
U. S. Atomic Energy Commission
National Reactor Testing Station
Idaho Falls, Idaho 83401

Abstract

Laboratory experiments have been conducted in an environmental chamber to evaluate the transfer to vegetation of krypton-85 which has been released to the atmosphere. A preliminary evaluation of the acute exposure case confirmed expectations that the air-to-grass transfer velocity was indeed small. Subsequent experiments were directed toward the evaluation of air-to-vegetation transfer under "global equilibrium" conditions in which the krypton-85 concentration remains approximately constant for extended periods of time. Edible vegetable greens (Swiss chard, lettuce, and turnip greens) and pasture grass were exposed to krypton-85 for periods up to 75 hours in length. It was found that the concentration of krypton-85 in vegetation reaches an equilibrium value in a relatively short time, probably within one hour. Transfer velocities computed assuming a 1-hour equilibration time range from 10^{-7} to 10^{-6} cm/sec; the values were not lognormally distributed. While these transfer velocities exceed the value initially obtained for the acute exposure case, the common assessment that neither animal forage nor human plant food is part of a significant exposure pathway for airborne krypton-85, has been confirmed.

INTRODUCTION

Concern about actual and projected local and global atmospheric concentrations of ^{85}Kr and other radioactive fission gases has not been limited to the potential doses from the direct exposure pathways of external irradiation and inhalation of contaminated air. The question of possible "biological concentrations" of airborne ^{85}Kr came to our attention as the result of questions raised regarding the possible radiological consequences of nuclear gas stimulation projects. This is not to say that the question had not been considered previously. It had and the common conclusion was that potential doses from indirect exposure pathways were so small that detailed evaluation was unneccessary. This belief persists today and, to our knowledge, radioactive noble gases have never been observed to "concentrate" in vegetation or animal components of the human food chain which have been sampled downwind from atmospheric testing locations, nuclear power reactors, fuel reprocessing plants, or sites of nuclear gas stimulation projects.

The expectation that airborne concentrations of ^{85}Kr and other noble gases are not significantly reduced by air-to-vegetation transfer is widely shared by those who employ these gases as tracers to evaluate atmospheric dispersion and mixing processes. Noble gas tracers are commonly termed "inert", a property which distinguishes them from the various particulate fluorescent tracers, which are known to interact with vegetation and other surfaces, and to bias the results of the dispersion experiments in which they were used. The use of ^{85}Kr as a meteorological tracer has been described (Nickola, *et al.*, 1970); studies of atmospheric mixing using ^{37}Ar have already been discussed at this Symposium (Wiest, *et al.*, 1973; and Machta, 1973).

Because of our previous experience in the evaluation of air-to-vegetation transfer of airborne contaminants under field conditions and in the laboratory (Pelletier, *et al.*, 1970 and Voilleque, *et al.*, 1971), we undertook the experimental evaluation of the air-to-vegetation transfer of ^{85}Kr using one of our environmental chambers. Our preliminary evaluation of the acute exposure case has been reported (Voilleque, *et al.*, 1970). The present paper presents the results of more detailed and longer duration experiments subsequently conducted to better define the air-to-vegetation transfer of ^{85}Kr.

MATERIALS AND METHODS

All vegetation exposed to ^{85}Kr was grown from seed in ~1.4 kg of sandy loam, contained in 25- by 25-cm pots whose depth was 14 cm. The vegetation was maintained in a growth room having a 16-hour photoperiod with an average light intensity of approximately 19,000 lm/m^2. The air temperature in the plant growth room was regulated to 24°C during the "day" and 13°C during the "night" period. The relative humidity averaged between 40 and 50%.

The Manchar Bromegrass, which is a common constituent of pasture grass in this area, had been cut back to a height of 10 cm one or more times, and was grown to a height of about 25 cm prior to exposure. Pots of (Fordhood Giant) Swiss chard and (Shogoin) turnip greens were both exposed when the plants had developed to the point when they would normally be cut for human consumption. The (Black Seeded Simpson, White Boston, and Great Lakes) lettuce was exposed when the plants were 7-13 cm high and could be cut for human consumption. White Boston and Great Lakes are head lettuce varieties; however, the plants were cut, as they frequently are by garderners, well before the development of the heads.

All exposures of vegetation to ^{85}Kr were conducted in a plexiglass exposure chamber whose dimensions are approximately 0.9 m high, 1.2 m wide, and 0.6 m deep. The chamber was maintained in a controlled environment laboratory and was illuminated by a 400-watt GE Lucalox lamp which produced about 50,000 lm/m^2 at plant level. After the vegetation was placed in the chamber, the chamber was sealed and the ^{85}Kr

was injected. The ^{85}Kr was mixed with chamber air using two 10-cm diameter fans which operated throughout the exposure period; wind was not simulated during these experiments. The relative humidity in the chamber increased from about 70% at the start of a typical experiment to 90% or greater by the end of the exposure period.

Samples of chamber air were drawn into evacuated glass vials which were counted in a calibrated well-type scintillation counter to determine the ^{85}Kr concentration at several times during the exposure period. The ^{85}Kr concentrations were also monitored continuously using a Geiger-Mueller tube with a ratemeter and strip chart recorder. The exposed vegetation was cut quickly after the pot was removed from the chamber, and either double bagged in polyethylene or placed in a glass jar which was tightly sealed with a screw-on top; the ^{85}Kr activity was then determined using a well counter calibrated for both sample configurations. It was found that ^{85}Kr was lost from the double polyethylene bags at a rate of about 55 percent per day and their use was discontinued; leakage from the sealed jars was not detectable in a 3-day period. Loss of ^{85}Kr from the samples was further limited by the normal practice of counting all samples within 4 hours following collection. Samples of unexposed vegetation of the same variety and stage of development were also collected and counted. All vegetation samples were subsequently oven dried to a constant weight, and the dried vegetation was weighed.

EXPERIMENTAL RESULTS AND DISCUSSION

A standard method of expressing results of experiments of this type employs a parameter usually called the "deposition velocity"; the term "transfer velocity" is perhaps more appropriate for gases and will be used in this discussion. The transfer velocity is considered to be an approximately constant parameter which describes the air-to-surface transfer of airborne contaminants. It is the ratio of the rate of transfer of the contaminant per unit surface area to the instantaneous air concentration at a standard height above the surface. The ratio has unit length/time; hence the designation of "velocity". In practice, the ratio is obtained by measuring the total quantity transferred per unit area and dividing that by the measured time-integrated air concentration at the specified height. In Equation (1), V_d (cm/sec) is the transfer velocity, C_ν (μCi/cm^2) is the activity transferred to the vegetation on a unit horizontal area, χ (μCi/cm^3) is the average air concentration and τ (sec) is the exposure time. The product $\chi - \tau$ is termed the time-integrated air concentration (Ψ, μCi-sec/cm^3).

$$V_d = \frac{C_\nu}{\chi - \tau} = \frac{C_\nu}{\Psi} \tag{1}$$

The mass of vegetation exposed to the contaminant has been found to be important for some transfer processes (Pelletier, *et al.*, 1970); so a second parameter, the normalized transfer velocity (V_D, cm^3/g-sec), is often computed and used in the same context. In Equation (2), D is the areal vegetation density (g/cm^2), computed using the dry weight of the vegetation.

$$V_D = \frac{V_d}{D} = \frac{C_\nu}{\Psi \text{-} D} \tag{2}$$

In this model, the transfer of radioactivity from air to vegetation is presumed to be a process which continues throughout the exposure period. The data in Tables 2 and 3 illustrate that this is not true for ^{85}Kr. V_d decreases with increasing Ψ for both Bromegrass and lettuce, implying that the ^{85}Kr concentration in vegetation reaches an equilibrium state, and that the ^{85}Kr activity found in vegetation will be related to the value of χ near the end of the exposure period. On the assumption that the same processes operate to increase or decrease C_ν as χ changes correspondingly, knowledge of the retention half-time permits an estimate of the equilibration period. The retention half-time for ^{85}Kr was estimated by measuring C_ν for exposed pots of vegetation removed to the normal laboratory environment for periods up to one hour after exposure. On the basis of limited measurements, the retention half-time is estimated to be 5-15 minutes. It is possible that (1) shorter lived components would be observed if more rapid sampling or "whole plant counting" techniques were employed, and (2) longer lived components would be noted if longer evaluation times were achieved by increasing the initial value of C_ν. Because it appears that C_ν will reach >90% of the equilibrium value within one hour after exposure to a new concentration of ^{85}Kr, the transfer velocities reported below have been computed using a 1-hour effective exposure time and the χ measured for the last hour before removal of the vegetation from the contaminated air has been employed. The effective time-integrated air concentration, Ψ_e, is then 3,600 χ μCi)sec/cm^3. This approach to reporting the results was selected because of the utility and widespread use of transfer velocities in the calculation of doses resulting from airborne radioactivity releases. The alternative of evaluating partition coefficients for the wet mass of vegetation or its water content is of some interest, but is not directly applicable to conventional hazard analysis techniques

and, for that reason, was not selected. Such an analysis would be further complicated by unmeasured variations in lipid content within the plants and in their waxy surface coatings.

Table 1 summarizes the experimental data obtained for the exposure of turnip greens and Swiss chard to ^{85}Kr. Both the actual (Ψ) and the effective(Ψ_e) time-integrated air concentrations were tabulated. As stated above, Ψ_e was used in the computations of V_d and V_D. For turnip greens, the mean values of transfer velocity and normalized transfer velocity are $(3.1 \pm 1.2)x10^{-6}$ cm/sec and $(5.0 \pm 2.0)x10^{-5}$ cm^3/g-sec, respectively (sample standard deviations are given). For Swiss chard the mean values of V_d and V_D were $(4.5 \pm 3.3)x10^{-7}$ cm/sec and $(6.4 \pm 4.2)x10^{-6} cm^3$/g-sec.

Tables 2 and 3 contain the data obtained on the transfer of ^{85}Kr to lettuce and Bromegrass. For lettuce, the mean transfer velocity was $(2.6 \pm 1.6)x10^{-6}$ cm/sec and the mean normalized transfer velocity was $(3.5 \pm 3.4)x10^{-4}$ cm^3/g-sec. Neither V_d nor V_D was found to be lognormally distributed when tested (a = .05) by the Kolmogorov-Smirnov method (Ong, *et al.*, 1968). For Bromegrass, the means of the 10 positive values of V_d and V_D were $(1.6 \pm 1.1)x10^{-6}$ cm/sec and $(1.6 \pm 0.9)x10^{-4}$ cm^3/g-sec, respectively; neither was lognormally distributed.

These transfer velocities are substantially larger than our first estimate (Voilleque, *et al.*, 1917); possible reasons for the difference can only be suggested. The exposure time for the first experiment was only 30 minutes; on the basis of present data, we presume the vegetation was not equilibrated with the ^{85}Kr in the chamber atmosphere. In addition, the ^{85}Kr contaminated air was pumped out of the chamber and replaced by clean air following the end of the exposure in the first experiment; this action surely served to further reduce the amount of ^{85}Kr observed in the exposed vegetation. Whatever the causes of the difference, the preponderance of evidence supports the higher transfer velocities reported here.

The data obtained indicate that the usual assessment of potential exposure pathways for ^{85}Kr and other radioactive noble gases is properly unconcerned with indirect exposure routes. Neither man's plant food consumption nor his consumption of herbivorous animals appears to be a significant route of exposure.

REFERENCES

Machta, L., (1973), *Argon-37 as a Measure of Atmospheric Vertical Mixing.* This Symposium.

Nickola, P. W., J. V. Ramsdell, Jr., and J. D. Ludwick, (1970), *Detailed Time Histories of Concentrations Resulting from Puff and Short-Period Releases of an Inert Radioactive Gas: A Volume of Atmospheric Diffusion Data,* USAEC Report BNWL-1272.

Ong, L. D. Y. and P. C. LeClare, (1968), *The Kolmogorov-Smirnov Test for the Lognormality of Sample Cumulative Frequency Distributions.* Health Phys. 14, 376.

Pelletier, C. A. and J. D. Zimbrick, (1970), *Kinetics of Environmental Radioiodine Transport Through the Milk-Food Chain in Environmental Surveillance in the Vicinity of Nuclear Facilities,* W. C. Reinig (Ed), Charles C. Thomas, p. 257.

Voilleque, P. G., D. R. Adams, and J. B. Echo, (1970), *Transfer of Krypton-85 from Air to Grass,* Health Phys., 19, 835.

Voilleque, P. G. and D. R. Adams, (1971), *Effect of Stomatal Opening on the Transfer of $^{131}I_2$ from Air to Grass.* Health Phys., 21, 771.

Wiest, W., H. Loosli, H. Deschger, R. Studer, and M. Wahlen, (1973), *Argon-37 Activity in Air Samples and Its Atmospheric Mixing,* This Symposium.

TABLE 1. Data on Transfer of ^{85}Kr to Turnip Greens and Swiss Chard.

Vegetation	C (μCi/cm²)	e(μCi-sec/cm³)(a)	V_d(cm/sec)(a)	D(g/cm²)(b)	V_D(cm³/g-sec)(a)	(μCi-sec/cm³)
Turnip Greens	$4.7 \pm .4x10^{-3}$	$1.02 \pm .15x10^{3}$	$4.6 \pm .8x10^{-6}$	$6.2 \pm .3x10^{-2}$	$7.4 \pm 1.3x10^{-5}$	$2.04 \pm .30x10^{3}$
Turnip Greens	$2.4 \pm .2x10^{-3}$	$1.02 \pm .15x10^{3}$	$2.4 \pm .4x10^{-6}$	$6.4 \pm .3x10^{-2}$	$3.8 \pm .6x10^{-5}$	$2.04 \pm .30x10^{3}$
Turnip Greens	$3.6 \pm .3x10^{-3}$	$1.02 \pm .15x10^{3}$	$3.5 \pm .6x10^{-6}$	$6.1 \pm .2x10^{-2}$	$5.7 \pm 1.0x10^{-5}$	$2.04 \pm .30x10^{3}$
Turnip Greens	$2.0 \pm .2x10^{-3}$	$1.02 \pm .15x10^{3}$	$2.0 \pm .3x10^{-6}$	$6.6 \pm .3x10^{-2}$	$3.0 \pm .5x10^{-5}$	$2.04 \pm .30x10^{3}$
Swiss Chard	$1.5 \pm .3x10^{-4}$	$9.6 \pm 1.3x10^{2}$	$1.6 \pm .4x10^{-7}$	$5.3 \pm .2x10^{-2}$	$3.0 \pm .8x10^{-6}$	$1.91 \pm .26x10^{3}$
Swiss Chard	$7.9 \pm 1.4x10^{-4}$	$9.6 \pm 1.3 x10^{2}$	$8.2 \pm 1.8x10^{-7}$	$7.8 \pm .3x10^{-2}$	$1.0 \pm .2x10^{-5}$	$1.91 \pm .26x10^{3}$
Swiss Chard	$6.1 \pm 1.1x10^{-4}$	$9.6 \pm 1.3 x10^{2}$	$6.4 \pm 1.4x10^{-7}$	$6.3 \pm .3x10^{-2}$	$1.0 \pm .2x10^{-5}$	$1.91 \pm .26x10^{3}$
Swiss Chard	$1.8 \pm .3x10^{-4}$	$9.6 \pm 1.3 x10^{2}$	$1.9 \pm .4x10^{-7}$	$7.4 \pm .3x10^{-2}$	$2.6 \pm .6x10^{-6}$	$1.91 \pm .26x10^{3}$

(a) Ψ_e is the effective time-integrated air concentrarion computed assuming a 1-hour equilibration time. Both V_d and V_D were computed using Ψ_e. The actual value of Ψ is given in the last column.

(b) Based on the dry weight of vegetation determined to $\pm$0.2 grams. The area of each pot was 625 ± 25 cm².

TABLE 2. Data on Transfer of ^{85}Kr to Lettuce.

Type	C (μCi/cm^2)	e(μCi-sec/cm^3)(a)	V_d(cm/sec)(a)	D(g/cm^2)(b)	V_D(cm^3/g-sec)(a)	(μCi-sec/cm^3)
GL	$1.9 \pm .3\times10^{-4}$	$77.0 \pm .7$	$2.5 \pm .4\times10^{-6}$	$2.6 \pm .1\times10^{-2}$	$9.6 \pm 1.6\times10^{-5}$	115.6 ± 1.1
GL	$8.4 \pm 1.5\times10^{-5}$	$77.0 \pm .7$	$1.1 \pm .2\times10^{-6}$	$3.3 \pm .1\times10^{-2}$	$3.3 \pm .6\times10^{-5}$	115.6 ± 1.1
GL	$4.0 \pm .7\times10^{-5}$	$77.0 \pm .7$	$6.2 \pm .9\times10^{-7}$	$2.8 \pm .1\times10^{-2}$	$1.9 \pm .3\times10^{-5}$	115.6 ± 1.1
GL	$6.3 \pm 1.1\times10^{-5}$	$77.0 \pm .7$	$8.2 \pm 1.4\times10^{-7}$	$2.4 \pm .1\times10^{-2}$	$3.4 \pm .6\times10^{-5}$	115.6 ± 1.1
WB	$1.4 \pm .2\times10^{-4}$	$54.7 \pm .5$	$2.6 \pm .4\times10^{-6}$	$2.9 \pm .1\times10^{-2}$	$9.0 \pm 1.4\times10^{-5}$	136.8 ± 1.3
WB	$7.5 \pm 1.2\times10^{-5}$	$54.7 \pm .5$	$1.4 \pm .2\times10^{-6}$	$3.0 \pm .1\times10^{-2}$	$4.7 \pm .7z10^{-5}$	$136.8 \pm .13$
WB	$8.2 \pm 1.3\times10^{-5}$	$54.7 \pm .5$	$1.5 \pm .2\times10^{-6}$	$3.0 \pm .1\times10^{-2}$	$5.0 \pm .7\times10^{-5}$	136.8 ± 1.3
WB	$4.6 \pm .7\times10^{-5}$	$54.7 \pm .5$	$8.4 \pm 1.3\times10^{-7}$	$3.1 \pm .1\times10^{-2}$	$2.7 \pm .4\times10^{-5}$	136.8 ± 1.3
BSS	$2.4 \pm .1\times10^{-4}$	84.2 ± 1.7	$2.9 \pm .1\times10^{-6}$	$4.6 \pm .4\times10^{-3}$	$6.3 \pm .6\times10^{-4}$	84.2 ± 1.7
BSS	$1.8 \pm .1\times10^{-4}$	59.4 ± 1.2	$3.0 \pm .2\times10^{-6}$	$6.1 \pm .4\times10^{-3}$	$4.9 \pm .5\times10^{-4}$	143.6 ± 2.1
BSS	$1.9 \pm .1\times10^{-4}$	$43.2 \pm .9$	$4.4 \pm .2\times10^{-6}$	$4.5 \pm .4\times10^{-3}$	$9.8 \pm 1.0\times10^{-4}$	186.8 ± 2.3
BSS	$1.3 \pm .1\times10^{-4}$	$38.9 \pm .8$	$3.3 \pm .3\times10^{-6}$	$4.0 \pm .4\times10^{-3}$	$8.3 \pm 1.1\times10^{-4}$	225.7 ± 2.4
BSS	$2.1 \pm .5\times10^{-4}$	33.8 ± 6.8	$6.2 \pm 1.9\times10^{-6}$	$7.5 \pm .4\times10^{-3}$	$8.3 \pm 2.6\times10^{-4}$	$7.5 \pm 1.5 \times10^{3}$
BSS	$8.7 \pm 2.0\times10^{-5}$	33.8 ± 6.8	$2.6 \pm .8\times10^{-6}$	$8.2 \pm .4\times10^{-3}$	$3.2 \pm 1.0\times10^{-4}$	$7.5 \pm 1.5 \times10^{3}$
BSS	$2.4 \pm .5\times10^{-4}$	53.6 ± 5.1	$4.5 \pm 1.0\times10^{-6}$	$8.2 \pm .4\times10^{-3}$	$5.5 \pm 1.2\times10^{-4}$	$1.48 \pm .14\times10^{3}$
BSS	$1.8 \pm .4\times10^{-4}$	53.6 ± 5.1	$3.4 \pm .8\times10^{-6}$	$5.8 \pm .4\times10^{-3}$	$5.9 \pm 1.4\times10^{-4}$	$1.48 \pm .14\times10^{3}$

(a) Ψ_e is the effective time-integrated air concentration computed assuming a 1-hour equilibration time. Both V_d and V_D were computed using Ψ_e. The actual value of Ψ is given in the last column.

(b) Based on the dry weight of vegetation determined to $\pm$ 0.2 grams. The area of each pot was 625 ± 25 cm^2.

TABLE 3. Data on Transfer of ^{85}Kr to Bromegrass.

C (μCi/cm^2)	e(μCi-sec/cm^3)(a)	V_d(cm/sec)(a)	D(g/cm^2)(b)	V_D(cm^3/g-sec)(a)	(μCi-sec/cm^3)
$6.7 \pm 1.2\times10^{-5}$	73.1 ± 2.2	$9.2 \pm 1.6\times10^{-7}$	$7.0 \pm .4 \times10^{-3}$	$1.3 \pm .2\times10^{-4}$	73.1 ± 2.2
$4.2 \pm 1.6\times10^{-5}$	61.6 ± 1.8	$6.8 \pm 2.6\times10^{-7}$	$9.8 \pm .5 \times10^{-3}$	$6.9 \pm 2.7\times10^{-5}$	134.7 ± 2.8
$4.5 \pm 1.9\times10^{-5}$	54.4 ± 1.6	$8.3 \pm 3.5\times10^{-7}$	$1.14 \pm .06\times10^{-2}$	$7.3 \pm 3.1\times10^{-5}$	189.1 ± 3.3
3.5×10^{-5}	41.0 ± 1.3	8.5×10^{-7}	$1.04 \pm .05\times10^{-2}$	8.2×10^{-5}	230.1 ± 3.5
$7.4 \pm 1.3\times10^{-5}$	78.8 ± 2.4	$9.4 \pm 1.7\times10^{-7}$	$7.8 \pm .5 \times10^{-3}$	$1.2 \pm .2\times10^{-4}$	78.8 ± 2.4
$5.0 \pm 1.0\times10^{-5}$	61.6 ± 1.9	$8.1 \pm 1.6\times10^{-7}$	$5.9 \pm .4 \times10^{-3}$	$1.4 \pm .3\times10^{-4}$	140.4 ± 3.1
3.1×10^{-5}	54.0 ± 1.7	5.7×10^{-7}	$9.3 \pm .5 \times10^{-3}$	6.1×10^{-5}	194.4 ± 3.5
$3.2 \pm 1.1\times10^{-5}$	46.8 ± 1.4	$6.8 \pm 2.3\times10^{-7}$	$6.7 \pm .4 \times10^{-3}$	$1.0 \pm .3\times10^{-4}$	241.2 ± 3.8
$6.9 \pm 1.8\times10^{-5}$	33.8 ± 0.9	$2.0 \pm .5\times10^{-6}$	$1.46 \pm .07\times10^{-2}$	$1.4 \pm .3\times10^{-4}$	$7.5 \pm 1.5 \times10^{3}$
$8.6 \pm 1.9\times10^{-5}$	$33.8 \pm .9$	$2.5 \pm .6\times10^{-6}$	$1.47 \pm .07\times10^{-2}$	$1.7 \pm .4\times10^{-4}$	$7.5 \pm 1.5 \times10^{3}$
$2.0 \pm .2\times10^{-4}$	53.6 ± 1.5	$3.7 \pm .4\times10^{-6}$	$1.18 \pm .06\times10^{-2}$	$3.1 \pm .4\times10^{-4}$	$1.48 \pm .14\times10^{3}$
$1.8 \pm .2\times10^{-4}$	53.6 ± 1.5	$3.4 \pm .4\times10^{-6}$	$1.04 \pm .05\times10^{-2}$	$3.3 \pm .4\times10^{-4}$	$1.48 \pm .14\times10^{3}$

(a) Ψ_e is the effective time-integrated air concentration computed assuming a 1-hour equilibration time. Both V_d and V_D computed using Ψ_e. The actual value of Ψ is given in the last column.

(b) Based on the dry weight of vegetation determined to $\pm$ 0.2 grams. The area of each pot was 625 ± 25 cm^2.

POSSIBLE EFFECTS OF NOBLE GAS EFFLUENTS FROM POWER REACTORS AND FUEL REPROCESSING PLANTS*

G. H. Whipple
School of Public Health
University of Michigan
Ann Arbor, Michigan 48104

Abstract

The noble radioactive gas of principal interest in the nuclear industry is krypton-85 because of its relatively large fission yield and its long half-life. This paper considers the various ways in which krypton-85 can deliver radiation doses to the human body; external irradiation by beta particles and gamma rays, and internal irradiation from the gas inside the respiratory tract and dissolved in body tissues. Equilibrium and transient conditions are discussed. The calculations summarized in this paper indicate that the present maximum permissible concentration of krypton-85 in public air (3×10^7 μCi/ml) delivers a dose rate of about 1/5 of that recommended by the ICRP. The long-term significance of krypton-85 and other noble radioactive gases from the nuclear power industry is reviewed.

INTRODUCTION

The noble radioactive gas of principal interest in the nuclear industry is krypton-85. This is so because of its relatively large fission yield (0.3%) and its half-life (10.8 years). The holdup delay at power reactors, and the delay between the removal of reactor fuel and its dissolution at the reprocessing plant eliminates, largely or completely, the other noble radioactive gases as contributors to off-site doses. For these reasons this paper is confined to consideration of the various ways in which krypton-85 can deliver radiation doses to the human body.

THE RADIOACTIVE DISINTEGRATION OF KRYPTON-85

Krypton-85 decays to rubidium-85, which is stable. The decay results in a beta particle with a maximum energy of 0.67 MeV, and no subsequent gamma ray in 99.6% of the disintegrations. The remaining 0.4% of the disintegrations give rise to a beta particle with a maximum energy of 0.16 MeV, followed by a gamma ray with an energy of 0.514 MeV. Thus, a gamma ray occurs only about 4 times for each 1,000 disintegrations, and the 0.67 MeV beta particle is the dominant radiation.

DOSE TO THE BODY FROM KRYPTON-85

The body may be exposed to the radiations of krypton-85 in four possible circumstances: (1) a cloud of the gas at some distance from the body; (2) a cloud of the gas completely enveloping the body; (3) the gas inside the respiratory tract; and (4) the gas dissolved in body tissues. These, I believe, are the only ways in which exposure to any appreciable degree is possible.

A CLOUD OF KRYPTON-85 AT SOME DISTANCE FROM THE BODY

This is the situation where a cloud or plume of gas is passing overhead. Since none of the beta particles emitted by krypton-85 can travel as far as 2 meters in air, there is no beta exposure from the overhead cloud; the only exposure is that from the infrequent gamma rays.

The dose rate from the overhead cloud is a function of the concentration of the krypton-85 in the cloud, the volume of the cloud, and its height above the ground. Just to get a feel for the numbers, the dose rate from a spherical cloud with a radius of 10 meters and with its center 100 meters above the ground, for a concentration of 1×10^{-6} μCi/ml, is about 5×10^{-7} milli-rad per hour. It will shortly become evident that this form of exposure is very small compared to the other three conditions.

*This paper is a summary of a study commissioned by the General Electric Company for the Midwest Fuel Recovery Plant in Illinois. The author takes pleasure in acknowledging this support and the permission to prepare this summary without condition.

A CLOUD OF KRYPTON-85 COMPLETELY ENVELOPING THE BODY

In an infinite cloud of krypton-85, or any other radioactive gas, the energy abosrbed per unit volume is equal to the energy emitted per unit volume. In such a cloud, a very small organism (say a mosquito) will receive a radiation dose at the rate of

$$D_m = 470\,C \text{ rad/hour} \qquad (1)$$

where

D_m = dose rate to the mosquito, rad/hour
C = concentration of ^{85}Kr, μCi/ml

Of this dose, 99% is delivered by the 0.67 MeV beta particles, which have a maximum range in tissue of 2.5 mm. Thus, the surface of a piece of tissue as small as a finger is irradiated only from the outer side. The mosquito is so small that the beta radiation passes through it and irradiates the surface from both the outer and inner sides almost equally. It follows that the dose rate to the skin of a person in an infinite cloud is just about half that to the mosquito.

$$D_s = Dm/2 = 240\,C \text{ rad/hour} \qquad (2)$$

The infrequent 0.514 MeV gamma ray and the bresstrahlung produced when the beta particles are stopped in tissue irradiate the entire body fairly uniformly. The whole body dose rate from the infinite cloud is approximately

$$D_w = 2\,C \text{ rad/hour} \qquad (3)$$

The dose to the sperm-producing cells of a man standing naked in this cloud is made up of the whole-body dose, given by eq. (3), and that portion of the skin dose, given by eq. (2), which penetrates the scrotum. The depth of the sperm producing cells below the surface of the skin has not, to my knowledge, been specified by the Standard Man. I am indebted to my associate Dr. A. P. Jacobson, who conferred intimately with several cadavers at the University Hospital, for the estimate that this depth is about 2.5 mm.

As has been stated previously, the maximum range of krypton-85 beta particles in tissue is 2.5 mm, at which depth, of course, the beta dose rate drops to zero. At a depth of 1.5 mm in tissue, the beta dose rate is just about 1/100 the surface dose rate. It seems unlikely, therefore, that krypton-85 beta particles contribute as much as 1% of the surface dose to sperm-producing cells. It is fashionable to be conservative (i.e. wrong, but on the high side) about these things, so I estimate that the genetically significant dose to a naked male in an infinite cloud of krypton-85 will not exceed

$$D_t \leq D_w + 0.01\,D_s = 4\,C \text{ rad/hour} \qquad (4)$$

KRYPTON-85 INSIDE THE RESPIRATORY TRACT

For the purpose of this estimation the respiratory tract is taken as a cylindrical trachea 10 cm long and 2 cm in diameter leading to a single, spherical lung 20 cm in diameter, which has a little larger volume than the vital capacity of the Standard Man. Since the dose rate tends to increase with volume, this simple model tends to overestimate the actual dose.

The dose rate to the inner surface of a sphere containing krypton-85 is about the same as that to the skin of a person standing in an infinite cloud (eq. 2), provided that the radius of the sphere is greater than the range of th beta particles in air (i.e., greater than 2 m). Geometric and depth-dose considerations indicate that as the radius of the sphere is reduced to less than 2 m, the dose rate drops, slowly at first and then more rapidly. These considerations lead to the estimate that the dose rate to the 20 cm diameter lung is somewhat less than half the skin dose, and that to the 2 cm diameter trachea is less than 1/10 the skin dose.

$$D_l \leq 120\,C \text{ rad/hour} \qquad (5)$$

$$D_a \leq 24\,C \text{ rad/hour} \qquad (6)$$

KRYPTON-85 DISSOLVED IN BODY TISSUE

Krypton is not highly soluble in water. The partition coefficient between water and air at 37° C is 0.052 (Hodgman, 1951), and that between blood and air is about 0.07 (Mellemgaard, *et al.*, 1962; and Muehlbaecher, *et al.*, 1966). The solubility of noble gases is considerably higher in fat and oil than it is in water. The partition coefficient between fat and air at 37°C for krypton appears to be about 0.5 (Lawrence, *et al.*, 1946; Yeh, *et al.*, 1963; and Kety, 1951). For tissues other than blood and fat there is little information. A value of 0.02 has been given for protein (Yeh, *et al.*, 1965), but the usual practice has been to use the blood value for all tissues other than fat.

Since 99% of the dose delivered by krypton-85 is attributable to its beta particles, which have a maximum range of 2.5 mm in tissue, a portion of tissue 5 mm on a side constitutes an infinite mass. Application of the same principles used to obtain the dose rate in an infinite cloud gives

$$D_i = 0.5\,G \text{ rad/hour} \qquad (7)$$

where

D_i = dose rate to the tissue containing ^{85}Kr, rad/hour
G = concentration of ^{85}Kr in the tissue, μCi/g

When the body has been exposed to a cloud of krypton-85 at a concentration of C(μCi/ml)long enough for equilibrium to be established, the relation between the concentration in tissue to that in the cloud is simply

$$G = PC \quad (8)$$

where

G ± concentration in tissue, μCi/g
C = concentration in air, μCi/ml
P = partition coefficient
P - 0.5 for fat
P = 0.07 for all other tissues

thus, for fat, the dose rate is

$$D_f = 0.25\,C \text{ rad/hour} \quad (9)$$

and for all other tissues is

$$D_o = 0.035\,C \text{ rad/hour} \quad (10)$$

SUMMARY OF EQUILIBRIUM DOSE RATES

Comparison of the dose rates given by the equations which have been developed to the maximum organ dose rates recommended for the public at large by the ICRP (1966) shows that the concentration of krypton-85 in air is limited equally by the dose rates to the skin and to the lung. The concentration which produces both these limiting dose rates is 1.5×10^{-6} μCi/ml, which is 5 times the present maximum concentration in public air (ICRP, 1966; and 10CFR). Dunster and Warner have noted this factor of 5 and suggested that the ICRP may increase the MPC accordingly (Dunster, *et al.,* 1970).

DOSE RATES UNDER NON-EQUILIBRIUM CONDITIONS

The first three exposure conditions (a cloud at some distance from the body, an enveloping cloud, and inside the respiratory tract) entail no delays for uptake and elimination. As a consequence, the dose rates from these exposure conditions follow the concentration of krypton-85 in air instantaneously and the dose is directly proportional to the period of exposure. Only in the case of krypton-85 dissolved in body tissue does the duration of exposure complicate the estimation of dose.

The exchange between krypton in the lung and that dissolved in blood is rapid for both uptake and elimination. Half-lives for these exchanges have been reported as being from 1 to 6 minutes (Whitton, 1968). The rates of exchange from blood to other tissues, and from these tissues back into blood, are considerably slower than the lung to blood rate. Half-lives for the transfer of krypton-85 from inhaled air to body fat range from 0.4 to 3 hours (Hytten, *et al.,* 1966; and Turkin, *et al.,* 199). The half-life for elimination of krypton-85 from fat appears to be considerably longer than that for uptake; i.e., 18 hours (Hytten, *et al.,* 1966).

If uptake and elimination occur at the same rates, the dose from krypton-85 dissolved in body tissues is simply the dose rate from the amount dissolved at equilibrium multiplied by the period of exposure, e.g.,

$$D_{ft} = D_f t \quad (11)$$

However, when elimination proceeds more slowly than uptake, the dose for short exposure periods is somewhat greater than is the case when elimination and uptake occur at equal rates.

Exposure periods of less than 100 hours do not reach equilibrium conditions in fat and, therefore, result in somewhat higher doses than would be the case if elimination took place at the same rate as uptake. In spite of this, the skin and the lung are still the limiting tissues, just as they are for equilibrium exposure conditions. In other words, the rapid uptake and slow elimination of krypton-85 in body fat do not change the conclusions based on steady state conditions.

LONG-TERM SIGNIFICANCE

The relations which have been developed between krypton-85 concentration in air and the dose rates to various organs and tissues have been applied to the emission rates expected from the General Electric Company's; Midwest Fuel Recovery Plant, in Illinois. The results show that the maximum off-site doses are about 9 milli-rem per year to the skin (the ICRP limit is 3,000 milli-rem per year), and 4.4 milli-rem per year to the lung (the ICRP limit is 1,500 milli-rem per year). Under the most adverse meteorological conditions, the dose to the skin might be as great as 8 milli-rem to the skin and 4 milli-rem to the lung if these conditions persisted for 15 hours.

A number of estimates have been made of the doses from krypton-85 released to the atmosphere as the result of nuclear power generation. The greatest uncertainty in these estimates is, quite naturally, the choice of the rate at which nuclear power will grow. Coleman, *et al.,* (1966) and Dunster, *et al.,*(1970) present a number of such estimates. These estimates differ in no significant way from the dose rates obtained by applying the relations in this paper to projected nuclear power growth. From all of these estimates it appears unlikely that the skin dose, world-wide, will exceed 10 milli-rem per year until after the year 2010 AD (34 million megawatts electric) if all the krypton-85 is released to the atmosphere.

The biological effects of 10 milli-rem per year to the skin of the world's population are, in my opinion, of little if any significance. Such effects, if they occur at all, will be swamped by the effects of natural, occupational, and domestic agents to the extent that their identification lies beyond the abilities of the most sophisticated epidemiologists and statisticians.

SUMMARY AND CONCLUSION

Examination of the possible ways a person may be exposed to airborne krypton-85 leads to the following conclusions, which apply under both equilibrium and transient conditions: exposure of skin and lung are equally limiting, and the appropriate maximum permissible concentration in public air is 1.5×10^{-6} μCi/ml, which is 5 times the presently accepted concentration.

Application of the dose-rate relations developed in this paper to the projected growth of nuclear power, in which all the krypton-85 is released to the atmosphere, leads to the estimate that the skin dose is unlikely to exceed 10 milli-rem per year, world-wide, before 2010 AD. The biological effects of this dose, if any, will be trivial and unmeasurable.

REFERENCES

Coleman, J.R. and R. Liberace, (1966), *Nuclear Power Production and Estimated Krypton-85 Levels.* Radiol. Health Data and Reports, 7:615-621.

Dunster, H.J. and B.F. Warner, (1970), *The Disposal of Noble Gas Fission Products from the Reprocessing of Nuclear Fuel.* AHSB (RP) R-101, Harwell, England.

Hodgman, C.D., (1951), ed., *Handbook of Chemistry and Physics,* 33rd ed. Chemical Rubber Publishing Co., Cleveland, p. 1482.

Hytten, F.E., K. Taylor and N. Taggart, (1966), *Measurement of Total Body Fat in Man by Absorption of ^{85}Kr.* Clin. Sci. 31:111-119.

Kety, S.S., (1951), *The Theory and Applications for the Exchange of Inert Gas at the Lungs and Tissues.* Pharm. Rev. 3:1.

Lawrence, H.H., *et al.,* **(1946),** *Preliminary Observations on the Narcotic Effects of Xenon with a Review of Values for Solubility of Gases in Water and Oils.* J. Physiol. 105:197.

Mellemgaard, K., N.A. Lassen and J. Georg, (1962), *Right-to-Left Shunts in Normal Man Determined by the Use of Tritium and Krypton-85.* J. Appl. Physical. 17:778.

Muehlbaecher, C.A., F.L. DeBon, and R.M. Featherstone, (1966), *Further Studies of Solubilities of Xenon and Cyclopropane in Blood and Protein Solutions.* Molec. Parmacol. 1:86-89.

Turking, A.D., *et al.,* **(1969),** *Radiation Hazards from Radioactive Inert Gases.* Symposium on Noble Gas Fission Products in the Nuclear Industry, Paris Oct. 1969, CONF-691039.

U.S. Atomic Energy Commission, Rules and Regulations, *10 CFR Part 20, Appendix B, Table II, Column 1.*

Whitton, J.T., (1968), *Dose Arising from Inhalation of Noble Gases,* Central Electricity Generating Board, Report RD/B/N/1274. Berkeley, England.

Yeh, S.Y. and R.E. Peterson, (1963), *Solubility of Carbon Dioxide, Krypton and Xenon in Lipids.* J. Pharm. Sci. 52:453-458.

Yeh, S.Y. and R.E. Peterson, (1965), *Solubility of Krypton and Xenon in Blood, Protein Solutions and Tissue Homogenates,* J. Appl. Physiol. 20:1041-1047.

RELATION BETWEEN CUMULATIVE EXPOSURE TO RADON-DAUGHTERS, LUNG DOSE, AND LUNG CANCER RISK

W. Jacobi
Institute for Radiation Protection
Munich, Germany

Abstract

The dose/exposure-ratios regarding the influence of uncombined radon-daughters for the bronchial region resulting from different dosimetric models are compared. For dose evaluation, the uncombined fraction of the total potential α-energy in the inhaled air seems to be a more suitable parameter than the uncombined activity-fraction of RaA only. The mean dose to the basal cell layer in the medium bronchi is probably not considerably higher than the mean dose to the total bronchial tree. Under normal conditions in mines, a ratio of 0.4 to 1.0 rad/WLM can be expected.

In the second part of the paper, the observed lung cancer-risks among uranium miners in the USA and the CSSR are discussed. Although the relative risk coefficient is similar for both groups, the absolute risk coefficient in the CSSR-group is significantly higher than in the USA-group of miners. On the basis of these data, an absolute lung cancer-risk of 10 to 20 cases/10^6 person-years per WLM is recommended for radiation protection purposes. Finally, the risk concept for the assessment of an exposure limit for uranium miners is discussed. The derived life time limit of 100 to 200 WLM for occupational exposure is comparable with the limit derived from the 15 rem/year-concept.

INTRODUCTION

An exposure limit for the inhalation of short-lived radon-daughters can be derived in two different ways:

(1) From the dose limit of 15 rem per year in the critical respiratory region, as it is recommended by the ICRP (dose concept).
(2) From the observed relationship between lung cancer risk and the cumulative radon exposure among uranium miners (risk concept).

In this paper some of the main problems with which we are confronted in the application of these concepts are outlined and discussed. They concern the relation between inhaled activity and dose in different respiratory regions, and between cumulative exposure and lung cancer-risk.

RELATION BETWEEN LUNG DOSE AND EXPOSURE

It is well known that the inhalation of radon-daughters results in an inhomogeneous dose and activity distribution in the respiratory tract — especially in the bronchial region. The first problem in the application of the dose concept is the suitable choice of the critical respiratory region to which the dose limit shall be referred. For other nuclides, the total lung or the total bronchial region is used as the reference organ. On the other hand, bronchogenic lung cancer among uranium miners is presumed to originate in the basal cells which line the basement membrane of the bronchial epithelium. With respect to lung cancer-risk, therefore, the mean dose to this basal cell layer seems to be the most reasonable reference quantity. In the following, the dose/exposure-ratios for these different reference regions are evaluated and compared.

1. Mean Dose in the Total Bronchial Region.

This dose can be calculated with sufficient accuracy on the basis of the new ICRP model for the deposition and clearance of soluble aerosols of clearance class D in the human lung (ICRP 1969; Jacobi, 1972a; and Jacobi; 1973). It should be emphasized that in the case of short-lived radon-daughters, the choice of the clearance class is rather uncritical for lung dose evaluation. Figure 1 shows the resulting ratio of the absorbed α-energy W in the tracheobronchial (T-B) or pulmonary (P) region to the inhaled potential α-energy P of the radon-daughter mixture. The curves in this figure refer to nose breathing and an AMAD of the vector aerosol of 0.2 μm.

In the left graph of Figure 1, this absorption yield is given as a function of the fraction f^1 of uncombined or free RaA atoms for different values of the air ventilation rate λ_V in the working area. This graph indicates that the relation between dose and the uncombined fraction of RaA activity depends on the ventilation rate. However, if this absorption yield is plotted as a function of the uncombined fraction f_p of the total potential - energy of the radon-daughter mixture, the curves for different ventilation rates converge into a straight line (see right graph in Figure 1). This leads to the conclusion, that the uncombined fraction f_p of the total potential energy is a more reasonable parameter than the uncombined fraction f_1 of RaA atoms.

From the absorption yield in Figure 1, the mean α-dose in the total bronchial and pulmonary region per WLM of cumulative exposure can be evaluated, taking into account a breathing rate of 20 l/min and a mass of 45 g or 955 g for the tracheobronchial region or the pulmonary region, respectively, as they are recommended

by the ICRP-task group for the "Reference Man" (ICRP, 1973). The resulting dose/exposure-ratio for radon- and thoron-daughters is shown in Figure 2 as a function of the uncombined fraction f_p of the total potential α-energy in the inhaled air.

As expected, the rad/WLM-ratio in the bronchial region increases linearly with the uncombined fraction f_p; for radon-daughters this ratio can be estimated from the relation (E = cumulative exposure):

$$D_{T\text{-}B}(\text{rad})/E(\text{WLM}) \cong 0.31\ (1+6\ f_p)$$

$$D_P(\text{rad})/E(\text{WLM}) \cong 0.16\ (1 - f_p)$$

As the uncombined fraction f_p of the total potential α-energy in air is considerably lower than the uncombined fraction f_1 of RaA atoms found in most working areas with unfiltered air is $f_p < 0.1$ — especially in mines; under normal conditions, a ratio of 0.4 to 0.5 rad/WLM or 4 to 5 rem/WLM (QF = 10) follows from the new ICRP lung model for the mean bronchial α-dose.

However, it should be kept in mind that the uncombined fraction increases with an increasing ventilation rate due to the reduction of the aerosol concentration and the decreasing RaB/RaA- and RaC/RaA-ratio in the air. This effect can be estimated on the basis of a box model which takes into account the removal of dust and activity by ventilation and wall deposition (Jacobi, 1972b). Figure 3 shows roughly the relationship between the rad/WLM-ratio and the rate of ventilation with clean air which should be expected in working areas with a high, intermediate, and low rate of aerosol production.

The increase of the rad/WLM-ratio with ventilation is of practical importance because it cancels out, to some extent, the dose reduction due to the decreasing concentration of radon-daughters in the air. Figure 4 shows this influence of ventilation in a relative scale. Due to the increasing uncombined fraction, the reduction of the bronchial dose with ventilation is not proportional to the reduction of the potential energy concentration in the air. It follows from this figure that ventilation rates of more than about 10 to 20 hours seem to be unreasonable, because the bronchial dose remains nearly constant in this ventilation range.

2. Dose to the Basal Cells in the Bronchi.

So far only the mean α-dose in the total tracheobronchial region has been considered; however, a large fraction of the absorbed α-energy in the T-B region is deposited in the mucus sheet and the rather insensitive layer of ciliated cells and goblet cells on the bronchial epithelium.

Several dosimetric models have been developed to estimate the dose from inhaled radon-daughters to the basal cells, where bronchogenic lung cancer is assumed to originate (Altshuler, *et al.*, 1964; Jacobi, 1964; Hague and Collinson, 1967; and Harley and Pasternack, 1972). The assumptions in these models, concerning the deposition pattern of the inhaled radon-daughters, the mucus flow-rate, and the position of the basal cells, are in part quite different due to our limited knowledge of these quantities in the different bronchial generations.

Nevertheless, these studies agree in the conclusion that the maximum α-dose in the basal cell layer is reached in the segmental-subsegmental bronchi (lung model of Landahl) or in the 4.0 to 9.0 airway generation (lung model of Weibel), respectively. The calculated absolute dose values are, however, different due to the different assumptions used in these models. The critical parameters in these models are (1) the depth of the basal cell layer below the mucus surface and (2) the uptake and distribution of radon-daughters in the mucus sheet, and the upper cell layers of the bronchial epithelium. The mean depth of the basal cells ranges probably from about 50 to 100 μm in the trachea and the main bronchi, 30 to 60 μm in the segmental-subsegmental bronchi, and 20 to 40 μm in the terminal bronchi.

In Figure 5 the variation range of the α-dose per WLM at a 30 to 60 μm depth in the segmental-subsegmental bronchi is given as it can be derived from the different models. The calculated values are plotted as a function of the uncombined fraction f_p of the total potential α-energy in the inhaled air, and are normalized for nose breathing at a rate of 20 l/min. The dose/exposure-ratios from the different models cover a range from about 0.2 to 10 rad/WLM. The more recent models (Harley and Pasternack, 1972) indicate that under normal mining conditions ($f_p < 0.1$), the mean α-dose in the basal cell layer of this critical bronchial region lies probably at the lower end of this range. A value of 0.5 to 1 rad/WLM = 5 to 10 rem/WLM seems to be a reasonable reference value for the conversion of exposure to the mean dose in the basal cell layer of the segmental-subsegmental bronchi. In the BEIR-report (1972) a conversion factor of 5 rem/WLM has been used.

A comparison with the previously derived conversion factor for the dose to the total bronchial region leads to the conclusion that the mean α-dose to the basal cell layer in the most exposed bronchial region is probably not considerably higher than the mean α-dose to the total bronchial tree.

This conclusion solves one of the main problems in the application of the ICRP dose limit of 15 rem/year. Taking into account a conversion factor of 0.4 to 1.0 rad/WLM, which range covers the results for both reference regions, this dose limit yields an exposure limit of 2 to 5 WLM per year, or an integral exposure of about 80 to 200 WLM during a working period of 40 years. The exposure limit of 0.3 WL or 4 WLM per year, which has been adopted for uranium miners in USA and other countries, falls in this range derived from the dose concept. However, as pointed out, this limit should be reduced in highly ventilated, dust-free working areas.

RELATION BETWEEN LUNG CANCER RISK AND CUMULATIVE RADON EXPOSURE

The annual dose limit of 15 rem recommended for the lung by the ICRP stems from radiation protection concepts prior to the introduction of a quantitative risk concept. The validity of these old concepts is now being seriously questioned. Therefore, this limit should be revised, if reliable data on the risk of lung cancer (LC) by inhalation of radon-daughters become available.

In recent years such results for two sufficiently large groups of persons have been published which enable us now to discuss the relationship between LC-risk and cumulative radon exposure. The first study group of about 3,400 white uranium miners in the Colorado-Plateau (USA), which was analyzed, mainly by Lundin, *et al.*, (1971). In this group, a total number of about 38,000 person-years of risk was reached during the observation period from 1951 to 1971. The second group was composed of uranium miners in the CSSR, for which group preliminary data about LC-risk versus the cumulative radon exposure were published recently by SEVC and PLACEK (1973). However, although the USA-data was published, data for the CSSR-group (the total number of miners and the absolute numbers of LC-cases) has not been published. Only the relative number of observed and expected LC-cases, normalized to 1,000 miners, are available, arranged in four exposure intervals: <100, 100 to 200, 200 to 400, > 400 WLM. This arrangement already indicates that the average cumulative exposure of the uranium miners in the CSSR was considerably lower than in the USA-group of uranium miners. However, the observation period from 1948 to 1970, and the total number of 34.511 person-years at risk for the CSSR-group, are comparable with the USA-group. This supports the assumption that the number of uranium miners in the CSSR-study group is comparable with that in the USA-study group.

For a direct comparison of both groups, the ratio of the observed to the expected LC-mortality can be quoted, which is shown in Figure 6 as a function of the cumulative exposure in WLM-units. The corresponding excess LC-mortality is given in Figure 7 for the USA-group and in Figure 8 for the CSSR-group of uranium miners. Note that in the USA-group (Figure 7) the excess LC-mortality is related to person-years, whereas in the CSSR-group (Figure 8) it is related to the number of persons. The marked observation points in the Figures 6 through 8 are plotted with their 95% confidence limit at the average of each exposure interval.

From the preliminary data for the CSSR-miners a significant dependence between excess LC-mortality and exposure can be stated already above 100 WLM, whereas for the USA-group of uranium miners in the observation period up to 1968 such a significant relationship could only be confirmed above 600 to 800 WLM (see Figure 6). However, the additional LC-cases which occurred in the USA-study group of miners in the last three years from 1968 to 1971 have shifted this significance limit to lower exposure values (see Figure 7,), taken from the BEIR-report (1972).

Taking into account the limits of error, the presently available data for both groups, therefore, do not indicate the existence of a practical exposure threshold above 100 to 200 WLM. The data also do not allow a reliable, quantitative distinction between a linear or nonlinear relationship between LC-incidence and cumulative radon exposure. The mean regression lines in Figures 7 and 8 indicate that a linear relationship in the considered exposure range cannot be excluded. At the present time, the recommendation of an exposure limit should be based, therefore, on the assumption of a linear exposure-risk curve.

It follows from Figure 6, that the mean, relative risk coefficient is nearly equal for both groups of uranium miners and results to $\alpha_{rel} \cong 0.009 + 0.003\ \mathrm{WLM}^{-1}$, corresponding with a mean "doubling exposure" of about 110 WLM. For comparison, it should be noted that the mean natural background level of radon-daughters in air leads to a cumulative exposure of about 4 to 5 WLM during a lifetime of 70 years. This means that only a few percent of the observed LC-mortality in our population can be attributed to irradiation of the lung by inhaled radon-daughters, if a linear extrapolation down to these low exposure values in generally accepted.

The absolute risk coefficient for the induction of lung cancer from inhaled radon-daughters can be derived from the slope of the mean regression lines given in Figures 7 and 8. For the USA-group of white uranium miners a mean value results as follows:

$$\alpha_{abs}(\text{USA-U-miners}) \cong 3 \pm 1 \ \frac{\text{LC-cases}}{\text{WLM} \times 10^6 \text{ person-years}}$$

Taking into account a conversion factor of 1 WLM = 5 rem for the dose equivalent to the critical bronchial region, this corresponds to about 0.6 LC-cases/rem x 10^6 person-years.

The mean slope of the excess LC-mortality among the CSSR-miners follows from Figure 8 to 170 ± 50 LC-cases per 10^6 persons per WLM. As the observation period and the number of person-years at risk is similar for both groups, it should be expected also that a rather similar time distribution exists for the start of uranium-mining. Under this assumption, the average number of years at risk per person of 38.622 person-years/3366 persons ≅ 12 years in the USA-group should be applicable also to the CSSR-group. Taking into account this conversion factor, an absolute risk coefficient follows:

$$\alpha_{abs}(\text{CSSR-U-miners}) \cong 14 \pm 4 \ \frac{\text{LC-cases}}{\text{WLM} \times 10^6 \text{ person-years}}$$

Compared with the USA-group, the absolute risk coefficient in the CSSR-group is significantly higher, although the relative risk coefficients are nearly equal.

The preliminary CSSR-data, furthermore, indicate an increase of the risk coefficients with the decreasing age of the miners at their start of uranium-mining. In addition, the real risk coefficients should be higher than the values given above due to the limited observation period of about 20 years. On the other hand, the LC-risk coefficient by radiation is probably considerably lower for non-smoking miners. Under these circumstances, an absolute risk coefficient of 10 to 20 LC-cases/WLM x 10^6 person-years seems to be a reasonable reference value for the assessment of the radon exposure limit to miners.

CONCLUSIONS

A strict application of the risk concept requires the assessment of the maximum acceptable radiation risk. With respect to the LC-risk of miners exposed to radon-daughters, this risk limit must comply with two different conditions.

Taking into account the strong variation of the natural background level of radon-daughters in air, the occupational exposure limit should be 1 to 2 orders of magnitude higher than the average background level. This means, that the limit for the occupational exposure of uranium miners, integrated over their total lifetimes, should not be fixed below about 100 WLM. This lower limit would cause a LC-risk by radiation comparable with the LC-risk from other sources (doubling exposure) and would yield an additional LC-risk of about 1,000 to 2,000 cases/10^6 person-years.

On the other hand, the average radiation risk of uranium miners should not exceed the average risk of death by other occupational diseases as it is observed among miners in conventional, safe-operated mines — especially coal mines. The latter level of risk is about 200 to 500 cases/10^6 person-years. This level corresponds to an average lifetime exposure of about 20 to 50 WLM averaged over all uranium miners. Taking into account the general recommendation of the ICRP that the average dose of radiation-exposed workers should be kept well below the recommended dose limit, an exposure limit of about 100 to 200 WLM for uranium miners seems to be acceptable.

The necessity to meet both of the above mentioned conditions reveals the narrow margin which is available for the assessment of an occupational exposure limit to radon-daughters. The resulting exposure limit on the basis of this risk concept is comparable with the limit which was derived from the ICRP-dose limit of 15 rem/year. This leads to the final conclusion that, on the basis of our present knowledge, the risk concept and the dose concept lead, within the limits of error, to the same value for the maximum permissible exposure to radon-daughters.

REFERENCES

Altshuler, B., N. Nelson, and M. Kuschner, (1964), Health Physics 10, 1137.

Haque, A. K. M. M., and A. J. L. Collinson, (1967), Health Physics 13, 431.

Harley, N. H. and B. S. Pasternack, (1972), Health Physics 23, 771.

Jacobi, W., (1964), Health Physics 10, 1163.

Jacobi, W., (1972a), Health Physics 23, 3.

Jacobi, W., (1973), Page 109-120 in *Health Physics Problems of International Contamination,* Hungarian Acad. of Sciences, Budapest 1973.

Jacobi, W., (1972b), Health Physics 22, 441.

Lundin, F. E., J. K. Wagoner, and V. E. Archer, (1971), 2 Radon-Daughter Exposure and Respiratory Cancer; Quantitative and Temporal Aspects, Nat. Inst. for Occup. Safety and Health — Nat. Inst. of Environmental Health Sciences, Joint Monograph No. 1.

Report of the Advisory Committee on the Biological Effects of Ionizing Radiations, (BEIR-report), (1972), Nat. Acad. of Sciences, Nat. Research Council (USA), Washington D.C., November 1972.

Report of the ICRP-task Group on Lung Dynamics, (1969), Health Physics 12, 173 (1966); revised at the ICRP-meeting, Oxford 1969.

Sevc, J. and V. Placek, (1973), Page 129-136 in *Health Physics Problems of Internal Contamination,* Hungarian Academy of Sciences, Budapest 1973.

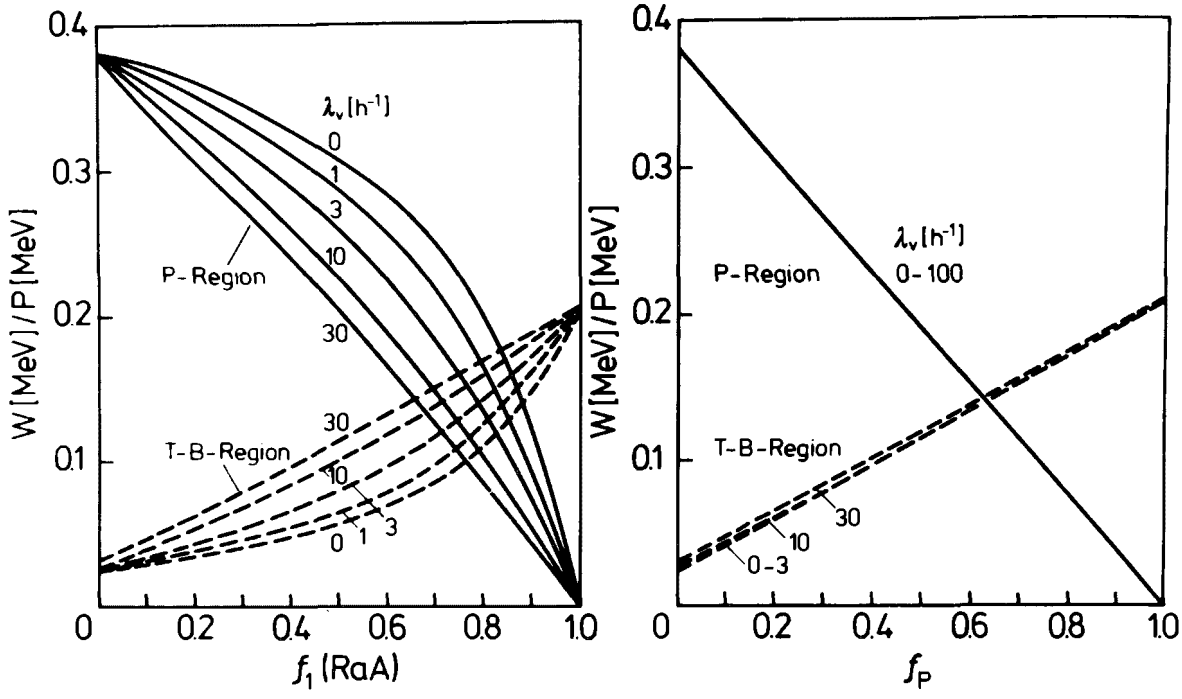

Figure 1. Fraction of the inhaled potential α-energy absorbed in the tracheobronchial and pulmonary region (see text).

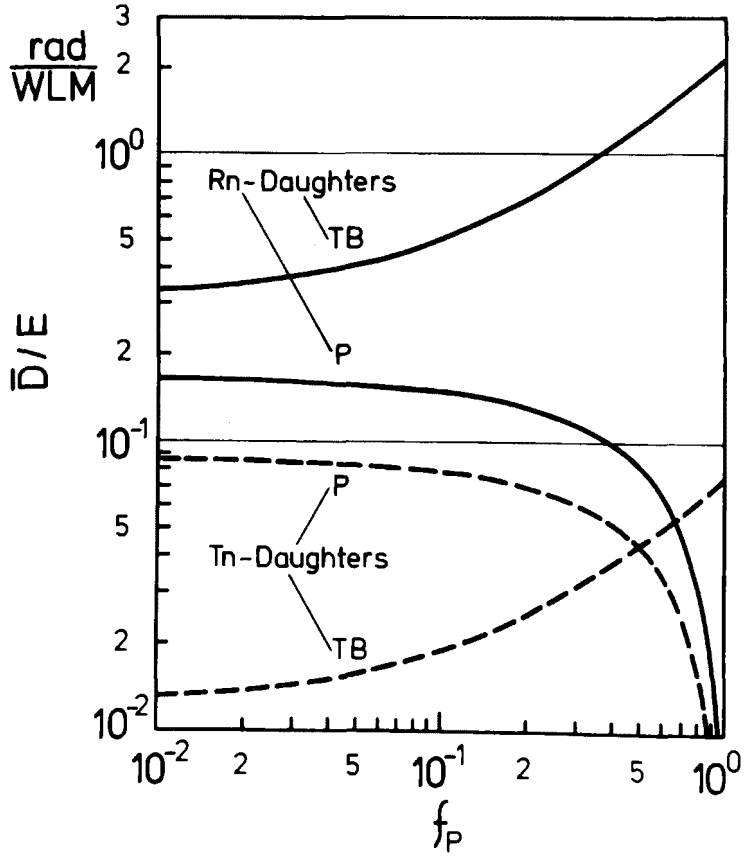

Figure 2. Mean α-dose per WLM in the tracheobronchial (T-B) and pulmonary (P) region as a function of the uncombined fraction fp of the potential α-energy in the inhaled air (ICRP-lung model).

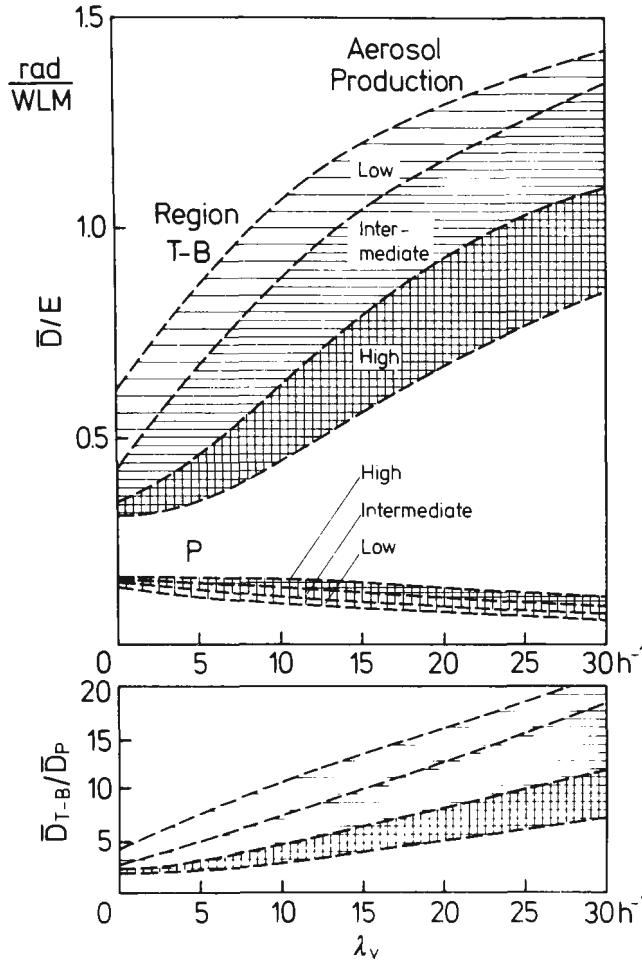

Figure 3. Expected mean α-dose per WLM to the total bronchial and pulmonary region as a function of the ventilation rate λ_V (box model).

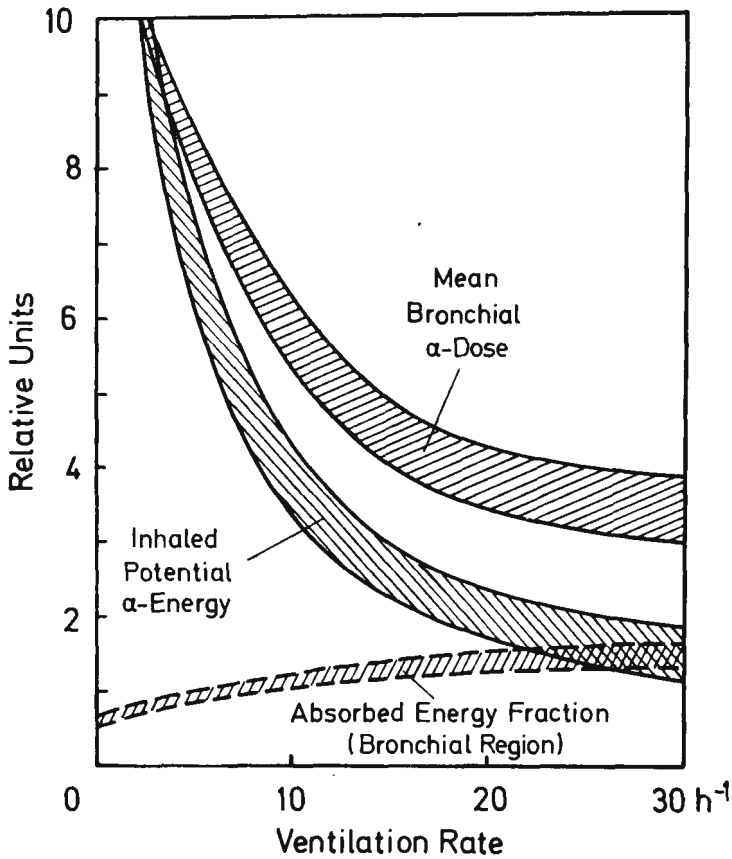

Figure 4. Estimated relative influence of ventilation on the potential energy concentration in air and the bronchial dose in a working area with constant rate of radon- and aerosol- production.

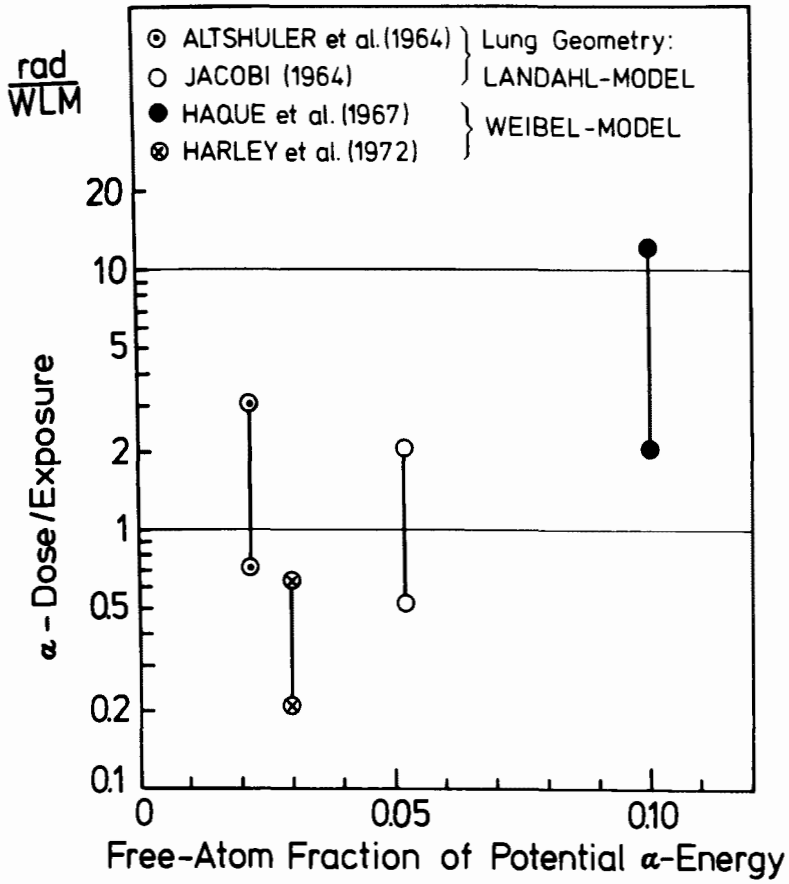

Figure 5. Mean dose to the basal cell layer in the segmental-subsegmental bronchi per WLM, calculated from different dosimetric models (v=20 l/min).

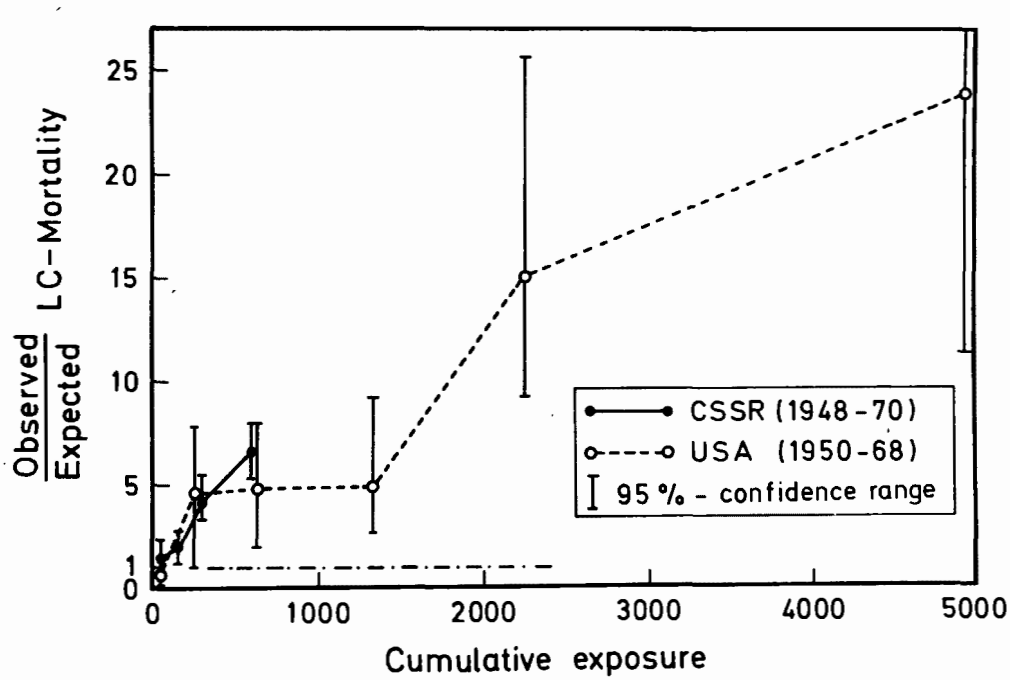

Figure 6. Relative lung cancer-risk among uranium miners in the USA and CSSR versus their cumulative exposure (in WLM-units).

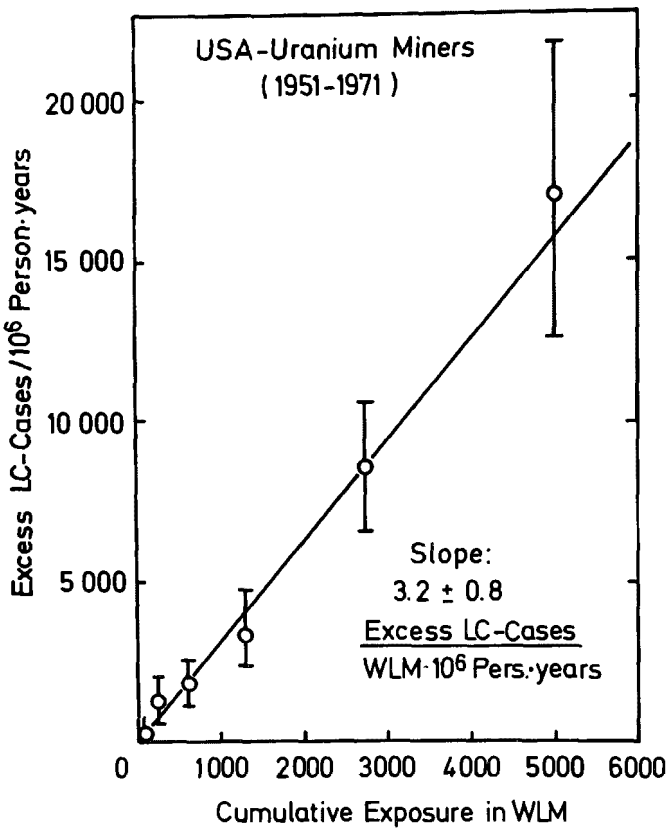

Figure 7. Additional lung cancer-risk among uranium miners in USA (from BEIR-report, 1972).

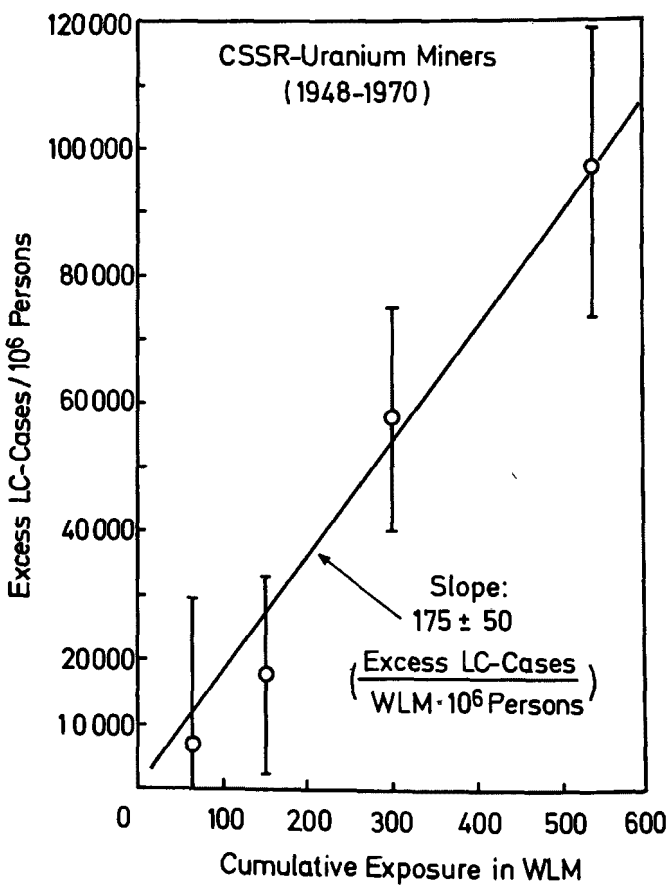

Figure 8. Additional lung cancer-risk among uranium miners in the CSSR (from *SEVC, et al.*, 1973).

THE BIOLOGICAL EFFECTS OF RADON ON THE LUNG*

D. A. Morken
University of Rochester
Rochester, New York 14642

Abstract

The biological effects of radon on the lung arise primarily from the alpha decay of the short-lived decay products of radon inhaled. Radon is chemically inert and so is distributed throughout the body according to its solubility in the various body tissues. The daughter products are isotopes of polonium, bismuth, and lead, which are treated individually by the tissues and fluids, within the confines of their brief half-lives.

Experiments with inhaled decay products indicate the dose to lung is much greater than to the rest of the body. Extensive injury was done to the bronchial tree, but the lesions did not lead to bronchial tumors. After irradiation ceased, these lesions were quickly repaired. Permanent changes, but no cancer, were seen in the region of the respiratory bronchioles.

Compared to other alpha emitters in the lung, the alpha radiation from radon is particularly inefficient in producing radiation-specific tumors. The conclusion is taken that the radiation effects of alpha emitters may be inconsequential compared to the chemical effects of the alpha emitters.

INTRODUCTION

The toxic effects from inhaled radon may result from the actions of three distinct radioactive agents. One of these is radon itself, a noble gas which becomes distributed throughout the body and delivers a radiological dose to all tissues from alpha particles. This radon is accompanied, however, by a series of short-lived radioactive decay products which are produced within the body. These products are isotopes of polonium, lead, and bismuth which may be treated by the body tissues to provide a distribution different from that of the parent radon. These products decay by alpha and beta particle and gamma ray emission, and provide a dose distribution different from that of the parent radon. These products of radon, produced within the body, provide a second radioactive agent. In practice the two agents occur together.

The decay of radon in the atmosphere produces these short-lived products as ions which become attached to dust particles. Inhalation of this radioactive dust results in the deposition of this radioactivity in the lung. By virtue of the short half-lives (3 to 30 minutes) and the parent-daughter relationship which exists among these products, they accumulate in the lung passages to provide a greater radiological dose than that from radon alone. This then provides a third agent which delivers a radiological dose to the lung only.

The inhalation of radon and its decay products present in uranium mines is believed to produce bronchial cancer in uranium miners. These miners exhibit an incidence of lung cancer greater than normal. Throughout the literature on the radiotoxic properties of radon occurs the suggestion that radon is somehow responsible for the lung cancer in miners; often radon is mentioned as a co-factor. Radon and its decay products are present in other kinds of mines, but bronchial or lung cancer has never been attributed to the presence of the radon. A large number of animal experiments over the past fifty years have been unable to confirm that radon or its decay products can cause lung cancer. Work with other alpha-emitting isotopes has been successful in producing neoplasia in the lung. A few experiments using radon combined with chemically toxic agents, generally silica, but including uranium mineral, may have demonstrated a potentiation or promotion of the tumorigenic properties of the chemical agents, or of the tumors themselves.

The biological effects of radon and its decay products contained within the whole animal are the subject of another paper presented in this Symposium. This paper summarizes the histopathology of the lung following inhalation by mice, dogs, and rats from an atmosphere which contained radon and dust, and compares this histology with that from experiments involving other alpha-active isotopes.

THE EXPERIMENTAL METHOD

The experimental animals are exposed in a large chamber to a radon atmosphere which is established by mixing radon from a generator with dusty air (normal room air) entering the chamber at a constant flow rate. The chamber has a volume of 2,000 liters, and the air flow, which can be adjusted over wide limits, is usually set near 40 liters per minute. The radon generator contains about 200 millicuries of radium in a dilute hydrochloric acid solution which is aerated continuously from a source of compressed air at about 300 milliliters per minute; this generator provides about 22 microcuries of radon per minute. The generated radon is scrubbed of acid and particulate material before being passed to the chamber. The radon concentration established in the chamber depends on the air flow through the chamber — for the 40 lpm flow the concentration is about 0.55 μCi/1 in the steady state.

The time taken to attain the steady state is related inversely to the air flow, and at 40 lpm amounts to about three hours. The radon decay products formed in the chamber become attached to the dust particles (normal room dust), also attaining a steady state. At 40 lpm air flow the concentrations of RaA, RaB, and RaC on dust become about 0.40, or 0.20, and 0.12 μCi/1, respectively. The chamber atmosphere is monitored hourly for radon, with activity recorded on a strip chart. The radon concentration is also measured daily, during the steady state, in an air sample taken with an evacuated ionization chamber, and is read with an electrometer.

**This paper is based on work performed under contract with the U.S. Atomic Energy Commission at the University of Rochester Atomic Energy Project and has been assigned Report No. UR-3490-384.*

The chamber atmosphere is occasionally sampled with a dust filter which is counted for alpha activity to provide estimates of the concentrations of RaA, RaB, and RaC in the chamber.

The exposure atmosphere is evaluated and reported in terms of the Working Level (WL) unit, which is derived from the concentrations of the airborne decay products of radon attached to dust, and which represents a dose rate. The cumulated exposure dose is represented by the Working Level Month (WLM) unit. The chamber is operated in the region of 1,800 WL, and the rate at which the dose is cumulated is about 11 WLM per hour of exposure.

For purposes of the radiobiologist, the radiation dose and dose rate to tissue are more meaningful, but less easy to determine. The radiological dose to lung can be estimated from a knowledge of the concentration of the decay products in the inhaled air, the breathing rate, the extent of deposition of the decay products in the lung, the lung weight, and the clearance rates which act on the dust or radioactivity. The air concentrations can be measured directly. The other quantities are not well established. For the present experiments, the radiological doses are estimated from measurements made on the lung and respiratory tract. This direct procedure removes the uncertainties associated with breathing rate, deposition, and clearance, but an uncertainty as to the amount of tissue involved remains.

Randomization methods are used to sort animals into experimental and control groups, and into the various dose categories. Following exposure, the animals were randomly sorted into a sacrifice schedule. Gross examinations were made of all tissues, but, generally, tissue sections were taken only from the lung. Mortality and weight were also followed, and in some cases the hemograms were examined.

EXPERIMENTS WITH MICE (Morken, *et al.*, 1971)

CAF_1 strain mice were used in these experiments; the mice were 20 weeks old when they entered the exposures. The mice were exposed to the radon atmosphere for three 50-hour periods each week for intervals which ranged from 8 weeks to life. The chamber air flow was about 45 lpm and the concentrations of radon, RaA, RaB, and RaC, in the steady state, were about 0.50, 0.45, 0.23, and 0.13 microcurie per liter, respectively. This represented 2,000 WL, and a dose cumulation rate of 1,800 WLM per week of exposure. Measurements on mice exposed for 24 hours, to attain the steady state, showed that the average dose rates from alpha acitivity were; whole body, 5.5 rad per week; lung-trachea-bronchi, 280 rad per week; kidney, 18 rad per week; liver, 2 rad per week; and gastro-intestinal tract, stomach and contents, 60 rad per week. The dose to bronchial tissue may have been 5 to 10 times as large as that to the entire lung, or as much as 2,800 rad per week, but only the average dose to the lung is used here. The exposures ranged, then, from 14,000 to 72,000 WLM, and the estimated doses to whole lung ranged from 2,000 rad to 11,000 rad.

For the first experiment mice were exposed continually throughout life (Morken, *et al.*, 1966). The median exposure lifespan was 35 weeks, which represented a 50% shortening of life. At 40 weeks of exposure, when only a few mice remained, these mice were taken for histopathologic study. A fairly extensive microscopic examination of all organs was performed. No lesions were found in any organs or tissues — except the respiratory tract. The lesions seen in the respiratory track were much the same in the animals examined.

The trachea section, taken at the level of the thyroid, displayed mucosal lesions which were hyperplastic, metaplastic, and destructive; many times all of these lesions were observed in the same animal. The hyperplastic changes consisted of a thickening of the mucosa with an increased number of cells which, in general, tended to maintain a columnar structure. There was a number of layers of nuclei, which extended to the surface of the mucosa, instead of the usual single layer near the basement membrane.

Squamous metaplasia consisted of areas of thickened mucosa made of cells resembling squamous epithelium, which was sometimes accompanied by keratinization. The destructive changes consisted of either a loss of mucosa or a single layer of elongated flat mucosal cells containing few nuclei; sometimes inflammatory changes were seen in the mucous glands. These metaplastic and destructive changes frequently occurred together.

The lesions observed in the major bronchi were similar to those of the trachea. Hyperplasia of the mucosa was seen in which the mucosal cells maintained their columnar structure, but the mucosa contained numerous layers of cells with nuclei extending to the surface. Squamous metaplasia was present, but not as marked as in the trachea. The principal change seen in the small bronchi was the presence of large hyperchromatic nuclei.

In the lung parenchyma, intra-alveolar edema was present in varying degrees in all animals. Foci of alveolar phagocytes were seen in all animals; some phagocytes contained a brown pigment. A few small foci of adenomatoid proliferation of bronchi accompanied by fibrosis were seen in a few animals.

The lesions of the bronchial mucosa may be summarized as destructive, hyperplastic, and metaplastic. No infiltration carcinoma was found, but many of the changes may be considered as precancerous. The lesions seen in the alveoli probably resulted, in part, from the failure of the ciliary action of the bronchial mucosa.

The exposure dose for these mice amounted to 72,000 WLM, and the average dose to lung was about 11,000 rad, cumulated to death. The destructive effect of continued irradiation at this level of 2,000 WL was most evident in the trachea and major bronchi.

In the second experiment, groups of mice were exposed for 15, 25, and 35 weeks. The exposure doses were 27,000, 45,000 and 63,000 WLM, respectively; the resulting lung doses ranged from 4200 to 9800 rad. The purpose for the histopathology in this experiment was to observe the injury immediately following the end of exposure and to observe, over a period of eight weeks, the repair of the injury. The 35-week exposure confirmed

the median lethal dose of the previous experiment, but life shortening was not found for the 15 and 25 weeks of exposure.

In the third experiment, groups of mice were exposed for 10, 15, 20, and 25 weeks. This was a pathology-only experiment, which involved sacrifices immediately following exposure of each group; and then, beginning at the mouse age of 60 weeks, sacrifices at intervals of 10 weeks until all the mice were used (this occurred at 110 weeks). The experiment was done to examine late effects following the relatively short exposure periods used. The exposure doses ranged from 18,000 to 45,000 WLM; the resulting lung doses ranged from 2,800 to 7,000 rad.

Age-control mice were also examined at each sacrifice. The pathological effects found in these experiments were not large. In general, lesions in the trachea and bronchi were similar to, but not as extensive as those observed in the previous experiment. The extent of the lesions seen immediately after exposure seemed proportional to the cumulated dose (or exposure duration); the repair was so rapid that by eight weeks post-exposure, the tissues appeared normal. The trachea showed only focal atypism of moderate degree. Nuclei were large, and the cytoplasm was diminished with loss of cilia immediately after exposure. Little or no squamous metaplasia was seen. None of the tracheal alterations was believed to be precancerous.

Changes in the large bronchi were less marked than in the trachea. The terminal bronchioles showed atypical changes in the cuboidal lining epithelium. With increased post-exposure time, the epithelium in many terminal bronchioles tended to become flattened or to disappear.

The tumors encountered were variants of those which appear spontaneously in this strain of mouse (adenomas and foci of adenomatosis), and were seen in some of the older controls for these experiments. These tumors were seen at considerably lower ages in mice exposed to radon than in the controls. No tumors were found after 25 weeks of exposure in any animal sacrificed between 25 and 100 weeks from the end of exposure. Most of the adenomas showed qualitative changes suggestive of a more malignant behavior — greater cellular anaplasia, a higher mitotic rate, and invasion of adjacent lung tissue.

Neoplastic lesions (tumorlets) were seen in mice sacrificed between zero and eight weeks after the 35-week exposure. Most of these were of a type not encountered after any of the lower doses. These consisted of ill-defined areas containing many small, often intra-alveolar, nests of bizarre cells. Sometimes these were multiple in one or more lobes, and some cells were of a squamous type associated with what appeared to be keratin. Other tumors in this group had a glandular pattern exhibiting local malignant features. These tumorlets did not appear in other groups, and have since been observed in control rats.

Non-specific pulmonary effects, perhaps attributable to the irradiation, consisting of edema, increased numbers of macrophages, and a few small foci of interstitial fibrosis, were observed in some lungs at long intervals after exposures of 25 weeks; edema and many large macrophages were noted in all the mice exposed for 35 weeks. Moderate to severe pneumonitis was seen in late age in both the controls and exposed mice.

EXPERIMENTS WITH DOGS (Morken, *et al.*, 1972)

Experiments with dogs were carried out to provide irradiated lungs which approach the dimensions of human lungs, and to use a longer-lived animal so that observation could extend over several years. The initial experiment involved 42 dogs exposed to doses from 200 to 10,000 WLM, delivered in one to 50 days. Histological examinations were conducted at zero, 1, 2, and 3 years post-exposure, for all dose levels. The radon atmosphere of 1,800 WL was about the same as used in the mouse experiments. Exposures were made daily for five days each week, at 20 hours each day. The rate of cumulation of dose was about 2000 WLM per day of exposure. Exposure periods were 1, 2, 4, 8, 15, and 50 days.

Chambered control dogs as well as age control dogs were included. The chamber control dogs spent their 20 hours per day in a chamber identical in size and operation to the radon chamber, but the generator contained no radium.

Randomization procedures were followed to place the dogs into the various dose categories, and into the sacrifice schedule. At sacrifice the dog lung was partially fixed with formalin in situ, and a prescribed protocol was followed to provide samples from the lung, respiratory tract, lymph nodes, nasal epithelium, and turbinates of the nose. Gross examinations of all organs were made.

Several dogs were exposed to the radon atmosphere for about 20 hours, and then killed immediately on removal from the chamber. The lungs, trachea, and major bifurcation were removed within a few minutes. These tissues were weighed and measured; the RaB and RaC were measured over a period of two hours. The counting data were resolved by decay curve analysis to provide the information needed to compute the dose rate to the trachea and lung.

The average dose rate to whole lung amounted to one millirad per hour per WL, or 0.17 rad per WLM, when the data were analyzed by a curve fitting procedure. The average dose in rad per WLM, with standard deviation, amounted to 0.22 ± 0.16 when considering zero clearance, and 0.26 ± 0.19 when considering a clearance effect. Individual lung doses ranged from 0.08 to 0.79 rad per WLM.

For the trachea and bifurcation, the volume used in the dose calculation was determined from the averaged inside dimensions of the sections and an alpha absorption layer thickness of 70 μm. These doses ranged from 0.28 to 12.5 rad per WLM (mean 4.73 ± 4.36 standard deviation) for trachea and from 0.36 to 20.7 (5.03 ± 6.20) rad per WLM, for the bifurcation. The average dose rate to the upper respiratory tract was about 30 times that to the alveolar region. For the dog, then, the alveolar doses ranged from 34 to 1,700 rad, while the tracheal doses ranged from 1,000 to 50,000 rad. The dose to the bronchi may have been greater than that to trachea.

No cancer has been found in these dogs. Pathologic changes were found only in the alveolar and bronchiolar regions of the lung. Even immediately after exposure, when the lesions produced directly by the

radiation should have been most evident, injury to the trachea and bronchial tree was absent. In the lung, the microscopic lesions observed at any dose were subtle, variable, very small spatially, widely separated, and involved only a small fraction of the lung substance. Immediately at the end of exposure no significant differences from age or chamber controls were apparent for doses from 200 to 10,000 WLM. At one and two years after exposure, there was a probable increasing relation to dose of small foci of chronic inflammation. At three years post exposure this relation had disappeared for doses to 800 WLM, but was still probable for the larger doses. The lesion at all doses appeared as small patches of thickened (fibrotic) alveolar walls, with some metaplasia of the alveolar cells, and some epithelial hyperplasia of the bronchioles. Chamber control dogs were not different from age control dogs.

Animals exposed to the same dose expressed in WLM are not likely to receive the same radiologic dose. The doses, normalized to the WLM dose, as described above, and estimated from lung measurements on eleven dogs, varied from 0.08 to 0.79, with the average near 0.2 rad per WLM. It is not unlikely that in some cases a lesser WLM dose may produce greater injury than would a greater dose, since the adjacent dose ratios of 2 and 3 used were less than the ratio of 10 found among the animals.

EXPERIMENTS WITH RATS (Morken, *et al.*, 1971)

These experiments were performed with rats exposed to a radon concentration near one microcurie per liter for five hours each day, five days each week, to a total of 600 hours. The chamber air flow was reduced to about 22 lpm in both the radon and the control chamber. Five hours from starting the daily exposure, the radon concentration attained the desired level of 1 μCi per liter. The concentrations of RaA, RaB, and RaC attained by five hours were 0.75, 0.53, and 0.43 microcurie per liter, respectively. For short exposures, the cumulated dose is related linearly to the hours of exposure to the steady state values. The steady state concentration attained for radon, RaA, RaB, and RaC were 1.4, 1.1, 0.78, and 0.63 microcuries per liter, respectively. The chamber operated at 7,300 WL and the exposure dose rate was 43 WLM per hour. In 600 hours the cumulated dose amounted to 25,800 WLM. If the factor of 0.17 rad per WLM found for the mouse and the dog is applied, the cumulated average dose to lung was about 4,300 rad. If the factor of 30 applies for the ratio of trachea-to-lung dose, the upper respiratory tract may have received a cumulated dose of 130,000 rad.

Radon-exposed, chamber control, and age control rats, both regular and pathogen-free, were used. Lung tissues were taken for histopathology examination following the death of the animal. By 12 months from the end of 6 months of exposure, no cancer was evident in the standard rat. Cancer was also not evident in the pathogen-free rats at 6 months after the end of 6 months of exposure. It is difficult to distinguish among the exposed, chamber controls, and age controls. This experiment is not yet complete, and further detailed study will be made when all the animal data are available.

A complete appraisal of each of these experiments will include descriptions of life shortening, weight changes, hemogram changes (in some cases), and, of course, details on the changes in the lung and other organs. These appraisals will be published elsewhere. For the purpose of this paper, only a brief description of the major effects in the lung has been provided.

The results of these experiments on mice, dogs, and rats are significant in several aspects. While extensive injury was done to the bronchial tree during irradiation by the alpha particles, the lesions did not lead to bronchial tumors or cancer — even with continued irradiation; and after irradiation ceased, these lesions were quickly repaired. Late effects did not appear in the bronchial tree. In the alveolar region, the injury was not immediately evident, but appeared later in life, whether or not the irradiation continued. Major, perhaps permanent, changes occurred in the region of the respiratory bronchioles.

The essentially negative character of the results seen here suggest that alpha irradiation is a particularly inefficient way to produce radiation-specific tumors, if such exist, in the lung or respiratory tract. Since the later effects seen here were similar to those reported to follow radon-only inhalation at a lung dose of only 300 rad (Morken, 1973), an uncertainty exists concerning the role played by the massive lung doses provided by the inhaled decay products of radon.

The relative ineffectiveness of irradiation by alpha particles to produce even microscopically visible evidence of radiation-specific tumors, or cancer in the lung, or to produce permanent alterations in the respiratory track which could lead to bronchial carcinoma, is impressive. The only apparent late and permanent changes occurred in the alveolar regions of the lung, for a wide range of doses, and for observation times to three years in the dog, and one to two years in the mouse and rat. These alveolar changes may eventually lead to cancer, but the cancer would be of peripheral origin, and not the kind generally expected in view of the large doses to the respiratory tract.

A few experiments using radon combined with chemically toxic dusts may have demonstrated a potentiation or promotion of the tumorigenic properties of the chemical agents or of the tumors themselves. Kushneva (1961) exposed rats to quartz dust, to radon, and to the dust with radon. The dust, 50 mg, was given by intratracheal injection. The radon was given by inhalation at 8 μCi per liter in three one-hour exposures. Experimental silicosis developed rapidly in the rats which received quartz dust alone. Rats which recieved radon alone displayed a general systemic response. Rats which received the dust-and-radon showed a more intense silicosis, and the author felt that, for the combination, the radon vitally influenced the development of the silicosis by way of increased numbers of nodules, acceleration of fibrosis., and increased metaplasia of the bronchial and alveolar epithelium. The radiation dose amounted to only a few rad.

Kilibarda, *et al.*, (1967) reported similar experiments, but with longer exposures to radon. Silica was given intratracheally as a sterile suspension at 15 mg per rat. These investigators reported that radon inhalation appeared to aid the silicogenic effect only when given after the silicotic nodules were formed; before that, radon had no effect on the process. Once the nodules were formed radon inhalation made them larger and more easily delineated from the parenchymal tissue. Radon alone had no effect in producing tumors. The whole body doses for radon exposures, which ranged from 180 to 900 hours at a concentration of 0.07 μ Ci per liter, amounted to only a few rad — whereas the lung doese were in the area of 3,000 WLM or about 600 rad.

French workers (Perraud, *et al.*, 1970) have also reported an enhancement of the effects produced in lung by silica, uranium mineral, and cerium. The authors found that the chemical must be given before the radon is given. Epidermoid carcinoma resulted in the uranium and cerium experiments. An estimate of the exposure dose for the cerium experiment, 540 hours at 0.7 μCi per liter, is 10,000 WLM at 3,700 WL for a tissue dose of 3,000 rad. The tumors appeared in 10 months in the bronchiolar/alveolar region.

Gates, *et al.*, (1961) reported that external gamma or x-irradiation increases the incidence of spontaneous tumors, but did not appear to produce new kinds of tumors; this radiation, then, provides a promotional or potentiation effect.

A few researchers believe that while radon may produce little or no effect by itself, it is a powerful stimulus to act on tumors already present.

The French workers also found that the chemical agent might not be required, and reported a 100% incidence of pulmonary carcinoma in pathogen-free rats exposed at 1 μCi per liter for 600 hours (6 months). Tumors appeared by 10 months from the start of the exposure. The exposure dose may have been as large as 25,000 WLM. The rat experiment reported in this paper reproduced the French experiment with a different type of radon generator; and, as reported here, no tumors or cancer have appeared in the rats; this experiment is not yet complete, however.

The ability of other kinds of alpha emitting isotopes to induce bronchial and pulmonary cancer is well documented and familiar. Reviews of these experiments are available (Gates, *et al.*, 1961; Albert, 1966; Bair, 1970; Sanders, *et al.*, 1970). Inhalation of polonium-210 by rats with doses estimated from 70 to 500 rad resulted in primary lung cancer within two months post-exposure. Inhaled plutonium-239 by dogs produced lung cancer by 150 days with doses from 9,000 to 23,000 rad. ^{239}Pu given intratracheally to mice produced fibrosarcoma at 500 days with a dose of 115 rad, and squamous cell carcinoma at 400 days with a dose of 2,300 rad. ^{239}Pu inhaled by mice produced bronchiolar carcinoma at 500 days with a dose of 600 rad; in rats, epidermoid carcinoma was evident by 250 days at a dose of a few thousand rad.

Inhalation of long-lived alpha emitters results in an irradiation which continues long after the inhalation has ceased. Doses are usually estimated to the time of appearance of the lesion. With radon inhalation the dose is accumulated entirely within the period of exposure, or inhalation. If a latent period operates, the radon exposure yields a valid dose — whereas the other materials do not. Thus, the tumor-producing doses may be considerably less than the estimated doses reported for other isotopes. With the continuously irradiating isotopes, it appears that tumors occur sooner for larger dose rates, but this idea has not been subjected to critical study.

A large number of experiments have been done with implanted sources. These are not considered here because the implant method involves the manufacture of a lesion which may become a part of the response if irradiation acts to promote lesions to tumors.

Thus it appears that relatively small doses of alpha radiation can produce tumors and cancer in the lung in relatively short periods of time, and especially within the lifetime of the mouse or rat. Since the radiation from radon or its decay products have not accomplished this, there may be some hesitation to label this tumor production a radiation effect.

The materials which have produced cancer are chemically reactive and long-lived so that appreciable amounts of the material are present throughout the exposure, compared to the radon exposures. The specific activity of polonium-210 is 4,300; that for plutonium-239 is 0.06. In contrast, the specific activities for the radon decay products range from 10^8 to 10^{16}; while for radon it is 10^5. In terms of a radiation-to-chemical exposure, the decay products are purer sources of radiation by factors of 10^5 to 10^{13} for polonium and 10^7 to 10^{15} for plutonium.

CONCLUSIONS

It appears reasonably easy to induce lung cancer with radionuclides of small specific activity (large specific mass). It has also been easy to induce lung tumors with non-radioactive chemical compounds. However, it has been extraordinarily difficult to produce even small long-lasting effects with alpha irradiation from radon and its decay products, and lung cancer has not been unequivocally demonstrated with radon.

Alpha radiation may promote chemically produced lesions leading to tumors and cancer, but the lesions must be there first. This suggests that alpha radiation may act indirectly through a systemic response — rather than directly on the cell.

Thus chemical induction of lung cancer by radioactive elements may be of greater importance than induction by alpha radiation. Threshold limits based on chemically active elements should not be applied to elements of greater radiation purity.

It would be prudent to study the probable chemical behavior with cells of the heavy metal isotopes, regardless of their radioactive natures. The use of radon may permit resolution of the effect into its radiological and chemical parts.

REFERENCES

Albert, R. E., (1966), *Thorium, Its Industrial Hygiene Aspects,* pp 100. Academic Press.

Bair, W. J., (1970), *Inhalation of Radionuclides and Carcinogenesis,* in Proceedings of the Conference on Inhalation Carcinogenesis, U. S. A. E. C. Division of Technical Information.

Gates, O. and S. Warren, (1961), *Histogenesis of Lung Carcinoma in Mice.* Arch. Pathology 71, 693.

Kilibarda, M., V. Visnjic, D. Panov, R. Radovanovic and L. Novak, (1967), *Deposition of Some Radon Daughters in Rats after Inhalation of Radon, with Special Consideration of the Simultaneous Influence of SiO2,* in Diagnosis and Treatment of Deposited Radionuclides, pp 222. Excerpta Medica Foundation.

Kushneva, B. S., (1961), *On the Problem of the Long Term Effects of the Combined Injury to Animals of Silicon Dioxide and Radon,* in AEC-tr-4473, pp 21-28.

Morken, D. A. and J. K. Scott, (1966), *The Effects on Mice of Continual Exposure to Radon and its Decay Products on Dust.* University of Rochester Atomic Energy Project, Report- UR-669.

Morken, D. A. and C. L. Yuile, (1971), (unpublished materials.)

Morken, D. A. and G. W. Casarett, (1972), (unpublished material).

Morken, D. A., (1973), *The Biological Effects of the Radioactive Noble Gases,* this Proceedings.

Perraud, R., J. Chameaud, R. Masse and J. Lafuma, (1970), *Cancers Pulmonaires Experimentaux chez le Rat Apres Inhalation de Radon Associe a des Poussieres non Radioactives.* C. R. Acad. Sci, Paris, 270, 2594.

Sanders, C. L., Jr., R. C. Thompson and W. J. Bair, (1970), *Lung Cancer: Dose Response Studies with Radionuclides,* in Proceedings of the Conference on Inhalation Carcinogenesis, pp 285-303. U. S. AEC Division of Technical Information.

BIOLOGICAL EFFECTS OF DAILY INHALATION OF RADON AND ITS SHORT-LIVED DAUGHTERS IN EXPERIMENTAL ANIMALS*

R. F. Palmer, B. O. Stuart, and R. E. Filipy
Biology Department
Battelle
Pacific Northwest Laboratories
Richland, WA 93352

Abstract

Syrian golden hamsters, C57BL mice, and specific-pathogen-free rats were exposed simultaneously in groups of 16 animals each for 90 hours per week to aerosols consisting of radon plus 3000-6000 Working Levels of radon-daughters with and without 18 mg/m^3 carnotite uranium ore dust. Condensation nuclei concentrations ranged from 2000-4000 per ml and from 90,000-120,000 per ml in the chamber without and with uranium ore dust, respectively. At 4 months of exposure only one of the rodents remained alive. Histopathology of radon-daughter exposed mice includes acute interstitial pneumonitis, severe pulmonary congestion, and supperative rhinitis; mice inhaling radon-daughters with ore showed these lesions plus macrophage proliferation, alveolar septal cell hyperplasia, and bronchial epithelial hyperplasia. Hamsters inhaling radon-daughters showed proliferating lesions characterzied by alveolar septal thickening, bronchiolar epithelial hyperplasia, septal fibrosis, and occasionally adenomatoid metaplasia and squamous metaplasia. Hamsters inhaling radon-daughters with ore dust showed similar effects plus granulomatous response and intense septal fibrosis. Rats inhaling radon-daughters showed lesions similar to those of hamsters but more focalized with classic radiation pneumonitis; rats exposed to radon-daughters with ore showed similar lesions, with greater consolidation and pneumoconiosis. These findings will be discussed in relation to pulmonary pathology in uranium miners.

INTRODUCTION

Initial studies in our laboratory with hamsters exposed for their lifespan to 30 Working Levels (WL) of radon-daughters produced only slight pulmonary responses. A Working Level (WL) is defined as any combination of short-lived radon-daughters in one liter of air that will result in the ultimate emission of 1.3 x 10^5 MeV of alpha energy from radioactive decay. Similar levels have been found in some areas of operating uranium mines. Lifespan exposures of hamsters to 600 WL radon-daughters with uranium ore dust caused pulmonary lesions, including vesicular emphysema, fibrosis, metaplasia, and adenomatous lesions with anaplasia. A subsequent experiment involved lifespan exposures of hamsters to 1,200 WL radon-daughters, diesel engine exhaust, and uranium ore dust. These hamsters showed more extensive and severe pulmonary lesions, with accelerated development of cuboidal and squamous metaplasia of the bronchial epithelium, and the appearance of squamous tumors.

Earlier studies (Morken and Scott, 1966) with mice exposed to 1,750 WL radon-daughters on room air dust (150 hrs/wk), showed a significant reduction of lifespan. Workers in France (Perraud, *et al.*, 1972) have reported peripheral tumors in the lungs of SPF rats after 500 hours of exposures to approximately 1 μCi per liter of radon, but interpretation of these results is extremely difficult because the levels of radon-daughters were not described, and no correlation to human exposure histories based on Working Levels (radon-daughter levels) was possible.

This paper presents the results of a pilot study that we conducted to correlate these results (obtained in three different laboratories) to provide direct interspecies comparison of the effects of exposure to identical aerosols, and to determine if there exists an increased sensitivity or resistance of one or more of these species of rodents. We prepared systems for simultaneous exposures of mice, hamsters, and SPF rats in the same chambers to high levels of radon-daughters, with and without concomitant exposure to uranium ore dust (carnotite). Exposure of the three species in these initial studies were made at levels of radon-daughters calculated to induce tumor production or acute death.

METHODS

The animals used in this study were SPF Wistar rats, Syrian-Golden hamsters, and C57 B1/6J mice. They were all males and approximately 100 days old at the start of exposures. The animals were individually housed in two types of compartmented, stainless steel mesh cages. There were 16 compartments for mice or hamsters in one type of cage, and 8 compartments for rats in the other type. Two cages of rats, one of hamsters, and one of mice were in each of the two exposure chambers. Ten control animals of each species were individually housed in the exposure room, but not in a chamber. Food and water were available to the animals at all times. The experimental design is shown in Table 1.

**This paper is based on research performed under U. S. Atomic Energy Commission Contract AT(45-1)-1830.*

The two exposure chambers were nearly cubical with volumes of 1,700 liters. As seen in Figure 1, the animal cages were supported on racks that positioned the bottoms of the cages 81 centimeters below the chamber inlets for radon or radon and uranium ore dust. Unfiltered room air entered at the top of each chamber, passed through the chambers, and left via outlets centered 20 cm above the chamber bottoms. These outlet air streams passed through valved flow meters and absolute filters, and were then discharged into a high-flow, low-vacuum system whose outlet was diluted in the building exhaust stack prior to discharge to the atmosphere.

A separate radon generator was used for each chamber. Saturated air bubbling through acid solutions of radium chloride at a rate of 150 ml/min swept radon from the generators through traps to remove acid vapor that may have been carried out of the generators. This radon laden air was filtered just prior to introduction into the chambers. The radon entered the center top of the chambers where it mixed with incoming room air in the case of Chamber 1, and with incoming room air and uranium ore dust in Chamber 2. The uranium ore dust was introduced into Chamber 2 by means of a Wright Dust Feed Mechanism mounted on top of the chamber. Ore dust with a count median diameter of 0.24 μm was maintained at a concentration of 18 $\pm$ 4 μg per liter in the chamber during exposure periods. This level was selected to coincide with those used in our previous studies, serving to lower the unattached radon-daughters to only a few percent.

Initial measurements in the empty chambers indicated that nearly twice as much radon would be required in Chamber 1 without ore dust in order to attain approximately equal Working Levels of radon-daughters in the two chambers. This was felt to be due to greater losses of radon-daughters to the walls of Chamber 1 than to those of Chamber 2 which contained the ore dust. As a consequence, one radon generator was loaded with approximately 1.3 Ci of radium and the other with approximately 0.7 Ci. With a total air flow of 35 liters per minute through each chamber, these levels of radium led to radon concentrations of 4.8 μCi/liter in Chamber 1 and 2.5 μCi/liter in Chamber 2.

Radon levels in the chambers were continuously monitored during exposures, and each chamber was sampled at least once during each exposure period for measurement of radon-daughter concentrations, using a two channel alpha analyzer employing a solid state surface barrier detector. Concentrations of condensation nuclei were measured one or more times during each exposure period using a Gardner nuclei counter. These concentrations ranged from 2,000 to 24,000 per ml in Chamber 1 and from 57,000 to 130,000 per ml in Chamber 2.

When animals were first introduced into the chambers, measured levels of radon-daughters and condensation nuclei showed little change in the chamber containing the aerosol of radon-daughters with uranium ore dust (Chamber 2). However, in Chamber 1, without uranium ore dust, radon-daughters were found to be reduced by a factor of at least four from levels observed in the empty chamber. Condensation nuclei were reduced from approximately 19,000 to 2,000 per ml. The radon level in the chamber remained at approximately 4.8 μCi per liter, however, so it was decided to continue the animal exposures with unequal Working Levels of radon-daughters in the two chambers.

The animals were exposed in the two chambers for approximately 90 hours per week, in two continuous 45-hour periods. All animals were weighed biweekly, and exposures were continued until all the animals had died or were sacrificed when moribund. At death the nose, trachea, lungs, liver, spleen, and kidneys of each animal were retained for histopathological investigation.

RESULTS

Table 2 shows the mean weights plus or minus the standard error of the means for the mice in the control and in the two exposure groups at various times after the start of exposures. As early as 55 days after the start of exposures, both exposure groups showed significant weight loss; i.e., 22% reduction from control animal weights. Table 3 shows the same data for hamsters. In this species, the reduction in weight did not occur as soon after the start of exposures, but it was just as dramatic as exposures progressed. As observed in the mice, the weights of the hamsters exposed to radon-daughters with uranium ore dust show greater reduction from control hamster weights than do those exposed to radon-daughters without ore dust. The weight data of exposed rats shown in Table 4 tell the same story. Significant reductions from control rat weights were seen in both exposure groups by 55 days after the start of exposures, with the greater weight reductions occurring in the rats exposed to radon-daughters with ore dust. It is evident that all three species showed a marked weight loss in both exposure groups, with those exposed to radon-daughters plus uranium ore dust showing more drastic effects in all three species.

Figure 2 shows the survival curves for each of the species exposed in Chamber 1, together with a curve showing the Cumulative Working Level Hours (CWLH) of radon-daughters to which they were exposed. The increase in the slope of the CWLH curve is a result of the radon-daughter concentrations increasing as the number of animals in the chamber decreases. The radon level in the chamber remained at $\sim$ 4.8 μCi/liter. It can be seen that the first death, a mouse, occurred only 25 days after the start of exposures. The last animal to die, a hamster, had been exposed to over 8 million CWLH of radon-daughters during the 178 days it survived after the start of exposures. The mice died earlier and at a faster rate than did rats and hamsters, but as the exposures continued the percent surviving showed little difference among the three species.

Figure 3 shows the survival curves for each of the species exposed to radon-daughters with uranium ore dust in Chamber 2. The nearly constant slope of the CWLH curve shows that the concentrations of radon-daughters in the chamber were little affected by the number of animals in the chamber. Half of the mice in this

group had died by 30 days after the start of exposures, compared to nearly 120 days before 1/2 of the rats and hamsters were dead. The first rat died 52 days after the start of exposures, at which time it had been exposed to ∿1.6 million CWLH of radon-daughters. The last hamster to die had been exposed to 7 million CWLH during the 144 days it survived after the start of exposures.

Table 5 shows the geometric mean survival times, and their 95% confidence limits, for the rats, hamsters, and mice in each of the two exposure chambers. All three species show significantly shorter survival times following exposure to radon-daughters with ore dust than they do following exposure to radon-daughters without ore dust.

Histopathological examination of tissues from the rats, hamsters, and mice reveals varying degrees of radiation pneumonitis due to inhalation of radon-daughters. The characteristic septal fibrosis, alveolar lining cells sloughed into alveolar lumena, and invasion by macrophages, as well as the atypical nuclei of alveolar septal cells, are illustrated in Figure 4. In animals exposed to uranium ore dust with radon-daughters, one sees a pulmonary response to particulate materials diagnosed as uranium ore pneumoconiosis. Macrophages laden with uranium ore dust, and the septal fibrosis characteristic of this lesion are shown in Figure 5. Bronchiolar epithelial hyperplasia was commonly seen in the lungs of animals exposed to radon-daughters.

Mice and rats seem less prone to the pulmonary lesions than hamsters, but are afflicted with quite severe lesions of the upper respiratory tract. Severe suppurative rhinitis and squamous metaplasia of nasal epithelium (Figure 6) was a common observation in the mice and rats used in this experiment. Dense exudate containing many neutrophils was seen in the nasal passages. Suppurative laryngitis and bronchitis were frequent observations in all three species, but were most severe in rats (Figure 7). Suppurative tracheitis was also quite common, and, in at least two mice, the tracheal epithelium had undergone a keratinizing squamous metaplasia (Figure 8). The squamous nature of the ordinarily columnar epithelial cells and the keratin layer are quite atypical of the trachea.

Hamsters also had a high incidence of rhinitis and laryngitis, but had a higher incidence of pulmonary consolidation due to septal cell hyperplasia, interstitial pneumonitis, and macrophage proliferation. An additional lesion found with approximately equal frequency in rats and hamsters was an adenomatoid metaplasia of alveolar epithelium. This lesion was found in small foci in rat lungs, but involved large areas in hamster lungs. In two hamsters exposed to radon-daughters without ore dust, the lesion had undergone squamous metaplasia (Figure 9). In view of previous observations in hamsters, this lesion is considered pre-malignant; i.e., a stage just previous to epidermoid carcinoma.

In all three species, the major differences between exposures to radon-daughters only and radon-daughters with uranium ore, seem to be the increased septal fibrosis and macrophage proliferation in the latter. The uranium ore dust particles also seem to cause a slightly higher incidence of pulmonary emphysema and septal cell hyperplasia than found in animals exposed to radon-daughters only.

DISCUSSION

This pilot study of the effects of inhalation of high levels of radon-daughters, with and without concomitant uranium ore dust, by three rodent species has shown several interesting results.

Exposures for 90 hours per week to radon-daughters ranging from 2,000 to 8,500 WL, with and without 18 μg per liter uranium ore dust, caused marked life-shortening in all three species. Marked reduction in body weights occurred in all three species, with weight losses of 30-50% of control animal values in all species after 3 1/2 months of exposures. Mice exposed to radon-daughters and ore dust were particularly susceptible in terms of mortality, although the lungs of these animals showed very little pathological change.

Classical radiation pneumonitis with alveolar septal fibrosis and occasional bronchiolar epithelial hyperplasia were the predominant deep lung lesions seen in all species. In contrast to hamsters exposed 30 hours per week to 1,200 WL of radon-daughters and uranium ore dust, proportionately more of the pathology was seen in the upper respiratory tracts of the hamsters in the present study. The contrast between markedly affected trachea and major bronchi vs. relatively little effects in deep lung was most evident in rats. Findings of severe suppurative laryngitis and bronchitis were frequent in rats, and may have been an important contributing factor to their death. These findings dictate further studies involving sacrafice and radioactivity analyses of tracheal and lung tissues to determine relative absorbed radiation doses at these sites for correlation with developing degenerative and proliferation changes of the respiratory tract in each species.

Our next experiment involves exposures of rats, hamsters, and mice during five, 6-hour periods per week. This lowered exposure rate may allow the animals to live long enough for proliferative epithelial changes to progress beyond the stage of squamous metaplasia to possible invasive tumor formation.

REFERENCES

Morken, D.A. and J.K. Scott, (1966), *The Effects on Mice of Continued Exposure to Radon and Its Decay Products on Dust.* UR-699. University of Rochester, New York.

Perraud, R., J. Chameaud and J. Lafuma, (1972), *Cancer Broncho-Pulmonaire Experimental Du Rat par Inhalation de Radon.* Extraits Francais Med Chir Thor, 26, 25-41.

TABLE 1. Experimental Design.

Group	Number of Animals	Exposure (90 Hours per Week)
1	16 of Each Species	2,000-8,500 WL Radon-Daughters
2	16 of Each Species	6,000-7,500 WL Radon-Daughters with Uranium Ore Dust (18 mg/m^3)
3	10 of Each Species	Controls (Not Housed in Chamber)

TABLE 2. Mouse Weights (Mean ± S.E. in Grams).

Days Since Start Of Exposures	Radon-Daughters	Daughters + Ore	Controls
0	27 ± 1	27 ± 1	28 ± 1
55	25 ± 1	25 ± 1	32 ± 1
111	23 ± 1	21	34 ± 2
132	19 ± 1	---	34 ± 2

TABLE 3. Hamster Weights (Mean ± S.E. in Grams).

Days Since Start Of Exposure	Radon-Daughters	Daughters + Ore	Controls
0	117 ± 3	120 ± 3	124 ± 3
55	121 ± 3	119 ± 4	128 ± 4
111	106 ± 4	99 ± 12	135 ± 3
132	93 ± 8	68	136 ± 3

TABLE 4. Rat Weights (Mean ± S.E. in Grams).

Days Since Start Of Exposures	Radon-Daughters	Daughters + Ore	Controls
0	466 ± 9	442 ± 7	470 ± 10
55	479 ± 9	439 ± 10	544 ± 12
111	407 ± 17	364 ± 26	600 ± 14
132	401 ± 23	321	616 ± 15

TABLE 5. Geometric Mean Survival Times (Days Since Start of Exposures With 95% Confidence Limits).

	Mice	Hamsters	Rats
Radon-Daughters	94^{120}_{73}	131^{149}_{115}	120^{132}_{109}
Daughters + Ore	43^{63}_{29}	107^{116}_{98}	105^{121}_{90}

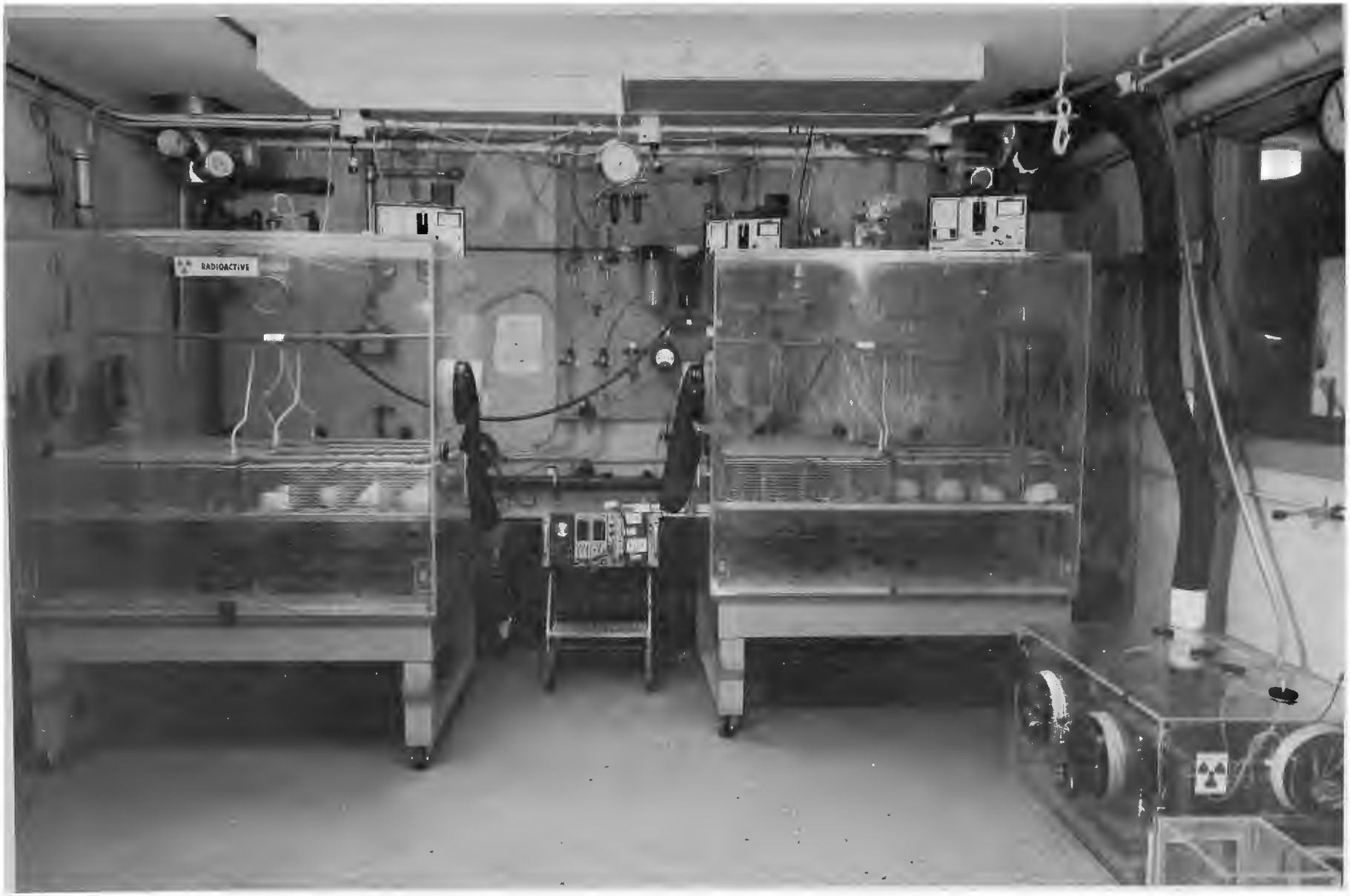

Figure 1. View of multi-species exposure chambers and glovebox containing the radon generators.

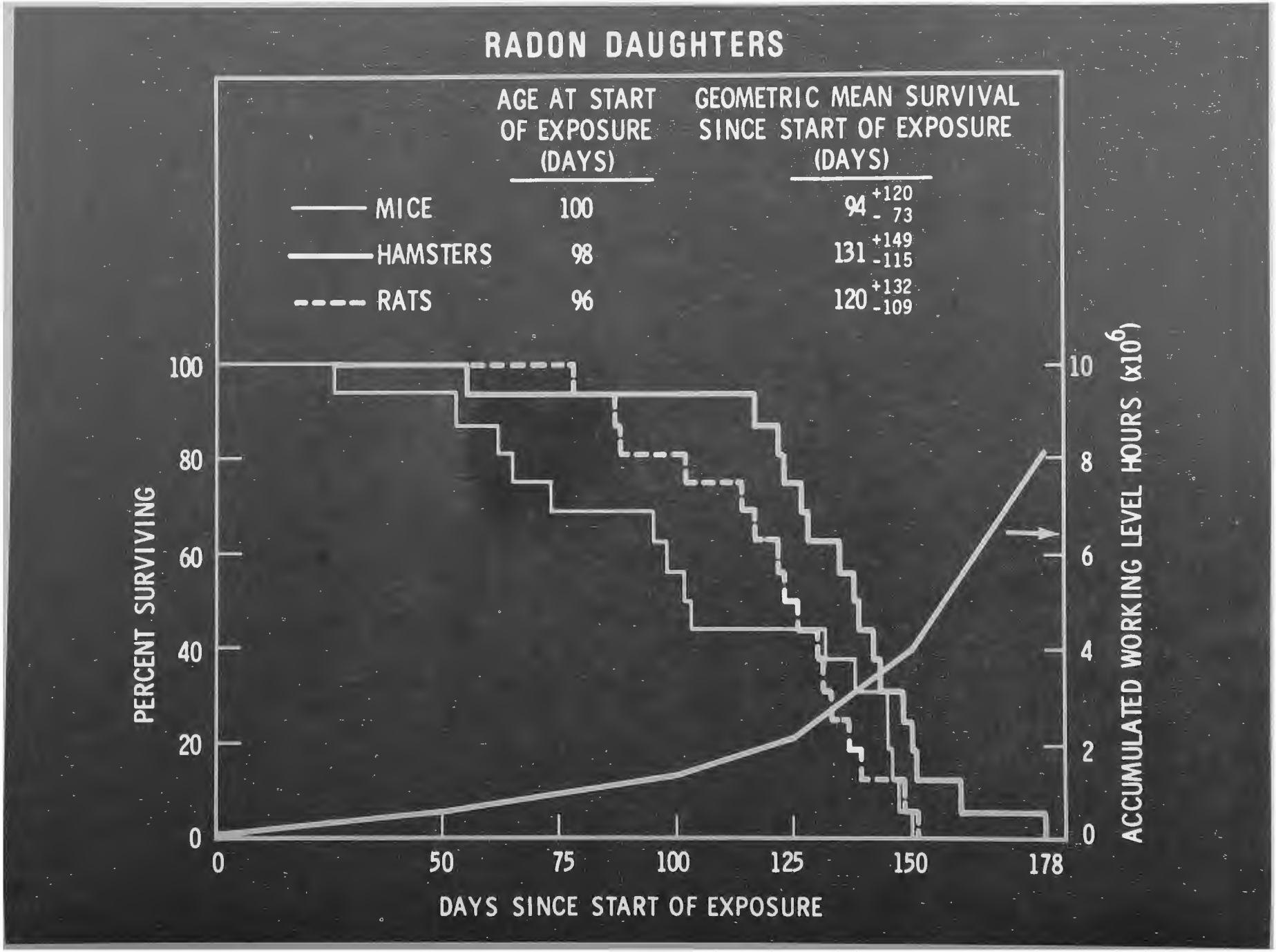

Figure 2. Survival curves of rats, hamsters, and mice exposed to radon-daughters without concomitant uranium ore dust, together with a curve showing the Cumulative Working Level Hours of radon-daughters to which they were exposed.

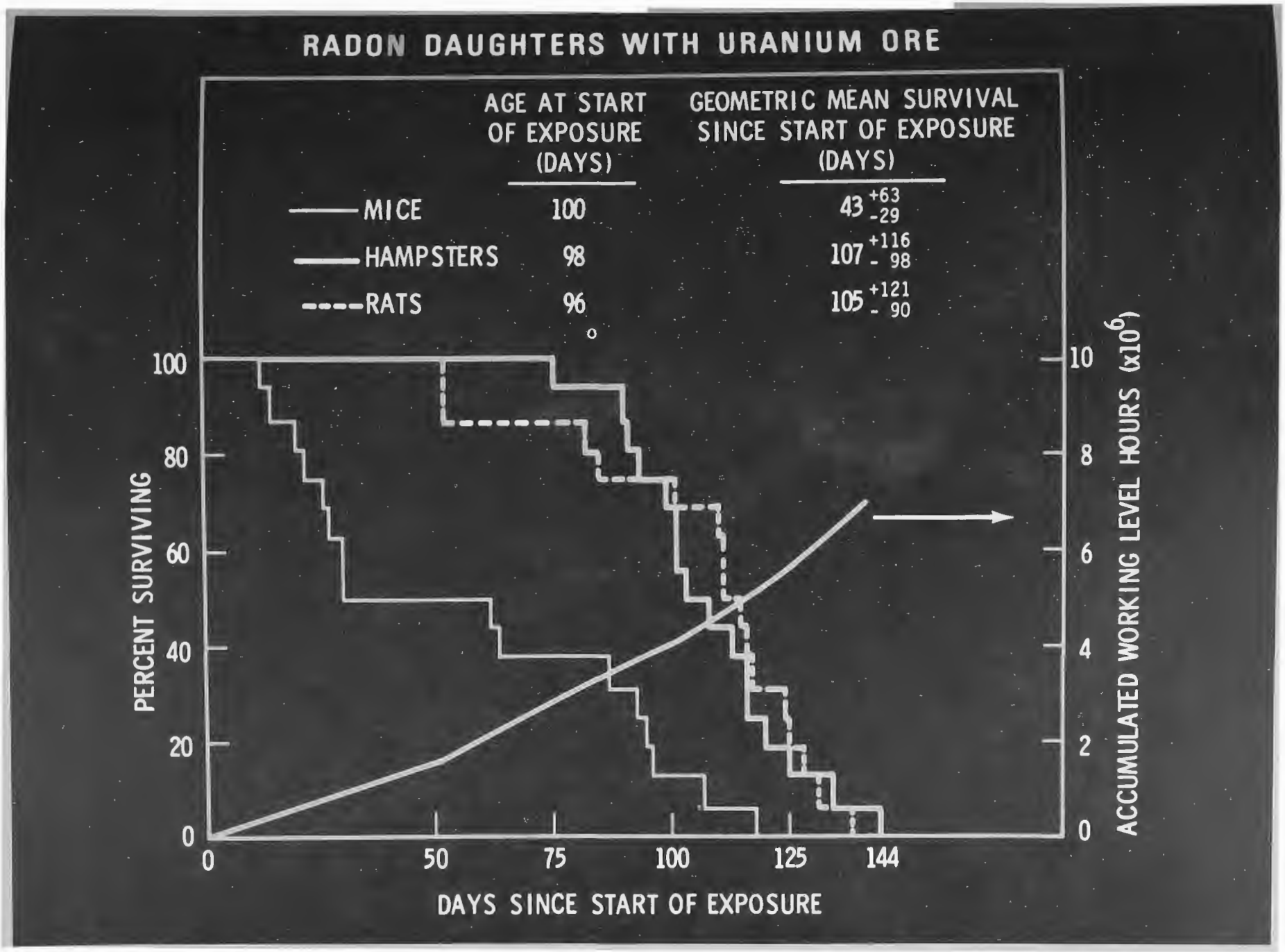

Figure 3. Survival curves of rats, hamsters, and mice exposed to radon-daughters with concomitant uranium ore dust, together with a curve showing the Cumulative Working Level Hours of radon-daughters to which they were exposed.

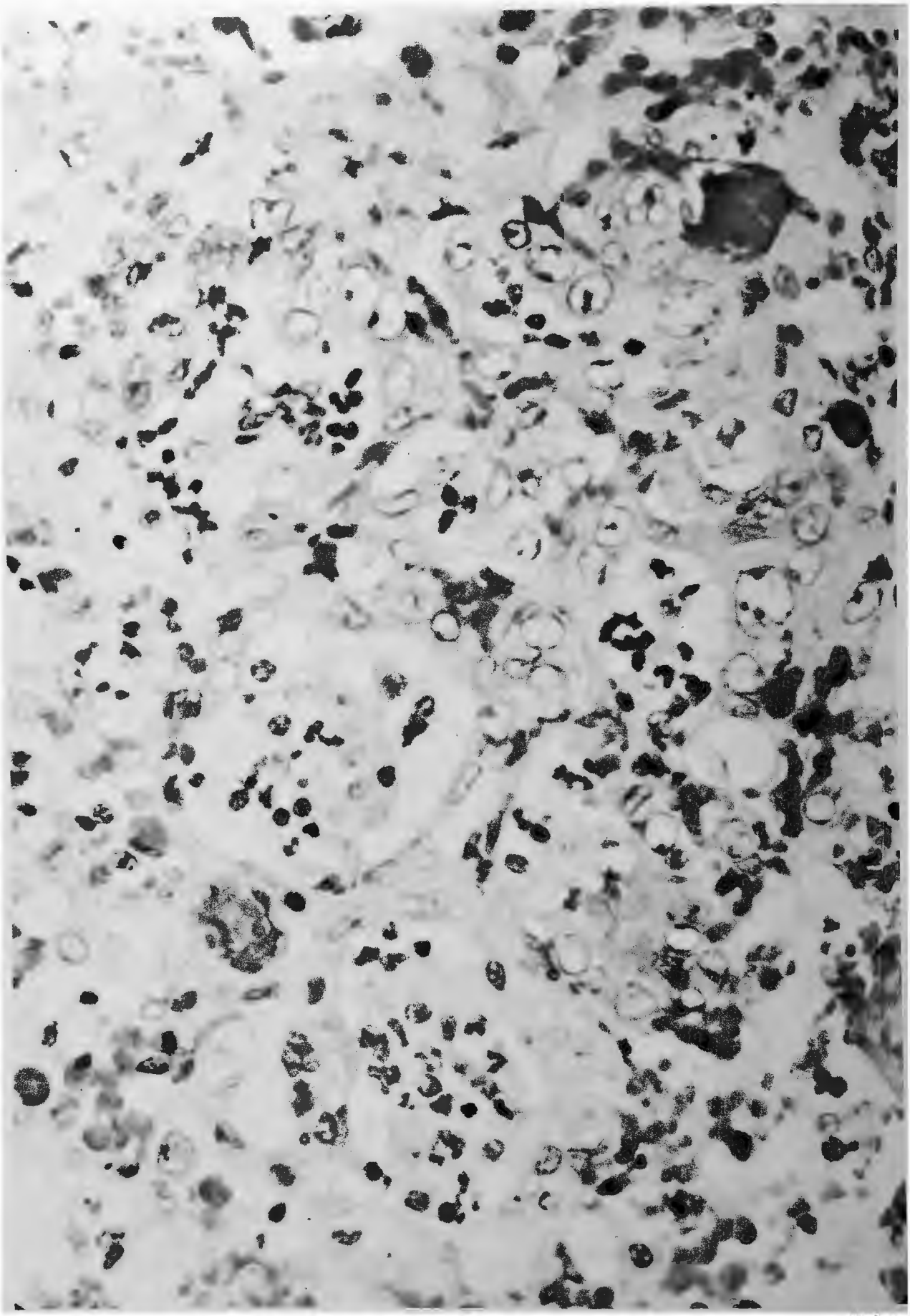

Figure 4. Radiation pneumonitis in hamster lung showing characteristic septal fibrosis, alveolar lining cells sloughed into alveolar lumena, invasion by macrophages, and atypical nuclei of alveolar septal cells. (H&E, 660X).

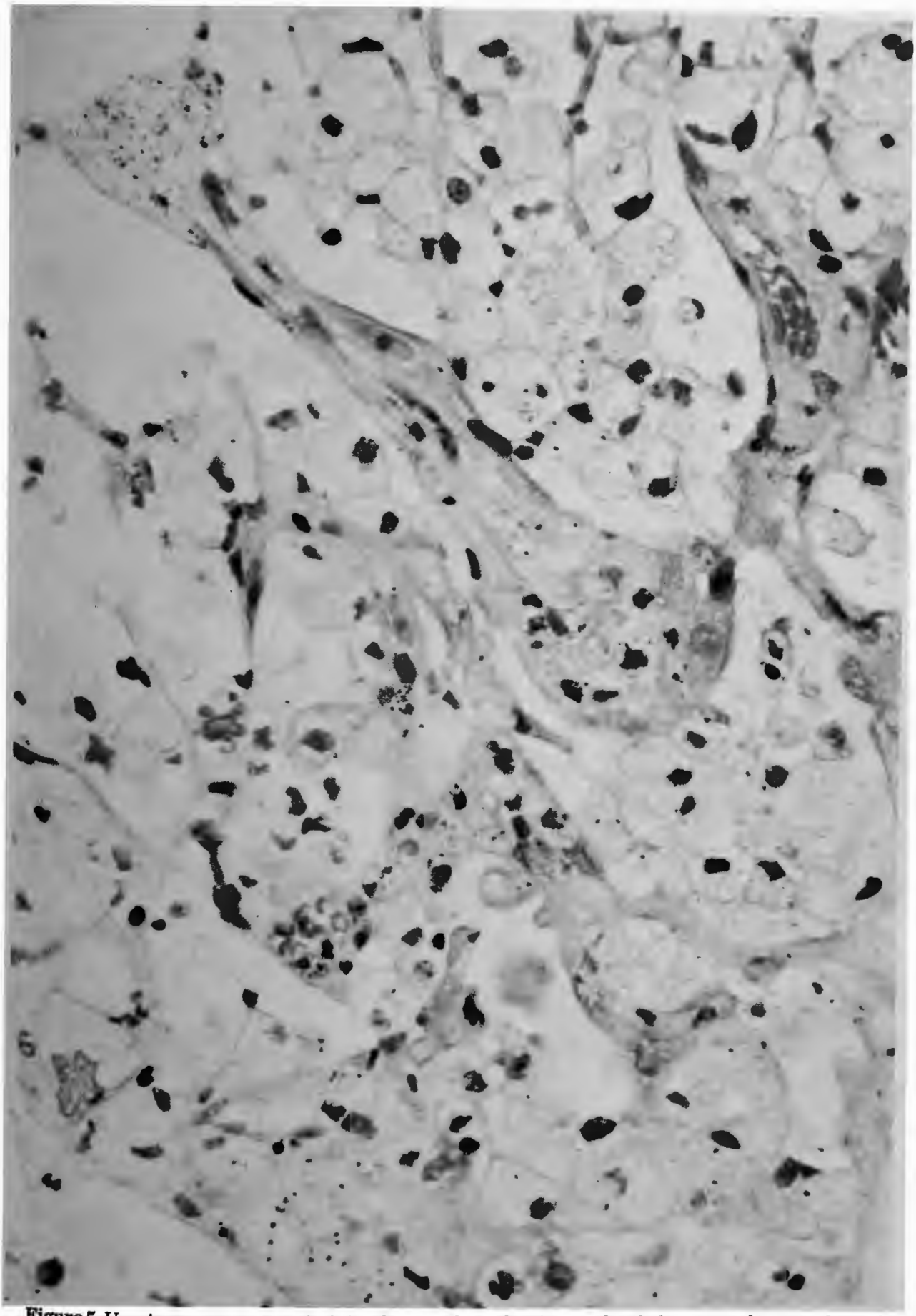

Figure 5. Uranium ore pneumoconiosis in a hamster lung showing ore dust laden macrophages and septal fibrosis (H&E, 660X).

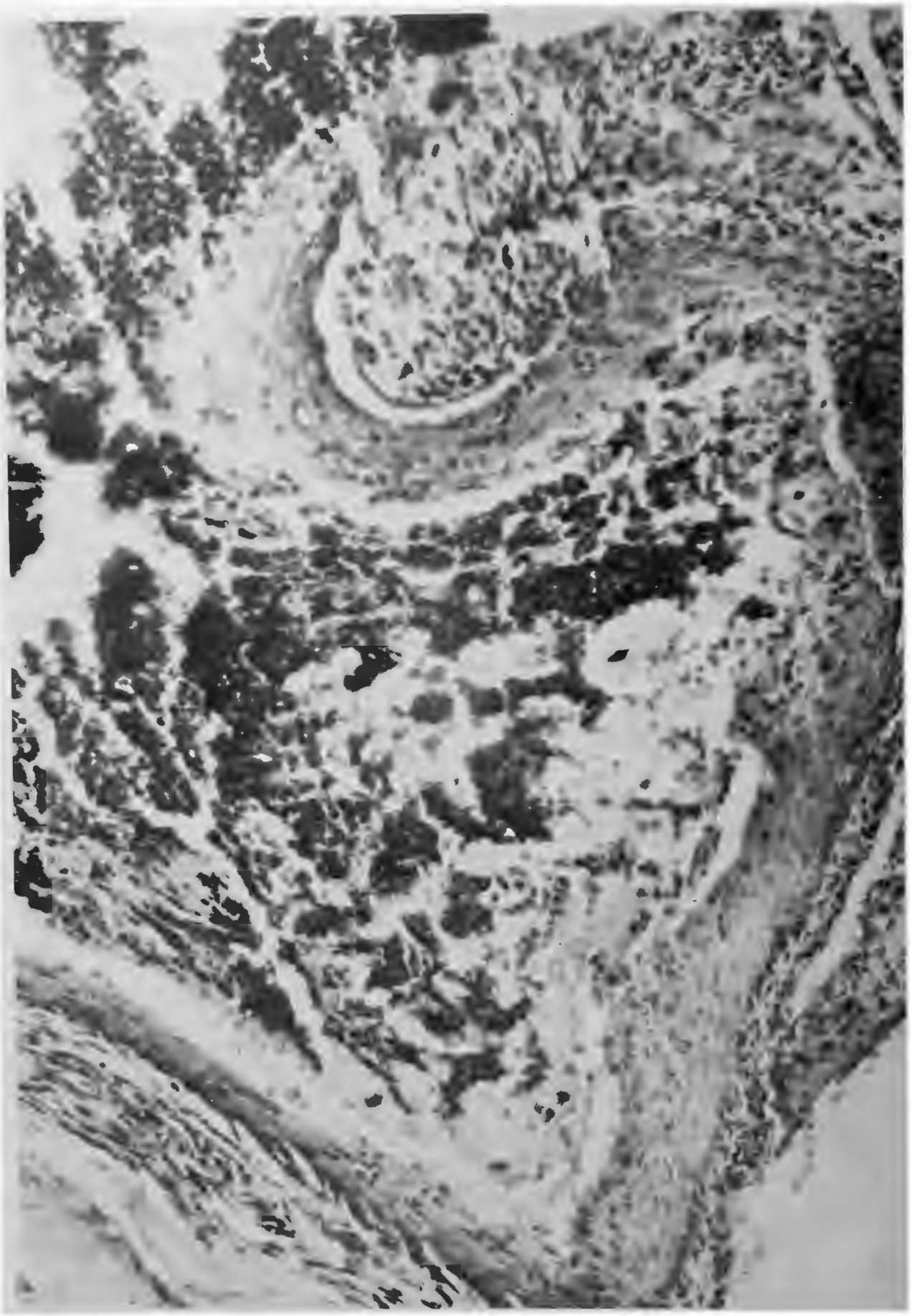

Figure 6. Suppurative rhinitis and squamous metaplasia of nasal epithelium seen in a mouse exposed to radon-daughters and uranium ore dust (H&E, 415X).

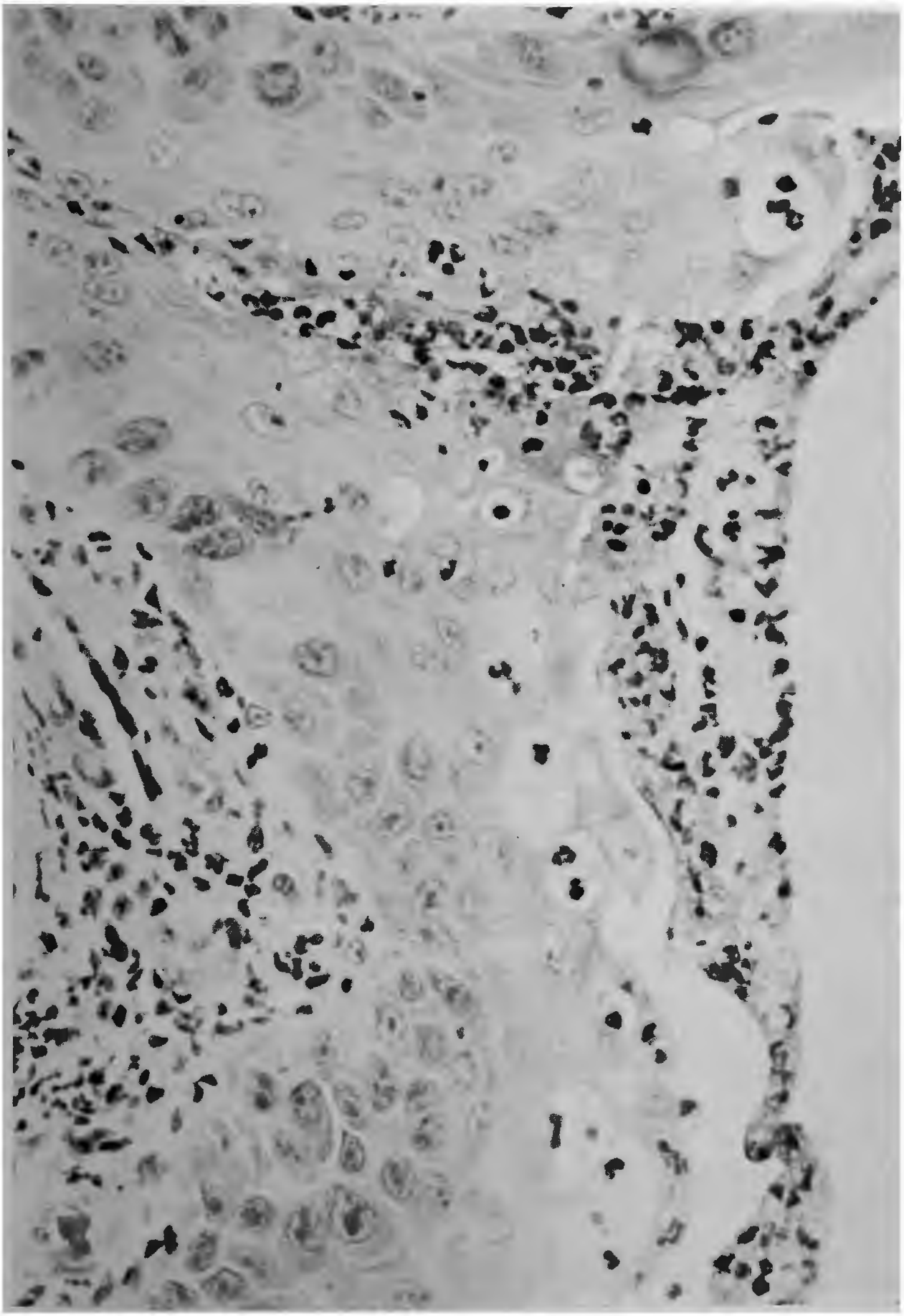

Figure 7. Suppurative laryngitis and bronchitis in a hamster (H&E, 660X).

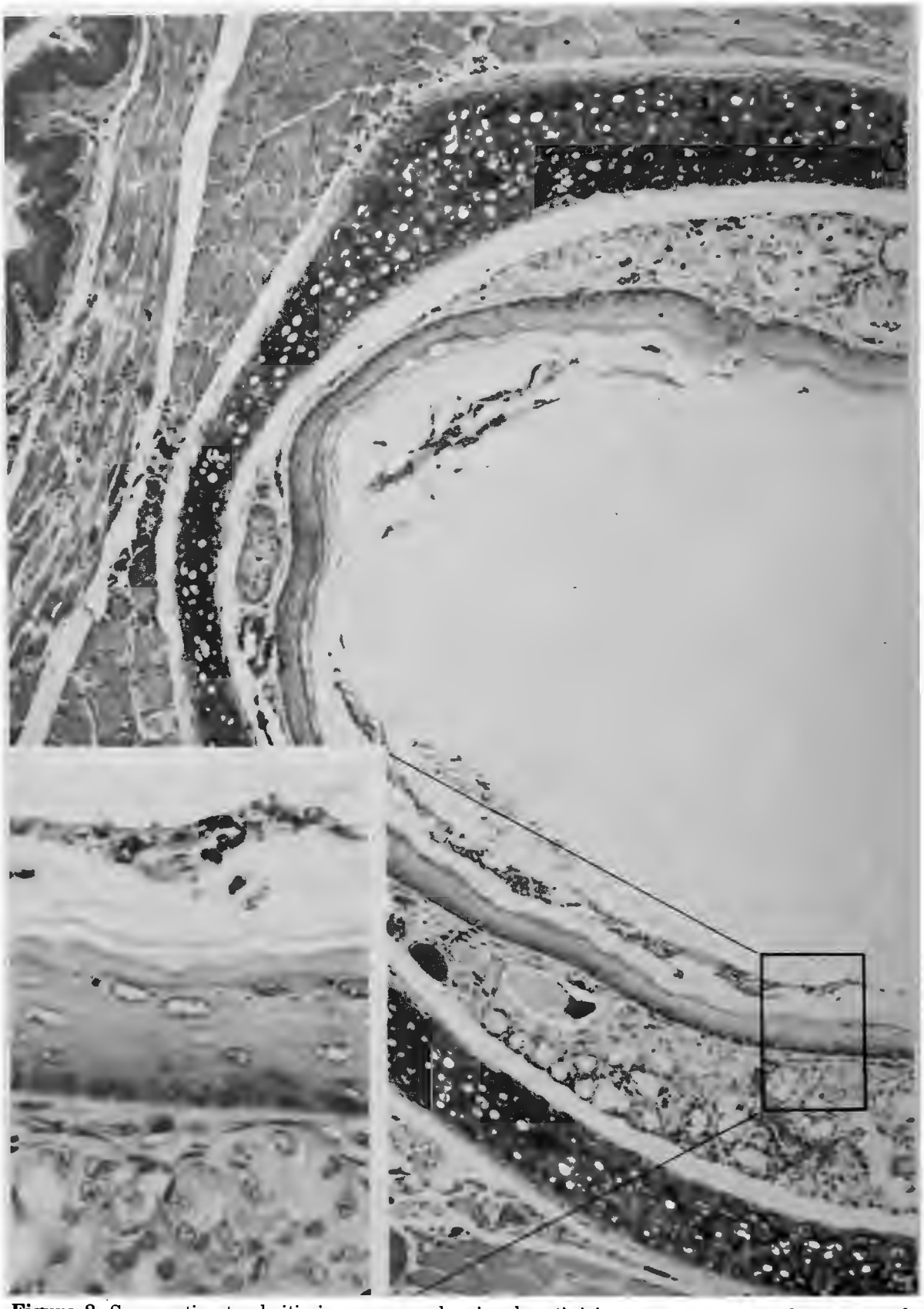

Figure 8. Suppurative tracheitis in a mouse showing keratinizing squamous metaplasia of tracheal epithelium (H&E, 120X; Insert X540).

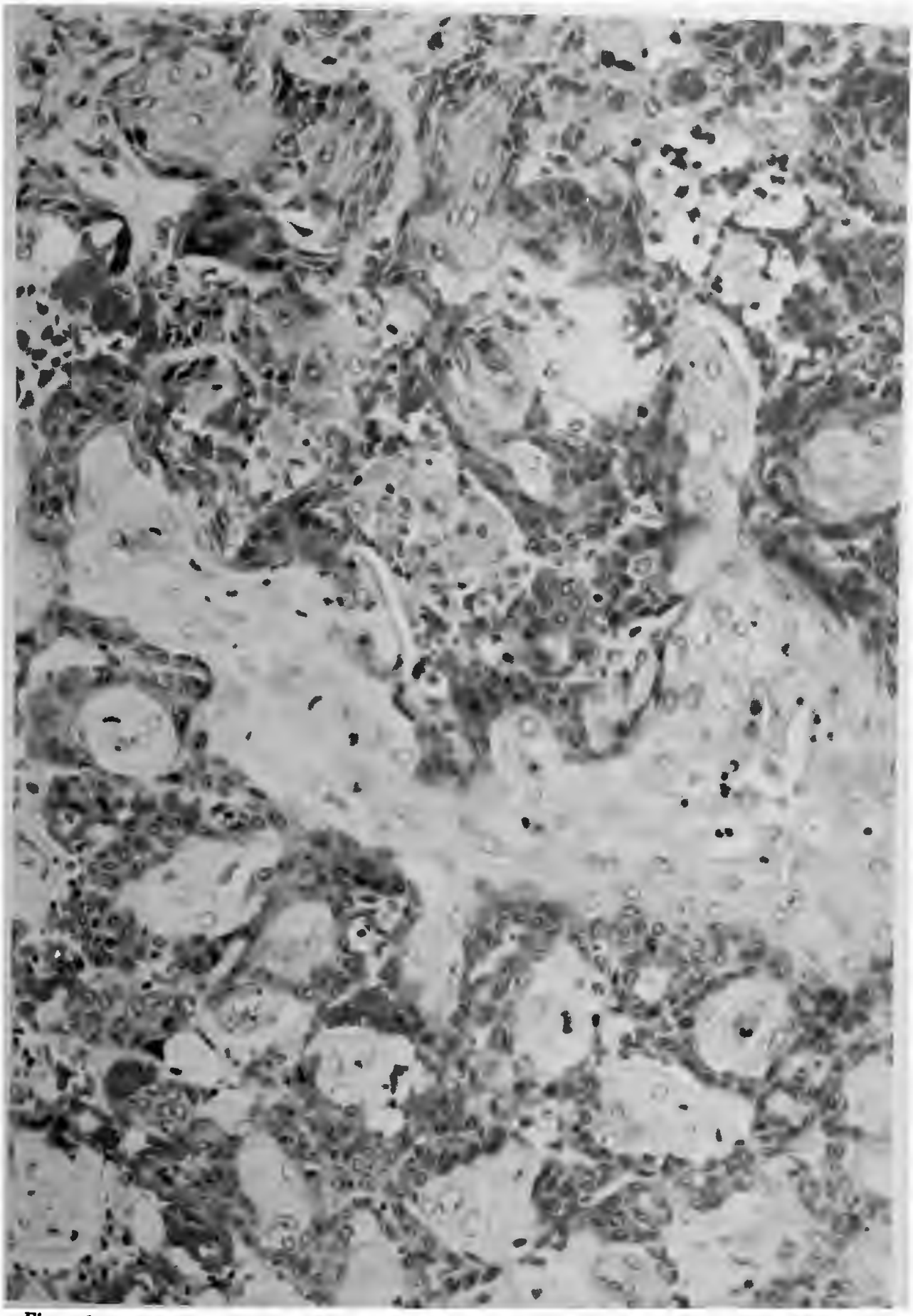

Figure 9. Squamous metaplasia of alveolar epithelium from the lung of a hamster (H&E, 330X).

EFFECT OF VENTILATION VARIABLES ON BREATH THORON OUTPUT*

J. E. Ballou
Biology Department
Battelle
Pacific Northwest Laboratories
Richland, WA 99352

Abstract

The radioactive noble gas thoron (^{220}Rn) was measured in the breath of dogs following intramuscular injection or inhalation of ^{228}Th enriched ThO_2. With increased ventilation the amount of exhaled thoron increased both in the injected dogs and in artificially ventilated lungs from dogs which had inhaled ThO_2. In general, thoron was washed from the lung more efficiently by the normal breathing maneuvers of the intact dogs than by artificial ventilation of their excised lungs. It was possible, however, to obtain marked variations in the thoron output by imposing rather bizarre ventilation patterns on the artificially ventilated lungs.

INTRODUCTION

The radioactive gas thoron (^{220}Rn) is a short-lived alpha emitting daughter product of the ^{232}Th decay series. Typical of the noble gases, thoron is retained to only a small extent in biological materials, and is excreted from the body via the exhaled air. Since a fraction of the thoron produced in the body is exhaled, analysis of the breath has long been of interest as a bioassay procedure for determining the amount of parent thorium compound retained in man. Breath analysis is particularly attractive because of the ease of collecting samples of the breath, and the high degree of sensitivity for detecting alpha radiation by conventional counting techniques. Breath analysis procedures are now available for detecting thoron in the range of 0.1 pCi per liter of exhaled air (Hursh, *et al.*, 1963). The detection limit for freshly inhaled natural thorium, based on breath thoron analysis, has been estimated by Tai-Pow (1969) to be 0.001 μCi or only 0.1 of a maximum permissible body burden.

It is of interest that past experience with human subjects administered ThO_2 (Thorotrast) has not shown a close agreement between the amount of thoron exhaled and the body burden of thorium. The variations in the thoron:thorium ratio are due in part to differences in the distribution of the thorium deposit as well as differences in the metabolism of the ^{232}Th decay products which alter the steady state amounts of the daughter products leading to thoron production. For example selective excretion or translocation of the Ra isotopes in the decay series $^{232}Th \rightarrow {}^{228}Ra \rightarrow {}^{228}Ac \rightarrow {}^{228}Th \rightarrow {}^{224}Ra \rightarrow {}^{220}Rn$ (thoron) may significantly alter the amount of thoron produced, and ultimately released to the breath from a fixed burden of ^{232}Th. The ratio of breath thoron to thorium burden varied by a factor of 10 in Thorotrast patients studied by Tai-Pow (1969). Results from several laboratories compiled by Hursh (1967) show a variation of about 3-fold in the fraction of thoron released by the breath of a variety of Thorotrast patients. The values of the ratio appeared to be influenced by the anatomical site of the thorium deposit relative to the lung, by the age of the thorium deposit, and by physiological parameters including the ventilation rate of the subjects. In general, the large range in variability in the thoron:thorium ratio can be attributed to the short physical half-life of thoron (55.6 sec) and the associated loss of thoron due to radioactive decay. As much as 90% of the thoron produced in the body may be lost by decay in the interval between its production and expulsion in the exhaled air. Losses of this magnitude are reported for predominantly nonpulmonary deposits of thorium, where thoron is produced systemically, diffuses into the circulating blood, and is transported via the blood to the blood-air interface in the lung. It is to be expected that breath thoron produced within the lung itself from inhaled thorium compounds would be less subject to decay losses, and probably influenced less by ventilation and distribution variables. Thus, measuring exhaled thoron may be particularly useful as a bioassay procedure for inhaled thorium burdens. In order to test this supposition, breath thoron was measured in dogs or their artificially ventilated excised lungs after inhalation of ThO_2 aerosols. Ventilation was varied to simulate a wide range of breathing patterns in lungs containing either freshly inhaled or well aged deposits of ThO_2.

METHODS

The method of thorium exposure and measurement was described in detail in an earlier publication by Ballou, *et al.*, (1972). Briefly, anesthetized dogs were administered by injection or inhalation of a ThO_2 dust enriched in ^{228}Th; the thoron in the breath was measured using a modification of the detector system developed by Hursh, *et al.*, (1963). In this procedure, breath thoron is adsorbed on a cold, activated charcoal surface, and the alpha disintigrations are detected with a NaI crystal faced with a ZnS screen. The lungs which were subjected to artificial ventilation were removed at necropsy in an expanded condition, and were maintained in a humid atmosphere at 37°C in a plastic box (artificial thorax) about 1 ft^3 in volume. Artificial ventilation of the excised lung was accomplished by negative pressure breathing using a respiratory pump to vary the

**This paper is based on work performed under contract with the United States Atomic Energy Commission at the University of Rochester Atomic Energy Project and has been assigned report number UR-3490-298.*

frequency and depth of the pressure excursions within the box. A second pump was employed to maintain the desired minimum negative box pressure, and thus the minimum lung expansion at end expiration. Ventilation frequency, minute volume and residual volume were varied during artificial ventilation. Thoron exhaled by the intact dog or by the artificially ventilated lung was introduced into the detector system (Figure 1a,b) and quantitated by comparison with a calibrated thoron source as described earlier by Ballou, *et al.*, 1972).

RESULTS AND DISCUSSION

The data in Table 1 illustrates the stability of the detector system during a series of 13 consecutive measurements using a ^{228}Th stearate thoron source prepared according to Hursh, *et al.*, (1966). Breathing through the thoron source was simulated using a respiratory pump. Since the dead space within the ^{228}Th stearate source was small ($\sim$10 ml) compared to the tidal volumes employed, losses due to radioactive decay were negligible and the washout of thoron produced within the source was complete for ventilation rates ranging from 0.75 to 2.62 liters per minute. After each measurement, the detector system was purged with air for 10 minutes to clear the system of thoron and allow time for the thoron to decay on the charcoal collecting surface. The detector efficiency was maintained satisfactorily, during this comparatively long series of consecutive measurements, as illustrated by the reproducibility of the source counts.

Also shown in Table 1 are data for two dogs (Dog M3 and Dog M4) injected intramuscularly with ThO_2 one month before exhaled thoron was measured. Again, the measurements were made consecutively on the same day for a given dog. Increasing the ventilation rate of Dog M3 by pressing on the chest, increased the thoron output by about 1/4. The observed increase in thoron output with increased ventilation is similar to that reported by Tai-Pow (1969) for Thorotrast patients containing systemic burdens of ThO_2. The response of Dog M4 to changes in ventilation was ambiguous in that hyperventilation induced by breathing CO_2 brought about an apparent decrease in exhaled thoron. Furthermore, although ventilation remained elevated about 50% after CO_2 was replaced by O_2, the amount of thoron collected from the breath remained at the normal level. These results suggested that high concentrations of CO_2 in the air stream may have impaired the detector efficiency. This was confirmed, also in Table 1, when the ^{228}Th stearate source was purged with CO_2. The source count was reduced roughly an order of magnitude when CO_2 was employed. The detector did not recover completely after the usual post-measurement purging with air indicating that a high level of CO_2, such as employed here, may interfere with thoron gas adsorption.

Preliminary studies with anesthetized dogs showed that ventilation changes could be fairly easily induced, but they could not be controlled or sufficiently prolonged to permit satisfactory measurement of exhaled thoron. Uniform breathing for a period of 6 minutes was required for an adequate measurement. For this reason, an *in vitro* system employing excised lungs in an artificial thorax was investigated as a means of varying ventilation under controlled conditions for extended periods of time.

The values in Table 2 compare thoron washout efficiencies for anesthetized dogs and their respective excised lungs at various times after inhalation of ThO_2. Washout efficiency was calculated as the ratio of the breath thoron (normalized to a ventilation of 1 l/min) and the ^{228}Th burden in the dog or isolated lung. Since these dogs were administered ThO_2 by inhalation, essentially all ThO_2 was retained in the lung and tracheobronchial lymph nodes. It should be made clear, however, that thoron is not produced directly by ^{228}Th decay, but rather is the daughter of ^{224}Ra ($T_{1/2}$= 3.64 days) a decay product of ^{228}Th. Therefore, ^{224}Ra in tissues other than lung contributed thoron to the dog's breath in excess of that produced solely from ^{224}Ra in the lung per se. In these animals, from 15 to 28% of the ^{224}Ra was translocated from the site of ^{228}Th deposition in the lung. The major extrapulmonary sources of thoron, which contributed to the higher thoron washout efficiency generally observed for the dogs in Table 2, was the gastrointestinal tract during the early post-exposure phase of lung clearance and the skeleton at later time periods. The quality of ventilation of the excised lung, that is the extent to which artificial ventilation reproduced ventilation of the lung by the intact dog, can not be directly inferred from the washout efficiencies because of the extrapulmonary sources of thoron. It is interesting, however, that although the lung was depleted as much as 28% in thoron precursor (^{224}Ra) in some cases, fairly close agreement in washout efficiencies was still obtained for the intact dogs and artificially ventilated lungs in Table 2. It is apparent that the major part of the exhaled thoron must have originated from ^{224}Ra in the lung in both the *in vivo* and *in vitro* preparations.

Probably the maximum ventilation effect on thoron washout to be expected is illustrated in Table 3 which summarizes the effects of radical changes in the depth and frequency of breathing of the excised lungs. Normal lung expansion, as judged by the size of the inflated lung at necropsy, was maintained by varying the artificial thorax pressure over the range of -1 to -4.5 inches of water. The lung was respired initially at approximately the same rate as the anesthetized dog, usually 12 to 15 breaths/minute; however, the dog's breathing frequency varied considerably depending on the state of anesthesia.

By manipulating the base line negative pressure in the box at end expiration, it was possible to control the residual volume in the lung, and investigate the effect of ventilating a fully expanded lung (lung 1), or a partially filled lung (lung 2) shown in Table 3. In both cases thoron washout was less efficient than when the lungs were ventilated within the normal pressure range. It seems clear that these exaggerated breathing maneuvers did not effectively ventilate the thorium deposits, or more accurately, the thoron sources in the lung parenchyma. It should be noted that the breath thoron recovered from Lung 1 (taken from Dog 1, Table 2) was only about 1/5 of that expected, possibly because of losses due to leaks in the system.

Increasing the frequency of respiration (lungs 3-6) was expected to yield maximum thoron washout since total ventilation increased and losses due to radioactive decay in the lung were minimized by decreasing the residence time of thoron in the lung. The total amount of thoron did generally increase as expected; however, only marginal increases or slightly decreased efficiency was observed — apparently because the quality of ventilation changed during rapid breathing. That is to say, the tidal volumes decreased at the higher frequencies, indicating that the lung was not able to fill and exhaust to the fullest extent during the limited time period between pressure changes within the aritficial thorax. Controlling the box pressure did not, therefore, control ventilation when the physical capacity of the lung to respond was exceeded.

Slower breathing (also lungs 3-6) was expected to decrease thoron washout by decreasing total ventilation and increasing thoron decay losses during the more prolonged breathing cycle. The expected decrease in thoron washout was observed in all cases. Furthermore, washout efficiencies decreased during slow breathing in all but one case (lung 3), and exhibited marginally higher values than rapid breathing in two cases (lungs 3 and 4). Although total ventilation decreased at the lower breathing frequencies the tidal volumes were generally greater since the longer breathing cycle permitted maximum filling and exhausting of the lung contents. Ventilation of the deep lung was undoubtedly improved by slow breathing as evidenced by the greater tidal volumes. A corresponding increase in breath thoron was not seen, however, because the residence time in lung was prolonged and more thoron was lost by decay.

CONCLUSIONS

The supposition that the amount of breath thoron released from inhaled thorium burdens would be relatively independent of variations in ventilation was not supported by the results of this study. Rather to the contrary, the artificially ventilated lungs which contained inhaled ThO_2 released comparatively more thoron in response to increased ventilation than either the dogs injected intramuscularly (Table 1) or the human Thorotrast patients studied by Tai-Pow (1969). It is apparent in the latter two cases that the amount of thoron exhaled in the breath was limited by the concentration of the radionuclide in the blood and the capacity of thoron to diffuse from the blood into the lung air spaces. It is conceivable, therefore, that a significant increase in ventilation could rapidly deplete the available thoron in the lung space and lower the thoron concentration in the exhaled air. This effect was observed to some degree in both the injected dog M3 and in the Thorotrast patients. The extreme case, illustrated by the thoron source in Table 1, demonstrates the complete lack of effect of increased ventilation when thoron was produced at a constant rate, and the total amount was washed out by less than maximum flow rates. The opposite relationship was observed in the lungs containing inhaled ThO_2. Although the amount of thoron generally increased as breathing frequency increased, the washout efficiency also increased, or remained relatively unchanged from the values obtained under more optimum breathing conditions. This probably means that total washout of the thoron produced in the lung was not achieved during artificial ventilation, and apparently was not achieved by at least two of the intact dogs shown in Table 2 (Dog 5 and Dog 8). This should be expected during normal breathing where only a fraction of the air in the lung is replaced during each breathing cycle. It should be mentioned that the animals employed in this study were anesthetized during thoron measurement and breathing was somewhat depressed from the normal ventilation value of about 2 L/min for a 10 kg dog.

From the practical viewpoint of bioassay for thorium burdens, the increased washout of thoron with increased ventilation has the advantage of increasing the sensitivity of thorium detection. It seems apparent also that the volume breathed should be recorded since the concentration of thoron relates best to the thorium burden. Assuming that the relationship between thoron concentration in the breath and the thorium lung burden remains fairly constant as in Table 3 (expressed here as washout efficiency), there may be an advantage in collecting exhaled thoron under maximum breathing conditions. This possibility is also suggested by the work of Tai-Pow (1969), who found the relationship between breath thoron concentration and thorium body burden to be less dependent on breathing rate than was the actual amount of thoron exhaled by his thorotrast subjects.

REFERENCES

Ballou, J. E. and J. B. Hursh, (1972), *The Measurement of Thoron in the Breath of Dogs Administered Inhaled or Injected ThO2.* Health Phys. 22:155-159.

Hursh, J. B. and A. I. Lovaas, (1963), *A Device for Measurement of Thoron in the Breath,* Health Phys. 9:621-627.

Hursh, J. B. And A. I. Lovaas, (1966), *Preparation of a Dry ^{228}Th Source of Thoron.* J. Inorg. Nucl. Chem. 29:599-600.

Hursh, J. B., (1967), *Loss of Thorium Daughter by Thorium Dioxide Patients.* Annal N. Y. Acad. Sc. 145:634-641.

Tai-Pow, J., (1969), *Measurement of Thoron in the Breath of Thorotrast Subjects.* Health Phys. 16:269-275.

TABLE 1. Effect of Changes in Breathing Pattern on Exhaled Thoron.

Thoron Source	Ventilation (L/Min)	Frequency Respiration/Min	Tidal Volume (ml)	Exhaled Thoron Counts/Min
^{228}Th Stearate(a)	1.67 (4) +	13	128.5	3,606 ± 171
	2.62 (4)	13	202	3,685 ± 125
	0.76 (4)	13	58.5	3,330 ± 240
	1.67 (1)	13	128.5	3,790
Dog M3(b)				
Normal Breathing	0.95	12	79	3,973
Chest Constricted	1.27	20	63.5	3,766
Normal Breathing	0.87	11	79	2,786
Dog M4(b)				
Normal Breathing	0.89	9	99	11,081
Breathing CO_2	2.06	25	82.5	3,964
Breathing O_2	1.24	10	124	10,417
Normal Breathing	1.40	16	87.5	12,137
^{228}Th Stearate(a)				
Purged with Air	1.43	13	110	3,686
Purged with CO_2	1.43	13	110	445
Purged with Air	1.43	13	110	3,192

(a) ^{228}Th stearate was enclosed in a container with approximately 10 ml dead space as described by Hursh, *et al.*, (1966).

(b) Dogs were injected intramuscularly with ThO_2 approximately 30 days before measurements.

+Number of measurements in parenthesis.

TABLE 2. Comparison of Normal and Artificial Ventilation on Thoron Washout from the Lung.

	Days After ThO_2 Inhalation	Ventilation (L/Min)	Breath Thoron (nCi)	^{228}Th Burden (nCi)	Washout Efficiency (nCi Thoron/L/Min/nCi ^{228}Th)
Dog 1	3	1.49	38.2	354(a)	0.0724
Excised Lung		0.68	7.95	352	0.0332
Dog 2	3	1.82	10.04	101.3	0.0545
Excised Lung		1.88	8.885	101	0.0465
Dog 3	7	0.98	8.95	98.6	0.0926
Excised Lung		1.11	7.19	96.4	0.0672
Dog 4	7	1.22	3.41	28	0.100
Excised Lung		1.15	2.16	27.6	0.0681
Dog 5	30	1.53	1.196	13.7	0.057
Excised Lung		0.90	0.726	13.6	0.0594
Dog 6	90	1.33	0.749	7.2	0.078
Excised Lung		1.44	0.676	7.2	0.0652
Dog 7	150	1.09	36.6	362	0.0928
Excised Lung		1.64	37.4	305	0.0749
Dog 8	150	1.61	0.802	6.97	0.0715
Excised Lung		1.61	1.08	6.93	0.097

(a) The burden for Dogs 1-8 excludes ^{228}Th in pelt and gastrointestinal tract.

TABLE 3. Ventilation Effects on Thoron Washout from the Artificially Ventilated Lung.

	Days After Exposure	Frequency (Resp/Min)	Tidal Vol. (ml)	Ventilation (L/Min)	Box Pressure (inches Water)	Breath Tn (nCi)	Washout Efficiency (nCiTn/L/Min/nCi ^{228}Th)
Lung 1	3	12	56.6	0.68	-1.1 to -5.2	7.95	0.033
(352)(a)		20	40.5	0.81	-5.0 -9.5	3.86	0.014
Lung 2	150	12	137	1.64	-1.1 -4.7	37.4	0.075
(305		13	94.8	1.23	-1.6 -2.7	16.6	0.044
		12	114	1.37	1.2 -5.7	40.2	0.096
		13	108	1.40	-1.1 -4.6	33	0.077
Lung 3	3	13	144	1.88	-1.4 -4.0	8.85	0.047
(101)		31	70.5	2.18	-1.5 -4.2	11.9	0.054
		42	55.7	2.34	-1.5 -4.2	11.53	0.049
		6	204	1.22	-1.2 -3.8	6.29	0.051
		13	141	1.83	-1.2 -3.8	8.8	0.048
Lung 4	7	13	88.5	1.15	-1.1 -4.4	2.16	0.068
(27.6)		18	65.5	1.18	-1.4 -4.6	1.72	0.053
		20	61	1.22	-1.5 -4.9	1.84	0.055
		7	84.4	0.59	-1.3 -4.8	0.896	0.055
Lung 5	90	12	120	1.44	-1.1 -4.1	0.676	0.065
(7.2)		20	76	1.52	-1.1 -4.2	0.735	0.067
		5	234	1.17	-1.1 -4.2	0.443	0.052
		12	124	1.49	-1.1 -4.2	0.574	0.054
Lung 6	150	40	40.3	1.61	-1.1 -4.2	1.08	0.097
(6.93)		13	85.5	1.11	-1.2 -4.2	0.652	0.085
		6	128	0.77	-1.1 -4.2	0.407	0.076
		37	39.2	1.45	-1.2 -4.2	1.24	0.123

(a) Values in parenthesis are nCi ^{228}Th in the lung.

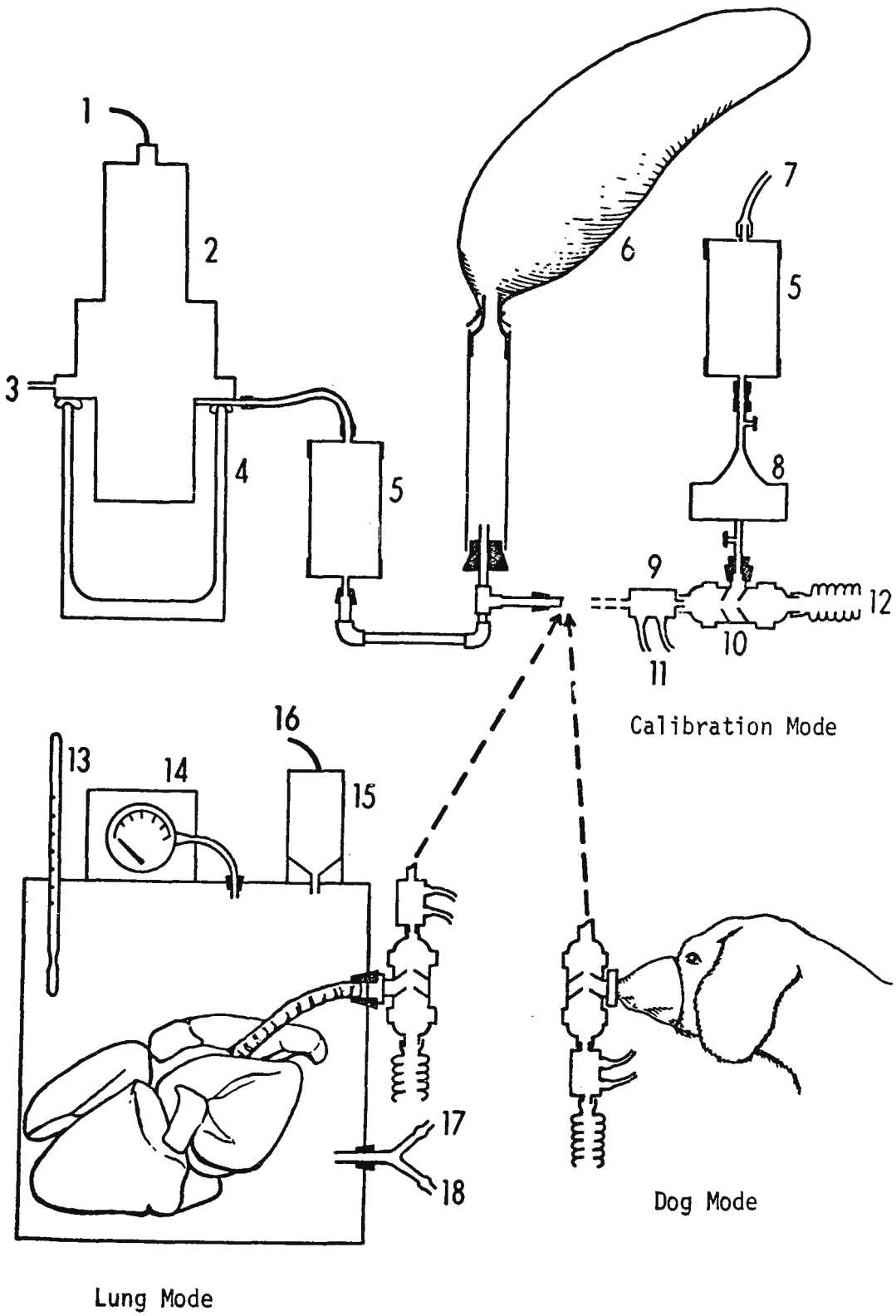

Figure 1a. Thoron Measurement Apparatus. (See Figure 1b for numerical breakdown of above.)

Figure 1b. Thoron Measurement Appratus.

1. To scaler
2. Thoron detector
3. To constant flow pump (4 l/min)
4. Dry ice-alcohol bath
5. Drying tube and CO_2 absorbant
6. Balloon air reservoir
7. To respiratory pump
8. Thoron source (^{228}Th stearate)
9. Pneumotachograph
10. Two-way Douglas valve
11. To pressure transducer and polygraph recorder
12. To spirometer air reservoir
13. Thermometer
14. Pressure gauge
15. Blood pressure transducer
16. To polygraph recorder
17. To pressure balance pump
18. To respiratory pump

A REVIEW OF THE URANIUM MINER EXPERIENCE IN THE UNITED STATES

A. W. Hilberg
Division of Medical Sciences
National Academy of Sciences
National Research Council
Washington, D. C.

Abstract

Mining of uranium ores on a very small scale began in the United States in 1898. In 1948 mining of uranium ores increased significantly as a result of the increasing demands of the atomic energy program, particularly, the weapons program. It was well-known that radioactivity was associated with uranium ore and potential health hazards had been identified as early as 1921. It was then suggested that the large number of lung cancers found in the Schneeberg miners could possibly be caused by ionizing radiation.

Radiation exposure to the lungs of uranium ore miners comes about because of varying concentrations of radon decay products in the mine atmosphere. Measurements of the amount of radioactivity in mine atmospheres began in the United States in 1950 and between 1951 and through 1968, approximately 43,000 measurements were made in about 2,500 uranium mines.

Periodic medical surveys were made starting in 1950, but it was not until 1954, that a concerted effort was made to examine all miners. At this time an epidemiological study was begun by the U.S. Public Health Service to determine the effects of uranium mining with particular emphasis on the problem of lung cancer induction.

The study of the miners, the results of which have been published, revealed a distinct and somewhat dramatic increase in lung cancer. This increase has been ascribed to the radiation exposure to radon-daughters. Because of the presence of a number of other potential occupational carcinogens in the dust of underground mines there has been some question as to whether radon and radon-daughters constitute the principal cause of increased lung cancer risk among these miners. However, the hypothesis that radiation exposure at least was a major contributor to the excess of lung cancers found in the miners cannot be disregarded and must be accepted pending more definitive data.

INTRODUCTION

In this review of the uranium miner experience in the United States, I will not dwell upon detailed statistical analyses of data concerning numbers of cases or numbers of measurements, nor will I discuss histological types of cancer. Instead, I will give enough data and, hopefully, enough background information, as well as information as up-to-date as I could find, in order to allow for some interpretation and general thoughts about what the uranium miner experience in the U. S. has been all about.

I will present no slides of charts, tables, or graphs. These may be found in great profusion in the several reports published on the subject. I am greatly indebted to these reports for much of the material I will present here. (See References Section.)

DISCUSSION

Pulmonary disease was noted among miners of ores containing uranium as early as 1597 by Agricola. The mines were located in the Erg Mountains of Central Europe in the Joachimstal and Schneeberg mining areas. With the beginning of modern pathological techniques in the 19th century, much of the pulmonary disease unique to the miners was identified as lung cancer. This high occurence of lung cancer among these miners was attributed to the high radiation levels in the mines by several authors (Ludwig, 1924; Hueper, 1942; Sikl, 1950; and Lundin, *et al.*, 1971).

The mining of uranium ores on a very small scale began in the United States in 1898. In 1948, the mining of uranium ores increased significantly as a result of the increasing demands of the atomic energy program — particularly the weapons program.

In a period dating from July 1950 through September 1968, a total of 509 deaths occurred among approximately 4,200 miners. In this group, there were 437 deaths among approximately 3,400 white miners and 72 deaths among approximately 800 non-white miners. The expected deaths (using a general population of the same area) would have been 277 among white and 90 among non-white. Thus, we note that the deaths in the white miner population are about double the normally expected death rate, while there is no particular difference in the non-white miner population. Certainly an increase of the magnitude of doubling a death rate must stimulate an interest concerning the causes or uniqueness of the environmental factors of the mining situation.

In 1949, a few radon measurements were made in the mines. Beginning in 1950, the U. S. Public Health Service and the Colorado State Health Department began taking samples of radon in mines. The real significance of radon-daughters in the atmosphere was not known at this time. Sampling of radon and radon-daughters has continued through the subsequent years with attempts to sample the atmospheres of all mines. From 1951 through 1968, approximately 43,000 measurements were made in about 2,500 uranium mines.

Periodic medical surveys were made, starting in 1950, but it was not until 1954 that a concerted effort was made to examine all miners. At this time, an epidemiological study was begun by the U. S. Public Health Service to determine the effects of uranium mining with particular emphasis on the problem of lung cancer induction. In 1971, approximately 150 cases of lung cancer were reported among uranium miners.

Because of the presence of a number of potential occupational carcinogens in the dust of underground mines, there has been some question as to whether radon and radon-daughters constitute the principal cause of increased risk among these miners. Pertinent to this issue is the fact that underground mining *per se* does not necessarily lead to an increase of lung cancer risk, a fact that has been well documented for underground coal miners in the United Kingdom. A recent study has investigated 5,500 potash miners in New Mexico, working in mines not associated with elevated concentrations of radon-daughter products in the air, and has shown no increased risk in such below-ground miners as compared with above-ground workers. (In both groups excess cigarette smoking could account for the increased lung cancer compared to the general population.) It is pertinent to point out that in those mining operations where a significant increase in respiratory cancer has been associated with inhalation of radon and its daughter products, the mineral constituents being mined were widely variable. Besides the uranium mines in Europe and the U.S.A., underground metal miners, fluorospar miners, and hematite miners have shown an excess respiratory cancer risk. In each of these populations, there was occupational exposure to elevated concentrations of radon which was also present in the mines. Thus, whether or not other agents such as arsenic, uranium, or fluoride may have been present in the air, the one constant relationship in these groups has been radon-daughter exposure and the incidence of lung cancer. In the early studies of the Bohemian pitchblende industry, some of the employees in milling operations developed lung cancer, as did miners, but their exposures to radon and radon-daughters, while probably significant, are not known with accuracy. In the U.S., uranium mill workers have not experienced an increased risk of lung cancer (presumably because good ventilation minimizes their exposure to radon-daughters).

Although most of the evidence relating radiation exposure to lung cancer in man pertains to internally deposited alpha-emitting radionuclides, such as radon-daughters and thoron and its short-lived daughters, there is some evidence of an excess lung cancer rate in individuals exposed to gamma- and x-radiation. Among the survivors of the atomic bombing in Hiroshima and Nagasaki, data are now available for the period up to 1970, which show the relative risk of cancer of the tracheobronchial tree for the period of 1955 to 1970 to be 1.4 times higher for doses of 10 rads or more than for lower doses. Difficulties exist in interpreting these data, however, one of which is the fact that the control group (i.e., those farthest from ground zero) the observed overall cancer rate was 50% higher than that expected for the Japanese at large. In addition, there is the question of neutron irradiation in the exposed individuals, which may have contributed significantly to the observed effects in view of the possibly high RBE of this component of the total dose.

An approximately two-fold increase in the relative risk of lung cancer was observed in the study by Court-Brown and Doll of patients with ankylosing spondylitis treated with x-ray therapy. In these cases, large doses of x-rays were delivered to the spine, and doses to the bronchial epithelium were estimated to average about 400 rads.

In a study of patients with tuberculosis, whether active or inactive, an increase in lung cancer of from 5- to 10-fold was found in comparison to the incidence in the general population. The possibility has been raised that the patients may have been exposed to fluoroscopy during treatment of the disease, and that this may account for their increased risk. In the absence of specific exposure information, however, and in view of the fact that there could also be a relationship between tuberculosis itself and the likelihood of developing lung cancer, little emphasis can be given to this study at present.

The incidence of lung cancer in x-ray technicians has been compared with that in pharmacy and medical technicians in the U.S. military service during World War II. Out of approximately 13,000 individuals who were present in both groups, 17 deaths from respiratory cancer were observed among the x-ray technicians as compared with four among the other groups. This difference is highly significant, but when the groups were compared with appropriate U.S. mortality statistics, a total of 12.4 cancers was expected from the x-ray technicians, which was not significantly lower than the 17 cases observed. Thus, the difference between groups may be due primarily to a decreased lung cancer incidence among the pharmacy and medical technicians, which is paradoxical and complicates interpretation of the data.

The various studies just cited tend to show that no matter what the source of radiation may be, there is circumstantial evidence of an increased risk of development of lung cancer from radiation exposure.

The experience through 1969 for all of the various underground mining groups in which an increased risk of cancer has been found, was summarized by Lundin, Wagoner, and Archer. Central to an interpretation of data from underground miners are a number of fundamental issues, which include the following:

(1) What exposures to radon-daughters have actually occurred?

(2) What is the rad dose to the critical cells from radon-daughters in the air?

(3) Is an increased risk observed at a dose rate below that equivalent to continuous occupational exposure to one working level of radon and radon-daughters?

(4) Is the dose-response curve at low doses linear, is it concave downward (i.e., giving a higher risk per rad at lower cumulative doses than at higher cumulative doses), or is there a true threshold for cancer production from a cumulative dose?

Considerable effort has been made to evaluate the radiation exposures of the various groups of miners in the Colorado Plateau area, with particular emphasis on previous underground mining experience not included in the category of uranium mining (a substantial number of the miners had such experience). Absent or infrequent samplings of air of some of the mines, especially in the early exposures prior to 1950, make estimates of cumulative dose only approximate at best; but it is unlikely that these estimates can be greatly improved at this time, and it is probable that in the aggregate the estimates of exposure are adequate to determine trends in the data. It should be emphasized that among these miners the dose rate was quite high in comparison to that in some of the other mining groups (about 10 working levels on the average). One "working level" (WL) in air is defined as any combination of short-lived radon-daughters (through Po-214, RaC') leading to total emission of 1.3 x 10^5 MeV of alpha energy per liter; the cumulative measurement of working level month (WLM) is defined as exposure at the rate of 1 WL for 170 hours. There has been criticism of the WL as an exposure index, because the state of equilibrium of the various nuclides in the chain is critical, especially with regard to the fraction present as free ions. This latter criticism remains valid, but it is fair to say that samples of mine air usually show relatively little contribution of unbound radon-daughters.

Estimates of the rad dose per WLM for basal cell layers of different segments of the bronchial epithelium have varied widely, from less than 0.1 rad per WLM to as much as 20 rad per WLM. A critical factor in these estimates is the thickness of the epithelial and mucous layers, an uncertain quantity in smokers with some degree of chronic bronchitis. The unpublished studies of Gastineau indicate that the normal epithelium of segmental and more proximal bronchi, where most radiogenic cancers have arisen, is thicker than had previously been assumed.

On the basis of the present evidence, 1 rad per WLM is probably close to the upper limit for a reasonably uniform dose to the basal cell layer of the epithelium of the larger bronchi on a probabilistic basis. In the presence of existing chronic bronchitis, the dose factor may well be substantially lower, owing to increased thickness of the mucous layer as well as of the epithelium.

So far as a limiting dose rate is concerned, the question is whether continuous exposure to less than 1 WL has been found in miners to be associated with increase in lung cancer risk. The problem is related to the possible influence of dose rate in latent period, and if latent periods of 20 to 30 years are found at the lowest exposures, no mining group has been under observation with known exposures at these levels for a long enough time to provide a definitive answer. The metal miners studied showed a cancer rate about three times that expected, with exposures at the time of the study well below a concentration of 1 WL, but this study indicates that earlier exposures before the mines were ventilated may well have been higher. The hematite miners studied, who have shown a risk of about 1.7 compared with controls, worked in mines where the radon concentrations are equivalent to WL concentrations of 1 WL or less, but until measurements of actual radon-daughter exposures and the influence of the hematite itself are determined, no final conclusion is possible. For the Colorado Plateau uranium miners in the lowest cumulative WLM exposure category whose dosage was usually received from several short periods of high working level exposures, no significant excess of cancer has appeared as yet. At present, the fact that the lowest exposure group shows only a slight increase in cancer rate above that expected makes the Colorado Plateau group inadequate to resolve this issue of the presence of a true threshold. Inspection of the composition of the study population indicates that the population at risk in this dose range (120 WLM) is now so small as to make it unlikely that even future follow-up will settle the matter.

There has been observed in the U.S. Colorado Plateau workers an inverse relationship between cumulative radiation dose and the latent period for cancer after initial exposure in the mines, but this effect is not very striking at the present time. The relationship of cigarette smoking to the latency period for lung cancer among uranium miners is not known.

A large body of experimental work has now been assembled relating the occurrence of lung cancer to ionizing radiation in animals. Although lung tumors are readily induced in animals by radiation exposure, not all of these may be relevant to the human disease, since peripheral adenocarcinomas are much more likely to occur in animals from whatever inciting stimulus is applied than are tumors comparable to squamous cell tumors in man.

For alpha-emitters, the lowest cumulative dose at which a rise in lung cancer has been observed experimentally was in rats given polonium-210 with a sodium chloride aerosol by inhalation. In this experiment, one squamous cell cancer occurred after 70 rads cumulative mean lung dose, and the dose-incidence relation was approximately linear at higher doses. For beta-emitters, the lowest dose associated with cancer induction was approximately 600 rads, in rats given cerium-144 salts by intratracheal installation. In these experiments, the dose-response curve appeared to be curvilinear (concave upward). An inherent difficulty in animal experiments, of course, is the short life span of the small rodents usually used; and, thus, the fact that only the cancers with short latent periods may be detected by this approach, a limitation which might be expected to produce a curvilinear dose-response curve of the kind observed.

A recent study reported in April 1973 concerning the effects in hamsters exposed to simulated uranium mine atmospheres showed invasive squamous cell carcinoma in a few hamsters receiving 6-hour daily exposure to 1,200 WL of radon-daughters with and without uranium ore dust for periods of 15 to 17 months.

The extensive studies of the U.S. uranium miners have attempted to establish as accurately as possible the exposure of each miner expressed in terms of WLM (working level month) defined as exposure to one working level during 170 hours each month, which corresponds to a probable dose of 1-2 rads to the bronchial epithelium.

The mortality experience of the white underground miners from 1950 to 1968 compared with that expected in the population of the four states shows an excess number of deaths (60 percent above expectation) — essentially due to a larger than expected numbers of violent causes (by 145 percent), and of lung cancers (by almost 500 percent). The mortality experience of the much smaller group of non-white miners over the same period is insufficient (72 deaths in all) to be informative.

The grouping of lung cancer cases in the uranium mines have generally been expressed in terms of WLM, that is: less than 120 WLM, 120-359 WLM, 360-839 WLM, 840-1,799 WLM, 1,800-3,719 WLM and greater than 3,720 WLM. There is an excess number of lung cancer cases in the uranium miners in all of the categories above 120 WLM.

The major uncertainty within the studies lies in the assessment of the exposure to the individual miners. This for the most part is due to the fact that large numbers of very small mines were operating at any one time. There were 450 mines employing an average of 2 miners in 1950, 850 mines with 3 miners in 1957, and 533 with an average of 5 miners in 1966. While the quality of the measurements made in the mines was considered to be good, the frequency of measurements was very unevenly distributed. In only 5 mines were more than 5 radon-daughter measurements made in 1950. 177 mines had measurements in 1962 and 110 in 1968. In many mines only one or two measurements were ever made. Thus, measurements often had to be inferred from circumstantial evidence, since actual measurements were not available. Since the amount of radon-daughters in air depends on many variables, including ventilation, meteorological conditions, and the quality of the ore, it is not possible to evaluate the errors that may have been involved in assessing the exposure of any particular miner.

An additional difficulty in interpreting the results arises from the fact that most of the miners included in the study were cigarette smokers. This difficulty can to some extent be circumvented by comparing the mortality in the miners with that in the population of the four states adjusted according to smoking habits as well as according to the factors mentioned previously. While the excess mortality over the expected mortality adjusted for smoking was somewhat reduced, the relation of the excess to the exposure remained basically unchanged.

The studies of the uranium miner experience in the U.S. show a definite increase in lung cancer risk in miners exposed to 120 working level months and above. They also demonstrate an over-all increase in mortality from all causes. The increases in mortality and in lung cancer risk have been demonstrated by a variety of analytic methods. Cigarette smoking, while possibly a factor in increasing the hazards of lung cancer, does not account for the excess lung cancer found in uranium miners. Approximately 78 percent of the miners were smokers, 22 percent non-smokers. Well over 90 percent of lung cancer deaths occurred in smokers. This would tend to indicate that cigarette smokers are particularly susceptible to lung cancer when exposed to the additional hazard of radiation exposure in the mines.

Uncertainties remain in an over-all evaluation of the uranium miners experience. Primarily, these are uncertainties concerned with physical measurements of mine air, the physical and physiologic processes in the lung, the possible interaction among several potentially harmful contaminents, such as radiation, diesel fuel, cigarette smoking, other ore dusts, and the unknown specificity of the causality of cancer in man.

In spite of these uncertainties, the evidence gained in the evaluation of the uranium miner experience in the U.S. leads to a summary of this report by quoting from the conclusions of the August 1968 Report of an Advisory Committee of the Division of Medical Sciences, National Academy of Sciences, National Research Council, as follows:

(1) "There appears to be a causal association between lung cancer and exposures of approximately 1,000 cumulative working level months (CWLM) and higher."

(2) "There is a statistically significant increase in the lung cancer risk for miners with approximately 100 to 400 cumulative working level months exposure."

(3) "The hypothesis is favored that radiation exposure at least contributed to the excess lung cancer observed in the miners in the 100 to 400 CWLM category."

I believe that with the evidence at hand there can be little doubt that exposure to radon and radon-daughters in the environment of a uranium mine certainly contributes to an increased risk of lung cancer induction after an unknown period of relatively constant exposure.

REFERENCES

The following references were used in the preparation of the paper. However, no specific reference points appear within the body of the paper.

An Assessment of the Economic Effects of Radiation Exposure Standards for Uranium Miners, (1970), Report to the Federal Radiation Council, Arthur D. Little, Inc.

Effects on Populations of Exposure to Low Levels of Ionizing Radiation, The (1972), Report of the Advisory Committee on the Biological Effects of Ionizing Radiations, Division of Medical Sciences, National Academy of Sciences — National Research Council.

Epidemiologic Studies of Uranium Miners, (1971), Report of the Ad Hoc Committee, Advisory Committee to the Federal Radiation Council. National Academy of Sciences — National Research Council.

Guidance for the Control of Radiation Hazards in Uranium Mining, (1967), Report No. 8, Revised. Staff Report of the Federal Radiation Council.

Ionizing Radiation: Levels and Effects, (1972), A Report of the United Nations Scientific Committee on the Effects of Atomic Radiation to the General Assembly, with Annexes. Volume II: Effects. United Nations 1972.

Late Somatic Effects of Ionizing Radiation, (1968), C. D. Van Cleave, School of Medicine, University of North Carolina, Chapel Hill, North Carolina.

Lundin, F. E., Jr., J. K. Wagoner, and V. E. Archer, (1971), *Radon-Daughter Exposure and Respiratory Cancer Quantitative and Temporal Aspects,* National Institute of Occupational Safety and Health, National Institute of Environmental Health Sciences. Joint Monograph No. 1. U. S. Department of Health, Education, and Welfare, Public Health Service.

Pacific Northwest Laboratory Annual Report for 1972 to the USAEC Division of Biological and Environmental Research, (1973), Volume I, Life Sciences, Part 1, Biological Sciences, Batelle Pacific Northwest Laboratories, Richland, Washington 99352.

Radiation Exposure of Uranium Miners, (1967), Summary Analysis of Hearings before the Subcommittee on Research, Development, and Radiation of the Joint Committee on Atomic Energy, Congress of the United States.

Radiation Exposure of Uranium Miners, (1968), A Report of an Advisory Committee from the Division of Medical Sciences:National Academy of Sciences — National Research Council — National Academy of Engineering, Washington, D.C.

Saccamanno, G., V. E. Archer, O. Auerbach, M. Kuschner, R. P. Saunders, and M. G. Klein, *(1971), Histologic Types of Lung Cancer Among Uranium Miners.* Cancer, March 1971, Vol. 27.

RADIOLOGICAL HEALTH SIGNIFICANCE OF RADON IN NATURAL GAS

R.H. Johnson, Jr., D.E. Bernhardt, N.S. Nelson, and H.W. Calley, Jr.
Office of Radiation Programs
Environmental Protection Agency
Washington, D.C. 20460

Abstract

Natural gas contains varying amounts of radon-222 which becomes dispersed within homes when natural gas is used in unvented appliances, such as kitchen ranges and space heaters. The average dose equivalent to the bronchial epithelium of an individual from use of natural gas in these appliances was estimated for typical exposure conditions to be 0.015 and 0.054 rem per year respectively. When extrapolated to the United States population at risk, the estimated population tracheobronchial dose equivalents were 1,874,000 and 854,000 person rems per year for these appliances, or a total of 2,728,000 person-rems per year.

A review of exposure conditions, lung model parameters, dose conversion factors, and health effects data indicated this population dose could possibly result in up to 15 deaths per year. For perspective, the concentrations and health effect consequences from use of natural gas containing radon were compared to current radon guides, natural background radon, and normal lung cancer mortality statistics. These comparisons indicated that natural gas radon represents about 0.9 to 1.5 percent of the guide of 0.33 pCi/l derived from ICRP No. 2, 0.3 to 3 percent of normal radon background, and 0.03 to 0.08 percent of normal lung cancer mortality. It was concluded that radon in natural gas does not contribute significantly to respiratory cancer mortality in the United States.

INTRODUCTION

Radon-222 is a radioactive gaseous daughter product of radium-226 found in naturally occurring uranium minerals throught the earth's crust. This heavy inert gas permeates porous geological formations, and is collected along with methane in production wells for natural gas. When this natural gas is used in unvented appliances, such as kitchen ranges and space heaters, a part of the combustion products and radon-222 are released within the home. This radon-222 constitutes an additional source of radiation in the home which has not been adequately evaluated for potential health effects.

In this assessment, potential health effects were derived following the sequential analysis outlined in Figure 1. This figure shows a generalized model and some of the factors which must be considered. Each of the four main phases of this model, radon concentrations, exposure conditions, dose calculations, and health effects estimates, have been reviewed in depth in a study by Johnson, *et al.*, (1973). This present paper constitutes a summary of some of the major findings of that study.

RADON CONCENTRATIONS IN NATURAL GAS

The average radon level in several natural gas production areas in the United States is 37 pCi/l as indicated in Table 1. However, from the range of concentrations shown in this table, it is apparent that many individual wells have levels 10 to 20 times the average value. There is also a considerable variation in radon concentrations at wells in different well fields ranging from a low of 5 pCi/l in the Gulf Coast to about 100 pCi/l in Texas, Kansas, Oklahoma, and California. These variations may be attributed to differences in regional distributions of uranium and individual well parameters such as location, depth, pressure, and production rate. It should also be noted that the average concentration calculated here does not account for the relative gas production volumes from different regions of the country. For example, the states of Texas, Louisiana, and Oklahoma produce 81 percent of the natural gas in the United States.

Radon levels at points of use have not been measured extensively, but some data are available for gas distribution lines (Table 2). These data indicate that average radon levels in various areas are 50 pCi/l or less with an overall average of 23 pCi/l. The highest levels were found in the Colorado and New Mexico areas where the transit times from production wells to consumers are short compared to the half-life for radon-222 of 3.83 days. The coastal regions furthest from natural gas sources have the lowest radon levels. This could be due to pipeline transmission time and storage which allows radon-222 to decay away. Also, most gas from production wells is processed to remove water, liquifiable hydrocarbons, and other gaseous products such as CO_2 and helium. This processing removes 30 to 75 percent of the radon with the liquid hydrocarbons (primarily propane).

RADON FROM USE OF NATURAL GAS IN HOMES

Radon concentrations in homes resulting from use of natural gas have not been measured; however, estimates may be made by determining the quantity of gas used, venting of gas appliances, house volume, and number of air changes per hour. The quantity of gas used, and the fraction of combustion products vented inside the home, depend on how the gas is used; i.e., for comfort heating, or ranges, water heaters, refrigerators, clothes dryers, etc. Most natural gas is used for comfort heating, but gas furnaces are normally vented outside the home. Conversely, gas kitchen ranges are normally vented into kitchen areas, and initial studies by Barton, *et al.*, (1970) indicate this is the main source of radon-222 from natural gas usage in homes. In addition, data compiled by T. F. Gesell (1973) indicate that there is also widespread use of unvented space heaters.

The use of these unvented appliances results in the dispersion of radon-222 along with the combustion products of natural gas within the home. The radon-222 decays to a radon-daughter product mixture which reaches an equilibrium concentration as a function of radioactive decay, dispersion, and removal processes. Tests by F. B. Johns at the National Environmental Research Center, Las Vegas, indicate that effectively there are no daughter products present in natural gas at the point of combustion because radon-daughters tend to plate out on any obstructing surfaces such as valves and walls of pipelines. Similar removal processes, and dilution by ventilation and mixing with outside air, reduce the daughter product concentrations in the home atmosphere below those which would be calculated for radioactive secular equilibrium with radon. A fraction of each daughter product also becomes attached to dust particles in the air. For specific aerosol conditions, the proportion of ions which remain free, or uncombined, reach a steady state for each decay product.

Using the exposure conditions postulated in Table 3, the following average radon-222 levels were calculated for use of natural gas in a typical home:

Unvented gas kitchen ranges	0.028 pCi/l
Unvented gas space heaters	0.010 pCi/l

CRITICAL MODE OF EXPOSURE AND RADON-222 DOSIMETRY

The primary hazard for radon-222 exposure is from inhalation and bronchial deposition of the alpha-emitting daughters ^{218}Po and ^{214}Po, commonly referred to as RaA and RaC', which release their alpha decay energy into tissues of the respiratory system. This was evidenced by uranium miners working in radon atmospheres who developed lung cancers believed to have occurred as a result of interaction of alpha particles with the basal layer cells of the bronchial epithelium (Lundin, *et al.*, 1971).

The dose to the critical tissue is estimated by the use of lung models which include functions of environmental conditions, anatomy, respiratory physiology, and radon-222 dosimetry. Some of the more important variables include the particle sizes and aerosol content of the atmosphere, home air change rate, free ion fraction, rate and depth of respiration, medical status of the individual, and the location of the precancerous cells at risk.

Variations in choice of lung model parameters and exposure conditions have led to a wide range of factors for converting radon concentrations to dose. A summary of these dose conversion factors (Johnson, *et al.*, 1973) shows a range from 12 to 140 rads per year for continuous exposure at one working level (WL). One WL is equivalent to 1.3×10^5 MeV of potential alpha energy per liter of air which would be available from radon-daughters (RaA through RaC') in secular equilibrium with radon-222 at a concentration of 100 pCi/l (Lundin, *et al.*, 1971). The conversion factor most closely representing exposure conditions expected in typical dwellings is 100 rads per year for continuous exposure at one WL.

DOSE TO AN INDIVIDUAL

The dose to a hypothetical individual exposed to radon and daughters from use of natural gas in unvented kitchen ranges was calculated by Barton, *et al.*, (1973) for the following set of exposure conditions (see also Table 3): a kitchen range gas usage of 0.765 m^3 per day; a 226.6 m^3 house; an air change rate of one per hour; no radon-daughters in the gas; the ratio of Rn, RaA, RaB, RaC (RaC') is 1, 0.8, 0.6, 0.4; free daughter ions of 8.5 percent; a dose conversion factor of 100 rads per WL; and a quality factor of 10. These conditions gave a dose of 0.0015 rads (dose equivalent of 0.015 rems) per person per year to the tracheobronchial epithelium due to inhalation of radon-daughters. Radon-222 itself contributes only about 0.5 percent of the dose for inhalation of radon and daughters together.

POPULATION DOSE EQUIVALENT

The average dose equivalent to the United States population was determined by extrapolation of the dose to a hypothetical individual. The population at risk was determined for each state from data compiled by Gesell (1973) from 1970 Census Bureau statistics. These data gave the number of dwellings with gas kitchen ranges

and unvented space heaters. The population at risk from the use of unvented kitchen ranges was determined by assuming four persons per dwelling; i.e., 4 x 31.2 x 10^6 = 124.8 million persons. The population tracheobronchial (T-B) dose in person-rems was then calculated by multiplying the population at risk times the individual dose equivalent. This gave 1.87 million person-rems per year from the use of gas kitchen ranges in the United States.

The population dose equivalent from use of unvented space heaters was determined by relating the average quantity of gas used in heaters to the quantity of gas used in ranges and the corresponding dose equivalent for ranges. The quantity of gas used by space heaters was calculated as 0.354 m^3 per degree-day for the average annual degree-days per year for each state. The average quantity of gas used by space heaters was 2.75 m^3 per day, compared to 0.765 m^3 per day for gas kitchen ranges. The average dose equivalent to an individual from use of space heaters was 0.054 rem per year. When extrapolated to the exposed population (15.8 million persons) the population T-B dose from space heaters was estimated as 0.854 million person-rems per year.

The total population T-B dose equivalent for exposure to radon-daughters from the use of natural gas in unvented kitchen ranges and space heaters was estimated as 2.73 million person-rems per year.

HEALTH EFFECTS ANALYSIS

This analysis was based on the absolute somatic and genetic risks from inhalation of radon-daughters as outlined in the report by the National Academy of Science on the biological effects of ionizing radiation (BEIR Report, 1972). The T-B dose effect of concern is lung carcinoma. Since lung cancer has such a high mortality rate, it is assumed that morbidity for this dose effect is equivalent to mortality.

The absolute risk from T-B dose was calculated from Table 3-2 of the BEIR report (1972) by multiplying the sum of the fractional risks by age times the expected plateau region. In this case, the plateau region, or time beyond the latent period during which the risk remains elevated, was taken as 30 years. The calculation for risk in terms of lung cancer deaths was based on the following analysis, where the adult risk for cancer of the lung from T-B dose is 1.3 deaths/million persons at risk/year/rem.

Age Group	Percent of Population	Proportion of Adult Risk	Fractional Risk deaths/10^6 persons/year/rem
10+	80	1	1.3 x 1 x 0.8 = 1.04
0-9	20	0.2	1.3 x 0.2 x 0.2 = 0.05
In Utero	1.3	5	1.3 x 5 x 0.013 = 0.08
			1.17

Annual Risk = 1.17 deaths/million persons/year/rem

This annual risk is then multiplied by 30 to estimate excess deaths for a plateau region of 30 years to give the absolute risk of 35 excess deaths/million persons/year/rem.

The potential health effects to the United States population at risk from use of natural gas containing radon in unvented appliances is determined by applying the absolute risk to the estimate of total population T-B dose equivalent. This gives an estimate of 95 excess deaths per year. However, the significance of this estimate should only be interpreted by comparison with other reference guides and after consideration for the uncertainties in this analysis.

DISCUSSION

The fundamental problem in an analysis of potential health effects as derived in this study is the necessity of extrapolating from a few measurements or reported values to average conditions for large populations. Because of inadequate information, values had to be estimated or assumptions made to represent typical exposure conditions or population at risk. The assumed values were normally selected so the calculated dose or health effects would be overestimated, i.e., conservative.

The possible variations of exposure conditions which could reasonably affect a large fraction of the population at risk were given previously in Table 3. The nature of corrections to adjust the estimated health effects for these possible variations in exposure conditions are listed in Table 4.

A review of the uncertainties in this analysis, and the significance of corrections for possible variations in exposure conditions (Johnson, *et al.*, 1973), indicate that the estimate of 95 excess deaths a year is probably conservative by up to a factor of 10. Therefore, a less conservative, but more realistic, estimate would be a

[1]Exposed through placental transfer of radioactivity in maternal blood.

possibility of 15 or less potential deaths per year from use of natural gas containing radon in unvented appliances. It should be further noted, however, that this estimate is based on a linear non-threshold dose response, and that no lung carcinomas have been confirmed at radon levels which could occur in homes using natural gas.

For further perspective as to the significance of radon in natural gas, the radon-222 concentrations and health effect consequences were compared to natural background radon, current radon guides, and normal lung cancer mortality statistics. It was determined that the use of natural gas containing radon-222 could increase the normal level of radon-222 in homes by 0.23 to 2.2 percent. These radon levels from natural gas represent about 0.9 to 1.5 percent of the guide of 0.33 pCi/l derived from ICRP No. 2 (1960). Also, an excess mortality of 95 deaths a year would be only 0.2 to 0.5 percent of normal annual respiratory cancer mortality. The more realistic estimate of 15 or less deaths a year would be only 0.03 to 0.08 percent of normal respiratory mortality.

It can be concluded from this assessment of potential health effects, that radon in natural gas does not contribute significantly to respiratory cancer mortality in the United States.

REFERENCES

Altshuler,B., N. Nelson, and M. Kuschner, (1964), *Estimation of Lung Tissue Dose from the Inhalation of Radon and Daughters, Health Physics,* 10-1137-1161.

Barton, C. J. (1971), *Radon in Air, Natural Gas, and House: A Preliminary Survey and Evaluation,* ORNL-CF-71-5-48.

Barton, C. J., R. E. Moore, and P. S. Rohwer, (1973), *Contribution of Radon in Natural Gas to the Natural Radioactivity Dose in Homes,* ORNL-TM 4154.

Bunce, L. A., and F. W. Sattler, (1966), *Radon-222 in Natural Gas, Radiological Health Data and Reports,* 7, 8, 441-444.

Fries, B. A., and K. H. Kilgren, (1972), *Radon in Natural Gas and Gas Liquids,* Chevron Research Company, California.

Gessel, T. F., (1973), Unpublished Data, University of Texas, School of Public Health, Houston, Texas.

International Commission on Radiological Protection, *(ICRP) (1960), Publication 2,* Pergamon Press, London.

Jacobi, W., (1972a), *Activity and Potential α-Energy of Radon-222 and Radon-220 Daughters in Different Air Atmospheres, Health Physics, 22,* 441-45.

Jacobi, (1972b), *Relations Between the Inhaled Potential α-Energy of Rn-222 and Rn-220 Daughters and the Absorbed -Energy in the Bronchial and Pulmonary Region, Health Physics, 23,* 3-11.

Johnson, R. H., Jr., D. E. Bernhardt, N. S. Nelson, and H. W. Calley, Jr., (1973), *Assessment of Potential Radiological Health Effects from Radon in Natural Gas, Environmental Protection Agency Document,* EPA-520/1-73-004, Office of Radiation Programs, Waterside Mall, Washington, D. C. 20460.

Lundin, F. E., Jr., J. K. Wagoner, and V. E. Archer, (1971), *Radon Daughter Exposure and Respiratory Cancer Quantitative and Temporal Aspects,* National Institute for Occupational Safety and Health, National Sciences, Joint Monograph No. 1, PB-204871, (NIOSH-M-71-1).

McBride, J. R., and D. H. Hill, (1969), *Off-Site Radiological Surveillance for Project Gasbuggy, June 1967-July 1968, Radiological Health Data and Reports,* 535-546.

Report of the Advisory Committee on the Biological Effects of Ionizing Radiations (BEIR Report 1972), Division of Medical Sciences, National Academy of Sciences, National Research Council, Washington, D. C., 20006, *The Effects on Populations of Exposure to Low Levels of Ionizing Radiation.*

Tsivoglou, E. C., H. E. Ayer, and D. A. Holaday (1953), *Occurrence of Nonequilibrium Atmosphere Mixtures of Radon and Its Daughter, Nucleonics,* 11, 40-45.

Table 1. Radon-222 Concentrations in Natural Gas at Production Wells.(a)

Area	Radon-222, pCi/l Average	Range
Colorado New Mexico	25	0.2-160
Texas, Kansas Oklahoma	<100	5-1450
Texas Panhandle	-----	10-520
Colorado	25.4	11-45
Project Gasbuggy Areas	15.8-29.4	12-59
California	-----	1-100
Gulf Coast	5	-----
Kansas	100	-----
Wyoming	10	-----
Overall Average	37	

(a) Johnson, *et al.*, (1973); Barton, *et al.*, (1971); Bunce, *et al.*, (1966); and Fries, *et al.*, (1972).

Table 2. Radon-222 Concentrations in Natural Gas Distribution Lines.(a)

Area	Radon-222, pCi/l Average	Range
Chicago	14.4	2.3-31.3
New York City	1.5	0.5-3.8
Denver	50.5	1.2-119
West Coast	15	1-100
Colorado	25	6.5-43
Nevada	8	5.8-10.4
New Mexico	45	10-53
Houston	8	1.4-14.3
Overall Average	23	

(a) Barton, *et al.*, (1973); McBride, *et al.*, (1969).

Table 3. Exposure Conditions and Possible Variation in Parameters.

Parameter	Condition for this(a) Analysis	Possible Variation(b)
Radon Concentration at Point of Use	20 pCi/l	10 - 100 pCi/l
Gas Appliances	Cooking Ranges Space Heaters	Could include Refrigerators, Clothes Dryers, etc.
Gas Use:		
Ranges	0.765 m^3/day	Up to 1.19 m^3/day
Heaters	0.354 m^3/degree-day	0.28-0.42 m^3/degree-day
Degree-Days	Average for Each State	± 25% within States
Appliance Venting	Unvented	Ranges could be Partly Vented
House Size	226.6 m^3	142-425 m^3
Air Change Rate	One per Hour	0.25 - 5 per Hour
Radon-Daughters:		
in Gas	No Daughters	1, 1, 1, 1(c)
in Home	1, 0.8, 0.6, 0.4(c)	1, 1, 1, 1 to 1.0, 0.5, 0.25, 0.1(c)
Percent Free RaA	8.5 Percent	5 to 25 Percent
Critical Mode of Exposure	Inhalation of Radon-Daughters	Radon Alone gives < 1% of Dose
Critical Organ	Bronchial Epithelium	Some Exposure Also to Nasopharynx, Lung, and Whole Body
Dose Conversion Factor(d)	100 rads/year for Continuous Exposure at 1 WL(100 pCi/l)	50-125 rads/year
Quality Factor	10	3-10

(a) These are intended to be typical average conditions — although some of the less well understood parameters were chosen to give a higher (or more conservative) dose estimate.

(b) These are reasonable variations which could be encountered for a large fraction of the exposure conditions or population at risk.

(c) Ratio of Rn, RaA, RaB, RaC (RaC').

(d) This factor includes assumptions for daughter equilibria, critical mode of exposure, lung model, and other dosimetry factors.

Table 4. Corrections to Adjust Estimated Health Effects for Different Exposure Conditions.

Parameter	Correction Multiplier
Air Changes per Hour (Barton, *et al.*, 1973)	6.01
0.25	6.01
1.0	1.0
2.0	0.339
Radon Activity	Linear(a)
Quantity of Gas Used	Linear
House Size	Linear
Daughter Equilibria (Tsivoglou, *et al.*, 1953)	
Ratio 1, 1, 1, 1	1.9
1, 0.9, 0.8, 0.7	1.3
1, 0.8, 0.6, 0.4	1.0
1, 0.75, 0.5, 0.3	0.84
1, 0.5, 0.25, 0.1	0.39
Percent Unattached RaA(b)	
3	0.75
8.5	1.0
10	1.3
25	2
Dose Conversion Factor	Linear
Quality Factor	Linear
Health Effects Conversion Factor	Linear

(a) A linear correction means the correction is proportional to the variation in the parameter.
(b) Estimated from Jacobi (1972 a, b) and Altshuler, *et al.*, (1964).

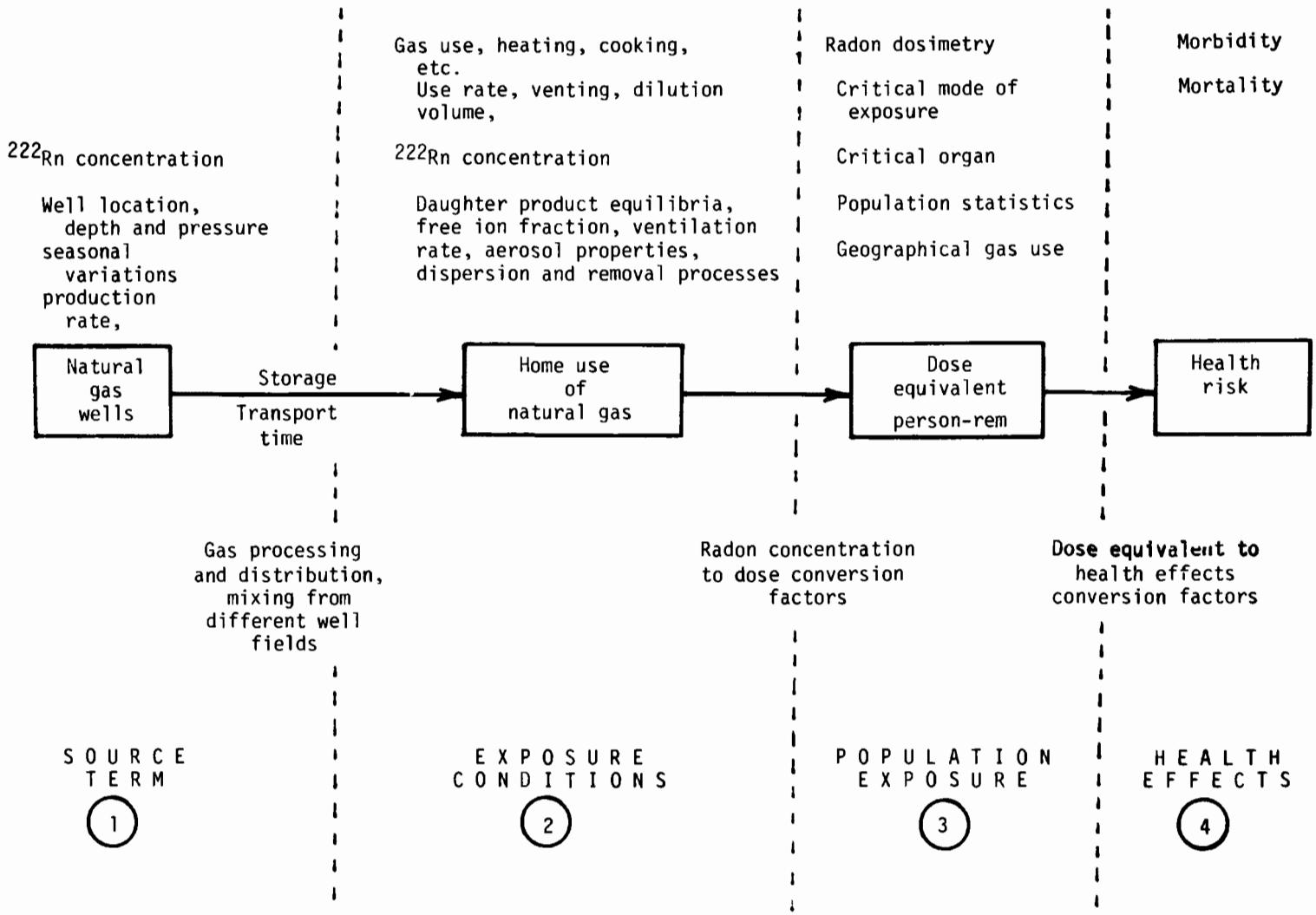

Figure 1. Model for estimating potential health effects from radon in natural gas.

VIII. Application of Noble Gases

UTILIZATION OF THE NOBLE GASES IN STUDIES OF UNDERGROUND NUCLEAR DETONATIONS*

C. F. Smith
Lawrence Livermore Laboratory
University of California
Livermore, California 94550

Abstract

The Livermore Gas Diagnostics Program employs a number of rare gas isotopes, both stable and radioactive, in its investigations of the phenomenology of underground nuclear detonations. Radioactive gases in a sample are radiochemically purified by elution chromatography, and the separated gases are radioassayed by gamma-ray spectrometry and by internal or thin-window beta proportional counting. Concentrations of the stable gases are determined by mass-spectrometry, following chemical removal of the reactive gases in the sample. The most general application of the noble gases is as device fraction indicators to provide a basis for estimating totals of chimney-gas components. All of the stable rare gases, except argon, have been used as tracers, as have xenon-127 and krypton-85. Argon-37 and krypton-85 have proven to be of particular value in the absence of a good tracer material as reference species for studies of chimney-gas chemistry. The rate of mixing of chimney gases, and the degree to which the sampled gas truly represents the underground gas mixture, can be studied with the aid of the fission-product gases. Radon-222 and helium are released to the cavity from the surrounding rock, and are, therefore, useful in studies of the interaction of the detonation with the surrounding medium.

INTRODUCTION

The gas diagnostics program at LLL was established to supplement conventional radiochemical techniques for obtaining device performance-evaluation data in support of test program activities. We provide analytical, interpretative, and diagnostic support for Plowshare gas-stimulation experiments, and we also perform a wide variety of service radiochemical measurements in conjunction with laboratory experiments in which gas tracers are used. Much of our effort requires measurement and interpretation of the concentration of noble gases in our samples. These species are present as products of nuclear reactions, as components of any air diluent of the samples, as tracer materials, or as combinations of these possibilities. We use both stable and radioactive components. Although the nature of our diagnostic application of the noble gases is unique, the procedures we have developed are of general applicability.

SAMPLING TECHNIQUES

Study of the phenomenology of an underground nuclear detonation requires collection of good-quality samples of the cavity and chimney gases over times extending from a few minutes to several weeks following detonation. The sampling system now used (Figure 1) basically consists of a reinforced rubber hose containing and fixed to a nonrotating wire rope that provides longitudinal strength and prevents crushing of the hose (Grens, 1972). The rope itself is a reasonably permeable gas path, even where the hose is compressed against it through regions of high soil compaction. Both the rope and hose terminate at a vacuum demand valve placed well downhole beneath the gas-containment stemming plug. This valve prevents passage of gas unless a vacuum can be applied from above, thus precluding the possibility of pressurized gas reaching the surface and providing a fail-safe closure of the system if the surface sampling equipment is not leak-tight. Other built-in safety features include a maximum allowable working pressure of the hose that is well in excess of any previously observed surface pressure. A deeply buried pressure relief valve ensures a safety factor of 6 or more in the upper portions of the sample system. Gas pumped through the system is totally contained either in pressurized sample cylinders or in underground tanks. Sampling operations are conducted in such a manner as to ensure compliance with the concept of total containment that characterizes explosive emplacement techniques currently in use.

Another often-used sampling scheme involves the use of production tubing placed in a postshot reentry drill hole. Although simple in concept, this technique suffers from the time delay imposed by the drilling schedule. At the test site, the delay can be days or weeks, which means a loss of the information obtained from short-lived radionuclides. In the case of gas-stimulation experiments, the delay has ranged from 1 month (Gasbuggy) to nearly a year (Rulison), and has precluded detection of all but the longer-lived gaseous radionuclides. To eliminate this loss of information, we emplaced a prompt gas-sampling system at Rio Blanco (Quong, 1972). This novel system consisted of about a mile of half-inch, stainless steel tubing containing a wire rope at its lower end, and three gas-block diaphrams that could be manually opened by back pressurization from the surface. Unfortunately, chimney gas was not collected by this system. Our first chimney gas samples are expected in early October 1973, following completion of drilling into the chimney.

**Work performed under the auspices of the U.S. Atomic Energy Commission.*

ANALYTICAL PROCEDURES

Samples are returned to Livermore for analyses. Typical sample volumes range from a few cubic centimeters to a few tens of liters, although several cubic meters of sample have been processed at times. Radionuclide concentrations range from background to a few hundred microcuries per milliliter. Needless to say, our processing equipment exists in isolated high- and low-level specialized versions.

The first step in the processing of an unknown sample is a germanium-diode gamma-ray scan of 10 to 20 ml of the gas. We have standardized this process to provide concentration measurements of the short-lived krypton isotopes (87, 88, 85m) and of xenon-135 against the background of other gamma ray-emitting nuclides in the gross fission product gas. In principle, it is possible to determine all of the krypton and xenon isotopes in a gross sample by a judiciously spaced series of counts. However, to save time, gain sensitivity, and improve measurement accuracy, we prefer purified krypton and xenon fractions of the sample for measurement of the longer-lived fission product gases.

Radiochemically and chemically pure fractions of a sample are prepared by elution chromatography. Helium is used as a carrier gas, and the separations are accomplished by manipulation of gas flow paths through controlled-temperature activated charcoal and molecular sieve (5A) columns (Momyer, 1960). Thermal conductivity and ionization-chamber detectors are used to monitor the progress of the elution. We have six high-level gas-separation systems, and two similar low-level systems.

The desired quantity of sample is mixed with appropriate carrier gases for trace components, and collected on activated charcoal at liquid nitrogen temperature. In general, the purification process consists of a series of initial group separations from the activated charcoal at temperatures ranging from liquid nitrogen to 350°C (Figure 2). A molecular sieve is used to obtain the final separation of each of the groups. A much simpler scheme is often used to obtain specific components of a moderately radioactive sample (e.g., krypton can be separated from air in a two-step process using only the charcoal column). Large samples require lower temperatures until the major constituent is eluted, and may require multiple elutions from the sieve traps to obtain species such as argon from air, or krypton from natural gas, in a pure form. Because of the large variety of sample sizes and compositions that we are asked to process, our systems have an excess of built-in versatility, and our techniques are modified accordingly. Simpler systems and techniques would suffice in a large number of specialized applications, where more-or-less routine analyses are required.

Counting systems used for the measurement of the radioactive constituents of the separated gas fractions are chosen according to their activity level. Low-level samples are counted in matched 0.8- and 0.5-liter anticoincidence shielded beta proportional counters, and the same tubes are operated on the alpha plateau to measure radon activity. More active samples are loaded into gas cells for thin-window beta counting or for gamma spectrometry. We use the latter two methods for the great majority of our noble gas samples.

We determine the gross chemical composition of our samples by mass spectrometry. The automated system now in routine use is applied to sample constitutents at 0.01% and higher concentrations (Crawford, et al., 1970 and 1971), and gas chromatography has also been used in specialized applications to determine trace components. We normally employ a sample enrichment process to gain sensitivity for the rare gases. As a first step, the total noble gas concentration in a sample is measured by monitoring the pressure decrease caused by the gettering of all reactive gases in a titanium sublimation pump. Enough sample to provide about 2ml(STP) of the noble gas mixture is metered into a reaction flask containing calcium metal. When molten, the calcium acts as a getter for all sample components except the noble gases. The residual gas from this concentration process is analyzed mass spectrometrically for the relative concentrations of the noble gases. In conjunction with the previously determined total noble gas concentration, this information is used to derive individual concentrations of each of the components. This technique has been applied to air, natural gas, and chimney gas samples, and has successfully been used to measure concentrations in the parts-per-billion range. (Newton, *et al.*, 1973).

NOBLE GAS TRACERS

Perhaps the single most important and useful application of the noble gases in our programs is in gas tracing. Mere measurement of the concentrations of species of interest in a series of samples is of little value unless one is able to identify and eliminate the effects of dilution, mixing, and chemical reactions that mask the interrelationship between the samples. To accomplish this unmasking we rely on selected noble gas tracers. These species are expected to be uniformly distributed within the cavity, are measurable over a wide range of dilution throughout the desired observation period, and are not subject to excessive and variable background corrections. Three classes of tracers can be defined: relative, internal diagnostic, and emplaced diagnostic.

Application of gas tracers in a relative sense is best illustrated by our gas-quality investigation for Project Rulison (Smith, 1971). During production testing, ^{85}Kr was used as an indicator of relative sample quality and of the extent of dilution due to the influx of formation gas into the chimney during production. It was also used as a common denominator for ratios used to investigate the significance of the changing composition of the produced gas.

A diagnostic tracer is a material present in the cavity in a known amount. It can be produced by the explosive, or emplaced with the explosive, and, of course, must also meet the requirements previously stated for a relative tracer. The "device fraction" is the ratio of the concentration of the tracer species in a sample to

its known total in the chimney. Its reciprocal is the volume of chimney gas at standard conditions. If estimates of chimney pressure and temperature are available, the reciprocal device fraction can be interpreted directly as chimney void volume, and can be used to estimate the cavity radius. Most importantly for diagnostic purposes, the total of any well-mixed component of the chimney gas is given by its concentration in a sample divided by the device fraction. These totals are the most tractable quantities available for providing device-performance estimates and for studying underground nuclear phenomenology.

Totals of internal diagnostic tracers must be either calculated or measured. The Rulison ^{85}Kr total, for example, was obtained from release estimates after production testing and was verified from chimney volume, pressure, and temperature estimates and the initial concentration. Krypton-85 was also used as a secondary tracer for the Gasbuggy gas-quality program (Smith, 1970a, b). In this case ^{127}Xe(the ^{127}Xe was produced by neutron capture in a xenon sample that had been enriched in the lighter xenon isotopes) was emplaced with the device to serve as the principal tracer. Because of its 36-day half-life, the ^{127}Xe was useful during only the initial shut-in period (6 months). Subsequent diagnostic tracing was based on the experimental total ^{85}Kr measured relative to the ^{127}Xe during this period. Internal tracer totals are sometimes estimated by calculation when measurements based on emplaced tracers are unavailable.

Normally, we prefer to emplace a unique tracer material with the explosive so that its total can be determined under controller conditions. Materials that have been used include ^{127}Xe, ^{85}Kr, ^{222}Rn, and stable neon, krypton, and xenon. All except ^{127}Xe require a background correction. This is obtained for ^{85}Kr from the ^{85m}Kr seen in the samples; for radon from helium, using the known preshot radon/helium soil ratio; and for the stable gases from argon in air or helium in natural gas, using known preshot tracer/argon or tracer/helium ratios.

Due in part to the expense and handling difficulties of radioactive tracers, and principally to the development of reliable trace-gas measurement techniques by Newton, *et al.,* (1973) we now rely almost entirely on stable gas tracers. The most notable example is the Rio Blanco gas-stimulation experiment, where each of the three explosives was emplaced with a unique tracer gas. When production testing is begun, we plan to use these tracers to monitor the degree of inter-chimney communication and, if possible, to gain some insight into characteristics of the individual chimneys. For gas diagnostics of test program events, we often use stable krypton and/or xenon as the emplaced tracer material.

NOBLE GASES FROM A NUCLEAR EXPLOSION

Our studies of nuclear detonations must treat at least five distinct sources of noble gases: (1) The fission process generates many krypton and xenon isotopes both directly and as a consequence of radioactive decay of their precursors; (2) helium isotopes are among the products of thermonuclear reactions; (3) neutrons generated by the detonation interact with components of the explosive, and of the surrounding medium, to create noble gas isotopes through nuclear reaction processes; (4) the detonation itself vaporizes, melts, and fractures the medium surrounding it, causing the release of soil gases to the chimney voids; and (5) air normally enters the chimney region to replace the condensing steam during the cooling process, and in doing so introduces an often significant quantity of noble gases that may be generally termed "background." Each of these sources can be characterized and quantitized, using the analytical procedures mentioned previously. The results of such a characterization constitute a viable gas-diagnostic program.

To obtain performance estimates for the explosive, we rely principally on those species expected to be present in the cavity at relatively early times following detonation. Prior to chimney collapse, dynamic mixing within the cavity assures a reasonably uniform mixture of detonation products and tracer gases, thus fulfilling a basic prerequisite for meaningful results. In practical terms, this limits diagnostic fission measurements to the krypton isotopes of mass 85, 87, and 88. Three of the four are short-lived, necessitating rapid sample recovery and analysis. If sampling times are early enough so that xenon isotopes measured in the gas are attributable to their independent fission yields, then these species can be used in diagnostics. At intermediate times, interpretation of the measured totals of xenon isotopes is complicated. The xenon precursor nuclides are predominately deposited on cool rock surfaces when the chimney collapses. Since chimney-gas mixing rates are considerably slower than cavity rates, and some entrapment of the gas may occur, the diagnostic application of the xenons during this period is questionable. In general, we prefer to use these isotopes to study the phenomenon of gas mixing rather than for diagnostics. However, in some cases, where late-time observations have been possible, we have been able to demonstrate that an appreciable fraction of the xenon was mixed with the gas, and have been able to extract diagnostic information from its measurement.

Since a significant fraction of the yield of a thermonuclear explosive is due to the fusion of deuterium and tritium to produce ^{4}He and a neutron, an experimental measurement of the device-produced helium is potentially useful in diagnostics. The measurement is complicated by the presence of "background" helium in the chimney gas from air and from soil. The argon content of a sample is a useful indicator of the amount of helium (and other noble gases) present due to air dilution. Amounts of helium and radon in the soil gas are related, since both are radiogenic. If the preshot helium/radon ratio for the detonation environment is known, then the radon in a sample becomes a useful indicator of the background helium contributed by the soil, and is also a useful indicator of the amount of rock that has been fractured by the detonation.

Neutrons produced by the detonation are eventually captured by materials in the device and its immediate surroundings. Although certain isotopes of each of the noble gases are potential products of these reactions, the most abundant such activation product is ^{37}Ar --- produced principally from calcium. Production of the ^{37}Ar occurs at zero time within the molten rock sphere around the explosive. It is, therefore, uniformly distributed

and well mixed with other detonation products in the expanding cavity. Because of this, we have found ^{37}Ar to be an extremely useful relative gas-tracer material, and we have also used it as an internal diagnostic tracer for samples that are too diluted to provide a useful stable gas-tracer measurement. In the latter application, the total ^{37}Ar must first be known from the results of measurements on good-quality samples, since calculational estimates of activation processes are quite imprecise.

CONCLUSION

Throughout this presentation I have attempted to provide a generalized summary of our gas-diagnostics program and of its utilization of the noble gases in studies of underground nuclear detonations. The results of some of these investigations have been published in connection with the Gasbuggy and Rulison experiments (Smith, 1970a and b, 1971 and 1972). The specifics of our investigations do not easily lend themselves to generalization, as each event is unique in itself in many ways. Such detailed presentation of our results is necessarily relegated to individualized topical presentations. My goal here has been to draw upon our experience in gas analysis techniques to describe concepts that are of general interest and applicability.

REFERENCES

Crawford, R., R. Stump, and J. Frazer (1970), *A Computerized Fully Automatic Analytical Mass Spectrometer,* Lawrence Livermore Laboratory, Rept. UCRL-50931, Part I (Mechanical Design).

Crawford, R., R. Stump, and J. Frazer (1971), *A Computerized Fully Automatic Analytical Mass Spectrometer,* Lawrence Livermore Laboratory, Rept. UCRL-50931, Part II (Electronic design).

Grens, J., G. Morris, and D. Skinner (1972), *The Technique of Obtaining Gas Samples from Underground Nuclear Detonations,* Lawrence Livermore Laboratory, Rept. UCID-15999.

Momyer, F. (1960), *The Radiochemistry of the Rare Gases,* Subcommittee on Radiochemistry — National Academy of Sciences, National Research Council, Rept. NAS-NS 3025.

Newton, J., F. Stephens, and R. Stump (1973), *Determination of Trace Noble Gases in Air and Natural Gas,* Lawrence Livermore Laboratory, Rept. UCRL-74695 (to be published); also to be published in "Proc. Noble Gases Symposium Las Vegas, Sept. 24-28, 1973."

Quong, R. (1972), *Project Definition, Chimney Gas Sampling System: Rio Blanco,* in "Project Rio Blanco Phase I Technical Studies," J. Toman and H. A. Tewes, Eds., Lawrence Livermore Laboratory, Rept. UCID-15968, Appendix I.

Smith, C. (1970a), *Gas Quality Analysis and Evaluation Program for Project Gasbuggy,* in "Proc. Symposium on Engineering with Nuclear Explosives, Las Vegas, Jan. 14-16, 1970" (CONF-700101), Vol I, p. 775.

Smith, C. (1970b), *Behavior of Radionuclides in Nuclear Gas Stimulation Techniques,* in "Proc. Symposium on Engineering with Nuclear Explosives, Las Vegas, Jan. 14-16, 1970" (CONF-700101), Vol. I, p. 818.

Smith, C. (1971), *Gas Analysis Results for Project Rulison Production Testing Samples,* Lawrence Livermore Laboratory, Rept. UCRL-51153.

Smith, C. (1972), *Chimney Gas Radiochemistry in Nuclear Gas Stimulation Applications,* "Nucl. Technol. 15,)) 85.

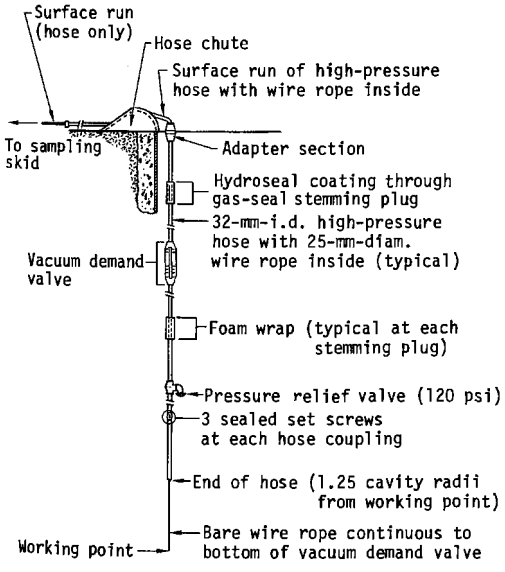

Figure 1. Gas-Sampling System.

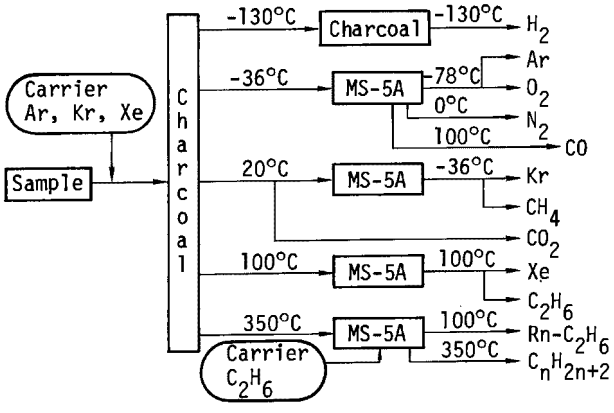

Figure 2. Gas-Analysis Separation Scheme.

RADON-222 MEASUREMENTS ABOARD AN AIRPLANE FOR THE DESCRIPTION OF ATMOSPHERIC DIFFUSION*

J. Bogen
II. Physics Institute
University of Heidelberg
Heidelberg, Germany**

ACKNOWLEDGEMENTS

The author expresses his thanks to Dr. G. Schumann, Head of the Laboratory for Environmental Radioactivity of the II. Physics Institute of the University of Heidelberg, for suggestions and advice in interpreting the results of the investigation. My thanks are also due to Dr. W. Roedel for helpful discussions. For assistance during equipment installation aboard the aircraft, as well as flight coordination, I wish to thank Dr. M. Reinhardt, Deutsche Forschungs- und Versuchsanstalt fur Luft- und Raumfahrt, Oberpfaffenhofen, Germany.

Abstract

Radon-222 is absorbed aboard an airplane in tubes filled with 50 g of selected charcoal and cooked in Dewars by carbon dioxyde and freon. After air collection at different heights up to 5 km, the tubes are evacuated and heated in the laboratory for desorption of the gas molecules and for transfer into a decay chamber covered with zinc-sulfide serving as a scintillator for the detection of alpha activity from radon-222 and its daughters. In general, the measurements show an exponential decrease of the concentration up to 5 km in height, if there is no cloud layer. The height for a reduction by a factor of two is about 900 meters. Assuming a constant diffusion coefficient K_0 up to 5 km, the measurements yield a K_0 of approximately 3.7×10^4 cm^2s^{-1}.

For flights in stratiform clouds a decrease is observed of the concentration up to a certain height, then radon-222 is again increasing or remains constant. This must be explained with respect to the meteorological situation. Assuming only a constant value for K_0 between the different flying heights, it was possible to appraise the development of the eddy diffusion coefficient with height.

INTRODUCTION

The radon isotopes ^{222}Rn, ^{220}Rn, and ^{219}Rn are the gaseous members in the naturally occurring decay chains ^{238}U, ^{232}Th, and ^{235}U. Due to the concentrations of their parent elements in the earth's crust, and their half-lives of 3.8 days (^{222}Rn), 54 seconds (^{220}Rn), and 3.9 seconds (^{219}Rn), the gaseous isotopes reach different heights in the atmosphere. Their daughter products are heavy metal ions which adhere rapidly to aerosol particles present in the atmosphere. In early measurements, the radioactivities of the aerosol particles deposited on filters were often used to estimate the radon concentrations in air. This presupposes some knowledge of the radioactive equilibrium between radon and its daughters. A recent discussion of the problems in this field is given by G. Schumann (1972).

Due to its long half-life, ^{222}Rn is a natural tracer in the troposphere. Dalu (1971) confirmed in laboratory experiments that the only removal mechanism of gaseous ^{222}Rn from an atmosphere consists in its radioactive decay — in contrast to its daughter products which are removed by rain-out, wash-out, and/or dry deposition. Thus, assuming a constant exhalation rate, the variations of the ^{222}Rn concentrations in the earth's atmosphere can be used for the description of turbulent diffusion — even inside the clouds or during precipitation.

In recent years, only a few measurements are known for determining ^{222}Rn height profiles in the atmosphere. Hosler (1969) calculated the ^{222}Rn concentration from the beta activity of ^{214}Pb and ^{214}Bi from filters exposed for 20 minutes at 1 meter and 91 meters on a meteorologically instrumented tower in Troysons Corner (Virginia, U.S.A.). The concentrations calculated for ^{222}Rn are corrected with respect to radioactive equilibrium.

Birot, *et al.*, (1970) measured the radioactivity of short-lived ^{222}Rn daughters deposited on filters aboard an airplane (Cessna TU-206) in the southwest of France, using a zinc-sulfide scintillation screen of 20 cm in diameter for the detection of the radioactivity. Wilkening (1970) collected air samples in evacuated stainless steel tanks of 34.4-, 16.4-, and 8.2-liter volumes with an aircraft (Queenair) in Central New Mexico, U.S.A., using the radon counting system of Johnson's Laboratories. Paffrath (1971) developed equipment for the measurement of α - and β - radioactivities of the radon-daughters deposited on filters aboard an airplane (Dornier DO-27) in the area of Munich, Germany.

**Part of this work was financially supported by the German Federal Ministry of the Interior (Schutzkommission).*

***Present address: Abteilung Strahlenschutz und Sicherheit, Gesellschaft fur Kernforschung Karlsruhe, Posfach 3640, 7500 Karlsruhe, Germany.*

In the following section, a system is described which is suitable for aircraft installation using ^{222}Rn adsorption on cooled charcoal. The system was developed at our Institute by Wenzel (1964) and improved by Bogen, *et al.*, (1970).

EXPERIMENTAL

Atmospheric air is sucked through a dry cell, a filter for aerosol retention, and cooled tubes filled with charcoal. During ground-level measurements, the air intake is outside the laboratory window (about 20 meters above the ground) and passes through polyethylene tubes. A vacuum pump is connected to the outlet of the charcoal filled tubes. When the ^{222}Rn enrichment system is installed in the aircraft used for the experiments (Queenair 65-65), a specifically designed emergency window is available for air suction from outside the cabin. During the flight, the output of the charcoal filled stainless-steel tubes is connected to the suction-air system of the aircraft, which generates an air stream of 4 liters per minute in the system. A total volume of 100 liters per sample is necessary. Figure 1 shows a schematic diagram of the arrangement.

Phosphorus-pentoxide granules are used as a drying agent mixed with a color indicator which shows the consumption of the agent. This is necessary because the adsorption coefficient of ^{222}Rn on charcoal depends on the water content of the air stream. Behind the dry cell, the dew point of the air is about -50 degrees Celsius. The cellulose asbestos fiber filter is necessary for retention of aerosols, as well as particulate matter from the drying agent. Differential and integral flow meters are inserted before connection to the stainless-steel tubes filled with 50 grams of charcoal. The tubes are closed on each side by a valve. The charcoal was selected for low ^{226}Ra content to avoid ^{222}Rn emanation from the adsorbens. The type used (Merck-Kohle Nr. 9624) showed a concentration of 2.7 fg of ^{226}Ra per gram of charcoal.

Before each experiment the stainless-steel tubes filled with charcoal are heated in a vacuum up to + 450°C for desorption of the gas molecules attached. Subsequently, six tubes are cooled to - 78°C in a Dewar vessel (stainless-steel) containing difluoro-dichloro-methane and dry ice. The beginning of the cooling period was at least one hour before the start of the experiment.

The Dewar vessel is mounted on an experimentation rack in the aircraft, and the air is sucked through polyethylene tubes from outside the aircraft cabin. After adsorption of ^{222}Rn at the desired height, the tubes are brought back to the laboratory; and after having been warmed up to room temperature, they are kept in the vacuum for 5 minutes. This causes no loss of ^{222}Rn, but reduces the gas volume desorbed from the charcoal after heating up to +450°C.

Figure 2 shows the radon measuring system consisting of two identical decay chambers (K I and K II) with a volume of 168 cm^3. The inner walls of the chamber are coated with silver-activated zinc-sulfide as the scintillator, which is viewed by a photomultiplier tube. The decay chambers are evacuated before every measurement. The gas desorbed from the charcoal is transferred to the decay chambers by opening the valves and flushing the charcoal with a stream of helium until atmospheric pressure is reached in the decay chamber.

The counting rate recorded on a scaler increases until radioactive equilibrium is reached between ^{222}Rn and its short-lived daughter products. Above 75% of the counting rate in equilibirum is reached within 30 minutes. The recorded counts are printed out automatically within preset time intervals.

The detection limit is on the order of one pCi per chamber volume, with a total error of about $\pm$ 10%.

During the flight, the air temperature was recorded automatically on a plotter, while the humidity was measured discontinuously by a dew-point hygrometer. The flight height was plotted using a barometric height recorder.

BASIC RELATIONS

The distribution of radon in the troposphere can be described rather well by the theory of eddy diffusion. Detailed discussions of the problems involved were given by Bolin (1962) and Jacobi and Andre (1963).

Assuming a constant exhalation rate (E) from the ground, which is independent of time, and a uniform horizontal distribution of ^{222}Rn, the vertical concentration profile can be described as a solution of the following differential equation — presupposing a negligible vertical wind velocity u_z.

$$(I) \quad \frac{\partial}{\partial z}\left(K_z \times \frac{\partial n}{\partial z}\right) - \lambda \times n = 0 \qquad (1)$$

K_z = vertical eddy diffusion coefficient [$cm^2 \times s^{-1}$]
n = ^{222}Rn concentration [atoms per volume]
λ = radioactive decay constant [s^{-1}]
E = exhalation rate [atoms x $cm^{-2} \times s^{-1}$]
c = $\lambda \times n$ = radioactivity concentration of ^{222}Rn [Ci x m^{-3}]

To solve eq. (1), the following assumptions are made:

(a) $\frac{\partial n}{\partial t} = 0$ ($\triangleq$ steady-state condition)

(b) $\frac{\partial n}{\partial x} = \frac{\partial n}{\partial y} = 0$ ($\hat{=}$ uniform horizontal distribution)

(c) $u_z = 0$ ($\hat{=}$ neglected vertical wind velocity)

The boundary conditions for Eq. (1) are:

(a) $\int_0^\infty \lambda \times n \times dz = E$ (This means that the total radioactivity found in a vertical air column is equal to the exhalation rate of the ground surface area.)

(b) $n \xrightarrow[(Z \to \infty)]{} 0$ (This means that the ^{222}Rn concentration decreases with increasing height as a consequence of the radioactive decay.)

Assuming a height-independent vertical diffusion coefficient, $K_z = K_c$, solution of Eq. (1) is:

$$n(Z) = \frac{E}{(\frac{\lambda}{K_c})^{1/2}} \times EXP\left[-(\frac{\lambda}{K_c})^{1/2} \times Z\right] \tag{2}$$

Considering concentration ratios in different heights, $Z_1 < Z_2$, the following equation becomes independent of the exhalation rate E:

$$\frac{n(Z_2)}{n(Z_1)} = EXP\left[-(\frac{\lambda}{K_c})^{1/2} \times (Z_2 - Z_1)\right] \tag{3}$$

Consequently, the boundary conditions must be valid for the height interval considered, and K_c is assumed to be constant in this interval.

For the vertical diffusion coefficient Eq. (3) yields:

$$K_c = \frac{\lambda \times (Z_2 - Z_1)^2}{\left[\ln(\frac{n(Z_2)}{n(Z_1)})\right]^2} \tag{4}$$

For theoretical considerations, the height intervals can be chosen infinitely small, and the height-dependent diffusion coefficient is the approximation of the step function for K_c, when $(Z_2 - Z_1) = \Delta Z$ approaches zero:

$$K_z = \lim_{\Delta Z \to 0} K_c \tag{5}$$

For measurements, the height intervals chosen for the determination of the ^{222}Rn concentration are always finite, and greater than zero. Using Eq. (4), one can determine the vertical diffusion coefficient step-by-step, always being independent of height within the chosen interval used for determination of the two concentrations.

One has to bear in mind all the presuppositions and boundary conditions which are necessary to get the solution of Eq. (1). If the measurements yield increasing concentrations with increasing height, one can only state that in this region no steadv-state solution is possible. This might be caused by advective processes, ($\partial n/\partial x \neq \partial n/\partial y \neq 0$) by a layer structure of the troposphere, ($\partial n/\partial t \neq 0$).

In the following paragraphs, a least squares fit to the measured ^{222}Rn radioactivity concentrations is calculated on the basis of Eq. (3). This implies the general expression for the concentration ratio:

$$\frac{n(Z_{i+1})}{n(Z_i)} = EXP\left(\alpha[Z_{i+1} - Z_i] + \beta\right) \tag{6}$$

$$i = 1, 2, 3 \ldots\ldots$$

The value β was chosen to yield 100%, if $Z_{i+1} = Z_i = 0$, and α is determined by a computer such that the square deviations of the measured values from Eq. (6) are minimum. Comparing Eqs. (6) and (3), one gets the relation:

$$\alpha \triangleq + \left(\frac{\lambda}{K_c}\right)^{1/2}$$

and this yields:

$$K_c \triangleq \frac{\lambda}{\alpha^2} \tag{7}$$

An estimate of the error for the vertical diffusion coefficient derived with respect to Eq. (4) depends on the accuracy of the radon concentration measurement, which is on the order of $\pm 10\%$, and on the error of the height determination, which is on the order of $\pm 5\%$. Considering the expression

$$\frac{\Delta K_c}{K_c} = \pm \left[\left(\frac{\partial K_c}{\partial z}\right)^2 \left(\frac{\Delta z}{z}\right)^2 + \left(\frac{\partial K_c}{\partial n}\right)^2 \left(\frac{\Delta n}{n}\right)^2 + \ldots \right]^{1/2}$$

one finds that the main contribution comes from the error of the concentration measurement. Using height intervals of about 1,000 meters, and assuming a decrease by a factor of two for the concentration within 1,000 meters, one gets:

$$\frac{\Delta K_c}{K_c} \approx \pm 40\,\%$$

This error is assumed during the following discussion on the K_c values derived.

RESULTS AND DISCUSSION

The ground-level radioactivity concentration of ^{222}Rn (shown in Figure 3), as well as the precipitation measured in Heidelberg, is plotted for all days on which a height profile of ^{222}Rn was measured aboard the airplane. At ground-level an average value of ^{222}Rn of 91 pCi m^{-3} ($\pm 10\%$) is found for these days. The ground-level concentrations are discussed now as a function of time with respect to the meteorological conditions.

On June 24, 1971, in the western part of a high-pressure area reaching from the North Sea to the eastern part of the Mediterranian Sea, warm humid air moved into Germany. No precipitation was registered in Heidelberg. There were fair-weather cumulus, with the base at 1,500 m and the tops at 2,600 m. Measurements were taken only outside the clouds.

On June 26, 1971 the ground-level concentration was somewhat lower than two days before. A high-pressure area was over Spain, and warm humid air moved into Germany from the southwest. No precipitation was registered in Heidelberg. There were cumulus clouds (base 1,200 m, tops 2,100 m) and a stratocumulus layer between 2,700 m and 3,200 m. Measurements were taken only outside the clouds.

On June 28, 1971 a low-pressure area lay over the Netherlands, and a warm-front crossed the southern part of Germany. This produced 7.1 mm precipitation in Heidelberg. The clouds were formed by a thick stratocumulus layer between 1,500 m and 4,000 m. The ground-level radon concentration was again lower than two days before due to 13.5 mm precipitation on June 27, 1971.

On June 30, 1971 a high-pressure area lay over England, and on its eastern part, cold maritime air moved into Germany. This caused an occlusion accompanied by 10.6 mm precipitation in Heidelberg. The ^{222}Rn concentration measured at ground-level was only slightly higher than the minimum value measured one day before. The clouds were formed by a stratocumulus layer between 1,100 m and 2,900 m

The ^{222}Rn profile of June 24, 1971 is plotted in Figure 4 as a function of the height. The ^{222}Rn concentrations are reported in percentages of the ground-level value, and are connected with a dashed line, while the fit to the measured values is plotted as a straight solid line. The diffusion coefficients calculated from the measured values are given in the lower part of Figure 4 with respect to the scale on the right. There, the broken line is used as a vision line to link the different K_c values derived from the measured concentrations. As can be seen, the ^{222}Rn concentration decreases by a factor of two for every 300 m within the height interval 0 m to 600 m. Considering the interval 600 m to 1,100 m, the concentration is constant within the error limits. In the height interval 1,100 m to 3,000 m, the reduction by a factor of two in the concentration is reached within 550 meters. The higher concentration gradient in the interval 0 m to 600 m corresponds to a lower value for the eddy diffusion coefficient compared to the height interval 1,100 m to 3,000 m. The constant ^{222}Rn concentration in the interval 600 m to 1,100 m does not allow the determination of a value for K_c.

Figure 5 shows the height-dependence of the ^{222}Rn radioactivity concentrations for June 26, 1971. Decreasing values are observed until reaching the 3,600 m height which is just above the stratocumulus layer. At the height of 5,200 m, the concentration of ^{222}Rn is higher than at 3,600 m. This indicates that, in the height interval from 3,600 m to 5,200 m, the troposphere is layered — meaning that an air parcel is present there

which should be associated to a lower height, assuming steady-state conditions. The eddy diffusion coefficient in the interval from 600 m to 3.600 m is lower than in the interval 0 m to 600 m. This indicates a reduced exchange in the region of the stratocumulus clouds.

Figure 6 shows the ^{222}Rn profile of June 28, 1971 which decreases to a height of 2500 m. This height is in the middle of the stratocumulus layer. In the upper part of this cloud, the ^{222}Rn concentration increases — indicating a change of the air mass. This presumption is supported by the meteorological situation discussed above. The decreasing values of the eddy diffusion coefficient K_C indicates a minor exchange between the different air masses.

The measured ^{222}Rn concentrations of June 29, 1971 in Figure 7 agree well with the exponential decrease required in theory. This yields nearly constant values for the vertical diffusion coefficient K_C. On that day, Germany was on the rear side of the low-pressure area mentioned for June 28, 1971. Precipitation composition of the air mass is homogeneous until the height of 3,600 meters. Due to the precipitation of the previous day, which ended 15 hours before the start of the flight on June 29, 1971, the ^{222}Rn concentration measured in the maritime air probably does not have the concentration corresponding to the normal exhalation rate of the Heidelberg area. Sappok (1971) measured an increase in concentration after precipitation on the order of 50% within 6 hours using ^{220}Rn as the tracer.

Figure 8 shows the ^{222}Rn profile on June 30, 1971 with decreasing values until a height of 1,500 m was reached. In the interval of 1,500 m to 2,400 m, an increase in concentration is observed. This indicates a change of the air mass. The air present in this height interval should either be associated to a lower altitude or, in other words, reaches this height faster than forecasted by the steady-state solution. This agrees with the meteorological situation which makes an occlusion responsible for the stratocumulus cloud. The eddy diffusion coefficient decreases in the lower part of the cloud. This indicates a low exchange between the different air masses.

Table 1 summarizes the values from the measurements of ^{222}Rn profiles, such as the height for reduction of the concentration by a factor of 2, as well as the diffusion coefficient derived from measured values and from the calculated mathematical fit.

In Figure 9, the vision lines, derived from the vertical diffusion coefficients calculated from the measured ^{222}Rn concentrations, are given as broken lines. These are constructed, assuming the calculated values of K_C plotted in the previous figures, for the middle of the height interval considered. The broader solid parts of these lines indicate a layer cloud, when present. For ground-level (Z=0), the molecular diffusion coefficient of ^{222}Rn in air is assumed (about 5.5×10^{-2} cm^2 s^{-1}). Measurements performed by Sappok (1971), using ^{220}Rn as the tracer, yield 1.2×10^3 cm^2 s^{-1} as an average value for the vertical eddy diffusion coefficient between 1 m and 6 m in height. This value is used in Figure 9. The method for these measurements is described by Bogen, *et al.*, (1972).

The broken lines in Figure 9 show two different types of height-dependence for the vertical diffusion coefficient. On June 24 and 29, 1971, when only fair-weather cumuli were present, the eddy diffusion coefficient seemed to increase rapidly within the first 500 meters above ground, and thereafter increased only relatively slowly.

On June 26, 28, and 30, 1971, when stratus clouds were present (indicated by the solid broader part of the lines in Figure 9), the diffusion coefficient seems to reach a maximum at a height which corresponds to the height of the cloud base. This indicates a change of the air mass or air parcel, respectively, and a low exchange through the boundary layer. The solid traced curves in Figure 9 represent values calculated by Jacobi and Andre (1963), who assumed special turbulence conditions in the ground-layer (0 to 1,000 m), the upper troposphere (1 km to 12 km), and the stratosphere (12 km to 30 km). These turbulence conditions are indicated by the characters I, W, N, S, which mean inversion, weak-, normal-, and strong-turbulence, respectively.

For June 24, 1971, the vertical eddy diffusion coefficient derived from measurements agrees well with the IWN-type of Jacobi and Andre's (1963) calculations, but no pronounced temperature inversion could be observed because the accuracy of the temperature measurement was not sufficient. One June 29, 1971, the development is similar to the NNN-type calculated by Jacobi and Andre (1963). The rest of the profiles measured yield a height-dependence of the diffusion coefficient which agrees in principle with the NWN-type of Jacobi and Andre's (1963). The profiles derived from the measured values of days with stratus clouds reach the maximum value of the eddy diffusion coefficient at a greater height than predicted by the calculations.

All measured ^{222}Rn concentrations are plotted in Figure 10 as percentages of the ground-level value (equivalent of 100%) as a function of the height. The mathematical fit for all these values is marked as a straight line, and yields a decrease by a factor of two in the ^{222}Rn concentration for a height of 986 meters (minimum value 300 m, maximum value 1,500 m). This means, for the case of a steady-state structure of the atmosphere, that ground-level air takes the half-life of ^{222}Rn (3.8 days) to reach a height of about 1,000 meters. This yields an averaged vertical eddy diffusion coefficient of about 4×10^4 cm^2 s^{-1} (minimum value 4×10^3 cm^2 s^{-1}, maximum value 1×10^5 cm^2 s^{-1}) for the Heidelberg area in June 1971.

SUMMARY

A method which uses adsorption of atmospheric ^{222}Rn on cooled charcoal is described. ^{222}Rn height profiles were determined using a specially equipped airplane in the area of Heidelberg from June 24 to 30, 1971. Basic relations of the eddy diffusion theory were used for interpretation of the results, and for determination of the vertical diffusion coefficient. The average ground-level radioactivity concentration of ^{222}Rn for the time mentioned was 91 pCi per cubic meter of air. An average decrease by a factor of two for the ^{222}Rn concentration

was found at 1,000 meters of height. This yields, for the height-independent vertical diffusion coefficient, an average value of 4 x 10^4 cm^2 s^{-1}. The derived development of the height-dependence of the vertical eddy diffusion coefficient showed a rapid increase within the first 500 meters above ground; above this height, it increased slowly when no stratiform clouds were present. A decrease in height was observed in the vertical eddy diffusion coefficient when stratiform clouds were present in the lower troposphere; this was probably due to meteorological conditions.

REFERENCES

Birot, A., B. Androuguer, and J. Fontan (1970), *Vertical Distribution of ^{222}Rn in the Atmosphere and its Use for Study of Exchange in the Lower Troposphere.* J. Geophys. Res. 75, 12 2373.

Bogen, J., G. Hoffmann, and G. Kirrstetter (1970), *Experimente zur Anreicherung von ^{222}Rn.* Jahresbericht II. Phys. Institut Heidelberg, (unpublished).

Bogen, M. Sappok, and G. Schumann (1972), *Measurements of Atmospheric Radon-220 Using Delayed Alpha-Particle Coicidences.* Arch. Met. Geophys. Biokl. Ser. A, 21 171.

Bolin, B. (1962), *Transfer and Circulation of Radioactivity in the Atmosphere,* in Nuclear Radiation in Geophysics (Ed. H. Israel and K. Krebs) p. 136, Springer Verlag, Berlin.

Dalu, G. A. and G. Dalu (1971), *An Experimental Check on the Removal of Radon.* Aerosol Sci 2 241.

Hosler, C. A. (1969), *Vertical Diffusivity from Radon Profiles.* J. Geophys. Res. 74 28 7018.

Jacobi, W. and K. Andre (1963), *The Vertical Distribution of ^{222}Rn, ^{220}Rn, and their Decay Products in the Atmosphere.* J. Geophys. Res. 68 13 3799.

Paffrath, D. (1971), *Untersuchung der Vertikalverteilung von Radonfolge-produkten in der Troposphare mit dem Flugzeug mit Anwendung auf den vertikalen turbulenten Austausch.* Bericht: DLR RB 71-68, Deutsche Forschungs- und Versuchsanstalt fur Luft- und Kaunfahrt, Oberpfaffenhofen, Germany.

Sappok, M. (1971), *Der Einfluβ meteorologischer Meβgröβen auf die Aktivitat des Thorons in der Atmosphare.* Diplomarbeit II. Physik. Institute Heidelberg (unpublished).

Schumann, G. (1972), *Radon Isotopes and Daughters in the Atmosphere.* Arch. Met. Geophys. Biokl. Ser. A, 21 149.

Wezel, K. P. (1964), *Messung des ^{222}Rn und seiner kurzlebigen Folgeprodukte in Bodennaher Luft.* Diplomarbeit, II. Physik Institute Heidelberg. (unpublished).

Wilkening, M. H. (1970), *^{222}Rn concentrations in Convective Patterns of a Mountain Environment.* J. Geophys. Res. 75 9 1733.

TABLE 1. Summarized Flight Data for the Determination of ^{222}Rn Radioactivity Concentrations in the Heidelberg Area. K_c(min,max) is Calculated from the Least Square Fit Values.

Date	Height Interval [meter] lower i	upper j	Height $\frac{c(Z_2)}{c(Z_1)} = 0,5$ meter	Vertical eddy diffusion coefficient $K_c(i,j)$ $[\frac{cm^2}{s}]$	K_c(min,max) $[\frac{cm^2}{s}]$
June 24, 1971	0	600	300	0.38×10^4	↓
	600	1,100	°°	ND	
	1,100	3,000	550	1.44×10^4	1.47×10^4
June 26, 1971	0	600	925	3.7×10^4	↓
	600	3,600	850	2.02×10^4	
	3,600	5,200	+	ND	5.08×10^4
June 28, 1971	0	1,300	850	2.56×10^4	↓
	1,300	2,000	500	1.37×10^4	
	2,000	2,500	350	5.78×10^4	
	2,500	3,600	+	ND	3.3×10^4
June 29, 1971	0	2,100	1,500	9.19×10^4	↓
	2,100	3,600	1,500	11.11×10^4	9.74×10^4
June 30, 1971	0	1,100	850	3.52×10^4	↓
	1,100	1.00	250	2.63×10^4	
	1,500	2,400	+	ND	6.07×10^4

+: increasing concentrations.
ND: not determined.

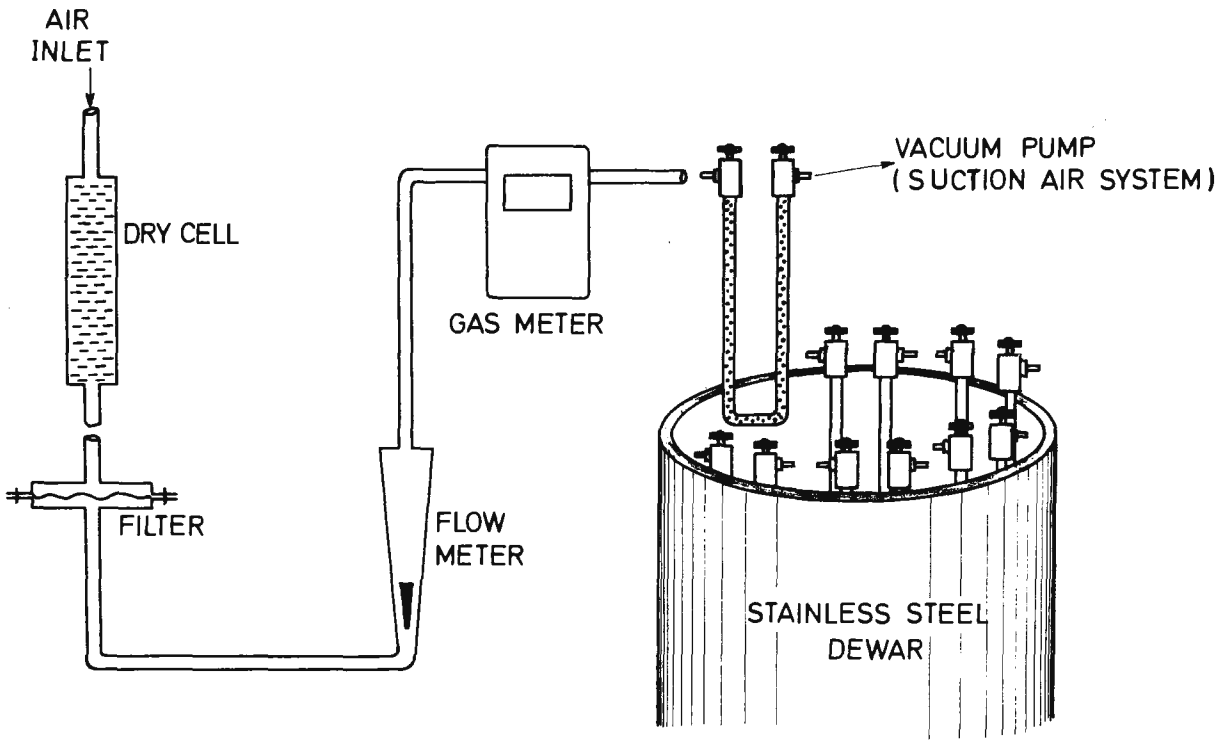

Figure 1. Schematic diagram of the ^{222}Rn enrichment system.

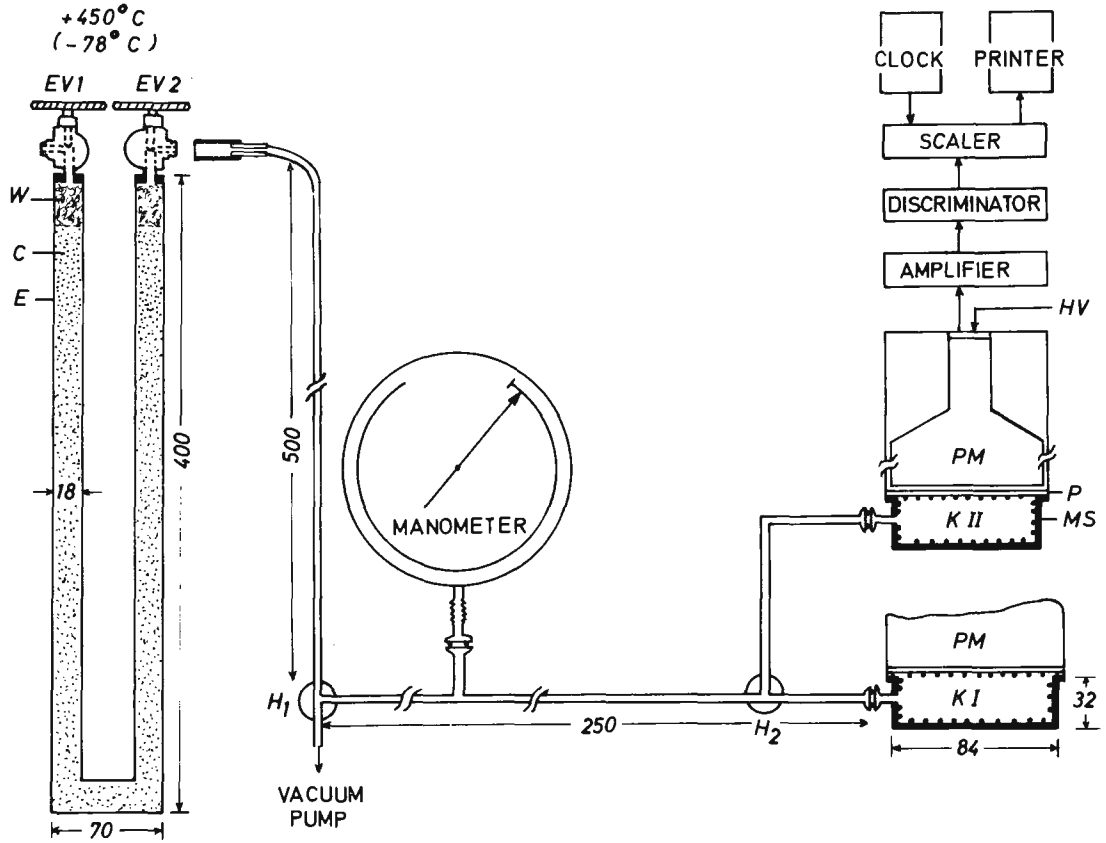

Figure 2. Schematic diagram of the ^{222}Rn measuring system. EV1, EV2, H1, H2 = valves, W = glass wool, C = charcoal, E = stainless-steel tube, KI, KII = decay chamber, MS = brass, P = Plexiglass (a methacrylate polymer), PM = photomultiplier, (dimensions in millimeters).

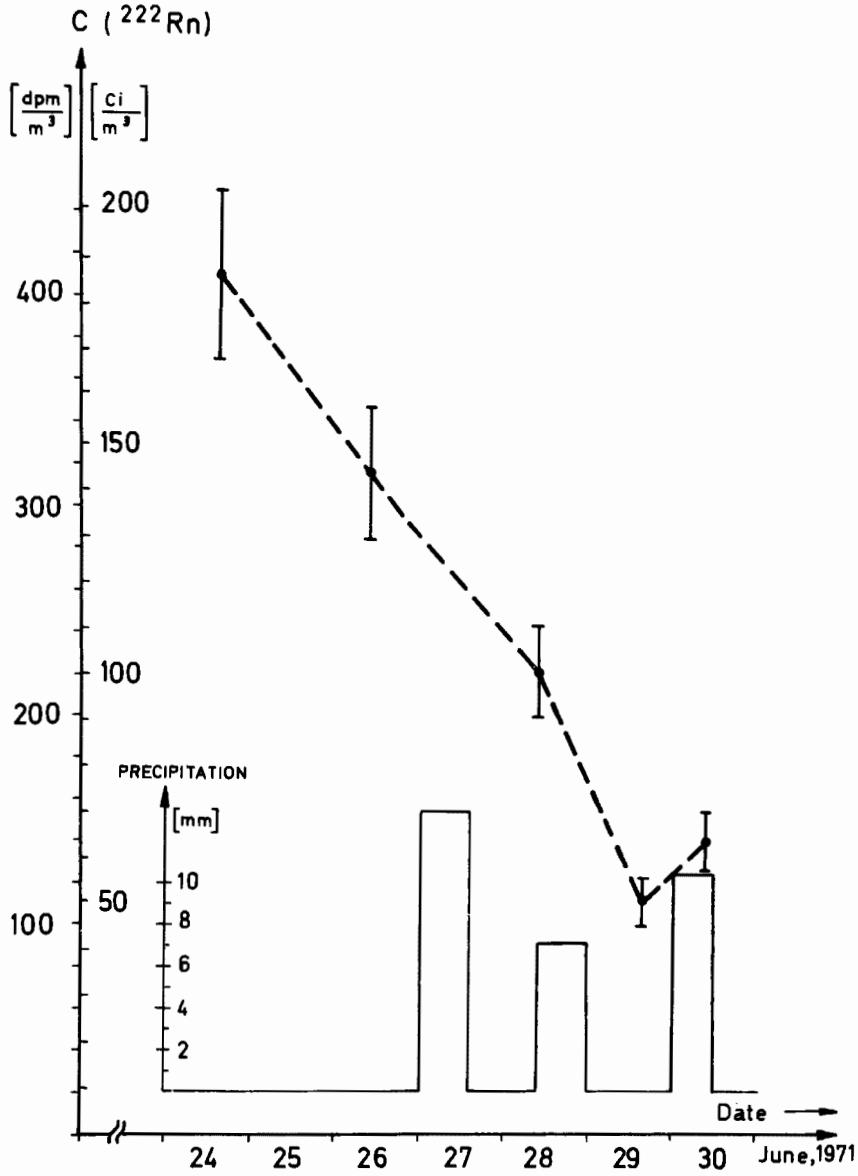

Figure 3. Radioactivity concentrations of ^{222}Rn and precipitation of June 24 to 30, 1971 registered at the Heidelberg ground-level station.

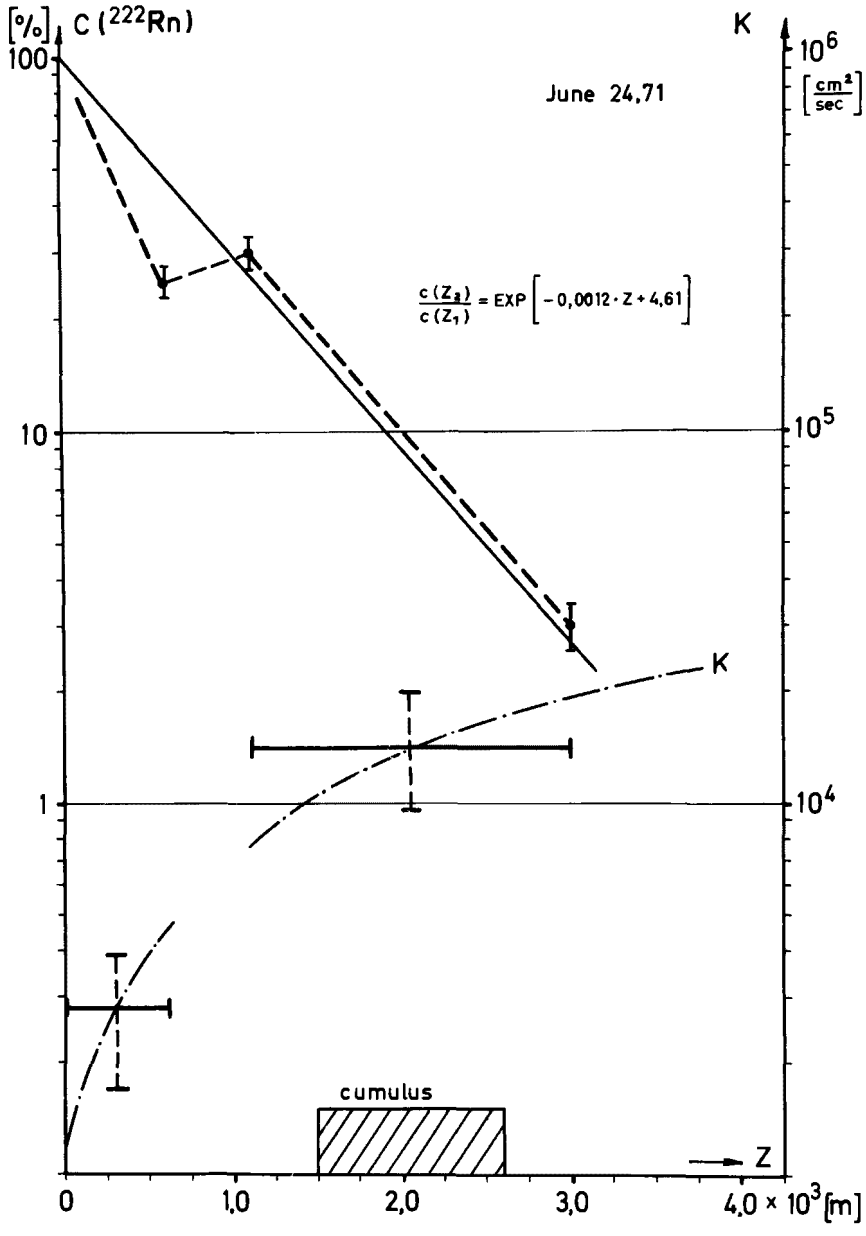

Figure 4. ^{222}Rn concentration of June 24, 1971 in percentages of the ground-level value and height-dependence of the vertical eddy diffusion coefficient K. The straight line gives the concentration calculated with a least squares fit program. The horizontal lines are the K_C values (of which the scale is on the right side) derived from the measured ^{222}Rn concentrations. The broken curve connects the K_C values at the centers of the height intervals.

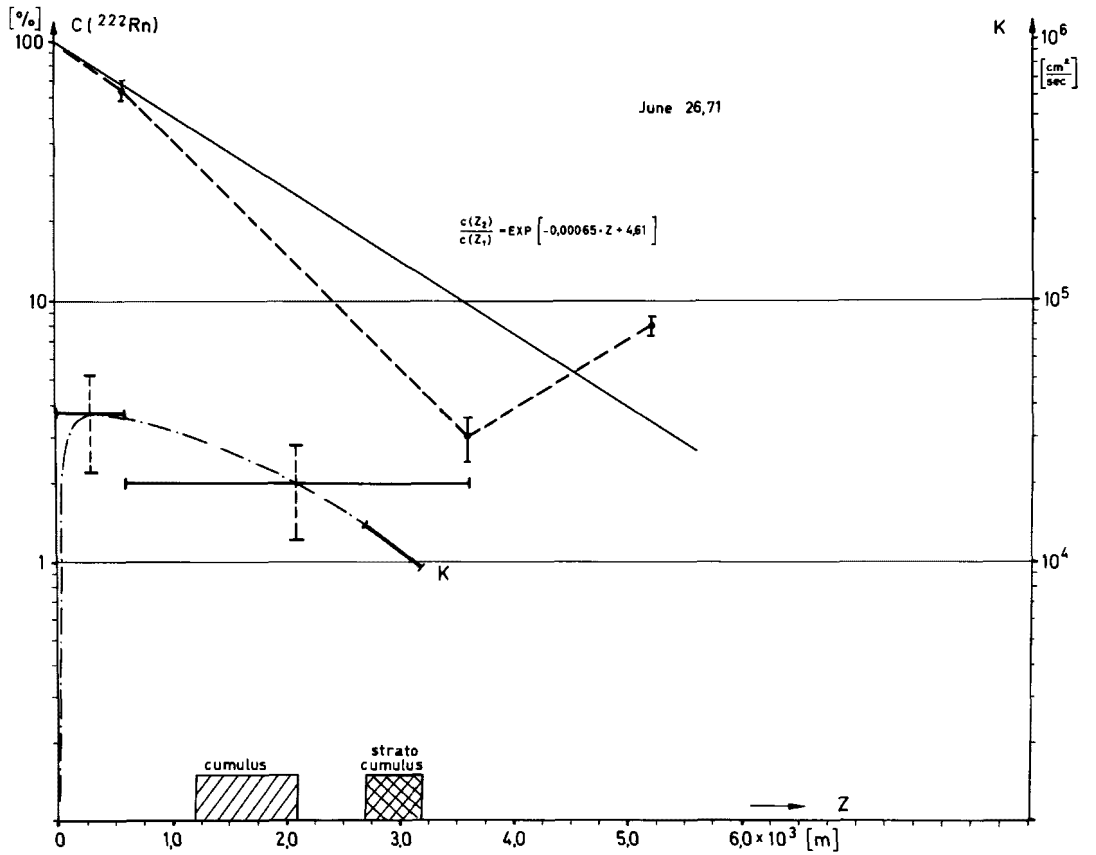

Figure 5. ^{222}Rn concentration of June 26, 1971 in percentages of the ground-level value and height-dependence of the vertical eddy diffusion coefficient K. The straight line gives the concentration calculated with a least squares fit program. The horizontal lines are the K_c values (of which the scale is on the right side) derived from the measured ^{222}Rn concentrations. The broken curve connects the K_c values at the centers of the height intervals.

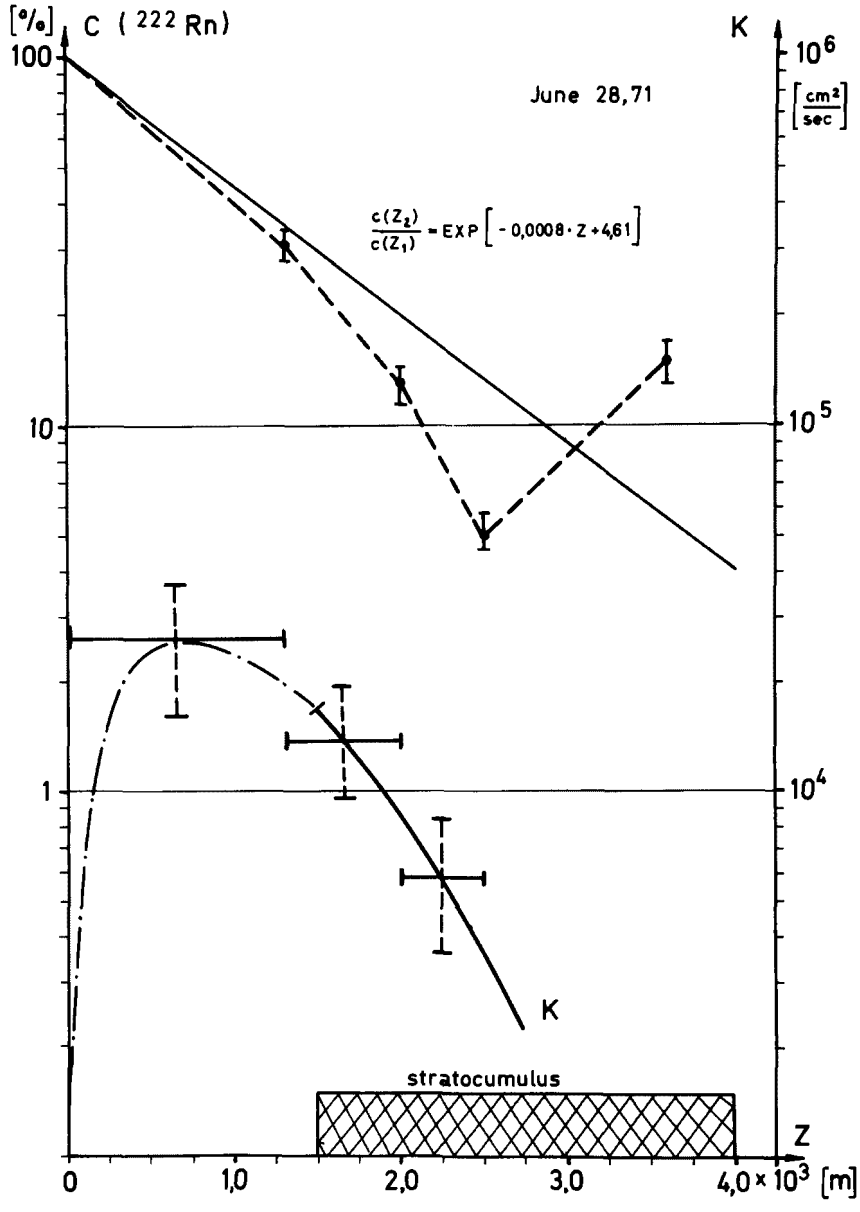

Figure 6. ^{222}Rn concentration of June 28, 1971 in percentages of the ground-level value and height-dependence of the vertical eddy diffusion coefficient K. The straight line gives the concentration calculated with a least squares fit program. The horizontal lines are the K_c values (of which the scale is on the right side) derived from the measured ^{222}Rn concentrations. The broken curve connects the K_c values at the centers of the height intervals.

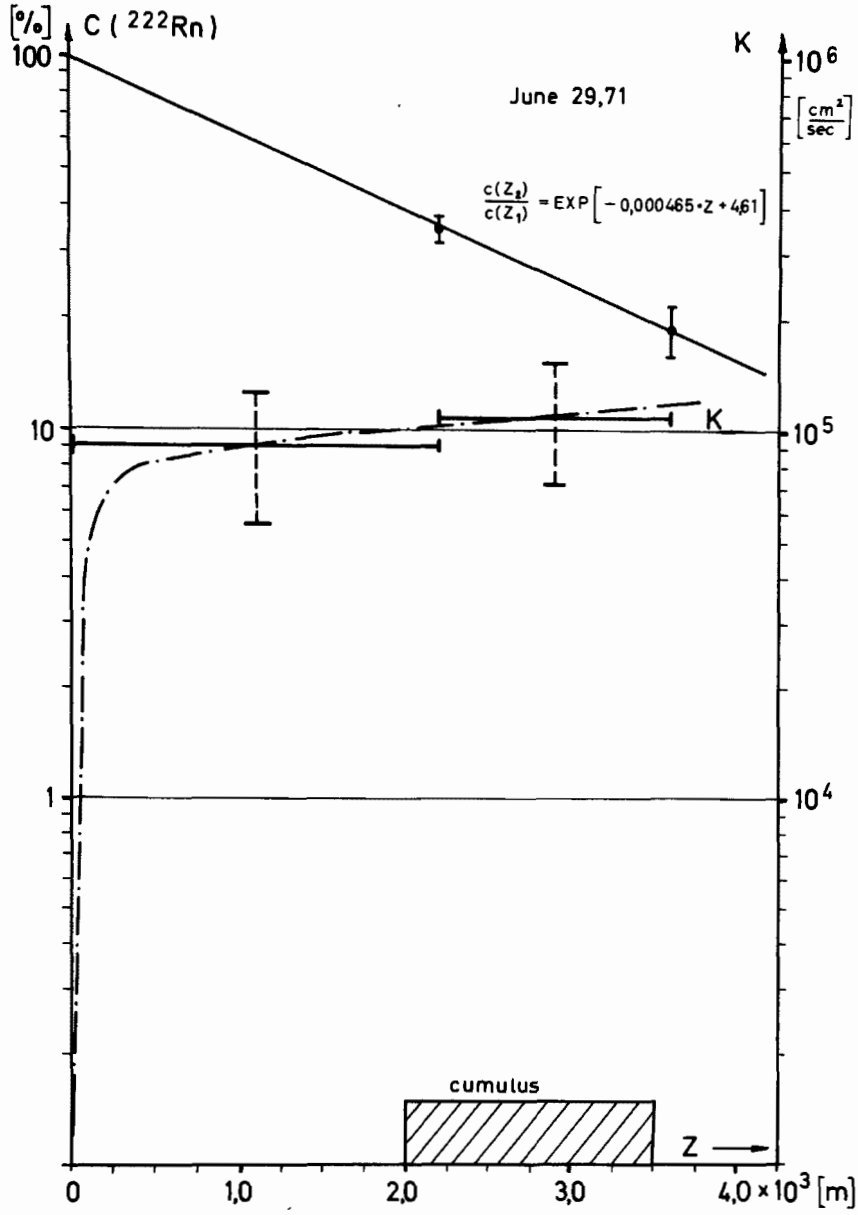

Figure 7. ^{222}Rn concentration of June 29, 1971 in percentages of the ground-level value and height-dependence of the vertical eddy diffusion coefficient K. The straight line gives the concentration calculated with a least squares fit program. The horizontal lines are the K_c values (of which the scale is on the right side) derived from the measured ^{222}Rn concentrations. The broken curve connects the K_c values at the centers of the height intervals.

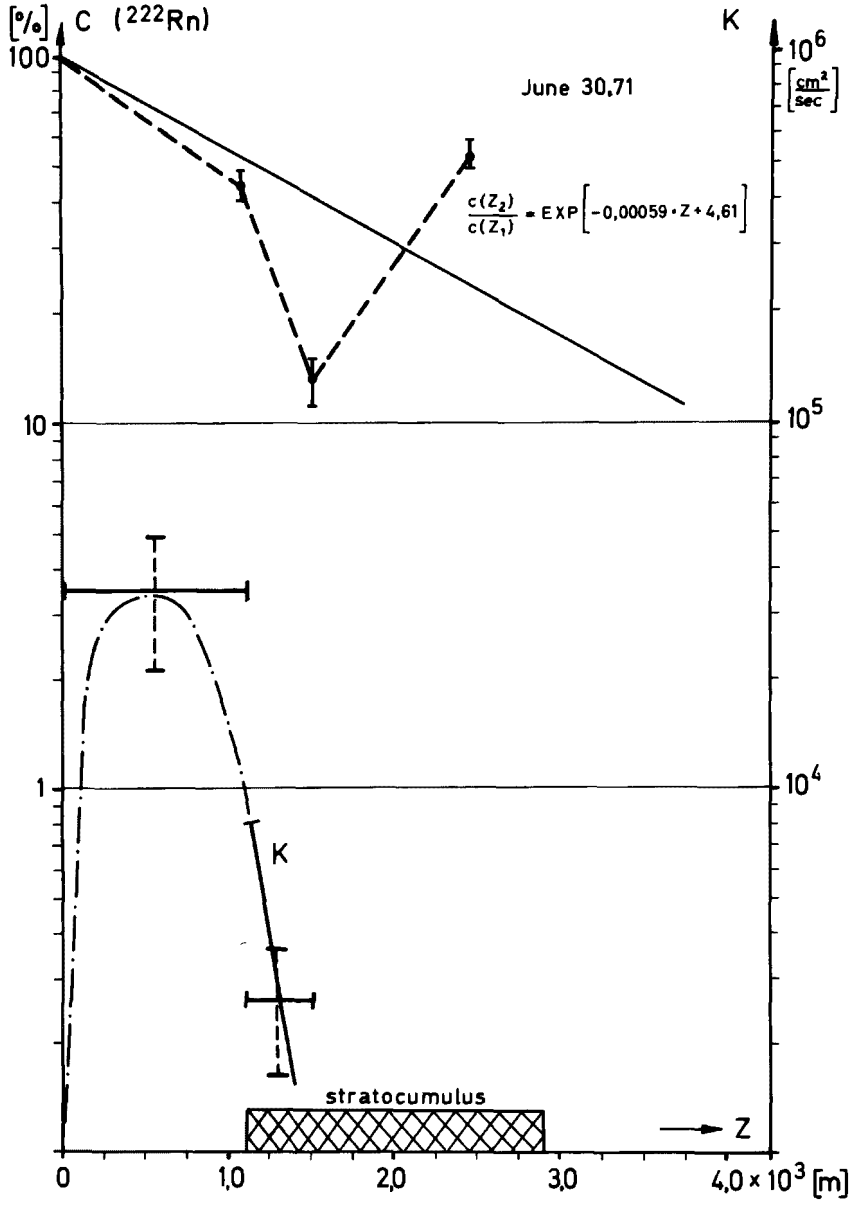

Figure 8. ^{222}Rn concentration of June 30, 1971 in percentages of the ground-level value and height-dependence of the vertical eddy diffusion coefficient K. The straight line gives the concentration calculated with a least squares fit program. The horizontal lines are the K_c values (of which the scale is on the right side) derived from the measured ^{222}Rn concentrations. The broken curve connects the K_c values at the centers of the height intervals.

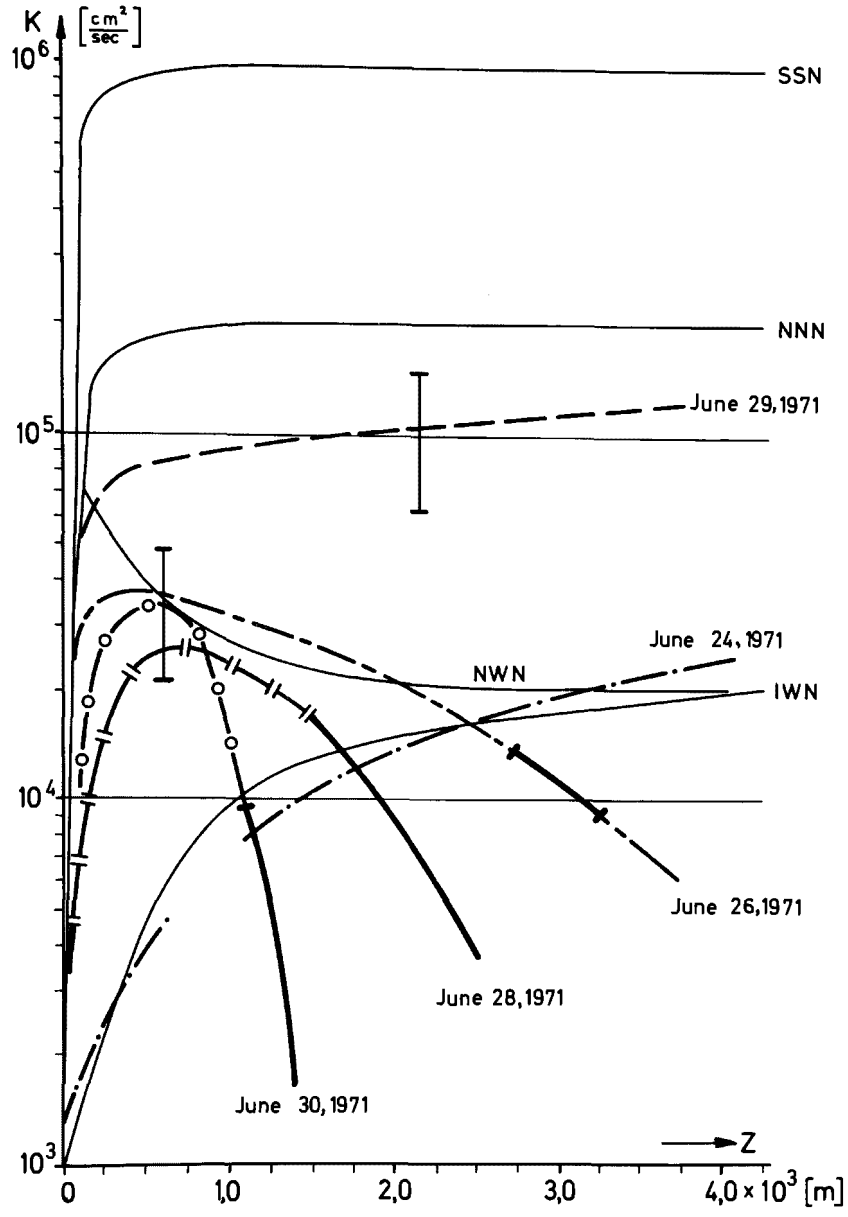

Figure 9. Height-dependence of the vertical eddy diffusion coefficient. Broken lines are derived from measured ^{222}Rn radioactivity concentrations (with indication of stratus clouds by broader solid parts). Solid lines: calculated values by Jacobi, *et al.*, (1963) for special turbulence conditions in the ground-layer, the upper troposphere, and the stratosphere, respectively. I, W, N, S, stand for inversion, weak-, normal-, strong-turbulence, respectively.

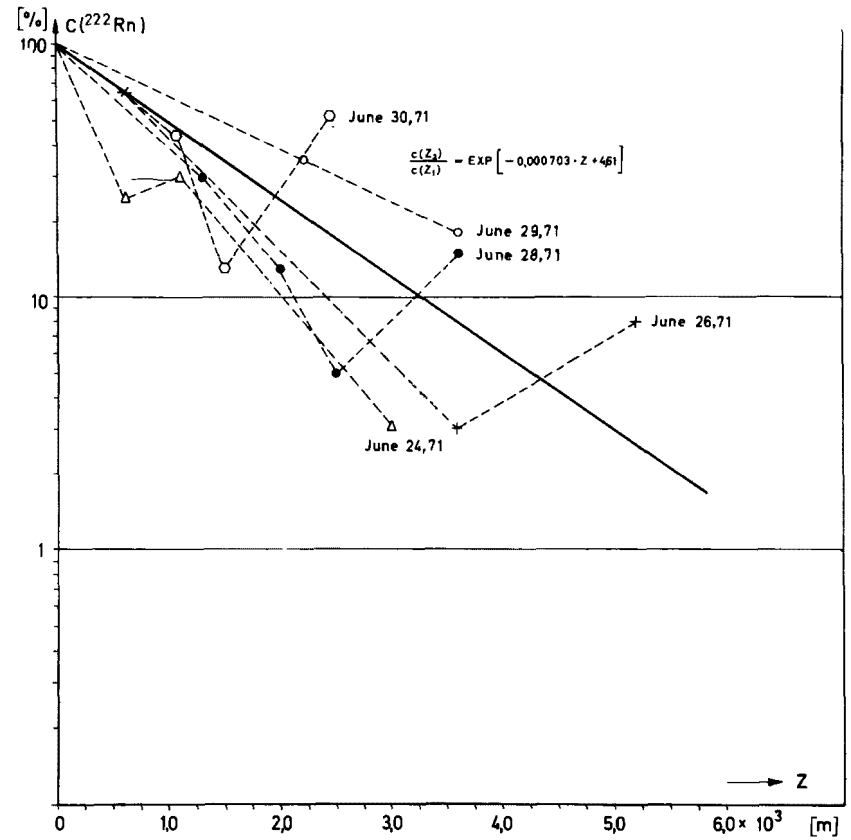

Figure 10. Radioactivity concentration profiles of ^{222}Rn in percentages of the ground-level value measured in June, 1971 in the Heidelberg area. The solid straight line represents the values calculated with the least squares fit to all measured values.

NOBLE GAS LASERS FOR AIR POLLUTION MONITORING

G. J. Linford
Laser Division
Hughes Aircraft Company
Culver City, California 90230

Abstract

Recent experiments with pulsed and continuous wave (CW) noble gas lasers have revealed that reliable, high gain laser oscillations at numerous infrared wavelengths can be achieved using a relatively simple laboratory apparatus. A total of more than eighty infrared neutral and ionized noble gas laser lines have been obtained using this equipment; eighteen of these noble gas laser lines were previously unreported. Despite the large number of noble gas laser lines, coincidences between laser lines and air pollution absorption lines are relatively rare, and hence some degree of spectral tuning is desirable in order to achieve coincidences between laser lines and pollutant absorption lines. In experiments performed here, it has been shown that a high-gain xenon laser can be tuned (using the Zeeman effect) over as much as 10 Å with applied dc magnetic fields of six kilogauss; furthermore, noble gas lasers may be tunable over more than 100 Å using strong, pulsed magnetic fields of at least sixty kilogauss. In spectral regions, where these noble gas laser lines are relatively closely spaced, the Zeeman effect may permit tuning from one laser wavelength to another. It has been shown here that high-gain noble gas laser lines can be tuned (via the Zeeman effect) into coincidence with absorption lines of selected pollutant gases.

INTRODUCTION

Among the most essential features of an effective air-pollution control system are unambiguous methods appropriate for detecting, identifying, and quantitatively measuring the concentrations and distributions of gaseous air pollutants. One highly useful technique for identifying and quantitatively measuring air pollutants is optical absorption spectroscopy. This paper presents the results obtained using noble gas lasers in absorption spectroscopic experiments conducted to (1) increase the number of available laser wavelengths; (2) tune individual laser lines over a narrow spectral region; and (3) demonstrate that quantitative data on the concentrations and distributions of selected air pollutants can be obtained with a noble gas laser absorption spectroscopic apparatus.

There have been a number of serious difficulties in the past that have been associated with using optical absorption spectroscopy for pollution measurements, most of which have been due to the use of incoherent light sources. With the technological development of laser sources, however, many of these difficulties are overcome, and the useful characteristics of absorption spectroscopy could be adapted from their former laboratory applications to actual field measurement situations.

Although laster oscillation has been achieved using a wide variety of solid-state, liquid, and gas lasers, the special requirements for air pollution monitoring equipment restrict the choice of laser sources to (1) continuously tunable lasers and/or (2) multiple wavelength, partially tunable lasers. This paper describes the work done in the latter category using noble gas lasers as narrow-band light sources for optical absorption spectroscopy.

Long optical path length absorption techniques using laser sources have a number of significant advantages over comparable incoherent optical detection techniques for the measurement and detection of air pollution. These advantages are:

(1) very narrow spectral line-widths permit extremely high resolution spectroscopic measurements to be obtained;

(2) the high laser radiances reduce the optical detection problems;

(3) the high beam collimation permits long optical path lengths to be monitored, thereby increasing the sensitivity;

(4) a capacity for unique identification of pollutant absorption lines is available using this technique; and

(5) laser sources offer the availability of coherent detection techniques (such as heterodyne detection).

Problems do remain, however, particularly those problems associated with band spectra, pressure broadening of fine spectral structures, etc.

The number and wide spectral dispersion of noble gas laser lines exceed those of all other discrete wavelength laser sources. To date, more than 400 neutral and ionized noble gas laser lines (Hdbk of Lasers, 1971) ranging in wavelength from the vacuum ultraviolet (xenon@0.1469μm) to the far infrared (neon@132.8μm). Tunable laser sources, notably dye lasers and optical parametric oscillators (OPO), are capable of covering specific spectral regions well, although, at present, not all spectral regions of interest are included. Thus, dye lasers cover the visible portion of the spectrum in detail, but, as yet, spectral coverage much beyond 1.0 micrometers is poor. OPO's have proven to be difficult to align and maintain, but OPO's are presently capable of generating optical radiation in the near visible and middle infrared portion of the spectrum.

The major absorption lines of atmospheric pollutants lie either in the ultraviolet (corresponding to atomic transitions within the atom constituents of the pollutant molecules) or in the infrared (corresponding to vibrations, rotations, torsions, etc., of the molecules themselves). Thus, aside from the oxides of nitrogen, most atmospheric pollutants appear to be nearly colorless, owing to the absence of absorption lines in the visible portion of the spectrum. Homonuclear molecules, such as N_2, are essentially free of absorption lines in the infrared, owing to the lack of a dipole moment; this is a convenient property, since it effectively eliminates homonuclear molecules from being detected (in the infrared), and homonuclear molecules are usually not sources of air pollution.

Although there are a large number of noble gas laser lines available, coincidences between these lines and individual absorption lines of pollutant gases are relatively rare. The advantage in having (1) numerous available laser lines and (2) a small degree of tunability of these lines is apparent since it is only necessary to tune a typical noble gas laser line from 10 to 100 Å before coincidence with a neighboring noble gas laser line can be achieved. In many cases, tuning a noble gas laser line by only 10 Å will bring that laser line into spectral coincidence with a pollutant absorption line. Noble gas laser lines are inherently fixed frequency/wavelength standards, unless the noble gas discharges are placed in relatively strong magnetic or electric fields. Recent experiments (Linford, 1973a) with a xenon laser oscillator placed inside a six kilogauss solenoid have indicated that a number of CW infrared xenon laser lines can be continuously tuned over a spectral interval of up to 11 Å using the Zeeman effect. These same experiments (Linford, 1973a) demonstrated that the 3.508 xenon laser line can be tuned into coincidence with an absorption line of formaldehyde with an applied magnetic field of approximately five kilogauss.

More than ten years have elapsed since laser oscillation was first reported in gas discharges of the neutral noble gases (Patel, *et al.,* 1962; Javan, *et al.,* 1961; and Faust, *et al.,* 1962). In spite of this, however, it has recently become apparent that a considerable number of new noble gas laser transitions may be available in addition to those previously reported in the literature. During the past two years, for example, the author has found a total of 18 new neutral argon, krypton, and xenon laser lines (Linford, 1972 and 1973b and c) using a relatively simple laser apparatus. Most of these new laser lines are located in spectral regions common to both the lasers and to spectral absorption lines of important atmospheric pollutants. As such, these new noble gas laser lines may be used as selective laser oscillators for differential absorption measurements of specific pollutant gases.

If a Zeeman-tuned noble gas laser is used as the probe laser source for such absorption measurements, laser oscillation at two wavelengths, λ_+ and λ_-, can be obtained. In general, only one of these two Zeeman-split laser lines will be tuned into coincidence with a spectrally-narrow pollutant absorption line, and, as a consequence, the laser line suffering the least absorption can serve as a comparison laser source for detailed differential absorption measurements (Linford, 1973a) for long atmospheric optical paths, such as the air over a polluted urban environment.

Additional simultaneous noble gas laser lines can be obtained by pulsing the laser discharge, although some electrical discharge instabilities result in a Zeeman-tuned laser owing to the interactions between the moving ions and electrons and the applied magnetic field. Pulsing the magnetic field permits higher (peak) magnetic fields to be obtained (thereby increasing the Zeeman-splitting of the laser lines), but synchronization of the pulsed magnetic field with a pulsed noble gas laser oscillator is necessary in order (1) to ensure that the laser oscillates when the (pulsed) magnetic field is maximum, and (2) to prevent the induced electric field associated with the increasing or collapsing magnetic field from extinguishing the noble gas electrical discharge.

The atomic energy level diagrams for argon, krypton, and xenon are quite complex, composed as they are of two relatively independent systems corresponding to the $^2P^o_{1/2}$ and $^2P^o_{3/2}$ parent ions, respectively. Radon is expected to be somewhat similar, although almost none of the energy levels corresponding to the $^2P^o_{1/2}$ parent ion is known (Moore, 1959). The plethora of energy levels available in the heavy noble gases allows a large number of laser lines to oscillate simultaneously. As discussed below, however, the noble gas lasers are inherently inefficient, owing to the location of the pertinent energy levels for laser oscillation relatively near the ionization limit(s) for these gases. Frequently, simultaneous laser oscillation at a number of wavelengths is inconvenient, and dispersive laser cavity elements are usually introduced to suppress these other laser lines.

Noble gas lasers cannot, in general, be used to detect the concentrations and distributions of the same noble gas used in the laser. As discussed in the following section, noble gas lasers are usually 4-level lasers, and the optical transition corresponding to a given laser line cannot be abosrbed by an identical atom in its ground state. In the case of the neutral argon laser, this property is an important one since argon represents almost one percent of the terrestrial atmosphere, a concentration many orders of magnitude greater than those expected for atmospheric pollutants.

In summary, noble gas lasers have been found to be promising optical sources for atmospheric pollution detection and measurement using selective spectral absorption techniques. Experiments and analyses have shown that the numerous noble gas laser lines can be:

(1) allowed to oscillate individually or simultaneously;
(2) Zeeman-tuned over spectral bands of up to 10 Å (using six kilogauss dc magnetic fields);
(3) transmitted over long optical paths in the atmosphere to provide great detection sensitivity;
(4) operated in those spectral bands common both to the laser and to important atmospheric pollutants; and,

(5) either pulsed or CW laser oscillation modes can be used depending upon the application and type of data processing system required.

Only a relatively simple laser apparatus and associated data processing system are required to obtain adequate data on the concentrations of atmospheric air pollutants. Details regarding the laser apparatus, data, and selected pollutant gases can be found in the following sections.

EXPERIMENTAL MEASUREMENTS AND RESULTS

Our noble gas laser experiments were designed to address three specific tasks:

(1) laser source development (conventional CW noble gas lasers, transverse-excited, atmospheric (TEA) pressure, pulsed noble gas lasers, and conventional low-pressure pulsed noble gas lasers);

(2) spectral tuning experiments of noble gas lasers (using applied magnetic fields to generate the Zeeman effect); and

(3) pollutant absorption experiments (using both intra-cavity and extra-cavity optical paths of variable length).

Most of our efforts were concentrated on the first area, laser source development, and, consequently, the following discussion emphasizes this work.

Several hundred neutral noble gas laser lines have been discovered during the past decade by a number of laser researchers (Hdbk. of Lasers, 1971). It was recognized early in our experiments, however, that there were four problems associated with implementing these numerous noble gas laser lines for air pollution monitoring applications:

(1) Some of these noble gas laser lines were obtained using laser apparatus of considerable size and complexity, and, as a consequence, this type of laser equipment may not be suitable for air pollution detection applications.

(2) Many of these noble gas laser lines fall into the extensive H_2O and CO_2 absorption bands in the terrestrial atmosphere — since H_2O and CO_2 are not considered to be pollutant species, those laser lines falling in these H_2O and CO_2 absorption bands cannot be used as laser sources for long atmospheric path length measurements.

(3) A considerable number of the known noble gas laser lines are too weak to be used successfully over long atmospheric paths, particularly if air turbulence is present.

(4) A few noble gas laser lines fall in spectral regions in which little or no pollutant absorption lines are present — these spectral regions are generally termed "windows" in the atmospheric absorption spectrum.

In order to automatically exclude those noble gas laser lines requiring an elaborate apparatus, we constructed a simple, relatively compact noble gas laser device having an active length of approximately 1.0 meter. Experiments were conducted in which noble gas pressure and discharge parameters were systematically varied, and the number, wavelengths, and output powers of the noble gas laser lines obtained with this equipment were carefully measured. In these experiments, our studies were restricted to the heavier noble gases (argon, krypton, and xenon) since the He/Ne laser had previously been subject to intensive development.

Some eighty noble gas laser lines were obtained; Tables 1, 2, and 3 list the pulsed laser lines obtained with argon, krypton, and xenon respectively. Table 4, 5, and 6 list the CW laser lines obtained with argon, krypton, and xenon lasers respectively. Note the remarkable dominance that xenon has over the two lighter noble gases. In particular, it was found that if xenon were allowed to remain in the laser apparatus overnight, xenon contamination of the apparatus occurred, presumably by the gas being strongly adsorbed on the inner surfaces of the laser plasma tube. Despite the fact that the contaminating xenon gas was present in very small fractions compared to the desired fill gas (fractions as small as 10^{-3} to 10^{-4} were estimated), the xenon laser spectrum generally dominated over the spectrum of the majority noble gas atoms. This dominance is attributed in part to the greater line strengths of many of the xenon laser lines and to the lower-lying energy levels in xenon.

Of the eighty noble gas laser lines obtained with our equipment, some 18 argon, krypton, and xenon laser lines were previously unreported. Many of these 18 new laser lines (Linford, 1972 and 1973b and c) fall in or near important pollutant absorption bands and lines — see Table 7 for a listing of the wavelengths, identifications, and estimated line strengths of these new lines.

A substantial number of the 80 noble gas laser lines obtained with our simple apparatus were observed to have adequate optical gains and output powers for air pollution monitoring applications, but only when operated in the pulsed mode. This necessity for pulsed operation may not be a disadvantage in practice, since electronic photodetector gating, lock-in amplifiers, etc., may be used to permit an acceptable signal-to-noise ratio to be achieved for an operational data-processing system.

1. Description of Laser Apparatus.

A general schematic of the laser apparatus used in many of our noble gas laser experiments is shown in Figure 1. As shown, a hot cathode/ring anode laser tube is fitted with a cryogenic pressure-control cold finger for regulating the tube pressure of xenon (Linford, 1973a). A heater coil wrapped around the cold finger allows surface temperatures to be varied from 77° to over 100°K. For CW laser operation, the noble gas apparatus was excited with a dc electrical discharge. When pulsed laser operation was desired, two circuits were used:

(1) a high voltage capacitor (C = 2 nF) was placed in parallel with the plasma tube electrodes and a large, 1.0 megohm, resistor was placed in series with a 15 kV high voltage power supply; and

(2) a hydrogen thyratron was used to apply controlled-duration high voltage pulses of variable current to the laser plasma tube.

The laser tube was placed inside a dc solenoid to permit axial magnetic fields up to 6 kilogauss to be applied to the laser tube. As discussed above, the six kilogauss applied magnetic field allowed us to tune a number of CW xenon laser transitions over bandwidths as great as 23 GHz (or 11 Å) using the Zeeman effect. Although as many as ten spectral components are obtained in Zeeman-split spontaneous emission spectra (in the case of the 3.508μm xenon laser transition), only two laser wavelengths, λ_+ and λ_-, were obtained when magnetic fields in excess of one kilogauss were applied to the laser tube. This convenient reduction in the number of oscillating laser lines in the Zeeman-split noble gas laser is attributed to spectral cross-relaxation processes occurring within the low-pressure noble gas discharge (Peressini and Linford, 1968).

The magnetically-induced spectral-splitting, $\delta\nu_m$, of a given Zeeman-split spontaneous spectral line can be calculated from the expression:

$$\delta\nu_m = \frac{eB}{2\pi m}\left[m_u g_u - (m_u - 1) g_\ell\right] \qquad (1)$$

where m_u is the magnetic quantum number of the upper energy level of the transition, g_u and g_ℓ are the Lande-g values of the upper and lower laser levels, respectively, and B is the applied magnetic field. In order to use equation (1) to calculate the spectral splitting effected by the applied magnetic field, it is necessary to either measure or calculate the values of the Lande-g coefficients.

The spectra of the neutral noble gases can be characterized most accurately by a j--ℓ coupling scheme (Racah, 1942). In the case of j--ℓ coupling, the orbital angular momemtum of the excited electron, ℓ_e, is coupled to the total angular momentum of the parent ion, j_p, to form a resultant intermediate quantum mechanical angular momentum, K. Thus:

$$K = j_p + \ell_e \qquad (2)$$

The total angular momentum, J, is then given by the vector sum:

$$J = K + s_e \qquad (3)$$

where s_e is the spin of the excited electron. Since only about half of the Lande-g values for equation (1) have been measured and reported for the noble gases (Moore, 1959), it was necessary to calculate the remaining Lande-g values using the j--ℓ coupling conditions. Under these circumstances,

$$g = \frac{2J+1}{2K+1} + 2\left[\frac{j_e(j_e+1) + K(K+1) - \ell_e(\ell_e+1)}{(2K+1)(2J+1)}\right](g_p - 1) \qquad (4)$$

where j_e is the total angular momentum of the excited electron and g_p is the Lande-g value of the appropriate parent ion. The Lande-g value, g_p, for the parent ion can be calculated from the ordinary Russell-Saunders coupling expression:

$$g_p = 1 + \frac{J(J+1) + S(S+1) - L(L+1)}{2J(J+1)} \qquad (5)$$

The spectra of the neutral noble gases (particularly the heavier noble gases) arise from two parent ions, $^2P^o_{1/2}$ and $^2P^o_{3/2}$. When appropriate values for the quantum numbers describing these two parent ions are inserted in equations (5) through (1), above, we found that the magnetic splitting factor, ζ, given by the expression:

$$\zeta = \frac{e}{2\pi m}\left[m_u g_u - (m_u - 1) g_\ell\right] \qquad (6)$$

can be calculated to be 1.25 MHz/gauss for the 3.51μm xenon laser line, 1.31 MHz/gauss for the 3.37μm xenon line, and 2.6 MHz/gauss for the 3.99μm xenon transition (Linford, 1973a). All but the last magnetic splitting factor agreed with the experimental measurements of the spectral splitting of these xenon laser lines. A

magnetic splitting factor of only 1.9 MHz/gauss was measured instead of the calculated 2.6 MHz/gauss for the 3.99μm xenon laser line. This relatively large error may be due to an incorrect Lande-g value in the Atomic Energy Levels (Moore, 1959).

The values of the magnetic splitting are quite substantial using a six kilogauss applied magnetic field (amounting to total line splittings of nearly 23 GHz, and 11 Å, in the case of the 3.99μm xenon laser line).

These magnetic splittings were measured in two ways: (1) for small fields and splittings, the heterodyne beats between the two Zeeman-split laser lines could be observed using a square-law photodetector (of sufficient speed) connected to a microwave spectrum analyzer for frequencies up to 1.2 GHz; and (2) for larger applied magnetic fields (and proportionally larger frequency splittings), a 3/4 meter Czerny-Turner monochromator (such as that shown in Figure 1) was used to measure the spectral splittings directly.

Photodetection of the noble gas laser lines was accomplished with one of three types of photodetectors (depending upon the wavelength region of interest). These photodetectors were:

(1) a photovoltaic InAs detector operated at 300°K with a spectral coverage of from 0.4μm to 3.5μm,
(2) a photovoltaic InSb detector operated at 77°K with a spectral coverage of from 0.4μm to 5.6μm, and
(3) a photoconductive gold-doped germanium detector covering the range 0.7μm to 11μm.

The photovoltaic InAs detector used in these experiments was an exceptionally fast detector — heterodyne beats between Zeeman-split laser lines having frequency differences as great as 1.2 GHz were observed. The other two detector types required liquid nitrogen cooling (to 77°K), were considerably slower, and their selection for these experiments was predicated primarily on their substantial photodetector sensitivities at wavelengths beyond the spectral cutoff of the InAs photodetector.

There were several techniques used to select the desired laser wavelengths reaching the photodetector. In the case of the Zeeman-tuned laser, the two Zeeman-split laser lines were circularly polarized, but of opposite helicities. By inserting a quarter-wave plate in the laser beam containing both laser lines, it was possible to convert the two circularly-polarized laser lines into two laser beams linearly polarized perpendicular to each other. A suitable prism analyzer could then separate these two wavelengths directly (Linford, 1973a).

For laser experiments employing more widely separated wavelengths, it was possible to use gratings, dicrotic beamsplitters, or suitable narrow-band interference filters to separate the two laser beams. The Littrow prism (shown in Figure 1) could be used to switch sequentially from one noble gas laser wavelength to another, providing that the wavelength differences between the two laser lines were sufficiently great (~ 0.5μm or better) in order to provide a sufficiently large dispersion factor.

Unfortunately, infrared noble gas lasers are inherently inefficient devices, particularly when the excitation mechanism uses conventional direct electron excitation from the (np) ground-state to excited (n + 1)s or (nd) states. As indicated in Figure 2, the first excited states, (n + 1)s, lie far above the (np) ground-state, and since laser oscillation takes place between two relatively closely-spaced energy levels, the theoretical quantum efficiency is necessarily low. Furthermore, since there are a number of possible energy levels within each multiplet, the resulting population inversions are spread among most of these energy levels. An example of this relatively complex energy level diagram is shown in Figure 3. The first excited states, the 5s levels, are located nearly 80,000 cm^{-1} above the 4p ground-state. The multiplicity of these population inversions gives rise to the useful multiple wavelength oscillation property of noble gas lasers. As shown in Figure 3, it is possible for numerous neutral krypton laser lines to oscillate simultaneously since these lines have neither upper nor lower laser levels in common.

The effects of isotopes on the oscillation characteristics of noble gas lasers predominantly affect the line-width of the laser amplifier. Thus, although the line-widths of the noble gas laser amplifiers are Doppler-broadened at the low pressures (P ~ 5–10 millitorr) used in conventional laser oscillators, the presence of naturally-occurring isotopic mixtures broadens the line-width further. This isotope effect is particularly interesting in the case of xenon which not only has nine stable, naturally-occurring isotopes, but also has approximately half of the naturally-occurring atoms composed of even-odd (xenon-129 and xenon-131) isotopes. Accordingly, naturally-occurring xenon not only displays a mass-shift, but also hyperfine structure in its spectra.

2. Radon Considered as an Active Laser Medium.

The incomplete term diagram of radon is very similar to those of xenon and krypton. Based on the pioneer work on radon by Rasmussen (1931 and 1932) only part of the term diagram of radon is known. Radon is the heaviest noble gas, having 86 electrons, no stable isotopes (radon-222 is the longest-lived isotope), and an average atomic weight of 222. Radon condenses at 211°K and freezes at 202°K, so that if an excess of gaseous radon were available in a laser tube, a cryogenic pressure control system similar to that used for xenon (see Figure 1) could be used to maintain the low gas pressures which are optimum for conventional heavy noble gas lasers (Linford, 1972).

Radon-222 is part of the radium decay scheme, is radioactive, and has a half-life of only 3.827 days — decaying by alpha emission with an energy of 5.5 MeV. The differential equation governing production of radon from radium is given by

$$\frac{dN_2}{dt} = \alpha_1 N_1(0) - \alpha_2 N_2 \qquad (7)$$

where N_2 is the population of radon, N_1 is the population of radium, and a_1 and a_2 are the mean reciprocal lifetimes of each element. If the production of radon from the parent element, radium, is considered to commence at t = 0, then the integral of equation (7) subject to the initial condition is simply

$$N_2(t) = \frac{N_1(0)a_1 \left[\exp(-a_1 t) - \exp(-a_2 t) \right]}{a_2 - a_1} \qquad (8)$$

which reduces to

$$N_2(t) = N_1(0)\left[\frac{a_1}{a_2}\right]\left[1 - \exp(-a_2 t)\right] \qquad (9)$$

since $a_2 \gg a_1$. As an asymptotic solution, $N_2(\infty) \rightarrow N_1 \frac{a_1}{a_2}$, so that the quantity of radon gas in equilibrium with the parent radium is essentially the ratio a1/a2 times the quantity of radium present. Approximately 10^{15} atoms of radon are required to fill a typical laser tube to a pressure of five millitorr, and, hence, some 1.5×10^{20} atoms of radium are required as a source — this corresponds to approximately 0.6 grams of radium. When allowances are made for radon gas adsorption by the laser tube walls, at least two grams of radium are required for a 0.3 cm bore gas discharge tube having a length of 50 cm ($V_{gas} = 3.5$ cm^3). An electrodeless laser tube would minimize the internal volume of the laser tube, and since rf excitation in excess of 10^9 Hz reduces gas adsorption, this type of excitation is recommended for any initial experiments conducted with radon.

We were unable to acquire a 2 gram source of radium to perform actual laser experiments with radon, but we did make some predictions as to the wavelengths and line strengths of the expected radon laser lines should a suitably-large source of radium become available in the future. The 2-gram radium source should be located in a detachable side-arm of the plasma tube so that the contaminated laser tube can be suitably disposed of after the experiment has been completed. The laser experiment should be performed approximately 2 to 3 days after the evacuated laser tube is attached to the radium-bearing sidearm. Beyond that period, accumulation in the discharge tube of the numerous daughter nuclei of radon would present a serious chemical contamination problem insofar as operation of the radon laser were concerned. Table 8 lists the pertinent wavelengths and estimated line-strengths for the strongest radon laser lines using xenon as a model.

Radon should be an excellent active laser medium. Its nearest relatives in the heavy noble gases all display strong, high-optical-gain laser lines, and the relatively great mass of radon reduces its Doppler-broadened line-width to, for example, 0.77 that of xenon and 0.29 that of neon. The narrowing of the laser line-width effectively increases the optical gain of the comparable transitions in radon. A further narrowing in the Doppler-broadened line-width of radon relative to xenon is caused by the lack of hyperfine or mass-shift line broadening mechanisms in the essentially single-isotope spectrum of radon.

3. Molecular Absorption Experiments.

In striving for simplicity of operation, our experimental laser configurations were designed to permit direct molecular absorption measurements to be made using selected pollutant gases. Referring to Figures 1 and 4, when a suitable sample gas was subjected to analysis by the noble gas laser apparatus, two laser wavelengths were generally used. One of the laser wavelengths was chosen such that it was absorbed more strongly than the other by the pollutant gas. The second wavelength then served as an intensity comparison standard. By measuring the relative intensities of these two laser wavelengths before and after they both passed through the absorbing sample of gas, it was possible to infer the relative concentration of the absorbing (pollutant) gas providing that:

(1) the optical path length, R, through the gas was known;
(2) the specific absorption coefficient at the specific wavelength, $a(\lambda)$, was known; and
(3) both the absorbed and comparison wavelengths were accurately measured and, hence, known.

Assuming that the comparison wavelength, λ_-, was negligibly absorbed by the pollutant gas and was initially of the same intensity, I_o, as the absorbed laser wavelength, λ_+, then the ratio of the two intensities after passage through the absorbing gas is simply

$$\epsilon = \frac{I_+}{I_o} = \exp(-2a(\lambda)\frac{N}{N_o} R) \qquad (10)$$

where the ratio, N/N_o, is the fractional molecular density of the pollutant gas in the laser beam. It is evident from equation (10) that if a measurable intensity ratio, I_+/I_o, can be obtained for a given molecular density fraction, N/N_o, in a small gas cell of given optical path length, R, then much greater detection sensitivities can be obtained by increasing R to distances of the order of 10 kilometers or more. This is true providing the deleterious effects of diffraction and atmospheric turbulence are either compensated or eliminated through careful optical design.

As a specific example, using the data of Hans (1971) for the pollutant gas CO, the intensity ratio, $\epsilon = 0.34$, when $N/N_o = 10^{-2}$, R = 10 cm, and a = 5.4 (when $\lambda_+ = 4.61\mu m$). If the optical path length, R, containing the polluting gas is increased by a factor of 10^5 (from 10 cm to 10^6cm), then the fractional pollutant molecular density, N/N_o, can be reduced by a factor of 10^5 also to produce a similar value of ϵ, the laser beam intensity ratio.

Our electronic data processing electronics used several techniques for comparing the relative intensities of the two laser lines, λ_+, and λ_-. These techniques utilized:

(1) a lock-in amplifier; and
(2) a real-time digital ratiometer.

Both of these instruments were capable of measuring intensity ratios, ϵ, of 0.99 or better, providing that the detected intensity fluctuations of the two laser beams were less than 10% of full intensity. If this maximum intensity ratio, $\epsilon_{max} = 0.99$, is inserted in equation (10) using the parameters given above for carbon monoxide, then the minimum molecular density fraction, N/N_o, of which the apparatus should be capable of detecting is reduced to only 8 parts per billion (8×10^{-9}).

Since the power supply for our dc solenoid magnet required 480V 3ϕ input power, we were unable to conduct Zeeman-tuned laser pollutant gas experiments over the long ranges (2 kilometers or more) required for sensitive operation of the equipment. Our laboratory experiments (Linford, 1973a), however, confirmed the relative sensitivity of the method for relatively short optical absorption cells (R~15cm), and we feel that the extrapolations noted above are justifiable. We have conducted a wide variety of noble gas laser experiments over ranges up to 30 kilometers through the terrestrial atmosphere (Linford, *et al.*, 1974) using a CW xenon laser similar to that used in our Zeeman-tuned laboratory laser experiments (Linford, 1973a). These long range laser experiments through the atmosphere included a unique class of experiments which can only be performed using laser amplifiers having large optical gains, such as the HF/DF chemical laser (Glaze and Linford, 1973) and the noble gas lasers described in this paper. These unique experiments used an optical configuration similar to that shown in Figure 1 with the exception that the front flat of the laser was removed. Laser oscillation was then achieved using the optical feed-back from the remote corner reflector — such an optical configuration is termed a "long laser" for obvious reasons (Linford, *et al.*, 1974). This method admits an increased sensitivity to atmospheric absorption above that calculated for the more conventional apparatus shown above in Figures 1 and 4. The increased absorption sensitivity is obtained because the absorbing gas is actually placed inside the laser cavity, and if the oscillation properties of the long laser are adjusted so as to place the laser near its oscillation threshold, then a substantial increase in the detection sensitivity of the laser can be obtained.

It should be emphasized that not all of the noble gas laser lines listed in Tables 1 through 7 can be used in either Zeeman-tuned or long laser pollutation monitoring applications. Only those noble gas laser lines having sufficient optical gain to attain laser oscillation threshold can be used in these relatively high-optical-loss laser configurations. More than two-thirds of the noble gas laser lines listed above in Tables 1 — 7 lacked sufficient optical gain to be used in either our Zeeman-tuned or long laser experiments using the relatively small, one meter, laser tubes constructed for our noble gas laser apparatus. Thus, the use of these more numerous lower gain noble gas laser lines for pollution monitoring applications is limited to those situations in which near-coincidences between a lower-gain laser line and pollutant absorption lines or bands occur. Many of these lower-gain laser lines fall in important bands, as can be seen by comparing Tables 1 — 7 with Table 9.

4. Summary of Experimental Results.

Our experiments have been conducted in three major areas:

(1) noble gas laser source study and development (resulted in the discovery and identification of 18 new noble gas laser lines);
(2) spectral tuning experiments (using the Zeeman effect to tune selected noble gas laser lines over bands as great as 11 Å); and
(3) pollutant absorption measurements (with selected absorbing gases).

Although the latter measurements were conducted using small, laboratory optical cells containing known quantities of absorbing gases, we concluded that the use of direct optical absorption detection is a sensitive method of measuring the concentrations and distributions of pollutant gases contained in long optical paths. Noble gas lasers are particularly useful in this context because:

(1) numerous noble gas laser lines are available in important pollutant bands; and
(2) some of these noble gas laser lines are partially tunable (using the Zeeman effect), thereby allowing them to be tuned into coincidence with a suitable, nearby pollutant absorption line.

Since direct optical absorption measurements can be made simply and relatively economically, it appears that further development of neutral noble gas lasers in air pollution monitoring applications should take place to permit these potentially useful devices to be more fully utilized. As shown in Figures 5 and 6, the general spectral coverage of the neutral noble gas lasers is excellent, particularly when compared with the relatively broad absorption bands of some important pollutants.

REFERENCES

Faust, W. L., *et al,* **(1962),** *Gas Maser Spectroscopy in the Infrared,* Applied Physics Letters, 1, 85.

Glaze, J. A. and G. J. Linford, (1973), *Design and Performance Characteristics of a Small Subsonic Flow HF Chemical Laser,* Review of Scientific Instruments, 44, 600.

Handbook of Lasers, **(1971),** The Chemical Rubber Co., pp. 183-242, Robert C. Weast, Editor.

Hanst, P. L., (1971), *Advances in Environmental Science and Technology,* John Wiley and Sons, pp. 91-213.

Javan, A., *et al.,* (1961), *Population Inversion and Continuous Optical Maser Oscillation in a Gas Discharge Containing a He — Ne Gas,* Physical Review Letters, 6, 106.

Linford, G. J., (1973), *Experimental Studies of A Zeeman-Tuned Xenon Laser Differential Absorption Apparatus,* Applied Optics, 12, 1130.

Linford, G. J.,(1972), *High-Gain Neutral Laser Lines in Pulsed Noble Gas Discharges,* IEEE Quamtum Electronics, QE-8, 477.

Linford, G. J., (1973b), *New Pulsed Laser Lines in Krypton,* IEEE Quantum Electronics, QE-9, 610.

Linford, G. J., (1973c), *New Pulsed and CW Laser Lines in the Heavy Noble Gases,* IEEE Quantum Electronics, QE-9, 611.

Linford, G. J., *et al.,* **(1974),** *Very Long Lasers,* Applied Optics, 13.

Moore, C. N., (1959), *Atomic Energy Levels,* Volumes 1, 2, and 3, National Bureau of Standards.

Patel, C. K. N., *et al.,* **(1962),** *Infrared Spectroscopy Using Stimulated Emission Techniques,* Physical Review Letters, 9, 102.

Peressini, E. R. and G. J. Linford, (1968), *Effect of Cross-Relaxation on the Spectral Flux and Population Inversion Distributions in a CW Laser Oscillator,* IEEE Quantum Electronics, QE-4, 657.

Racah, G., (1942), *On a New Type of Vector Coupling in Complex Spectra,* Physical Review, 61, 537.

Rasmussen, E., (1931), *Das Bogenspectrum der Radiumemanation,* Zeitschrift fur Physik, 76, 494.

Rasmussen, E., (1932), *Uber das Bogenspectrum der Radiumemanation,* Zeitschrift fur Physik, 77, 312.

TABLE 1. Observed Argon Pulsed Laser Lines.

No.	λ (Micrometers)	Transition	Current	Output	Comments
1	0.4579	$(^3P)4p^2S^0 1/2—(^3P)4s^2 1/2$	M	M	Argon II
2	0.4764	$(^3P)4p^2P^0 3/2—(^3P)4s^2P1/2$	M	M	Argon II
3	0.4879	$(^3P)4p^2D^0 5/2—(^3P)4s^2P3/2$	M	H	Argon II
4	0.4965	$(^3P)4p^2D^0 3/2—(^3P)4s^2P1/2$	M	M	Argon II
5	0.5017	$(^1D)4p^2F^0 5/2—(^3P)3d^2D3/2$	M	H	Argon II
6	0.5145	$(^3P)4p^4D^0 5/2—(^3P)4s^2P3/2$	M	M	Argon II
7	1.214	$3d'(3/2)^0 1—4p'(3/2)1$	M	M	Argon I
8	1.240	$3d(3/2)1^0—4p(3/2)1$	M	W	Argon I
9	1.270	$3d'(3/2)1^0—4p'(3/2)1$	M	M	Argon I
10	1.280	$3d(5/2)2^0—4p(5/2)2$	M	W	Argon I
11	1.694	$3d(3/2)2^0—4p(3/2)2$	M	M	Argon I
12	1.792	$\{3d(1/2)1^0—4p(3/2)2$ $3d(1/2)0^0—4p(3/2)1\}$	M	H	Argon I
13	2.062	$3d(3/2)2^0—4p'(3/2)2$	M	M	Argon I
14	2.314	$3d(1/2)1^0—4p'(1/2)1$	M	M	Argon I
15	2.397	$3d(1/2)0^0—4p'(1/2)1$	M	M	Argon I
16	2.551	$5p(1/2)0—5s(3/2)1^0$	M	M	Argon I
17	2.567	$5p'(1/2)0—5s'(1/2)1^0$	H	H	Argon I
18	2.715	$5s(3/2)2^0—5p(3/2)1$	M	M	Argon I
19	3.135	$5p(1/2)1—5s(3/2)2^0$	M	M	Argon I
20	3.630	$6s'(1/2)1^0—5p'(3/2)1$	M	W	Argon I
21	3.700	$6s'(1/2)1^0—5p'(1/2)1$	M	W	Argon I
22	3.708	$4d(3/2)1^0—5p(3/2)1$	M	H	Argon I
23	3.713	$6s'(1/2)1^0—5p'(3/2)2$	M	M	Argon I
24	5.020	$6p'(3/2)1—4d'(5/2)2^0$	L	W	Argon I

L=Low W=Weak M=Moderate H=High

TABLE 2. Observed Krypton Pulsed Laser Lines.

No.	λ (Micrometers)	Transition	Current	Output	Comments
1	0.4762.43	$(^3P)5p^2D^0 3/2—(^3P)5s^2P1/2$	M	W	Krypton I
2	0.7603	$5p(3/2)2—5s(3/2)2^0$	M	W	Krypton I
3	0.8115	$5p(5/2)3—5s(3/2)2^0$	M	W	Krypton I
4	1.318	$6s(3/2)1^0—5p(5/2)2$	M	W	Krypton I
5	1.362	$4d(3/2)1^0—5p(5/2)1$	M	M	Krypton I
6	1.443	$6s(3/2)1^0—5p(3/2)1$	M	M	Krypton I
7	1.476	$6s(3/2)1^0—5p(5/2)2$	M	M	Krypton I
8	1.4962	$4d(3/2)1^0—5p(3/2)1$	M	M	Krypton I
9	1.5326	$4d(3/2)1^0—5p(3/2)2$	M	M	Krypton I
10	1.685	$4d(7/2)3^0—5p(5/2)3$	M	W	Krypton I
11	1.690	$4d(1/2)1^0—5p(1/2)1$	M	W	Krypton I
12	1.785	$4d(1/2)0^0—5p(1/2)1$	M	M	Krypton I
13	1.819	$4d'(5/2)3^0—5p'(3/2)2$	M	M	Krypton I
14	2.190	$4d(3/2)2^0—5p(3/2)2$	M	H	Krypton I
15	2.248	$\{8d(5/2)2^0—4f(7/2)3$ $8d(7/2)3^0—4f(5/2)2\}$	M	M	Krypton I
16	2.523	$4d(1/2)1^0—5p(3/2)2$	M	H	Krypton I
17	2.8655	$6p(5/2)3—6s(3/2)2^0$	M	M	Krypton I
18	3.774	$7s(3/2)1^0—6p(5/2)2$	M	W	Krypton I
19	3.956	$5d(3/2)1^0—6p(5/2)2$	M	M	Krypton I
20	4.068	$7s(3/2)1^0—6p(3/2)1$	M	M	Krypton I
21	4.142	$7s(3/2)1^0—6p(3/2)2$	M	W	Krypton I
22	4.375	$5d(3/2)1^0—6p(3/2)2$	M	W	Krypton I
23	4.998	$4d'(3/2)1^0—6p(1/2)1$	M	W	Krypton I

W=Weak M=Moderate H=High

TABLE 3. Observed Pulsed Xenon Laser Lines.

No.	λ (Micrometers)	Transition	Watts	Current	Comments
1	0.4954	Unknown	10	H	Xenon IV?
2	0.5159	Unknown	10	H	Xenon IV?
3	0.5352	Unknown	10^2	H	Xenon IV?
4	0.5971	$(^1D)6p^2P^0 3/2—(^1D)6s^2D3/2$		H	Xenon II
5	0.8716	$(^3P)6p4D^0 3/2—(^3P)5d^2P3/2$		M	Xenon II
6	0.9059	Unknown		M	Xenon II?
7	0.904	$6p(5/2)2—6s(3/2)2^0$	10^{-4}	L	Xenon I
8	1.6053	$7s(3/2)1^0—6p(3/2)2$	10^{-1}	M	Xenon I
9	1.732	$5d(3/2)1^0—6p(5/2)2$	10	H	Xenon I
10	2.027	$5d(3/2)1^0—6p(3/2)1$	10	H	Xenon I
11	2.515	$7d(7/2)4^0—7p(5/2)3$	10^{-1}	M	Xenon I
12	2.627	$5d(5/2)2^0—6p(5/2)2$	10^{-1}	M	Xenon I
13	2.652	$5d(3/2)1^0—6p(1/2)0$	10	H	Xenon I
14	2.661	$5d'(3/2)1^0—6p'(1/2)0$	10^{-4}	M	Xenon I
15	2.859	$7p(3/2)2—7s(3/2)2^0$	10^{-2}	M	Xenon I
16	3.108	$5d(5/2)3^0—6p(3/2)2$	10^{-1}	M	Xenon I
17	3.275	$5d(3/2)2^0—6p(1/2)1$	10	M	Xenon I
18	3.367	$5d(5/2)2^0—6p(3/2)1$	1.0	M	Xenon I
19	3.508	$5d(7/2)3^0—6p(5/2)2$	5.0	M	Xenon I
20	3.622	$5d'(3/2)2^0—7p(3/2)2$	10^{-3}	M	Xenon I
21	3.651	$7p(1/2)1—7s(3/2)2^0$	10^{-3}	M	Xenon I
22	3.680	$5d(1/2)1^0—6p(1/2)1$	10^{-1}	L	Xenon I
23	3.686	$5d(5/2)2^0—6p(3/2)2$	10^{-4}	M	Xenon I
24	3.870	$5d'(5/2)3^0—6p'(3/2)2$	10^{-3}		Xenon I
25	3.895	$5d(7/2)3^0—6p(5/2)3$	10^{-3}		Xenon I
26	3.996	$5d(1/2)0^0—6p(1/2)1$	10^{-2}		Xenon I
27	4.153	$5d'(5/2)2^0—7p(3/2)1$	10^{-2}		Xenon I
28	4.539	$5d(3/2)2^0—6p(5/2)2$	10^{-1}	M	Xenon I
29	4.661	$5d'(3/2)2^0—6p'(1/2)1$	10^{-1}	H	Xenon I
30	5.024	$5d'(5/2)2^0—6p'(3/2)2$	10^{-4}	L	Xenon I
31	5.575	$5d(7/2)4^0—6p(5/2)3$	10^{-1}	M	Xenon I
32	7.316	$5d(3/2)2^0—6p(3/2)1$	10^{-4}	M	Xenon I
33	9.006	$5d(3/2)2^0—6p(3/2)2$	10^{-4}	M	Xenon I

L=Low M=Moderate H=High

TABLE 4. CW Argon Laser Lines.

No.	Wavelength (in micrometers)	Transition	Relative Output Power
1	1.694	$3d(3/2)^0_2—4p(3/2)2$	1.0
2	2.061	$3d(3/2)^0_2—4p'(3/2)2$	4.4
3	2.549	$5p(5/2)_3—3d(7/2)^0_3$	3.5
4	2.563	$6d'(3/2)^0_2—6p(5/2)3$	3.2
5	3.133	$5p(1/2)1—5s(3/2)^0_2$	6.1

NOTE: The data presented in this Table were taken using the same laser apparatus used to take the xenon laser data listed in Table 6. The fewer number of CW laser lines obtained with argon and krypton was a consistent observation made during the course of these experiments.

TABLE 5. CW Krypton Laser Lines.

No.	Wavelengths (in micrometers)	Transition	Relative Output Power
1	2.19	$4d(3/2)^{o}_{2}-5p(3/2)2$	7.1
2	2.523	$4d(1/2)^{o}_{1}-5p(3/2)2$	5.3

TABLE 6. CW Xenon Laser Lines.

No.	Wavelength (in micrometers)	Transition	Output Power*
1	2.026	$5d(3/2)^{o}_{1}—6p(3/2)$	10
1	2.627	$5d(5/2)^{o}_{2}—6p(5/2)2$	3
3	2.651	$5d(3/2)^{o}_{1}—6p(1/2)o$	6
4	3.108	$5d(5/2)^{o}_{3}—6p(3/2)2$	8
5	3.275	$5d(3/2)^{o}_{2}—6p(1/2)1$	10
6	3.367	$5d(5/2)^{o}_{2}—6p(3/2)1$	20
7	3.508	$5d(7/2)^{o}_{3}—6p(5/2)2$	50
8	3.622	$5d'(3/2)^{o}_{3}—7p(3/2)2$	2**
9	3.652	$7p(1/2)1—7s(3/2)^{0}$	1**
10	3.680	$5d(1/2)^{o}_{1}—6p(1/2)1$	12
11	3.870	$5d'(5/2)^{o}_{3}—6p'(3/2)2$	2**
12	3.997	$5d(1/2)^{o}_{0}—6p(1/2)1$	6
13	4.153	$5d'(5/2)^{o}_{2}—7p(3/2)1$	4
14	4.539	$5d(3/2)^{o}_{2}—6p(5/2)2$	1, 10+
15	4.611	$5d'(3/2)^{o}_{2}—6p'(1/2)1$	3
16	5.024	$5d'(5/2)^{o}_{2}—6p'(3/2)2$	5
17	5.575	$5d(7/2)^{o}_{4}—6p(5/2)3$	9

* In Tables 4, 5, and 6, each output power unit = 100 μwatts.

** These lines had relatively low optical gains, and as a consequence required special efforts to obtain oscillation with the one-meter laser tubes.

+ The indicated output power could be obtained only when the Littrow prism was used to suppress most of the laser oscillation at the competing 3.508μm xenon laser line.

TABLE 7. Recently Discovered Noble Gas Laser Lines.

No.	λ (Micrometers)	Transition	Element	Strength	Mode
1	0.7603	5p(3/2)2—5s(3/2)2⁰	Krypton	W	P
2	1.4962	4d(3/2)1⁰—5p(3/2)1	Krypton	M	P
3	1.5326	4d(3/2)1⁰—5p(3/2)2	Krypton	M	P
4	2.248	8d(5/2)2⁰—4f(7/2)3 (7/2)3⁰—4f(5/2)2	Krypton	M	P
5	2.515	7d(7/2)4⁰—7p(5/2)-nn		M	P
6	2.715	5s(3/2)2⁰—5p(3/2)1	Argon	M	P
7	2.859	7p(3/2)2—7s(3/2)2⁰	Xenon	M	P
8	3.630	6s'(1/2)1⁰—5p'(3/2)1	Argon	W	P
9	3.700	6s'(1/2)1⁰—5p'(1/2)1	Argon	W	P
10	3.708	4d(3/2)1⁰—5p(3/2)1	Argon	S	P
11	3.713	6s'(1/2)1⁰—5p'(3/2)2	Argon	M	P
12	3.774	7s(3/2)1⁰—6p(5/2)2	Krypton	W	P
13	3.956	5d(3/2)1⁰—6p(5/2)2	Krypton	M	P
14	4.068	7s(3/2)1⁰—6p(3/2)1	Krypton	M	P
15	4.142	7s(3/2)1⁰—6p(3/2)2	Krypton	W	P
16	4.998	4d'(3/2)1⁰—6p(1/2)1	Krypton	W	P
17	5.020	6p'(3/2)1—4d'(5/2)2⁰	Argon	W	P
18	5.024	5d'(5/2)2⁰—6p'(3/2)2	Xenon	M	CW,P

W=Weak M=Moderate S=Strong

TABLE 8. Projected Radon Laser Lines.

No.	Wavelength (in micrometers)	Transition	Xenon Laser Analogy	Theoretical Line Strength
1	5.68	$6d(7/2)^0_4$—7p(5/2)3	5.57μm	54.0
2	2.68	$6d(7/2)^0_3$—7p(5/2)2	3.51μm	40.0
3	3.92*	$6d(5/2)^0_3$—7p(3/2)2	3.11μm	29.4
4	3.63*	$6d(5/2)^0_2$—7p(3/2)1	3.37μm	18.9
5	6.90	$6d(3/2)^0_2$—7p(3/2)2	9.00μm	14.4
6	2.56	$6d(3/2)^0_2$—7p(1/2)1	3.275μm	12.5
7	3.71	$6d(1/2)^0_1$—7p(1/2)1	3.68μm	10.0
8	8.53*	$6d(3/2)^0_1$—7p(3/2)1	2.026μm	8.0

* These projected radon laser lines are only approximately correct since the 6d energy levels are unknown at the present time (Moore, 1959).

TABLE 9. Absorption Bands of Common Pollutants.

Pollutant	Spectral Band (Micrometers)	Structure
Methane	3.1—3.4	Fine
	7.3—8.0	
Ethane	3.2—3.5	Fine
Acetalaldehyde	3.2—3.8	Moderate
Formaldenyde	3.1—3.7	Fine
Ammonia	10.2—11.2	Moderate
Hydrogen Chloride	3.1—3.7	Fine
Nitric Oxide	5.1—5.6	Fine
Sulphur Dioxide	3.8—4.2	Moderate
	7.2—7.5	
Carbon Monoxide	4.4—4.9	Fine
Ozone	9.3—10.0	Moderate
Propane	3.3—3.6	Coarse
Methanol	9.5—10.2	Fine
Ethylene	10.1—11.2	
Propylene	3.2—3.5	Moderate
Nitrogen Oxide (No)	5.0—5.4	Moderate
Hydrogen Bromide	3.9—4.2	Moderate
Butane	3.3—3.6	Coarse
Hexane	3.3—3.5	Coarse
Pentane	3.3—3.6	Coarse
Nitrogen Dioxide	3.4—3.5	Fine
Acetylene	2.9—3.1	Fine

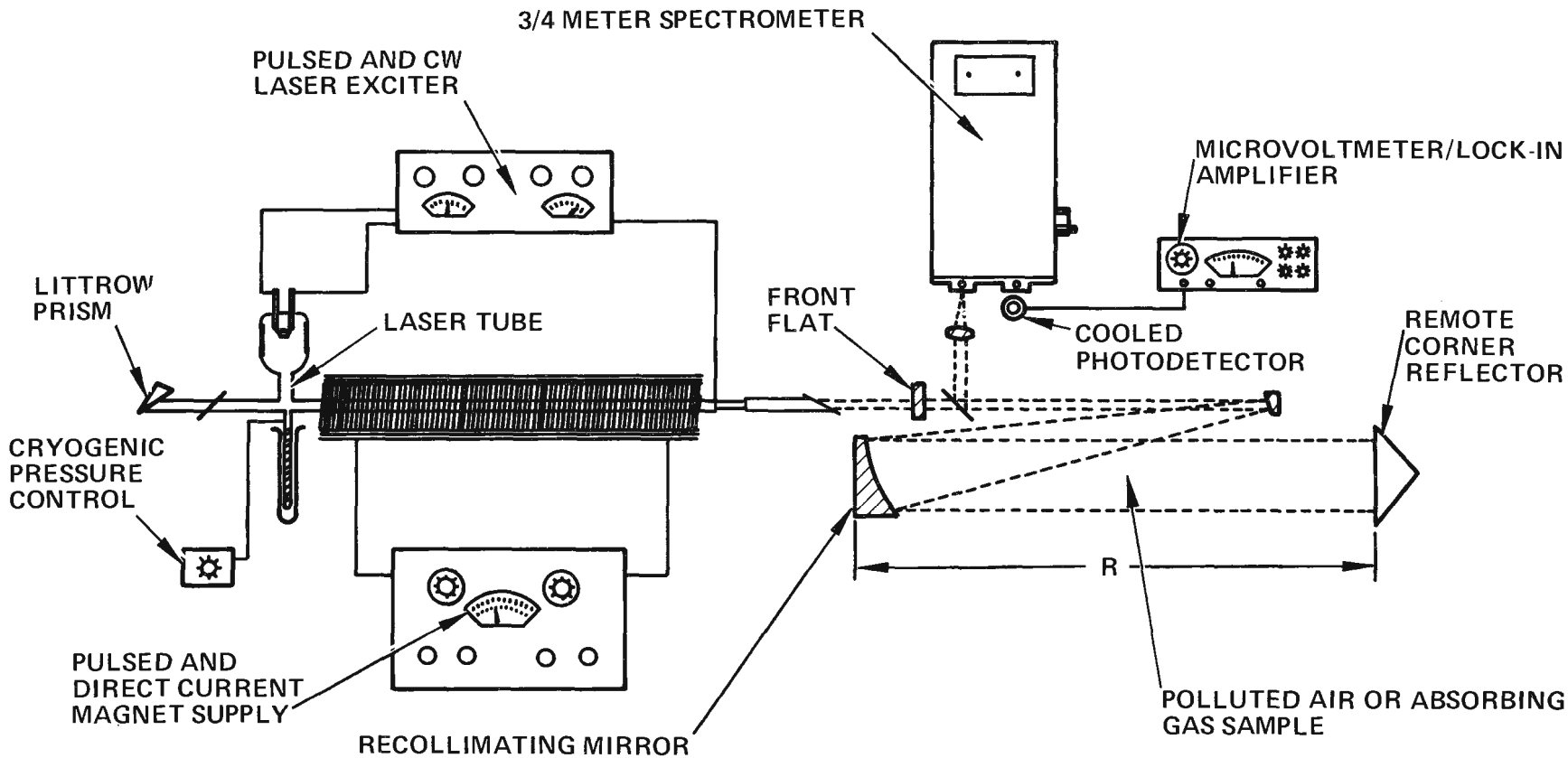

Figure 1. Schematic of Pulsed and CW Noble Gas Laser Monitoring System.

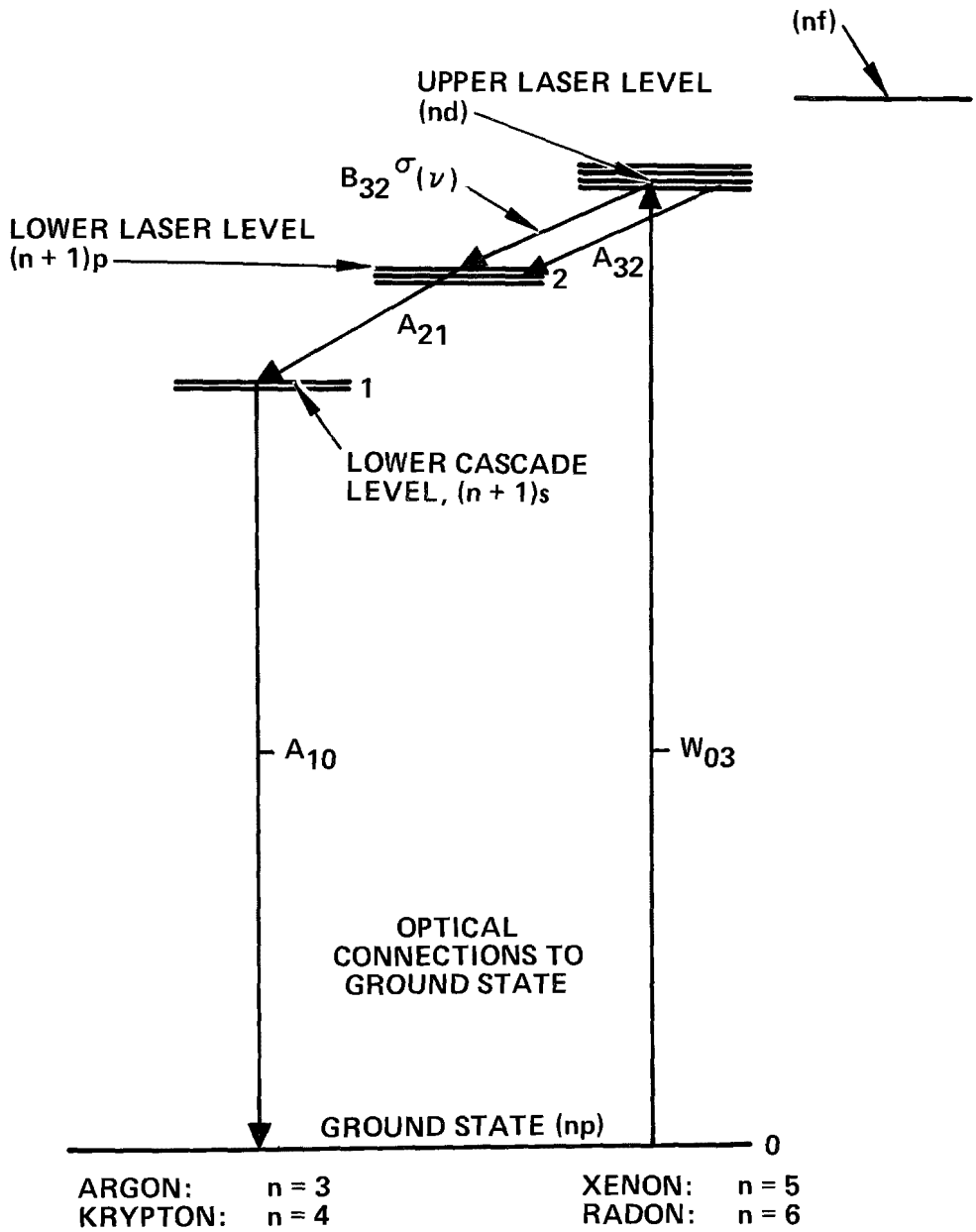

Figure 2. Noble Gas Laser Energy Diagram.

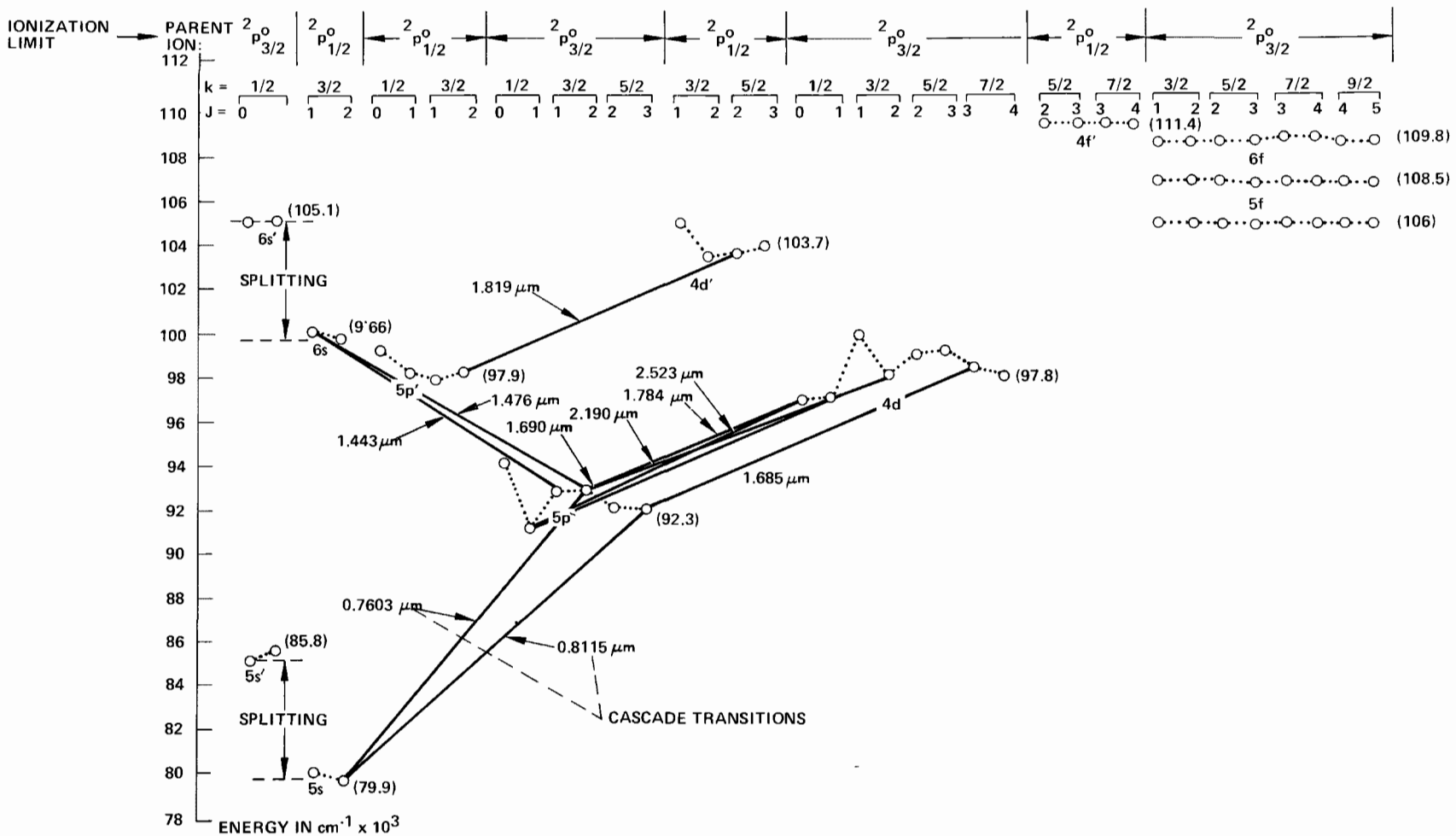

Figure 3. Energy Level Diagram of Neutral Krypton.

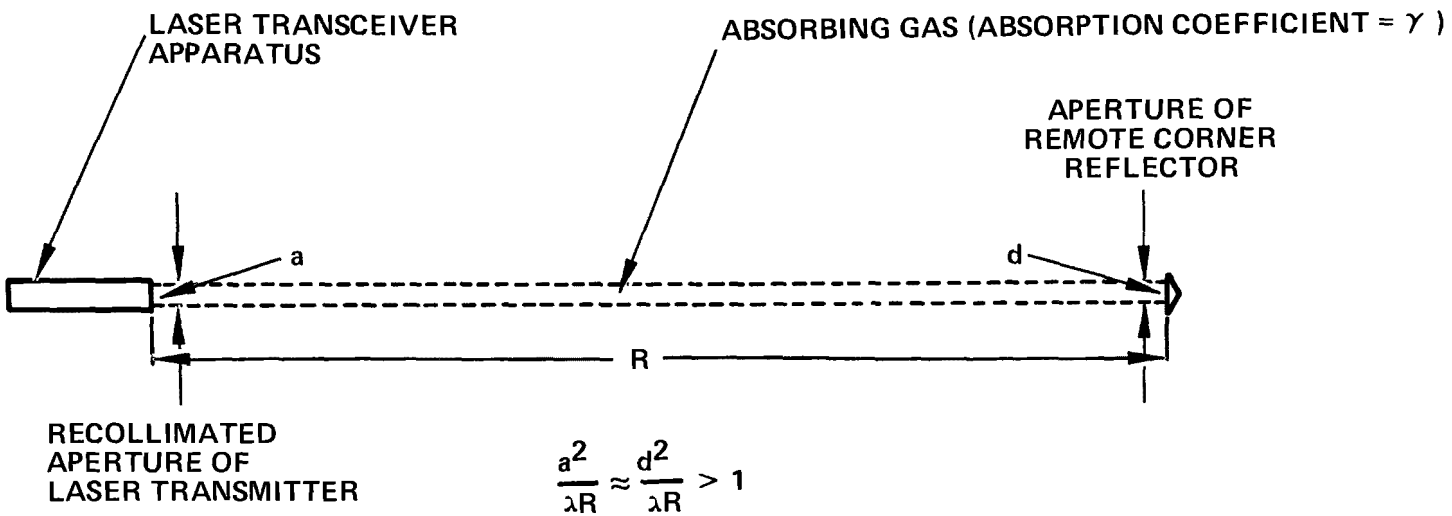

Figure 4. Schematic of Remote Monitoring Laser Apparatus.

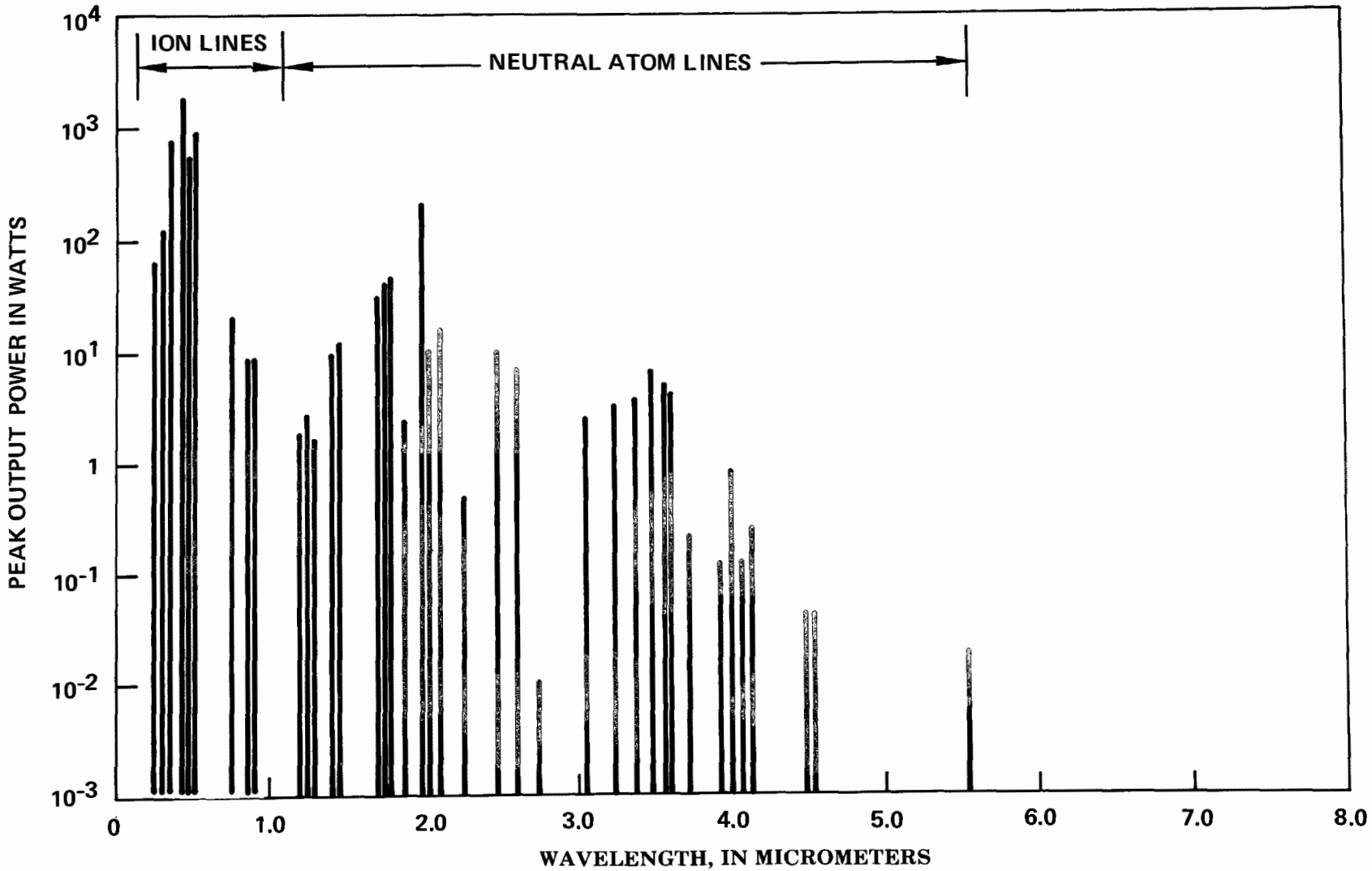

Figure 5. Spectral Distribution of Pulsed Noble Gas Laser Lines.

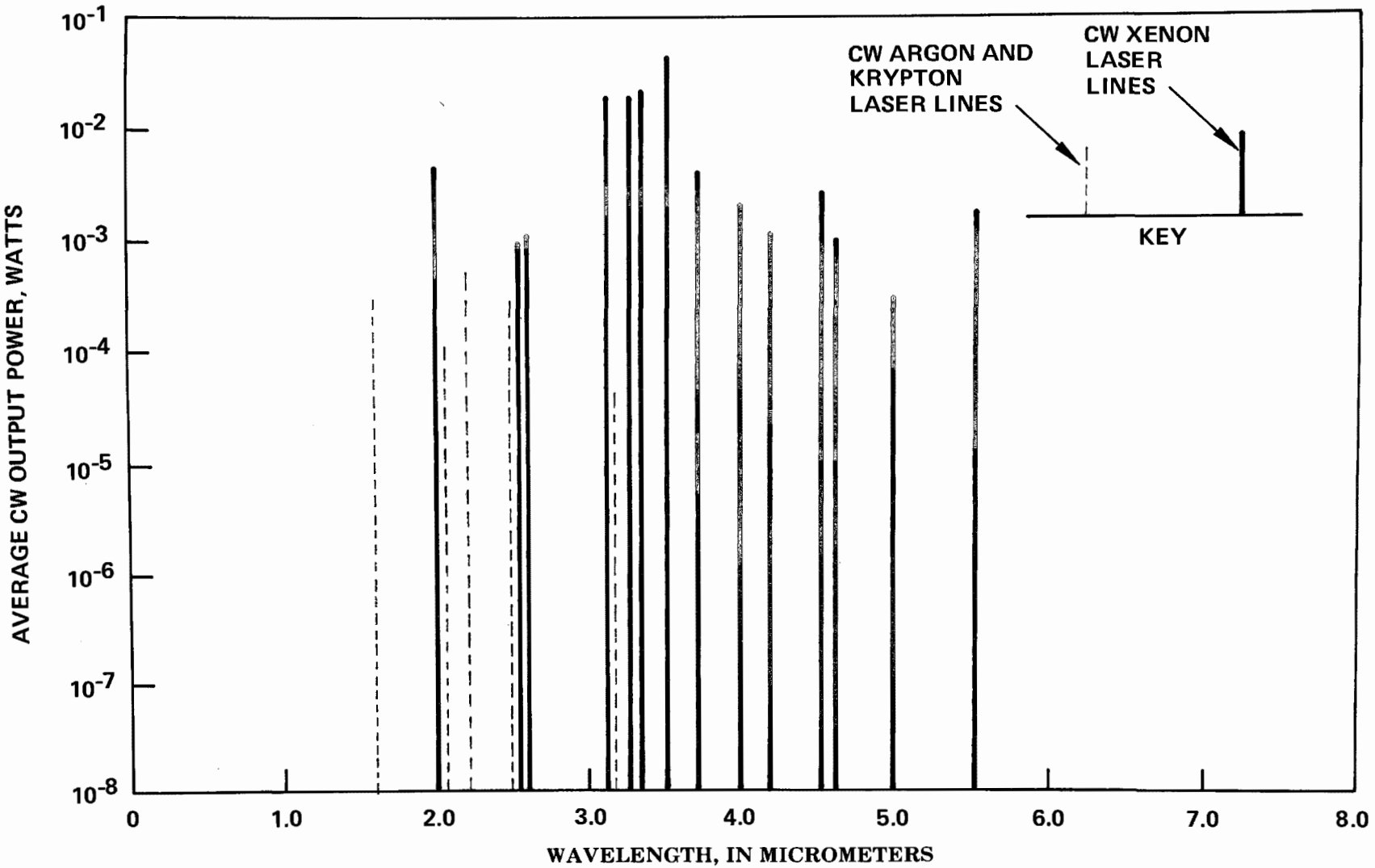

Figure 6. Spectral Coverage of CW Noble Gas Laser Lines.

ENRICHED STABLE ISOTOPES OF THE NOBLE GASES AND THEIR USES

C.F. Eck
Monsanto Research Corporation
Mound Laboratory*
Miamisburg, Ohio 45342

Abstract

Isotopes of the noble gases were initially discovered in the early part of this century. Since then the natural abundances of 23 stable isotopes have been measured. Two of these isotopes occur naturally at above 99 mole % isotopic concentration. For enrichment of noble gas stable isotopes, thermal diffusion is the common separation method. Six of the isotopes have been enriched to 99 mole %. Most of the others have been enriched in varying degrees ranging from 20 to 95 mole %. The uses of these isotopes are varied. Natural helium and argon, which are greater than 99% helium-4 and argon-40 respectively, are used widely in industry. The others are used in limited quantities. Some of the unique uses are in low-temperature refrigeration, gas tagging, and chemical analysis of surfaces. The isotopes are used in research and development work, directly in experiments and indirectly as components of systems for performing experimental work. Some of the common uses include lasers, preparation of radioisotopes, and studies of nuclear reactions, properties, and isotope effects, as well as isotope dilution and tracer work.

INTRODUCTION

Noble gases are an interesting group of elements. They are the most recently discovered natural stable elements. At that time, the end of the last century, radioactivity was also discovered, and there was great interest in identifying the various radioactive materials and their decay products. Spectroscopic studies were made of numerous materials. Among these was neon. In 1912 Sir J. J. Thomson studied its spectral lines and noticed two distinct lines. These were provisionally identified as neon-20 and neon-22, and called isotopes by Soddy. Thus, one of the noble gases, discovered only 14 years earlier played a part in demonstrating the existence of stable isotopes. Since then all the isotopes of the noble gases have been discovered. High enrichments of many of these isotopes have become available, and they are being used for many purposes. This paper reviews the noble gas stable isotopes, their separation methods, current separation and availability, and their uses.

After Thomson discovered two isotopes of neon, the spectra of many elements were studied. By 1922, Aston reported a provisional third isotope of neon, two isotopes of argon, all six isotopes of krypton, and seven isotopes of xenon with two provisional additional ones. Helium-3 was produced artificially and identified before it had been found in natural helium. In 1934 Vaughn measured its natural abundance to be less than one part in 35,000.

In 1939 Alvarez, *et al.*, showed that helium-3 isotopic abundance was greater in atmospheric helium than in gas-well helium. Table 1 shows the chronology of the discovery of the isotopes. All of these isotopes are found in air. Natural abundance data from Walton, *et al.*, (1966) for neon and from Lederer, *et al.*, (1967) for the other noble gases are given in Table 2.

Another source of some of these stable isotopes is the nuclear reactor industry. Materials from this source are isotopes of helium, krypton, and xenon. The isotopes of the first element result from excited-state lithium-7 disintegrating into helium-4 and tritium which in turn decays to helium-3. The helium-3 is separated from the resulting helium-3/helium-4 mixture. Isotopic abundances of fission product krypton and xenon are given in Table 3.

As noted in Table 2, two of these 23 stable isotopes, helium-4 and argon-40, already occur in nature at concentrations above 99 mole %. The other isotopes vary in isotopic concentrations from 630 ppm for argon-38 to 90.5 mole % for neon-20.

SEPARATION METHODS AND ENRICHMENT

Various methods have been tried to separate the noble gas stable isotopes. They include charcoal adsorption, diffusion, distillation, electromagnetic separation, gas centrifugation, gas chromatography, glow discharge, superfluidity, and thermal diffusion. The one commonly used is thermal diffusion.

Helium isotope separation studies have included diffusion, distillation, superfluid flow, and thermal diffusion. Natural abundance of helium-3 is so low that the helium mixture from the nuclear industry is used as feed to enrich helium-3 to above 99% by thermal diffusion (Anon, 1963 and Baker, 1965).

Early separations of neon-20 and -22 were achieved by diffusion through porous walls and distillation. Later Dickel, *et al.*, (1940) devised the thermogravitational column, and used the thermal diffusion effect to separate neon-20 and neon-22. This column consisted of a vertical glass tube with cooling water on the outside and with a hot electrically heated center wire. The temperature gradient between the hot wire and cool wall caused a concentration gradient, which was increased by the convection effect in the vertical system. This way they

**Mound Laboratory is operated by Monsanto Research Corporation for the U.S. Atomic Energy Commission under Contract No. AT-33-1-GEN-53.*

obtained high enrichments and reasonable separation rates. Subsequently, Clusius, *et al.*, (1956a) used an auxiliary gas, deuterated methane, in a thermal diffusion column to separate the middle isotope, neon-21 of the ternary system.

Methods used for separation of argon isotopes were Hertz diffusion method in flowing mercury vapor, thermal diffusion, and distillation. Thermal diffusion by Clusius, *et al.*, (1956b) enriched argon-36 to above 99% at reasonable separation rates. The middle isotope, argon-38, was also isolated above 99% in the thermal diffusion column by using the auxiliary gas, deuterium chloride.

Krypton has six isotopes; they are not as easily separated as the binary and ternary mixtures. Gas centrifugation and thermal diffusion have been used. Clusius, *et al.*, (1943-3) enriched krypton-86 to 99.5% and krypton-84 to 98.2% by thermal diffusion. Using the same method Blais, *et al.*, (1956) enriched krypton-78 to 44.9% and krypton-80 to 69.8%. Using hydrogen bromides as auxiliary gases in a thermal diffusion column, Clusius, *et al.*, (1957) enriched krypton-78 to 60.5%.

Xenon's nine isotopes with their high mass values are more difficult to separate than the krypton isotopes. Groth, *et al.*, (1939) tried to separate these isotopes in a direct current glow discharge unsuccessfully. The gas centrifuge was used with some success by Beyerle, *et al.*, (1949) and Hertz, *et al.*, (1954). Using a thermal diffusion column 48 meters long, Clusius, *et al.*, (1955) were able to enrich xenon-136 to 99%. Hechtl, *et al.*, (1967) used electromagnetic separation to isolate small quantities of xenon-131 to 99%. A production method used to obtain a stable xenon isotope was irradiation of iodine-127 to make xenon-128 of over 99% concentration (Haase, 1970). Xenon-124, which has a low natural abundance, has been enriched to 65% by thermal diffusion (Mound, 1969). During this enrichment, the isotope xenon-129 was concentrated to 60%. The preceding isotopes have been enriched using natural abundance feed gases. Fission xenon has been used as feed to a thermal diffusion system to enrich xenon-131 to 60% in liter quantities (Mound, 1967).

Table 4 shows the chronology of enrichment of noble gas stable isotopes. Table 5 shows the status and enrichment of these various isotopes. The scale of availability is divided roughly as follows:

Preparative — liter (STP) quantities
Experimental — milliliter (STP) quantities

As shown in the table, only six of the isotopes are available in liter quantities at enrichment of 99% or more. All of the preparative scale enrichments are being done by thermal diffusion at Mound Laboratory. Subsequent to the experimental development of the thermogravitational column by Clusius, Mound Laboratory used it for helium-3 enrichment, and later expanded its use to cascaded systems for the rest of the noble gas isotopes. Time-wise, these stable isotopes have not been available for more than 1-2 decades. Since then, many uses have developed in research and development work and some in specific applications. The uses of helium-4 and argon-40 will not be discussed since they have been available naturally for over half a century at high enrichments, and their uses have been reported widely.

PRESENT USES OF THE NOBLE GASES

Helium-3 is being used in a variety of ways. Its unique properties have made it the object of many studies in low-temperature physics and related work. As the most fugacious gas known with a normal boiling point of 3.2°K, helium-3 has been useful as a refrigerant in cryostats to achieve temperatures less than 1°K. (Cowen, 1964, Fruneau, *et al.*, 1967). For relatively large loads, a recirculating helium-3 refrigerator has been developed (Wilkes, 1972). Because of its high vapor pressure, 10,000 times greater than that of helium-4 at 0.5°K (Keller, 1969), helium-3 has been used as a vapor pressure standard temperature scale for low-temperatures (Sydoriak, 1964). The development of a dilution type refrigerator using helium-3/helium-4, and the effect from phase change, has allowed the maintenance of temperature at millidegrees Kelvin (Hall, 1966, Radebaugh, *et al.*, 1971). In physics of quantum phenomena at low-temperature, helium-3 has been used for considerable study of itself to clarify its uniqueness (Keller, 1969). This has included properties of liquid helium-3, critical phenomena, and study of dilute solutions of helium-3/helium-4.

In nuclear work where helium-4 causes interference in measurement of deuterium, helium-3 is used, for example, as a scattering gas in measuring total collision cross sections at thermal energies by molecular-beam scattering of deuterium by helium (Moore, *et al.*, 1967). A large use is for neutron detection and neutron spectrometry. Upon exposure to neutrons, helium-3 reacts to form tritium. The cross section for this reaction varies smoothly over a wide range and has a large value of 5,400 barns for thermal neutrons (Price, 1964). Also, there are no excited products, only tritium and a proton. The tritium decays with the emission of beta particles; these particles can readily be detected on a counter (Heiberg, 1967 and Myers, 1967). Helium-3 has advantages of sensitivity, high-temperature efficiency, and moderate voltage requirements at increased pressures. Neutron detectors filled with this isotope are used in applications such as oil well logging (Eaton, *et al.*, 1969). Helium-3 is also useful for neutron spectrometry (Batchelor, *et al.*, 1955; Manning, *et al.*, 1965; and Sayres, 1964).

An interesting application is its use in activation analysis. Helium-3 ions require less energy than protons as a bombarding particle and it has found use in analyses for oxygen (Lyon, 1964; Vialatte, *et al.*, 1972), fluorine (Lee, *et al.*, 1971), and carbon (Sanders, 1971). These ions do not penetrate deeply, permitting surface analysis only. Sensitivities of this method for many elements have been determined (Ricci, *et al.*, 1967 and Lutz, *et al.*, 1972).

Radioisotopes are being used increasingly in medical studies. Helium-3 as a bombarding particle serves for surface analysis as noted above, but also, the same helium-3 proton reaction serves to make fluorine-18 from oxygen-16. The fluorine-18 in this case is used in bone scanning for diagnostic study (Blau, 1962 and Tilbury, *et al.*, 1970). Other radioisotopes made by using helium-3 as a projectile are iron-52 for metabolism and bone marrow function, selenium-73 for sulfur substitute, rubidium-81 for splenic volume, and iodine-123 for thyroid and blood metabolism studies (Jester, 1972).

There are many methods for leak detection in vessels. Turner (1968) has reported a unique method for using helium-3 for large vessel leak measurement. Injection first of a known amount of helium-4 is made into a vessel pressurized with a carrier gas, and later, similarly, helium-3 is injected. The isotope ratio allows calculation of the percent leakage. This is useful when vacuum leak testing is inappropriate and accessibility a problem.

A recent use of noble gases is in lasers. Helium-neon gas lasers have found many applications in industry and scientific research, such as mechanical alignment, surveying, seismometry, holography, polarimetry, interferometry, and optical communications. These lasers can be improved by the use of the enriched isotopes, helium-3 and neon-20. At maximum output, helium-3 in place of helium-4 increases the power of such a laser by about 25% (White, 1963). Use of neon-20 and neon-22 allows the shifting of the maximum of the gain curve to the desired frequency of the laser beam (Schweitzer, 1968). In addition to uses in lasers, neon isotopes are used in nuclear reaction studies, nuclear magnetic resonance studies, and property measurements. Due to the ternary mixture of natural neon, it has been suggested that the normal boiling point of neon-20 be used to define a fixed point on the temperature scale (Furukawa, 1972).

The most interesting use of argon isotopes is the application of argon-38 to the dating of meteorites and other minerals. In this method, the decay of potassium-40 to argon-40 is measured by analysis of the resulting product using the isotope dilution method (Rankana, 1963). The final result for radiogenic argon is adjusted for the presence of atmospheric isotopes, such as argon-40, by the use of isotope ratios resulting from injecting argon-36 and argon-38 tracers. The argon-38/argon-36 ratio shows the atmospheric contaminant, and the argon-40/argon-36 ratio allows calculation of the radiogenic argon-40 quantity (Dalrymple, 1969). Large numbers of tracers are used in an experiment, but each tracer aliquot is small, being 10^{-5} STP milliliters (Reynolds, *et al.*, 1966).

Specific uses of krypton isotopes include the international wavelength standard, leak location in nuclear fuel elements, and preparation of radioisotopes. After study of several isotopes (Bruce, *et al.*, 1961), a multiple (1,650,763.73) of the wavelength in vacuum of the orange light of krypton-86, given off at the triple point (63°K) of nitrogen, has been used as the international standard for the length of the meter (Baird, *et al.*, 1961). This allows each laboratory to set up its own unit for this standard if desired. Krypton isotopes are used increasingly in the preparation of radioactive isotopes. Krypton-84 undergoes the proton, neutron reaction to make rubidium-84, which is used in myocardium scanning (Jester, *et al.*, 1972). Preparation of other rubidium and strontium isotopes are being considered.

One of the problems in operating a fast breeder reactor is to determine which fuel elements have developed a leak, when a leak is detected. This allows planning for replacement of the leaky fuel pin. A method using stable isotope tags has been developed by Argonne National Laboratory for the EBR-II fast reactor (Walker, *et al.*, 1969). In this method, a specific volume with a unique ratio of stable isotopes (xenon-124, xenon-126, xenon-128, and xenon-129) is injected into a feed element and the element is sealed (Henault, 1969). If at some future time, the element develops a leak, the gas with the unique ratio of isotopes goes into the cover gas of the reactor. A mass spectrometer analysis of the recovered tag gas establishes the element that is leaking (Henault, *et al.*, 1970a,b). Analysis of tag burnup has been made and includes the study of krypton isotopes (Boulette, 1972). The light krypton and xenon isotopes allow a sufficient number of unique isotope ratios to provide the necessary location points in the core of a fast breeder reactor. For the Fast Flux Test Facility being built at Hanford, this method has been refined to the use of a krypton capsule and a xenon capsule, each containing a specific volume and a unique ratio of isotopes (Cash, *et al.*, 1972). These capsules are inserted into a fuel element. The element is sealed, and the capsules punctured. The identification of a leak is made in the same way as with the EBR-II.

In addition to fuel element gas tags, xenon isotopes are used for radioisotope manufacture, nuclear physics studies, and scintillation counters. Xenon-124, when irradited with neutrons, is converted to iodine-125 (Jester, *et al.*, 1972). This radioactive isotope is particularly useful as a portable x-ray unit (Graham, 1970). It is also used in medical tests on thyroid function. Xenon-136 in a lamp would emit a normal frequency with extreme sharpness because the hyperfine structure is missing (Clusius, *et al.*, 1955).

This has been a brief survey highlighting some of the unique ways in which stable isotopes are used. In addition to these specific uses of noble gas isotopes, they are used in the basic study of their properties (physical, thermodynamic, and transport), in the study of reaction phenomena (energy levels, cross sections, yields), and for analytical standards.

REFERENCES

Alvarez, L. W. and R. Cornog (1939), *Helium and Hydrogen of Mass 3*, Phys. Rev., 56, Ser. 2, 613.
Anon (1963), *Thermal Diffusion Recovers Helium-3 Isotope*, Chem. Eng., 70, Nov. 25, 1963, 64-6.
Aston, F. W. (1922), *List of Elements and Their Isotopes*. Proc. Phys. Soc. London, 34, 197.

Baird, K. M. and D. S. Smith(1962), *Primary Standard of Length*, J. Opt. Soc. Am., 52, 507-14.
Baker, P. S.(1965). *Research Materials Coordination and Planning Meeting*, ORNL-TM-1047, Oak Ridge National Laboratory, Oak Ridge, Tennessee.
Batchelor, R., R. Aves and T. H. R. Shyrme(1955), *Helium -3 Filled Proportional Counter for Neutron Spectrometry*, Rev. Sci. Inst., 26, 1037-47.
Beyerle, K., *et al.***(1949),** *Gas Centrifuges: Enrichment of Isotopes of Xenon, Krypton, and Selenium with the Centrifugal Process*, Chem. Ing. Tech., 21, 331-4.
Bezella, W. A.(1968). *Analysis of the Fission Gases Released Within Spent Yankee Fuel Rods*, USAEC Report WCAp-6087, Westinghouse Electric Corp., February, 1969.
Blais, N. C. and W. W. Watson(1956),(d.p.) *Reactions with Krypton-78 and Krypton-80*, Phys. Rev., 104, 202.
Blau, M., W. Nagler and M. A. Bender,(1962). *Fluorine-18: A New Isotope for Bone Scanning*, J. Nucl. Med., 3, 332-3.
Boulette, E. T., R. E. Schenter and F. Schmittroth(1972), *Gas Tag Burnup Analysis for Fuel Failure Location and Detection in the FTR*, HEDL-TME-72-93, Hanford Engineering Development Laboratory, Richland, Washington.
Bruce, C. F. and R. M. Hill(1961). *Wavelengths of Krypton-86, Mercury-198, and Cadmium-114*, Austral, J. Phys., 14, 64-88.
Cash, R. J., F. E. Holt and Y. S. Tang,(1972), *FFTF Fuel Failure Location System Recommendations and Rationale*, HEDL-TME-72-96, Hanford Engineering Development Laboratory, Richland, Washington and Westinghouse Advanced Reactor Design.
Clusius, K., H. H. Buhler, H. Hurzeler and E. Schumacher,(1955), The Separation Tube. XVI. *Preparation of the Isotope Xenon-136*, Z. Naturforsch., 19a, 809-14.
Clusius, K. and G. Dickel(1942-3), Separation Tube. IV. *Preparation of the Isotopes Krypton-84 and Krypton-86*, Z. physik. Chem., B 52, 348-68, and B 53, 178.
Clusius, K., M. Huber, H. Hurzeler and E. F. Schumacher(1956), *Preparation of the Rare Isotope Neon-21*, J. Chem. Phys., 24, 167-8.
Clusius, K. and H. U. Hostettler(1957), The Separation Tube XIX, *The Enrichment of the Isotopes Bromine-79 and Bromine-81*, Z. Naturforsch, 12a, 974-82.
Clusius, K., E. Schumacher, H. Hurzeler and H. V. Hostettler(1956b), Separation Tube. XVIII. *Preparation of the Pure Rare Isotopes of Argon, Argon-36, and Argon-38*, Z. Naturforsch, 11a, 709-15.
Cowen, J. A.(1964), *Simple Glass He-3 Cryostat for EJR and NMR*, Rev. Sci. Inst., 35, 914-5.
Dalrymple, G. B. and M. A. Lanphere(1969), *Potassium-Argon Dating*, W. H. Freeman and Co., San Francisco, California.
Dickel, G. and K. Clusius(1940), The Separation Tube. III. *Production of 2.5 Liters of Pure Isotope Neon-22 and Neon-20*, Z. physik Chem., B 48, 50-62.
Eaton, E. and D. Leslie(1969), *Nuclear Radiation Techniques in Oil Well Logging*, World Petroleum, 40, 54-60.
Fruneau, M., Lacaze and L. Weil(1967), *Helium-3 Cryostat with Adsorption Pump*, Cryogenics, 7, 135-7.
Furukawa, G. T.(1972), *Vapor Pressures of Neon-20 and Neon-22*, Metrologia, 8, 11.
Graham, D.,(1970), *Use of Radioactive Iodine-125 for Dental Identification in Mass Disasters*, J. of Forensic Sci., 15, 553-64.
Groth, W. and P. Harteck(1939), *Experiments on Separation of Isotope Molecules in a Direct-Current Glow Discharge*, Naturwissenschaften, 27, 390-1.
Hasse, D. W.(1970), *Xenon-128 Production Process Development*, DUN-SA-145, Douglas United Nuclear, Inc., Richland, Washington.
Hall, H. E., P. J. Ford and K. Thompson(1966), *Helium-3 Dilution Refrigerator*, Cryogenics, 6, 80-8.
Hechtl, E. and F. P. Vierbock,(1967), *Electromagnetic Separation of Highly Enriched Noble Gas Isotopes in Multimilligram Quantities*, Nucl. Instr. Methods, 48, 323.
Heiberg, E.,(1967), *The Helium-3 Counter as a Detector of Time-of-Flight Measurements of Thermal Neutron Spectra*, Nucl. Instrum. Methods, 52, 175-6.
Henault, P. B., G. J. Bernstein, L. F. Coleman, E. R. Ebersole, W. V. Larson and W. W. Smith, (1969), *Identification of Failed Fuel Elements by Xenon Tag*, Trans. Am. Nucl. Soc., 12, 102-3.
Henault, P. B., E. R. Ebersole, M. T. Laug, R. Villarreal and D. E. Walker, (1970a), *Progress in Xenon Tagging*, Trans. Am. Nucl. Soc., 13, 797-8.
Hertz, G. and E. Nann(1954). *New Results on the Isotope Separation of Heavy Gases in the Gas Ultra Centrifuge*. Z. Elektrochem., 58, 612-16.
Keller, W. E.(1969), *Helium-3 and Helium-4*, Plenum Press, New York, New York.
Jester, W. A., G. L. Jackson, B. K. Lee, J. S. Burkle and D. Jarrell,(1972), *Nuclear Engineering Applications in Medical Science*, Isot. and Rad. Tech., 9, Summer 1972, 485-99.
Lederer, C. M., J. M. Hollander and I. Perlman(1967), *Table of Isotopes*. Sixth Edition. John Wiley and Sons, Inc., New York, New York.
Lee, D. M., J. F. Lamb and S. S. Markowitz(1972), *Rapid Non-Destructive Method of Fluorine Analysis by Helium-3 Activation*, Anal. Chem., 43, 542-5.
Lutz, G. T., R. J. Boreni, R. S. Maddock and J. Wing, (1972), *Activation Analysis — A Bibliography through 1972*, NBS Tech. Note 467, U.S. National Bureau of Standards, Washington, D.C.

Lyon, W. S., Jr.(1964), *Guide to Activation Analysis,* D. Van Nostrand Company, Inc., Princeton, N. J.
Manning, A. W., T. B. Jeter, H. Schuckler and W. Sluck(1965), *Helium-3 Spectrometer Characteristics and Applications,* Nucleonics, 23, April, 1965, 69-71.
Moore, G. E., S. Datz and F. van der Valk(1967), *Total Scattering Cross Sections of Hydrogen and Deuterium by Helium,* J. Chem. Phys., 46, 2012-13.
Mound(1967), *Stable Gaseous Isotope Separation and Purification,* April-June, 1966, MLM-1353, Mound Laboratory, Miamisburg, Ohio.
Mound(1969), *Stable Gaseous Isotope Separation and Purification,* July-September, 1968, MLM-1529, Mound Laboratory, Miamisburg, Ohio.
Myers, J. E.(1967), *High-Temperature Helium-3 Detectors,* IEEE Trans. Nucl. Sci., 14, 416-21.
Price, W. J.(1964), *Nuclear Radiation Detection,* McGraw-Hill Book Co., New York, New York.
Radebaugh, R. and J. D. Siegworth(1971), *Dilution Refrigerator Technology,* Cryogenics, 11, 368-84.
Rankama, K.(1963), *Progress in Isotope Geology,* Interscience Publishers, New York, New York.
Reynolds, J. H. and R. Spira(1966). *Individual Tracers for Isotope Dilution Analysis of Rare Gases,* Nucl. Instr. Methods, 42, 225-8.
Ricci, E. and R. L. Hahn(1967), *Sensitivities for Activation Analysis of 15 Light Elements with 18MeV Helium-3 Particles,* Analytical Chem. 39, 794-7.
Sanders, W. M.(1971), *Techniques for Active Helium-3 Activation Analysis for Carbon and Oxygen,* LA-4833, Los Alamos Scientific Laboratory, Los Alamos, New Mexico.
Sayres, A.(1964), *Helium-3 Fast Neutron Spectrometer with Extended Energy Range;* Trans. Am. Nucl. Soc., 7, 372-3.
Schweitzer, W. G., Jr.(1968), *Saturated Absorption by Neon Inside a 6328 Å Laser with a Mixture of Neon Isotopes in its Gain Tube,* App. Phys. Let., 13, 367-8.
Sydoriak, S. G.(1964), *1962 Helium-3 Scale of Temperature,* J. Res. Nat. Bur. Stand., 68 A, 547-88.
Tilbury, R. S., J. R. Dahl., J. P. Mamacos, and J. S. Laughlin(1970), *Fluorine-18 Production for Medical Use by Helium-3 Bombardment of Water,* Int. J. Appl. Radiat. Isot., 21, 277-81.
Turner, S.(1968), *Measurement of Leakage from Large Pressurized Components Using Helium Isotopes,* TRG Report 1195(R), United Kingdom Atomic Energy Authority, The Reactor Group, HQ, Risley, Warrington, Lancs, U.K.
Vaughn, A. L., J. H. Williams and J. T. Tate(1934), *Isotopic Abundance Ratios of Carbon, Nitrogen, Argon, Neon, and Helium,* Phys. Rev., 46 Ser. 2, 327.
Vialatte, B. and G. Revel(1972), *Determination of Oxygen in Aluminum by Helium-3 Activation,* Anal. Chem., 44, 1077-9.
Walker, D. E., P. J. Halfman and J. H. Sanecki(1969), *Xenon Tagging of Instrumented Fuel Capsules for Use in EBR-II.,* Nat. Sym. Develop. Irrad. Test Technol., 3rd, 59-70.
Walton, R., Jr. and A. E. Cameron,(1966), *The Isotopic Composition of Atmospheric Neon,* Naturforschung, 21a, 115-119.
White, A. D.(1963), *Increased Power Output of the 6328 A Gas Maser,* Proceedings of the IEEE, 51, 1669.
Wilkes, W. R.(1972), *A 200 mW Recirculating Helium-3 Refrigerator,* Cryogenics, 12, 180-3.

TABLE 1. Chronology of Discovery of Noble Gas Stable Isotopes.

1919	Neon-20	1922	Xenon-124
	Neon-22		Xenon-126
1920	Helium-4	1923	Xenon-128
	Argon-36		Xenon-130
	Argon-40		
	Krypton-78	1928	Neon-21
	Krypton-80		
	Krypton-82	1934	Argon-38
	Krypton-83		
	Krypton-84	1939	Helium-3
	Krypton-86		
	Xenon-129		
	Xenon-131		
	Xenon-132		
	Xenon-134		
	Xenon-136		

TABLE 2. Natural Abundance of Stable Isotopes of Noble Gases.

Isotope	Natural Abundance (Mole %)
Helium-3	1.3×10^{-4}
Helium-4	99.9999
Neon-20	90.5
Neon-21	0.27
Neon-22	9.23
Argon-36	0.337
Argon-38	0.063
Argon-40	99.600
Krypton-78	0.35
Krypton-80	2.27
Krypton-82	11.56
Krypton-83	11.55
Krypton-84	56.90
Krypton-86	17.37
Xenon-124	0.096
Xenon-126	0.090
Xenon-128	1.92
Xenon-129	26.44
Xenon-130	4.08
Xenon-131	21.18
Xenon-132	26.89
Xenon-134	10.44
Xenon-136	8.87

TABLE 4. Chronology of Enrichments of Noble Gas Stable Isotopes.

Year	Isotope	Enrichment Mole %
1940	Neon-20	99.8 (1950: 99.95)
	Neon-22	99.7 (1960: 99.92)
1942	Krypton-84	98.2
	Krypton-86	99.5
1955	Xenon-136	99.0
1956	Neon-21	99.6
	Argon-36	99.9 (1962: 99.99)
	Argon-38	99.6 (1959: 99.98)
	Krypton-80	69.8
1957	Krypton-78	60.5
1967	Xenon-131	99
	Xenon-129	60
1969	Xenon-124	65
1971	Argon-40	99.98
1973	Krypton-82	77

TABLE 3. Fission Noble Gas Isotopes (Bezella, 1968).

Fission Krypton		Fission Xenon	
Krypton-78	--	Xenon-124	--
Krypton-80	--	Xenon-126	-
Krypton-82	0.2 Mole %	Xenon-128	0.15 Mole %
Krypton-83	11 " "	Xenon-129	
Krypton-84	31 " "	Xenon-130	
Krypton-85*	6 " "	Xenon-131	8 " "
Krypton-86	52 " "	Xenon-132	22 " "
		Xenon-134	29 " "
		Xenon-136	41 " "

*Radioactive

TABLE 5. Enriched Stable Isotopes of Noble Gases.

Isotope	Enrich. Mole %	Method	Scale
Helium-3	99.98	Thermal diffusion	Preparative
Neon-20	99.95	Thermal diffusion	Preparative
Neon-21	90	" "	"
	99.6	Thermal diffusion & auxiliary gas	Experimental
Neon-22	99.9	Thermal diffusion	Preparative
Argon-36	99.5	Thermal diffusion	Preparative
Argon-38	95	" "	"
	99.6	" " and auxiliary gas	Experimental
Argon-40	99.95	Thermal diffusion	Preparative
Krypton-78	50	Thermal diffusion	Preparative
	60.5	Thermal diffusion and auxiliary gas	Experimental
Krypton-80	69.8	Thermal diffusion	Experimental
Krypton-82	70	" "	Preparative
Krypton-84	90	Thermal diffusion	Preparative
	98.2	" "	Experimental
Krypton-86	99.	" "	Preparative
	99.5	" "	Experimental
Xenon-124	20	Thermal diffusion	Preparative
	65	" "	Experimental
Xenon-126	10	" "	Preparative
Xenon-128	99	Irradiation of I-127	Experimental
Xenon-129	60	Thermal diffusion	Preparative
Xenon-131	60	Thermal diffusion	Preparative
	99	Electromagnetic sep.	Experimental
Xenon-132	38	Thermal diffusion	Preparative
Xenon-134	27	" "	"
Xenon-136	99	" "	"

NOBLE GASES IN NUCLEAR MEDICINE

M. Calderon and J.A. Burdine
Baylor College of Medicine and
St. Luke's Episcopal-Texas Children's Hospitals
Houston, Texas

ACKNOWLEDGEMENTS

We are indebted to Professor Linda Monroe and Jane Demos for assistance in preparation of the manuscript and illustrations.

Abstract

Radioactive noble gases have made a significant contribution to diagnostic nuclear medicine. In the area of regional assessment of pulmonary function, ^{133}Xe has had its greatest clinical impact. Following a breath of ^{133}Xe gas, pulmonary ventilation can be measured using a scintillation camera or other appropriate radiation detector. If ^{133}Xe dissolved in saline is injected intravenously, both pulmonary capillary perfusion and ventilation can be measured since 90% of the highly insoluble xenon escapes into the alveoli during the first passage through the lungs. Radionuclide pulmonary function tests provide the first qualitative means of assessing lung ventilation and blood flow on a regional basis, and have recently been extended to include quantification of various parameters of lung function by means of a small computer interfaced to the scintillation camera.

^{133}Xe is also used in the measurement of organ blood flow following injection into a vessel leading into an organ such as the brain, heart, kidneys, or muscles.

INTRODUCTION

The field of nuclear medicine originated in the early 1920's when George Hevesy and Hermann Blumgart applied naturally occurring radioisotopes to the study of physiological phenomena. Since the introduction of the cyclotron and the development of nuclear reactors, the Atomic Energy Commission and other governmental agencies such as the Food and Drug Administration have provided significant support for activities in this area of medicine. As a result, in less than a quarter of a century, nuclear medicine has become the fastest growing major specialty concerned with diagnostic and therapeutic patient care.

The use of radioactive noble gases such as isotopes of xenon and krypton has become increasingly important in both the research and clinical activities of nuclear medicine. The most widely used gas has been ^{133}Xe, primarily because of its more abundant availability. ^{133}Xe is reactor produced as a fission product of ^{235}U. With a half-life of 5.2 days, this radionuclide decays by beta emission with a maximum energy of 346 keV, and a primary gamma photon of 81 keV to stable ^{133}Cs. As is true with other noble gases, ^{133}Xe is virtually non-reactive and freely diffusible. Under high pressure or in a vacuum, the gas can be dissolved in aqueous or saline solution, and in this form is used for the study of several important physiological parameters. ^{127}Xe has also been used, and has several significant advantages in terms of physical characteristics such as its pure gamma emission. However, this material is accelerator produced and therefore has very limited availability.

APPLICATIONS

The two most important applications of radioactive xenon are in the measurement of organ or tissue blood flow, and the assessment of pulmonary function. When ^{133}Xe is injected into a blood vessel leading into an organ such as the brain, heart, kidneys, or even muscles, the dissolved gas rapidly diffuses from the blood into the tissues (Figure 1). The relative distribution between tissue and blood is a constant for the particular histologic or cellular structure involved, and may be numerically expressed by a partition coefficient. As the bolus of radioactive gas passes through the organ, equilibrium with the tissue occurs transiently, followed by a rapid decrease in the blood level of xenon within the organ. The extravascular xenon at this point begins to diffuse back into the blood, with the rate of xenon clearance from the organ being proportional to the rate of blood flow. Very little xenon recirculates during the next phase of the cardiac cycle, since more than 90% of the xenon passing through the lungs is cleared by ventilation. The rate of clearance of the radioactive xenon from the organ is determined by appropriately positioned scintillation detectors. If the tissue-to-blood partition coefficient for the particular organ is known, the specific perfusion fraction in ml/gram of tissue can be calculated from the clearance half-time. The general equation is:

$$\underset{\text{(ml/g/min)}}{\text{OBF}} = \lambda \frac{\log_e 2}{T\,1/2\ \text{(min)}}$$

Where OBF = Organ blood flow

λ = Partition coefficient

$\frac{\log_e 2}{T\,1/2\ \text{(min)}}$ = Clearance rate

The concept of exponential clearance is basic to stochastic or kinetic analysis of this type. The formula is based upon the initial slope of the washout, assuming a single exponential function. Organs such as the brain with different rates of perfusion to gray and white matter create the need for a multi-exponential approach. Through these techniques, the first quantitative information concerning regional blood flow has been obtained in patients with cerebral vascular disease, as well as those with coronary artery disease before and after infarction.

Of even greater clinical significance has been the study of pulmonary function with radioactive noble gases, particularly ^{133}Xe. Until such techniques came into being, the regional distribution of blood flow and ventilation could not be measured by conventional pulmonary function studies. Consequently, the pulmonary physiologist has been severly limited in the type of information he could obtain concerning the pathogenesis of pulmonary disease. Because of the amazing functional reserve of the lungs, many patients experience a disease process which goes undetected for years, until the point at which significant signs and symptoms occur. Radionuclide studies of pulmonary function have offered the potential for filling most of this void.

When ^{133}Xe is injected intravenously, the gas passes through the heart into the vascular system within the lungs (Figure 2). At this point, more than 90% of the gas diffuses into the alveoli, the small sacs which constitute the great majority of the lung volume, and/or the ventilatory unit which is most distal from the ambient atmosphere. While the patient holds his breath, the initial distribution of injected gas is proportional on a regional basis to perfusion or blood flow. Utilizing a sophisticated radiation detecting device called a scintillation camera, the distribution of radioactivity in a patient's lungs is displayed on a cathode ray tube, and may be photographed. The scintillation camera consists basically of a large sodium iodide crystal viewed by nineteen photomultiplier tubes which are in turn connected to a x-y pulse locator. This device, by recording the relative distribution of pulmonary blood flow, enables the physician to diagnose perfusion abnormalities which have been caused by blood clots or emboli, as well as the destructive changes inherent in pulmonary emphysema. Such testing is rapid, safe, and relatively simple. Because of these characteristics, the tests are readily applicable to children. In addition, the information provided is not available through other modalities.

A normal pulmonary perfusion scintiphoto is illustrated in Figure 3. Note the regular distribution of the injected gas with a gradient that follows the actual hydrostatic distribution of the blood flow.

Figure 4 is a ^{133}Xe perfusion image obtained in a patient with a pulmonary embolus, a condition in which blood clots in the lungs occlude branches of the pulmonary arteries. This disease has been reported to be the most common cause of sudden death in hospitalized patients.

In addition to perfusion or blood flow, the other essential mechanism involved in the exchange of oxygen and carbon dioxide by the lungs is ventilation. Ventilation may be defined as the transfer of gases to and from the alveoli by the bronchial tree in connection with the ambient atmosphere. This critical parameter of pulmonary function can be monitored in two ways using radioactive xenon gas. First, the rate of washout of injected xenon during a perfusion study is directly proportional to ventilation. Any abnormalities of ventilation will appear on the scintillation camera photographs as retained or "trapped" radioactivity in this patient.

Ventilation may also be measured by observing the distribution of radioactive xenon in the lungs after a single breath inhalation of the gas (Figure 5). Ordinarily regional ventilation and, therefore, gas concentration is relatively uniform, with a slight preponderance toward the lower or basal portion of each lung.

Patients with chronic obstructive pulmonary disease such as the individual in Figure 6 with emphysema have an uneven gas distribution produced by airway obstruction and parenchymal destruction. In addition, a "ball-valve" phenomenon may occur, whereby gas passing into lung regions on inspiration has trouble exiting during expiration. Such "trapping" is common in these diseases.

Radionuclide pulmonary function tests have provided the first qualitative means of assessing regional lung ventilation and blood flow, and have been extremely useful clinically. However, quantitative values would be helpful for research purposes and to follow the clinical progress of a particular patient's disease. In addition, other parameters of pulmonary function such as regional gas exchange which depend upon the coupling of ventilation of perfusion are not readily appreciated from the static scan images. To gain important new information derived from the basic imaging studies, we have designed in our laboratories a multipurpose minicomputer system for computation of quantitative values of pulmonary function.

The computer system is interfaced directly to the scintillation camera. Appropriate gas dispensing equipment such as this spirometer is located in proximity to the patient. Raw data are processed by the computer to obtain indices which express regional ventilation and perfusion per unit volume of lung, with the information displayed as a functional image of color-coded contours, each contour representing a different level of ventilation or perfusion. The color sequence begins with the red end of the spectrum as a maximum value, and decreases to blue for a minimal level. The functional images illustrate that the area of greatest perfusion in the upright patient is located in the lower portion of both lungs, reflecting the hydrostatic distribution of the column of blood. Ventilation is also located somewhat more toward the lung base, but because of pressure differences within the lung parenchyma itself. In a patient with pulmonary embolism or blood clots within the lung, large perfusion defects are noted due to the clot, with essentially normal ventilation. In patients with pulmonary emphysema, diffuse abnormalities in ventilation and perfusion are present.

The physiologic coupling of ventilation to perfusion is critical for adequate exchange of oxygen and carbon dioxide between the alveoli and blood. The basic abnormality in many lung diseases is an uneven influence of

these two parameters of pulmonary function. To determine the efficiency of such coupling and therefore to reflect imbalances, a functional image of the ventilation-perfusion (V/Q) ratio decreases in a stepwise fashion in the normal patient. In the patient with pulmonary embolism, ventilation predominates in the areas where blood flow has been obstructed by a clot. In the patient with pulmonary embolism, the normal stepwise sequence has been disrupted, because of destruction of the lung tissue.

In summary, some of the most important tests in clinical medicine are now based upon the use of noble gases. With the development of new instrumentation including sophisticated data processing systems, these important radionuclides will undoubtedly assume an even greater importance in medicine during the next few years.

REFERENCES

Ball, W. C., *et al.*, **(1962),** *Regional Pulmonary Function Studies with Xenon-133.* J. Clin. Invest. 41:519-531.

Burdine, J. A., *et al.*, **(1972),** *Functional Pulmonary Imaging.* J. Nucl. Med. 13:933-938.

Cannon, P. J., R. B. Dell, and E. M. Dwyer, Jr., (1972), *Measurement of Regional Myocardial Perfusion in Man with* ^{133}*Xe and a Scintillation Camera.* J. Clin. Invest. 51:964-977.

Hoffer, P. B., *et al.*, **(1973),** *Improved Xenon Images with* ^{127}*Xe.* J. Nucl. Med. 14:172-174.

Lassen, N. A., (1967), *On the Theory of the Local Clearance Method of Measurement of Blood Flow including a Discussion of its Application to Various Tissues.* Acta Medica Scandanavica Suppl. 472:136-144.

Wagner, H. N., Jr., (1964), *Regional Blood Flow Measurements with Krypton-85 and Xenon-133.* In Dynamic Clinical Studies with Radioisotopes, AEC Symposium #3.

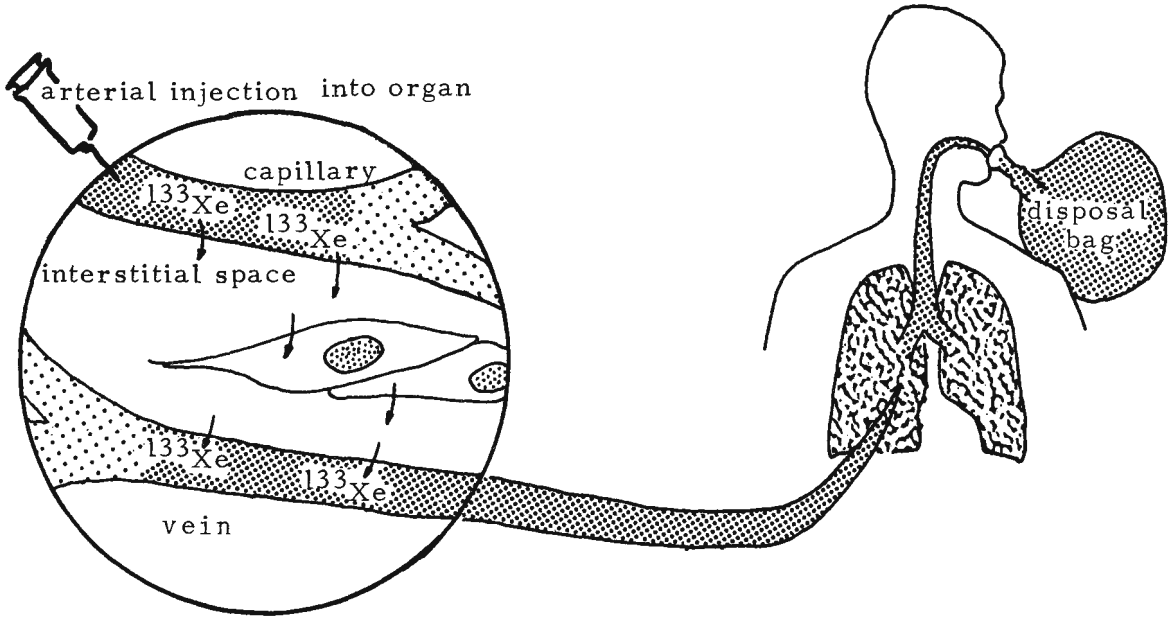

Figure 1. Schematic representation of an intra-arterial injection of ^{133}Xe solution for the measurement of organ blood flow. The partition coefficient for ^{133}Xe between tissue and blood is constant for the particular histologic structure.

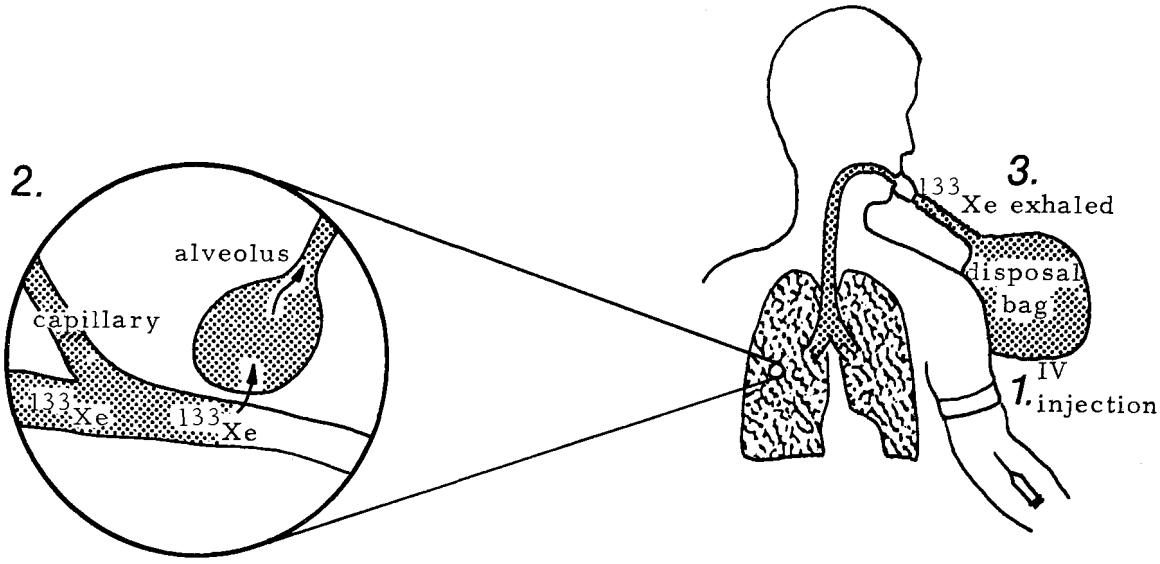

Figure 2. Schematic representation of an intravenous injection of ^{133}Xe in saline. More than 90% of the ^{133}Xe is cleared by ventilation on the first passage through the lungs.

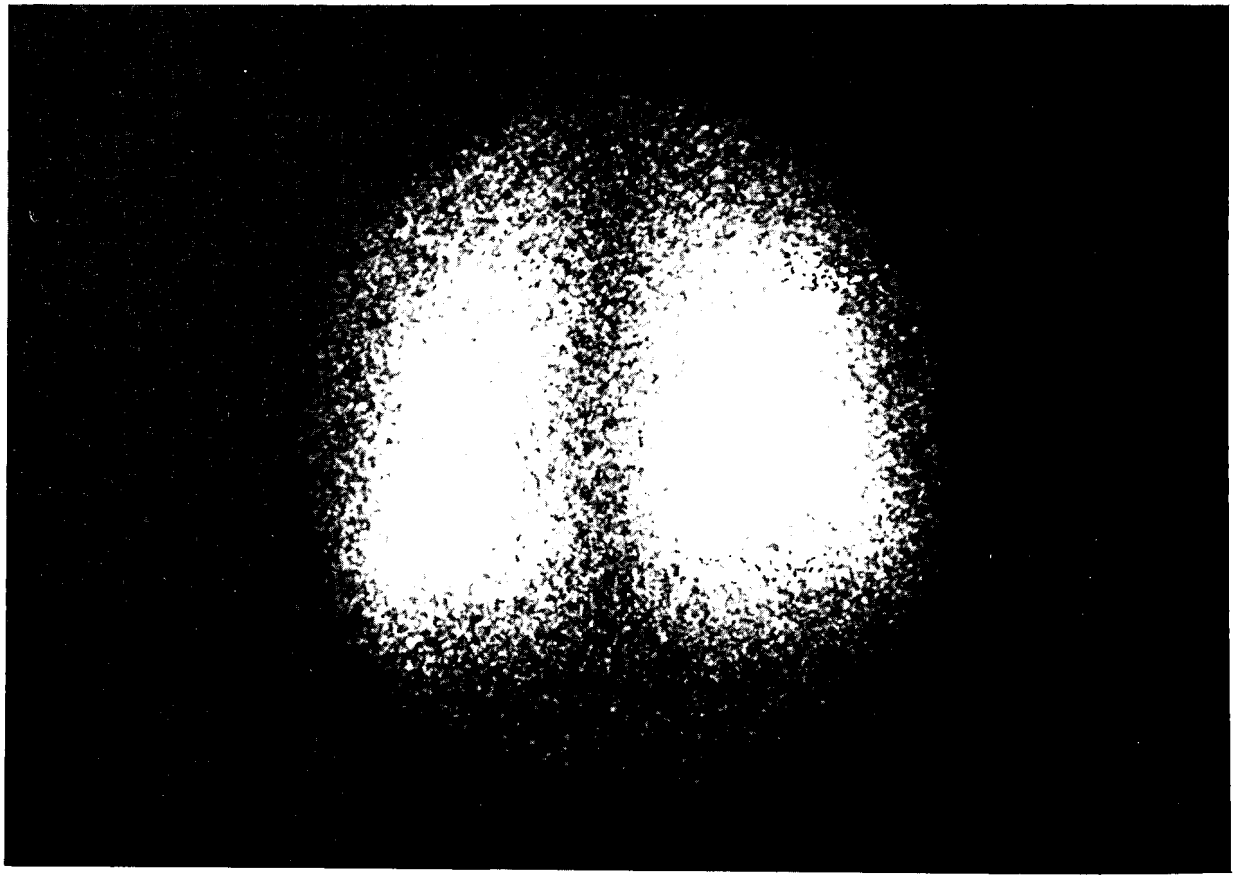

Figure 3. Normal ^{133}Xe pulmonary perfusion scintiphoto recorded during breath holding.

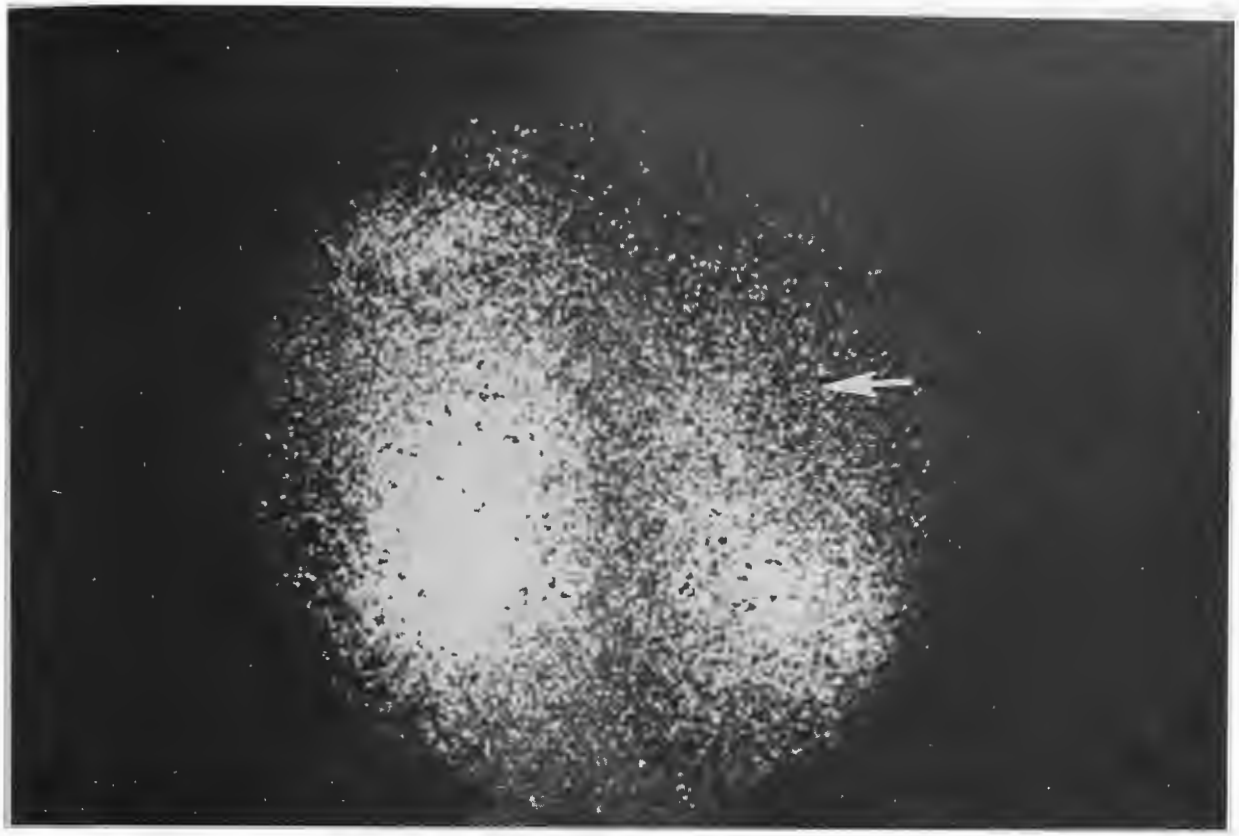

Figure 4. ^{133}Xe perfusion image in a patient with pulmonary embolism. Arrow indicates an area of perfusion deficit produced by a blood clot in a branch of the pulmonary artery.

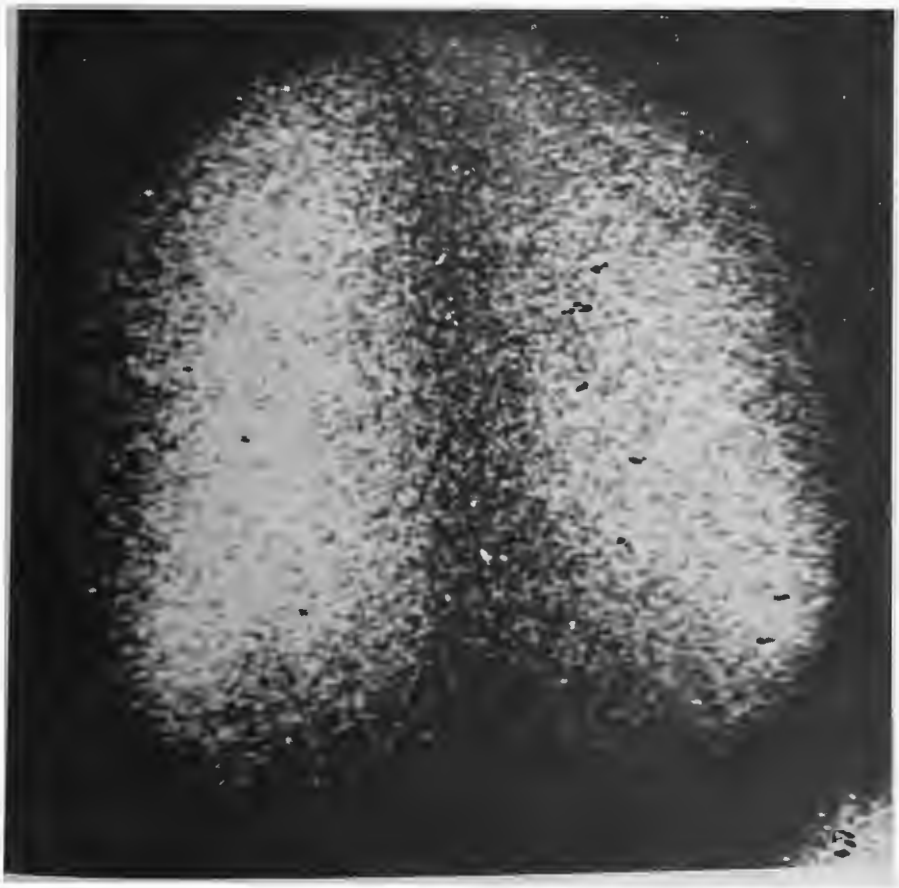

Figure 5. Normal ^{133}Xe pulmonary ventilation scintiphoto obtained during breath holding following a single deep inspiration of the gas.

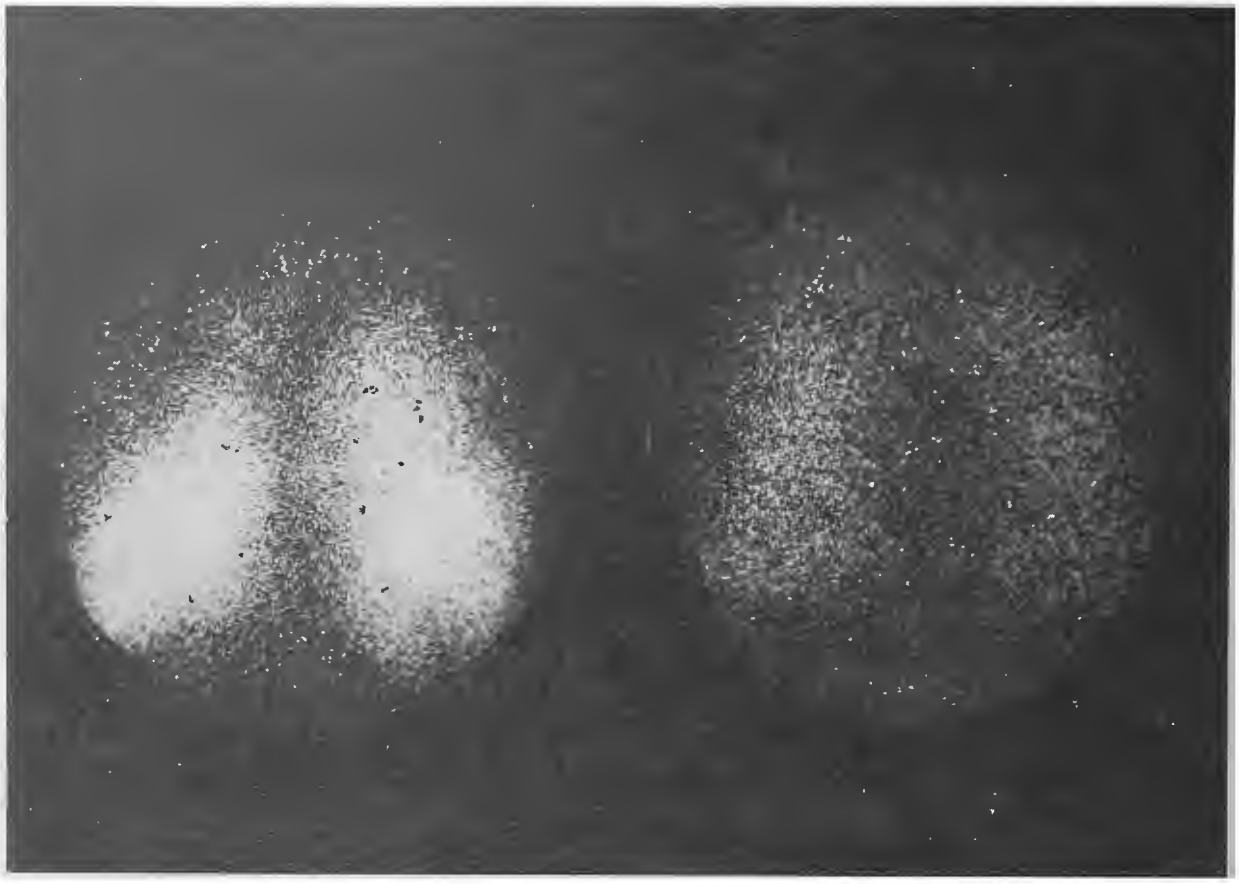

Figure 6. Ventilatory images in a patient with emphysema. The breath holding image (left) shows areas of lung destruction, while the image obtained during subsequent ventilatory washout (right) demonstrates gas trapping indicative of airway obstruction.

HELIUM — ITS CONSERVATION AND ITS POTENTIAL FOR FUTURE YEARS

C. Laverick
Argonne National Laboratory
Argonne, Illinois

ACKNOWLEDGEMENTS

Information from the Department of Interior, Congressional hearings, the excellent opinion of Judge Frank Theis of the U.S. Kansas District Court on June 11, 1973, and the many discussions and reports generated by the National Science Foundation, Helium Study Advisory Committee (see Figure 2) and Participants, have been freely used in generating the cross section of the helium problem presented here. In particular, thanks are due to Harold Lipper, Chief, Division of Helium, U.S. Bureau of Mines; David M. Evans, Director, Potential Gas Committee, Mineral Resources Institute, Colorado School of Mines; John K. Hulm and H. Richard Howland of the Westinghouse Systems Research Directorate; and representatives of the gas companies and distributors involved. Further information can be obtained from members of the Helium Study Advisory Committee.

Abstract

Some of the past history of the U.S. helium conservation program is outlined giving the Administration's reasons for cancelling the helium storage contracts. The helium demand for current technologies is given, and rough estimates of demands for these and newly developing technologies are presented for future years. The objectives of the current National Science Foundation's Helium Study are stated, and some developing conclusions for further discussion are outlined. The dilemma between current economic and conservationist philosophy is outlined. While a substantial gain in long-term cash return for the program is possible by the time the stored helium has been sold, the principal concern seems to be the short-term cash flow, with its substantial borrowings from the Treasury (more than $320 million by June, 1973), due in part to the way the Interior chose to administer the program, and in part due to the fact that substantial investments are usually necessary to yield even greater, longer term revenue. Some thoughts on these aspects of the program are expressed.

While it is inappropriate to second guess NSF helium study conclusions which have yet to be reached, it is almost certain that helium will be needed in substantial quantities beyond the turn of the century if the leading world nations are to continue to develop as post-industrial societies. New helium-based technologies can reduce our energy and resource needs for any given energy base. A conservative estimate of U.S. demand from 2000 to 2050 A.D. is about 136 billion cubic feet with total world demand for the same period in excess of 500 billion cubic feet. The U.S. has the most substantial world reserves and, with good husbandry, could supply a significant portion of this demand, with associated favorable international trading aspects. The desirability of such a situation should be self-evident in view of the current impact of the policies of the oil exporting nations on life in the United States.

INTRODUCTION

Helium is considered essential to several national programs now under way or being contemplated. These programs have potential positive consequences for the future well being of our society, and include providing options in energy conversion, transmission, and utilization, enhancing mass transportation, revolutionizing ship design, providing space ship propulsion options, enhancing the mass to weight ratio of large aircraft, developing new techniques for water purification and ore separation, improving instrumentation, and advancing basic science.

Organizations deeply involved include the National Science Foundation, DOD, DOI, DOT, AEC, OST*, The electrical power, gas, petroleum, and coal industries, and the Federal Power Commission, Programs already planned or underway involve commitments in excess of $200 million for superconductivity alone in the next 15 years, and on the order of several hundred billion dollars in the years ahead, when large scale usage becomes commonplace.

At the moment these uses for new technologies comprise less than 10% of the helium demand, and it is anticipated that this will continue to be so to the end of this century.

HELIUM DEMAND

1. Established Technologies.

Helium demand since 1960 increased from 420 million cubic feet through a peak of 922 million cubic feet in 1969, due to the vigorous space program (unforeseen when the 1960 Helium Act was passed), to 601 million cubic feet in 1972.

**Department of Defense, Department of Interior, Department of Transportation, Atomic Energy Commission, Office of Science and Technology.*

The principal current uses listed for 1970 by the Bureau of Mines, with the volume used in each case in millions of cubic feet, are:

(a) Aerospace (purging and pressurization), 237;
(b) Inert protective atmospheres, 68;
(c) Research, 65;
(d) Welding, 63;
(e) Lifting gas, 45;
(f) Leak detection, 42;
(g) Low-temperature science and engineering (cryogenics), 33;
(h) Chromatography (for rapid, accurate gas analysis in many major industries), 14;
(i) Heat transfer, 9;
(j) Synthetic breathing mixtures, 4;
(k) Medical and other, 7; and
(l) Exports, 60.

The Bureau of Mines estimates the total demand for these uses, less exports, to be between 1.4 and 3.6 billion cubic feet in 2000 A.D. This is based on applying an annual 1.6% population increase and 4.5% new construction, as a matter of judgement, to the 1968 demand base.

Stanford Research Institute uses a different (they claim more accurate) forecasting technique. Assuming an ample supply at present prices,they predict that annual demand will exceed 3 billion cubic feet by 2000, 12 billion cubic feet by 2025, and 44 billion cubic feet by 2050 — an annual growth rate of about 5.5%. This includes estimates for use in some new technologies. They predict a lower demand, approximately 1/2 to 1/3 of the above, based on assumptions of price escalation. These must not be confused with high- and low-range demands as used by the Interior. The price is assumed to be $75/Mcf in 1975 and 1985, $150 in 2000, $300 in 2025, and $600 in 2050, in actual, not constant, dollars. Under these conditions, a predicted demand of 2.4 billion cubic feet is expected in 2000, 6.2 billion in 2025, and 16.5 billion in 2050.

2. New Technologies.

Helium demand for some, but not all, new technologies is projected by Stanford Research Institute. It is not considered by the Bureau of Mines. These new technologies involving helium may help ameliorate future national energy, transportation, and resource problems. Many of these helium uses involve the use of liquid helium to provide the low-temperature environment (about 4 to 18°K) for superconductors. Superconductivity is the ability of many materials to transmit electrical energy, or conduct electricity, with no loss except for the refrigeration energy needed to keep them cold. Some superconductors conduct electricity at no loss even in high magnetic fields, and are used as windings in the new high-efficiency, high current density, superconducting magnets, and superconducting rotating machines.

Examples of new technologies using helium, or requiring helium-cooled superconductors, and under active development are:

Electrical Power. Fusion reactors, MHD peaking plants, large rotating machinery, gas-cooled fission and fission breeder reactors, liquid metal fast breeder reactors, and superconducting AC and DC urban and long distance underground power transmission lines.

Transportation. Superconducting generators in high-performance aircraft and space devices, precision instrumentation, high-speed magnetically levitated ground transportation, flexible high-performance naval and mercantile marine and submarine propulsion systems, hybrid airship/airplane, high-load capacity systems.

Industrial, Resource Utilization and Waste Treatment. Ore separation, water purification, rolling mill motors, low-voltage high-current superconducting electrolysis systems for aluminum plants, or a future national hydrogen economy system, rain making in arid coastal regions (not superconducting — involves making a tall helium supported chimney to condense moisture from air).

Computers. Compact, high-density, low-power dissipation, superconducting memories.

THE U.S. HELIUM PROGRAM

The U.S. Helium Storage Contracts were finally formally terminated in December, 1973, after more than four years debate and litigation.

Early History

As increasing helium demands threatened to outstrip the production capacity of the Bureau of Mines, concern arose regarding the future ability to meet mobilization needs and the casual wastage of the natural resource. In 1957, the Director, Office of Defense Mobilization, recommended to the Secretary of Interior that a working group be established to determine the feasibility of making the conservation aspect of the helium program the primary, rather than the incidental, objective of the Department of Interior.

A working group was subsequently established, comprised of representatives from the Departments of Commerce, Defense, and Interior, Atomic Energy Commission, Office of Defense Mobilization, Bureau of the Budget, and Federal Power Commission. Headed by then Undersecretary of Interior, O. Hatfield Chilson, the group compiled a study entitled "Cost of Implementation of a National Helium Conservation Policy." (The Chilson Report, January 24, 1958.) As a result of the study, a national helium conservation policy was subsequently recommended to President Eisenhower and formally approved on April 25, 1958.

Due to the magnitude of expense involved in accomplishing the conservation program, the Report recommended that:

(1) private industry be encouraged to participate in the program by entering long-term contracts with the Government which would give the companies a reasonable return on their capital investment and, at the same time, help to defray the overall costs of the program;

(2) the Secretary be authorized to set the price for the helium at a level which would enable the Department of Interior to cover all costs incurred in carrying out the provisions of the program;

(3) all federal agencies and contractors purchase all major requirements of helium from the Secretary; and

(4) the private companies participating in the program be prohibited from selling any helium to any purchaser other than the Secretary at a price lower than the lowest price paid by any government agency.

In 1958 the Department of Interior proposed legislation to Congress for the implementation of the recommended conservation program. This was not acted upon, however, and redrafted proposals were subsequently submitted to Congress on July 27, 1959. After lengthy hearings and incidental revisions and amendments of the proposed bill, a legislative amendment was adopted on September 13, 1960, to be known as "An Act to Amend the Helium Act of March 3, 1925, as amended, for the defense, security, and the general welfare of the United States."The Act became effective on March 1, 1961, and a limitation on the annual contracting authority of 47.5 million dollars was established by the Act of August 3, 1961 (75 Stat. 246, 253).

The 1960 Helium Act Amendments authorized the Secretary of the Interior to enter into long-term contracts for the acquisition, processing, transportation, or conservation of helium, not exceeding twenty-five years. In addition, he was given the power to acquire, by eminent domain, helium contained in helium-bearing natural gas, and so much of such gas as was necessarily removed in the extraction process; if he were unable to acquire helium otherwise upon reasonable terms and at the fair market value. In an attempt to make the program self-liquidating, the Act provided for a comprehensive system similar to that recommended by the Chilson Report. The Secretary was given authority to set his own price for the helium that he sold, and to establish and promulgate such rules and regulations, consistent with the directions of the Act, which were necessary to carry out its provisions.

The helium conservation program apparently ran smoothly until some time in 1968. After the passage of the 1960 Act, however, several private companies had begun their own helium extraction outside of the government program. Because the Secretary's price for helium reflected not only direct extraction costs, but also a portion of the costs involved in the administration of the conservation program, the Secretary's price for helium exceeded the private producers' price. As the private companies' sales increased, the Secretary's sales decreased, despite increased overall demand. In response to this situation, the Secretary proposed regulations which would have forbidden government agencies and their contractors from purchasing their major requirements of helium from any source other than the Secretary, or private companies "eligible" under the regulations. These regulations were considered illegal in a subsequent court action. The Court noted, however, that the Secretary's purpose could be accomplished by obtaining an Executive Order requiring that such provisions be included in all contracts entered into by government agencies. An Executive Order was requested of the President by the Interior, but was never obtained.

The Secretary's termination statement, which is based on the Department's final environmental statement, and the comments received from the private contractors, recognized that:

(1) the direct result of the decision to terminate the contracts will be that the Government will forego the storage of an estimated 20 billion cubic feet of helium which will be "wasted" or "depleted" if the contractors do not continue to extract and store the helium, prior to delivery of the natural gas to fuel markets;

(2) natural gas — primarily fuel gas — is the only known source of helium other than the atmosphere, an environmentally and economically inferior source;

(3) the currently proved "helium-rich" natural gas reserves (containing at least 0.3% helium) will probably be exhausted before the turn of the century;

(4) it is unknown exactly how much, if any, "lean" helium-bearing natural gas will be available after the year 2000;

(5) present studies predict large demands for helium for environmentally beneficial uses beginning around the turn of the century which could rapidly deplete the helium supply then in storage; and

(6) assuming a lack of supply at a later time, future environmentally beneficial technological advancements might be precluded due to unacceptably adverse environmental effects of recovery from other sources.

In contrast to the above possibilities, the Secretary's statement notes that:

(1) government demand for helium has decreased consistently since 1966, and is presently below the 1961 level;

(2) present technological advancement enables recovery of helium from "lean" sources of helium-bearing natural gas expected to be available in large quantities in the future;

(3) the Bureau of Mines estimated a total of 17 to 24 billion cubic feet of probable shut-in "helium-rich" reserves (i.e., found in natural gas fields not being exploited for present fuel purposes);

(4) including the helium currently in storage, in shut-in government reserves, which are expected to be recoverable from government-owned plants, have total reserves of approximately 44.5 billion cubic feet;

(5) storage of recoverable helium at today's costs does not necessarily assure "low-cost" helium in the future;

(6) the forecasted large demands for the future are "speculative" and of questionable reliability;

(7) government agencies' estimates for future helium demands would not require removal of helium presently in storage "to meet essential government needs" until well into the next century; and

(8) assuming the estimated total future demands were to materialize at the beginning of the next century, as predicted, the storage now of an additional 20 billion cubic feet of helium would merely delay, rather than foreclose, the necessity of obtaining helium from presently unknown or environmentally disadvantageous sources.

On the basis of the above assumptions, the Secretary determined that there had been a substantial diminution in helium requirements for essential government activities, and that the termination was therefore authorized under Section 12.1 of the contracts, since the purposes of the Helium Act Amendments of 1960 had been satisfied.

HELIUM SUPPLY

Future helium supply and discovery must be largely a matter of conjecture. The helium abundance in the earth's crust is not known while the atmosphere constitutes a virtually infinite supply at the low-concentration of about six parts per million. The energy investment required to obtain pure helium from the atmosphere is large, being about 26 gigawatt years per billion standard cubic feet (scf) of gaseous helium. Extraction of helium from gas streams that are not commercially attractive as heating gases is probably not economic. Helium availability from gases which have a satisfactory thermal content must be expressed in terms of cost of extraction. The conclusions of David Evans, Potential Gas Committee, in this regard are as follows:

(1) The proved and probable helium reserves of the United States are estimated to be 161 billion cubic feet at a price of $35.00 per Mcf. With the exception of 52 billion cubic feet of helium in underground storage or in shut-in fields (probable supply), this helium will have been wasted with produced natural gas in the next 30 years.

(2) It is estimated that 194 billion cubic feet of helium is present in gas in the Rocky Mountains area that could be recovered for from $50 to $80 per Mcf. This includes 3 billion cubic feet of helium in the non-flammable gas of the Tip Top field, Wyoming, as well as helium contained in natural gas averaging .205 percent helium in the rest of the Potential Gas Committee Areas H and I. (See map in Figure 1.)

(3) The estimate for the Tip Top field is based upon one well. The Tip Top structure is large, and future drilling could prove up ten times more helium than is reported here on the basis of one well.

(4) Helium can be recovered from natural gas containing 0.1 percent helium for about $143/Mcf. There is an estimated 113 billion cubic feet of helium in gas of this concentration in the eastern part of the U.S. (Areas A, B, and C).

(5) Another 375 billion cubic feet of helium is contained in the natural gas of the Midcontinent Region (Areas D, J-North, and J-South). The helium concentration of this gas averages .091 to .094 percent. Since this concentration is only slightly less than .1 percent, which costs $143/Mcf to recover, the price is roughly estimated at $150/Mcf.

(6) The costs involved in gathering and recovering helium from gas containing less than approximately 0.1 percent helium are considered prohibitive. It would be cheaper to recover helium from the atmosphere for between $500 and $1,700/Mcf, depending upon whether the helium was the byproduct of separating oxygen and neon from air, or whether helium alone was recovered.

H. R. Howland of Westinghouse has noted that the cost of helium is much less sensitive to plant operating costs than capital costs. There are economies of scale, and the use of complex petrochemical plants with helium-nitrogen mixtures as a final byproduct, also reduces helium price. Using a 280 million cubic feet per day plant as a basis, Howland interprets the varied data as leading to a price of $95 to $130 per Mcf per 0.1% helium content gas, and judges $110/Mcf as a fairly reasonable figure. A. Francis of Linde states that for helium concentrations between 0.01% and 0.1%, the unit cost of helium extraction will be approximately inverse to the helium concentration. That is, about $180 per Mcf for 0.08% He; $250 for 0.06%; $500 for 0.03%; $1,000 for 0.015%; and over $2,000 for 0.007%. Howland has extrapolated this to 0.5%, which may be questionable, and quotes slightly different figures. These are: $21 per Mcf for 0.528% He; $46 for 0.240%; $110 for 0.1%; $733 for 0.015%; and $1,690 for 0.0065%. He notes that the free market price of helium, bulk Grade A, (f.o.b.), has been about $20/Mcf for the past two years.

NSF HELIUM STUDY

To assist in ordering the confusion and resolving the controversy, a brief, intense study was proposed with the objectives of:

(1) examining the outlook for helium supply and demand;
(2) determining ways of preventing compromise of critical U.S. technology by limited helium availability; and
(3) specifying goals and estimated helium requirements for likely helium-based developments — especially superconducting electrotechnology.

This study is in progress, and definite conclusions have not yet been reached.

HELIUM STUDY DEMAND ESTIMATES — NEW TECHNOLOGIES

At the July Advisory Committee meeting of the Helium Study, the estimates for various technologies were:

Fusion Power (C. E. Taylor, Livermore). He assumes 1,400 gigawatts of fusion power by 2020, giving an inventory of 35 to 100 billion cubic feet (complete recovery) based on 1,300 scf/megawatt electric. It might be possible to cut this by a factor of 10 with further design work. We chose 50 billion cubic feet as a modest estimate to 2050, which is more pessimistic than the Taylor figure.
Fission Reactor Cooling. There is little loss, assuming reasonable capture and recycle precautions, but by 2000 the inventory will be about 1 billion cubic feet. We did not extend this figure for the years to 2050, but clearly some will be needed.
Ore Separation (R. Powell, NBS). There are few ore separation plants in this country, and a slight rise in the price of helium could make the use of superconducting magnets for this purpose uneconomical. P. Marsden claims that superconducting magnets are not necessary for this purpose.
Water Purification (R. Powell, NBS). This use may not materialize as a large scale application of superconducting magnets.
Magnetically Levitated Trains (J. Harding, DOT). Assuming 300 miles of track in the Northeast corridor, the inventory would be approximately 52.5×10^6 scf over a period of 10 years. This assumes that high-speed ground transportation with magnetic levitation is of little interest to the United States.
Defense Department. Accepting DOD estimates for 2000 A.D. through 2019 A.D. as 1.6 Mcf, this implies 4 Mcf to 2050, assuming no increase in demand rate from 2019.

SUMMARY OF U.S. DOMESTIC HELIUM REQUIREMENTS (2000-2050)

Annual helium demand for conventional uses = 1.4×10^9 scf/year (BuMines' low forecast). Assume it holds flat for 2000-2050.

Category	Cumulative Demand x 10^9 scf
Conventional uses	70
Fusion	50
Transmission	11
Defense	4
Other	1
	136

This total ignores: rotating machines, marine uses, airborne, fission reactor cooling, ore separation, water purification, levitating trains, and exports in the interests of a conservative estimate for newly emerging technologies.

Assuming the U.S. with its advanced industrial society of 200 million to be a typical bloc, we can discern Europe, U.S.S.R. and Japan, Australia and New Zealand to be blocs which will develop similar requirements for helium. Thus, a conservative world helium requirement from 2000 to 2050 might be about 500 billion cubic feet.

It should be noted that the helium inventory for superconducting power transmission and fusion reactor magnets is helium stored and conserved, since every effort will be made to make the leakage rates as low as possible.

Prevailing Economic Philosophy Versus the Conservationist Approach

The economist wonders who will pay now, the conservationist and the scientist knows it must be someone else.

Professor Preston, in his 1969 testimony on the Federal Helium Program before the Joint Economic Committee of the Subcommittee on Economy in Government, emphasizes that the choice of an appropriate interest rate is absolutely critical to the decision problem at hand. In this connection, he references the contribution of Professor Baumol[1] to the compendium of papers already published by the committee. In fact, he is right. The 10% rate being applied to new programs by OMB makes the financial picture for a self-supporting helium program hopeless. By contrast, the Government never paid 6¼% interest until 1969, while the current rate for Treasury Bills and Notes is about 7%, reflecting a real rate of 3% plus an inflationary factor

Baumol asserts that "the correct discount rate for the evaluation of a government project is the percentage rate of return that the resources utilized would otherwise provide in the private sector." He continues, "It is difficult to quarrel with the conservationists view that the destruction of irreplacable natural resources imposes a heavy cost on our posterity. . . . this is precisely the legitimate ground on which conservationists urge increased care in avoiding depletion of our resources. But, it is not legitimate to jump from the valid point that one generation has no right to use up wastefully the resources that cannot be replaced by its successors, to the questionable conclusion that each generation is constrained to engage in overall efforts to support its posterity beyond the level that is indicated by the free market . For that is precisely what is involved in a program of low discount rates . . . . We are therefore wealthier than our predecessors and it can quite safely be predicted that our successors will be richer than we. In effect, then, the subsidization of a program of added investment amounts to a transfer of additional resources from the poor to the rich. It would take inputs whose produce would be available for consumption today and make them available tomorrow when the supply of consumer goods is likely to be so much more abundant than at present."

This then is the attitude which presumably led the White House and the OMB to cancel the Helium Storage Contracts. It is based on the views of short-term economics and prevailing economic opinion. Recent events with regard to the energy crisis may lead to a reappraisal of this type of economic thought, since we can now see more clearly that future resources may not be more abundant than at present.

An alternate view is that expressed by Senator Jackson prior to the passage of NEPA. "The needs and aspirations of future generations make it our duty to build a sound and operable foundation of national objectives for the management of our resources for our children and their children. The future of succeeding generations in this country is in our hands. It will be shaped by the choices we make. We will not and they cannot escape the consequences of our choices." (115 Cong. Rec. S17451, December, 1969.)

Again NEPA requires that federal agencies "Use all practical means, consistent with other essential considerations of national policy, to improve and coordinate federal plans, functions, programs, and resources to the end that the nation may . . .

(1) "fulfill the responsibilities of each generation as trustee of the environment for succeeding generations;

(2) achieve a reasonable balance between population and resource use which will permit high standards of living and a wide sharing of life's amenities; and

(3) enhance the quality of renewable resources and approach the maximum attainable recycling of depletable resources."

Thus, we see that the helium conservation problem resolves into a conflict between conventionally acceptable economic thinking and the desires of conservationists.

Finally, we must note the implied assumption in the economic thinking. "We are richer than our fathers, and will be poorer than our sons. The supply of consumer goods will be much more abundant tomorrow than today." This view while not widely shared by those who take a broader view of the problem, and even by many who do not, assumes that the best way to assure national survival, and a good future, is to do our best in present activities and planning to ensure that such a desirable state of affairs will come to pass. In the case of helium, we are dealing with an irreplaceable resource, or at least a resource which will cost one hundred times or more to retrieve from the atmosphere. It would require the present electrical generating capacity of the United States to produce 13 billion cubic feet per year of helium from air. It is a resource which is presently produced as an incidental to the country's need for natural gas, and which is required as a necessary component of several new technologies essential for the country's air, sea, and land defense, its energy needs, and, as an option, for its high-speed and transportation needs. About 96% of the helium resources in fuel gases containing 0.3% helium or more will be dissipated by 1985.

SHORT-RANGE POSSIBILITIES FOR THE HELIUM STORAGE PROGRAM

The economic subcommittee of the helium study asked Westinghouse to examine the effect of short-term tax measures. Their conclusions were that:

(1) the Conservation Program can be made financially self-amortizing as far as the U.S. government is concerned, from present to to the end of the present phase (1983);

(2) continuation of the program on the above basis will ensure an adequate supply of helium for presently developed uses well into the 21st century; and

(3) continuation of the program will enable the U.S. to buy time and to keep open certain important technological options relative to the energy crisis. These options will be foreclosed by cancellation.

[1]*On the Discount Rate for Public Projects by William J. Baumol, Professor of Economics at Princeton University.*

TENTATIVE FINDINGS FROM WESTINGHOUSE STUDY

(1) In the short run (0-10 years), if the conservation program is cancelled, there will be a massive wash-out of gas producers as an annual capacity of five times current usage hits the open market. Some distributors with long-term purchase contracts will be affected.

(2) If the contracts are cancelled, helium will be cheap — perhaps 2/3 current prices — until 1995-2000, when the rich streams are exhausted.

(3) At $100-120/Mcf, helium will be available in reasonable quantities until 2020 or so, even in the absence of stockpile sales. (All prices in 1973 constant dollars.)

(4) Shrinking supplies of depleting gas streams will begin to pinch helium availability in 2030+, forcing reliance on shut-in reserves of non-fuel helium bearing gas, or recovery of helium as a byproduct of oxygen separation from air at a price of $200-500/Mcf. Crudely projected growth of the oxygen separation industry shows that from 0.5 to 4 times current (1973) usage will be available in 2030+.

(5) The length of time the stockpile in the Cliffside field lasts depends crucially on the pricing policy of the Helium Activity. A "cost-pricing" policy will discourage construction of extraction plants, and lead to early depletion of the stockpile. An "alternate-source" pricing policy will stretch the length of time it lasts.

(6) An important unknown factor in projections of helium demand is whether or not superconductors can be devised which exhibit this superconducting property in liquid hydrogen, or at higher temperatures.

EXTRACTS FROM THE HELIUM ACT

Title - "An Act to Amend the Helium Act of March 3, 1925, as Amended for the Defense, Security, and the General Welfare of the United States."

From Section 4: "The Secretary is authorized to . . . conduct or contract with private parties, for experimentation and research, to discover helium supplies and to improve processes and methods of helium utilization."

From Section 7: "The Secretary of Defense and the Chairman of the Atomic Energy Commission may each designate representatives to cooperate with the Secretary in carrying out the purposes of this Act, and shall have complete right of access to plants, data, and accounts."

From Section 15: Section 15 of the Act is captioned specifically "Individual Enterprise in Developing Helium." No statement that this is the object of the Act appears anywhere in that section.

The section states "it is the sense of the Congress that it is in the national interest to foster and encourage individual enterprise in the development and distribution of supplies of helium, and at the same time provide, within economic limits, through the administration of this Act, a sustained supply of helium which, together with supplies available otherwise, will be sufficient to provide for essential government activities."

The Interior has maintained that the purpose of the Act is to provide helium for essential government activities, and relies on a portion of Section 15 for that. The Denver Appellate Court accepted this view. Key witnesses at the March 1973 Court of Claims hearing, Northern Helex v U.S., insisted that the Act was for the General Welfare of the United States. These witnesses were the principal originators and administrators of the Act.

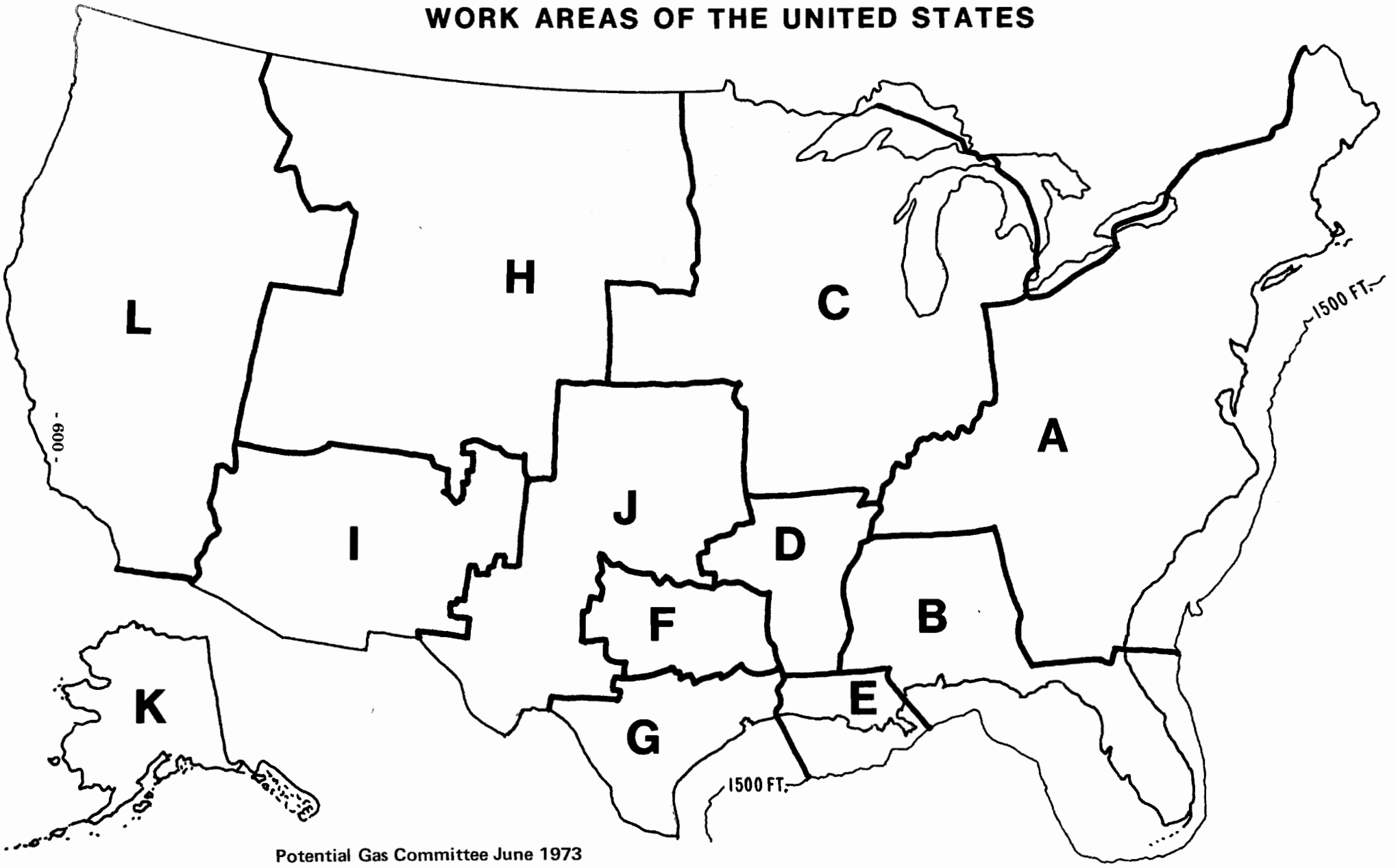
WORK AREAS OF THE UNITED STATES
L
H
C
A
I
J
D
F
B
E
G
K
-600-
1500 FT.
1500 FT.
Potential Gas Committee June 1973

Figure 1.

Figure 2. 1973 NSF Helium Study Advisory Committee.

Dr. John Andelin
Science Adviser
Office of Congressman McCormack
1205 Longworth House Office Building
Washington, D. C. 20510

Dr. Brian C. Belanger
Div. of Applied Technology
US AEC
Washingon, D. C. 20545

Mr. Bascom Birmingham, Director
NBS Boulder Laboratories
Boulder, Colorado 80302

Dr. F. H. Buttner
Battelle Columbus Laboratories
505 King Avenue
Columbus, Ohio 43201

Dr. Paul Craig
National Science Foundation - RANN
1800 G. Street
Washington, D. C. 20550

Mr. David Evans, Director
Mineral Resources Institute
Colorado School of Mines Foundation Inc.
Golden, Colorado 80401

Dr. Edward Hammel
Los Alamos Scientific Laboratory
P. O. Box 1663
Los Alamos, New Mexico 87544

Mr. M. Hathaway
Office of Senator James McClure
Room 437, Old Senate Office Building
Washington, D. C. 20510

Dr. John K. Hulm
Westinghouse Research Laboratory
Pittsburgh, Pa. 15235

Mr. Charles Laverick - Chairman
Argonne National Laboratory
9700 S. Cass Avenue
Argonne, Illinois 60439

Mr. Frank C. Nicholson
Northern Natural Gas Company
Suite 503
1133 - 15th Street, NW
Washington, D. C. 20005

Dr. James Nicol
Arthur D. Little, Inc.
25 Acorn Park
Cambridge, Mass. 02140

Dr. Charlotte Price
Department of Economics
Sarah Lawrence College
Bronxville, New York

Mr. C. E. Taylor
Lawrence Livermore Laboratory
Box 808, L-384
Livermore, California 94550

IX. Protection Against Radioactive Noble Gases

RADIATION PROTECTION IN URANIUM MINES — A REVIEW

D. A. Holaday
Environmental Sciences Laboratory
Mount Sinai School of Medicine
City University of New York
New York, New York

Abstract

The consequences of the exposures to external and internal radiation which can occur in the mining of uranium ores are well-documented. Methods for evaluating and controlling these hazards have been developed by health protection agencies and the uranium mining companies. These procedures have been described in numerous reports from a number of the uranium-producing countries. The only feasible procedure for reducing exposure to external radiation is limitation of working time. Controls of radon and radon-daughters are directed at reducing influx of radon and dilution ventilation to supply uncontaminated air to working areas. Many different methods are employed depending on the particular circumstances. There is no "typical" uranium mine so the health protection group must adjust procedures to fit the conditions in each situation. Control of long-lived radioactive dust is usually accomplished by the dust-suppression methods used to control silica dust. In some circumstances, where high-grade ore is being mined, additional controls may be required to reduce concentrations of long-lived alpha emitting elements to acceptable levels.

INTRODUCTION

Radiation protection in uranium mines is of great theoretical and practical interest, and has been studied extensively for many years by mine radiation safety personnel and research investigators. The basis for this interest is that uranium miners comprise the only group in the nuclear energy industry in which radiation exposures have resulted in significant health effects, and for which exposure control procedures are difficult to implement and maintain.

Uranium miners are exposed to external and internal radiation from radon and its short-lived daughters, as well as to long-lived radioactive elements of the uranium family. Since exposures to radon and its daughters are considered to present the most serious health hazards, a brief review of this area is presented in this paper. However, other radiation sources should not be ignored because in some exposure situations they may also require consideration and control.

DISCUSSION

Of the numerous studies of procedures for controlling radon reported in the world literature, it is only possible to mention a few of them in this paper. A Russian monograph (Bykovsky, 1963) contains a rather complete discussion on the subject. Additionally, a two-volume manual issued by the U. S. Bureau of Mines (Rock and Walker, 1970) is the most comprehensive treatise written in English. The ICRP will be issuing a manual on uranium mines which hopefully will describe the current state of scientific knowledge. The aforesaid documents, and the references given therein, will repay careful study by radiation safety and mine ventilation officers.

The two basic principles which must be observed in designing radon control programs is (1) to limit the influx of radon into working areas as much as possible, and (2) to remove it from working areas as expeditiously as possible. In many respects the problem is similar to that encountered in gassy coal mines where the ventilation practices and criteria used are more applicable to uranium mines than to those which are standard for metal mines.

The proper planning of mine design and operational methods is an important first step in radon control. The methods to be used in ore extraction, and the ventilation system employed, should be designed together. Many of our existing mines have severe control problems because they were opened before the importance of controlling radon was appreciated. They were planned to remove ore as rapidly and economically as possible with existing metal mine ventilation criteria. These mines are now mature operations; it would be a time-consuming and costly process to make improvements in their ventilation. The final design of a mine is usually a compromise between the wishes of the production superintendent and the ventilation engineers.

Ideally, the mining system should be designed to keep all working areas uncontaminated. This would involve development to the furthest extent of the ore bodies with air courses and haulageways driven in barren rock. The ore is extracted by retreating toward air inlets with the used air rejected to return air courses. Unfortunately, this is only an ideal condition. Ore bodies change in grade, occur in unexpected locations, and radon emission rates vary widely depending on the porosity and the degree of fracturing in the host rocks. Thus, a continued assessment of conditions, and continued efforts to correct conditions, are required. An ideal mining design also keeps open working areas at a minimum, limits the amount of broken ore stored underground at the lowest feasible level, and minimizes spillage of ore during transport. All of these precautions reduce the emission of radon into working areas.

Sealants to reduce emission of radon have been investigated; several materials have been found which are essentially impervious to this gas. Expanded polyurethane foams are now used to assist in sealing off worked out areas, particularly those which have been back-filled with mill tailings (which still contain most of the original radium). The sealing of large areas such as air courses has been tried experimentally in metal mines. The main problem is in the preparation of rock surfaces to obtain good coating adherence. This is merely an operational detail, but one that can be very troublesome. Another problem, for example, is that all persons in the area where urethane foams are being sprayed must wear the correct respirators. Plastic films which are impervious to radon have been studied by the U. S. Bureau of Mines and Colorado State University. Some of these materials show promise and may be useful for such applications as temporary stoppings and for covering piles of broken ore which are awaiting transport.

As stated earlier, ventilation air should be moved through active areas and to return air courses as expeditiously as possible. The shorter the residence time of the air, the less the ingrowth of radon-daughters. Every effort must be made to course the air directly to active stopes, and to prevent the recirculation of the contaminated air. This requires that inactive and abandoned stopes should be closed off by temporary or permanent stoppings. Such areas can be potent sources of contamination, and also waste ventilation air. Experience has shown, that wherever possible, such closed areas should be kept under negative pressure. As ground movement and changes in air pressure loosen stoppings, a routine inspection and repair program is required to maintain the integrity of the seals.

In addition to programs for reducing radon emission, supplying clean air, and removing contaminated air, considerable work has been done on methods of decontaminating mine air to extend its useful life. The approaches which have been tested in mines are the removal of radon-daughters either by filtration or by electrostatic precipitation. Either method is effective, but there are limitations on their utility. The basic limitation, of course, is the atmospheric concentration of radon. This must be low enough for the treated air to be used for at least a few minutes before the ingrowth of daughters makes it unacceptable.

It has been found that with cleaned air in which a large fraction of the daughters exist as unattached atoms, plate-out on walls is large enough to make the air usable significantly longer than theory predicts. The most troublesome problems have been due to equipment failures. Filters clog with dust and soot, and are seriously affected by water mist and vapors. Present electrostatic precipitators do not seem to have been designed to withstand mine conditions. Obviously, the use of air cleaning procedures will be limited to special situations, but considering the problems involved in extending ventilation systems, the idea is attractive.

An even more fundamental approach would be the removal of radon from the air. Several papers in this symposium have discussed adsorption of noble gases, and more on this topic is presented in this session. In my opinion, radon removal methods merit further investigation.

Environmental conditions in uranium mines can now be evaluated more accurately and in greater depth than was possible even three years ago. Among others significant work has been done at the Nuclear Research Center in France (Lopez, *et al.*, 1970), at the A.E.C. Health and Safety Laboratory (Breslin, *et al.*, 1969) in the U. S. A. to develop instrumentation and procedures for measuring radon emission rates, atmospheric radon concentrations, radon-daughter ratios, fractions of unattached atoms and number concentrations, and size distribution characteristics of mine aerosols. While most of these methods are too elaborate for routine use, they can be employed by control personnel. Information obtained by their use would certainly assist in evaluating the degree of radiation hazards in mines.

Methods for measuring individual exposures to radon-daughters have been studied, and two papers in this symposium report work on dosimeters. In my opinion, such devices would also be useful as area monitors, and might reduce the amount of air sampling which is now necessary. If reliable personal dosimeters can be developed, the task of estimating and controlling individual exposures can be simplified. At present, these records are generated from air concentration measurements and time-occupancy data. Not only is this an uncertain process, which involves handling a large amount of data, but the possibility of overlooking brief, high-level exposures is always present.

Inevitably there will be situations where personal protective equipment is required to prevent the over-exposure of the miners. Typically such situations will occur in limited areas where men must enter to install auxiliary ventilation or to perform other work to correct conditions. For such relatively brief operations, respirators equipped with filters which will remove radon-daughters are available. The atmospheric concentration limits for which each type of respirator is suitable will be detailed in the forthcoming ICRP manual. Battery powered devices, which will blow filtered air to a hood, have recently been approved. In at least one of these, the final air cleaner is a HEPA filter. This equipment is more cumbersome than the usual respirators, but there is no resistance to breathing or restriction to vision, and the filtering efficiency is very high. Such devices would seem to be particularly suitable for use by mine geologists, mine surveyors, or other men who enter inactive mine areas. However, in such situations, the atmospheric concentrations of radon may become of real concern, and protection against the gas may also be required. Self-contained breathing apparatus or air-supplied respirators have been used. The effectiveness of gas masks equipped with charcoal-filled canisters for protection against radon has been studied by HASL, and the conditions under which they are satisfactory have been defined.

As we still have no firm definition of what a "safe" level of exposure to radon and radon-daughters would be, the objective is to reduce atmospheric concentrations to the lowest feasible levels.

REFERENCES

Breslin, A.J., A.C. George and M.S. Weinstein, (1969), *Investigation of the Radiological Characteristics of Uranium Mine Atmospheres,* USAEC, HASL-220.

Bykovsky, A.V., (1963), *Occupational Hygiene in Underground Uranium Mines,* Moscow, 1963 (in Russian).

Lopez, A., A. Chapius, J. Fontan, E. Billiard and G.J. Macklain, (1970), *Measurement of the State of Equilibrium Between Radon and its Daughters in the Uranium Mines,* Aerosol Science, I, 225.

Rock, R.L. and D.K. Walker, (1970), *Controlling Employee Exposure to Alpha Radiation in Underground Uranium Mines,* U.S. Dept. of Interior, Bureau of Mines, Two volumes.

RADON PROTECTION IN URANIUM MINES

J. Pradel
Nuclear Research Center
Atomic Energy Commission
Fontenay-Aux-Roses, France

Abstract

In uranium mines, radon is present with its daughter products which may be fixed on different particles, the form of which is described. It is well-known that uranium miners may contract some pulmonary diseases when radon-daughter concentrations are too high during long periods. The origin of lung cancer is confirmed by animal experiments.

To have a good protection, practical limits for radon and radon-daughter concentrations are established and individual monitoring is initiated. This monitoring must be well-fitted because the actual levels are almost up to maximum permissible levels.

Ventilation is the most important technique to control radon and radon-daughter concentrations. Some ventilation investigations in an experimental mine are described.

INTRODUCTION

Radon-222 is present naturally in uranium mines. This radioactive gas and its daughters, which are also radioactive, contaminate the air and very likely contribute to the excess in the number of lung cancer cases observed among populations of miners who have worked in poorly ventilated atmospheres. The importance of this problem, therefore, necessitates a thorough knowledge about the behavior of radon, constant surveillance of its concentrations, and the implementation of effective control measures.

BEHAVIOR OF RADON AND OF ITS DAUGHTER PRODUCTS IN MINE AIR

Radon-222, an element in the uranium-238 chain, is a noble gas with a half-life of 3.8 days, which is produced by the decay of the radium-226 dispersed in uranium rocks. Formed within the rock, radon gas fills all the available openings and may be released into uranium mines by various routes. Primarily, the retained gas is liberated when rock is fractured — especially at the time of blasting. The gas can also enter the working environment through underground water into which it has mixed.

After having passed into the mine's atmosphere, radon decays into short-lived radioactive products (all with half-lives of less than 30 minutes) in the form of ultrafine solid particles which attach themselves to other particles. This attachment brings about the formation of a radioactive aerosol with physical characteristics that determine its probability of retention in the respiratory system, and thus its toxicity.

1. Formation of a Radioactive Aerosol Present in a Mine.

Radon decays into polonium-218 (Ra A). At the time of its formation, it is a recoil atom which possesses an initial energy on the order of 100 keV. Although these atoms are produced by alpha-disintegration, around 80 per cent reach the thermal level in the form of positive ions. The remaining 20 percent are present as ultrafine neutral particles with perhaps a small percentage of negative ions, the presence of which has not yet been proved with certainty.

Many authors have been able to show that these "primary particles" have, at their origin, high diffusion coefficients on the order of 10^{-1} cm^2 s^{-1} for the neutral particles and 5.4×10^{-2} cm^2 s^{-1} for the small ions. But, in fact, various molecules are quickly attached to these particles. For the charged particles in the open air, it can be shown that these clusters become distributed into several groups of distinct and preferential mobility (K = 2.1 - 1.35 - 0.88 - 0.55 - 0.43 cm^2 s^{-1} V^{-1}). These results have not been confirmed for the electrically neutral particles because the current measurement techniques are not selective enough. This illustrates, therefore, that before attaching themselves to the nuclei or dust particles, the radon-daughters can exist as ultrafine particles during a time span which depends upon the concentration of the other particles present.

It should be noted that together these ultrafine and primary particles constitute what is customarily called free ions or uncombined particles. The value of the diffusion coefficient is, in general, taken to be 5.4×10^{-2} cm^2 s^{-1}; while it should be much lower, the actual value probably being between 5.4×10^{-2} cm^2 s^{-1}, as in outside air. In the absence of data for mine air, it seems more justified to adopt the value 1.5×10^{-2} cm^2 s^{-1}.

Because of their high diffusion coefficients, the ultrafine particles (with radii of less than 10^{-3} μm are going to attach themselves to the condensation nuclei and dust particles present in the air; the attachment being a function not only of the number, but also of the dimensions and electrical charge of the nuclei and of the dust particles. It can therefore be seen that the total concentration of non-radioactive particles and knowledge of the particle size distribution and the charged state of these particles are necessary to study the evolution of radon decay products and to determine the risks associated with them. Therefore, if one wants to study the evolution of these particles, one should be equally interested not only in the radioactive products, but also in the physical characteristics of all the aerosols present in the air of the mine. Because the concentration and

the characteristics of these particles in a given place depend upon their mode of formation (blasting, slushing, haulage), the place they are formed (stope, drift), and the path followed by the air in arriving at a given spot, one can see the hazards in determining the nature of exposure relevant.

2. Data Concerning Mine Aerosols.

The particle concentration inside a mine is essentially variable, but it is high in all cases. The following results can be given for French mines (obtained with condensation nuclei counters [CEA-SEERI] which enable the detection of particles greater than $10^{-3}\mu m$).

(a) outside the mine: 3,000 to 5,000 particles per cm^3.
(b) in the nonworking areas of the mine: 3,000 to 5,000 particles per cm^3.
(c) in the drifts: 40,000 to 70,000 particles per cm^3.
(d) in the working areas: 10^5 particles per cm^3.
(e) after blasting 2×10^6 particles per cm^3.

These measurements were carried out on the radioactive particles using Zeleny tubes. Diffusion batteries and filters make it possible to have a general idea of the characteristics of a radioactive aerosol in a mine. In the working areas where an important amount of radon, condensation nuclei, and dust are emitted, an extremely rapid evolution of the aerosol, by coagulation for the finest particles and sedimentation for the largest particles, is produced. In this high-particle-density atmosphere, the ultrafine radioactive aerosol activity represents, on the average, 3 per cent of the equilibrium activity of RaA, while still being almost always 10 per cent — except in the case of a work stoppage in the mine when values on the order of 25 per cent can be found. As one gets further away from the work area, the particle concentration decreases under the affects of sedimentation, turbulent diffusion, and impaction; the aerosol evolves continuously toward an equilibrium. In that way the count median diameter (on the order of 0.2 μm) tends toward a value of 0.07 μm, with the whole range of particle size being between 0.01 and 0.4 μm.

3. State of Equilibrium Between Radon and its Decay Products.

Radon decays with a 3.8-day half-life; its three principal short-lived decay products are RaA, RaB, and RaC, the mean lives of which are much shorter than radon and are found in the air in proportions varying with the age of radon; i.e., with the elapsed time since its diffusion into the atmosphere. The equilibrium fractions, f_A, f_B, f_C, are defined as the ratios of the activity of the respective decay products A, B, or C to that of radon.
Five hundred measurements in the French mines gave the following results:

	f_A	f_B	f_C
(a) upper value	1	0.73	0.43
(b) lower value	0.08	0.04	0.02
(c) mean value	0.50	0.30	0.15

It should be noted that most of the measurements were made in the drifts so that the mean value for the whole mine is lower than that given here.

STANDARDS AND MONITORING

The hazards of radon and its decay products have been proved mainly by:

(a) early studies on the mortality of miners in the Schneeberg and Joachimstal areas, which show that fifty percent of the miners had lung cancers;
(b) a recent U.S. study pointing to an excess of deaths from lung cancer in a population of about 3,000 miners; and
(c) the experimental induction of lung cancers in animals exposed to radon and its decay products (Perraud, *et al.*, 1972).

Various recommendations were issued since 1940, but there is currently some confusion on the choice of maximum permissible concentrations for radon and its daughters.
The ICRP in 1959 proposed $3 \times 10^{-6}/(1 + 1{,}000\ f)\ \mu Ci\ cm^{-3}$ as a limit for the radon concentration for a 40-hour weekly exposure; f being the ratio of Ra A; f also being assumed to be equal to ten per cent; the MPC obtained is $3 \times 10^{-8}\mu Ci\ cm^{-3}$. The IAEA limit has remained at $3 \times 10^{-7}\mu Ci\ cm^{-3}$. On the other hand, the U.S. Public Health Service introduced the concept of "working level" (WL), which is linked to the total alpha energy liberated by the products of radon when they decay. One WL corresponds to any combination of short-lived products in one liter of air that delivers 1.3×10^5 MeV of alpha energy, for instance $10^{-10}\mu Ci\ l^{-1}$ of Ra A in equilibrium with Ra B and Ra C. The WL and the corresponding integrated unit called Working Level Month (WLM) are more and

more widely used. From the viewpoint of monitoring, this unit has in practice several drawbacks, and it should only be adopted if it is derived from adequate biological knowledge. For example, if the hazard is associated with the presence of uncombined particles, the total alpha energy is not representative at all, whereas the radon concentration is. It is thus urgent for the ICRP to provide precise recommendations because, as a consequence, the monitoring could be substantially modified.

Radon monitoring is carried out very easily; the air sample is taken by filling a vial, the inside of which is covered with zinc sulfide; the measurement is made outside the mine without any restriction to the delay time. A great number of samples can be taken, and that is the only way in which a precise and constant surveillance of all the working areas can be done.

On the other hand, measurement of the total alpha energy necessitates the use of pumps, filters, and portable detectors in the difficult conditions of the mine. The measurements are subject to errors and must be performed *in situ*; the person in charge of the monitoring, subjected to various kinds of pressure, tends to interpret and modify the results obtained, which is not the case when radon is measured because it is performed outside of the mine by personnel not directly concerned with the consequences of the result.

The calculation of the activities inhaled by each miner is made from local measurements, taking into account the time spent in the various locations.

The procedure is to be replaced with a technique of personal monitoring which we have just started to use. This personal monitoring is performed with portable instruments (Figure 1) which use a filtering device enabling the separate measurement of the alpha particles of Ra A and Ra C with a LR 115 (Kodak-Pathe) cellulose nitrate detector (Chapuis, *et al.*, 1972). However, it is likely that, at least at the beginning, this personal monitoring will be used only for a few miners with the aim of "adjusting" the results obtained from the local radon measurements and the periods of time spent by each miner in each location.

MONITORING RESULTS

In 1972, 36,000 measurements were carried out in France; the average dose to the population of 621 miners corresponds to a radon concentration of $1.45 \times 10^{-7} \mu Ci\ cm^{-3}$ during 2,112 hours.

From the results of about 1,000 simultaneous measurements of radon and total alpha energy in 1972, it can be estimated that the average dose corresponds to about 3 WLM, but this is not true for the most exposed individual for which the dose is likely to be higher by a factor of two to three.

The following remark has to be made on that point: in the U.S. epidemiological survey, the dose received by the workers was, in general, assessed in a very inaccurate way, and, in fact, the dose estimated was the average dose, and not that to the most exposed worker for whom the exposure results from exceptional working conditions. If one wishes to derive a standard from this survey, the value obtained would be an average value, and it would be admissible to tolerate a value higher by a factor of 2 to 3 for the most exposed workers.

MEANS OF PROTECTION

Techniques widely used in uranium mines are ventilation, isolation of sources, and elimination of the polluted waters. As a result, the doses received by the miners are considerably lower than those corresponding to the former conditions that brought about an excess of lung cancers. In order to further improve the working conditions, we found it necessary to build an experimental mine which allows us to test various techniques under any required conditions.

The first results obtained deal with the influence of ventilation (Pradel, *et al.*, 1973). It has been observed (Figures 2 and 3) that:

(a) at a given flow rate, the radon concentration in mine air is lower when the pressure in the mine is positive than when it is negative; the reduction factor increases from 0.5 to 0.9 when the flow rate increases from 2 to 10 $m^3 s^{-1}$;

(b) at a given flow rate, the concentration expressed in working levels is also lower when the pressure in the mine is positive; the reduction factor is constant and equal to 0.7 when the flow rate is higher than 3 $m^3 s^{-1}$;

(c) the radon flux is reduced by about twenty-five per cent when the pressure in the mine is positive.

Another test showed that, at a constant flow rate (2 $m^3 s^{-1}$), the radon flux decreases from 9.2×10^{-7} Ci s^{-1} to 7.4, 7.3, and 5.7×10^{-7} Ci s^{-1} when the differential pressure increases from -45 millibars to -2, + 2, and + 56 millibars, respectively.

These values may not apply to all mines but they confirm that overpressurizing the uranium mines brings about, in many cases, a significant decrease in the radon levels.

CONCLUSIONS

Radon protection in the uranium mines is important because an excess in lung cancer rate can be observed among miners working under poor conditions. It is difficult, but urgent, to set up a precise standard. The following physical data can be of use in order to define this standard:

(a) the proportion of uncombined ultrafine particles should be taken to be equal to 3 per cent of equilibrium Ra A activity instead of 10 per cent; and

(b) the diffusion coefficient is likely to be close to 1.5×10^{-2} cm^2 s^{-1}, and is not equal to 5.4×10^{-2} cm^2 s^{-1}.

The standard should not use as a unit the total potential alpha energy, unless biological data justify it; these measurements are more difficult to carry out than those of radon concentration, the latter being a better representative of the concentration of the uncombined ultrafine particles.

If one hopes to lower the pollution levels, new control measures must be looked for. Overpressurizing the mines can already be considered effective.

As to monitoring, because the first tests were satisfactory, the use of personal detectors can be foreseen, at least for part of the miners.

REFERENCES

Billard, F., J. Bricard, G. Madelaine and J. Pradel, (1965), *Etude Experimentale de la Charge Electrique des Aerosols Ultrafins par Marquage Radioactif*, Journal de Physique 26, n° t.

Billard, F., G. Madelaine, A. Chapuis, J. Fontan and A. Lopez, (1971), *Contribution a l'etude de la Pollution de l'atmosphere des Mines d'uranium*, Radioprotection 6; 45-61.

Bricard, J., P. Girod and J. Pradel, (1965), *Etat de Charge des Aerosols Ultrafins en Milieu Faiblement Ionise*, Journal de Physique 26.

Bricard, J., F. Billard, D. Blanc, M. Cabane and J. Fontan, (1966), *Structure Detaillee du Spectre Granulometrique des Petits Ions Radioactifs*, Compte-Rendu a l'Academie des Sciences de Paris 263.

Chamberlain, A. C. and E. Dyson, (1956), *The Dose to the Trachea and Bronchi from the Decay Products of Radon and Thoron*, British Journal of Radiology 3171.

Chapuis, A., A. Lopez, J. Fontan, F. Billard and G. Madelaine, (1970), *Spectre Granulometrique des Aerosols Radioactifs dans une Mine d'uranium*, Aerosol Science 1: 243.

Chapuis, A., (1971), *These Docteur es Sciences, Toulouse.*

Chapuis, A., D. Dajlevic, P. Duport and G. Soudain, (1972), *Dosimetrie du Radon, Bucarest.*

Chapuis, A., A. Lopez, J. Fontan and G. Madelaine, (1973), *Determination de la Fraction d'activite Existant sous forme de Ra A non Attache dans l'atmosphere d'une Mine d'uranium.* Health Physics 25: 59-65.

Lopez, A., A. Chapuis, J. Fontan, F. Billard and G. Madelaine, *Measure de l'etat d'equilibre entre le Radon et ses Descendants dans les Mines d'uranium.*

Perraud, R., J. Chameau, J. Lafuma, R. Masse and J. Chretien, (1972), *Cancer Bronchopulmonaire Experimental du Rat par Inhalation de Radon.* Comparaison avec les aspects histologiques des cancers humains. Journal Francais de Medecine et de Chirurgie thoracique 26: 25-41.

Porstendorfer, J., (1968), *Geladene und Neutrale Radon Folgeprodukte in Luft.* Zeit. fur Physik 384-396.

Pradel, J., P. Zettwoog, G. Madelaine and Y. Francois, (1973), *Quelques Donnees Nouvelles Concernant la Protection des Mineurs dans les Mines d'uranium.* Third International Congress of the International Radiation Protection Association (IRPA), Washington, D.C.

Raabe, O. G., (1968), *The Absorption of Radon-Daughters to some Polydisperse Submicron Polystyrene Aerosols*, Health Physics 14: 397-416.

Renoux, A., (1965), *These Docteur es Sciences, Paris*, also Commissariat a l'Energie Atomique (CEA) report n° 2771.

Figure 1. Individual radon monitoring apparatus.

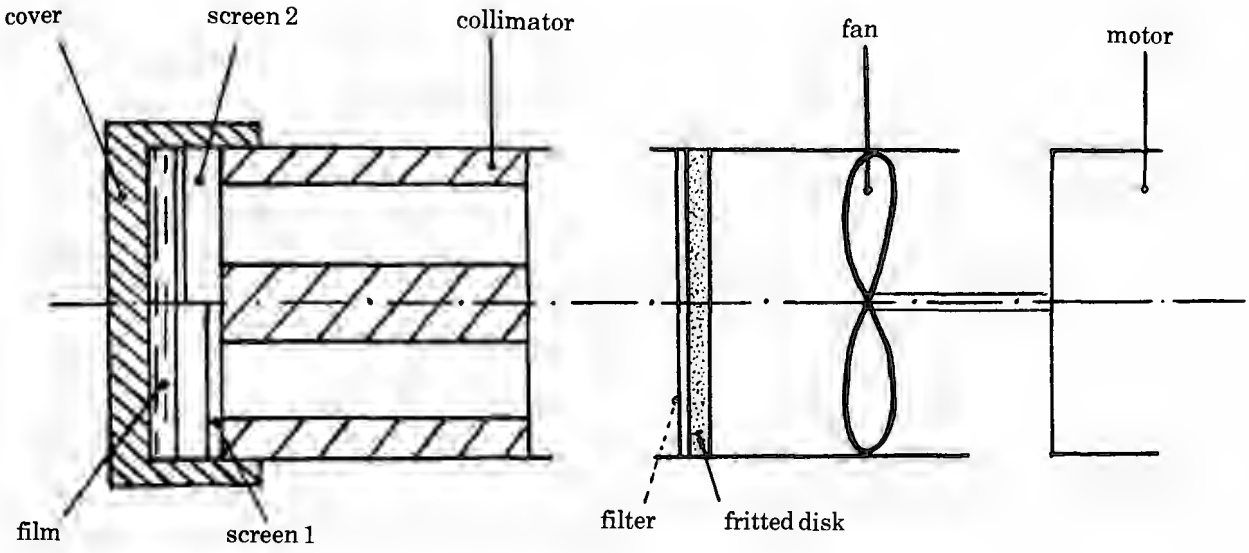

- Schéma de principe de la tête de prélèvement

(a) Design of the sampling head.

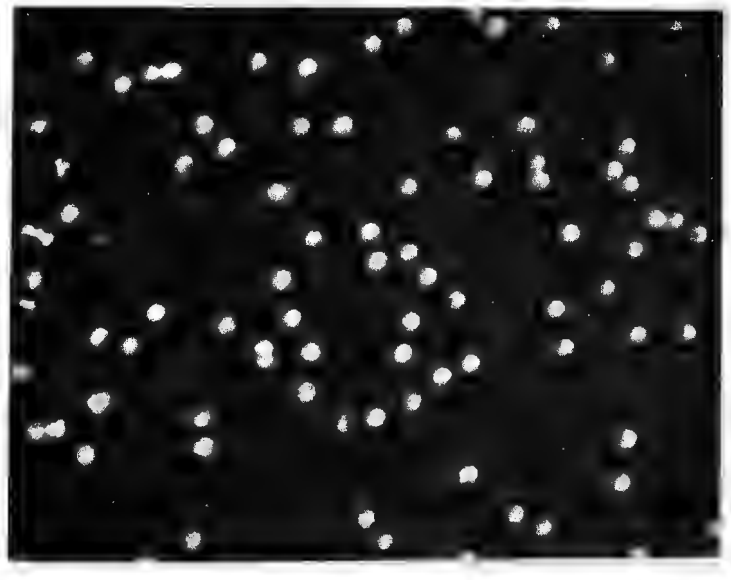

(b) Ra A alpha tracks in Kodak-Pathe LR115 cellulose nitrate detector.

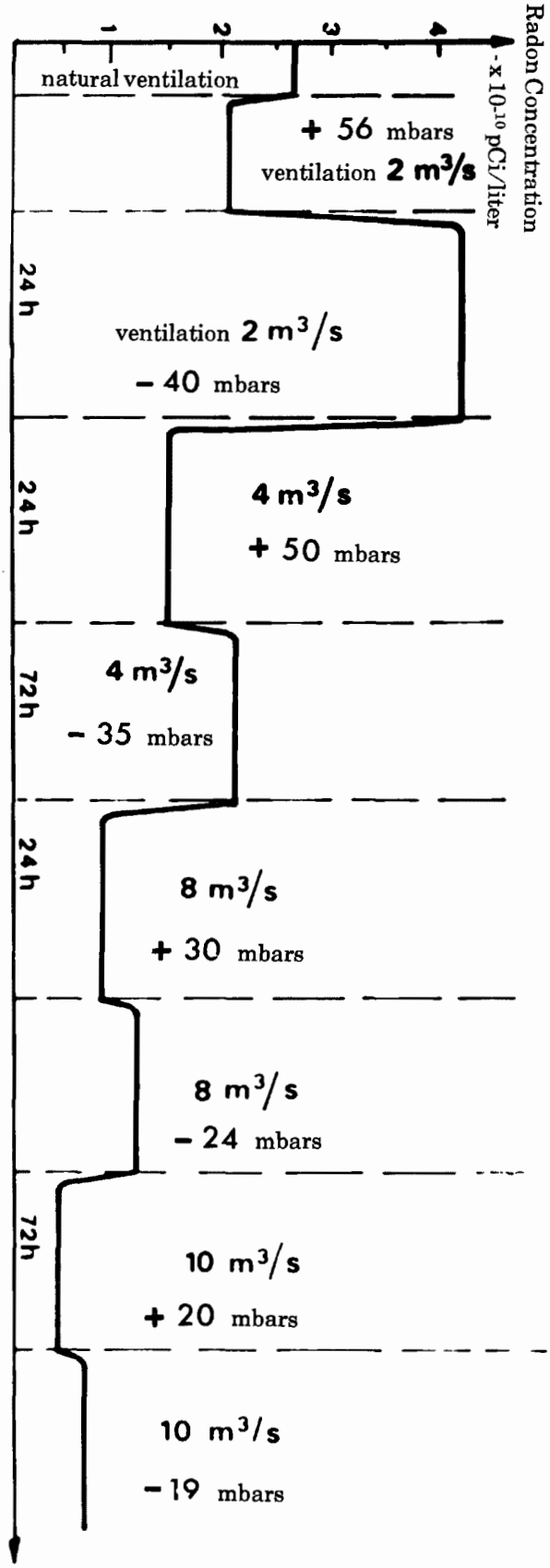

Figure 2. Influence of the mode of ventilation on the radon concentration.

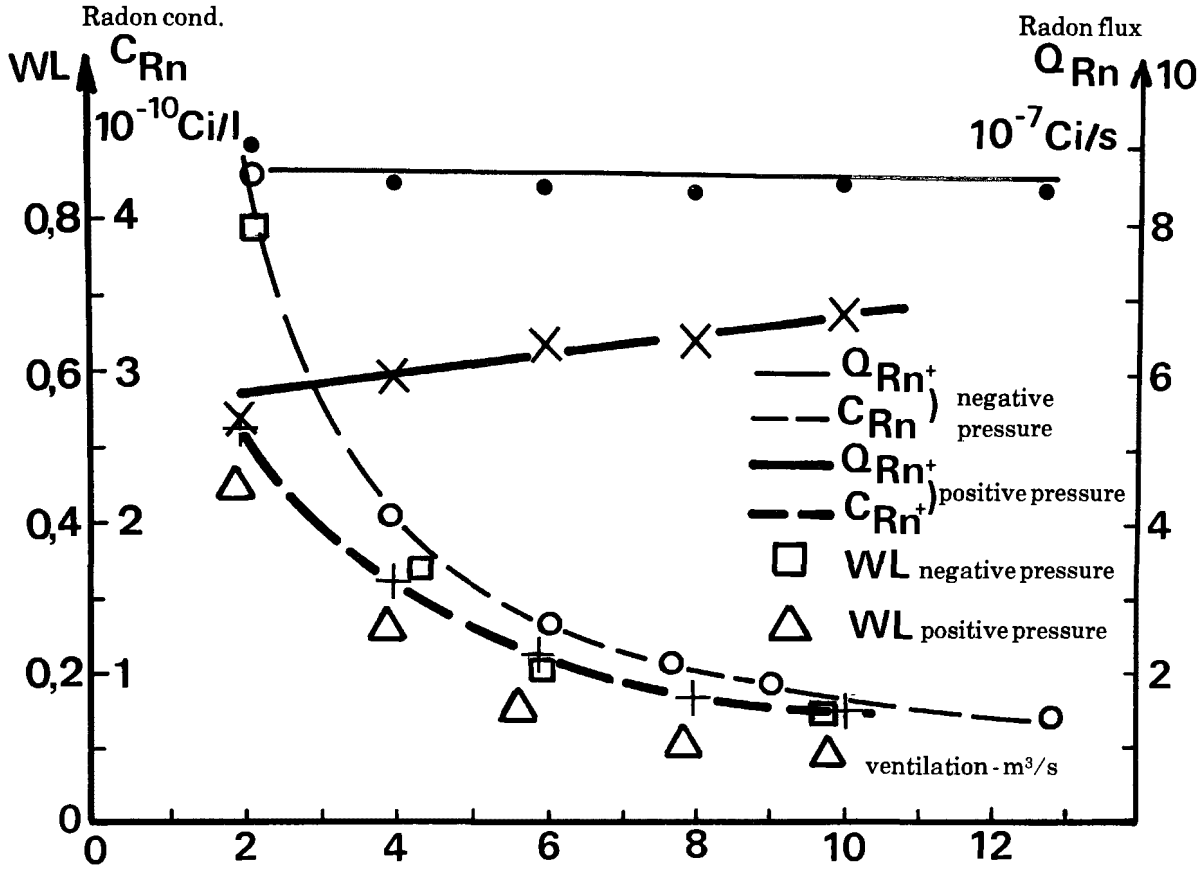

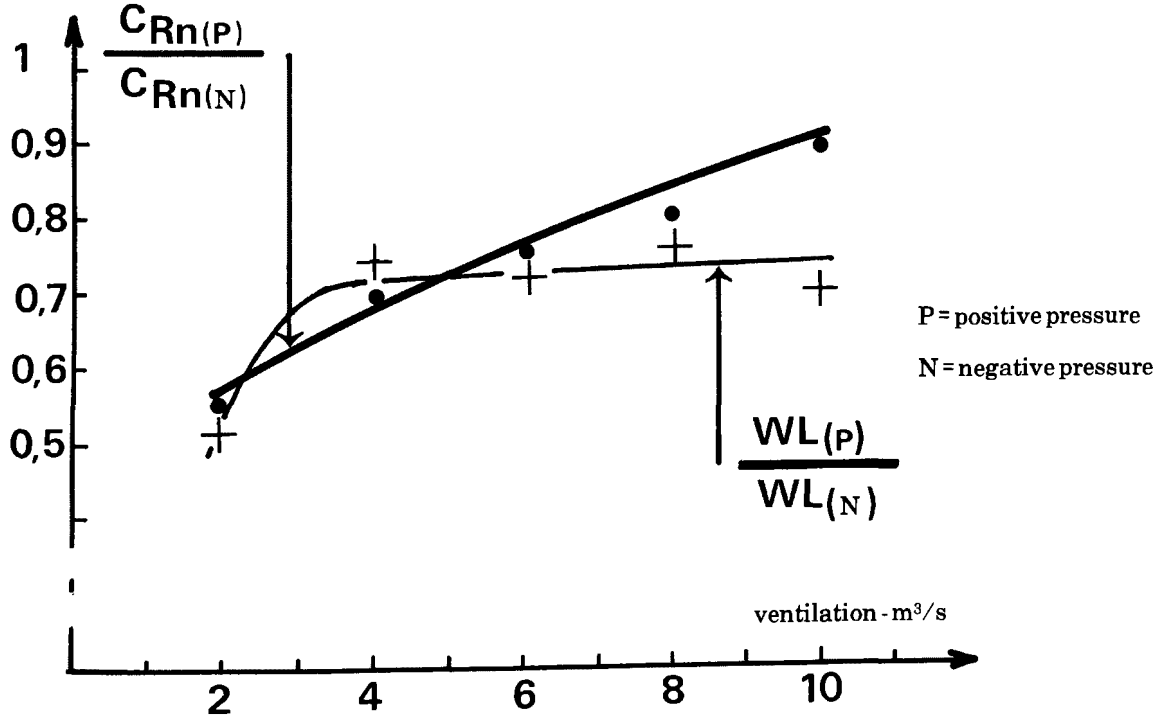

Figure 3. Variations of radon concentration (C_{Rn}), radon flux (Q_{Rn}), and potential alpha energy (WL) with pressure.

SOME RADIOLOGICAL HEALTH ASPECTS OF RADON-222 IN LIQUIFIED PETROLEUM GAS*

T. F. Gesell
School of Public Health
University of Texas
Houston, Texas

ACKNOWLEDGEMENT

The author wishes to acknowledge professor John A. S. Adams for consultation; Mr. Carl Mullins, Mr. Dickie Burgess, Mr. Steve Bryan and Mr. Bobby Lane for their assistance in collecting and analyzing the samples; and Miss Susan Bettes for technical aid in the preparation of the manuscript.

Abstract

Natural Gas (NG) produced at the wellhead contains varying quantities of radon-222. Previous studies of wellhead gas from several gas fields have indicated concentrations ranging to 1450 pCi/l at standard temperature and pressure. When natural gas is processed to remove impurities and heavier, more valuable hydrocarbons, the radon becomes concentrated in the ethane and propane fractions. This concentration apparently takes place during fractionation because of the similar boiling points of radon, propane, and ethane. Liquified Petroleum Gas (LPG), which is widely used as a domestic fuel and as a chemical feedstock is composed principally of propane and ethane. Potential human exposure to radon-222 and its progeny contained in NG and LPG can occur in a variety of ways to both occupational groups and to members of the general public. The paper includes an identification of the pathways of human exposure, the results of approximately 400 measurements of radon-222 concentrations in retail LPG and domestic NG supplies, and measurements of radon-222 concentrations in gas processing plant streams. An exposure model for the domestic fuel usage pathway is also presented.

INTRODUCTION

Radioactivity in natural gases was first reported for Canadian gas in 1904 (Slatterly and McLennan, 1918). At that time, it was suggested that helium, a known product of radioactive decay, might be associated with the radioactivity. Somewhat later, a systematic survey was made of Canadian natural gases (Slatterly and McLennan, 1918) in an effort to find a relation between helium concentrations and radioactivity. The radioactivity was reported to be due to "radium emanation", now known to be radon-222. Other reports were made on the radioactivity of American and European natural gases in the years between 1904 and 1918.

Although no strong correlation between radon-222 and helium concentrations was found in the 1904-1918 studies, interest in a possible correlation was revived in the 1940's and early 1950's resulting in a series of papers dealing with radon and helium concentrations in U. S. natural gases (Faul, *et al.*, 1952 and Pierce, *et al.*, 1955). A comprehensive survey of radon-222 and helium concentrations in the Texas Panhandle Field gases was issued by the U. S. Geological Survey (Pierce, *et al.*, 1964).

Subsequently, Bunce and Sattler (1966) and McBride and Hill (1969) dealt with radon concentrations in natural gas in the San Juan Basin, located in southwestern Colorado and northwestern New Mexico. These papers are significant because, unlike the previous papers, the potential for exposure of population groups to radon-222 via the natural gas pathway was explicitly recognized. These investigations determined that the Project Gasbuggy nuclear stimulation experiment did not raise the radon-222 concentrations in the neighboring wells above the naturally occuring levels.

Subsequent to these wellhead studies, two papers have mentioned the possibility of radon release from gas fired electric power generating stations (Fish, 1969 and Terrill, *et al.*, 1967).

The studies reported in the literature give an indication of the magnitude and range of radon-222 concentrations to be found in natural gas. Table 1 summarizes some of the reported results. Discounting the values reported at "reservoir temperature and pressure", it is seen that wellhead natural gas exhibits radon-222 concentrations ranging from nearly zero to 1450 pCi/liter at STP.

The foregoing review of the literature demonstrates that we have a general, but by no means comprehensive, knowledge of radon-222 concentrations in wellhead natural gas. For the purposes of this study, however, knowledge of radon-222 levels at wellhead is insufficient. Wellhead data give no indication of the distribution of radon-222 in the products of gas processing plants. Owing to the fact that the boiling point of radon lies between that of propane and ethane (Table 2), which are the principal constituents of LPG sold commercially (Table 3), one may expect the concentration of radon to be greater in the LPG products than in other natural gas products. Any activity in these products would, of course, be diminished by the delays from actual production, processing and delivery according to the half-life of radon-222 (3.82 days). Wellhead data of the type existing in the literature are also of little use in evaluating occupational radiation exposure due to radon.

**Work supported by Atlantic Richfield Co., Dow Chemical Co., Esso Production Research, Phillips Petroleum Co., Shell Oil Co., Texaco Inc., and the Texas State Department of Health.*

POTENTIAL PATHWAYS FOR HUMAN EXPOSURE

Radon-222 and its daughter products emit alpha, beta, and gamma radiation. Occupational exposure to external radiation can occur in the vicinity of gas processing or transport equipment where high radon-222 and concentrations exist. The internal exposure of the lung to radon-222 and daughter radiations can occur whenever radon bearing gases or combustion products are released and inhaled by workers. Another internal exposure possiblity exists whenever gas processing equipment is disassembled for repair. Lengthy exposure of the internal surfaces of such equipment could result in the buildup of the long-lived radon-daughters lead-210 and polonium-210. Ordinary cleaning procedures could then create an aerosol containing these isotopes and result in a respiratory exposure.

Population exposure to external radiation could occur in the vicinity of domestic LPG storage tanks. Internal exposure to the lung could occur whenever combustion products of radon-containing fuel gases are present in the atmosphere. While this situation occurs at limited concentrations in the general environment, the highest levels of individual exposure would occur whenever radon-containing LPG or NG is burned without a flue inside dwellings or other occupied buildings. This situation occurs with gas cooking, unvented gas space heating or unvented gas hot water heating. An indication of the magnitude of the exposed population may be gained from the U. S. Census data of 1970 (U. S. Bureau of the Census, 1970) which lists 5,314,082 dwellings containing LPG fueled ranges, 3,14,164 dwellings containing LPG fueled hot water heaters, and 3,949,420 dwellings containing unvented heaters. Most unvented heaters burn either NG or LPG.

An estimate of population exposure due to radon in LPG should be based on field data collected as close to the point of use as is practicable. This paper reports the results of radon-222 concentrations measured in retail LPG (propane) samples gathered in fourteen southern and western states. Regular weekly samples were gathered from seven Houston, Texas area-retailers for a period of one year in order that seasonal dependencies could be studied. Individual grab samples were obtained from the other geographic areas over an eight-month period. The results are compared with standards and with natural background levels for radon in air with the aid of an exposure model based principally upon fuel usage and ventilation conditions.

SAMPLING AND MEASUREMENT

Sampling cylinders were obtained specifically for this project. Before use, each of the 1 ½ gallon cylinders was tested to assure that no radon-222 would be introduced to the samples from radium in the construction materials of the cylinders. This test was accomplished by introducing known radon-free LPG into each cylinder and after 24 hours, removing a sample for analysis. The results of these analyses showed no measurable radioactivity, and it was, therefore, concluded that any activity found in subsequent samples contained in these cylinders would be exclusively from the LPG being studied.

Retail LPG was sampled by simply purchasing LPG at the "bottle stations" or "dispensers" operated by retail dealers. The dealers filled the sample bottles in exactly the same fashion that they filled LPG bottles presented by their customers.

Samples of LPG obtained by purchase from retail dealers at their bottle stations are obviously representative of LPG purchased in the same fashion by members of the general public. These customers include owners of permanent house trailers and recreational vehicles. Most LPG consumed by the general public, however, is delivered to residential and commercial sites by truck. The extent to which our samples at the bottle stations are representative of the LPG delivered by truck is dependent upon the practices of the individual retailers. A typical retailer designated by code number 2, operates his business in the manner shown in Figure 1. The #2 bottle station where we obtained our samples is filled at the end of each day with the same gas from the same trucks that deliver to residential and commercial customers. Thus, due to radioactive decay, the radon concentration of the bottle station LPG would be lower to an extent dependent upon turnover rate, than that delivered by the trucks.

Another common practice employed by some LPG retailers is to fill gas bottles from the same main retail storage tanks that serve the trucks. Samples obtained from these dealers would be highly representative of the LPG delivered to the consumer. A third, less common practice is to fill LPG bottles directly from the trucks used to deliver gas to residential customers. This practice usually exists among the smaller dealers. Thus, dependent upon the practices of the retailers, our LPG samples are similar or somewhat older in age than the LPG delivered to the consumer. Consequently, the measured radon concentrations represent, on the average, the lower limit of radon concentrations to be found in delivered LPG.

The radon concentration of the samples was measured using the Lucas Method (Lucas, 1957). Special cells whose curved interior surfaces are coated with a phosphor are filled with gaseous LPG (expanded from a liquid aliquot) to atmospheric pressure. After three hours (to allow the daughter products to reach transient equilibrium with the radon) the cells are placed in contact with a photomultiplier tube and the pulses counted with a scaler. The analytical equipment was calibrated using a National Bureau of Standards radium solution.

Error is due to error in calibration coupled with error produced by counting statistics. A standard counting time of 90 minutes is used so no error due to counting statistics is greater for the lower concentrations. Counting statistics errors range from σ = 1% for 300 pCi/1 to σ = 17% for 1 pCi/1. Our limit of detection is taken as 0.5 pCi/liter which is approximately 2σ above background. Calibration error is

related to the 1% error given by the National Bureau of Standards for the radium solution plus any error in transfer of the radon to the Lucas cell. The new data produced by the counting instruments are expressed in counts per minute. This number is converted to picocuries per liter at STP at the time of sampling using the following formula.

$$Y = \frac{XP_o T}{VfPT_o} \; EXP(.693t/t_{1/2})$$

where

- Y = Radon concentration in picocuries per liter
- X = Counting rate of sample in counts per minute
- V = Volume of Lucas cell = 0.096 liters
- f = Calibration factor in counts per minute per picocurie
- P = Barometric pressure at time of transfer in mm of Hg
- P_o = Standard pressure (760 mm Hg)
- T_o = Standard temperature on the absolute scale (273° K)
- T = Ambient temperature at time of transfer on the absolute scale in °K
- t = Elapsed time between collection and analysis of sample in hours
- $t_{1/2}$ = Half-life of radon-222, (91.8 hours)

RESULTS OF THE SURVEY

The survey of radon-222 concentrations in LPG was done in three phases. Initially, thrice weekly and later weekly samples from the seven identified major Houston area LPG retailers were collected and analyzed. This program continued for one calendar year. After the weekly sampling and analysis had become routine, the second phase collection and analysis of grab samples from other areas in Texas was begun. In the third phase the analytical equipment was installed in a motor coach and samples from other places in the United States were collected and analyzed.

It was determined that the population group most likely to receive the highest exposures to radon-222 and its daughters from this pathway would be those persons living in dwellings utilizing unvented space heaters. Furthermore, the exposure would be directly related to the usage of the heaters. Accordingly, an index was devised which consisted of the product of the average number of degree days of heating required in a geographic area multiplied by the number of unvented heaters in use in the same area. The distribution of this index is shown in Figure 2.

Another major factor that influenced our sampling was the distribution of gas processing plants which produce LPG. The hypothesis was that due to radioactive decay, retail LPG sold near the production would generally exhibit higher radon levels than LPG sold far away from the production. LPG production areas are shown in Figure 3 where each dot represents one gas processing plant. Thus, we wished to include areas near and far from production. These constraints plus operational factors resulted in the sample locations shown in Figure 4. Each dot represents one sample except for the Houston, Texas area where each dot represents one of the seven regularly sampled retailers.

The weekly results of the Houston survey have been averaged into monthly intervals and are presented in Table 4. Also included are column and row averages. Retailer #7 was consistently low so sampling was discontinued after six months. For purposes of the averages retailer #7 was taken as 0.5 pCi/liter for February through June. The data are characterized by a large amount of scatter within and among dealers. This scatter is not too surprising in view of the number of factors that control the radon in LPG. These factors include the radon concentrations in the wellhead gas, the elapsed time between processing and entry into the wholesale market, the elapsed time between entry into the wholesale market and delivery to the retail dealer and delivery to the consumer.

Of the seven retailers sampled, No. 6 is on the average much higher in radon concentration than the others and No. 7 is on the average much lower than the others. Inquiry revealed that retail dealership #6 obtains its propane directly from a gas processing plant and that retail dealership #7 receives its propane from an underground storage well. The other five retailers obtain their gas from wholesale distributors. Thus, the radon concentrations in the propane of the several retailers are entirely consistant with their individual supply practices.

Figure 5 is a second order regression analysis of the monthly averages of the Houston area dealers. The pronounced dip in the activity during the winter months is in all probability due to the higher winter consumption rate and consequent appearance on the market of previously stored LPG. This interpretation is consistent with the known practices of the dealers and wholesalers. It is worthwhile noting that the average concentration during the heating season is approximately one-half of the concentration during the summer months. Thus, the existing practice (at least in the Houston, Texas area) of storing during the summer and using from storage during the winter serves to reduce the exposure of those who utilize LPG in unvented heating from what it would be if production were simply adjusted to demand.

The results of all the non-Houston retail propane samples are grouped by region and presented in Figure 6. In each region, the top number is the maximum concentration observed, the middle number is the mean of all samples in the region and the bottom number is the lowest concentration observed. The most remarkable feature of this distribution is the difference in radon concentrations in the Eastern and Western parts of the United States. Two major factors affect the concentration of radon in retail LPG, concentration at the point of manufacture and the time required to deliver the gas to the consumer. The low concentrations found in the two eastern-most regions could potentially be explained in terms of longer transport and storage times since these areas are fairly far from any major production. The low concentrations found in Louisiana and Arkansas, in view of the large amount of gas processing in Louisiana, have to be interpreted in terms of low concentrations in the sources.

The variation of radon in LPG with distance from a major gas processing area was examined by dividing non-Houston samples into three categories according to whether they were taken within less than 25 miles, between 25 and 200 miles, or greater than two hundred miles from a major gas processing area. The results are shown in Table 5. The differences were tested by the non-parametric Wilcoxon two sample test (Baily, 1971). The mean for the 25-200 mile category was found to be significantly less ($P < 0.1$) than the mean for the 25 mile category and, the mean for the > 200 mile category was found to be significantly less ($P < 0.01$) than the mean for the 25-200 mile category. This result suggests (but by no means demonstrates) that the unsampled northern states would tend to have lower radon concentrations than the sampled states since they are, with few exceptions, farther from the major gas processing areas than the sampled states.

The variation of radon in LPG with the type of container (retail storage tank, truck, or small tank) from which the sample was drawn was also examined. Only Texas was included in this examination, because in the other regions very few samples were obtained from trucks. Retailers fill bottles brought to their locations either from the same, generally large, (>10,000 gal) tanks from which they fill their own delivery trucks, from the delivery trucks themselves or from special "bottle stations" which are supplied by small (generally < 2,000 gal) tanks. The "bottle stations" are typically filled from the retail trucks. Thus, the LPG in the bottle stations would tend to be older, on the average, than the LPG in the trucks and that in the trucks slightly older than the LPG in the large storage tanks. The Texas samples (non-Houston) were categorized and averaged and the results presented in Table 6. The mean of the truck samples, although smaller than that of the large tank samples, was not significantly smaller. The mean of the small tank samples is significantly smaller ($P<0.01$) than both the truck samples and the large tank samples. Significance was tested with the non-parametric Wilcoxon Two Sample Test (Baily, 1971). This finding is consistent with the operational practices of the LPG retailers described above in that the samples which are anticipated to be older have, on the average, lower radon concentrations.

A third major independent variable, the initial concentration has not been examined yet, but is clearly related. Surveys of some ten gas processing plants in various parts of the U. S. have been completed and more are planned. When completed, these surveys should permit us to account for the variation associated with initial concentration.

HUMAN EXPOSURE

Human exposure should be evaluated in terms of the maximum possible exposure to an individual and in terms of population exposure. In this section, the maximum concentration that could occur in a dwelling is estimated, the worst annual average concentration is estimated, and a method for estimating population dose is suggested.

When propane is burned, the principal combustion products are water and carbon dioxide. For every volume (at STP) of propane burned, one volume (at STP) of carbon dioxide results. Carbon dioxide is a well understood and recognized pollutant, and it is reasonable to relate the radon concentration in a building due to combustion of LPG to the CO_2 level due to the same combustion. The CO_2 content of a dwelling due to heating with unvented appliances is a function of the amount of gas burned per unit time, the volume of the room and the degree of ventilation or infiltration.

The American Society of Heating and Air Conditioning Engineers, (ASHRAE, 1963) provides a table (Table 7) relating the number of air changes per hour due to infiltration (all windows and doors closed) to the nature of the room. If we consider a well-sealed house, then an average of one air change per hour for the entire house is not unreasonable.

Jacobs, *et al.*, (1972) have computed, on the basis of the insulation properties of normal construction materials, the home dilution factors for several types of dwellings, assuming the use of unvented heating and the use of natural gas. They assumed one air change per hour and an indoor/outdoor temperature differential of 80°F. We have made a linear extrapolation of these computations for three dwelling types and present the results in Figure 7. These results are approximately correct for propane also. Dwelling type No. 1 is a 10' by 10' shack with one door and two windows. Dwelling type No. 2 is a normally constructed 1,000 square-foot house with rock wool insulation. Dwelling type No. 3 is a 1,000 square-foot, extremely well designed and built house with storm windows and doors. It is seen that with this model even under the most adverse circumstances (i.e., poor construction and 100°F. indoor/outdoor temperature differential) the average indoor CO_2 concentration due to heating does not exceed about 1.2%.

The model, however, leaves much to be desired. For example, the infiltration rate is assumed to be one air change per hour for all three types of dwellings, whereas common sense would dictate that a dwelling with excellent insulation, storm windows, and storm doors would have fewer air changes per hour due to infiltration than a poorly constructed dwelling. The effect of this sort of correction would cause the lines in Figure 7 to converge, thus reducing the disparity among the dwelling types. A second difficulty with the model is that there is no provision for local variations within the dwelling. There would certainly be concentration gradients, but they would be difficult to predict or measure.

The radon levels to be expected in room air can be related to the radon levels to be found in LPG (assumed to be propane) and the CO_2 levels found in the room using simple stoichiometry. The results presented in Figure 8 are the maximum permissible concentrations of radon-222 in air for members of the general population as recommended by three different organizations (International Commission on Radiological Protection, 1959; National Committee on Radiation Protection, 1959; and the U. S. Atomic Energy Commission, 1965). At the present time, only the highest value, given by the USAEC Rules and Regulations, (U. S. Atomic Energy Commission, 165) carry the force of law. It is of significance, however, that the maximum permissible exposure of miners to radon and radon-daughters was recently reduced by a factor of three, (Federal Radiation Council, 1969) largely on the basis of epidemiological work which demonstrated that the old standard was unsafe with respect to the induction of lung cancer. It is not improbable that the maximum permissible exposure for members of the general population may be reduced at some future time. A conservative approach would be to take 1 pCi/liter as an assumed upper bound.

If we take the worst case example, the highest measured radon concentration of 1288 pCi/liter, and further assume that this LPG is burned in a type 1 dwelling (see Figure 7) at a 80°F indoor/outdoor temperature differential, then the CO_2 content of the model dwelling would be about 1% and the associated radon concentration (from Figure 8) would be approximately 4.5 pCi/liter, which is somewhat greater than the AEC Standard.

The standards are written for yearly averages, however, so it is more appropriate to estimate the worst possible yearly average exposure. We shall assume that LPG is delivered monthly throughout the year (industry practice) and that each time it is delivered, the radon concentration, C_o is 1,288 pCi/liter (our highest measured value). Then, the average concentration in LPG, $\bar{C}$, over each 30-day period would be related to the half-life of radon ($\tau_{1/2}$ = 3.825 days) and the delivery interval, 30 days by

$$\bar{C} = C_o \frac{1}{30} \int_0^{30} \exp\left(\frac{-0.693\,t}{\tau_{1/2}}\right) dt$$

$$\bar{C} = C_o\,(0.183) = 235 \text{ PCi/liter.}$$

The estimate of 4.5 pCi/liter for the maximum instantaneous radon level was based on 80°F indoor/outdoor temperature differential. If this differential were maintained for one year, there would be a requirement for 80°F x 365 days/yr = 29,200 degree days of heating. The highest reported heating requirement for a city in the contiguous United States (ASHRAE, 1970) is 10,000 degree days for Duluth, Minnesota. Thus, a maximum yearly average concentration may be estimated by adjusting the instantaneous maximum for the actual average radon concentration in the gas and for the actual annual heating requirements.

$$(\bar{C}_{\text{air max}}) = (C_{\text{air max}}) \times \frac{10{,}000}{29{,}200} \times \frac{235}{1288}$$

$$= (C_{\text{air max}}) \times 0.062 \qquad 0.28 \text{ pCi/liter.}$$

This result is below all of the suggested standards for population exposure to radon-222. Furthermore, it is within the range of normal indoor radon levels (0.05-3 pCi/liter) reported by UNSCEAR (1962).

It is conservative to assume that the effects of radiation vary linearly with exposure, so it is appropriate to estimate the population dose in terms of man-rads. To do this, it is necessary to know the relationship between radon concentration and dose. It has been recognized that in the case of radiation exposure to the lung, the short-lived daughters of radon-222 are much more important than radon itself (Hague and Collinson, 1967). Radon is an inert gas and is subject to fewer removal processes than are its daughter products which are not inert gases and which are often ionized. Thus, in room air or mine air, transient equilibrium between radon and its daughter products usually does not exist. For these reasons, the quantity "working level" (WL) was introduced to define a certain quantity of radon-daughters (U. S. Public Health Service, 1957). A working level is defined as any combination of short-lived radon-daughters in one liter of air which results in the ultimate emission of 1.3×10^5 MeV of alpha particle energy. It is also equal to the alpha energy released by the radon-daughters in secular equilibrium with 100 pCi/liter of radon-222. The current exposure level permitted to uranium miners is equivalent to 40 hours per week at 1/3 WL (Federal Radiation Council, 1969).

The principal health hazard that has been associated with the respiration of radon-daughters is carcinoma of the lung. The target cells have been identified as the basal cells of the bronchial epithelium (lining of the bronchial tubes). A considerable amount of work has been done in an effort to find a model that will relate ambient radon-daughter concentrations to the dose delivered to the basal cells of the bronchial epithelium by

the deposited daughter products. Studies on this subject have been done by Jacobi (1964 and 1972), Altshuler, *et al.,* (1964), Hague and Collinson (1967), Parker (1969), and Harley and Pasternack (1972).

The relationship between radon-daughters and dose to the bronchial epithelium is dependent upon a number of complex factors. These factors include:

(1) The state of equilibrium between radon and its various daughters.
(2) The particle size-distribution of the radon-daughters.
(3) The deposition of radon-daughters in the respiratory tract.
(4) The clearance of radon-daughters from the respiratory tract.

The literature up to 1968 has been reviewed by Parker (1969). He concludes, for typical uranium mine atmospheres, that the most probable relation between the working level and the absorbed dose to the bronchial epithelium is 7 rads per working level month (WLM). He further concludes that this value is probably accurate only to a factor of three.

Barton, *et al.,* (1973) has estimated the dose to the bronchial epithelium due to the burning of 27 ft^3/day of NG containing 20 pCi/liter of radon in a kitchen range located in a 8,000 ft^3 dwelling with one air change per hour. They assume a concentration-dose conversion factor of 100 rad/yr at one working level. For the case of one air change per hour, they calculate a dose rate of 15 millirem per year assuming no radon-daughters in the combustion products.

In the same type of dwelling, approximately 12.5 ft^3 of NG are required per degree day of heating. The heating value per unit volume of propane (LPG) is some 2 1/2 times that of methane (NG), so the Barton, *et al.,* (1973) values would be applicable to LPG with a radon concentration of 50 pCi/liter. Thus, we may estimate for the stated conditions, that the unit dose equivalent rate use of an LPG burning range is

$$\dot{H}_{lr} = \frac{15\,\text{mrem/yr}}{50\,\text{pCi/liter}} = 0.3\ \frac{\text{mrem/yr}}{\text{pCi/liter}}$$

and for unvented heating is

$$\dot{H}_{lh} = 0.3\ \frac{(\text{mrem/yr}}{\text{pCi/liter}}\ \text{range} \times \frac{12.5\,(\text{ft}^3/\text{degree-day}}{27\,(\text{ft}^3/\text{day})} \div 365\ \text{day/yr.}$$

$$= 0.00038\ \frac{(\text{mrem/yr})}{(\text{pCi/liter})\,(\text{degree-day/year})}\,.$$

These coefficients may then be employed with demographic data to estimate the population dose due to domestic use of LPG in man-rem. The country would be divided into regions small enough to have similar heating requirements. The population dose equivalent rate (mrem/yr) for the ith region, $_i$, would be given by

$$\dot{H}_i = C_i f_i (\dot{H}_{lr})_i\ (n_r)_i\ m_i + C_i f_i (\dot{H}_{lh})_i B_i (n_h)_i m_i$$

where C_i is the estimated average radon concentration of delivered propane, f_i accounts for radioactive decay in the domestic storage tanks ($f = 0.183$ for monthly deliveries), $(n_r)_i$ is the number of dwellings utilizing LPG burning ranges in the region, m_i is the average number of persons per dwelling, B_i is the average number of degree days of heating required per year and $(n_h)_i$ is the number of dwellings utilizing LPG in unvented heating.

The population dose equivalent rate would then be estimated by summing over all N regions.

$$\dot{H} = \sum_{i=1}^{N} C_i f_i m_i\ [(\dot{H}_{lr})_i (n_r)_i + (\dot{H}_{lh})_i B_i (n_h)_i]$$

At the present time we are prevented from finding $\dot{H}$ because $(n_h)_i$ is not reported by the Bureau of the Census. Computer tapes of census data which would enable us to obtain $(n_h)_i$ are on order, however, and $\dot{H}$ will be reported in a future publication.

In conclusion, given the available information, radon in LPG does not pose a threat to the individual exposed person. We do not anticipate that the population dose will be of significance either, but judgment is reserved until $\dot{H}$ is estimated.

REFERENCES

Altshuler, B., N. Nelson, and M. Kuschner, (1964), *Estimation of Lung Tissue Dose from the Inhalation of Radon-Daughters,* Health Physics 10:1137-1161.

ASHRAE (1963), *ASHRAE Guide and Data Book; Fundamentals and Equipment,* New York: American Society of Heating, Refrigeration, and Air Conditioning Engineers, Inc., p. 432.

ASHRAE (1970), *ASHRAE Guide and Data Book; Systems,* New York: American Society of Heating, Refrigeration, and Air Conditioning Engineers, Inc., p. 619.

Baily, D. E., (1971), *Probability and Statistics*, John Wiley and Sons, New York. p. 393.

Barton, C. J., R. E. Moore, and P. S. Rohwer, (1973), *Contribution of Radon in Natural Gas to the Natural Radioactivity Dose in Homes*. Oak Ridge National Laboratory Report TM-4154.

Bunce, L. A. and F. W. Satler, (1966) *Radon-222 in Natural Gas*, Radiological Health Data and Reports, 7:441-444.

Faul, H., G. B. Gott, G. E. Manger, J. W. Mytton, and A. W. Sakakura, (1954), *Radon and Helium in Natural Gas*, International Geological Congress. 19th, Algiers 1952, Comptes rendus, Sec. 9, Pt. 9, 339-349.

Federal Radiation Countil, (1969), *Federal Register* 34(10):576-577.

Fish, B. R., (1969), *Radiation in Perspective; The Role of Nuclear Energy in the Control of Air Pollution.* Nuclear Safety 10:119-130.

Hague, A. K. M. M. and A. J. L. Collinson, (1967), *Radiation dose to the Respiratory System due to Radon and its Daughter Products*, Health Physics, 13:431-443.

Harley, N. H. and B. S. Pasternack, (1972), *Alpha Absorption Measurements Applied to Lung Dose from Radon-Daughters*. Health Physics 23:771-782.

International Commission on Radiological Protection, (1959), *Recommendations of the International Commission on Radiological Protection on Permissible Dose for Internal Radiation.* Report No. 2, Pergamon Press, New York, N. Y.

Jacobi, W., (1964), *The Dose to the Human Respiratory Tract by Inhalation of Short-Lived Radon-222 and Radon-220 decay products*, Health Physics 10:1163-1175.

Jacobi, W., (1972), *Activity and Potential Alpha Energy of Radon-222 and Radon-220 Daughters in Different Air Atmospheres*. Health Physics 22:441-450.

Jacobs, D. G., E. G. Struxness, M. J. Kelly, and C. R. Bowman, (1972), *Consideration of the Radiological Impact from the Hypothetical Use of Contaminated Natural Gas from Nuclearly-Stimulated* Reservoirs, Health Physics 22:429-440.

Lucas, H. F., (1957), *Improved Low-Level Alpha-Scintillation Counter for Radon*, Review of Scientific Instruments 28:680-683.

McBride, J. R. and D. Hill, (1969), *Off-Site Radiological Surveillance for Project Gasbuggy*, Radiological Health Data and Reports 10:535-546.

National Committee on Radiation Protection, (1959), *Maximum Permissible Body Burdens and Maximum Permissible Concentrations of Radionuclides in Air and Water for Occupational Exposure*, NBS Handbook 69.

National Council on Radiation Protection, (1971), *Basic Radiation Protection Criteria*, NCRP Publication No. 39.

Parker, H. M., (1969), *The Dilema of Lung Dosimetry*, Health Physics 16:553-561.

Pierce, A. P., G. B. Gott, and J. W. Mytton, (1964), *Uranium and Helium in the Panhandle gas Field in Texas and Adjacent Areas*, U. S. Geological Survey Professional Paper 454-G.

Pierce, A. P., J. W. Mytton, and G. B. Gott, (1955), *Radioactive Elements and their Daughter Products in the Texas Panhandle and Other Oil and Gas Fields in the United States*, Geology of Uranium and Thorium, InternationalConference.

Satterly, J. and J. C. McLennan, (1918), *The Radioactivity of the Natural Gases of Canada*, Royal Society of Canada Transactions 12, Series 3, p. 153-160.

Terrill, J. G., E.D. Harward, and I. P. Leggett, (1967), *Environmental Aspects of Nuclear and Conventional Power Plants*. Industrial Medicine and Surgery 36:412-419.

UNSCEAR, (1962), *Report of the United Nations Scientific Committee on the Effects of Atomic Radiation*, General Assembly, Official Records, Seventeenth Session, Supplement No. 16 (A/5216).

U. S. Atomic Energy Commission, (1965), *Title 10 of the Code of Federal Regulations, Park 20, Rules and Regulations*, Washington, D. C., U. S. Government Printing Office.

U. S. Bureau of the Census, (1970), *Census of Housing: 1970; Detailed Housing Characteristics, Final Report HC(1)-B-1, United States Summary.*

U. S. Public Health Service, (1957), *Control of Radon-Daughters in Uranium Mines and Calculations on Biological Effects*, U. S. Public Health Service Publication 494.

TABLE 1. Radon-222 Concentration of Wellhead Natural Gases.

STUDY				RADON-222 CONCENTRATION (picocuries/liter @ s.t.p.)		
AUTHOR(S)	YEAR REPORTED	GEOGRAPHIC AREA	NUMBER OF ANALYSES	MINIMUM	MAXIMUM	AVERAGE
Satterly and McLennon	1918	Ontario, Canada	21	4	800	169
Satterly and McLennon	1918	Alberta, Canada	16	10	205	62
Satterly and McLennon	1918	British Columbia				
Satterly and McLennon	1918	British Columbia, Canada	3	390	540	473
Paul, et. al.	1951	Texas Panhandle	≅ 500	≅10	≅ 520	---
Pierce, et. al.	1955	U.S.A.	"66 fields"	<100*	10,000*	460*
Pierce, et. al.	1964	Texas Panhandle	≅ 500	<5	1,450	≅ 100
Bunce and Sattler	1966	SW Colorado; NW New Mexico	307	0.2	158.8	24.6
McBride and Hill	1969	SW Colorado; NW New Mexico	42	0.33	57.5	16.4

*Reported at "reservoir temperature and pressure"; the pressure and temperature were not stated, but 200-300 psi is typical.

TABLE 2. Boiling Point of LPG Constituents and Radon.

NAME	FORMULA	BOILING POINT (°C)
METHANE	CH_4	-161.5
ETHANE	$(CH_3)_2$	- 88.3
RADON	Rn	- 61.8
PROPANE	$(CH_3)(CH_2)(CH_3)$	- 42.2
ISOBUTANE	$(CH_3)_3(CH)$	- 10.2
BUTANE	$(CH_3)_3(CH_2)_2(CH_3)$	- 0.5

TABLE 3. Constituents of Retail LPG in Percent.*

RETAILER CODE	CH_4 METHANE	C_2H_6 ETHANE	C_3H_8 PROPANE	C_4H_{10} n-BUTANE	C_4H_{10} i-BUTANE
1	2.0	9.5	88.0	0.5	---
2	0.2	3.8	95.9	1.5	---
3	0.2	3.8	96.0	---	---
4	1.8	6.0	91.5	0.7	---
5	0.5	7.2	91.3	0.5	0.5
6	0.44	2.8	25.58	0.16	---

*Samples taken during week of Nov. 26, 1972 and analyzed using gas chromatography.

TABLE 4. Radon Concentrations of Retail LPG (pCi/l) in the Houston, Texas Area: Monthly Averages of Weekly Samples.

MONTH	RETAILER CODE NUMBER							AVERAGE
	1	2	3	4	5	6	7	
July, 1972	9.4	5.6	6.0	130.9	57.6	233.4	<0.5	63.3
August	63.1	62.1	41.6	160.4	32.6	197.0	0.7	79.7
September	27.7	42.5	10.0	79.4	23.2	148.0	<0.5	47.3
October	20.3	48.3	30.2	85.8	34.4	163.7	4.6	55.3
November	17.9	27.8	63.8	48.4	14.9	220.4	4.1	56.7
December	6.2	43.9	25.6	2.9	9.7	176.6	3.4	38.3
January, 1973	3.4	33.0	2.2	0.6	41.6	139.2	<0.5*	32.4
February	53.0	26.6	21.2	11.0	11.5	167.2	<0.5*	41.8
March	80.6	30.5	10.5	40.3	3.5	204.9	<0.5*	52.9
April	105.6	55.8	6.0	77.7	30.2	149.3	<0.5*	60.7
May	78.3	10.8	46.4	59.4	38.7	178.2	<0.5*	59.3
June	115.0	37.5	34.8	25.8	23.3	173.6	<0.5*	58.8
Average	48.4	35.4	24.9	50.1	26.8	179.3	1.4	53.7

*Sampling for this retailer was discontinued after December, 1972 and values of 0.5 were assumed thereafter for averaging purposes.

TABLE 5. Relationship Between Radon-222 Concentration in LPG and Distance From a Major Gas Processing Area.

DISTANCE (miles)	NO. OF SAMPLES	AVERAGE CONCENTRATION (pCi/liter)
<25	103	87.8
25-200	23	63.7
200	31	45.6

TABLE 6. Relationship Between Radon-222 Concentration in LPG and the Type of Container From Which the Sample was Obtained.

CONTAINER	NO. OF SAMPLES	AVERAGE CONCENTRATION (pCi/liter)
Large Tank	21	162.9
Truck	20	125.8
Small Tank	30	31.4

TABLE 7. Air Changes Taking Place Under Average Conditions in Residences, Exclusive of Air Provided for Ventilation.*

KIND OF ROOM OR BUILDING	Number of Air Changes Taking Place per Hour
Rooms with no windows or exterior doors	1/2
Rooms with windows or exterior doors on one side	1
Rooms with windows or exterior doors on two sides	1 1/2
Rooms with windows or exterior doors on three sides	2
Entrance Halls	2

*For rooms with weatherstripped windows or with storm sash, use 2/3 these values.

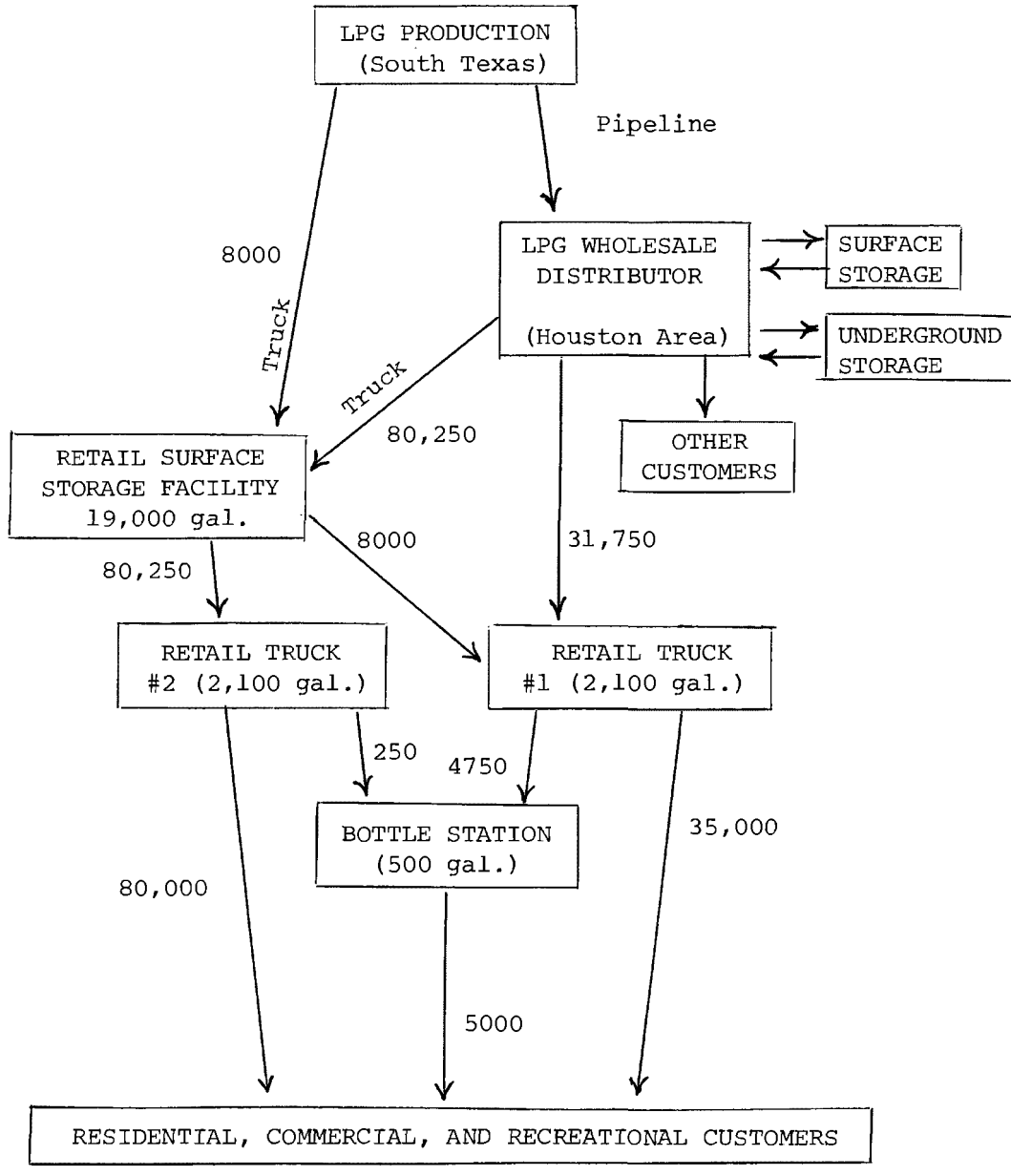

Figure 1. Distribution network for Retailer #2. The numerals adjacent to the arrows represent the approximate gallons of LPG moved per month along the various pathways during a typical winter season.

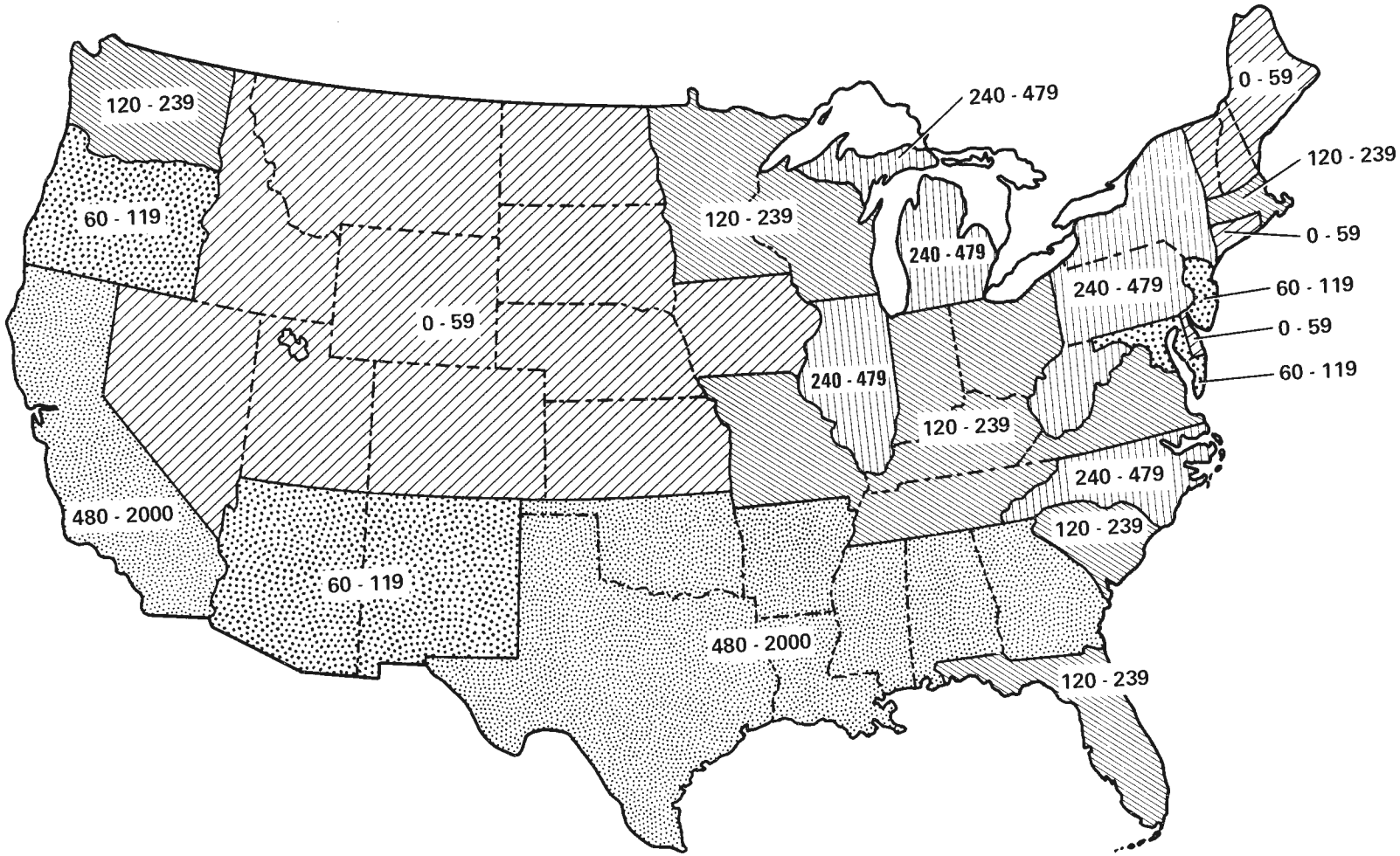

Figure 2. Distribution of the exposure index (degree days) X (unvented heaters) by state for the contiguous United States. The values are expressed in millions.

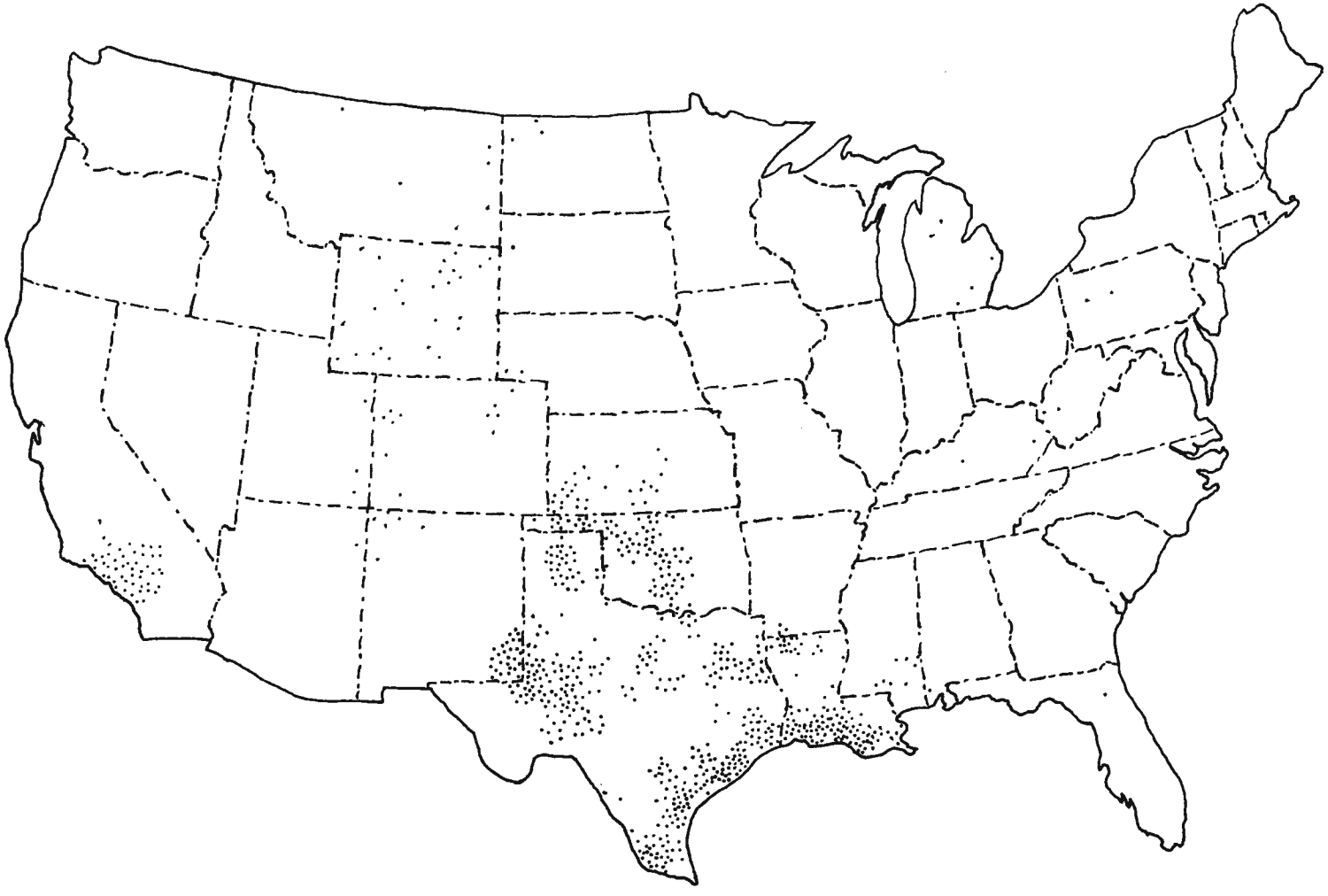

Figure 3. Distribution of gas processing plants in the contiguous United States. Each dot represents one gas processing plant.

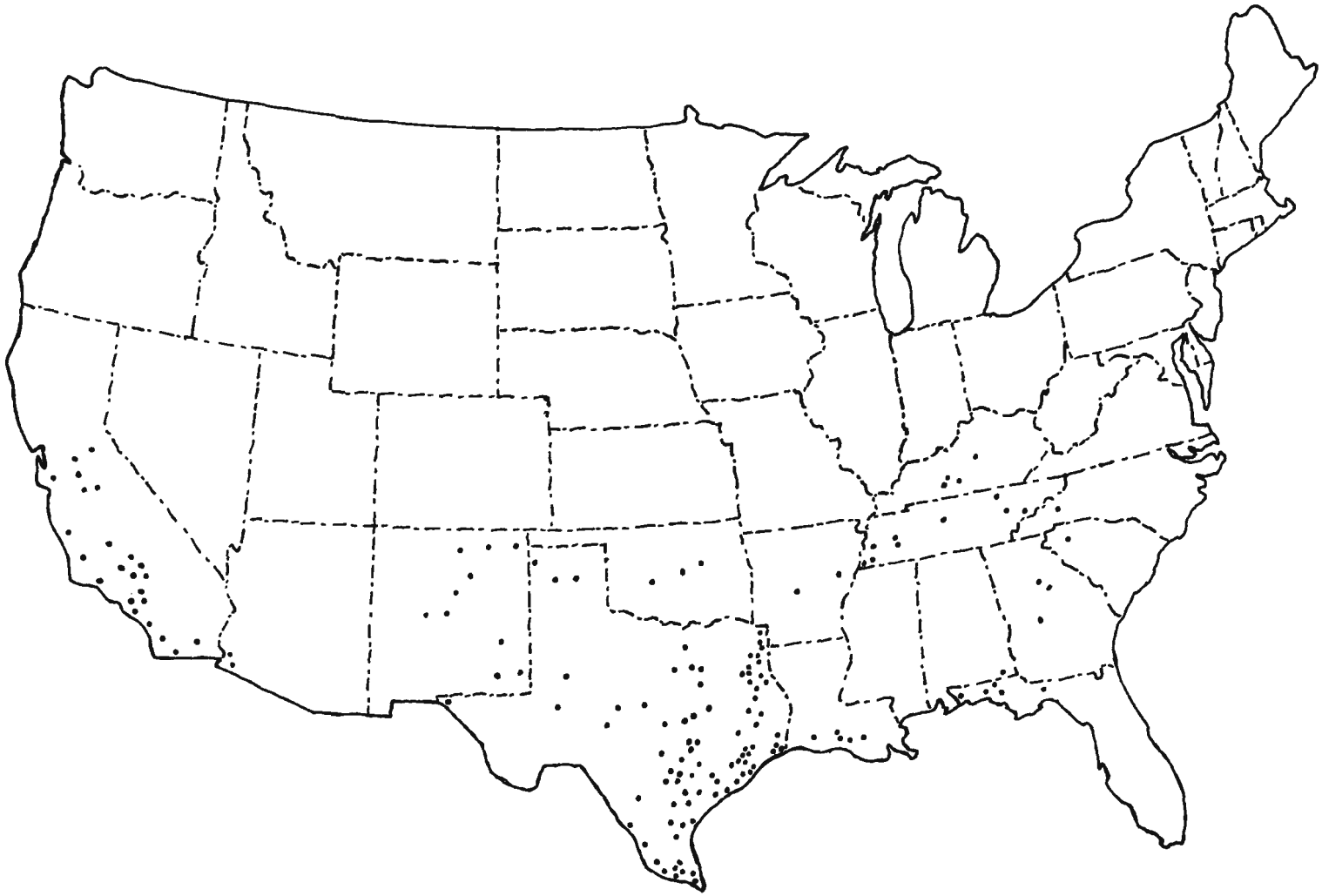

Figure 4. Distribution of retail LPG sample sites. Each dot represents one sample except in the Houston, Texas area where each dot represents one of the seven regularly sampled retailers.

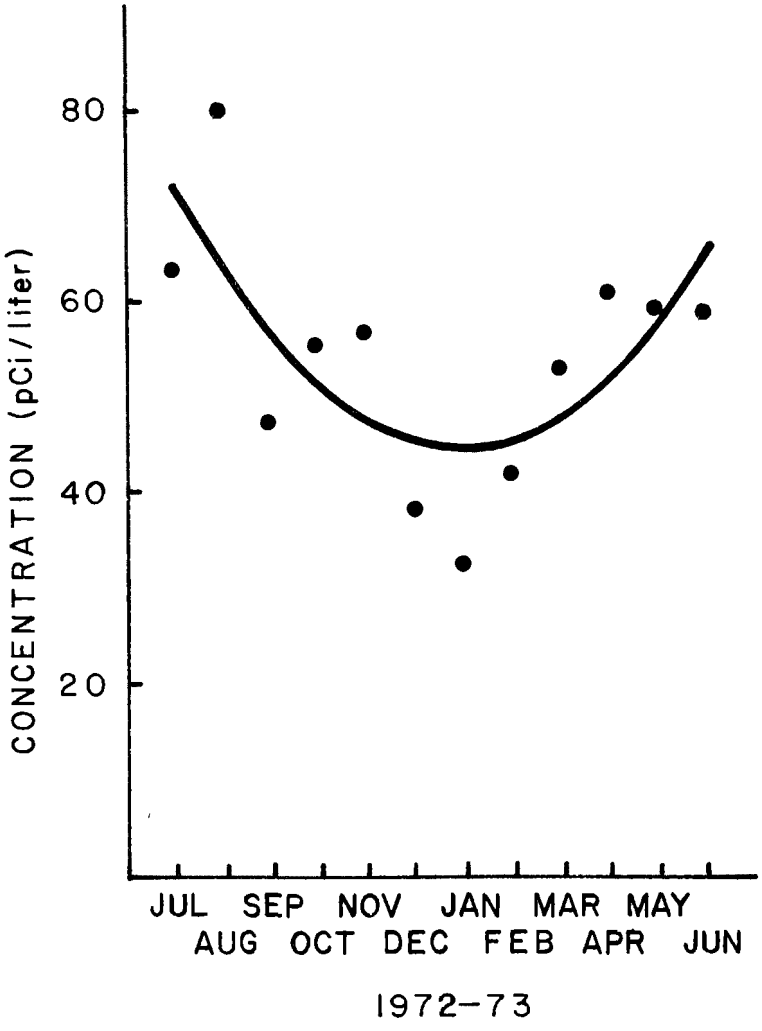

Figure 5. Second order regression analysis of the monthly average values of radon concentrations found in weekly Houston, Texas area retail LPG samples.

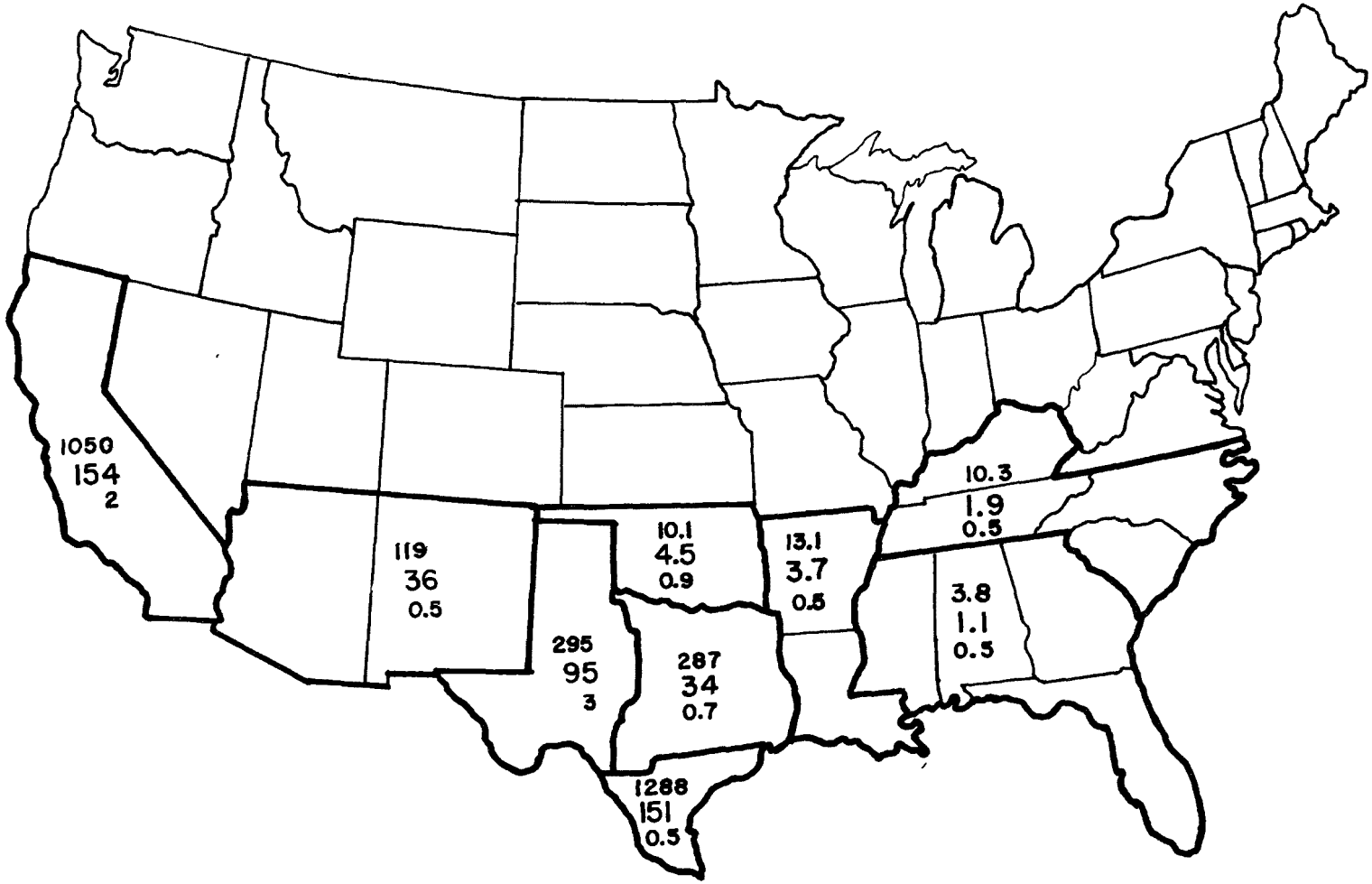

Figure 6. Distribution by region of radon concentrations found in retail LPG samples. The three numbers in each region represent, respectively, the maximum, mean, and minimum concentrations (pCi/liter).

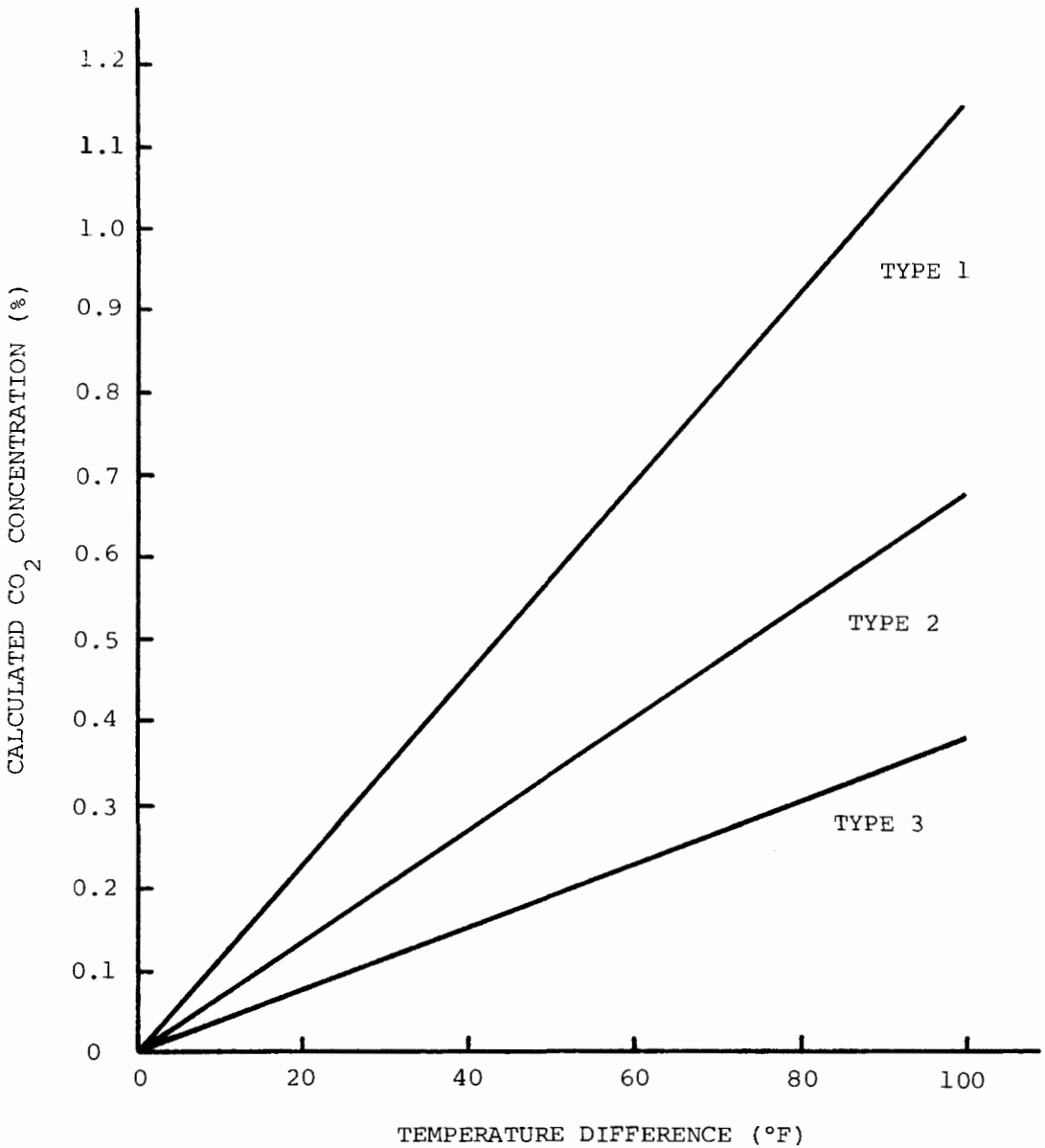

Figure 7. Calculated CO_2 concentrations vs indoor-outdoor temperature differences, for three dwelling types assuming the use of unvented heating and one air change per hour.

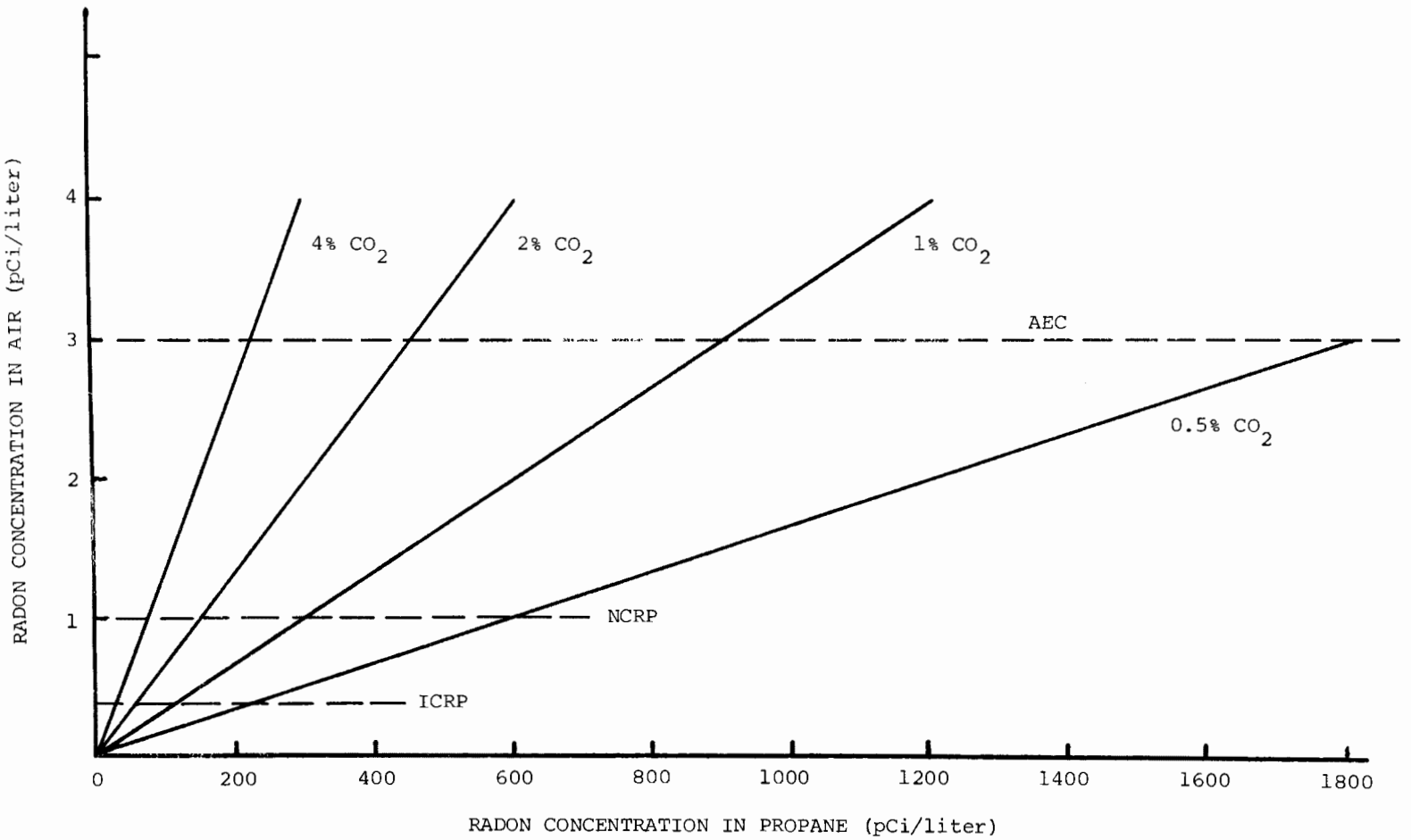

Figure 8. Theoretical concentrations of radon contributed by combustion vs concentration in propane for several assumed CO_2 concentrations.

PERSONNEL DOSIMETRY OF RADON AND RADON-DAUGHTERS*

K. Becker
Health Physics Division
Oak Ridge National Laboratory
Oak Ridge, Tennessee 37830

Abstract

During the past five years there has been increasing interest in monitoring the individual exposure of persons to radon and, more importantly, the radon progeny attached to aerosol particles. Several devices have been proposed. These include the following:

(1) passive detectors based on nuclear track emulsions and track etching foils;
(2) semi-active systems in which the aerosols are collected electrostatically and detected by scintillator/film combinations or track etching; and
(3) active systems based on the collection of aerosols on a filter, and integrating measurement of the alpha flux from the filter by TLD or track films.

All these systems have drawbacks, which have been minimized in a small active system based on alpha particle track etching which was originally developed at ORNL in 1969. Since then it has undergone substantial laboratory and field testing, and has been subjected to various improvements. The system is briefly discussed.

PASSIVE DETECTORS

Various authors in the U.S., Germany, and the Soviet Union (Geiger, 1967; Jacobi and Koeppe, 1968; Markov, *et al.*, 1970; and Evans, 1972) suggested the use of nuclear track emulsions and visual alpha particle counting in the microscope. In a special radon film badge (Geiger, 1967 and Evans, 1972), a Kodak NTA film was separated from a central recess by a light-tight window sufficiently thin to permit the passage of alpha particles, with the radon-containing air diffusing into the recess. A coefficient of variation of ±30% for one MPC-week was claimed in early laboratory tests (Geiger, 1967), but other laboratory and field tests (White, 1969) did not produce satisfactory results, largely because of intense fading in the NTA emulsion. In high-humidity areas, such a badge cannot be used for more than 2-3 days without a change of film, but a week of exposure at MPC would be required for a ± 30% statistical error.

Several groups have, therefore, studied the feasibility of the use of sensitive polymers (mostly cellulosics such as cellulose nitrate, acetate, triacetate, or acetobutyrate) in which alpha particles are detected by track etching (for a recent review on track etching dosimetry see Becker, 1972). The latent tracks in such detectors are sufficiently stable (Figure 1) and are easily countable — either by visual scanning (Becker, 1969) or automatic spark-counting of the etched perforations in ~15 um cellulose nitrate films. In a cellulose triacetate foil of 3 cm^2, for example, exposure to one weekly MPC of radon in equilibrium with its progeny produces ≅100 tracks (Becker, 1969). The aerosol-attached radon-daughters can be excluded by placing a filter between the foil and the environment. Detectors containing one foil which is exposed to unfiltered air, and one exposed to filtered air (Figure 2[a]) were found to be sufficiently sensitive (Becker, 1970), but not accurate enough under simulated field conditions.

Since those early experiments, various other authors in the U. S. (Lovett, 1969 and Alter and Price, 1972), Poland (Domanski, *et al.*, 1973), Japan (Kurosawa, 1972), and France (Anno and Commancy, 1971) exposed open, unprotected foils — mostly of cellulose nitrate — to radon-containing atmospheres. This method, although simple and inexpensive, seems unlikely to provide sufficiently precise data. Single detectors are unable to distinguish between radon gas and attached daughter products. Also, in field tests, contamination of the foils by dust, oil films from the exhaust of diesel engines, etc., lead to grossly erroneous results (White, 1969).

SEMI-ACTIVE SYSTEMS

Several semi-active systems for a more sensitive and/or selective measurement of the radon progeny have been investigated. Thermal precipitation of aerosol particles on the plastic detector opposite to a heating device did not result in a substantial increase in sensitivity, largely because increased latent alpha track fading took place at elevated temperatures (Auxier, *et al.*, 1971). Electrostatic deposition did not turn out to be very practical at high humidities in our experiments, but others (Costa-Ribeiro, *et al.*, 1969) have proposed a rather bulky battery-operated electrostatic collection device. It is based on the collection of radium A from the decay of pure, filtered radon on a charged thin hemispherical aluminum foil, and a scintillator behind the foil

**Research sponsored by the U.S. Atomic Energy Commission under contract with the Union Carbide Corporation.*

which converts the alpha particle energy into light flashes to be integrated by means of a conventional photographic film. Unfortunately, this procedure results in a pronounced exposure-rate dependence of the response due to the reciprocity failure of photographic emulsions.

ACTIVE DETECTORS

Active radon progeny personnel dosimeters are usually based on the collection of aerosols on the surface of suitable filters through which ambient air is forced, and subsequent integrating measurement of the alpha particles emitted from these aerosols. One such system in which TLD-impregnated Teflon discs are used as detectors has been developed at Colorado State University (McCord, *et al.*, 1969 and Schiager and Savigner, 1972). It can be made sufficiently sensitive (permitting measurements in the 0.1 to 10 MPC range), but the substantial air-flow which is necessary requires a fairly large and heavy pumping system and battery. There have also been problems with the accuracy of such detectors in laboratory as well as field tests (White, 1969 and Schiager and Savigner, 1972) probably related to clogging of the filter, fading of the TLD's, and other inherent inaccuracies of TLD.

In another system which has been developed by our group at Oak Ridge (Becker, 1970 and Auxier, *et al.*, 1971) a 15 μm cellulose nitrate foil to be evaluated by spark-counting (Johnson, *et al.*, 1970) is used for alpha particle detection. The sensitivity of this system, which permits the detection of single alpha particles, is so high that only a small air flow is required, and clogging of the filter is minimized. A schematical diagram of this small (115 x 23 mm) and light-weight (67 g) device is given in Figure 2(b) and a photograph is presented in Figure 3. The details of its construction have been described in an earlier publication (Auxier, *et al.*, 1971). A rechargable battery operates the motor without loss of efficiency for 12-15 hours, which is more than sufficient for an 8-hour shift. The dosimeter can easily be attached to a miner's helmet (Figure 4).

During tests at HASL, the performance of this detector turned out to be satisfactory in comparison to other detectors which were simultaneously tested (White, 1970), but some problems were also uncovered. For example, the speed of several of the initially used motors was not very uniform; there were occasional air-leaks around the filter edges, and the reproducibility of the cellulose nitrate foil preparation was less than desirable. The mechanical problems have since been corrected, and improved cellulose nitrate foils have been prepared (Lupica, 1974), because the commercially available 18 μm cellulose nitrate (LR 115 made by Kodak-Pathe, France) appears to be too thin for reproducible spark-counting results.

Similar systems have since been tested also in Germany (Haider and Jacobi, 1972) and France (Chapuis, *et al.*, 1972). Various additional parameters such as the effect of distance between the alpha source and the detector foil on the alpha particle spectrum and, consequently, the registration efficiency (Figure 5) have been investigated and have helped to improve the performance.

With the radon progeny concentration in the air of a typical mine fluctuating substantially with location and time, stationary or portable instruments provide only a very crude estimate of an individual miner's lung exposure. A light-weight, reliable personnel dosimeter which does not require an outside power source is highly desirable and apparently feasible, but some additional de-bugging and testing efforts may be required before a sufficiently rugged version of such a dosimeter can go into large-scale production and use.

REFERENCES

Alter, H. W. and P. B. Price, (1972), U. S. Patent 3, 665 194.

Anno, J. and L. Commanay, (1971), Am. Phys. Biol. Med. 5, 65.

Auxier, J. A., *et al.*, **(1971),** Health Phys. 21, 126.

Becker, K., (1969), Health Phys. 16, 113.

Becker, K., (1972), Chapter 2 in *Topics in Radiat. Dosimetry* (F. H. Attix, Ed.), Academic Press, New York.

Becker, K., (1970), in ORNL-4446, p. 266; and U. S. Patent 3, 505, 523.

Chapuis, A. M., D. Dajlevic, P. Duport, and G. Soudain, (1972), *Proceed. 8th Internat. Conf. Nucl. Photography*, Bucharest 1972.

Costa-Ribeiro, C. Thomas, R. T. Drew, M. E. Wrenn, and M. Eisenbud, (1969), Health Phys. 17, 193.

Domanski, T., W. Chruscielewski, and J. Liniecki, (1973), Health Phys., in press.

Evans, R. D., (1972), U. S. Patent 3, 655, 975.

Geiger, E. L., (1967), Health Phys. 13, 407.

Haider, B. and W. Jacobi, (1972), Rep. BMBW-FB K 72-14.

Jacobi, W. and P. Koeppe, (1968), Atomkernenergie 13, 429.

Johnson, D. R., R. H. Boyett, and K. Becker, (1970), Health Phys. 18, 424.

Kurosawa, R., (1972), Hoken Butsuri 7, 105.

Lovett, D. B., (1969), Health Phys. 16, 623.

Lupica, S. B., (1974), To be published.

Markov, K. P., N. V. Ryabou, and K. N. Stas, (1970), Tr. Soyuznogo Nack. Issied. Inst. Priborostr. 12, 184.

McCurdy, D. E., K. J. Schiager, and E. D. Flack, (1969), Health Phys. 17, 415.

Schiager, K. J., and N. F. Savignac, (1972), Rep. C00-150-21.

White, O., (1969), AEC-HASL Techn. Mem. 69-23A, and pers. comm.

White, O., Jr., (1970), AEC-HASL Techn. Mem. 70-3.

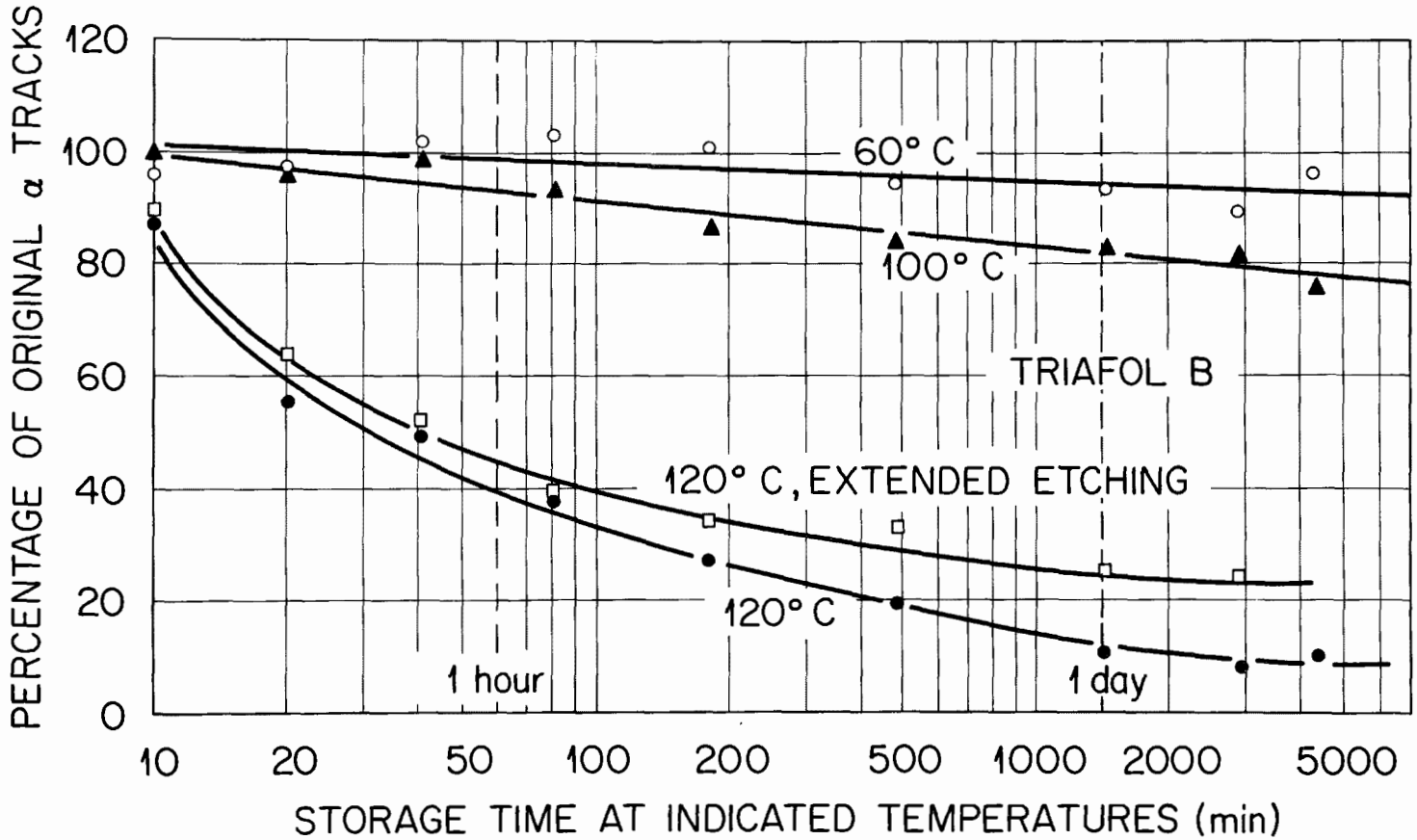

Figure 1. Percentage of original alpha particle etch pits in cellulose acetobutyrate (Triafol B made by Bayer, Leverkusen, Germany) which remains visible after storage of the foil at different temperatures between exposure and etching.

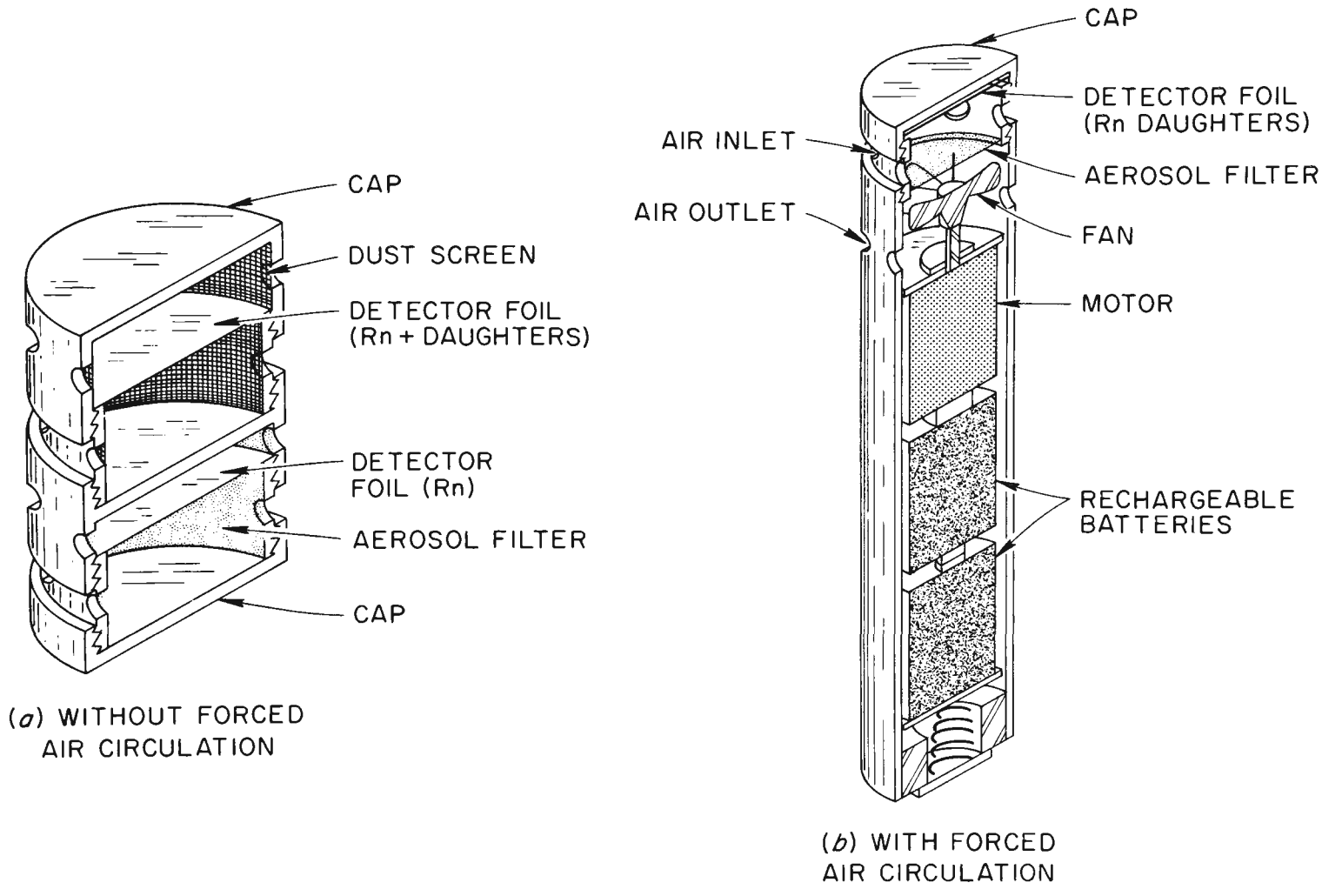

Figure 2. Schematical diagram of a "passive" two-foil radon and radon progeny detector (left), and of the "active" ORNL radon progeny personnel dosimeter (right).

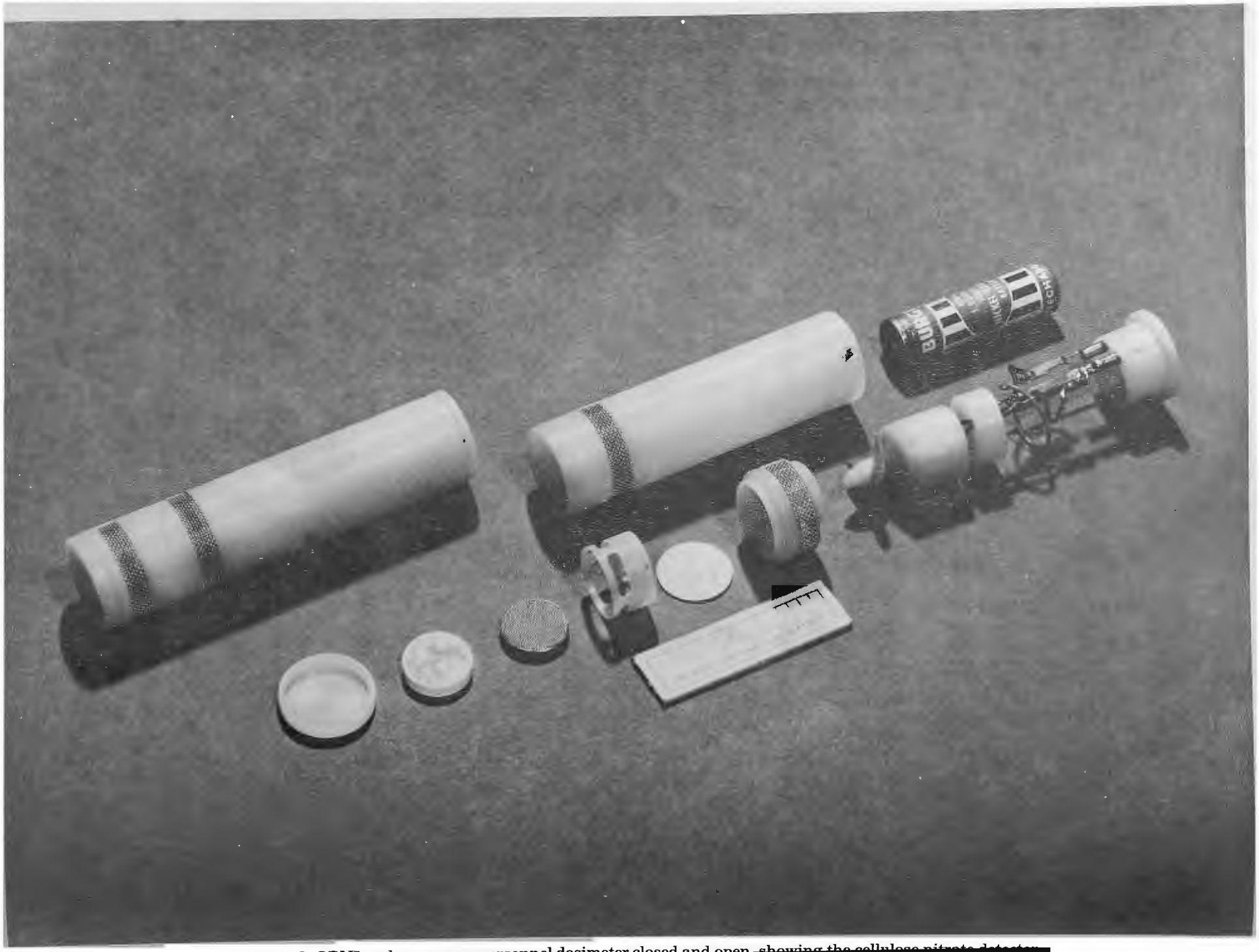

Figure 3. ORNL radon progeny personnel dosimeter closed and open, showing the cellulose nitrate detector

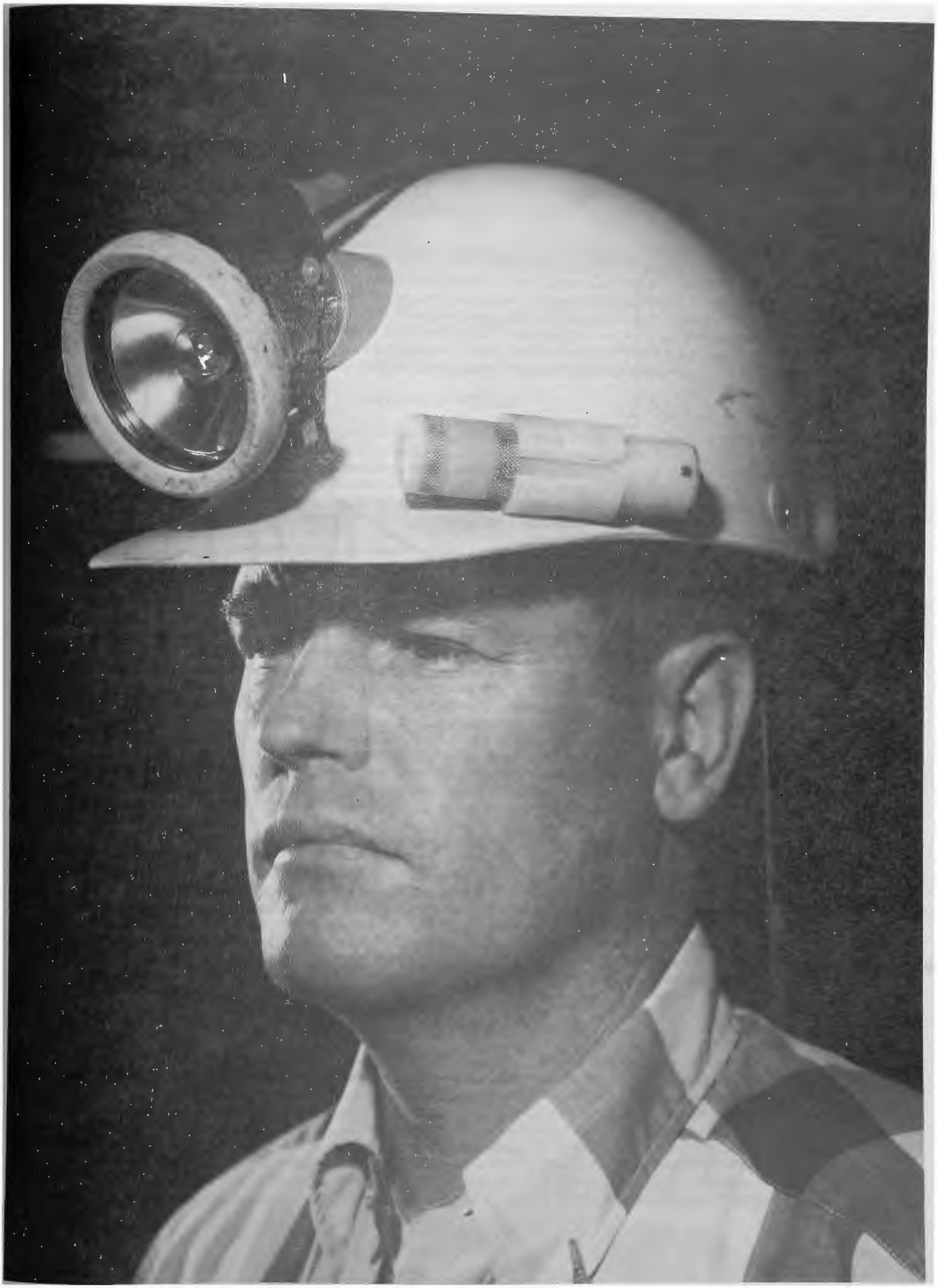

Figure 4. Dosimeter attached to a miner's helmet.

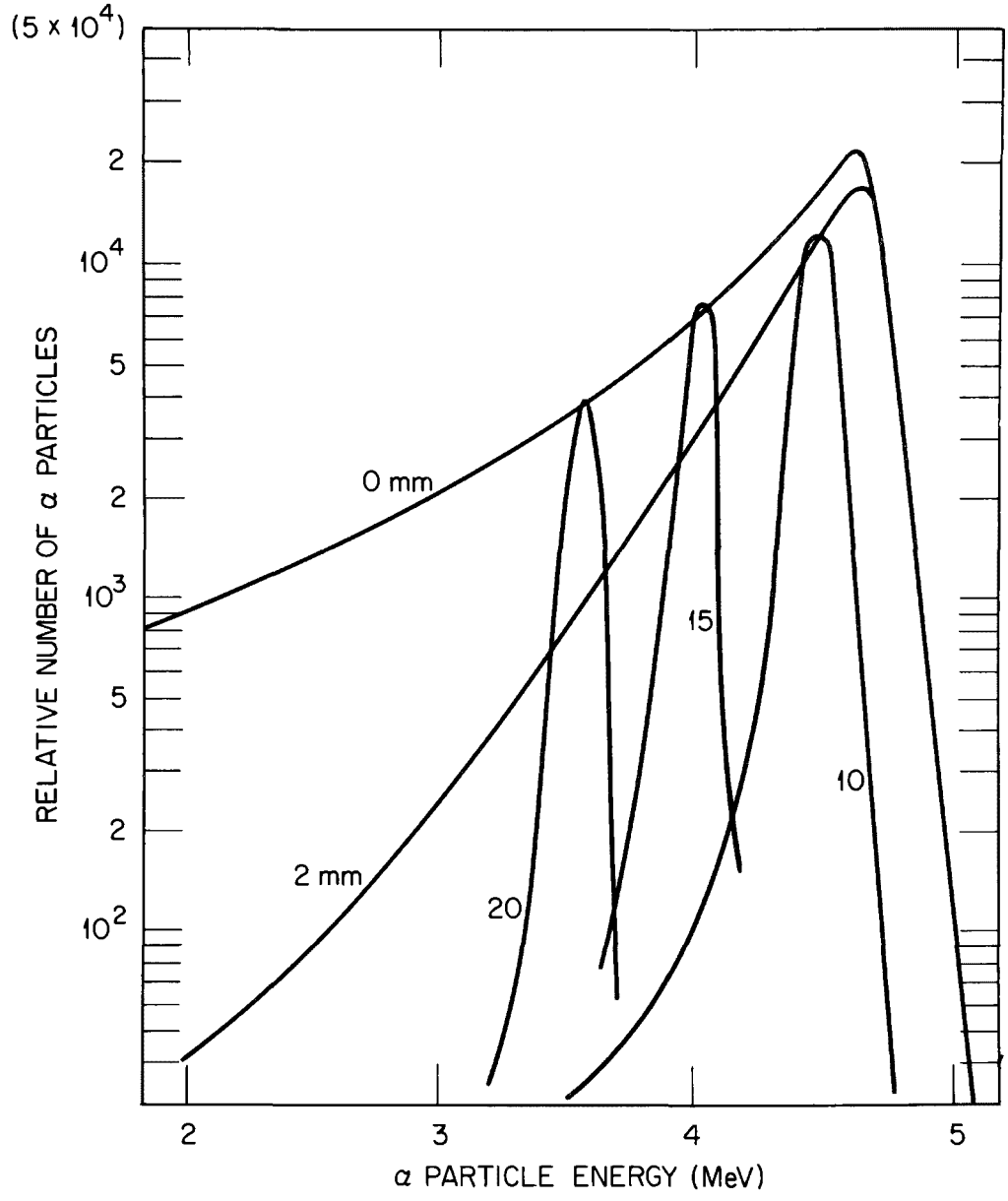

Figure 5. Variation of the original alpha particle spectrum from radon-daughter products as a function of the distance between source and detector in air (Chapuis, *et al.*, 1972).

RADON ADSORPTION BY ACTIVATED CARBON IN URANIUM MINES

J.W. Thomas
Health and Safety Laboratory
U.S. Atomic Energy Commission
New York, N.Y. 10014

Abstract

A brief study was made of the feasibility of using activated carbon to remove radon in uranium mines with the use of a multiple bed-temperature cycling process. Air containing radon is passed through a carbon bed at ambient temperature until the bed is considered exhausted. The bed is then heated to about 120°C and the radon desorbed, using a much smaller volume of air than was used during adsorption. The desorbed radon, after cooling, is passed into a second bed. Since the capacity of the carbon depends primarily on the volume of air passed into it rather than the quantity of radon adsorbed, the second bed will adsorb much more radon than the first. Multiple stages of this process are possible. It was extrapolated from experiments that about 10 liters per minute or more of air could be purified continuously of radon per liter of carbon.

INTRODUCTION

This investigation is a preliminary study of the feasibility of using activated carbon to remove radon in uranium mines. Although radon-daughters are the principal inhalation hazard, rather than radon itself, removal of the daughters alone is unsatisfactory since unacceptable concentration levels of the daughters are rapidly produced from relatively small amounts of radon. At present, the radon-daughter hazard is controlled by high air ventilation rates. This can be quite expensive, particularly for deep mines, since long ventilating shafts and large exhaust blowers are required. It appears, therefore, that alternate methods of control could present an advantage.

The use of carbon to remove radon in mines has been previously considered (Coleman, *et al.*, 1956; Fusamura, *et al.*, 1963; and Schroeder, *et al.*, 1968), but it was concluded that the quantity of carbon required would be excessive. These previous investigations, however, did not consider the possibility of amplifying the capacity of carbon for removing radon by an adsorption-desorption process, such as the multiple bed-temperature cycling process described in this work.

A basic principle of the present process is that the rate of penetration, or breakthrough, of a noble gas through a carbon bed is independent of the noble gas concentration when the gas is present in low concentration. This has been verified for krypton and xenon (Siegwarth, *et al.*, 1972) and for radon in preliminary experiments in this laboratory. It follows from this that a given quantity of carbon will purify a given quantity of air, regardless of the radon concentrations in the entering air.

Let this air cleaning capacity be expressed as Φ volumes of air cleanable by a unit volume of carbon. Hence, if Φ liters of air are passed through a unit volume carbon bed at mine radon concentration, the flow stopped, the radon driven off in $\Phi/10$ liters of air by application of heat, and the effluent cooled and passed into a second bed the same size as the first, the second bed would be able to accept 10 "charges" of enriched radon from the first bed. Hence, the process is said to have an "amplifying factor" of 10; that is, the second bed would have a capacity of cleaning 10 Φ volumes of the original air. Extending the process, a third bed would have a capacity of cleaning 100 Φ volumes of original air, a fourth (Φ = 1,000) volumes, etc. Hence, it is seen that such a multiple bed-temperature cycling process could amplify the radon adsorption capacity of carbon by several orders of magnitude.

It was already known from previous work that a good grade of activated carbon would purify about 1,000 volumes of air of radon per unit volume of carbon (Φ = 1,000). The presence of water vapor and carbon dioxide was deleterious, but not excessively so. Experiments also confirmed that Φ did not depend on the radon concentration. Hence the principal objective of the present work was to ascertain the quantity of air needed in the desorbing step to drive off the adsorbed radon and to determine the amplifying factor, defined as the volume of air cleaned on the adsorption step divided by the air volume used for desorption. If the amplifying factor of the process could be made sufficiently high, without excessive heating and cooling requirements, the process could have practical application.

APPARATUS AND PROCEDURE

The process consists of an adsorption step and a desorption step. In the adsorption step a radon-air mixture is passed into a carbon bed at a known flow rate, radon concentration, and humidity, and the "transmission" vs. time curve determined. This dimensionless, fractional transmission T is defined as the concentration of radon in the carbon bed effluent divided by the influent concentration at any time. Details of the adsorption test apparatus are shown in Figure 1. Radon was generated by bubbling air saturated with water at 1 l/min through a radium chloride solution containing several millicuries of ^{226}Ra. The rate of production of radon was found to be about 900,000 pCi/min. An "aerosol canister" containing two layers of high-efficiency filter paper was used downstream of the bubbler to remove any entrained aerosol from the radium bubbler. The main air supply for the apparatus entered through flow meter F-1 at 69 l/min and was humidified to about 9.0

mg/l by means of the humidifying tubes shown in the figure. The total flow influent to the test chamber was 69 + 1 = 70 l/min, which provided a radon concentration of about 900,000/70 = 13,000 pCi/l. The carbon bed (actually a gas mask canister) was tested at a flow of 56.6 l/min, which was maintained by two flow meters, F-3 at 48.6 l/min and F-4 at 8 l/min. The 8 l/min flow line was needed to measure radon concentrations in the effluent from the test canister. This line was provided with a bypass, so that the total flow of 56.6 l/min could be maintained whether or not a concentration sample was being obtained.

To prepare for an adsorption test, the air flow was turned on through flow meters F-1 and F-2, and about 2 or 3 hours allowed for the establishment of equilibrium conditions. The waiting period is necessary to allow time for accumulated radon in the radium bubbler to be swept out into the hood, and to allow the water in the humidifier to reach an equilibrium temperature. It was found that after the waiting period the apparatus would produce a constant (± 5%) radon concentration for 24 hours/day for a period of days or weeks, with replenishment of the water-level in the water saturators and humidifying tubes every few days. Immediately prior to the test, the input radon concentration was measured at 8 l/min using the two-filter method (Thomas, *et al.*, 1970), sampling from line 1 of the figure. Usually four determinations were taken prior to a test, and four after completion of the test. After establishing the input radon concentration, the canister was attached to line 2 of the figure and the radon concentration in the canister output determined continuously to permit calculation of radon transmission. Transmission curves were plotted from the test data by considering the average transmission obtained over the three-minute sampling period to be the instantaneous transmission at the midpoint of the sampling period.

The carbon bed tested was that of a commercial gas mask canister. This canister contained about 900 ml (400 grams) of activated carbon (Witco Chemicals Co., Type AC-337, 6/16 mesh). This is a petroleum base carbon and has a surface area of about 1,400 m^2/g. The carbon bed in the canister was nearly rectangular, with a cross sectional area of about 60 cm^2 perpendicular to the direction of air flow, and height of about 15 cm in the direction of air flow. Hence, the superficial air velocity through the bed was 56,600/(60)(60) = 15.7 cm/s.

The desorption test apparatus was relatively simple, Figure 2. Heating or cooling air was supplied by a small blower equipped with an electrical resistance heater (Heat Gun Model 301, Master Appliance Corp., Racine, Wis.). This device supplied a blast of air at about 120 l/min, and by means of a variable transformer on the resistance heater of the gun, temperatures could be controlled up to about 250°C. The nozzle of the gun was installed through the side of a 20-liter container and the canister placed inside for heating. A water condenser was placed in the canister effluent line to collect the several grams of water which are evolved in each desorption step. A capillary type flow meter was used to measure flow rate, and a standard wet test meter to register total volume of desorbing air. Two protective canisters in series were inserted downstream of the apparatus as shown in the figure. These canisters permitted confirmation that a second carbon bed would accept many charges of radon from the canister undergoing desorption, and they also prevented evolution of radon into the laboratory.

The desorption procedure was as follows: the canister was removed from the adsorption apparatus and placed in the air bath, pre-set at the desired temperature. Immediately, air from the hot air bath was drawn through the canister at a low flow rate of about 1 l/min. Theoretically, it is inefficient to pull air through the canister while it is still at room temperature, as there is little radon desorption per unit volume of desorbing air and the capacity of the second bed for radon is thereby partially wasted. However, it was necessary to pull air at a low flow through the canister at the start of the heating step; otherwise the gases evolved from the carbon, as it heats up, would go out the canister inlet. As these gases constitute part of the desorbed air volume, their volume must be measured by the downstream wet meter.

After a preliminary heating time of about 15 to 25 minutes, at the low flow rate the air flow through the system is increased to sweep off most of the adsorbed radon from the hot carbon. From the total volume of desorption air and the volume of air cleaned in the adsorption step, the amplifying factor of the process was calculated. The temperature of the carbon in the heating step was not measured directly, but was estimated roughly from the temperature of the air entering and leaving the canister. After the heating period, the canister was removed from the hot air bath and cooled for 15 minutes. The total desorption time, including cooling, was 45 minutes in each test series.

RESULTS AND DISCUSSION

Four series of tests were done using the same canister. The same adsorption procedure, but a different desorption procedure, was used in each series of four to six replicate runs. This method was adopted to obtain transmission curves in each series that were reproducible and not affected by the treatment of the previous test series. Figures 3-6 show the adsorption transmission curves for the four different series. In each of the figures only two of the adsorption runs are plotted. Data from the other runs, except for the first one or two, fell on the same line and show that the process was highly reproducible.

All of the figures show a characteristic shape; the transmission at zero adsorption time is moderate or high; this drops and then again rises with time. The initial transmission in test series MT-2 and MT-4 was greater than unity. This may be understood by consideration of process details. During desorption, the radon concentration in the gas phase of the carbon bed is higher than during adsorption, because of the higher temperature. Hence, if desorption is incomplete and the canister is still warm, the initial adsorption flow can sweep off the high radon concentration and result in transmissions over unity. The initial high transmission could have been avoided by use of more desorbing air, but probably the advantage gained in the adsorption

step thereby would have been more than neutralized by the increased quantity of desorbing air required. In all four series, the flow of desorbing air was in the same direction as it was in the adsorption test. In retrospect, it would have been better to have used reverse flushing which would have effected higher desorption efficiency, since at the end of the adsorption step the radon concentration in the carbon is higher at the inlet of the carbon bed than at the exit.

The transmission curves of each figure were integrated graphically to obtain the fraction F of the total input radon adsorbed by the canister in the 40-minute test period. The quantity of interest is the net amount of air completely cleaned of radon in the adsorption step, since, for example, cleaning X liters of air per minute at 50% efficiency is as effective in reducing ambient radon concentrations as is cleaning X/2 liters per minute at 100% efficiency. The volume of air completely cleaned V_A, was therefore calculated from the flow rate and test time to be

$$V_A = (56.6)(40)(F) = 2{,}264\,F \text{ liters}$$

A summary of results for the four test series is given in Table 1. As previously mentioned, two different flow rates were used during desorption. The flow rates given are approximate, hence, the total desorption volume, V_D, which was measured with an accurate wet test meter, does not agree exactly with the volume calculated from the flow rates. The temperatures listed are those of the air entering the canister (the air bath temperature) and of the air leaving the canister. The latter values have a range, since the air flow was started immediately after insertion of the cold canister into the hot air bath. From these inlet and outlet temperatures it was estimated that the average carbon temperature was about 100°C for the 120°C air bath temperature and 120°C for the 150°C air bath temperature. The last column shows the amplifying factor obtained for the different desorption treatments. Comparison of test series MT-1 and MT-2 shows an improvement of about a factor of 2 in amplification by reducing the desorption air volume from 248 liters to 101 liters. This reduced desorption volume more than compensated for the resulting decrease in net volume of air cleaned in the adsorption step, which dropped from 1,630 to 1,290 liters. Test series MT-3 was done to determine the gain that could be achieved by increasing heat; for an estimated increase of 20°C in average carbon temperature, the amplifying factor rose from 12.8 to 16.1 due to lower transmission on the adsorption step. The last test series MT-4, was done to see if the desorbing air volume could be further reduced without affecting the adsorption transmission curve too adversely. The somewhat lower net volume of air cleaned on the adsorption step was more than compensated for by the decrease in desorption air volume and the amplifying factor increased from 16.1 to 23.4. It seemed apparent that the amplifying factor of the process could be further increased by other modifications of desorbing conditions.

Let us consider the application of the results of test series MT-4 to a hypothetical system containing 4 carbon beds, to estimate the net quantity of air which could be cleaned continuously per liter of carbon. The process is assumed to have three one-liter carbon beds and one two-liter bed, and is designed to clean 60 l/min of air at 80% radon removal efficiency. Two primary carbon beds A and B operate alternately in parallel at 60 l/min during the 45-minute adsorption time, and at an average flow rate of 2 l/min during the desorption time, also 45 minutes. Since the radon removal efficiency is 80%, the net quantity of air cleaned in the adsorption step (V_A) is (60) (0.80) (45) = 2,160 liters. The quantity of desorption air used (V_D) is (45) (2) or 90 liters. Hence, the amplification factor is 2,160/90 = 24. The primary beds A and B are desorbed into bed C, which also contains one liter of carbon. With the amplifying factor of 24, this bed has the capacity to remove 24 charges of desorbed radon over a time period of 24 x 45 minutes, or 18 hours, before requiring desorption. After the 45 minute desorption of bed C, at 2 l/min, beds A and B are put back on stream, with bed C receiving the desorbed radon from beds A and B as before. This system results in beds A and B operating 96% of the time.

Bed D receives one charge of desorbed radon from bed C every 18.75 hours. If it contained one liter of carbon as do beds A, B, and C, it would have an amplifying factor of 24, and a holdup time of 18.75 days. To avoid the necessity of desorbing this bed, it is made to contain 2 liters of carbon and, hence, has a holdup time of 37.5 days, or about 10 radon half-lives. The flow from bed D will, therefore, contain negligible amounts of radon.

The overall process, including the flow from beds C and D, removes about 80% of the radon in 60 l/min of incoming air with the use of 5 liters of carbon. Hence, the net cleaning capacity of this hypothetical system is about 10 l/min per liter of carbon. It seems very probable that optimization of the system, particularly of desorbing conditions, could greatly increase the efficiency of the process. The process was evaluated with the adsorption taking place at room temperature, about 25°C. Better performance would be expected at the lower temperatures existing in mines.

REFERENCES

Coleman, R. D., H. L. Kusnetz, P. F. Woolrich, and D. A. Holaday (1956), *Radon and Radon-Daughter Hazards in Mine Atmospheres*, Amer. Ind. Hyg. Assoc. Quart. 17, 405.

Fusamura, N., R. Kurosawa, and S. Ono (1963), *On the Study of Radon Removal with Active Carbon*, Nippon Kogyo Kai 79, 590. (Sandia Translation SC-T-64-904, Sandia Base, Albuquerque, N. M.).

Schroeder, G. L., P. Groer, M. M. Costello, and R. D. Evans (1968), *Refreshing and Secondary Use of Mine Air*, in *Radium and Mesothorium Poisoning and Dosimetry and Instrumentation Techniques in Applied Radioactivity*, Report MIT-952-5, p. 323, Massachusetts Institute of Technology, Cambridge, Mass.

Siegwarth, D. P., C. K. Neulander, R. T. Pao, and M. Siegler (1972), *Measurement of Dynamic Adsorption Coefficients for Noble Gases on Activated Carbon*; in the Proceedings of the Twelfth Air Cleaning Conference, p. 28. Available from the National Technical Information Service, U. S. Dept. of Commerce, Springfield, Va.

Thomas, J. W. and P. C. LeClare (1970), *A Study of the Two-Filter Method for Radon-222*, Health Phys. 10, 113.

TABLE 1. Summary of Results.

Test Series	Adsorption Step F	Adsorption Step V_A (liters)	Desorption Step Time (min)	Desorption Step Flow Rate l/min	Desorption Step Temperatures In (°C)	Desorption Step Temperatures Out (°C)	V_D (liters)	Amplification Factor V_D/V_A
MT-1	0.72	1,630	15 15	10 16	120 120	30 to 70 75 to 95	248	6.6
MT-2	0.57	1,290	25 5	1 16	120 120	30 to 75 75 to 85	101	12.8
MT-3	0.57	1,610	25 5	1 16	150 150	30 to 85 85 to 100	100	16.1
MT-4	0.58	1,310	25 5	1 6.4	150 150	30 to 85 85 to 100	56	23.4

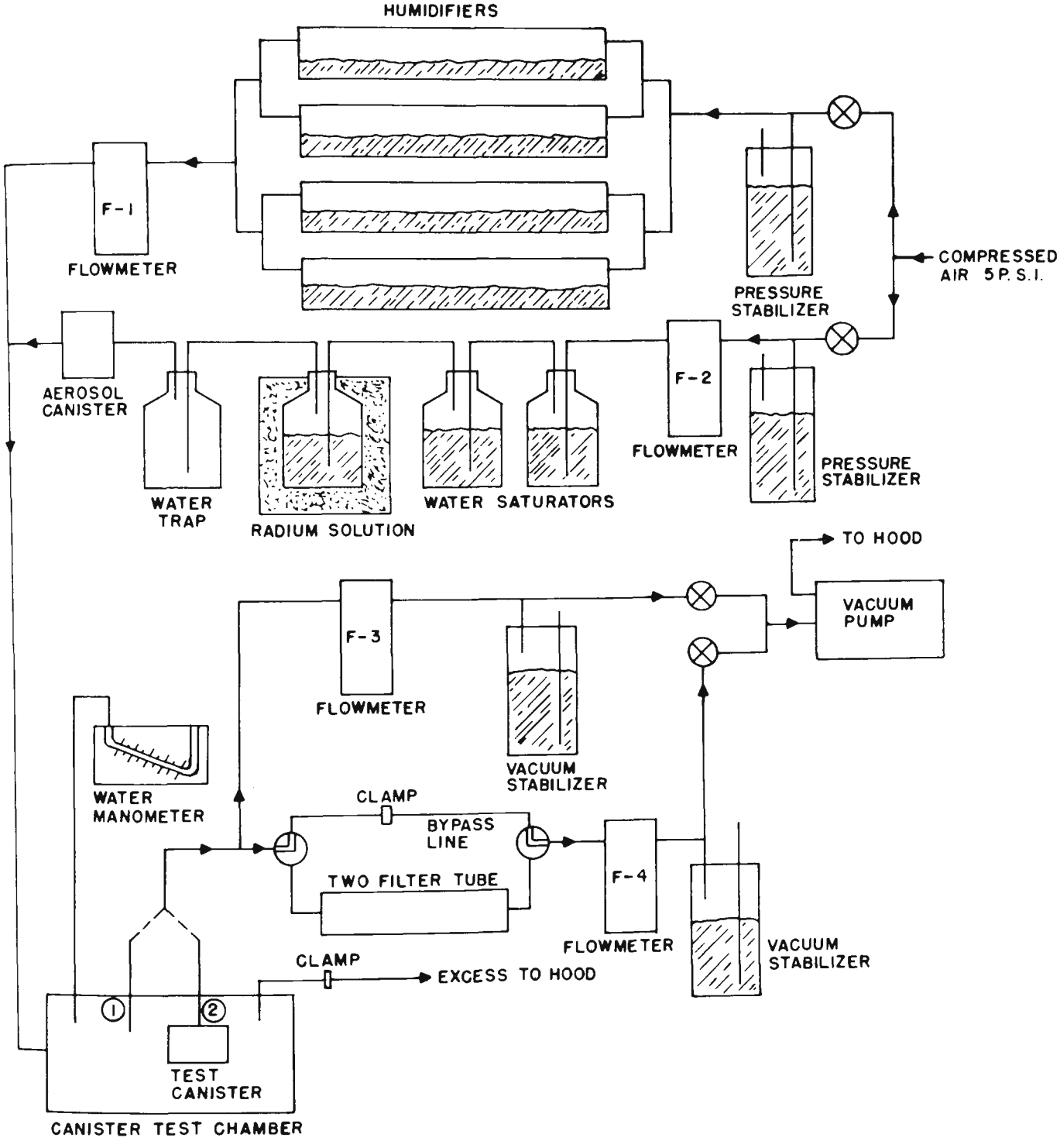

Figure 1. Radon adsorption apparatus.

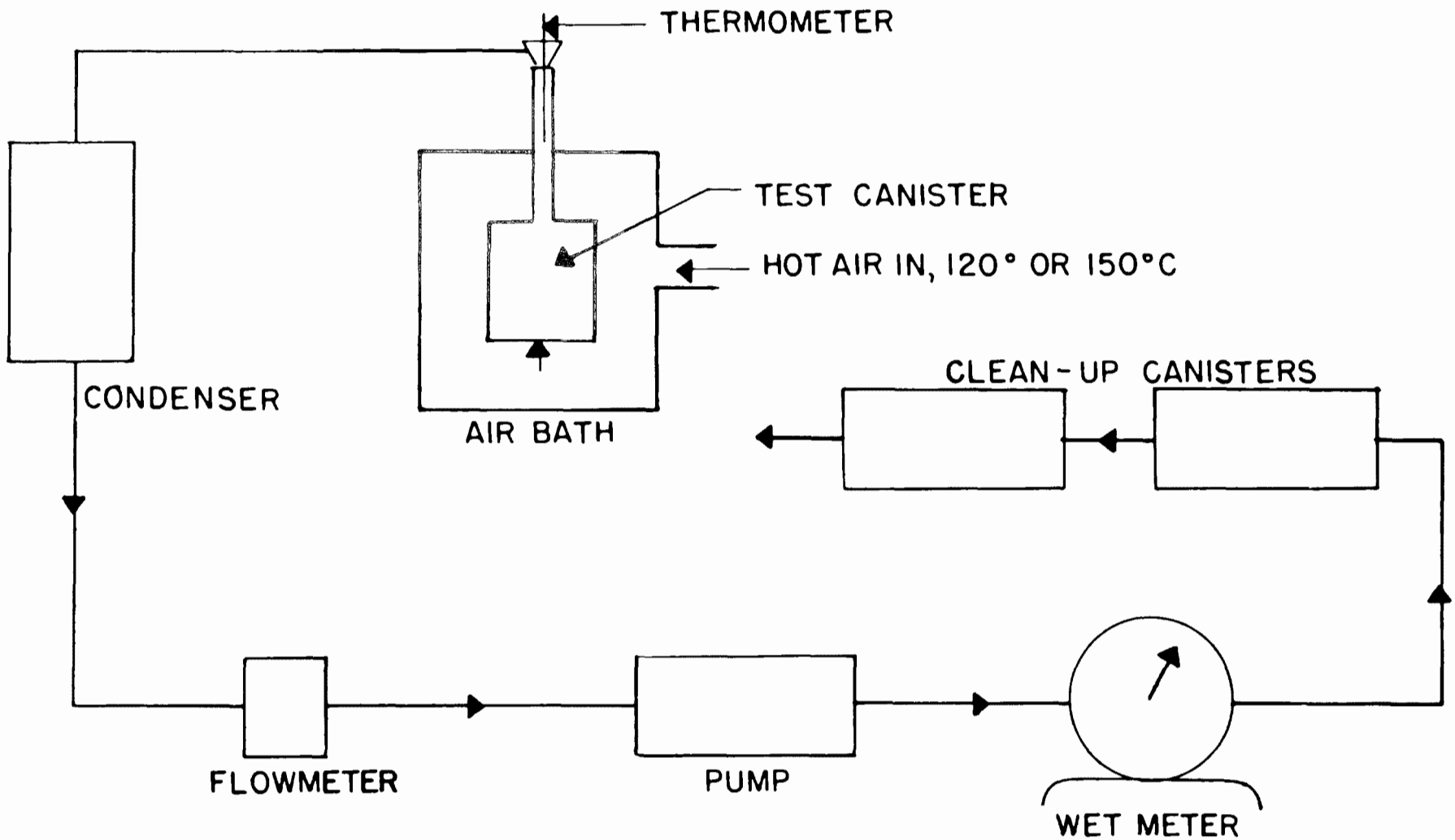

Figure 2. Radon desorption apparatus.

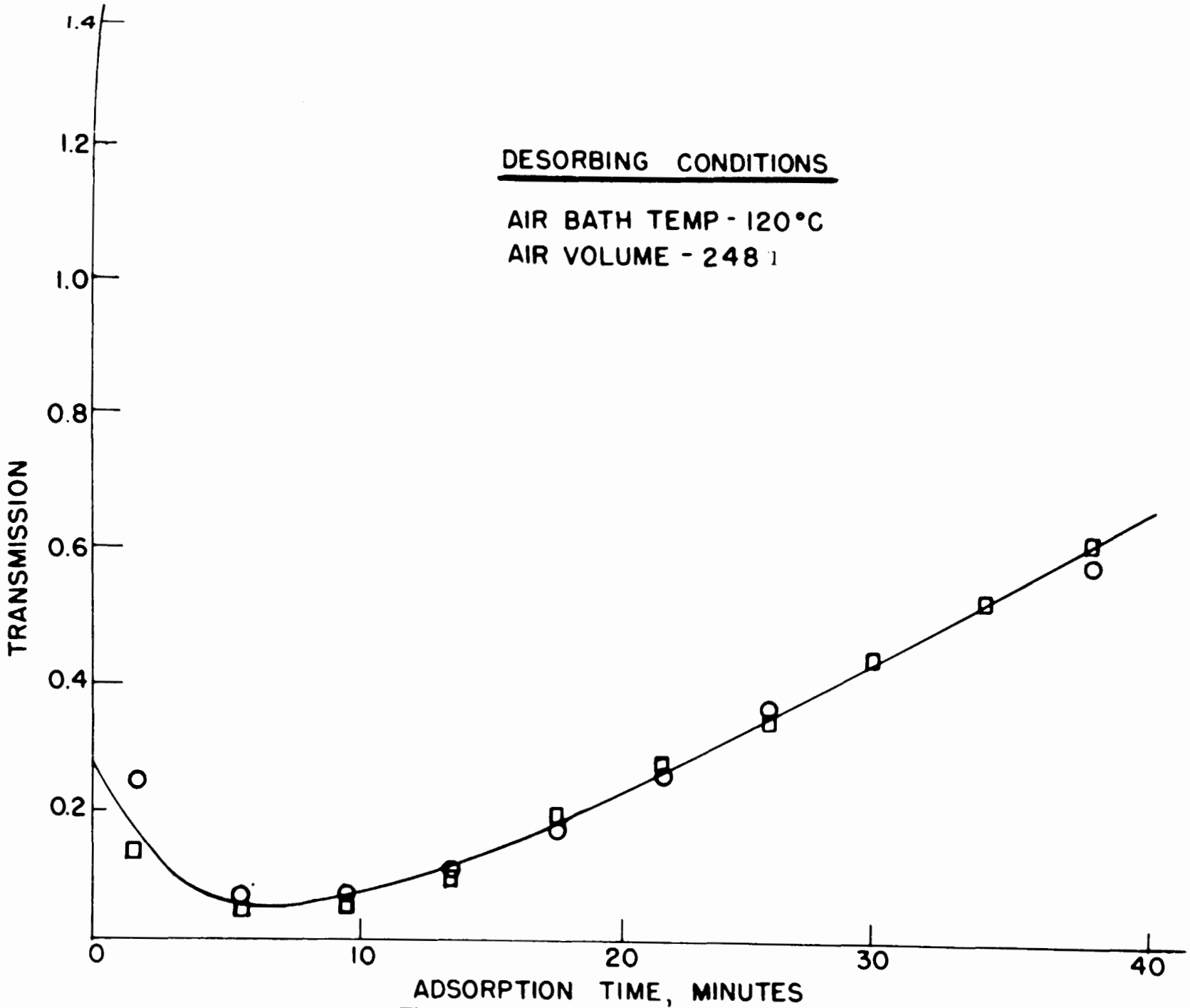

Figure 3. Transmission curve, test series MT-1.

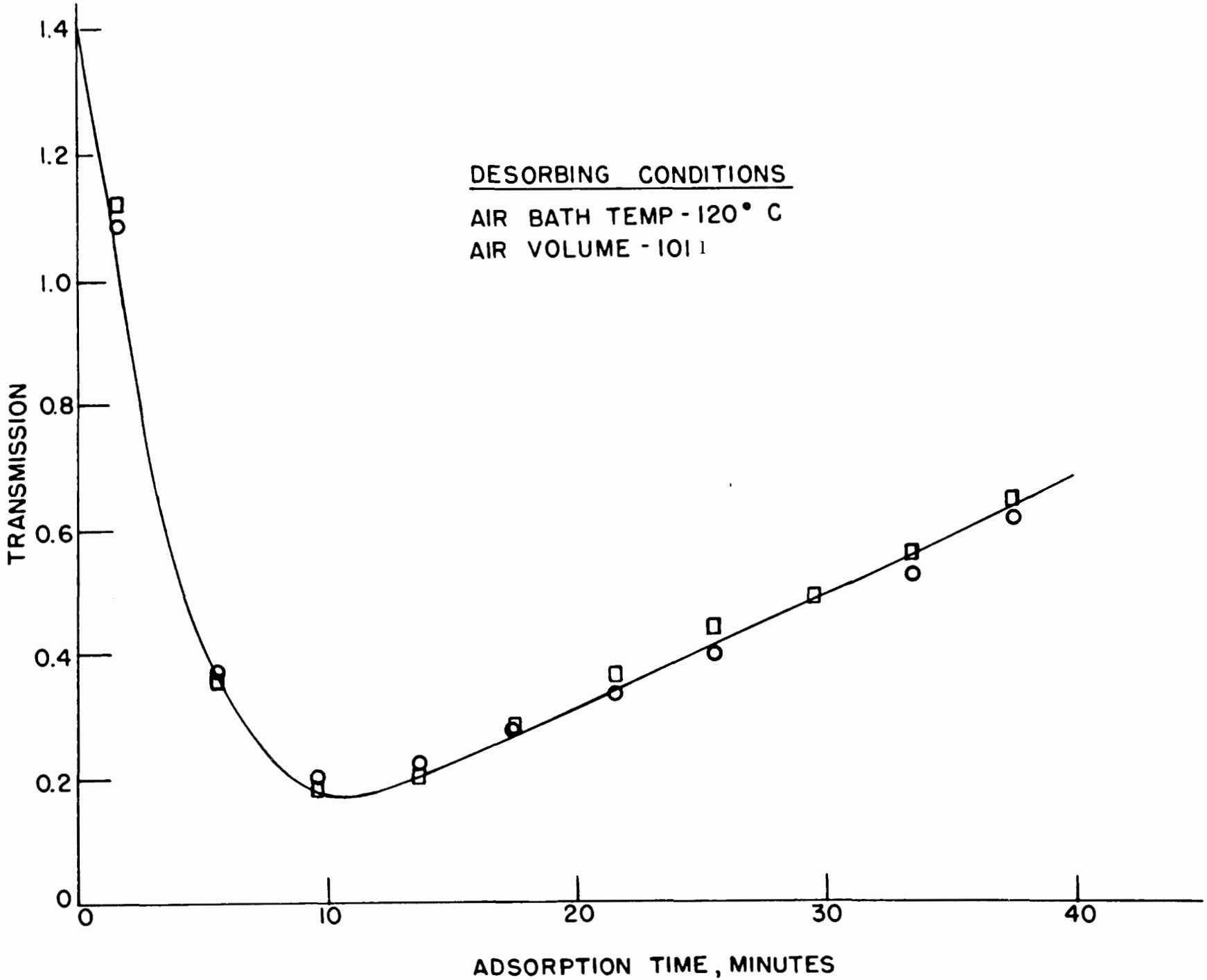

Figure 4. Transmission curve, test series MT-2.

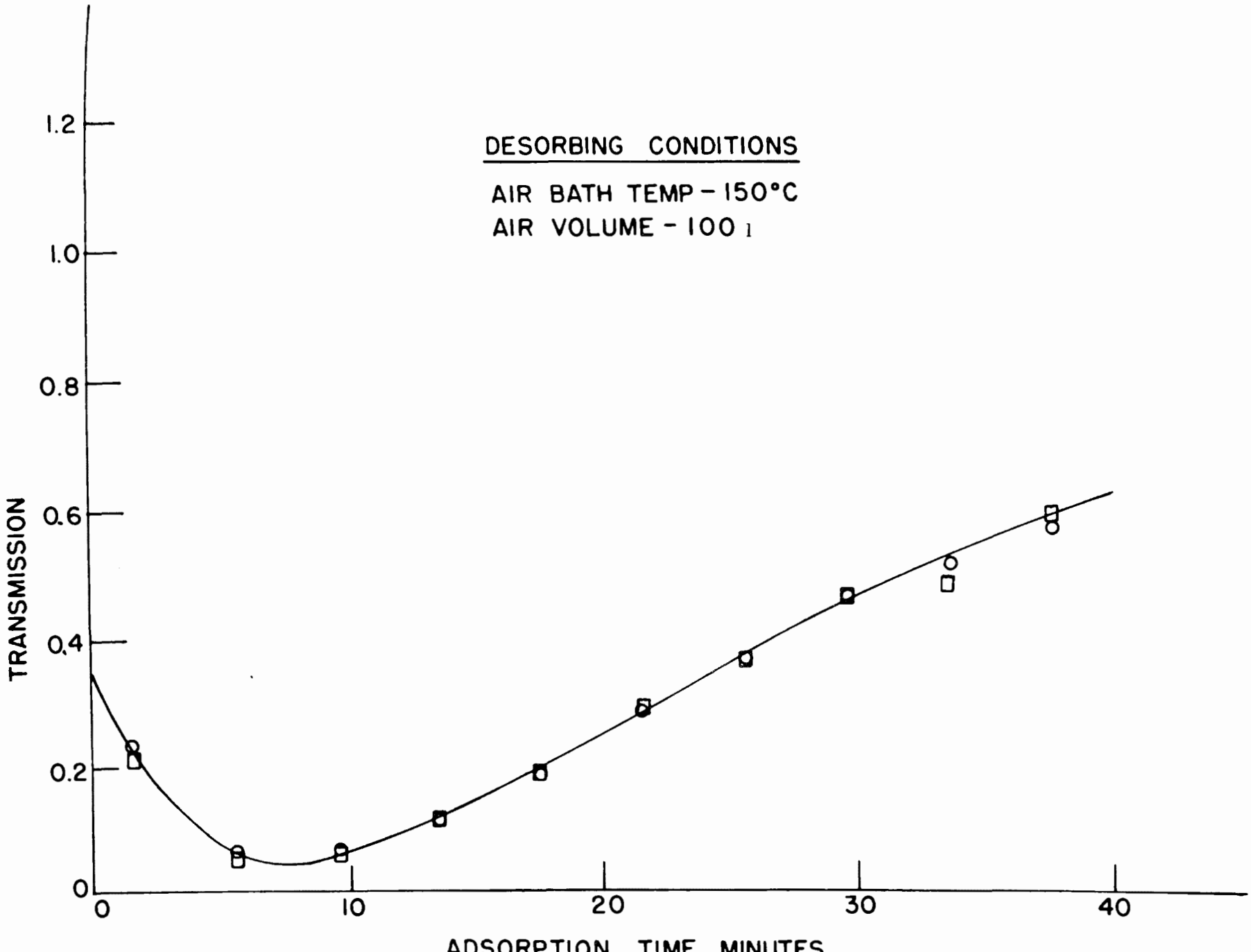

Figure 5. Transmission curve, test series MT-3.

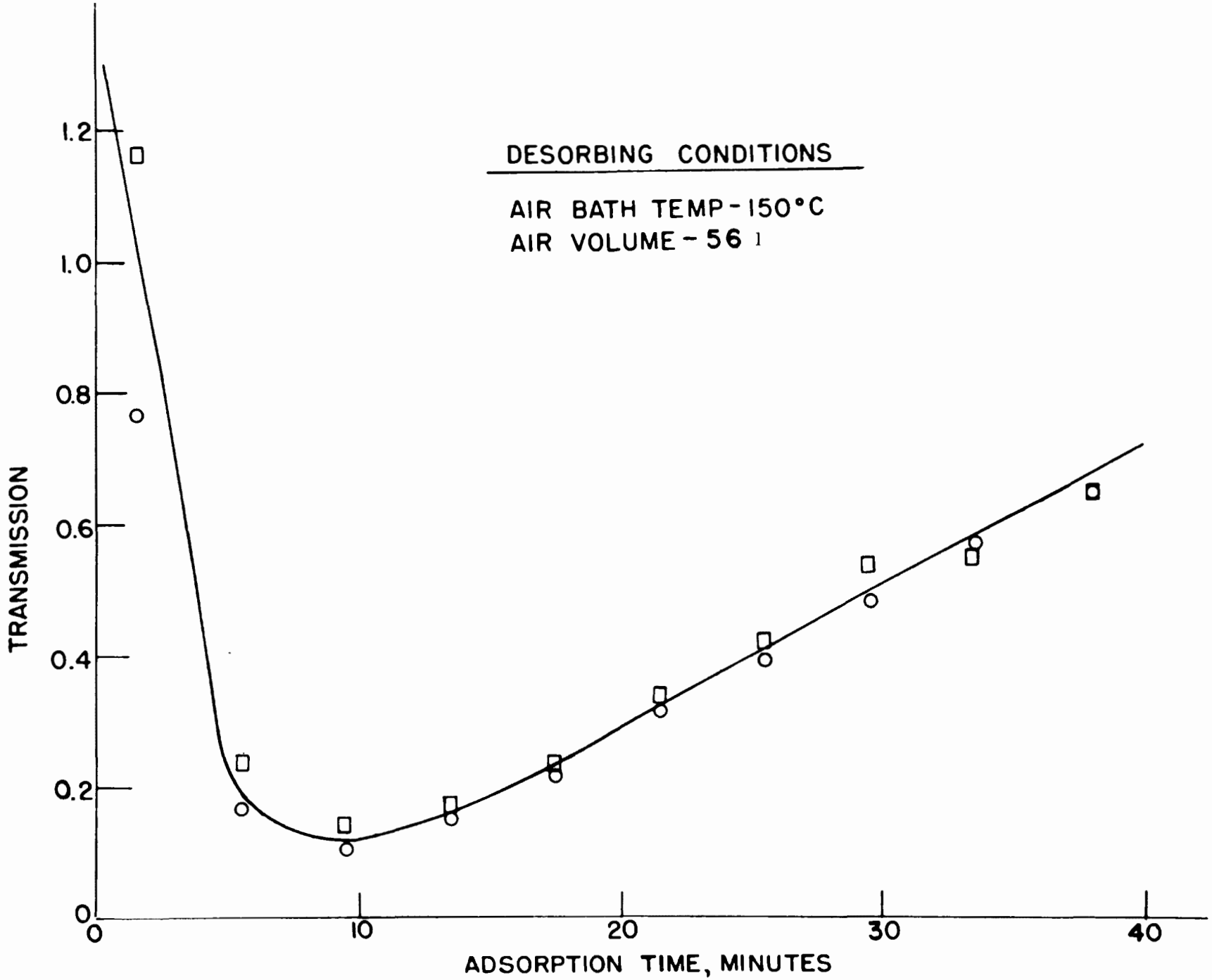

Figure 6. Transmission curve, test series MT-4.

X. Environmental Standards for Noble Gases

ENVIRONMENTAL RADIATION STANDARDS CONSIDERATIONS FOR KRYPTON-85 AND RADON

J. E. Martin and W. A. Mills
Criteria and Standards Division
Office of Radiation Programs
Environmental Protection Agency
Washington, D. C. 20460

Abstract

To ensure adequate public health protection, the Environmental Protection Agency is charged with the responsibility of establishing appropriate standards for controlling radioactive materials in the environment. Two noble gases are presently of interest to EPA, namely naturally occurring radon (radon-222) and fission-produced krypton (krypton-85). To establish standards pertaining to these gases, information on source concentration, source control and effectiveness, and estimates of health effects must be utilized when available. From this viewpoint, the control of krypton emission from nuclear fuel reprocessing plants and the concentrations of radon in natural gas will be discussed.

INTRODUCTION

Two important noble gases associated with the natural existence and use of uranium are radon-222 and krypton-85. Although radon and its decay products have always existed in the world's atmosphere, especially over the land areas, the discovery of uranium fission energy has introduced significant new situations whereby man is exposed to radiation from radon and its decay products. This use and the projected future accelerated use of uranium and its fissile by-products as energy resources result in the creation of krypton-85 and several other noble gases as fission products. In contrast to radon, krypton-85 did not exist, for all practical purposes, in the atmosphere until after the discovery of fission in the late 1930's. This radionuclide is, however, being generated and discharged to the environment at an increased rate because of the growth of nuclear power. The purpose of this paper is to examine some of the more important considerations for environmental radiation standards for these two important noble gases in terms of uses of uranium and by-product material to produce energy.

CONSIDERATIONS FOR KRYPTON-85

1. Environmental Sources of Krypton.

The environmental sources of krypton are all related to nuclear fission. Although spontaneous fission of uranium in the earth may result in trace quantities of krypton-85 in the earth's atmosphere, the first major source of krypton-85 in the environment was the testing of nuclear weapons which began in the late 1940's. Most of the krypton-85 in the environment produced from this source occurred in a relatively short period from about 1956 to 1962. Since most tests have been conducted underground since 1962, the significance of this source has decreased considerably although the krypton introduced into the atmosphere in this relatively short period still persists, decaying with a half-life of 10.7 years. Not all of the weapons-related krypton-85 came directly from the nuclear detonations themselves, but appreciable quantities also resulted from chemical processing of reactor fuel from the production reactors which supported the production of fuel for the weapons program. By about 1962, these activities resulted in an ambient level of krypton-85 in the atmosphere of about 6-8 pCi/m (Ehhalt, *et al.*, 1964).

The largest contributor of krypton-85 to the environment at the present time is the generation of electricity by nuclear fission. Several countries have a nuclear power program. This energy source is expected to increase rapidly over the next several decades with a concomitant increase in krypton-85 levels especially if current control practices continue. With the exception of small amounts retained for radioisotope use, all krypton-85 currently produced eventually finds its way to the atmosphere. The major source is the chemical reprocessing plant which breaks the containment barrier of spent reactor fuel to reclaim unfissioned uranium and other products. The U.S. nuclear industry alone is estimated to produce about 10 billion curies of krypton-85 by the year 2020 (EPA, 1973), all of which would be discharged to the atmosphere under current control practices.

Reactors also routinely discharge krypton-85 to the atmosphere; however, the quantities are small in comparison to those from fuel reprocessing plants. This minimal contribution is attributed to good fuel design which contains most gases until they either decay or the fuel is reprocessed.

Another potential source of krypton-85 in man's environment is that which contaminates natural gas which comes from gas fields developed with nuclear explosives. It is difficult, however, to project the amount of this source at the present time although standards would need to be developed for its use if appreciable quantities of natural gas are developed by this means.

2. Radiation Standards for Krypton-85.

Radiation standards for krypton-85 are currently based on a limitation of 500 millirems per year to the total body of an individual in the general public or a concentration limit which would maintain the exposure to any

individual below this annual dose. For population groups the limit is 170 millirems per year (Fed. Reg., 1967). Because of siting factors and the discharge from tall stacks, all of the sources thus far have been able to meet this standard for individuals on an annual basis, and still discharge all the krypton-85 produced. The result, however, of these discharges has been a gradual accumulation of krypton-85 in the earth's atmosphere since it readily mixes with the atmosphere and distributes over the entire globe. Since the nuclide has a 10.7-year half-life, its persistence in the environment will be for several decades. This factor and the increasing generation of krypton by various sources result in long-term low-level exposure of large populations throughout the entire world.

Because of its rapid dispersion in the earth's atmosphere and the fact that it will expose all individuals in the world at a low dose rate, neither the current perspective or standard based on annual dose to an individual is sufficient to describe or control the public health impact of the discharge of krypton-85 to the environment. The current and proposed expanded development of nuclear energy use which will release long-lived krypton-85 requires, therefore, the development of a broader environmental assessment that encompasses the entire radiological impact of this pollutant. This assessment requires a projection of the migration of the radionuclide through the environment over long periods of time, and a determination of the potential dose to populations (measured in person-rems), and the associated health effects expected to occur throughout this migration. All individual exposures, however small, should be included so that all of the impact on society is assessed, and the exposure of future generations implied by the essentially irreversible environmental commitments should be recognized. The population dose resulting from such an assessment can be termed an "environmental dose commitment". In the setting of standards for such radionuclides, it is important to recognize this long-term radiation risk, in addition to the present one of annual exposures of individuals, and to implement appropriate controls to minimize it.

The environmental dose commitment for krypton-85, estimated to be produced by the nuclear power industry through the year 2020, has been determined (EPA, 1973) and the results are shown in terms of committed health effects in Figure 1. This analysis of the committed health effects is based on the prudent assumption that the public health impact of radiation dose follows a linear hypothesis down to zero. Although it is recognized that data are not available to either prove or disprove this assumption, it provides the only sound basis for developing standards to protect public health. Within this framework, the only totally risk-free level of radiation exposure is zero; a standard set at any other level must be justified on the basis that the activity producing the radiation exposure provides sufficient offsetting benefits. This perspective and others on the risks due to exposures to ionizing radiation were recently analyzed quantitatively by the Committee on Biological Effects of Ionizing Radiation (BEIR Committee) formed by the National Academy of Sciences' National Research Council (BEIR, 1972).

The data in Figure 1 represent the sum of effects for the population within 80 kilometers of projected fuel reprocessing plants in the U. S., the U. S. population, and the world population. Most of the resulting dose and the effects from krypton-85 are due to the worldwide distribution of this source outside the U. S. The doses to individuals outside the U. S. are quite small, usually less than 1 millirem/yr; however, it is the cumulative wide-spread impact on a population this large that results in health effects of this magnitude. The health effects were calculated utilizing the BEIR Committee data and were derived from the total person-rem commitment to the world population over a 100-year decay period after a release occurs. The exposure pathway model was quite straightforward because of the rapid mixing of krypton-85 in the atmosphere; the most significant error, perhaps, is in the estimate of the projected world population over the 150-year period considered.

Standards for controlling krypton-85 from nuclear energy sources should consider the availability of technology, its effectiveness, and its cost in terms of reducing the total population impact of releases of krypton over the time that it can be estimated to persist in the environment. Since fuel reprocessing plants represent the major source of krypton-85, it is the first point to consider control. Several processes can be used to remove krypton-85 from fuel reprocessing plant effluents; however, none of these have been demonstrated on a commercial scale. Sufficient information exists, however, to project the effectiveness of such technologies and the cost of their application as shown in Table 1. Since one fuel reprocessing plant of current design can support 45 to 50 large nuclear power plants, the cost of this control is less than 0.1% of the cost of generating electric power (EPA, 1973). It appears, therefore, that the impact is sufficient and the cost-effectiveness of control is good enough to warrant serious consideration of reducing krypton-85 discharges from fuel reprocessing plants. Reductions of 99% and more appear possible depending, of course, on the performance characteristics of the equipment once installed. Such a 100-fold reduction in the discharge of krypton-85 by the year 1985 would substantially reduce the projected health effects committed from this source as shown in Figure 2. These data indicate quite clearly the effect such control would have on the health effects committed by this source.

Nuclear power reactors also discharge krypton-85; however, the quantities are generally less than 1,000 curies per year per plant (EPA, 1973). The annual dose to an individual in the public from such discharges is less than about 1 millirem and most of this is surface dose to the skin, not to viable tissue or to genetically significant organs. Such discharges result in a 100-year dose commitment of less than 1 person-rem from one year of operation of one of these power plants. The total health effects committed through the year 2000 from nuclear power reactors themselves are generally less than approximately 5 effects (EPA, 1973). Since the technologies to remove krypton-85 at reactors would have to be applied to each individual plant at a cost in the range of 0.5 to 1 million dollars per plant, the public health protection gained does not appear to justify the cost that would be involved.

CONSIDERATIONS FOR RADON

1. Environmental Sources of Radon.

The environmental sources of radon, other than the natural background levels, are directly related to processes which disturb uranium deposits or which remove it from the ground and prepare it for other uses. For example, when uranium is extracted from ore at a mill, more than 99 percent of the ore material becomes the mill wastes or tailings, a slurry of sandlike material in waste solutions which are accumulated to form a tailings pile. More than 97 percent of the radioactive decay products of uranium and about 4 percent of the uranium from the ore remain in these tailings. The concentration of radium-226 in the tailings averages about 700 pCi/g, indicating an inventory of about 56,000 curies of radium-226 in a representative pile. The radon-222 decay product of radium-226 emanates from such a pile at an average of about 500 pCi/m^2-s, representing a total release of radon gas of more than 130,000 Ci/yr. Because of the presence in the tailings of thorium-230, which by its decay maintains the radium inventory, the radioactivity in the tailings will remain almost constant for thousands of years. As of 1970, there were more than 80 million metric tons of tailings occupying more than 2,100 acres of land (EPA, 1973).

The emanation rate of radon from tailings piles is also influenced by whether the pile is wet or dry. If the pile is saturated with water or under water, the water tends to prevent the escape of the radon gas by a factor of about 25. This indicates a release rate of about 22 pCi/m^2-s for a radium concentration of 560 pCi/g. For comparison, the natural background release rate is about 1 pCi/m^2-s in most parts of the U. S.; it may be one hundred times greater, or more, over uranium deposits (Pearson, 1967). The radon release rate at any one location is also known to vary over a factor of 10 due to the effects of weather, i. e., wind speed, barometric pressure, atmosphere stability, rainfall, and snow cover.

A significant source of radon which has received considerable attention is that in underground uranium mines. Although this source represents occupational exposures which are currently controlled by standards, the exhausting of the mines to meet exposure standards represents a concentrated point source of radon and associated decay products which can expose local populations at varying rates.

Radon also exists in natural gas and at concentrations that may be quite high at the point of use if the travel time between the well and the point of use is short. A recent study (Levels, 1972) of radon in natural gas indicates considerable variation in the concentration levels at points of use in the U. S. with an overall average of about 23 pCi/l.

The use of tailings as fill and construction materials represents a rather special source of exposure to the public from radon. The presence of tailings under buildings in the Colorado area has prompted remedial action in several locations because of the public exposures which occur. Most buildings contain materials which emanate radon. Some of these materials, such as various granites, have quite high radon emanation rates. Indoor concentrations due to building material emanation have been found to be typically 3 to 4 times the outdoor levels (Levels. 1972).

The largest source of radon in the environment, of course, is due to the ambient levels produced by the widespread distribution of uranium and its decay products in the earth's crust. The ambient radon level goes through a daily cycle of concentrations ranging from 0.03 to 3.50 pCi/l with the average U.S. level being about 0.3 pCi/l (Pearson, 1967).

2. Standards for Radon-222.

The standards for radon-222 and its decay products are most often given in terms of a working level (WL). One WL is the total potential alpha energy from any combination of short-lived radon-daughters (through RaC') that impart 1.3 x 10^5 MeV per liter of air. This level was first proposed by the U. S. Public Health Service in 1957 as a level which was thought to be safe, yet not unnecessarily restrictive to industrial operations (Holaday, *et al.*, 1957). The Federal Radiation Council and the Environmental Protection Agency (Fed. Reg., 1971 and FRC, 1967) recently recommended that the standard for exposure to miners be 4 working level months per year (WLM). One WLM is the exposure resulting from inhalation of air containing a radon-daughter concentration of 1 WL for 170 working hours.

The working level is often related to radon activity by calculating the number of radon-daughter disintegrations required to impart 1.3 x 10^5 MeV of alpha energy. A concentration of 100 pCi/l radon-222 in secular equilibrium with daughter products RaA, RaB, RaC (RaC') will produce 1 WL. The working level definition is often misunderstood as a unit of radon concentration when, in fact, it is a concentration of only the short-lived daughters RaA, RaB, RaC, (RaC'). It can be applied to any mixture of these decay products. The conversion of 1 WL per 100 pCi/l radon-222 applies only for secular equilibrium of radon and daughters. The guides for control of radon have been primarily oriented towards health protection of uranium miners. These guides have undergone several changes over the years as the potential for lung carcinomas from radon-daughters became better understood. Guides for continuous exposure of the general public vary from 0.3 to 3 pCi/l. The lowest recommendation of 0.3 pCi/1 is derived from ICRP No. 9, par. 72, 1966, (ICRP, 1966). This was derived as 1/30 of the radon-222 guide for continuous occupation exposure. The upper level of 3 pCi/l is derived from 10 CFR 20.

Another instance of protection recommendations for the public is the issuance of guidelines by the U. S. Surgeon General regarding levels at which remedial action should be undertaken to remove tailings from under buildings (JCAE, 1971). The guidelines are directly related to measured working levels inside the structures. At levels below 0.01 WL no action is recommended; at levels above 0.05 WL action should be

considered. In the range between these values it is recommended that all relevant factors be weighted in a decision as to whether to remove the tailings.

3. Public Health Impact.

The public health impact of radon is difficult to determine exactlv because of a number of factors. Pure radon-222 is not nearly as hazardous as radon and its daughters together. Being a noble gas radon does not remain in the lungs and, in addition, radon is not in intimate contact with the tissue. In the event of a disintegration of radon, the alpha energy is likely to be expended into a non-critical area of the lung. Radon-daughters, in particular polonium-218 and polonium-214, which are not noble gas elements, have chemical and physical properties that cause them to be absorbed into the bronchial epithelium of the lung, leading to high dose rates to the region of the lung where tumors arise. Radiation dose caused by radon is therefore a function of the state of equilibrium between radon and its daughters at the time of exposure; it is not enough simply to know the radon-222 concentration alone. Furthermore, the dose rate in air with relatively little particulate matter will be higher from radon-daughters than for rather dirty air because more daughters will be present as ions rather than adsorbed onto particles. In western states where tailing piles are located, and where air is presumably lowest in aerosol concentration of radon-222, the dose rate should be higher than in more industrial areas. Air conditioning may serve the same purpose by removing significant numbers of particles from the air.

The critical biological target in the lung is assumed to be the nuclei of the basal cells of the bronchial epithelium. Alpha particles have a limited range in tissue. To reach the basal cells they must penetrate first a mucus layer, then certain other cells. The bronchial epithelium shows extreme variations in thickness because it tends to fold upon itself. In addition, there is to be expected natural variation in thickness of both the mucus layer and the intervening cells if a population of all age groups is considered. It is therefore a matter of some controversy to determine exactly the depth the alpha particle must penetrate to deliver a critical exposure. Given these difficulties, it should be clear that radon dosimetry does not give a simple correlation between the radon-222 concentration in air and the radiation dose delivered to the lung. Inclusion of all these factors yields a range of conversion factors relating air concentration and lung dose. The factor that appears most suitable for general environmental exposure conditions appears to be that a steady concentration of 1 pCi/m^3 of radon in air will produce 4 millirem to the lung.

Uranium tailings piles represent an unusual radiation exposure situation for the public. Even though such piles are currently stabilized after they are filled by covering them with soil and plantings of some sort, they can be expected to emanate radon at a rate close to that from a dry pile. Since the piles contain radium with a half-life of 1620 years, their emanation will continue for thousands of years. The radium will also be replenished by the decay of thorium-230. Such piles represent, therefore, an irreversible source of environmental contamination to the atmosphere of local areas by radon-222 and its decay products. Data from two representative piles are shown in Table 2 which indicate that the lung doses of individuals near the piles can be quite substantial. The health effects committed to surrounding populations can be expected to be significant if estimated for long periods of time.

The only control method currently used for tailings piles is to stabilize them; however, this procedure only affects erosion of other radioactive materials. Perhaps the only controls that would appreciably affect the amount of radon and daughters entering the environment over the long-term from the use of uranium in nuclear energy programs would be to return the tailings deep underground to contain radon emanation or remove radium (the radon precursor) in the uranium mill. Neither the cost nor the effectiveness of either of these methods is known at the present time. In view of the radiation exposures over the long-term, however, it appears prudent to further consider methods of reducing the discharge of radon from uranium mill wastes.

SUMMARY

Both krypton-85 and radon-222 and its resultant daughters represent long-term health effect commitments as a result of current practices in the use of uranium and its by-products as an energy resource. New standards and concepts which recognize and control long-term environmental dose commitments are needed for each of these radionuclides. Effective controls can be required at reasonable costs for krypton-85 at fuel reprocessing plants, the major source of environmental levels of krypton-85 in the future. No such controls have been developed, however, for the discharge of radon from mine shafts or tailings piles, although future consideration of methods to limit such discharges to the environment appear warranted. Natural gas contaminated by krypton-85 is difficult to control, but as yet no new standards appear to be required. Radon-222 and its daughters in natural gas should receive further emphasis with regard to controlling the levels that exist at the point of use.

REFERENCES

Effects on Populations of Exposure to Low Levels of Ionizing Radiation, The, **(1972)**, Report of the Advisory Committee on the Biological Effects of Ionizing Radiations (BEIR), National Academy of Sciences, Washington, D.C.

Ehhalf, D., K. O. Munnich, W. Roether, J. Scholoch, and W. Stich, (1964), *Krypton-85 in the Atmosphere,* Proceedings of the Third International Conference on the Peaceful Uses of Atomic Energy, 14:45-47.

Environmental Analysis of the Uranium Fuel Cycle — Part I (Fuel Supply), Part II (Nuclear Reactors), Part III (Fuel Reprocessing), **(1973),** Report No. EPA-520/9-73-003, Environmental Protection Agency, Washington, D.C.

Environmental Protection Agency, (1971), *Underground Mining of Uranium Ore,* Radiation Protection Guidance for Federal Agencies, Fed. Reg., 36, 101.

Federal Radiation Council, Radiation Protection Guidance for Federal Agencies, (1967), *Memorandum for the President,* Fed. Reg., 32, 147.

Guidance for the Control of Radiation Hazards in Uranium Mining, **(1967),** Report No. 8 revised, Staff Report of the Federal Radiation Council.

Holaday, D.A., D.E. Rushing, R.D. Coleman, P.F. Woolrich, H.L. Kusnetz, and W.F. Dale, (1957), *Control of Radon and Daughters in Uranium Mines and Calculations on Biological Effects,* Public Health Service Publication, No. 494.

International Commission on Radiological Protection, (1966), *Recommendations of the International Commission on Radiological Protection,* Adopted September 17, 1965, ICRP Publication 9, Pergamon Press, London.

JCAE Hearings, (1971), *Use of Uranium Mill Tailings for Construction Purposes,* October 28 and 29, 1971, p. 52.

Pearson, J. E., (1967), *Natural Environmental Radioactivity for Radon-222,* Environmental Health Series, Public Health Service Public No. 999-RH-26.

A Report of the United Nations Scientific Committee on the Effects of Atomic Radiation for the General Assembly, (1972), *Ionizing Radiation: Levels and Effects,* Vol. 1: Levels, United Nations, New York.

TABLE 1. Summary of Health Effects and Costs of Krypton-85 Controls for a 5 MT/Yr Fuel Reprocessing Plant.

Removal System	Cost	Health Effects Averted
Cryogenic Distillation	$11.5 million	270[1]/
Cryogenic Absorption	$12.1 million	270[1]/
Freon Adsorption	$ 6.4 million	270[1]/

1/∿ 60% mortality expected from induced cancers and other serious effects.

TABLE 2. Public Health Impact of Dry Tailings Piles.

	GRAND JUNCTION	SALT LAKE CITY
Ra-226 (Ci)	1.700	1670
Ra-222 (Ci/yr)	5,600	13,500
Size (acres)	55	107
Doses (mrem/yr)*		
Background	2400	620
Avg. Individual	800	380
Max. Individual	3200	1140
At 1 km	320	760

*Dose conversion factor of 1 pCi/m^3 radon-222 =4 mrem/yr.

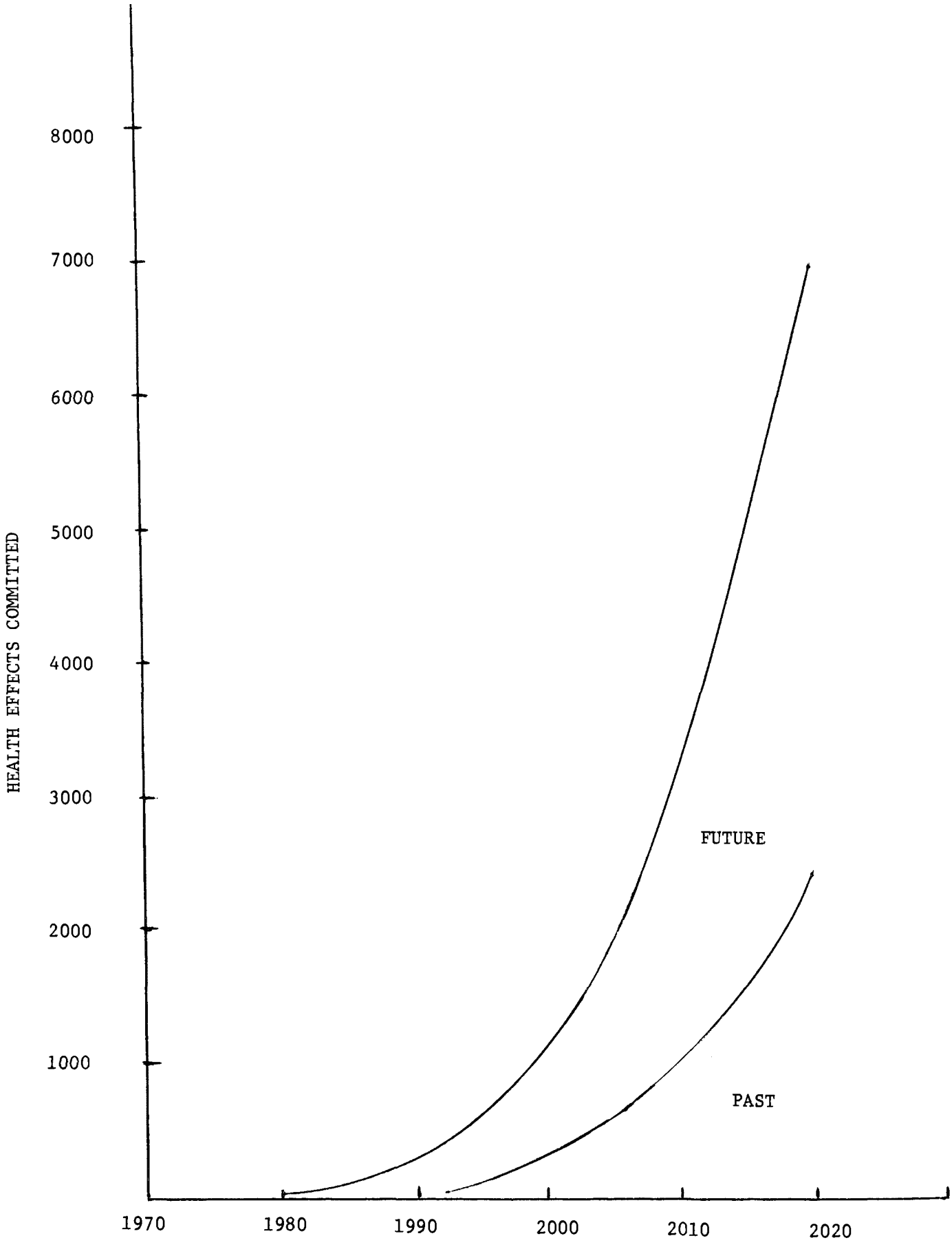

Figure 1. Estimated Past and Future Health Effects Committed by Krypton-85 Releases from the United States Fuel Reprocessing Industry.

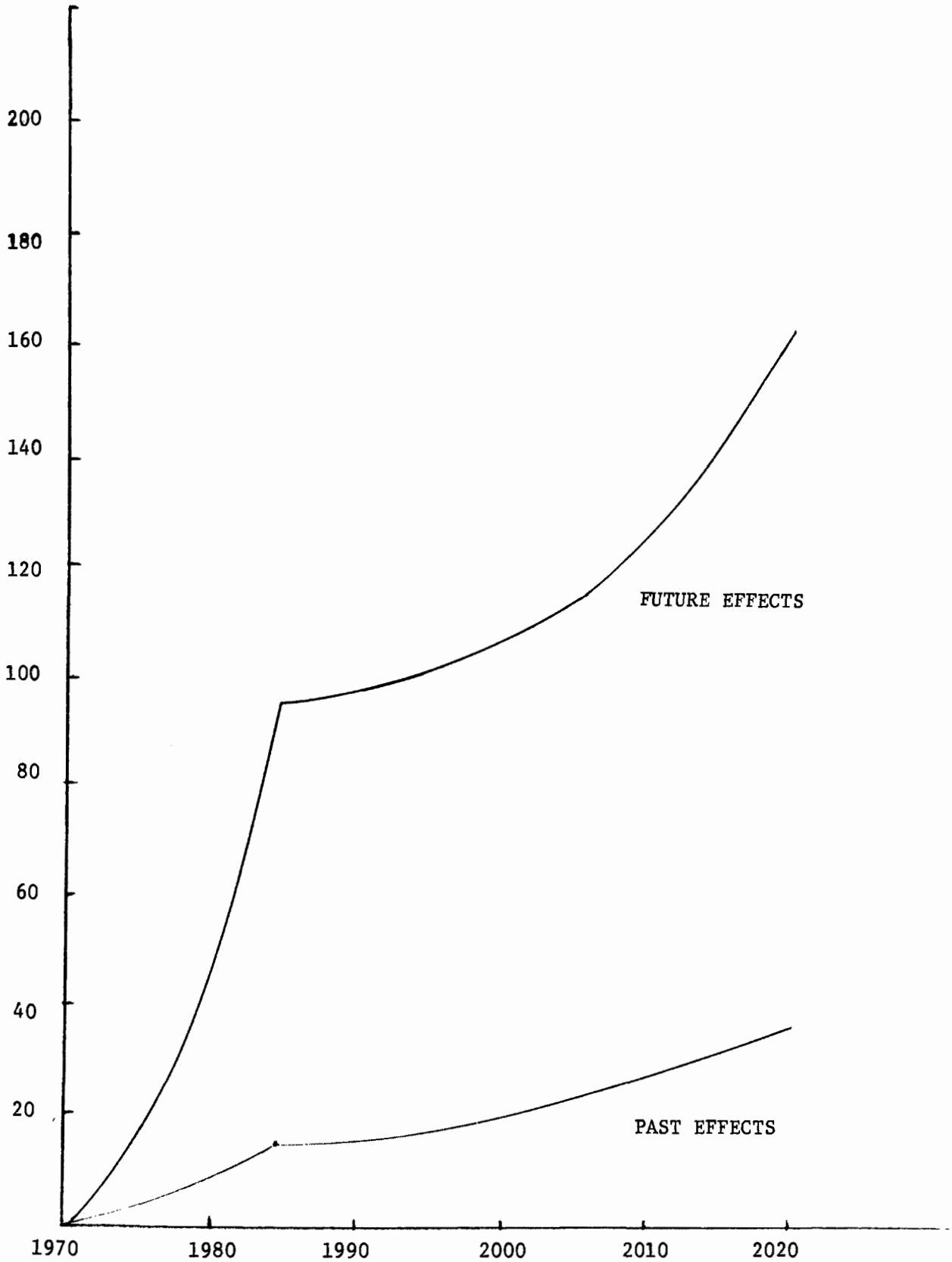

Figure 2. Estimated Past and Future Health Effects Committed by Krypton-85 Released from the U. S. Fuel Reprocessing Industry, with 99% Removal.

CONSIDERATIONS IN SITING LONG-TERM RADIOACTIVE NOBLE GAS STORAGE FACILITIES*

J.J. Cohen and K.R. Peterson
Lawrence Livermore Laboratory
University of California
Livermore, California

Abstract

Projections of future fission reactor capacity indicate that the present practice of releasing radioactive noble gases (primarily krypton-85) to the atmosphere cannot safely be allowed to continue indefinitely. Ongoing research programs are developing methods of extracting and concentrating these waste gases so they may be stored for extended periods, thereby allowing them to decay to relatively safe levels.

Anticipating the need for facilities specifically designed for long-term storage of noble gases, we have reviewed some factors which might be considered in developing optimum siting criteria. Among these factors are, above- vs. below-ground storage, meteorology, geography, and demography. The objective used in these considerations is minimization of resulting population doses, both long- and short-term, from a major release, either "instantaneous" or "continuous," from the various facilities.

Those sites considered are remote islands, continental shorelines, mountain tops, deep water, and inland low-population-density areas.

Assuming an equal probability of containment failure at each of the site options, we conclude that siting is relatively inconsequential for long-term population doses. Siting, however, is important for short-term exposures to local populations, especially where there might be a possibility of exceeding Radiation Protection Guides. The relative significance of long- vs. short-term doses resulting from exposures to radioactive noble gases is also discussed.

INTRODUCTION

Of those noble gases produced in nuclear reactor operations, only ^{85}Kr is considered to have significant long-term health effects because of its chemical stability, long half-life, high production rate, and its relative hazard. Figure 1 gives the projected production rate and total accumulation for ^{85}Kr through the remainder of this century (ORNL, 1970).

In normal operations, only minute quantities of ^{85}Kr are released at the reactor itself. Almost all of the ^{85}Kr is released at nuclear fuel reprocessing plants during the chopping and dissolving operations. At present, essentially all of this gas is released to the atmosphere. Figure 2 shows the projected individual dose rates for both skin and whole body resulting from exposure to accumulated ^{85}Kr, assuming present practices of atmospheric release are continued. At current levels of reactor operation, this practice is considered to be acceptable; however, based upon projections for future reactor usage and resultant exposures, it appears to be the general consensus that the practice cannot be allowed to continue indefinitely. Figure 3 shows the projected worldwide population dose based on data from the previous figure plus predicted world population growth (UN, 1966). The point at which measures to prevent the release will become necessary has not as yet been defined, but it appears reasonable to assume that sooner or later the routine release of ^{85}Kr to the atmosphere from fuel reprocessing plants will be prohibited.

COST-BENEFIT ANALYSIS

The application of cost-benefit analysis can be used to gain some insight into the advisability of instituting preventive measures. Table 1 gives some data on the effects of ^{85}Kr atmospheric releases. These data have been derived by assuming the following:

(1) Concentration-to-dose conversion factors have been calculated from data given by Dunster, *et al.*, (1970). These are 1.4×10^4 and 2.1×10^6 rem/yr per Ci/m^3 for whole body and skin, respectively.

(2) The mass of the atmosphere is taken to be 5×10^{21} gm, which at conditions of standard temperature and pressure occupies a volume of 4.2×10^{18} m^3 (USGS, 1967).

(3) For this cost-benefit analysis we assume that the released ^{85}Kr mixes instantaneously with the entire atmosphere to a uniform concentration. The significance of atmospheric diffusion of released gas to the point of uniform mixing will be discussed later in this paper.

(4) The only process by which atmospheric levels of ^{85}Kr are diminished is by radioactive decay. Therefore, the mean atmospheric residence time for ^{85}Kr is essentially its mean radiological life, approximately 15.5 yrs. This implies that there is no sink in nature that removes ^{85}Kr and renders it biologically unavailable.

It can be determined from these data that the total whole body dose resulting from each curie of ^{85}Kr released to the atmosphere will average

$$\frac{1.4 \times 10^4 \ \frac{\text{rem-m}^3}{\text{Ci-yr}}}{4.2 \times 10^{18} \ \text{m}^3} \times 15.5 \text{ yrs} = 5.2 \times 10^{-14} \text{ rem/Ci.}$$

**Work performed under the auspices of the U. S. Atomic Energy Commission.*

Determination of total population dose is based on an assumed uniform exposure to the entire world population taken as 3.5 billion people. Therefore, the total population dose integrated to infinite time is 1.8×10^4 man-rem per curie for whole body and 0.027 for skin.

The monetary cost for biological damage due to radiation exposure has been estimated by various authors to be somewhere in the low hundreds of dollars per man-rem (Cohen, 1973). For purposes of this report we have assumed a cost of $250 per man-rem for whole body exposure. For skin exposure this value is estimated at approximately $40 per man-rem, based on the ratio (factor of 6) between the ICRP maximum permissible dose (MPD) criteria for whole body and skin (ICRP, 1966). This implies that roughly equivalent damage is done to an individual by his exposure to MPD levels of either 0.5 rem/yr to the whole body or 3.0 rem/yr to the skin. Using these data, one may estimate the cost for biological damage due to ^{85}Kr based on either whole body or skin exposure to be roughly $0.05 or $1.00 per curie, respectively. Essentially this implies that skin may be considered to be the critical organ for ^{85}Kr exposure. For each curie released to the atmosphere, the resultant biological damage cost to all humanity over all time is approximately one dollar. Expenditures for prevention of ^{85}Kr release in excess of this figure would therefore not be considered to be cost effective.

RELEASE PREVENTION COSTS

Having estimated the effect of ^{85}Kr release, we shall next estimate the cost of release prevention. Continued research has been performed on methods for ^{85}Kr removal and storage. Other papers given in this symposium deal extensively with this topic. Estimates on ^{85}Kr treatment costs have been provided by Slansky, *et al.*, (1969), Davis (1973), and Davis, *et al.*, (1973). From these data we can conservatively assume that for a 1,500 ton/yr fuel reprocessing plant, ^{85}Kr treatment facilities can be installed at a capital cost of $2,000,000 and operated at a cost of $200/ton of fuel processed. Further, assuming a plant life of 20 yrs, an interest rate of 12%, and a content of 10^4 Ci of ^{85}Kr per ton of spent fuel, we calculate a prorated capital cost of approximately 2¢/Ci and an operating cost of 2¢/Ci, giving a total cost of 4¢/Ci for ^{85}Kr release prevention. Using this estimate, we have performed the cost benefit analysis shown in Table 2. Comparing estimated biological damage costs against release prevention costs, we derived a cost benefit ratio of roughly 25. This analysis also allows us to estimate the cost effectiveness for ^{85}Kr treatment to be $220/man-rem of whole body dose averted, or roughly $1.50 for each man-rem of skin exposure averted. To gain some perspective on the significance of these figures, we can compare them with cost estimates for other activities. As previously discussed, a suggested guideline for cost effectiveness is considered to be $250/man-rem of whole body dose averted, and $40 /man-rem of skin dose averted. Hull (1972) has estimated a cost of between $1,000 and $1,000,000/ man-rem averted as the cost for compliance with the currently proposed light-water reactor standards. It appears from these figures that, even under present conditions, it would be reasonable to require implementation of measures to prevent the release of ^{85}Kr from fuel reprocessing plants. Such a requirement certainly seems consistent with "as low as practicable" guidelines, especially when compared to the proposed standards for light-water reactors.

STORAGE OPTIONS

In any event, whenever prevention of atmospheric release becomes a requirement, some options for the accomplishment of this objective must be evaluated. These are diagrammed in Figure 4. Having decided to retain rather than release ^{85}Kr, we must consider whether to do so in some concentrated form or to retain the entire off-gas volume in which it is carried.

Another option is whether or not to store the gases at the surface or at an underground storage facility. The main trade-off here is between greater assurance of retention plus easier surveillance at surface facilities as opposed to lower cost for underground storage.

Finally, we must decide whether to store the retained gas at the point of collection or to transport it a centralized facility specifically designed for long-term storage. Selection of the best options will depend on prevailing costs and political attitudes at the time the decision is made. At such time, a thorough cost-benefit analysis of the various options should, of course, be made. We shall not attempt such an analysis here. For purposes of this study we shall assume that ^{85}Kr is extracted from fuel reprocessing offgas streams and stored in pressurized tanks at a centralized facility for the extended periods of time necessary to allow for decay to innocuous levels. This assumption would appear to be consistent with present AEC philosophy as expressed in its nuclear waste management policy, in which storage of solidified high-level waste at centralized repositories is required (Fed. Reg., 1970).

SITING CRITERIA

Anticipating the need for some centralized radioactive noble gas storage facility, we have reviewed some of the factors that might be considered in developing optimum siting criteria. The facility we envision will be used for the receipt and long-term storage of pressure tanks of extracted noble gas that have been collected at various fuel reprocessing plants throughout the country and perhaps the world. From the work of Dunster, *et al.*,(1970) and from various other considerations, it would seem reasonable to assume that each tank or container of gas would initially contain approximately 1 MCi of ^{85}Kr. On this basis, roughly 20 containers per year would be generated at present, and by the turn of the century this figure would rise to approximately 80 containers per year. At 1 MCi per container, the output of decay heat would be no more than 1.6 kW, which should prove to be quite manageable, with cooling accomplished either by submersion of the containers in water or by maintaining sufficient air flow in the storage area to dissipate this heat by convection.

In determining safety criteria for siting the storage facility, we have assumed that in normal operation there would be no routine releases of radioactive gas. The only assumed mechanism for release would be from accidental or inadvertent containment failure.

With the possible exception of sabotage, we do not consider the simultaneous leakage of more than one container to be credible. If massive multicontainer leakage were a major concern, then the entire concept of centralized storage would not be prudent, since this would constitute a policy of "putting all one's eggs in one basket." For purposes of radiation safety, therefore, the siting criteria that we have selected assume the leakage of 1 MCi of ^{85}Kr over a relatively short period of time. The siting objectives are twofold: first, to assure that in the event of such leakage, no individual at or near the fence line receives a dose in excess of MPC standards; and, second, to minimize resultant total population doses.

MAXIMUM ACCIDENT DOSES

To evaluate fence line dose criteria, we have calculated the total leakage required to exceed maximum permissible dose criteria for both accident and routine conditions, conservatively assuming a dilution factor (X/Q) of 10^{-6} sec/m^3 between the point of release and the fence line. The results of these calculations are given in Table 3. From these data we conclude, that even for routine release conditions, one may release as much as 45 MCi without exceeding the 3 rem skin dose at the fence line. Therefore, our assumed maximum container capacity of 1 MCi appears to be well within these limits.

POPULATION DOSE CONSIDERATIONS

Our second radiation safety criterion is that in the event of leakage, total population dose (man-rem) will be minimized. With this objective in mind, geographic siting becomes critical. A number of factors, all of which are to some extent interrelated, determine the type of storage site that will minimize population dose in the event of an accidental release. These are:

1. Meteorology.

Meteorology — or, more precisely, the diffusion climatology of the area surrounding the storage site — determines the rate of dilution and the resultant effluent concentrations as a function of time and distance from the release site. Rapid diffusion accompanied by lower individual doses is favored by those locations experiencing a combination of the following factors:

(a) Strong surface winds, relatively variable in direction.
(b) Strong daytime heating resulting in neutral or unstable temperature lapse rates.
(c) A relative absence of night-time temperature inversions.
(d) A site that is elevated with respect to surrounding locations.

2. Geography.

Geographic factors that would tend to affect potential population dose are:

(a) The distribution of population with respect to the storage site.
(b) Topographical features that would affect the rate of dilution of effluents prior to their arrival at population centers.

POTENTIAL SITES

From these considerations we have chosen to consider five hypothetical storage sites within the jurisdiction of the United States. These sites are evaluated on the assumption that a 1 MCi release of ^{85}Kr occurs over a period of a few days or less. It is further assumed that the release occurs at a time when the surface wind direction is the most probable one for the particular site. The hypothetical sites selected for evaluation are:

1. A Remote Island Site.

Because of its relatively low population and distance from any major population center, Johnston Island, southwest of Hawaii, was chosen as a hypothetical site. The Marshall Islands, over 1000 km distant, are the most likely point of first exposure, since surface winds in this area blow consistently towards the west. In our analysis we assume that before reaching the Marshall Islands, the plume of ^{85}Kr would loop into the middle-latitude westerlies and then move toward the east.

2. A Coastal Site.

Cape Hatteras, North Carolina has been selected as a hypothetical site since the prevailing winds at this location are usually offshore, but are not as directionally persistent as those at Johnston Island. Although our primary evaluation is based on most probable meteorological conditions, we have in this case also performed a calculation assuming onshore winds.

3. A Remote Desert Inland Site.

The Fort Irwin Military Reservation in the Mojave Desert of California was selected as a hypothetical site in this category. There are no population centers within 150 km in all directions. The average winds are toward Nevada; a "worst case" would occur with winds toward Los Angeles. Dose estimates are presented for both cases.

4. A Mountain Top Site.

Mt. Whitney, California was selected as a hypothetical site in this category. We have assumed that an all-weather road could be built to the summit and that the storage facility could be sited there at an elevation of approximately 4,400 m. The advantage of an elevated site, of course, is that it would allow for a maximum turbulent mixing of an effluent plume prior to its arrival at any population center. Average and "worst case" winds are similar to those for the Mojave Desert, due to their proximity. Both cases have been included in the dose calculations.

5. A Metropolitan Site.

Although it is not considered credible that the storage facility would actually be located within a major population center, we have evaluated such a site to determine an upper limit to man-rem estimates. For this purpose, an analysis was performed for a facility located in downtown Chicago, Illinois.

CALCULATIONS

The hypothetical sites and their prevailing wind directions are shown in Figure 5. The calculational model used to determine population dose was developed by Knox, *et al.*, (1972). The model has been adapted for use in this study according to the following assumptions:

1. The release occurs at an elevation of 10 m above ground.
2. The effluent stream is eventually dispersed over the entire troposphere of the Northern Hemisphere with a depth of about 15 km. (The model used is applicable only to a hemisphere.) Since the Northern Hemisphere contains about 90% of the world population, the calculated population doses will therefore be conservatively large. Population statistics were obtained from 1970 census figures.

Calculation of doses within 1,000 km followed the method of Knox (1971) in which functional relationships with distance were developed, except that winds were sector-averaged over 22.5 degrees. The close-in equation for man-rem, D_P, is

$$D_p = \int_0^{\pi/8} \int_{r_o}^{r} D_o \, R(r) \, p r dr d\theta,$$

where

D_o = individual dose at r_o (1 km), rem,

$R(r)$ = ratio of dilution factors at r to r_o, expressed as functional ratios [see Knox (1971) for full discussion],

p = population density, people/km,

r = distance downwind, km,

r_o = distance to site boundary, km, and

θ = azimuthal angle, radians.

Values of R(r) and population density used in this analysis are shown in Table 4.

Beyond 1,000 km, Knox, *et al.*, (1972) developed an intermediate-range solution. It is assumed that the ^{85}Kr effluent is transported at 40 km/hr, spreading throughout the troposphere horizontally at a rate of 220 km/day (half-width) for the first few days and then at a rate proportional to $t^{1/2}$. If D_o is the site boundary dose, then the total dose is

$$D_i = D_o \left(\frac{D_i}{D_o}\right)^1 \left(1 + e^{-\lambda} + e^{-2\lambda} + \ldots\ldots + e^{-n\lambda}\right)$$

$$= D_o \left(\frac{D_i}{D_o}\right)^1 (15.5),$$

where

$$\left(\frac{D_i}{D_o}\right)^1 \text{ is the first-year individual dose.}$$

Table 5 provides summary values of population doses to 1,000 km and for three continents. Long-range Northern Hemisphere population doses out to infinite time are also given. These calculations assume a uniform mass concentration of ^{85}Kr in the atmosphere and a mean residence time of 15.5 yrs.

It is apparent that the worldwide population dose is rather insensitive to storage site. The largest Northern Hemisphere dose (for a Chicago location) is about 1-1/3 times the smallest dose (for a remote island site). The important siting criterion appears to be the avoidance of a location where a large number of people residing nearby might receive large individual doses.

SUMMARY AND CONCLUSIONS

1. Cost-benefit analysis indicates that it would be prudent policy to require the prevention of ^{85}Kr release from fuel reprocessing plants at the present time, assuming this can be accomplished at a cost amounting to less than $1.00/Ci.
2. We have discussed options for accomplishment of ^{85}Kr release prevention from fuel reprocessing plants. No value judgments have been attempted in evaluating these options. However, it has been assumed that a policy of concentrating effluent noble gases, retaining them in pressurized storage tanks, and storing them for long periods at some centralized facility will be adopted. Such a policy would appear to be consistent with current AEC policy on high-level waste management.
3. Criteria for siting a long-term noble gas storage facility should include assurance that in the event of a containment failure: (a) Maximum permissible dose guidelines (0.5 rem/yr for whole body and 3.0 rem/yr for skin) are not exceeded. (b) Resultant population doses (man-rem) are minimized.
4. Five hypothetical sites have been evaluated to estimate population doses in the event of leakage. From this analysis it appears that geographic siting may be considered relatively unimportant.
5. Site selection should be based on cost-benefit studies considering: (a) Transportation and handling costs. (b) Maintenance and surveillance costs. (c) Resultant health benefits derived in terms of potential population dose averted.

REFERENCES

Cohen, J. J., (1973), *On Determining the Cost of Radiation Exposure to Populations for Purposes of Cost-Benefit Analyses,* Health Physics, vol. 25, p. 527.

Davis, J. S., (1973), personal communication.

Davis, J. S., and J. R. Martin, (1973), *A Cryogenic Approach to Fuel Reprocessing Gaseous Radwaste Treatment.* This Symposium.

Dunster, H. J. and B. F. Warner, (1970), *The Disposal of Noble Gas Fission Products From the Reprocessing of Nuclear Fuel,* AHSB(RP) R101, United Kingdom Atomic Energy Authority (UKAEA), Harwell.

Federal Regulation No. 222, **(1970),** *Policy Relating to the Siting of Fuel Reprocessing Plants and Related Waste Management Facilities,* vol. 35.

Hull, A. P., (1972), *Reactor Effluents: As Low as Practicable or as Low as Reasonable,* Nuclear News, vol. 16(11), p. 53.

International Commission on Radiological Protection (ICRP), **(1966),** *Recommendations of the International Commission on Radiological Protection,* Publication No. 9, Pergamon Press.

Knox, J. B., (1971), *Airborne Radiation from the Nuclear Power Industry,* Nuclear News, vol. 14(2).

Knox, J. B. and K. R. Peterson, (1972), *Estimates of Dose to Northern Hemisphere Population Groups from ^{85}Kr Emitted by a Single Nuclear Fuel-Reprocessing Plant,* Nuclear Safety, vol. 13(2).

Oak Ridge National Laboratory (ORNL), **(1970),** *Siting of Fuel Reprocessing Plants and Waste Management Facilities,* Rept. ORNL-4451.

Slansky, C., H. K. Peterson, and V. G. Johnson, (1969), *Nuclear Power Growth Spurs Interest in Fuel Plant Wastes,* Environ. Sci. Technol., vol. 3, p. 446.

United Nations (U.N.), **(1966),** Demographic Yearbook.

U. S. Geological Survey (USGS), **(1967),** *Data on Geochemistry: Composition of the Earth's Crust,* USGS-440-D, sixth edition, Washington, D.C.

TABLE 1. ^{85}Kr Exposure Data.

	Whole body	Skin	Units
Concentration — dose conversion factor	1.4×10^{4}	2.1×10^{6}	$\frac{\text{rem-m}^3}{\text{Ci-yr}}$
Total individual dose due to atmospheric ^{85}Kr	5.2×10^{-14}	7.8×10^{-12}	rem/Ci
Total population dose due to atmospheric ^{85}Kr (world population = 3.5×10^{9})	1.8×10^{-4}	0.027	man-rem/Ci
Maximum permissible dose	0.5	3.0	rem/yr
Cost of biological damage	250.	40.	$/man-rem
Estimated biological damage cost per unit release	0.05	1.00	$/Ci

Assumptions:

1. Instantaneous uniform atmospheric mixing
2. AtmVol = 4.2×10^{18} m^3
3. World population (1970) = 3.5×10^{9}
4. Mean atm residence time (^{85}Kr) = 15.5 yr

TABLE 2. Cost-Benefit Analysis.

1. Estimated Cost for ^{85}Kr extraction and storage:

   $0.04/Ci

2. Estimated Benefit due to ^{85}Kr release averted:

   $1.00/Ci

3. Benefit/cost ratio:

   $$\frac{1.00}{0.04} = 25$$

4. Cost effectiveness for exposure prevention:

   For whole body:

   $$\$0.04/\text{Ci} \times \frac{1}{1.8 \times 10^{-4}} \text{ Ci/man-rem} \cong \$220/\text{man-rem averted}$$

   For skin:

   $$\$0.04/\text{Ci} \times \frac{1}{0.027} \text{ Ci/man-rem} \cong \$1.50/\text{man-rem averted}$$

TABLE 3. ^{85}Kr Accidental Release.[a]

Maximum allowable fence line dose (rem)	Maximum allowable container capacity (10^6 Ci) - assume fence line $\frac{\chi}{Q} = 10^{-6}$ sec/m^3
25 (whole body)	56,000.
0.5 (whole body)	1,100.
150 (skin)	2,250.
3 (skin)	45.

[a] Assume the entire contents of one container is released.

TABLE 4. Population Densities and Functional Relationships R(r) for Calculating Population Doses to 1,000 km.

		1970 population density (people/km^2)							
		Island	Coast		Desert		Mountain		City
Distance (km)	R(r)	Most probable	Most probable	Worst case	Most probable	Worst case	Most probable	Worst case	Most probable
1-3	1	0	0	7	5	5			
1-3	1	0	0	7	5	5	0	0	2,500
3-10	$(3r_0/r)^2$	0	0	7	5	5	0	0	2,500
10-20	$(3r_0/r)^2$	0	0	7	10	10	0	0	2,200
20-100	$0.4\, r_0/r$	0	0	20	15	25	15	25	800
100-1000	$0.4\, r_0/r$	0	0	70	50	200	40	200	70

TABLE 5. Population Whole Body Doses for a 1 MCi Release of ^{85}Kr.

	Population whole body dose (man-rem)							
	Johnston Is.	Cape Hatteras		Mojave Desert		Mt. Whitney		Chicago
Distance or Continent	Most probable	Most probable	Worst case	Most probable	Worst case	Most probable	Worst case	Most probable
1 to 1000 km	0	0	45	31	120	26	120	210
North America	40	40	40	40	40	40	40	40
Europe	92	92	92	92	92	92	92	92
Asia	460	460	460	460	460	460	460	460
Northern Hemisphere total	590	590	637	623	712	618	712	802

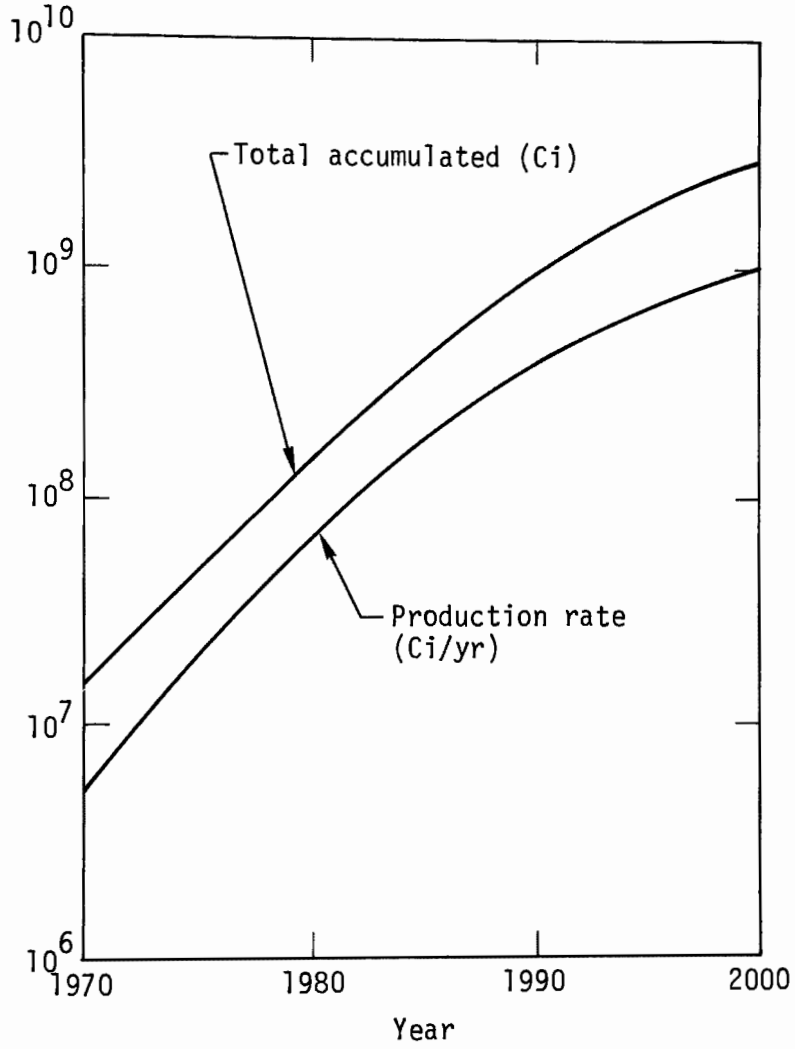

Figure 1. Projected worldwide ^{85}Kr production. Data from ORNL (1970).

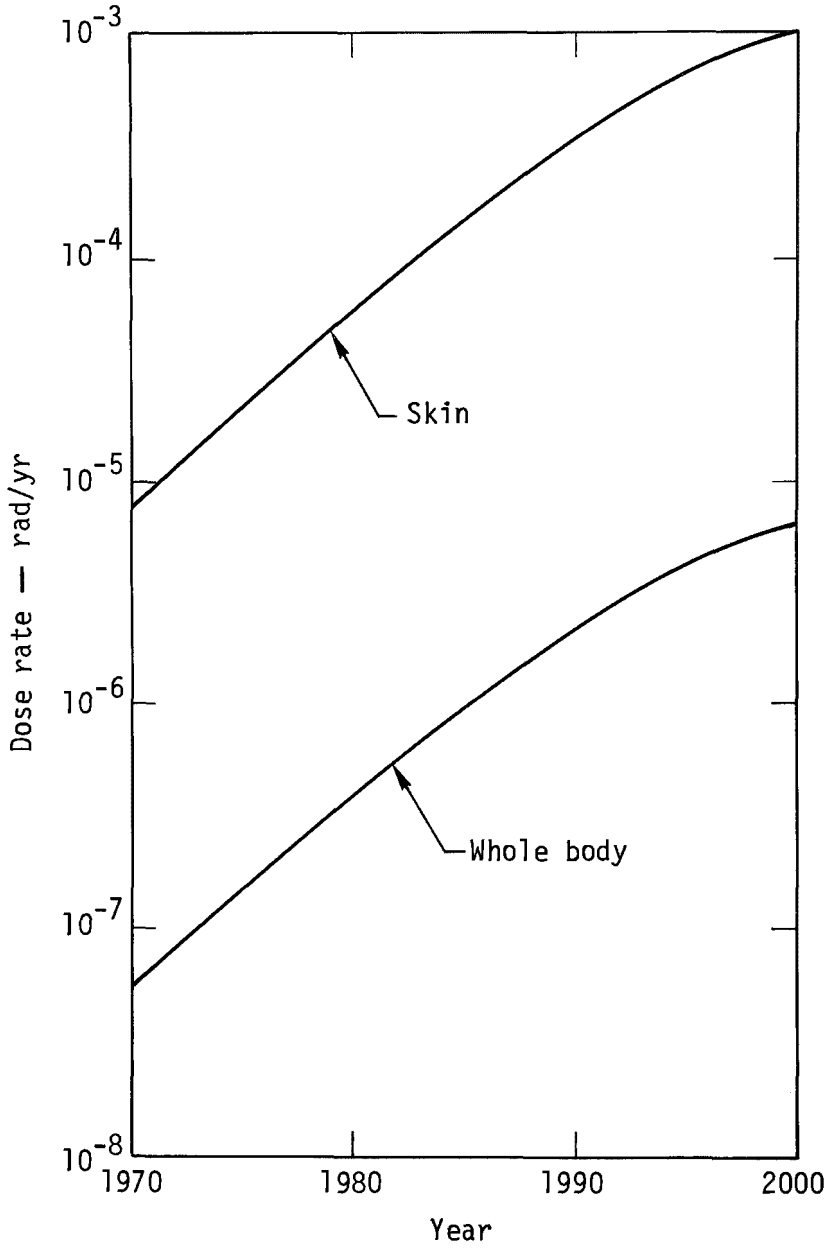

Figure 2. Projected worldwide individual dose due to atmospheric ^{85}Kr.

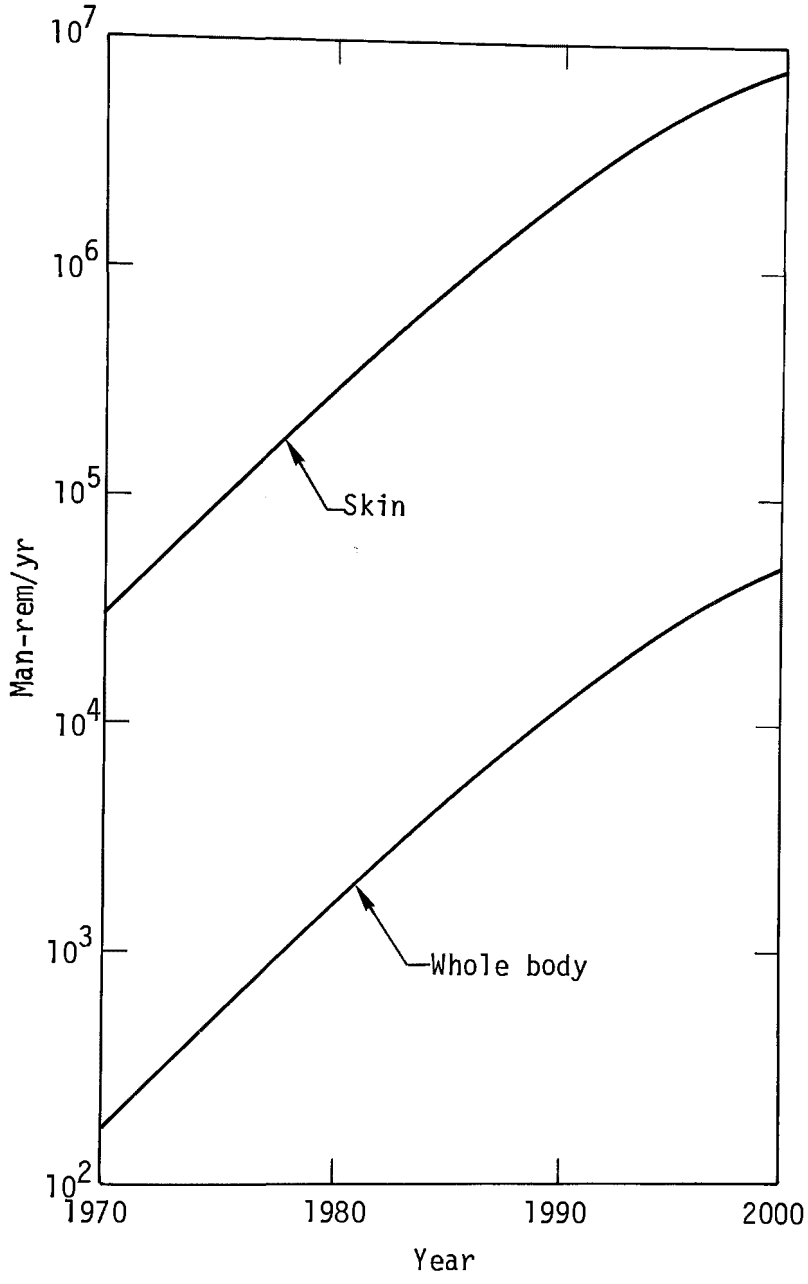

Figure 3. Projected worldwide population dose due to atmospheric ^{85}Kr.

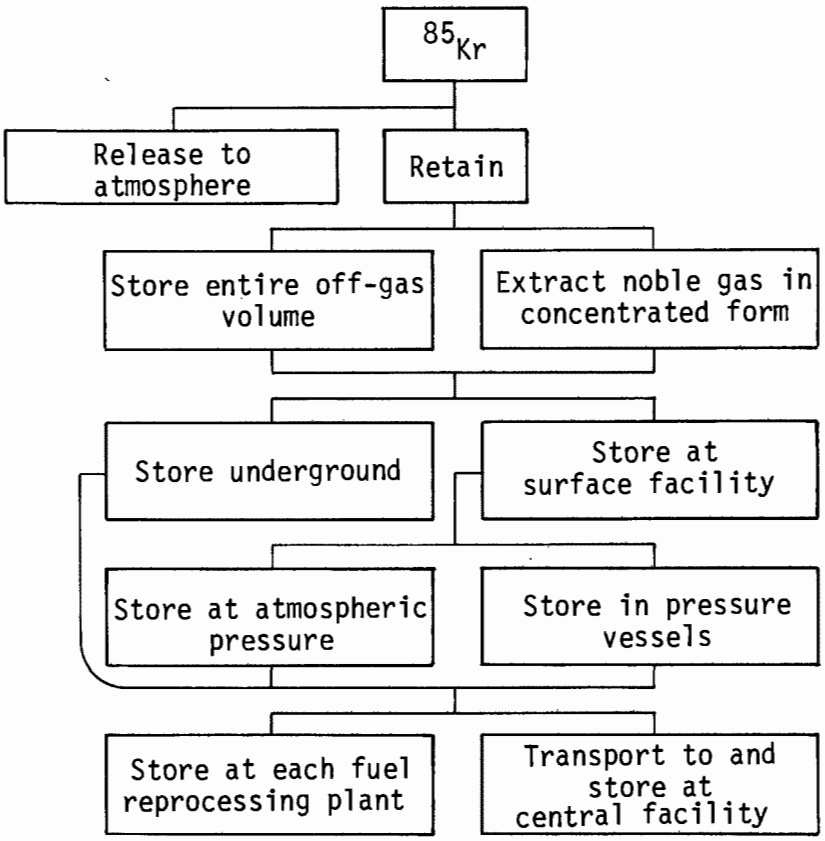

Figure 4. ^{85}Kr treatment options.

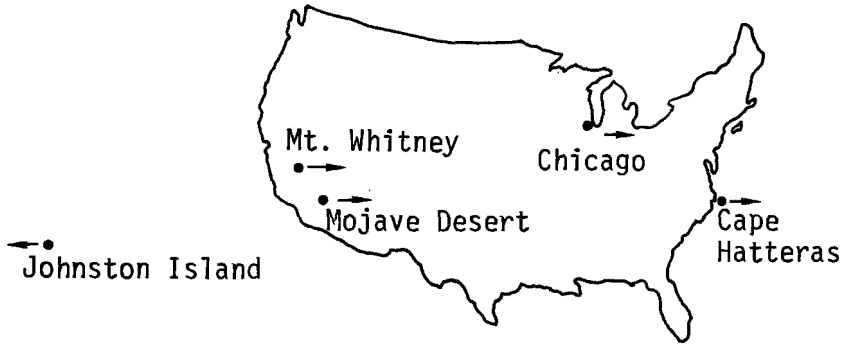

Figure 5. Potential storage sites (arrows indicate prevailing wind directions).

SELF ABSORPTION AND GEOMETRIC CORRECTION FACTORS FOR REACTOR OFF-GAS SAMPLES RELATIVE TO NBS STANDARDS*

R. F. Coley[1,2] and N. A. Frigerio[2]
[1]Commonwealth Edison Company
Chicago, Illinois
[2]Argonne National Laboratory
Argonne, Illinois

Abstract

Although they can be counted in identical bottles using identical counting systems, real gas samples differ from the NBS solution standards (e. g., mock reactor off-gas) in two respects — geometry and self absorption. Because both detector and source are real and finite, the simple "narrow beam" linear attenuation coefficient approximations currently used in the industry are quite inadequate for correction. Accordingly, the well-tested, complete-analog program, BIM 130, was used to compute the fraction of photons, and the photon energy spectra, reaching typical detectors used in the industry. Using this method, it was possible to correct the given NBS standard activity to its effective activity relative to a gas sample in an identical bottle. Factors were much closer to unity than predictions based on "narrow beam" linear attenuation coefficient approximations. At 80 keV, for example, such approximations gave 0.76, whereas the factor proved to be 1.03 for a 3" x 3" NaI(Tl) crystal and a 3 cm distance. Results are presented for various gamma energies of interest from 80 keV to 1,830 keV, and for the commonly used industrial distances of 3, 10, and 30 cm from the bottom of the sample bottle to the top of the detector container. Complete spectra for photons entering the detectors, as well as factors derived from these for typical NaI(Tl) and Ge(Li) detector resolutions, are given.

INTRODUCTION

A problem familiar to those associated with the nuclear power industry is that of the quantitative determination of the amounts of noble fission gas nuclides in reactor off-gas samples. Typically, reactor off-gas grab samples are collected in 15 ml serum vials for subsequent measurements using a gamma detector and multichannel analyzer system. Because of the wide ranges in both activity and isotopic composition experienced for such samples, the power plant analyst requires efficiency calibration data for various source-to-detector distances — 3, 10, and 30 cm being typical.

DISCUSSION

Recently, the National Bureau of Standards, with the support of the Atomic Energy Commission (ICONS, 1972), issued relatively inexpensive, mixed-radionuclide, gamma standards in 15 ml serum vials. Experimentally, one can use a multichannel analyzer system to compare the count rates from two bottles, one of known activity (the NBS standard), the other containing an off-gas samples. The absolute gamma activities in the off-gas sample could be simply obtained from the count rate ratio were it not for two factors: (1) the gas and the liquid are not identical in geometry; e. g., the extension upwards is higher for the gas than for the liquid and (2) self absorption and scatter are also greater within the liquid than within the gas. Because both NBS standards and samples can be counted in identical bottles using identical counting systems, a general set of geometry-self absorption correction factors for such samples might be a welcome step towards the long needed standardization of industrial techniques in this area.

The assumption that the effects of the glass between the photons leaving the source medium and the detector is the same for two identical bottles is not quite true. Measurements performed at the National Bureau of Standards have indicated that up to 25% of a group of such standards fell outside of 1.5% of the mean activity value, when measured one inch over a 3" x 3" NaI(Tl) detector (Coursey, 1973). However, such small errors are not usually of concern within the nuclear power industry.

The essential question is: For a given number of source photons, how many leave the source in such a direction as to be counted within the photopeak, for liquid and for gas? The number of photons leaving the liquid source per unit time may be expressed as: $N_l = k_l A_l$, where k_l is the fraction actually emerging from the liquid and A_l is the known emission rate. Similarly, for the gas source: $N_g = k_g A_g$. In order the compute k_l and k_g, the complete-analog program BIM 130, which has been shown to give excellent agreement with experimental values in both simple and complex systems (Frigerio, *et al.*, 1969 and 1973a and b), was used. In addition, the program was utilized to compute the photon energy spectra reaching the two most common types of detectors in use in the industry, NaI(Tl) and Ge(Li). Table 1 presents the spectrum reaching the detector for each of several photon energies emitted from the 12.4 ml right circular cylinder liquid source of radius 1.14 cm and a height of 3.037 cm representing the NBS serum vial source. Interactions within the 14.4 ml volume representing an off-gas sample, in the same serum vial, proved to be negligible (for 10^6 source photons there were only 5 photoelectric and 94 compton events within the source medium). Thus, the spectra of Table 1 represent the net spectral differences between liquid and vapor phase samples counted in the same vial using the same counting systems.

The fraction of source photons emergent from the liquid and from the gas samples, and striking the detector, were computed for a 3" x 3" NaI(Tl) crystal and for a 46.2 ml true coaxial, right circular cylinder of Ge(Li) with a diameter of 42.7 mm. These fractions are given in Table 2 for distances of 3, 10, and 30 cm from the bottom of

**Work supported, in part, by the U. S. Atomic Energy Commission.*

the vial to the top of the detector can. They represent the fraction of photons which would be counted within the photopeak for summation from the low energy channel (valley) indicated. The lower energy bounds for these summations were chosen to agree with actual experimental data obtained at operating nuclear units.

The ratios of the liquid fractions given, to the corresponding gas fractions, yield the desired correction factors, k_l/k_g. These are given in Table 3.

Thus, the activity of an unknown gas source, A_g, is given by:

$$A_g = (k_l/k_g)(N_g/N_l)A_l$$

where A_l is the liquid source activity, as given by NBS, (N_g/N_l) is the observed ratio of count rates, and (k_l/k_g) is the correction factor as given in Table 3.

Several features of Table 3 may be noted. First of all, the correction factors are greatly different than those from approximations obtained using "narrow beam" linear attenuation coefficients. At 80 keV, for example, such an approximation gives a single correction factor of 1.32 for an average photon path length in water equal to one-half the source height. That is, with u equal to 0.184 cm^{-1} for 80 keV and t equal to 1.52 cm in water, e^{ut} equals 1.32 (Hubbell, 1969). This may be contrasted with the corresponding values for a NaI(Tl) detector in Table 3, 1.03 to 0.97 as a function of distance to the detector. Such disagreement is a consequence of the fact that many of the "narrow beam attenuated" events are associated with scatter at small angles, with resultant small changes in energy (see spectra of Table 1). Thus, for real sources and finite detectors, a significant fraction of these scattered photons reach the detector, and remain within the photopeak. This fraction decreases with increasing energy so that, for example, (k_l/k_g) at 3 cm from a 3" x 3" NaI(Tl) detector drops from 1.03 at 80 keV to a minimum of 0.96 at 400 keV. This may be called the "photopeak effect".

At the same time, the total cross section also decreases with increasing energy, rendering the liquid more and more transparent to emitted photons. As this "transparency effect" becomes more pronounced (k_l/k_g) rises toward an asymptote of approximately one. Note also that the centroid of a liquid source is closer to the detector than the centroid of a gas source in the same vial. This results in (k_a/k_g) values which can, and should be greater than one either at low energies (photopeak effect dominating) or at high energies (transparency effect dominating). The much higher resolution of the Ge(Li) detector mitigates the photopeak effect very noticeably, so that for a Ge(Li) detector (k_l/k_g) rises monotonically toward unity without an evident minimum.

From the standpoint of the industrial user, the correction factors themselves are so close to one another that correction for specific energies is probably not warranted. Because off-gas samples are almost invariably measured at less than 550 keV, it is recommended that the 250 keV (k_l/k_g) values be used as adequate average correction factors for plant off-gas measurements.

REFERENCES

Coursey, B. M., (1973), private communication.

Frigerio, N. A. and M. H. Branson, (1969), *Current Research in Depth Dose Computations*, Proceedings of the Symposium on Neutrons in Radiobiology, Oak Ridge, Tennessee, 11-14 November, 1969, USAEC Report CONF-691106, p. 95.

Frigerio, N. A., R. F. Coley, and M. H. Branson, (1973), *Depth Dose Determinations. II. A Monte Carlo Program and a Standard Man Phantom for Neutron and Gamma Computations*, Phys. Med. Biol., vol. 18, no. 1, p. 53.

Frigerio, N. A. and R. F Coley, (1973), *Depth Dose Determinations. III. Standard Man Phantom and Various Gamma Sources*, Phys. Med. Biol., vol. 18, no. 2, p. 187.

Hubbel, J. H., (1969), *Photon Cross Sections, Attenuation Coefficients, and Energy Absorption Coefficients From 10 keV to 100 GeV*, NSRDS-NBS 29.

Information Center On Nuclear Standards (ICONS), (1972), *New Standards for Environmental Monitoring of Radioactivity*, Nuclear Standards News, October, 1972, (American Nuclear Society).

TABLE 1. Spectra Inbound to Detectors for Various Monoenergetic Sources (a).

keV (b)	counts	keV	counts	keV	counts	keV	counts	keV	counts	keV	counts
80	83,537	150	96,114	190	86,819	250	88,076	400	89,749	525	90,759
75	4,449	145	1,520	185	1,016	245	565	395	219	520	142
70	3,248	140	1,406	180	938	240	566	390	215	515	124
65	3,124	135	1,180	175	862	235	563	385	236	510	126
60	3,790	130	1,051	170	802	230	490	380	223	505	138
55	593	125	978	165	723	225	460	375	215	500	122
50	464	120	977	160	699	220	496	370	212	495	165
45	103	115	848	155	686	215	473	365	191	490	164
40	30	110	893	150	614	210	473	360	215	485	146
35	5	105	1,075	145	606	205	391	355	244	480	141
30	2	100	1,210	140	561	200	424	350	221	475	146
<30	0	95	1,476	135	572	195	371	345	216	470	120
		90	425	130	591	190	392	340	187	465	118
		85	202	125	703	185	365	335	190	460	127
		80	194	120	796	180	319	330	187	455	135
		75	178	115	864	175	333	325	200	450	127
		70	111	110	1,008	170	351	320	197	445	140
		65	33	105	389	165	365	315	170	440	121
		<60	33	<100	689	<160	4,503	<310	6,707	<435	6,938
sum(c)	99,345	sum	99,904	sum	99,938	sum	99,976	sum	99,994	sum	99,999

keV	counts	keV	counts	keV	counts	keV	counts	keV	counts
660	91,608	840	92,418	1,335	93,912	1,590	94,438	1,830	94,750
645	251	825	170	1,320	73	1,575	43	1,815	33
630	278	810	163	1,305	73	1,560	60	1,800	37
615	238	795	185	1,290	64	1,545	58	1,785	30
600	246	780	137	1,275	73	1,530	56	1,770	39
585	237	765	145	1,260	73	1,515	53	1,755	29
570	233	750	165	1,245	58	1,500	53	1,740	27
555	239	735	143	1,230	60	1,485	41	1,725	28
540	221	720	188	1,215	87	1,470	54	1,710	39
525	242	705	150	1,200	65	1,455	48	1,695	32
510	237	690	161	1,185	61	1,440	31	1,680	35
495	237	675	142	1,170	63	1,425	44	1,665	37
480	227	660	168	1,155	57	1,410	47	1,650	40
465	195	645	138	1,140	70	1,395	53	1,635	42
450	231	630	136	1,125	62	1,380	52	1,620	32
435	254	615	143	1,110	66	1,365	46	1,605	36
420	218	600	161	1,095	70	1,350	55	1,590	25
<405	4,379	<585	4,952	<1,080	4,936	<1,335	4,740	<1,575	4,702
sum	100,000	sum-	99,998	sum	100,000	sum	100,000	sum	100,000

(a) The source consisted of a 12.2 ml right circular cylinder of water with a radius of 1.14 cm and a height of 3.037 cm. The spectra proved to be independent of both detector size and source-to-detector distance, to less than 0.03%.

(b) The listed keV is the minimum energy for that channel. Thus, the first channel contains only unmodified photons.

(c) The listed sum represents the total number of photons reaching the detector. The difference between this sum and 100,000 is the number of photoelectric events that occurred within the water.

TABLE 2. Percent of Source Photons Counted Within Photopeak.

12.4 ml liquid source								
	3" x 3" NaI(Tl)				46.2 ml Ge(Li)			
keV (a)	**keV (b)**	**3 cm (c)**	**10 cm**	**30 cm**	**keV (b)**	**3 cm**	**10 cm**	**30 cm**
80	50	10.2	2.24	0.316	75	3.19	0.646	0.0830
150	110	9.73	2.14	0.310	145	3.20	0.611	0.0950
190	145	9.68	2.15	0.304	185	3.21	0.623	0.0775
250	200	9.64	2.11	0.337	245	3.22	0.638	0.110
400	335	9.55	2.17	0.324	395	3.33	0.677	0.103
525	445	9.61	2.17	0.318	520	3.36	0.664	0.0880
660	570	9.67	2.17	0.319	645	3.39	0.649	0.0870
840	735	9.70	2.13	0.294	835	3.39	0.655	0.0785
1,335	1,215	9.90	2.20	0.315	1,320	0.690	0.0945	
1,590	1,455	9.95	2.29	0.334	1,575	3.57	0.719	0.111
1,830	1,695	9.89	2.18	0.319	1,815	3.49	0.670	0.104

14.4 ml off-gas source							
3" x 3" NaI(Tl)				46.2 ml Ge(Li)			
keV	**3 cm**	**10 cm**	**30 cm**	**keV**	**3 cm**	**10 cm**	**30 cm**
d	9.95	2.29	0.344	d	3.55	0.717	0.107

(a) Initial source photon energy.

(b) Low energy channel used for beginning of photopeak summation.

(c) Distance from bottom of sample vial to top of detector can.

(d) For a gas sample, essentially all photons are unmodified. Thus, the fractions are not a function of initial photon energy.

TABLE 3. Combined Factors for Geometry and Self Absorption.

	(k_1/k_g)					
	3" x 3" NaI(Tl)			46.2 ml Ge(Li)		
keV	**3 cm**	**10 cm**	**30 cm**	**3 cm**	**10 cm**	**30 cm**
80	1.03	1.00	0.97	0.90	0.87	0.82
150	0.98	0.95	0.92	0.90	0.87	0.82
190	0.97	0.94	0.91	0.90	0.87	0.82
250	0.97	0.94	0.91	0.91	0.88	0.83
400	0.96	0.93	0.90	0.94	0.91	0.86
525	0.97	0.94	0.91	0.95	0.92	0.87
660	0.97	0.94	0.91	0.97	0.94	0.89
840	0.98	0.95	0.92	0.99	0.96	0.91
1,000 to 2,000	1.00	0.97	0.94	1.00	0.97	0.92

XI. Round Table Discussion of Noble Gases

NOBLE GASES FROM NUCLEAR REACTORS: CONTAINMENT VS. ENVIRONMENTAL RELEASE

During the Symposium, a round table discussion was held on the subject of noble gases, in general, and krypton-85, in particular. The members of the panel were: V.P. Bond, M. Eisenbud, C.C. Gamertsfelder, and E.C. Tsivoglou. Chairman was A.A. Moghissi.

MOGHISSI: Welcome to the panel discussion. I believe the stage is set for a very interesting and fruitful discussion. Before I get started, let me introduce the panel. On my extreme right is Dr. Carl C. Gamertsfelder, a technical assistant to the Director of Regulatory Standards of the U. S. Atomic Commission. He received his Ph.D. in Radiation Physics from the University of Missouri in 1941 and soon afterwards joined the Radiological Laboratory of Chicago. He also served at Oak Ridge National Laboratory in 1943, and at Hanford in 1944. On these three assignments he was involved in various developments in health physics and, most particularly, in matters related to production of plutonium for weapons. In 1952, he joined the aircraft nuclear propulsion project. In that capacity, he was concerned with safety analysis, metallurigical studies, and application of atomic energy. In 1964, he performed aerospace safety analysis on nuclear power projects and since late 1969 he has been with the Atomic Energy Commission.

On the extreme left is Dr. Merrill Eisenbud. He is Professor of Environmental Medicine and Director of the Laboratory for Environmental Studies at New York University Medical Center. He joined the University's faculty in 1959 following a 12-year career with the Atomic Energy Commission during most of which he served as the Director of Health and Safety Laboratory. From 1936 to 1947, he served as an industrial hygienist on the staff of the Liberty Mutual Life Insurance Company where he was engaged in studies of chemical and radiation hazards in industry. For two years, from 1968 to 1970, Dr. Eisenbud served as the first Environmental Protection Administrator for New York City. In that capacity, he had the primary responsibility for the Departments of Sanitation, Air Resources and Water Resources. Dr. Eisenbud holds a degree in Electrical Engineering from New York University and two honorary doctorates from Fairly Dickerson University and Catholic University of Rio de Janeiro. He is a member of many National and International Committees concerned with Public Health. Dr. Eisenbud is the author of numerous papers, including a textbook on Environmental Radioactivity, the second edition of which just appeared.

Next to him, on my left, is Dr. Victor Bond, who is the Associate Director of Life Sciences and Chemistry at Brookhaven National Laboratory in Upton, New York. He is internationally known as an expert in the field of nuclear medicine, radiation biology and therapy. Dr. Bond served as a medical officer in the U. S. Navy from 1945 to 1954. For six of these years, he was head of the Experimental Pathology Branch of the Naval Radiological Defense Laboratory in San Francisco. Following his tour of duty with the Navy, Dr. Bond joined the staff of the Brookhaven National Laboratory's Medical Research Center. He held increasingly responsible positions at Brookhaven until he was appointed in his present position as Associate Director of the Laboratory in 1967. Dr. Bond is also an Adjunct Professor of Radiology at Columbia University and Adjunct Professor of Medicine at the State University of New York at Stony Brook. Dr. Bond is a member of a large number of national and international organizations. He has published over 250 papers. He has contributed to many books and monographs. Most of us who have been in this business have referred to them for a long time. If I may add a personal note, Dr. Bond has given a number of ideas which I have used in my research.

Last, but not least, on my right, is Dr. Tsivoglou. Dr. Ernest Tsivoglou is a Professor of Civil Engineering at the Georgia Institute of Technology in Atlanta, Georgia, where he has been a member of the faculty for the past 7 years. Before joining the faculty of Georgia Tech, Dr. Tsivoglou was with the U.S. Public Health Service from 1949 to 1966 in Cincinnati and Columbus, Ohio, and Salt Lake City, Utah. In the Public Health Service, he was a Sanitary Engineer Director, and was Chief of Physical and Engineering Sciences in the Division of Water Supply and Pollution Control. He had various assignments in his Public Health Service career working in stream sanitation, radioactive waste control, studies of the fate of pollutants in the environment and research in the kinetics of natural processes. He also provided technical assistance and consultation to State, Federal, and other National agencies. Dr. Tsivoglou is largely responsible for the recurrence of the discussion on environmental radiation standards and emission standards from power reactors.

Here are the members of our panel; now I would like to ask them, one by one, to give a brief statement of their ideas, positions, what else they want to say in terms of the theme of our panel discussion, after which time I would appreciate receiving questions.

EISENBUD: I will confine myself to the subject of krypton-85 because this panel is supposed to discuss the pros and cons of containment versus release of krypton-85, the long-lived Noble Gases, of which there is only one. We are working in a field in which information is accumulating more rapidly than the risk. We talk about the projected per capita dose rates for the year 2050, but that is a long way off. We are dealing with a 10.5-year-half-life nuclide which, at the present time, is being produced in relatively modest amounts. I know, for example, that the present world-wide estimate for 1970 was a production of 6.6 MCi. This will go to 102 MCi in 1980 and up to 1000 MCi by the year 2000 and so on, into the next century.

We are talking, so far as National policy is concerned, about a relatively small number of plants that are the principal sources of krypton-85. It has been noted by several speakers that the reactors put out about 0.1% or less of the krypton-85 so that 99.9% or more will be released by relatively few fuel reprocessing plants. I believe

that what is needed is a sort of interim national policy which should be reevaluated every 5 or 10 years. From my point of view, there is no question that this would call for a containment of the krypton-85 in some form by the fuel reprocessing plants. Whether this would need to be done in the long-term, would depend on how a number of important questions are answered in the future. I didn't hear any of the speakers question the validity of the risk coefficients that have been used by the various speakers and which have their origin in the BEIR Report. I would certainly hope, and this is what I mean when I say the *information will accumulate* more rapidly than the risk, that, in the next decade, the biologists would give us answers to some fundamental questions, such as: Is there dose rate dependence, and should the risk coefficients, which are based on relatively massive exposure, be modified accordingly? For a given dose rate, is there a linearity, and is there a threshold?

When we talk about the genetic effects of radiation and such diseases as leukemia in humans, these are very difficult questions to answer. I would hope that Dr. Bond might address himself to this question. One difficulty is that the leukemia incidence is normally something like six cases per hundred thousand people per year: It is a relatively rare disease. But skin cancer is the most common of the neoplasms, and, incidently, one that is rarely fatal. If the skin is that sensitive to cancer so that we need to be concerned about per capita doses of the order of one to ten mrem per year, it should be possible by epidemiological techniques in a population as large as the atomic energy workers to see if they have a higher incidence of skin cancer. The incidence of skin cancer in the general population is very high compared to leukemia. It is estimated that one out of four light-skinned Australians develop one or more basal carcinomas by the time they are 65 years old. Thus, there is a much larger epidemiological base. For example, the uranium refinery workers who handled natural uranium and were exposed to the distilled daughter products in the course of the process, received relatively high skin doses. This group should be studied.

In summary, there are some fundamental questions, mainly of a biological nature, which will determine whether or not the radiation exposure of the order of background are significant. We should bear in mind that these levels will not be approached until sometime in the next century and our National policy should be developed accordingly. If my calculations are correct, the present per capita skin dose from krypton-85 is about 27 μrem per year and this will increase by 1980 to 0.6 mrem per year, and then to a little less than 1 mrem per year by the year 1990. Thus, 17 or 18 years from now, the dose will still be less than 1 mrem per year on a per capita basis. This would give us time to get the basic biological information and to make the decision as to what the National policy should be.

BOND: First, I would like to thank our Chairman for his very generous introduction. I do not have a prepared statement and there is little that I can say that has not already been said. I would like, in essence, to repeat several points that have been made.

First, let me state that I believe in the approach that has been used, of "as low as practicable" and that, "no radiation exposure should be given or allowed without good reason and compensating benefits." I also think that if we are exposed to a number of risks, this in no way gives us license to be cavalier about exposure to other risks. However, I also believe in looking at risks in context and in the philosophy of "as low as reasonable" as well as "low as practicable."

Let me remind you of what was stated this morning. The speakers agreed that the principal dose from krypton-85 was to the skin, and that dose to internal organs was a couple of orders of magnitude less than the dose to the skin. The figures that were given were of the order of a few mrem sometime in the next century. The dose to the whole body would be one or two orders of magnitude below that. In other words, we are talking about a small fraction of one mrem per year to the whole body.

We heard certain data on biological effects. With respect to the effects of radiation on the skin, no increase in skin cancer in those exposed in Hiroshima and Nagasaki have been reported, and a period of approximately 30 years has elapsed. The exposure was, of course, at high doses and dose rates and included neutron irradiation in the exposure in Hiroshima. The report of the Biological Effects of Ionizing Radiation (BEIR) Committee of the NAS/NRC (1972) presented data on a number of cancers which were well-known to result from exposure to radiation delivered at high doses and dose rates. The data were insufficient to provide risk estimates for skin cancer.

Numerical risk estimates for a number of other types of cancer were obtained as upper limit risk values by interpolation between data obtained at high doses and the natural incidence at background exposure levels. The BEIR Committee, however, which was very conservative in its approach, did not feel that the data available were adequate to provide risk estimates for skin cancer. This goes along with results available from some of Dr. Eisenbud's associates, on effects of exposure on the skin of animals. The curves appear definitely to be curvilinear, with increasing slope with increasing dose. There also appears to be a dose rate effect which generally follows curvilinearity. Also, United Nations Scientific Committee on Effects of Atomic Radiation (UNSCEAR Report 1972) which opined on the same data that the BEIR Committee reviewed, provided no risk estimates for skin cancer. The UNSCEAR Committee, however, unlike the BEIR Committee refused to provide risk estimates for any type of cancer for exposure at low doses and dose rates. This was done on the basis that the data obtained in man apply only at the high doses and dose rates at which they were obtained, and that the risk estimates obtained at low doses and dose rates obtained by interpolation very likely overestimate the true risk by a considerable margin. In summary, the risk of skin cancer, following exposure, is minimal, indeed.

Now, with respect to the removal of krypton, and the approaches to removing it from power plants and from reprocessing plants. From what I heard today, it is expensive to do this. Dr. Cohen said that the releases from power plants represent only a very small fraction of that from reprocessing plants. Let me remind you that, even into the next century, the average dose is 1 mrem per year. As a taxpayer, it seems to me that our money could be better spent than outfitting power plants to prevent the release of this isotope. I think that we could achieve much more real reduction in the mortality rate by spending this money elsewhere rather than spending our money to prevent imaginary deaths from this isotope.

So, my position then is similar to that of Dr. Eisenbud. I would have to be shown much more than I have been shown that there is a biological hazard, or that the dose is higher than has been shown, before I would become an advocate of outfitting power plants to reduce the release of krypton-85. I would have questions about outfitting the fuel reprocessing plants, but feel less strongly about that. Thank you.

GAMERTSFELDER: I am beginning to feel a little bit like Hoyt Whipple this morning, and people who have talked about all the things that are hard to talk about. I would say, in respect to removing krypton from the power plant emissions, that the AEC has not considered doing it at present. There would be no point in doing it until there were some effort put into removing it from the major source, which is the reprocessing plant. Now with respect to reprocessing plants, the AEC has no definite plans to remove krypton, but the people who are operating reprocessing plants have been told and have cooperated in providing enough space in their plants so that, in the future, when the equipment is developed, it could be put in. The bulk of exposure results from releases of krypton in countries other than the United States. It seems to me that if it becomes technically desirable as well as morally desirable to remove krypton from our fuel reprocessing plants, there should be some kind of international cooperation. We could get a lot more by getting some cooperation from our neighbors. I do not know if I have enough information to say when these things ought to take place. I would leave that to, I guess, the State Department.

TSIVOGLOU: I do have some prepared comments that I would like to make before we get to the question period. I feel like everybody else here on the platform that all my stuff has been stolen before the discussion got to me, but that happens. If you will bear with me, I would like to read these comments, because I find I stay out of trouble better that way.

The question of containment versus environmental release is far from new in the pollution control business. The same old question has been raised in connection with virtually every pollutant that has appeared on the scene. And it has been the principal question that I have contended with since I began working in this field some 20 years or so ago. The arguments from both the proponents and the opponents of environmental release are still also much the same. I don't think anybody here will be surprised to find that I am opposed to a policy of unnecessary environmental dispersal of the radioactive noble gases that result from nuclear power generation. We have seen a lot of progress in the last few years, let me say in the last four or five years. I recall as though it were yesterday the arguments in Minnesota that there was no technology available to reduce the stack releases from nuclear power plants; that the cost of doing so would be outrageous and would stifle the growth of the industry; and that releases up to the AEC limits would not hurt anybody anyway. Yet, in the short space of four years, we have seen the development of an excellent containment technology. We have seen that the actual costs are not that unreasonable. The industry still seems to be in a healthy state. And there has been a sharp reduction in the release limits that used to be regarded as acceptable.

It appears to me that the earlier real problems associated with noble gas releases from reactors are solved in the large sense and under much improved control, and that such releases can be expected to be truly minimal in the future. Therefore, I would like to confine my remarks here to the matter of release of krypton-85 from fuel recovery plants. We all seem to agree that that is the major noble gas problem that confronts us. Now, I too have a few numbers. They are crude numbers and I will duck as rapidly as possible later if anybody tries to pin me down on all of the assumptions, on which exponential curves I have used, and what references I am citing. An eight hundred megawatt nuclear generating plant of the Dresden-II type will have something like a half million curies of krypton-85 in the fuel rods after an initial twelve months of operation at full capacity. A considerably larger inventory will accumulate as operation continues, depending upon the operating level, frequency of fuel changes, and so on. There should be very little loss, we all agree on that, so that essentially all of that krypton-85 will go to a fuel recovery plant. The current generation of commercial fuel recovery plants envisions release to the atmosphere of all krypton-85 received. The Allied Gulf Plant at Barnwell, South Carolina, expects an atmospheric release in the neighborhood of about twelve million curies a year when operating at full capacity. The GE Midwest Fuel Recovery Plant projects an annual release of about three and a half million curies, but I understand that is operating one shift. The Nuclear Field Services Plant in New York State is currently shutdown for improvements. With the backlog of fuel that is accumulating for processing it seems safe to assume that all of these recovery plants, all three, will be operating at full capacity as soon as possible. So that within a very short time, with only those three plants in full-capacity operation, we can expect a combined release of 20 to 30 million curies a year of krypton-85. And that is the immediate future. As more generating plants come on line over the next two decades or so, there will be an increasing need for fuel recovery capacity, and the annual krypton-85 release will increase accordingly. By the end of the century then, according to my horseback numbers, if we go on the way we are, we alone will have released somewhere around a half a billion or more curies of krypton-85 to the environment. Let us admit right off the bat that it would undoubtedly be most difficult to prevent the escape of some of this gas and there are bound to be

occasional small releases. I am not an adherent of the currently popular zero-pollution cult either. I am a physicist among other things, and to me zero is an absolute, not a hazy concept. It is a word that is being used just a little too loosely today by politicans and, sometimes, by people who should know better. However, to me, the proponents of unrestrained environmental release represent the extreme opposite. Now they would leave future generations a legacy of world-wide contamination that I have to regard as inexcuseable. Perhaps the key to this problem is the matter of need. If I were able to convince myself that we were incapable of developing a suitable technology for krypton-85 containment or so destitute of money that we could not afford to contain it, then perhaps I might be more willing to go along for a time with a temporary policy of environmental release. But, I simply do not believe that such a real and honest need exists.

Let me recall briefly some of the arguments. The arguments against containment involve again the question of available technology (do we know how to do it?), the matter of whether we can afford the cost, the question of proof of harm, and the possibility of accidental release of the stored krypton-85.

Perhaps this example will help explain my attitude a little better. About two years ago, I published a paper in which I called for containment of krypton-85 from fuel recovery plants. Shortly thereafter, I was told by representatives of the industry "we would be glad to capture and store the krypton-85, but there is no practical technology available that is applicable on a full scale for a plant just like ours." It seems to me I am being presented with the question of which came first, the chicken or the egg. Of course, the technology needed to be developed just as it needed to be developed four years ago to control the stack releases from boiling water reactors. I have too much faith, in essence, in the skills of our engineers and scientists to accept the argument that there is no available technology. From what I see of the program, and from what I have heard here and in the halls, I gather that there is fairly general agreement now that the technology is available, or can be very shortly. As for the cost, coming up with a cost that is reasonable appears to me to be an integral part of developing a practical technology for containment. The problem of potential accidents with the stored krypton-85 is also technological in nature: I can't belive that we are unable to design a storage facility that can safely contain or disperse the relatively small quantities of gas that might escape if a tank were to rupture. And so I come finally to the old proof of harm argument, like who would be hurt anyway if we were to release it all? I must confess that I cannot prove and I would not attempt to that a billion or two curies of krypton-85 in the world environment will harm anybody. But I also must confess that I do not have infinite faith in the wisdom of those who decide what is safe and what isn't. To gamble now that no future harm can result from a policy of environmental release, to be so certain of our infinite wisdom, is to me to gamble with the well-being of future generations.

It is well, too, to remember that these little gambles can add up to larger ones. Krypton-85 is not the only radioisotope that we have around. And so I come back to the matter of need. In my view, the only acceptable justification for a policy of environmental release of krypton-85 would be a real and convincing proof of need. Unless I can convince myself that environmental release is a real and pressing necessity, I am unwilling to gamble, even in a small way, with the well-being of future generations. I am afraid I remain unconvinced that there is a need. I think we will know, in a very short time, whether our technological people are capable of developing containment processes that are effective, reasonable in cost, and safe. If my faith in their skill proves to be unfounded, I will hang my head.

MOGHISSI: Thank you members of the panel. Now is the time for questioning.

NEWMAN: I am Bob Newman with Allied Gulf Nuclear Services. When we first announced to the Commissioners of the AEC in February of 1968 that we intended to build a plant in Barnwell, South Carolina, we made the commitment that the plant would be designed to accommodate krypton capture facilities as far as space is concerned, connections, penetrations, and so forth. It was qualified; it is still qualified. We need to know when the cost benefit study or risk benefit or both warrants such an installation, when the technology is available, and when criteria and methods of storage are developed. I can tell you that when our plant in Barnwell goes into operation, it will have incorporated in it facilities for pollution abatement in excess of sixty million dollars. I do not think we are skimping, nor are we trying to delay. We, in our present climate, accept the linear dose relationship. We have our doubts, but we see no choice at the present time but to accept it. We especially have doubts, as has been brought out here, on the effect of low exposures to the skin from krypton. Even so, we are going ahead and assume it can be used as a basis. We do not think the Industry should respond to emotion. I was in Washington, talking to one of the Agencies. One of the first questions that came up was, "when are you going to start capturing krypton?" I say, "why? why should we?" The answer was simply, "the public demands it." Not one technical reason, not one justification, not one health related reason for capturing it, but the public demands it. I do not think the Industry can go on this way. There is a finite limit to the number of dollars we have. I want to see our dollars spent in the right way to do the most good. We agree with the principle of "as low as practicable." Licensing boards now are applying this to workers as well as to the public. I think one can opine from authoritative sources, projections of future doses of krypton-85 for the year 2000 vary by almost two orders of magnitude. I think this is one problem that we are faced with. The experts should be able to get together and say this is a reasonable projection and a realistic projection on which we can do our planning. I second the suggestion that as much work should be done as practical on defining what is the consequence of the skin exposure to very low levels of radiation. Are they important? How does one attach a dollar value to them? What is the value of a man-rem of very low level skin dose?

I do not think there is technology available which we would want to recommend to our management. I am sure there is at least one person in this room that disagrees with me from the comments I heard before. I do not think that we can obtain designer assistance for a technology which we could license through the AEC, meeting all their safety requirements. I am a chemical engineer. I have spent most of my career in the chemical business. I know the countless times the gas purification systems have failed because of trace impurities not recognized. You can synthesize a gas mixture and demonstrate a purification system. But, as in the case of krypton recovery facilities in operation today, trace impurities can lick you. The long-term storage has not really been looked at. Yes, it is feasible, but it has not really been addressed and engineered and the safety implications considered. Accidents do have to be looked at, we do not have enough knowledge yet to really assess the potential nor the consequences of an accident. Dr. Morgan, I will agree, the health physicists have done a fantastic job, but if you have radiochemical plant processes, from time to time, you have to do some maintenance and you are going to get some exposure. Is it safe? I think it is safe. Is it as low as practicable? I do not know, but still it is a trade-off.

MOGHISSI: Please make your statement brief and put your questions to the panel.

NEWMAN: I would like the panel to answer the following questions: 1. Define how the public can be educated in the real life of the potential consequences of krypton release. 2. How can the Industry, and that is used in the broad sense, the whole nuclear community, obtain well defined and supportable numbers on which we can make projections and plans. 3. How can we get the AEC, or maybe EPA, to set forth the overall criteria to which krypton recovery facilities should be addressed and on which you would base your decision to install the krypton recovery facilities including how does one weigh one number vs. another when they are not in consistent units. And, finally, can we get this whole thing on a real life basis and eliminate, at least within our own house, the emotion and hysteria?

MOGHISSI: Does any one of the panel members volunteer to answer all these questions?

EISENBUD: I cannot answer any of them, but I would like to ask one more question which I think perhaps Dr. Gamertsfelder can answer. Is there a krypton recovery system in existence today which the Commission is prepared to license?

MOGHISSI: The question is for Dr. Gamertsfelder. The last question first and then we go on to the other questions.

GAMERTSFELDER: I know of none and I do not think our licensing people know of any either. I do not think the research work has been done to clean up the gas streams that the krypton collection system would have to have before it could be operated. The initial stream has nitrogen oxides, hydrogen, oxygen, and various other things which have to be looked at from a safety standpoint as well as from an economic one.

TSIVOGLOU: I thought I heard a littler earlier from Jim Martin of EPA, that EPA has reached a conclusion that there is a technology, that is either available or very close to it, for krypton removal from fuel recovery plants. I even thought I heard him put a figure of about ten million dollars on it which, let us suppose, is optimistic — perhaps it will cost somewhat more than that. So I am a little confused really in the sense of what stage of technology we are. I presume that the EPA and AEC have been working together and are aware of everything that everybody else is doing. Perhaps somebody from EPA would like to comment on the stage of their investigations in the technology.

MOGHISSI: Before the somebody from EPA comes, there is somebody from Industry who would like to make a statement.

DAVIS: (Linde) Two years ago when the fuel reprocessing plant in Morris, Ill., went out for bids for a krypton-85 recovery system, we provided them with a commercially proven system using components that have been used for the last 50 years in the chemical industry which would give krypton recovery within 99%. Cryogenic systems and their present state-of-the-art are such that there are probably over a thousand plants in the world, some processing over twelve million cubic feet of gas an hour, and these plants operate 99% on stream time. For the Morris facility, we were talking about $800,000 for installed equipment or purchased equipment, and probably $1,500,000 in installed units and utilities. Operating costs are about two to three hundred dollars per day. I think that our paper in this Symposium shows that technology is here, it comes from a different area and has been used and proven thoroughly in many other applications outside the nuclear industry. We have the technology and even though its components are drawn from other fields, it is available.

MOGHISSI: Is Jim Martin here? Jim, a question was put to you. EPA has made a decision to recommend the collection of krypton from fuel reprocessing plants. Has this decision been discussed with the AEC?

MARTIN: Carl (Gamertsfelder) can answer that question for you. Yes, it definitely has been. The AEC does raise points that are fair. We do not blame them one bit for being unsure that the system can be made, not only

to perform to meet an environmental standard, but also that it can be made to perform in a way that it won't blow up in somebody's face. I submit that these are technical problems that can be overcome within a reasonable time. What is lacking is the decision to get on with the solution of those technical problems. Now, as an Agency, we are trying to be quite fair in allowing or recommending a time period that is reasonable to work toward those solutions. But, we are ready to bite the bullet and say it has got to come out. Once you get moving, it may not perform at 99%. You may have leakage, you may only get 90%, but until you start, you are not going to get these problems solved and I think that what has been holding us up, perhaps the starting of this particular approach, has been the conviction that is tied to the things that I tried to point out in my paper at this Symposium. We have not really looked at the total impact of the decision. In view of the comments from Linde, and several other places, we are not convinced that the arguments that the technology is not available are valid. We are prepared to admit that it's not demonstrated, but we believe that we are close to it.

EISENBUD: My instinct would lead me to believe that this is why we should not freeze the National policy around a single piece of equipment or a single performance standard. When I said that I thought that the information was accumulating faster than the risk, I was not talking entirely about the biological information; I meant the engineering information too. It might be useful, as a matter of National policy, to go through a 5- or 10-year period of demonstration of these plants seeing to it that one installation uses cryogenics, if this seems reasonable. I think the technology will eventually prove to be feasible from what I have seen from the literature. I think that we are probably almost there. I would hate to see us making the same mistake in the nuclear industry as they have made in the automobile industry in mandating a short time table for emissions controls which will lead to installation of ineffective hardware which will not do the job in the long-run.

BOND: I agree with Dr. Eisenbud. I do not see a reason for a crash program or for hasty regulations in this area. The low doses to which we are exposed in the present state of the technology are such that we have plenty of time to evaluate more thoroughly than has been done up to the present. I would also bring up something that was touched on several times and that has to do with the trade-off in risk — real vs. hypothetical risk; if the material is concentrated versus dispersing it widely. It has been stated that if one wishes to spend the necessary amount of money, the gas can be concentrated with a minimum exposure rate to the individuals concerned. However, I would expect that the cost would be considerable. While, perhaps, all persons are created equal, not all man-rems are. If we concentrate the material, we now have large amounts of radioactive isotopes and large amounts of radiation in a single location. I have dealt enough with accidents generally, and with nuclear installations to appreciate fully the human element. Accidents have occurred and they will occur. I do not have much faith in probabilities of accidents. I know that accidents have occurred where it is inconceivable that they could have occurred and substantial exposures have been sustained. What I am getting at, basically, is that what we may be trading is an unsubstantiated hypothetical risk from the material widely dispersed versus a strong possibility of a real obvious hazard to individuals resulting from the concentration and storage of the materials.

TSIVOGLOU: I would like to clarify something. I did not intend to call for a "crash program." I do not think that is what Dr. Martin of EPA was speaking about either. I have not heard anybody here, including myself, say that a crash program is necessary. I have heard people indicate that what we really need is a decision to go ahead. Because we do not even have a decision to go ahead yet, I am with Merrill Eisenbud, completely. In the sense of a time lapse, if we, today, got a decision to go ahead, from the way things have gone, it looks like five years is the minimum before there will be anything in operation. So, nobody is calling for a crash program.

GESELL: I am with the University of Texas School of Public Health. I just had the thunder stolen out of my question. Both the AEC and the EPA have a history of supporting research on technology for preventing environmental contamination, for instance, the research on the emergency core cooling. I was wondering if there were any plans, and I am addressing this to any spokesman from EPA or AEC who might be here, for support and funding research on krypton removal.

MOGHISSI: Carl, I think you would be the right person to answer that question.

GAMERTSFELDER: I cannot say that there are funds available at the present time. I know the subject is being discussed within the AEC, but decisions of that kind are not made by a few people discussing it. It takes time.

MOGHISSI: Any more comments?

BENDIXSEN: (Allied Chemical, Idaho) The last comments have been very interesting to me since we happen to be recovering krypton-85 in a distillation facility. Who is going to fund the first demonstration facility — EPA, AEC, or the industry? I do not count the unit we are operating as the first unit. Anyone who has looked at the reports we have published knows that we do not say that, and if they look at our efficiencies, they know that it is not the demonstration unit. Since we have a good representation on the panel, I would like to ask who is going to fund it? I might tell you right at the moment, there is not any funding for a demonstration unit. There is funding at Oak Ridge for a certain development work for a liquid carbon dioxide.

There has been some for a fluorocarbon system. There is no funding at all for a cryogenic system within the AEC. There has just begun this last fiscal year some funding to start looking at the containment and disposal of krypton-85. But let me return to my initial question. Who should fund it? EPA, AEC, or Industry?

EISENBUD: I will volunteer to answer this question because it is something that I feel very strongly about. I think that the National policy to put the AEC into the R&D business, for the first 20 or 25 years in the so-called atomic era was very sound, and could be justified. But we now have a nuclear industry which is building 30 or 40 reactors a year. At the present time, more than 200 nuclear power plants will be built in the next six or seven years, It is a fifty or hundred billion dollar industry. That industry consists of four or five manufacturers and two or three reprocessors. I suggest that Industry should set up the money to fund the research and not expect Uncle Sam to do it for you.

TSIVOGLOU: I cannot resist saying Amen.

BENDIXSEN: Let me point out that I am employed by the Government too. I am employed by Allied Chemical, but we are under subcontract to the AEC. I only do what they have told us to do and fund us to do at the moment.

EISENBUD: Pardon me if I point my finger. Your Company is one of the largest industries in the world. You have got to get together and develop the mechanisms for doing this internally.

BENDIXSEN: Please do not take my words as a member employee of Allied Chemical as any position of Allied Chemical. I have spent the last eight years in the same office and I have worked for three different companies. Those three companies have had the same subcontract with the AEC. So my company loyalty should not mean that I am stating something for Allied Chemical.

DEMPSEY: I am with the Division of Waste Management and Transportation. We are the Division responsible for evaluating and developing containment technology and we have a program with Allied Chemical at present. They finished a study on their cryogenic technology and put costs down for making a full stage system. Our plan is to go on to a demonstration by 1979. In the meantime, we are looking at the storage aspects.

PRETRE: (Switzerland) I would like to support what Dr. Bond has just said. May I recall that there is on one side, the general public, and, on the other, the personnel of the plant. The man-rem situation now is roughly as follows: For the public around the plant, the exposure between one and ten man-rem per year and for the personnel in the plant it is between one hundred and one thousand man-rem per year. That means the dose in the plant is two orders of magnitude higher than the dose outside the plant, It seems, therefore, that we have already passed the optimum. It is also important to realize that the man-rem for the personnel in the plant are real man-rem absorbed at high dose rates. On the other side, the few man-rem absorbed by the public are calculated and if they are really absorbed, they are at low dose rates. So, any additional retention of radioactivity in the plant will increase the total of man-rem instead of decreasing it. Therefore, it might be completely wrong to further concentrate all the radioactivity at the same point.

STRONG: I am with the Atomic Energy Commission, Licensing. I would like to address my question to Drs. Eisenbud and Bond. I was intrigued by Dr. Eisenbud's comment that he expected that, within the reasonably near future, we might expect information from biological studies that would resolve current problems regarding thresholds for cancer reduction: Linear versus other probability functions, etc. I wonder if you would expand on this and perhaps indicate what might represent reasonably conclusive evidence.

BOND: Let me say that at the time the BEIR Committee was reviewing data available to them, relatively little — this might be surprising to you — but relatively small amounts of data on late effects in animals were available to that group. A few years ago, a large amount of work, financed by the Atomic Energy Commission, was undertaken to evaluate such things as the shape of dose effect curves for different types of tumors in animals, the possibility of dose rate effect, RBE, and so forth. These experiments took years to complete. The data had not become available at the time of the BEIR Committee or the UNSCEAR Committee's deliberations. As a result, members of the BEIR Committee paid very little attention to animal data in their deliberations. They paid most attention to the relatively poor data available on the human. The UNSCEAR Committee, on the other hand, paid more attention to animal data, even then available, and took a far less conservative position in their report than did the BEIR Committee. Since the publication of these reports, data from these experiments that have been in preparation, are becoming available. These data are not published, as yet, but I have seen preprints. I will give you my interpretation that the data indicate that the bulk of animal tumors will show a curvilinear dose-effect relationship with increasing slope. They also indicate that a dose rate factor will apply in a number of situations. In addition, there are techniques open to us now at a very fundamental level to evaluate better, both somatic and genetic effects of radiation. I would expect, over the next few years, the data available to us and our ability to interpret these data, will be markedly improved over what they were at the time of the BEIR and UNSCEAR reports were written.

EISENBUD: It would be presumptuous of me to say that I agree with what Dr. Bond says, but I certainly do. I would add one more point. There is an admirable tendency now to reevaluate old animal and human data. A recent paper by two of my own colleagues, Drs. Albert and Altshuler, looked at not only radiation tumors, but cigarette smoking. In examining both the human data and the animal data, they have shown that as the dose goes down, the delay in onset of the tumor is longer. Of course, Robley Evans was the first to point this out, and he coined a term "practical threshold." He pointed out that the radium dial painters who had lower body burdens of radium took longer to develop the bone cancers. So, that in theory, if the incubation period is longer than the life of the person, the dose cannot be termed carcinogenic, because death will result from other causes.

KIRK: (EPA) I hate to muddy the waters at all, but there was a paper several years ago by Dunster and Warner in which they stated the opinion that the first group that would start receiving significant radiation exposure to krypton would probably be the people in the air products industries, recovering the krypton from the air. We may be trading off a high radiation dose to a segment of the population in the radiation industry to avoid a higher man-rem dose to a segment of a population outside of the nuclear industry.

SOLDAT: I am with Battelle Northwest, Richland, Washington. I would like to make two points. First, I do not want anyone to leave the room with the impression that the utility industry is sponsoring absolutely no research and development effort in terms of nuclear safety. This is an impression that might be gained from some of the things that were said here today. And second, I would like to restate what Dr. Bengston of the ICRP stated two weeks ago at the meeting of the International Radiation Protection Association. He said that it is perfectly logical to use reasoning that was used in the BEIR Report to arrive at dose limits. But, it is not equally logical to use such ultra conservative reasoning to calculate the effects of these doses.

MARTIN: (EPA) I raised another question earlier that fits into this argument of looking at the long-term commitment of the decision to dispose of pollutants in a certain way. It involves radon from our monuments called "tailing piles." I would like to have the panel comment on that, while I think we have bogged down in a morass here on krypton-85 and the battle lines and the opinion lines are pretty well drawn. Could we have some comment on radon?

BOND: I cannot comment, in depth, and would like to say only that I have been rather surprised at the time delay in effecting measures to reduce the exposure of miners. It was known many many years ago, in the last century, in deep mines in Europe, that miners did develop lung cancer. This was associated with radiation exposure. Yet, this went on for years without effective protection and it is only recently that adequate measures have been put into effect. I would also like to say that, with the exposure to radon, the doses received by the bronchial epithelium of the miners are quite high and very much higher than what we are talking about from krypton. Furthermore, exposure from radon is to alpha emitters, not beta emitters, so the problems are not comparable, at all, in that respect.

TSIVOGLOU: I feel some urge to comment since I guess the first nuclear work I did involved studies of radon and its daughter products in uranium mines back in 1952. Dr. Bond commented very justly on the long-time delay between the time we knew what to do, and the time anyone actually got down to work and began to try to protect uranium miners. My recollection of the time delay is something like 15 or 18 years. We knew in 1953 or 1954 that if we ventilated a uranium mine we could cut these doses down. This is a good example because it is the crux of the matter that we have here about krypton. The time delay occurred because we could not get a decision anywhere to go ahead and do something, because people argued and kept arguing. The Atomic Energy Commission, under the Atomic Energy Act, had no authority, it said, to do anything. The Public Health Service, at that time, felt that it did not have jurisdiction within a state boundary. And yet, the States in the early fifties and mid-fifties had no competence in the nuclear field. Who was to advise them? How was anybody to get a decision? It took 15 or 17 years to get a decision, and you know who made it? The Department of Labor under the Walsh-Healy Act. This is the same problem that bothers me now. And it is the problem that Jim Martin brought up on containment of krypton-85. No one wants a crash program, but I think we do have an urgent need for a decision.

EISENBUD: Well Dr. Tsivoglou, if you and I ever found ourselves on the same platform back in the Minnesota days, and I am surprised that we didn't because I thought you and I were on every platform and in every discussion group during the late 60's. You were then arguing against the right of the Federal government to preempt health and safety in respect to these matters, had we been on the same platform, and knowing of your experience, I would have pointed out to you, Ernie, that the reason that mess in the Southwest developed, which was absolutely inexcusable, was because of a quirk in the law which made it possible for the AEC to interpret that the State should regulate that particular problem. Since 1936 or 1937, established by NCRP for a completely different reason, there was a radon standard which may have been arrived at in the wrong way since we were not very sophisticated, but the recommended value prior to World War II was not too far off. Had it been adopted by the States, there would be several hundred men alive today who have since died of lung cancer.

TSIVOGLOU: That is absolutely correct. Had the standard for occupational protection that was available been adopted, it would have worked. However, the States had no competence in this field. In 1953 and thereabouts, there were not a lot of experts who even knew how to calculate simple radioactive decay. Merrill, if I heard you right, I think I may have been accused of saying I want the Feds to preempt now, although I did not in Minnesota. I think the Feds need to preempt where the States are not capable. However, I make no apology for my position in Minnesota, I think the States, many of them, have gotten to the point where they are entirely competent to regulate in the nuclear field. So that - I am a States-righter, let us face it.

BOND: I would submit that the parallel drawn by Dr. Tsivoglou is dubious, to say the least. What I mean is that, with the uranium miners, there was very little, if any, question that real harm was being done. The doses were high. The miners did have lung cancer. The role of smoking was and still is incompletely evaluated, but there was no question that those exposures to radon represented an occupational exposure resulting in serious damage. The problem should have been taken care of. Now contrast that with the krypton problem. As we have gone into many times during this meeting, the dose from this source is well below even current so-called "population standards" for the general public. Harm has not been demonstrated. It has been calculated that at these low doses in mice, the number of animals that would be required to determine an effect would be up in the billions, so high that one could not possibly conduct the experiment. So that, on the one hand, we are dealing with a real hazard; on the other hand, we are dealing with a supposed hazard.

HOLADAY: I am going to surprise you Alan (Moghissi) and not discuss the history of the uranium miner business because my blood pressure can get a lot higher than Ernie's (Tsivoglou). I will just make one comment. There is enough blame in that whole business to pass around and everybody from the Department of Labor, down to any State Bureau of Mines, all the way through, can pick up his proper share and there is still plenty left. What I came up here for was to speak to the question that was asked about the "tailing piles" of radon which all the panel carefully ducked around. This is one of those things that, looking at it, you can see no real excuse for not taking care of it. I personally cannot get concerned about the amount of radon released from a "tailing pile" in Shiprock, New Mexico, compared with what is coming out of a few hundred square miles around that place. In other words, you can completely stop the radon emission from that source and you will never notice the difference. The problem of controlling abandoned "tailing piles" from mines is not new. It has been taken care of, many times, merely on the basis that the stuff blowing around was a nuisance to the community and the area. The people who owned the mill hauled in dirt and covered it up and stabilized the thing just on the basis of being a good neighbor. I suspect that, here, the problem is that if they came back and stabilized them, their lawyers would tell them that somebody will say that they are admitting guilt. The problem is a simple one to cure. It just costs money.

MORGAN: I would like to comment on some of the remarks of my good friend, Vic Bond. I would interpret what he said that he is somewhat depreciating the application of the linear hypothesis at low doses and low dose rates. I am not sure whether Vic was in attendance at the meetings of the Congress of the International Radiation Protection Association in Washington, a few days back. At that Congress, there were some very well known and respected persons who presented some reasons why, at low doses and low dose rates, theoretically at least, one might expect a much greater risk per rem than at higher doses and dose rates. Also, at the hearings in Aliquippa, Pennsylvania, in response to allegations of Sternglass, that the Shippingport nuclear power plant had damaged the neighboring population, Dr. Bross brought out some of this research results of the tri-state studies which indicate that, in a population, there are critical groups such as those with asthma who seem to suffer far more from the effects of low doses of radiation than the average member of the population. One might argue that we are not concerned in these statistics with small groups, but this group of asthmatics is not a small group in a world population. So, I for one, would feel much more comfortable if, in the next decade, we would think in terms of developing techniques to remove the krypton-85, get rid of these 10 mrem per year to the skin and, in the meantime, hope that we have been overly conservative and protecting these critical segments of the population.

BOND: I do not know to whom at the IRPA meeting Dr. Morgan was referring to specifically. I have seen reports of several individuals who do feel that, perhaps, the risk is greater at low doses and dose rates than the linear hypothesis would indicate. Oftidal, for instance, was one. Others have attempted to repeat that work and have been unable to. I have seen estimates of this nature derived from the data in Hiroshima and Nagaskai. These data are heavily weighed by a neutron radiation component. In other words, the people were not exposed to a single radiation and, therefore, conclusions drawn from these data on the effects of low-LET radiations, to my mind, are not valid. With respect to Bross in Buffalo, there are others who very seriously disagree with his work and with his conclusions. (P. G. Smith, *et al.*, British Medical Journal, 27 May 1973; Hollacher, T. C., M. E. J. Med., 287:887, 1972). Bross started with leukemic children and claimed that the relative risk of this disease from *in-utero* exposure was greater in those with a "marker" (viral or bacterial infection; allergy) disease. Those who disagree start with children who have a "marker" disease and find no greater incidence of leukemia in those irradiated *in-utero* versus those not exposed. The conclusion is that the markers are associated with leukemia, irradiated or not, and that *in-utero* exposure is a "red herring." In summary, I know of no convincing data indicating that the "linear hypothesis" is other than conservative with respect to exposure at low doses and dose rates.

CHIRIWOLU: (Gibbs and Hill) The tendency here, today, seems to be that we should not be bothered by any release as long as it is not proven to be harmful. I think we should go the other way around. As long as it is not definitely proven to be harmless, we should try to separate it and contain it till we know it is safe to release it.

STEINDLER: (Argonne) There has been remarkably little practical information that has come out of this panel discussion. I am wondering if the costs of a krypton retention system, like waste management cost, in general, are going to be passed on to the guy who turns on the electricity. Can we get an estimate of what fraction of the power costs you anticipate to be involved in the krypton system?

EISENBUD: I will answer that by saying that I do not think anybody here really knows and I do not think it really matters. This argument has been used in such a way that you simply pile engineered safeguard upon engineered safeguard until far beyond the importance to the additional cost of power, is the fact that you end up with a plant that becomes very difficult to operate. I believe that many of the operating problems of the present generation of nuclear reactors is because of the application of redundant safeguards. They simply provide more and more opportunities for something to go wrong.

MOGHISSI: Carl, would you like to volunteer to give an answer if you have any number?

GAMERTSFELDER: Give me a few minutes. I might have a rough number. Based on certain comparisons with radioactive waste systems for power plants, I made a very rough calculation for krypton removal from reprocessing plants. The cost would be a very small fraction of a cent per kWh, somewhere in the neighborhood of 10^{-4} to 10^{-3} cent per kWh.

MATUSZEK: (New York Health Department) Unfortunately, what might come to the public, out of this discussion, is that there should be a major National policy to go to containment, particularly as Jim Martin is proposing it and Ernie (Tsivoglou) is in general agreement. Unfortunately we are not an island. Unless EPA plans to build a plastic dome around the United States, this reinforces what Carl Gamertsfelder said, just briefly, in his comments, that the rest of the world may not agree with us. The result of all this National policy, including time, effort, research, and money may be an inconsequential reduction of the dose to the world population.

SNYDER: (Oak Ridge) I was going to raise the same question, but I will try to phrase it slightly different. By one of the estimates used today, the present reactors going into commission will be operating in the year 2000 or there abouts and, consequently, if this pattern persists, then you are faced with an industry which is saddled with a policy and this is very difficult to reverse. We have seen it in the case of radon. We have seen it in the medical profession and so on. In other words, it is more difficult to reverse a policy once it is entrenched or, at least, I think that is the general course of experience, than it is to take steps in time. Now, the question is how close are we to that time. And I think perhaps the panel might wish to comment on this point.

EISENBUD: I have a few numbers that I could read. I thought I gave them earlier. It is true Walt (Snyder), that the reactors we are building today will be operating in the twenty-first century. However, the reactors that are already built are delivering a per capita dose of approximately 27 μrad per year. And if we made no change in technology, by the year 2000, the dose from the thousand reactors that will be operating in the world, will be 2.7 mrem per year. I have tried to make the point that, in my opinion, we have five years to formulate a National policy which will give us hardware that will do the job effectively without trade-offs that may be undesirable.

NELSON: (Environmental Protection Agency) There were some comments made earlier on the trade-off between the anticipated dose to the radiation workers which compared with the low, but nevertheless, existent dose to the general population. I would like to query the panel on this subject. The radiation worker is working voluntarily at his task whereas the general dose is given to anyone who happens to be downwind of the source.

TSIVOGLOU: Of course this is part of what has bothered me for a long time. In our great wisdom, we are making decisions for all of the general public and what we think they ought to be exposed to, where they do not understand what is going on in the first place, and where they have no real participation in a decision. I am afraid of decisions like that. I do not like to decide that the whole public can absorb such and such dose without knowing what I am doing. And I think Neil Nelson made the point that the radiation worker knows, we hope he knows, what he is doing, and he is a radiation worker by his own free choice. When it comes to how much radiation dose we will subject people to, we are tending not to give people any choice.

BOND: I think both of these considerations work out better in theory than in practice. I question, very much, that most radiation workers appreciate what the risk is. Sure, an effort is made, particularly recently, to explain this to them, but I am not sure how much they appreciate it. The other thing is, I am not sure how much we, in the practical world, really have choices. For instance, if we do not want to drive or ride in a car, we, in principle, have that option. I would ask anyone to become practical about it and see if you can get along in this modern day world without driving a car. Again, I think these arguments are fine, in theory, but, in practice,

they break down. The public, at large, does benefit from power generation, so there is that trade-off. Finally, why should any group force large expenditures on the public to save them from the hypothetical risk when, if they were informed and had a choice, they might well prefer to expend the money to reduce the real and serious risks to which they are exposed.

MOGHISSI: If I may put the last question of the day. I was recently invited to talk in a civic club. One of the very nice ladies put a question to me which I am going to put to the panel. The question is as follows: The release of krypton-85 by industrialized nations violates the spirit of the Test Ban Treaty because, and that was the way she put it, the risk is being given to the total population of the world, while the benefit goes to selected nations; those who have the capability for fuel reprocessing.

EISENBUD: We have a case in New York, where a power plant is planned 70-80 miles from New York City. The people there are saying, why should we be inconvenienced to build a plant to provide New York City with electricity for their subway? It is a very challenging question. The less developed parts of New York get some benefit from the industry and the commerce in New York City, just as developing countries, are getting the benefits of U. S. technology.

That lady had a very good question which we are going to hear more and more. Power plants are being proposed at sites where local people will not benefit from them, particularly, if a public agency is building them, in which case, they do not even pay taxes.

MOGHISSI: Thank you very much, members of the panel. On behalf of the organizers of this Symposium, I would like to express to the audience my appreciation for the excellent cooperation. I am particularly appreciative to the panel members for their frank and clear answers.

GPO 694-527/8